Guide to Meteorological Instruments and Methods of Observation

2014 edition

Updated in 2017

WORLD
METEOROLOGICAL
ORGANIZATION

Guide to Meteorological Instruments and Methods of Observation

2014 edition

Updated in 2017

WORLD
METEOROLOGICAL
ORGANIZATION

WMO-No. 8

PUBLICATION REVISION TRACK RECORD

Date	Part/ chapter/ section	Purpose of amendment	Proposed by	Approved by
May 2017	Part II, Chapter 5	Addition of new annex comprising the text of common WMO/ISO standard on ground-based remote sensing of wind by heterodyne pulsed Doppler lidar (equivalent of 28902-2:2017(E))	president of CIMO following consultation with WMO Members	Decision 35 (EC-69)

CONTENTS

PREFACE

One of the purposes of the World Meteorological Organization (WMO) is to coordinate the activities of its Members in the generation of data and information on weather, climate and water, according to internationally agreed standards. With this in mind, each session of the World Meteorological Congress adopts Technical Regulations which lay down the meteorological practices and procedures to be followed by WMO Members. The Technical Regulations are supplemented by a number of Manuals and Guides which describe in more detail the practices and procedures. Manuals contain standard and recommended practices that Members are required and urged to follow, respectively. Guides, such as this one, contain practices that Members are invited to follow or implement in establishing and conducting their arrangements for compliance with the Technical Regulations, and in otherwise developing meteorological and hydrological services in their respective countries. Whereas the regulatory material (Technical Regulations and Manuals) describe what is to be done and who is to do it, the purpose of the Guides is to provide information on how best to do it.

The implementation of the WMO Integrated Global Observing System (WIGOS) relies on the standardization of meteorological and related observations, aiming at uniformity in the practices and procedures employed worldwide and at better accuracy of the observations. The uniform, traceable and high-quality observational data represent an essential input for most WMO applications, such as climate monitoring, nowcasting and severe weather forecasting, thereby facilitating the improvement of the well-being of societies of all nations.

The first edition of the *Guide to Meteorological Instruments and Methods of Observation* (WMO-No. 8) was published in 1954 and consisted of twelve chapters. Since then, standardization has remained a key concern of the Commission for Instruments and Methods of Observation (CIMO) activities. The Commission continuously reviews the contents of the Guide and ensures that its regular update incorporates modern guidance material which reflects the rapid development of technologies and their implementation in the field of meteorological instruments and methods of observation.
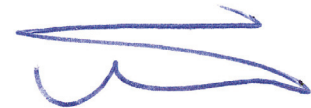
This Guide is a key resource that provides a description of most instruments, systems and techniques in regular use, from the simplest to the most complex and sophisticated, but does not attempt to deal with methods and instruments used only for research. The purpose of the Guide is to provide best practices, procedures and the basic capabilities of instruments and systems for assisting National Meteorological and Hydrological Services and other interested users operating observing systems in the preparation of their manuals and procedures to meet their specific needs for measurements and observations. The Guide intentionally restricts standardization to the essential requirements only, and confines recommendations to the general features most common to various configurations of a given instrument or measurement system, thus enabling wide areas for further development. The Guide is the authoritative reference for all matters related to instrumentation and methods of observation in the context of WIGOS.

This persistent work of experts has resulted in the 2014 edition of the Guide, which was approved by CIMO at its sixteenth session, held in Saint Petersburg, Russian Federation, in July 2014. In addition to almost all chapters being updated, the new edition includes a number of fully revised chapters and an extensive new part on space-based observations. The important impact of the recent Minamata Convention on Mercury of the United Nations Environment Programme in regard to mercury-based instruments is particularly highlighted in the relevant chapters.

The current Guide consists of 38 chapters distributed over the following four parts: Measurement of Meteorological Variables, Observing Systems, Space-based Observations, and Quality Assurance and Management of Observing Systems.

In the process of updating the CIMO Guide, WMO has benefited from the excellent collaboration that took place between CIMO and the Commission for Atmospheric Sciences, the Joint WMO/IOC Technical Commission for Oceanography and Marine Meteorology, the Commission for Basic Systems and the Global Climate Observing System, which provided significant contributions to the new edition of the Guide.

On behalf of the World Meteorological Organization, I would like to take the opportunity to express my sincere gratitude to CIMO and to all involved experts, whose tremendous efforts have enabled the publication of this new edition.

(Petteri Taalas)
Secretary-General

PART I. MEASUREMENT OF METEOROLOGICAL VARIABLES

PART CONTENTS

Page

CHAPTER CONTENTS

CHAPTER 1. GENERAL

1.1 METEOROLOGICAL OBSERVATIONS

1.1.1 General

Meteorological (and related environmental and geophysical) observations are made for a variety of reasons. They are used for the real-time preparation of weather analyses, forecasts and severe weather warnings, for the study of climate, for local weather-dependent operations (for example, local aerodrome flying operations, construction work on land and at sea), for hydrology and agricultural meteorology, and for research in meteorology and climatology. The purpose of the *Guide to Meteorological Instruments and Methods of Observation* is to support these activities by giving advice on good practices for meteorological measurements and observations.

There are many other sources of additional advice, and users should refer to the references placed at the end of each chapter for a bibliography of theory and practice relating to instruments and methods of observation. The references also contain national practices, national and international standards, and specific literature. They also include reports published by the World Meteorological Organization (WMO) for the Commission for Instruments and Methods of Observation (CIMO) on technical conferences, instrumentation, and international comparisons of instruments. Many other Manuals and Guides issued by WMO refer to particular applications of meteorological observations (see especially those relating to the Global Observing System (WMO, 2010*c*, 2010*e*), aeronautical meteorology (WMO, 2014), hydrology (WMO, 2008), agricultural meteorology (WMO, 2010*b*) and climatology (WMO, 2011*a*).

Quality assurance and maintenance are of special interest for instrument measurements. Throughout this Guide many recommendations are made in order to meet the stated performance requirements. Particularly, Part IV of this Guide is dedicated to quality assurance and management of observing systems. It is recognized that quality management and training of instrument specialists is of utmost importance. Therefore, on the recommendation of CIMO,[1] several regional associations of WMO have set up Regional Instrument Centres (RICs) to maintain standards and provide advice regarding meteorological measurements. Their terms of reference and locations are given in Annex 1.A. In addition, on the recommendation of the Joint WMO/IOC Technical Commission for Oceanography and Marine Meteorology[2] (WMO, 2010*a*) a network of Regional Marine Instrument Centres has been set up to provide for similar functions regarding marine meteorology and other related oceanographic measurements. Their terms of reference and locations are given in Part II, Chapter 4, Annex 4.A.

The definitions and standards stated in this Guide (see section 1.5.1) will always conform to internationally adopted standards. Basic documents to be referred to are the *International Meteorological Vocabulary* (WMO, 1992) and the *International Vocabulary of Metrology – Basic and General Concepts and Associated Terms (VIM)* (JCGM, 2012).

1.1.2 Representativeness

The representativeness of an observation is the degree to which it accurately describes the value of the variable needed for a specific purpose. Therefore, it is not a fixed quality of any observation, but results from joint appraisal of instrumentation, measurement interval and exposure against the requirements of some particular application. For instance, synoptic observations should typically be representative of an area up to 100 km around the station, but for small-scale or local applications the considered area may have dimensions of 10 km or less.

---

[1] Recommended by the Commission for Instruments and Methods of Observation at its ninth session (1985) through Recommendation 19 (CIMO-IX).

[2] Recommended by the Joint WMO/IOC Technical Commission for Oceanography and Marine Meteorology at its third session (2009) through Recommendation 1 (JCOMM-III).

In particular, applications have their own preferred timescales and space scales for averaging, station density and resolution of phenomena — small for agricultural meteorology, large for global long-range forecasting. Forecasting scales are closely related to the timescales of the phenomena; thus, shorter-range weather forecasts require more frequent observations from a denser network over a limited area in order to detect any small-scale phenomena and their quick development. Using various sources (WMO, 2001, 2010e; Orlanski, 1975), horizontal meteorological scales may be classified as follows, with a factor two uncertainty:

(a) Microscale (less than 100 m) for agricultural meteorology, for example, evaporation;

(b) Toposcale or local scale (100–3 km), for example, air pollution, tornadoes;

(c) Mesoscale (3–100 km), for example, thunderstorms, sea and mountain breezes;

(d) Large scale (100–3 000 km), for example, fronts, various cyclones, cloud clusters;

(e) Planetary scale (larger than 3 000 km), for example, long upper tropospheric waves.

Section 1.6 discusses the required and achievable uncertainties of instrument systems. The stated achievable uncertainties can be obtained with good instrument systems that are properly operated, but are not always obtained in practice. Good observing practices require skill, training, equipment and support, which are not always available in sufficient degree. The measurement intervals required vary by application: minutes for aviation, hours for agriculture, and days for climate description. Data storage arrangements are a compromise between available capacity and user needs.

Good exposure, which is representative on scales from a few metres to 100 km, is difficult to achieve (see section 1.3). Errors of unrepresentative exposure may be much larger than those expected from the instrument system in isolation. A station in a hilly or coastal location is likely to be unrepresentative on the large scale or mesoscale. However, good homogeneity of observations in time may enable users to employ data even from unrepresentative stations for climate studies.

Annex 1.B discusses site representativeness in further detail and provides guidelines on the classification of surface observing sites on land to indicate their representativeness for the measurement of different variables. This classification has several objectives:

(a) To improve the selection of a site and the location of a sensor within a site in order to optimize representativeness by applying some objective criteria;

(b) To help in the construction of a network and the selection of its sites:

  (i) Not only for meteorological services but also, for example, for road services;

  (ii) To avoid inappropriate positioning of instruments;

(c) To document the site representativeness with an easy-to-use criterion:

  (i) It is clear that a single number is not enough to fully document the environment and representativeness of a site. Additional information is necessary such as a map, pictures or a description of the surroundings;

  (ii) Despite this numerical value, the site classification is not only a ranking system. Class 1 sites are preferred, but sites in other classes are still valuable for many applications;

(d) To help users benefit from metadata when using observations data. If the metadata are too complex, they may discourage appropriate use.

1.1.3   **Metadata**

The purpose of this Guide and related WMO publications is to ensure reliability of observations by standardization. However, local resources and circumstances may cause deviations from the agreed standards of instrumentation and exposure. A typical example is that of regions with much snowfall, where the instruments are mounted higher than usual so that they can be useful in winter as well as summer.

Users of meteorological observations often need to know the actual exposure, type and condition of the equipment and its operation; and perhaps the circumstances of the observations. This is now particularly significant in the study of climate, in which detailed station histories have to be examined. Metadata (data about data) should be kept concerning all of the station establishment and maintenance matters described in section 1.3, and concerning changes which occur, including calibration and maintenance history and the changes in terms of exposure and staff (WMO, 2003). Metadata are especially important for elements which are particularly sensitive to exposure, such as precipitation, wind and temperature. One very basic form of metadata is information on the existence, availability and quality of meteorological data and of the metadata about them.

1.2   **METEOROLOGICAL OBSERVING SYSTEMS**

The requirements for observational data may be met using in situ measurements or remote-sensing (including space-borne) systems, according to the ability of the various sensing systems to measure the elements needed. The requirements in terms of global, regional and national scales and according to the application area are described in WMO (2010*e*). The Global Observing System, designed to meet these requirements, is composed of the surface-based subsystem and the space-based subsystem. The surface-based subsystem comprises a wide variety of types of stations according to the particular application (for example, surface synoptic station, upper-air station, climatological station, and so on). The space-based subsystem comprises a number of spacecraft with on-board sounding missions and the associated ground segment for command, control and data reception. The succeeding paragraphs and chapters in this Guide deal with the surface-based system and, to a lesser extent, with the space-based subsystem. To derive certain meteorological observations by automated systems, for example, present weather, a so-called "multi-sensor" approach is necessary, where an algorithm is applied to compute the result from the outputs of several sensors.

1.3   **GENERAL REQUIREMENTS OF A METEOROLOGICAL STATION**

The requirements for elements to be observed according to the type of station and observing network are detailed in WMO (2010*e*). In this section, the observational requirements of a typical climatological station or a surface synoptic network station are considered.

The following elements are observed at a station making surface observations (the chapters refer to Part I of the Guide):

    Present weather (Chapter 14)
    Past weather (Chapter 14)
    Wind direction and speed (Chapter 5)
    Cloud amount (Chapter 15)
    Cloud type (Chapter 15)
    Cloud-base height (Chapter 15)
    Visibility (Chapter 9)
    Temperature (Chapter 2)
    Relative humidity (Chapter 4)
    Atmospheric pressure (Chapter 3)
    Precipitation (Chapter 6)

Snow cover (Chapter 6)
Sunshine and/or solar radiation (Chapters 7, 8)
Soil temperature (Chapter 2)
Evaporation (Chapter 10)

Instruments exist which can measure all of these elements, except cloud type. However, with current technology, instruments for present and past weather, cloud amount and height, and snow cover are not able to make observations of the whole range of phenomena, whereas human observers are able to do so.

Some meteorological stations take upper-air measurements (Part I, Chapters 12 and 13), measurements of soil moisture (Part I, Chapter 11), ozone and atmospheric composition (Part I, Chapter 16), and some make use of special instrument systems as described in Part II of this Guide.

Details of observing methods and appropriate instrumentation are contained in the succeeding chapters of this Guide.

1.3.1 Automatic weather stations

Most of the elements required for synoptic, climatological or aeronautical purposes can be measured by automatic instrumentation (Part II, Chapter 1).

As the capabilities of automatic systems increase, the ratio of purely automatic weather stations to observer-staffed weather stations (with or without automatic instrumentation) increases steadily. The guidance in the following paragraphs regarding siting and exposure, changes of instrumentation, and inspection and maintenance apply equally to automatic weather stations and staffed weather stations.

1.3.2 Observers

Meteorological observers are required for a number of reasons, as follows:

(a) To make synoptic and/or climatological observations to the required uncertainty and representativeness with the aid of appropriate instruments;

(b) To maintain instruments, metadata documentation and observing sites in good order;

(c) To code and dispatch observations (in the absence of automatic coding and communication systems);

(d) To maintain in situ recording devices, including the changing of charts when provided;

(e) To make or collate weekly and/or monthly records of climatological data where automatic systems are unavailable or inadequate;

(f) To provide supplementary or back-up observations when automatic equipment does not make observations of all required elements, or when it is out of service;

(g) To respond to public and professional enquiries.

Observers should be trained and/or certified by an authorized Meteorological Service to establish their competence to make observations to the required standards. They should have the ability to interpret instructions for the use of instrumental and manual techniques that apply to their own particular observing systems. Guidance on the instrument training requirements for observers will be given in Part IV, Chapter 5.

1.3.3   **Siting and exposure**

1.3.3.1   *Site selection*

Meteorological observing stations are designed so that representative measurements (or observations) can be taken according to the type of station involved. Thus, a station in the synoptic network should make observations to meet synoptic-scale requirements, whereas an aviation meteorological observing station should make observations that describe the conditions specific to the local (aerodrome) site. Where stations are used for several purposes, for example, aviation, synoptic and climatological purposes, the most stringent requirement will dictate the precise location of an observing site and its associated sensors. A detailed study on siting and exposure is published in WMO (1993).

As an example, the following considerations apply to the selection of site and instrument exposure requirements for a typical synoptic or climatological station in a regional or national network:

(a)   Outdoor instruments should be installed on a level piece of ground, preferably no smaller than 25 m x 25 m where there are many installations, but in cases where there are relatively few installations (as in Figure 1.1) the area may be considerably smaller, for example, 10 m x 7 m (the enclosure). The ground should be covered with short grass or a surface representative of the locality, and surrounded by open fencing or palings to exclude unauthorized persons. Within the enclosure, a bare patch of ground of about 2 m x 2 m is reserved for observations of the state of the ground and of soil temperature at depths of equal to or less than 20 cm (Part I, Chapter 2) (soil temperatures at depths greater than 20 cm can be measured outside this bare patch of ground). An example of the layout of such a station is given in Figure 1.1 (taken from WMO, 2010*c*);
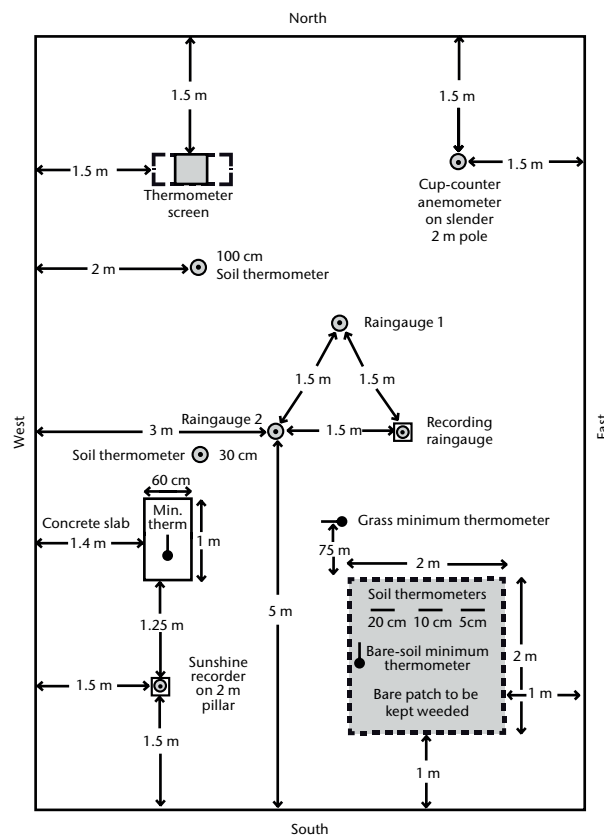
Figure 1.1. Layout of an observing station in the northern hemisphere showing minimum distances between installations

(b)   There should be no steeply sloping ground in the vicinity, and the site should not be in a hollow. If these conditions are not met, the observations may show peculiarities of entirely local significance;

(c)   The site should be well away from trees, buildings, walls or other obstructions. The distance of any such obstacle (including fencing) from the raingauge should not be less than twice the height of the object above the rim of the gauge, and preferably four times the height;

(d)   The sunshine recorder, raingauge and anemometer must be exposed according to their requirements, preferably on the same site as the other instruments;

(e)   It should be noted that the enclosure may not be the best place from which to estimate the wind speed and direction; another observing point, more exposed to the wind, may be desirable;

(f)   Very open sites which are satisfactory for most instruments are unsuitable for raingauges. For such sites, the rainfall catch is reduced in conditions other than light winds and some degree of shelter is needed;

(g)   If in the instrument enclosure surroundings, maybe at some distance, objects like trees or buildings obstruct the horizon significantly, alternative viewpoints should be selected for observations of sunshine or radiation;

(h)   The position used for observing cloud and visibility should be as open as possible and command the widest possible view of the sky and the surrounding country;

(i)   At coastal stations, it is desirable that the station command a view of the open sea. However, the station should not be too near the edge of a cliff because the wind eddies created by the cliff will affect the wind and precipitation measurements;

(j)   Night observations of cloud and visibility are best made from a site unaffected by extraneous lighting.

It is obvious that some of the above considerations are somewhat contradictory and require compromise solutions. Detailed information appropriate to specific instruments and measurements is given in the succeeding chapters.

1.3.3.2   *Coordinates of the station*

The position of a station referred to in the World Geodetic System 1984 (WGS-84) and its Earth Geodetic Model 1996 (EGM96) must be accurately known and recorded.[3] The coordinates of a station are (as required by WMO, 2010*c*):

(a)   The latitude in degrees, minutes and integer seconds;

(b)   The longitude in degrees, minutes and integer seconds;

(c)   The height of the station above mean sea level,[4] namely, the elevation of the station, in metres (up to two decimals).

These coordinates refer to the plot on which the observations are taken and may not be the same as those of the town, village or airfield after which the station is named. If a higher resolution of the coordinates is desired, the same practice applied to elevation can be followed, as explained below.

---

[3]   For an explanation of the WGS-84 and recording issues, see ICAO (2002).
[4]   Mean sea level (MSL) is defined in WMO (1992). The fixed reference level of MSL should be a well-defined geoid, like the WGS-84 Earth Geodetic Model 1996 (EGM96) [Geoid: the equipotential surface of the Earth's gravity field which best fits, in a least squares sense, global MSL].

The elevation of the station is defined as the height above mean sea level of the ground on which the raingauge stands or, if there is no raingauge, the ground beneath the thermometer screen. If there is neither raingauge nor screen, it is the average level of terrain in the vicinity of the station. If the station reports pressure, the elevation to which the station pressure relates must be separately specified. It is the datum level to which barometric reports at the station refer; such barometric values being termed "station pressure" and understood to refer to the given level for the purpose of maintaining continuity in the pressure records (WMO, 2010f).

If a station is located at an aerodrome, other elevations must be specified (see Part II, Chapter 2, and WMO, 2014). Definitions of measures of height and mean sea level are given in WMO (1992).

1.3.3.3   *Operating equipment in extreme environments*

Continuous observations during and after extreme hydrometeorological events are extremely important both to support recovery efforts and to prepare for future events. Mitigation strategies for common hazards are described in Annex 1.D.

1.3.4   **Changes of instrumentation and homogeneity**

The characteristics of an observing site will generally change over time, for example, through the growth of trees or erection of buildings on adjacent plots. Sites should be chosen to minimize these effects, if possible. Documentation of the geography of the site and its exposure should be kept and regularly updated as a component of the metadata (see Annex 1.C and WMO, 2003).

It is especially important to minimize the effects of changes of instrument and/or changes in the siting of specific instruments. Although the static characteristics of new instruments might be well understood, when they are deployed operationally they can introduce apparent changes in site climatology. In order to guard against this eventuality, observations from new instruments should be compared over an extended interval (at least one year; see the *Guide to Climatological Practices* (WMO, 2011a)) before the old measurement system is taken out of service. The same applies when there has been a change of site. Where this procedure is impractical at all sites, it is essential to carry out comparisons at selected representative sites to attempt to deduce changes in measurement data which might be a result of changing technology or enforced site changes.

1.3.5   **Inspection and maintenance**

1.3.5.1   *Inspection of stations*

All synoptic land stations and principal climatological stations should be inspected no less than once every two years. Agricultural meteorological and special stations should be inspected at intervals sufficiently short to ensure the maintenance of a high standard of observations and the correct functioning of instruments.

The principal objective of such inspections is to ascertain that:

(a)   The siting and exposure of instruments are known, acceptable and adequately documented;

(b)   Instruments are of the approved type, in good order, and regularly verified against standards, as necessary;

(c)   There is uniformity in the methods of observation and the procedures for calculating derived quantities from the observations;

(d)   The observers are competent to carry out their duties;

(e)   The metadata information is up to date.

Further information on the standardization of instruments is given in section 1.5.

1.3.5.2   *Maintenance*

Observing sites and instruments should be maintained regularly so that the quality of observations does not deteriorate significantly between station inspections. Routine (preventive) maintenance schedules include regular "housekeeping" at observing sites (for example, grass cutting and cleaning of exposed instrument surfaces) and manufacturers' recommended checks on automatic instruments. Routine quality control checks carried out at the station or at a central point should be designed to detect equipment faults at the earliest possible stage. Depending on the nature of the fault and the type of station, corrective maintenance (instrument replacement or repair) should be conducted according to agreed priorities and timescales. As part of the metadata, it is especially important that a log be kept of instrument faults, exposure changes, and remedial action taken where data are used for climatological purposes.

Further information on station inspection and management can be found in WMO (2010*c*).

1.4   **GENERAL REQUIREMENTS OF INSTRUMENTS**

1.4.1   **Desirable characteristics**

The most important requirements for meteorological instruments are the following:

(a)   Uncertainty, according to the stated requirement for the particular variable;

(b)   Reliability and stability;

(c)   Convenience of operation, calibration and maintenance;

(d)   Simplicity of design which is consistent with requirements;

(e)   Durability;

(f)   Acceptable cost of instrument, consumables and spare parts;

(g)   Safe for staff and the environment.

With regard to the first two requirements, it is important that an instrument should be able to maintain a known uncertainty over a long period. This is much better than having a high level of initial confidence (meaning low uncertainty) that cannot be retained for long under operating conditions.

Initial calibrations of instruments will, in general, reveal departures from the ideal output, necessitating corrections to observed data during normal operations. It is important that the corrections should be retained with the instruments at the observing site and that clear guidance be given to observers for their use.

Simplicity, strength of construction, and convenience of operation and maintenance are important since most meteorological instruments are in continuous use year in, year out, and may be located far away from good repair facilities. Robust construction is especially desirable for instruments that are wholly or partially exposed to the weather. Adherence to such characteristics will often reduce the overall cost of providing good observations, outweighing the initial cost.

Appropriate safety procedures must be implemented when using instruments containing dangerous chemicals (see in particular guidance on mercury (Part I, Chapter 3, 3.2.7) and hazardous chemicals (Part II, Chapter 8, 8.5 and 8.6). The Minamata Convention on Mercury of the United Nations Environment Programme (UNEP) entered into force in October 2013 and will have a significant impact on the use of mercury for meteorological applications.

1.4.2   Recording instruments

In many of the recording instruments used in meteorology, the motion of the sensing element is magnified by levers that move a pen on a chart on a clock-driven drum. Such recorders should be as free as possible from friction, not only in the bearings, but also between the pen and paper. Some means of adjusting the pressure of the pen on the paper should be provided, but this pressure should be reduced to a minimum consistent with a continuous legible trace. Means should also be provided in clock-driven recorders for making time marks. In the design of recording instruments that will be used in cold climates, particular care must be taken to ensure that their performance is not adversely affected by extreme cold and moisture, and that routine procedures (time marks, and so forth) can be carried out by the observers while wearing gloves.

Recording instruments should be compared frequently with instruments of the direct-reading type.

An increasing number of instruments make use of electronic recording in magnetic media or in semiconductor microcircuits. Many of the same considerations given for bearings, friction and cold-weather servicing apply to the mechanical components of such instruments.

1.5   MEASUREMENT STANDARDS AND DEFINITIONS

1.5.1   Definitions of standards of measurement

The term "standard" and other similar terms denote the various instruments, methods and scales used to establish the uncertainty of measurements. A nomenclature for standards of measurement is given in the *International Vocabulary of Metrology – Basic and General Concepts and Associated Terms (VIM)*, which was prepared simultaneously by the International Bureau of Weights and Measures (BIPM), the International Electrotechnical Commission (IEC), the International Federation of Clinical Chemistry and Laboratory Medicine (IFCC), the International Laboratory Accreditation Cooperation (ILAC), the International Organization for Standardization (ISO), the International Union of Pure and Applied Chemistry (IUPAC), the International Union of Pure and Applied Physics (IUPAP) and the International Organization of Legal Metrology (OIML), and issued by the Joint Committee for Guides in Metrology (JCGM). The current version is JCGM 200:2012, available at http://www.bipm.org/en/publications/guides/vim.html. Some of the definitions are as follows:

Measurement standard: Realization of the definition of a given quantity, with stated quantity value and associated measurement uncertainty, used as a reference.

> Example 1: 1 kg mass measurement standard with an associated standard measurement uncertainty of 3 μg

> Example 2: 100 Ω measurement standard resistor with an associated standard measurement uncertainty of 1 $\mu\Omega$

International measurement standard (international standard): Measurement standard recognized by signatories to an international agreement and intended to serve worldwide.

> Example 1: The international prototype of the kilogramme

National measurement standard (national standard): Measurement standard recognized by national authorities to serve in a State or economy as the basis for assigning quantity values to other measurement standards for the kind of quantity concerned.

Primary measurement standard (primary standard): Measurement standard established using a primary reference measurement procedure, or created as an artefact, chosen by convention.

> Example 1: Primary measurement standard of amount-of-substance concentration prepared by dissolving a known amount of substance of a chemical component to a known volume of solution

> Example 2: Primary measurement standard for pressure based on separate measurements of force and area

Secondary measurement standard (secondary standard): Measurement standard established through calibration with respect to a primary measurement standard for a quantity of the same kind.

Reference measurement standard (reference standard): Measurement standard designated for the calibration of other measurement standards for quantities of a given kind in a given organization or at a given location.

Working measurement standard (working standard): Measurement standard that is used routinely to calibrate or verify measuring instruments or measuring systems.

Notes:
1. A working measurement standard is usually calibrated with respect to a reference measurement standard.
2. In relation to verification, the terms "check standard" or "control standard" are also sometimes used.

Transfer measurement device (transfer device): Device used as an intermediary to compare measurement standards.

Note: Sometimes, measurement standards are used as transfer devices.

Travelling measurement standard (travelling standard): Measurement standard, sometimes of special construction, intended for transport between different locations.

Collective standard: A set of similar material measures or measuring instruments fulfilling, by their combined use, the role of a standard.

> Example: The World Radiometric Reference

Notes:
1. A collective standard is usually intended to provide a single value of a quantity.
2. The value provided by a collective standard is an appropriate mean of the values provided by the individual instruments.

Traceability: A property of the result of a measurement or the value of a standard whereby it can be related to stated references, usually national or international standards, through an unbroken chain of comparisons all having stated uncertainties.

Metrological traceability: A property of a measurement result whereby the result can be related to a reference through a documented unbroken chain of calibrations, each contributing to the measurement uncertainty.

Calibration: Operation that, under specified conditions, in a first step, establishes a relation between the quantity values with measurement uncertainties provided by measurement standards and corresponding indications with associated measurement uncertainties and, in a second step, uses this information to establish a relation for obtaining a measurement result from an indication.

Notes:

1. A calibration may be expressed by a statement, calibration function, calibration diagram, calibration curve, or calibration table. In some cases, it may consist of an additive or multiplicative correction of the indication with associated measurement uncertainty.

2. Calibration should not be confused with adjustment of a measuring system, often mistakenly called "self-calibration", nor with verification of calibration.

1.5.2   Procedures for standardization

In order to control effectively the standardization of meteorological instruments on a national and international scale, a system of national and regional standards has been adopted by WMO. The standardization of meteorological and related environmental measurements and assurance of the traceability of individual Members' standards to the International System of Units (SI) can be supported by Regional Instrument Centres (Annex 1.A). The locations of the regional standards for pressure and radiation are given in Part I, Chapter 3 (Annex 3.B), and Part I, Chapter 7 (Annex 7.C), respectively. In general, regional standards are designated by the regional associations, and national standards by the individual Members. Unless otherwise specified, instruments designated as regional and national standards should be compared by means of travelling standards at least once every five years. It is not essential for the instruments used as travelling standards to possess the uncertainty of primary or secondary standards; they should, however, be sufficiently robust to withstand transportation without changing their calibration.

Similarly, the instruments in operational use at a Service should be periodically compared directly or indirectly with the national standards. Comparisons of instruments within a Service should, as far as possible, be made at the time when the instruments are issued to a station and subsequently during each regular inspection of the station, as recommended in section 1.3.5. Portable standard instruments used by inspectors should be checked against the standard instruments of the Service before and after each tour of inspection.

Comparisons should be carried out between operational instruments of different designs (or principles of operation) to ensure homogeneity of measurements over space and time (see section 1.3.4).

1.5.3   Symbols, units and constants

1.5.3.1   *Symbols and units*

Instrument measurements produce numerical values. The purpose of these measurements is to obtain physical or meteorological quantities representing the state of the local atmosphere. For meteorological practices, instrument readings represent variables, such as "atmospheric pressure", "air temperature" or "wind speed". A variable with symbol a is usually represented in the form $a = \{a\} \cdot [a]$, where $\{a\}$ stands for the numerical value and $[a]$ stands for the symbol for the unit. General principles concerning quantities, units and symbols are stated in ISO (2009) and IUPAP (1987). The International System of Units should be used as the system of units for the evaluation of meteorological elements included in reports for international exchange. This system is published and updated by BIPM (2006). Guides for the use of SI are issued by the National Institute of Standards and Technology (NIST, 2008) and ISO (2009). Variables not defined as an international symbol by the International System of Quantities (ISQ), but commonly used in meteorology can be found in the *International Meteorological Tables* (WMO, 1966) and relevant chapters in this Guide.

The following units should be used for meteorological observations:

(a)   Atmospheric pressure, p, in hectopascals (hPa);[5]

---

[5]   The unit "pascal" is the principal SI derived unit for the pressure quantity. The unit and symbol "bar" is a unit outside the SI system; in every document where it is used, this unit (bar) should be defined in relation to the SI. Its continued use is not encouraged. By definition, 1 mbar (millibar) = 1 hPa (hectopascal).

(b) Temperature, t, in degrees Celsius (°C) or T in kelvins (K);

Note: The Celsius and kelvin temperature scales should conform to the actual definition of the International Temperature Scale (ITS-90, see BIPM, 1990).

(c) Wind speed, in both surface and upper-air observations, in metres per second (m s^{-1});

(d) Wind direction in degrees clockwise from true north or on the scale 0–36, where 36 is the wind from true north and 09 the wind from true east (°);

(e) Relative humidity, U, in per cent (%);

(f) Precipitation (total amount) in millimetres (mm) or kilograms per square metre (kg m^{-2});[6]

(g) Precipitation intensity, R_i, in millimetres per hour (mm h^{-1}) or kilograms per square metre per second (kg m^{-2} s^{-1});[7]

(h) Snow water equivalent in kilograms per square metre (kg m^{-2});

(i) Evaporation in millimetres (mm);

(j) Visibility in metres (m);

(k) Irradiance in watts per square metre and radiant exposure in joules per square metre (W m^{-2}, J m^{-2});

(l) Duration of sunshine in hours (h);

(m) Cloud height in metres (m);

(n) Cloud amount in oktas;

(o) Geopotential, used in upper-air observations, in standard geopotential metres (m').

Note: Height, level or altitude are presented with respect to a well-defined reference. Typical references are Mean Sea Level (MSL), station altitude or the 1 013.2 hPa plane.

The standard geopotential metre is defined as 0.980 665 of the dynamic metre; for levels in the troposphere, the geopotential is close in numerical value to the height expressed in metres.

1.5.3.2 *Constants*

The following constants have been adopted for meteorological use:

(a) Absolute temperature of the normal ice point T_0 = 273.15 K (t = 0.00 °C);

(b) Absolute temperature of the triple point of water T = 273.16 K (t = 0.01 °C), by definition of ITS-90;

(c) Standard acceleration of gravity (g_n) = 9.806 65 m s^{-2};

(d) Density of mercury at 0 °C = 1.359 51 $\cdot$ 10^4 kg m^{-3}.

The values of other constants are given in WMO (1966, 2011b).

---

[6] Assuming that 1 mm equals 1 kg m^{-2} independent of temperature.
[7] Recommendation 3 (CBS-XII), Annex 1, adopted through Resolution 4 (EC-LIII).

1.6   UNCERTAINTY OF MEASUREMENTS

1.6.1   Meteorological measurements

1.6.1.1   *General*

This section deals with definitions that are relevant to the assessment of accuracy and the measurement of uncertainties in physical measurements, and concludes with statements of required and achievable uncertainties in meteorology. First, it discusses some issues that arise particularly in meteorological measurements.

The term *measurement* is carefully defined in section 1.6.2, but in most of this Guide it is used less strictly to mean the process of measurement or its result, which may also be called an "observation". A *sample* is a single measurement, typically one of a series of spot or instantaneous readings of a sensor system, from which an average or smoothed value is derived to make an observation. For a more theoretical approach to this discussion, see Part IV, Chapters 2 and 3.

The terms *accuracy*, *error* and *uncertainty* are carefully defined in section 1.6.2, which explains that accuracy is a qualitative term, the numerical expression of which is uncertainty. This is good practice and is the form followed in this Guide. Formerly, the common and less precise use of accuracy was as in "an accuracy of ±x", which should read "an uncertainty of x".

1.6.1.2   *Sources and estimates of error*

The sources of error in the various meteorological measurements are discussed in specific detail in the following chapters of this Guide, but in general they may be seen as accumulating through the chain of traceability and the measurement conditions.

It is convenient to take air temperature as an example to discuss how errors arise, but it is not difficult to adapt the following argument to pressure, wind and other meteorological quantities. For temperature, the sources of error in an individual measurement are as follows:

(a)   Errors in the international, national and working standards, and in the comparisons made between them. These may be assumed to be negligible for meteorological applications;

(b)   Errors in the comparisons made between the working, travelling and/or check standards and the field instruments in the laboratory or in liquid baths in the field (if that is how the traceability is established). These are small if the practice is good (say ±0.1 K uncertainty at the 95% confidence level, including the errors in (a) above), but may quite easily be larger, depending on the skill of the operator and the quality of the equipment;

(c)   Non-linearity, drift, repeatability and reproducibility in the field thermometer and its transducer (depending on the type of thermometer element);

(d)   The effectiveness of the heat transfer between the thermometer element and the air in the thermometer shelter, which should ensure that the element is at thermal equilibrium with the air (related to system time-constant or lag coefficient). In a well-designed aspirated shelter this error will be very small, but it may be large otherwise;

(e)   The effectiveness of the thermometer shelter, which should ensure that the air in the shelter is at the same temperature as the air immediately surrounding it. In a well-designed case this error is small, but the difference between an effective and an ineffective shelter may be 3 °C or more in some circumstances;

(f)   The exposure, which should ensure that the shelter is at a temperature which is representative of the region to be monitored. Nearby sources and heat sinks (buildings, other unrepresentative surfaces below and around the shelter) and topography (hills, land-

water boundaries) may introduce large errors. The station metadata should contain a good and regularly updated description of exposure (see Annex 1.C) to inform data users about possible exposure errors.

Systematic and random errors both arise at all the above-mentioned stages. The effects of the error sources (d) to (f) can be kept small if operations are very careful and if convenient terrain for siting is available; otherwise these error sources may contribute to a very large overall error. However, they are sometimes overlooked in the discussion of errors, as though the laboratory calibration of the sensor could define the total error completely.

Establishing the true value is difficult in meteorology (Linacre, 1992). Well-designed instrument comparisons in the field may establish the characteristics of instruments to give a good estimate of uncertainty arising from stages (a) to (e) above. If station exposure has been documented adequately, the effects of imperfect exposure can be corrected systematically for some parameters (for example, wind; see WMO, 2002) and should be estimated for others.

Comparing station data against numerically analysed fields using neighbouring stations is an effective operational quality control procedure, if there are sufficient reliable stations in the region. Differences between the individual observations at the station and the values interpolated from the analysed field are due to errors in the field as well as to the performance of the station. However, over a period, the average error at each point in the analysed field may be assumed to be zero if the surrounding stations are adequate for a sound analysis. In that case, the mean and standard deviation of the differences between the station and the analysed field may be calculated, and these may be taken as the errors in the station measurement system (including effects of exposure). The uncertainty in the estimate of the mean value in the long term may, thus, be made quite small (if the circumstances at the station do not change), and this is the basis of climate change studies.

1.6.2   **Definitions of measurements and measurement errors**

The following terminology relating to the accuracy of measurements is based on JCGM (2012), which contains many definitions applicable to the practices of meteorological observations. Very useful and detailed practical guidance on the calculation and expression of uncertainty in measurements is given in ISO/IEC (2008) / JCGM (2008).

Measurement: The process of experimentally obtaining one or more quantity values that can reasonably be attributed to a quantity.

Note: The operations may be performed automatically.

Result of a measurement: A set of quantity values being attributed to a measurand together with any other available relevant information.

Notes:
1.   When a result is given, it should be made clear whether it refers to the indication, the uncorrected result or the corrected result, and whether several values are averaged.
2.   A complete statement of the result of a measurement includes information about the uncertainty of the measurement.

Corrected result: The result of a measurement after correction for systematic error.

Value (of a quantity): A number and reference together expressing the magnitude of a quantity.

    Example: Length of a rod: 5.34 m

True value (of a quantity): The quantity value consistent with the definition of a quantity.

$$< true\ value > = < measured\ value > \pm < uncertainty >$$

Notes:
1.   This is a value that would be obtained by a perfect measurement.
2.   True values are by nature indeterminate.

Accuracy (of a measurement): A qualitative term referring to the closeness of agreement between a measured quantity value and a true quantity value of a measurand. The accuracy of a measurement is sometimes understood as the closeness of agreement between measured quantity values that are being attributed to the measurand. It is possible to refer to an instrument or a measurement as having a high accuracy, but the quantitative measure of the accuracy is expressed in terms of uncertainty.

Uncertainty: A non-negative parameter characterizing the dispersion of the quantity values being attributed to a measurand, based on the information used.

Repeatability: The closeness of agreement between indications or measured quantity values obtained on the same or similar objects under a set of conditions that includes the same measurement procedure, same operators, same measuring system, same operating conditions and same location, and replicate measurements over a short period of time.

Note: Relevant statistical terms are given in ISO (1994*a*) and ISO (1994*b*).

Reproducibility: The closeness of agreement between indications or measured quantity values obtained on the same or similar objects under a set of conditions that includes different locations, operators and measuring systems, and replicate measurements.

Error (of measurement): Measured quantity value minus a reference quantity value.

Instrumental bias: Average of replicate indications minus a reference quantity value.

Random error: The component of measurement error that in replicate measurements varies in an unpredictable manner.

Notes:
1.   Random measurement error equals measurement error minus systematic measurement error.
2.   A reference quantity value for a random measurement error is the average that would ensue from an infinite number of replicate measurements of the same measurand.

Systematic error: The component of measurement error that in replicate measurements remains constant or varies in a predictable manner.

Notes:
1.   Systematic measurement error equals measurement error minus random measurement error.
2.   Like true value, systematic error and its causes cannot be completely known.

Correction: Compensation for an estimated systematic effect.

Some definitions are also repeated in Part IV, Chapter 4 for convenience.

1.6.3   **Characteristics of instruments**

Some other properties of instruments which must be understood when considering their uncertainty are taken from JCGM (2012).

Sensitivity: Quotient of the change in an indication of a measuring system and the corresponding change in a value of a quantity being measured.

Note: The sensitivity of a measuring system can depend on the value of the quantity being measured.

Discrimination threshold: The largest change in a value of a quantity being measured that causes no detectable change in the corresponding indication.

Resolution: The smallest change in a quantity being measured that causes a perceptible change in the corresponding indication.

Hysteresis: The property of a measuring instrument whereby its response to a given stimulus depends on the sequence of preceding stimuli.

Stability (of an instrument): The property of a measuring instrument whereby its metrological properties remain constant in time.

Drift: A continuous or incremental change over time in indication due to changes in metrological properties of a measuring instrument.

Step response time: The duration between the instant when an input quantity value of a measuring instrument or measuring system is subjected to an abrupt change between two specified constant quantity values and the instant when a corresponding indication settles within specified limits around its final steady value.

The following other definitions are used frequently in meteorology:

Statements of response time: The time for 90% of the step change is often given. The time for 50% of the step change is sometimes referred to as the half-time.

Calculation of response time: In most simple systems, the response to a step change is:

$$Y = A\left(1 - e^{-t/\tau}\right) \tag{1.1}$$

where Y is the change after elapsed time t; A is the amplitude of the step change applied; t is the elapsed time from the step change; and τ is a characteristic variable of the system having the dimension of time.

The variable τ is referred to as the time constant or the lag coefficient. It is the time taken, after a step change, for the instrument to reach $1/e$ of the final steady reading.

In other systems, the response is more complicated and will not be considered here (see also Part IV, Chapter 2).

Lag error: The error that a set of measurements may possess due to the finite response time of the observing instrument.

1.6.4 The measurement uncertainties of a single instrument

ISO/IEC (2008) / JCGM (2008) should be used for the expression and calculation of uncertainties. It gives a detailed practical account of definitions and methods of reporting, and a comprehensive description of suitable statistical methods, with many illustrative examples.

1.6.4.1 The statistical distributions of observations

To determine the uncertainty of any individual measurement, a statistical approach is to be considered in the first place. For this purpose, the following definitions are stated (ISO/IEC (2008) / JCGM (2008); JCGM, 2012):

(a) Standard uncertainty;

(b) Expanded uncertainty;

(c) Variance, standard deviation;

(d) Statistical coverage interval.
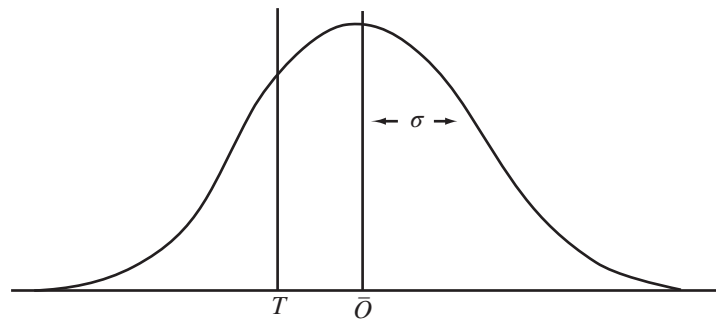
Figure 1.2. The distribution of data in an instrument comparison

If n comparisons of an operational instrument are made with the measured variable and all other significant variables held constant, if the best estimate of the true value is established by use of a reference standard, and if the measured variable has a Gaussian distribution,[8] the results may be displayed as in Figure 1.2.

In this figure, T is the true value, $\bar{O}$ is the mean of the n values O observed with one instrument, and σ is the standard deviation of the observed values with respect to their mean values.

In this situation, the following characteristics can be identified:

(a)   The systematic error, often termed bias, given by the algebraic difference $\bar{O} - T$. Systematic errors cannot be eliminated but may often be reduced. A correction factor can be applied to compensate for the systematic effect. Typically, appropriate calibrations and adjustments should be performed to eliminate the systematic errors of sensors. Systematic errors due to environmental or siting effects can only be reduced;

(b)   The random error, which arises from unpredictable or stochastic temporal and spatial variations. The measure of this random effect can be expressed by the standard deviation σ determined after n measurements, where n should be large enough. In principle, σ is a measure for the uncertainty of $\bar{O}$;

(c)   The accuracy of measurement, which is the closeness of the agreement between the result of a measurement and a true value of the measurand. The accuracy of a measuring instrument is the ability to give responses close to a true value. Note that "accuracy" is a qualitative concept;

(d)   The uncertainty of measurement, which represents a parameter associated with the result of a measurement, that characterizes the dispersion of the values that could be reasonably attributed to the measurand. The uncertainties associated with the random and systematic effects that give rise to the error can be evaluated to express the uncertainty of measurement.

1.6.4.2   *Estimating the true value*

In normal practice, observations are used to make an estimate of the true value. If a systematic error does not exist or has been removed from the data, the true value can be approximated by taking the mean of a very large number of carefully executed independent measurements. When fewer measurements are available, their mean has a distribution of its own and only certain

---

8   However, note that several meteorological variables do not follow a Gaussian distribution. See section 1.6.4.2.3.

limits within which the true value can be expected to lie can be indicated. In order to do this, it is necessary to choose a statistical probability (level of confidence) for the limits, and the error distribution of the means must be known.

A very useful and clear explanation of this notion and related subjects is given by Natrella (1966). Further discussion is given by Eisenhart (1963).

1.6.4.2.1 Estimating the true value – n large

When the number of n observations is large, the distribution of the means of samples is Gaussian, even when the observational errors themselves are not. In this situation, or when the distribution of the means of samples is known to be Gaussian for other reasons, the limits between which the true value of the mean can be expected to lie are obtained from:

Upper limit:
$$L_U = \bar{X} + k \cdot \frac{\sigma}{\sqrt{n}} \qquad (1.2)$$

Lower limit:
$$L_L = \bar{X} - k \cdot \frac{\sigma}{\sqrt{n}} \qquad (1.3)$$

where $\bar{X}$ is the average of the observations $\bar{O}$ corrected for systematic error; σ is the standard deviation of the whole population; and k is a factor, according to the chosen level of confidence, which can be calculated using the normal distribution function.

Some values of k are as follows:

Level of confidence	90%	95%	99%
k	1.645	1.960	2.575

The level of confidence used in the table above is for the condition that the true value will not be outside the one particular limit (upper or lower) to be computed. When stating the level of confidence that the true value will lie between both limits, both the upper and lower outside zones have to be considered. With this in mind, it can be seen that k takes the value 1.96 for a 95% probability, and that the true value of the mean lies between the limits L_U and L_L.

1.6.4.2.2 Estimating the true value – n small

When n is small, the means of samples conform to Student's t distribution provided that the observational errors have a Gaussian or near-Gaussian distribution. In this situation, and for a chosen level of confidence, the upper and lower limits can be obtained from:

Upper limit:
$$L_U \approx \bar{X} + t \cdot \frac{\hat{\sigma}}{\sqrt{n}} \qquad (1.4)$$

Lower limit:
$$L_L \approx \bar{X} - t \cdot \frac{\hat{\sigma}}{\sqrt{n}} \qquad (1.5)$$

where t is a factor (Student's t) which depends upon the chosen level of confidence and the number n of measurements; and $\hat{\sigma}$ is the estimate of the standard deviation of the whole population, made from the measurements obtained, using:

$$\hat{\sigma}^2 = \frac{\sum_{i=1}^{n}\left(X_i - \bar{X}\right)^2}{n-1} = \frac{n}{n-1} \cdot \sigma_0^2 \qquad (1.6)$$

where X_i is an individual value O_i corrected for systematic error.

Some values of t are as follows:

Level of confidence	90%	95%	99%
df			
1	6.314	12.706	63.657
4	2.132	2.776	4.604
8	1.860	2.306	3.355
60	1.671	2.000	2.660

where *df* is the degrees of freedom related to the number of measurements by $df = n - 1$. The level of confidence used in this table is for the condition that the true value will not be outside the one particular limit (upper or lower) to be computed. When stating the level of confidence that the true value will lie between the two limits, allowance has to be made for the case in which *n* is large. With this in mind, it can be seen that *t* takes the value 2.306 for a 95% probability that the true value lies between the limits L_U and L_L, when the estimate is made from nine measurements ($df = 8$).

The values of *t* approach the values of *k* as *n* becomes large, and it can be seen that the values of *k* are very nearly equalled by the values of *t* when *df* equals 60. For this reason, tables of *k* (rather than tables of *t*) are quite often used when the number of measurements of a mean value is greater than 60 or so.

1.6.4.2.3 Estimating the true value – additional remarks

Investigators should consider whether or not the distribution of errors is likely to be Gaussian. The distribution of some variables themselves, such as sunshine, visibility, humidity and ceiling, is not Gaussian and their mathematical treatment must, therefore, be made according to rules valid for each particular distribution (Brooks and Carruthers, 1953).

In practice, observations contain both random and systematic errors. In every case, the observed mean value has to be corrected for the systematic error insofar as it is known. When doing this, the estimate of the true value remains inaccurate because of the random errors as indicated by the expressions and because of any unknown component of the systematic error. Limits should be set to the uncertainty of the systematic error and should be added to those for random errors to obtain the overall uncertainty. However, unless the uncertainty of the systematic error can be expressed in probability terms and combined suitably with the random error, the level of confidence is not known. It is desirable, therefore, that the systematic error be fully determined.

1.6.4.3 *Expressing the uncertainty*

If random and systematic effects are recognized, but reduction or corrections are not possible or not applied, the resulting uncertainty of the measurement should be estimated. This uncertainty is determined after an estimation of the uncertainty arising from random effects and from imperfect correction of the result for systematic effects. It is common practice to express the uncertainty as "expanded uncertainty" in relation to the "statistical coverage interval". To be consistent with common practice in metrology, the 95% confidence level, or $k = 2$, should be used for all types of measurements, namely:

$$< expanded\ uncertainty > = k \cdot \sigma = 2 \cdot \sigma \tag{1.7}$$

As a result, the true value, defined in section 1.6.2, will be expressed as:

$$< true\ value > = < measured\ value > \pm < expanded\ uncertainty > = < measured\ value > \pm 2\sigma$$

1.6.4.4 *Measurements of discrete values*

While the state of the atmosphere may be described well by physical variables or quantities, a number of meteorological phenomena are expressed in terms of discrete values. Typical examples of such values are the detection of sunshine, precipitation or lightning and freezing precipitation. All these parameters can only be expressed by "yes" or "no". For a number of parameters, all of which are members of the group of present weather phenomena, more than two possibilities exist. For instance, discrimination between drizzle, rain, snow, hail and their combinations is required when reporting present weather. For these practices, uncertainty calculations like those stated above are not applicable. Some of these parameters are related to a numerical threshold value (for example, sunshine detection using direct radiation intensity), and the determination of the uncertainty of any derived variable (for example, sunshine duration) can be calculated from the estimated uncertainty of the source variable (for example, direct radiation intensity). However, this method is applicable only for derived parameters, and not for the typical present weather phenomena. Although a simple numerical approach cannot be presented, a number of statistical techniques are available to determine the quality of such observations. Such techniques are based on comparisons of two datasets, with one set defined as a reference. Such a comparison results in a contingency matrix, representing the cross-related frequencies of the mutual phenomena. In its most simple form, when a variable is Boolean ("yes" or "no"), such a matrix is a two by two matrix with the number of equal occurrences in the elements of the diagonal axis and the "missing hits" and "false alarms" in the other elements. Such a matrix makes it possible to derive verification scores or indices to be representative for the quality of the observation. This technique is described by Murphy and Katz (1985). An overview is given by Kok (2000).

1.6.5 Accuracy requirements

1.6.5.1 *General*

The uncertainty with which a meteorological variable should be measured varies with the specific purpose for which the measurement is required. In general, the limits of performance of a measuring device or system will be determined by the variability of the element to be measured on the spatial and temporal scales appropriate to the application.

Any measurement can be regarded as made up of two parts: the signal and the noise. The signal constitutes the quantity which is to be determined, and the noise is the part which is irrelevant. The noise may arise in several ways: from observational error, because the observation is not made at the right time and place, or because short-period or small-scale irregularities occur in the observed quantity which are irrelevant to the observations and need to be smoothed out. Assuming that the observational error could be reduced at will, the noise arising from other causes would set a limit to the accuracy. Further refinement in the observing technique would improve the measurement of the noise but would not give much better results for the signal.

At the other extreme, an instrument – the error of which is greater than the amplitude of the signal itself – can give little or no information about the signal. Thus, for various purposes, the amplitudes of the noise and the signal serve, respectively, to determine:

(a)   The limits of performance beyond which improvement is unnecessary;

(b)   The limits of performance below which the data obtained would be of negligible value.

This argument, defining and determining limits (a) and (b) above, was developed extensively for upper-air data by WMO (1970). However, statements of requirements are usually derived not from such reasoning but from perceptions of practically attainable performance, on the one hand, and the needs of the data users, on the other.

1.6.5.2   ***Required and achievable performance***

The performance of a measuring system includes its reliability, capital, recurrent and lifetime cost, and spatial resolution, but the performance under discussion here is confined to uncertainty (including scale resolution) and resolution in time.

Various statements of requirements have been made, and both needs and capability change with time. The statements given in Annex 1.E are the most authoritative at the time of writing, and may be taken as useful guides for development, but they are not fully definitive.

The requirements for the variables most commonly used in synoptic, aviation and marine meteorology, and in climatology are summarized in Annex 1.E.[9] It gives requirements only for surface measurements that are exchanged internationally. Details on the observational data requirements for Global Data-processing and Forecasting System Centres for global and regional exchange are given in WMO (2010*d*). The uncertainty requirement for wind measurements is given separately for speed and direction because that is how wind is reported.

The ability of individual sensors or observing systems to meet the stated requirements is changing constantly as instrumentation and observing technology advance. The characteristics of typical sensors or systems currently available are given in Annex 1.E.[10] It should be noted that the achievable operational uncertainty in many cases does not meet the stated requirements. For some of the quantities, these uncertainties are achievable only with the highest quality equipment and procedures.

Uncertainty requirements for upper-air measurements are dealt with in Part I, Chapter 12.

––––––––––––

[9]   Established by the CBS Expert Team on Requirements for Data from Automatic Weather Stations (2004) and approved by the president of CIMO for inclusion in this Guide after consultation with the presidents of the other technical commissions.
[10] Established by the CIMO Expert Team on Surface Technology and Measurement Techniques (2004) and confirmed for inclusion in this Guide by the president of CIMO.

ANNEX 1.A. REGIONAL INSTRUMENT CENTRES

1.　　　　Considering the need for the regular calibration and maintenance of meteorological instruments to meet the increasing needs for high-quality meteorological and hydrological data, the need for building the hierarchy of the traceability of measurements to the International System of Units (SI) standards, Members' requirements for the standardization of meteorological and related environmental instruments, the need for international instrument comparisons and evaluations in support of worldwide data compatibility and homogeneity, the need for training instrument experts and the role played by Regional Instrument Centres (RICs) in the Global Earth Observing System of Systems, the Natural Disaster Prevention and Mitigation Programme and other WMO cross-cutting programmes, it has been recommended that:[1]

A.　　　　**Regional Instrument Centres with full capabilities and functions** should have the following capabilities to carry out their corresponding functions:

Capabilities:

(a)　A RIC must have, or have access to, the necessary facilities and laboratory equipment to perform the functions necessary for the calibration of meteorological and related environmental instruments;

(b)　A RIC must maintain a set of meteorological standard instruments and establish the traceability of its own measurement standards and measuring instruments to the SI;

(c)　A RIC must have qualified managerial and technical staff with the necessary experience to fulfil its functions;

(d)　A RIC must develop its individual technical procedures for the calibration of meteorological and related environmental instruments using calibration equipment employed by the RIC;

(e)　A RIC must develop its individual quality assurance procedures;

(f)　A RIC must participate in, or organize, inter-laboratory comparisons of standard calibration instruments and methods;

(g)　A RIC must, when appropriate, utilize the resources and capabilities of the Region according to the Region's best interests;

(h)　A RIC must, as far as possible, apply international standards applicable for calibration laboratories, such as ISO/IEC 17025;

(i)　A recognized authority must assess a RIC, at least every five years, to verify its capabilities and performance;

Corresponding functions:

(j)　A RIC must assist Members of the Region in calibrating their national meteorological standards and related environmental monitoring instruments;

(k)　A RIC must participate in, or organize, WMO and/or regional instrument intercomparisons, following relevant CIMO recommendations;

(l)　According to relevant recommendations on the WMO Quality Management Framework, a RIC must make a positive contribution to Members regarding the quality of measurements;

---

[1]　Recommended by the Commission for Instruments and Methods of Observation at its fourteenth session, held in 2006.

(m)   A RIC must advise Members on enquiries regarding instrument performance, maintenance and the availability of relevant guidance materials;

(n)   A RIC must actively participate, or assist, in the organization of regional workshops on meteorological and related environmental instruments;

(o)   The RIC must cooperate with other RICs in the standardization of meteorological and related environmental measurements;

(p)   A RIC must regularly inform Members and report,[2] on an annual basis, to the president of the regional association and to the WMO Secretariat on the services offered to Members and activities carried out.

B.   **Regional Instrument Centres with basic capabilities and functions** should have the following capabilities to carry out their corresponding functions:

Capabilities:

(a)   A RIC must have the necessary facilities and laboratory equipment to perform the functions necessary for the calibration of meteorological and related environmental instruments;

(b)   A RIC must maintain a set of meteorological standard instruments[3] and establish the traceability of its own measurement standards and measuring instruments to the SI;

(c)   A RIC must have qualified managerial and technical staff with the necessary experience to fulfil its functions;

(d)   A RIC must develop its individual technical procedures for the calibration of meteorological and related environmental instruments using calibration equipment employed by the RIC;

(e)   A RIC must develop its individual quality assurance procedures;

(f)   A RIC must participate in, or organize, inter-laboratory comparisons of standard calibration instruments and methods;

(g)   A RIC must, when appropriate, utilize the resources and capabilities of the Region according to the Region's best interests;

(h)   A RIC must, as far as possible, apply international standards applicable for calibration laboratories, such as ISO/IEC 17025;

(i)   A recognized authority must assess a RIC, at least every five years, to verify its capabilities and performance;

Corresponding functions:

(j)   A RIC must assist Members of the Region in calibrating their national standard meteorological and related environmental monitoring instruments according to **Capabilities** (b);

(k)   According to relevant recommendations on the WMO Quality Management Framework, a RIC must make a positive contribution to Members regarding the quality of measurements;

---

[2]   A Web-based approach is recommended.
[3]   For calibrating one or more of the following variables: temperature, humidity, pressure or others specified by the Region.

(l)   A RIC must advise Members on enquiries regarding instrument performance, maintenance and the availability of relevant guidance materials;

(m)   The RIC must cooperate with other RICs in the standardization of meteorological and related environmental instruments;

(n)   A RIC must regularly inform Members and report,[4] on an annual basis, to the president of the regional association and to the WMO Secretariat on the services offered to Members and activities carried out.

2.   The following RICs have been designated by the regional associations (RAs) concerned: Algiers (Algeria), Cairo (Egypt), Casablanca (Morocco), Nairobi (Kenya) and Gaborone (Botswana) for RA I (Africa); Beijing (China) and Tsukuba (Japan) for RA II (Asia); Buenos Aires (Argentina) for RA III (South America); Bridgetown (Barbados) and San José (Costa Rica) for RA IV (North America, Central America and the Caribbean); Manila (Philippines) and Melbourne (Australia) for RA V (South-West Pacific); Bratislava (Slovakia), Ljubljana (Slovenia) and Toulouse (France) for RA VI (Europe).

---

[4]   A Web-based approach is recommended.

ANNEX 1.B. SITING CLASSIFICATIONS FOR SURFACE OBSERVING STATIONS ON LAND

(The text of the common ISO/WMO standard 19289:2014(E))

INTRODUCTION

The environmental conditions of a site[1] may influence measurement results. These conditions must be carefully analysed, in addition to assessing characteristics of the instrument itself, so as to avoid distorting the measurement results and affecting their representativeness, particularly when a site is supposed to be representative of a large area (i.e. 100 to 1 000 km^2).

1.   SCOPE

This annex[2] indicates exposure rules for various sensors. But what should be done when these conditions are not fulfilled?

There are sites that do not respect the recommended exposure rules. Consequently, a classification has been established to help determine the given site's representativeness on a small scale (impact of the surrounding environment). Hence, a class 1 site can be considered as a reference site. A class 5 site is a site where nearby obstacles create an inappropriate environment for a meteorological measurement that is intended to be representative of a wide area (at least tens of km^2). The smaller the siting class, the higher the representativeness of the measurement for a wide area. In a perfect world, all sites would be in class 1, but the real world is not perfect and some compromises are necessary. A site with a poor class number (large number) can still be valuable for a specific application needing a measurement in this particular site, including its local obstacles.

The classification process helps the actors and managers of a network to better take into consideration the exposure rules, and thus it often improves the siting. At least, the siting environment is known and documented in the metadata. It is obviously possible and recommended to fully document the site, but the risk is that a fully documented site may increase the complexity of the metadata, which would often restrict their operational use. That is why this siting classification is defined to condense the information and facilitate the operational use of this metadata information.

A site as a whole has no single classification number. Each parameter being measured at a site has its own class, and is sometimes different from the others. If a global classification of a site is required, the maximum value of the parameters' classes can be used.

The rating of each site should be reviewed periodically as environmental circumstances can change over a period of time. A systematic yearly visual check is recommended: if some aspects of the environment have changed, a new classification process is necessary.

A complete update of the site classes should be done at least every five years.

In the following text, the classification is (occasionally) completed with an estimated uncertainty due to siting, which has to be added in the uncertainty budget of the measurement. This estimation is coming from bibliographic studies and/or some comparative tests.

The primary objective of this classification is to document the presence of obstacles close to the measurement site. Therefore, natural relief of the landscape may not be taken into account, if far

---

[1]   A "site" is defined as the place where the instrument is installed.
[2]   Whereas this is referred to as an annex in the WMO *Guide to Meteorological Instruments and Methods of Observation* (WMO-No. 8), it is referred to as a standard in the ISO document.

away (i.e. > 1 km). A method to judge if the relief is representative of the surrounding area is the following: does a move of the station by 500 m change the class obtained? If the answer is no, the relief is a natural characteristic of the area and is not taken into account.

Complex terrain or urban areas generally lead to high class numbers. In such cases, an additional flag "S" can be added to class numbers 4 or 5 to indicate specific environment or application (i.e. 4S).

2.   AIR TEMPERATURE AND HUMIDITY

2.1   General

Sensors situated inside a screen should be mounted at a height determined by the meteorological service (within 1.25 to 2 m as indicated in the WMO *Guide to Meteorological Instruments and Methods of Observation* (WMO-No. 8)). The height should never be less than 1.25 m. The respect of the higher limit is less stringent, as the temperature gradient versus height is decreasing with height. For example, the difference in temperature for sensors located between 1.5 and 2 m is less than 0.2 °C.

The main discrepancies are caused by unnatural surfaces and shading:

(a)   Obstacles around the screen influence the irradiative balance of the screen. A screen close to a vertical obstacle may be shaded from the solar radiation or "protected" against the night radiative cooling of the air, by receiving the warmer infrared radiation from this obstacle or influenced by reflected radiation;

(b)   Neighbouring artificial surfaces may heat the air and should be avoided. The extent of their influence depends on the wind conditions, as wind affects the extent of air exchange. Unnatural or artificial surfaces to take into account are heat sources, reflective surfaces (for example buildings, concrete surfaces, car parks) and water or moisture sources (for example, ponds, lakes, irrigated areas).

Shading by nearby obstacles should be avoided. Shading due to natural relief is not taken into account for the classification (see above).

The indicated vegetation growth height represents the height of the vegetation maintained in a "routine" manner. A distinction is made between structural vegetation height (per type of vegetation present on the site) and height resulting from poor maintenance. Classification of the given site is therefore made on the assumption of regular maintenance (unless such maintenance is not practicable).

2.2   Class 1

(a)   Flat, horizontal land, surrounded by an open space, slope less than ⅓ (19°);

(b)   Ground covered with natural and low vegetation (< 10 cm) representative of the region;

(c)   Measurement point situated:

  (i)   At more than 100 m from heat sources or reflective surfaces (buildings, concrete surfaces, car parks, etc.);

  (ii)   At more than 100 m from an expanse of water (unless significant of the region);

  (iii) Away from all projected shade when the sun is higher than 5°.

A source of heat (or expanse of water) is considered to have an impact if it occupies more than 10% of the surface within a circular radius of 100 m surrounding the screen, makes up 5% of an annulus of 10–30 m, or covers 1% of a 10 m radius area.
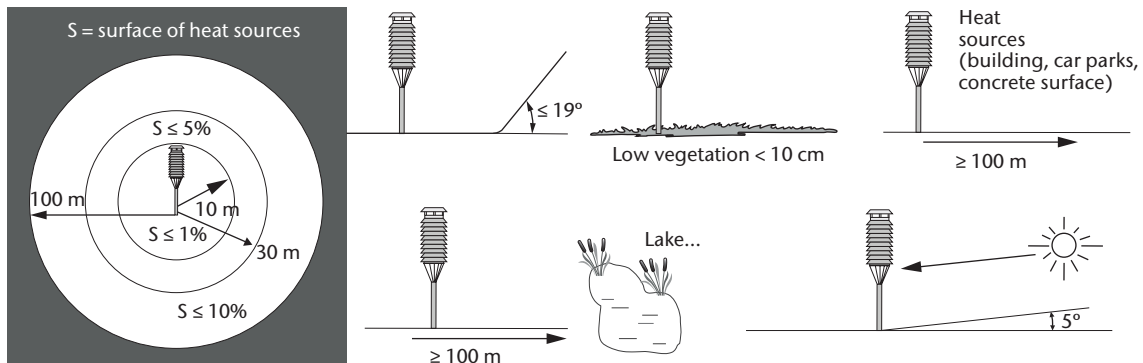
Figure 1.B.1. Criteria for air temperature and humidity for class 1 sites

2.3   **Class 2**

(a)   Flat, horizontal land, surrounded by an open space, slope inclination less than ⅓ (19°);

(b)   Ground covered with natural and low vegetation (< 10 cm) representative of the region;

(c)   Measurement point situated:

   (i)   At more than 30 m from artificial heat sources or reflective surfaces (buildings, concrete surfaces, car parks, etc.);

   (ii)   At more than 30 m from an expanse of water (unless significant of the region);

   (iii) Away from all projected shade when the sun is higher than 7°.

A source of heat (or expanse of water) is considered to have an impact if it occupies more than 10% of the surface within a radius of 30 m surrounding the screen, makes up 5% of an annulus of 5–10 m, or covers 1% of a 5 m radius area.
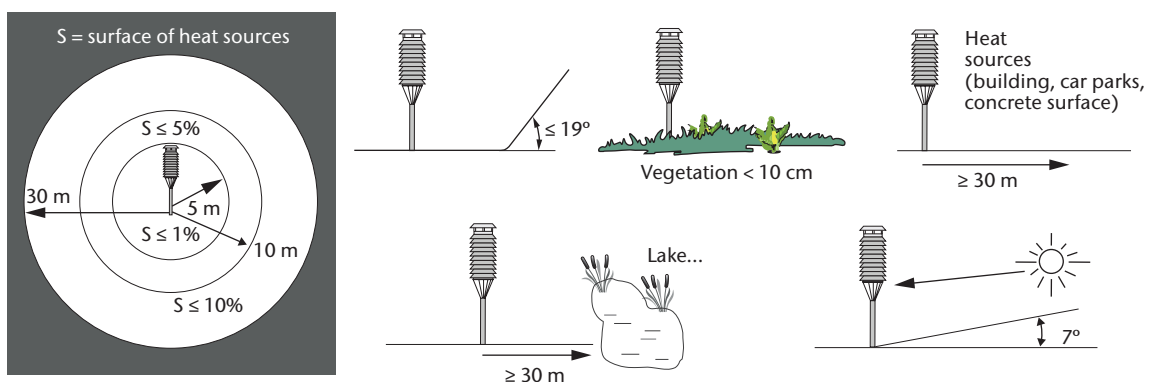
Figure 1.B.2. Criteria for air temperature and humidity for class 2 sites

2.4   **Class 3 (additional estimated uncertainty added by siting up to 1 °C)**

(a)   Ground covered with natural and low vegetation (< 25 cm) representative of the region;

(b)   Measurement point situated:

   (i)   At more than 10 m from artificial heat sources and reflective surfaces (buildings, concrete surfaces, car parks, etc.);

(ii)   At more than 10 m from an expanse of water (unless significant of the region);

(iii)   Away from all projected shade when the sun is higher than 7°.

A source of heat (or expanse of water) is considered to have an impact if it occupies more than 10% of the surface within a radius of 10 m surrounding the screen or makes up 5% of a 5 m radius area.
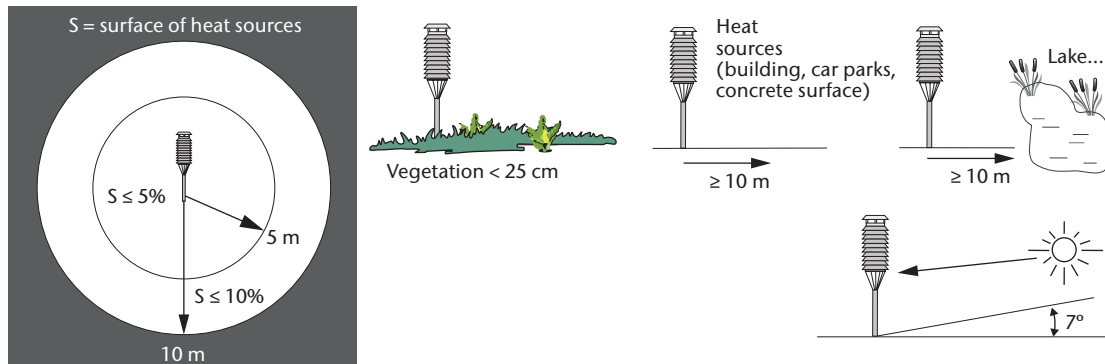
Figure 1.B.3. Criteria for air temperature and humidity for class 3 sites

2.5   **Class 4 (additional estimated uncertainty added by siting up to 2 °C)**

(a)   Close, artificial heat sources and reflective surfaces (buildings, concrete surfaces, car parks, etc.) or expanse of water (unless significant of the region), occupying:

(i)   Less than 50% of the surface within a 10 m radius around the screen;

(ii)   Less than 30% of the surface within a 3 m radius around the screen;

(b)   Away from all projected shade when the sun is higher than 20°.
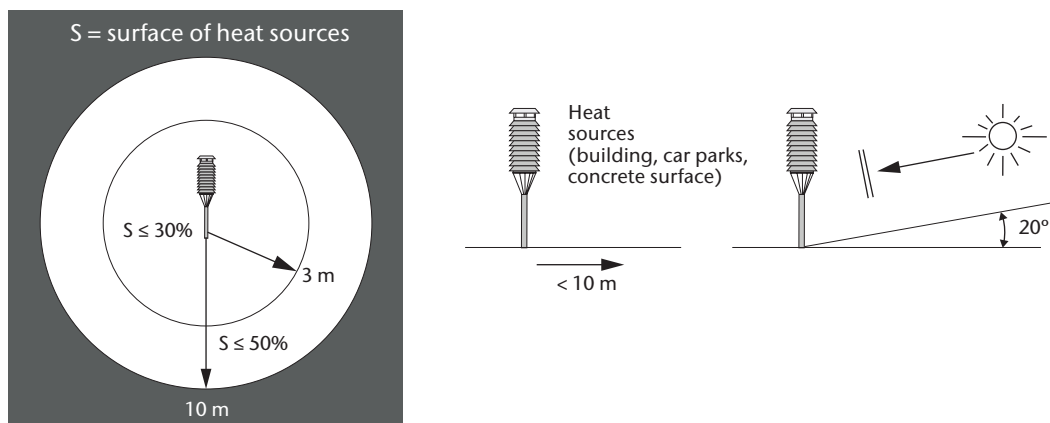
Figure 1.B.4. Criteria for air temperature and humidity for class 4 sites

2.6   **Class 5 (additional estimated uncertainty added by siting up to 5 °C)**

Site not meeting the requirements of class 4.

3.   PRECIPITATION

3.1   General

Wind is the greatest source of disturbance in precipitation measurements, due to the effect of the instrument on the airflow. Unless raingauges are artificially protected against wind, for instance by a wind shield, the best sites are often found in clearings within forests or orchards, among trees, in scrub or shrub forests, or where other objects act as an effective windbreak for winds from all directions. Ideal conditions for the installation are those where equipment is set up in an area surrounded uniformly by obstacles of uniform height. An obstacle is an object with an effective angular width of 10° or more.

The choice of such a site is not compatible with constraints in respect of the height of other measuring equipment. Such conditions are practically unrealistic. If obstacles are not uniform, they are prone to generate turbulence, which distorts measurements; this effect is more pronounced for solid precipitation. This is the reason why more realistic rules of elevation impose a certain distance from any obstacles. The orientation of such obstacles with respect to prevailing wind direction is deliberately not taken into account. Indeed, heavy precipitation is often associated with convective factors, whereby the wind direction is not necessarily that of the prevailing wind. Obstacles are considered of uniform height if the ratio between the highest and lowest height is less than 2.

Reference for the heights of obstacles is the catchment's height of the raingauge.

3.2   Class 1

(a)   Flat, horizontal land, surrounded by an open area, slope less than ⅓ (19°). The raingauge shall be surrounded by low obstacles of uniform height, that is subtending elevation angles between 14° and 26° (obstacles at a distance between 2 and 4 times their height);

(b)   Flat, horizontal land, surrounded by an open area, slope less than ⅓ (19°). For a raingauge artificially protected against wind, the instrument does not necessarily need to be protected by obstacles of uniform height. In this case, any other obstacles must be situated at a distance of at least 4 times their height.

or:
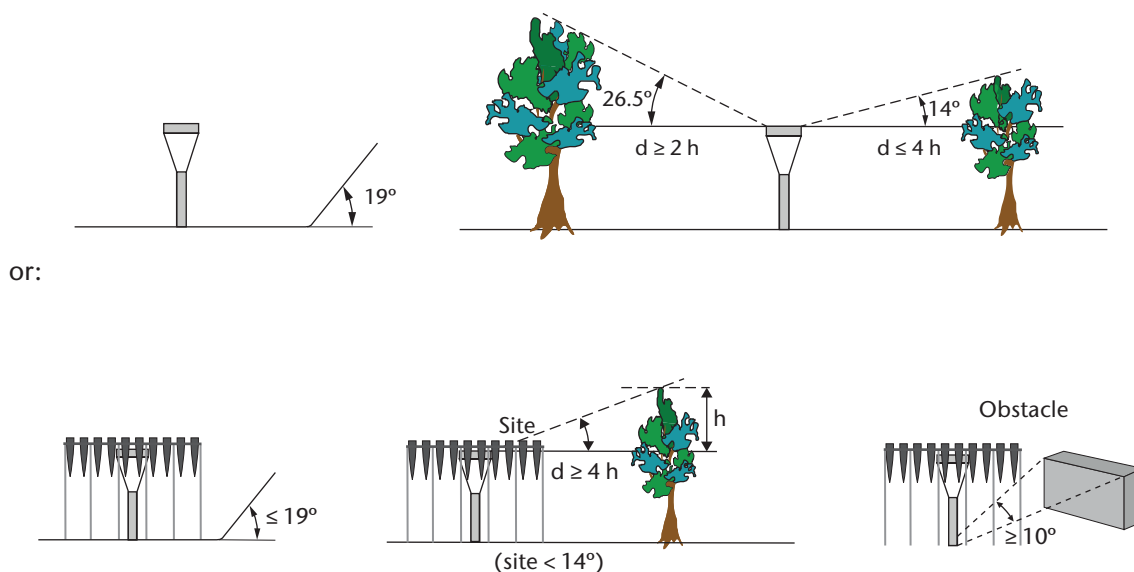
Figure 1.B.5. Criteria for precipitation for class 1 sites

3.3 **Class 2 (additional estimated uncertainty added by siting up to 5%)**

(a) Flat, horizontal land, surrounded by an open area, slope less than ⅓ (19°);

(b) Possible obstacles must be situated at a distance at least twice the height of the obstacle (with respect to the catchment's height of the raingauge).
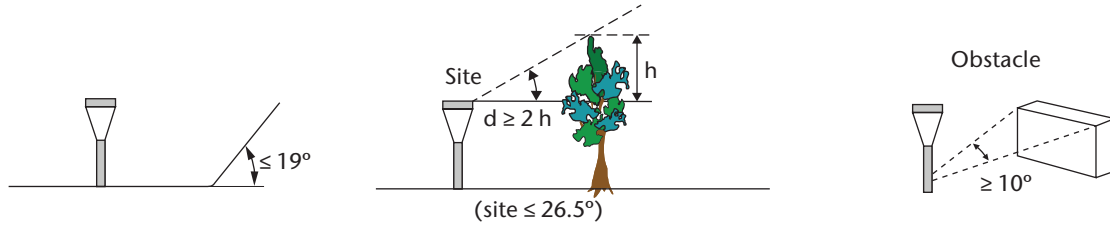
Figure 1.B.6. Criteria for precipitation for class 2 sites

3.4 **Class 3 (additional estimated uncertainty added by siting up to 15%)**

(a) Land is surrounded by an open area, slope less than ½ (≤ 30°);

(b) Possible obstacles must be situated at a distance greater than the height of the obstacle.
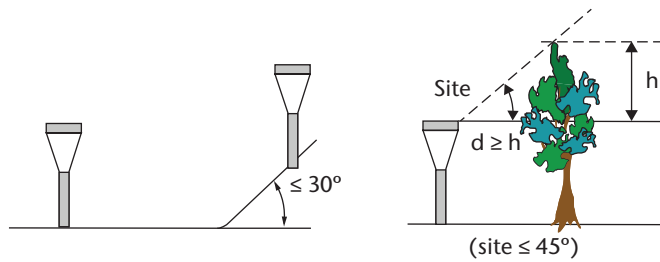
Figure 1.B.7. Criteria for precipitation for class 3 sites

3.5 **Class 4 (additional estimated uncertainty added by siting up to 25%)**

(a) Steeply sloping land (> 30°);

(b) Possible obstacles must be situated at a distance greater than one half (½) the height of the obstacle.
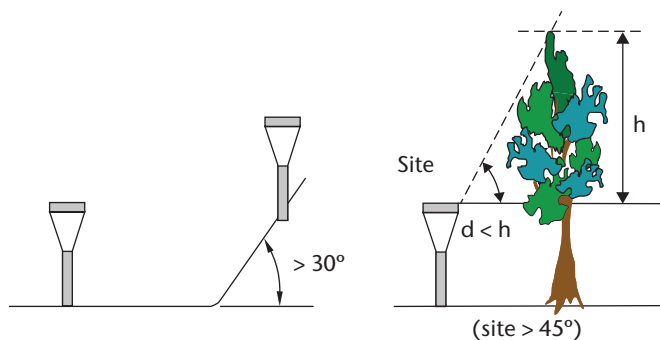
Figure 1.B.8. Criteria for precipitation for class 4 sites

3.6 **Class 5 (additional estimated uncertainty added by siting up to 100%)**

Obstacles situated closer than one half (½) their height (tree, roof, wall, etc.).
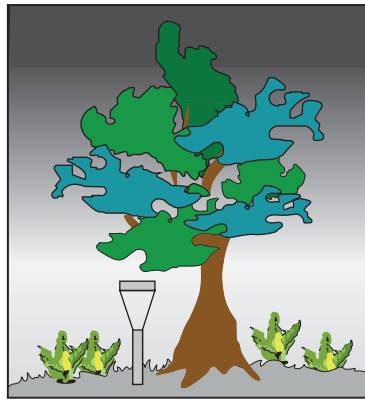
Figure 1.B.9. Criteria for precipitation for class 5 sites

4. SURFACE WIND

4.1 General

Conventional elevation rules stipulate that sensors should be placed 10 m above ground surface level and on open ground. Open ground here represents a surface where obstacles are situated at a minimum distance equal to at least 10 times their height.

4.2 Roughness

Wind measurements are disturbed not only by surrounding obstacles; terrain roughness also plays a role. WMO defines wind blowing at a geometrical height of 10 m and with a roughness length of 0.03 m as the surface wind for land stations.

This is regarded as a reference wind for which exact conditions are known (10 m height and roughness length of 0.03 m).

Therefore, roughness around the measuring site has to be documented. Roughness should be used to convert the measuring wind to the reference wind, but this procedure can be applied only when the obstacles are not too close. Roughness-related matters and correction procedure are described in the WMO *Guide to Meteorological Instruments and Methods of Observation* (WMO-No. 8), Part I, Chapter 5.

The roughness classification, reproduced from the annex in the WMO *Guide to Meteorological Instruments and Methods of Observation* (WMO-No. 8), Part I, Chapter 5, is recalled here:

**Terrain classification from Davenport (1960) adapted by Wieringa (1980*b*)
in terms of aerodynamic roughness length z_0**

Class index	Short terrain description	z_0 (m)
1	Open sea, fetch at least 5 km	0.000 2
2	Mud flats, snow; no vegetation, no obstacles	0.005
3	Open flat terrain; grass, few isolated obstacles	0.03
4	Low crops; occasional large obstacles, $x/H > 20$	0.10

Class index	Short terrain description	z_0 (m)
5	High crops; scattered obstacles, $15 < x/H < 20$	0.25
6	Parkland, bushes; numerous obstacles, $x/H \approx 10$	0.5
7	Regular large obstacle coverage (suburb, forest)	1.0
8	City centre with high- and low-rise buildings	≥ 2

Note: Here x is a typical upwind obstacle distance and H is the height of the corresponding major obstacles. For more detailed and updated terrain class descriptions see Davenport et al. (2000).

4.3 Environment classification

The presence of obstacles, including vegetation, (almost invariably) means a reduction in average wind readings, but less significantly affects wind gusts.

The following classification assumes measurement at 10 m, which is the standard elevation for meteorological measurement.

When measurements are carried out at lower height (such as measurements carried out at 2 m, as is sometimes the case for agroclimatological purposes), a class 4 or 5 (see below) is to be used, with flag S (Specific situation).

Where numerous obstacles higher than 2 m are present, it is recommended that sensors be placed 10 m above the average height of the obstacles. This method allows the influence of the adjacent obstacles to be minimized. This method represents a permanent solution for partly eliminating the influence of certain obstacles. It inconveniently imposes the necessity for higher masts that are not standard and consequently are more expensive. It must be considered for certain sites and where used, the height of obstacles to be taken into account is that above the level situated 10 m below the sensors (e.g. for an anemometer installed at a 13 m height, the reference "ground" level of the obstacles is at a 3 m height; an obstacle of 7 m is considered to have an effective height of 4 m).

In the following, an object is considered to be an obstacle if its effective angular width is over 10°. Tall, thin obstacles, that is with an effective angular width less than 10° and a height greater than 8 m, also need to be taken into account when considering class 1 to 3, as mentioned below. Under some circumstances, a cluster of tall, thin obstacles will have a similar effect to a single wider obstacle and will need to be considered as such.

Changes of altitude (positive or negative) in the landscape which are not representative of the landscape are considered as obstacles.

4.4 Class 1

(a) The mast should be located at a distance equal to at least 30 times the height of surrounding obstacles;

(b) Sensors should be situated at a minimum distance of 15 times the width of thin obstacles (mast, thin tree) higher than 8 m;

Single obstacles lower than 4 m can be ignored.

Roughness class index is less than or equal to 4 (roughness length ≤ 0.1 m).

d ≥ 30 h (site ≤ 1.9°)

Large obstacle

≥ 10°

Thin obstacle > 8 m

Width

≥ 15 Width

Obstacles lower than 4 m ignored
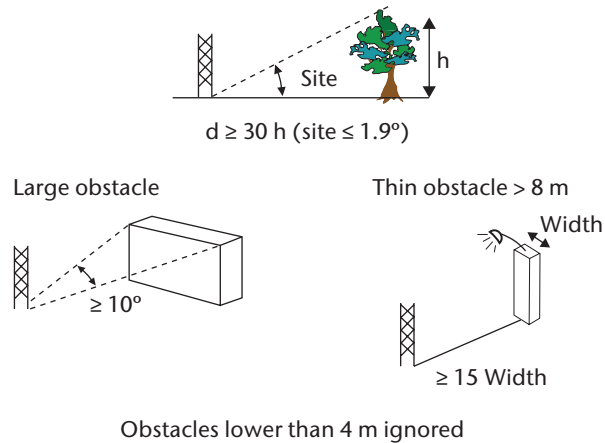
Figure 1.B.10. Criteria for surface wind for class 1 sites

4.5   **Class 2 (additional estimated uncertainty added by siting up to 30%, possibility to apply correction)**

(a)   The mast should be located at a distance of at least 10 times the height of the surrounding obstacles;

(b)   Sensors should be situated at a minimum distance of 15 times the width of thin obstacles (mast, thin tree) over 8 m high;

Single obstacles lower than 4 m can be ignored.

Roughness class index is less than or equal to 5 (roughness length ≤ 0.25 m).

Thin obstacle > 8 m

d ≥ 10 h (site ≤ 5.7°)

Width

≥ 15 Width

≥ 10°

Obstacles lower than 4 m ignored
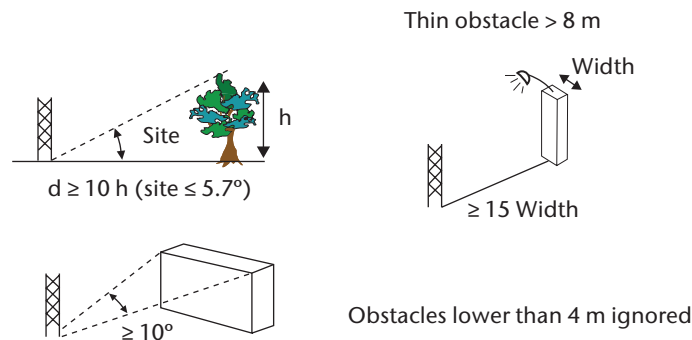
Figure 1.B.11. Criteria for surface wind for class 2 sites

Note: When the mast is located at a distance of at least 20 times the height of the surrounding obstacles, a correction (see the WMO *Guide to Meteorological Instruments and Methods of Observation* (WMO-No. 8), Part I, Chapter 5) can be applied. For nearer obstacles, a correction may be applied in some situations.

4.6   **Class 3 (additional estimated uncertainty added by siting up to 50%, correction cannot be applied)**

(a)   The mast should be located at a distance of at least 5 times the height of surrounding obstacles;

(b)   Sensors should be situated at a minimum distance of 10 times the width of thin obstacles (mast, thin tree) higher than 8 m.

Single obstacles lower than 5 m can be ignored.
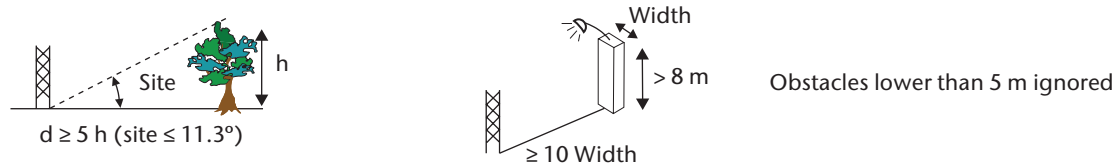
Figure 1.B.12. Criteria for surface wind for class 3 sites

4.7 **Class 4 (additional estimated uncertainty added by siting greater than 50%)**

(a) The mast should be located at a distance of at least 2.5 times the height of surrounding obstacles;

(b) No obstacle with an angular width larger than 60° and a height greater than 10 m, within a 40 m distance.

Single obstacles lower than 6 m can be ignored, only for measurements at 10 m or above.
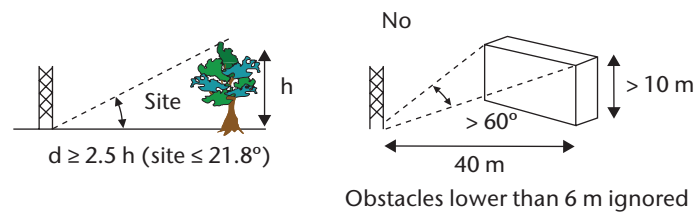
Figure 1.B.13. Criteria for surface wind for class 4 sites

4.8 **Class 5 (additional estimated uncertainty cannot be defined)**

Site not meeting the requirements of class 4.

5. **GLOBAL AND DIFFUSE RADIATION**

5.1 **General**

Close obstacles have to be avoided. Shading due to the natural relief is not taken into account for the classification. Non-reflecting obstacles below the visible horizon can be neglected.

An obstacle is considered as reflecting if its albedo is greater than 0.5.

The reference position for elevation angles is the sensitive element of the instrument.

5.2 **Class 1**

(a) No shade projected onto the sensor when the sun is at an angular height of over 5°. For regions with latitude ≥ 60°, this limit is decreased to 3°;

(b) No non-shading reflecting obstacles with an angular height above 5° and a total angular width above 10°.
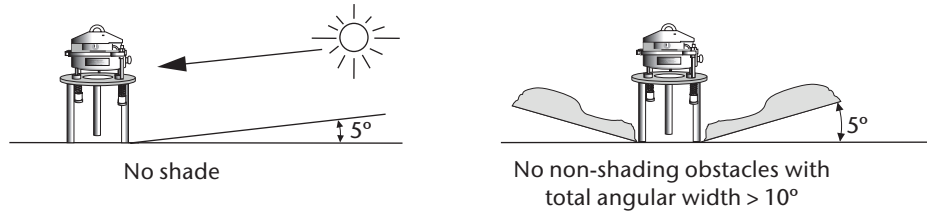
Figure 1.B.14. Criteria for global and diffuse radiation for class 1 sites

5.3　　　Class 2

(a)　No shade projected onto the sensor when the sun is at an angular height of over 7°. For regions with latitude ≥ 60°, this limit is decreased to 5°;

(b)　No non-shading reflecting obstacles with an angular height above 7° and a total angular width above 20°.
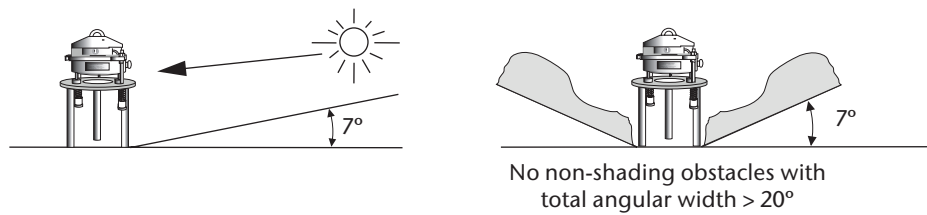
Figure 1.B.15. Criteria for global and diffuse radiation for class 2 sites

5.4　　　Class 3

(a)　No shade projected onto the sensor when the sun is at an angular height of over 10°. For regions with latitude ≥ 60°, this limit is decreased to 7°;

(b)　No non-shading reflecting obstacles with an angular height above 15° and a total angular width above 45°.
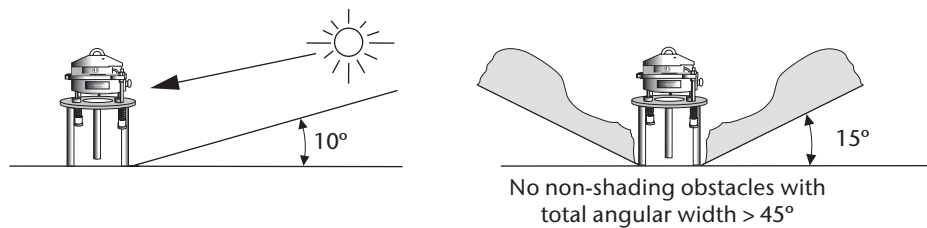
Figure 1.B.16. Criteria for global and diffuse radiation for class 3 sites

5.5　　　Class 4

No shade projected during more than 30% of the daytime, for any day of the year.

Figure 1.B.17. Criteria for global and diffuse radiation for class 4 sites

5.6   **Class 5**

Shade projected during more than 30% of the daytime, for at least one day of the year.

6.   **DIRECT RADIATION AND SUNSHINE DURATION**

6.1   **General**

Close obstacles have to be avoided. Shading due to the natural relief is not taken into account for the classification. Obstacles below the visible horizon can be neglected.

The reference position for angles is the sensitive element of the instrument.

6.2   **Class 1**

No shade projected onto the sensor when the sun is at an angular height of over 3°.
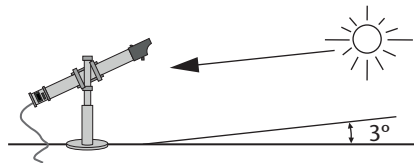
Figure 1.B.18. Criteria for direct radiation and sunshine duration for class 1 sites

6.3   **Class 2**

No shade projected onto the sensor when the sun is at an angular height of over 5°.
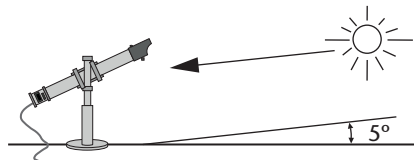
Figure 1.B.19. Criteria for direct radiation and sunshine duration for class 2 sites

6.4   **Class 3**

No shade projected onto the sensor when the sun is at an angular height of over 7°.
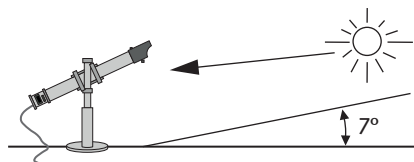
Figure 1.B.20. Criteria for direct radiation and sunshine duration for class 3 sites

6.5   **Class 4**

No shade projected during more than 30% of the daytime, for any day of the year.

≤ 30% of daytime

No shade for more than 30% of daytime
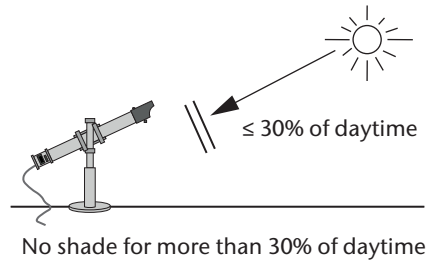
Figure 1.B.21. Criteria for direct radiation and sunshine duration for class 4 sites

6.6   **Class 5**

Shade projected during more than 30% of the daytime, for at least one day of the year.

––––––––––––

ANNEX 1.C. STATION EXPOSURE DESCRIPTION

The accuracy with which an observation describes the state of a selected part of the atmosphere is not the same as the uncertainty of the instrument, because the value of the observation also depends on the instrument's exposure to the atmosphere. This is not a technical matter, so its description is the responsibility of the station observer or attendant. In practice, an ideal site with perfect exposure is seldom available and, unless the actual exposure is adequately documented, the reliability of observations cannot be determined (WMO, 2002).

Station metadata should contain the following aspects of instrument exposure:

(a)   Height of the instruments above the surface (or below it, for soil temperature);

(b)   Type of sheltering and degree of ventilation for temperature and humidity;

(c)   Degree of interference from other instruments or objects (masts, ventilators);

(d)   Microscale and toposcale surroundings of the instrument, in particular:

    (i)   The state of the enclosure's surface, influencing temperature and humidity; nearby major obstacles (buildings, fences, trees) and their size;

    (ii)   The degree of horizon obstruction for sunshine and radiation observations;

    (iii)   Surrounding terrain roughness and major vegetation, influencing the wind;

    (iv)   All toposcale terrain features such as small slopes, pavements, water surfaces;

    (v)   Major mesoscale terrain features, such as coasts, mountains or urbanization.

Most of these matters will be semi-permanent, but any significant changes (growth of vegetation, new buildings) should be recorded in the station logbook, and dated.

For documenting the toposcale exposure, a map with a scale not larger than 1:25 000 showing contours of ≈ 1 m elevation differences is desirable. On this map the locations of buildings and trees (with height), surface cover and installed instruments should be marked. At map edges, major distant terrain features (for example, built-up areas, woods, open water, hills) should be indicated. Photographs are useful if they are not merely close-ups of the instrument or shelter, but are taken at sufficient distance to show the instrument and its terrain background. Such photographs should be taken from all cardinal directions.

The necessary minimum metadata for instrument exposure can be provided by filling in the template given on the next page for every station in a network (see the figure below). An example of how to do this is shown in WMO (2003). The classes used here for describing terrain roughness are given in Part I, Chapter 5, of the Guide. A more extensive description of metadata matters is given in WMO (2010c).

Station   Update

Elevation   Latitude   Longitude

0   200 m

□ Enclosure

▨ Building

// Road

x x
x Trees, bushes

(12) Height (m) of obstacle

+⌒3 Elevation contour

N

Radiation horizon

1 : 6   8°
1 : 10   4°
1 : 20   0°

N   E   S   W   N

Temperature and humidity: Sensor height
                              Artificial ventilation?   yes/no

Surface cover under screen

Soil under screen

Precipitation: Gauge rim height

Wind: Anemometer height   Free-standing?   yes/no

(if "no" above: building height   , width   , length

Terrain roughness class: to N   ,to E   , to S,   to W

Remarks:

General template for station exposure metadata

ANNEX 1.D. OPERATING EQUIPMENT IN EXTREME ENVIRONMENTS

1. Extreme winds (tornadoes, hurricanes)

Aerodynamic shapes can be used to improve the survivability of instruments and structures. Weighted shaped disks on the ground can help keep instrumentation in place during tornadoes. Shaped balloons can enable tethersonde operation in hurricane-force winds.

Masts can have additional stays fitted. All cabling should be well tied down and supported. Shielding should be put in place to protect equipment from wind-blown debris, including large objects (that can cause impact damage) and smaller particles like dust and sand (that can cause erosive damage).

Sensors that can survive high wind speeds should be selected. Wind sensors using the measurement principle of pressure difference (pitot tubes), the principle of sound propagation (ultrasonic wind sensors) or thermal cooling eliminate the vulnerabilities associated with moving parts. Nevertheless, some cup anemometers, wind vanes and propeller anemometers have been designed to operate during extreme wind events.

2. Floods and storm surges

Low-lying areas should be avoided as site locations. Sensors can be raised on pilings to prevent damage due to surface-water flow and debris. Foundations should be constructed using resilient materials and oriented parallel to any expected surface flow to minimize hydrostatic pressures. Electrical connections should be raised above predicted flood levels or contained within suitable waterproof housings (designed to suitable Ingress Protection (IP) ratings).

3. Fire

Non-combustible materials, generally metal and concrete, should be used wherever practicable. Equipment openings should include screening to prevent sparks from entering cavities – as long as measurement exposure is not compromised.

4. Icing

Heat and/or airflow over sensors is commonly used to keep sensors free of ice. Some manufacturers include built-in sensor heating with varying heat amounts depending on expected icing severity. Sensors without built-in heating can still be heated by applying heat tape directly to surfaces (electrical resistance elements embedded in a flexible sheet or by use of nichrome wire). Note that for wind sensors, it is generally easier to heat those with no moving parts (such as ultrasonic wind sensors). Another method is to spray a low freezing-point fluid (such as ethanol) on sensors during icing events. In heavy icing conditions, none of these methods may prevent ice build-up.

Icing on mounting structures can disturb the airflow and measurement environment even when the sensors themselves are ice-free. Minimizing the surface area of these structures can help. De-icing them also may be necessary.

The method used to mitigate ice accretion should not affect the sensor measurement or the measurements being made by adjacent sensors. For example, the heating of a sensor must not affect nearby air temperature or relative humidity measurements. One approach is to heat for a period, let the sensor cool, take a measurement and repeat.

5. Solar radiation heating and erosion

In locations where sensors, cabinets and cabling receive high levels of solar radiation, and in particular high levels of ultraviolet (UV) exposure, some materials will break down and lose structural integrity. The use of alternative materials like metals, hardwoods and UV-stabilized plastics will often lead to much longer equipment and structure lifetimes.

In warmer climates and where there are high levels of solar radiation, cabinets can heat up internally to levels that exceed the operating specifications of equipment, thereby compromising data values and equipment reliability. Vents and/or forced venting (with appropriate filters) or small air-conditioning systems can be employed to reduce heat build-up. Peltier coolers also can be used to transfer heat out of enclosures without exposing the contents to external airflow.

Solar shades, cable conduits or simply burying equipment can also be used where sensor measurement exposure will not be compromised.

6. Electrical transients (lightning)

Lightning protection systems generally involve four components – a collector exposed at the highest point of the structure, a conduction path to earth, a discharge system of the current into the ground and a surge protection device for sensitive equipment.

Different types of collectors may be used effectively. Two common types are the Franklin Rod and the Spline Ball. The Franklin Rod encourages a lightning strike to follow a predetermined path to the ground. The Spline Ball prevents a direct strike before it occurs by dissipating charge build-up. Both approaches work. Depending on the size and height of the structure to be protected, one or more collectors and conduction paths may be needed, with generally one set for each vertical face of the structure.

The grounding path to earth should be made of highly conductive material (often copper) of sufficient capacity to handle the extremely high but brief currents involved in a lightning strike. Each element of this path, including connections, must have this capacity. Every attempt should be made to minimize the electrical resistance of the connection to earth ground. Bends in the path should be minimized and should never be more than 45 degrees. Even if the structure itself is metal and grounded, a separate low impedance ground conductor is recommended.

The discharge system can be a simple pole (usually a copper alloy) introduced vertically into the ground for soils with sufficient electrical conductivity. Salts may be added to increase the local soil's conductivity. Contact with the water table is desirable. In extreme cases, such as surfaces of rock or sand, a horizontal web of conductive material may be placed on or under the surface surrounding the structure.

Surge protection for sensitive equipment is desirable. There are many varieties of devices and they must be used in accordance with manufacturer specifications. Both differential-mode (between wires) and common-mode (between wires/equipment and earth ground) protection devices are available. Common-mode protection relies on a high-quality earth ground. These surges are generally most destructive and characterized by elevated voltages on wires/equipment with respect to the earth ground. It is also possible for a nearby strike to propagate through the earth itself, raising its potential above the equipment. These are more likely where there are poor earth grounds and grounding materials. Isolating working grounds from earth grounds is advantageous. In some cases, inductive arrays between working and earth grounds can help protect against these problems. Shielded data cables, connected to ground only at one end, should be used to reduce the likelihood of induced transients in signal lines.

For equipment that connects to third-party infrastructure such as telephone lines and mains power lines, uses power from generators or has long cable runs between sensors and modules, there is a risk of direct or induced electrical transients in cables. Appropriate transient protection

and/or isolation devices placed where cables enter equipment and at both ends of long cables are recommended. Careful attention must be paid when earthing transient protection devices so that earth potential equalization is achieved for each system being protected.

7. Corrosion (high salt, geothermal and humid environments)

Equipment installed in locations with high or moderate corrosive atmospheres can suffer from data errors due to sensor malfunction and reduction in equipment reliability.

Common problems include:

(a)   Foreign chemical build-up on sensing elements, such as relative humidity sensing elements;

(b)   High friction in sensor bearings;

(c)   Seized bearings, hinges, latches, screws and terminals;

(d)   Mould and corrosion on circuit boards;

(e)   High-resistance terminal connections;

(f)   Structural failure of mounts and clamps.

Mitigating strategies should include:

(a)   Use of suitable materials such as stainless steel, galvanized steel and appropriate plastics;

(b)   Protection of connectors and clamps using grease/oil impregnated tape or similar;

(c)   Careful selection of metal types at joints or use of isolating separators and lubricants (high viscosity grease) to ensure that electrolysis is minimized.

8. Security (against human or wildlife interference)

Tampering and theft of equipment can be minimized by installing appropriate security structures such as protective fences, or by installing non-removable fittings so that high-value modules like solar panels cannot be removed without the appropriate keys or tools.

Some soft infrastructure like plastics and cable sheaths can be easily damaged by wildlife, for example by birds chewing through cable. This can be mitigated by using armoured cables or enclosing cables in toughened conduit.

Physical crushing or misalignment of sensors due to the rubbing of sensors and structures by large animals can be mitigated by setting up appropriate livestock fencing.

9. Loss of infrastructure

During extreme weather and geophysical events, mains power may become unavailable for many days. An appropriate battery backup design should be made so that equipment continues to operate until power is restored or workers can visit the site and replace batteries.

Furthermore, during extreme weather and geophysical events, telecommunications networks may become inoperative or overloaded for many days. Outages may only affect one operator, so using various operators and communications paths may be a useful option, such as having both cellular and satellite communications at a station. Similarly, redundant and/or quick-deploy systems can help minimize damage from extreme events.

10. General

Regular maintenance as described in Part I, Chapter 1, 1.3.5 will increase the resilience of structures to extreme events.

Characterization of instrument response to extreme events may enable data to be used even when operating beyond manufacturer specifications and is to be encouraged whenever possible. Post-calibration of damaged sensors may enable recovery of data recorded during extreme events.

Adherence to these guidelines does not guarantee network operation through extreme events. Human operators can reduce data loss, though extreme conditions are often associated with high risk to human life. Some amount of data loss in these conditions is expected.

_____

ANNEX 1.E. OPERATIONAL MEASUREMENT UNCERTAINTY REQUIREMENTS AND INSTRUMENT PERFORMANCE

(See explanatory notes at the end of the table; numbers in the top row indicate column numbers.)

1	*2*	*3*	*4*	*5*	*6*	*7*	*8*	*9*
Variable	Range	Reported resolution	Mode of measurement/ observation	Required measurement uncertainty	Sensor time-constant	Output averaging time	Achievable measurement uncertainty	Remarks
1. Temperature								
1.1 Air temperature	–80 – +60 °C	0.1 K	I	0.3 K for ≤ –40 °C 0.1 K for > –40 °C and ≤ +40 °C 0.3 K for > +40 °C	20 s	1 min	0.2 K	Achievable uncertainty and effective time-constant may be affected by the design of the thermometer solar radiation screen Time constant depends on the airflow over the sensor
1.2 Extremes of air temperature	–80 – +60 °C	0.1 K	I	0.5 K for ≤ –40 °C 0.3 K for > –40 °C and ≤ +40 °C 0.5 K for > +40 °C	20 s	1 min	0.2 K	
1.3 Sea-surface temperature	–2 – +40 °C	0.1 K	I	0.1 K	20 s	1 min	0.2 K	
1.4 Soil temperature	–50 – +50 °C	0.1 K	I		20 s	1 min	0.2 K	

	1	*2*	*3*	*4*	*5*	*6*	*7*	*8*	*9*
	Variable	*Range*	*Reported resolution*	*Mode of measurement/ observation*	*Required measurement uncertainty*	*Sensor time- constant*	*Output averaging time*	*Achievable measurement uncertainty*	*Remarks*
2.	**Humidity**								
2.1	Dewpoint temperature	–80 – +35 °C	0.1 K	I	0.1 K	20 s	1 min	0.25 K	Measurement uncertainty depends on the deviation from air temperature
						Wet-bulb temperature (psychrometer)			
2.2	Relative humidity	0 – 100%	1%	I	1%	20 s	1 min	0.2 K	If measured directly and in combination with air temperature (dry bulb) Large errors are possible due to aspiration and cleanliness problems (see also note 11) Threshold of 0 °C to be noticed for wet bulb
						Solid state and others			
						40 s	1 min	3%	Time constant and achievable uncertainty of solid-state sensors may show significant temperature and humidity dependence

1	*2*	*3*	*4*	*5*	*6*	*7*	*8*	*9*
Variable	Range	Reported resolution	Mode of measurement/ observation	Required measurement uncertainty	Sensor time-constant	Output averaging time	Achievable measurement uncertainty	Remarks
3. Atmospheric pressure								
3.1 Pressure	500 – 1 080 hPa	0.1 hPa	I	0.1 hPa	2 s	1 min	0.15 hPa	Both station pressure and MSL pressure Measurement uncertainty is seriously affected by dynamic pressure due to wind if no precautions are taken Inadequate temperature compensation of the transducer may affect the measurement uncertainty significantly MSL pressure is affected by the uncertainty in altitude of the barometer for measurements onboard ships
3.2 Tendency	Not specified	0.1 hPa	I	0.2 hPa			0.2 hPa	Difference between instantaneous values

	1	2	3	4	5	6	7	8	9
	Variable	Range	Reported resolution	Mode of measurement/ observation	Required measurement uncertainty	Sensor time-constant	Output averaging time	Achievable measurement uncertainty	Remarks
4.	**Clouds**								
4.1	Cloud amount	0/8 – 8/8	1/8	I	1/8	n/a		2/8	Period clustering algorithms may be used to estimate low cloud amount automatically
4.2	Height of cloud base	0 m – 30 km	10 m	I	10 m for ≤ 100 m 10% for > 100 m	n/a		~10 m	Achievable measurement uncertainty can be determined with a hard target. No clear definition exists for instrumentally measured cloud-base height (e.g. based on penetration depth or significant discontinuity in the extinction profile) Significant bias during precipitation
4.3	Height of cloud top	Not available							

1	2	3	4	5	6	7	8	9
Variable	Range	Reported resolution	Mode of measurement/ observation	Required measurement uncertainty	Sensor time-constant	Output averaging time	Achievable measurement uncertainty	Remarks
5. Wind								
5.1 Speed	0 – 75 m s^{-1}	0.5 m s^{-1}	A	0.5 m s^{-1} for ≤ 5 m s^{-1} 10% for > 5 m s^{-1}	Distance constant 2 – 5 m	2 and/or 10 min	0.5 m s^{-1} for ≤ 5 m s^{-1} 10% for > 5 m s^{-1}	Average over 2 and/or 10 min Non-linear devices. Care needed in design of averaging process
5.2 Direction	0 – 360°	1°	A	5°	Damping ratio > 0.3	2 and/or 10 min	5°	Distance constant is usually expressed as response length Averages computed over Cartesian components (see Part IV, Chapter 3, 3.6 of this Guide) When using ultrasonic anemometers, no distance constant or time constant is needed. For moving mobile stations, the movement of the station needs to be taken into account, inclusive of its uncertainty.
5.3 Gusts	0.1 – 150 m s^{-1}	0.1 m s^{-1}	A	10%		3 s	0.5 m s^{-1} for ≤ 5 m s^{-1} 10% for > 5 m s^{-1}	Highest 3 s average should be recorded

	1	2	3	4	5	6	7	8	9
	Variable	Range	Reported resolution	Mode of measurement/ observation	Required measurement uncertainty	Sensor time-constant	Output averaging time	Achievable measurement uncertainty	Remarks
6.	**Precipitation**								
6.1	Amount (daily)	0 – 500 mm	0.1 mm	T	0.1 mm for ≤ 5 mm 2% for > 5 mm	n/a	n/a	The larger of 5% or 0.1 mm	Quantity based on daily amounts Measurement uncertainty depends on aerodynamic collection efficiency of gauges and evaporation losses in heated gauges
6.2	Depth of snow	0 – 25 m	1 cm	I	1 cm for ≤ 20 cm 5% for > 20 cm	< 10 s	1 min	1 cm	Average depth over an area representative of the observing site
6.3	Thickness of ice accretion on ships	Not specified	1 cm	I	1 cm for ≤ 10 cm 10% for > 10 cm				
6.4	Precipitation intensity	0.02 mm h^{-1} – 2 000 mm h^{-1}	0.1 mm h^{-1}	I	(trace): n/a for 0.02 – 0.2 mm h^{-1} 0.1 mm h^{-1} for 0.2 – 2 mm h^{-1} 5% for > 2 mm h^{-1}	< 30 s	1 min	Under constant flow conditions in laboratory, 5% above 2 mm/h, 2% above 10 mm/h In field, 5 mm/h and 5% above 100 mm/h	Uncertainty values for liquid precipitation only Uncertainty is seriously affected by wind Sensors may show significant non-linear behaviour For < 0.2 mm h^{-1}: detection only (yes/no) sensor time-constant is significantly affected during solid precipitation using catchment type of gauges
6.5	Precipitation duration (daily)	0 – 24 h	60 s	T	n/a	60 s			Threshold value of 0.02 mm/h

	1	2	3	4	5	6	7	8	9
	Variable	*Range*	*Reported resolution*	*Mode of measurement/ observation*	*Required measurement uncertainty*	*Sensor time-constant*	*Output averaging time*	*Achievable measurement uncertainty*	*Remarks*
7.	**Radiation**								
7.1	Sunshine duration (daily)	0 – 24 h	60 s	T	0.1 h	20 s	n/a	The larger of 0.1 h or 2%	
7.2	Net radiation, radiant exposure (daily)	Not specified	1 J m^{-2}	T	0.4 MJ m^{-2} for ≤ 8 MJ m^{-2} 5% for > 8 MJ m^{-2}	20 s	n/a	15%	Radiant exposure expressed as daily sums (amount) of (net) radiation Best achievable operational uncertainty is obtained by combining the measurements of two pyranometers and two pyrgeometers
7.3	Global downward/ upward solar radiation	Not specified	1 J m^{-2}	T	2%	20 s	n/a	5% (daily) 8% (hourly)	Daily total exposure
7.4	Downward/ upward long-wave radiation at Earth surface	Not specified	1 J m^{-2}	T	5%	20 s	n/a	10%	

	1	*2*	*3*	*4*	*5*	*6*	*7*	*8*	*9*
	Variable	*Range*	*Reported resolution*	*Mode of measurement/ observation*	*Required measurement uncertainty*	*Sensor time-constant*	*Output averaging time*	*Achievable measurement uncertainty*	*Remarks*
8.	**Visibility**								
8.1	Meteorological optical range (MOR)	10 m – 100 km	1 m	I	50 m for ≤ 600 m 10% for > 600 m – ≤ 1 500 m 20% for > 1 500 m	< 30 s	1 and 10 min	The larger of 20 m or 20%	Achievable measurement uncertainty may depend on the cause of obscuration Quantity to be averaged: extinction coefficient (see Part IV, Chapter 3, 3.6 of this Guide). Preference for averaging logarithmic values
8.2	Runway visual range (RVR)	10 m – 2 000 m	1 m	A	10 m for ≤ 400 m 25 m for > 400 m – ≤ 800 m 10% for > 800 m	< 30 s	1 and 10 min	The larger of 20 m or 20%	In accordance with WMO-No. 49, Volume II, Attachment A (2004 ed.) and ICAO Doc 9328-AN/908 (second ed., 2000) New versions of these documents may exist, specifying other values.
8.3	Background luminance	0 – 40 000 cd m^{-2}	1 cd m^{-2}	I		30 s	1 min	10%	Related to 8.2 RVR

1	*2*	*3*	*4*	*5*	*6*	*7*	*8*	*9*
Variable	*Range*	*Reported resolution*	*Mode of measurement/ observation*	*Required measurement uncertainty*	*Sensor time-constant*	*Output averaging time*	*Achievable measurement uncertainty*	*Remarks*
9. Waves								
9.1 Significant wave height	0 – 50 m	0.1 m	A	0.5 m for ≤ 5 m 10% for > 5 m	0.5 s	20 min	0.5 m for ≤ 5 m 10% for > 5 m	Average over 20 min for instrumental measurements
9.2 Wave period	0 – 100 s	1 s	A	0.5 s	0.5 s	20 min	0.5 s	Average over 20 min for instrumental measurements
9.3 Wave direction	0 – 360°	1°	A	10°	0.5 s	20 min	20°	Average over 20 min for instrumental measurements
10. Evaporation								
10.1 Amount of pan evaporation	0 – 100 mm	0.1 mm	T	0.1 mm for ≤ 5 mm 2% for > 5 mm	n/a			

Notes:

1. Column 1 gives the basic variable.
2. Column 2 gives the common range for most variables; limits depend on local climatological conditions.
3. Column 3 gives the most stringent resolution as determined by the *Manual on Codes* (WMO-No. 306).
4. In column 4:
   I = Instantaneous: In order to exclude the natural small-scale variability and the noise, an average value over a period of 1 min is considered as a minimum and most suitable; averages over periods of up to 10 min are acceptable.
   A = Averaging: Average values over a fixed period, as specified by the coding requirements.
   T = Totals: Totals over a fixed period, as specified by coding requirements.
5. Column 5 gives the recommended measurement uncertainty requirements for general operational use, i.e. of Level II data according to FM 12, 13, 14, 15 and its BUFR equivalents. They have been adopted by all eight technical commissions and are applicable for synoptic, aeronautical, agricultural and marine meteorology, hydrology, climatology, etc. These requirements are applicable for both manned and automatic weather stations as defined in the *Manual on the Global Observing System* (WMO-No. 544). Individual applications may have less stringent requirements. The stated value of required measurement uncertainty represents the uncertainty of the reported value with respect to the true value and indicates the interval in which the true value lies with a stated probability. The recommended probability level is 95% ($k = 2$), which corresponds to the 2σ level for a normal (Gaussian) distribution of the variable. The assumption that all known corrections are taken into account implies that the errors in reported values will have a mean value (or bias) close to zero. Any residual bias should be small compared with the stated measurement uncertainty requirement. The true value is the value which, under operational conditions, perfectly characterizes the variable to be measured/observed over the representative time interval, area and/or volume required, taking into account siting and exposure.

Notes *(cont.)*

6. Columns 2 to 5 refer to the requirements established by the CBS Expert Team on Requirements for Data from Automatic Weather Stations in 2004.
7. Columns 6 to 8 refer to the typical operational performance established by the CIMO Expert Team on Surface Technology and Measurement Techniques in 2004.
8. Achievable measurement uncertainty (column 8) is based on sensor performance under nominal and recommended exposure that can be achieved in operational practice. It should be regarded as a practical aid to users in defining achievable and affordable requirements.
9. n/a = not applicable.
10. The term *uncertainty* has preference over *accuracy* (i.e. uncertainty is in accordance with ISO/IEC/JCGM standards on the uncertainty of measurements (ISO/IEC (2008) / JCGM (2008)).
11. Dewpoint temperature, relative humidity and air temperature are linked, and thus their uncertainties are linked. When averaging, preference is given to absolute humidity as the principal variable.

REFERENCES AND FURTHER READING

Brooks, C.E.P. and N. Carruthers, 1953: *Handbook of Statistical Methods in Meteorology.* MO 538, Meteorological Office, London.

Bureau International des Poids et Mesures, 2006: *The International System of Units (SI).* BIPM, Sèvres/Paris.

Bureau International des Poids et Mesures/Comité Consultatif de Thermométrie, 1990: The International Temperature Scale of 1990 (ITS-90) (H. Preston Thomas). *Metrologia*, 27:3–10.

Eisenhart, C., 1963: Realistic evaluation of the precision and accuracy of instrument calibration systems. National Bureau of Standards–C, Engineering and Instrumentation, *Journal of Research*, 67C(2).

International Civil Aviation Organization, 2002: *World Geodetic System – 1984 (WGS-84) Manual.* ICAO Doc 9674–AN/946, Quebec.

International Organization for Standardization, 1994*a*: *Accuracy (Trueness and Precision) of Measurement Methods and Results – Part 1: General Principles and Definitions*, ISO 5725-1:1994/Cor.1:1998. Geneva.

———, 1994*b*: *Accuracy (Trueness and Precision) of Measurement Methods and Results – Part 2: Basic Method for the Determination of Repeatability and Reproducibility of a Standard Measurement Method*, ISO 5725-2:1994/Cor.1:2002. Geneva.

———, 2009: *Quantities and Units – Part 1: General*, ISO 80000-1:2009. Geneva.

International Organization for Standardization/International Electrotechnical Commission, 2008: *Uncertainty of Measurement – Part 3: Guide to the Expression of Uncertainty in Measurement*, ISO/IEC Guide 98-3:2008, Incl. Suppl. 1:2008/Cor 1:2009, Suppl. 1:2008, Suppl. 2:2011. Geneva. (equivalent to: Joint Committee for Guides in Metrology, 2008: *Evaluation of Measurement Data – Guide to the Expression of Uncertainty in Measurement*, JCGM 100:2008, Corrected in 2010).

International Union of Pure and Applied Physics, 1987: *Symbols, Units, Nomenclature and Fundamental Constants in Physics.* SUNAMCO Document IUPAP-25 (E.R. Cohen and P. Giacomo), reprinted from Physica 146A, pp. 1–68.

Joint Committee for Guides in Metrology, 2012: *International Vocabulary of Metrology – Basic and General Concepts and Associated Terms (VIM).* JCGM 200:2012.

Kok, C.J., 2000: *On the Behaviour of a Few Popular Verification Scores in Yes/No Forecasting.* Scientific Report. WR-2000-04. KNMI, De Bilt.

Linacre, E., 1992: *Climate Data and Resources – A Reference and Guide.* Routledge, London.

Murphy, A.H. and R.W. Katz (eds.), 1985: *Probability, Statistics and Decision Making in the Atmospheric Sciences.* Westview Press, Boulder.

National Institute of Standards and Technology, 2008: *Guide for the Use of the International System of Units (SI)* (A. Thompson and B.N. Taylor). NIST Special Publication No. 811, Gaithersburg, United States of America.

Natrella, M.G., 1966: *Experimental Statistics.* National Bureau of Standards Handbook 91, Washington DC.

Orlanski, I., 1975: A rational subdivision of scales for atmospheric processes. *Bulletin of the American Meteorological Society*, 56:527–530.

World Meteorological Organization, 1966: *International Meteorological Tables* (S. Letestu, ed.) (1973 amendment). (WMO-No. 188, TP. 94). Geneva.

———, 1970: *Performance Requirements of Aerological Instruments: an Assessment Based on Atmospheric Variability* (C.L. Hawson). Technical Note No. 112 (WMO-No. 267, TP. 151). Geneva.

———, 1992: *International Meteorological Vocabulary* (WMO-No. 182). Geneva.

———, 1993: *Siting and Exposure of Meteorological Instruments* (J. Ehinger). Instruments and Observing Methods Report No. 55 (WMO/TD-No. 589). Geneva.

———, 2001: *Lecture Notes for Training Agricultural Meteorological Personnel* (J. Wieringa and J. Lomas) (WMO-No. 551). Geneva.

———, 2002: Station exposure metadata needed for judging and improving the quality of observations of wind, temperature and other parameters (J. Wieringa and E. Rudel). *Papers Presented at the WMO Technical Conference on Meteorological and Environmental Instruments and Methods of Observation (TECO-2002)* Instruments and Observing Methods Report No. 75 (WMO/TD-No. 1123). Geneva.

———, 2003: *Guidelines on Climate Metadata and Homogenization* (P. Llansó, ed.). World Climate Data and Monitoring Programme (WCDMP) Series Report No. 53 (WMO/TD-No. 1186). Geneva.

———, 2008: *Guide to Hydrological Practices* (WMO-No. 168), Volume I. Geneva.

———, 2010*a*: *Abridged Final Report with Resolutions and Recommendations of the Third Session of the Joint WMO/ IOC Technical Commission for Oceanography and Marine Meteorology* (WMO-No. 1049). Geneva.

———, 2010*b*: *Guide to Agricultural Meteorological Practices* (WMO-No. 134). Geneva.

———, 2010*c*: *Guide to the Global Observing System* (WMO-No. 488). Geneva.

———, 2010*d*: *Manual on the Global Data-processing and Forecasting System* (WMO-No. 485), Volume I, Appendix II-2. Geneva.

———, 2010*e*: *Manual on the Global Observing System* (WMO-No. 544), Volume I. Geneva.

———, 2010*f*: *Weather Reporting* (WMO-No. 9), Volume A. Geneva.

———, 2011*a*: *Guide to Climatological Practices* (WMO-No. 100). Geneva.

———, 2011*b*: *Technical Regulations* (WMO-No. 49), Volume I, Appendix A. Geneva.

———, 2014: *Guide to Meteorological Observing and Information Distribution Systems for Aviation Weather Services* (WMO-No. 731). Geneva.

_____

CHAPTER CONTENTS

CHAPTER 2. MEASUREMENT OF TEMPERATURE

2.1 GENERAL

2.1.1 Definition

WMO (1992) defines temperature as a physical quantity characterizing the mean random motion of molecules in a physical body. Temperature is characterized by the behaviour whereby two bodies in thermal contact tend to an equal temperature. Thus, temperature represents the thermodynamic state of a body, and its value is determined by the direction of the net flow of heat between two bodies. In such a system, the body which overall loses heat to the other is said to be at the higher temperature. Defining the physical quantity temperature in relation to the "state of a body" however is difficult. A solution is found by defining an internationally approved temperature scale based on universal freezing and triple points.[1] The current such scale is the International Temperature Scale of 1990 (ITS-90),[2] in which temperature is expressed as t_{90} (Celsius temperature) or T_{90} (kelvin temperature). For the meteorological range (–95 °C to +60 °C), t_{90} is defined by means of a well-specified set of platinum resistance thermometers calibrated at a series of defining fixed points and using specified interpolation procedures (BIPM, 1989, 1990).

For meteorological purposes, temperatures are measured for a number of media. The most common variable measured is air temperature (at various heights). Other variables are ground, soil, grass minimum and seawater temperature. WMO (1992) defines air temperature as "the temperature indicated by a thermometer exposed to the air in a place sheltered from direct solar radiation". Although this definition cannot be used as the definition of the thermodynamic quantity itself, it is suitable for most applications.

2.1.2 Units and scales

The thermodynamic temperature (T), with units of kelvin (K) (also defined as "kelvin temperature"), is the basic temperature. The kelvin is the fraction 1/273.16 of the thermodynamic temperature of the triple point of water. The temperature (t), in degrees Celsius (or "Celsius temperature") defined by equation 2.1, is used for most meteorological purposes (from the ice-point secondary reference in Table 2.A.2 in the annex):

$$t/°\mathrm{C} = T/\mathrm{K} - 273.15 \tag{2.1}$$

A temperature difference of one degree Celsius (°C) unit is equal to one kelvin (K) unit. Note that the unit K is used without the degree symbol.

In the thermodynamic scale of temperature, measurements are expressed as differences from absolute zero (0 K), the temperature at which the molecules of any substance possess no kinetic energy. The scale of temperature in general use since 1990 is the ITS-90 (see the annex), which is based on assigned values for the temperatures of a number of reproducible equilibrium states (see Table 2.A.1 in the annex) and on specified standard instruments calibrated at those temperatures. The ITS was chosen in such a way that the temperature measured against it is identical to the thermodynamic temperature, with any difference being within the present limits of measurement uncertainty. In addition to the defining fixed points of the ITS, other secondary reference points are available (see Table 2.A.2 in the annex). Temperatures of meteorological interest are obtained by interpolating between the fixed points by applying the standard formulae in the annex.

---

[1] The authoritative body for this scale is the International Bureau of Weights and Measures/Bureau International des Poids et Mesures (BIPM), Sèvres (Paris); see http://www.bipm.org. BIPM's Consultative Committee for Thermometry (CCT) is the executive body responsible for establishing and realizing the ITS.

[2] Practical information on ITS-90 can be found on the ITS-90 website: http://www.its-90.com.

2.1.3   Meteorological requirements

2.1.3.1   *General*

Meteorological requirements for temperature measurements primarily relate to the following:

(a)   The air near the Earth's surface;

(b)   The surface of the ground;

(c)   The soil at various depths;

(d)   The surface levels of the sea and lakes;

(e)   The upper air.

These measurements are required, either jointly or independently and locally or globally, for input to numerical weather prediction models, for hydrological and agricultural purposes, and as indicators of climatic variability. Local temperature also has direct physiological significance for the day-to-day activities of the world's population. Measurements of temperature may be required as continuous records or may be sampled at different time intervals. This chapter deals with requirements relating to (a), (b) and (c).

2.1.3.2   *Accuracy requirements*

The range, reported resolution and required uncertainty for temperature measurements are detailed in Part I, Chapter 1, of this Guide. In practice, it may not be economical to provide thermometers that meet the required performance directly. Instead, cheaper thermometers, calibrated against a laboratory standard, are used with corrections being applied to their readings as necessary. It is necessary to limit the size of the corrections to keep residual errors within bounds. Also, the operational range of the thermometer will be chosen to reflect the local climatic range. As an example, the table below gives an acceptable range of calibration and errors for thermometers covering a typical measurement range.

Example of possible thermometer characteristics

Thermometer type	Ordinary	Maximum	Minimum
Span of scale (°C)	–30 to 45	–30 to 50	–40 to 40
Range of calibration (°C)	–30 to 40	–25 to 40	–30 to 30
Maximum error	< 0.2 K	0.2 K	0.3 K
Maximum difference between maximum and minimum correction within the range	0.2 K	0.3 K	0.5 K
Maximum variation of correction within any interval of 10 °C	0.1 K	0.1 K	0.1 K

All temperature-measuring instruments should be issued with a certificate confirming compliance with the appropriate uncertainty or performance specification, or a calibration certificate that gives the corrections that must be applied to meet the required uncertainty. This initial testing and calibration should be performed by an accredited calibration laboratory. Temperature-measuring instruments should also be checked subsequently at regular intervals, the exact apparatus used for this calibration being dependent on the instrument or sensor to be calibrated.

2.1.3.3   *Response times of thermometers*

For routine meteorological observations there is no advantage in using thermometers with a very small time-constant or lag coefficient, since the temperature of the air continually fluctuates up to one or two degrees within a few seconds. Thus, obtaining a representative reading with such a thermometer would require taking the mean of a number of readings, whereas a thermometer with a larger time-constant tends to smooth out the rapid fluctuations. Too long a time constant, however, may result in errors when long-period changes of temperature occur. It is recommended that the time constant, defined as the time required by the thermometer to register 63.2% of a step change in air temperature, should be 20 s. The time constant depends on the airflow over the sensor.

2.1.3.4   *Recording the circumstances in which measurements are taken*

Temperature is one of the meteorological quantities whose measurements are particularly sensitive to exposure. For climate studies in particular, temperature measurements are affected by the state of the surroundings, by vegetation, by the presence of buildings and other objects, by ground cover, by the condition of, and changes in, the design of the radiation shield or screen, and by other changes in equipment (WMO, 2011). It is important that records should be kept not only of the temperature data, but also of the circumstances in which the measurements are taken. Such information is known as metadata (data about data; see Part I, Chapter 1, Annex 1.C).

2.1.4   **Measurement methods**

In order to measure the temperature of an object, a thermometer can be brought to the same temperature as the object (namely, into thermodynamic equilibrium with it), and the temperature of the thermometer itself can then be measured. Alternatively, the temperature can be determined by a radiometer without the need for thermal equilibrium.

Any physical property of a substance which is a function of temperature can be used as the basis of a thermometer. The properties most widely used in meteorological thermometers are thermal expansion and the change in electrical resistance with temperature. Radiometric thermometers operate in the infrared part of the electromagnetic spectrum and are used, among other applications, for temperature measurements from satellites. A special technique to determine the air temperature using ultrasonic sampling, developed to determine air speeds, also provides the average speeds of the air molecules, and as a consequence its temperature (WMO, 2002*a*).

Thermometers which indicate the prevailing temperature are often known as ordinary thermometers, while those which indicate extreme temperature over a period of time are called maximum or minimum thermometers.

There are various standard texts on instrument design and laboratory practice for the measurement of temperature thermometry, such as Jones (1992) and Middleton and Spilhaus (1960). Considering the concepts of thermometry, care should be taken that, for meteorological applications, only specific technologies are applicable because of constraints determined by the typical climate or environment.

2.1.4.1   *Thermometer exposure and siting*

Radiation from the sun, clouds, the ground and other surrounding objects passes through the air without appreciably changing its temperature, but a thermometer exposed freely in the open can absorb considerable radiation. As a consequence, its temperature may differ from the true air temperature, with the difference depending on the radiation intensity and on the ratio of absorbed radiation to dissipated heat. For some thermometer elements, such as the very fine wire used in an open-wire resistance thermometer, the difference may be very small or even negligible. However, with the more usual operational thermometers the temperature difference may reach 25 K under extremely unfavourable conditions. Therefore, in order to ensure that the

thermometer is at true air temperature it is necessary to protect the thermometer from radiation by a screen or shield that also serves to support the thermometer. This screen also shelters it from precipitation while allowing the free circulation of air around it, and prevents accidental damage. Precipitation on the sensor will, depending on the local airflow, depress the sensor temperature, causing it to behave as a wet-bulb thermometer. Maintaining free circulation may, however, be difficult to achieve under conditions of rime ice accretion. Practices for reducing observational errors under such conditions will vary and may involve the use of special designs of screens or temperature-measuring instruments, including artificial ventilation. Nevertheless, in the case of artificial ventilation, care should be taken to avoid unpredictable influences caused by wet deposition in combination with evaporation during precipitation, drizzle, fog, and the like. An overview of concepts of temperature measurement applicable for operational practices is given by Sparks (1970).

In order to achieve representative results when comparing thermometer readings at different places and at different times, a standardized exposure of the screen and, hence, of the thermometer itself is also indispensable. For general meteorological work, the observed air temperature should be representative of the free air conditions surrounding the station over as large an area as possible, at a height of between 1.25 and 2 m above ground level. The height above ground level is specified because large vertical temperature gradients may exist in the lowest layers of the atmosphere. The best site for the measurements is, therefore, over level ground, freely exposed to sunshine and wind and not shielded by, or close to, trees, buildings and other obstructions. Sites on steep slopes or in hollows are subject to exceptional conditions and should be avoided. In towns and cities, local peculiarities are expected to be more marked than in rural districts. Temperature observations on the top of buildings are of doubtful significance and use because of the variable vertical temperature gradient and the effect of the building itself on the temperature distribution.

The siting classification for surface observing stations on land (see Part I, Chapter 1, Annex 1.B of this Guide) provides additional guidance on the selection of a site and the location of a thermometer within a site to optimize representativeness.

2.1.4.2   *Temperature standards*

Laboratory standards

Primary standard thermometers will be held and maintained at national standards laboratories. A national meteorological or other accredited calibration laboratory will have, as a working standard, a high-grade platinum resistance thermometer, traceable to the national standard. The uncertainty of this thermometer may be checked periodically in a water triple-point cell. The triple point of water is defined exactly and can be reproduced in a triple-point cell with an uncertainty of $1 \cdot 10^{-4}$ K.

Field standards

The WMO reference psychrometer (WMO, 1992) is the reference instrument for determining the relationship between the air temperature measured by conventional surface instruments and the true air temperature. This instrument has been designed to be used as a free-standing instrument and not for deployment within a screen or shelter; it is the most accurate instrument available for evaluating and comparing instrument systems. It is not intended for continuous use in routine meteorological operations and is capable of providing a temperature measurement with an uncertainty of 0.04 K (at the 95% confidence level). See Part I, Chapter 4, for further information.

2.2 LIQUID-IN-GLASS THERMOMETERS

2.2.1 General description

For routine observations of air temperature, including maximum, minimum and wet-bulb temperatures, liquid-in-glass thermometers are still commonly used. Such thermometers make use of the differential expansion of a pure liquid with respect to its glass container to indicate the temperature. The stem is a tube which has a fine bore attached to the main bulb; the volume of liquid in the thermometer is such that the bulb is filled completely but the stem is only partially filled at all temperatures to be measured. The changes in volume of the liquid with respect to its container are indicated by changes in the liquid column; by calibration with respect to a standard thermometer, a scale of temperature can be marked on the stem, or on a separate scale tightly attached to the stem.

The liquid used depends on the required temperature range; mercury[3] is generally used for temperatures above its freezing point (–38.9 °C), while ethyl alcohol or other pure organic liquids are used for lower temperatures. The glass should be one of the normal or borosilicate glasses approved for use in thermometers. The glass bulb is made as thin as is consistent with reasonable strength to facilitate the conduction of heat to and from the bulb and its contents. A narrower bore provides greater movement of liquid in the stem for a given temperature change, but reduces the useful temperature range of the thermometer for a given stem length. The thermometer should be suitably annealed before it is graduated in order to minimize the slow changes that occur in the glass with ageing.

There are four main types of construction for meteorological thermometers, as follows:

(a) The sheathed type with the scale engraved on the thermometer stem;

(b) The sheathed type with the scale engraved on an opal glass strip attached to the thermometer tube inside the sheath;

(c) The unsheathed type with the graduation marks on the stem and mounted on a metal, porcelain or wooden back carrying the scale numbers;

(d) The unsheathed type with the scale engraved on the stem.

The stems of some thermometers are lens-fronted to provide a magnified image of the mercury thread.

Types (a) and (b) have the advantage over types (c) and (d) that their scale markings are protected from wear. For types (c) and (d), the markings may have to be reblackened from time to time; on the other hand, such thermometers are easier to make than types (a) and (b). Types (a) and (d) have the advantage of being less susceptible to parallax errors (see section 2.2.4). An overview of thermometers, designed for use in meteorological practices is given by HMSO (1980).

Whichever type is adopted, the sheath or mounting should not be unduly bulky as this would keep the heat capacity high. At the same time, the sheath or mounting should be sufficiently robust to withstand the normal risks associated with handling and transit.

For mercury-in-glass thermometers, especially maximum thermometers, it is important that the vacuum above the mercury column be nearly perfect. All thermometers should be graduated for total immersion, with the exception of thermometers for measuring soil temperature. The special requirements of thermometers for various purposes are dealt with hereafter under the appropriate headings.

---

[3] Advice concerning the safe use of mercury is given in Part I, Chapter 3, 3.2.7. The Minamata Convention on Mercury of the United Nations Environment Programme entered into force in October 2013 and will have a significant impact on the use of mercury for meteorological applications.

2.2.1.1   *Ordinary (station) thermometers*

This is the most accurate instrument of all meteorological thermometers. Usually it is a mercury-in-glass-type thermometer. Its scale markings have an increment of 0.2 K or 0.5 K, and the scale is longer than that of the other meteorological thermometers.

The ordinary thermometer is used in a thermometer screen to avoid radiation errors. A support keeps it in a vertical position with the bulb at the lower end. The form of the bulb is that of a cylinder or an onion.

A pair of ordinary thermometers can be used as a psychrometer if one of them is fitted with a wet-bulb[4] sleeve.

2.2.1.2   *Maximum thermometers*

The recommended type for maximum thermometers is a mercury-in-glass thermometer with a constriction in the bore between the bulb and the beginning of the scale. This constriction prevents the mercury column from receding with falling temperatures. However, observers can reset by holding it firmly, bulb-end downwards, and swinging their arm until the mercury column is reunited. A maximum thermometer should be mounted at an angle of about 2° from the horizontal position, with the bulb at the lower end to ensure that the mercury column rests against the constriction without gravity forcing it to pass. It is desirable to have a widening of the bore at the top of the stem to enable parts of the column which have become separated to be easily united.

2.2.1.3   *Minimum thermometers*

As regards minimum thermometers, the most common instrument is a spirit thermometer with a dark glass index, about 2 cm long, immersed in the spirit. Since some air is left in the tube of a spirit thermometer, a safety chamber should be provided at the upper end which should be large enough to allow the instrument to withstand a temperature of 50 °C without being damaged. Minimum thermometers should be supported in a similar manner to maximum thermometers, in a near-horizontal position. Various liquids can be used in minimum thermometers, such as ethyl alcohol, pentane and toluol. It is important that the liquid should be as pure as possible since the presence of certain impurities increases the tendency of the liquid to polymerize with exposure to light and after the passage of time; such polymerization causes a change in calibration. In the case of ethyl alcohol, for example, the alcohol should be completely free of acetone.

Minimum thermometers are also exposed to obtain grass minimum temperature.

2.2.1.4   *Soil thermometers*

For measuring soil temperatures at depths of 20 cm or less, mercury-in-glass thermometers, with their stems bent at right angles, or any other suitable angle, below the lowest graduation, are in common use. The thermometer bulb is sunk into the ground to the required depth, and the scale is read with the thermometer in situ. These thermometers are graduated for immersion up to the measuring depth. Since the remainder of the thermometer is kept at air temperature, a safety chamber should be provided at the end of the stem for the expansion of the mercury.

For measuring temperature at depths of over 20 cm, mercury-in-glass thermometers, mounted on wooden, glass or plastic tubes, with their bulbs embedded in wax or metallic paint, are recommended. The thermometer-tube assemblies are then suspended or slipped in thin-walled metal or plastic tubes sunk into the ground to the required depth. In cold climates, the tops of the outer tubes should extend above the ground to a height greater than the expected depth of snow cover.

---

[4]   Wet-bulb temperatures are explained in Part I, Chapter 4.

The technique of using vertical steel tubes is unsuitable for measuring the diurnal variation of soil temperature, particularly in dry soil, and calculations of soil thermal properties based on such measurements could be significantly in error because they will conduct heat from the surface layer.

The large time-constant due to the increased heat capacity enables the thermometers to be removed from the outer tubes and read before their temperature has had time to change appreciably from the soil temperature.

When the ground is covered by snow, and in order that the observer may approach the line of thermometers without disturbing the snow cover, it is recommended that a lightweight bridge be constructed parallel to the line of thermometers. The bridge should be designed so that the deck can be removed between readings without affecting the snow cover.

2.2.2   Measurement procedures

2.2.2.1   *Reading ordinary thermometers*

Thermometers should be read as rapidly as possible in order to avoid changes of temperature caused by the observer's presence. Since the liquid meniscus, or index, and the thermometer scale are not on the same plane, care must be taken to avoid parallax errors. These will occur unless the observer ensures that the straight line from his/her eye to the meniscus, or index, is at a right angle to the thermometer stem. Since thermometer scales are not normally subdivided to less than one fifth of a degree, readings to the nearest tenth of a degree, which are essential in psychrometry, must be made by estimation. Corrections for scale errors, if any, should be applied to the readings. Maximum and minimum thermometers should be read and set at least twice daily. Their readings should be compared frequently with those of an ordinary thermometer in order to ensure that no serious errors develop.

2.2.2.2   *Measuring grass minimum temperatures*

The grass minimum temperature is the lowest temperature reached overnight by a thermometer freely exposed to the sky just above short grass. The temperature is measured with a minimum thermometer such as that described in section 2.2.1.3. The thermometer should be mounted on suitable supports so that it is inclined at an angle of about 2° from the horizontal position, with the bulb lower than the stem, 25 to 50 mm above the ground and in contact with the tips of the grass. When the ground is covered with snow, the thermometer should be supported immediately above the surface of the snow, as near to it as possible without actually touching it.

Normally, the thermometer is exposed at the last observation hour before sunset, and the reading is taken the next morning. The instrument is kept within a screen or indoors during the day. However, at stations where an observer is not available near sunset, it may be necessary to leave the thermometer exposed throughout the day. In strong sunshine, exposing the thermometer in this way can cause the spirit to distil and collect in the top of the bore. This effect can be minimized by fitting a cotton sock on a black metal shield over the safety chamber end of the thermometer; this shield absorbs more radiation and consequently reaches a higher temperature than the rest of the thermometer. Thus, any vapour will condense lower down the bore at the top of the spirit column.

2.2.2.3   *Measuring soil temperatures*

The standard depths for soil temperature measurements are 5, 10, 20, 50 and 100 cm below the surface; additional depths may be included. The site for such measurements should be a level plot of bare ground (about 75 cm^2) and typical of the surrounding soil for which information is required. If the surface is not representative of the general surroundings, its extent should

not be less than 100 m². When the ground is covered with snow, it is desirable to measure the temperature of the snow cover as well. Where snow is rare, the snow may be removed before taking the readings and then replaced.

When describing a site for soil temperature measurements, the soil type, soil cover and the degree and direction of the ground's slope should be recorded. Whenever possible, the physical soil constants, such as bulk density, thermal conductivity and the moisture content at field capacity, should be indicated. The level of the water table (if within 5 m of the surface) and the soil structure should also be included.

At agricultural meteorological stations, the continuous recording of soil temperatures and air temperatures at different levels in the layer adjacent to the soil (from ground level up to about 10 m above the upper limit of prevailing vegetation) is desirable.

2.2.3　　Thermometer siting and exposure

Both ordinary thermometers and maximum and minimum thermometers are always exposed in a thermometer screen placed on a support. Extreme thermometers are mounted on suitable supports so that they are inclined at an angle of about 2° from the horizontal position, with the bulb being lower than the stem.

The siting and exposure of grass minimum thermometers is as prescribed in section 2.2.2.2. At a station where snow is persistent and of varying depth, it is possible to use a support that allows the thermometers to be raised or lowered to maintain the correct height above the snow surface.

2.2.4　　Sources of error in liquid-in-glass thermometers

The main sources of error common to all liquid-in-glass thermometers are the following:

(a)　Elastic errors;

(b)　Errors caused by the emergent stem;

(c)　Parallax and gross reading errors;

(d)　Changes in the volume of the bulb produced by exterior or interior pressure;

(e)　Capillarity;

(f)　Errors in scale division and calibration;

(g)　Inequalities in the expansion of the liquid and glass over the range considered.

The last three errors can be minimized by the manufacturer and included in the corrections to be applied to the observed values. Some consideration needs to be given to the first three errors. Error (d) does not usually arise when the thermometers are used for meteorological purposes.

2.2.4.1　　*Elastic errors*

There are two kinds of elastic errors, namely reversible and irreversible errors. The first is of importance only when a thermometer is exposed to a large temperature range in a short period of time. Thus, if a thermometer is checked at the steam point and shortly afterwards at the ice point, it will read slightly too low at first and then the indicated temperature will rise slowly to the correct value. This error depends on the quality of the glass employed in the thermometer, and may be as much as 1 K (with glass of the highest quality it should be only 0.03 K) and would be proportionately less for smaller ranges of temperature. The effect is of no importance in meteorological measurements, apart from the possibility of error in the original calibration.

The irreversible changes may be more significant. The thermometer bulb tends to contract slowly over a period of years and, thus, causes the zero to rise. The greatest change will take place in the first year, after which the rate of change will gradually decrease. This alteration can be reduced by subjecting the bulb to heat treatment and by using the most suitable glass. Even with glass of the highest quality, the change may be about 0.01 K per year at first. For accurate work, and especially with inspector or check thermometers, the zero should be redetermined at the recommended intervals and the necessary corrections applied.

2.2.4.2   *Errors caused by the emergent stem*

A thermometer used to measure air temperature is usually completely surrounded by air at an approximately uniform temperature, and is calibrated by immersing the thermometer either completely or only to the top of the mercury column (namely, calibrated by complete or partial immersion). When such a thermometer is used to determine the temperature of a medium which does not surround the stem, so that the effective temperature of the stem is different from that of the bulb, an error will result.

For meteorological applications, the most likely circumstance where this might be encountered is when checking the calibration of an ordinary thermometer in a vessel containing another liquid at a temperature significantly different from ambient temperature and only the bulb or lower part of the stem is immersed.

2.2.4.3   *Parallax and gross reading errors*

If the thermometer is not viewed on the plane that is perpendicular to the stem of the thermometer, parallax errors will arise. The error increases with the thickness of the thermometer stem and the angle between the actual and the correct line of sight. This error can be avoided only by taking great care when making an observation. With mercury-in-glass thermometers suspended vertically, as in an ordinary screen, the thermometer must be viewed at the horizontal level of the top of the mercury column.

Errors can also occur because observers usually disturb the surroundings in some way when they approach to read the thermometer. It is, therefore, necessary for observers to take the readings to the nearest tenth of a degree as soon as possible. Gross reading errors are usually 1°, 5° or 10° in magnitude. Such errors will be avoided if observers recheck the tens and units figure after taking their initial reading.

2.2.4.4   *Errors due to differential expansion*

The coefficient of cubical expansion of mercury is $1.82 \cdot 10^{-4}$ K^{-1}, and that of most glass lies between $1.0 \cdot 10^{-5}$ and $3.0 \cdot 10^{-5}$ K^{-1}. The expansion coefficient of the glass is, thus, an important fraction of that of mercury and cannot be neglected. As neither the coefficients of cubical expansion of mercury and glass nor the cross-sectional area of the bore of the stem are strictly constant over the range of temperature and length of the stem being used, the scale value of unit length of the stem varies along the stem, and the thermometer has to be calibrated by the manufacturer against a standard thermometer before it can be used.

2.2.4.5   *Errors associated with spirit thermometers*

The expansion coefficients of the liquids used in spirit thermometers are very much larger than those of mercury, and their freezing points are much lower (ethyl alcohol freezes at –115 °C). Spirit is used in minimum thermometers because it is colourless and because its larger expansion coefficient enables a larger bore to be used. Spirit thermometers are less accurate than mercury thermometers of similar cost and quality. In addition to having the general disadvantages of liquid-in-glass thermometers, spirit thermometers have some peculiarities to themselves:

(a) Adhesion of the spirit to the glass: Unlike mercury, organic liquids generally wet the glass. Therefore, when the temperature falls rapidly, a certain amount of the liquid may remain on the walls of the bore, causing the thermometer to read low. The liquid gradually drains down the bore if the thermometer is suspended vertically;

(b) Breaking of the liquid column: Drops of the liquid often form in the upper part of the thermometer stem by a process of evaporation and condensation. These can be reunited with the main column, but errors may be caused at the beginning of the process before it is noticed. The column is also often broken during transport. This error is reduced during manufacture by sealing off the thermometer at its lowest temperature so that it contains the maximum amount of air in the stem;

(c) Slow changes in the liquid: The organic liquids used tend to polymerize with age and exposure to light, with a consequent gradual diminution in liquid volume. This effect is speeded up by the presence of impurities; in particular, the presence of acetone in ethyl alcohol has been shown to be very deleterious. Great care has therefore to be taken over the preparation of the liquid for the thermometers. This effect may also be increased if dyes are used to colour the liquid to make it more visible.

The reduction of errors caused by breakage in the liquid column and the general care of spirit thermometers are dealt with later in this chapter.

2.2.5 Comparison and calibration in the field and laboratory

2.2.5.1 *Laboratory calibration*

Laboratory calibrations of thermometers should be carried out by accredited calibration laboratories. For liquid-in-glass thermometers, a liquid bath should be employed, within which it should be possible to maintain the temperature at any desired values within the required range. The rate of temperature change within the liquid should not exceed the recommended limits, and the calibration apparatus should be provided with a means of stirring the liquid. The reference thermometers and thermometers being calibrated should be suspended independently of the container and fully immersed, and should not touch the sides.

Sufficient measurements should be taken to ensure that the corrections to be applied represent the performance of the thermometer under normal conditions, with errors due to interpolation at any intermediate point not exceeding the non-systematic errors (see Part IV, Chapter 4).

2.2.5.2 *Field checks and calibration*

All liquid-in-glass thermometers experience gradual changes of zero. For this reason, it is desirable to check them at regular intervals, usually about once every two years. The thermometers should be stored in an upright position at room temperature for at least 24 h before the checking process begins.

The ice point may be checked by almost filling a Dewar flask with crushed ice made from distilled water and moistening it with more distilled water. The space between the ice pieces as well as the bottom of the vessel should be free from air. The water should remain 2 cm beneath the ice surface. An ordinary Thermos flask will accommodate the total immersion of most thermometers up to their ice point. The thermometers should be inserted so that as little of the mercury or spirit column as possible emerges from the ice. An interval of at least 15 min should elapse to allow the thermometer to take up the temperature of the melting ice before a reading of the indicated temperature is taken. Each thermometer should be moved backwards and forwards through the mixture and immediately read to a tenth part of the scale interval. Further readings at 5 min intervals should be taken and a mean value computed.

Other points in the range can be covered by reference to a travelling standard or inspector thermometer. Comparison should be made by immersing the reference thermometer and the

thermometer, or thermometers, to be calibrated in a deep vessel of water. It is generally better to work indoors, especially if the sun is shining, and the best results will be obtained if the water is at, or close to, ambient temperature.

Each thermometer is compared with the reference thermometer; thermometers of the same type can be compared with each other. For each comparison, the thermometers are held with their bulbs close together, moved backwards and forwards through the water for about 1 min, and then read. It must be possible to read both thermometers without changing the depth of immersion; subject to this, the bulbs should be as deep in the water as possible. Most meteorological thermometers are calibrated for total immersion; provided that the difference between the water and air temperature is not more than 5 K, the emergent stem correction should be negligible. Often, with the bulbs at the same depth, the tops of the columns of mercury (or other liquid) in the reference thermometer and the thermometer being checked will not be very close together. Particular care should therefore be taken to avoid parallax errors.

These comparisons should be made at least three times for each pair of thermometers. For each set of comparisons, the mean of the differences between readings should not exceed the tolerances specified in the table in section 2.1.3.2.

Soil thermometers may be calibrated in this manner, but should be left in the water for at least 30 min to allow the wax in which the bulbs are embedded to take up the temperature of the water. The large time-constant of the soil thermometer makes it difficult to conduct a satisfactory check unless the temperature of the water can be kept very steady. If the calibration is carefully carried out in water whose temperature does not change by more than 1 K in 30 min, the difference from the corrected reading of the reference thermometer should not exceed 0.25 K.

2.2.6 **Corrections**

When initially issued, thermometers identified by a serial number should be provided with either a dated certificate confirming compliance with the uncertainty requirement, or a dated calibration certificate giving the corrections that should be applied to the readings to achieve the required uncertainty.

In general, if the errors at selected points in the range of a thermometer (for example, 0 °C, 10 °C, 20 °C) are all within 0.05 K, no corrections will be necessary and the thermometers can be used directly as ordinary thermometers in naturally ventilated screens and as maximum, minimum, soil or grass minimum thermometers. If the errors at these selected points are greater than 0.05 K, a table of corrections should be available to the observer at the place of reading, together with unambiguous instructions on how these corrections should be applied.

Thermometers for which certificates would normally be issued are those:

(a)   For use in ventilated psychrometers;

(b)   For use by inspectors as travelling standards;

(c)   For laboratory calibration references;

(d)   For special purposes for which the application of corrections is justified.

For psychrometric use, identical thermometers should be selected.

2.2.7 Maintenance

2.2.7.1 *Breakage in the liquid column*

The most common fault encountered is the breaking of the liquid column, especially during transit. This is most likely to occur in spirit (minimum) thermometers. Other problems associated with these thermometers are adhesion of the spirit to the glass and the formation by distillation of drops of spirit in the support part of the bore.

A broken liquid column can usually be reunited by holding the thermometer bulb-end downward and tapping the thermometer lightly and rapidly against the fingers or something else which is elastic and not too hard. The tapping should be continued for some time (5 min if necessary), and afterwards the thermometer should be hung, or stood, upright in a suitable container, bulb downward, for at least 1 h to allow any spirit adhering to the glass to drain down to the main column. If such treatment is not successful, a more drastic method is to cool the bulb in a freezing mixture of ice and salt, while keeping the upper part of the stem warm; the liquid will slowly distil back to the main column. Alternatively, the thermometer may be held upright with its bulb in a vessel of warm water, while the stem is tapped or shaken from the water as soon as the top of the spirit column reaches the safety chamber at the top of the stem. Great care must be taken when using this method as there is a risk of bursting the thermometer if the spirit expands into the safety chamber.

2.2.7.2 *Scale illegibility*

Another shortcoming of unsheathed liquid-in-glass thermometers is that with time their scale can become illegible. This can be corrected at the station by rubbing the scale with a dark crayon or black lead pencil.

2.2.8 Safety

Mercury, which is the liquid most commonly used in liquid-in-glass thermometers, is poisonous if swallowed or if its vapour is inhaled. If a thermometer is broken and the droplets of mercury are not removed there is some danger to health, especially in confined spaces. (Advice on cleaning up after a breakage is given in Part I, Chapter 3, in section 3.2 on mercury barometers.) There may also be restrictions on the carriage of mercury thermometers on aircraft, or special precautions that must be taken to prevent the escape of mercury in the event of a breakage. The advice of the appropriate authority or carrier should be sought.

2.3 MECHANICAL THERMOGRAPHS

2.3.1 General description

The types of mechanical thermographs still commonly used are supplied with bimetallic or Bourdon-tube sensors since these are relatively inexpensive, reliable and portable. However, they are not readily adapted for remote or electronic recording. Such thermographs incorporate a rotating chart mechanism common to the family of classic recording instruments. In general, thermographs should be capable of operating over a range of about 60 K or even 80 K if they are to be used in continental climates. A scale value is needed such that the temperature can be read to 0.2 K without difficulty on a reasonably sized chart. To achieve this, provisions should be made for altering the zero setting of the instrument according to the season. The maximum error of a thermograph should not exceed 1 K.

2.3.1.1 *Bimetallic thermograph*

In bimetallic thermographs, the movement of the recording pen is controlled by the change in curvature of a bimetallic strip or helix, one end of which is rigidly fixed to an arm attached to the frame. A means of finely adjusting this arm should be provided so that the zero of the instrument can be altered when necessary. In addition, the instrument should be provided with a means of altering the scale value by adjusting the length of the lever that transfers the movement of the bimetal to the pen; this adjustment is best left to authorized personnel. The bimetallic element should be adequately protected from corrosion; this is best done by heavy copper, nickel or chromium plating, although a coat of lacquer may be adequate in some climates. A typical time-constant of about 25 s is obtained at an air speed of 5 m s^{-1}.

2.3.1.2 *Bourdon-tube thermograph*

The general arrangement is similar to that of the bimetallic type but its temperature-sensitive element is in the form of a curved metal tube of flat, elliptical section, filled with alcohol. The Bourdon tube is less sensitive than the bimetallic element and usually requires a multiplying level mechanism to give sufficient scale value. A typical time-constant is about 6 s at an air speed of 5 m s^{-1}.

2.3.2 Measurement procedures

In order to improve the resolution of the reading, thermographs will often be set, in different seasons, to one of two different ranges with corresponding charts. The exact date for changing from one set of charts to the other will vary according to the locality. However, when the change is made the instrument will need to be adjusted. This should be done either in the screen on a cloudy, windy day at a time when the temperature is practically constant or in a room where the temperature is constant. The adjustment is made by loosening the screw holding the pen arm to the pen spindle, moving the pen arm to the correct position and retightening, the screws. The instrument should then be left as is before rechecking, and any further adjustments made as necessary.

2.3.3 Exposure and siting

These instruments should be exposed in a large thermometer screen.

2.3.4 Sources of error

In the thermograph mechanism itself, friction is the main source of error. One cause of this is bad alignment of the helix with respect to the spindle. Unless accurately placed, the helix acts as a powerful spring and, if rigidly anchored, pushes the main spindle against one side of the bearings. With modern instruments this should not be a serious problem. Friction between the pen and the chart can be kept to a minimum by suitably adjusting the gate suspension.

2.3.5 Comparison and calibration

2.3.5.1 *Laboratory calibration*

There are two basic methods for the laboratory calibration of bimetallic thermographs. They may be checked by fixing them in a position with the bimetallic element in a bath of water. Alternatively, the thermograph may be placed in a commercial calibration chamber equipped with an air temperature control mechanism, a fan and a reference thermometer.

Comparisons should be made at two temperatures; from these, any necessary changes in the zero and magnification can be found. Scale adjustments should be performed by authorized personnel, and only after reference to the appropriate manufacturer's instrument handbook.

2.3.5.2 *Field comparison*

The time constant of the instrument may be as low as one half that of the ordinary mercury thermometer, so that routine comparisons of the readings of the dry bulb and the thermograph at fixed hours will, in general, not produce exact agreement even if the instrument is working perfectly. A better procedure is to check the reading of the instrument on a suitable day at a time when the temperature is almost constant (usually a cloudy, windy day) or, alternatively, to compare the minimum readings of the thermograph trace with the reading of the minimum thermometer exposed in the same screen. Any necessary adjustment can then be made by means of the setting screw.

2.3.6 **Corrections**

Thermographs would not normally be issued with correction certificates. If station checks show an instrument to have excessive errors, and if these cannot be adjusted locally, the instrument should be returned to an appropriate calibration laboratory for repair and recalibration.

2.3.7 **Maintenance**

Routine maintenance will involve an inspection of the general external condition, the play in the bearings, the inclination of the recording arm, the set of the pen, and the angle between the magnification arm and recording arm, and a check of the chart-drum clock timing. Such examinations should be performed in accordance with the recommendations of the manufacturer. In general, the helix should be handled carefully to avoid mechanical damage and should be kept clean. The bearings of the spindle should also be kept clean and oiled at intervals using a small amount of clock oil. The instrument is mechanically very simple and, provided that precautions are taken to keep the friction to a minimum and prevent corrosion, it should give good service.

2.4 **ELECTRICAL THERMOMETERS**

2.4.1 **General description**

Electrical instruments are in widespread use in meteorology for measuring temperatures. Their main virtue lies in their ability to provide an output signal suitable for use in remote indication, recording, storage, or transmission of temperature data. The most frequently used sensors are electrical resistance elements, semiconductor thermometers (thermistors) and thermocouples.

2.4.1.1 *Electrical resistance thermometers*

A measurement of the electrical resistance of a material whose resistance varies in a known manner with the temperature of the material can be used to represent the temperature.

For small temperature changes, the increase in resistance of pure metals is proportional to the change in temperature, as expressed in equation 2.2:

$$R_T = R_0 \left[1 + \alpha \left(T - T_0 \right) \right] \tag{2.2}$$

where $(T - T_0)$ is small; R_T is the resistance of a fixed amount of the metal at temperature T; R_0 is its resistance at a reference temperature T_0, and α is the temperature coefficient of resistance in the vicinity of T_0.

With 0 °C as the reference temperature, equation 2.2 becomes:

$$R_T = R_0\left(1 + \alpha \cdot t\right) \tag{2.3}$$

For larger temperature changes and for certain metallic alloys, equation 2.4 expresses the relationship more accurately:

$$R_T = R_0\left[1 + \alpha\left(T - T_0\right) + \beta\left(T - T_0\right)^2\right] \tag{2.4}$$

With 0 °C as the reference temperature, equation 2.4 becomes:

$$R_T = R_0\left(1 + \alpha \cdot t + \beta \cdot t^2\right) \tag{2.5}$$

These equations give the proportional change in resistance of an actual thermometer, so that values for the coefficients α and β can be found by calibration of the thermometer concerned. Based on these results, the inverse function, namely, t as a function of R, can be derived. Such a function may be expressed in terms of a power series of $(R_0 - R_T)$, namely, $t = t\,(R_0 - R_T) = c_1\,(R_0 - R_T) + c_2\,(R_0 - R_T)^2 + \ldots$

A good metal resistance thermometer will satisfy the following requirements:

(a)   Its physical and chemical properties will remain the same through the temperature measurement range;

(b)   Its resistance will increase steadily with increasing temperature without any discontinuities in the range of measurement;

(c)   External influences such as humidity, corrosion or physical deformations will not alter its resistance appreciably;

(d)   Its characteristics will remain stable over a period of two years or more;

(e)   Its resistance and thermal coefficient should be large enough to be useful in a measuring circuit.

Pure platinum best satisfies the foregoing requirements. Thus, it is used for the primary standard thermometers needed for transferring the ITS-90 between instrument locations. Platinum thermometers are also used for secondary standards and for operational sensors.

Practical thermometers are artificially aged before use and are commonly made from platinum alloys, nickel and occasionally tungsten for meteorological purposes. Usually they are hermetically sealed in a ceramic sheath. Their time constant is smaller than that of liquid-in-glass thermometers.

2.4.1.2   *Semiconductor thermometers*

Another type of resistance element in common use is the thermistor. This is a semiconductor with a relatively large temperature coefficient of resistance, which may be either positive or negative depending upon the actual material. Mixtures of sintered metallic oxides are suitable for making practical thermistors, which usually take the form of small discs, rods or spheres and are often glass-coated. The general expression for the temperature dependence of the resistance, R, of the thermistor is given in equation 2.6:

$$R = a \exp\left(b/T\right) \tag{2.6}$$

where a and b are constants and T is the temperature of the thermistor in kelvins.

The advantages of thermistors from a thermometric point of view are as follows:

(a)   The large temperature coefficient of resistance enables the voltage applied across a resistance bridge to be reduced while attaining the same sensitivity, thus reducing or even eliminating the need to account for the resistance of the leads and its changes;

(b)   The elements can be made very small, so their very low thermal capacities can yield a small time-constant. However, very small thermistors with their low thermal capacity have the disadvantage that, for a given dissipation, the self-heating effect is greater than for large thermometers. Thus, care must be taken to keep the power dissipation small.

A typical thermistor has a resistance which varies by a factor of 100 or 200 over the temperature range –40 °C to 40 °C.

2.4.1.3   *Thermocouples*

In 1821 Seebeck discovered that a very small contact electromotive force was set up at the place where two different metals touched. If a simple circuit is made with two metals and with the conjunction at the same temperature, there will be no resultant electromotive force in the circuit because the two electromotive forces, one at each junction, will exactly oppose and cancel one another. If the temperature of one junction is altered, the two electromotive forces no longer balance and there is a net electromotive force set up in the circuit; a current will then flow. When there are several junctions, the resultant electromotive force is the algebraic sum of the individual electromotive forces. The magnitude and sign of the contact electromotive force set up at any one junction depend on the types of metals joined and the temperature of the junction point, and may be empirically represented for any two metals by the expression:

$$(E_T - E_S) = \alpha(T - T_S) + \beta(T - T_S)^2 \tag{2.7}$$

where E_T is the contact electromotive force at a temperature T and E_s is the electromotive force at some standard temperature T_s, α and β being constants. If there are two junctions at temperatures T_1 and T_2, the net electromotive force E_n (the thermal electromotive force) is given by $(E_1 - E_2)$, where E_1 is the electromotive force at temperature T_1 and E_2 is the contact electromotive force temperature T_2. E_n can also be represented by a quadratic formula of the type given for $(E_T - E_s)$ to a good approximation:

$$E_n = E_1 - E_2 \tag{2.8}$$
$$E_n = a(T_1 - T_2) + b(T_1 - T_2)^2 \tag{2.9}$$

where a and b are constants for the two metals concerned. For most meteorological purposes, it is often possible to neglect the value of b, as it is always small compared with a.

Thermocouples are made by welding or soldering together wires of the metals concerned. These junctions can be made very small and with negligible heat capacity.

When used to measure temperature, a measurement is taken of the electromotive force set up when one junction is maintained at a standard known temperature and the other junction is allowed to take the temperature whose value is required. This electromotive force can be directly related to the difference in temperature between the two junctions by previous calibration of the system, and thus the unknown temperature is found by adding this difference algebraically to the known standard temperature.

In meteorology, thermocouples are mostly used when a thermometer of very small time-constant, of the order of 1 or 2 s, and capable of remote reading and recording is required, usually for special research tasks. A disadvantage, if the absolute temperature is required, is the necessity for a constant-temperature enclosure for both the cold junction and ancillary apparatus for the measurements of the electromotive force that has been set up; thermocouples are best suited for the measurement of differential temperatures, since this complication does not arise. Very high accuracy can be achieved with suitably sensitive apparatus, but frequent calibration is

necessary. Copper-constantan or iron-constantan combinations are suitable for meteorological work, as the electromotive force produced per degree Celsius is higher than with rarer and more expensive metals, which are normally used at high temperatures.

2.4.2 Measurements procedures

2.4.2.1 *Electrical resistance thermometers*

Electrical resistance thermometers may be connected to a variety of electrical measurement circuits, many of which are variations of resistance bridge circuits in either balanced or unbalanced form. In a balanced bridge, an accurate potentiometer is adjusted until no current flows in an indicator, with the position of the potentiometer arm being related to the temperature. In an unbalanced bridge, the out-of-balance current may be measured by a galvanometer; however, this current is not simply a function of the temperature and depends in part on other effects. An alternative which avoids this situation is to use a constant current source to power the bridge and to measure the out-of-balance voltage to obtain the temperature reading.

In the case of remote measuring, it should be taken into consideration that the wire between the resistance thermometer and the bridge also forms a resistance that alters depending on the temperature. Suitable precautions can be taken to avoid such errors.

Digital voltmeters can be used in conjunction with a constant current source to measure the temperature-dependent voltage drop across the thermometer element; the output can be scaled directly in temperature. Also, the digital output can be stored or transmitted without loss of accuracy and, thus, be available for further use. The digital output of the digital voltmeters can be subsequently converted back to an analogue voltage, if desired, to feed a recorder, for example.

2.4.2.2 *Thermocouples*

There are two main methods of measuring the electromotive force produced by thermocouples:

(a) By measuring the current produced in the circuit with a sensitive galvanometer;

(b) By balancing the thermoelectric electromotive force with a known electromotive force, so that no current actually flows through the thermocouples themselves.

In method (a), the galvanometer is connected directly in series with the two junctions. Method (b) will generally be used if a measuring uncertainty of better than 0.5% is required. This procedure does not depend on the magnitude of, or changes in, the line resistance since no current flows in the balanced condition.

2.4.3 Exposure and siting

The requirements relating to the exposure and siting of electrical thermometers will, in general, be the same as those for liquid-in-glass thermometers (see section 2.2.3). Exceptions include the following:

(a) The measurement of extreme values: Separate maximum and minimum thermometers may no longer be required if the electrical thermometer is connected to a continuously operating data recording system;

(b) The measurement of surface temperatures: The radiative properties of electrical thermometers will be different from liquid-in-glass thermometers. Electrical thermometers

exposed as grass minimum (or other surface) thermometers will, therefore, record different values from similarly exposed conventional thermometers. These differences may be minimized by placing the electrical thermometer within a glass sheath;

(c)   The measurement of soil temperatures: The use of mercury-in-glass thermometers in vertical steel tubes is quite unsuitable for the measurement of the diurnal variation of soil temperature because of heat conduction from the surface. It is possible to obtain readings that are much more representative by deploying electrical thermometers in brass plugs, inserted at the required depth into an undisturbed vertical soil face, the latter having been exposed by trenching. Electrical connections are brought out through plastic tubes via the trench, which is then refilled in such a way to restore, as far as possible, the original strata and drainage characteristics.

2.4.4   Sources of error

2.4.4.1   *Electrical resistance thermometers*

The main sources of error in a temperature measurement taken with electrical resistance thermometers are the following:

(a)   Self-heating of the thermometer element;

(b)   Inadequate compensation for lead resistance;

(c)   Inadequate compensation for non-linearities in the sensor or processing instrument;

(d)   Sudden changes in switch contact resistances.

Self-heating occurs because the passage of a current through the resistance element produces heat and, thus, the temperature of the thermometer element becomes higher than that of the surrounding medium.

The resistance of the connecting leads will introduce an error in the temperature reading. This will become more significant for long leads, for example, when the resistance thermometer is located at some distance from the measuring instrument; the reading errors will also vary as the temperature of the cables changes. These errors can be compensated for by using extra conductors, ballast resistors and an appropriate bridge network. To reduce errors, it is highly recommended to use four-wire platinum resistance thermometers.

Neither the electrical resistance thermometer nor the thermistor is linear over an extended temperature range but may approximate a linear output if the range is limited. Provision must, therefore, be made to compensate for such non-linearities. This is most likely to be required for thermistors, to achieve a usable meteorological range of measurement.

Sudden changes in switch contact resistance can occur as switches age. They may be variable and can go undetected unless regular system calibration checks are performed (see section 2.4.5).

2.4.4.2   *Thermocouples*

The main sources of error in the measurement of temperature using thermocouples are the following:

(a)   Changes in the resistances of the connecting leads with temperature. This effect may be minimized by keeping all the leads as short and compact as possible, and well insulated;

(b)   Conduction along the leads from the junction when there is a temperature gradient in the vicinity of the temperature measuring point;

(c)   Stray secondary thermal electromotive forces due to the use of metals that are different from the thermocouple metals in the connecting circuit. The temperature differences in the remainder of the circuit must, therefore, be kept as low as possible; this is especially important when the electromotive forces to be measured are small (periodical recalibration will be necessary to allow for this);

(d)   Leakage currents can occur from neighbouring power circuits. This can be minimized by suitable screening of the leads;

(e)   Galvanic currents can be set up if any leads or junctions are allowed to get wet;

(f)   Changes in temperature in the galvanometer alter its characteristics (chiefly by changing its resistance). This will not affect the readings by the potentiometric method to any degree, but will affect direct-reading instruments. This effect can be minimized by keeping the temperature of the galvanometer as near as possible to that at which the circuit was calibrated;

(g)   In the potentiometric measurement, changes in the electromotive force of the standard cell against which the potentiometer current is adjusted and changes in the potentiometer current between adjustments will cause corresponding errors in the measured electromotive force. These errors will normally be small, provided that the standard cell is treated correctly, and that adjustments of the potentiometer current are made just before taking a temperature measurement.

Errors (a) and (f) emphasize the superiority of the potentiometric method when a very high degree of accuracy is required.

2.4.5   **Comparison and calibration**

2.4.5.1   *Electrical resistance thermometers*

The basic techniques and procedures for the laboratory calibration and field checking of electrical thermometers will be the same as for liquid-in-glass thermometers (see section 2.2.5). In general, however, it will not be possible to bring a resistance thermometer indoors since checks should include the thermometer's normal electrical leads. Checks will therefore have to be carried out with the thermometers in the screen. Accurate comparative measurements of the temperatures indicated by the electrical thermometer and a reference mercury-in-glass or local indicating resistance thermometer will be difficult to achieve unless two observers are present. Since the measurement instrument is an integral part of the electrical thermometer, its calibration may be checked by substituting the resistance thermometer by an accurate decade resistance box and by applying resistances equivalent to fixed 5 K temperature increments over the operational temperature range. The error at any point should not exceed 0.1 K. This work would normally be performed by a servicing technician.

2.4.5.2   *Thermocouples*

The calibration and checking of thermocouples require the hot and cold junctions to be maintained at accurately known temperatures. The techniques and instrumentation necessary to undertake this work are generally very specialized and will not be described here.

2.4.6   **Corrections**

When initially issued, electrical thermometers (which have a serial number) should be provided with either:

(a)   A dated certificate confirming compliance with the appropriate standard; or

(b)　A dated calibration certificate giving the actual resistance at fixed points in the temperature range. These resistances should be used when checking the uncertainty of the measuring instrument or system interface before and during operation. The magnitude of the resistance difference from the nominal value should not, in general, be greater than an equivalent temperature error of 0.1 or 0.2 K.

2.4.7　　　Maintenance

The regular field checks should identify any changes in system calibration. These may occur as a result of long-term changes in the electrical characteristics of the thermometer, degradation of the electrical cables or their connections, changes in the contact resistance of switches or changes in the electrical characteristics of the measuring equipment. Identification of the exact source and correction of such errors will require specialized equipment and training and should be undertaken only by a maintenance technician.

2.5　　　RADIATION SHIELDS

A radiation shield or screen should be designed to provide an enclosure with an internal temperature that is both uniform and the same as that of the outside air. It should completely surround the thermometers and exclude radiant heat, precipitation and other phenomena that might influence the measurement.

Screens with forced ventilation, in which air is drawn over the thermometer element by a fan, may help to avoid biases when the microclimate inside the screen deviates from the surrounding air mass. Such a deviation only occurs when the natural wind speed is very low (< 1 m s^{-1}). When such artificial ventilation is used, care should be taken to prevent the deposition of aerosols and rain droplets on the sensor which decrease its temperature towards the wet-bulb temperature. Manufacturers of artificially ventilated radiation shields are encouraged to provide a clear indication (such as an LED light) of the fan status directly on the screen or on the control unit or data logger to allow maintenance staff to check whether the fan is functioning properly by visual inspection. Additionally, the fan status and preferably the fan speed should be provided in the data output for automatic monitoring purposes.

As a shield material, highly polished, non-oxidized metal is favourable because of its high reflectivity and low heat absorption. Nevertheless, thermally insulating plastic-based material is preferable because of its simple maintenance requirements. Thermally insulating material must be used if the system relies on natural ventilation.

The performance of a screen (response behaviour and microclimate effects introducing unwanted biases) depends predominantly on its design, in which care must be taken to ensure both radiation protection and sufficient ventilation. Since the start of meteorological temperature measurements, very diverse types of screens have been designed. Following the introduction of temperature measurements taken in automatic weather stations, the variety of these designs has increased significantly (see WMO, 1998*a*). Because of differences in specific applications, the degree of automation and climatology, it is difficult to recommend one specific type of design suitable for worldwide measurements. Nevertheless, many investigations and intercomparisons on designs and their performance have been carried out. A clear overview of screen designs is given by WMO (1972). Results of thermometer screen intercomparisons are reported by Andersson and Mattison (1991), Sparks (2001), WMO (1998*b*, 1998*c*, 1998*d*, 2000*a*, 2000*b*, 2002*b*, 2002*c*, 2002*d*, 2011) and Zanghi (1987).

An international standard (ISO/DIS 17714) defines most relevant screen types and describes the methods to determine or compare screen performances (ISO, 2007).

2.5.1   Louvred screens

Most of the numerous varieties of louvred screen rely on natural ventilation. The walls of such a screen should preferably be double-louvred and the floor should be made of staggered boards, but other types of construction may be found to meet the above requirements. The roof should be double-layered, with provisions for ventilation of the space between the two layers. In cold climates, owing to the high reflectivity of snow (up to 88%), the screen should also have a double floor. At the same time, however, the floor should easily drop or tilt so that any snow entering the screen during a storm can be removed.

The size and construction of the screen should be such that it keeps the heat capacity as low as practicable and allows ample space between the instruments and the walls. The latter feature excludes all possibility of direct contact between the thermometer sensing elements and the walls, and is particularly important in the tropics where insolation may heat the sides to the extent that an appreciable temperature gradient is caused in the screen. Direct contact between the sensing elements and the thermometer mounting should also be avoided. The screen should be painted both inside and outside with white, non-hygroscopic paint.

When double walls are provided, the layer of air between them serves to reduce the amount of heat that would otherwise be conducted from the outer wall to the inner enclosure, especially in strong sunshine. When the wind is appreciable, the air between the walls is changed continually so that the conduction of heat inwards from the outer walls is further decreased.

The free circulation of air throughout the screen helps the temperature of the inner wall adapt to ambient air changes. In this way, the influence of the inner wall upon the temperature of the thermometer is reduced. Also, the free circulation of air within the screen enables the thermometer to follow the ambient air changes more quickly than if radiative exchanges alone were operative. However, the air circulating through the screen spends a finite time in contact with the outer walls and may have its temperature altered thereby. This effect becomes appreciable when the wind is light and the temperature of the outer wall is markedly different from the air temperature. Thus, the temperature of the air in a screen can be expected to be higher than the true air temperature on a day of strong sunshine and calm wind, and slightly lower on a clear, calm night, with errors perhaps reaching 2.5 and –0.5 K, respectively, in extreme cases. Additional errors may be introduced by cooling due to evaporation from a wet screen after rain. All these errors also have a direct influence on the readings of other instruments inside the screen, such as hygrometers, evaporimeters, and the like.

Errors due to variations in natural ventilation can be reduced if the screen is fitted with a suitably designed forced ventilation system that maintains a constant and known ventilation rate, at least at low wind speeds. Care should be taken in the design of such systems to ensure that heat from the fan or an electrical motor does not affect the screen temperature.

In general, only one door is needed, with the screen being placed so that the sun does not shine on the thermometers when the door is open at the times of observation. In the tropics, two doors are necessary for use during different periods of the year. Likewise, in polar regions (where the sun is at a low angle) precautions should be taken to protect the inside of the screen from the direct rays of the sun either by a form of shading or by using a screen which is mounted so that it can be turned to an appropriate angle while the door is open for readings.

Although most screens are still made of wood, some recent designs using plastic materials offer greater protection against radiation effects because of an improved louvre design that provides a better airflow. In any case, the screen and stand should be constructed of sturdy materials and should be firmly installed so that errors in maximum and minimum thermometer readings caused by wind vibration are kept to a minimum. In some areas where wind vibration cannot be entirely damped, elastic mounting brackets are recommended. The ground cover beneath the screen should be grass or, in places where grass does not grow, the natural surface of the area.

The screen should be kept clean and repainted regularly; in many places, repainting the screen once every two years is sufficient, but in areas subject to atmospheric pollution it may be necessary to repaint it at least once a year.

2.5.2   **Other artificially ventilated shields**

The main alternative to exposure in a louvred screen, which is either naturally or artificially ventilated, is to shield the thermometer bulb from direct radiation by placing it on the axis of two concentric cylindrical shields and drawing a current of air (with a speed between 2.5 and 10 m s^{-1}) between the shields and past the thermometer bulb. This type of exposure is normal in aspirated psychrometers (see Part I, Chapter 4). In principle, the shields should be made of a thermally insulating material, although in the Assmann psychrometer the shields are made of highly polished metal to reduce the absorption of solar radiation. The inner shield is kept in contact with a moving stream of air on both sides so that its temperature, and consequently that of the thermometer, can approximate very closely to that of the air. Such shields are usually mounted with their axes in a vertical position. The amount of direct radiation from the ground entering through the base of such shields is small and can be reduced by extending the base of the shields appreciably below the thermometer bulb. When the artificial ventilation is provided by an electrically driven fan, care should be taken to prevent any heat from the motor and fan from reaching the thermometers.

The design of the WMO reference psychrometer takes careful account of the effects of radiation and the use of artificial ventilation and shielding to ensure that the thermometer element is at equilibrium at the true air temperature (see Part I, Chapter 4).

———————

ANNEX. DEFINING THE FIXED POINTS OF THE INTERNATIONAL TEMPERATURE SCALE OF 1990

The fixed points of the International Temperature Scale of 1990 (ITS-90) of interest to meteorological measurements are contained in Table 2.A.1, while secondary reference points of interest to meteorological measurements are contained in Table 2.A.2.

The standard method of interpolating between the fixed points uses formulae to establish the relation between indications of the standard instruments and the values of the ITS-90 (BIPM, 1990). The standard instrument used from –259.34 °C to 961.78 °C is a platinum resistance thermometer.

An alternative practical method for ITS-90 approximation in platinum resistance thermometer calibration (determination of R_0, A, B and C, see equation below) is to obtain resistance-temperature data by making a comparison with a calibrated standard platinum resistance thermometer at numerous temperatures in the range of interest and then fit a polynomial to the data by a least-squares technique.

The relationship between the resistance of the platinum resistance thermometer under calibration and the temperature measured with a reference thermometer is described with an interpolation equation. The Callendar–Van Dusen equation is generally accepted as the interpolation equation for industrial platinum resistance thermometers (defined in the IEC 60751, see IEC (2008)) rather than for standard platinum resistance thermometers:

$$R_t = R_0 \left(1 + A \cdot t + B \cdot t^2 + C \cdot (t - 100) \cdot t^3 \right)$$

where R_t is the resistance at temperature t of a platinum wire, R_0 is its resistance at 0 °C (ice point) and A, B and C ($C = 0$ for $t > 0$ °C) are constants which are found using the least-squares method on the data acquired during the calibration.

Table 2.A.1. Defining fixed points on the ITS-90

Equilibrium state	Assigned value of ITS	
	K	°C
Equilibrium between the solid, liquid and vapour phases of argon (triple point of argon)	83.805 8	–189.344 2
Equilibrium between the solid, liquid and vapour phases of mercury (triple point of mercury)	234.315 6	–38.834 4
Equilibrium between the solid, liquid and vapour phases of water (triple point of water)	273.160 0	0.01
Equilibrium between the solid and liquid phases of gallium (melting point of gallium)	302.914 6	29.764 6
Equilibrium between the solid and liquid phases of indium (freezing point of indium)	429.748 5	156.598 5

Table 2.A.2. Secondary reference points and their temperatures on the ITS-90

Equilibrium state	Assigned value of ITS	
	K	˚C
Equilibrium between the solid and vapour phases of carbon dioxide (sublimation point of carbon dioxide) at standard atmospheric pressure p_0 (1 013.25 hPa).		
The temperature t as a function of the vapour pressure of carbon dioxide is given by the equation:		
$t = [1.210\ 36 \cdot 10^{-2}\ (p - p_0) - 8.912\ 26 \cdot 10^{-6}(p - p_0)_2 - 78.464]\ °C$		
where p is the atmospheric pressure in hPa, in the temperature range 194 to 195 K	194.686	–78.464
Equilibrium between the solid and liquid phases of mercury (freezing point of mercury) at standard atmospheric pressure	234.296	–38.854
Equilibrium between ice and air-saturated water (ice-point) at standard atmospheric pressure	273.150	0.00
Equilibrium between the solid, liquid and vapour phases of phenoxybenzene (diphenyl ether) (triple point of phenoxybenzene)	300.014	26.864

REFERENCES AND FURTHER READING

Andersson, T. and I. Mattison, 1991: *A Field Test of Thermometer Screens*. SMHI Report No. RMK 62, Norrköping.

Bureau International des Poids et Mesures, 1989: *Procès-Verbaux du Comité International des Poids et Mesures*, 78th meeting, 1989, Paris (available from http://www.bipm.org/utils/common/pdf/its-90/ITS-90.pdf).

Bureau International des Poids et Mesures/Comité Consultatif de Thermométrie, 1990: The International Temperature Scale of 1990 (ITS-90) (H. Preston-Thomas). *Metrologia*, 27:3–10 (amended version) (available from http://www.bipm.org/utils/common/pdf/its-90/ITS-90_metrologia.pdf).

Her Majesty's Stationery Office (HMSO)/Meteorological Office, 1980: *Handbook of Meteorological Instruments*, Volume 2: Measurement of temperature, London.

International Electrotechnical Commission, 2008: *Industrial Platinum Resistance Thermometers and Platinum Temperature Sensors*, IEC 60751:2008. Geneva.

International Organization for Standardization, 2007: *Meteorology – Air Temperature Measurements – Test Methods for Comparing the Performance of Thermometer Shields/Screens and Defining Important Characteristics*, ISO/DIS 17714:2007. Geneva.

Jones, E.B., 1992: *Jones' Instrument Technology*. Volume 2: Measurement of temperature and chemical composition, Butterworths-Heinemann, Oxford.

Middleton, W.E.K. and A.F. Spilhaus, 1960: *Meteorological Instruments*. University of Toronto Press.

Sparks, W.R., 1970: Current concepts of temperature measurement applicable to synoptic networks. *Meteorological Monographs*, 11(33):247–251.

———, 2001: Field trial of Metspec screens. *Technical Report TR19*, Met Office/OD, Wokingham, United Kingdom of Great Britain and Northern Ireland.

World Meteorological Organization, 1972: *The Effect of Thermometer Screen Design on the Observed Temperature* (W.R. Sparks). (WMO-No. 315). Geneva.

———, 1992: *Measurement of Temperature and Humidity: Specification, Construction, Properties and Use of the WMO Reference Psychrometer* (R.G. Wylie and T. Lalas). Technical Note No. 194 (WMO-No. 759). Geneva.

———, 1998a: *Recent Changes in Thermometer Screen Design and their Impact* (A. Barnett, D.B. Hatton and D.W. Jones). Instruments and Observing Methods Report No. 66 (WMO/TD-No. 871). Geneva.

———, 1998b: An investigation of temperature screens and their impact on temperature measurements (J. Warne). *Papers Presented at the WMO Technical Conference on Meteorological and Environmental Instruments and Methods of Observation (TECO-98)*. Instruments and Observing Methods Report No. 70 (WMO/TD-No. 877). Geneva.

———, 1998c: A thermometer screen intercomparison (J.P. van der Meulen). *Papers Presented at the WMO Technical Conference on Meteorological and Environmental Instruments and Methods of Observation (TECO-98)*. Instruments and Observing Methods Report No. 70 (WMO/TD-No. 877). Geneva.

———, 1998d: Comparison of meteorological screens for temperature measurement (G. Lefebvre). *Papers Presented at the WMO Technical Conference on Meteorological and Environmental Instruments and Methods of Observation (TECO-98)*. Instruments and Observing Methods Report No. 70 (WMO/TD-No. 877). Geneva.

———, 2000a: A comparison of air temperature radiation screens by field experiments and computational fluid dynamics (CFD) simulations (A. Spetalen, C. Lofseik and P. Ø. Nordli). *Papers Presented at the WMO Technical Conference on Meteorological and Environmental Instruments and Methods of Observation (TECO-2000)*. Instruments and Observing Methods Report No. 74 (WMO/TD-No. 1028). Geneva.

———, 2000b: Temperature measurements: Some considerations for the intercomparison of radiation screens (J.P. van der Meulen). *Papers Presented at the WMO Technical Conference on Meteorological and Environmental Instruments and Methods of Observation (TECO-2000)*. Instruments and Observing Methods Report No. 74 (WMO/TD-No. 1028). Geneva.

———, 2002a: Measurement of temperature with wind sensors during severe winter conditions (M. Musa, S. Suter, R. Hyvönen, M. Leroy, J. Rast and B. Tammelin). *Papers Presented at the WMO Technical Conference on Meteorological and Environmental Instruments and Methods of Observation (TECO-2002)*. Instruments and Observing Methods Report No. 75 (WMO/TD-No. 1123). Geneva.

——, 2002*b*: Norwegian national thermometer screen intercomparison (M.H. Larre and K. Hegg). *Papers Presented at the WMO Technical Conference on Meteorological and Environmental Instruments and Methods of Observation (TECO-2002)*. Instruments and Observing Methods Report No. 75 (WMO/TD-No. 1123). Geneva.

——, 2002*c*: Results of an intercomparison of wooden and plastic thermometer screens (D.B. Hatton). *Papers Presented at the WMO Technical Conference on Meteorological and Environmental Instruments and Methods of Observation (TECO-2002)*. Instruments and Observing Methods Report No. 75 (WMO/TD-No. 1123). Geneva.

——, 2002*d*: Temperature and humidity measurements during icing conditions (M. Leroy, B. Tammelin, R. Hyvönen, J. Rast and M. Musa). *Papers Presented at the WMO Technical Conference on Meteorological and Environmental Instruments and Methods of Observation (TECO-2002)*. Instruments and Observing Methods Report No. 75 (WMO/TD-No. 1123). Geneva.

——, 2011: *WMO Field Intercomparison of Thermometer Screens/Shields and Humidity Measuring Instruments* (M. Lacombe, D. Bousri, M. Leroy and M. Mezred). Instruments and Observing Methods Report No. 106 (WMO/TD-No. 1579). Geneva.

Zanghi, F., 1987: *Comparaison des Abris Météorologiques*. Technical Memorandum No. 11, Météo-France/SETIM, Trappes.

———————

CHAPTER CONTENTS

CHAPTER 3. MEASUREMENT OF ATMOSPHERIC PRESSURE

3.1 GENERAL

3.1.1 Definition

The atmospheric pressure on a given surface is the force per unit area exerted by virtue of the weight of the atmosphere above. The pressure is thus equal to the weight of a vertical column of air above a horizontal projection of the surface, extending to the outer limit of the atmosphere.

Apart from the actual pressure, pressure trend or tendency has to be determined as well. Pressure tendency is the character and amount of atmospheric pressure change for a 3 h or other specified period ending at the time of observation. Pressure tendency is composed of two parts, namely the pressure change and the pressure characteristic. The pressure change is the net difference between pressure readings at the beginning and end of a specified interval of time. The pressure characteristic is an indication of how the pressure has changed during that period of time, for example, decreasing then increasing, or increasing and then increasing more rapidly.

3.1.2 Units and scales

The basic unit for atmospheric pressure measurements is the pascal (Pa) (or newton per square metre). It is accepted practice to add the prefix "hecto" to this unit when reporting pressure for meteorological purposes, making the hectopascal (hPa), equal to 100 Pa, the preferred terminology. This is largely because one hectopascal equals one millibar (mbar), the formerly used unit.

The scales of all barometers used for meteorological purposes should be graduated in hPa. Some barometers are graduated in "millimetres or inches of mercury under standard conditions", $(mm\ Hg)_n$ and $(in\ Hg)_n$, respectively. When it is clear from the context that standard conditions are implied, the briefer terms "millimetre of mercury" or "inch of mercury" may be used. Under these standard conditions, a column of mercury having a true scale height of 760 $(mm\ Hg)_n$ exerts a pressure of 1 013.250 hPa.

The following conversion factors will then apply:

> 1 hPa = 0.750 062 $(mm\ Hg)_n$
> 1 $(mm\ Hg)_n$ = 1.333 224 hPa

In the case where the conventional engineering relationship between the inch and the millimetre is assumed, namely 1 in = 25.4 mm, the following conversion factors are obtained:

> 1 hPa = 0.029 530 $(in\ Hg)_n$
> 1 $(in\ Hg)_n$ = 33.863 9 hPa
> 1 $(mm\ Hg)_n$ = 0.039 370 08 $(in\ Hg)_n$

Scales on mercury barometers for meteorological purposes should be so graduated that they yield true pressure readings directly in standard units when the entire instrument is maintained at a standard temperature of 0 °C and the standard value of gravity is 9.806 65 m s^{-2}.

Barometers may have more than one scale engraved on them, for example, hPa and mm Hg, or hPa and in Hg, provided that the barometer is correctly calibrated under standard conditions.

Pressure data should be expressed in hectopascals. Hereafter in this chapter only the unit hectopascal will be used.

3.1.3   Meteorological requirements

Analysed pressure fields are a fundamental requirement of the science of meteorology. It is imperative that these pressure fields be accurately defined as they form the basis for all subsequent predictions of the state of the atmosphere. Pressure measurements must be as accurate as technology will allow, within realistic financial constraints, and there must be uniformity in the measurement and calibration procedures across national boundaries.

The level of accuracy needed for pressure measurements to satisfy the requirements of various meteorological applications has been identified by the respective WMO commissions and is outlined in Part I, Chapter 1, Annex 1.E, which is the primary reference for measurement specifications in this Guide. The requirements are as follows:

> Measuring range: 500 – 1 080 hPa (both station pressure and mean sea-level pressure)
> Required target uncertainty: 0.1 hPa
> Reporting resolution: 0.1 hPa
> Sensor time-constant: 20 s (for most modern barometers, 2 s is achievable – see Part I, Chapter 1, Annex 1.E)
> Output averaging time: 1 min

The above requirements should be considered achievable for new barometers in a strictly controlled environment, such as those available in a properly equipped laboratory. They provide an appropriate target accuracy for barometers to meet before their installation in an operational environment.

For barometers installed in an operational environment, practical constraints will require well-designed equipment for a National Meteorological Service to maintain this target accuracy. Not only the barometer itself, but the exposure also requires special attention. Nevertheless, the performance of the operational network station barometer, when calibrated against a standard barometer whose index errors are known and allowed for, should not be below the stated criteria.

3.1.4   Methods of measurement and observation

For meteorological purposes, atmospheric pressure is generally measured with electronic barometers, mercury barometers, aneroid barometers or hypsometers. The latter class of instruments, which depends on the relationship between the boiling point of a liquid and the atmospheric pressure, has so far seen only limited application and will not be discussed in depth in this publication. A very useful discussion of the performance of digital barometers (which mostly have electronic read-out) is found in WMO (1992).

Meteorological pressure instruments (barometers) are suitable for use as operational instruments for measuring atmospheric pressure if they meet the following requirements:

(a)   The instruments must be calibrated or controlled regularly against a (working) standard barometer using approved procedures. The period between two calibrations must be short enough to ensure that the total absolute measurement error will meet the accuracy requirements defined in this chapter;

(b)   Any variations in the accuracy (long-term and short-term) must be much smaller than the tolerances outlined in section 3.1.3. If some instruments have a history of a drift in calibration, they will be suitable operationally only if the period between calibrations is short enough to ensure the required measurement accuracy at all times;

(c)   Instrument readings should not be affected by temperature variations. Instruments are suitable only if:

(i)   Procedures for correcting the readings for temperature effects will ensure the required accuracy; and/or

(ii)   The pressure sensor is placed in an environment where the temperature is stabilized so that the required accuracy will be met.

Some instruments measure the temperature of the pressure sensor in order to compensate for temperature effects. It is necessary to control and calibrate these temperature-compensating functions as part of the standard calibration activity;

(d)   The instrument must be placed in an environment where external effects will not lead to measurement errors. These effects include wind, radiation/temperature, shocks and vibrations, fluctuations in the electrical power supply and pressure shocks. Great care must be taken when selecting a position for the instrument, particularly for mercury barometers.

It is important that every meteorological observer should fully understand these effects and be able to assess whether any of them are affecting the accuracy of the readings of the barometer in use;

(e)   The instrument should be quick and easy to read. Instruments must be designed so that the standard deviation of their readings is less than one third of the stated absolute accuracy;

(f)   If the instrument has to be calibrated away from its operational location, the method of transportation employed must not affect the stability or accuracy of the barometer. Effects which may alter the calibration of the barometer include mechanical shocks and vibrations, and displacement from the vertical and large pressure variations such as may be encountered during transportation by air.

Most barometers with recent designs make use of transducers which transform the sensor response into pressure-related quantities. These are subsequently processed by using appropriate electrical integration circuits or data-acquisition systems with appropriate smoothing algorithms. A time constant of about 10 s (and definitely no greater than 20 s) is desirable for most synoptic barometer applications. For mercury barometers, the time constant is generally not important.

There are several general methods for measuring atmospheric pressure which will be outlined in the following paragraphs.

Historically, the most extensively used method for measuring the pressure of the atmosphere involves balancing it against the weight of a column of liquid. For various reasons, the required accuracy can be conveniently attained only if the liquid used is mercury. Mercury barometers are, in general, regarded as having good long-term stability and accuracy, but are now losing favour to equally accurate electronic barometers, which are easier to read.

A membrane of elastic substance, held at the edges, will be deformed if the pressure on one side is greater than on the other. In practice, this is achieved by using a completely or partially evacuated closed metal capsule containing a strong metal spring to prevent the capsule from collapsing due to external atmospheric pressure. Mechanical or electrical means are used to measure the deformation caused by the pressure differential between the inside and outside of the capsule. This is the principle of the well-known aneroid barometer.

Pressure sensor elements comprising thin-walled nickel alloy cylinders, surrounded by a vacuum, have been developed. The natural resonant frequency of these cylinders varies as a function of the difference in pressure between the inside of the cylinder, which is at ambient atmospheric pressure, and the outside of the cylinder, which is maintained as a vacuum.

Absolute pressure transducers, which use a crystalline quartz element, are becoming more commonly used. Pressure exerted via flexible bellows on the crystal face causes a compressive force on the crystal. On account of the crystal's piezoresistive properties, the application of pressure alters the balance of an active Wheatstone bridge. Balancing the bridge enables accurate determination of the pressure. These types of pressure transducers are virtually free of hysteresis effects.

The boiling point of a liquid is a function of the pressure under which it boils. Once this function has been determined, the temperature at which the liquid boils may be used in a hypsometer to determine the atmospheric pressure.

3.2   MERCURY BAROMETERS

There is an increasing move away from the use of mercury barometers because mercury vapour is highly toxic; free mercury is corrosive to the aluminium alloys used in air frames (for these reasons there are regulations proscribing the handling or carriage of mercury barometers in some countries); special lead glass is required for the tube; the barometer is very delicate and difficult to transport; it is difficult to maintain the instrument and to clean the mercury; the instrument must be read and corrections applied manually; and other pressure sensors of equivalent accuracy and stability with electronic read-out are now commonly available.

3.2.1   Construction requirements

The basic principle of a mercury barometer is that the pressure of the atmosphere is balanced against the weight of a column of mercury. In some barometers, the mercury column is weighed on a balance, but, for normal meteorological purposes, the length of the mercury column is measured against a scale graduated in units of pressure.

There are several types of mercury barometers in use at meteorological stations, with the fixed cistern and the Fortin types being the most common. The length to be measured is the distance between the top of the mercury column and the upper surface of the mercury in the cistern. Any change in the length of the mercury column is, of course, accompanied by a change in the level of the mercury in the cistern. In the Fortin barometer, the level of the mercury in the cistern can be adjusted to bring it into contact with an ivory pointer, the tip of which is at the zero of the barometer scale. In the fixed-cistern barometer, often called the Kew-pattern barometer, the mercury in the cistern does not need to be adjusted as the scale engraved on the barometer is constructed to allow for changes in the level of the mercury in the cistern.

3.2.2   General requirements

The main requirements of a good mercury station barometer include the following:

(a)   Its accuracy should not vary over long periods. In particular, its hysteresis effects should remain small;

(b)   It should be quick and easy to read, and readings should be corrected for all known effects. The observers employing these corrections must understand their significance to ensure that the corrections applied are correct and not, in fact, causing a deterioration in the accuracy of the readings;

(c)   It should be transportable without a loss of accuracy;

(d)   The bore of the tube should not be less than 7 mm and should preferably be 9 mm;

(e)   The tube should be prepared and filled under vacuum. The purity of the mercury is of considerable significance. It should be double-distilled, degreased, repeatedly washed, and filtered;

(f)   The actual temperature for which the scale is assumed to give correct readings, at standard gravity, should be engraved upon the barometer. The scale should preferably be calibrated to give correct readings at 0 °C;

(g)   The meniscus should not be flat unless the bore of the tube is large (greater than 20 mm);

(h)   For a marine barometer, the error at any point should not exceed 0.5 hPa.

The response time for mercury barometers at land stations is usually very small compared with that of marine barometers and instruments for measuring temperature, humidity and wind.

3.2.3   Standard conditions

Given that the length of the mercury column of a barometer depends on other factors, especially on temperature and gravity, in addition to the atmospheric pressure, it is necessary to specify the standard conditions under which the barometer should theoretically yield true pressure readings. The following standards are laid down in the international barometer conventions.

3.2.3.1   *Standard temperature and density of mercury*

The standard temperature to which mercury barometer readings are reduced to remove errors associated with the temperature-induced change in the density of mercury is 0 °C.

The standard density of mercury at 0 °C is taken to be $1.359\,51 \cdot 10^4$ kg m^{-3} and, for the purpose of calculating absolute pressure using the hydrostatic equation, the mercury in the column of a barometer is treated as an incompressible fluid.

The density of impure mercury is different from that of pure mercury. Hence, a barometer containing impure mercury will produce reading errors as the indicated pressure is proportional to the density of mercury.

3.2.3.2   *Standard gravity*

Barometric readings have to be reduced from the local acceleration of gravity to standard (normal) gravity. The value of standard gravity (g_n) is regarded as a conventional constant, $g_n = 9.806\,65$ m s^{-2}.

Note: The need to adopt an arbitrary reference value for the acceleration of gravity is explained in WMO (1966). This value cannot be precisely related to the measured or theoretical value of the acceleration of gravity in specified conditions, for example, sea level at latitude 45°, because such values are likely to change as new experimental data become available.

3.2.4   Reading mercury barometers

When making an observation with a mercury barometer, the attached thermometer should be read first. This reading should be taken as quickly as possible, as the temperature of the thermometer may rise owing to the presence of the observer. The barometer should be tapped a few times with the finger in two places, one adjacent to the meniscus and the other near the cistern, so as to stabilize the mercury surfaces. If the barometer is not of a fixed-cistern type, the necessary adjustment should be made to bring the mercury in the cistern into contact with the fiducial pointer. Lastly, the vernier should be set to the meniscus and the reading taken. The vernier is correctly adjusted when its horizontal lower edge appears to be touching the highest part of the meniscus; with a magnifying glass it should be possible to see an exceedingly narrow strip of light between the vernier and the top of the mercury surface. Under no circumstances should the vernier "cut off" the top of the meniscus. The observer's eye should be in such a position that both front and back lower edges of the vernier are in the line of vision.

3.2.4.1   *Accuracy of readings*

The reading should be taken to the nearest 0.1 hPa. Usually it is not possible to read the vernier to any greater accuracy.

Optical and digital systems have been developed to improve the reading of mercury barometers. Although they normally ease the observations, such systems may also introduce new sources of error, unless they have been carefully designed and calibrated.

3.2.4.2   *Changes in index correction*

Any change in the index correction shown during an inspection should be considered on its merits, keeping in mind the following:

(a)   The history of the barometer;

(b)   The experience of the inspector in comparison work;

(c)   The magnitude of the observed change;

(d)   The standard deviation of the differences;

(e)   The availability of a spare barometer at the station, the correction of which is known with accuracy;

(f)   The behaviour of travelling standards during the tour;

(g)   The agreement, or otherwise, of the pressure readings of the station with those of neighbouring stations on the daily synoptic chart if the change is accepted;

(h)   Whether or not the instrument was cleaned before comparison.

Changes in index errors of station barometers, referred to as drift, are caused by:

(a)   Variations in the capillary depression of the mercury surfaces due to contamination of the mercury. In areas of severe atmospheric pollution from industrial sources, mercury contamination may constitute a serious problem and may require relatively frequent cleaning of the mercury and the barometer cistern;

(b)   The rise of air bubbles through the mercury column to the space above.

These changes may be erratic, or consistently positive or negative, depending on the cause.

Changes in index correction are also caused by:

(a)   Observer error resulting from failure to tap the barometer before taking the reading and improper setting of the vernier and fiducial point;

(b)   Lack of temperature equilibrium in either the station barometer or the travelling standard;

(c)   Non-simultaneity of readings when the pressure is changing rapidly.

Such changes can be caused by accidental displacement of the adjustable scale and the shrinkage or loosening of fiducial points in Fortin-type barometers.

3.2.4.3   *Permissible changes in index correction*

Changes in index correction should be treated as follows:

(a)   A change in correction within 0.1 hPa may be neglected unless persistent;

(b)   A change in correction exceeding 0.1 hPa but not exceeding 0.3 hPa may be provisionally accepted unless confirmed by at least one subsequent inspection;

(c)   A change in correction exceeding 0.3 hPa may be accepted provisionally only if the barometer is cleaned and a spare barometer with known correction is not available. This barometer should be replaced as soon as a correctly calibrated barometer becomes available.

Barometers with changes in index correction identified in (b) and (c) above warrant close attention. They should be recalibrated or replaced as soon as practicable.

The same criteria apply to changes in the index corrections of the travelling standards as those applied as to station barometers. A change in correction of less than 0.1 hPa may be neglected unless persistent. A larger change in correction should be confirmed and accepted only after repeated comparisons. The "before" and "after" tour index corrections of the travelling standard should not differ by more than 0.1 hPa. Only barometers with a long history of consistent corrections should, therefore, be used as travelling standards.

3.2.5   Correction of barometer readings to standard conditions

In order to transform barometer readings taken at different times and different places into usable atmospheric pressure values, the following corrections should be made:

(a)   Correction for index error;

(b)   Correction for gravity;

(c)   Correction for temperature.

For a large number of operational meteorological applications, it is possible to obtain acceptable results by following the barometer manufacturer's instructions, provided that it is clear that these procedures give pressure readings of the required uncertainty. However, if these results are not satisfactory or if higher precision is required, detailed procedures should be followed to correct for the above factors; these procedures are described in Annex 3.A.

3.2.6   Errors and faults with mercury barometers

3.2.6.1   *Uncertainties as to the temperature of the instrument*

The temperature indicated by the attached thermometer will not usually be identical to the mean temperature of the mercury, the scale and the cistern. The resultant error can be reduced by favourable exposure and by using a suitable observation procedure. Attention is drawn to the frequent existence of a large, stable vertical temperature gradient in a room, which may cause a considerable difference between the temperature of the upper and lower parts of the barometer. An electric fan can prevent such a temperature distribution but may cause local pressure variations and should be switched off before an observation is made. Under normal conditions, the error associated with the temperature reduction will not exceed 0.1 hPa if such precautions are taken.

3.2.6.2   *Defective vacuum space*

It is usually assumed that there is a perfect vacuum, or only a negligible amount of gas, above the mercury column when the instrument is calibrated. Any change in this respect will cause an error in pressure readings. A rough test for the presence of gas in the barometer tube can be made by tilting the tube and listening for the click when the mercury reaches the top, or by examining the closed end for the presence of a bubble, which should not exceed 1.5 mm in diameter when the barometer is inclined. The existence of water vapour cannot be detected in this way, as it is condensed when the volume decreases. According to Boyle's Law, the error caused by air and

unsaturated water vapour in the space will be inversely proportional to the volume above the mercury. The only satisfactory way to overcome this error is by conducting a recalibration over the entire scale; if the error is large, the barometer tube should be refilled or replaced.

3.2.6.3   *The capillary depression of the mercury surfaces*

The height of the meniscus and the capillary depression,[1] for a given tube, may change with the ageing of the glass tube, mercury contamination, pressure tendency, and the position of the mercury in the tube. As far as is practicable, the mean height of the meniscus should be observed during the original calibration and noted on the barometer certificate. No corrections should be made for departures from the original meniscus height, and the information should be used only as an indication of the need, or otherwise, to overhaul or recalibrate the barometer. A 1 mm change in the height of the meniscus (from 1.8 to 0.8 mm) for an 8 mm tube may cause an error of about 0.5 hPa in the pressure readings.

It should be noted that large variations in the angle of contact between the mercury and the wall of the cistern in a fixed-cistern barometer may cause small but appreciable errors in the observed pressure.

3.2.6.4   *Lack of verticality*

If the bottom of a symmetrical barometer of normal length (about 90 cm), which hangs freely, is displaced by about 6 mm from the vertical position, the indicated pressure will be about 0.02 hPa too high. Such barometers generally hang more truly vertical than this.

In the case of an asymmetrical barometer, however, this source of error is more critical. For example, if the fiducial pointer in the cistern is about 12 mm from the axis, the cistern needs to be displaced by only about 1 mm from the vertical to cause an error of 0.02 hPa.

3.2.6.5   *General accuracy of the corrected pressure readings*

The standard deviation of a single, corrected barometer reading at an ordinary meteorological station should be within 0.1 hPa. This error will mainly be the result of the unavoidable uncertainty in the instrument correction, the uncertainty concerning the temperature of the instrument, and the error caused by the pumping effect of wind gusts on the mercury surface.

3.2.7   **Safety precautions for the use of mercury**

Mercury is used in relatively large quantities in barometers and, because it is poisonous, must be handled with care. Elemental mercury is a liquid at temperatures and pressures experienced at the Earth's surface. Mercury vapour forms in the air whenever liquid mercury is present. Mercury can be absorbed through the skin in both liquid and gaseous states and can be inhaled as a vapour. The properties of mercury are described by Sax (1975). In many countries, precautions for its use are prescribed by regulations governing the handling of hazardous goods. The Minamata Convention on Mercury of the United Nations Environment Programme (UNEP) entered into force in October 2013 and will have a significant impact on the use of mercury for meteorological applications.

A large dose of mercury may cause acute poisoning. It can also accumulate in the body's hard and soft tissues and prolonged exposure to even a low dose can cause long-term damage to organs, or even death. Mercury mainly affects the central nervous system, and the mouth and gums, with symptoms that include pain, loosening of teeth, allergic reactions, tremors and psychological disturbance.

---

[1]   Capillary depression is a reduction in height of the meniscus of a liquid contained in a tube where the liquid (such as mercury) does not wet the walls of the tube. The meniscus is shaped convex upward.

For barometric applications, the main risks occur in laboratories where barometers are frequently emptied or filled. There may also be problems in meteorological stations if quantities of mercury, for example from a broken barometer, are allowed to remain in places where it may continuously vaporize into an enclosed room where people work.

A danger exists even if the mercury is properly contained and if it is cleaned up after an accident. The following points must be considered when using mercury:

(a)   Vessels containing mercury must be well sealed and not likely to leak or easily break, and must be regularly inspected;

(b)   The floor of a room where mercury is stored or used in large quantities should have a sealed, impervious and crack-free floor covering, such as PVC. Small cracks in the floor, such as those between floor tiles, will trap mercury droplets. It is preferable to have the flooring material curving up the walls by approximately 10 cm, leaving no joint between the floor and the walls at floor level;

(c)   Mercury must not be stored in a metal container as it reacts with almost all metals, except iron, forming an amalgam which may also be hazardous. Mercury should not come into contact with any other metallic object;

(d)   Mercury must not be stored with other chemicals, especially amines, ammonia or acetylene;

(e)   Large quantities of mercury should always be stored and handled in a well-ventilated room. The raw material should be handled in a good-quality fume cupboard;

(f)   Mercury should never be stored near a heat source of any kind as it has a relatively low boiling point (357 °C) and may produce hazardous concentrations of toxic vapour, especially during a fire;

(g)   If mercury is handled, the room where it is used and the personnel using it should be regularly tested to determine if hazardous quantities of mercury are being encountered.

Under the Minamata Convention, imports and exports of mercury will no longer be allowed. In this context, the production, import and export of mercury-added products such as thermometers will be stopped by 2020. The Convention states that "[e]ach party shall not allow, by taking appropriate measures, the manufacture, import or export of mercury-added products listed in Part I of Annex A [of the Convention] after the phase-out date specified for those products" (UNEP, 2013). More specifically, this list includes:

> The following non-electronic measuring devices except non-electronic measuring devices installed in large-scale equipment or those used for high precision measurement, where no suitable mercury-free alternative is available:
>
> (a)   barometers;
>
> (b)   hygrometers;
>
> (c)   manometers;
>
> (d)   thermometers;
>
> (e)   sphygmomanometers.

3.2.7.1   *Spillages and disposal*

The two common methods of cleaning up mercury spillages are either with a suitable aspirated pick-up system, as outlined below, or by adsorption/amalgamation of the mercury onto a powder.

Mercury should be cleaned up immediately. The operator should wear PVC gloves or gauntlets, safety goggles and, for significant spills, a respirator fitted with a mercury vapour cartridge.

Depending upon how large the spillage is, the mercury will be picked up by using a vacuum system; an adsorption kit should then be used to clean up the small droplets. The use of an adsorption kit is imperative because, during a spillage, dozens of small droplets of less than 0.02 mm in diameter will adhere to surfaces and cannot be efficiently removed with a vacuum system.

In an aspirated pick-up system, the mercury is drawn through a small-diameter plastic tube into a glass flask with approximately 3 cm of water in the bottom, with the tube opening being below the water line in the flask. One end of a larger diameter plastic tube is connected to the air space above the water in the flask, and the other end is connected to a vacuum cleaner or vacuum pump. The water prevents the mercury vapour or droplets from being drawn into the vacuum cleaner or pump. The slurry is then placed in a clearly labelled plastic container for disposal.

By using adsorption material, a variety of compounds can be used to adsorb or amalgamate mercury. These include zinc powder, sulphur flour or activated carbon. Commercial kits are available for cleaning up mercury spills. The powder is sprinkled on the spill and allowed to adsorb or amalgamate the mercury. The resulting powder is swept up and placed in a clearly labelled plastic container for disposal.

The collected mercury can be either disposed of or recovered. Details on how to dispose of mercury can be obtained from local authorities and/or the supplier. The supplier can also advise on recovery and purification.

3.2.7.2 *Fire*

Mercury will not burn but does give off significant concentrations of toxic fumes. After a fire, the mercury vapour will condense on the nearest cool surfaces, contaminating large areas and being adsorbed onto open surfaces, such as carbonized timber. During a fire, evacuate the area and remain upwind of any fumes. Advise the fire authorities of the location and quantity of mercury involved.

3.2.7.3 *Transportation*

The transportation by air of mercury or instruments containing mercury is regulated by the International Air Transport Association. Airlines will provide the specific conditions for such transport upon request. Transportation by rail or road is usually governed by the hazardous material regulations in each country.

In general, metallic mercury must be packed in glass or plastic containers. The containers should be packed with sufficient cushioning to prevent breakage and should be clearly labelled. Mercury-containing instruments should be packed in a strong cushioned case which is leak-proof and impervious to mercury.

3.3 ELECTRONIC BAROMETERS

Most barometers with recent designs make use of transducers which transform the sensor response into a pressure-related electrical quantity in the form of either analogue signals, for example, voltage (DC or AC with a frequency related to the actual pressure), or digital signals, for example, pulse frequency or with standard data communication protocols such as RS232, RS422, RS485 or IEEE488. Analogue signals can be displayed on a variety of electronic meters. Monitors and data-acquisition systems, such as those used in automatic weather stations, are frequently used to display digital outputs or digitized analogue outputs.

Current digital barometer technology employs various levels of redundancy to improve the long-term stability and accuracy of the measurements. One technique is to use three independently operating sensors under centralized microprocessor control. Even higher stability and

reliability can be achieved by using three completely independent barometers, incorporating three sets of pressure transducers and microprocessors. Each configuration has automatic temperature compensation from internally mounted temperature sensors. Triple redundancy ensures excellent long-term stability and measurement accuracy, even in the most demanding applications. These approaches allow for continuous monitoring and verification of the individual sensor performances.

The use of digital barometers introduces some particular operational requirements, especially when they are used with automatic weather stations, and formal recommendations exist to ensure good practice (see the *Abridged Final Report of the Eleventh Session of the Commission for Instruments and Methods of Observation* (WMO-No. 807), Annex VII). Meteorological organizations should:

(a)   Control or re-adjust the calibration setting of digital barometers upon receipt and repeat these operations regularly (annually, until the rate of drift is determined);

(b)   Ensure regular calibration of digital barometers and investigate the possibility of using calibration facilities available nationally for this purpose;

(c)   Consider that certain types of digital barometers may be used as travelling standards because of their portability and good short-term stability;

(d)   Consider that the selection of a specific type of digital barometer should not only be based on stated instrument specifications but also on environmental conditions and maintenance facilities.

Manufacturers should:

(a)   Improve the temperature independence and the long-term stability of digital barometers;

(b)   Use standardized communication interfaces and protocols for data transmission;

(c)   Enable the power supply of a digital barometer to function over a large range of DC voltages (for example, 5 to 28 VDC).

3.3.1   Aneroid displacement transducers

Contact-free measurement of the displacement of the aneroid capsule is a virtual necessity as regards precision pressure-measuring instruments for meteorological applications. A wide variety of such transducers are in use, including capacitive displacement detectors, potentiometric displacement detectors, strain gauges placed at strategic points on the sensor, and force-balanced servo-systems which keep the sensor dimensions constant regardless of pressure.

All sensitive components must be encased in a die-cast housing. This housing must be kept at a constant temperature by an electronically controlled heater. Condensation of water must be completely prevented. An effective technique is to put a hygroscopic agent, such as silica gel crystals, into the die-cast housing and to prevent water vapour diffusion into the housing by connecting a long plastic tube (approximately 25 m) with a bore of 2 mm or less between the pressure port and a static head (see section 3.8.1).

The pressure-sensor housing must be airtight, allowing external connection to the compartment where the pressure is to be measured.

3.3.2 Digital piezoresistive barometers

Measurements of atmospheric pressure have become possible by utilizing the piezoelectric (piezoresistive) effect. A common configuration features four measuring resistors placed onto the flexible surface of a monolithic silicon substratum interconnected to form a Wheatstone bridge circuit.

Axially loaded crystalline quartz elements are used in digital piezoresistive barometers and are a type of absolute pressure transducer. Crystalline quartz has been chosen because of its piezoelectric properties, stable frequency characteristics, small temperature effects and precisely reproducible frequency characteristics. Pressure applied to an inlet port causes an upward axial force by means of flexible bellows, thus resulting in a compressive force on the quartz crystal element. Since the crystal element is a substantially rigid membrane, the entire mechanical structure is constrained to minute deflections, thereby virtually eliminating mechanical hysteresis.

The fully active Wheatstone bridge mentioned above may consist either of semiconductor strain gauges or piezoresistive gauges. The strain gauges are either bonded to a thin circular diaphragm, which is clamped along its circumference, or atomically diffused into a silicon diaphragm configuration. In the case of diffused devices, the silicon integrated chip itself is the diaphragm. Applied pressure presents a distributed load to the diaphragm which, in turn, provides bending stress and resultant strains to which the strain gauges react. This stress creates a strain that is proportional to the applied pressure and which results in a bridge imbalance. The bridge output is then proportional to the net difference in pressure acting upon the diaphragm.

This mode of operation is based on the fact that the atmospheric pressure acts on the sensor element covering a small evacuated cell, through which the resistors are submitted to compressive and tensile stresses. By the piezoelectric effect, the values of resistance change proportionally with atmospheric pressure. To eliminate temperature errors, the sensor often incorporates a built-in thermostat.

The output from the Wheatstone bridge, which is fed from a direct-current source, is transduced into a standard signal by an appropriate amplifier. A light-emitting diode or liquid crystal display usually presents the measured pressure values.

In a modern version of the pressure transducer using a piezoelectric transducer, two resonance frequencies of the piezoelectric element are determined. By calculating a linear function of these frequencies and with an appropriate set of variables obtained after calibration, a pressure is calculated by a microprocessor which is independent of the temperature of the sensor.

3.3.3 Cylindrical resonator barometers

Cylindrical resonator barometers use a sensing element which is a thin-walled cylinder of nickel alloy. This is electromagnetically maintained in a "hoop" mode of vibration. The input pressure is sensed by the variation it produces in the natural resonant frequency of the vibrating mechanical system. Cylinder wall movement is sensed by a pick-up coil whose signal is amplified and fed back to a drive coil. The air pressure to be measured is admitted to the inside of the cylinder, with a vacuum reference maintained on the outside. The natural resonant frequency of vibration then varies precisely with the stress set up in the wall due to the pressure difference across it. An increase in pressure gives rise to an increase in frequency.

The thin cylinder has sufficient rigidity and mass to cater for the pressure ranges over which it is designed to operate, and is mounted on a solid base. The cylinder is placed in a vacuum chamber and its inlet is connected to the free atmosphere for meteorological applications. Since there is a unique relationship between the natural resonant frequency of the cylinder and the pressure, the atmospheric pressure can be calculated from the measured resonant frequency. However, this relationship, determined during calibration, depends on the temperature and the density of the gas. Temperature compensation is therefore required and the air should be dried before it enters the inlet.

3.3.4   **Reading electronic barometers**

An electronic barometer measures the atmospheric pressure of the surrounding space or any space that is connected to it via a tube. In general, the barometer should be set to read the pressure at the level of the instrument. On board a ship or at low-level land stations, however, the instrument may be set to indicate the pressure at mean sea level, provided that the difference between the station pressure and the sea-level pressure can be regarded as constant.

Electronic barometers give accurate readings on a digital read-out, normally scaled in hPa but readily adaptable to other units, if required. Provision can usually be made for digital recording. Trend in pressure changes can be presented if the unit is microprocessor-controlled.

The accuracy of electronic barometers depends on the accuracy of the barometer's calibration, the effectiveness of the barometer's temperature compensation (residual air method, temperature measurement and correction, use of a thermostat) and the drift with time of the barometer's calibration.

Circuits may be attached to primary transducers which correct the primary output for sensor non-linearities and temperature effects and which convert output to standard units. Standard modern barometer versions comprise the barometer sensor, the microcomputer unit (including the display) and an interface circuit to communicate with any data logger or automatic weather station.

Electronic barometers which have more than one transducer or sensing element generally calculate a weighted mean of the outputs from each of the sensors and establish the resultant pressure with a resolution of 0.1 hPa. During calibration, each of the sensing elements can be checked with a resolution of 0.01 hPa. This should not lead operators to believe that the sensor accuracy is better than 0.1 hPa (see section 3.10.3.4).

3.3.5   **Errors and faults with electronic barometers**

3.3.5.1   *Calibration drift*

Calibration drift is one of the key sources of error with electronic barometers. It is often greater when the barometer is new and decreases with the passage of time. Step jumps in calibration may occur.

In order to maintain the acceptable performance of a barometer, the calibration corrections applied to the readings must be checked at relatively frequent intervals, for example, annually, for early detection and replacement of defective sensors.

The need to check frequently the calibration of electronic barometers imposes an additional burden on National Meteorological Services, particularly on those with extensive barometer networks. The ongoing cost of calibration must be taken into consideration when planning to replace mercury barometers with electronic barometers.

3.3.5.2   *Temperature*

Electronic barometers must be kept at a constant temperature if the calibration is to be maintained. It is also preferable that the temperature be near the calibration temperature. However, many commercially available electronic barometers are not temperature-controlled and are prone to greater error. Most depend on accurate temperature measurement of the sensing element and electronic correction of the pressure. This assumes that there are no thermal gradients within the sensing element of the barometer. In situations where the temperature changes reasonably quickly, this can result in short-term hysteresis errors in the measured pressure.

The change in calibration is also highly dependent on the thermal history of the barometer. Prolonged exposure to temperatures that differ from the calibration temperature can result in medium to long-term calibration shifts.

The electronics of the barometer can also introduce errors if it is not held at the same temperature as the sensor element. Electronic barometers are very often used in extreme climatic conditions, especially in automatic weather stations. In these situations, the barometer can be exposed to temperatures well in excess of its manufacturer's design and calibration specifications.

3.3.5.3   *Electrical interference*

As with all sensitive electronic measurement devices, electronic barometers should be shielded and kept away from sources of strong magnetic fields, such as transformers, computers, radar, and so forth. Although this is not often a problem, it can cause an increase in noise, with a resultant decrease in the precision of the device.

3.3.5.4   *Nature of operation*

Apparent changes in the calibration of an electronic barometer can be caused by differences in the way in which the barometer is operated during calibration, as compared with its operational use. A pressure read on a barometer that is run continuously and, therefore, warmed up will read differently from that read in a pulsed fashion every few seconds.

3.4   ANEROID BAROMETERS

3.4.1   Construction requirements

The greatest advantages of conventional aneroid barometers over mercury barometers are their compactness and portability, which make them particularly convenient for use at sea or in the field. The principal components are a closed metal chamber, completely or partly evacuated, and a strong spring system that prevents the chamber from collapsing under the external atmospheric pressure. At any given pressure, there will be an equilibrium between the force caused by the spring and that of the external pressure.

The aneroid chamber may be made of materials (steel or beryllium copper) that have elastic properties such that the chamber itself can act as a spring.

A means is required to detect and display the changes in deflection which occur. This may be a system of levers that amplify the deflections and drive a pointer over a scale graduated to indicate the pressure. Alternatively, a ray of light may be deviated over the scale. Instead of these mechanical analogue techniques, certain barometers are provided with a manually operated micrometer whose counter indicates the pressure directly in tenths of a hectopascal. A reading is taken when a luminous indicator signals that the micrometer has just made contact with the aneroid. This type of aneroid is portable and robust.

3.4.2   Accuracy requirements

The chief requirements of a good aneroid barometer are as follows:

(a)   It should be compensated for temperature so that the reading does not change by more than 0.3 hPa for a change in temperature of 30 K;

(b)   The scale errors at any point should not exceed 0.3 hPa and should remain within this tolerance over periods of at least one year, when in normal use;

(c)   The hysteresis should be sufficiently small to ensure that the difference in reading before a change in pressure of 50 hPa and after a return to the original value does not exceed 0.3 hPa;

(d)   It should be capable of withstanding ordinary transit risks without introducing inaccuracies beyond the limits specified above.

3.4.3   Reading aneroid barometers

3.4.3.1   *Accuracy of readings*

An aneroid barometer should always be read in the same orientation (vertical or horizontal) as during calibration. It should be tapped lightly before being read. As far as possible, it should be read to the nearest 0.1 hPa. Optical and digital devices are available for improving the reading accuracy and reducing the errors caused by mechanical levers.

3.4.3.2   *Corrections applied to aneroid barometers*

In general, aneroid barometers should be set to read the pressure at the level of the instrument. On board a ship or at low-lying land stations, however, the instrument may be set to indicate the pressure at mean sea level, provided that the difference between the station pressure and the sea-level pressure can be regarded as constant. The readings should be corrected for instrumental errors, but the instrument is usually assumed to be sufficiently compensated for temperature, and it needs no correction for gravity.

3.4.4   Errors and faults with aneroid barometers

3.4.4.1   *Incomplete compensation for temperature*

In an aneroid barometer, if the spring is weakened by an increase in temperature, the pressure indicated by the instrument will be too high. This effect is generally compensated for in one of the following ways:

(a)   By means of a bimetallic link in the lever system; or

(b)   By leaving a certain amount of gas inside the aneroid chamber.

In most ordinary aneroid barometers, the compensation obtained by these methods is complete only at one particular compensation pressure. It is desirable that all aneroid barometers and barographs used at meteorological stations should be properly compensated for temperatures over the full range of pressure. In digital read-out systems suitable for automation, such complete corrections can be applied as part of the electronic system.

3.4.4.2   *Elasticity errors*

An aneroid barometer may be subjected to a large and rapid change in pressure. For example, a strong gust of wind would cause an aneroid barometer to experience a rapid increase in pressure followed by a more gradual return to the original value. In such circumstances, the instrument will, owing to hysteresis, indicate a slightly different reading from the true pressure; a considerable time may elapse before this difference becomes negligible. However, since aneroids and barographs at surface stations are not usually directly exposed to such pressure changes, their hysteresis errors are not excessive.

There is also a secular error caused by slow changes in the metal of the aneroid capsule. This effect can be allowed for only by comparison at regular intervals, for example, annually, with a standard barometer. A good aneroid barometer should retain an accuracy of 0.1 hPa over

a period of one year or more. In order to detect departures from this accuracy by individual barometers, a regular inspection procedure with calibration and adjustment as necessary should be instituted.

3.5   BAROGRAPHS

3.5.1   General requirements

Of the various types of barographs, only the aneroid barograph will be dealt with in detail here. For synoptic purposes, it is recommended that charts for barographs:

(a)   Be graduated in hPa;

(b)   Be readable to 0.1 hPa;

(c)   Have a scale factor of 10 hPa to 1.5 cm on the chart.

In addition, the following requirements are desirable:

(a)   The barograph should employ a first-class aneroid unit (see section 3.5.2);

(b)   The barograph should be compensated for temperature, so that the reading does not change by more than 1 hPa for a 20 K change in temperature;

(c)   Scale errors should not exceed 1.5 hPa at any point;

(d)   Hysteresis should be sufficiently small to ensure that the difference in reading before a change in pressure of 50 hPa and after a return to the original value does not exceed 1 hPa;

(e)   There should be a time-marking arrangement that allows the marks to be made without lifting the cover;

(f)   The pen arm should be pivoted in a "gate", the axis of which should be inclined in such a way that the pen rests on the chart through the effects of gravity. A means of adjustment should be provided for setting the position of the pen.

Marine barographs are subject to special requirements, which are considered in Part II, Chapter 4.

3.5.2   Construction of barographs

The principle of the aneroid barograph is similar to that of the aneroid barometer, except that a recording pen is used instead of a pointer. This involves some change in the design of the capsule stack, and usually means a decrease in the overall magnification and an increase in the number and size of the capsules used.

The "control" of the barograph may be expressed as the force required to move the pointer over one unit of the scale (1 hPa) and is, thus, equal to the force required to prevent the pen from moving when the pressure changes by 1 hPa. It is a measure of the effect that friction is likely to have on the details of the record.

The force required to overcome the movement of the capsule when the pressure changes by 1 hPa is 100 A newtons, where A is the effective cross-sectional area of the capsule in square metres. If the magnification is X, the force necessary to keep the pen from moving is 100 A/X newtons and varies as A/X. For a given type of capsule and scale value, the value of X will be largely independent of A, so that the control of a barograph pen may be considered to vary approximately with the effective cross-sectional area of the capsule.

3.5.3   Sources of error and inaccuracy

In addition to the sources of error mentioned for the aneroid (see section 3.4.4), the friction between the pen and the paper is important. The control of the pen depends largely on the effective cross-section of the aneroid. In a well-made barograph, the friction of the pen is appreciably greater than the total friction at all the pivots and bearings of the instrument; special attention should, therefore, be given to reduce such errors, for example, by having a sufficiently large aneroid capsule.

A first-class barograph should be capable of an uncertainty of about 0.2 hPa after corrections have been applied and should not alter for a period of one or two months. The barometric change read from such a barograph should usually be obtained within the same limits.

3.5.4   Instruments with data-processing capability

A barometer suitable for automated reading can be linked to a computer, typically a microprocessor, which can be programmed to provide suitably sampled data. These data, in turn, can be presented graphically to provide records similar to those supplied by a barograph. Models are available that print their own scales, thereby eliminating one source of error.

3.5.5   Reading a barograph

The barograph should be read without touching the instrument. The time mark and any inspection of the instrument involving lifting the cover, and so on, should always be made after the reading is completed.

3.5.5.1   *Accuracy of readings*

The chart should be read to the nearest 0.1 hPa. The barometric change should be obtained within the same resolution limits.

3.5.5.2   *Corrections to be applied to barograph readings*

The temperature compensation of each individual instrument should be tested before the instrument is used, and the scale factor should be adjusted by testing in a vacuum chamber. If the barograph is used only to find the barometric change, the corrections are not usually applied to the readings. In this case, the accurate setting of the pen position is not important. When absolute pressure values are required from the barograph, the record should be compared with the corrected readings of a mercury barometer or a good aneroid barometer at least once every 24 h and the desired values found by interpolation.

3.6   BOURDON-TUBE BAROMETERS

Bourdon-tube barometers usually consist of a sensor element that, as for an aneroid capsule, changes its shape under the influence of pressure changes (pressure transducers) and a transducer that transforms the changes into a form directly usable by the observer. The display may be remote from the sensor. Precise and stable digital instruments with quartz Bourdon tubes are used as working reference barometers in calibration laboratories.

3.7 BAROMETRIC CHANGE

Two methods are available to stations making observations at least every 3 h as follows:

(a)   The change can be read from the barograph; or

(b)   The change can be obtained from appropriate readings of the barometer, corrected to station level. If the choice is between an ordinary mercury barometer and a first-class open-scale barograph, the latter should be selected for the reasons outlined below.

The error of a single barometric reading is mainly random, assuming that the barometer functions perfectly. Therefore, when two independent readings are subtracted to find the amount of change, the errors may be cumulative. Barograph errors are partly systematic in nature, so that in the relatively short period of 3 h, the errors are likely to have the same sign and would, therefore, be diminished by subtraction.

A further reason for using the barograph is the convenience of avoiding the need to correct barometric readings to station level. In any case, the barograph must be used to ascertain the characteristic of the barometric change.

Barometers with digital displays are also very suitable for determining the magnitude and character of a pressure change.

3.8 GENERAL EXPOSURE REQUIREMENTS

It is important that the location of barometers at observation stations be selected with great care. The main requirements of the place of exposure are uniform temperature, good light, a draught-free environment, a solid and vertical mounting, and protection against rough handling. The instrument should, therefore, be hung or placed in a room in which the temperature is constant, or changes only slowly, and in which gradients of temperature do not occur. The barometer should be shielded from direct sunshine at all times and should not be placed near any heating apparatus or where there is a draught.

3.8.1 The effect of wind

It should be noted that the effects of wind apply to all types of barometers. More information on wind effects is found in Liu and Darkow (1989).

A barometer will not give a true reading of the static pressure if it is influenced by gusty wind. Its reading will fluctuate with the wind speed and direction and with the magnitude and sign of the fluctuations, depending also on the nature of the room's openings and their position in relation to the direction of the wind. At sea, error is always present due to the ship's motion. A similar problem will arise if the barometer is installed in an air-conditioned room.

Wind can often cause dynamic changes of pressure in the room where the barometer is placed. These fluctuations are superimposed on the static pressure and, with strong and gusty wind, may amount to 2 or 3 hPa. It is usually impractical to correct for such fluctuations because the "pumping" effect on the mercury surface is dependent on both the direction and the force of the wind, as well as on the local circumstances of the barometer's location. Thus, the "mean value" does not only represent the true static pressure. When comparing barometers in different buildings, the possibility of a difference in readings due to the wind effect should be borne in mind.

It is possible to overcome this effect to a very large extent by using a static head between the exterior atmosphere and the inlet port of the sensor. Details concerning the operating principles of static heads can be found in several publications (Miksad, 1976; United States Weather Bureau, 1963). For a mercury barometer, the barometer cistern must be made airtight except for a lead

to a special head exposed to the atmosphere and designed to ensure that the pressure inside is true static pressure. Aneroid and electronic barometers usually have simple connections to allow for the use of a static head, which should be located in an open environment not affected by the proximity of buildings. The design of such a head requires careful attention. Static pressure heads are commercially available, but there is no published literature on intercomparisons to demonstrate their performance.

3.8.2 The effects of air conditioning

Air conditioning may create a significant pressure differential between the inside and outside of a room. Therefore, if a barometer is to be installed in an air-conditioned room, it is advisable to use a static head with the barometer which will couple it to the air outside the building.

3.9 BAROMETER EXPOSURE

3.9.1 Exposure of mercury barometers

The general exposure requirements of mercury barometers have been outlined in the preceding sections. Mercury barometers have additional exposure requirements above those already mentioned. It is always preferable to hang the mercury barometer on an inside wall. For very accurate work, the best position would be in an unheated basement room with no windows and with a small electric fan to prevent any stratification of temperature.

In order to obtain uniform lighting conditions for reading the barometer, it is advisable to use artificial lighting for all observations. For this purpose, some sort of illuminator – which can provide a white and slightly luminous background for the mercury meniscus and, if necessary, for the fiducial point – may be provided. If no illuminator is used, care should be taken to provide the meniscus and the fiducial point with a light background, by such means as pieces of milk glass, white celluloid, or a sheet of white paper. Artificial light should also be provided for reading the barometer scale and the attached thermometer. Care should, however, be taken to guard against heating the barometer with artificial light during a barometer reading.

The barometer should be mounted in a place where it is not subject to vibration, preferably on a solid wall. The instrument must be mounted with the mercury column in a vertical position. Errors due to departure from verticality are more critical for asymmetric barometers. Such barometers should be mounted with their longest axis vertical in order that a true setting of the mercury surface to the fiducial point remains correct even when the instruments are tilted from the vertical.

To protect the barometer from rough handling, dust and air currents, it is recommended that the instrument be placed in a box furnished with a hinged door with provisions for sufficient ventilation to prevent stratification of the air inside.

Great care should be taken when transporting a mercury barometer. The safest method is to carry the barometer upside down in a wooden case furnished with a sling. If the barometer cannot be accompanied by a responsible person, it ought to be transported in a suitable sprung crate with the cistern uppermost. The barometer should not be subject to violent movements and must always be turned over very slowly. Special precautions must be taken for some individual types of barometers before the instrument is turned over.

3.9.2 Exposure of electronic barometers

Electronic barometers require a clean, dry atmosphere that is free of corrosive substances. The barometer should also be kept at a constant temperature (see section 3.3.5.2). The instrument

should be mounted in such a manner as to avoid mechanical shock and vibration. It should also be mounted away from electromagnetic sources, where this is not possible, the wires and casing should be shielded.

Barometers with digital read-outs should be mounted where there is good general lighting, but should not face a window or other strong light sources.

3.9.3   Exposure of aneroid barometers

The exposure requirements for aneroid barometers are similar to those for mercury barometers (see section 3.9.1) owing to the fact that such instruments may not be perfectly compensated for the effects of temperature. The place selected for mounting the device should preferably have a fairly uniform temperature throughout the day. Therefore, a location is required where the barometer is shielded from the direct rays of the sun and from other sources of either heat or cold, which can cause abrupt and marked changes in its temperature.

At land stations, it is an advantage to have the aneroid barometer installed in the vicinity of a mercury barometer for cross-checking and standardization purposes (see section 3.10).

3.9.4   Exposure of barographs

The barograph should be installed where it is protected from sudden changes in temperature and from vibration and dust. It should not be exposed to direct sunshine. The barograph should also be placed at a location where it is unlikely to be tampered with by unauthorized persons. Mounting the barograph on a sponge rubber cushion is a convenient means of reducing the effects of vibration. The site selected should be clean and dry. The air should also be relatively free of substances which would cause corrosion, fouling of the mechanism, and the like.

It is important to mount the instrument so that its face will be at a convenient height to be read at eye-level under normal operating conditions with a view to minimizing the effects of parallax. The exposure ought to be such that the barometer is uniformly illuminated, with artificial lighting being provided if necessary.

If a barograph has to be transported by air or transported at a high altitude, the pen arm should be disconnected and precautions should be taken to ensure that the mechanism is able to withstand the overload caused by exceeding the normal measuring range of the instrument.

3.10   COMPARISON, CALIBRATION AND MAINTENANCE

3.10.1   General requirements of a barometer comparison

In view of the importance of accurate pressure observations, especially for aeronautical and synoptic purposes, and of the various possible errors to which barometers are subject, all station barometers should be checked regularly by an inspector. Some guidance is given in the following sections regarding the equipment to be used for checks, the frequency with which these should be carried out, and other related topics. Where precision aneroid barometers are used as station barometers, they should be checked frequently (at least once every week) against a mercury or digital barometer, and a permanent record of all such checks should be kept on a suitable card or in a special logbook.

Alternatively, mercury barometers can be dispensed with if a daily comparison, both with a second aneroid barometer kept at the station and with analysed pressures in the vicinity, is undertaken. This should be supported by six monthly checks with a travelling standard.

The following symbols may be used to denote various categories of barometers in a National Meteorological Service:

A: A primary or secondary standard barometer capable of independent determination of pressure to an uncertainty of 0.05 hPa or less;

B: A working standard barometer of a design suitable for routine pressure comparisons and with known errors, which have been established by comparison with a primary or secondary standard;

C: A reference standard barometer used for comparisons of travelling standard and station barometers at field supervising stations of a National Meteorological Service;

S: A barometer (mercury, aneroid, electronic) located at an ordinary meteorological station;

P: A mercury barometer of good quality and accuracy, which may be carried from one station to another and still retain calibration;

N: A portable precision aneroid barometer of first quality;

Q: A portable precision digital barometer of first quality, to be used as a travelling standard (Q stands for quality);

M: A portable microbarograph of good quality and accuracy.

In order that barometer correction programmes be conducted on the same basis by all National Meteorological Services, it is desirable that uniform practices be followed in the quality of the equipment used, the frequency of comparisons, the procedures to be followed, the permissible changes in index correction, and the criteria for remedial action.

3.10.2 Equipment used for barometer comparisons

3.10.2.1 *Primary standard barometer (A)*

There are different opinions regarding the best type of primary standard barometer (WMO, 2010*c*). Two types are outlined in the following paragraphs.

One possible primary standard for atmospheric pressure consists of a precision dead weight tester that produces a calibrated pressure related to the precision weights used and the local gravity field. This type of barometer is relatively simple and does not suffer from the problem of excessive drift experienced by mercury barometers in a polluted environment.

The primary standard barometer may well be a high-quality mercury barometer specially designed for that purpose. The primary standard mercury barometer must have a high vacuum, contain very pure mercury with a well-known density maintained at a constant temperature, and be located in an environment where pollution effects are prevented. The barometer also needs a calibrated measure (scale) and an optical read-out facility. These types of barometers measure absolute pressure with high absolute accuracy, while dead weight testers are gauge pressure measuring instruments.

Considering the cost of such primary standards and the constraints on their use and maintenance, these barometers are most frequently used in high-level calibration laboratories.

3.10.2.2 *Working standard barometer (B)*

The working and reference standards, and the travelling standards used to compare barometers, should have high stability over long periods. These standards may be either mercury or electronic barometers. In the case of mercury barometers, they should have a tube with at least

a 12 mm bore. It is also desirable that barometers be instruments in which the vacuum can be checked. They should be fully and carefully corrected for all known errors, which should have been established by two or more recent comparisons with barometers of a higher category.

3.10.2.3   *Travelling standard barometer (C)*

A reliable travelling standard barometer must retain its index correction during transit to within 0.1 hPa. It should be standardized with reference to the working or reference standard before and after each tour. Once standardized, it should on no account be opened or adjusted in any fashion until after the final comparison at the station of origin of the tour. A travelling standard barometer needs to be carried in a high-quality, cushioned travelling case to protect it during transit.

Considering the restrictions on mercury transportation and the ongoing development of digital barometers, National Meteorological Services may use an appropriate high-precision digital barometer as a travelling standard barometer. In this case, the National Meteorological Service should regularly control the drift of such instruments by conducting regular comparisons with working or reference standards.

If a mercury travelling standard is used, before the beginning of a tour it should be examined carefully and checked to ensure that the mercury in the tube and cistern is clean, that there are no bubbles in the tube, and that the vacuum above the mercury in the tube is good. Every care should be taken in handling, packing and transporting travelling standards so that there is the least possible cause for any change, however slight, in their index correction. Quick, jerky movements which might cause air bubbles from the tube cistern to rise in the tube should be avoided. Mercury travelling standards should be carried in a suitably cushioned leather or metal case, with the cistern end always higher than the tube.

3.10.2.4   *Specifications of portable mercury barometers (P)*

If a mercury barometer is to be used as a category P barometer, it must be designed so that the vacuum can be checked or so that a good degree of vacuum can be established at the top of the tube with a vacuum pump. A check valve for sealing the tube is essential. It should also have the property of high stability over long periods and have a tube with at least a 12 mm bore. Another desirable feature is a means of determining whether the quantity of mercury in the fixed cistern has remained constant since the original filling.

Also, a well-built Fortin-type barometer with a tube bore of at least 9 mm, but preferably 12 mm, can be used as a travelling standard. The degree of accuracy (as regards repeatability) considered necessary for a travelling standard is about 0.1 hPa. Category P barometers should be calibrated over a wide pressure and temperature range, covering all possible values likely to be encountered.

3.10.2.5   *Specifications of portable electronic barometers (Q)*

Portable electronic barometers have now reached the level of development and reliability to allow them to be used as a category Q barometer. The barometer must have a history of reliability with low drift corrections, as determined by several comparisons with a standard barometer both over a period of one year or more and over the maximum pressure range in which the barometer must be expected to operate.

Electronic barometers with multiple pressure transducers under independent microprocessor control are preferred. The temperature-compensation mechanism for the barometer must be proven to be accurate. The method for taking measurements from the pressure transducer must be contact-free and the barometer itself sufficiently robust to withstand the type of shock that may be encountered during transportation.

3.10.3   **Barometer comparison**

3.10.3.1   *International barometer comparison*

Great importance is attached to international barometer comparisons. The WMO Automatic Digital Barometer Intercomparison was carried out in De Bilt (Netherlands) from 1989 to 1991. Only by such comparisons is it possible to ensure consistency in the national standards of pressure-measuring instruments and thus prevent discontinuities in pressure data across international boundaries. The recommended procedure for such comparisons is given in section 3.10.4.

The programme of comparisons includes the following:

(a)   Comparison of national working standard B with primary or secondary standard barometer A, at least once every two years. If barometers A and B are located at the same centre, no travelling standards are required;

(b)   Comparison of reference standard C with national working standard B, at least once every two years by means of travelling standards;

(c)   Comparison of station barometer S with reference standard C, at least once every year, by means of travelling standards, or by comparison with the working standard B, every one to two years, depending upon the known characteristics of the barometers being used. It is a matter of policy whether the comparison occurs at the station or at a central calibration facility. In the latter case, travelling standards are not required.

It should be understood that the error of each barometer at the end of any link in a chain of comparison is determined with respect to the primary or secondary standard barometer A, so that the results of corrected barometric pressure readings are on an absolute basis at each stage.

3.10.3.2   *Inspection of station barometers*

For the inspection of station barometers, Fortin barometers with a tube bore of 9 mm are suitable; however, note section 3.2.7.3 on restrictions on the carriage of mercury instruments. Electronic barometers may also be used as travelling standards, provided that they have the necessary stability and accuracy.

3.10.3.3   *Procedure for the comparison of mercury barometers*

The instructions given in previous sections should be generally followed. All normal precautions necessary while setting and reading barometers should be enforced with great care. Investigations show that readings averaging within 0.05 hPa can normally be achieved in a barometer comparison if adequate precautions are taken.

Comparative readings of the barometers should be entered in appropriate forms. A permanent record of all checks should be attached to the instrument and should include such information as the date of the check, the temperature and pressure at which the comparison was made, and the correction obtained.

Reports of barometer comparisons should be forwarded to the National Meteorological Service for evaluating errors, computing and issuing corrections, and determining the need for remedial action. Continuous records of the comparison data should be kept for each station barometer for a study of its performance over a period of years and for the detection of defects. Tabular and/or graphical records are useful visual tools for a barometer quality control programme.

3.10.3.4 *Checking electronic barometers*

At the current state of development, it is important to calibrate electronic barometers at intervals of about one year. It is standard procedure to calibrate an electronic barometer at a calibration facility immediately before its dispatch to a meteorological observation station. At the station, a number of comparison readings of pressure between the electronic barometer and the travelling standard should be taken at different pressures (either over an adequate period of time or using a pressure generator). The readings should be taken with all barometers at the same height, when the wind speed is less than 12 m s^{-1} and when the pressure is either steady or changing by less than 1 hPa h^{-1}. Any electronic barometer whose mean difference from the travelling standard exceeds 0.25 hPa should be regarded as unserviceable and returned to the calibration facility for recalibration.

If at all possible, it is advisable to install two independent electronic barometers at a meteorological observing station, with one barometer preferably having a history of low drift. This barometer is identified by the calibration facility staff from its calibration history and is identified as a low-drift barometer. With the arrival of each new barometer at a station, a set of comparison readings are taken, as described above, and the mean difference between the low-drift barometer and the new barometer is established. Once this is accomplished, daily readings from both barometers should be taken and a running sum of 25 differences calculated. If the new barometer and the low-drift barometer exhibit different rates of drift, the sums of the 25 differences will change. If a station has one mercury barometer and one electronic barometer, it would be normal for the mercury barometer to be the low-drift barometer. The low drift of the mercury barometer should still be verified by regular calibration checks.

These checks do not represent an inspection or a new calibration of the electronic barometer. Every National Meteorological Service should establish detailed inspection and calibration procedures for its electronic barometers, with the above method being used as a practical guide.

3.10.4 **General procedure recommended for the comparison of barometers at different locations**

The comparison of barometers is essential and should be undertaken in the following ways:

(a) If barometer "1" is to be compared with barometer "2", a qualified person should carry the travelling standard(s), preferably of the P or Q category, from barometer "1" to barometer "2", and then return to "1", thus closing the circuit. This procedure is applicable both between and within countries. Barometer "1" is usually at the central laboratory of a national standards organization or at the laboratory of a National Meteorological Service. Barometer "2" is at some other location. The carrying of category N and M standards is optional, and M may be omitted if microbarographs of good quality are installed at the two locations;

(b) For standardization purposes, the travelling standards should be placed next to the barometer to be compared and all the instruments given equal exposure for at least 24 h before official comparative readings are begun. An air current from an electric fan played on the instruments will aid in equalizing their temperature. The temperature of the room should be kept as uniform as practicable;

> Note: The fan should be turned off before comparisons are made.

(c) Comparative readings should not be taken if category M standards show the pressure to be fluctuating rapidly. Preference should be given to barometrically quiet periods (pressure steady or changing only slowly) for making the comparisons;

(d) Comparative readings should be taken at uniform intervals of no less than 15 min in duration;

(e) Experience indicates that at least five comparative readings are required for category S barometers at ordinary stations. At least 10 comparative barometer readings are required for barometers in categories A, B or C for standardization purposes;

(f) If meteorological conditions permit, the comparative readings in the latter cases should be taken at different pressures covering both high and low pressures;

(g) Records should include the attached thermometer observations, the readings of the travelling standards and barometers being compared, the wind speed, direction and gustiness, the corrections for gravity, temperature and instrumental error, the actual elevation above sea level of the zero point of the barometers, and the latitude, longitude, place name and date and time of observations;

(h) The readings of category N barometers, if used, should include the readings of two or more precision aneroid barometers, corrected to a common reference, if standardization against instruments of category A or B shows them to differ in calibration. The correct readings of the aneroid barometers must be in agreement within tolerances appropriate to the instrument, otherwise the comparisons will be regarded as invalid;

(i) With respect to comparisons using travelling standards, barometer "1" must be the highest class of standard barometer available at the point of departure. Barometer "1" should be of category A, B or B_r (see section 3.10.5.1), with category C being the lowest acceptable quality. Two sets of comparisons of the travelling standards are necessary with barometer "1", at the following points in time:

   (i) Before the travelling standards are carried by hand from where barometer "1" is located to the place where barometer "2" is located;

   (ii) After the return of the travelling standards to their point of origin, following transit to and from the location of barometer "2". The "before" and "after" comparisons should be checked against each other. If agreement with barometer "1" is within satisfactory tolerances for each of the instruments involved, it can be assumed that the comparisons between the travelling standards and barometer "2" are also within the required tolerances, provided that due care has been taken during all phases of the comparison process. However, if there is a significant disagreement or if a known mishap has occurred which might have affected the instruments, or if the validity of the comparison data is in question for any reason, the comparison exercise is deemed invalid and the whole process must be repeated;

(j) As far as practical, all discrepancies should finally be expressed with respect to a primary or secondary reading of a category A barometer. This will ensure a common basis for all comparisons. In each case, the report of comparisons should indicate the standard used;

   Note: When a programme involving the elimination of residual barometric errors is adopted, there will be a homogeneous system of barometric observational data conforming to a single standard, which will permit the elimination of errors in horizontal pressure gradients from instrumental sources.

(k) Comparisons are necessary both before and after the relocation of barometers at a laboratory or a station, or the cleaning of the mercury, to ensure early detection of the development of a defect.

3.10.5   Regional barometer comparison

3.10.5.1   *Nomenclature and symbols*

Symbols denoting barometer categories are as follows:

A_r: A barometer of category A which has been selected by regional agreement as a reference standard for barometers of that Region;

B_r: A barometer of category B which the National Meteorological Services of the Region agree to use as the standard barometer for that Region, in the event that the category A barometer is unavailable in the Region.

Annex 3.B contains the list of regional standard barometers.

3.10.5.2   *System of interregional comparison*

The following measures must be considered when planning interregional comparisons:

(a)   Member countries in each Region will designate a primary or secondary standard barometer A to serve as A_r for the Region. If a primary or secondary barometer is not available within the Region, a category B barometer will be designated jointly as the regional standard barometer for that Region, with the barometer so chosen being denoted by the symbol B_r. Relative costs will determine whether a Region may deem it advantageous to designate more than one standard barometer;

(b)   A competent person carrying travelling standard barometers will travel from a central station equipped with a barometer of category A_r to a nearby Region equipped with a barometer of at least category B or B_r. A comparison of the barometers should then be performed. When the comparison is made in ambient conditions, it should be done in accordance with the method outlined in section 3.10.3. Otherwise, in presence of a pressure generator, the comparison may be made for several pressure calibration points covering the whole range and over several cycles. This makes it possible to define the accuracy of the standards at different pressure levels and determine some metrological characteristics such as hysteresis, repeatability and reproducibility. For the purposes of verification and intercomparison, it is sometimes desirable to repeat the process by comparing the B_r barometer with a barometer of category A_r from a different Region;

(c)   Copies of the comparison records should be transmitted to each of the central stations equipped with a category A barometer and to the station where the barometer B or B_r compared is located. Summaries of the comparison results should be forwarded to all National Meteorological Services in the Region where the barometer B or B_r is located.

3.10.5.3   *System of international comparison within a Region*

The following measures must be considered when planning international comparisons:

(a)   Each National Meteorological Service will compare its category B barometer with the category A barometer within the Region, if available, using the system outlined in section 3.10.4. Where possible, preference should be given to the category A barometer for the Region as the standard instrument for the area;

(b)   When a category A barometer is not available in the Region, the category B barometers of the respective National Meteorological Service of the Region will be compared with the category B_r barometer for the Region, in accordance with section 3.10.4;

(c)   When a competent person is engaged in the execution of the programme to compare barometers of categories B with B_r, it is desirable that additional en route comparisons be made with barometers of categories B and C, while the person is travelling both to and from the station where the instrument B_r for the Region is located;

(d)   Copies of records and summaries of comparisons will be prepared and forwarded to interested agencies as outlined in paragraph 3.10.5.2 (c).

3.11   ADJUSTMENT OF BAROMETER READINGS TO OTHER LEVELS

In order to compare barometer readings taken at stations at different altitudes, it is necessary to reduce them to the same level. Various methods are in use for carrying out this reduction, but WMO has not yet recommended a particular method, except in the case of low-level stations.

The recommended method is described in WMO (1954, 1964, 1968). WMO (1966) contains a comprehensive set of formulae that may be used for calculations involving pressure.

3.11.1   Standard levels

The observed atmospheric pressure should be reduced to mean sea level (see Part I, Chapter 1) for all stations where this can be done with reasonable accuracy. Where this is not possible, a station should, by regional agreement, report either the geopotential of an agreed "constant pressure level" or the pressure reduced to an agreed datum for the station. The level chosen for each station should be reported to the WMO Secretariat for promulgation.

Reduction formula for sea-level pressure feasible for stations below 750 m (from WMO, 1964, p. 22, equation 2):

$$\log_{10}\frac{p_0}{p_s} = \frac{K_p \cdot H_p}{T_{mv}} = \frac{K_p \cdot H_p}{T_s + \dfrac{a \cdot H_p}{2} + e_s \cdot C_h} \tag{3.1}$$

where p_0 is the pressure reduced to sea level in hPa; p_s is the station pressure in hPa; K_p is the constant = 0.014 827 5 K/gpm; H_p is the station elevation in gpm; T_{mv} is the mean virtual temperature of the fictitious air column below station level in K, ($T_{mv} = T_s + (a \cdot H_p)/2 + e_s \cdot C_h$); T_s is the station temperature in K; $T_s = 273.15 + t$, t is the station temperature in °C; a is the assumed lapse-rate in the fictitious air column extending from sea level to the level of the station elevation level = 0.006 5 K/gpm; e_s is the vapour pressure at the station in hPa; and C_h is the coefficient = 0.12 K/hPa.

The same formula is often used in the exponential form:

$$p_0 = p_s \cdot \exp\left(\frac{\dfrac{g_n}{R} \cdot H_p}{T_s + \dfrac{a \cdot H_p}{2} + e_s \cdot C_h}\right) \tag{3.2}$$

where g_n is the standard acceleration of gravity = 9.806 65 m s^{-2} and R is the gas constant of dry air = 287.05 J/kg/K.

3.11.2   Low-level stations

At low-level stations (namely, those at a height of less than 50 m above mean sea level), pressure readings should be reduced to mean sea level by adding to the station pressure a reduction constant C given by the following expression:

$$C = p \cdot H_p/\left(29.27 T_v\right) \tag{3.3}$$

where p is the observed station pressure in hectopascals; H_p is the station elevation in metres; and T_v is the mean annual normal value of virtual temperature at the station in kelvins.

Note: The virtual temperature of damp air is the temperature at which dry air of the same pressure would have the same density as the damp air. WMO (1966) contains virtual temperature increments of saturated moist air for various pressures and temperatures.

This procedure should be employed only at stations of such low elevation that when the absolute extreme values of virtual temperature are substituted for T_v in the equation, the deviation of the result due to the other approximations of the equation (used for height rather than standard geopotential, and with C to be small compared with p) is negligible in comparison.

### 3.12	**PRESSURE TENDENCY AND PRESSURE TENDENCY CHARACTERISTIC**

At surface synoptic observing stations, pressure tendency and the pressure tendency characteristic should be derived from pressure observations from the last 3 h (over 24 h in tropical regions). Typically, the pressure tendency characteristic can be expressed by the shape of the curve recorded by a barograph during the 3 h period preceding an observation (WMO, 2010*b*). In the case of hourly observations, the amount and characteristic can be based on only four observations, and misinterpretations may result. Therefore, it is recommended that the characteristic should be determined on a higher frequency of observations, for example with 10 min intervals (WMO, 1985). Nine types of pressure tendency characteristics are defined (see WMO, 2010*a*, p. II-4-8).

ANNEX 3.A. CORRECTION OF BAROMETER READINGS TO STANDARD CONDITIONS

Correction for index error

The residual errors in the graduation of the scale of a barometer should be determined by comparison with a standard instrument. They may include errors due to inaccurate positioning or subdividing of the scale, capillarity and imperfect vacuum. Certificates of comparison with the standard should state the corrections to be applied for index error at no fewer than four points of the scale, for example, at every 50 hPa. In a good barometer, these corrections should not exceed a few tenths of a hectopascal.

Corrections for gravity

The reading of a mercury barometer at a given pressure and temperature depends upon the value of gravity, which in turn varies with latitude and altitude. Barometers for meteorological applications are calibrated to yield true pressure readings at the standard gravity of 9.806 65 m s^{-2} and their readings at any other value of gravity must be corrected. The following method is recommended for reducing such barometer readings to standard gravity. Let B be the observed reading of the mercury barometer, B_t the barometer reading reduced to standard temperature but not to standard gravity, and corrected for instrumental errors, B_n be the barometer reading reduced to standard gravity and standard temperature, and corrected for instrumental errors, B_{ca} be the climatological average of B_t at the station, $g_{\varphi H}$ the local acceleration of gravity (in m s^{-2}) at a station at latitude φ and elevation H above sea level, and g_n the standard acceleration of gravity, 9.806 65 m s^{-2}.

The following relations are appropriate:

$$B_n = B_t \left(g_{\varphi H} / g_n \right)$$
(3.A.1)

or:

$$B_n = B_t + B_t \left[\left(g_{\varphi H} / g_n \right) - 1 \right]$$
(3.A.2)

The approximate equation 3.A.3 may be used, provided that the results obtained do not differ by more than 0.1 hPa from the results that would be obtained with the aid of equation 3.A.2:

$$B_n = B_t + B_{ca} \left[\left(g_{\varphi H} / g_n \right) - 1 \right]$$
(3.A.3)

The local acceleration of gravity $g_{\varphi H}$ should be determined by the procedure outlined in the following section. The values so derived should be referred to as being on the International Gravity Standardization Net 1971 (IGSN71).

Determining local acceleration of gravity

In order to determine the local value of the acceleration of gravity at a station to a satisfactory degree of precision, one of two techniques should be used. These techniques involve, in the first case, the use of a gravimeter (an instrument for measuring the difference between the values of the acceleration of gravity at two points) and, in the second case, the use of the so-called Bouguer anomalies. Preference should be given to the gravimeter method. If neither of these methods can be applied, the local acceleration of gravity may be calculated using a simple model of the Earth.

Use of a gravimeter

Suppose g_1 represents the known local acceleration of gravity at a certain point O, usually a gravity base station established by a geodetic organization, where g_1 is on the IGSN71, and suppose further that g represents the unknown local acceleration of gravity on the meteorological gravity system at some other point X for which the value g is desired. Let Δg denote the difference in gravity acceleration at the two places, as observed by means of a gravimeter. That is, Δg is the value at point X minus the value at point O on a consistent system. Then, g is given by equation 3.A.4:

$$g = g_1 + \Delta g \tag{3.A.4}$$

Use of Bouguer anomalies

If a gravimeter is not available, interpolated Bouguer anomalies (A_B) may be used to obtain g at a given point. It is necessary that a contour chart of these anomalies be available from a geodetic organization or from a network of gravity stations spaced at a density of at least one station per 10 000 km² (no more than a 100 km distance between stations) in the vicinity of the point.

Gravity networks of somewhat less density can be used as a basis provided that a geodetic organization considers that this method is expected to yield more reliable results than those that could be obtained by using a gravimeter.

The definition of the Bouguer anomaly (A_B) is derivable from equation 3.A.5:

$$g_s = \left(g_{\varphi,0} \right) s - C \cdot H + A_B \tag{3.A.5}$$

where $(g_{\varphi,0})s$ is the theoretical value of the acceleration of gravity at latitude φ at sea level, as given by the formula actually used in computing the Bouguer anomaly. This formula expresses the value as a function of latitude in some systems. H is the elevation of the station (in metres) above sea level at which g_s is measured, g_s is the observed value of the acceleration of gravity (in m s⁻²); A_B is the Bouguer anomaly (in m s⁻²); and C is the elevation correction factor used in computing the Bouguer anomaly (for example, using a crustal specific gravity of 2.67, this factor is 0.000 001 968 m s⁻²).

When g is desired for a given station and has not been measured, the value of g_s should be computed by means of equation 3.A.5, provided that the appropriate value of A_B for the locality of the station can be interpolated from the aforementioned contour charts or from data representing the Bouguer anomalies supplied by a suitable network of gravity stations, as defined.

Calculating local acceleration of gravity

If neither of the preceding methods can be applied, the local value may be calculated less accurately according to a simple model. According to the Geodetic Reference System 1980, the theoretical value ($g_{\varphi,0}$) of the acceleration of gravity at mean sea level at geographic latitude, φ, is computed by means of equation 3.A.6:

$$g_{\varphi,0} = 9.806\,20 \left(1 - 0.002\,644\,2 \cos 2\varphi + 0.000\,005\,8 \cos^2 2\varphi \right) \tag{3.A.6}$$

The local value of the acceleration of gravity at a given point on the surface of the ground at a land station is computed by means of equation 3.A.7:

$$g = g_{\varphi,0} - 0.000\,003\,086\,H + 0.000\,001\,118 \left(H - H' \right) \tag{3.A.7}$$

where g is the calculated local value of the acceleration of gravity, in m s⁻², at a given point; $g_{\varphi,0}$ is the theoretical value of the acceleration of gravity in m s⁻² at mean sea level at geographic latitude φ, computed according to equation 3.A.6 above; H is the actual elevation of the given point, in metres above mean sea level; and H' is the absolute value in metres of the difference between the height of the given point and the mean height of the actual surface of the terrain included within a circle whose radius is about 150 km, centred at the given point.

The local value of the acceleration of gravity at a given point within height H above mean sea level of not more than about 10 km, and where that point lies over the sea water surface, is computed by means of equation 3.A.8:

$$g = g_{\varphi,0} - 0.000\,003\,086\,H - 0.000\,006\,88\,(D - D')$$ (3.A.8)

where D is the depth of water in metres below the given point; and D' is the mean depth of water, in metres, included within a circle whose radius is about 150 km centred at the given point.

At stations or points on or near the coast, the local value of acceleration of gravity should be calculated, so far as practicable, through the use of equations 3.A.7 and 3.A.8 on a pro rata basis, weighting the last term of equation 3.A.7 according to the relative area of land included within the specified circle, and weighting the last term of equation 3.A.8 according to the relative area of the sea included within the circle. The values thus obtained are then combined algebraically to obtain a correction which is applied to the final term in the right-hand side of both equations, as shown in equation 3.A.9:

$$g = g_{\varphi,0} - 0.000\,003\,086\,H + 0.000\,001\,118\,\alpha$$
$$(H - H') - 0.000\,006\,88\,(1 - \alpha)(D - D')$$ (3.A.9)

where α is the fraction of land area in the specified area, and H' and D' refer to the actual land and water areas, respectively.

Corrections for temperature

Barometer readings must be corrected to the values that would have been obtained if the mercury and the scale had been at their standard temperatures. The standard temperature for mercury barometers is 0 °C. With reference to scales, some barometers have scales which read accurately at this same temperature, but some read accurately at 20 °C.

The temperature correction necessary for adjustable cistern barometers (Fortin-type barometers) is different from that required for fixed-cistern barometers, though the principle reasons leading to the necessity for temperature corrections are the same for both types, namely, the fact that the coefficient of cubic thermal expansion of mercury is different from the coefficient of linear thermal expansion of the scale. Thus, a certain correction term is required for both types of mercury barometer.

A fixed-cistern barometer requires an additional correction. The reason for this is that an increase in temperature of the instrument causes an increase both in the volume of the mercury and in the cross-sectional areas of the (iron) cistern and the (glass) tube. Owing to these area changes, the apparent rise of the mercury resulting from a temperature increase is less than would be the case if the areas remained constant. This is because some of the mercury from the barometer goes to occupy the capacity increment produced by the expansion of the cistern and tube.

The scale of a fixed-cistern barometer must, for a variety of reasons, undergo a calibration check against a primary standard barometer of the adjustable-cistern type. Some manufacturers decrease the volume of mercury by such an amount that the readings of the test barometer agree with the readings of the standard barometer at 20 °C. Correction tables can be generated for fixed-cistern barometers using the readings from a primary standard barometer whose scales are accurate when 20 °C is used as the reference temperature.

Temperature corrections for mercury barometers

Researchers have conducted exhaustive studies for temperature corrections for mercury barometers, the results of which are summarized below:

1. (a) Scale correct at 0 °C and additionally $\quad C_t \quad = -B\,(\alpha - \beta) \cdot t$
   (b) Hg volume correct at 0 °C $\quad\quad\quad\quad C_{t,V} = -B\,(\alpha - \beta) \cdot t - (\alpha - 3\eta) \cdot t \cdot 4V/3A$

2. Scale correct at 0 °C and
   Hg volume correct at 20 °C $\quad\quad\quad\quad C_{t,V} = -B\,(\alpha - \beta) \cdot t - (\alpha - 3\eta) \cdot (t - 20) \cdot 4V/3A$

3. (a) Scale correct at 20 °C $\quad\quad\quad\quad\quad C_t \quad = -B\,[\alpha \cdot t - \beta \cdot (t - 20)]$
   (b) Hg volume correct at 0 °C $\quad\quad\quad\quad C_{t,V} = -B\,[\alpha \cdot t - \beta \cdot (t - 20)] - (\alpha - 3\eta) \cdot t \cdot (4V/3A)$
   (c) Hg volume decreasing by an amount
   equivalent to 0.36 hPa $\quad\quad\quad\quad\quad C_{t,V} = -B\,(\alpha - \beta) \cdot t - (\alpha - 3\eta) \cdot t \cdot (4V/3A)$

4. Scale correct at 20 °C and
   (a) Hg volume correct at 20 °C $\quad\quad\quad C_{t,V} = -B\,[\alpha \cdot t - \beta\,(t - 20)] - (\alpha - 3\eta) \cdot (t - 20) \cdot (4V/3A)$
   (b) Hg volume decreasing by an amount
   equivalent to 0.36 hPa $\quad\quad\quad\quad\quad C_{t,V} = -B\,(\alpha - \beta) \cdot t - (\alpha - 3\eta) \cdot (t - 20) \cdot (4V/3A)$

where:

$C_t \quad$ = temperature correction;

$C_{t,V} \quad$ = additional correction for fixed-cistern barometers;

$B \quad$ = observed barometer reading;

$V \quad$ = total volume of mercury in the fixed-cistern barometer;

$A \quad$ = effective cross-sectional area of the cistern;

$t \quad$ = temperature;

$\alpha \quad$ = cubic thermal expansion of mercury;

$\beta \quad$ = coefficient of linear thermal expansion of the scale;

$\eta \quad$ = coefficient of linear thermal expansion of the cistern.

————————

ANNEX 3.B. REGIONAL STANDARD BAROMETERS

WMO Region	Location	Category[a]
I	Cairo, Egypt	A_r
	Casablanca, Morocco	A_r
	Dakar, Senegal	A_r
	Douala, Cameroon	A_r
	Kinshasa/Binza, Democratic Republic of the Congo	A_r
	Nairobi, Kenya	A_r
	Oran, Algeria	A_r
II	Calcutta, India	B_r
III	Buenos Aires, Argentina	B_r
	Maracay, Venezuela (Bolivarian Republic of)	B_r
	Rio de Janeiro, Brazil	A_r
IV	Miami, Florida, United States (subregional)	A_r
	San Juan, Puerto Rico (subregional)	A_r
	Toronto, Canada (subregional)	A_r
	Washington DC (Gaithersburg, Maryland), United States	A_r
V	Melbourne, Australia	A_r
VI	Hamburg, Germany	A_r
	London, United Kingdom	A_r
	St Petersburg, Russian Federation	A_r
	Toulouse, France	A_r

Note:
a   For category definitions, see section 3.10.5.1.

REFERENCES AND FURTHER READING

Liu, H. and G. Darkow, 1989: Wind effect on measured atmospheric pressure. *Journal of Atmospheric and Oceanic Technology*, 6(1):5–12.

Miksad, R., 1976: An omni-directional static pressure probe. *Journal of Applied Meteorology*, 15:1215–1225.

Sax, N.I., 1975: *Dangerous Properties of Industrial Materials*. Van Nostrand Reinhold Co., New York.

United Nations Environment Programme, 2013: *Minamata Convention on Mercury*. Geneva, United Nations.

United States Weather Bureau, 1963: *Manual of Barometry* (WBAN). 1, US Government Printing Office, Washington DC.

World Meteorological Organization, 1954: *Reduction of Atmospheric Pressure: Preliminary Report on Problems Involved*. Technical Note No. 7 (WMO-No. 36, TP. 12). Geneva.

———, 1964: *Note on the Standardization of Pressure Reduction Methods in the International Network of Synoptic Stations: Report of a Working Group of the Commission for Synoptic Meteorology*. Technical Note No. 61 (WMO-No. 154, TP. 74). Geneva.

———, 1966: *International Meteorological Tables* (S. Letestu, ed.) (1973 amendment). (WMO-No. 188, TP. 94). Geneva.

———, 1968: *Methods in Use for the Reduction of Atmospheric Pressure*. Technical Note No. 91 (WMO-No. 226, TP. 120). Geneva.

———, 1985: "Pressure tendency" and "discontinuity in wind" – discussion of two algorithms used in Swedish automatic weather stations (L. Bergman, T. Hovberg and H. Wibeck). *Papers Presented at the Third WMO Technical Conference on Instruments and Methods of Observation (TECIMO-III)*. Instruments and Observing Methods Report No. 22 (WMO/TD-No. 50). Geneva.

———, 1992: *The WMO Automatic Digital Barometer Intercomparison* (J.P. van der Meulen). Instruments and Observing Methods Report No. 46 (WMO/TD-No. 474). Geneva.

———, 2010a: *Manual on the Global Data-processing and Forecasting System* (WMO-No. 485), Volume I. Geneva.

———, 2010b: *Manual on the Global Observing System* (WMO-No. 544), Volume I. Geneva.

———, 2010c: *Guidance on Instrumentation for Calibration Laboratories, Including RICs* (D. Groselj). Instruments and Observing Methods Report No. 101 (WMO/TD-No. 1543). Geneva.

———, 2014: *Guide to Meteorological Observing and Information Distribution Systems for Aviation Weather Services* (WMO-No. 731). Geneva.

———————

CHAPTER CONTENTS

CHAPTER 4. MEASUREMENT OF HUMIDITY

4.1   GENERAL

The measurement of atmospheric humidity, and often its continuous recording, is an important requirement in most areas of meteorological activity. This chapter deals with the measurement of humidity at or near the Earth's surface. There are many different methods in use, and there is extensive literature on the subject. An old but still useful wide-ranging account of the techniques is given in Wexler (1965).

4.1.1   Definitions

The definitions of the terms used in this chapter follow those given in the WMO *Technical Regulations* (WMO 2011*a*, Appendix B), the text of which is reproduced in Annex 4.A.

The simple definitions of the most frequently used quantities in humidity measurements are as follows:

Mixing ratio r: The ratio between the mass of water vapour and the mass of dry air;

Specific humidity q: The ratio between the mass of water vapour and the mass of moist air;

Dewpoint temperature T_d: The temperature at which moist air saturated with respect to water at a given pressure has a saturation mixing ratio equal to the given mixing ratio;

Relative humidity U: The ratio in % of the observed vapour pressure to the saturation vapour pressure with respect to water at the same temperature and pressure;

Vapour pressure e': The partial pressure of water vapour in air;

Saturation vapour pressures e'_w and e'_i: Vapour pressures in air in equilibrium with the surface of water and ice, respectively.

Annex 4.B provides the formulae for the computation of various measures of humidity. These versions of the formulae and coefficients were adopted by WMO in 1990.[1] They are convenient for computation and sufficiently accurate for all normal meteorological applications (WMO, 1989*a*).

More accurate and detailed formulations of these and other quantities may be found in Sonntag (1990, 1994). Other detailed formulations[2] are presented in WMO (1966, introductions to tables 4.8–10) and WMO (2011*a*, Appendix A).

4.1.2   Units and scales

The following units and symbols are normally used for expressing the most commonly used quantities associated with water vapour in the atmosphere:

(a)   Mixing ratio *r* and specific humidity *q* (in kg kg^{-1});

(b)   Vapour pressure in air *e'*, e'_w, e'_i and pressure *p* (in hPa);

---

[1]   Adopted by the Executive Council at its forty-second session through Resolution 6 (EC-XLII).
[2]   Adopted by the Fourth Congress through Resolution 19 (Cg-IV).

(c)   Temperature T, wet-bulb temperature T_w, dewpoint temperature T_d, and frost-point
      temperature T_f (in K);

(d)   Temperature t, wet-bulb temperature t_w, dewpoint temperature t_d, and frost-point
      temperature t_f (in °C);

(e)   Relative humidity U (in %).

4.1.3   Meteorological requirements

Humidity measurements at the Earth's surface are required for meteorological analysis and
forecasting, for climate studies, and for many special applications in hydrology, agriculture,
aeronautical services and environmental studies, in general. They are particularly important
because of their relevance to the changes of state of water in the atmosphere.

General requirements for the range, resolution and accuracy of humidity measurements are
given in Part I, Chapter 1, Annex 1.E. The achievable uncertainties listed in the table refer to good
quality instruments that are well operated and maintained. In practice, these are not easy to
achieve. In particular, the psychrometer in a thermometer shelter without forced ventilation, still
in widespread use, may have significantly lower performance.

For most purposes, time constants of the order of 1 min are appropriate for humidity
measurements. The response times readily available with operational instruments are discussed
in section 4.1.4.9.

4.1.4   Measurement methods

A general review of the state of the art in the field of hygrometry is given by Sonntag (1994).

4.1.4.1   *Hygrometers*

Any instrument for measuring humidity is known as a hygrometer. The physical principles most
widely employed for hygrometry are given in sections 4.1.4.4 to 4.1.4.8. More information on the
different methods is found in Wexler (1965). The report of a WMO international comparison of
various hygrometers is given in WMO (1989*b*).

4.1.4.2   *Exposure: general comments*

The general requirements for the exposure of humidity sensors are similar to those for
temperature sensors, and a suitably positioned thermometer screen may be used for that
purpose. Particular requirements include:

(a)   Protection from direct solar radiation, atmospheric contaminants, rain and wind;

(b)   Avoidance of the creation of a local microclimate within the sensor housing structure or
      sampling device. Note that wood and many synthetic materials will adsorb or desorb water
      vapour according to the atmospheric humidity.

Exposures appropriate to particular instruments are described in sections 4.2 to 4.7.

The siting classification for surface observing stations on land (see Part I, Chapter 1, Annex 1.B
of this Guide) provides additional guidance on the selection of a site and the location of a
hygrometer within a site to optimize representativeness.

4.1.4.3   *Sources of error: general comments*

Errors in the measurement of humidity may be caused by the following:

(a)   Modification of the air sample, for example, by heat or water-vapour source or sink;

(b)   Contamination of the sensor, for example, by dirt, sea spray;

(c)   Calibration error, including pressure correction, temperature coefficient of sensor, and electrical interface;

(d)   Inappropriate treatment of water/ice phase;

(e)   Poor instrument design, for example, stem heat conduction in the wet-bulb thermometer;

(f)   Incorrect operation, for example, failure to achieve stable equilibrium;

(g)   Inappropriate sampling and/or averaging intervals.

The time constant of the sensor, the time-averaging of the output and the data requirement should be consistent.

The different types of humidity sensors vary in their susceptibility to, and the significance of, each of the above; further discussion will be found in the appropriate sections of this chapter.

4.1.4.4   *Gravimetric hygrometry*

This method uses the absorption of water vapour by a desiccant from a known volume of air (gravimetric hygrometer; used for primary standards only). Some details are given in section 4.9.

The gravimetric method yields an absolute measure of the water-vapour content of an air sample in terms of its humidity mixing ratio. This is obtained by first removing the water vapour from the sample. The mass of the water vapour is determined by weighing the drying agent before and after absorbing the vapour. The mass of the dry sample is determined either by weighing or by measuring its volume.

The method is restricted to providing an absolute calibration reference standard, and such apparatus is found mostly in national calibration standards laboratories.

4.1.4.5   *Condensation methods*

4.1.4.5.1   **Chilled-mirror method (dewpoint or frost-point hygrometer)**

When moist air at temperature T, pressure p and mixing ratio r_w (or r_i) is cooled, it eventually reaches its saturation point with respect to water (or to ice at lower temperatures) and a deposit of dew (or frost) can be detected on a solid non-hygroscopic surface. The temperature of this saturation point is the dewpoint temperature T_d (or the frost-point T_f).

The chilled-mirror hygrometer are used to measure T_d or T_f. The most widely used systems employ a small polished-metal reflecting surface, cooled electrically by using a Peltier-effect device, and sense condensation with an optical detector.

Instruments using condensation method are used for observational purposes and might also be used as working standards and/or reference standards (see section 4.4).

4.1.4.5.2 Heated salt-solution method (vapour equilibrium hygrometer, known as the dew cell)

The equilibrium vapour pressure at the surface of a saturated salt solution is less than that for a similar surface of pure water at the same temperature. This effect is exhibited by all salt solutions but particularly by lithium chloride, which has an exceptionally low equilibrium vapour pressure.

An aqueous salt solution (whose equilibrium vapour pressure is below the ambient vapour pressure) may be heated until a temperature is reached at which its equilibrium vapour pressure exceeds the ambient vapour pressure. At this point, the balance will shift from condensation to evaporation and eventually there will be a phase transition from the liquid solution to a solid hydrate (crystalline) form. The transition point may be detected through a characteristic decrease in the electrical conductivity of the solution as it crystallizes. The temperature of the solution at which the ambient vapour pressure is reached provides a measure of the ambient vapour pressure. For this purpose, a thermometer is placed in good thermal contact with the solution. The ambient dewpoint (namely, with respect to a plane surface of pure water) may be determined by using empirical data relating vapour pressure to temperature for pure water and for salt solutions. The most frequently used salt solution for this type of sensor is lithium chloride.

This method is used for observational purposes, especially for automatic weather stations (see section 4.5).

4.1.4.6 *The psychrometric method*

A psychrometer consists essentially of two thermometers exposed side by side, with the surface of the sensing element of one being covered by a thin film of water or ice and termed the wet or ice bulb, as appropriate. The sensing element of the second thermometer is simply exposed to the air and is termed the dry bulb. This method is still widely used and is described in detail in section 4.2.

Owing to evaporation of water from the wet bulb, the temperature measured by the wet-bulb thermometer is generally lower than that measured by the dry bulb. The difference in the temperatures measured by the pair of thermometers is a measure of the humidity of the air; the lower the ambient humidity, the greater the rate of evaporation and, consequently, the greater the depression of the wet-bulb temperature below the dry-bulb temperature. The size of the wet-bulb depression is related to the ambient humidity by a psychrometer formula.

This method is in widespread use for observational purposes. Instruments using the psychrometric method are also commonly used as working standards.

4.1.4.7 *Sorption methods*

Certain materials interact with water vapour and undergo a change in a chemical or physical property that is sufficiently reversible for use as a sensor of ambient humidity. Water vapour may be adsorbed or absorbed by the material, adsorption being the taking up of one substance at the surface of another and absorption being the penetration of a substance into the body of another. A hygroscopic substance is one that characteristically absorbs water vapour from the surrounding atmosphere, by virtue of having a saturation vapour pressure that is lower than that of the surrounding atmosphere. For absorption to take place, a necessary condition requires that the ambient vapour pressure of the atmosphere exceeds the saturation vapour pressure of the substance. The following are two properties of sorption:

(a) Changes in the dimensions of hygroscopic materials: Certain materials vary dimensionally with humidity. Natural fibres tend to exhibit the greatest proportional change and, when coupled to a mechanical lever system, can be incorporated into an analogue linear displacement transducer. Such a transducer may be designed to move a pointer over a scale to provide a visual display, or be an electromechanical device which provides an electrical output.

Human hair is the most widely used material for this type of humidity sensor. Synthetic fibres may be used in place of human hair. Because of the very long lag time for synthetic fibres, such sensors should never be used below 10 °C. The hair hygrometer is described in section 4.3.

Goldbeater's skin (an organic membrane obtained from the gut of domestic animals) has properties similar to those of human hair and has been used for humidity measurements, though most commonly in devices for taking upper-air measurement.

(b) Changes in electrical properties of hygroscopic materials: Certain hygroscopic materials exhibit changes in their electrical properties in response to a change in the ambient relative humidity with only a small temperature dependence. Commonly used methods making use of these properties are described in section 4.6.

Electrical relative humidity sensors are increasingly used for remote-reading applications, particularly where a direct display of relative humidity is required.

Properties commonly exploited in the measurement of relative humidity include sensors made from chemically treated plastic material having an electrically conductive surface layer (electrical resistance) and sensors based upon the variation of the dielectric properties of a solid, hygroscopic material in relation to the ambient relative humidity (electrical capacitance).

4.1.4.8 *Absorption of electromagnetic radiation by water vapour (ultraviolet and infrared absorption hygrometers)*

The water molecule absorbs electromagnetic radiation in a range of wavebands and discrete wavelengths; this property can be exploited to obtain a measure of the molecular concentration of water vapour in a gas. The most useful regions of the electromagnetic spectrum for this purpose lie in the ultraviolet and infrared regions, and the principle of the method is to determine the attenuation of radiation in a waveband that is specific to water-vapour absorption, along the path between a source of the radiation and a receiving device. There are two principal methods for determining the degree of attenuation of the radiation, namely:

(a) The transmission of narrowband radiation at a fixed intensity to a calibrated receiver;

(b) The transmission of radiation at two wavelengths, one of which is strongly absorbed by water vapour and the other is either not absorbed or only very weakly absorbed.

Both types of instruments require frequent calibration and are more suitable for measuring changes in vapour concentration rather than absolute levels. Their use remains restricted to research activities; a brief account of these instruments is given in section 4.7.

4.1.4.9 *Time constants of humidity sensors*

The specification of the time constant for a humidity sensor implies that the response of the sensor to a step change in humidity is consistent with a known function. In general usage, the term refers to the time taken for the sensor to indicate 63.2% ($1/e$) of a step change in the measurand (in this case humidity), and assumes that the sensor has a first-order response to changes in the measurand (namely, the rate of change of the measurement is proportional to the difference between the measurement and the measurand). It is then possible to predict that 99.3% of the change will take place after a period of five time constants in duration.

Table 4.1 gives $1/e$ time-constant values typical for various types of humidity sensor.

Table 4.1. Time constants for humidity sensors

85% relative humidity	1/e time constant (s)		
Sensor type	20 °C	0 °C	–20 °C
Ordinary human hair	32	75	440
Rolled hair	10	10	12
Goldbeater's skin	10	16	140
Electrical capacitance	1–10	1–10	1–10
Electrical resistance	1–10	—	—
Assmann psychrometer			
Condensation hygrometers	30–50	30–50	30–50
Electrolytic hygrometers			
Optical hygrometer	< 0.01	< 0.01	< 0.01

Note: The first-order relation does not hold particularly well for sorption sensors since the forcing agent for vapour equilibrium, the local gradient of vapour pressure, is dependent upon the local migration of water vapour molecules within the body of a solid humidity element. In general, a first-order response will be most closely exhibited by those sensors having a thin active element.

4.1.4.10   ***Maintenance: general comments***

The following maintenance procedures should be considered:

(a)   Cleanliness: Sensors and housings should be kept clean. Some sensors, for example, chilled-mirror and hair hygrometers, may be cleaned with distilled water and this should be carried out regularly. Others, notably those having some form of electrolyte coating, but also some with a polymeric substrate, may on no account be treated in this way. The provision of clear instructions for observers and maintenance staff is vital;

(b)   Checking and calibration of field instruments: Regular calibration is required for all humidity sensors in the field. For psychrometers and dewpoint hygrometers, which use a temperature detector, the calibration of the detector can be checked whenever the regular maintenance routine is performed. A comparison with a working reference hygrometer, such as an Assmann psychrometer, should also be performed at least once a month.

Saturated salt solutions have applications with sensors that require only a small sample volume. A very stable ambient temperature is required and it is difficult to be confident about their use in the field.

The use of a standard type of aspirated psychrometer, such as the Assmann, as a field reference has the advantage that its own integrity can be verified by comparing the dry- and wet-bulb thermometers, and that adequate aspiration may be expected from a healthy sounding fan. The reference instrument should itself be calibrated at intervals that are appropriate to its type.

It is important to check the calibration of electrical interfaces regularly and throughout their operational range. A simulator may be used in place of the sensor for this purpose. However, it will still be necessary to calibrate the ensemble at selected points, since the combination of calibration errors for sensor and interface which are individually within specification may be outside the specification for the ensemble.

Detailed maintenance requirements specific to each class of hygrometer described in this chapter are included in the appropriate section.

4.1.4.11 *Protective filters*

A protective filter is commonly used to protect a humidity sensor from contaminants that may adversely affect its performance. Where a sensor is not artificially aspirated, the use of a filter tends to slow the response rate of the sensor by preventing the bulk movement of air and by relying upon molecular diffusion through the filter material. Although the diffusion of water vapour through some materials, such as some cellulose products, is theoretically more rapid than for still air, porous hydrophobic membranes achieve better diffusion rates in practice. The pore size should be sufficiently small to trap harmful aerosol particles (in a maritime environment sea-salt particles may be present in significant quantity down to a diameter of 0.1 μm) and the porosity should be sufficient to allow an adequate diffusion rate.

The size of the filter, as well as its porosity, affects the overall diffusion rate. Diffusion will be enhanced by aspiration, but it must be remembered that this technique relies upon maintaining low air pressure on the sensing side of the filter, and that this can have a significant effect on the measurement.

Non-aspirated sensors should, in general, be protected using a hydrophobic, inert material. High-porosity polymer membranes made from an expanded form of polytetrafluoroethylene have been used successfully for this purpose in a variety of situations and are fairly robust.

Sintered metal filters may be used, but they should be heated to avoid problems with condensation within the material. This is not normally appropriate for a relative humidity sensor, but is quite acceptable for a dewpoint sensor. Sintered metal filters are robust and well suited for aspirated applications, which allow the use of a filter having a large surface area and, consequently, an acceptably small pressure differential.

Where diffusion is not enhanced by artificial aspiration, the relation of the surface area of the filter to the volume of the air being sampled by the sensor must be considered. In the case of a typical sorption sensor composed of a flat substrate, a flat membrane positioned close to the sensor surface will provide the optimum configuration. In the case of a cylindrical sensing surface, a cylindrical filter is appropriate.

4.2 THE PSYCHROMETER

4.2.1 General considerations

4.2.1.1 *Psychrometric formulae and tables*

The following paragraphs summarize the existing practice in drawing up psychrometric tables.

The usual practice is to derive the vapour pressure e' under the conditions of observation from the following semi-empirical psychrometric formulae:

$$e' = e'_w \left(p, T_w \right) - Ap \left(T - T_w \right) \tag{4.1}$$

and:

$$e' = e'_i \left(p, T_i \right) - Ap \left(T - T_i \right) \tag{4.2}$$

where e'_w is the saturation vapour pressure with respect to water at temperature T_w and pressure p of the wet bulb; e'_i is the saturation vapour pressure with respect to ice at temperature T_i and pressure p of the ice bulb; p is the pressure of the air; T the temperature of the dry bulb; and A is the psychrometer coefficient. (The latter is preferred to the term "psychrometer constant", which is a misnomer.)

The wet-bulb thermometer temperature T_w for most instruments is not identical to the thermodynamic wet-bulb temperature, defined in Annex 4.A, which depends only upon p, T and r (the humidity mixing ratio). The temperature measured by a practical wet-bulb

thermometer depends also upon a number of variables that are influenced by the dynamics of heat transfer across a liquid/gas interface (in which the gas must be characterized in terms of its component laminar and turbulent layers). The description of a satisfactory thermodynamic model is beyond the scope of this publication. The inequality of the thermodynamic and measured wet-bulb temperatures is resolved in practice through the empirical determination of the psychrometer coefficient A (see section 4.2.6).

In general, the coefficient A depends upon the design of the psychrometer (in particular the wet-bulb system), the rate of airflow past the wet bulb (termed the ventilation rate), and the air temperature and its humidity. At low rates of ventilation, A depends markedly upon the ventilation rate. However, at ventilation rates of 3 to 5 m s^{-1} (for thermometers of conventional dimensions) or higher, the value of A becomes substantially independent of the ventilation rate and is practically the same for well-designed psychrometers. The value of A does not, then, depend very much on temperature or humidity and its dependence on these variables is usually considered unimportant. A is smaller when the wet bulb is coated with ice than when it is covered with water.

The formulae and coefficients appropriate for the various forms of psychrometer are discussed in the following sections.

4.2.1.2　　*The specification of a psychrometer*

The equipment used for psychrometric observations should, as far as practicable, conform with the following recommendations (see sections 4.2.3 and 4.2.6):

(a)　At sea level, and in the case where the thermometers are of the types ordinarily used at meteorological stations, air should be drawn past the thermometer bulbs at a rate of no less than 2.2 m s^{-1} and no greater than 10 m s^{-1}. For appreciably different altitudes, these air speed limits should be adjusted in inverse proportion to the density of the atmosphere;

(b)　The wet and dry bulbs must be protected from radiation, preferably by a minimum of two shields. In a psychrometer with forced ventilation, such as the Assmann, the shields may be of polished, unpainted metal, separated from the rest of the apparatus by insulating material. Thermally insulating material is preferable in principle and must be used in psychrometers which rely on natural ventilation;

(c)　If the psychrometer is exposed in a louvred screen with forced ventilation, separate ventilation ducts should be provided for the two thermometers. The entrance to the ducts should be located so as to yield a measurement of the true ambient temperature, and the air should be exhausted above the screen in such a way as to prevent recirculation;

(d)　The greatest care should be taken to prevent the transfer of significant amounts of heat from an aspirating motor to the thermometers;

(e)　The water reservoir and wick should be arranged in such a way that the water will reach the bulb with sensibly the wet-bulb temperature, so as not to affect the temperature of the dry bulb.

4.2.1.3　　*The wet-bulb sleeve*

The wet bulb usually has a cotton wick, or similar fabric, fitting closely around the sensing element in order to maintain an even covering of water, which is either applied directly or by some form of capillary feed from a reservoir. The wick commonly takes the form of a sleeve that has a good fit around the bulb and extends at least 2 cm up the stem of the thermometer.

The fabric used to cover the wet bulb should be thin but closely woven. Before installation, it should be washed thoroughly in an aqueous solution of sodium bicarbonate ($NaHCO_3$), at a dilution of 5 g per litre, and rinsed several times in distilled water. Alternatively, a solution of pure detergent in water may be used. If a wick is to be employed, it should be similarly treated.

Any visible contamination of the wick or the wet-bulb sleeve should be considered an absolute indication of the necessity for its replacement. Great care should be exercised in handling the sleeve and wick to prevent contamination from hands. Distilled water should be used for the wet bulb.

The proper management of the wet bulb is particularly important. Observers should be encouraged to change the wet-bulb sleeve and wick regularly. These should be replaced at least once a week for all psychrometers that are continuously exposed. At places near the sea and in dusty or industrialized districts it may be necessary to replace these items more frequently. The water supply should be checked frequently and replaced or replenished as required.

Under hot, dry conditions, it can be an advantage to wet the covering with water from a porous vessel. This will cause the water to be pre-cooled by evaporation from the porous surface. The vessel should be kept in the shade, but not in the immediate vicinity of the psychrometer.

4.2.1.4 *Operation of the wet bulb below freezing*

The psychrometer is difficult to operate at temperatures below freezing, but it is used in climates where such temperatures occur. A wick cannot be used to convey water from a reservoir to the wet-bulb sleeve by capillary action when the wet-bulb temperature is below 0 °C. Under these conditions, care should be taken to form only a thin layer of ice on the sleeve. It is an absolute necessity that the thermometers be artificially ventilated; if they are not, the management of the wet bulb will be extremely difficult.

The water should, as far as possible, have a temperature close to freezing point. If a button of ice forms at the lowest part of the bulb, it should be immersed in water long enough to melt the ice.

The time required for the wet bulb to reach a steady reading after the sleeve is wetted depends on the ventilation rate and the actual wet-bulb temperature. An unventilated thermometer usually requires from 15 to 45 min, while an aspirated thermometer will require a much shorter period. It is essential that the formation of a new ice film on the bulb be made at an appropriate time. If hourly observations are being made with a simple psychrometer, it will usually be preferable to form a new coating of ice just after each observation. If the observations are made at longer intervals, the observer should visit the screen sufficiently in advance of each observation to form a new ice film on the bulb. The wet bulb of the aspirated and sling psychrometers should be moistened immediately before use.

The evaporation of an ice film may be prevented or slowed by enclosing the wet bulb in a small glass tube, or by stopping the ventilation inlet of the wet bulb between intervals. (Note that the latter course should not be taken if the circumstances are such that the ventilating fan would overheat.)

The effect of supercooled water on the wet bulb may be dealt with in two ways:

(a)   By using different tables when the wet bulb is coated with ice and with supercooled water, respectively. To find out which table should be used, the wet bulb should be touched with a snow crystal, a pencil or other object, just after each observation is completed. If the temperature rises towards 0 °C, and then commences to fall again, it can be assumed that the water on the wet bulb was supercooled at the time of the observation;

(b)   By using a table appropriate for an ice-covered wet bulb and inducing the freezing of supercooled water in the same way as for method (a). In order to save time and to ensure that the wet bulb is ice-covered, the observer should make a point of initiating the freezing of the water at each observation as soon as possible after moistening the bulb. From the

behaviour of the wetted thermometer at the freezing point it may usually be determined whether the bulb is covered by ice or by supercooled water. The recommended procedure, however, is to initiate the freezing of the water at each observation when the wet-bulb temperature is assumed to be below 0 °C, regardless of whether the behaviour of the thermometer after moistening has been observed or not.

Although the first method is usually the quickest, it requires two tables and this may cause some confusion.

4.2.1.5 *General procedure for making observations*

The procedures outlined in Part I, Chapter 2, for the measurement of temperature should be followed, in addition to the following procedures:

(a)   If the wet-bulb sleeve, wick or water has to be changed, this should be done sufficiently in advance of the observation. The period required for the correct wet-bulb temperature to be attained will depend upon the type of psychrometer;

(b)   The thermometers should be read to the nearest tenth of a degree;

(c)   When making an observation, the readings of the two thermometers should, as far as possible, be taken simultaneously, and it should be ascertained that the wet bulb is receiving a sufficient water supply.

4.2.1.6 *Use of electrical resistance thermometers*

Precision platinum electrical resistance thermometers are widely used in place of mercury-in-glass thermometers, in particular where remote reading and continuous measurements are required. It is necessary to ensure that the devices, and the interfacing electrical circuits selected, meet the performance requirements. These are detailed in Part I, Chapter 2. Particular care should always be taken with regard to self-heating effects in electrical thermometers.

The psychrometric formulae in Annex 4.B used for Assmann aspiration psychrometers are also valid if platinum resistance thermometers are used in place of the mercury-in-glass instruments, with different configurations of elements and thermometers. The formula for water on the wet bulb is also valid for some transversely ventilated psychrometers (WMO, 1989*a*).

4.2.1.7 *Sources of error in psychrometry*

The following main sources of error must be considered:

(a)   Index errors of the thermometers: It is very important in psychrometric measurements that the index errors of the thermometers be known over the actual temperature range and that corrections for these errors be applied to the readings before the humidity tables are used.

Any other errors in the wet-bulb or ice-bulb temperature caused by other influences will appear in the same way as index errors.

Table 4.2 shows the error in relative humidity $\varepsilon\,(U)$, derived from wet- and ice-bulb measurements having errors $\varepsilon\,(t_x)$, where x is water for $t > 0$ °C and ice for $t < 0$ °C, respectively of 0.5 and 0.1 K, for a relative humidity U of 50% and a range of true air temperatures (where the dry-bulb reading is assumed to give the true air temperature).

(b)   Thermometer lag coefficients: To obtain the highest accuracy with a psychrometer it is desirable to arrange for the wet and dry bulbs to have approximately the same lag coefficient; with thermometers having the same bulb size, the wet bulb has an appreciably smaller lag than the dry bulb.

Table 4.2. Error in derived relative humidity resulting from wet- and ice-bulb index errors $\varepsilon\ (t_x)$ for $U = 50\%$

Air temperature in °C	Error in relative humidity, $\varepsilon\ (U)$ in % due to an error in wet- or ice-bulb temperature	
	$\varepsilon\ (t_x) = 0.5\ K$	$\varepsilon\ (t_x) = 0.1\ K$
–30	60	12
–20	27	5
–10	14	3
0	8	2
10	5	1
20	4	0.5
30	3	0.5
40	2	0.5
50	2	0

(c)   Errors relating to ventilation: Errors due to insufficient ventilation become much more serious through the use of inappropriate humidity tables (see sections covering individual psychrometer types).

(d)   Errors due to excessive covering of ice on the wet bulb: Since a thick coating of ice will increase the lag of the thermometer, it should be removed immediately by dipping the bulb into distilled water.

(e)   Errors due to contamination of the wet-bulb sleeve or to impure water: Large errors may be caused by the presence of substances that alter the vapour pressure of water. The wet bulb with its covering sleeve should be washed at regular intervals in distilled water to remove soluble impurities. This procedure is more frequently necessary in some regions than others, for example, at or near the sea or in areas subject to air pollution.

(f)   Errors due to heat conduction from the thermometer stem to the wet-bulb system: The conduction of heat from the thermometer stem to the wet bulb will reduce the wet-bulb depression and lead to determinations of humidity that are too high. The effect is most pronounced at low relative humidity but can be effectively eliminated by extending the wet-bulb sleeve at least 2 cm beyond the bulb up the stem of the thermometer.

4.2.2   **The Assmann aspirated psychrometer**

4.2.2.1   *Description*

Two mercury-in-glass thermometers, mounted vertically side by side in a chromium- or nickel-plated polished metal frame, are connected by ducts to an aspirator. The aspirator may be driven by a spring or an electric motor. One thermometer bulb has a well-fitted muslin wick which, before use, is moistened with distilled water. Each thermometer is located inside a pair of coaxial metal tubes, highly polished inside and out, which screen the bulbs from external thermal radiation. The tubes are all thermally insulated from each other.

A WMO international intercomparison of Assmann-type psychrometers from 10 countries (WMO, 1989*a*) showed that there is good agreement between dry- and wet-bulb temperatures of psychrometers with the dimensional specifications close to the original specification, and with aspiration rates above 2.2 m s⁻¹. Not all commercially available instruments fully comply. A more

detailed discussion is found in WMO (1989*a*). The performance of the Assmann psychrometer in the field may be as good as the achievable accuracy stated in Part I, Chapter 1, Annex 1.E of this Guide, and with great care it can be significantly improved.

Annex 4.B lists standard formulae for the computation of measures of humidity using an Assmann psychrometer,[3] which are the bases of some of the other artificially ventilated psychrometers, in the absence of well-established alternatives.

4.2.2.2   *Observation procedure*

The wick, which must be free of grease, is moistened with distilled water. Dirty or crusty wicks should be replaced. Care should be taken not to introduce a water bridge between the wick and the radiation shield.

The mercury columns of the thermometers should be inspected for breaks, which should be closed up or the thermometer should be replaced.

The instrument is normally operated with the thermometers held vertically. The thermometer stems should be protected from solar radiation by turning the instrument so that the lateral shields are in line with the sun. The instrument should be tilted so that the inlet ducts open into the wind, but care should be taken so that solar radiation does not fall on the thermometer bulbs. A wind screen is necessary in very windy conditions when the rotation of the aspirator is otherwise affected.

The psychrometer should be in thermal equilibrium with the surrounding air. At air temperatures above 0 °C, at least three measurements at 1 min intervals should be taken following an aspiration period. Below 0 °C it is necessary to wait until the freezing process has finished, and to observe whether there is water or ice on the wick. During the freezing and thawing processes the wet-bulb temperature remains constant at 0 °C. In the case of outdoor measurements, several measurements should be taken and the average taken. Thermometer readings should be made with a resolution of 0.1 K or better.

A summary of the observation procedure is as follows:

(a)   Moisten the wet bulb;

(b)   Wind the clockwork motor (or start the electric motor);

(c)   Wait 2 or 3 min or until the wet-bulb reading has become steady;

(d)   Read the dry bulb;

(e)   Read the wet bulb;

(f)   Check the reading of the dry bulb.

4.2.2.3   *Exposure and siting*

Observations should be made in an open area with the instrument either suspended from a clamp or attached using a bracket to a thin post, or held with one hand at arm's length with the inlets slightly inclined into the wind. The inlets should be at a height of 1.25 to 2 m above ground for normal measurements of air temperature and humidity.

Great care should be taken to prevent the presence of the observer or any other nearby sources of heat and water vapour, such as the exhaust pipe of a motor vehicle, from having an influence on the readings.

---

[3]   Recommended by the Commission for Instruments and Methods of Observation at its tenth session (1989).

4.2.2.4   *Calibration*

The ventilation system should be checked regularly, at least once per month.

The calibration of the thermometers should also be checked regularly. The two may be compared together, with both thermometers measuring the dry-bulb temperature. Comparison with a certified reference thermometer should be performed at least once a year.

4.2.2.5   *Maintenance*

Between readings, the instrument should be stored in an unheated room or be otherwise protected from precipitation and strong insolation. When not in use, the instrument should be stored indoors in a sturdy packing case such as that supplied by the manufacturer.

4.2.3   Screen psychrometer

4.2.3.1   *Description*

Two mercury-in-glass thermometers are mounted vertically in a thermometer screen. The diameter of the sensing bulbs should be about 10 mm. One of the bulbs is fitted with a wet-bulb sleeve, which should fit closely to the bulb and extend at least 20 mm up the stem beyond it. If a wick and water reservoir are used to keep the wet-bulb sleeve in a moist condition, the reservoir should preferably be placed to the side of the thermometer and with the mouth at the same level as, or slightly lower than, the top of the thermometer bulb. The wick should be kept as straight as possible and its length should be such that water reaches the bulb with sensibly the wet-bulb temperature and in sufficient (but not excessive) quantity. If no wick is used, the wet bulb should be protected from dirt by enclosing the bulb in a small glass tube between readings.

It is recommended that screen psychrometers be artificially aspirated. Both thermometers should be aspirated at an air speed of about 3 m s^{-1}. Both spring-wound and electrically driven aspirators are in common use. The air should be drawn in horizontally across the bulbs, rather than vertically, and exhausted in such a way as to avoid recirculation.

The performance of the screen psychrometer may be much worse than that shown in Part I, Chapter 1, Annex 1.E of this Guide, especially in light winds if the screen is not artificially ventilated.

The psychrometric formulae given in section 4.2.1.1 apply to screen psychrometers, but the coefficients are quite uncertain. A summary of some of the formulae in use is given by Bindon (1965). If there is artificial ventilation at 3 m s^{-1} or more across the wet bulb, the values given in Annex 4.B may be applied, with a psychrometer coefficient of 6.53 · 10^{-4} K^{-1} for water. However, values from 6.50 to 6.78 · 10^{-4} are in use for wet bulbs above 0 °C, and 5.70 to 6.53 · 10^{-4} for below 0 °C. For a naturally ventilated screen psychrometer, coefficients in use range from 7.7 to 8.0 · 10^{-4} above freezing and 6.8 to 7.2 · 10^{-4} for below freezing when there is some air movement in the screen, which is probably nearly always the case. However, coefficients up to 12 · 10^{-4} for water and 10.6 · 10^{-4} for ice have been advocated for when there is no air movement.

The psychrometer coefficient appropriate for a particular configuration of screen, shape of wet bulb and degree of ventilation may be determined by comparison with a suitable working or reference standard, but there will be a wide scatter in the data, and a very large experiment would be necessary to obtain a stable result. Even when a coefficient has been obtained by such an experiment, the confidence limits for any single observation will be wide, and there would be little justification for departing from established national practices.

4.2.3.2 *Special observation procedures*

The procedures described in section 4.2.1.5 apply to the screen psychrometer. In the case of a naturally aspirated wet bulb, provided that the water reservoir has about the same temperature as the air, the correct wet-bulb temperature will be attained approximately 15 min after fitting a new sleeve; if the water temperature differs substantially from that of the air, it may be necessary to wait for 30 min.

4.2.3.3 *Exposure and siting*

The exposure and siting of the screen are described in Part I, Chapter 2.

4.2.4 **Sling or whirling psychrometers**

4.2.4.1 *Description*

A small portable type of whirling or sling psychrometer consists of two mercury-in-glass thermometers mounted on a sturdy frame, which is provided with a handle and spindle, and located at the furthest end from the thermometer bulbs, by means of which the frame and thermometers may be rotated rapidly about a horizontal axis.

The wet-bulb arrangement varies according to individual design. Some designs shield the thermometer bulbs from direct insolation, and these are to be preferred for meteorological measurements.

The psychrometric formulae in Annex 4.B may be used.

4.2.4.2 *Observation procedure*

The following guidelines should be applied:

(a) All instructions with regard to the handling of Assmann aspirated psychrometers apply also to sling psychrometers;

(b) Sling psychrometers lacking radiation shields for the thermometer bulbs should be shielded from direct insolation in some other way;

(c) Thermometers should be read at once after aspiration ceases because the wet-bulb temperature will begin to rise immediately, and the thermometers are likely to be subject to insolation effects.

4.2.5 **Heated psychrometer**

The principle of the heated psychrometer is that the water-vapour content of an air mass does not change if it is heated. This property may be exploited to the advantage of the psychrometer by avoiding the need to maintain an ice bulb under freezing conditions.

4.2.5.1 *Description*

Air is drawn into a duct where it passes over an electrical heating element and then into a measuring chamber containing both dry- and wet-bulb thermometers and a water reservoir. The heating element control circuit ensures that the air temperature does not fall below a certain level, which might typically be 10 °C. The temperature of the water reservoir is maintained in a similar way. Thus, neither the water in the reservoir nor the water at the wick should freeze, provided that the wet-bulb depression is less than 10 K, and that the continuous operation of

the psychrometer is secured even if the air temperature is below 0 °C. At temperatures above 10 °C the heater may be automatically switched off, when the instrument reverts to normal psychrometric operation.

Electrical thermometers are used so that they may be entirely enclosed within the measuring chamber and without the need for visual readings.

A second dry-bulb thermometer is located at the inlet of the duct to provide a measurement of the ambient air temperature. Thus, the ambient relative humidity may be determined.

The psychrometric thermometer bulbs are axially aspirated at an air velocity in the region of 3 m s^{-1}.

4.2.5.2 *Observation procedure*

A heated psychrometer would be suitable for automatic weather stations.

4.2.5.3 *Exposure and siting*

The instrument itself should be mounted outside a thermometer screen. The air inlet, where ambient air temperature is measured, should be inside the screen.

4.2.6 **The WMO reference psychrometer**

The reference psychrometer and procedures for its operation are described in WMO (1992). The wet- and dry-bulb elements are enclosed in an aspirated shield, for use as a free-standing instrument. Its significant characteristic is that the psychrometer coefficient is calculable from the theory of heat and mass exchanges at the wet bulb, and is different from the coefficient for other psychrometers, with a value of $6.53 \cdot 10^{-4}$ K^{-1} at 50% relative humidity, 20 °C and 1 000 hPa. Its wet-bulb temperature is very close to the theoretical value (see Annex 4.A, paragraphs 18 and 19). This is achieved by ensuring that the evaporation at the wet bulb is very efficient and that extraneous heating is minimized. The nature of the airflow over the wet bulb is controlled by careful shaping of the duct and the bulb, and by controlling the ventilation rate. The double shield is highly reflective externally, and blackened on the inside, and the thermometer elements are insulated and separated by a shield. The shields and the wet-bulb element (which contains the thermometer) are made of stainless steel to minimize thermal conduction.

The procedures for the use of the reference psychrometer ensure that the wet bulb is completely free of grease, even in the monomolecular layers that always arise from handling any part of the apparatus with the fingers. This is probably the main reason for the close relation of the coefficient to the theoretical value, and its difference from the psychrometer coefficients of other instruments.

The reference psychrometer is capable of great accuracy, 0.38% uncertainty in relative humidity at 50% relative humidity and 20 °C. It has also been adopted as the WMO reference thermometer. It is designed for use in the field but is not suitable for routine use. It should be operated only by staff accustomed to very precise laboratory work. Its use as a reference instrument is discussed in section 4.9.7.

4.3 THE HAIR HYGROMETER

4.3.1 General considerations

Any absorbing material tends to equilibrium with its environment in terms of both temperature and humidity. The water-vapour pressure at the surface of the material is determined by the temperature and the amount of water bound by the material. Any difference between this pressure and the water-vapour pressure of the surrounding air will be equalized by the exchange of water molecules.

The change in the length of hair has been found to be a function primarily of the change in relative humidity with respect to liquid water (both above and below an air temperature of 0 °C), with an increase of about 2% to 2.5% when the humidity changes from 0% to 100%. By rolling the hairs to produce an elliptical cross-section and by dissolving out the fatty substances with alcohol, the ratio of the surface area to the enclosed volume increases and yields a decreased lag coefficient which is particularly relevant for use at low air temperatures. This procedure also results in a more linear response function, although the tensile strength is reduced. For accurate measurements, a single hair element is to be preferred, but a bundle of hairs is commonly used to provide a degree of ruggedness. Chemical treatment with barium (BaS) or sodium sulphide (Na_2S) yields further linearity of response.

The hair hygrograph or hygrometer is considered to be a satisfactory instrument for use in situations or during periods where extreme and very low humidities are seldom or never found. The mechanism of the instrument should be as simple as possible, even if this makes it necessary to have a non-linear scale. This is especially important in industrial regions, since air pollutants may act on the surface of the moving parts of the mechanism and increase friction between them.

The rate of response of the hair hygrometer is very dependent on air temperature. At –10 °C the lag of the instrument is approximately three times greater than the lag at 10 °C. For air temperatures between 0 °C and 30 °C and relative humidities between 20% and 80% a good hygrograph should indicate 90% of a sudden change in humidity within about 3 min.

A good hygrograph in perfect condition should be capable of recording relative humidity at moderate temperatures with an uncertainty of ±3%. At low temperatures, the uncertainty will be greater.

Using hair pre-treated by rolling (as described above) is a requirement if useful information is to be obtained at low temperatures.

4.3.2 Description

The detailed mechanism of hair hygrometers varies according to the manufacturer. Some instruments incorporate a transducer to provide an electrical signal, and these may also provide a linearizing function so that the overall response of the instrument is linear with respect to changes in relative humidity.

The most commonly used hair hygrometer is the hygrograph. This employs a bundle of hairs held under slight tension by a small spring and connected to a pen arm in such a way as to magnify a change in the length of the bundle. A pen at the end of the pen arm is in contact with a paper chart fitted around a metal cylinder and registers the angular displacement of the arm. The cylinder rotates about its axis at a constant rate determined by a mechanical clock movement. The rate of rotation is usually one revolution either per week or per day. The chart has a scaled time axis that extends round the circumference of the cylinder and a scaled humidity axis parallel to the axis of the cylinder. The cylinder normally stands vertically.

The mechanism connecting the pen arm to the hair bundle may incorporate specially designed cams that translate the non-linear extension of the hair in response to humidity changes into a linear angular displacement of the arm.

The hair used in hygrometers may be of synthetic fibre. Where human hair is used it is normally first treated as described in section 4.3.1 to improve both the linearity of its response and the response lag, although this does result in a lower tensile strength.

The pen arm and clock assembly are normally housed in a box with glass panels which allow the registered humidity to be observed without disturbing the instrument, and with one end open to allow the hair element to be exposed in free space outside the limits of the box. The sides of the box are separate from the solid base, but the end opposite the hair element is attached to it by a hinge. This arrangement allows free access to the clock cylinder and hair element. The element may be protected by an open mesh cage.

4.3.3 Observation procedure

The hair hygrometer should always be tapped lightly before being read in order to free any tension in the mechanical system. The hygrograph should, as far as possible, not be touched between changes of the charts except in order to make time marks.

Both the hygrometer and the hygrograph can normally be read to the nearest 1% of relative humidity. Attention is drawn to the fact that the hair hygrometer measures relative humidity with respect to saturation over liquid water even at air temperatures below 0 °C.

The humidity of the air may change very rapidly and, therefore, accurate setting of time marks on a hygrograph is very important. In making the marks, the pen arm should be moved only in the direction of decreasing humidity on the chart. This is done so that the hairs are slackened by the displacement and, to bring the pen back to its correct position, the restoring force is applied by the tensioning spring. However, the effect of hysteresis may be evidenced in the failure of the pen to return to its original position.

4.3.4 Exposure and siting

The hygrograph or hygrometer should be exposed in a thermometer screen. Ammonia is very destructive to natural hair. Exposure in the immediate vicinity of stables and industrial plants using ammonia should be avoided.

When used in polar regions, the hygrograph should preferably be exposed in a special thermometer screen which provides the instrument with sufficient protection against precipitation and drifting snow. For example, a cover for the thermometer screen can be made of fine-meshed net (Mullergas) as a precautionary measure to prevent the accumulation of snow crystals on the hairs and the bearing surfaces of the mechanical linkage. This method can be used only if there is no risk of the net being wetted by melting snow crystals.

4.3.5 Sources of error

4.3.5.1 *Changes in zero offset*

For various reasons which are poorly understood, the hygrograph is liable to change its zero. The most likely cause is that excess tension has been induced in the hairs. For instance, the hairs may be stretched if time marks are made in the direction of increasing humidity on the chart or if the hygrograph mechanism sticks during decreasing humidity. The zero may also change if the hygrograph is kept in very dry air for a long time, but the change may be reversed by placing the instrument in a saturated atmosphere for a sufficient length of time.

4.3.5.2　*Errors due to contamination of the hair*

Most kinds of dust will cause appreciable errors in observations (perhaps as much as 15% relative humidity). In most cases this may be eliminated, or at least reduced, by cleaning and washing the hairs. However, the harmful substances found in dust may also be destructive to hair (see section 4.3.4).

4.3.5.3　*Hysteresis*

Hysteresis is exhibited both in the response of the hair element and in the recording mechanism of the hair hygrometer. Hysteresis in the recording mechanism is reduced through the use of a hair bundle, which allows a greater loading force to overcome friction. It should be remembered that the displacement magnification of the pen arm lever applies also to the frictional force between the pen and paper, and to overcome this force it requires a proportionately higher tension in the hair. The correct setting of the tensioning spring is also required to minimize hysteresis, as is the correct operation of all parts of the transducing linkage. The main fulcrum and any linearizing mechanism in the linkage introduce much of the total friction.

Hysteresis in the hair element is normally a short-term effect related to the absorption–desorption processes and is not a large source of error once vapour pressure equilibrium is established (see section 4.3.5.1 in respect of prolonged exposure at low humidity).

4.3.6　**Calibration and comparisons**

The readings of a hygrograph should be checked as frequently as is practical. In the case where wet- and dry-bulb thermometers are housed in the same thermometer screen, these may be used to provide a comparison whenever suitable steady conditions prevail, but otherwise field comparisons have limited value due to the difference in response rate of the instruments.

Accurate calibration can only be obtained through the use of an environmental chamber and by comparison with reference instruments.

The 100% humidity point may be checked, preferably indoors with a steady air temperature, by surrounding the instrument with a saturated cloth (though the correct reading will not be obtained if a significant mass of liquid water droplets forms on the hairs).

The ambient indoor humidity may provide a low relative humidity checkpoint for comparison against a reference aspirated psychrometer. A series of readings should be obtained.

Long-term stability and bias may be appraised by presenting comparisons with a reference aspirated psychrometer in terms of a correlation function.

4.3.7　**Maintenance**

Observers should be encouraged to keep the hygrometer clean.

The hair should be washed at frequent intervals using distilled water on a soft brush to remove accumulated dust or soluble contaminants. At no time should the hair be touched by fingers. The bearings of the mechanism should be kept clean and a small amount of clock oil should be applied occasionally. The bearing surfaces of any linearizing mechanism will contribute largely to the total friction in the linkage, which may be minimized by polishing the surfaces with graphite. This procedure may be carried out by using a piece of blotting paper rubbed with a lead pencil.

With proper care, the hairs may last for several years in a temperate climate and when not subject to severe atmospheric pollution. Recalibration and adjustment will be required when hairs are replaced.

4.4 THE CHILLED-MIRROR DEWPOINT HYGROMETER

4.4.1 General considerations

4.4.1.1 *Theory*

The dewpoint (or frost-point) hygrometer is used to measure the temperature at which moist air, when cooled, reaches saturation and a deposit of dew (or ice) can be detected on a solid surface, which usually is a mirror. The deposit is normally detected optically. The principle of the measurement is described in section 4.1.4.5 and below.

The thermodynamic dewpoint is defined for a plane surface of pure water. In practice, water droplets have curved surfaces, over which the saturation vapour pressure is higher than for the plane surface (known as the Kelvin effect). Hydrophobic contaminants will exaggerate the effect, while soluble ones will have the opposite effect and lower the saturation vapour pressure (the Raoult effect). The Kelvin and Raoult effects (which, respectively, raise and lower the apparent dewpoint) are minimized if the critical droplet size adopted is large rather than small; this reduces the curvature effect directly and reduces the Raoult effect by lowering the concentration of a soluble contaminant.

4.4.1.2 *Principles*

When moist air at temperature T, pressure p and mixing ratio r_w (or r_i) is cooled, it eventually reaches its saturation point with respect to a free water surface (or to a free ice surface at lower temperatures) and a deposit of dew (or frost) can be detected on a solid non-hygroscopic surface. The temperature of this saturation point is called the thermodynamic dewpoint temperature T_d (or the thermodynamic frost-point temperature T_f). The corresponding saturation vapour pressure with respect to water e'_w (or ice e'_i) is a function of T_d (or T_f), as shown in the following equations:

$$e'_w\left(p,T_d\right) = f\left(p\right)\cdot e_w\left(T_d\right) = \frac{r\cdot p}{0.621\,98 + r} \tag{4.3}$$

$$e'_i\left(p,T_f\right) = f\left(p\right)\cdot e_i\left(T_f\right) = \frac{r\cdot p}{0.621\,98 + r} \tag{4.4}$$

The hygrometer measures T_d or T_f. Despite the great dynamic range of moisture in the troposphere, this instrument is capable of detecting both very high and very low concentrations of water vapour by means of a thermal sensor alone.

Cooling using a low-boiling-point liquid has been used but is now largely superseded except for very low water-vapour concentrations.

It follows from the above that it must also be possible to determine whether the deposit is supercooled liquid or ice when the surface temperature is at or below freezing point.

The chilled-mirror hygrometer is used for meteorological measurements and as a reference instrument both in the field and in the laboratory.

4.4.2 Description

4.4.2.1 *Sensor assembly*

The most widely used systems employ a small polished-metal reflecting surface, cooled electrically using a Peltier-effect device. The sensor consists of a thin metallic mirror of small (2 to 5 mm) diameter that is thermally regulated using a cooling assembly (and possibly a heater), with a temperature sensor (thermocouple or platinum resistance thermometer) embedded on the underside of the mirror. The mirror should have a high thermal conductance,

optical reflectivity and corrosion resistance combined with a low permeability to water vapour. Suitable materials used include gold, rhodium-plated silver, chromium-plated copper and stainless steel.

The mirror should be equipped with a (preferably automatic) device for detecting contaminants that may increase or decrease the apparent dewpoint (see section 4.4.2.2), so that they may be removed.

4.4.2.2 *Optical detection assembly*

An electro-optical system is usually employed to detect the formation of condensate and to provide the input to the servo-control system to regulate the temperature of the mirror. A narrow beam of light is directed at the mirror at an angle of incidence of about 55°. The light source may be incandescent but is now commonly a light-emitting diode. In simple systems, the intensity of the directly reflected light is detected by a photodetector that regulates the cooling and heating assembly through a servo-control. The specular reflectivity of the surface decreases as the thickness of the deposit increases; cooling should cease while the deposit is thin, with a reduction in reflectance in the range of 5% to 40%. More elaborate systems use an auxiliary photodetector which detects the light scattered by the deposit; the two detectors are capable of very precise control. A second, uncooled, mirror may be used to improve the control system.

Greatest precision is obtained by controlling the mirror to a temperature at which condensate neither accumulates nor dissipates; however, in practice, the servo-system will oscillate around this temperature. The response time of the mirror to heating and cooling is critical in respect of the amplitude of the oscillation, and should be of the order of 1 to 2 s. The airflow rate is also important for maintaining a stable deposit on the mirror. It is possible to determine the temperature at which condensation occurs with a precision of 0.05 K.

It is feasible, but a time-consuming and skilled task, to observe the formation of droplets by using a microscope and to regulate the mirror temperature under manual control.

4.4.2.3 *Thermal control assembly*

A Peltier-effect thermo-junction device provides a simple reversible heat pump; the polarity of direct current energization determines whether heat is pumped to, or from, the mirror. The device is bonded to, and in good thermal contact with, the underside of the mirror. For very low dewpoints, a multistage Peltier device may be required.

Thermal control is achieved by using an electrical servo-system that takes as input the signal from the optical detector subsystem. Modern systems operate under microprocessor control.

A low-boiling-point fluid, such as liquid nitrogen, may be used to provide cooling, but this technique is no longer widely used. Similarly, electrical resistance wire may be used for heating but has now been superseded with the advent of small Peltier devices.

4.4.2.4 *Temperature display system*

The mirror temperature, as measured by the electrical thermometer embedded beneath the mirror surface, is presented to the observer as the dewpoint of the air sample. Commercial instruments normally include an electrical interface for the mirror thermometer and a digital display, but may also provide digital and analogue electrical outputs for use with data-logging equipment. A chart recorder is particularly useful for monitoring the performance of the instrument in the case where the analogue output provides a continuous registration of the mirror thermometer signal but the digital display does not.

4.4.2.5 *Auxiliary systems*

A microscope may be incorporated to provide a visual method to discriminate between supercooled water droplets and ice crystals for mirror temperatures below 0 °C. Some instruments have a detector mounted on the mirror surface to provide an automatic procedure for this purpose (for example, capacitive sensor), while others employ a method based on reflectance.

A microprocessor-based system may incorporate algorithms to calculate and display relative humidity. In this case, it is important that the instrument should discriminate correctly between a water and an ice deposit.

Many instruments provide an automatic procedure for minimizing the effects of contamination. This may be a regular heating cycle in which volatile contaminants are evaporated and removed in the air stream. Systems with a wiper to automatically clean the mirror by means of a wiper are also in use.

For meteorological measurements, and in most laboratory applications, a small pump is required to draw the sampled air through the measuring chamber. A regulating device is also required to set the flow at a rate that is consistent with the stable operation of the mirror temperature servo-control system and at an acceptable rate of response to changes in humidity. The optimum flow rate is dependent upon the moisture content of the air sample and is normally within the range of 0.25 to 1 l min^{-1}.

4.4.3 Observation procedure

The correct operation of a dewpoint hygrometer depends upon achieving an appropriate volume airflow rate through the measuring chamber. The setting of a regulator for this purpose, usually a throttling device located downstream of the measuring chamber, is likely to require adjustment to accommodate diurnal variations in air temperature. Adjustment of the airflow will disturb the operation of the hygrometer, and it may even be advisable to initiate a heating cycle. Both measures should be taken with sufficient time in order for a stable operation to be achieved before a reading is taken. The amount of time required will depend upon the control cycle of the individual instrument. The manufacturer's instructions should be consulted to provide appropriate guidance on the airflow rate to be set and on details of the instrument's control cycle.

The condition of the mirror should be checked frequently; the mirror should be cleaned as necessary. The stable operation of the instrument does not necessarily imply that the mirror is clean. It should be washed with distilled water and dried carefully by wiping it with a soft cloth or cotton dabstick to remove any soluble contaminant. Care must be taken not to scratch the surface of the mirror, most particularly where the surface has a thin plating to protect the substrate or where an ice/liquid detector is incorporated. If an air filter is not in use, cleaning should be performed at least daily. If an air filter is in use, its condition should be inspected at each observation. The observer should take care not to stand next to the air inlet or to allow the outlet to become blocked.

For readings at, or below, 0 °C the observer should determine whether the mirror condensate is supercooled water or ice. If no automatic indication is given, the mirror must be observed. From time to time the operation of any automatic system should be verified.

An uncertainty of ±0.3 K over a wide dewpoint range (–60 °C to 50 °C) is specified for the best instruments.

4.4.4 Exposure and siting

The criteria for the siting of the sensor unit are similar to those for any aspirated hygrometer, although less stringent than for either a psychrometer or a relative humidity sensor, considering

the fact that the dew or frost point of an air sample is unaffected by changes to the ambient temperature provided that it remains above the dewpoint at all times. For this reason, a temperature screen is not required. The sensor should be exposed in an open space and may be mounted on a post, within a protective housing structure, with an air inlet at the required level.

An air-sampling system is required. This is normally a small pump that must draw air from the outlet port of the measuring chamber and eject it away from the inlet duct. Recirculation of the airflow should be avoided as this represents a poor sampling technique, although under stable operation the water-vapour content at the outlet should be effectively identical to that at the inlet. Recirculation may be avoided by fixing the outlet above the inlet, although this may not be effective under radiative atmospheric conditions when a negative air temperature lapse rate exists.

An air filter should be provided for continuous outdoor operations. It must be capable of allowing an adequate throughflow of air without a large blocking factor, as this may result in a significant drop in air pressure and affect the condensation temperature in the measuring chamber. A sintered metal filter may be used in this application to capture all but the smallest aerosol particles. A metal filter has the advantage that it may be heated easily by an electrical element in order to keep it dry under all conditions. It is more robust than the membrane-type filter and more suited to passing the relatively high airflow rates required by the chilled-mirror method as compared with the sorption method. On the other hand, a metallic filter may be more susceptible to corrosion by atmospheric pollutants than some membrane filters.

4.4.5 Calibration

Regular comparisons against a reference instrument, such as an Assmann psychrometer or another chilled-mirror hygrometer, should be made as the operation of a field chilled mirror is subject to a number of influences which may degrade its performance. An instrument continuously in the field should be the subject of weekly check measurements. As the opportunity arises, its operation at both dew and frost points should be verified. When the mirror temperature is below 0 °C the deposit should be inspected visually, if this is possible, to determine whether it is of supercooled water or ice.

A useful check is to compare the mirror temperature measurement with the air temperature while the thermal control system of the hygrometer is inactive. The instrument should be aspirated, and the air temperature measured at the mouth of the hygrometer air intake. This check is best performed under stable, non-condensing conditions. In bright sunshine, the sensor and duct should be shaded and allowed to come to equilibrium. The aspiration rate may be increased for this test.

An independent field calibration of the mirror thermometer interface may be performed by simulating the thermometer signal. In the case of a platinum resistance thermometer, a standard platinum resistance simulation box, or a decade resistance box and a set of appropriate tables, may be used. A special simulator interface for the hygrometer control unit may also be required.

4.5 THE LITHIUM CHLORIDE HEATED CONDENSATION HYGROMETER (DEW CELL)

4.5.1 General considerations

4.5.1.1 *Principles*

The physical principles of the heated salt-solution method are discussed in section 4.1.4.5.2. The equilibrium vapour pressure at the surface of a saturated lithium chloride solution is exceptionally low. As a consequence, a solution of lithium chloride is extremely hygroscopic under typical conditions of surface atmospheric humidity; if the ambient vapour pressure

exceeds the equilibrium vapour pressure of the solution, water vapour will condense over it (for example, at 0 °C water vapour condenses over a plane surface of a saturated solution of lithium chloride to only 15% relative humidity).

A thermodynamically self-regulating device may be achieved if the solution is heated directly by passing an electrical current through it from a constant-voltage device. An alternating current should be used to prevent polarization of the solution. As the electrical conductivity decreases, so will the heating current, and an equilibrium point will be reached whereby a constant temperature is maintained; any cooling of the solution will result in the condensation of water vapour, thus causing an increase in conductivity and an increase in heating current, which will reverse the cooling trend. Heating beyond the balance point will evaporate water vapour until the consequent fall in conductivity reduces the electrical heating to the point where it is exceeded by heat losses, and cooling ensues.

It follows from the above that there is a lower limit to the ambient vapour pressure that may be measured in this way at any given temperature. Below this value, the salt solution would have to be cooled in order for water vapour to condense. This would be equivalent to the chilled-mirror method except that, in the latter case, condensation takes place at a lower temperature when saturation is achieved with respect to a pure water surface, namely, at the ambient dewpoint.

A degree of uncertainty is inherent in the method due to the existence of four different hydrates of lithium chloride. At certain critical temperatures, two of the hydrates may be in equilibrium with the aqueous phase, and the equilibrium temperature achieved by heating is affected according to the hydrate transition that follows. The most serious ambiguity for meteorological purposes occurs for ambient dewpoint temperatures below –12 °C. For an ambient dewpoint of –23 °C, the potential difference in equilibrium temperature, according to which one of the two hydrate-solution transitions takes place, results in an uncertainty of ±3.5 K in the derived dewpoint value.

4.5.1.2   *Description*

The dew-cell hygrometer measures the temperature at which the equilibrium vapour pressure for a saturated solution of lithium chloride is equal to the ambient water-vapour pressure. Empirical transformation equations, based on saturation vapour pressure data for lithium chloride solution and for pure water, provide for the derivation of the ambient water vapour and dewpoint with respect to a plane surface of pure water. The dewpoint temperature range of –12 °C to 25 °C results in dew-cell temperatures in the range of 17 °C to 71 °C.

4.5.1.3   *Sensors with direct heating*

The sensor consists of a tube, or bobbin, with a resistance thermometer fitted axially within. The external surface of the tube is covered with a glass fibre material (usually tape wound around and along the tube) that is soaked with an aqueous solution of lithium chloride, sometimes combined with potassium chloride. Bifilar silver or gold wire is wound over the covering of the bobbin, with equal spacing between the turns. An alternating electrical current source is connected to the two ends of the bifilar winding; this is commonly derived from the normal electrical supply (50 or 60 Hz). The lithium chloride solution is electrically conductive to a degree determined by the concentration of solute. A current passes between adjacent bifilar windings, which act as electrodes, and through the solution. The current heats the solution, which increases in temperature.

Except under conditions of extremely low humidity, the ambient vapour pressure will be higher than the equilibrium vapour pressure over the solution of lithium chloride at ambient air temperature, and water vapour will condense onto the solution. As the solution is heated by the electrical current, a temperature will eventually be reached above which the equilibrium vapour pressure exceeds the ambient vapour pressure, evaporation will begin, and the concentration of the solution will increase.

An operational equilibrium temperature exists for the instrument, depending upon the ambient water-vapour pressure. Above the equilibrium temperature, evaporation will increase the concentration of the solution, and the electrical current and the heating will decrease and allow heat losses to cause the temperature of the solution to fall. Below the equilibrium temperature, condensation will decrease the concentration of the solution, and the electrical current and the heating will increase and cause the temperature of the solution to rise. At the equilibrium temperature, neither evaporation nor condensation occurs because the equilibrium vapour pressure and the ambient vapour pressure are equal.

In practice, the equilibrium temperature measured is influenced by individual characteristics of sensor construction and has a tendency to be higher than that predicted from equilibrium vapour-pressure data for a saturated solution of lithium chloride. However, reproducibility is sufficiently good to allow the use of a standard transfer function for all sensors constructed to a given specification.

Strong ventilation affects the heat transfer characteristics of the sensor, and fluctuations in ventilation lead to unstable operation.

In order to minimize the risk of excessive current when switching on the hygrometer (as the resistance of the solution at ambient temperature is rather low), a current-limiting device, in the form of a small lamp, is normally connected to the heater element. The lamp is chosen so that, at normal bobbin-operating currents, the filament resistance will be low enough for the hygrometer to function properly, while the operating current for the incandescent lamp (even allowing for a bobbin-offering no electrical resistance) is below a value that might damage the heating element.

The equilibrium vapour pressure for saturated lithium chloride depends upon the hydrate being in equilibrium with the aqueous solution. In the range of solution temperatures corresponding to dewpoints of –12 °C to 41 °C monohydrate normally occurs. Below –12 °C, dihydrate forms, and above 41 °C, anhydrous lithium chloride forms. Close to the transition points, the operation of the hygrometer is unstable and the readings ambiguous. However, the –12 °C lower dewpoint limit may be extended to –30 °C by the addition of a small amount of potassium chloride (KCl).

4.5.1.4   *Sensors with indirect heating*

Improved accuracy, compared with the arrangement described in section 4.5.1.2, may be obtained when a solution of lithium chloride is heated indirectly. The conductance of the solution is measured between two platinum electrodes and provides control of a heating coil.

4.5.2   **Operational procedure**

Readings of the equilibrium temperature of the bobbin are taken and a transfer function applied to obtain the dewpoint temperature.

Disturbing the sensor should be avoided as the equilibrium temperature is sensitive to changes in heat losses at the bobbin surface.

The instrument should be energized continuously. If allowed to cool below the equilibrium temperature for any length of time, condensation will occur and the electrolyte will drip off.

Check measurements with a working reference hygrometer must be taken at regular intervals and the instrument must be cleaned and retreated with a lithium chloride solution, as necessary.

A current-limiting device should be installed if not provided by the manufacturer, otherwise the high current may damage the sensor when the instrument is powered-up.

4.5.3 Exposure and siting

The hygrometer should be located in an open area in a housing structure which protects it from the effects of wind and rain. A system for providing a steady aspiration rate is required.

The heat from the hygrometer may affect other instruments; this should be taken into account when choosing its location.

The operation of the instrument will be affected by atmospheric pollutants, particularly substances which dissociate in solutions and produce a significant ion concentration.

4.5.4 Sources of error

An electrical resistance thermometer is required for measuring the equilibrium temperature; the usual sources of error for thermometry are present.

The equilibrium temperature achieved is determined by the properties of the solute, and significant amounts of contaminant will have an unpredictable effect.

Variations in aspiration affect the heat exchange mechanisms and, thus, the stability of operation of the instrument. A steady aspiration rate is required for a stable operation.

4.5.5 Field inspection and calibration

A field inspection should be performed at least once a month, by means of comparison with a working standard instrument. Calibration of the bobbin thermometer and temperature display should be performed regularly, as for other operational thermometers and display systems.

4.5.6 Maintenance

The lithium chloride should be renewed regularly. This may be required once a month, but will depend upon the level of atmospheric pollution. When renewing the solution, the bobbin should be washed with distilled water and fresh solution subsequently applied. The housing structure should be cleaned at the same time.

Fresh solution may be prepared by mixing five parts by weight of anhydrous lithium chloride with 100 parts by weight of distilled water. This is equivalent to 1 g of anhydrous lithium chloride to 20 ml of water.

The temperature-sensing apparatus should be maintained in accordance with the recommendations for electrical instruments used for making air temperature measurements, but bearing in mind the difference in the range of temperatures measured.

4.6 ELECTRICAL RESISTIVE AND CAPACITIVE HYGROMETERS

4.6.1 General considerations

Certain hygroscopic materials exhibit changes in their electrical properties in response to a change in the ambient relative humidity with only a small temperature dependence.

Electrical relative humidity sensors are increasingly used for remote-reading applications, particularly where a direct display of relative humidity is required. Since many of them have very non-linear responses to changes in humidity, the manufacturers often supply them with special data-processing and display systems.

4.6.2 Electrical resistance

Sensors made from chemically treated plastic material having an electrically conductive surface layer on the non-conductive substrate may be used for meteorological purposes. The surface resistivity varies according to the ambient relative humidity. The process of adsorption, rather than absorption, is dominant because the humidity-sensitive part of such a sensor is restricted to the surface layer. As a result, this type of sensor is capable of responding rapidly to a change in ambient humidity.

This class of sensor includes various electrolytic types in which the availability of conductive ions in a hygroscopic electrolyte is a function of the amount of adsorbed water vapour. The electrolyte may take various physical forms, such as liquid or gel solutions, or an ion-exchange resin. The change in impedance to an alternating current, rather than to a direct current, is measured in order to avoid polarization of the electrolyte. Low-frequency supply can be used, given that the DC resistance is to be measured, and therefore it is possible to employ quite long leads between the sensor and its electrical interface.

4.6.3 Electrical capacitance

The method is based upon the variation of the dielectric properties of a solid, hygroscopic material in relation to the ambient relative humidity. Polymeric materials are most widely used for this purpose. The water bound in the polymer alters its dielectric properties owing to the large dipole moment of the water molecule.

The active part of the humidity sensor consists of a polymer foil sandwiched between two electrodes to form a capacitor. The electrical impedance of this capacitor provides a measure of relative humidity. The nominal value of capacitance may be only a few or several hundred picofarads, depending upon the size of the electrodes and the thickness of the dielectric. This will, in turn, influence the range of excitation frequency used to measure the impedance of the device, which is normally at least several kilohertz and, thus, requires that short connections be made between the sensor and the electrical interface to minimize the effect of stray capacitance. Therefore, capacitance sensors normally have the electrical interface built into the probe, and it is necessary to consider the effect of environmental temperature on the performance of the circuit components.

4.6.4 Observation procedure

Sensors based on changes in the electronic properties of hygroscopic materials are frequently used for the remote reading of relative humidity and also for automatic weather stations.

4.6.5 Exposure and siting

The sensors should be mounted inside a thermometer screen. The manufacturer's advice regarding the mounting of the actual sensor should be followed. The use of protective filters is mandatory. Direct contact with liquid water will seriously harm sensors using hygroscopic electrolyte as a sensor element. Great care should be taken to prevent liquid water from reaching the sensitive element of such sensors.

4.6.6 Field inspection and calibration

Field inspections and laboratory calibrations should be carried out as for hair hygrometers. Suitable auxiliary equipment to enable checks by means of salt solutions is available for most sensors of this type.

4.6.7 Maintenance

Observers should be encouraged to maintain the hygrometer in clean conditions (see section 4.1.4.10).

4.7 HYGROMETERS USING ABSORPTION OF ELECTROMAGNETIC RADIATION

The water molecule absorbs electromagnetic radiation (EMR) in a range of wavebands and discrete wavelengths; this property can be exploited to obtain a measure of the molecular concentration of water vapour in a gas. The most useful regions of the electromagnetic spectrum, for this purpose, lie in the ultraviolet and infrared regions. Therefore, the techniques are often classified as optical hygrometry or, more correctly, EMR absorption hygrometry.

The method makes use of measurements of the attenuation of radiation in a waveband specific to water-vapour absorption, along the path between a source of the radiation and a receiving device. There are two principal methods for determining the degree of attenuation of the radiation as follows:

(a) Transmission of narrowband radiation at a fixed intensity to a calibrated receiver: The most commonly used source of radiation is hydrogen gas; the emission spectrum of hydrogen includes the Lyman-Alpha line at 121.6 nm, which coincides with a water-vapour absorption band in the ultraviolet region where there is little absorption by other common atmospheric gases. The measuring path is typically a few centimetres in length;

(b) Transmission of radiation at two wavelengths, one of which is strongly absorbed by water vapour and the other being either not absorbed or only very weakly absorbed: If a single source is used to generate the radiation at both wavelengths, the ratio of their emitted intensities may be accurately known, so that the attenuation at the absorbed wavelength can be determined by measuring the ratio of their intensities at the receiver. The most widely used source for this technique is a tungsten lamp, filtered to isolate a pair of wavelengths in the infrared region. The measuring path is normally greater than 1 m.

Both types of EMR absorption hygrometers require frequent calibration and are more suitable for measuring changes in vapour concentration than absolute levels. The most widespread application of the EMR absorption hygrometer is to monitor very high frequency variations in humidity, since the method does not require the detector to achieve vapour-pressure equilibrium with the sample. The time constant of an optical hygrometer is typically just a few milliseconds. The use of optical hygrometers remains restricted to research activities.

4.8 SAFETY

Chemical agents are widely used in the measurement of humidity. The properties of such agents should always be made known to the personnel handling them. All chemicals should be kept in secure and clearly labelled containers and stored in an appropriate environment. Instructions concerning the use of toxic materials may be prescribed by local authorities.

Saturated salt solutions are widely used in the measurement of humidity. The notes that follow give some guidance for the safe use of some commonly used salts:

(a) Barium chloride ($BaCl_2$): Colourless crystals; very soluble in water; stable, but may emit toxic fumes in a fire; no hazardous reaction with water, acids, bases, oxidizers or with combustible materials; ingestion causes nausea, vomiting, stomach pains and diarrhoea; harmful if inhaled as dust and if it comes into contact with the skin; irritating to eyes; treat with copious amounts of water and obtain medical attention if ingested;

(b)   Calcium chloride ($CaCl_2$): Colourless crystals; deliquescent; very soluble in water, dissolves with increase in heat; will initiate exothermic polymerization of methyl vinyl ether; can react with zinc to liberate hydrogen; no hazardous reactions with acids, bases, oxidizers or combustibles; irritating to the skin, eyes and respiratory system; ingestion causes gastric irritation; ingestion of large amounts can lead to hypercalcaemia, dehydration and renal damage; treat with copious amounts of water and obtain medical attention;

(c)   Lithium chloride (LiCl): Colourless crystals; stable if kept dry; very soluble in water; may emit toxic fumes in a fire; ingestion may affect ionic balance of blood leading to anorexia, diarrhoea, vomiting, dizziness and central nervous system disturbances; kidney damage may result if sodium intake is low (provide plenty of drinking water and obtain medical attention); no hazardous reactions with water, acids, bases, oxidizers or combustibles;

(d)   Magnesium nitrate ($Mg(NO_3)_2$): Colourless crystals; deliquescent; very soluble in water; may ignite combustible material; can react vigorously with deoxidizers, can decompose spontaneously in dimethylformamide; may emit toxic fumes in a fire (fight the fire with a water spray); ingestion of large quantities can have fatal effects (provide plenty of drinking water and obtain medical attention); may irritate the skin and eyes (wash with water);

(e)   Potassium nitrate (KNO_3): White crystals or crystalline powder; very soluble in water; stable but may emit toxic fumes in a fire (fight the fire with a water spray); ingestion of large quantities causes vomiting, but it is rapidly excreted in urine (provide plenty of drinking water); may irritate eyes (wash with water); no hazardous reaction with water, acids, bases, oxidizers or combustibles;

(f)   Sodium chloride (NaCl): Colourless crystals or white powder; very soluble in water; stable; no hazardous reaction with water, acids, bases, oxidizers or combustibles; ingestion of large amounts may cause diarrhoea, nausea, vomiting, deep and rapid breathing and convulsions (in severe cases obtain medical attention).

Advice concerning the safe use of mercury is given in Part I, Chapter 3, 3.2.7.

4.9   STANDARD INSTRUMENTS AND CALIBRATION

4.9.1   Principles involved in the calibration of hygrometers

Precision in the calibration of humidity sensors entails special problems, to a great extent owing to the relatively small quantity of water vapour which can exist in an air sample at normal temperatures, but also due to the general difficulty of isolating and containing gases and, more particularly, vapour. An ordered hierarchy of international traceability in humidity standards is only now emerging.

An absolute standard for humidity (namely, a realization of the physical definition for the quantity of humidity) can be achieved by gravimetric hygrometry. The reference psychrometer (within its limited range) is also a form of primary standard, in that its performance is calculable. The calibration of secondary, reference and working standards involves several steps. Table 4.3 shows a summary of humidity standard instruments and their performances.

A practical field inspection is most frequently done by means of well-designed aspirated psychrometers and dewpoint sensors or capacitive hygrometers as working standards. These specific types of standards must be traceable to the higher levels of standards by careful calibrations. Any instrument used as a standard must be individually calibrated for all variables involved in calculating humidity (air temperature, wet-bulb temperature, dewpoint temperature, and so forth). Other factors affecting performance, such as airflow, must also be checked.

4.9.2 **Calibration intervals and methods**

Regular calibration is required for all humidity sensors in the field. For psychrometers and dewpoint hygrometers that use a temperature detector, calibration can be checked whenever a regular maintenance routine is performed. Comparison with a working standard, such as an Assmann psychrometer, should be performed at least once a month.

The use of a standard type of aspirated psychrometer, such as the Assmann, as a working standard has the advantage that its integrity can be verified by comparing the dry- and wet-bulb thermometers, and that adequate aspiration may be expected from a healthy sounding fan. The reference instrument should itself be calibrated at an interval appropriate to its type.

Saturated salt solutions can be applied with sensors that require only a small-volume sample. A very stable ambient temperature is required and it is difficult to be confident about their use in the field. When using salt solutions for control purposes, it should be borne in mind that the nominal humidity value given for the salt solution itself is not traceable to any primary standard.

Table 4.3. Standard instruments for the measurement of humidity

Standard instrument	Dewpoint temperature		Relative humidity (%)	
	Range (°C)	Uncertainty (K)	Range	Uncertainty
Primary standard				
Requirement	–60 to –15 –15 to 40	0.3 0.1	5 to 100 5 to 100	0.2 0.2
Gravimetric hygrometer	–60 to –35 –35 to 35 35 to 60	0.25 0.03 0.25		
Standard two-temperature humidity generator	–75 to –15 –15 to 30 30 to 80	0.25 0.1 0.2		
Standard two-pressure humidity generator	–75 to 30	0.2		
Secondary standard				
Requirement	–80 to –15 –15 to 40	0.75 0.25	5 to 100	0.5
Chilled-mirror hygrometer	–60 to 40	0.15		
Reference psychrometer			5 to 100	0.6
Reference standard				
Requirement	–80 to –15 –15 to 40	1.0 0.3	5 to 100	1.5
Reference psychrometer			5 to 100	0.6
Chilled-mirror hygrometer	–60 to 40	0.3		
Working standard				
Requirement	–15 to 40	0.5	5 to 100	2
Assmann psychrometer	–10 to 25		40 to 90	1
Chilled-mirror hygrometer	–10 to 30	0.5		

4.9.3   Laboratory calibration

Laboratory calibration is essential for maintaining accuracy in the following ways:

(a)   Field and working standard instruments: Laboratory calibration of field and working standard instruments should be carried out on the same regular basis as for other operational thermometers. For this purpose, the chilled-mirror sensor device may be considered separately from the control unit. The mirror thermometer should be calibrated independently and the control unit should be calibrated on the same regular basis as other items of precision electronic equipment. The calibration of a field instrument in a humidity generator is not strictly necessary if the components have been calibrated separately, as described previously.

       The correct operation of an instrument may be verified under stable room conditions by comparison with a reference instrument, such as an Assmann psychrometer or a standard chilled-mirror hygrometer. If the field instrument incorporates an ice detector, the correct operation of this system should be verified.

(b)   Reference and standard instruments: Laboratory calibration of reference and standard instruments requires a precision humidity generator and a suitable transfer standard hygrometer. Two-pressure and two-temperature humidity generators are able to deliver a suitable controlled flow of air at a predetermined temperature and dewpoint. The calibration should be performed at least every 12 months and over the full range of the reference application for the instrument. The calibration of the mirror thermometer and the temperature display system should be performed independently at least once every 12 months.

4.9.4   Primary standards

4.9.4.1   *Gravimetric hygrometry*

The gravimetric method yields an absolute measure of the water-vapour content of an air sample in terms of its humidity mixing ratio. This is obtained by first removing the water vapour from the sample using a known mass of a drying agent, such as anhydrous phosphorous pentoxide (P_2O_5) or magnesium perchlorate ($Mg(ClO_4)_2$). The mass of the water vapour is determined by weighing the drying agent before and after absorbing the vapour. The mass of the dry sample is determined either by weighing (after liquefaction to render the volume of the sample manageable) or by measuring its volume (and having knowledge of its density).

The complexity of the apparatus required to accurately carry out the procedure described limits the application of this method to the laboratory environment. In addition, a substantial volume sample of air is required for accurate measurements to be taken and a practical apparatus requires a steady flow of the humid gas for a number of hours, depending upon the humidity, in order to remove a sufficient mass of water vapour for an accurate weighing measurement. As a consequence, the method is restricted to providing an absolute calibration reference standard. Such an apparatus is found mostly in national calibration standards laboratories.

4.9.4.2   *Dynamic two-pressure standard humidity generator*

This laboratory apparatus serves to provide a source of humid gas whose relative humidity is determined on an absolute basis. A stream of the carrier gas is passed through a saturating chamber at pressure P_1 and allowed to expand isothermally in a second chamber at a lower pressure P_2. Both chambers are maintained at the same temperature in an oil bath. The relative humidity of the water vapour-gas mixture is straightforwardly related to the total pressures in each of the two chambers through Dalton's law of partial pressures; the partial pressure e' of the vapour in the low-pressure chamber will have the same relation to the saturation vapour pressure e'_w as the total pressure in the high-pressure saturator has to the total pressure in the low-pressure chamber. Thus, the relative humidity U_w is given by:

$$U_w = 100 \cdot e'/e'_w = 100 \cdot P_1/P_2 \qquad (4.5)$$

The relation also holds for the solid phase if the gas is saturated with respect to ice at pressure P_1:

$$U_i = 100 \cdot e'/e'_i = 100 \cdot P_1/P_2 \qquad (4.6)$$

4.9.4.3 *Dynamic two-temperature standard humidity generator*

This laboratory apparatus provides a stream of humid gas at temperature T_1 having a dew- or frost-point temperature T_2. Two temperature-controlled baths, each equipped with heat exchangers and one with a saturator containing either water or ice, are used first to saturate the air-stream at temperature T_1 and then to heat it isobarically to temperature T_2. In practical designs, the air-stream is continuously circulated to ensure saturation. Test instruments draw off air at temperature T_2 and a flow rate that is small in proportion to the main circulation.

4.9.5 Secondary standards

A secondary standard instrument should be carefully maintained and removed from the calibration laboratory only for the purpose of calibration with a primary standard or for intercomparison with other secondary standards. Secondary standards may be used as transfer standards from the primary standards.

A chilled-mirror hygrometer may be used as a secondary standard instrument under controlled conditions of air temperature, humidity and pressure. For this purpose, it should be calibrated from a recognized accredited laboratory, giving uncertainty limits throughout the operational range of the instrument. This calibration must be directly traceable to a primary standard and should be renewed at an appropriate interval (usually once every 12 months).

General considerations for chilled-mirror hygrometers are discussed in section 4.4. This method presents a fundamental technique for determining atmospheric humidity. Provided that the instrument is maintained and operated correctly, following the manufacturer's instructions, it can provide a primary measurement of dew or frost point within limits of uncertainty determined by the correspondence between the mirror surface temperature at the appropriate point of the condensation/evaporation cycle and the temperature registered by the mirror thermometer at the observation time. The Kelvin and Raoult effects upon the condensation temperature must be taken into consideration, and any change of the air pressure resulting from the sampling technique must be taken into account by using the equations given in section 4.4.1.2.

4.9.6 Working standards (and field reference instruments)

A chilled-mirror hygrometer or an Assmann psychrometer may be used as a working standard for comparisons under ambient conditions in the field or the laboratory. For this purpose, it is necessary to have performed comparisons at least at the reference standard level. The comparisons should be performed at least once every 12 months under stable room conditions. The working standard will require a suitable aspiration device to sample the air.

4.9.7 The WMO reference psychrometer

This type of psychrometer is essentially a primary standard because its performance is calculable. However, its main use is as a highly accurate reference instrument, specifically for type-testing other instrument systems in the field. It is intended for use as a free-standing instrument, alongside the screen or other field instruments, and must be made precisely to its general specification and operated by skilled staff experienced in precise laboratory work; careful attention should be given to aspiration and to preventing the wet bulb from being contaminated by contact with fingers or other objects. There are, however, simple tests by which the readings may be validated at any time, and these should be used frequently during the operation. The psychrometer's description and operating instructions are given in WMO (1992).

4.9.8 Salt solution

A salt solution creates characteristic values of the relative humidity in the air above it. The values of relative humidity are dependent on the chemical structure of the salt, the salt concentration and the temperature. Two types of salt solutions are available:

(a) Unsaturated salt solution, which comes in the form of ampoules of solution, generates an atmosphere with a certain relative humidity. These ampoules are generally used to soak a pad in a housing designed for exposing a sensor to the humidity produced.

(b) Saturated salt solution maintains a stable concentration of relative humidity if both phases of the salt exist: if the solution is saturated with salt and some salt remains in the solid phase. In this case, the vapour pressure depends only on temperature.

Vessels containing saturated solutions of appropriate salts may be used to calibrate relative humidity sensors. Commonly used salts and their saturation relative humidities at 25 °C are as follows:

Barium chloride ($BaCl_2$): 90.3%
Sodium chloride (NaCl): 75.3%
Magnesium nitrate ($Mg(NO_3)_2$): 52.9%
Calcium chloride ($CaCl_2$): 29.0%
Lithium chloride (LiCl): 11.1%

It is important that the surface area of the solution is large compared to that of the sensor element and the enclosed volume of air so that equilibrium may be achieved quickly; an airtight access port is required for the test sensor. The temperature of the vessel should be measured and maintained at a constant level as the saturation humidity for most salts has a significant temperature coefficient.

Care should be taken when using saturated salt solutions. The degree of toxicity and corrosivity of salt solutions should be known to the personnel dealing with them. The salts listed above may all be used quite safely, but it is nevertheless important to avoid contact with the skin, and to avoid ingestion and splashing into the eyes. The salts should always be kept in secure and clearly labelled containers which detail any hazards involved. Care should be taken when dissolving calcium chloride crystals in water, as much heat is evolved. Section 4.8 deals with chemical hazards in greater detail.

Saturated salt solutions provide a practical method for adjusting a certain type of hygrometer (capacitive), but for calibration purposes a reference instrument should also be used.

_____

ANNEX 4.A. DEFINITIONS AND SPECIFICATIONS OF WATER VAPOUR IN THE ATMOSPHERE

(adapted from the Technical Regulations (WMO-No. 49), Volume I, Appendix B)

(1)   ***The mixing ratio r*** of moist air is the ratio of the mass m_v of water vapour to the mass m_a of dry air with which the water vapour is associated:

$$r = \frac{m_v}{m_a} \tag{4.A.1}$$

(2)   ***The specific humidity, mass concentration*** or ***moisture content q*** of moist air is the ratio of the mass m_v of water vapour to the mass $m_v + m_a$ of moist air in which the mass of water vapour m_v is contained:

$$q = \frac{m_v}{m_v + m_a} \tag{4.A.2}$$

(3)   ***Vapour concentration (density of water vapour in a mixture)*** or ***absolute humidity***: For a mixture of water vapour and dry air the vapour concentration ρ_v is defined as the ratio of the mass of vapour m_v to the volume V occupied by the mixture:

$$\rho_v = \frac{m_v}{V} \tag{4.A.3}$$

(4)   ***Mole fraction of the water vapour of a sample of moist air***: The mole fraction x_v of the water vapour of a sample of moist air, composed of a mass m_a of dry air and a mass m_v of water vapour, is defined by the ratio of the number of moles of water vapour ($n_v = m_v/M_v$) to the total number of moles of the sample $n_v + n_a$, where n_a indicates the number of moles of dry air ($n_a = m_a/M_a$) of the sample concerned. This gives:

$$x_v = \frac{n_v}{n_a + n_v} \tag{4.A.4}$$

or:

$$x_v = \frac{r}{0.621\,98 + r} \tag{4.A.5}$$

where r is merely the mixing ratio ($r = m_v/m_a$) of the water vapour of the sample of moist air.

(5)   ***The vapour pressure e'*** of water vapour in moist air at total pressure p and with mixing ratio r is defined by:

$$e' = \frac{r}{0.621\,98 + r}\, p = x_v \cdot p \tag{4.A.6}$$

(6)   ***Saturation***: Moist air at a given temperature and pressure is said to be saturated if its mixing ratio is such that the moist air can coexist in neutral equilibrium with an associated condensed phase (liquid or solid) at the same temperature and pressure, the surface of separation being plane.

(7)   ***Saturation mixing ratio***: The symbol r_w denotes the saturation mixing ratio of moist air with respect to a plane surface of the associated liquid phase. The symbol r_i denotes the saturation mixing ratio of moist air with respect to a plane surface of the associated solid phase. The associated liquid and solid phases referred to consist of almost pure water and almost pure ice, respectively, there being some dissolved air in each.

(8)   ***Saturation vapour pressure in the pure phase***: The saturation vapour pressure e_w of pure aqueous vapour with respect to water is the pressure of the vapour when in a state of neutral equilibrium with a plane surface of pure water at the same temperature and pressure; similarly for e_i with respect to ice; e_w and e_i are temperature-dependent functions only, namely:

$$e_w = e_w(T) \tag{4.A.7}$$
$$e_i = e_i(T) \tag{4.A.8}$$

(9)   *Mole fraction of water vapour in moist air saturated with respect to water*: The mole fraction of water vapour in moist air saturated with respect to water, at pressure p and temperature T, is the mole fraction x_{vw} of the water vapour of a sample of moist air, at the same pressure p and the same temperature T, that is in stable equilibrium in the presence of a plane surface of water containing the amount of dissolved air corresponding to equilibrium. Similarly, x_{vi} will be used to indicate the saturation mole fraction with respect to a plane surface of ice containing the amount of dissolved air corresponding to equilibrium.

(10)   *Saturation vapour pressure of moist air*: The saturation vapour pressure with respect to water e'_w of moist air at pressure p and temperature T is defined by:

$$e'_w = \frac{r_w}{0.621\,98 + r_w}\, p = x_{vw} \cdot p \tag{4.A.9}$$

Similarly, the saturation vapour pressure with respect to ice e'_i of moist air at pressure p and temperature T is defined by:

$$e'_i = \frac{r_i}{0.621\,98 + r_i}\, p = x_{vi} \cdot p \tag{4.A.10}$$

(11)   *Relations between saturation vapour pressures of the pure phase and of moist air*: In the meteorological range of pressure and temperature the following relations hold with an error of 0.5% or less:

$$e'_w = e_w \tag{4.A.11}$$
$$e'_i = e_i \tag{4.A.12}$$

(12)   *The thermodynamic dewpoint temperature T_d* of moist air at pressure p and with mixing ratio r is the temperature at which moist air, saturated with respect to water at the given pressure, has a saturation mixing ratio r_w equal to the given mixing ratio r.

(13)   *The thermodynamic frost-point temperature T_f* of moist air at pressure p and mixing ratio r is the temperature at which moist air, saturated with respect to ice at the given pressure, has a saturation mixing ratio r_i equal to the given ratio r.

(14)   *The dewpoint and frost-point temperatures* so defined are related to the mixing ratio r and pressure p by the respective equations:

$$e'_w\left(p, T_d\right) = f\left(p\right) \cdot e_w\left(T_d\right) = x_v \cdot p = \frac{r \cdot p}{0.621\,98 + r} \tag{4.A.13}$$
$$e'_i\left(p, T_f\right) = f\left(p\right) \cdot e_i\left(T_f\right) = x_v \cdot p = \frac{r \cdot p}{0.621\,98 + r} \tag{4.A.14}$$

(15)[1]   *The relative humidity U_w with respect to water of moist air* at pressure p and temperature T is the ratio in % of the vapour mole fraction x_v to the vapour mole fraction x_{vw} which the air would have if it were saturated with respect to water at the same pressure p and temperature T. Accordingly:

$$U_w = 100 \left(\frac{x_v}{x_{vw}}\right)_{p,T} = 100 \left(\frac{p x_v}{p x_{vw}}\right)_{p,T} = 100 \left(\frac{e'}{e'_w}\right)_{p,T} \tag{4.A.15}$$

where subscripts p, T indicate that each term is subject to identical conditions of pressure and temperature. The last expression is formally similar to the classic definition based on the assumption of Dalton's law of partial pressures.

U_w is also related to the mixing ratio r by:

$$U_w = 100 \frac{r}{r_w} \cdot \frac{0.621\,98 + r_w}{0.621\,98 + r} \tag{4.A.16}$$

where r_w is the saturation mixing ratio at the pressure and temperature of the moist air.

(16)[1]   **The relative humidity U_i with respect to ice of moist air** at pressure p and temperature T is the ratio in % of the vapour mole fraction x_v to the vapour mole fraction x_{vi} which the air would have if it were saturated with respect to ice at the same pressure p and temperature T. Corresponding to the defining equation in paragraph 15:

$$U_i = 100 \left(\frac{x_v}{x_{vi}} \right)_{p,T} = 100 \left(\frac{px_v}{px_{vi}} \right)_{p,T} = 100 \left(\frac{e'}{e'_i} \right)_{p,T}$$ (4.A.17)

(17)   **Relative humidity at temperatures less than 0 °C** is to be evaluated with respect to water. The advantages of this procedure are as follows:

(a)   Most hygrometers which are essentially responsive to the relative humidity indicate relative humidity with respect to water at all temperatures;

(b)   The majority of clouds at temperatures below 0 °C consist of water, or mainly of water;

(c)   Relative humidities greater than 100% would in general not be observed. This is of particular importance in synoptic weather messages, since the atmosphere is often supersaturated with respect to ice at temperatures below 0 °C;

(d)   The majority of existing records of relative humidity at temperatures below 0 °C are expressed on a basis of saturation with respect to water.

(18)   **The thermodynamic wet-bulb temperature of moist air** at pressure p, temperature T and mixing ratio r is the temperature T_w attained by the moist air when brought adiabatically to saturation at pressure p by the evaporation into the moist air of liquid water at pressure p and temperature T_w and containing the amount of dissolved air corresponding to equilibrium with saturated air of the same pressure and temperature. T_w is defined by the equation:

$$h(p,T,r) + \left[r_w(p,T_w) - r \right] h_w(p,T_w) = h(p,T_w, r_w(p,T_w))$$ (4.A.18)

where $r_w(p,T_w)$ is the mixing ratio of saturated moist air at pressure p and temperature T_w; $h_w(p,T_w)$ is the enthalpy[2] of 1 gram of pure water at pressure p and temperature T_w; $h(p,T,r)$ is the enthalpy of $1 + r_w$ grams of moist air, composed of 1 gram of dry air and r grams of water vapour, at pressure p and temperature T; and $h(p,T_w, r_w(p,T_w))$ is the enthalpy of $1 + r_w$ grams of saturated air, composed of 1 gram of dry air and r_w grams of water vapour, at pressure p and temperature T_w. (This is a function of p and T_w only and may appropriately be denoted by $h_{sw}(p,T_w)$.)

If air and water vapour are regarded as ideal gases with constant specific heats, the above equation becomes:

$$T - T_w = \frac{\left[r_w(p,T_w) - r \right] L_v(T_w)}{c_{pa} + r c_{pv}}$$ (4.A.19)

where $L_v(T_w)$ is the heat of vaporization of water at temperature T_w, c_{pa} is the specific heat of dry air at constant pressure; and c_{pv} is the specific heat of water vapour at constant pressure.

Note: Thermodynamic wet-bulb temperature as here defined has for some time been called "temperature of adiabatic saturation" by air-conditioning engineers.

(19)   **The thermodynamic ice-bulb temperature of moist air** at pressure p, temperature T and mixing ratio r is the temperature T_i at which pure ice at pressure p must be evaporated into the moist air in order to saturate it adiabatically at pressure p and temperature T_i. The saturation is with respect to ice. T_i is defined by the equation:

$$h(p,T,r) + \left[r_i(p,T_i) - r \right] h_i(p,T_i) = h(p,T_i, r_i(p,T_i))$$ (4.A.20)

---

1   Equations 4.A.15 and 4.A.17 do not apply to moist air when pressure p is less than the saturation vapour pressure of pure water and ice, respectively, at temperature T.
2   The enthalpy of a system in equilibrium at pressure p and temperature T is defined as $E + pV$, where E is the internal energy of the system and V is its volume. The sum of the enthalpies of the phases of a closed system is conserved in adiabatic isobaric processes.

where $r_i(p,T_i)$ is the mixing ratio of saturated moist air at pressure p and temperature T_i; $h_i(p,T_i)$ is the enthalpy of 1 gram of pure ice at pressure p and temperature T_i; $h(p,T,r)$ is the enthalpy of $1 + r$ grams of moist air, composed of 1 gram of dry air and r grams of water vapour, at pressure p and temperature T; and $h(p,T_i,r_i(p,T_i))$ is the enthalpy of $1 + r_i$ grams of saturated air, composed of 1 gram of dry air and r_i grams of water vapour, at pressure p and temperature T_i. (This is a function of p and T_i only, and may appropriately be denoted by $h_{si}(p,T_i)$.)

If air and water vapour are regarded as ideal gases with constant specific heats, the above equation becomes:

$$T - T_i = \frac{\left[r_i\left(p,T_i \right) - r \right] L_s\left(T_i \right)}{c_p + rc_{pv}} \tag{4.A.21}$$

where $L_s(T_i)$ is the heat of sublimation of ice at temperature T_i.

The relationship between T_w and T_i as defined and the wet-bulb or ice-bulb temperature as indicated by a particular psychrometer is a matter to be determined by carefully controlled experiment, taking into account the various variables concerned, for example, ventilation, size of thermometer bulb and radiation.

———————————

ANNEX 4.B. FORMULAE FOR THE COMPUTATION OF MEASURES OF HUMIDITY

(see also section 4.1.2)

Saturation vapour pressure:

$e_w(t) = 6.112 \exp [17.62\, t/(243.12 + t)]$ 　　　　　　　　Water (–45 °C to 60 °C) (pure phase)

$e'_w(p,t) = f(p) \cdot e_w(t)$ 　　　　　　　　Moist air

$e_i(t) = 6.112 \exp [22.46\, t/(272.62 + t)]$ 　　　　　　　　Ice (–65 °C to 0 °C) (pure phase)

$e'_i(p,t) = f(p) \cdot e_i(t)$ 　　　　　　　　Moist air

$f(p) = 1.001\,6 + 3.15 \cdot 10^{-6}\, p - 0.074\, p^{-1}$ 　　　　　　　　[see note]

Dewpoint and frost point:

$$t_d = \frac{243.12 \cdot \ln\left[e'/6.112 f(p)\right]}{17.62 - \ln\left[e'/6.112 f(p)\right]}$$ 　　　　　　　　Water (–45 °C to 60 °C)

$$t_f = \frac{272.62 \cdot \ln\left[e'/6.112 f(p)\right]}{22.46 - \ln\left[e'/6.112 f(p)\right]}$$ 　　　　　　　　Ice (–65 °C to 0 °C)

Psychrometric formulae for the Assmann psychrometer:

$e' = e'_w(p,t_w) - 6.53 \cdot 10^{-4} \cdot (1 + 0.000\,944\, t_w) \cdot p \cdot (t - t_w)$ 　　　Water

$e' = e'_i(p,t_i) - 5.75 \cdot 10^{-4} \cdot p \cdot (t - t_i)$ 　　　Ice

Relative humidity:

$U = 100\, e'/e'_w(p,t)$ %

$U = 100\, e'_w(p,t_d)/e'_w(p,t)$ %

Units applied:

t　　　= air temperature (dry-bulb temperature);

t_w　　　= wet-bulb temperature;

t_i　　　= ice-bulb temperature;

t_d　　　= dewpoint temperature;

t_f　　　= frost-point temperature;

p　　　= pressure of moist air;

$e_w(t)$　　= saturation vapour pressure in the pure phase with regard to water at the dry-bulb temperature;

$e_w(t_w)$ = saturation vapour pressure in the pure phase with regard to water at the wet-bulb temperature;

$e_i(t)$ = saturation vapour pressure in the pure phase with regard to ice at the dry-bulb temperature;

$e_i(t_i)$ = saturation vapour pressure in the pure phase with regard to ice at the ice-bulb temperature;

$e'_w(t)$ = saturation vapour pressure of moist air with regard to water at the dry-bulb temperature;

$e'_w(t_w)$ = saturation vapour pressure of moist air with regard to water at the wet-bulb temperature;

$e'_i(t)$ = saturation vapour pressure of moist air with regard to ice at the dry-bulb temperature;

$e'_i(t_i)$ = saturation vapour pressure of moist air with regard to ice at the ice-bulb temperature;

U = relative humidity.

Note: In fact, f is a function of both pressure and temperature, i.e. $f = f(p, t)$, as explained in WMO (1966) in the introduction to Table 4.10. In practice, the temperature dependency (±0.1%) is much lower with respect to pressure (0% to +0.6%). Therefore, the temperature dependency may be omitted in the formula above (see also WMO (1989a), Chapter 10). This formula, however, should be used only for pressure around 1 000 hPa (i.e. surface measurements) and not for upper-air measurements, for which WMO (1966), Table 4.10 should be used.

———————————

REFERENCES AND FURTHER READING

Anderson, P.S., 1995: Mechanism for the behavior of hydroactive materials used in humidity sensors. *J. Atmos. Oceanic Technol.*, 12:662–667.

Bindon, H.H., 1965: A critical review of tables and charts used in psychrometry. In: *Humidity and Moisture* (A. Wexler, ed.), Reinhold, New York, 1:3–15.

Ingleby, B., D. Moore, C. Sloan and R. Dunn, 2013: Evolution and Accuracy of Surface Humidity Reports. *J. Atmos. Oceanic Technol.*, 30:2025–2043.

Sonntag, D., 1990: Important new values of the physical constants of 1986, vapour pressure formulations based on the ITS-90 and psychrometer formulae. *Zeitschrift für Meteorologie*, 40(5):340–344.

———, 1994: Advancements in the field of hygrometry. *Zeitschrift für Meteorologie*, 3(2):51–66.

Wexler, A. (ed.), 1965: *Humidity and Moisture*. Volumes 1 and 3, Reinhold, New York.

World Meteorological Organization, 1966: *International Meteorological Tables* (S. Letestu, ed.) (1973 amendment). (WMO-No. 188, TP. 94). Geneva.

———, 1989*a*: *WMO Assmann Aspiration Psychrometer Intercomparison* (D. Sonntag). Instruments and Observing Methods Report No. 34 (WMO/TD-No. 289). Geneva.

———, 1989*b*: *WMO International Hygrometer Intercomparison* (J. Skaar, K. Hegg, T. Moe and K. Smedstud). Instruments and Observing Methods Report No. 38 (WMO/TD-No. 316). Geneva.

———, 1992: *Measurement of Temperature and Humidity: Specification, Construction, Properties and Use of the WMO Reference Psychrometer* (R.G. Wylie and T. Lalas). Technical Note No. 194 (WMO-No. 759). Geneva.

———, 2011*a*: *Technical Regulations* (WMO-No. 49), Volume I. Geneva.

———, 2011*b*: *WMO Field Intercomparison of Thermometer Screens/Shields and Humidity Measuring Instruments* (M. Lacombe, D. Bousri, M. Leroy and M. Mezred). Instruments and Observing Methods Report No. 106 (WMO/TD-No. 1579). Geneva.

———————

CHAPTER CONTENTS

CHAPTER 5. MEASUREMENT OF SURFACE WIND

5.1   GENERAL

5.1.1   Definitions

The following definitions are used in this chapter (see Mazzarella, 1972, for more details).

Wind velocity is a three-dimensional vector quantity with small-scale random fluctuations in space and time superimposed upon a larger-scale organized flow. It is considered in this form in relation to, for example, airborne pollution and the landing of aircraft. For the purpose of this Guide, however, surface wind will be considered mainly as a two-dimensional vector quantity specified by two numbers representing direction and speed. The extent to which wind is characterized by rapid fluctuations is referred to as gustiness, and single fluctuations are called gusts.

Most users of wind data require the averaged horizontal wind, usually expressed in polar coordinates as speed and direction. More and more applications also require information on the variability or gustiness of the wind. For this purpose, three quantities are used, namely the peak gust and the standard deviations of wind speed and direction.

Averaged quantities are quantities (for example, horizontal wind speed) that are averaged over a period of 10 to 60 min. This chapter deals mainly with averages over 10 min intervals, as used for forecasting purposes. Climatological statistics usually require averages over each entire hour, day and night. Aeronautical applications often use shorter averaging intervals (see Part II, Chapter 2). Averaging periods shorter than a few minutes do not sufficiently smooth the usually occurring natural turbulent fluctuations of wind; therefore, 1 min "averages" should be described as long gusts.

Peak gust is the maximum observed wind speed over a specified time interval. With hourly weather reports, the peak gust refers to the wind extreme in the last full hour.

Gust duration is a measure of the duration of the observed peak gust. The duration is determined by the response of the measuring system. Slowly responding systems smear out the extremes and measure long smooth gusts; fast response systems may indicate sharp wave-front gusts with a short duration.

For the definition of gust duration an ideal measuring chain is used, namely a single filter that takes a running average over t_0 seconds of the incoming wind signal. Extremes detected behind such a filter are defined as peak gusts with duration t_0. Other measuring systems with various filtering elements are said to measure gusts with duration t_0 when a running average filter with integration time t_0 would have produced an extreme with the same height (see Beljaars, 1987; WMO, 1987 for further discussion).

Standard deviation is:

$$s_u = \sqrt{\overline{\left(u_i - U\right)^2}} = \sqrt{\left(\left(\sum\left(u_i^2\right) - \left(\sum u_i\right)^2 / n\right) / n\right)} \tag{5.1}$$

where u is a time-dependent signal (for example, horizontal wind speed) with average U and an overbar indicates time-averaging over n samples u_i. The standard deviation is used to characterize the magnitude of the fluctuations in a particular signal.

Time constant (of a first-order system) is the time required for a device to detect and indicate about 63% of a step-function change.

Response length is approximately the passage of wind (in metres) required for the output of a wind-speed sensor to indicate about 63% of a step-function change of the input speed.

Critical damping (of a sensor such as a wind vane, having a response best described by a second-order differential equation) is the value of damping which gives the most rapid transient response to a step change without overshoot.

Damping ratio is the ratio of the actual damping to the critical damping.

Undamped natural wavelength is the passage of wind that would be required by a vane to go through one period of an oscillation if there were no damping. It is less than the actual "damped" wavelength by a factor $\sqrt{(1-D^2)}$ if D is the damping ratio.

Variable wind with no mean wind direction is wind where the total variation from the mean wind direction during the previous 10 minutes is 60° or more, and less than 180°, and the wind speed is less than 6 km/h (3 kt), or when the total variation is 180° or more.

5.1.2   Units and scales

Wind speed should be reported to a resolution of 0.5 m s^{-1} or in knots (0.515 m s^{-1}) to the nearest unit, and should represent, for synoptic reports, an average over 10 min. Averages over a shorter period are necessary for certain aeronautical purposes (see Part II, Chapter 2).

In traditional codes, wind direction should be reported in degrees true to the nearest 10°, using a 01 ... 36 code (for example, code 2 means that the wind direction is between 15° and 25°), and should represent an average over 10 min (see Part II, Chapter 2). In BUFR code, wind direction should be reported in degrees true, with resolution 1°. Wind direction is defined as the direction from which the wind blows, and is measured clockwise from geographical north, namely, true north (based on the World Geodetic System 1984 (WGS-84) and its Earth Geodetic Model 1996 (EGM96)).

"Calm" should be reported when the average wind speed is less than 1 kt. The direction in this case is coded as 00.

Wind direction at stations within 1° of the North Pole or 1° of the South Pole should be measured so that the azimuth ring should be aligned with its zero coinciding with the Greenwich 0° meridian.

5.1.3   Meteorological requirements

Wind observations or measurements are required for weather monitoring and forecasting, for wind-load climatology, for probability of wind damage and estimation of wind energy, and as part of the estimation of surface fluxes, for example, evaporation for air pollution dispersion and agricultural applications. Performance requirements are given in Part I, Chapter 1, Annex 1.E. An accuracy for horizontal speed of 0.5 m s^{-1} below 5 m s^{-1} and better than 10% above 5 m s^{-1} is usually sufficient. Wind direction should be measured with an accuracy of 5°. Apart from mean wind speed and direction, many applications require standard deviations and extremes (see section 5.8.2). The required accuracy is easily obtained with modern instrumentation. The most difficult aspect of wind measurement is the exposure of the anemometer. Since it is nearly impossible to find a location where the wind speed is representative of a large area, it is recommended that estimates of exposure errors be made (requirements on siting and exposure are provided in section 5.9 and in Part I, Chapter 1, Annex 1.B).

Many applications require information about the gustiness of the wind. Such applications provide "nowcasts" for aircraft take-off and landing, wind-load climatology, air pollution dispersion problems and exposure correction. Two variables are suitable for routine reading, namely the standard deviation of wind speed and direction and the 3 s peak gust (see Recommendations 3 and 4 (CIMO-X) (WMO, 1990)).

5.1.4   **Methods of measurement and observation**

Surface wind is usually measured by a wind vane and cup or propeller anemometer. When the instrumentation is temporarily out of operation or when it is not provided, the direction and force of the wind may be estimated subjectively (Tables 5.1 and 5.2 provide wind speed equivalents in common use for estimations).

The instruments and techniques specifically discussed here are only a few of the more convenient ones available and do not comprise a complete list. The references and further reading at the end of this chapter provide a good literature on this subject.

The sensors briefly described below are cup-rotor and propeller anemometers, and direction vanes. Cup and vane, propeller and vane, and propellers alone are common combinations. Other classic sensors, such as the pitot tube, are less used now for routine measurements but can perform satisfactorily, while new types being developed or currently in use as research tools may become practical for routine measurement with advanced technology.

Table 5.1. Wind speed equivalents

Beaufort scale number and description	Wind speed equivalent at a standard height of 10 m above open flat ground				Specifications for estimating speed over land
	(kt)	(m s⁻¹)	(km h⁻¹)	(mi h⁻¹)	
0 Calm	< 1	0 – 0.2	< 1	< 1	Calm; smoke rises vertically
1 Light air	1 – 3	0.3 – 1.5	1 – 5	1 – 3	Direction of wind shown by smoke-drift but not by wind vanes
2 Light breeze	4 – 6	1.6 – 3.3	6 – 11	4 – 7	Wind felt on face; leaves rustle; ordinary vanes moved by wind
3 Gentle breeze	7 – 10	3.4 – 5.4	12 – 19	8 – 12	Leaves and small twigs in constant motion; wind extends light flag
4 Moderate breeze	11 – 16	5.5 – 7.9	20 – 28	13 – 18	Raises dust and loose paper; small branches are moved
5 Fresh breeze	17 – 21	8.0 – 10.7	29 – 38	19 – 24	Small trees in leaf begin to sway, crested wavelets form on inland waters
6 Strong breeze	22 – 27	10.8 – 13.8	39 – 49	25 – 31	Large branches in motion; whistling heard in telegraph wires; umbrellas used with difficulty
7 Near gale	28 – 33	13.9 – 17.1	50 – 61	32 – 38	Whole trees in motion; inconvenience felt when walking against the wind
8 Gale	34 – 40	17.2 – 20.7	62 – 74	39 – 46	Breaks twigs off trees; generally impedes progress
9 Strong gale	41 – 47	20.8 – 24.4	75 – 88	47 – 54	Slight structural damage occurs (chimney-pots and slates removed)
10 Storm	48 – 55	24.5 – 28.4	89 – 102	55 – 63	Seldom experienced inland; trees uprooted; considerable structural damage occurs
11 Violent storm	56 – 63	28.5 – 32.6	103 – 117	64 – 72	Very rarely experienced; accompanied by widespread damage
12 Hurricane	64 and over	32.7 and over	118 and over	73 and over	

Table 5.2. Wind speed equivalents for arctic areas and areas where there is no vegetation

Beaufort scale number and description	Wind speed equivalent at a standard height of 10 m above open flat ground				Specifications for estimating speed for arctic areas and areas where there is no vegetation
	(kt)	(m s⁻¹)	(km h⁻¹)	(mi h⁻¹)	
0 Calm	< 1	0 – 0.2	< 1	< 1	
1 Light air	1 – 3	0.3 – 1.5	1 – 5	1 – 3	No noticeable wind; smoke rises nearly vertically
2 Light breeze	4 – 6	1.6 – 3.3	6 – 11	4 – 7	Wind felt on face, leaves rustle
3 Gentle breeze	7 – 10	3.4 – 5.4	12 – 19	8 – 12	Hair is disturbed, clothing flaps
4 Moderate breeze	11 – 16	5.5 – 7.9	20 – 28	13 – 18	Dust and loose paper raised, hair disarranged
5 Fresh breeze	17 – 21	8.0 – 10.7	29 – 38	19 – 24	Force of wind felt on body; limit of agreeable wind on land
6 Strong breeze	22 – 27	10.8 – 13.8	39 – 49	25 – 31	Some inconvenience in walking
7 Near gale	28 – 33	13.9 – 17.1	50 – 61	32 – 38	Difficulty when walking against wind
8 Gale	34 – 40	17.2 – 20.7	62 – 74	39 – 46	Difficulty with balance in walking
9 Strong gale	41 – 47	20.8 – 24.4	75 – 88	47 – 54	Danger in being blown over
10 Storm	48 – 55	24.5 – 28.4	89 – 102	55 – 63	Trees uprooted, considerable structural damage
11 Violent storm	56 – 63	28.5 – 32.6	103 – 117	64 – 72	
12 Hurricane	64 and over	32.7 and over	118 and over	73 and over	

For nearly all applications, it is necessary to measure the averages of wind speed and direction. Many applications also need gustiness data. A wind-measuring system, therefore, consists not only of a sensor, but also of a processing and recording system. The processing takes care of the averaging and the computation of the standard deviations and extremes. In its simplest form, the processing can be done by writing the wind signal with a pen recorder and estimating the mean and extreme by reading the record.

5.2　　ESTIMATION OF WIND

In the absence of equipment for measuring wind, the observations must be made by estimation. The errors in observations made in this way may be large, but, provided that the observations are used with caution, the method may be justified as providing data that would otherwise not be available in any way. If either temporarily or permanently the wind data of some stations are obtained by estimation instead of measurement, this fact should be documented in station records made accessible to data users.

5.2.1　　Wind speed

Estimates are based on the effect of the wind on movable objects. Almost anything which is supported so that it is free to move under the influence of the wind can be used, but the descriptive specifications given in the Beaufort scale of wind force, as reproduced in the tables, will be found especially useful.

In order to make the estimates, the observer (and the wind-susceptible object) must stand on flat open terrain as far as possible from obstructions. It must always be remembered that even small obstructions cause serious changes in wind speed and deviations in wind direction, especially at their lee side.

5.2.2   Wind direction

In the case of an absence of instruments, or when the instrumental equipment is unserviceable, the direction should be estimated by observing the drift of smoke from an elevated chimney, the movement of leaves, and so on, in an open situation, or a streamer or pennant fixed to a tall flagstaff. In addition, the wind drogue at an airport may be used when the wind speed is sufficient to move such a device.

Whichever of these aids is used, errors due to perspective are liable to be made unless the observer stands vertically below the indicator. Care should be taken to guard against mistaking local eddies caused by buildings, and the like, for the general drift of the wind.

In an open location, the surface wind direction can be estimated rather accurately by facing the wind. The direction of the movement of clouds, however low, should not be taken into account.

5.2.3   Wind fluctuations

No attempt should be made to estimate peak gusts or standard deviations without proper instruments and recording devices.

5.3   SIMPLE INSTRUMENTAL METHODS

At stations where orthodox anemometers cannot be installed it may be possible to provide some very low-cost, simple instruments that help the observer take measurements that are somewhat more reliable than those obtained by unaided estimation.

5.3.1   Wind speed

Simple hand-held anemometers, if they are used, should be set up and read in accordance with the maker's instructions. The measurement should be taken from a point well exposed to the wind, and not in the lee of obstructions such as buildings, trees and hillocks. If this is not possible, the measurement point should be a good distance from obstructions, namely at least 10 times the obstruction height and upwind or sideways by at least twice the obstruction height.

5.3.2   Wind direction

Direction may be estimated from a vane (or banner) mounted on a pole that has pointers indicating the principal points of the compass. The vane is observed from below, and wind direction may be estimated to the nearest of the 16 points of the compass. If the vane oscillates in the wind, the wind direction must be estimated as the average direction about which the oscillations occur.

5.4   CUP AND PROPELLER SENSORS

Cup and propeller anemometers are commonly used to determine wind speed and consist of two sub-assemblies: the rotor and the signal generator. In well-designed systems, the angular velocity of the cup or propeller rotor is directly proportional to the wind speed, or, more

precisely, in the case of the propeller rotor, to the component of the wind speed parallel to the axis of rotation. Also, in well-designed anemometers, the calibration linearity is independent of air density, has good zero and range stability, and is easily reproduced in a manufacturing process. Near the starting threshold, say for wind speeds of less than 4 m s^{-1}, the calibration of cup anemometers can deviate substantially from linearity, if the arm connecting the cup to the rotation axis is much longer than the diameter of the cup (Patterson, 1926).

The nature of the response of the cup and propeller-type wind-speed sensors to changes in wind speed can be characterized by a response length, the magnitude of which is directly proportional to the moment of inertia of the rotor and, in addition, depends on a number of geometric factors (Busch and Kristensen, 1976; Coppin, 1982).

For almost all cup and propeller-type wind sensors, the response is faster for acceleration than for deceleration, so that the average speed of these rotors overestimates the actual average wind speed. Moreover, vertical velocity fluctuations can cause overspeeding of cup anemometers as a result of reduced cup interference in oblique flow (MacCready, 1966). The total overspeeding can be as much as 10% for some designs and turbulent wind conditions (cup anemometers at 10 m height with a response length of 5 m over very rough terrain; Coppin, 1982). This effect can be minimized by choosing fast-response anemometers, either cup anemometers of a design verified as having a good cosine response or propeller vanes that have virtually no vertical component of overspeeding. In case that performance cannot be investigated in a wind tunnel, operational anemometers can be compared in the field with a calibrated anemometer (Albers et al., 2000).

Since both cup and propeller rotors turn with an angular velocity that is directly proportional to speed or to the axial component, they are particularly convenient for driving a wide variety of signal generators. Alternating and direct current generators, optical and magnetic pulse generators, and turn-counting dials and registers have been used (WMO, 2001). The choice of signal generator or transducer depends largely on the type of data processor and read-out to be used. Care should be taken to ensure that the bearings and signal generator have low starting and running frictional torques, and that the moment of inertia of the signal generator does not reduce the response too much. In cases of long-distance transmission, voltage signals decrease due to cable resistance losses and are therefore inferior to pulse frequency signals, which are not so affected during transmission.

The required and achievable characteristics for wind-speed sensors are included in Part I, Chapter 1, Annex 1.E.

5.5   WIND-DIRECTION VANES

For the purpose of obtaining a satisfactory measurement, a wind vane will be suitable if it is well balanced so as not to have a preferred position in case the axis is not vertical. Multiple vane fins should preferably be parallel to the vane axis, because a vane with two fins at angles > 10° to its axis has two equilibrium positions which each differ significantly from the real wind direction (Wieringa and van Lindert, 1971).

The response of the usual underdamped wind vane to a sudden change in wind direction is normally characterized by overshoot and oscillation about its true position, with the amplitude decreasing approximately exponentially. Two variables are used to define this response: the "undamped natural frequency" or "wavelength" and the "damping ratio", the ratio of the actual damping to the critical damping (MacCready, 1966; Mazzarella, 1972). A damping ratio between 0.3 and 0.7 is considered to be good and as having not too much overshoot, and a reasonably fast response (Wieringa, 1967). Where a relatively long period average is to be computed from data captured at short intervals, it is self-evident that lower damping ratios may be acceptable.

The signal generator is essentially a shaft-angle transducer, and many varieties have been employed. Potentiometers, alternating and direct current synchros, digital angle-encoder discs, direct reading dials and rotary switches have been used to advantage. The choice of signal

generator is largely a matter of the type of data processor and read-out used. Care should be taken to ensure that the bearings and signal generator have low starting and running frictional torques. The simplest recording method is to have a sheet mounted around a cylinder rotating with the vane axis, on which a writing instrument slowly travels downward.

The absolute accuracy of direction measurement also depends on the care with which the instrument has been aligned to true north. The required and achievable characteristics for wind-direction vanes are included in Part I, Chapter 1, Annex 1.E.

5.6   OTHER WIND SENSORS

Many physical principles can be used to measure wind speed and direction, all of which have their own merits and problems. New systems often have been developed for specific purposes, such as small-scale fluctuations and air pollution studies (see for example, Smith (1980)). The following are other types of sensors:

(a)   Pitot tube anemometers, which measure the overpressure in a tube that is kept aligned with the wind vector by means of a direction vane (see Gold (1936) and WMO (1984*a*) for a description of the Dines anemometer). The Dines linearizing recording system deals with the speed averaging problem caused by the quadratic relation between wind speed and pressure, and it also provides useful gustiness records without requiring electrical power;

(b)   Sonic anemometers, which measure the time between emission and reception of an ultrasonic pulse travelling over a fixed distance (Kaimal, 1980). Because sonic anemometers have no moving parts owing to their principle, they have high durability and little accuracy deterioration;

(c)   Hot-disc anemometers are recently developed solid-state instruments which measure the temperature gradient across a chip arrangement. This provides both wind speed and direction at accuracies within the specification of Part I, Chapter 1, Annex 1.E (Van Oudheusden and Huijsing, 1991; Makinwa et al., 2001). They are sturdy, and steady in calibration, but operational experience is limited so far;

(d)   Hot-wire anemometers measure the cooling of thin heated wires. Operationally they are rather unreliable, both because of excessive fragility and because their calibration changes rather fast in unclean or wet surroundings. They are not recommended for use in precipitation;

(e)   Antique swinging-plate vanes are a little better than no instrument at all;

(f)   Remote wind-sensing techniques with sound (sodar), light (lidar) or electromagnetic waves (radar) are uncommon in routine meteorological networks and will not be discussed in this Guide. Details are provided in Lenschow (1986).

5.7   SENSORS AND SENSOR COMBINATIONS FOR COMPONENT RESOLUTION

Propellers which respond only to the wind speed component that is parallel to the axis of rotation of the rotor can be mounted orthogonally to produce two read-outs which are directly proportional to the components in the axis directions. Other sensors, such as twin-axis sonic anemometers, perform the same function at the expense of more sophisticated electronic adjuncts. Orthogonal propellers have the disadvantage that exact cosine response (namely, pure component sensitivity) is difficult to attain. A cup anemometer/vane combination or a propeller vane can also be used as a component device when the velocity components are computed from the measured wind speed and direction.

5.8   **DATA-PROCESSING METHODS**

Signals from anemometer/vane combinations can be processed and averaged in many different ways. Before considering the aspects of the entire wind-measuring chain (exposure, sensing, transmission, filtering, recording and processing), it is useful to discuss the problem of averaging. This Guide deals with the following outputs: averaged horizontal wind (components or speed/direction), standard deviations and peak gust.

5.8.1   **Averaging**

The averaging of wind vectors or their components is straightforward in principle, but there are a few problems associated with it. The first is that the mean vector speed in the average wind direction U is less than the average of all instantaneous wind speeds by a small amount, generally a few % (MacCready, 1966; Wieringa, 1980a). If necessary, this may be corrected if the standard deviation of wind direction s_d is measured; for the ratio of U, and the averaged instantaneous wind speeds is (Frenkiel, 1951):

$$U \Big/ \overline{\sqrt{\left(u_i^2 + v_i^2\right)}} = 1 - s_d^2 / 2 \qquad (5.2)$$

This effect of crosswind turbulence is often confused with the overestimation (overspeeding), causing distortion in the standard deviation s_u (see section 5.4).

The second problem is the discontinuity of the wind direction between 0° and 360°. This problem can be solved either by recording on a cylinder or by extending the recorder range (for example to 540° with an automatic device switching the range from 0 to 360 and from 540 to 180), or by a computer algorithm that makes successive samples continuous by adding or subtracting 360° when necessary. The fact that the first-order response of a cup anemometer and the second-order response of a vane cannot be fully matched is a problem of minor importance, because the response differences are reflected only in the high-frequency part of the fluctuations.

From the fundamental point of view, component averaging is preferable over the independent averaging of speed and direction. However, the differences are very small and, for most applications, component averages can easily be derived from average speed and direction. This also applies to the corresponding standard deviations. From the technical point of view, the independent treatment of speed and direction is preferable for a number of reasons. First of all, the processing of the signal for speed and direction is independent, which implies that the operation of one instrument can continue even when the other drops out. Secondly, this data reduction is simpler than in those cases where components have to be computed. Lastly, the independent treatment of speed and direction is compatible with common usage (including SYNOP and SHIP coding).

The averages of horizontal wind speed can be obtained with a number of both mechanical and electrical devices. Perhaps the simplest example is a mechanical rotation-counting register on a cup anemometer commonly used to measure the passage of wind during a chosen averaging time interval. At the other end of the complexity spectrum, electrical pulse generators drive special-purpose digital processors, which can easily calculate averages, peak gusts and standard deviations.

If wind speed and direction are recorded as continuous graphs, an observer can estimate 10 min averages fairly accurately from a pen recording. The recorded wind trace can also be used to read peak gusts. The reading of dials or meters gives a feel for the wind speed and its variability, but is subject to large errors when averages are needed. Instantaneous read-outs are, therefore, less suitable to obtain 10 min averages for standard weather reports.

5.8.2 Peak gusts and standard deviations

The computation or recording of wind fluctuations is extremely sensitive to the dynamic response of all the elements of the measuring chain, including response length and damping ratio of the sensors. Additionally, the dynamic response of the system as a whole determines the duration of peak gusts, as defined in section 5.1.1. Slowly responding systems spread out the extremes and indicate wide gusts with small amplitude, whereas fast-response systems record high and narrow peaks (gusts of short duration). It is clear that the dynamic response of wind systems has to be carefully designed to obtain gusts or standard deviations that are accurate, reliable and compatible between stations.

Before specifying the appropriate response characteristics of wind-measuring systems, it is necessary to define the gust duration as required by the application. Wind extremes are mainly used for warning purposes and for the climatology of extreme loads on buildings, constructions and aircraft. It is important to realize that the shortest gusts have neither the time nor the horizontal extent to exert their full damaging effect on large constructions. WMO (1987) concludes that a gust duration of about 3 s accommodates most potential users. Gusts that persist for about 3 s correspond to a "wind run" (duration multiplied by the average wind speed) of the order of 50 to 100 m in strong wind conditions. This is sufficient to engulf structures of ordinary suburban/urban size and to expose them to the full load of a potentially damaging gust.

The standard deviation of wind direction and wind speed can easily be computed with microcomputer-based equipment by taking samples of the signals at intervals of about 1 s. Sampling frequencies should not be too great, because the sensor itself provides smoothing over a multiple of its response distance (Wieringa, 1980b). A sampling frequency of 0.25 Hz is suitable in most cases, but depends on the response distance of the sensor and the wind speed. Part IV, Chapter 2, includes a detailed discussion of the theory of sampling sensor signals.

Simultaneous computation of the standard deviation of the horizontal wind speed over 10 min together with the detection of gusts with a duration of a few seconds gives interesting requirements for electronic filters. The gusts are most critical with regard to filtering, so in practice the system is optimized for them. Any low-pass filter used for the detection of peak gusts measured by fast anemometers, smoothing over a few seconds, may reduce the standard deviation by up to 10%. This can be corrected if the filtering variables in the measuring chain are well documented. Often, in practice, the reduction is less because the standard deviation increases if the average wind speed shows a positive or negative trend. Alternatively, the unfiltered signal can be recorded separately for the purpose of measuring an unbiased standard deviation. In the next section, recommendations are made for wind-measuring systems with exact values for the filter variables.

In order to determine peak gusts accurately, it is desirable to sample the filtered wind signal every 0.25 s (frequency 4 Hz). Lower sampling frequencies can be used, but it should be realized that the estimate of the extreme will generally be lower as the extreme in the filtered signal may occur between samples.

Apart from the wind vane inertial damping, any further filtering should be avoided for wind direction. This means that the standard deviation of wind direction can be determined within 2% with most wind vanes.

Accurate computation of the standard deviation of wind direction requires a minimum resolution of the digitization process, which is often done on the shaft of the vane by means of a digital encoder. A 7 bit resolution is quite sufficient here because then a 5° unit for the standard deviation can still be measured with an accuracy of 1% (WMO, 1987).

5.8.3   Recommendations for the design of wind-measuring systems[1]

Wind-measuring systems can be designed in many different ways; it is impossible to cover all design options in this Guide. Two common examples are given here, one with mainly analogue signal treatment and the other with digital signal processing (WMO, 1987).

The first system consists of an anemometer with a response length of 5 m, a pulse generator that generates pulses at a frequency proportional to the rotation rate of the anemometer (preferably several pulses per rotation), a counting device that counts the pulses at intervals of 0.25 s, and a microprocessor that computes averages and standard deviation over 10 min intervals on the basis of 0.25 s samples. The extreme has to be determined from 3 s averages, namely, by averaging over the last 12 samples. This averaging has to be done every 0.25 s (namely, overlapping 3 s averages every 0.25 s). The wind direction is measured with a vane that has an undamped wavelength of 5 m, a damping ratio of 0.3, and a 7 bit digital encoder that is sampled every second. Averages and standard deviations are computed over 10 min intervals, where successive samples are checked for continuity. If two successive samples differ by more than 180°, the difference is decreased by adding or subtracting 360° from the second sample. With response lengths of 5 m for the anemometer and the wind vane (damping ratio 0.3, undamped wavelength 10 m), the standard deviations of wind speed and wind direction are reduced by about 7% and 2%, respectively. The gust duration corresponding to the entire measuring chain (as defined in section 5.1.1) is about 3 s.

The second system consists of an anemometer with a response length of 5 m, a voltage generator producing a voltage proportional to the rotation rate of the anemometer, analogue-to-digital conversion every second, and the digital processing of samples. The wind-direction part consists of a vane with an undamped wavelength of 5 m and a damping ratio of 0.3, followed by analogue-to-digital conversion every second and digital computation of averages and standard deviations. To determine peak gusts the voltage is filtered with a first-order filter with a time constant of 1 s and analogue-to-digital conversion every 0.25 s. With regard to filtering, this system is slightly different from the first one in that standard deviations of wind speed and direction are filtered by 12% and 2%, respectively, while again the gust duration is about 3 s. This system can also be operated with a pen recorder connected to the analogue output instead of the analogue-to-digital converter. Only averages and extremes can be read now, and the gust duration is about 3 s, unless the pen recorder responds more slowly than the first-order filter.

The signal-processing procedure, as described above, is in accordance with Recommendation 3 (CIMO-X) (WMO, 1990) and guarantees optimal accuracy. The procedure, however, is fairly complicated and demanding as it involves overlapping averages and a relatively high sampling frequency. For many applications, it is quite acceptable to reduce the sampling rate down to one sample every 3 s, provided that the wind signal has been averaged over 3 s intervals (namely, non-overlapping averaging intervals). The resulting gust duration is about 5 s and the reduction in standard deviation is 12% (Beljaars, 1987; WMO, 1987).

5.9   EXPOSURE OF WIND INSTRUMENTS

5.9.1   General problems

Wind speed increases considerably with height, particularly over rough terrain. For this reason, a standard height of 10 m above open terrain is specified for the exposure of wind instruments. For wind direction, the corresponding shift over such a height interval is relatively small and can be ignored in surface wind measurements. An optimum wind observation location is one where the observed wind is representative of the wind over an area of at least a few kilometres, or can easily be corrected to make it representative.

For terrain that is uneven, contains obstacles, or is non-homogeneous in surface cover, both wind speed and direction can be affected considerably. Corrections are often possible, and the tools

---

[1]   Recommended by the Commission for Instruments and Methods of Observation at its tenth session (1989).

to compute such corrections are becoming available. To improve the applicability of wind data, essential information to perform such corrections should be transmitted to the users in addition to the direct measurements.

5.9.2 Anemometers over land

The standard exposure of wind instruments over level, open terrain is 10 m above the ground. Open terrain is defined as an area where the distance between the anemometer and any obstruction is at least 10 times the height of the obstruction. Wind measurements that are taken in the direct wake of tree rows, buildings or any other obstacle are of little value and contain little information about the unperturbed wind. Since wakes can easily extend downwind to 12 or 15 times the obstacle height, the requirement of 10 obstruction heights is an absolute minimum. In practice, it is often difficult to find a good or even acceptable location for a wind station. The importance of optimizing the location can hardly be overstressed; nonetheless, it is difficult to give universal guidelines. In some cases, however, the data can be largely corrected for obstructions, as follows:

(a) Obstacles at a distance of more than 30 times their height: no correction needs to be applied;

(b) Obstacles at a distance of more than 20 times their height: correction can be applied;

(c) Obstacles at a distance of more than 10 times their height: correction may be applied in some situations, taking special care.

It should be noted that when the distance is less than 20 times the height of the obstacle, the measured value before correction can be erroneous by up to 25%; when the distance is about 10 times the height of the obstacle, the measured value can in some cases even indicate the opposite direction.

Detailed information on the exposure correction is provided in paragraph 5.9.4.

In Table 5.3, the classification of wind observing sites based on siting and exposure is summarized. Full details on the siting classification for surface observing stations on land, which provides additional guidance on the selection of a site and the location of a wind sensor within a site to optimize representativeness, can be found in Part I, Chapter 1, Annex 1.B of this Guide.

Table 5.3. Classification of wind observing sites based on siting and exposure

Class	Distance of mast to surrounding obstacles[a] (with height h)	Distance of sensors to thin obstacles[b] (with height > 8 m, width w)	Roughness class index[c]	Ignore single obstacles below x m
1	≥ 30 h	≥ 15 w	2 – 4 (roughness length ≤ 0.1 m)	$x = 4$
2	≥ 10 h	≥ 15 w	2 – 5 (roughness length ≤ 0.25 m)	$x = 4$
3	≥ 5 h	≥ 10 w		$x = 5$
4	≥ 2.5 h	No obstacle with angular width > 60° and height > 10 m within 40 m distance		$x = 6$, if measurement at ≥ 10 m
5	Not meeting requirements of any other class			

Notes:
a   An obstacle is defined as an object having an angular width > 10°.
b   A thin obstacle is for instance a mast, thin tree or lamp post.
c   Roughness is defined in the annex of this chapter.

Two aspects are very important. First, the sensors should be kept away from local obstructions as much as possible. When wind measurements are taken on the side of masts or towers rather than at their top, the instruments should be placed on booms with a length of at least three mast or tower widths (Gill et al., 1967). When wind instruments are placed on top of a building, they should be raised at least one building width above the top. Secondly, the local situation should be well documented (Wieringa, 1983). There should at least be a map of the station surroundings within a radius of 2 km, documenting obstacle and vegetation locations and height, terrain elevation changes, and so forth. Changes in the surroundings, such as the construction of buildings or growth of trees nearby, should be explicitly recorded in station logbooks. Station instrumentation should be specified in detail.

Where standard exposure is unobtainable, the anemometer may be installed at such a height that its indications should not be too much affected by local obstructions and represent as far as possible how the wind at 10 m would be if there were no obstructions in the vicinity. If the terrain varies little with azimuth, this may be effected by placing the anemometer at a height exceeding 10 m by an amount depending on the effective surface roughness length z_0 of the surroundings (see the annex): about 13 m if $z_0 = 0.1$ m, and about 19 m if $z_0 = 0.5$ m. Wieringa (1980b) shows that the strategy of anemometer height increase does not work well if local sheltering varies strongly with azimuth. Simple calculation procedures now exist to determine the effect of local topography (Walmsley et al., 1990), and the climatology of the gustiness records can be used to determine exposure corrections in inhomogeneous surroundings (Verkaik, 2000). Evans and Lee (1981) and Grimmond et al. (1998) discuss the problem in urban areas (see also Part II, Chapter 9).

In freezing weather, special precautions must be taken to keep the wind sensors free from sleet and ice accumulations. In some localities it may be desirable to provide some form of artificial heating for the exposed parts such as a thermostatically controlled infrared radiator. Sleet and ice shields have been designed for particular types of wind equipment (see Curran et al., 1977).

5.9.3   Anemometers at sea

There is an increasing requirement for instrumental measurements of wind over the sea, especially by means of automatic unattended systems (see also Part II, Chapter 4). This task presents special problems since the standard exposure height of 10 m specified for land use cannot always be achieved in a marine environment owing to the state of the sea and/or tidal height variation. The obvious extrapolation of the exposure criteria for land sites leads to the idea that, on moored buoys, the anemometer should be mounted 10 m above the waterline of the buoy. However, other sources of error are often more significant than those arising from different exposure heights (for a review, see WMO, 1981). On fixed platforms and ships, it is of the utmost importance that wind sensors be exposed sufficiently high above the platform and its superstructure to avoid the often extensive influence of the platform on the local wind structure. In general, it is never safe to assume that a wind sensor is unaffected by the platform structure, even if it is exposed at least 10 m above the height of the tallest obstruction on the platform, unless the platform is relatively small. WMO (1981) concludes that, at sea, good exposure should have higher priority in obtaining accurate and useful measurements than standardization of the measurements at 10 m (WMO, 1989). Despite careful siting, it is often impossible in practice to avoid exposure errors. In order to allow height and flow distortion corrections to be made, it is very important to keep a record and detailed information about anemometer location and platform or ship type (shape, dimension). If wind speed is measured at a height significantly greater than 10 m (namely, when the appropriate reduction factor would be > 1.2), a reduction to the 10 m level should be performed according to the procedures recommended in the following paragraph, and using the constant for "open sea" in the table of the annex.

5.9.4   Exposure correction

Surface wind measurements without exposure problems hardly exist. The requirement of open, level terrain is difficult to meet, and most wind stations over land are perturbed by topographic effects or surface cover, or by both (WMO, 1987; Wieringa, 1996).

It is clear that exposure errors pose problems to users of wind data and often make the data useless. This problem is particularly serious in numerical forecast models where there is a tendency to analyse the wind and pressure fields separately. Surface winds, however, can be used for initialization only if they are representative of a large area. This means that errors due to local exposure and/or non-standard measurement height must be removed.

The correction of wind readings for local exposure can be performed only with measurements of reasonable quality at locations that are not too rough ($z_0 \leq 0.5$ m) and reasonably level. No attempt should be made to correct measurements that have hardly any relation to a regional average. For example, a wind station in a deep valley, where the flow is dominated by katabatic effects, may be important for local forecasts, but cannot be used as a regionally representative wind.

If U is the wind speed measured at height z, the corrected wind speed U_c which would be indicated locally at 10 m above terrain with roughness z_0 follows from:

$$U_c = U \cdot C_F \cdot C_T \cdot \frac{\ln(10/z_{0u})}{\ln(z/z_{0u})} \cdot \frac{\ln(60/z_{0u})\ln(10/z_0)}{\ln(10/z_{0u})\ln(60/z_0)} \tag{5.3}$$

where C_F is the flow distortion correction; C_T is the correction factor due to topographic effects; z_{0u} is the effective roughness length of the terrain upstream of the measurement station, and z_0 is roughness length in the application (for example, a grid box value in a numerical forecast model). In this expression, z, z_0 and z_{0u} are specified in metres. The different correction terms represent the following:

(a)   Flow distortion: The correction factor C_F accounts for flow distortion by nearby big objects. This is particularly important for anemometers on buildings, ships, and platforms at sea. The best way of finding C_F as a function of wind direction is by means of model simulation in a wind tunnel (Mollo-Christensen and Seesholtz, 1967). Estimates based on potential flow around simple configurations can also be applied (Wyngaard, 1981; WMO, 1984b). For measurements on top of a free-standing mast, flow distortion is negligible ($C_F = 1$).

(b)   Topographic correction: This correction accounts for terrain height effects around the wind station. C_T is the ratio of the regionally averaged wind speed (averaged over ridges and valleys at 10 m above local terrain) and the wind speed measured at the wind station. In the example of an isolated hill with a station at the top of the hill, C_T should be less than 1 to correct for the speed-up induced by the hill, to make the result representative of the area rather than of the hill top only. C_T equals 1 for flat terrain. For isolated hills and ridges, estimates of C_T can be made with the help of simple guidelines (Taylor and Lee, 1984). In more complicated topography, model computations are needed on the basis of detailed height contour maps of the terrain surrounding the wind stations (Walmsley et al., 1990). Such computations are fairly complicated but need to be done only once for a single station and lead to a semi-permanent table of C_T as a function of wind direction.

(c)   Non-standard measurement height: This effect is simply included in the U_c formula by assuming a logarithmic profile combined with the roughness length z_{0u} of the upstream terrain. For stations over sea, this reduction to standard height can be important, but stability corrections are relatively small there, justifying the logarithmic form of the reduction.

(d)   Roughness effects: Upstream roughness effects as well as the effects of surface obstacles can be corrected by extrapolating the wind speed logarithmic profile to a height of 60 m with the station specific effective roughness length z_{0u} and by interpolating back to 10 m with the roughness length z_0 necessary for the application. The roughness length z_{0u} should be representative of a 2 km fetch upwind of the wind station; the value usually depends on wind direction. The annex discusses how to estimate z_{0u}.

If flow distortion and topography problems are negligible or have been corrected, apply the (c) to (d) exposure correction by formula 5.3 towards $z = 10$ m and $z_0 = 0.03$ m. Corrected wind speeds then will be equivalent to those which would have been measured at a local hypothetical wind station conforming fully with WMO requirements (10 m over open terrain). Wind speeds

corrected in this way are called potential wind speeds (WMO, 2001). Two comments are appropriate here. First, the extrapolation height of 60 m should not be seen as a very firm value. Heights between 40 and 80 m would have been acceptable; 60 m is about the correct magnitude in relation to the 2 km fetch for which z_{0u} is representative and has proved to give satisfactory results (Wieringa, 1986). Secondly, stability-related changes in the wind profile cannot be neglected over the height range from 10 to 60 m, but the effect of stability is relatively small in the present formulation because the stability corrections in the transformations upwards and downwards cancel out. A practical example of the application of wind measurement correction in an operational context is given in WMO (2000) and WMO (2001). Although most of the exposure correction can be directly applied to the measurements, both unadjusted (Level I) data and adjusted (Level II) data are to be disseminated.

5.10 CALIBRATION AND MAINTENANCE

A fully reliable calibration of cup, propeller and vane anemometers is possible only in a wind tunnel; the performance of such instruments is now well known and the manufacturer's calibration can be relied upon for most purposes, when the instrument is in good condition. Wind-tunnel tests are useful for special projects or for type-testing new models. For more information, see the International Organization for Standardization (ISO) standards (ISO 16622:2002 and ISO 17713-1:2007).

In the field, anemometers are prone to deterioration and regular inspections are advisable. A change in sensor characteristics leading to a deterioration in wind data quality may occur as a result of physical damage, an increase in bearing friction from the ingress of dust, corrosion, or degradation of the transduction process (for example, a reduction in the output of a cup or propeller generator as a result of brush wear).

The inspection of analogue traces will show faults as indicated by incorrect zero, stepped traces due to friction, noise (which may be evident at low wind speeds), low sensitivity (at low speeds), and irregular or reduced variability of recorded wind.

Instruments should be inspected for physical damage, by checking the zero of the anemometer system by holding the cups or propeller, and by checking vane orientation by holding it fixed in a predetermined position or positions. Repairs to the sensors are usually only practicable in a workshop.

System checks should regularly be carried out on the electrical and electronic components of electrical recording or telemetering instruments. Zero and range checks should be made on both the speed and direction systems.

———————

ANNEX. THE EFFECTIVE ROUGHNESS LENGTH

For the purpose of exposure correction, a roughness length z_0 that represents the terrain over 2 km of upstream fetch is needed as a function of wind direction. The quality of the roughness correction is very much dependent on the accuracy of this roughness length.

Over sea, the task is relatively simple because of the uniform fetch. The so-called Charnock relation can be applied. It expresses the sea surface roughness to the friction velocity $u*$ and the gravitational acceleration g by means of $z_{0u} = \alpha\, u*^2/g$, where α is an empirical constant approximately equal to 0.014. The friction velocity relates to the neutral wind profile by means of $U(z) = (u*/\kappa) \ln (z/z_{0u})$, where κ is the Von Karman constant (0.4) and z is the measurement height. These two equations have to be solved iteratively, which can be done by starting with $z_{0u} = 0.000\ 1$, computing $u*$ from the log-profile, evaluating z_{0u} again, and repeating this a few times.

The surface roughness length over land depends on the surface cover and land use and is often difficult to estimate. A subjective way of determining z_{0u} is by a visual survey of the terrain around the wind station with the help of the table below, the validity of which has been recently corroborated (Davenport et al., 2000). Choosing wind direction sectors of 30° up to a distance of 2 km is most convenient. With very non-homogeneous fetch conditions, an effective roughness should be determined by averaging ln (z_{0u}) rather than z_{0u} itself.

The best way of determining z_{0u} is with the help of about one year of climatology of the standard deviations. The standard deviations of wind speed and wind direction are related to the upstream roughness over a few kilometres and can be used for an objective estimate of z_{0u}. Both the standard deviation of wind speed s_u and the standard deviation of wind direction s_d (in radians) can be employed by means of the following formulae:

$$s_u/U = c_u\kappa \left[\ln\left(z/z_{0u}\right)\right]^{-1} \qquad\qquad 5.\text{A}.1$$

$$s_d/U = c_v\kappa \left[\ln\left(z/z_{0u}\right)\right]^{-1} \qquad\qquad 5.\text{A}.2$$

where $c_u = 2.2$ and $c_v = 1.9$ and $\kappa = 0.4$ for unfiltered measurements of s_u and s_d. For the measuring systems described in section 5.8.3, the standard deviation of wind speed is filtered by about 12%, and that of wind direction by about 2%, which implies that c_u and c_v reduce to 1.94 and 1.86, respectively. In order to apply the above equations, it is necessary to select strong wind cases ($U > 4$ m s^{-1}) and to average s_u/U and/or s_d over all available data per wind sector class (30° wide) and per season (surface roughness depends, for example, on tree foliage). The values of z_{0u} can now be determined with the above equations, where comparison of the results from s_u and s_d give some idea of the accuracy obtained.

In cases where no standard deviation information is available, but the maximum gust is determined per wind speed averaging period (either 10 min or 1 h), the ratios of these maximum gusts to the averages in the same period (gust factors) can also be used to determine z_{0u} (Verkaik, 2000). Knowledge of system dynamics, namely, the response length of the sensor and the response time of the recording chain, is required for this approach.

**Terrain classification from Davenport (1960) adapted by Wieringa (1980b)
in terms of aerodynamic roughness length z_0**

Class index	Short terrain description	z_0 (m)
1	Open sea, fetch at least 5 km	0.000 2
2	Mud flats, snow; no vegetation, no obstacles	0.005
3	Open flat terrain; grass, few isolated obstacles	0.03
4	Low crops; occasional large obstacles, $x/H > 20$	0.10
5	High crops; scattered obstacles, $15 < x/H < 20$	0.25
6	Parkland, bushes; numerous obstacles, $x/H \approx 10$	0.5
7	Regular large obstacle coverage (suburb, forest)	1.0
8	City centre with high- and low-rise buildings	≥ 2

Note: Here x is a typical upwind obstacle distance and H is the height of the corresponding major obstacles. For more detailed and updated terrain class descriptions see Davenport et al. (2000) (see also Part II, Chapter 9, Table 9.2).

——————————

REFERENCES AND FURTHER READING

Ackermann, G.R., 1983: Means and standard deviations of horizontal wind components. *Journal of Climate and Applied Meteorology*, 22:959–961.

Albers, A., H. Klug and D. Westermann, 2000: Outdoor comparison of cup anemometers. *DEWI Magazin*, No. 17.

Beljaars, A.C.M., 1987: The influence of sampling and filtering on measured wind gusts. *Journal of Atmospheric and Oceanic Technology*, 4:613–626.

Busch, N.E. and L. Kristensen, 1976: Cup anemometer overspeeding. *Journal of Applied Meteorology*, 15:1328–1332.

Coppin, P.A., 1982: An examination of cup anemometer overspeeding. *Meteorologische Rundschau*, 35:1–11.

Curran, J.C., G.E. Peckham, D. Smith, A.S. Thom, J.S.G. McCulloch and I.C. Strangeways, 1977: Cairngorm summit automatic weather station. *Weather*, 32:60–63.

Davenport, A.G., 1960: Rationale for determining design wind velocities. *Journal of the Structural Division*, American Society of Civil Engineers, 86:39–68.

Davenport, A.G., C.S.B. Grimmond, T.R. Oke and J. Wieringa, 2000: Estimating the roughness of cities and sheltered country. *Preprints of the Twelfth American Meteorological Society Conference on Applied Climatology* (Asheville, NC, United States), pp. 96–99.

Evans, R.A. and B.E. Lee, 1981: The problems of anemometer exposure in urban areas: a wind-tunnel study. *Meteorological Magazine*, 110:188–189.

Frenkiel, F.N., 1951: Frequency distributions of velocities in turbulent flow. *Journal of Meteorology*, 8:316–320.

Gill, G.C., L.E. Olsson, J. Sela and M. Suda, 1967: Accuracy of wind measurements on towers or stacks. *Bulletin of the American Meteorological Society*, 48:665–674.

Gold, E., 1936: Wind in Britain: The Dines anemometer and some notable records during the last 40 years. *Quarterly Journal of the Royal Meteorological Society*, 62:167–206.

Grimmond, C.S.B., T.S. King, M. Roth and T.R. Oke, 1998: Aerodynamic roughness of urban areas derived from wind observations. *Boundary-Layer Meteorology*, 89:1–24.

International Organization for Standardization, 2002: *Meteorology – Sonic Anemometers/Thermometers – Acceptance Test Methods for Mean Wind Measurements*, ISO 16622:2002. Geneva.

———, 2007: *Meteorology – Wind Measurements – Part I: Wind Tunnel Test Methods for Rotating Anemometer Performance*, ISO 17713-1:2007. Geneva.

Kaimal, J.C., 1980: Sonic anemometers. In: *Air-sea Interaction: Instruments and Methods* (F. Dobson, L. Hasse and R. Davis, eds.). Plenum Press, New York, pp. 81–96.

Lenschow, D.H. (ed.), 1986: *Probing the Atmospheric Boundary Layer*. American Meteorological Society, Boston.

MacCready, P.B., 1966: Mean wind speed measurements in turbulence. *Journal of Applied Meteorology*, 5:219–225.

MacCready, P.B. and H.R. Jex, 1964: Response characteristics and meteorological utilization of propeller and vane wind sensors. *Journal of Applied Meteorology*, 3:182–193.

Makinwa, K.A.A., J.H. Huijsing and A. Hagedoorn, 2001: Industrial design of a solid-state wind sensor. *Proceedings of the First ISA/IEEE Conference* (Houston, November 2001), pp. 68–71.

Mazzarella, D.A., 1972: An inventory of specifications for wind-measuring instruments. *Bulletin of the American Meteorological Society*, 53:860–871.

Mollo-Christensen, E. and J.R. Seesholtz, 1967: Wind tunnel measurements of the wind disturbance field of a model of the Buzzards Bay Entrance Light Tower. *Journal of Geophysical Research*, 72:3549–3556.

Patterson, J., 1926: The cup anemometer. *Transactions of the Royal Society of Canada*, 20(III):1–54.

Smith, S.D., 1980: Dynamic anemometers. In: *Air-sea Interaction: Instruments and Methods* (F. Dobson, L. Hasse and R. Davis, eds.). Plenum Press, New York, pp. 65–80.

Taylor, P.A. and R.J. Lee, 1984: Simple guidelines for estimating wind speed variations due to small scale topographic features. *Climatological Bulletin*, Canadian Meteorological and Oceanographic Society, 18:3–22.

Van Oudheusden, B.W. and J.H. Huijsing, 1991: Microelectronic thermal anemometer for the measurement of surface wind. *Journal of Atmospheric and Oceanic Technology*, 8:374–384.

Verkaik, J.W., 2000: Evaluation of two gustiness models for exposure correction calculations. *Journal of Applied Meteorology*, 39:1613–1626.

Walmsley, J.L., I.B. Troen, D.P. Lalas and P.J. Mason, 1990: Surface-layer flow in complex terrain: Comparison of models and full-scale observations. *Boundary-Layer Meteorology*, 52:259–281.

Wieringa, J., 1967: Evaluation and design of wind vanes. *Journal of Applied Meteorology*, 6:1114–1122.

——, 1980*a*: A revaluation of the Kansas mast influence on measurements of stress and cup anemometer overspeeding. *Boundary-Layer Meteorology*, 18:411–430.

——, 1980*b*: Representativeness of wind observations at airports. *Bulletin of the American Meteorological Society*, 61:962–971.

——, 1983: Description requirements for assessment of non-ideal wind stations, for example Aachen. *Journal of Wind Engineering and Industrial Aerodynamics*,11:121–131.

——, 1986: Roughness-dependent geographical interpolation of surface wind speed averages. *Quarterly Journal of the Royal Meteorological Society*, 112:867–889.

——, 1996: Does representative wind information exist? *Journal of Wind Engineering and Industrial Aerodynamics*, 65:1–12.

Wieringa, J. and F.X.C.M. van Lindert, 1971: Application limits of double-pin and coupled wind vanes. *Journal of Applied Meteorology*, 10:137–145.

World Meteorological Organization, 1981: *Review of Reference Height for and Averaging Time of Surface Wind Measurements at Sea* (F.W. Dobson). Marine Meteorology and Related Oceanographic Activities Report No. 3. Geneva.

——, 1984*a*: *Compendium of Lecture Notes for Training Class IV Meteorological Personnel* (B.J. Retallack). (WMO-No. 266), Volume II. Geneva.

——, 1984*b*: Distortion of the wind field by the Cabauw Meteorological Tower (H.R.A. Wessels). *Papers Presented at the WMO Technical Conference on Instruments and Cost-effective Meteorological Observations (TECEMO)*. Instruments and Observing Methods Report No. 15. Geneva.

——, 1987: *The Measurement of Gustiness at Routine Wind Stations: A Review* (A.C.M. Beljaars). Instruments and Observing Methods Report No. 31. Geneva.

——, 1989: *Wind Measurements Reduction to a Standard Level* (R.J. Shearman and A.A. Zelenko). Marine Meteorology and Related Oceanographic Activities Report No. 22 (WMO/TD-No. 311). Geneva.

——, 1990: *Abridged Final Report of the Tenth Session of the Commission for Instruments and Methods of Observation* (WMO-No. 727). Geneva.

——, 1991: *Guidance on the Establishment of Algorithms for Use in Synoptic Automatic Weather Stations: Processing of Surface Wind Data* (D. Painting). Report of the CIMO Working Group on Surface Measurements, Instruments and Observing Methods Report No. 47 (WMO/TD-No. 452). Geneva.

——, 2000: Wind measurements: Potential wind speed derived from wind speed fluctuations measurements, and the representativity of wind stations (J.P. van der Meulen). *Papers Presented at the WMO Technical Conference on Meteorological and Environmental Instruments and Methods of Observation (TECO-2000)*. Instruments and Observing Methods Report No. 74 (WMO/TD-No. 1028). Geneva.

——, 2001: *Lecture Notes for Training Agricultural Meteorological Personnel* (J. Wieringa and J. Lomas) (WMO-No. 551). Geneva.

——, 2011: *Manual on Codes* (WMO-No. 306), Volume I.1. Geneva.

Wyngaard, J.C., 1981: The effects of probe-induced flow distortion on atmospheric turbulence measurements. *Journal of Applied Meteorology*, 20:784–794.

CHAPTER CONTENTS

CHAPTER 6. MEASUREMENT OF PRECIPITATION

6.1 GENERAL

This chapter describes the well-known methods of precipitation measurements at ground stations.

It also addresses precipitation intensity measurements (in particular the rate of rainfall or rainfall intensity) due to the rapidly increasing need for such measurements for the interpretation of rainfall patterns, rainfall event modelling and forecasts.

This chapter does not discuss measurements which attempt to define the structure and character of precipitation, or which require specialized instrumentation, which are not standard meteorological observations (such as drop size distribution). Marine and radar measurements are discussed in Part II, Chapters 4 and 7 respectively, while space-based observations are discussed in Part III.

Information on precipitation measurements which includes, in particular, more detail on snow cover measurements can also be found in WMO (1992*a*, 1998).

The general problem of representativeness is particularly acute in the measurement of precipitation. Precipitation measurements are particularly sensitive to exposure, wind and topography, and metadata describing the circumstances of the measurements are particularly important for users of the data.

The analysis of precipitation data is much easier and more reliable if the same gauges and siting criteria are used throughout the networks. This should be a major consideration in designing networks.

6.1.1 Definitions

Precipitation is defined as the liquid or solid products of the condensation of water vapour falling from clouds or deposited from air onto the ground. It includes rain, hail, snow, dew, rime, hoar frost and fog precipitation. The total amount of precipitation which reaches the ground in a stated period is expressed in terms of the vertical depth of water (or water equivalent in the case of solid forms) to which it would cover a horizontal projection of the Earth's surface. Snowfall is also expressed by the depth of fresh, newly fallen snow covering an even horizontal surface (see section 6.7).

Precipitation intensity is defined as the amount of precipitation collected per unit time interval. According to this definition, precipitation intensity data can be derived from the measurement of precipitation amount using an ordinary precipitation gauge. In that sense, precipitation intensity is a secondary parameter, derived from the primary parameter precipitation amount. However, precipitation intensity can also be measured directly (see section 6.1.4.1).

6.1.2 Units and scales

The unit of precipitation is linear depth, usually in millimetres (volume/area), or kg m^{-2} (mass/area) for liquid precipitation. Daily amounts of precipitation should be read to the nearest 0.2 mm and, if feasible, to the nearest 0.1 mm; weekly or monthly amounts should be read to the nearest 1 mm (at least). Daily measurements of precipitation should be taken at fixed times common to the entire network or networks of interest. Less than 0.1 mm (0.2 mm in the United States) is generally referred to as a trace.

Snowfall measurements are taken in units of centimetres and tenths, to the nearest 0.2 cm. Less than 0.2 cm is generally called a trace. The depth of snow on the ground is usually measured daily in whole centimetres.

The measurement unit of rainfall intensity is linear depth per hour, usually in millimetres per hour (mm h^{-1}). Rainfall intensity is normally measured or derived over one-minute time intervals due to the high variability of intensity from minute to minute.

6.1.3 Meteorological and hydrological requirements

Part I, Chapter 1, Annex 1.E gives a broad statement of the requirements for accuracy, range and resolution for precipitation measurements. It gives the larger of 5% or 0.1 mm as the achievable measurement uncertainty of daily amounts, 1 cm as the achievable uncertainty of depth of snow, and 5 mm h^{-1} for rates of up to 100 mm h^{-1} and 5% for rates above 100 mm h^{-1} as the achievable uncertainties of precipitation intensity in the field (all uncertainties at the 95% confidence level). In addition, for precipitation intensity, Part I, Chapter 1, Annex 1.E gives the achievable uncertainties under constant flow conditions in the laboratory (5% above 2 mm h^{-1} or 2% above 10 mm h^{-1}).

The common observation times are hourly, three-hourly and daily, for synoptic, climatological and hydrological purposes. For some purposes, such as the design and management of urban drainage systems, forecasting and mitigation of flash floods, transport safety measures, and in general most of the applications where rainfall data are sought in real time, a much greater time resolution is required to measure very high rainfall rates over very short periods (typically 1 min for rainfall intensity). For some other applications, storage gauges are used with observation intervals of weeks or months or even a year in mountains and deserts.

6.1.4 Measurement methods

6.1.4.1 *Instruments*

Precipitation gauges (or raingauges if only liquid precipitation can be measured) are the most common instruments used to measure precipitation. Generally, an open receptacle with vertical sides is used, usually in the form of a right cylinder, with a funnel if its main purpose is to measure rain. Since various sizes and shapes of orifice and gauge heights are used in different countries, the measurements are not strictly comparable (WMO, 1989*a*). The volume or weight of the catch is measured, the latter in particular for solid precipitation. The gauge orifice may be at one of many specified heights above the ground or at the same level as the surrounding ground. The orifice must be placed above the maximum expected depth of snow cover, and above the height of significant potential in-splashing from the ground. For solid precipitation measurement, the orifice is above the ground and an artificial shield should be placed around it. The most commonly used elevation height in more than 100 countries varies between 0.5 and 1.5 m (WMO, 1989*a*).

The measurement of precipitation is very sensitive to exposure, and in particular to wind. Section 6.2 discusses exposure, while section 6.4 discusses at some length the errors to which precipitation gauges are prone, and the corrections that may be applied.

Rainfall intensity can be either derived from the measurement of precipitation amount using a recording raingauge (see section 6.5) or measured directly. The latter can be done, for example, by using a gauge and measuring the flow of the captured water, measuring the accretion of collected water as a function of time, or using some optical principles of measurement. A number of techniques for determining precipitation amount are based on these direct intensity measurements by integrating the measured intensity over a certain time interval.

This chapter also describes some other special techniques for measuring other types of precipitation (dew, ice, and the like) and snow cover. Some new techniques which are appearing in operational use are not described here, for example, the optical raingauge, which makes

use of optical scattering. Useful sources of information on new methods under development are the reports of recurrent conferences, such as the international workshops on precipitation measurement (Slovak Hydrometeorological Institute and Swiss Federal Institute of Technology, 1993; WMO, 1989*b*) and the Technical Conference on Meteorological and Environmental Instruments and Methods of Observation (TECO), and the instrument intercomparisons organized by the Commission for Instruments and Methods of Observation (WMO, 1998).

Point measurements of precipitation serve as the primary source of data for areal analysis. However, even the best measurement of precipitation at one point is only representative of a limited area, the size of which is a function of the length of the accumulation period, the physiographic homogeneity of the region, local topography and the precipitation-producing process. Radar and, more recently, satellites are used to define and quantify the spatial distribution of precipitation. In principle, a suitable integration of all three sources of areal precipitation data into national precipitation networks (automatic gauges, radar, and satellite) can be expected to provide sufficiently accurate areal precipitation estimates on an operational basis for a wide range of precipitation data users.

Instruments that detect and identify precipitation, as distinct from measuring it, may be used as present weather detectors, and are referred to in Part I, Chapter 14.

6.1.4.2   *Reference gauges and intercomparisons*

Several types of gauges have been used as reference gauges. The main feature of their design is that of reducing or controlling the effect of wind on the catch, which is the main reason for the different behaviours of gauges. They are chosen also to reduce the other errors discussed in section 6.4.

Ground-level gauges are used as reference gauges for liquid precipitation measurement. Because of the absence of wind-induced error, they generally show more precipitation than any elevated gauge (WMO, 1984, 2009). The gauge is placed in a pit with the gauge rim at ground level, sufficiently distant from the nearest edge of the pit to avoid in-splashing. A strong plastic or metal anti-splash grid with a central opening for the gauge should span the pit. Provision should be made for draining the pit. A description and drawings of a standard pit gauge are given in Annex 6.C and more details are provided in WMO (2009) and the EN 13798:2010 standard (CEN, 2010).

The reference gauge for solid precipitation is the gauge known as the Double Fence Intercomparison Reference. It has octagonal vertical double fences surrounding a Tretyakov gauge, which itself has a particular form of wind-deflecting shield. Drawings and a description are given by Goodison et al. (1989) and in WMO (1985, 1998).

Recommendations for comparisons of precipitation gauges against the reference gauges are given in Annex 6.A.

6.1.4.3   *Documentation*

The measurement of precipitation is particularly sensitive to gauge exposure, so metadata about the measurements must be recorded meticulously to compile a comprehensive station history, in order to be available for climate and other studies and quality assurance.

Section 6.2 discusses the site information that must be kept, namely detailed site descriptions, including vertical angles to significant obstacles around the gauge, gauge configuration, height of the gauge orifice above ground and height of the wind speed measuring instrument above ground.

Changes in observational techniques for precipitation, mainly the use of a different type of precipitation gauge and a change of gauge site or installation height, can cause temporal inhomogeneities in precipitation time series (see Part IV, Chapter 2). The use of differing types

of gauges and site exposures causes spatial inhomogeneities. This is due to the systematic errors of precipitation measurement, mainly the wind-induced error. Since adjustment techniques based on statistics can remove the inhomogeneities relative to the measurements of surrounding gauges, the correction of precipitation measurements for the wind-induced error can reduce the bias of measured values.

The following sections (especially section 6.4) on the various instrument types discuss the corrections that may be applied to precipitation measurements. Such corrections have uncertainties, and the original records and the correction formulae should be kept.

Any changes in the observation methods should also be documented.

6.2 SITING AND EXPOSURE

All methods for measuring precipitation should aim to obtain a sample that is representative of the true amount falling over the area which the measurement is intended to represent, whether on the synoptic scale, mesoscale or microscale. The choice of site, as well as the systematic measurement error, is, therefore, important. For a discussion of the effects of the site, see Sevruk and Zahlavova (1994).

The location of precipitation stations within the area of interest is important, because the number and locations of the gauge sites determine how well the measurements represent the actual amount of precipitation falling in the area. Areal representativeness is discussed at length in WMO (1992a), for rain and snow. WMO (2008) gives an introduction to the literature on the calculation of areal precipitation and corrections for topography.

The effects on the wind field of the immediate surroundings of the site can give rise to local excesses and deficiencies in precipitation. In general, objects should not be closer to the gauge than a distance of twice their height above the gauge orifice. For each site, the average vertical angle of obstacles should be estimated, and a site plan should be made. Sites on a slope or the roof of a building should be avoided. Sites selected for measuring snowfall and/or snow cover should be in areas sheltered as much as possible from the wind. The best sites are often found in clearings within forests or orchards, among trees, in scrub or shrub forests, or where other objects act as an effective wind-break for winds from all directions.

Preferably, however, the effects of the wind, and of the site on the wind, can be reduced by using a ground-level gauge for liquid precipitation or by making the airflow horizontal above the gauge orifice using the following techniques (listed in order of decreasing effectiveness):

(a)   In areas with homogeneous dense vegetation; the height of such vegetation should be kept at the same level as the gauge orifice by regular clipping;

(b)   In other areas, by simulating the effect in (a) through the use of appropriate fence structures;

(c)   By using windshields around the gauge.

The surface surrounding the precipitation gauge can be covered with short grass, gravel or shingle, but hard, flat surfaces, such as concrete, should be avoided to prevent excessive in-splashing.

A classification of measurement sites has been developed in order to quantify and document the influence of the surrounding environment (see Part I, Chapter 1, Annex 1.B of this Guide). This classification uses a relatively simple description of the (land-based) sites.

6.3   NON-RECORDING PRECIPITATION GAUGES

6.3.1   Ordinary gauges

6.3.1.1   *Instruments*

The commonly used precipitation gauge consists of a collector placed above a funnel leading into a container where the accumulated water and melted snow are stored between observation times. Different gauge shapes are in use worldwide as shown in Figure 6.1. Where solid precipitation is common and substantial, a number of special modifications are used to improve the accuracy of measurements. Such modifications include the removal of the raingauge funnel at the beginning of the snow season or the provision of a special snow fence (see WMO, 1998) to protect the catch from blowing out. Windshields around the gauge reduce the error caused by deformation of the wind field above the gauge and by snow drifting into the gauge. They are advisable for rain and essential for snow. A wide variety of gauges are in use (see WMO, 1989*a*).

The stored water is either collected in a measure or poured from the container into a measure, or its level in the container is measured directly with a graduated stick. The size of the collector orifice is not critical for liquid precipitation, but an area of at least 200 cm^2 is required if solid forms of precipitation are expected in significant quantity. An area of 200 to 500 cm^2 will probably be found most convenient. The most important requirements of a gauge are as follows:

(a)   The rim of the collector should have a sharp edge and should fall away vertically on the inside, and be steeply bevelled on the outside; the design of gauges used for measuring snow should be such that any narrowing of the orifice caused by accumulated wet snow about the rim is small;

(b)   The area of the orifice should be known to the nearest 0.5%, and the construction should be such that this area remains constant while the gauge is in normal use;
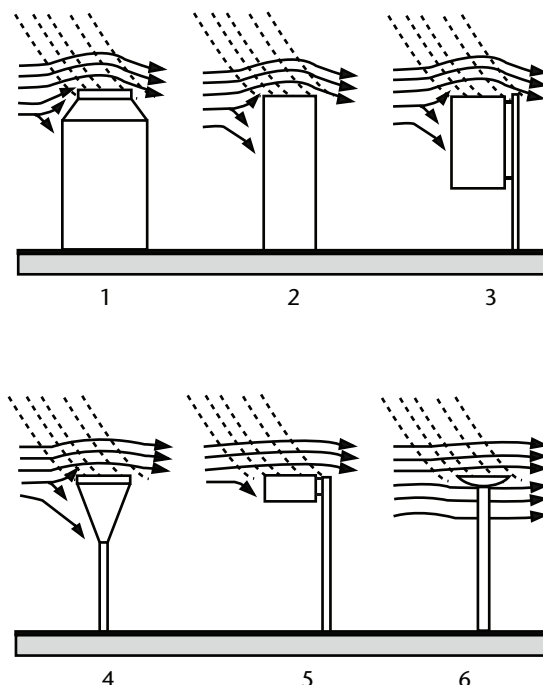
Figure 6.1. Different shapes of standard precipitation gauges. The solid lines show streamlines and the dashed lines show the trajectories of precipitation particles. The first gauge shows the largest wind field deformation above the gauge orifice, and the last gauge the smallest. Consequently, the wind-induced error for the first gauge is larger than for the last gauge.

Source: Sevruk and Nespor (1994)

(c)   The collector should be designed to prevent rain from splashing in and out. This can be achieved if the vertical wall is sufficiently deep and the slope of the funnel is sufficiently steep (at least 45%). Suitable arrangements are shown in Figure 6.2;

(d)   The construction should be such as to minimize wetting errors. This can be done by choosing the proper material and minimizing the total inner surface of the collector;

(e)   The container should have a narrow entrance and be sufficiently protected from radiation to minimize the loss of water by evaporation. Precipitation gauges used in locations where only weekly or monthly readings are practicable should be similar in design to the type used for daily measurements, but with a container of larger capacity and stronger construction.

The measuring cylinder should be made of clear glass or plastic which has a suitable coefficient of thermal expansion and should be clearly marked to show the size or type of gauge with which it is to be used. Its diameter should be less than 33% of that of the rim of the gauge; the smaller the relative diameter, the greater the precision of measurement. The graduations should be finely engraved; in general, there should be marks at 0.2 mm intervals and clearly figured lines at each whole millimetre. It is also desirable that the line corresponding to 0.1 mm be marked. The maximum error of the graduations should not exceed ±0.05 mm at or above the 2 mm graduation mark and ±0.02 mm below this mark.

To measure small precipitation amounts with adequate precision, the inside diameter of the measuring cylinder should taper off at its base. In all measurements, the bottom of the water meniscus should define the water level, and the cylinder should be kept vertical when reading, to avoid parallax errors. Repetition of the main graduation lines on the back of the measure is also helpful for reducing such errors.

Dip-rods should be made of cedar wood, or another suitable material that does not absorb water appreciably and possesses only a small capillary effect. Wooden dip-rods are unsuitable if oil has been added to the collector to suppress evaporation. When this is the case, rods made of metal or other materials from which oil can be readily cleaned must be used. Non-metallic rods should be provided with a brass foot to avoid wear and be graduated according to the relative areas of cross-section of the gauge orifice and the collector; graduations should be marked at least every 10 mm and include an allowance for the displacement caused by the rod itself. The maximum error in the dip-rod graduation should not exceed ±0.5 mm at any point. A dip-rod measurement should be checked using a volumetric measure, wherever possible.

6.3.1.2   *Operation*

The measuring cylinder must be kept vertical when it is being read, and the observer must be aware of parallax errors. Snow collected in non-recording precipitation gauges should be either weighed or melted immediately after each observation and then measured using a standard
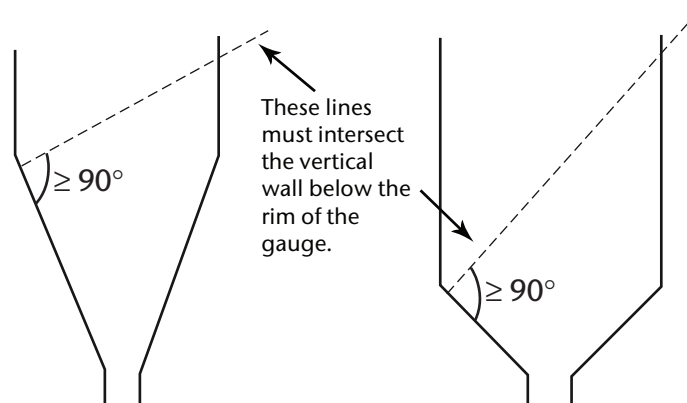
Figure 6.2. Suitable collectors for raingauges

graduated measuring cylinder. It is also possible to measure precipitation catch by accurate weighing, a procedure which has several advantages. The total weight of the can and contents is measured and the known weight of the can is subtracted. There is little likelihood of spilling the water and any water adhering to the can is included in the weight. The commonly used methods are, however, simpler and cheaper.

6.3.1.3 *Calibration and maintenance*

The graduation of the measuring cylinder or stick must, of course, be consistent with the chosen size of the collector. The calibration of the gauge, therefore, includes checking the diameter of the gauge orifice and ensuring that it is within allowable tolerances. It also includes volumetric checks of the measuring cylinder or stick.

Routine maintenance should include, at all times, keeping the gauge level in order to prevent an out-of-level gauge (see Rinehart, 1983; Sevruk, 1984). As required, the outer container of the gauge and the graduate should be kept clean at all times both inside and outside by using a long-handled brush, soapy water and a clean water rinse. Worn, damaged or broken parts should be replaced, as required. The vegetation around the gauge should be kept trimmed to 5 cm (where applicable). The exposure should be checked and recorded.

6.3.2 **Storage gauges**

Storage gauges are used to measure total seasonal precipitation in remote and sparsely inhabited areas. Such gauges consist of a collector above a funnel, leading into a container that is large enough to store the seasonal catch (or the monthly catch in wet areas). A layer of no less than 5 mm of a suitable oil or other evaporation suppressant should be placed in the container to reduce evaporation (WMO, 1972). This layer should allow the free passage of precipitation into the solution below it.

An antifreeze solution may be placed in the container to convert any snow which falls into the gauge into a liquid state. It is important that the antifreeze solution remain dispersed. A mixture of 37.5% by weight of commercial calcium chloride (78% purity) and 62.5% water makes a satisfactory antifreeze solution. Alternatively, aqueous solutions of ethylene glycol or of an ethylene glycol and methanol mixture can be used. While more expensive, the latter solutions are less corrosive than calcium chloride and give antifreeze protection over a much wider range of dilution resulting from subsequent precipitation. The volume of the solution initially placed in the container should not exceed 33% of the total volume of the gauge.

In some countries, this antifreeze and oil solution is considered toxic waste and, therefore, harmful to the environment. Guidelines for the disposal of toxic substances should be obtained from local environmental protection authorities.

The seasonal precipitation catch is determined by weighing or measuring the volume of the contents of the container (as with ordinary gauges; see section 6.3.1). The amount of oil and antifreeze solution placed in the container at the beginning of the season and any contraction in the case of volumetric measurements must be carefully taken into account. Corrections may be applied as with ordinary gauges.

The operation and maintenance of storage gauges in remote areas pose several problems, such as the capping of the gauge by snow or difficulty in locating the gauge for recording the measurement, and so on, which require specific monitoring. Particular attention should be paid to assessing the quality of data from such gauges.

6.4 PRECIPITATION GAUGE ERRORS AND CORRECTIONS

It is convenient to discuss at this point the errors and corrections that apply in some degree to most precipitation gauges, whether they are recording or non-recording gauges. The particular cases of recording gauges are discussed in section 6.5.

Comprehensive accounts of errors and corrections can be found in WMO (1982, 1984, 1986; specifically for snow, 1998; and specifically for rainfall intensity, 2006, 2009). Details of the models currently used for adjusting raw precipitation data in Canada, Denmark, Finland, the Russian Federation, Switzerland and the United States are given in WMO (1982). WMO (1989*a*) gives a description of how the errors occur. There are collected conference papers on the topic in WMO (1986, 1989*b*). Details on the improvement of the reliability of rainfall intensity measurements as obtained by traditional tipping-bucket gauges, weighing gauges and other types of gauges (optical, floating/siphoning, etc.) are given in WMO (2006, 2009).

The amount of precipitation measured by commonly used gauges may be less than the actual precipitation reaching the ground by up to 30% or more. Systematic losses will vary by type of precipitation (snow, mixed snow and rain, and rain). The systematic error of solid precipitation measurements is commonly large and may be of an order of magnitude greater than that normally associated with liquid precipitation measurements.

For many hydrological purposes it is necessary first to make adjustments to the data in order to allow for the error before making the calculations. The adjustments cannot, of course, be exact (and may even increase the error). Thus, the original data should always be kept as the basic archives both to maintain continuity and to serve as the best base for future improved adjustments if, and when, they become possible.

The traditional assessment of errors in precipitation gauges refers to so-called weather-related errors. It is well recognized that the measurement of liquid precipitation at the ground is affected by different sources of systematic and random errors, mainly due to wind-, wetting- and evaporation-induced losses (see WMO, 1982) which make the measurement of light to moderate rainfall scarcely reliable in the absence of an accurate calibration. Wind-induced errors still have an influence on rainfall intensities of the order of 20–50 mm h^{-1} with an incidence of about 5% observed in some intercomparison stations in central Europe (WMO, 1984). Sampling errors due to the discrete nature of the rain measurement are also recognized to be dependent on the bucket size (for tipping-bucket gauges) and sampling interval or instrument response time, though not on precipitation intensity, and can be analytically evaluated (Colli et al., 2013*a*).

The true amount of precipitation may be estimated by correcting for some or all of the various error terms listed below:

(a) Error due to systematic wind field deformation above the gauge orifice: typically 2% to 10% for rain and 10% to 50% for snow;

(b) Error due to the wetting loss on the internal walls of the collector;

(c) Error due to the wetting loss in the container when it is emptied: typically 2% to 15% in summer and 1% to 8% in winter, for (b) and (c) together;

(d) Error due to evaporation from the container (most important in hot climates): 0% to 4%;

(e) Error due to blowing and drifting snow;

(f) Error due to the in- and out-splashing of water: 1% to 2%;

(g) Systematic mechanical and sampling errors, and dynamic effects errors (i.e. systematic delay due to instrument response time): typically 5% to 15% for rainfall intensity, or even more in high-rate events (see WMO, 2009);

(h) Random observational and instrumental errors, including incorrect gauge reading times.

The first seven error components are systematic and are listed in order of general importance. The net error due to blowing and drifting snow and to in- and out-splashing of water can be either negative or positive, while net systematic errors due to the wind field and other factors are negative. Since the errors listed as (e) and (f) above are generally difficult to quantify, the general model for adjusting data from most gauges, originally proposed by WMO (1982) and later modified by Legates and Willmott (1990), can be written as:

$$P_k = k_r P_{cr} + k_s P_{cs} = k_r \left(P_{gr} + \Delta P_{1r} + \Delta P_{2r} + \Delta P_{3r} + \Delta P_{4r} \right) + k_s \left(P_{gs} + \Delta P_{1s} + \Delta P_{2s} + \Delta P_{3s} + \Delta P_{4s} \right) \quad (6.1)$$

where subscripts r and s refer to liquid (rain) and solid (snow) precipitation, respectively; P_k is the adjusted precipitation amount; k (see Figure 6.3) is the adjustment factor for the effects of wind field deformation; P_c is the amount of precipitation caught by the gauge collector; P_g is the measured amount of precipitation in the gauge; ΔP_1 is the adjustment for the wetting loss on the internal walls of the collector; ΔP_2 is the adjustment for wetting loss in the container after emptying; ΔP_3 is the adjustment for evaporation from the container; and ΔP_4 is the adjustment for systematic mechanical errors.

Errors due to the weather conditions at the collector, as well as those related to wetting, splashing and evaporation, are typically referred to as catching errors. They indicate the ability of the instrument to collect the exact amount of water according to the definition of precipitation at the ground, that is, the total water falling over the projection of the collector's area over the ground. Systematic mechanical and sampling errors, typically referred to as quantification errors, are related to the ability of the instrument to sense correctly the amount of water collected by the instrument. The WMO laboratory and field intercomparisons on rainfall intensity gauges (WMO 2006, 2009) both contributed to the assessment of quantification errors and documented
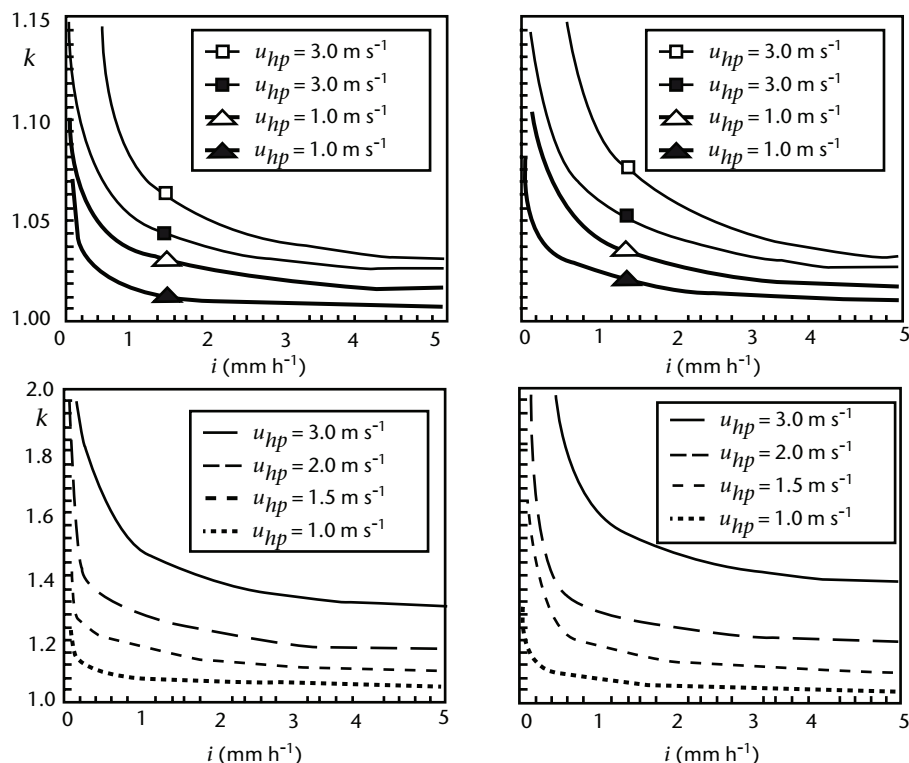
Figure 6.3. Conversion factor k defined as the ratio of "correct" to measured precipitation for rain (top) and snow (bottom) for two unshielded gauges in dependency of wind speed u_{hp}, intensity i and type of weather situation according to Nespor and Sevruk (1999). On the left is the German Hellmann manual standard gauge, and on the right the recording, tipping-bucket gauge by Lambrecht. Void symbols in the top diagrams refer to orographic rain, and black ones to showers. Note the different scales for rain and snow. For shielded gauges, k can be reduced to 50% and 70% for snow and mixed precipitation, respectively (WMO, 1998). The heat losses are not considered in the diagrams (in Switzerland they vary with altitude between 10% and 50% of the measured values of fresh snow).

laboratory and field calibration methods for identifying and/or correcting quantification errors in rainfall intensity measurements. Obviously, these errors may derive from very different aspects of the sensing phase since the instruments may differ in the measuring principle applied, construction details, operational solutions and so forth.

The corrections of precipitation measurement errors are applied to daily or monthly totals or, in some practices, to individual precipitation events.

When dealing with precipitation intensity measurements, systematic mechanical errors can be properly corrected through a standardized laboratory calibration referred to as a dynamic calibration in steady-state conditions of the reference flow rate (Niemczynowicz, 1986; WMO, 2009). For more details, see Annex 6.D.

In general, the supplementary data needed to make adjustments related to weather conditions include the wind speed at the gauge orifice during precipitation, drop size, precipitation intensity, air temperature and humidity, and the characteristics of the gauge site. Although temperature has some effect on gauge undercatch, the effect is significantly less than the effects of wind speed at gauge height (Yang et al., 1993; Yang et al., 1995). Wind speed and precipitation type or intensity may be sufficient variables to determine the corrections. Wind speed alone is sometimes used. At sites where such observations are not made, interpolation between the observations made at adjacent sites may be used for making such adjustments, but with caution, and for monthly rainfall data only.

For most precipitation gauges, wind speed is the most important environmental factor contributing to the under-measurement of solid precipitation. These data must be derived from standard meteorological observations at the site in order to provide daily adjustments. In particular, if wind speed is not measured at gauge orifice height, it can be derived by using a mean wind speed reduction procedure after having knowledge of the roughness of the surrounding surface and the angular height of surrounding obstacles. A suggested scheme is shown in Annex 6.B.[1] This scheme is very site-dependent, and estimation requires a good knowledge of the station and gauge location. Shielded gauges catch more precipitation than their unshielded counterparts, especially for solid precipitation. Therefore, gauges should be shielded either naturally (for example, forest clearing) or artificially (for example, Alter, Canadian Nipher type, Tretyakov windshield) to minimize the adverse effect of wind speed on measurements of solid precipitation (for some information on shield design, refer to WMO, 1998, 2008). The type of windshield configuration, as well as gauge type, will alter the relationship between wind speeds and catch efficiency and have implications on data homogeneity.

Wetting loss (Sevruk, 1974a) is another cumulative systematic loss from manual gauges which varies with precipitation and gauge type; its magnitude is also a function of the number of times the gauge is emptied. Average wetting loss can be up to 0.2 mm per observation. At synoptic stations where precipitation is measured every 6 h, this can become a very significant loss. In some countries, wetting loss has been calculated to be 15% to 20% of the measured winter precipitation. Correction for wetting loss at the time of observation is a feasible alternative. Wetting loss can be kept low in a well-designed gauge. The methodology to determine the wetting loss of manual gauges (WMO, 1998) would suffice. It is recommended that the wetting loss for manual gauges be re-examined periodically (for example, every 5 years) as it tends to change with the age of the collector. The internal surfaces should be of a material which can be kept smooth and clean; paint, for example, is unsuitable, but baked enamel is satisfactory. Seams in the construction should be kept to a minimum.

Evaporation losses (Sevruk, 1974b) vary by gauge type, climatic zone and time of year. Evaporation loss is a problem with gauges that do not have a funnel device in the bucket, especially in late spring at mid-latitudes. Losses of over 0.8 mm per day have been reported. Losses during winter are much less than during comparable summer months, ranging from 0.1 to 0.2 mm per day. These losses, however, are cumulative. In a well-designed gauge, only a small

---

[1]   A wind reduction scheme recommended by the Commission for Instruments and Methods of Observation at its eleventh session (1994).

water surface is exposed, its ventilation is minimized, and the water temperature is kept low by a reflective outer surface. In storage and accumulating recording gauges, errors associated with evaporation can be virtually eliminated through the use of oil in the collector.

It is clear that, in order to achieve data compatibility when using different gauge types and shielding during all weather conditions, corrections to the actual measurements are necessary. In all cases where precipitation measurements are adjusted in an attempt to reduce errors, it is strongly recommended that both the measured and adjusted values be published.

6.5　　RECORDING PRECIPITATION GAUGES

Recording precipitation automatically has the advantage that it can provide better time resolution than manual measurements, and it is possible to reduce the evaporation and wetting losses. These readings are of course subject to the wind effects discussed in section 6.4.

Three types of automatic precipitation recorders are in general use, namely the weighing-recording type, the tilting or tipping-bucket type, and the float type. Only the weighing type is satisfactory for measuring all kinds of precipitation, the use of the other two types being for the most part limited to the measurement of rainfall. Some new automatic gauges that measure precipitation without using moving parts are available. These gauges use devices such as capacitance probes, pressure transducers, and optical or small radar devices to provide an electronic signal that is proportional to the precipitation equivalent. The clock device that times intervals and dates the time record is a very important component of the recorder.

Because of the high variability of precipitation intensity over a 1 min timescale, a single 1 min rainfall intensity value is not representative of a longer time period. Therefore, 1 min rainfall intensity should not be used in a temporal sampling scheme, such as one synoptic measurement every one or three hours. Very good time synchronization, better than 10 s, is required between the reference time and the different instruments of the observing station.

6.5.1　　Weighing-recording gauge

6.5.1.1　　*Instruments*

In these instruments, the weight of a container, together with the precipitation accumulated therein, is recorded continuously, either by means of a spring mechanism or with a system of balance weights. All precipitation, both liquid and solid, is recorded as it falls. This type of gauge normally has no provision for emptying itself; the capacity (namely, the maximum accumulation between recharge) ranges from 250 to 1 500 mm depending on the model. Low-capacity models should be avoided in areas where the maximum accumulation could occur over short periods of time. The gauges must be maintained to minimize evaporation losses, which can be accomplished by adding sufficient oil or other evaporation suppressants inside the container to form a film over the water surface. Any difficulties arising from oscillation of the balance in strong winds can be reduced by suitably programming a microprocessor to eliminate this effect on the readings. Such weighing gauges are particularly useful for recording snow, hail, and mixtures of snow and rain, since the solid precipitation does not need to be melted before it can be recorded. For winter operation, the catchment container is charged with an antifreeze solution (see section 6.3.2) to dissolve the solid contents. The amount of antifreeze depends on the expected amount of precipitation and the minimum temperature expected at the time of minimum dilution. These instruments do not use any moving mechanical parts in the weighing mechanism; only elastic deformation occurs. Therefore, mechanical degradation and the resulting need for maintenance are significantly reduced.

The digitized output signal is generally averaged and filtered. Precipitation intensity can also be calculated from the differences between two or more consecutive weight measurements. The accuracy of these types of gauges is related directly to their measuring and/or recording characteristics, which can vary with manufacturer.

Many instruments have data output that contain diagnostic parameters which are very useful for further evaluations of measured data and for data quality control.

6.5.1.2   *Errors and corrections*

Except for error due to the wetting loss in the container when it is emptied, weighing-recording gauges are susceptible to all of the other sources of error discussed in section 6.4. It should also be noted that automatic recording gauges alone cannot identify the type of precipitation. A significant problem with this type of gauge is that precipitation, particularly freezing rain or wet snow, can stick to the inside of the gauge orifice and not fall into the bucket until later. This severely limits the ability of weighing-recording gauges to provide accurate timing of precipitation events. Another common fault with weighing-type gauges is wind pumping. This usually occurs during high winds when turbulent air currents passing over and around the catchment container cause oscillations in the weighing mechanism. Errors associated with such anomalous recordings can be minimized by averaging readings over short time intervals usually ranging from 1 to 5 min. Timing errors in the instrument clock may assign the catch to the wrong period or date. Some weighing-recording gauges may also exhibit some temperature sensitivity in the weighing mechanism that adds a component to the output which is proportional to the diurnal temperature cycle.

Some potential errors in manual methods of precipitation measurement can be eliminated or at least minimized by using weighing-recording gauges. Random measurement errors associated with human observer error and certain systematic errors, particularly evaporation and wetting loss, are minimized. In some countries, trace observations are officially given a value of zero, thus resulting in a biased underestimate of the seasonal precipitation total. This problem is minimized with weighing-type gauges, since even very small amounts of precipitation will accumulate over time.

A fundamental characteristic of weighing-recording gauges when measuring precipitation intensity is the response time (filtering process included), which leads to measurement errors (systematic delay). The response times, available in operation manuals or evaluated during a previous WMO intercomparison (WMO, 2009), are of the order of six seconds to a few minutes depending on the gauge's design and model. The 1 min precipitation intensity resolution of weighing-recording gauges can be very different from gauge to gauge and depends on the transducer resolution. Such gauges may also exhibit a limit or discrimination threshold for precipitation intensity.

The correction of weighing gauge data on an hourly or daily basis may be more difficult than on longer time periods, such as monthly climatological summaries. Ancillary data from automatic weather stations, such as wind at gauge height, air temperature, present weather or snow depth, will be useful in interpreting and correcting accurately the precipitation measurements from automatic gauges.

6.5.1.3   *Calibration and maintenance*

Weighing-recording gauges usually have few moving parts and, therefore, should seldom require calibration. Calibration commonly involves the use of a series of weights which, when placed in the bucket or catchment container, provide a predetermined value equivalent to an amount of precipitation. Calibrations should normally be done in a laboratory setting and should follow the manufacturer's instructions.

An alternative procedure for calibrating weighing-recording gauges when dealing with precipitation intensity measurements is given in Annex 6.D. This calibration, referred to as a dynamic calibration in steady-state conditions of the reference flow rates, is performed to evaluate the measurement errors of the weighing gauge. This procedure can also be used to assess the dynamic response of the weighing gauge by performing the classic step-response test, that is, by providing the instrument with a reference flow rate showing a single abrupt change from zero to a given equivalent rainfall rate. Moreover, the repeating of the dynamic calibration

in unsteady conditions (time-varying reference flow rates as a simulation of real-world events) permits a finer calibration of weighing gauges (especially for systematic delays due to the instrument's response time) and could lead to improved dynamic performance and accuracy in real-world events (Colli et al., 2013*b*).

Routine maintenance should be conducted every three to four months, depending on precipitation conditions at the site. Both the exterior and interior of the gauge should be inspected for loose or broken parts and to ensure that the gauge is level. Any manual read-out should be checked against the removable data record to ensure consistency before removing and annotating the record. The bucket or catchment container should be emptied, inspected, cleaned, if required, and recharged with oil for rainfall-only operation or with antifreeze and oil if solid precipitation is expected (see section 6.3.2). The recording device should be set to zero in order to make maximum use of the gauge range. The digital memory as well as the power supply should be checked and replaced, if required. Timing intervals and dates of record must be checked.

A proper field calibration, and field calibration check or field inspection should also be conducted on a regular basis as part of the routine maintenance and check, taking into account site and operational constraints. For rainfall intensity gauges, a recommended procedure by means of a portable device for reference flow rates is given in Annex 6.E.

6.5.2 Tipping-bucket gauge

The tipping-bucket raingauge is used for measuring accumulated totals and the rate of rainfall. Suitable intensity-dependent corrections (see section 6.5.2.2) should be applied to improve the accuracy of the intensity measurements and to overcome the underestimation of intensity for high rainfall rates and the overestimation of intensity for low rainfall rates, both of which are typical in non-corrected tipping-bucket gauges.

6.5.2.1 *Instruments*

The principle behind the operation of this instrument is simple. A tipping-bucket raingauge uses a metallic or plastic twin bucket balance to measure the incoming water in portions of equal weight. When one bucket is full, its centre of mass is outside the pivot and the balance tips, dumping the collected water and bringing the other bucket into position to collect. The bucket compartments are shaped in such a way that the water is emptied from the lower one. The water mass content of the bucket is constant (m [g]). Therefore, by using the density of water ($\rho = 1$ g/cm^3), the corresponding volume (V [cm^3]) is derived from the weight of the water and, consequently, the corresponding accumulation height (h [mm]) is retrieved by using the area of the collector (S [cm^2]). The equation is:

$$V = m/\rho = h \cdot S \tag{6.2}$$

Thus, by using the density of water, h is calculated, where 1 mm corresponds to 1 g of water over an area of 10 cm^2 . To have detailed records of precipitation, the amount of rain should not exceed 0.2 mm. For a gauge area of 1 000 cm^2, this corresponds to a bucket content of 20 g of water.

The raw output is a contact closure (reed switch or relay contact), so each tip produces an electrical impulse as a signal output which must be recorded by a data logger or an analogue-to-digital converter (data acquisition system equipped with reed switch reading ports). This mechanism provides a continuous measurement without manual interaction.

The rainfall intensity of non-corrected tipping-bucket gauges is calculated based on the number of tips in a periodic sampling rate (typically 6 or 10 s) and averaged over a chosen time interval (for example, 1 min). In this way, an intensity value is available every minute that represents the intensity of the past minute or minutes. This sampling scheme reduces the uncertainty of the average. In addition, the rainfall intensity resolution depends on the size of the bucket and the

chosen time interval. For example, a tip equivalent to 0.2 mm leads to a 1 min rainfall intensity resolution of 12 mm h^{-1} which is constant over the measurement range of the gauge if no intensity-dependent corrections are applied.

The bucket takes a small but finite time to tip and, during the first half of its motion, additional rain may enter the compartment that already contains the calculated amount of rainfall. The water losses during the tipping movement indicate a systematic mechanical error that is rather a function of the intensity itself and can be appreciable during heavy rainfall (> 100 mm h^{-1}). However, this can be corrected by using a calibration procedure as given in Annex 6.D and applying a correction curve or algorithm (see section 6.4). An alternative simple method is to use a device like a siphon at the foot of the funnel to direct the water to the buckets at a controlled rate. This smoothes out the intensity peaks of very short-period rainfall. Alternatively, a device can be added to accelerate the tipping action; essentially, a small blade is impacted by the water falling from the collector and is used to apply an additional force to the bucket, varying with rainfall intensity.

The tipping-bucket gauge is particularly convenient for automatic weather stations because it lends itself to digital methods. The pulse generated by a contact closure can be monitored by a data logger, preferably including the time the tips occurred, to calculate a corrected rainfall intensity, which can then be used to retrieve the precipitation amount over selected periods. It may also be used with a chart recorder.

6.5.2.2   *Errors and corrections*

Since the tipping-bucket raingauge has sources of error which differ somewhat from those of other gauges, special precautions and corrections are advisable. Some sources of error include the following:

(a)   The loss of water during the tipping action in heavy rain; this can be considerably reduced by conducting a dynamic calibration (see Annex 6.D) and applying an intensity-dependent correction;

(b)   With the usual bucket design, the exposed water surface is large in relation to its volume, meaning that appreciable evaporation losses can occur, especially in hot regions. This error may be significant in light rain;

(c)   The discontinuous nature of the record may not provide satisfactory data during light drizzle or very light rain. In particular, the time of onset and cessation of precipitation cannot be accurately determined;

(d)   Water may adhere to both the walls and the lip of the bucket, resulting in rain residue in the bucket and additional weight to be overcome by the tipping action. Tests on waxed buckets produced a 4% reduction in the volume required to tip the balance compared with non-waxed buckets. Volumetric calibration can change, without adjustment of the calibration screws, by variation of bucket wettability through surface oxidation or contamination by impurities and variations in surface tension;

(e)   The stream of water falling from the funnel onto the exposed bucket may cause over-reading, depending on the size, shape and position of the nozzle;

(f)   The instrument is particularly prone to bearing friction and to having an improperly balanced bucket because the gauge is not level;

(g)   The limited repeatability at various rainfall intensities of the inter-tip time interval due to low stability of the mechanics of the buckets (i.e. bucket movement) degrades the measurements; this systematic mechanical effect can be investigated by means of specific tests recording a series of inter-tip time intervals that make it possible to estimate the mechanical precision of the bucket (see Colli et al., 2013*b*); such errors may be reduced by improving the construction quality of the gauges;

(h)   The sampling errors of tipping-bucket gauges (Habib et al., 2001) have an additional strong impact on field performance under light precipitation regimes; these errors consist in a delay of the tipping-bucket mechanism in assigning the collected amount of water to the corresponding time interval; different calculation techniques exist for reducing the impact of sampling errors and providing rainfall intensity measurements at a higher resolution than the tipping-bucket gauges' sensitivity would allow (see Colli et al., 2013*a*).

Careful calibration can provide corrections for the systematic parts of these errors. Effective corrections for improving the measurement of rainfall intensity (WMO, 2009), and consequently the corresponding accumulated amount, consist in performing a dynamic calibration and applying correction curves (see section 6.4), for example by applying a software correction or an algorithm in the data acquisition system. Alternatively, they can involve conducting a linearization procedure in the instrument's electronics circuit (generating an intensity-dependent emission of extra pulses) or through a mechanism (for example, small deflectors that induce a dynamic pressure which increases with intensity, allowing the tip to occur before the bucket is full). In WMO (2009), it is shown that linearization by extra electronic pulses is well suited for measuring precipitation amount but less so for measuring intensity. On the other hand, mechanical linearization compensates for the loss of water during the movement of the balance and greatly minimizes the intensity underestimation during high-rate events. The software correction (correction curve or algorithm) resulted in being the most effective method for correcting systematic mechanical errors.

The measurements from tipping-bucket raingauges may be corrected for effects of exposure in the same way as other types of precipitation gauge.

Heating devices can be used to allow for measurements during the cold season, particularly of solid precipitation. However, the performance of heated tipping-bucket gauges has been found to be very poor as a result of large errors due to both wind and evaporation of melting snow. Therefore, these types of gauges are not recommended for use in winter precipitation measurement in regions where temperatures fall below 0 °C for prolonged periods.

6.5.2.3   *Calibration and maintenance*

Calibration of the tipping bucket is usually accomplished by passing a known amount of water through the tipping mechanism at various rates and by adjusting the mechanism to the known volume. This procedure should be followed under laboratory conditions. The recommended calibration procedure for these gauges is available in Annex 6.D.

A proper field calibration, and field calibration check or field inspection should also be conducted on a regular basis as part of the routine maintenance and check, taking into account site and operational constraints. For catchment type rainfall intensity gauges, a recommended procedure by means of a portable device for reference flow rates is given in Annex 6.E.

Owing to the numerous error sources, the collection characteristics and calibration of tipping-bucket raingauges are a complex interaction of many variables. Daily comparisons with the standard raingauge can provide useful correction factors, and is good practice. The correction factors may vary from station to station. Correction factors are generally greater than 1.0 (under-reading) for low-intensity rain, and less than 1.0 (over-reading) for high-intensity rain. The relationship between the correction factor and intensity is not linear but forms a curve.

Routine maintenance should include cleaning the accumulated dirt and debris from funnel and buckets, as well as ensuring that the gauge is level. It is highly recommended that the tipping mechanism be replaced with a newly calibrated unit on an annual basis. Timing intervals and dates of records must be checked.

6.5.3 Float gauge

In this type of instrument, the rain passes into a float chamber containing a light float. As the level of the water within the chamber rises, the vertical movement of the float is transmitted, by a suitable mechanism, to the movement of a pen on a chart or a digital transducer. By suitably adjusting the dimensions of the collector orifice, the float and the float chamber, any desired chart scale can be used.

In order to provide a record over a useful period (24 h are normally required) either the float chamber has to be very large (in which case a compressed scale on the chart or other recording medium is obtained), or a mechanism must be provided for emptying the float chamber automatically and quickly whenever it becomes full, so that the chart pen or other indicator returns to zero. Usually a siphoning arrangement is used. The actual siphoning process should begin precisely at the predetermined level with no tendency for the water to dribble over at either the beginning or the end of the siphoning period, which should not be longer than 15 s. In some instruments, the float chamber assembly is mounted on knife edges so that the full chamber overbalances; the surge of the water assists the siphoning process, and, when the chamber is empty, it returns to its original position. Other rain recorders have a forced siphon which operates in less than 5 s. One type of forced siphon has a small chamber that is separate from the main chamber and accommodates the rain that falls during siphoning. This chamber empties into the main chamber when siphoning ceases, thus ensuring a correct record of total rainfall.

A heating device (preferably controlled by a thermostat) should be installed inside the gauge if there is a possibility that water might freeze in the float chamber during the winter. This will prevent damage to the float and float chamber and will enable rain to be recorded during that period. A small heating element or electric lamp is suitable where a mains supply of electricity is available, otherwise other sources of power may be employed. One convenient method uses a short heating strip wound around the collecting chamber and connected to a large-capacity battery. The amount of heat supplied should be kept to the minimum necessary in order to prevent freezing, because the heat may reduce the accuracy of the observations by stimulating vertical air movements above the gauge and increasing evaporation losses.

A large undercatch by unshielded heated gauges, caused by the wind and the evaporation of melting snow, has been reported in some countries, as is the case for weighing gauges (see section 6.5.1.2).

Apart from the fact that calibration is performed using a known volume of water, the maintenance procedures for this gauge are similar to those of the weighing-recording gauge (see section 6.5.1.3).

6.6 MEASUREMENT OF DEW, ICE ACCUMULATION AND FOG PRECIPITATION

6.6.1 Measurement of dew and leaf wetness

The deposition of dew is essentially a nocturnal phenomenon and, although relatively small in amount and locally variable, is of much interest in arid zones; in very arid regions, it may be of the same order of magnitude as the rainfall. The exposure of plant leaves to liquid moisture from dew, fog and precipitation also plays an important role in plant disease, insect activity, and the harvesting and curing of crops.

In order to assess the hydrological contribution of dew, it is necessary to distinguish between dew formed:

(a)   As a result of the downward transport of atmospheric moisture condensed on cooled surfaces, known as dew-fall;

(b)　　By water vapour evaporated from the soil and plants and condensed on cooled surfaces, known as distillation dew;

(c)　　As water exuded by leaves, known as guttation.

All three forms of dew may contribute simultaneously to the observed dew, although only the first provides additional water to the surface, and the latter usually results in a net loss. A further source of moisture results from fog or cloud droplets being collected by leaves and twigs and reaching the ground by dripping or by stem flow.

The amount of dew deposited on a given surface in a stated period is usually expressed in units of kg m^{-2} or in millimetres depth of dew. Whenever possible, the amount should be measured to the nearest tenth of a millimetre.

Leaf wetness may be described as light, moderate or heavy, but its most important measures are the time of onset or duration.

A review of the instruments designed for measuring dew and the duration of leaf wetness, as well as a bibliography, is given in WMO (1992*b*).

The following methods for the measurement of leaf wetness are considered.

The amount of dew depends critically on the properties of the surface, such as its radiative properties, size and aspect (horizontal or vertical). It may be measured by exposing a plate or surface, which can be natural or artificial, with known or standardized properties, and assessing the amount of dew by weighing it, visually observing it, or making use of some other quantity such as electrical conductivity. The problem lies in the choice of the surface, because the results obtained instrumentally are not necessarily representative of the dew deposit on the surrounding objects. Empirical relationships between the instrumental measurements and the deposition of dew on a natural surface should, therefore, be established for each particular set of surface and exposure conditions; empirical relationships should also be established to distinguish between the processes of dew formation if that is important for the particular application.

A number of instruments are in use for the direct measurement of the occurrence, amount and duration of leaf wetness and dew. Dew-duration recorders use either elements which themselves change in such a manner as to indicate or record the wetness period, or electrical sensors in which the electrical conductivity of the surface of natural or artificial leaves changes in the presence of water resulting from rain, snow, wet fog or dew. In dew balances, the amount of moisture deposited in the form of precipitation or dew is weighed and recorded. In most instruments providing a continuous trace, it is possible to distinguish between moisture deposits caused by fog, dew or rain by considering the type of trace. The only certain method of measuring net dew-fall by itself is through the use of a very sensitive lysimeter (see Part I, Chapter 10).

In WMO (1992*b*) two particular electronic instruments for measuring leaf wetness are advocated for development as reference instruments, and various leaf-wetting simulation models are proposed. Some use an energy balance approach (the inverse of evaporation models), while others use correlations. Many of them require micrometeorological measurements. Unfortunately, there is no recognized standard method of measurement to verify them.

6.6.2　　　　Measurement of ice accumulation

Ice can accumulate on surfaces as a result of several phenomena. Ice accumulation from freezing precipitation, often referred to as glaze, is the most dangerous type of icing condition. It may cause extensive damage to trees, shrubs and telephone and power lines, and create hazardous conditions on roads and runways. Hoar frost (commonly called frost) forms when air with a dewpoint temperature below freezing is brought to saturation by cooling. Hoar frost is a deposit of interlocking ice crystals formed by direct sublimation on objects, usually of small diameter,

such as tree branches, plant stems, leaf edges, wires, poles, and so forth. Rime is a white or milky and opaque granular deposit of ice formed by the rapid freezing of supercooled water drops as they come into contact with an exposed object.

6.6.2.1   *Measurement methods*

At meteorological stations, the observation of ice accumulation is generally more qualitative than quantitative, primarily due to the lack of a suitable sensor. Ice accretion indicators, usually made of anodized aluminium, are used to observe and report the occurrence of freezing precipitation, frost or rime icing.

Observations of ice accumulation can include both the measurement of the dimensions and the weight of the ice deposit as well as a visual description of its appearance. These observations are particularly important in mountainous areas where such accumulation on the windward side of a mountain may exceed the normal precipitation. A system consisting of rods and stakes with two pairs of parallel wires (one pair oriented north-south and the other east-west) can be used to accumulate ice. The wires may be suspended at any level, and the upper wire of each pair should be removable. At the time of observation, both upper wires are removed, placed in a special container, and taken indoors for melting and weighing of the deposit. The cross-section of the deposit is measured on the permanently fixed lower wires.

Recording instruments are used in some countries for continuous registration of rime. A vertical or horizontal rod, ring or plate is used as the sensor, and the increase in the amount of rime with time is recorded on a chart. A simple device called an ice-scope is used to determine the appearance and presence of rime and hoar frost on a snow surface. The ice-scope consists of a round plywood disc, 30 cm in diameter, which can be moved up or down and set at any height on a vertical rod fixed in the ground. Normally, the disc is set flush with the snow surface to collect the rime and hoar frost. Rime is also collected on a 20 cm diameter ring fixed on the rod, 20 cm from its upper end. A wire or thread 0.2 to 0.3 mm in diameter, stretched between the ring and the top end of the rod, is used for the observation of rime deposits. If necessary, each sensor can be removed and weighed.

In the ISO 12494:2001 standard (ISO, 2001), which applies to ice accretion on all kinds of structures except electrical overhead line conductors, a standard ice-measuring device is described as follows:

(a)   A smooth cylinder with a diameter of 30 mm placed with the axis vertical and rotating around the axis. The cylinder length should be a minimum of 0.5 m, but, if heavy ice accretion is expected, the length should be 1 m;

(b)   The cylinder is placed 10 m above terrain;

(c)   Recordings of ice weight may be performed automatically.

In Fikke et al. (2007), several types of ice detectors are identified, some of which are used for the start and end of icing periods while others are also able to quantify the ice accretion rate (usually expressed in kg m^{-2} h^{-1}). Many sensors are based on the measurement of the ice mass on a vertical tube used as a target for icing. An optical sensor (infrared beam) detects the change of reflecting properties of a target tube when covered with ice. Another sensor, widely used for freezing rain, consists of a vibrating probe. Ice accreted on this probe changes the vibrating frequency, which allows both the detection of icing conditions and an estimate of the ice accretion rate. An internal probe heater is applied to melt the ice and keep the sensor within its operational limits.

6.6.2.2 *Ice on pavements*

Sensors have been developed and are in operation to detect and describe ice on roads and runways, and to support warning and maintenance programmes. Part II, Chapter 10 provides more specific information on this subject.

With a combination of measurements, it is possible to detect dry and wet snow and various forms of ice. One sensor using two electrodes embedded in the road, flush with the surface, measures the electrical conductivity of the surface and readily distinguishes between dry and wet surfaces. A second measurement, of ionic polarizability, determines the ability of the surface, to hold an electrical charge; a small charge is passed between a pair of electrodes for a short time, and the same electrodes measure the residual charge, which is higher when there is an electrolyte with free ions, such as salty water. The polarizability and conductivity measurements together can distinguish between dry, moist and wet surfaces, frost, snow, white ice and some de-icing chemicals. However, because the polarizability of the non-crystalline black ice is indistinguishable from water under some conditions, the dangerous black ice state can still not be detected with the two sensors. In at least one system, this problem has been solved by adding a third specialized capacitive measurement which detects the unique structure of black ice.

The above method is a passive technique. There is an active in situ technique that uses either a heating element, or both heating and cooling elements, to melt or freeze any ice or liquid present on the surface. Simultaneous measurements of temperature and of the heat energy involved in the thaw-freeze cycle are used to determine the presence of ice and to estimate the freezing point of the mixture on the surface.

Most in situ systems include a thermometer to measure the road surface temperature. The quality of the measurement depends critically on the mounting (especially the materials) and exposure, and care must be taken to avoid radiation errors.

There are two remote-sensing methods under development which lend themselves to car-mounted systems. The first method is based on the reflection of infrared and microwave radiation at several frequencies (about 3 000 nm and 3 GHz, respectively). The microwave reflections can determine the thickness of the water layer (and hence the risk of aquaplaning), but not the ice condition. Two infrared frequencies can be used to distinguish between dry, wet and icy conditions. It has also been demonstrated that the magnitude of reflected power at wavelengths around 2 000 nm depends on the thickness of the ice layer.

The second method applies pattern recognition techniques to the reflection of laser light from the pavement, to distinguish between dry and wet surfaces, and black ice.

6.6.3 Measurement of fog precipitation

Fog consists of minute water droplets suspended in the atmosphere to form a cloud at the Earth's surface. Fog droplets have diameters from about 1 to 40 μm and fall velocities from less than 1 to approximately 5 cm s^{-1}. In fact, the fall speed of fog droplets is so low that, even in light winds, the drops will travel almost horizontally. When fog is present, horizontal visibility is less than 1 km; it is rarely observed when the temperature and dewpoint differ by more than 2 °C.

Meteorologists are generally more concerned with fog as an obstruction to vision than as a form of precipitation. However, from a hydrological standpoint, some forested high-elevation areas experience frequent episodes of fog as a result of the advection of clouds over the surface of the mountain, where the consideration of precipitation alone may seriously underestimate the water input to the watershed (Stadtmuller and Agudelo, 1990). More recently, the recognition of fog as a water supply source in upland areas (Schemenauer and Cereceda, 1994*a*) and as a wet deposition pathway (Schemenauer and Cereceda, 1991; Vong et al., 1991) has led to the requirement for standardizing methods and units of measurement. The following methods for the measurement of fog precipitation are considered.

Although there have been a great number of measurements for the collection of fog by trees and various types of collectors over the last century, it is difficult to compare the collection rates quantitatively. The most widely used fog-measuring instrument consists of a vertical wire mesh cylinder centrally fixed on the top of a raingauge in such a way that it is fully exposed to the free flow of the air. The cylinder is 10 cm in diameter and 22 cm in height, and the mesh is 0.2 cm by 0.2 cm (Grunow, 1960). The droplets from the moisture-laden air are deposited on the mesh and drop down into the gauge collector where they are measured or registered in the same way as rainfall. Some problems with this instrument are its small size, the lack of representativeness with respect to vegetation, the storage of water in the small openings in the mesh, and the ability of precipitation to enter directly into the raingauge portion, which confounds the measurement of fog deposition. In addition, the calculation of fog precipitation by simply subtracting the amount of rain in a standard raingauge (Grunow, 1963) from that in the fog collector leads to erroneous results whenever wind is present.

An inexpensive, 1 m^2 standard fog collector and standard unit of measurement is proposed by Schemenauer and Cereceda (1994*b*) to quantify the importance of fog deposition to forested high-elevation areas and to measure the potential collection rates in denuded or desert mountain ranges. The collector consists of a flat panel made of a durable polypropylene mesh and mounted with its base 2 m above the ground. The collector is coupled to a tipping-bucket raingauge to determine deposition rates. When wind speed measurements are taken in conjunction with the fog collector, reasonable estimates of the proportions of fog and rain being deposited on the vertical mesh panel can be taken. The output of this collector results in litres of water. Since the surface area is 1 m^2, this gives a collection in l m^{-2}.

6.7 MEASUREMENT OF SNOWFALL AND SNOW COVER

The authoritative texts on this topic are WMO (2008) and WMO (1992*a*), which cover the hydrological aspects, including the procedures, for snow surveying on snow courses. The following is a brief account of some simple and well-known methods, and a brief review of the instrumentation.

Snowfall is the depth of freshly fallen snow deposited over a specified period (generally 24 h). Thus, snowfall does not include the deposition of drifting or blowing snow. For the purposes of depth measurements, the term "snow" should also include ice pellets, glaze, hail, and sheet ice formed directly or indirectly from precipitation. Snow depth usually means the total depth of snow on the ground at the time of observation.

The water equivalent of a snow cover is the vertical depth of the water that would be obtained by melting the snow cover.

6.7.1 Snowfall depth

Direct measurements of the depth of fresh snow on open ground are taken with a graduated ruler or scale. A sufficient number of vertical measurements should be made in places where drifting is considered absent in order to provide a representative average. Where the extensive drifting of snow has occurred, a greater number of measurements are needed to obtain a representative depth. Special precautions should be taken so as not to measure any previously fallen snow. This can be done by sweeping a suitable patch clear beforehand or by covering the top of the old snow surface with a piece of suitable material (such as wood with a slightly rough surface, painted white) and measuring the depth accumulated on it. On a sloping surface (to be avoided, if possible) measurements should still be taken with the measuring rod vertical. If there is a layer of old snow, it would be incorrect to calculate the depth of the new snow from the difference between two consecutive measurements of total depth of snow since lying snow tends to become compressed and to suffer ablation.

6.7.2　　　　Direct measurements of snow cover depth

Depth measurements of snow cover or snow accumulated on the ground are taken with a snow ruler or similar graduated rod which is pushed down through the snow to the ground surface. It may be difficult to obtain representative depth measurements using this method in open areas since the snow cover drifts and is redistributed under the effects of the wind, and may have embedded ice layers that limit penetration with a ruler. Care should be taken to ensure that the total depth is measured, including the depth of any ice layers which may be present. A number of measurements are taken and averaged at each observing station.

A number of snow stakes, painted with rings of alternate colours or another suitable scale, provide a convenient means of measuring the total depth of snow on the ground, especially in remote regions. The depth of snow at the stake or marker may be observed from distant ground points or from aircraft by means of binoculars or telescopes. The stakes should be painted white to minimize the undue melting of the snow immediately surrounding them. Aerial snow depth markers are vertical poles (of variable length, depending on the maximum snow depth) with horizontal cross-arms mounted at fixed heights on the poles and oriented according to the point of observation.

The development of an inexpensive ultrasonic ranging device to provide reliable snow depth measurements at automatic stations has provided a feasible alternative to the standard observation, both for snow depth and fresh snowfall (Goodison et al., 1988). Several ultrasonic models exist on the market and are commonly used with automatic systems. This type of sensor can also be utilized to control the quality of automatic recording gauge measurements by providing additional details on the type, amount and timing of precipitation. It is capable of an uncertainty of ±1 cm.

The temperature correction formula for ultrasonic snow depth measurement is:

$$d = d_r \sqrt{\frac{T}{273.15}} \tag{6.3}$$

where d is the snow depth in cm; d_r is the raw value of snow depth in cm; T is the air temperature in K; and $T = 273.15 + t$, t is the air temperature in °C.

Another recent new design uses a modulated visible laser beam and determines the distance to the ground by comparing phase information. The measurement of the distance is independent of air temperature, but may depend on the penetration of the laser beam in the snow surface according to the type of snow. The laser spot is also very small, increasing the importance of ground surface representativeness.

Selecting an area with natural vegetation can create issues, so it may be better to use a stable and controlled surface, such as an artificial lawn, in good thermal contact with the ground. Some National Meteorological and Hydrological Services have reported good results from using a snow plate (see WMO, 2010).

6.7.3　　　　Direct measurements of snow water equivalent

The standard method of measuring water equivalent is by gravimetric measurement using a snow tube to obtain a sample core. This method serves as the basis for snow surveys, a common procedure in many countries for obtaining a measure of water equivalent. The method consists of either melting each sample and measuring its liquid content or by weighing the frozen sample. A measured quantity of warm water or a heat source can be used to melt the sample.

Cylindrical samples of fresh snow may be taken with a suitable snow sampler and either weighed or melted. Details of the available instruments and sampling techniques are described in WMO (2008). Often a standard raingauge overflow can be used for this method.

Snowgauges measure snowfall water equivalent directly. Essentially, any non-recording precipitation gauges can also be used to measure the water equivalent of solid precipitation.

Snow collected in these types of gauges should be either weighed or melted immediately after each observation, as described in section 6.3.1.2. The recording-weighing gauge will catch solid forms of precipitation as well as liquid forms, and record the water equivalent in the same manner as liquid forms (see section 6.5.1).

The water equivalent of solid precipitation can also be estimated using the depth of fresh snowfall. This measurement is converted to water equivalent by using an appropriate specific density. Although the relationship stating that 1 cm of fresh snow equals the equivalent of 1 mm of water may be used with caution for long-term average values, it may be highly inaccurate for a single measurement, as the specific density ratio of snow may vary between 0.03 and 0.4.

6.7.4   Snow pillows

Snow pillows of various dimensions and materials are used to measure the weight of the snow that accumulates on the pillow. The most common pillows are flat circular containers (with a diameter of 3.7 m) made of rubberized material and filled with an antifreeze mixture of methyl alcohol and water or a methanol-glycol-water solution. The pillow is installed on the surface of the ground, flush with the ground, or buried under a thin layer of soil or sand. In order to prevent damage to the equipment and to preserve the snow cover in its natural condition, it is recommended that the site be fenced in. Under normal conditions, snow pillows can be used for 10 years or more.

Hydrostatic pressure inside the pillow is a measure of the weight of the snow on the pillow. Measuring the hydrostatic pressure by means of a float-operated liquid-level recorder or a pressure transducer provides a method of continuous measurement of the water equivalent of the snow cover. Variations in the accuracy of the measurements may be induced by temperature changes. In shallow snow cover, diurnal temperature changes may cause expansion or contraction of the fluid in the pillow, thus giving spurious indications of snowfall or snow melt. In deep mountain areas, diurnal temperature fluctuations are unimportant, except at the beginning and end of the snow season. The access tube to the measurement unit should be installed in a temperature-controlled shelter or in the ground to reduce the temperature effects.

In situ and/or telemetry data-acquisition systems can be installed to provide continuous measurements of snow water equivalent through the use of charts or digital recorders.

Snow pillow measurements differ from those taken with standard snow tubes, especially during the snow-melt period. They are most reliable when the snow cover does not contain ice layers, which can cause "bridging" above the pillows.

A comparison of the water equivalent of snow determined by a snow pillow with measurements taken by the standard method of weighing shows that these may differ by 5% to 10%.

6.7.5   Radioisotope snowgauges

Nuclear gauges measure the total water equivalent of the snow cover and/or provide a density profile. They are a non-destructive method of sampling and are adaptable to in situ recording and/or telemetry systems. Nearly all systems operate on the principle that water, snow or ice attenuates radiation. As with other methods of point measurement, siting in a representative location is critical for interpreting and applying point measurements as areal indices.

The gauges used to measure total water content consist of a radiation detector and a source, which is either natural or artificial. One part (for example, the detector/source) of the system is located at the base of the snowpack, and the other at a height greater than the maximum expected snow depth. As snow accumulates, the count rate decreases in proportion to the water equivalent of the snowpack. Systems using an artificial source of radiation are used at fixed locations to obtain measurements only for that site. A system using naturally occurring uranium as a ring source around a single pole detector has been successfully used to measure packs of up to 500 mm of water equivalent, or a depth of 150 cm.

A profiling radioactive snowgauge at a fixed location provides data on total snow water equivalent and density and permits an accurate study of the water movements and density changes that occur with time in a snowpack (Armstrong, 1976). A profiling gauge consists of two parallel vertical access tubes, spaced approximately 66 cm apart, which extend from a cement base in the ground to a height above the maximum expected depth of snow. A gamma ray source is suspended in one tube, and a scintillation gamma-ray detector, attached to a photomultiplier tube, in the other. The source and detector are set at equal depths within the snow cover and a measurement is taken. Vertical density profiles of the snow cover are obtained by taking measurements at depth increments of about 2 cm. A portable gauge (Young, 1976) which measures the density of the snow cover by backscatter, rather than transmission of the gamma rays, offers a practical alternative to digging deep snow pits, while instrument portability makes it possible to assess areal variations of density and water equivalent.

6.7.6 Natural gamma radiation

The method of gamma radiation snow surveying is based on the attenuation by snow of gamma radiation emanating from natural radioactive elements in the top layer of the soil. The greater the water equivalent of the snow, the more the radiation is attenuated. Terrestrial gamma surveys can consist of a point measurement at a remote location, a series of point measurements, or a selected traverse over a region (Loijens, 1975). The method can also be used on aircraft. The equipment includes a portable gamma-ray spectrometer that utilizes a small scintillation crystal to measure the rays in a wide spectrum and in three spectral windows (namely, potassium, uranium and thorium emissions). With this method, measurements of gamma levels are required at the point, or along the traverse, prior to snow cover. In order to obtain absolute estimates of the snow water equivalent, it is necessary to correct the readings for soil moisture changes in the upper 10 to 20 cm of soil for variations in background radiation resulting from cosmic rays, instrument drift and the washout of radon gas (which is a source of gamma radiation) in precipitation with subsequent build-up in the soil or snow. Also, in order to determine the relationship between spectrometer count rates and water equivalent, supplementary snow water equivalent measurements are initially required. Snow tube measurements are the common reference standard.

The natural gamma method can be used for snowpacks which have up to 300 mm water equivalent; with appropriate corrections, its precision is ±20 mm. The advantage of this method over the use of artificial radiation sources is the absence of a radiation risk.

6.7.7 Cosmic-Ray Snow Sensor

The Cosmic-Ray Snow Sensor provides a real-time measurement of the snow water equivalent by measuring the absorption of the cosmic-ray neutrons by the snowpack water. These neutrons are produced by the interaction of cosmic rays with the atmosphere and water. The incoming cosmic ray may fluctuate, up to 20%, over periods of a few days to a few months. A 20% variation of the incoming flux has approximately the same effect as the absorption of about 250 mm of water. Therefore, a snow-free reference signal is necessary to account for the natural variations of the cosmic ray. A single reference measurement may be used for a close network of sensors.

A local calibration of each device with on-site snow gauge measurements appears to be essential. With these precautions, the accuracy and reliability of the Cosmic-Ray Snow Sensor measurement are fully satisfying (Paquet and Laval, 2006).

————————————

ANNEX 6.A. PRECIPITATION INTERCOMPARISON SITES

The following text regarding precipitation intercomparison sites is based on statements made by the Commission for Instruments and Methods of Observation at its eleventh session in 1994 and updated following its fifteenth session in 2010:

The Commission recognized the benefits of national precipitation sites or centres where past, current and future instruments and methods of observation for precipitation can be assessed on an ongoing basis at evaluation stations. These stations should:

(a)   Operate the WMO recommended gauge configurations for rain (Reference Raingauge Pit) and snow (Double Fence Intercomparison Reference (DFIR)). Installation and operation will follow specifications of the WMO precipitation intercomparisons. A DFIR installation is not required when only rain is observed;

(b)   Operate past, current and new types of operational precipitation gauges or other methods of observation according to standard operating procedures and evaluate the accuracy and performance against WMO recommended reference instruments;

(c)   Take auxiliary meteorological measurements which will allow the development and tests for the application of precipitation correction procedures;

(d)   Provide quality control of data and archive all precipitation intercomparison data, including the related meteorological observations and the metadata, in a readily acceptable format, preferably digital;

(e)   Operate continuously for a minimum of 10 years;

(f)   Test all precipitation correction procedures available (especially those outlined in the final reports of the WMO intercomparisons) on the measurement of rain and solid precipitation;

(g)   Facilitate the conduct of research studies on precipitation measurements. It is not expected that the centres provide calibration or verification of instruments. They should make recommendations on national observation standards and should assess the impact of changes in observational methods on the homogeneity of precipitation time series in the region. The site would provide a reference standard for calibrating and validating radar or remote-sensing observations of precipitation.

––––––––––––

ANNEX 6.B. SUGGESTED CORRECTION PROCEDURES FOR PRECIPITATION MEASUREMENTS

The following text regarding the correction procedures for precipitation measurements is based on statements made by the Commission for Instruments and Methods of Observation at its eleventh session in 1994:

The correction methods are based on simplified physical concepts as presented in WMO (1987). They depend on the type of precipitation gauge applied. The effect of wind on a particular type of gauge has been assessed by using intercomparison measurements with the WMO reference gauges – the pit gauge for rain and the Double Fence Intercomparison Reference (DFIR) for snow as is shown in WMO (1984) and by the results of the WMO Solid Precipitation Measurement Intercomparison (WMO, 1998). The reduction of wind speed to the level of the gauge orifice should be made according to the following formula:

$$u_{hp} = \left(\log h z_0^{-1} \right) \cdot \left(\log H z_0^{-1} \right)^{-1} \cdot \left(1 - 0.024\alpha \right) u_H$$

where u_{hp} is the wind speed at the level of the gauge orifice; h is the height of the gauge orifice above ground; z_0 is the roughness length (0.01 m for winter and 0.03 m for summer); H is the height of the wind speed measuring instrument above ground; u_H is the wind speed measured at the height H above ground; and α is the average vertical angle of obstacles around the gauge.

The latter depends on the exposure of the gauge site and can be based either on the average value of direct measurements, on one of the eight main directions of the wind rose of the vertical angle of obstacles (in 360°) around the gauge, or on the classification of the exposure using metadata as stored in the archives of Meteorological Services. The classes are as follows:

Class	Angle	Description
Exposed site	0–5	Only a few small obstacles such as bushes, group of trees, a house
Mainly exposed site	6–12	Small groups of trees or bushes or one or two houses
Mainly protected site	13–19	Parks, forest edges, village centres, farms, group of houses, yards
Protected site	20–26	Young forest, small forest clearing, park with big trees, city centres, closed deep valleys, strongly rugged terrain, leeward of big hills

Wetting losses occur with the moistening of the inner walls of the precipitation gauge. They depend on the shape and the material of the gauge, as well as on the type and frequency of precipitation. For example, for the Hellmann gauge they amount to an average of 0.3 mm on a rainy and 0.15 mm on a snowy day; the respective values for the Tretyakov gauge are 0.2 mm and 0.1 mm. Information on wetting losses for other types of gauges can be found in WMO (1982).

––––––––––––––

ANNEX 6.C. STANDARD REFERENCE RAINGAUGE PIT

Reference raingauges are installed in a well-drained pit according to the design and specifications reported in the EN 13798:2010 standard (CEN, 2010) to minimize environmental interference on measured rainfall intensities and protect against in-splash by a metal or plastic grating. The buried or sunken gauge (see Koschmider, 1934; Sieck et al., 2007) is expected to show a higher rainfall reading than a gauge above ground, with possible differences of 10% or more, when both instruments are working perfectly and accurately. Pits are preferably sited on ground level to avoid possible surface runoff (see general configuration in Figure 6.C.1). The pit should be deep enough to accommodate the raingauge and to level the gauge's collector with the top of the grating (ground level) and centre it. The design of the pit takes into account dimensions of the raingauge and its method of installation. The base of the pit should have a recess (extra pit) to allow water to be drained. The square space of the grating is also adapted according to the raingauge collector's diameter in order to satisfy the standard requirements reported in CEN (2010). The sides of the pit are formed of bricks and concrete and are supported to prevent collapse. Supporting walls are built around the edges and a grating of approximately 1 875 x 1 875 x 120 mm (L x W x H) is installed on the pit walls with the possibility to be lifted to give access to the raingauge for checks and maintenance operations. The grating distance is approximately 120–125 mm. The grating is strong enough to walk on, to maintain its shape without distortion. To prevent in-splash from the top surface of the grating, the strips of the grating are at least 2 mm thick and the distance between the edge of the central square and the ground is greater than 600 mm (for further details see CEN, 2010). In Figure 6.C.2, an example of a realization of four standard reference raingauge pits is provided, as reported in WMO (2009).
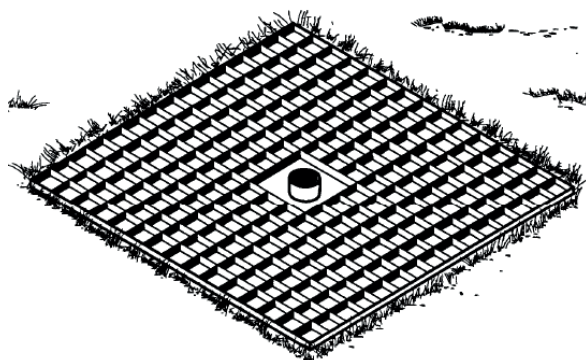
Figure 6.C.1. A raingauge pit and its grating (ground level configuration)
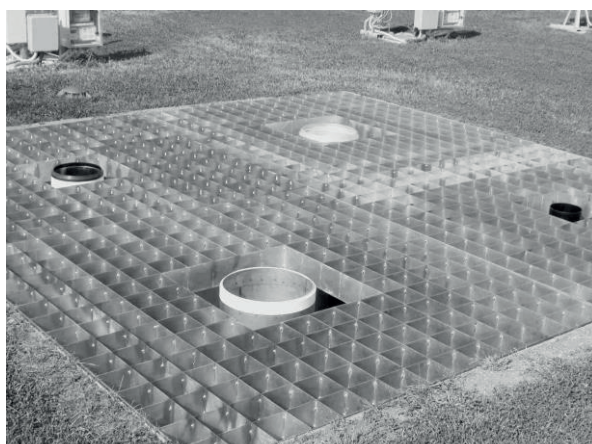
Figure 6.C.2. Realization of the reference raingauge pits at Vigna di Valle, Italy (2007) during the WMO Field Intercomparison of Rainfall Intensity Gauges

————————

ANNEX 6.D. STANDARDIZED PROCEDURE FOR LABORATORY CALIBRATION OF CATCHMENT TYPE RAINFALL INTENSITY GAUGES

1.   Principles

The calibration laboratory should be well prepared to perform calibrations of instruments to be used for operational practices. Apart from a well-designed reference system, the calibration procedures should be documented in full detail and set-up and staff should be well prepared before starting any calibration activity (see the ISO/IEC 17025 standard (ISO/IEC, 2005) for details). The result of any calibration will be a calibration certificate presenting the results of the calibration (including corrections to be applied), allowing a compliance check with the relevant WMO recommendations.

This certificate should also contain the measurement uncertainty for rainfall intensity. It should document the traceability of the rainfall intensity reference, the environmental conditions, such as temperature, and the applied time-averaging method.

Rainfall intensity gauges should be calibrated using a calibration system that:

(a)   Has the capability of generating a constant water flow at various flow rates corresponding to the entire operational range of measurement (recommended range: from 0.2 mm h^{-1} up to 2 000 mm h^{-1});

(b)   Is able to measure the flow by weighing the amount of water over a given period of time;

(c)   Is able to measure the output of the calibrated instrument at regular intervals or when a pulse occurs, which is typical for the majority of tipping-bucket raingauges.

2.   Requirements

(a)   The calibration system should be designed to obtain uncertainties less than 1% for the generated rainfall intensity, and such performances should be reported and detailed;

(b)   In case of tipping-bucket raingauges, correct and suitable balancing of the buckets should be verified in order to guarantee a minimal variance of the tipping duration during the measurement process;

(c)   At least five reference intensities suitably spaced to cover the whole operating range of the instrument should be used;

(d)   The number of rainfall intensity reference setting points should be large enough to be able to determine a fitting curve by interpolation. The reference setting should be selected and well spaced so that the calibration curve can be established by interpolation in such a way that the uncertainty of the fitting curve is less than the required measurement uncertainty for the full range;

(e)   The calculation of flow rate is based on the measurements of mass and time;

(f)   The measurement of mass is better than 0.1%;

(g)   The duration of any test should be long enough to guarantee an uncertainty of less than 1% on the generated intensity;

(h)   The maximum time resolution for the measurement of rainfall intensities should be 1 s;

(i)   The following issues must be considered for any related laboratory activity in addressing possible error sources:

(i)   The water quality/purity used for calibration should be well defined;

(ii)   The reproducibility of the calibration conditions should be a priority;

(iii) Suitable control and recording equipment should be used (such as PC-controlled);

(iv)   All acquisition systems must comply with electromagnetic compatibility to avoid parasitic pulses;

(j)   The quantity, for which measurements of precipitation are generally reported, is height expressed in millimetres although weighing gauges measure mass. Since the density of rain depends on ambient temperature, the relationship between mass and the equivalent height of rainfall introduces an inaccuracy that must be taken into account during calibration and uncertainty calculation;

(k)   The environmental conditions during each calibration must be noted and recorded:

(i)   Date and hour (start/end);

(ii)   Air temperature [°C];

(iii) Water temperature [°C];

(iv)   Atmospheric pressure [hPa];

(v)   Ambient relative humidity [%];

(vi)   Any special condition that may be relevant to calibration (for example, vibrations);

(vii) Evaporation losses must be estimated [mm];

(l)   The number of tests performed for each instrument, their description in terms of time units and/or number of tips must be documented.

3.   **Procedure from data interpretation**

(a)   The results should be presented in the form of a graph where the relative error is plotted against the reference intensity. The relative error is evaluated for each reference flow rate as:

$$e = \frac{I_m - I_r}{I_r} \cdot 100\%$$

where I_m is the intensity measured by the instrument and I_r the actual reference intensity provided to the instrument;

(b)   Ideally five tests, but a minimum of three, should be performed for each set of reference intensities, so that five error figures are associated with each instrument. The average error and the average values of I_r and I_m are obtained by discarding the minimum and the maximum value of e obtained for each reference flow rate, then evaluating the arithmetic mean of the three remaining errors and reference intensity values. For each reference intensity, an error bar encompassing all the five error values used to obtain the average figures should be reported;

(c)   In addition, I_r versus I_m can be plotted, where I_m and I_r are average values, calculated as indicated above; all data are fitted with an interpolating curve, obtained as the best fit (linear, power law or second order polynomial are acceptable);

(d)   In the graphs presenting the results, the ±5% limits must be drawn to allow an easy comparison of the results with the WMO recommendations;

(e)   In case water storage should occur for an intensity below the maximum declared intensity, the intensity at which water storage begins should be documented in the calibration certificate and intensities above this limit should not be considered;

(f)   In addition to measurements based on constant flow rates, the step response of each non-tipping-bucket raingauge instrument should be determined. The step response should be measured by switching between two different constant flows, namely from 0 mm h^{-1} to the reference intensity and back to 0 mm h^{-1}. The constant flow should be applied until the output signal of the instrument is stabilized, that is, when the further changes or fluctuation in the established rainfall intensity can be neglected with respect to the stated measurement uncertainty of the reference system. The sampling rate must be at least one per minute for those instruments that allow it. The time before stabilization is assumed as a measure of the delay of the instrument in measuring the reference rainfall intensity. Less than one minute delay is required for accurate rainfall intensity measurements. The response time should always be documented in the calibration certificate.

4.   Uncertainty calculation

The following sources of the measurement uncertainty should be considered and quantified:

(a)   Flow generator: Uncertainty on the flow steadiness deriving from possible variations in the constant flow generation mechanism, including pressure difference inside water content and in distribution pipes;

(b)   Flow measuring devices (both reference and device under calibration): Uncertainties due to the weighing apparatus, to time measurement and delays in acquisition and data processing and to the variation of experimental and ambient conditions such as temperature and relative humidity.

These two sources of uncertainty are independent from each other; therefore a separate analysis can be performed, and results can be then combined into the uncertainty budget.

———————

ANNEX 6.E. PROCEDURE FOR FIELD CALIBRATION OF CATCHMENT TYPE RAINFALL INTENSITY GAUGES

The field calibration is part of a routine field maintenance and check and should be performed on a regular basis. Its main purpose is to verify the operational status of precipitation gauges: to detect malfunctions, output anomalies and calibration drifts over time or between two laboratory calibrations. Field calibrations also provide valuable insight for data analysis and interpretation. The procedure is based on the same principles as laboratory calibration (given in Annex 6.D), using the generation of constant intensity (stationary reference flow) within the gauge's range of operational use.

A field calibrator is typically composed of a cylindrical water tank of suitable capacity, a combination of air intakes and output nozzles for different rainfall intensities, and an electronic system to calculate the emptying time (see figure below). A suitable combination of air intakes and nozzles must be selected based on the precipitation gauge collector size and the intensity value chosen for the calibration. By opening the top tap and bottom nozzle, a constant flow is conveyed to the funnel of the gauge and, through the time of emptying and the conversion table (volume–time–intensity), it is possible to retrieve the reference intensity. Air intakes provide the pressure compensation, thus maintaining a constant push.

From an operational viewpoint, the portable field calibrator permits rapid tests due to its very simple operation. The calibrator does not contain any sophisticated components and therefore provides a cost-effective solution for the metrological verification of precipitation intensity instruments.

The repeatability of the field calibrator (and its accuracy) should be rigorously assessed in a laboratory before the operational use. The uncertainty should preferably be expressed as relative expanded uncertainty in relation to the statistical coverage interval (95% confidence level, $k = 2$) and should be lower than 2%.

A statistical analysis of relative errors with respect to the field reference flow of the calibrator should be conducted for each field-calibrated precipitation gauge. At least 25–30 data points (normally 1 min intensity values in mm h^{-1}) should be recorded for each reference intensity (selected by the field calibrator). This makes it possible to assume a normal distribution of the data around the mean value and to better estimate the average and improve the accuracy of the results (central limit theorem). All tests must be performed in environmental conditions without precipitation or fog and with low wind flows (to avoid dynamic pressure perturbations to air intakes). The reference intensity should always be started at the beginning of a minute synchronized with the instrument clock or data-logger timer (official/station time-stamp).
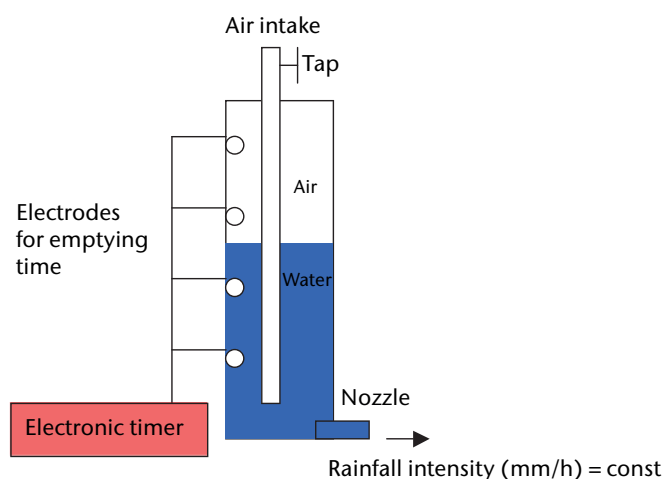
A simplified scheme of a portable field calibrator

The minimum set of statistical parameters and metadata to be reported after each field calibration is listed below:

(a) Date and time;

(b) Reference intensity in mm h⁻¹ (I_{ref}): constant intensity generated by the field calibrator;

(c) Average ($avgI$) of intensity values (I_{1min}) in mm h⁻¹ of the precipitation gauge during the calibration, calculated as follows:

$$avgI = \frac{1}{N} \sum_{j=1}^{N} \left(I_{1min}^{j} \right)$$

(6.E.1)

(d) Extremes (namely $I_{+CL95\%}$, $I_{-CL95\%}$) of an interval [$avgI – \delta(95\%)$; $avgI + \delta(95\%)$] = [$I_{+CL95\%}$; $I_{-CL95\%}$] corresponding to the 95% confidence level. The amplitude $\delta(95\%)$ is the half-width of the confidence interval calculated according to a normal or Student's t probability distribution of samples (it includes a calculation of the standard deviation);

(e) Relative error in percentage of the average intensity, calculated as follows:

$$RE_{avgI} = 100 \cdot \left(\frac{avgI - I_{ref}}{I_{ref}} \right)$$

(6.E.2)

(f) Relative errors in percentage of $I_{+CL95\%}$ and $I_{-CL95\%}$, calculated as follows:

$$RE_{+CL95\%} = 100 \cdot \left(\frac{I_{+CL95\%} - I_{ref}}{I_{ref}} \right)$$

(6.E.3)

$$RE_{-CL95\%} = 100 \cdot \left(\frac{I_{-CL95\%} - I_{ref}}{I_{ref}} \right)$$

(6.E.4)

The last three statistical parameters are used to calculate the gauge's relative errors with regard to intensity with an uncertainty interval at the 95% confidence level for each reference intensity used during the calibration. The regular repetition of the field calibration and the comparison of results makes it possible to evaluate the stability of the calibration status and possible anomalies.

————————

REFERENCES AND FURTHER READING

Armstrong, R.L., 1976: The application of isotopic profiling snow-gauge data to avalanche research. *Proceedings of the Forty-fourth Annual Western Snow Conference*, Atmospheric Environment Service, Canada, pp. 12–19.

Colli, M., L.G. Lanza and P.W. Chan, 2013*a*: Co-located tipping-bucket and optical drop counter RI measurements and a simulated correction algorithm. *Atmospheric Research*, 119:3–12.

Colli, M., L.G. Lanza and P. La Barbera, 2013*b*: Performance of a weighing rain gauge under laboratory simulated time-varying reference rainfall rates. *Atmospheric Research*, 131:3–12.

European Committee for Standardization (CEN), 2010: *Hydrometry – Specification for a Reference Raingauge Pit*, EN 13798:2010.

Fikke, S., G. Ronsten, A. Heimo, S. Kunz, M. Ostrozlik, P.E. Persson, J. Sabata, B. Wareing, B. Wichura, J. Chum, T. Laakso, K. Säntti and L. Makkonen, 2007: *COST-727: Atmospheric Icing on Structures; Measurements and data collection on icing: State of the Art*, MeteoSwiss, No. 75.

Goodison, B.E., J.R. Metcalfe, R.A. Wilson and K. Jones, 1988: The Canadian automatic snow depth sensor: A performance update. *Proceedings of the Fifty-sixth Annual Western Snow Conference*, Atmospheric Environment Service, Canada, pp. 178–181.

Goodison, B.E., B. Sevruk and S. Klemm, 1989: WMO solid precipitation measurement intercomparison: Objectives, methodology and analysis. In: International Association of Hydrological Sciences, 1989: *Atmospheric deposition. Proceedings*, Baltimore Symposium (May, 1989), IAHS Publication No. 179, Wallingford.

Grunow, J., 1960: The productiveness of fog precipitation in relation to the cloud droplet spectrum. In: American Geophysical Union, 1960, *Physics of precipitation*. Geophysical Monograph No. 5, *Proceedings of the Cloud Physics Conference* (3–5 June 1959, Woods Hole, Massachusetts), Publication No. 746, pp. 110–117.

———, 1963: *Weltweite Messungen des Nebelniederschlags nach der Hohenpeissenberger Methode*. In: International Union of Geodesy and Geophysics, General Assembly (Berkeley, California, 19–31 August 1963), International Association of Scientific Hydrology Publication No. 65, pp. 324–342.

Habib, E., W.F. Krajewski and A. Kruger, 2001: Sampling errors of tipping-bucket rain gauge measurements. *Journal of Hydrologic Engineering*, 6:159–166.

International Organization for Standardization, 2001: *Atmospheric Icing of Structures*, ISO 12494:2001. Geneva.

International Organization for Standardization/International Electrotechnical Commission, 2005: *General Requirements for the Competence of Testing and Calibration Laboratories*, ISO/IEC 17025:2005/ Cor 1:2006. Geneva.

Koschmieder, H., 1934: Methods and results of definite rain measurements; III. Danzig Report (1). *Monthly Weather Review*, 62:5–7.

Legates, D.R. and C.J. Willmott, 1990: Mean seasonal and spatial variability in gauge-corrected, global precipitation. *Int. J. Climatology*, 10:111–127.

Loijens, H.S., 1975: Measurements of snow water equivalent and soil moisture by natural gamma radiation. *Proceedings of the Canadian Hydrological Symposium-75* (11–14 August 1975, Winnipeg), pp. 43–50.

Nespor, V. and B. Sevruk, 1999: Estimation of wind-induced error of rainfall gauge measurements using a numerical simulation. *Journal of Atmospheric and Oceanic Technology*, 16(4):450–464.

Niemczynowicz, J., 1986: The dynamic calibration of tipping-bucket raingauges. *Nordic Hydrology*, 17:203–214.

Paquet, E. and M.T. Laval, 2006: Operation feedback and prospects of EDF Cosmic-Ray Snow Sensors, *La Houille Blanche*, 2:113–119.

Rinehart, R.E., 1983: Out-of-level instruments: Errors in hydrometeor spectra and precipitation measurements. *Journal of Climate and Applied Meteorology*, 22:1404–1410.

Schemenauer, R.S. and P. Cereceda, 1991: Fog water collection in arid coastal locations. *Ambio*, 20(7):303–308.

———, 1994*a*: Fog collection's role in water planning for developing countries. *Natural Resources Forum*, 18(2):91–100.

———, 1994*b*: A proposed standard fog collector for use in high-elevation regions. *Journal of Applied Meteorology*, 33(11):1313–1322.

Sevruk, B., 1974*a*: Correction for the wetting loss of a Hellman precipitation gauge. *Hydrological Sciences Bulletin*, 19(4):549–559.

———, 1974*b*: Evaporation losses from containers of Hellman precipitation gauges. *Hydrological Sciences Bulletin*, 19(2):231–236.

———, 1984: Comments on "Out-of-level instruments: Errors in hydrometeor spectra and precipitation measurements". *Journal of Climate and Applied Meteorology*, 23:988–989.

Sevruk, B. and V. Nespor, 1994: The effect of dimensions and shape of precipitation gauges on the wind-induced error. In: *Global Precipitation and Climate Change* (M. Desbois and F. Desalmand, eds.). NATO ASI Series, Springer Verlag, Berlin, I26:231–246.

Sevruk, B. and L. Zahlavova, 1994: Classification system of precipitation gauge site exposure: Evaluation and application. *International Journal of Climatology*, 14(6):681–689.

Sieck, L.C., S.J. Burges and M. Steiner, 2007: Challenges in obtaining reliable measurements of point rainfall. *Water Resources Research*, 43:1–23.

Slovak Hydrometeorological Institute and Swiss Federal Institute of Technology, 1993: Precipitation measurement and quality control. *Proceedings of the International Symposium on Precipitation and Evaporation* (B. Sevruk and M. Lapin, eds.) (Bratislava, 20–24 September 1993), Volume I, Bratislava and Zurich.

Smith, J.L., H.G. Halverson and R.A. Jones, 1972: *Central Sierra Profiling Snowgauge: A Guide to Fabrication and Operation*. USAEC Report TID-25986, National Technical Information Service, U.S. Department of Commerce, Washington DC.

Stadtmuller, T. and N. Agudelo, 1990: Amount and variability of cloud moisture input in a tropical cloud forest. In: *Proceedings of the Lausanne Symposia* (August/November), IAHS Publication No. 193, Wallingford.

Vong, R.J., J.T. Sigmon and S.F. Mueller, 1991: Cloud water deposition to Appalachian forests. *Environmental Science and Technology*, 25(6):1014–1021.

World Meteorological Organization, 1972: Evaporation losses from storage gauges (B. Sevruk). In: *Distribution of Precipitation in Mountainous Areas*, Geilo Symposium (Norway, 31 July–5 August 1972), Volume II – technical papers (WMO-No. 326). Geneva.

———, 1982: *Methods of Correction for Systematic Error in Point Precipitation Measurement for Operational Use* (B. Sevruk). Operational Hydrology Report No. 21 (WMO-No. 589). Geneva.

———, 1984: *International Comparison of National Precipitation Gauges with a Reference Pit Gauge* (B. Sevruk and W.R. Hamon). Instruments and Observing Methods Report No. 17 (WMO/TD-No. 38). Geneva.

———, 1985: *International Organizing Committee for the WMO Solid Precipitation Measurement Intercomparison*. Final report of the first session (distributed to participants only). Geneva.

———, 1986: *Papers Presented at the Workshop on the Correction of Precipitation Measurements* (B. Sevruk, ed.) (Zurich, Switzerland, 1–3 April 1985). Instruments and Observing Methods Report No. 25 (WMO/TD-No. 104). Geneva.

———, 1987: *Instruments Development Inquiry* (E. Prokhorov). Instruments and Observing Methods Report No. 24 (WMO/TD-No. 231). Geneva.

———, 1989*a*: *Catalogue of National Standard Precipitation Gauges* (B. Sevruk and S. Klemm). Instruments and Observing Methods Report No. 39 (WMO/TD-No. 313). Geneva.

———, 1989*b*: *International Workshop on Precipitation Measurements* (B. Sevruk, ed.) (St Moritz, Switzerland, 3–7 December 1989). Instruments and Observing Methods Report No. 48 (WMO/TD-No. 328). Geneva.

———, 1992*a*: *Snow Cover Measurements and Areal Assessment of Precipitation and Soil Moisture* (B. Sevruk, ed.). Operational Hydrology Report No. 35 (WMO-No. 749). Geneva.

———, 1992*b*: *Report on the Measurement of Leaf Wetness* (R.R. Getz). Agricultural Meteorology Report No. 38 (WMO/TD-No. 478). Geneva.

———, 1998: *WMO Solid Precipitation Measurement Intercomparison: Final Report* (B.E. Goodison, P.Y.T. Louie and D. Yang). Instruments and Observing Methods Report No. 67 (WMO/TD-No. 872). Geneva.

———, 2006: *WMO Laboratory Intercomparison of Rainfall Intensity Gauges* (L.G. Lanza, M. Leroy, C. Alexandropoulos, L. Stagi and W. Wauben). Instruments and Observing Methods Report No. 84 (WMO/TD-No. 1304). Geneva.

———, 2008: *Guide to Hydrological Practices* (WMO-No. 168), Volume I. Geneva.

———, 2009: *WMO Field Intercomparison of Rainfall Intensity Gauges* (E. Vuerich, C. Monesi, L.G. Lanza, L. Stagi, E. Lanzinger). Instruments and Observing Methods Report No. 99 (WMO/TD-No. 1504). Geneva.

———, 2010: Optimized snow plates and snow grids for automatic and manual snow depth measurements (E. Lanzinger and M. Theel). *Paper presented at the WMO Technical Conference on Meteorological and Environmental Instruments and Methods of Observation (TECO-2010).* Instruments and Observing Methods Report No. 104 (WMO/TD-No. 1546). Geneva.

Yang, D., J.R. Metcalfe, B.E. Goodison and E. Mekis, 1993: True Snowfall: An evaluation of the Double Fence Intercomparison Reference Gauge. *Proceedings of the Fiftieth Eastern Snow Conference*, Quebec City, 8–10 June 1993, Quebec, Canada, pp. 105–111.

Yang, D., B.E. Goodison, J.R. Metcalfe, V.S. Golubev, E. Elomaa, T. Gunther, R. Bates, T. Pangburn, C.L. Hanson, D. Emerson, V. Copaciu and J. Milkovic, 1995: Accuracy of Tretyakov precipitation gauge: results of WMO intercomparison. *Hydrological Processes*, 9:877–895.

Young, G.J., 1976: A portable profiling snow-gauge: Results of field tests on glaciers. *Proceedings of the Forty-fourth Annual Western Snow Conference*, Atmospheric Environment Service, Canada, pp. 7–11.

CHAPTER CONTENTS

CHAPTER 7. MEASUREMENT OF RADIATION

7.1 GENERAL

The various fluxes of radiation to and from the Earth's surface are among the most important variables in the heat economy of the Earth as a whole and at any individual place at the Earth's surface or in the atmosphere. Radiation measurements are used for the following purposes:

(a) To study the transformation of energy within the Earth–atmosphere system and its variation in time and space;

(b) To analyse the properties and distribution of the atmosphere with regard to its constituents, such as aerosols, water vapour, ozone, and so on;

(c) To study the distribution and variations of incoming, outgoing and net radiation;

(d) To satisfy the needs of biological, medical, agricultural, architectural and industrial activities with respect to radiation;

(e) To verify satellite radiation measurements and algorithms.

Such applications require a widely distributed regular series of records of solar and terrestrial surface radiation components and the derivation of representative measures of the net radiation. In addition to the publication of serial values for individual observing stations, an essential objective must be the production of comprehensive radiation climatologies, whereby the daily and seasonal variations of the various radiation constituents of the general thermal budget may be more precisely evaluated and their relationships with other meteorological elements better understood.

A very useful account of the operation and design of networks of radiation stations is contained in WMO (1986). Part IV of this CIMO Guide describes the scientific principles of the measurements and gives advice on quality assurance, which is most important for radiation measurements. The *Baseline Surface Radiation Network (BSRN) Operations Manual* (WMO, 1998) gives an overview of the latest state of radiation measurements.

Following normal practice in this field, errors and uncertainties are expressed in this chapter as a 66% confidence interval of the difference from the true quantity, which is similar to a standard deviation of the population of values. Where needed, specific uncertainty confidence intervals are indicated and uncertainties are estimated using the International Organization for Standardization method (ISO/IEC, 2008 / JCGM, 2008). For example, 95% uncertainty implies that the stated uncertainty is for a confidence interval of 95%.

7.1.1 Definitions

Annex 7.A contains the nomenclature of radiometric and photometric quantities. It is based on definitions recommended by the International Radiation Commission of the International Association of Meteorology and Atmospheric Sciences and by the International Commission on Illumination (CIE). Annex 7.B gives the meteorological radiation quantities, symbols and definitions.

Radiation quantities may be classified into two groups according to their origin, namely solar and terrestrial radiation. In the context of this chapter, "radiation" can imply a process or apply to multiple quantities. For example, "solar radiation" could mean solar energy, solar exposure or solar irradiance (see Annex 7.B).

Solar energy is the electromagnetic energy emitted by the sun. The solar radiation incident on the top of the terrestrial atmosphere is called extraterrestrial solar radiation; 97% of which is confined to the spectral range 290 to 3 000 nm is called solar (or sometimes short-wave) radiation. Part of the extra-terrestrial solar radiation penetrates through the atmosphere to the Earth's surface, while part of it is scattered and/or absorbed by the gas molecules, aerosol particles, cloud droplets and cloud crystals in the atmosphere.

Terrestrial radiation is the long-wave electromagnetic energy emitted by the Earth's surface and by the gases, aerosols and clouds of the atmosphere; it is also partly absorbed within the atmosphere. For a temperature of 300 K, 99.99% of the power of the terrestrial radiation has a wavelength longer than 3 000 nm and about 99% longer than 5 000 nm. For lower temperatures, the spectrum is shifted to longer wavelengths.

Since the spectral distributions of solar and terrestrial radiation overlap very little, they can very often be treated separately in measurements and computations. In meteorology, the sum of both types is called total radiation.

Light is the radiation visible to the human eye. The spectral range of visible radiation is defined by the spectral luminous efficiency for the standard observer. The lower limit is taken to be between 360 and 400 nm, and the upper limit between 760 and 830 nm (CIE, 1987). The radiation of wavelengths shorter than about 400 nm is called ultraviolet (UV), and longer than about 800 nm, infrared radiation. The UV range is sometimes divided into three sub-ranges (IEC, 1987):

> UV-A: 315–400 nm
> UV-B: 280–315 nm
> UV-C: 100–280 nm

7.1.2   Units and scales

7.1.2.1   *Units*

The International System of Units (SI) is to be preferred for meteorological radiation variables. A general list of the units is given in Annexes 7.A and 7.B.

7.1.2.2   *Standardization*

The responsibility for the calibration of radiometric instruments rests with the World, Regional and National Radiation Centres, the specifications for which are given in Annex 7.C. Furthermore, the World Radiation Centre (WRC) at Davos is responsible for maintaining the basic reference, the World Standard Group (WSG) of instruments, which is used to establish the World Radiometric Reference (WRR). During international comparisons, organized every five years, the standards of the regional centres are compared with the WSG, and their calibration factors are adjusted to the WRR. They, in turn, are used to transmit the WRR periodically to the national centres, which calibrate their network instruments using their own standards.

Definition of the World Radiometric Reference

In the past, several radiation references or scales have been used in meteorology, namely the Ångström scale of 1905, the Smithsonian scale of 1913, and the international pyrheliometric scale of 1956 (IPS 1956). The developments in absolute radiometry in recent years have very much reduced the uncertainty of radiation measurements. With the results of many comparisons of 15 individual absolute pyrheliometers of 10 different types, a WRR has been defined. The old scales can be transferred into the WRR using the following factors:

$$\frac{WRR}{Angstrom\ scale\ 1905} = 1.026$$

$$\frac{WRR}{Smithsonian\ scale\ 1913} = 0.977$$

$$\frac{WRR}{IPS\ 1956} = 1.022$$

The WRR is accepted as representing the physical units of total irradiance within 0.3% (99% uncertainty of the measured value).

Realization of the World Radiometric Reference: World Standard Group

In order to guarantee the long-term stability of the new reference, a group of at least four absolute pyrheliometers of different design is used as the WSG. At the time of incorporation into this group, the instruments are given a reduction factor to correct their readings to the WRR. To qualify for membership of this group, a radiometer must fulfil the following specifications:

(a)   Stability must be better than 0.2% of the measured value over timescales of decades;

(b)   The 95% uncertainty of the series of measurements with the instrument must lie within the limits of the uncertainty of the WRR;

(c)   The instrument has to have a different design from the other WSG instruments.

To meet the stability criteria, the instruments of the WSG are the subjects of an intercomparison at least once a year, and, for this reason, WSG is kept at the WRC Davos.

Computation of world radiometric reference values

In order to calibrate radiometric instruments, the reading of a WSG instrument, or one that is directly traceable to the WSG, should be used. During international pyrheliometer comparisons (IPCs), the WRR value is calculated from the mean of at least three participating instruments of the WSG. To yield WRR values, the readings of the WSG instruments are always corrected with the individual reduction factor, which is determined at the time of their incorporation into the WSG. Since the calculation of the mean value of the WSG, serving as the reference, may be jeopardized by the failure of one or more radiometers belonging to the WSG, the Commission for Instruments and Methods of Observation resolved[1] that at each IPC an ad hoc group should be established comprising the Rapporteur on Meteorological Radiation Instruments (or designate) and at least five members, including the chairperson. The director of the comparison must participate in the group's meetings as an expert. The group should discuss the preliminary results of the comparison, based on criteria defined by the WRC, evaluate the reference and recommend the updating of the calibration factors.

7.1.3   **Meteorological requirements**

7.1.3.1   *Data to be reported*

Irradiance and radiant exposure are the quantities most commonly recorded and archived, with averages and totals of over 1 h. There are also many requirements for data over shorter periods, down to 1 min or even tens of seconds (for some energy applications). Daily totals of radiant exposure are frequently used, but these are expressed as a mean daily irradiance. Measurements of atmospheric extinction must be made with very short response times to reduce the uncertainties arising from variations in air mass.

---

[1]   Recommended by the Commission for Instruments and Methods of Observation at its eleventh session (1994).

For radiation measurements, it is particularly important to record and make available information about the circumstances of the observations. This includes the type and traceability of the instrument, its calibration history, and its location in space and time, spatial exposure and maintenance record.

7.1.3.2 *Uncertainty*

There are no formally agreed statements of required uncertainty for most radiation quantities, but uncertainty is discussed in the sections of this chapter dealing with the various types of measurements, and best practice uncertainties are stated for the Global Climate Observing System's Baseline Surface Radiation Network (see WMO, 1998). It may be said generally that good quality measurements are difficult to achieve in practice, and for routine operations they can be achieved only with modern equipment and redundant measurements. Some systems still in use fall short of best practice, the lesser performance having been acceptable for many applications. However, data of the highest quality are increasingly in demand.

Statements of uncertainty for net radiation and radiant exposure are given in Part I, Chapter 1, Annex 1.E. The required 95% uncertainty for radiant exposure for a day, stated by WMO for international exchange, is 0.4 MJ m^{-2} for $\leq$ 8 MJ m^{-2} and 5% for > 8 MJ m^{-2}.

7.1.3.3 *Sampling and recording*

The uncertainty requirements can best be satisfied by making observations at a sampling period less than the $1/e$ time constant of the instrument, even when the data to be finally recorded are integrated totals for periods of up to 1 h, or more. The data points may be integrated totals or an average flux calculated from individual samples. Digital data systems are greatly to be preferred. Chart recorders and other types of integrators are much less convenient, and the resultant quantities are difficult to maintain at adequate levels of uncertainty.

7.1.3.4 *Times of observation*

In a worldwide network of radiation measurements, it is important that the data be homogeneous not only for calibration, but also for the times of observation. Therefore, all radiation measurements should be referred to what is known in some countries as local apparent time, and in others as true solar time. However, standard or universal time is attractive for automatic systems because it is easier to use, but is acceptable only if a reduction of the data to true solar time does not introduce a significant loss of information (that is to say, if the sampling and storage rates are high enough, as indicated in section 7.1.3.3 above). See Annex 7.D for useful formulae for the conversion from standard to solar time.

7.1.4 **Measurement methods**

Meteorological radiation instruments are classified using various criteria, namely the type of variable to be measured, the field of view, the spectral response, the main use, and the like. The most important types of classifications are listed in Table 7.1. The quality of the instruments is characterized by items (a) to (h) below. The instruments and their operation are described in sections 7.2 to 7.4 below. WMO (1986) provides a detailed account of instruments and the principles according to which they operate.

Absolute radiometers are self-calibrating, meaning that the irradiance falling on the sensor is replaced by electrical power, which can be accurately measured. The substitution, however, cannot be perfect; the deviation from the ideal case determines the uncertainty of the radiation measurement.

Most radiation sensors, however, are not absolute and must be calibrated against an absolute instrument. The uncertainty of the measured value, therefore, depends on the following factors, all of which should be known for a well-characterized instrument:

(a)   Resolution, namely, the smallest change in the radiation quantity which can be detected by the instrument;

(b)   Drifts of sensitivity (the ratio of electrical output signal to the irradiance applied) over time;

(c)   Changes in sensitivity owing to changes of environmental variables, such as temperature, humidity, pressure and wind;

(d)   Non-linearity of response, namely, changes in sensitivity associated with variations in irradiance;

(e)   Deviation of the spectral response from that postulated, namely the blackness of the receiving surface, the effect of the aperture window, and so on;

(f)   Deviation of the directional response from that postulated, namely cosine response and azimuth response;

Table 7.1. Meteorological radiation instruments

Instrument classification	Parameter to be measured	Main use	Viewing angle (sr) (see Figure 7.1)
Absolute pyrheliometer	Direct solar radiation	Primary standard	5×10^{-3} (approx. 2.5° half angle)
Pyrheliometer	Direct solar radiation	(a) Secondary standard for calibrations (b) Network	5×10^{-3} to 2.5×10^{-2}
Spectral pyrheliometer	Direct solar radiation in broad spectral bands (e.g. with OG 530, RG 630, etc. filters)	Network	5×10^{-3} to 2.5×10^{-2}
Sunphotometer	Direct solar radiation in narrow spectral bands (e.g. at 500 ± 2.5 nm, 368 ± 2.5 nm)	(a) Standard (b) Network	1×10^{-3} to 1×10^{-2} (approx. 2.3° full angle)
Pyranometer	(a) Global (solar) radiation (b) Diffuse sky (solar) radiation (c) Reflected solar radiation	(a) Working standard (b) Network	2π
Spectral pyranometer	Global (solar) radiation in broadband spectral ranges (e.g. with OG 530, RG 630, etc. filters)	Network	2π
Net pyranometer	Net global (solar) radiation	(a) Working standard (b) Network	4π
Pyrgeometer	(a) Upward long-wave radiation (downward-looking) (b) Downward long-wave radiation (upward-looking)	Network	2π
Pyrradiometer	Total radiation	Working standard	2π
Net pyrradiometer	Net total radiation	Network	4π

(g)   Time constant of the instrument or the measuring system;

(h)   Uncertainties in the auxiliary equipment.

Instruments should be selected according to their end-use and the required uncertainty of the derived quantity. Certain instruments perform better for particular climates, irradiances and solar positions.

7.2   MEASUREMENT OF DIRECT SOLAR RADIATION

Direct solar radiation is measured by means of pyrheliometers, the receiving surfaces of which are arranged to be normal to the solar direction. By means of apertures, only the radiation from the sun and a narrow annulus of sky is measured, the latter radiation component is sometimes referred to as circumsolar radiation or aureole radiation. In modern instruments, this extends out to a half-angle of about 2.5° on some models, and to about 5° from the sun's centre (corresponding, respectively, to $6 \cdot 10^{-3}$ and $2.4 \cdot 10^{-2}$ sr). The pyrheliometer mount must allow for the rapid and smooth adjustment of the azimuth and elevation angles. A sighting device is usually included in which a small spot of light or solar image falls upon a mark in the centre of the target when the receiving surface is exactly normal to the direct solar beam. For continuous recording, it is advisable to use automatic sun-following equipment (sun tracker).

For all new designs of direct solar radiation instruments it is recommended that the opening half-angle be 2.5° ($6 \cdot 10^{-3}$ sr) and the slope angle 1°. For the definition of these angles refer to Figure 7.1.

During the comparison of instruments with different view-limiting geometries, the aureole radiation influences the readings more significantly for larger slope and aperture angles. The difference can be as great as 2% between the two apertures mentioned above for an air mass of 1.0. In order to enable climatological comparison of direct solar radiation data during different seasons, it may be necessary to reduce all data to a mean Sun–Earth distance:

$$E_N = E / R^2 \tag{7.1}$$

where E_N is the solar radiation, normalized to the mean Sun–Earth distance, which is defined to be one astronomical unit (AU) (see Annex 7.D); E is the measured direct solar radiation; and R is the Sun–Earth distance in astronomical units.
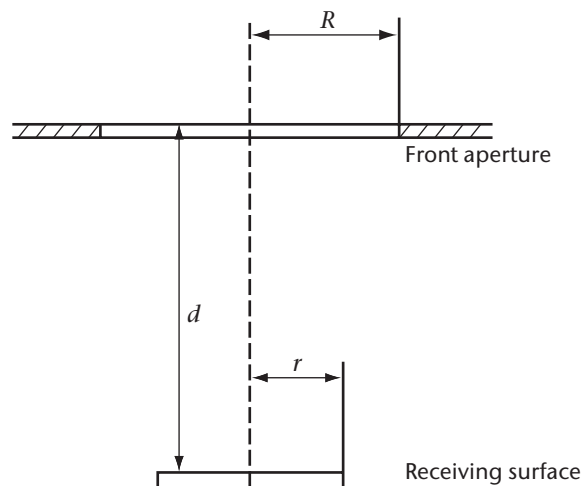
Figure 7.1. View-limiting geometry: The opening half-angle is arctan R/d; the slope angle is arctan $(R–r)/d$.

7.2.1 Direct solar radiation

Some of the characteristics of operational pyrheliometers (other than primary standards) are given in Table 7.2 (adapted from ISO, 1990*a*), with indicative estimates of the uncertainties of measurements made with them if they are used with appropriate expertise and quality control. Cheaper pyrheliometers are available (see ISO, 1990*a*), but without effort to characterize their response the resulting uncertainties reduce the quality of the data, and, given that a sun tracker is required, in most cases the incremental cost for a good pyrheliometer is minor. The estimated uncertainties are based on the following assumptions:

(a) Instruments are well-maintained, correctly aligned and clean;

(b) 1 min and 1 h figures are for clear-sky irradiances at solar noon;

(c) Daily exposure values are for clear days at mid-latitudes.

7.2.1.1 Primary standard pyrheliometers

An absolute pyrheliometer can define the scale of total irradiance without resorting to reference sources or radiators. The limits of uncertainty of the definition must be known; the quality of this

Table 7.2. Characteristics of operational pyrheliometers

Characteristic		High quality[a]	Good quality[b]
Response time (95% response)		< 15 s	< 30 s
Zero offset (response to 5 K h^{-1} change in ambient temperature)		2 W m^{-2}	4 W m^{-2}
Resolution (smallest detectable change in W m^{-2})		0.51	1
Stability (percentage of full scale, change/year)		0.1	0.5
Temperature response (percentage maximum error due to change of ambient temperature within an interval of 50 K)		1	2
Non-linearity (percentage deviation from the responsivity at 500 W m^{-2} due to the change of irradiance within 100 W m^{-2} to 1 100 W m^{-2})		0.2	0.5
Spectral sensitivity (percentage deviation of the product of spectral absorptance and spectral transmittance from the corresponding mean within the range 300 to 3 000 nm)		0.5	1.0
Tilt response (percentage deviation from the responsivity at 0° tilt (horizontal) due to change in tilt from 0° to 90° at 1 000 W m^{-2})		0.2	0.5
Achievable uncertainty, 95% confidence level (see above)			
1 min totals	%	0.9	1.8
	kJ m^{-2}	0.56	1
1 h totals	%	0.7	1.5
	kJ m^{-2}	21	54
Daily totals	%	0.5	1.0
	kJ m^{-2}	200	400

Notes:
a Near state of the art; suitable for use as a working standard; maintainable only at stations with special facilities and staff.
b Acceptable for network operations.

knowledge determines the reliability of an absolute pyrheliometer. Only specialized laboratories should operate and maintain primary standards. Details of their construction and operation are given in WMO (1986). However, for the sake of completeness, a brief account is given here.

All absolute pyrheliometers of modern design use cavities as receivers and electrically calibrated, differential heat-flux meters as sensors. At present, this combination has proved to yield the lowest uncertainty possible for the radiation levels encountered in solar radiation measurements (namely, up to 1.5 kW m^{-2}).

Normally, the electrical calibration is performed by replacing the radiative power by electrical power, which is dissipated in a heater winding as close as possible to where the absorption of solar radiation takes place.

The uncertainties of such an instrument's measurements are determined by a close examination of the physical properties of the instrument and by performing laboratory measurements and/or model calculations to determine the deviations from ideal behaviour, that is, how perfectly the electrical substitution can be achieved. This procedure is called characterization of the instrument.

The following specification should be met by an absolute pyrheliometer (an individual instrument, not a type) to be designated and used as a primary standard:

(a)   At least one instrument out of a series of manufactured radiometers has to be fully characterized. The 95% uncertainty of this characterization should be less than 2 W m^{-2} under the clear-sky conditions suitable for calibration (see ISO, 1990*a*). The 95% uncertainty (for all components of the uncertainty) for a series of measurements should not exceed 4 W m^{-2} for any measured value;

(b)   Each individual instrument of the series must be compared with the one which has been characterized, and no individual instrument should deviate from this instrument by more than the characterization uncertainty as determined in (a) above;

(c)   A detailed description of the results of such comparisons and of the characterization of the instrument should be made available upon request;

(d)   Traceability to the WRR by comparison with the WSG or some carefully established reference with traceability to the WSG is needed in order to prove that the design is within the state of the art. The latter is fulfilled if the 95% uncertainty for a series of measurements traceable to the WRR is less than 1 W m^{-2}.

7.2.1.2   *Secondary standard pyrheliometers*

An absolute pyrheliometer which does not meet the specification for a primary standard or which is not fully characterized can be used as a secondary standard if it is calibrated by comparison with the WSG with a 95% uncertainty for a series of measurements less than 1 W m^{-2}.

Other types of instruments with measurement uncertainties similar or approaching those for primary standards may be used as secondary standards.

The Ångström compensation pyrheliometer has been, and still is, used as a convenient secondary standard instrument for the calibration of pyranometers and other pyrheliometers. It was designed by K. Ångström as an absolute instrument, and the Ångström scale of 1905 was based on it; now it is used as a secondary standard and must be calibrated against a standard instrument.

The sensor consists of two platinized manganin strips, each of which is about 18 mm long, 2 mm wide and about 0.02 mm thick. They are blackened with a coating of candle soot or with an optical matt black paint. A thermo-junction of copper-constantan is attached to the back of

Table 7.3. View-limiting geometry of Ångström pyrheliometers

Angle	Vertical	Horizontal
Opening half-angle	5° – 8°	~2°
Slope angle	0.7° – 1.0°	1.2° – 1.6°

each strip so that the temperature difference between the strips can be indicated by a sensitive galvanometer or an electrical micro-voltmeter. The dimensions of the strip and front diaphragm yield opening half-angles and slope angles as listed in Table 7.3.

The measurement set consists of three or more cycles, during which the left- or right-hand strip is alternately shaded from or exposed to the direct solar beam. The shaded strip is heated by an electric current, which is adjusted in such a way that the thermal electromagnetic force of the thermocouple and, hence, the temperature difference between the two strips approximate zero. Before and after a measuring sequence, the zero is checked either by shading or by exposing both strips simultaneously. Depending on which of these methods is used and on the operating instructions of the manufacturer, the irradiance calculation differs slightly. The method adopted for the IPCs uses the following formula:

$$E = K \cdot i_L \cdot i_R \qquad\qquad (7.2)$$

where E is the irradiance in W m^{-2}; K is the calibration constant determined by comparison with a primary standard (W m^{-2} A^{-2}); and i_L i_R is the current in amperes measured with the left- or right-hand strip exposed to the direct solar beam, respectively.

Before and after each series of measurements, the zero of the system is adjusted electrically by using either of the foregoing methods, the zeros being called "cold" (shaded) or "hot" (exposed), as appropriate. Normally, the first reading, say i_R, is excluded and only the following $i_L - i_R$ pairs are used to calculate the irradiance. When comparing such a pyrheliometer with other instruments, the irradiance derived from the currents corresponds to the geometric mean of the solar irradiances at the times of the readings of i_L and i_R.

The auxiliary instrumentation consists of a power supply, a current-regulating device, a nullmeter and a current monitor.

The sensitivity of the nullmeter should be about 0.05 · 10^{-6} A per scale division for a low-input impedance (< 10 Ω), or about 0.5 μV with a high-input impedance (> 10 kΩ). Under these conditions, a temperature difference of about 0.05 K between the junction of the copper-constantan thermocouple causes a deflection of one scale division, which indicates that one of the strips is receiving an excess heat supply amounting to about 0.3%.

The uncertainty of the derived direct solar irradiance is highly dependent on the qualities of the current-measuring device, whether a moving-coil milliammeter or a digital multimeter which measures the voltage across a standard resistor, and on the operator's skill. The fractional error in the output value of irradiance is twice as large as the fractional error in the reading of the electric current. The heating current is directed to either strip by means of a switch and is normally controlled by separate rheostats in each circuit. The switch can also cut the current off so that the zero can be determined. The resolution of the rheostats should be sufficient to allow the nullmeter to be adjusted to within one half of a scale division.

7.2.1.3   *Field and network pyrheliometers*

These pyrheliometers generally make use of a thermopile as the detector. They have similar view-limiting geometry as standard pyrheliometers. Older models tend to have larger fields of view and slope angles. These design features were primarily designed to reduce the need for accurate sun tracking. However, the larger the slope (and opening) angle, the larger the amount of aureole radiation sensed by the detector; this amount may reach several % for high optical depths and large limiting angles. With new designs of sun trackers, including computer-assisted

trackers in both passive and active (sun-seeking) configurations, the need for larger slope angles is unnecessary. However, a slope angle of 1° is still required to ensure that the energy from the direct solar beam is distributed evenly on the detector; and allows for minor sun tracker pointing errors of the order of 0.1°.

The intended use of the pyrheliometer may dictate the selection of a particular type of instrument. Some manually oriented models, such as the Linke Fuessner Actinometer, are used mainly for spot measurements, while others such as the EKO, Eppley, Kipp and Zonen, and Middleton types are designed specifically for the long-term monitoring of direct irradiance. Before deploying an instrument, the user must consider the significant differences found among operational pyrheliometers as follows:

(a)   The field of view of the instrument;

(b)   Whether the instrument measures both the long-wave and short-wave portion of the spectrum (namely, whether the aperture is open or covered with a glass or quartz window);

(c)   The temperature compensation or correction methods;

(d)   The magnitude and variation of the zero irradiance signal;

(e)   If the instrument can be installed on an automated tracking system for long-term monitoring;

(f)   If, for the calibration of other operational pyrheliometers, differences (a) to (c) above are the same, and if the pyrheliometer is of the quality required to calibrate other network instruments.

7.2.1.4   *Calibration of pyrheliometers*

All pyrheliometers, other than absolute pyrheliometers, must be calibrated by comparison using the sun as the source with a pyrheliometer that has traceability to the WSG and a likely uncertainty of calibration equal to or better than the pyrheliometer being calibrated.

As all solar radiation data must be referred to the WRR, absolute pyrheliometers also use a factor determined by comparison with the WSG and not their individually determined one. After such a comparison (for example, during the periodically organized IPCs) such a pyrheliometer can be used as a standard to calibrate, again by comparison with the sun as a source, secondary standards and field pyrheliometers. Secondary standards can also be used to calibrate field instruments, but with increased uncertainty.

The quality of sun-source calibrations may depend on the aureole influence if instruments with different view-limiting geometries are compared. Also, the quality of the results will depend on the variability of the solar irradiance, if the time constants and zero irradiance signals of the pyrheliometers are significantly different. Lastly, environmental conditions, such as temperature, pressure and net long-wave irradiance, can influence the results. If a very high quality of calibration is required, only data taken during very clear and stable days should be used.

The procedures for the calibration of field pyrheliometers are given in an ISO standard (ISO, 1990*b*).

From recent experience at IPCs, a period of five years between traceable calibrations to the WSG should suffice for primary and secondary standards. Field pyrheliometers should be calibrated every one to two years; the more prolonged the use and the more rigorous the conditions, the more often they should be calibrated.

7.2.2 **Exposure**

For continuous recording and reduced uncertainties, an accurate sun tracker that is not influenced by environmental conditions is essential. Sun tracking to within 0.2° is required, and the instruments should be inspected at least once a day, and more frequently if weather conditions so demand (with protection against adverse conditions).

The principal exposure requirement for monitoring direct solar radiation is freedom from obstructions to the solar beam at all times and seasons of the year. Furthermore, the site should be chosen so that the incidence of fog, smoke and airborne pollution is as typical as possible of the surrounding area.

For continuous observations, typically a window is used to protect the sensor and optical elements against rain, snow, and so forth. Care must be taken to ensure that such a window is kept clean and that condensation does not appear on the inside.

7.3 **MEASUREMENT OF GLOBAL AND DIFFUSE SKY RADIATION**

The solar radiation received from a solid angle of 2π sr on a horizontal surface is referred to as global radiation. This includes radiation received directly from the solid angle of the sun's disc, as well as diffuse sky radiation that has been scattered in traversing the atmosphere.

The instrument needed for measuring solar radiation from a solid angle of 2π sr into a plane surface and a spectral range from 300 to 3 000 nm is the pyranometer. The pyranometer is sometimes used to measure solar radiation on surfaces inclined in the horizontal and in the inverted position to measure reflected global radiation. When measuring the diffuse sky component of solar radiation, the direct solar component is screened from the pyranometer by a shading device (see section 7.3.3.3).

Pyranometers normally use thermo-electric, photoelectric, pyro-electric or bimetallic elements as sensors. Since pyranometers are exposed continually in all weather conditions they must be robust in design and resist the corrosive effects of humid air (especially near the sea). The receiver should be hermetically sealed inside its casing, or the casing must be easy to take off so that any condensed moisture can be removed. Where the receiver is not permanently sealed, a desiccator is usually fitted in the base of the instrument. The properties of pyranometers which are of concern when evaluating the uncertainty and quality of radiation measurement are: sensitivity, stability, response time, cosine response, azimuth response, linearity, temperature response, thermal offset, zero irradiance signal and spectral response. Further advice on the use of pyranometers is given in ISO (1990c) and WMO (1998).

Table 7.4 (adapted from ISO, 1990a) describes the characteristics of pyranometers of various levels of performance, with the uncertainties that may be achieved with appropriate facilities, well-trained staff and good quality control under the sky conditions outlined in 7.2.1.

7.3.1 **Calibration of pyranometers**

The calibration of a pyranometer consists of the determination of one or more calibration factors and the dependence of these on environmental conditions, such as:

(a) Angular distribution of irradiance;

(b) Calibration methods;

(c) Directional response of the instrument;

(d) Inclination of instrument;

(e)   Irradiance level;

(f)   Net long-wave irradiance for thermal offset correction;

(g)   Spectral distribution of irradiance;

(h)   Temperature;

(i)   Temporal variation.

The users of pyranometers must recognize that the uncertainty of observations will increase when the sensor exposure conditions deviate from the conditions in which the pyranometer was calibrated.

Normally, it is necessary to specify the test environmental conditions, which can be quite different for different applications. The method and conditions must also be given in some detail in the calibration certificate.

Table 7.4. Characteristics of operational pyranometers

Characteristic	High quality[a]	Good quality[b]	Moderate quality[c]
Response time (95% response)	< 15 s	< 30 s	< 60 s
Zero offset:			
(a) Response to 200 W m^{-2} net thermal radiation (ventilated)	7 W m^{-2}	15 W m^{-2}	30 W m^{-2}
(b) Response to 5 K h^{-1} change in ambient temperature	2 W m^{-2}	4 W m^{-2}	8 W m^{-2}
Resolution (smallest detectable change)	1 W m^{-2}	5 W m^{-2}	10 W m^{-2}
Stability (change per year, percentage of full scale)	0.8	1.5	3.0
Directional response for beam radiation (the range of errors caused by assuming that the normal incidence responsivity is valid for all directions when measuring, from any direction, a beam radiation whose normal incidence irradiance is 1 000 W m^{-2})	10 W m^{-2}	20 W m^{-2}	30 W m^{-2}
Temperature response (percentage maximum error due to any change of ambient temperature within an interval of 50 K)	2	4	8
Non-linearity (percentage deviation from the responsivity at 500 W m^{-2} due to any change of irradiance within the range 100 to 1 000 W m^{-2})	0.5	1	3
Spectral sensitivity (percentage deviation of the product of spectral absorptance and spectral transmittance from the corresponding mean within the range 300 to 3 000 nm)	2	5	10
Tilt response (percentage deviation from the responsivity at 0° tilt (horizontal) due to change in tilt from 0° to 90° at 1 000 W m^{-2})	0.5	2	5
Achievable uncertainty (95% confidence level):			
Hourly totals	3%	8%	20%
Daily totals	2%	5%	10%

Notes:
a   Near state of the art; suitable for use as a working standard; maintainable only at stations with special facilities and staff.
b   Acceptable for network operations.
c   Suitable for low-cost networks where moderate to low performance is acceptable.

There are a variety of methods for calibrating pyranometers using the sun or laboratory sources. These include the following:

(a)   By comparison with a standard pyrheliometer for the direct solar irradiance and a calibrated shaded pyranometer for the diffuse sky irradiance;

(b)   By comparison with a standard pyrheliometer using the sun as a source, with a removable shading disc for the pyranometer;

(c)   With a standard pyrheliometer using the sun as a source and two pyranometers to be calibrated alternately measuring global and diffuse irradiance;

(d)   By comparison with a standard pyranometer using the sun as a source, under other natural conditions of exposure (for example, a uniform cloudy sky and direct solar irradiance not statistically different from zero);

(e)   In the laboratory, on an optical bench with an artificial source, either normal incidence or at some specified azimuth and elevation, by comparison with a similar pyranometer previously calibrated outdoors;

(f)   In the laboratory, with the aid of an integrating chamber simulating diffuse sky radiation, by comparison with a similar type of pyranometer previously calibrated outdoors.

These are not the only methods; (a), (b) and (c) and (d) are commonly used. However, it is essential that, except for (b), either the zero irradiance signals for all instruments are known or pairs of identical model pyranometers in identical configurations are used. Ignoring these offsets and differences can bias the results significantly.

Method (c) is considered to give very good results without the need for a calibrated pyranometer.

It is difficult to determine a specific number of measurements on which to base the calculation of the pyranometer calibration factor. However, the standard error of the mean can be calculated and should be less than the desired limit when sufficient readings have been taken under the desired conditions. The principal variations (apart from fluctuations due to atmospheric conditions and observing limitations) in the derived calibration factor are due to the following:

(a)   Departures from the cosine law response, particularly at solar elevations of less than 10° (for this reason it is better to restrict calibration work to occasions when the solar elevation exceeds 30°);

(b)   The ambient temperature;

(c)   Imperfect levelling of the receiver surface;

(d)   Non-linearity of instrument response;

(e)   The net long-wave irradiance between the detector and the sky.

The pyranometer should be calibrated only in the position of use.

When using the sun as the source, the apparent solar elevation should be measured or computed (to the nearest 0.01°) for this period from solar time (see Annex 7.D). The mean instrument or ambient temperature should also be noted.

7.3.1.1   *By reference to a standard pyrheliometer and a shaded reference pyranometer*

In this method, described in ISO (1993), the pyranometer's response to global irradiance is calibrated against the sum of separate measurements of the direct and diffuse components.

Periods with clear skies and steady radiation (as judged from the record) should be selected. The vertical component of the direct solar irradiance is determined from the pyrheliometer output, and the diffuse sky irradiance is measured with a second pyranometer that is continuously shaded from the sun. The direct component is eliminated from the diffuse sky pyranometer by shading the whole outer dome of the instrument with a disc of sufficient size mounted on a slender rod and held some distance away. The diameter of the disc and its distance from the receiver surface should be chosen in such a way that the screened angle approximately equals the aperture angles of the pyrheliometer. Rather than using the radius of the pyranometer sensor, the radius of the outer dome should be used to calculate the slope angle of the shading disc and pyranometer combination. This shading arrangement occludes a close approximation of both the direct solar beam and the circumsolar sky irradiance as sensed by the pyrheliometer.

On a clear day, the diffuse sky irradiance is less than 15% of the global irradiance; hence, the calibration factor of the reference pyranometer does not need to be known very accurately. However, care must be taken to ensure that the zero irradiance signals from both pyranometers are accounted for, given that for some pyranometers under clear sky conditions the zero irradiance signal can be as high as 15% of the diffuse sky irradiance.

The calibration factor is then calculated according to:

$$E \cdot \sin h + V_s k_s = V \cdot k \tag{7.3}$$

or:

$$k = (E \sin h + V_s k_s)/V \tag{7.4}$$

where E is the direct solar irradiance measured with the pyrheliometer (W m^{-2}), V is the global irradiance output of the pyranometer to be calibrated (μV); V_s is the diffuse sky irradiance output of the shaded reference pyranometer (μV), h is the apparent solar elevation at the time of reading; k is the calibration factor of the pyranometer to be calibrated (W m^{-2} μV^{-1}); and k_s is the calibration factor of the shaded reference pyranometer (W m^{-2} μV^{-1}), and all the signal measurements are taken simultaneously.

The direct, diffuse and global components will change during the comparison, and care must be taken with the appropriate sampling and averaging to ensure that representative values are used.

7.3.1.2 *By reference to a standard pyrheliometer*

This method, described in ISO (1993), is similar to the method of the preceding paragraph, except that the diffuse sky irradiance signal is measured by the same pyranometer. The direct component is eliminated temporarily from the pyranometer by shading the whole outer dome of the instrument as described in section 7.3.1.1. The period required for occulting depends on the steadiness of the radiation flux and the response time of the pyranometer, including the time interval needed to bring the temperature and long-wave emission of the glass dome to equilibrium; 10 times the thermopile 1/e time constant of the pyranometer should generally be sufficient.

The difference between the representative shaded and unshaded outputs from the pyranometer is due to the vertical component of direct solar irradiance E measured by the pyrheliometer. Thus:

$$E \cdot \sin h = (V_{un} - V_s) \cdot k \tag{7.5}$$

or:

$$k = (E \cdot \sin h)/(V_{un} - V_s) \tag{7.6}$$

where E is the representative direct solar irradiance at normal incidence measured by the pyrheliometer (W m^{-2}); V_{un} is the representative output signal of the pyranometer (μV) when in unshaded (or global) irradiance mode; V_s is the representative output signal of the pyranometer (μV) when in shaded (or diffuse sky) irradiance mode; h is the apparent solar elevation, and k is the calibration factor (W m^{-2} μV^{-1}), which is the inverse of the sensitivity (μV W^{-1} m^2).

Both the direct and diffuse components will change during the comparison, and care must be taken with the appropriate sampling and averaging to ensure that representative values of the shaded and unshaded outputs are used for the calculation. To reduce uncertainties associated with representative signals, a continuous series of shade and un-shade cycles should be performed and time-interpolated values used to reduce temporal changes in global and diffuse sky irradiance. Since the same pyranometer is being used in differential mode, and the difference in zero irradiance signals for global and diffuse sky irradiance is negligible, there is no need to account for zero irradiances in equation 7.6.

7.3.1.3   *Alternate calibration using a pyrheliometer*

This method uses the same instrumental set-up as the method described in section 7.3.1.1, but only requires the pyrheliometer to provide calibrated irradiance data (E), and the two pyranometers are assumed to be un-calibrated (Forgan, 1996). The method calibrates both pyranometers by solving a pair of simultaneous equations analogous to equation 7.3. Irradiance signal data are initially collected with the pyrheliometer and one pyranometer (pyranometer A) measures global irradiance signals (V_{gA}) and the other pyranometer (pyranometer B) measures diffuse irradiance signals (V_{dB}) over a range of solar zenith angles in clear sky conditions. After sufficient data have been collected in the initial configuration, the pyranometers are exchanged so that pyranometer A, which initially measured the global irradiance signal, now measures the diffuse irradiance signal (V_{dA}), and vice versa with regard to pyranometer B. The assumption is made that for each pyranometer the diffuse (k_d) and global (k_g) calibration coefficients are equal, and the calibration coefficient for pyranometer A is given by:

$$k_A = k_{gA} = k_{dA} \tag{7.7}$$

with an identical assumption for pyranometer B coefficients. Then for a time t_0 in the initial period a modified version of equation 7.3 is:

$$E(t_0)\sin(h(t_0)) = k_A V_{gA}(t_0) - k_B V_{dB}(t_0) \tag{7.8}$$

For time t_1 in the alternate period when the pyranometers are exchanged:

$$E(t_1)\sin(h(t_1)) = k_B V_{gB}(t_1) - k_A V_{dA}(t_1) \tag{7.9}$$

As the only unknowns in equations 7.8 and 7.9 are k_A and k_B, these can be solved for any pair of times (t_0, t_1). Pairs covering a range of solar elevations provide an indication of the directional response. The resultant calibration information for both pyranometers is representative of the global calibration coefficients and produces almost identical information to method 7.3.1.1, but without the need for a calibrated pyranometer.

As with method 7.3.1.1, to produce coefficients with minimum uncertainty this alternate method requires that the irradiance signals from the pyranometers be adjusted to remove any estimated zero irradiance offset. To reduce uncertainties due to changing directional response it is recommended to use a pair of pyranometers of the same model and observation pairs when $\sin h (t_0) \sim \sin h (t_1)$.

The method is ideally suited to automatic field monitoring situations where three solar irradiance components (direct, diffuse and global) are monitored continuously. Experience suggests that the data collection necessary for the application of this method may be conducted during as little as one day with the exchange of instruments taking place around solar noon. However, at a field site, the extended periods and days either side of the instrument change may be used for data selection, provided that the pyrheliometer has a valid calibration.

7.3.1.4   *By comparison with a reference pyranometer*

As described in ISO (1992), this method entails the simultaneous operation of two pyranometers mounted horizontally, side by side, outdoors for a sufficiently long period to acquire representative results. If the instruments are of the same model and monitoring configuration, only one or two days should be sufficient. The more pronounced the difference between the types of pyranometer configurations, the longer the period of comparison required. A long

period, however, could be replaced by several shorter periods covering typical conditions (clear, cloudy, overcast, rainfall, snowfall, and so on). The derivation of the instrument factor is straightforward, but, in the case of different pyranometer models, the resultant uncertainty is more likely to be a reflection of the difference in model, rather than the stability of the instrument being calibrated. Data selection should be carried out when irradiances are relatively high and varying slowly. Each mean value of the ratio R of the response of the test instrument to that of the reference instrument may be used to calculate $k = R \cdot k_r$, where k_r is the calibration factor of the reference, and k is the calibration factor being derived. During a sampling period, provided that the time between measurements is less than the $1/e$ time constant of the pyranometers, data collection can occur during times of fluctuating irradiance.

The mean temperature of the instruments or the ambient temperature should be recorded during all outdoor calibration work to allow for any temperature effects.

7.3.1.5   *By comparison in the laboratory*

There are two methods which involve laboratory-maintained artificial light sources providing either direct or diffuse irradiance. In both cases, the test pyranometer and a reference standard pyranometer are exposed under the same conditions.

In one method, the pyranometers are exposed to a stabilized tungsten-filament lamp installed at the end of an optical bench. A practical source for this type of work is a 0.5 to 1.0 kW halogen lamp mounted in a water-cooled housing with forced ventilation and with its emission limited to the solar spectrum by a quartz window. This kind of lamp can be used if the standard and the instrument to be calibrated have the same spectral response. For general calibrations, a high-pressure xenon lamp with filters to give an approximate solar spectrum should be used. When calibrating pyranometers in this way, reflection effects should be excluded from the instruments by using black screens. The usual procedure is to install the reference instrument and measure the radiant flux. The reference is then removed and the measurement repeated using the test instrument. The reference is then replaced and another determination is made. Repeated alternation with the reference should produce a set of measurement data of good precision (about 0.5%).

In the other method, the calibration procedure uses an integrating light system, such as a sphere or hemisphere illuminated by tungsten lamps, with the inner surface coated with highly reflective diffuse-white paint. This offers the advantage of simultaneous exposure of the reference pyranometer and the instrument to be calibrated. Since the sphere or hemisphere simulates a sky with an approximately uniform radiance, the angle errors of the instrument at 45° dominate. As the cosine error at these angles is normally low, the repeatability of integrating-sphere measurements is generally within 0.5%. As for the source used to illuminate the sphere, the same considerations apply as for the first method.

7.3.1.6   *Routine checks on calibration factors*

There are several methods for checking the constancy of pyranometer calibration, depending upon the equipment available at a particular station. Every opportunity to check the performance of pyranometers in the field must be seized.

At field stations where carefully preserved standards (either pyrheliometers or pyranometers) are available, the basic calibration procedures described above may be employed. Where standards are not available, other techniques can be used. If there is a simultaneous record of direct solar radiation, the two records can be examined for consistency by the method used for direct standardization, as explained in section 7.3.1.2. This simple check should be applied frequently.

If there are simultaneous records of global and diffuse sky radiation, the two records should be frequently examined for consistency. In periods of total cloud the global and diffuse sky radiation should be identical, and these periods can be used when a shading disc is used for monitoring

diffuse sky radiation. When using shading bands it is recommended that the band be removed so that the diffuse sky pyranometer is measuring global radiation and its data can be compared to simultaneous data from the global pyranometer.

The record may be verified with the aid of a travelling working standard sent from the central station of the network or from a nearby station. Lastly, if calibrations are not performed at the site, the pyranometer can be exchanged for a similar one sent from the calibration facility. Either of the last two methods should be used at least once a year. Pyranometers used for measuring reflected solar radiation should be moved into an upright position and checked using the methods described above.

7.3.2 **Performance of pyranometers**

Considerable care and attention to details are required to attain the desirable standard of uncertainty. A number of properties of pyranometers and measurement systems should be evaluated so that the uncertainty of the resultant data can be estimated. For example, it has been demonstrated that, for a continuous record of global radiation without ancillary measurements of diffuse sky and direct radiation, an uncertainty better than 5% in daily totals represents the result of good and careful work. Similarly, when a protocol similar to that proposed by WMO (1998) is used, uncertainties for daily total can be of the order of 2%.

7.3.2.1 *Sensor levelling*

For accurate global radiation measurements with a pyranometer it is essential that the spirit level indicate when the plane of the thermopile is horizontal. This can be tested in the laboratory on an optical levelling table using a collimated lamp beam at about a 20° elevation. The levelling screws of the instrument are adjusted until the response is as constant as possible during rotation of the sensor in the azimuth. The spirit-level is then readjusted, if necessary, to indicate the horizontal plane. This is called radiometric levelling and should be the same as physical levelling of the thermopile. However, this may not be true if the quality of the thermopile surface is not uniform.

7.3.2.2 *Change of sensitivity due to ambient temperature variation*

Thermopile instruments exhibit changes in sensitivity with variations in instrument temperature. Some instruments are equipped with integrated temperature compensation circuits in an effort to maintain a constant response over a large range of temperatures. The temperature coefficient of sensitivity may be measured in a temperature-controlled chamber. The temperature in the chamber is varied over a suitable range in 10 °C steps and held steady at each step until the response of the pyranometers has stabilized. The data are then fitted with a smooth curve. If the maximum percentage difference due to temperature response over the operational ambient range is 2% or more, a correction should be applied on the basis of the fit of the data.

If no temperature chamber is available, the standardization method with pyrheliometers (see section 7.3.1.1, 7.3.1.2 or 7.3.1.3) can be used at different ambient temperatures. Attention should be paid to the fact that not only the temperature, but also, for example, the cosine response (namely, the effect of solar elevation) and non-linearity (namely, variations of solar irradiance) can change the sensitivity.

7.3.2.3 *Variation of response with orientation*

The calibration factor of a pyranometer may very well be different when the instrument is used in an orientation other than that in which it was calibrated. Inclination testing of pyranometers can be conducted in the laboratory or with the standardization method described in section 7.3.1.1

or 7.3.1.2. It is recommended that the pyranometer be calibrated in the orientation in which it will be used. A correction for tilting is not recommended unless the instrument's response has been characterized for a variety of conditions.

7.3.2.4 *Variation of response with angle of incidence*

The dependence of the directional response of the sensor upon solar elevation and azimuth is usually known as the Lambert cosine response and the azimuth response, respectively. Ideally, the solar irradiance response of the receiver should be proportional to the cosine of the zenith angle of the solar beam, and constant for all azimuth angles. For pyranometers, it is recommended that the cosine error (or percentage difference from ideal cosine response) be specified for at least two solar elevation angles, preferably 30° and 10°. A better way of prescribing the directional response is given in Table 7.4, which specifies the permissible error for all angles.

Only lamp sources should be used to determine the variation of response with the angle of incidence, because the spectral distribution of the sun changes with the angle of elevation. Using the sun as a source, an apparent variation of response with solar elevation angle could be observed which, in fact, is a variation due to non-homogeneous spectral response.

7.3.2.5 *Uncertainties in hourly and daily totals*

As most pyranometers in a network are used to determine hourly or daily exposures (or exposures expressed as mean irradiances), it is evident that the uncertainties in these values are important.

Table 7.4 lists the expected maximum deviation from the true value, excluding calibration errors. The types of pyranometers in the third column of Table 7.4 (namely, those of moderate quality) are not suitable for hourly or daily totals, although they may be suitable for monthly and yearly totals.

7.3.3 **Installation and maintenance of pyranometers**

The site selected to expose a pyranometer should be free from any obstruction above the plane of the sensing element and, at the same time, should be readily accessible. If it is impracticable to obtain such an exposure, the site must be as free as possible of obstructions that may shadow it at any time in the year. The pyranometer should not be close to light-coloured walls or other objects likely to reflect solar energy onto it; nor should it be exposed to artificial radiation sources.

In most places, a flat roof provides a good location for mounting the radiometer stand. If such a site cannot be obtained, a stand placed some distance from buildings or other obstructions should be used. If practicable, the site should be chosen so that no obstruction, in particular within the azimuth range of sunrise and sunset over the year, should have an elevation exceeding 5°. Other obstructions should not reduce the total solar angle by more than 0.5 sr. At stations where this is not possible, complete details of the horizon and the solid angle subtended should be included in the description of the station.

A site survey should be carried out before the initial installation of a pyranometer whenever its location is changed or if a significant change occurs with regard to any surrounding obstructions. An excellent method of doing this is to use a survey camera that provides azimuthal and elevation grid lines on the negative. A series of exposures should be made to identify the angular elevation above the plane of the receiving surface of the pyranometer and the angular range in azimuth of all obstructions throughout the full 360° around the pyranometer. If a survey camera is not available, the angular outline of obscuring objects may be mapped out by means of a theodolite or a compass and clinometer combination.

The description of the station should include the altitude of the pyranometer above sea level (that is, the altitude of the station plus the height of pyranometer above the ground), together with its geographical longitude and latitude. It is also most useful to have a site plan, drawn to scale, showing the position of the recorder, the pyranometer, and all connecting cables.

The accessibility of instrumentation for frequent inspection is probably the most important single consideration when choosing a site. It is most desirable that pyranometers and recorders be inspected at least daily, and preferably more often.

The foregoing remarks apply equally to the exposure of pyranometers on ships, towers and buoys. The exposure of pyranometers on these platforms is a very difficult and sometimes hazardous undertaking. Seldom can an instrument be mounted where it is not affected by at least one significant obstruction (for example, a tower). Because of platform motion, pyranometers are subject to wave motion and vibration. Precautions should be taken, therefore, to ensure that the plane of the sensor is kept horizontal and that severe vibration is minimized. This usually requires the pyranometer to be mounted on suitably designed gimbals.

7.3.3.1 *Correction for obstructions to a free horizon*

If the direct solar beam is obstructed (which is readily detected on cloudless days), the record should be corrected wherever possible to reduce uncertainty.

Only when there are separate records of global and diffuse sky radiation can the diffuse sky component of the record be corrected for obstructions. The procedure requires first that the diffuse sky record be corrected, and the global record subsequently adjusted. The fraction of the sky itself which is obscured should not be computed, but rather the fraction of the irradiance coming from that part of the sky which is obscured. Since the diffuse sky radiation from elevations below 5° contributes less than 1% to the diffuse sky radiation, it can normally be neglected. Attention should be concentrated on objects subtending angles of 10° or more, as well as those which might intercept the solar beam at any time. In addition, it must be borne in mind that light-coloured objects can reflect solar radiation onto the receiver.

Strictly speaking, when determining corrections for the loss of diffuse sky radiation due to obstacles, the variance in sky radiance over the hemisphere should be taken into account. However, the only practical procedure is to assume that the radiance is isotropic, that is, the same from all parts of the sky. In order to determine the relative reduction in diffuse sky irradiance for obscuring objects of finite size, the following expression may be used:

$$\Delta E_{\text{sky}} = \pi^{-1} \int_{\phi} \int_{\Theta} \sin\theta \cos\theta d\,\theta d\,\varphi \tag{7.10}$$

where θ is the angle of elevation; ϕ is the azimuth angle, Θ is the extent in elevation of the object; and φ is the extent in azimuth of the object.

The expression is valid only for obstructions with a black surface facing the pyranometer. For other objects, the correction has to be multiplied by a reduction factor depending on the reflectivity of the object. Snow glare from a low sun may even lead to an opposite sign for the correction.

7.3.3.2 *Installation of pyranometers for measuring global radiation*

A pyranometer should be securely attached to whatever mounting stand is available, using the holes provided in the tripod legs or in the baseplate. Precautions should always be taken to avoid subjecting the instrument to mechanical shocks or vibration during installation. This operation is best effected as follows. First, the pyranometer should be oriented so that the emerging leads or the connector are located poleward of the receiving surface. This minimizes heating of the electrical connections by the sun. Instruments with Moll-Gorcynski thermopiles should be oriented so that the line of thermo-junctions (the long side of the rectangular thermopile) points east-west. This constraint sometimes conflicts with the first, depending on the type of

instrument, and should have priority since the connector could be shaded, if necessary. When towers are nearby, the instrument should be situated on the side of the tower towards the Equator, and as far away from the tower as practical.

Radiation reflected from the ground or the base should not be allowed to irradiate the instrument body from underneath. A cylindrical shading device can be used, but care should be taken to ensure that natural ventilation still occurs and is sufficient to maintain the instrument body at ambient temperature.

The pyranometer should then be secured lightly with screws or bolts and levelled with the aid of the levelling screws and spirit-level provided. After this, the retaining screws should be tightened, taking care that the setting is not disturbed so that, when properly exposed, the receiving surface is horizontal, as indicated by the spirit-level.

The stand or platform should be sufficiently rigid so that the instrument is protected from severe shocks and the horizontal position of the receiver surface is not changed, especially during periods of high winds and strong solar energy.

The cable connecting the pyranometer to its recorder should have twin conductors and be waterproof. The cable should be firmly secured to the mounting stand to minimize rupture or intermittent disconnection in windy weather. Wherever possible, the cable should be properly buried and protected underground if the recorder is located at a distance. The use of shielded cable is recommended; the pyranometer, cable and recorder being connected by a very low resistance conductor to a common ground. As with other types of thermo-electric devices, care must be exercised to obtain a permanent copper-to-copper junction between all connections prior to soldering. All exposed junctions must be weatherproof and protected from physical damage. After identification of the circuit polarity, the other extremity of the cable may be connected to the data-collection system in accordance with the relevant instructions.

7.3.3.3   *Installation of pyranometers for measuring diffuse sky radiation*

For measuring or recording separate diffuse sky radiation, the direct solar radiation must be screened from the sensor by a shading device. Where continuous records are required, the pyranometer is usually shaded either by a small metal disc held in the sun's beam by a sun tracker, or by a shadow band mounted on a polar axis.

The first method entails the rotation of a slender arm synchronized with the sun's apparent motion. If tracking is based on sun-synchronous motors or solar almanacs, frequent inspection is essential to ensure proper operation and adjustment, since spurious records are otherwise difficult to detect. Sun trackers with sun-seeking systems minimize the likelihood of such problems. The second method involves frequent personal attention at the site and significant corrections to the record on account of the appreciable screening of diffuse sky radiation by the shading arrangement. Assumptions about the sky radiance distribution and band dimensions are required to correct for the band and increase the uncertainty of the derived diffuse sky radiation compared to that using a sun-seeking disc system. Annex 7.E provides details on the construction of a shading ring and the necessary corrections to be applied.

A significant error source for diffuse sky radiation data is the zero irradiance signal. In clear sky conditions the zero irradiance signal is the equivalent of 5 to 10 W m^{-2} depending on the pyranometer model, and could approach 15% of the diffuse sky irradiance. The *Baseline Surface Radiation Network (BSRN) Operations Manual* (WMO, 1998) provides methods to minimize the influence of the zero irradiance signal.

The installation of a diffuse sky pyranometer is similar to that of a pyranometer which measures global radiation. However, there is the complication of an equatorial mount or shadow-band stand. The distance to a neighbouring pyranometer should be sufficient to guarantee that the shading ring or disc never shadows it. This may be more important at high latitudes where the sun angle can be very low.

Since the diffuse sky radiation from a cloudless sky may be less than one tenth of the global radiation, careful attention should be given to the sensitivity of the recording system.

7.3.3.4   *Installation of pyranometers for measuring reflected radiation*

The height above the surface should be 1 to 2 m. In summer time, the ground should be covered by grass that is kept short. For regions with snow in winter, a mechanism should be available to adjust the height of the pyranometer in order to maintain a constant separation between the snow and the instrument. Although the mounting device is within the field of view of the instrument, it should be designed to cause less than 2% error in the measurement. Access to the pyranometer for levelling should be possible without disturbing the surface beneath, especially if it is snow.

7.3.3.5   *Maintenance of pyranometers*

Pyranometers in continuous operation should be inspected at least once a day and perhaps more frequently, for example when meteorological observations are being made. During these inspections, the glass dome of the instrument should be wiped clean and dry (care should be taken not to disturb routine measurements during the daytime). If frozen snow, glazed frost, hoar frost or rime is present, an attempt should be made to remove the deposit very gently (at least temporarily), with the sparing use of a de-icing fluid, before wiping the glass clean. A daily check should also ensure that the instrument is level, that there is no condensation inside the dome, and that the sensing surfaces are still black.

In some networks, the exposed dome of the pyranometer is ventilated continuously by a blower to avoid or minimize deposits in cold weather, and to minimize the temperature difference between the dome and the case. The temperature difference between the ventilating air and the ambient air should not be more than about 1 K. If local pollution or sand forms a deposit on the dome, it should be wiped very gently, preferably after blowing off most of the loose material or after wetting it a little, in order to prevent the surface from being scratched. Such abrasive action can appreciably alter the original transmission properties of the material. Desiccators should be kept charged with active material (usually a colour-indicating silica gel).

7.3.3.6   *Installation and maintenance of pyranometers on special platforms*

Very special care should be taken when installing equipment on such diverse platforms as ships, buoys, towers and aircraft. Radiation sensors mounted on ships should be provided with gimbals because of the substantial motion of the platform.

If a tower is employed exclusively for radiation equipment, it may be capped by a rigid platform on which the sensors can be mounted. Obstructions to the horizon should be kept to the side of the platform farthest from the Equator, and booms for holding albedometers should extend towards the Equator.

Radiation sensors should be mounted as high as is practicable above the water surface on ships, buoys and towers, in order to keep the effects of water spray to a minimum.

Radiation measurements have been taken successfully from aircraft for a number of years. Care must be exercised, however, in selecting the correct pyranometer and proper exposure.

Particular attention must be paid during installation, especially for systems that are difficult to access, to ensure the reliability of the observations. It may be desirable, therefore, to provide a certain amount of redundancy by installing duplicate measuring systems at certain critical sites.

7.4 MEASUREMENT OF TOTAL AND LONG-WAVE RADIATION

The measurement of total radiation includes both short wavelengths of solar origin (300 to 3 000 nm) and longer wavelengths of terrestrial and atmospheric origin (3 000 to 100 000 nm). The instruments used for this purpose are pyrradiometers. They may be used for measuring either upward or downward radiation flux components, and a pair of them may be used to measure the differences between the two, which is the net radiation. Single-sensor pyrradiometers, with an active surface on both sides, are also used for measuring net radiation. Pyrradiometer sensors must have a constant sensitivity across the whole wavelength range from 300 to 100 000 nm.

The measurement of long-wave radiation can be accomplished either directly using pyrgeometers, or indirectly by subtracting the measured global radiation from the total radiation measured. Most pyrgeometers eliminate the short wavelengths by means of filters which have approximately constant transparency to long wavelengths while being almost opaque to the shorter wavelengths (300 to 3 000 nm). Some pyrgeometers – either without filters or filters that do not eliminate radiation below 3 000 nm – can be used only during the night.

The long-wave flux L^- measured by a pyrgeometer or a pyrradiometer has two components, the black-body flux from the surface temperature of the sensing element and the net radiative flux measured by the receiver:

$$L^- = L^* + \sigma T_s^4 \tag{7.11}$$

σ is the Stefan-Boltzmann constant (5.670 4 · 10^{-8} W m^{-2} K^{-1}); T_s is the underlying surface temperature (K); L^- is the irradiance measured either by a reference pyrgeometer or calculated from the temperature of the black-body cavity capping the upper receiver (W m^{-2}); L^* is the net radiative flux at the receiver (W m^{-2}). Measuring the short-wave component measured by a pyrradiometer follows the description in 7.3.

7.4.1 Instruments for the measurement of long-wave radiation

Over the last decade, significant advances have been made in the measurement of terrestrial radiation by pyrgeometers particularly with the advent of the silicon domed pyrgeometer, and as a result pyrgeometers provide the highest accuracy measurements of terrestrial radiation. Nevertheless, the measurement of terrestrial radiation is still more difficult and less understood than the measurement of solar irradiance, Table 7.5 provides an analysis of the sources of errors.

Pyrgeometers have developed in two forms. In the first form, the thermopile receiving surface is covered with a hemispheric dome inside which an interference filter is deposited. In the second form, the thermopile is covered with a flat plate on which the interference filter is deposited. In both cases, the surface on which the interference filter is deposited is made of silicon. The first style of instrument provides a full hemispheric field of view, while for the second a 150° field of view is typical and the hemispheric flux is modelled using the manufacturer's procedures. The argument used for the latter method is that the deposition of filters on the inside of a hemisphere has greater imprecision than the modelling of the flux below 30° elevations. Both types of instruments are operated on the principle that the measured output signal is the difference between the irradiance emitted from the source and the black-body radiative temperature of the instrument. In general, pyrgeometer derived terrestrial radiation can be approximated by a modification to equation 7.11:

$$L^- = L^* + k_2 \sigma T_s^4 + k_3 \sigma \left(T_d^4 - T_s^4 \right) \tag{7.12}$$

where k_2 takes into account the emission properties of the thermopile and uncertainties of the temperature measurement of the cold surface of the thermopile; k_3 is the instrument dome sensitivity to infrared irradiance (μV/(W m^{-2})); and T_d is the detector temperature (K).

The net radiative flux measured by the receiver, L^*, is defined as:

$$L^* = U/C \left(1 + k_1 \sigma T_s^4 \right) \tag{7.13}$$

where C is the sensitivity of the receiver ($\mu V/(W\ m^{-2})$), and k_1 is a residual temperature coefficient of the receiver. While state-of-the-art pyrgeometers have a temperature correction circuitry implemented in their receiver to bring k_1 very close to zero (as described in section 7.3.2.2), it is still recommended to determine k_1 by a laboratory characterization as described in section 7.4.3.

Several recent comparisons have been made using instruments of similar manufacture in a variety of measurement configurations. These studies have indicated that, following careful calibration, fluxes measured at night agree to within ±1 W m^{-2}, but in periods of high solar energy the difference between unshaded instruments can be significant. The reason for the differences is that the silicon dome and the associated interference filter may transmit solar radiation and is not a perfect reflector of solar energy. Thus, a solar contribution may reach the sensor and solar heating of the dome occurs. By shading the instrument similarly to that used for diffuse solar measurements, ventilating it as recommended by ISO (1990*a*), and measuring the temperature of the dome and the instrument case, this discrepancy can be reduced to ±2 W m^{-2}. Based upon these and other comparisons, the following recommendations should be followed for the measurement of long-wave radiation:

(a)   When using pyrgeometers that have a built-in battery circuit to emulate the black-body condition of the instrument, extreme care must be taken to ensure that the battery is well maintained. Even a small change in the battery voltage will significantly increase the measurement error. If at all possible, the battery should be removed from the instrument, and the case and dome temperatures of the instrument should be measured according to the manufacturer's instructions;

(b)   Where possible, both the case and dome temperatures of the instrument should be measured and used in the determination of irradiance;

(c)   The instrument should be ventilated;

(d)   For best results, the instrument should be shaded from direct solar irradiance by a small sun-tracking disc as used for diffuse sky radiation measurement.

These instruments should be calibrated at national or regional calibration centres by using reference pyrgeometers traceable to the World Infrared Standard Group of Pyrgeometers (WISG) of the WRC Davos.

7.4.2   Instruments for the measurement of total radiation

One problem with instruments for measuring total radiation is that there are no absorbers which have a completely constant sensitivity over the extended range of wavelengths concerned. Similarly, it is difficult to find suitable filters that have constant transmission between 300 and 100 000 nm. Therefore, the recommended practice for measuring total radiation is to perform simultaneous separate measurements of short- and long-wave radiation using a pyranometer and a pyrgeometer, respectively.

The use of thermally sensitive sensors requires a good knowledge of the heat budget of the sensor. Otherwise, it is necessary to reduce sensor convective heat losses to near zero by protecting the sensor from the direct influence of the wind. The technical difficulties linked with such heat losses are largely responsible for the fact that net radiative fluxes are determined less precisely than global radiation fluxes. In fact, different laboratories have developed their own pyrradiometers on technical bases which they consider to be the most effective for reducing the convective heat transfer in the sensor. During the last few decades, pyrradiometers have been built which, although not perfect, embody good measurement principles. Thus, there is a great variety of pyrradiometers employing different methods for eliminating, or allowing for, wind effects, as follows:

(a)   No protection, in which case empirical formulae are used to correct for wind effects;

(b)   Determination of wind effects by the use of electrical heating;

(c)   Stabilization of wind effects through artificial ventilation;

(d)   Elimination of wind effects by protecting the sensor from the wind.

The long-wave component of a pyrradiometer is described in equation 7.11.

Table 7.5 provides an analysis of the sources of error arising in pyrradiometric measurements and proposes methods for determining these errors.

Table 7.5. Sources of error in pyrradiometric measurements

Elements influencing the measurements	Nature of influence on pyrradiometers		Effects on the precision of measurements	Methods for determining these characteristics
	with domes	without domes		
Screening properties	Spectral characteristics of transmission	None	(a) Spectral variations in calibration coefficient (b) The effect of reduced incident radiation on the detector due to short-wave diffusion in the domes (depends on thickness) (c) Ageing and other variations in the sensors	(a) Determine spectrally the extinction in the screen (b) Measure the effect of diffuse sky radiation or measure the effect with a varying angle of incidence (c) Spectral analysis: compare with a new dome; determine the extinction of the dome
Convection effects	Changes due to non-radiative energy exchanges: sensor-dome environment (thermal resistance)	Changes due to non-radiative energy exchanges: sensor-air (variation in areal exchange coefficient)	Uncontrolled changes due to wind gusts are critical in computing the radiative flux divergence in the lowest layer of the atmosphere	Study the dynamic behaviour of the instrument as a function of temperature and speed in a wind tunnel
Effects of hydrometeors (rain, snow, fog, dew, frost) and dust	Variation of the spectral transmission plus the non-radiative heat exchange by conduction and change	Variation of the spectral character of the sensor and of the dissipation of heat by evaporation	Changes due to variations in the spectral characteristics of the sensor and to non-radiative energy transfers	Study the influence of forced ventilation on the effects
Properties of the sensor surface (emissivity)	Depends on the spectral absorption of the blackening substance on the sensor		Changes in calibration coefficient (a) As a function of spectral response (b) As a function of intensity and azimuth of incident radiation (c) As a function of temperature effects	(a) Spectrophoto-metric analysis of the calibration of the absorbing surfaces (b) Measure the sensor's sensitivity variability with the angle of incidence

Elements influencing the measurements	Nature of influence on pyrradiometers		Effects on the precision of measurements	Methods for determining these characteristics
	with domes	without domes		
Temperature effects	Non-linearity of the sensor as a function of temperature		A temperature coefficient is required	Study the influence of forced ventilation on these effects
Asymmetry effects	(a) Differences between the thermal capacities and resistance of the upward- and downward-facing sensors (b) Differences in ventilation of the upward- and downward-facing sensors (c) Control and regulation of sensor levelling		(a) Influence on the time constant of the instrument (b) Error in the determination of the calibration factors for the two sensors	(a) Control the thermal capacity of the two sensor surfaces (b) Control the time constant over a narrow temperature range

It is difficult to determine the uncertainty likely to be obtained in practice. In situ comparisons at different sites between different designs of pyrradiometer yield results manifesting differences of up to 5% to 10% under the best conditions. In order to improve such results, an exhaustive laboratory study should precede the in situ comparison in order to determine the different effects separately.

Deriving total radiation by independently measuring the short-wave and long-wave components achieves the highest accuracies and is recommended over the pyrradiometer measurements. Short-wave radiation can be measured using the methods outlined in 7.2 and 7.3, while long-wave radiation can be measured with pyrgeometers.

Table 7.6 lists the characteristics of pyrradiometers of various levels of performance, and the uncertainties to be expected in the measurements obtained from them.

7.4.3   Calibration of pyrgeometers

Pyrradiometers and net pyrradiometers can be calibrated for short-wave radiation using the same methods as those used for pyranometers (see section 7.3.1) using the sun and sky as the source. In the case of one-sensor net pyrradiometers, the downward-looking side must be covered by a cavity of known and steady temperature.

Table 7.6. Characteristics of operational pyrradiometers

Characteristic	High quality[a]	Good quality[b]	Moderate quality[c]
Resolution (W m^{-2})	1	5	10
Stability (annual change; % of full scale)	2%	5%	10%
Cosine response error at 10° elevation	3%	7%	15%
Azimuth error at 10° elevation (additional to cosine error) (deviation from mean)	3%	5%	10%
Temperature dependence (–20 °C to 40 °C) (deviation from mean)	1%	2%	5%
Non-linearity (deviation from mean)	0.5%	2%	5%
Variation in spectral sensitivity integrated over 200 nm intervals from 300 to 75 000 nm	2%	5%	10%

Notes:
a   Near state of the art; maintainable only at stations with special facilities and specialist staff.
b   Acceptable for network operations.
c   Suitable for low-cost networks where moderate to low performance.

Long-wave radiation calibration of reference radiometers is best done in the laboratory with black-body cavities, but night-time comparison to reference instruments is preferred for network measurements. In the case of calibration of the sensor the downward flux L^- is measured separately by using a pyrgeometer or provided by a black-body cavity. In which case, signal V from the net radiative flux received by the instrument (via equation 7.11) amounts to:

$$V = L^* \cdot K \text{ or } K = V/L^* \tag{7.14}$$

where V is the output of the instrument (μV); and K is sensitivity ($\mu V/(W\ m^{-2})$).

The instrument sensitivities should be checked periodically in situ by careful selection of well-described environmental conditions with slowly varying fluxes. Pyrgeometers should also be checked periodically to ensure that the transmission of short-wave radiation has not changed.

The symmetry of net pyrradiometers requires regular checking. This is done by inverting the instrument, or the pair of instruments, in situ and noting any difference in output. Differences of greater than 2% of the likely full scale between the two directions demand instrument recalibration because either the ventilation rates or absorption factors have become significantly different for the two sensors. Such tests should also be carried out during calibration or installation.

7.4.4 Installation of pyrradiometers and pyrgeometers

Pyrradiometers and pyrgeometers are generally installed at a site which is free from obstructions, or at least has no obstruction with an angular size greater than 5° in any direction, and which has a low sun angle at all times during the year.

A daily check of the instruments should ensure that:

(a) The instrument is level;

(b) Each sensor and its protection devices are kept clean and free from dew, frost, snow and rain;

(c) The domes do not retain water (any internal condensation should be dried up);

(d) The black receiver surfaces have emissivities very close to 1.

Since it is not generally possible to directly measure the reflected solar radiation and the upward long-wave radiation exactly at the surface level, it is necessary to place the pyrradiometers, or pyranometers and pyrgeometers at a suitable distance from the ground to measure these upward components. Such measurements integrate the radiation emitted by the surface beneath the sensor. For those instruments which have an angle of view of 2π sr and are installed 2 m above the surface, 90% of all the radiation measured is emitted by a circular surface underneath having a diameter of 12 m (this figure is 95% for a diameter of 17.5 m and 99% for one of 39.8 m), assuming that the sensor uses a cosine detector.

This characteristic of integrating the input over a relatively large circular surface is advantageous when the terrain has large local variations in emittance, provided that the net pyrradiometer can be installed far enough from the surface to achieve a field of view which is representative of the local terrain. The output of a sensor located too close to the surface will show large effects caused by its own shadow, in addition to the observation of an unrepresentative portion of the terrain. On the other hand, the readings from a net pyrradiometer located too far from the surface can be rendered unrepresentative of the fluxes near that surface because of the existence of undetected radiative flux divergences. Usually a height of 2 m above short homogeneous vegetation is adopted, while in the case of tall vegetation, such as a forest, the height should be sufficient to eliminate local surface heterogeneities adequately.

7.4.5 Recording and data reduction

In general, the text in section 7.1.3 applies to pyrradiometers and pyrgeometers. Furthermore, the following effects can specifically influence the readings of these radiometers, and they should be recorded:

(a) The effect of hydrometeors on non-protected and non-ventilated instruments (rain, snow, dew, frost);

(b) The effect of wind and air temperature;

(c) The drift of zero of the data system. This is much more important for pyrradiometers, which can yield negative values, than for pyranometers, where the zero irradiance signal is itself a property of the net irradiance at the sensor surface.

Special attention should be paid to the position of instruments if the derived long-wave radiation requires subtraction of the solar irradiance component measured by a pyranometer; the pyrradiometer and pyranometer should be positioned within 5 m of each other and in such a way that they are essentially influenced in the same way by their environment.

7.5 MEASUREMENT OF SPECIAL RADIATION QUANTITIES

7.5.1 Measurement of daylight

Illuminance is the incident flux of radiant energy that emanates from a source with wavelengths between 380 and 780 nm and is weighted by the response of the human eye to energy in this wavelength region. The CIE has defined the response of the human eye to photons with a peak responsivity at 555 nm. Figure 7.2 and Table 7.7 provide the relative response of the human eye normalized to this frequency. Luminous efficacy is defined as the relationship between radiant emittance (W m^{-2}) and luminous emittance (lm). It is a function of the relative luminous sensitivity $V(\lambda)$ of the human eye and a normalizing factor K_m (683) describing the number of lumens emitted per watt of electromagnetic radiation from a monochromatic source of 555.19 nm (the freezing point of platinum), as follows:

$$\Phi_v = K_m \int_{380}^{780} \Phi(\lambda) V(\lambda) d\lambda \qquad (7.15)$$

where Φ_v is the luminous flux (lm m^{-2} or lx); $\Phi(\lambda)$ is the spectral radiant flux (W m^{-2} nm^{-1}); $V(\lambda)$ is the sensitivity of the human eye; and K_m is the normalizing constant relating luminous to radiation quantities. Thus, 99% of the visible radiation lies between 400 and 730 nm.
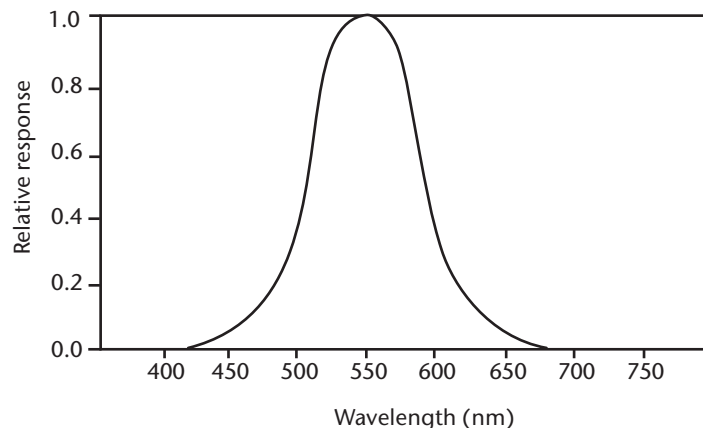
Figure 7.2. Relative luminous sensitivity $V(\lambda)$ of the human eye for photopic vision

**Table 7.7. Photopic spectral luminous efficiency values
(unity at wavelength of maximum efficacy)**

Wavelength (nm)	Photopic V(λ)	Wavelength (nm)	Photopic V(λ)
380	0.000 04	590	0.757
390	0.000 12	600	0.631
400	0.000 4	610	0.503
410	0.001 2	620	0.381
420	0.004 0	630	0.265
430	0.011 6	640	0.175
440	0.023	650	0.107
450	0.038	660	0.061
460	0.060	670	0.032
470	0.091	680	0.017
480	0.139	690	0.008 2
490	0.208	700	0.004 1
500	0.323	710	0.002 1
510	0.503	720	0.001 05
520	0.710	730	0.000 52
530	0.862	740	0.000 25
540	0.954	750	0.000 12
550	0.995	760	0.000 06
560	0.995	770	0.000 03
570	0.952	780	0.000 015
580	0.870		

Quantities and units for luminous variables are given in Annex 7.A.

7.5.1.1   *Instruments*

Illuminance meters comprise a photovoltaic detector, one or more filters to yield sensitivity according to the $V(\lambda)$ curve, and often a temperature control circuit to maintain signal stability. The CIE has developed a detailed guide to the measurement of daylight (CIE, 1994) which describes expected practices in the installation of equipment, instrument characterization, data-acquisition procedures and initial quality control.

The measurement of global illuminance parallels the measurement of global irradiance. However, the standard illuminance meter must be temperature controlled or corrected from at least –10 °C to 40 °C. Furthermore, it must be ventilated to prevent condensation and/or frost from coating the outer surface of the sensing element. Illuminance meters should normally be able to measure fluxes over the range 1 to 20 000 lx. Within this range, uncertainties should remain within the limits of Table 7.8. These values are based upon CIE recommendations (CIE, 1987), but only for uncertainties associated with high-quality illuminance meters specifically intended for external daylight measurements.

Table 7.8. Specification of illuminance meters

Specification	Uncertainty percentage
$V(\lambda)$ match	2.5
UV response	0.2
IR response	0.2
Cosine response	1.5
Fatigue at 10 klx	0.1
Temperature coefficient	0.1 K^{-1}
Linearity	0.2
Settling time	0.1 s

Diffuse sky illuminance can be measured following the same principles used for the measurement of diffuse sky irradiance. Direct illuminance measurements should be taken with instruments having a field of view whose open half-angle is no greater than 2.85° and whose slope angle is less than 1.76°.

7.5.1.2   *Calibration*

Calibrations should be traceable to a Standard Illuminant A following the procedures outlined in CIE (1987). Such equipment is normally available only at national standards laboratories. The calibration and tests of specification should be performed yearly. These should also include tests to determine ageing, zero setting drift, mechanical stability and climatic stability. It is also recommended that a field standard be used to check calibrations at each measurement site between laboratory calibrations.

7.5.1.3   *Recording and data reduction*

The CIE has recommended that the following climatological variables be recorded:

(a)   Global and diffuse sky daylight illuminance on horizontal and vertical surfaces;

(b)   Illuminance of the direct solar beam;

(c)   Sky luminance for 0.08 sr intervals (about 10° · 10°) all over the hemisphere;

(d)   Photopic albedo of characteristic surfaces such as grass, earth and snow.

Hourly or daily integrated values are usually needed. The hourly values should be referenced to true solar time. For the presentation of sky luminance data, stereographic maps depicting isolines of equal luminance are most useful.

7.6   **MEASUREMENT OF UV RADIATION**

Measurements of solar UV radiation are in demand because of its effects on the environment and human health, and because of the enhancement of radiation at the Earth's surface as a result of ozone depletion (Kerr and McElroy, 1993) and changes in other parameters like clouds and aerosols. The UV spectrum is conventionally divided into three parts, as follows:

(a)   UV-A is the band with wavelengths of 315 to 400 nm, namely, just outside the visible spectrum. It is usually[2] less biologically active, and its intensity at the Earth's surface does not vary significantly with atmospheric ozone content;

(b)   UV-B is defined as radiation in the 280 to 315 nm band. It is biologically active and its intensity at the Earth's surface depends on the atmospheric ozone column, depending on wavelength. A frequently used expression of its biological activity is its erythemal effect, which is the extent to which it causes the reddening of human skin;

(c)   UV-C, in wavelengths of 100 to 280 nm, is completely absorbed in the atmosphere and does not occur naturally at the Earth's surface.

UV-B is the band on which most interest is centred for measurements of UV radiation. An alternative, but now non-standard, definition of the boundary between UV-A and UV-B is 320 nm rather than 315 nm.

Measuring UV radiation is difficult because of the small amount of energy reaching the Earth's surface, the variability due to changes in stratospheric ozone levels, and the rapid increase in the magnitude of the flux with increasing wavelength. Figure 7.3 illustrates changes in the spectral irradiance between 290 and 325 nm at the top of the atmosphere and at the surface in $W\ m^{-2}\ nm^{-1}$. Global UV irradiance is strongly affected by atmospheric phenomena such as clouds, and to a lesser extent by atmospheric aerosols.

The influence of surrounding surfaces is also significant because of multiple scattering. This is especially the case in snow-covered areas.

Difficulties in the standardization of UV radiation measurement stem from the variety of uses to which the measurements are put (WMO, 2003, 2011). Unlike most meteorological measurements, standards based upon global needs have not yet been reached. In many countries, measurements of UV radiation are not taken by Meteorological Services, but by health or environmental protection authorities. This leads to further difficulties in the standardization of instruments and methods of observation. Standards are necessary for compatible observations, quality assurance and quality control of measurements, and data archiving, as well as for connecting measurements with the user communities (WMO, 2003).
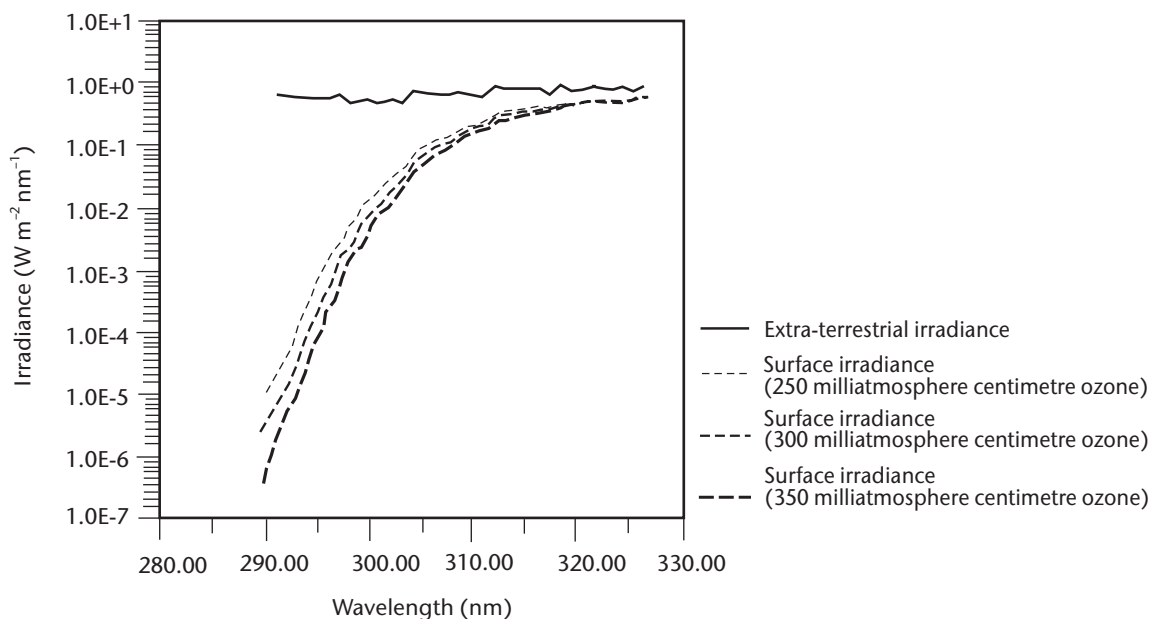
Figure 7.3. Model results illustrating the effect of increasing ozone levels on the transmission of UV-B radiation through the atmosphere

---

[2]   The phytoplankton photosynthesis action spectrum, for example, has an important component in the UV-A.

Guidelines and standard procedures have been developed on how to characterize and calibrate UV broadband instruments, spectroradiometers and filter radiometers used to measure solar UV irradiance (see WMO, 1996, 1999*a*, 1999*b*, 2001, 2008, 2010*a*). Although not available commercially yet, guides and standard procedures have also been developed for array spectroradiometers (WMO, 2010*b*). Application of the recommended procedures for data quality assurance performed at sites operating instruments for solar UV radiation measurements will ensure a valuable UV radiation database. This is needed to derive a climatology of solar UV irradiance in space and time for studies of the Earth's climate. Recommendations for measuring sites and instrument specifications are also provided in these documents. Requirements for UV-B measurements were put forward in the WMO GAW Programme (WMO, 1993, 2001, 2003, 2010*a*, 2010*b*, 2011). For UV-B global spectral irradiance, requirements depend on the objective. Specifications for less demanding objectives are reproduced in Table 7.9 (WMO, 2001).

The following instrument descriptions are provided for general information and for assistance in selecting appropriate instrumentation.

7.6.1   **Instruments**

Three general types of instruments are available commercially for the measurement of UV radiation. The first class of instruments use broadband filters. These instruments integrate over either the UV-B or UV-A spectrum or the entire broadband UV region responsible for affecting human health. The second class of instruments use one or more interference filters to integrate over discrete portions of the UV-A and/or UV-B spectrum. The third class of instruments are spectroradiometers that measure across a pre-defined portion of the spectrum sequentially, or simultaneously, using a fixed passband.

7.6.1.1   *Broadband sensors*

Most, but not all, broadband sensors are designed to measure a UV spectrum that is weighted by the erythemal function proposed by McKinlay and Diffey (1987) and reproduced in Figure 7.4. Another action spectrum found in some instruments is that of Parrish et al. (1982). Two methods (and their variations) are used to accomplish this hardware weighting.

One of the means of obtaining erythemal weighting is to first filter out nearly all visible wavelength light using UV-transmitting, black-glass blocking filters. The remaining radiation then strikes a UV-sensitive phosphor. In turn, the green light emitted by the phosphor is filtered again by using coloured glass to remove any non-green visible light before impinging on a gallium arsenic or a gallium arsenic phosphorus photodiode. The quality of the instrument is dependent on such items as the quality of the outside protective quartz dome, the cosine response of the instrument, the temperature stability, and the ability of the manufacturer to match the erythemal curve with a combination of glass and diode characteristics. Instrument temperature stability is crucial, both with respect to the electronics and the response of the phosphor to incident UV radiation. Phosphor efficiency decreases by approximately 0.5% K^{-1} and its wavelength response curve is shifted by approximately 1 nm longer every 10 K. This latter effect is particularly important because of the steepness of the radiation curve at these wavelengths.

More recently, instruments have been developed to measure erythemally weighted UV irradiance using thin film metal interference filter technology and specially developed silicon photodiodes. These overcome many problems associated with phosphor technology, but must contend with very low photodiode signal levels and filter stability.

Other broadband instruments use one or the other measurement technology to measure the complete spectra by using either a combination of glass filters or interference filters. The bandpass is as narrow as 20 nm full-width half-maximum (FWHM) to as wide as 80 nm FWHM for instruments measuring a combination of UV-A and UV-B radiation. Some manufacturers of these instruments provide simple algorithms to approximate erythemal dosage from the unweighted measurements.

Table 7.9. GAW Programme requirements for UV-B global spectral irradiance measurements

Characteristic	Requirements
Cosine error[a]	(a) < ±10% for incidence angles < 60° (b) < ±10% for integrated isotropic radiance
Minimum spectral range	290–325 nm[b]
Bandwidth (FWHM)	< 1 nm
Wavelength precision	< ±0.05 nm
Wavelength accuracy	< ±0.1 nm
Slit function	< 10^{-3} of maximum at 2.5 FWHM away from centre
Sampling wavelength interval	< FWHM
Maximum irradiance	> 1 W m^{-2} nm^{-1} at 325 nm and, if applicable, 2 W m^{-2} nm^{-1} at 400 nm (noon maximum)
Detection threshold	< 5 · 10^{-5} W m^{-2} nm^{-1} (for signal-to-noise ratio (SNR) = 1 at 1 nm FWHM)
Stray light	< 5 · 10^{-4} W m^{-2} nm^{-1} when the instrument is exposed to the sun at minimum solar zenith angle
Instrument temperature	Monitored and sufficiently stable to maintain overall instrument stability
Scanning duration	< 10 min per spectrum, e.g. for ease of comparison with models
Overall calibration uncertainty[c]	< ±10% (unless limited by detection threshold)
Scan date and time	Recorded with each spectrum such that timing is known to within 10 s at each wavelength
Ancillary measurements required	Direct normal spectral irradiance or diffuse spectral irradiance Total ozone column, e.g. derived from measurements of direct normal spectral irradiance Erythemally weighted irradiance, measured with a broadband radiometer Atmospheric pressure Cloud amount Illuminance, measured with a luxmeter Direct irradiance at normal incidence measured with a pyrheliometer Visibility
Data frequency	At least one scan per hour and additionally a scan at local solar noon

Notes:
a   Smaller cosine errors would be desirable, but are unrealistic for the majority of the instruments that are currently in use.
b   The overall calibration uncertainty is expressed at 95% confidence level and includes all uncertainties associated with the irradiance calibration (for example, uncertainty of the standard lamps, transfer uncertainties, alignment errors during calibration, and drift of the instrument between calibrations). For more details, see Bernhard and Seckmeyer (1999), Cordero et al. (2008), and Cordero et al. (2013).
c   An extension to longer wavelengths is desirable for the establishment of a UV climatology with respect to biological applications, see WMO (2001, 2010*b*).

The basic maintenance of these instruments consists of ensuring that the domes are cleaned, the instrument is levelled, the desiccant (if provided) is active, and the heating/cooling system is working correctly, if so equipped. Quality control and quality assurance as well as detailed maintenance should be done by well-experienced staff.
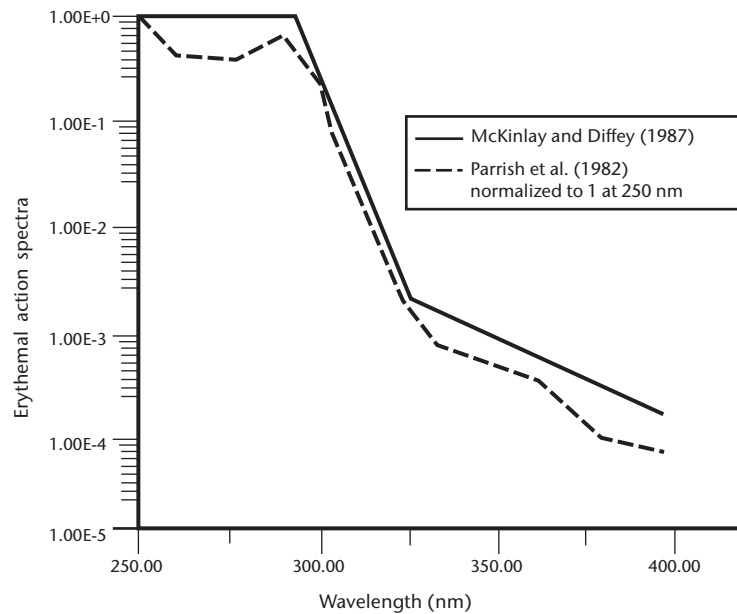
Figure 7.4. Erythemal curves

Source: Parrish et al. (1982) and McKinlay and Diffey (1987)

7.6.1.2 *Narrowband sensors*

The definition of narrowband for this classification of instrument is vague. The widest bandwidth for instruments in this category is 10 nm FWHM. The narrowest bandwidth at present for commercial instruments is of the order of 2 nm FWHM (WMO, 2010*a*).

These sensors use one or more interference filters to obtain information about a portion of the UV spectra. The simplest instruments consist of a single filter, usually at a wavelength that can be measured by a good-quality, UV enhanced photodiode, although more than one filter is desirable. Specifications required for this type of instrument (WMO, 2010*a*) are given in Table 7.10. Wavelengths near 305 nm are typical for such instruments. The out-of-band rejection of such filters should be equal to, or greater than, 10^{-6} throughout the sensitive region of the detector. Higher quality instruments of this type either use Peltier cooling to maintain a constant temperature near 20 °C or heaters to increase the instrument filter and diode temperatures to above normal ambient temperatures, usually 40 °C. However, the latter alternative markedly reduces the life of interference filters. A modification of this type of instrument uses a photomultiplier tube instead of the photodiode. This allows the accurate measurement of energy from shorter wavelengths and lower intensities at all measured wavelengths.

Manufacturers of instruments that use more than a single filter often provide a means of reconstructing the complete UV spectrum and determining biologically effective doses for a variety of action spectra, the total column ozone amount and cloud attenuation, through modelled relationships developed around the measured wavelengths (WMO, 2010*a*). Single wavelength instruments are used similarly to supplement the temporal and spatial resolution of more sophisticated spectrometer networks or for long-term accurate monitoring of specific bands to detect trends in the radiation environment.

The construction of the instruments must be such that the radiation passes through the filter close to normal incidence so that wavelength shifting to shorter wavelengths is avoided. For example, a 10° departure from normal incidence may cause a wavelength shift of 1.5 nm, depending on the refractive index of the filter. The effect of temperature can also be significant in altering the central wavelength by about 0.012 nm K^{-1} on very narrow filters (< 1 nm).

Maintenance for simple one-filter instruments is similar to that of the broadband instruments. For instruments that have multiple filters in a moving wheel assembly, maintenance will include

Table 7.10. Requirements for UV-B global narrowband irradiance measurements

Characteristic	Requirements
Stray light including sensitivity to visible and infrared radiation	< 1% contribution to the signal of wavelengths outside 2.5 FWHM for a solar zenith angle less than 70°
Stability over time on timescales up to a year	Signal change: Currently in use: better than 5% Desired: 2%
Minimum number of channels	At least one channel with centre wavelength < 310 nm and at least one with centre wavelength > 330 nm
Maximum irradiance	Signal of the instruments must not saturate at radiation levels encountered on the Earth's surface
Detection threshold	SNR = 3 for irradiance at solar zenith angle of 80° and total ozone column of 300 Dobson units
Instrument temperature	Monitored and sufficiently stable to maintain overall instrument stability
Response time	< 1 s
Multiplexing time	< 1 s
Accuracy of time	Better than ±10 s
Sampling frequency	≤ 1 min
Levelling	< 0.2°
Calibration uncertainty	< 10% (unless limited by detection threshold)

determining whether or not the filter wheel is properly aligned. Regular testing of the high-voltage power supply for photomultiplier-equipped instruments and checking the quality of the filters are also recommended.

7.6.1.3   *Spectroradiometers*

The most sophisticated commercial instruments are those that use either ruled or holographic gratings to disperse the incident energy into a spectrum. The low energy of the UV radiation compared with that in the visible spectrum necessitates a strong out-of-band rejection. This is achieved by using a double monochromator or by blocking filters, which transmit only UV radiation, in conjunction with a single monochromator. A photomultiplier tube is most commonly used to measure the output from the monochromator (WMO, 2001). Some less expensive instruments use photodiode or charge-coupled detector arrays (WMO, 2010*b*), enabling the measurement of an entire spectral region of interest at the same time. These instruments are unable to measure energy in the shortest wavelengths of the UV-B radiation and generally have more problems associated with stray light.

Monitoring instruments are now available with several self-checking features. Electronic tests include checking the operation of the photomultiplier and the analogue to digital conversion. Tests to determine whether the optics of the instrument are functioning properly include testing the instrument by using internal mercury lamps and standard quartz halogen lamps. While these do not give absolute calibration data, they provide the operator with information on the stability of the instrument both with respect to spectral alignment and intensity.

Commercially available instruments are constructed to provide measurement capabilities from approximately 290 nm to the mid-visible wavelengths, depending upon the type of construction and configuration. The bandwidth of the measurements is usually between 0.5 and 2.0 nm. The time required to complete a full scan across the grating depends upon both the wavelength resolution and the total spectrum to be measured. Scan times to perform a spectral scan across

the UV region and part of the visible region (290 to 450 nm) with small wavelength steps range from less than 1 min per scan with modern fast scanning spectroradiometers to about 10 min for some types of conventional high-quality spectroradiometers.

For routine monitoring of UV radiation it is recommended that the instrument either be environmentally protected or developed in such a manner that the energy incident on a receiver is transmitted to a spectrometer housed in a controlled climate. In both cases, care must be taken in the development of optics so that uniform responsivity is maintained down to low solar elevations.

The maintenance of spectroradiometers designed for monitoring UV-B radiation requires well-trained on-site operators who will care for the instruments. It is crucial to follow the manufacturer's maintenance instructions because of the complexity of this instrument.

7.6.2　　**Calibration**

The calibration of all sensors in the UV-B is both very important and difficult. Guidelines on the calibration of UV spectroradiometers and UV filter radiometers have been given in WMO (1996, 1999*a*, 1999*b*, 2001, 2008, 2010*a*, 2010*b*) and in the relevant scientific literature. Spectroradiometers must be calibrated against standard lamps, which have to be traceable to national standards laboratories. Many countries do not have laboratories capable of characterizing lamps in the UV. In these countries, lamps are usually traceable to the National Institute of Standards and Technology in the United States or to the Physikalisch-Technische Bundesanstalt in Germany.

It is estimated that a 5% uncertainty in spot measurements at 300 nm can be achieved only under the most rigorous conditions at the present time. The uncertainty of measurements of daily totals is about the same, using best practice. Fast changes in cloud cover and/or cloud optical depths at the measuring site require fast spectral scans and small sampling time steps between subsequent spectral scans, in order to obtain representative daily totals of spectral UV irradiance. Measurements of erythemal irradiance would have uncertainties typically in the range 5% to 20%, depending on a number of factors, including the quality of the procedures and the equipment. The sources of error are discussed in the following paragraphs and include:

(a)　Uncertainties associated with standard lamps;

(b)　The stability of instruments, including the stability of the spectral filter and, in older instruments, temperature coefficients;

(c)　Cosine error effects;

(d)　The fact that the calibration of an instrument varies with wavelength, and that:

　　(i)　The spectrum of a standard lamp is not the same as the spectrum being measured;

　　(ii)　The spectrum of the UV-B irradiance being measured varies greatly with the solar zenith angle.

The use of standard lamps as calibration sources leads to large uncertainties at the shortest wavelengths, even if the transfer of the calibration is perfect. For example, at 350 nm the uncertainty associated with the standard irradiance is of the order of 1.3%; when transferred to a standard lamp, another 0.7% uncertainty is added. Uncertainties in calibration decrease with increasing wavelength. Consideration must also be given to the set-up and handling of standard lamps. Even variations as small as 1% in the current, for example, can lead to errors in the UV flux of 10% or more at the shortest wavelengths. Inaccurate distance measurements between the lamp and the instrument being calibrated can also lead to errors in the order of 1% as the inverse square law applies to the calibration. Webb et al. (1994) discuss various aspects of uncertainty as related to the use of standard lamps in the calibration of UV or visible spectroradiometers.

The problems associated with broadband instruments stem from: (a) the complex set of filters used to integrate the incoming radiation into the erythemal signal; and (b) the fact that the spectral nature of the atmosphere changes with air mass and ozone amount. Even if the characterization of the instrument by using calibrated lamp sources is perfect, the difference between the measured solar spectrum and the lamp spectrum affects the uncertainty of the final measurements. The use of high-output deuterium lamps, a double monochromator and careful filter selection will help in the characterization of these instruments, but the number of laboratories capable of calibrating these devices is extremely limited. Different calibration methods for broadband instruments are described in WMO (2008).

Trap detectors could potentially be used effectively for narrowband sensors, but have been used only in research projects to date. In recalibrating these instruments, whether they have a single filter or multiple filters, care must be taken to ensure that the spectral characteristics of the filters have not shifted over time. Different methods for calibrating narrowband sensors, as well as their advantages and disadvantages, are described in WMO (2010a).

Spectroradiometers should be calibrated in the same position as that in which the measurements are to be taken, as many spectroradiometers are adversely affected by changes in orientation. The calibration of a spectroradiometer should also include testing the accuracy of the wavelength positioning of the monochromator, checking for any changes in internal optical alignment and cleanliness, and an overall test of the electronics. The out-of-band rejection needs to be characterized, possibly by scanning a helium cadmium laser ($\lambda = 325$ nm), only once, as it usually does not change with time.

Most filter instrument manufacturers indicate a calibration frequency of once a year. Spectroradiometers should be calibrated at least twice a year and more frequently if they do not have the ability to perform self-checks on the photomultiplier output or the wavelength selection. In all cases, absolute calibrations of the instruments should be performed by qualified technicians at the sites on a regular time schedule. The sources used for calibration must guarantee that the calibration can be traced back to absolute radiation standards kept at national metrological institutes. If the results of quality assurance routines applied at the sites indicate a significant change in an instrument's performance or changes of its calibration level over time, an additional calibration may be needed in between two regular calibrations. All calibrations should be based on expertise and documentation available at the site and on the guidelines and procedures such as those published in WMO (1996, 1999a, 1999b, 2001, 2008, 2010a, 2010b). In addition to absolute calibrations of instruments, intercomparisons between the sources used for calibration, for example, calibration lamps, and the measuring instruments are useful to detect and remove inconsistencies or systematic differences between station instruments at different sites.

───────────

ANNEX 7.A. NOMENCLATURE OF RADIOMETRIC AND PHOTOMETRIC QUANTITIES

(1) Radiometric quantities

Name	Symbol	Unit	Relation	Remarks
Radiant energy	Q, (W)	J = W s	–	–
Radiant flux	Φ, (P)	W	$\Phi = \dfrac{dQ}{dt}$	Power
Radiant flux density	(M), (E)	W m^{-2}	$\dfrac{d\Phi}{dA} = \dfrac{d^2Q}{dA \cdot dt}$	Radiant flux of any origin crossing an area element
Radiant exitance	M	W m^{-2}	$M = \dfrac{d\Phi}{dA}$	Radiant flux of any origin emerging from an area element
Irradiance	E	W m^{-2}	$E = \dfrac{d\Phi}{dA}$	Radiant flux of any origin incident onto an area element
Radiance	L	W m^{-2} sr^{-1}	$L = \dfrac{d^2\Phi}{d\Omega \cdot dA \cdot \cos\theta}$	The radiance is a conservative quantity in an optical system
Radiant exposure	H	J m^{-2}	$H = \dfrac{dQ}{dA} = \displaystyle\int_{t_1}^{t_2} Edt$	May be used for daily sums of global radiation, etc.
Radiant intensity	I	W sr^{-1}	$I = \dfrac{d\Phi}{d\Omega}$	May be used only for radiation outgoing from "point sources"

(2) Photometric quantities

Name	Symbol	Unit
Quantity of light	Q_v	lm · s
Luminous flux	Φ_v	lm
Luminous exitance	M_v	lm m^{-2}
Illuminance	E_v	lm m^{-2} = lx
Light exposure	H_v	lm m^{-2} s = lx · s
Luminous intensity	I_v	lm sr^{-1} = cd
Luminance	L_v	lm m^{-2} s r^{-1} = cdm^{-2}
Luminous flux density	$(M_v ; E_v)$	lm m^{-2}

(3) Optical characteristics

Characteristic	Symbol	Definition	Remarks
Emissivity	ε	$\varepsilon = \dfrac{M_\varepsilon}{M_{\varepsilon=1}}$	$\varepsilon = 1$ for a black-body
Absorptance	α	$\alpha = \dfrac{\Phi_a}{\Phi_i}$	Φ_a and Φ_i are the absorbed and incident radiant flux, respectively
Reflectance	ρ	$\rho = \dfrac{\Phi_r}{\Phi_i}$	Φ_r is the reflected radiant flux
Transmittance	τ	$\tau = \dfrac{\Phi_t}{\Phi_i}$	Φ_t is the radiant flux transmitted through a layer or a surface
Optical depth	δ	$\tau = e^{-\delta}$	In the atmosphere, δ is defined in the vertical. Optical thickness equals $\delta/\cos\theta$, where θ is the apparent zenith angle

_____

ANNEX 7.B. METEOROLOGICAL RADIATION QUANTITIES, SYMBOLS AND DEFINITIONS

Quantity	Symbol	Relation	Definitions and remarks	Units
Downward radiation	$\Phi{\downarrow}$[a]	$\Phi{\downarrow} = \Phi_g{\downarrow} + \Phi_l{\downarrow}$	Downward radiant flux	W
	$Q{\downarrow}$	$Q{\downarrow} = Q_g{\downarrow} + Q_l{\downarrow}$	" radiant energy	J (W s)
	$M{\downarrow}$	$M{\downarrow} = M_g{\downarrow} + M_l{\downarrow}$	" radiant exitance[b]	W m^{-2}
	$E{\downarrow}$	$E{\downarrow} = E_g{\downarrow} + E_l{\downarrow}$	" irradiance	W m^{-2}
	$L{\downarrow}$	$L{\downarrow} = L_g{\downarrow} + L_l{\downarrow}$	" radiance	W m^{-2} sr^{-1}
	$H{\downarrow}$	$H{\downarrow} = H_g{\downarrow} + H_l{\downarrow}$ (g = global) (l = long wave)	" radiant exposure for a specified time interval	J m^{-2} per time interval
Upward radiation	$\Phi{\uparrow}$[a]	$\Phi{\uparrow} = \Phi_r{\uparrow} + \Phi_l{\uparrow}$	Upward radiant flux	W
	$Q{\uparrow}$	$Q{\uparrow} = Q_r{\uparrow} + Q_l{\uparrow}$	" radiant energy	J (W s)
	$M{\uparrow}$	$M{\uparrow} = M_r{\uparrow} + M_l{\uparrow}$	" radiant exitance	W m^{-2}
	$E{\uparrow}$	$E{\uparrow} = E_r{\uparrow} + E_l{\uparrow}$	" irradiance	W m^{-2}
	$L{\uparrow}$	$L{\uparrow} = L_r{\uparrow} + L_l{\uparrow}$	" radiance	W m^{-2} sr^{-1}
	$H{\uparrow}$	$H{\uparrow} = H_r{\uparrow} + H_l{\uparrow}$	" radiant energy per unit area for a specified time interval	J m^{-2} per time interval
Global radiation	$E_g{\downarrow}$	$E_g{\downarrow} = E \cos \theta_{\odot} + E_d{\downarrow}$	Hemispherical irradiance on a horizontal surface ($\theta_{\odot}$ = *apparent solar zenith angle*)[c]	W m^{-2}
Sky radiation: downward diffuse solar radiation	$\Phi_d{\downarrow}$ $Q_d{\downarrow}$ $M_d{\downarrow}$ $E_d{\downarrow}$ $L_d{\downarrow}$ $H_d{\downarrow}$		Subscript d = diffuse	As for downward radiation
Upward/downward long-wave radiation	$\Phi_l{\uparrow}$, $\Phi_l{\downarrow}$ $Q_l{\uparrow}$, $Q_l{\downarrow}$ $M_l{\uparrow}$, $M_l{\downarrow}$ $E_l{\uparrow}$, $E_l{\downarrow}$ $H_l{\uparrow}$, $H_l{\downarrow}$		Subscript l = long wave. If only atmospheric radiation is considered, the subscript a may be added, e.g., $\Phi_{l,a}{\uparrow}\sigma\sigma$	As for downward radiation

Quantity	Symbol	Relation	Definitions and remarks	Units
Reflected solar radiation	$\varPhi_r\uparrow$ $Q_r\uparrow$ $M_r\uparrow$ $E_r\uparrow$ $L_r\uparrow$ $H_r\uparrow$		Subscript r = reflected (the subscript s (specular) and d (diffuse) may be used, if a distinction is to be made between these two components)	As for downward radiation
Net radiation	$\varPhi^*$ Q^* M^* E^* L^* H^*	$\varPhi^* = \varPhi\downarrow - \varPhi\uparrow$ $Q^* = Q\downarrow - Q\uparrow$ $M^* = M\downarrow - M\uparrow$ $E^* = E\downarrow - E\uparrow$ $L^* = L\downarrow - L\uparrow$ $H^* = H\downarrow - H\uparrow$	The subscript g or l is to be added to each of the symbols if only short-wave or long-wave net radiation quantities are considered	As for downward radiation
Direct solar radiation	E	$E = E_0\tau$ $\tau = e^{-\delta/\cos\theta_\odot}$	τ = atmospheric transmittance δ = optical depth (vertical)	W m^{-2}
Solar constant	E_0		Solar irradiance, normalized to mean Sun–Earth distance	W m^{-2}

Notes:

a   The symbols – or + could be used instead of ↓ or ↑ (e.g., $\varPhi^+ = \varPhi\uparrow$).

b   Exitance is radiant flux emerging from the unit area; irradiance is radiant flux received per unit area. For flux density in general, the symbol M or E can be used. Although not specifically recommended, the symbol F, defined as $\varPhi$/area, may also be introduced.

c   In the case of inclined surfaces, $\theta_\odot$ is the angle between the normal to the surface and the direction to the sun.

ANNEX 7.C. SPECIFICATIONS FOR WORLD, REGIONAL AND NATIONAL RADIATION CENTRES

World Radiation Centres

The World Radiation Centres were designated by the Executive Committee at its thirtieth session in 1978 through Resolution 11 (EC-XXX) to serve as centres for the international calibration of meteorological radiation standards within the global network and to maintain the standard instruments for this purpose.

A World Radiation Centre shall fulfil the following requirements. It shall either:

(a) Possess and maintain a group of at least three stable absolute pyrheliometers, with a traceable 95% uncertainty of less than 1 W m^{-2} to the World Radiometric Reference, and in stable, clear sun conditions with direct irradiances above 700 W m^{-2}, 95% of any single measurements of direct solar irradiance will be expected to be within 4 W m^{-2} of the irradiance. The World Radiation Centre Davos is requested to maintain the World Standard Group for realization of the World Radiometric Reference;

(b) It shall undertake to train specialists in radiation;

(c) The staff of the centre should provide for continuity and include qualified scientists with wide experience in radiation;

(d) It shall take all steps necessary to ensure, at all times, the highest possible quality of its standards and testing equipment;

(e) It shall serve as a centre for the transfer of the World Radiometric Reference to the regional centres;

(f) It shall have the necessary laboratory and outdoor facilities for the simultaneous comparison of large numbers of instruments and for data reduction;

(g) It shall follow closely or initiate developments leading to improved standards and/or methods in meteorological radiometry;

(h) It shall be assessed by an international agency or by CIMO experts, at least every five years, to verify traceability of the direct solar radiation measurements;

or:

(a) Provide and maintain an archive for solar radiation data from all the Member States of WMO;

(b) The staff of the centre should provide for continuity and include qualified scientists with wide experience in radiation;

(c) It shall take all steps necessary to ensure, at all times, the highest possible quality of, and access to, its database;

(d) It shall be assessed by an international agency or by CIMO experts, at least every five years.

Regional Radiation Centres

A Regional Radiation Centre is a centre designated by a regional association to serve as a centre for intraregional comparisons of radiation instruments within the Region and to maintain the standard instrument necessary for this purpose.

A Regional Radiation Centre shall satisfy the following conditions before it is designated as such and shall continue to fulfil them after being designated:

(a)   It shall possess and maintain a standard group of at least three stable pyrheliometers, with a traceable 95% uncertainty of less than 1 W m^{-2} to the World Standard Group, and in stable, clear sun conditions with direct irradiances above 700 W m^{-2}, 95% of any single measurements of direct solar irradiance will be expected to be within 6 W m^{-2} of the irradiance;

(b)   One of the radiometers shall be compared through a WMO/CIMO sanctioned comparison, or calibrated, at least once every five years against the World Standard Group;

(c)   The standard radiometers shall be intercompared at least once a year to check the stability of the individual instruments. If the mean ratio, based on at least 100 measurements, and with a 95% uncertainty less than 0.1%, has changed by more than 0.2%, and if the erroneous instrument cannot be identified, a recalibration at one of the World Radiation Centres must be performed prior to further use as a standard;

(d)   It shall have, or have access to, the necessary facilities and laboratory equipment for checking and maintaining the accuracy of the auxiliary measuring equipment;

(e)   It shall provide the necessary outdoor facilities for simultaneous comparison of national standard radiometers from the Region;

(f)   The staff of the centre should provide for continuity and include a qualified scientist with wide experience in radiation;

(g)   It shall be assessed by a national or international agency or by CIMO experts, at least every five years, to verify traceability of the direct solar radiation measurements.

National Radiation Centres

A National Radiation Centre is a centre designated at the national level to serve as a centre for the calibration, standardization and checking of the instruments used in the national network of radiation stations and for maintaining the national standard instrument necessary for this purpose.

A National Radiation Centre shall satisfy the following requirements:

(a)   It shall possess and maintain at least two pyrheliometers for use as a national reference for the calibration of radiation instruments in the national network of radiation stations with a traceable 95% uncertainty of less than 4 W m^{-2} to the regional representation of the World Radiometric Reference, and in stable, clear sun conditions with direct irradiances above 700 W m^{-2}, 95% of any single measurements of direct solar irradiance will be expected to be within 20 W m^{-2} of the irradiance;

(b)   One of the national standard radiometers shall be compared with a regional standard at least once every five years;

(c)   The national standard radiometers shall be intercompared at least once a year to check the stability of the individual instruments. If the mean ratio, based on at least

100 measurements, and with a 95% uncertainty less than 0.2%, has changed by more than 0.6% and if the erroneous instrument cannot be identified, a recalibration at one of the Regional Radiation Centres must be performed prior to further use as a standard;

(d)   It shall have or, have access to, the necessary facilities and equipment for checking the performance of the instruments used in the national network;

(e)   The staff of the centre should provide for continuity and include a qualified scientist with experience in radiation.

National Radiation Centres shall be responsible for preparing and keeping up to date all necessary technical information for the operation and maintenance of the national network of radiation stations.

Arrangements should be made for the collection of the results of all radiation measurements taken in the national network of radiation stations, and for the regular scrutiny of these results with a view to ensuring their accuracy and reliability. If this work is done by some other body, the National Radiation Centre shall maintain close liaison with the body in question.

List of World and Regional Radiation Centres

World Radiation Centres

Davos	(Switzerland)
St Petersburg (see note)	(Russian Federation)

Regional Radiation Centres

Region I (Africa):

Cairo	(Egypt)
Khartoum	(Sudan)
Kinshasa	(Democratic Republic of the Congo)
Lagos	(Nigeria)
Tamanrasset	(Algeria)
Tunis	(Tunisia)

Region II (Asia):

Pune	(India)
Tokyo	(Japan)

Region III (South America):

Buenos Aires	(Argentina)
Santiago	(Chile)
Huayao	(Peru)

Region IV (North America, Central America and the Caribbean):

Toronto	(Canada)
Boulder	(United States)
Mexico City/Colima	(Mexico)

Region V (South-West Pacific):

Melbourne	(Australia)

Region VI (Europe):

Budapest	(Hungary)
Davos	(Switzerland)
St Petersburg	(Russian Federation)
Norrköping	(Sweden)
Toulouse/Carpentras	(France)
Uccle	(Belgium)
Lindenberg	(Germany)

Note: The Centre in St Petersburg is mainly operated as a World Radiation Data Centre under the Global Atmosphere Watch Strategic Plan.

———————

ANNEX 7.D. USEFUL FORMULAE

General

All astronomical data can be derived from tables in the nautical almanacs or ephemeris tables. However, approximate formulae are presented for practical use. Michalsky (1988*a*, 1988*b*) compared several sets of approximate formulae and found that the best are the equations presented as convenient approximations in the *Astronomical Almanac* (United States Naval Observatory, 1993). They are reproduced here for convenience.

The position of the sun

To determine the actual location of the sun, the following input values are required:

(a)   Year;

(b)   Day of year (for example, 1 February is day 32);

(c)   Fractional hour in universal time (UT) (for example, hours + minute/60 + number of hours from Greenwich);

(d)   Latitude in degrees (north positive);

(e)   Longitude in degrees (east positive).

To determine the Julian date (JD), the *Astronomical Almanac* determines the present JD from a prime JD set at noon 1 January 2000 UT. This JD is 2 451 545.0. The JD to be determined can be found from:

$$JD = 2\ 432\ 917.5 + delta \cdot 365 + leap + day + hour/24$$

where:

delta = year – 1949
leap = integer portion of (delta/4)

The constant 2 432 917.5 is the JD for 0000 1 January 1949 and is simply used for convenience.

Using the above time, the ecliptic coordinates can be calculated according to the following steps (L, g and l are in degrees):

(a) n = JD – 2 451 545;

(b) L (mean longitude) = 280.460 + 0.985 647 4 $\cdot$ n ($0 \leq L < 360°$);

(c) g (mean anomaly) = 357.528 + 0.985 600 3 $\cdot$ n ($0 \leq g < 360°$);

(d) l (ecliptic longitude) = L + 1.915 $\cdot$ sin (g) + 0.020 $\cdot$ sin ($2g$) ($0 \leq l < 360°$);

(e) ep (obliquity of the ecliptic) = 23.439 – 0.000 000 4 $\cdot$ n (degrees).

It should be noted that the specifications indicate that all multiples of 360° should be added or subtracted until the final value falls within the specified range.

From the above equations, the celestial coordinates can be calculated – the right ascension (*ra*) and the declination (*dec*) – by:

$$\tan(ra) = \cos(ep) \cdot \sin(l) / \cos(l)$$
$$\sin(dec) = \sin(ep) \cdot \sin(l)$$

To convert from celestial coordinates to local coordinates, that is, right ascension and declination to azimuth (*A*) and altitude (*a*), it is convenient to use the local hour angle (*h*). This is calculated by first determining the Greenwich mean sidereal time (GMST, in hours) and the local mean sidereal time (LMST, in hours):

$$\mathrm{GMST} = 6.697\,375 + 0.065\,709\,824\,2 \cdot n + \mathrm{hour}\,(\mathrm{UT})$$

where: $0 \le \mathrm{GMST} < 24\mathrm{h}$

$$\mathrm{LMST} = \mathrm{GMST} + (\text{east longitude}) / (15° \mathrm{h}^{-1})$$

From the LMST, the hour angle (*ha*) is calculated as (*ha* and *ra* are in degrees):

$$ha = 15 \cdot \mathrm{LMST} - ra \qquad\qquad (-12 \le ha < 12\mathrm{h})$$

Before the sun reaches the meridian, the hour angle is negative. Caution should be observed when using this term, because it is opposite to what some solar researchers use.

The calculations of the solar elevation (*el*) and the solar azimuth (*az*) follow (*az* and *el* are in degrees):

$$\sin(el) = \sin(dec) \cdot \sin(\mathrm{lat}) + \cos(dec) \cdot \cos(\mathrm{lat}) \cdot \cos(ha)$$

and:

$$\sin(az) = -\cos(dec) \cdot \sin(ha) / \cos(el)$$
$$\cos(az) = (\sin(dec) - \sin(el) \cdot \sin(\mathrm{lat})) / (\cos(el) \cdot \cos(\mathrm{lat}))$$

where the azimuth is from 0° north, positive through east.

To take into account atmospheric refraction, and derive the apparent solar elevation (*h*) or the apparent solar zenith angle, the *Astronomical Almanac* proposes the following equations:

(a)   A simple expression for refraction *r* for zenith angles less than 75°:

$$r = 0°.004\,52\,P \tan z / (273 + T)$$

where *z* is the zenith distance in degrees; *P* is the pressure in hectopascals; and *T* is the temperature in °C.

(b)   For zenith angles greater than 75° and altitudes below 15°, the following approximate formula is recommended:

$$r = \frac{P\left(0.159\,4 + 0.019\,6a + 0.000\,02a^2\right)}{\left[(273 + T)\left(1 + 0.505a + 0.084\,5a^2\right)\right]}$$

where *a* is the elevation (90° – *z*) where $h = el + r$ and the apparent solar zenith angle $z_0 = z + r$.

Sun–Earth distance

The present-day eccentricity of the orbit of the Earth around the Sun is small but significant to the extent that the square of the Sun–Earth distance *R* and, therefore, the solar irradiance at the Earth, varies by 3.3% from the mean. In astronomical units (AU), to an uncertainty of 10^{-4}:

$$R = 1.000\,14 - 0.016\,71 \cdot \cos(g) - 0.000\,14 \cdot \cos(2g)$$

where g is the mean anomaly and is defined above. The solar eccentricity is defined as the mean Sun–Earth distance (1 AU, R_0) divided by the actual Sun–Earth distance squared:

$$E_0 = \left(R_0/R\right)^2$$

Air mass

In calculations of extinction, the path length through the atmosphere, which is called the absolute optical air mass, must be known. The relative air mass for an arbitrary atmospheric constituent, m, is the ratio of the air mass along the slant path to the air mass in the vertical direction; hence, it is a normalizing factor. In a plane parallel, non-refracting atmosphere m is equal to $1/\sin h_0$ or $1/\cos z_0$.

Local apparent time

The mean solar time, on which our civil time is based, is derived from the motion of an imaginary body called the mean sun, which is considered as moving at uniform speed in the celestial equator at a rate equal to the average rate of movement of the true sun. The difference between this fixed time reference and the variable local apparent time is called the equation of time, Eq, which may be positive or negative depending on the relative position of the true mean sun. Thus:

$$LAT = LMT + Eq = CT + LC + Eq$$

where LAT is the local apparent time (also known as TST, true solar time), LMT is the local mean time; CT is the civil time (referred to a standard meridian, thus also called standard time); and LC is the longitude correction (4 min for every degree). LC is positive if the local meridian is east of the standard and vice versa.

For the computation of Eq, in minutes, the following approximation may be used:

$$Eq = 0.017\,2 + 0.428\,1 \cos \Theta_0 - 7.351\,5 \sin \Theta_0 - 3.349\,5 \cos 2\Theta_0 - 9.361\,9 \sin 2\Theta_0$$

where $\Theta_0 = 2\,\pi d_n/365$ in radians or $\Theta_0 = 360\,d_n/365$ in degrees, and where d_n is the day number ranging from 0 on 1 January to 364 on 31 December for a normal year or to 365 for a leap year. The maximum error of this approximation is 35 s (which is excessive for some purposes, such as air-mass determination).

———————

ANNEX 7.E. DIFFUSE SKY RADIATION – CORRECTION FOR A SHADING RING

The shading ring is mounted on two rails oriented parallel to the Earth's axis, in such a way that the centre of the ring coincides with the pyranometer during the equinox. The diameter of the ring ranges from 0.5 to 1.5 m and the ratio of the width to the radius b/r ranges from 0.09 to 0.35. The adjustment of the ring to the solar declination is made by sliding the ring along the rails. The length of the shading band and the height of the mounting of the rails relative to the pyranometer are determined from the solar position during the summer solstice; the higher the latitude, the longer the shadow band and the lower the rails.

Several authors, for example, Drummond (1956), Dehne (1980) and Le Baron et al. (1980), have proposed formulae for operational corrections to the sky radiation accounting for the part not measured due to the shadow band. For a ring with $b/r < 0.2$, the radiation D_v lost during a day can be expressed as:

$$D_v \approx \frac{b}{r}\cos^3\delta \int_{t_{rise}}^{t_{set}} L(t)\cdot\sin h_\odot (t)\, dt$$

where δ is the declination of the sun; t is the hour angle of the sun; t_{rise} and t_{set} are the hour angle at sunrise and sunset, respectively, for a mathematical horizon (Φ being the geographic latitude, $t_{rise} = -t_{set}$ and $\cos t_{rise} = -\tan\Phi \cdot \tan\delta$); $L(t)$ is the sky radiance during the day; and $h_\odot$ is the solar elevation.

With this expression and some assumptions on the sky radiance, a correction factor f can be determined:

$$f = \frac{1}{1 - \dfrac{D_v}{D}}$$

D being the unobscured sky radiation. In the figure below, an example of this correction factor is given for both a clear and an overcast sky, compared with the corresponding empirical curves. It is evident that the deviations from the theoretical curves depend on climatological factors of the station and should be determined experimentally by comparing the instrument equipped with a shading ring with an instrument shaded by a continuously traced disc. If no experimental data are available for the station, data computed for the overcast case with the corresponding b/r should be used. Thus:

$$\frac{D_v}{D_{overcast}} = \frac{b}{r}\cos^3\delta\left(t_{set} - t_{rise}\right)\cdot\sin\Phi\cdot\sin\delta + \cos\Phi\cdot\cos\delta\cdot\left(\sin t_{set} - \sin t_{rise}\right)$$

where δ is the declination of the sun; Φ is the geographic latitude; and t_{rise} and t_{set} are the solar hour angle for set and rise, respectively (for details, see above).
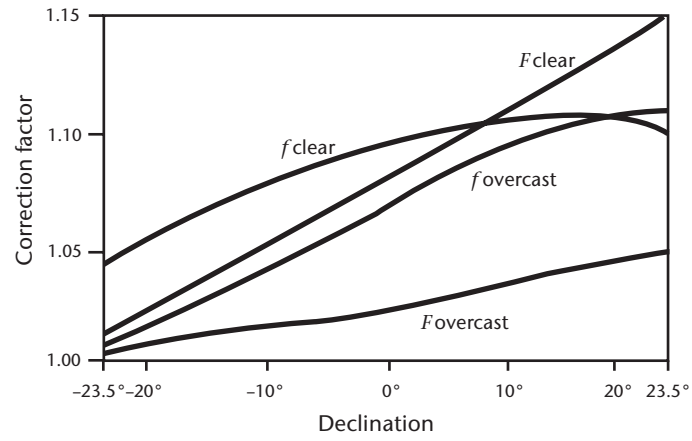
Comparison of calculated and empirically determined correction factors for a shading ring, with $b/r = 0.169$; f indicates calculated curves and F indicates empirical ones.

Source: Dehne (1980)

REFERENCES AND FURTHER READING

Bass, A.M. and R.J. Paur, 1985: The ultraviolet cross-sections of ozone: I. The Measurements. *Atmospheric Ozone* (C.S. Zerefos and A. Ghazi, eds.), Reidel, Dordrecht, pp. 606–610.

Bernhard, G. and G. Seckmeyer, 1999: Uncertainty of measurements of spectral solar UV irradiance. *Journal of Geophysical Research: Atmospheres*, 104(D12):14321–14345.

Bodhaine, B.A., N.B. Wood, E.G. Dutton and J.R. Slusser, 1999: On Rayleigh optical depth calculations. *Journal of Atmospheric and Oceanic Technology*, 16:1854–1861.

Cordero R.R., G. Seckmeyer, A. Damiani, F. Labbe and D. Laroze, 2013: Monte Carlo-based uncertainties of surface UV estimates from models and from spectroradiometers. *Metrologia*, 50(5):L1–L5.

Cordero R.R., G. Seckmeyer, D. Pissulla, L. DaSilva and F. Labbe, 2008: Uncertainty evaluation of spectral UV irradiance measurements. *Measurement Science and Technology*, 19(4):1–15.

Dehne, K., 1980: Vorschlag zur standardisierten Reduktion der Daten verschiedener nationaler Himmelsstrahlungs-Messnetze. *Annalen der Meteorologie* (Neue Folge), 16:57–59.

Drummond, A.J., 1956: On the measurement of sky radiation. *Archiv für Meteorologie, Geophysik und Bioklimatologie*, Serie B, 7:413–436.

Forgan, B.W., 1996: A new method for calibrating reference and field pyranometers. *Journal of Atmospheric and Oceanic Technology*, 13:638–645.

Frouin, R., P.-Y. Deschamps and P. Lecomte, 1990: Determination from space of atmospheric total water vapour amounts by differential absorption near 940 nm: Theory and airborne verification. *Journal of Applied Meteorology*, 29:448–460.

International Commission on Illumination, 1987: *Methods of Characterizing Illuminance Meters and Luminance Meters*, CIE 69-1987. Vienna.

———, 1994: *Guide to Recommended Practice of Daylight Measurement*, CIE 108-1994. Vienna.

International Electrotechnical Commission, 1987: *International Electrotechnical Vocabulary*, Chapter 845: Lighting, IEC 60050-845. Geneva.

International Organization for Standardization, 1990*a*: *Solar Energy – Specification and Classification of Instruments for Measuring Hemispherical Solar and Direct Solar Radiation*, ISO 9060:1990. Geneva.

———, 1990*b*: *Solar Energy – Calibration of Field Pyrheliometers by Comparison to a Reference Pyrheliometer*, ISO 9059:1990. Geneva.

———, 1990*c*: *Solar Energy – Field Pyranometers – Recommended Practice for Use*, ISO/TR 9901:1990. Geneva.

———, 1992: *Solar Energy – Calibration of Field Pyranometers by Comparison to a Reference Pyranometer*, ISO 9847:1992. Geneva.

———, 1993: *Solar Energy – Calibration of a Pyranometer Using a Pyrheliometer*, ISO 9846:1993. Geneva.

International Organization for Standardization/International Electrotechnical Commission, 2008: *Uncertainty of Measurement – Part 3: Guide to the Expression of Uncertainty in Measurement*, ISO/IEC Guide 98-3:2008, Incl. Suppl. 1:2008/Cor 1:2009, Suppl. 1:2008, Suppl. 2:2011. Geneva. (equivalent to: Joint Committee for Guides in Metrology, 2008: *Evaluation of Measurement Data – Guide to the Expression of Uncertainty in Measurement*, JCGM 100:2008, Corrected in 2010).

Kerr, J.B. and T.C. McElroy, 1993: Evidence for large upward trends of ultraviolet-B radiation linked to ozone depletion. *Science*, 262:1032–1034.

Le Baron, B.A., W.A. Peterson and I. Dirmhirn, 1980: Corrections for diffuse irradiance measured with shadowbands. *Solar Energy*, 25:1–13.

McKinlay, A.F. and B.L. Diffey, 1987: A reference action spectrum for ultraviolet induced erythema in human skin. In: *Human Exposure to Ultraviolet Radiation: Risks and Regulations* (W.F. Passchier and B.F.M. Bosnjakovic, eds.), Elsevier, Amsterdam, pp. 83–87.

Michalsky, J.J., 1988*a:* The astronomical almanac's algorithm for approximate solar position (1950–2050). *Solar Energy*, 40(3):227–235.

———, 1988*b*: Errata. The astronomical almanac's algorithm for approximate solar position (1950–2050). *Solar Energy*, 41(1):113.

Parrish, J.A., K.F. Jaenicke and R.R. Anderson, 1982: Erythema and melanogenesis action spectra of normal human skin. *Photochemistry and Photobiology*, 36:187–191.

Rüedi, I., 2001: *International Pyrheliometer Comparison IPC-IX, Results and Symposium*. MeteoSwiss Working Report No. 197, Davos and Zurich.

Schneider, W., G.K. Moortgat, G.S. Tyndall and J.P. Burrows, 1987: Absorption cross-sections of NO_2 in the UV and visible region (200–700 nm) at 298 K. *Journal of Photochemistry and Photobiology, A: Chemistry*, 40:195–217.

United States Naval Observatory, 1993: *The Astronomical Almanac*, Nautical Almanac Office, Washington DC.

Vigroux, E., 1953: Contribution à l'étude expérimentale de l'absorption de l'ozone. *Annales de Physique*, 8:709–762.

Webb, A.R., B.G. Gardiner, M. Blumthaler and P. Foster, 1994: A laboratory investigation of two ultraviolet spectroradiometers. *Photochemistry and Photobiology*, 60(1):84–90.

World Meteorological Organization, 1986: *Revised Instruction Manual on Radiation Instruments and Measurements*. World Climate Research Programme Publications Series No. 7 (WMO/TD-No. 149). Geneva.

———, 1993: *Report of the Second Meeting of the Ozone Research Managers of the Parties to the Vienna Convention for the Protection of the Ozone Layer* (Geneva, 10–12 March 1993). WMO Global Ozone Research and Monitoring Project Report No. 32. Geneva.

———, 1996: *WMO/UMAP Workshop on Broad-band UV Radiometers* (Garmisch-Partenkirchen, Germany, 22–23 April 1996). Global Atmosphere Watch Report No. 120 (WMO/TD-No. 894). Geneva.

———, 1998: *Baseline Surface Radiation Network (BSRN): Operations Manual* (WMO/TD-No. 879). Geneva.

———, 1999a: *Guidelines for Site Quality Control of UV Monitoring*. Global Atmosphere Watch Report No. 126 (WMO/TD-No. 884). Geneva.

———, 1999b: *Report of the LAP/COST/WMO Intercomparison of Erythemal Radiometers* (Thessaloniki, Greece, 13–23 September 1999). Global Atmosphere Watch Report No. 141 (WMO/TD-No. 1051). Geneva.

———, 2001: *Instruments to Measure Solar Ultraviolet Radiation. Part 1: Spectral Instruments*. Global Atmosphere Watch Report No. 125 (WMO/TD-No. 1066). Geneva.

———, 2003: *Quality Assurance in Monitoring Solar Ultraviolet Radiation: the State of the Art*. Global Atmosphere Watch Report No. 146 (WMO/TD-No. 1180). Geneva.

———, 2005: *WMO/GAW Experts Workshop on a Global Surface-based Network for Long Term Observations of Column Aerosol Optical Properties* (Davos, Switzerland, 8–10 March 2004). Global Atmosphere Watch Report No. 162 (WMO/TD-No. 1287). Geneva.

———, 2008: *Instruments to Measure Solar Ultraviolet Radiation – Part 2: Broadband Instruments Measuring Erythemally Weighted Solar Irradiance*. Global Atmosphere Watch Report No. 164 (WMO/TD-No. 1289). Geneva.

———, 2010a: *Instruments to Measure Solar Ultraviolet Radiation – Part 3: Multi-channel Filter Instruments*. Global Atmosphere Watch Report No. 190 (WMO/TD-No. 1537). Geneva.

———, 2010b: *Instruments to Measure Solar Ultraviolet Radiation – Part 4: Array Spectroradiometers*. Global Atmosphere Watch Report No. 191 (WMO/TD-No. 1538). Geneva.

———, 2011: *Data Quality Objectives (DQO) for Solar Ultraviolet Radiation Measurements – Part I* (Addendum to *Quality Assurance in Monitoring Solar Ultraviolet Radiation: State of the Art*, GAW Report No. 146). Global Atmosphere Watch Report No. 198. Geneva.

CHAPTER CONTENTS

CHAPTER 8. MEASUREMENT OF SUNSHINE DURATION

8.1 GENERAL

The term "sunshine" is associated with the brightness of the solar disc exceeding the background of diffuse sky light, or, as is better observed by the human eye, with the appearance of shadows behind illuminated objects. As such, the term is related more to visual radiation than to energy radiated at other wavelengths, although both aspects are inseparable. In practice, however, the first definition was established directly by the relatively simple Campbell-Stokes sunshine recorder (see section 8.2.3), which detects sunshine if the beam of solar energy concentrated by a special lens is able to burn a special dark paper card. This recorder was already introduced in meteorological stations in 1880 and is still used in many networks. Since no international regulations on the dimensions and quality of the special parts were established, applying different laws of the principle gave different sunshine duration values.

In order to homogenize the data of the worldwide network for sunshine duration, a special design of the Campbell-Stokes sunshine recorder, the so-called interim reference sunshine recorder (IRSR), was recommended as the reference (WMO, 1962). The improvement made by this "hardware definition" was effective only during the interim period needed for finding a precise physical definition allowing for both designing automatic sunshine recorders and approximating the "scale" represented by the IRSR as near as possible. With regard to the latter, the settlement of a direct solar threshold irradiance corresponding to the burning threshold of the Campbell-Stokes recorders was strongly advised. Investigations at different stations showed that the threshold irradiance for burning the card varied between 70 and 280 W m^{-2} (Bider, 1958; Baumgartner, 1979). However, further investigations, especially performed with the IRSR in France, resulted in a mean value of 120 W m^{-2}, which was finally proposed as the threshold of direct solar irradiance to distinguish bright sunshine.[1] With regard to the spread of test results, a threshold accuracy of 20% in instrument specifications is accepted. A pyrheliometer was recommended as the reference sensor for the detection of the threshold irradiance. For future refinement of the reference, the settlement of the field-of-view angle of the pyrheliometer seems to be necessary (see Part I, Chapter 7, 7.2 and 7.2.1.3).

8.1.1 Definition

According to WMO (2010),[2] sunshine duration during a given period is defined as the sum of the time for which the direct solar irradiance exceeds 120 W m^{-2}.

8.1.2 Units and scales

The physical quantity of sunshine duration (SD) is, evidently, time. The units used are seconds or hours. For climatological purposes, derived terms such as "hours per day" or "daily sunshine hours" are used, as well as percentage quantities, such as "relative daily sunshine duration", where SD may be related to the extra-terrestrial possible, or to the maximum possible, sunshine duration (SD_0 and SD_{max}, respectively). The measurement period (day, decade, month, year, and so on) is an important addendum to the unit.

---

[1] Recommended by the Commission for Instruments and Methods of Observation at its eighth session (1981) through Recommendation 10 (CIMO-VIII).
[2] Recommended by the Commission for Instruments and Methods of Observation at its tenth session (1989) through Recommendation 16 (CIMO-X).

8.1.3 Meteorological requirements

Performance requirements are given in Part I, Chapter 1. Hours of sunshine should be measured with an uncertainty of ±0.1 h and a resolution of 0.1 h.

Since the number and steepness of the threshold transitions of direct solar radiation determine the possible uncertainty of sunshine duration, the meteorological requirements on sunshine recorders are essentially correlated with the climatological cloudiness conditions (WMO, 1985).

In the case of a cloudless sky, only the hourly values at sunrise or sunset can (depending on the amount of dust) be erroneous because of an imperfectly adjusted threshold or spectral dependencies.

In the case of scattered clouds (cumulus, stratocumulus), the steepness of the transition is high and the irradiance measured from the cloudy sky with a pyrheliometer is generally lower than 80 W m^{-2}; that means low requirements on the threshold adjustment. But the field-of-view angle of the recorder can influence the result if bright cloud clusters are near the sun.

The highest precision is required if high cloud layers (cirrus, altostratus) with small variations of the optical thickness attenuate the direct solar irradiance around the level of about 120 W m^{-2}. The field-of-view angle is effective as well as the precision of the threshold adjustment.

The requirements on sunshine recorders vary, depending on site and season, according to the dominant cloud formation. The latter can be roughly described by three ranges of relative daily sunshine duration SD/SD_0 (see section 8.1.2), namely "cloudy sky" by ($0 \leq SD/SD_0 < 0.3$), "scattered clouds" by ($0.3 \leq SD/SD_0 < 0.7$) and "fair weather" by ($0.7 \leq SD/SD_0 \leq 1.0$). The results for dominant clouded sky generally show the highest percentage of deviations from the reference.

8.1.3.1 Application of sunshine duration data

One of the first applications of SD data was to characterize the climate of sites, especially of health resorts. This also takes into account the psychological effect of strong solar light on human well-being. It is still used by some local authorities to promote tourist destinations.

The description of past weather conditions, for instance of a month, usually contains the course of daily SD data.

For these fields of application, an uncertainty of about 10% of mean SD values seemed to be acceptable over many decades.

8.1.3.2 Correlations to other meteorological variables

The most important correlation between sunshine duration and global solar radiation G is described by the so-called Ångström formula:

$$G/G_0 = a + b \cdot \left(SD/SD_0 \right) \tag{8.1}$$

where G/G_0 is the so-called clearness index (related to the extra-terrestrial global irradiation), SD/SD_0 is the corresponding sunshine duration (related to the extra-terrestrial possible SD value), and a and b are constants which have to be determined monthly. The uncertainty of the monthly means of daily global irradiation derived in this way from Campbell-Stokes data was found to be lower than 10% in summer, and rose up to 30% in winter, as reported for German stations (Golchert, 1981).

The Ångström formula implies the inverse correlation between cloud amount and sunshine duration. This relationship is not fulfilled for high and thin cloudiness and obviously not for cloud fields which do not cover the sun, so that the degree of inverse correlation depends first

of all on the magnitude of the statistical data collected (Stanghellini, 1981; Angell, 1990). The improvement of the accuracy of SD data should reduce the scattering of the statistical results, but even perfect data can generate sufficient results only on a statistical basis.

8.1.3.3 *Requirement of automated records*

Since electrical power is available in an increasing number of places, the advantage of the Campbell-Stokes recorder of being self-sufficient is of decreasing importance. Furthermore, the required daily maintenance requirement of replacing the burn card makes the use of Campbell-Stokes recorders problematic at either automatic weather stations or stations with reduced numbers of personnel. Another essential reason to replace Campbell-Stokes recorders by new automated measurement procedures is to avoid the expense of visual evaluations and to obtain more precise results on data carriers permitting direct computerized data processing.

8.1.4 **Measurement methods**

The principles used for measuring sunshine duration and the pertinent types of instruments are briefly listed in the following methods:

(a) Pyrheliometric method: Pyrheliometric detection of the transition of direct solar irradiance through the 120 W m^{-2} threshold (according to Recommendation 10 (CIMO-VIII)). Duration values are readable from time counters triggered by the appropriate upward and downward transitions.

Type of instrument: Pyrheliometer combined with an electronic or computerized threshold discriminator and a time-counting device.

(b) Pyranometric method:

(i) Pyranometric measurement of global (G) and diffuse (D) solar irradiance to derive the direct solar irradiance as the WMO threshold discriminator value and further as in (a) above.

Type of instrument: Radiometer systems of two fitted pyranometers and one sunshade device combined with an electronic or computerized threshold discriminator and a time-counting device.

(ii) Pyranometric measurement of global (G) solar irradiance to estimate sunshine duration.

Type of instrument: A pyranometer combined with an electronic or computerized device which is able to deliver 10 min means as well as minimum and maximum global (G) solar irradiance within those 10 min, or alternatively to deliver 1 min means of global (G) solar irradiance.

(c) Burn method: Threshold effect of burning paper caused by focused direct solar radiation (heat effect of absorbed solar energy). The duration is read from the total burn length.

Type of instrument: Campbell-Stokes sunshine recorders, especially the recommended version, namely the IRSR (see section 8.2).

(d) Contrast method: Discrimination of the insolation contrasts between some sensors in different positions to the sun with the aid of a specific difference of the sensor output signals which corresponds to an equivalent of the WMO recommended threshold (determined by comparisons with reference SD values) and further as in (b) above.

Type of instrument: Specially designed multi-sensor detectors (mostly equipped with photovoltaic cells) combined with an electronic discriminator and a time counter.

(e)   Scanning method: Discrimination of the irradiance received from continuously scanned, small sky sectors with regard to an equivalent of the WMO recommended irradiance threshold (determined by comparisons with reference *SD* values).

Type of instrument: One-sensor receivers equipped with a special scanning device (rotating diaphragm or mirror, for instance) and combined with an electronic discriminator and a time-counting device.

The sunshine duration measurement methods described in the following paragraphs are examples of ways to achieve the above-mentioned principles. Instruments using these methods, with the exception of the Foster switch recorder, participated in the WMO Automatic Sunshine Duration Measurement Comparison in Hamburg from 1988 to 1989 and in the comparison of pyranometers and electronic sunshine duration recorders of Regional Association VI in Budapest in 1984 (WMO, 1986).

The description of the Campbell-Stokes sunshine recorder in section 8.2.3 is relatively detailed since this instrument is still widely used in national networks, and the specifications and evaluation rules recommended by WMO should be considered (however, note that this method is no longer recommended,[3] since the duration of bright sunshine is not recorded with sufficient consistency).

A historical review of sunshine recorders is given in Coulson (1975), Hameed and Pittalwala (1989) and Sonntag and Behrens (1992).

8.2   INSTRUMENTS AND SENSORS

8.2.1   Pyrheliometric method

8.2.1.1   *General*

This method, which represents a direct consequence of the WMO definition of sunshine (see section 8.1.1) and is, therefore, recommended to obtain reference values of sunshine duration, requires a weatherproof pyrheliometer and a reliable solar tracker to point the radiometer automatically or at least semi-automatically to the position of the sun. The method can be modified by the choice of pyrheliometer, the field-of-view angle of which influences the irradiance measured when clouds surround the sun.

The sunshine threshold can be monitored by the continuous comparison of the pyrheliometer output with the threshold equivalent voltage $V_{th} = 120\ \text{W m}^{-2} \cdot R\ \mu V\ \text{W}^{-1}\ \text{m}^2$, which is calculable from the responsivity R of the pyrheliometer. A threshold transition is detected if $\Delta V = V - V_{th}$ changes its sign. The connected time counter is running when $\Delta V > 0$.

8.2.1.2   *Sources of error*

The field-of-view angle is not yet settled by agreed definitions (see Part I, Chapter 7, 7.2 and 7.2.1.3). Greater differences between the results of two pyrheliometers with different field-of-view angles are possible, especially if the sun is surrounded by clouds. Furthermore, typical errors of pyrheliometers, namely tilt effect, temperature dependence, non-linearity and zero-offset, depend on the class of the pyrheliometer. Larger errors appear if the alignment to the sun is not precise or if the entrance window is covered by rain or snow.

---

[3]   See Recommendation 10 (CIMO-VIII).

8.2.2 Pyranometric method

8.2.2.1 *General*

The pyranometric method to derive sunshine duration data is based on the fundamental relationship between the direct solar radiation (I) and the global (G) and diffuse (D) solar radiation:

$$I \cdot \cos\zeta = G - D \qquad (8.2)$$

where ζ is the solar zenith angle and $I \cdot \cos\zeta$ is the horizontal component of I. To fulfil equation 8.2 exactly, the shaded field-of-view angle of the pyranometer for measuring D must be equal to the field-of-view angle of the pyrheliometer (see Part I, Chapter 7). Furthermore, the spectral ranges, as well as the time constants of the pyrheliometers and pyranometers, should be as similar as possible.

In the absence of a sun-tracking pyrheliometer, but where computer-assisted pyranometric measurements of G and D are available, the WMO sunshine criterion can be expressed according to equation 8.2 by:

$$(G-D)\big/\cos\zeta > 120 \text{ W m}^{-2} \qquad (8.3)$$

which is applicable to instantaneous readings.

The modifications of this method in different stations concern first of all:

(a) The choice of pyranometer;

(b) The shading device applied (shade ring or shade disc with solar tracker) and its shade geometry (shade angle);

(c) The correction of shade-ring losses.

As a special modification, the replacement of the criterion in equation 8.3 by a statistically derived parameterization formula (to avoid the determination of the solar zenith angle) for applications in more simple data-acquisition systems should be mentioned (Sonntag and Behrens, 1992).

Different algorithms, based on different assumptions, can be used to estimate sunshine duration from the measurement of only one pyranometer.

The Slob and Monna method (Slob and Monna, 1991) is based on two assumptions on the relation between irradiance and cloudiness, as follows:

(a) A rather accurate calculation of the potential global irradiance at the Earth's surface based on the calculated value of the extra-terrestrial irradiation (G_0) by taking into account extinction in the atmosphere. The attenuation factor depends on the solar elevation h and the turbidity T of the atmosphere. The ratio between the measured global irradiance and this calculated value of the clear sky global irradiance is a good measure for the presence of clouds;

(b) An evident difference between the minimum and maximum value of the global irradiance, measured during a 10 min interval, presumes a temporary eclipse of the sun by clouds. On the other hand, in the case of no such difference, there is no sunshine or continuous sunshine during the 10 min interval (namely, $SD = 0$ or $SD = 10$ min).

Based on these assumptions, an algorithm can be used (Slob and Monna, 1991) to calculate the daily SD from the sum of 10 min SD. Within this algorithm, SD is determined for succeeding 10 min intervals (namely, $SD_{10'} = f \cdot 10$ min, where f is the fraction of the interval with sunshine, $0 \leq f \leq 1$). The attenuation factor largely depends on the optical path of the sunlight travelling through the atmosphere. Because this path is related to the elevation of the sun, $h = 90° - z$, the algorithm discriminates between three time zones. Although usually $f = 0$ or $f = 1$, special

attention is given to $0 < f < 1$. This algorithm is given in Annex 8.A. The uncertainty is about 0.6 h for daily sums, though recent work (Hinssen and Knap, 2007; WMO, 2012) showed that the expanded uncertainty ($k = 2$) on daily totals can exceed 1 h.

The Carpentras method assumes the possibility of parameterizing and calculating over 1 min intervals an irradiance threshold (G_{thr}) of G as a function of the most frequent in situ conditions of atmospheric turbidity and solar elevation (h). The corresponding algorithm of this method is given in Annex 8.B. The achievable expanded uncertainty ($k = 2$) for daily totals is about 0.7 h (WMO, 2012).

The application of the Carpentras method can be optimized by using 1 min average global and direct irradiances (used as reference) for a few consecutive years (at least four), which makes it possible to determine the coefficients for the parameterization of the 1 min G_{thr} for the specific location. This minimizes the total relative error of daily SD calculated by the Carpentras method over a long period of time (years) by using the SD cumulative differences, and also provides an evaluation of the achievable uncertainty of the Carpentras method (Morel et al., 2012).

8.2.2.2 *Sources of error*

According to equation 8.3, the measuring errors in global and diffuse solar irradiance are propagated by the calculation of direct solar irradiance and are strongly amplified with increasing solar zenith angles. Therefore, the accuracy of corrections for losses of diffuse solar energy by the use of shade rings (WMO, 1984*a*) and the choice of pyranometer quality is of importance to reduce the uncertainty level of the results.

8.2.3 **The Campbell-Stokes sunshine recorder (burn method)**

The Campbell-Stokes sunshine recorder consists essentially of a glass sphere mounted concentrically in a section of a spherical bowl, the diameter of which is such that the sun's rays are focused sharply on a card held in grooves in the bowl. The method of supporting the sphere differs according to whether the instrument is operated in polar, temperate or tropical latitudes. To obtain useful results, both the spherical segment and the sphere should be made with great precision, the mounting being so designed that the sphere can be accurately centred therein. Three overlapping pairs of grooves are provided in the spherical segment so that the cards can be suitable for different seasons of the year (one pair for both equinoxes), their length and shape being selected to suit the geometrical optics of the system. It should be noted that the aforementioned problem of burns obtained under variable cloud conditions indicates that this instrument, and indeed any instrument using this method, does not provide accurate data of sunshine duration.

The table below summarizes the main specifications and requirements for a Campbell-Stokes sunshine recorder of the IRSR grade.

8.2.3.1 *Adjustments*

In installing the recorder, the following adjustments are necessary:

(a)   The base must be levelled;

(b)   The spherical segment should be adjusted so that the centre line of the equinoctial card lies in the celestial equator (the scale of latitude marked on the bowl support facilitates this task);

(c)   The vertical plan through the centre of the sphere and the noon mark on the spherical segment must be in the plane of the geographic meridian (north-south adjustment).

A recorder is best tested for (c) above by observing the image of the sun at the local apparent noon; if the instrument is correctly adjusted, the image should fall on the noon mark of the spherical segment or card.

Campbell-Stokes recorder (IRSR grade) specifications

Glass sphere	Spherical segment	Record cards
Shape: Uniform	Material: Gunmetal or equivalent durability	Material: Good quality pasteboard not affected appreciably by moisture
Diameter: 10 cm	Radius: 73 mm	Width: Accurate to within 0.3 mm
Colour: Very pale or colourless	Additional specifications:	Thickness: 0.4 ± 0.05 mm
Refractive index: 1.52 ± 0.02	(a) Central noon line engraved transversely across inner surface	Moisture effect: Within 2%
Focal length: 75 mm for sodium "D" light	(b) Adjustment for inclination of segment to horizontal according to latitude	Colour: Dark, homogeneous, no difference detected in diffuse daylight
	(c) Double base with provision for levelling and azimuth setting	Graduations: Hour-lines printed in black

8.2.3.2　　*Evaluation*

In order to obtain uniform results from Campbell-Stokes recorders, it is especially important to conform closely to the following directions for measuring the IRSR records. The daily total duration of bright sunshine should be determined by marking off on the edge of a card of the same curvature the lengths corresponding to each mark and by measuring the total length obtained along the card at the level of the recording to the nearest tenth of an hour. The evaluation of the record should be made as follows:

(a)	In the case of a clear burn with round ends, the length should be reduced at each end by an amount equal to half the radius of curvature of the end of the burn; this will normally correspond to a reduction of the overall length of each burn by 0.1 h;

(b)	In the case of circular burns, the length measured should be equal to half the diameter of the burn. If more than one circular burn occurs on the daily record, it is sufficient to consider two or three burns as equivalent to 0.1 h of sunshine; four, five, six burns as equivalent to 0.2 h of sunshine; and so on in steps of 0.1 h;

(c)	Where the mark is only a narrow line, the whole length of this mark should be measured, even when the card is only slightly discoloured;

(d)	Where a clear burn is temporarily reduced in width by at least a third, an amount of 0.1 h should be subtracted from the total length for each such reduction in width, but the maximum subtracted should not exceed one half of the total length of the burn.

In order to assess the random and systematic errors made while evaluating the records and to ensure the objectivity of the results of the comparison, it is recommended that the evaluations corresponding to each one of the instruments compared be made successively and independently by two or more persons trained in this type of work.

8.2.3.3   *Special versions*

Since the standard Campbell-Stokes sunshine recorder does not record all the sunshine received during the summer months at stations with latitudes higher than about 65°, some countries use modified versions.

One possibility is to use two Campbell-Stokes recorders operated back to back, one of them being installed in the standard manner, while the other should be installed facing north.

In many climates, it may be necessary to heat the device to prevent the deposition of frost and dew. Comparisons in climates like that of northern Europe between heated and normally operated instruments have shown that the amount of sunshine not measured by a normal version, but recorded by a heated device, is about 1% of the monthly mean in summer and about 5% to 10% of the monthly mean in winter.

8.2.3.4   *Sources of error*

The errors of this recorder are mainly generated by the dependence on the temperature and humidity of the burn card as well as by the overburning effect, especially in the case of scattered clouds (Ikeda et al., 1986).

The morning values are frequently affected by dew or frost at middle and high latitudes.

8.2.4   Contrast-evaluating devices

The Foster sunshine switch is an optical device that was introduced operationally in the network of the United States in 1953 (Foster and Foskett, 1953). It consists of a pair of selenium photocells, one of which is shielded from direct sunshine by a shade ring. The cells are corrected so that in the absence of the direct solar beam no signal is produced. The switch is activated when the direct solar irradiance exceeds about 85 W m^{-2} (Hameed and Pittalwala, 1989). The position of the shade ring requires adjustments only four times a year to allow for seasonal changes in the sun's apparent path across the sky.

8.2.5   Contrast-evaluating and scanning devices

8.2.5.1   *General*

A number of different opto-electronic sensors, namely contrast-evaluating and scanning devices (see, for example, WMO, 1984*b*), were compared during the WMO Automatic Sunshine Duration Measurement Comparison at the Regional Radiation Centre of Regional Association VI in Hamburg (Germany) from 1988 to 1989. The report of this comparison contains detailed descriptions of all the instruments and sensors that participated in this event.

8.2.5.2   *Sources of error*

The distribution of cloudiness over the sky or solar radiation reflected by the surroundings can influence the results because of the different procedures to evaluate the contrast and the relatively large field-of-view angles of the cells in the arrays used. Silicon photovoltaic cells without filters typically have the maximum responsivity in the near-infrared, and the results, therefore, depend on the spectrum of the direct solar radiation.

Since the relatively small, slit-shaped, rectangular field-of-view angles of this device differ considerably from the circular-symmetrical one of the reference pyrheliometer, the cloud distribution around the sun can cause deviations from the reference values.

Because of the small field of view, an imperfect glass dome may be a specific source of uncertainty. The spectral responsivity of the sensor should also be considered in addition to solar elevation error. At present, only one of the commercial recorders using a pyroelectric detector is thought to be free of spectral effects.

8.3 EXPOSURE OF SUNSHINE DETECTORS

The three essential aspects for the correct exposure of sunshine detectors are as follows:

(a) The detectors should be firmly fixed to a rigid support. This is not required for the SONI (WMO, 1984*b*) sensors that are designed also for use on buoys;

(b) The detector should provide an uninterrupted view of the sun at all times of the year throughout the whole period when the sun is more than 3° above the horizon. This recommendation can be modified in the following cases:

   (i) Small antennas or other obstructions of small angular width (≤2°) are acceptable if no alternative site is available. In this case, the position, elevation and angular width of obstructions should be well documented and the potential loss of sunshine hours during particular hours and days should be estimated by the astronomical calculation of the apparent solar path;

   (ii) In mountainous regions (valleys, for instance), natural obstructions are acceptable as a factor of the local climate and should be well documented, as mentioned above;

(c) The site should be free of surrounding surfaces that could reflect a significant amount of direct solar radiation to the detector. Reflected radiation can influence mainly the results of the contrast-measuring devices. To overcome this interference, white or gloss paint should be avoided and nearby surfaces should either be kept free of snow or screened.

The adjustment of the detector axis is mentioned above. For some detectors, the manufacturers recommend tilting the axis, depending on the season.

The siting classification for surface observing stations on land (see Part I, Chapter 1, Annex 1.B of this Guide) provides additional guidance on the selection of a site and the location of a sunshine detector within a site in order to optimize representativeness.

8.4 GENERAL SOURCES OF ERROR

The uncertainty of sunshine duration recorded using different types of instrument and methods was demonstrated as deviations from reference values in WMO for the weather conditions of Hamburg (Germany) in 1988–1989.

The reference values are also somewhat uncertain because of the uncertainty of the calibration factor of the pyrheliometer used and the dimensions of its field-of-view angle (dependency on the aureole). For single values, the time constant should also be considered.

General sources of uncertainty are as follows:

(a) The calibration of the recorder (adjustment of the irradiance threshold equivalent (see section 8.5));

(b) The typical variation of the recorder response due to meteorological conditions (for example, temperature, cloudiness, dust) and the position of the sun (for example, errors of direction, solar spectrum);

(c)   The poor adjustment and instability of important parts of the instrument;

(d)   The simplified or erroneous evaluation of the values measured;

(e)   Erroneous time-counting procedures;

(f)   Dirt and moisture on optical and sensing surfaces;

(g)   Poor quality of maintenance.

8.5   CALIBRATION

The following general remarks should be made before the various calibration methods are described:

(a)   No standardized method to calibrate SD detectors is available;

(b)   For outdoor calibrations, the pyrheliometric method has to be used to obtain reference data;

(c)   Because of the differences between the design of the SD detectors and the reference instrument, as well as with regard to the natural variability of the measuring conditions, calibration results must be determined by long-term comparisons (some months);

(d)   Generally the calibration of SD detectors requires a specific procedure to adjust their threshold value (electronically for opto-electric devices, by software for pyranometric systems);

(e)   For opto-electric devices with an analogue output, the duration of the calibration period should be relatively short;

(f)   The indoor method (using a lamp) is recommended primarily for regular testing of the stability of field instruments.

8.5.1   Outdoor methods

8.5.1.1   *Comparison of sunshine duration data*

Reference values SD_{ref} have to be measured simultaneously with the sunshine duration values SD_{cal} of the detector to be calibrated. The reference instrument used should be a pyrheliometer on a solar tracker combined with an irradiance threshold discriminator (see section 8.1.4). Alternatively, a regularly recalibrated sunshine recorder of selected precision may be used. Since the accuracy requirement of the sunshine threshold of a detector varies with the meteorological conditions (see section 8.1.3), the comparison results must be derived statistically from datasets covering long periods.

If the method is applied to the total dataset of a period (with typical cloudiness conditions), the first calibration result is the ratio $q_{tot} = \Sigma_{tot}\, SD_{ref}/\Sigma_{tot}\, SD_{cal}$.

For $q > 1$ or $q < 1$, the threshold equivalent voltage has to be adjusted to lower and higher values, respectively. Since the amount of the required adjustment is not strongly correlated to q_{tot}, further comparison periods are necessary to validate iteratively the approach to the ideal threshold by approximation of $q_{tot} = 1$. The duration of a total calibration period may be three to six months at European mid-latitudes. Therefore, the facilities to calibrate network detectors should permit the calibration of several detectors simultaneously. (The use of q_{tot} as a correction factor for the $\Sigma\, SD$ values gives reliable results only if the periods to be evaluated have the same cloud formation as during the calibration period. Therefore, this method is not recommended.)

If the method is applied to datasets which are selected according to specific measurement conditions (for example, cloudiness, solar elevation angle, relative sunshine duration, daytime), it may be possible, for instance, to find factors $q_{sel} = \Sigma_{sel} SD_{ref}/\Sigma_{sel} SD_{cal}$ statistically for different types of cloudiness. The factors could also be used to correct datasets for which the cloudiness is clearly specified.

On the other hand, an adjustment of the threshold equivalent voltage is recommended, especially if q_{sel} values for worse cloudiness conditions (such as cirrus and altostratus) are considered. An iterative procedure to validate the adjustment is also necessary; depending on the weather, some weeks or months of comparison may be needed.

8.5.1.2   *Comparison of analogue signals*

This method is restricted to SD detectors which have an analogue output that responds linearly to the received direct solar irradiance, at least in the range <500 W m^{-2}. The comparison between the reference irradiance measured by a pyrheliometer and the simultaneously measured analogue output should be performed at cloudless hours or other intervals with slowly variable direct solar irradiance below 500 W m^{-2}.

The linear regression analysis of such a dataset generates a best-fit line from which the threshold equivalent voltage at 120 W m^{-2} can be derived. If this calibration result deviates from the certified voltage by more than ±20%, the threshold of the detector should be adjusted to the new value.

For detectors with a pronounced spectral response, the measured data at low solar elevation angles around 120 W m^{-2} should be eliminated because of the stronger non-linearity caused by the spectrum, unless the threshold voltage at sunrise and sunset is of special interest. The threshold equivalent voltage has to be extrapolated from higher irradiance values.

8.5.1.3   *Mean effective irradiance threshold method*

The so-called mean effective irradiance threshold (MEIT) method is based on the determination of an hourly mean effective irradiance threshold I_m for the detector to be calibrated.

As a first step of this method, SD values SD_{ref} (h_k, $I(n)$) have to be determined from computer-controlled pyrheliometric measurements for hours h_k and fictitious threshold irradiances $I(n)$ between 60 and 240 W m^{-2} (this means that $I(n) = (60 + n)$ W m^{-2} with $n = 0, 1, 2, ... 180$). As a second step, the hourly SD value $SD(h_k)$ of the detector must be compared with the SD_{ref} (h_k, $I(n)$) to find the $n = n_k$ for which $SD(h_k)$ equals SD_{ref} (h_k, $I(n_k)$). $I(n_k)$ represents the MEIT value of the hour h_k: $I_m(h_k) = (60 + n_k)$ W m^{-2}. If n_k is not found directly, it has to be interpolated from adjacent values.

The third step is the adjustment of the threshold equivalent voltage of the recorder if the relative deviation between a MEIT value I_m and the ideal threshold 120 W m^{-2} is larger than ±20%. The mean value should be a monthly average, for instance, because of the large spread of the deviations of hourly MEIT values.

The method is not applicable to hours with dominant fast threshold transitions; the average gradient of an hour should be lower than 5 W m^{-2} s^{-1}. The MEIT values are not representative of the total dataset of the calibration period.

8.5.2   **Indoor method**

Since the simulation of the distribution of direct and diffuse solar fluxes is difficult indoors, only a "spare calibration" can be recommended which is applicable for SD detectors with an adjustable threshold equivalent voltage. The laboratory test equipment consists of a stabilized

radiation source (preferably with an approximated solar spectrum) and a stand for a precise local adjustment of the *SD* detector as well as of an *SD* detector (carefully calibrated outdoors) which is used as reference. Reference and test detectors should be of the same model.

At the beginning of the test procedure, the reference detector is positioned precisely in the beam of the lamp so that 120 W m^{-2} is indicated by an analogue output or by the usual "sunshine switch". Afterwards, the reference device is replaced precisely by the test device, whose threshold voltage must be adjusted to activate the switch, or to get a 120 W m^{-2} equivalent. The repeatability of the results should be tested by further exchanges of the instruments.

8.6   MAINTENANCE

The required maintenance routine for technicians consists of the following:

(a)   Cleaning: The daily cleaning of the respective entrance windows is necessary for all detectors, especially for scanning devices with small field-of-view angles. Instruments without equipment to prevent dew and frost should be cleared more than once on certain days;

(b)   Checking: The rotation of special (scanning) parts as well as the data-acquisition system should be checked daily;

(c)   Exchange of record: In Campbell-Stokes sunshine recorders, the burn card must be exchanged daily; in other devices, the appropriate data carriers have to be replaced regularly;

(d)   Adjustments: Adjustments are required if a seasonal change of the tilt of the detector is recommended by the manufacturer, or possibly after severe storms.

Special parts of the detectors and of the data-acquisition systems used should undergo maintenance by trained technicians or engineers according to the appropriate instruction manuals.

––––––––––––––

ANNEX 8.A. ALGORITHM TO ESTIMATE SUNSHINE DURATION FROM DIRECT GLOBAL IRRADIANCE MEASUREMENTS

(see Slob and Monna, 1991)

The estimation of the daily SD is based on the sum of the fractions f of 10 min intervals, namely, $SD = \Sigma\, SD_{10}$, where $SD_{10} = f \leq 10$ min. In practice $f = 0$ (no sunshine at all, overcast) or 1 (only sunshine, no clouds), but special attention is given to $0 < f < 1$ (partly sunshine, part clouded). Because the correlation between SD and the global irradiation, measured horizontally, depends on the elevation of the sun (h), discrimination is made in the first place in terms of sin (h).

The following variables are applicable:

h Elevation angle of the sun in degrees
G Global irradiance on a horizontal surface in W m^{-2}
I Direct irradiance on a surface perpendicular to the direction of the sun in W m^{-2}
D Diffuse radiation on a horizontal surface in W m^{-2}
T_L "Linke" – turbidity (dimensionless)

For the measured values of G it holds that:

G represents a 10 min average of the measured global irradiance
G_{min} represents the minimum value of the global irradiance, measured during the 10 min interval
G_{max} represents the maximum value of the global irradiance, measured during the 10 min interval ($G_{min} \leq G \leq G_{max}$)

Equations used:

G_0 $= I_0 \sin (h)$, $I_0 = 1\,367$ W m^{-2} (for extra-terrestrial irradiance)
I $= I_0 \exp (-T_L/(0.9 + 9.4 \sin (h)))$, $I_0 = 1\,367$ W m^{-2}
c $= (G - D)/(I \sin (h))$, where
      $T_L = 4$ and
      $D = 1.2\, G_{min}$ if $(1.2\, G_{min} < 0.4)$ else
      $D = 0.4$

Sun elevation	sin (h)<0.1, $h < 5.7°$	0.1 ≤ sin (h) ≤ 0.3, 5.7° ≤ h ≤ 17.5°		sin (h) ≥ 0.3, h ≥ 17.5°					
Other criteria	No further decision criteria	Is $G/G_0 \leq \{0.2 + \sin (h)/3 + \exp (-T_L/(0.9 + 9.4 \sin (h)))\}$ with $T_L = 6$?		Is $G_{max}/G_0 < 0.4$?					
				If "yes"	If "no"				
					Is $G_{min}/G_0 > \{0.3 + \exp (-T_L/(0.9 + 9.4 \sin (h)))\}$ with $T_L = 10$?				
		If "yes"	If "no"		If "yes"	If "no"			
						Is $G_{max}/G_0 > \{0.3 + \exp (-T_L/(0.9 + 9.4 \sin (h)))\}$ and $G_{max} - G_{min} < 0.1\, G_0$ with $T_L = 10$?			
							If "yes"	If "no"	
								$c < 0$	$0 \leq c \leq 1$	$c > 1$
Result	$f = 0$	$f = 0$	$f = 1$	$f = 0$	$f = 1$	$f = 1$	$f = 0$	$f = c$	$f = 1$

――――――――

ANNEX 8.B. ALGORITHM TO ESTIMATE SUNSHINE DURATION FROM 1 MIN GLOBAL IRRADIANCE MEASUREMENTS

(Carpentras method; see WMO, 1998, 2012)

This method, developed at the WMO Regional Radiation Centre of Carpentras (France) and described by Oliviéri (WMO, 1998), consists of an algorithm that calculates the SD every minute through the measurement of 1 min means of global irradiance (G) compared with a threshold value (G_{thr}) that is parameterized by two coefficients (A, B) and the solar elevation h (specifically sin (h)).

The following variables are applicable:

h Elevation angle of the sun in degrees (see Part I, Chapter 7, Annex 7.D)
G Global irradiance on a horizontal surface in W m^{-2} (1 s sampled, 1 min averaged)

Equations used:

$$G_{thr} = F_c \times \text{Mod}$$
$$\text{Mod} = 1\,080\,(\sin\,(h))^{1.25}$$
$$F_c = A + B\cos\,(2\pi d/365)$$

where Mod represents the global irradiance obtained from a cloudless day model (clear sky and mean value of turbidity); F_c represents a factor, the empirical value of which is close to 0.7; and d is the day number of the annual sequence.

The F_c factor, generally varying between 0.5 and 0.8, depends on the climatic conditions of the location, and the A, B coefficients can be empirically calculated by long-term comparison between SD and pyrheliometer measurements (Morel et al., 2012). Alternatively, the presence of near or, even better, co-located instruments for atmospheric turbidity permits an improved determination of the F_c factor. A variability of the A and B coefficients has been observed in relation to latitude (B tends towards negative values for the southern hemisphere, while A decreases with latitude).

The algorithm is run every minute and can be expressed as follows:

Sun elevation	$h < 3°$	$h \geq 3°$	
Criteria	No decision	Is $G \geq G_{thr}$?	
		If "yes"	If "no"
Result	$SD = 0$ min	$SD = 1$ min	$SD = 0$ min

The solar elevation must be calculated every minute contemporarily to the sun hour angle, right ascension and geocentric declination according to the astronomical formulae reported in Part I, Chapter 7, Annex 7.D.

The data filtering ($h \geq 3°$) is applied before the execution of the main test and permits the filtering of errors due to the imperfection of the model, the height of the sun (low heights) and the atmospheric refraction. A tolerance of 3° above the horizon is accepted for the requirement that the SD detectors have an uninterrupted view of the sun at all times of the year. The errors introduced by the data filtering on h produce a small underestimation that, due to their systematic nature, can be corrected after a long period of measurements. A comparison of this method with other methods and with reference SD data is reported in WMO (2012).

REFERENCES AND FURTHER READING

Angell, J.K., 1990: Variation in United States cloudiness and sunshine duration between 1950 and the drought year of 1988. *Journal of Climate*, 3:296–308.

Baumgartner, T., 1979: Die Schwellenintensität des Sonnenscheinautographen Campbell-Stokes an wolkenlosen Tagen. *Arbeitsberichte der Schweizerischen Meteorologischen Zentralanstalt*, No. 84, Zürich.

Bider, M., 1958: Über die Genauigkeit der Registrierungen des Sonnenscheinautographen Campbell-Stokes. *Archiv für Meteorologie, Geophysik und Bioklimatologie*, Serie B, 9(2):199–230.

Coulson, K.L., 1975: *Solar and Terrestrial Radiation. Methods and Measurements*. Academic Press, New York, pp. 215–233.

Dyson, P., 2003: *Investigation of the Uncertainty of Sunshine Duration in the Solar and Terrestrial Radiation Network*. Instrument Test Report 674, Commonwealth Bureau of Meteorology.

Foster, N.B. and L.W. Foskett, 1953: A photoelectric sunshine recorder. *Bulletin of the American Meteorological Society*, 34:212–215.

Golchert, H.J., 1981: Mittlere Monatliche Global-strahlungsverteilungen in der Bundesrepublik Deutschland. *Meteorologische Rundschau*, 34:143–151.

Hameed, S. and I. Pittalwala, 1989: An investigation of the instrumental effects on the historical sunshine record of the United States. *Journal of Climate*, 2:101–104.

Hinssen, Y.B.L. and W.H. Knap, 2007: Comparison of pyranometric and pyrheliometric methods for the determination of sunshine duration. *Journal of Atmospheric and Oceanic Technology*, 24(5):835–846.

Ikeda, K., T. Aoshima and Y. Miyake, 1986: Development of a new sunshine-duration meter. *Journal of the Meteorological Society of Japan*, 64(6):987–993.

Jaenicke, R. and F. Kasten, 1978: Estimation of atmospheric turbidity from the burned traces of the Campbell-Stokes sunshine recorder. *Applied Optics*, 17:2617–2621.

Morel, J.P., E. Vueric h, J. Oliviéri and S. Mevel, 2012: Sunshine duration measurements using the Carpentras method. Baseline Surface Radiation Network meeting, Postdam, Germany, 1–3 August 2012.

Painter, H.E., 1981: The performance of a Campbell-Stokes sunshine recorder compared with a simultaneous record of normal incidence irradiance. *The Meteorological Magazine*, 110:102–109.

Slob, W.H. and W.A.A. Monna, 1991: *Bepaling van een directe en diffuse straling en van zonneschijnduur uit 10-minuutwaarden van de globale straling*. KNMI TR136, de Bilt.

Sonntag, D. and K. Behrens, 1992: Ermittlung der Sonnenscheindauer aus pyranometrisch gemessenen Bestrahlungsstärken der Global-und Himmelsstrahlung. *Berichte des Deutschen Wetterdienstes*, No. 181.

Stanghellini, C., 1981: A simple method for evaluating sunshine duration by cloudiness observations. *Journal of Applied Meteorology*, 20:320–323.

World Meteorological Organization, 1962: *Abridged Final Report of the Third Session of the Commission for Instruments and Methods of Observation* (WMO-No. 116, R.P. 48). Geneva.

——, 1982: *Abridged Final Report of the Eighth Session of the Commission for Instruments and Methods of Observation* (WMO-No. 590). Geneva.

——, 1984a: Diffuse solar radiation measured by the shade ring method improved by a new correction formula (K. Dehne). *Papers Presented at the WMO Technical Conference on Instruments and Cost-effective Meteorological Observations (TECEMO)*. Instruments and Observing Methods Report No. 15. Geneva.

——, 1984b: A new sunshine duration sensor (P. Lindner). *Papers Presented at the WMO Technical Conference on Instruments and Cost-effective Meteorological Observations (TECEMO)*. Instruments and Observing Methods Report No. 15. Geneva.

——, 1985: Dependence on threshold solar irradiance of measured sunshine duration (K. Dehne). *Papers Presented at the Third WMO Technical Conference on Instruments and Methods of Observation (TECIMO-III)*. Instruments and Observing Methods Report No. 22 (WMO/TD-No. 50). Geneva.

——, 1986: *Radiation and Sunshine Duration Measurements: Comparison of Pyranometers and Electronic Sunshine Duration Recorders of RA VI* (G. Major). Instruments and Observing Methods Report No. 16 (WMO/TD-No. 146). Geneva.

——, 1990: *Abridged Final Report of the Tenth Session of the Commission for Instruments and Methods of Observation* (WMO-No. 727). Geneva.

———, 1998: Sunshine duration measurement using a pyranometer (J.C. Oliviéri). *Papers Presented at the WMO Technical Conference on Meteorological and Environmental Instruments and Methods of Observation (TECO-98)*. Instruments and Observing Methods Report No. 70 (WMO/TD-No. 877). Geneva.

———, 2010: *Manual on the Global Observing System* (WMO-No. 544), Volume I. Geneva.

———, 2012: Updating and development of methods for worldwide accurate measurements of sunshine duration (E. Vuerich, J.P. Morel, S. Mevel, J. Oliviéri). *Paper presented at the WMO Technical Conference on Meteorological and Environmental Instruments and Methods of Observation (TECO-2012)*. Instruments and Observing Methods Report No. 109. Geneva.

———————————

CHAPTER CONTENTS

CHAPTER 9. MEASUREMENT OF VISIBILITY

9.1   GENERAL

9.1.1   Definitions

Visibility was first defined for meteorological purposes as a quantity to be estimated by a human observer, and observations made in that way are widely used. However, the estimation of visibility is affected by many subjective and physical factors. The essential meteorological quantity, which is the transparency of the atmosphere, can be measured objectively and is represented by the meteorological optical range (MOR).

The *meteorological optical range* is the length of path in the atmosphere required to reduce the luminous flux in a collimated beam from an incandescent lamp, at a colour temperature of 2 700 K, to 5% of its original value, the luminous flux being evaluated by means of the photometric luminosity function of the International Commission on Illumination (CIE).

Visibility, meteorological visibility (by day) and meteorological visibility at night[1] are defined as the greatest distance at which a black object of suitable dimensions (located on the ground) can be seen and recognized when observed against the horizon sky during daylight or could be seen and recognized during the night if the general illumination were raised to the normal daylight level (WMO, 1992*a*, 2010*a*).

Visual range (meteorological): Distance at which the contrast of a given object with respect to its background is just equal to the contrast threshold of an observer (WMO, 1992*a*).

Airlight is light from the sun and the sky which is scattered into the eyes of an observer by atmospheric suspensoids (and, to a slight extent, by air molecules) lying in the observer's cone of vision. That is, airlight reaches the eye in the same manner as diffuse sky radiation reaches the Earth's surface. Airlight is the fundamental factor limiting the daytime horizontal visibility for black objects, because its contributions, integrated along the cone of vision from eye to object, raise the apparent luminance of a sufficiently remote black object to a level which is indistinguishable from that of the background sky. Contrary to subjective estimates, most of the airlight entering observers' eyes originates in portions of their cone of vision lying rather close to them.

The following four photometric qualities are defined in detail in various standards, such as by the International Electrotechnical Commission (IEC, 1987):

(a)   *Luminous flux* (symbol: F (or Φ); unit: lumen) is a quantity derived from radiant flux by evaluating the radiation according to its action upon the International Commission on Illumination standard photometric observer;

(b)   *Luminous intensity* (symbol: I; unit: candela or lm sr^{-1}) is luminous flux per unit solid angle;

(c)   *Luminance* (symbol: L; unit: cd m^{-2}) is luminous intensity per unit area;

(d)   *Illuminance* (symbol: E; unit: lux or lm m^{-2}) is luminous flux per unit area.

---

[1]   To avoid confusion, visibility at night should not be defined in general as "the greatest distance at which lights of specified moderate intensity can be seen and identified" (see the *Abridged Final Report of the Eleventh Session of the Commission for Instruments and Methods of Observation* (WMO-No. 807)). If visibility should be reported based on the assessment of light sources, it is recommended that a visual range should be defined by specifying precisely the appropriate light intensity and its application, like runway visual range. Nevertheless, at its eleventh session CIMO agreed that further investigations were necessary in order to resolve the practical difficulties of the application of this definition.

The *extinction coefficient* (symbol σ) is the proportion of luminous flux lost by a collimated beam, emitted by an incandescent source at a colour temperature of 2 700 K, while travelling the length of a unit distance in the atmosphere. The coefficient is a measure of the attenuation due to both absorption and scattering.

The *luminance contrast* (symbol C) is the ratio of the difference between the luminance of an object and its background and the luminance of the background.

The *contrast threshold* (symbol ε) is the minimum value of the luminance contrast that the human eye can detect, namely, the value which allows an object to be distinguished from its background. The contrast threshold varies with the individual.

The *illuminance threshold* (symbol E_t) is the smallest illuminance, required by the eye, for the detection of point sources of light against a background of specified luminance. The value of E_t, therefore, varies according to lighting conditions.

The *transmission factor* (symbol T) is defined, for a collimated beam from an incandescent source at a colour temperature of 2 700 K, as the fraction of luminous flux which remains in the beam after traversing an optical path of a given length in the atmosphere. The transmission factor is also called the transmission coefficient. The terms transmittance or transmissive power of the atmosphere are also used when the path is defined, that is, of a specific length (for example, in the case of a transmissometer). In this case, T is often multiplied by 100 and expressed in %.

An *aerodrome* is a defined area on land or water (including any buildings, installations and equipment) intended to be used either wholly or in part for the arrival, departure and surface movement of aircraft (International Civil Aviation Organization, 2013).

9.1.2   **Units and scales**

The meteorological visibility or MOR is expressed in metres or kilometres. The measurement range varies according to the application. While for synoptic meteorological requirements, the scale of MOR readings extends from below 100 m to more than 70 km, the measurement range may be more restricted for other applications. This is the case for civil aviation, where the upper limit may be 10 km. This range may be further reduced when applied to the measurement of runway visual range representing landing and take-off conditions in reduced visibility. Runway visual range is required only between 50 and 1 500 m (see Part II, Chapter 2). For other applications, such as road or sea traffic, different limits may be applied according to both the requirements and the locations where the measurements are taken.

The errors of visibility measurements increase in proportion to the visibility, and measurement scales take this into account. This fact is reflected in the code used for synoptic reports by the use of three linear segments with decreasing resolution, namely, 100 to 5 000 m in steps of 100 m, 6 to 30 km in steps of 1 km, and 35 to 70 km in steps of 5 km. This scale allows visibility to be reported with a better resolution than the accuracy of the measurement, except when visibility is less than about 1 000 m.

9.1.3   **Meteorological requirements**

The concept of visibility is used extensively in meteorology in two distinct ways. First, it is one of the elements identifying air-mass characteristics, especially for the needs of synoptic meteorology and climatology. Here, visibility must be representative of the optical state of the atmosphere. Secondly, it is an operational variable which corresponds to specific criteria or special applications. For this purpose, it is expressed directly in terms of the distance at which specific markers or lights can be seen.

One of the most important special applications is found in meteorological services to aviation (see Part II, Chapter 2).

The measure of visibility used in meteorology should be free from the influence of extra-meteorological conditions; it must be simply related to intuitive concepts of visibility and to the distance at which common objects can be seen under normal conditions. MOR has been defined to meet these requirements, as it is convenient for the use of instrumental methods by day and night, and as the relations between MOR and other measures of visibility are well understood. MOR has been formally adopted by WMO as the measure of visibility for both general and aeronautical uses (WMO, 2014). It is also recognized by the International Electrotechnical Commission (IEC, 1987) for application in atmospheric optics and visual signalling.

MOR is related to the intuitive concept of visibility through the contrast threshold. In 1924, Koschmieder, followed by Helmholtz, proposed a value of 0.02 for ε. Other values have been proposed by other authors. They vary from 0.007 7 to 0.06, or even 0.2. The smaller value yields a larger estimate of the visibility for given atmospheric conditions. For aeronautical requirements, it is accepted that ε is higher than 0.02, and it is taken as 0.05 since, for a pilot, the contrast of an object (runway markings) with respect to the surrounding terrain is much lower than that of an object against the horizon. It is assumed that, when an observer can just see and recognize a black object against the horizon, the apparent contrast of the object is 0.05, and, as explained below, this leads to the choice of 0.05 as the transmission factor adopted in the definition of MOR.

Accuracy requirements are discussed in Part I, Chapter 1.

9.1.4 Measurement methods

Visibility is a complex psycho-physical phenomenon, governed mainly by the atmospheric extinction coefficient associated with solid and liquid particles held in suspension in the atmosphere; the extinction is caused primarily by scattering rather than by absorption of the light. Its estimation is subject to variations in individual perception and interpretative ability, as well as the light source characteristics and the transmission factor. Thus, any visual estimate of visibility is subjective.

When visibility is estimated by a human observer it depends not only on the photometric and dimensional characteristics of the object which is, or should be, perceived, but also on the observer's contrast threshold. At night, it depends on the intensity of the light sources, the background illuminance and, if estimated by an observer, the adaptation of the observer's eyes to darkness and the observer's illuminance threshold. The estimation of visibility at night is particularly problematic. The first definition of visibility at night in section 9.1.1 is given in terms of equivalent daytime visibility in order to ensure that no artificial changes occur in estimating the visibility at dawn and twilight. The second definition has practical applications especially for aeronautical requirements, but it is not the same as the first and usually gives different results. Both are evidently imprecise.

Instrumental methods measure the extinction coefficient from which the MOR may be calculated. The visibility may then be calculated from knowledge of the contrast and illuminance thresholds, or by assigning agreed values to them. It has been pointed out by Sheppard (1983) that:

> [s]trict adherence to the definition (of MOR) would require mounting a transmitter and receiver of appropriate spectral characteristics on two platforms which could be separated, for example along a railroad, until the transmittance was 5 per cent. Any other approach gives only an estimate of MOR.

However, fixed instruments are used on the assumption that the extinction coefficient is independent of distance. Some instruments measure attenuation directly and others measure the scattering of light to derive the extinction coefficient. These are described in section 9.3. The brief analysis of the physics of visibility in this chapter may be useful for understanding the relations between the various measures of the extinction coefficient, and for considering the instruments used to measure it.
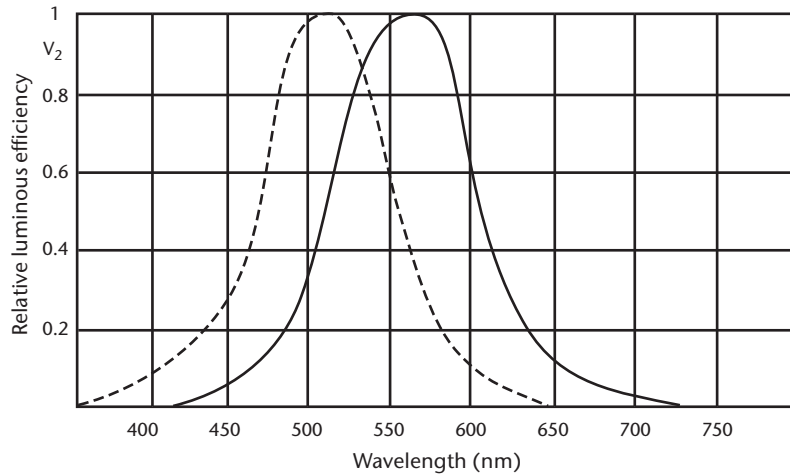
Figure 9.1. Relative luminous efficiency of the human eye for monochromatic radiation. The continuous line indicates daytime vision, while the broken line indicates night-time vision.

Visual perception – photopic and scotopic vision

The conditions of visual perception are based on the measurement of the photopic efficiency of the human eye with respect to monochromatic radiation in the visible light spectrum. The terms *photopic vision* and *scotopic vision* refer to daytime and night-time conditions, respectively.

The adjective *photopic* refers to the state of accommodation of the eye for daytime conditions of ambient luminance. More precisely, the photopic state is defined as the visual response of an observer with normal sight to the stimulus of light incident on the retinal fovea (the most sensitive central part of the retina). The fovea permits fine details and colours to be distinguished under such conditions of adaptation.

In the case of photopic vision (vision by means of the fovea), the relative luminous efficiency of the eye varies with the wavelength of the incident light. The luminous efficiency of the eye in photopic vision is at a maximum for a wavelength of 555 nm. The response curve for the relative efficiency of the eye at the various wavelengths of the visible spectrum may be established by taking the efficiency at a wavelength of 555 nm as a reference value. The curve in Figure 9.1, adopted by the International Commission on Illumination for an average normal observer, is therefore obtained.

Night-time vision is said to be scotopic (vision involving the rods of the retina instead of the fovea). The rods, the peripheral part of the retina, have no sensitivity to colour or fine details, but are particularly sensitive to low light intensities. In scotopic vision, maximum luminous efficiency corresponds to a wavelength of 507 nm.

Scotopic vision requires a long period of accommodation, up to 30 min, whereas photopic vision requires only 2 min.

Basic equations

The basic equation for visibility measurements is the Bouguer-Lambert law:

$$F = F_0 \, e^{-\sigma x} \tag{9.1}$$

where F is the luminous flux received after a length of path x in the atmosphere and F_0 is the flux for $x = 0$. Differentiating, we obtain:

$$\sigma = \frac{-dF}{F} \cdot \frac{1}{dx} \tag{9.2}$$

Note that this law is valid only for monochromatic light, but may be applied to a spectral flux to a good approximation. The transmission factor is:

$$T = F/F_0 \tag{9.3}$$

Mathematical relationships between MOR and the different variables representing the optical state of the atmosphere may be deduced from the Bouguer-Lambert law. The relationship between the transmission factor and MOR is valid for fog droplets, but when visibility is reduced by other hydrometeors (such as rain or snow) or lithometeors (such as blowing sand), MOR values should be treated with more care.

From equations 9.1 and 9.3 we may write:

$$T = F / F_0 = e^{-\sigma x} \tag{9.4}$$

If this law is applied to the MOR definition $T = 0.05$, then $x = P$ and the following may be written:

$$T = 0.05 = e^{-\sigma P} \tag{9.5}$$

Hence, the mathematical relation of MOR to the extinction coefficient is:

$$P = (1/\sigma) \cdot \ln(1/0.05) \approx 3/\sigma \tag{9.6}$$

where ln is the log to base e or the natural logarithm. When combining equation 9.4, after being deduced from the Bouguer-Lambert law, and equation 9.6, the following equation is obtained:

$$P = x \cdot \ln(0.05)/\ln(T) \tag{9.7}$$

This equation is used as a basis for measuring MOR with transmissometers where x is, in this case, equal to the transmissometer baseline a in equation 9.14.

Meteorological visibility in daylight

The contrast of luminance is:

$$C = \frac{L_b - L_h}{L_h} \tag{9.8}$$

where L_h is the luminance of the horizon, and L_b is the luminance of the object.

The luminance of the horizon arises from the airlight scattered from the atmosphere along the observer's line of sight.

It should be noted that, if the object is darker than the horizon, C is negative, and that, if the object is black ($L_b = 0$), $C = -1$.

In 1924, Koschmieder established a relationship, which later became known as Koschmieder's law, between the apparent contrast (C_x) of an object, seen against the horizon sky by a distant observer, and its inherent contrast (C_0), namely, the contrast that the object would have against the horizon when seen from very short range. Koschmieder's relationship can be written as:

$$C_x = C_0 \, e^{-\sigma x} \tag{9.9}$$

This relationship is valid provided that the scatter coefficient is independent of the azimuth angle and that there is uniform illumination along the whole path between the observer, the object and the horizon.

If a black object is viewed against the horizon ($C_0 = -1$) and the apparent contrast is -0.05, equation 9.9 reduces to:

$$0.05 = e^{-\sigma x} \tag{9.10}$$

Comparing this result with equation 9.5 shows that when the magnitude of the apparent contrast of a black object, seen against the horizon, is 0.05, that object is at MOR (P).

Meteorological visibility at night

The distance at which a light (a night visibility marker) can be seen at night is not simply related to MOR. It depends not only on MOR and the intensity of the light, but also on the illuminance at the observer's eye from all other light sources.

In 1876, Allard proposed the law of attenuation of light from a point source of known intensity (I) as a function of distance (x) and extinction coefficient (σ). The illuminance (E) of a point light source is given by:

$$E = I \cdot x^{-2} \cdot e^{-\sigma x} \tag{9.11}$$

When the light is just visible, $E = E_t$ and the following may be written:

$$\sigma = (1/x) \cdot \ln \left\{ I \middle/ \left(E_t \cdot x^2 \right) \right\} \tag{9.12}$$

Noting that $P = (1/\sigma) \cdot \ln (1/0.05)$ in equation 9.6, we may write:

$$P = x \cdot \ln (1/0.05) \middle/ \ln \left(I \middle/ \left(E_t \cdot x^2 \right) \right) \tag{9.13}$$

The relationship between MOR and the distance at which lights can be seen is described in section 9.2.3, while the application of this equation to visual observations is described in section 9.2.

9.2 VISUAL ESTIMATION OF METEOROLOGICAL OPTICAL RANGE

9.2.1 General

A meteorological observer can make a visual estimation of MOR using natural or man-made objects (groups of trees, rocks, towers, steeples, churches, lights, and so forth).

Each station should prepare a plan of the objects used for observation, showing their distances and bearings from the observer. The plan should include objects suitable for daytime observations and objects suitable for night-time observations. The observer must also give special attention to significant directional variations of MOR.

Observations should be made by observers who have "normal" vision and have received suitable training. The observations should normally be made without any additional optical devices (binoculars, telescope, theodolite, and the like) and, preferably, not through a window, especially when objects or lights are observed at night. The eye of the observer should be at a normal height above the ground (about 1.5 m); observations should, thus, not be made from the upper storeys of control towers or other high buildings. This is particularly important when visibility is poor.

When visibility varies in different directions, the value recorded or reported may depend on the use to be made of the report. In synoptic messages, the lower value should be reported, but in reports for aviation the guidance in WMO (2014) should be followed.

9.2.2 Estimation of meteorological optical range by day

For daytime observations, the visual estimation of visibility gives a good approximation of the true value of MOR.

Provided that they meet the following requirements, objects at as many different distances as possible should be selected for observation during the day. Only black, or nearly black, objects which stand out on the horizon against the sky should be chosen. Light-coloured objects or objects located close to a terrestrial background should be avoided as far as possible. This is particularly important when the sun is shining on the object. Provided that the albedo of the

object does not exceed about 25%, no error larger than 3% will be caused if the sky is overcast, but it may be much larger if the sun is shining. Thus, a white house would be unsuitable, but a group of dark trees would be satisfactory, except when brightly illuminated by sunlight. If an object against a terrestrial background has to be used, it should stand well in front of the background, namely, at a distance at least half that of the object from the point of observation. A tree at the edge of a wood, for example, would not be suitable for visibility observations.

For observations to be representative, they should be made using objects subtending an angle of no less than 0.5° at the observer's eye. An object subtending an angle less than this becomes invisible at a shorter distance than would large objects in the same circumstances. It may be useful to note that a hole of 7.5 mm in diameter, punched in a card and held at arm's length, subtends this angle approximately; a visibility object viewed through such an aperture should, therefore, completely fill it. At the same time, however, such an object should not subtend an angle of more than 5°.

9.2.3   Estimation of meteorological optical range at night

Methods which may be used to estimate MOR at night from visual observations of the distance of perception of light sources are described below.

Any source of light may be used as a visibility object, provided that the intensity in the direction of observation is well defined and known. However, it is generally desirable to use lights which can be regarded as point sources, and whose intensity is not greater in any one more favoured direction than in another and not confined to a solid angle which is too small. Care must be taken to ensure the mechanical and optical stability of the light source.

A distinction should be made between sources known as point sources, in the vicinity of which there is no other source or area of light, and clusters of lights, even though separated from each other. In the latter case, such an arrangement may affect the visibility of each source considered separately. For measurements of visibility at night, only the use of suitably distributed point sources is recommended.

It should be noted that observations at night, using illuminated objects, may be affected appreciably by the illumination of the surroundings, by the physiological effects of dazzling, and by other lights, even when these are outside the field of vision and, more especially, if the observation is made through a window. Thus, an accurate and reliable observation can be made only from a dark and suitably chosen location.

Furthermore, the importance of physiological factors cannot be overlooked, since these are an important source of measurement dispersion. It is essential that only qualified observers with normal vision take such measurements. In addition, it is necessary to allow a period of adaptation (usually from 5 to 15 min) during which the eyes become accustomed to the darkness.

For practical purposes, the relationship between the distance of perception of a light source at night and the value of MOR can be expressed in two different ways, as follows:

(a)   For each value of MOR, by giving the value of luminous intensity of the light, so that there is a direct correspondence between the distance where it is barely visible and the value of MOR;

(b)   For a light of a given luminous intensity, by giving the correspondence between the distance of perception of the light and the value of MOR.

The second relationship is easier and also more practical to use since it would not be an easy matter to install light sources of differing intensities at different distances. The method involves using light sources which either exist or are installed around the station and replacing I, x and E_t in equation 9.13 by the corresponding values of the available light sources. In this way, the Meteorological Services can draw up tables giving values of MOR as a function of background

luminance and the light sources of known intensity. The values to be assigned to the illuminance threshold E_t vary considerably in accordance with the ambient luminance. The following values, considered as average observer values, should be used:

(a) $10^{-6.0}$ lux at twilight and at dawn, or when there is appreciable light from artificial sources;

(b) $10^{-6.7}$ lux in moonlight, or when it is not yet quite dark;

(c) $10^{-7.5}$ lux in complete darkness, or with no light other than starlight.

Tables 9.1 and 9.2 give the relations between MOR and the distance of perception of light sources for each of the above methods for different observation conditions. They have been compiled to guide Meteorological Services in the selection or installation of lights for night visibility observations and in the preparation of instructions for their observers for the computation of MOR values.

Table 9.1. Relation between MOR and intensity of a just-visible point source for three values of E_t

MOR	Luminous intensity (candela) of lamps only just visible at distances given in column P		
P (m)	Twilight ($E_t = 10^{-6.0}$)	Moonlight ($E_t = 10^{-6.7}$)	Complete darkness ($E_t = 10^{-7.5}$)
100	0.2	0.04	0.006
200	0.8	0.16	0.025
500	5	1	0.16
1 000	20	4	0.63
2 000	80	16	2.5
5 000	500	100	16
10 000	2 000	400	63
20 000	8 000	1 600	253
50 000	50 000	10 000	1 580

Table 9.2. Relation between MOR and the distance at which a 100 cd point source is just visible for three values of E_t

MOR	Distance of perception (metres) of a lamp of 100 cd as a function of MOR value		
P (m)	Twilight ($E_t = 10^{-6.0}$)	Moonlight ($E_t = 10^{-6.7}$)	Complete darkness ($E_t = 10^{-7.5}$)
100	250	290	345
200	420	500	605
500	830	1 030	1 270
1 000	1 340	1 720	2 170
2 000	2 090	2 780	3 650
5 000	3 500	5 000	6 970
10 000	4 850	7 400	10 900
20 000	6 260	10 300	16 400
50 000	7 900	14 500	25 900

An ordinary 100 W incandescent bulb provides a light source of approximately 100 cd.

In view of the substantial differences caused by relatively small variations in the values of the visual illuminance threshold and by different conditions of general illumination, it is clear that Table 9.2 is not intended to provide an absolute criterion of visibility, but indicates the need for calibrating the lights used for night-time estimation of MOR so as to ensure as far as possible that night observations made in different locations and by different Services are comparable.

9.2.4 **Estimation of meteorological optical range in the absence of distant objects**

At certain locations (open plains, ships, and so forth), or when the horizon is restricted (valley or cirque), or in the absence of suitable visibility objects, it is impossible to make direct estimations, except for relatively low visibilities. In such cases, unless instrumental methods are available, values of MOR higher than those for which visibility points are available have to be estimated from the general transparency of the atmosphere. This can be done by noting the degree of clarity with which the most distant visibility objects stand out. Distinct outlines and features, with little or no fuzziness of colours, are an indication that MOR is greater than the distance between the visibility object and the observer. On the other hand, indistinct visibility objects are an indication of the presence of haze or of other phenomena reducing MOR.

9.2.5 **Accuracy of visual observations**

General

Observations of objects should be made by observers who have been suitably trained and have what is usually referred to as normal vision. This human factor has considerable significance in the estimation of visibility under given atmospheric conditions, since the perception and visual interpretation capacity vary from one individual to another.

Accuracy of daytime visual estimates of meteorological optical range

Observations show that estimates of MOR based on instrumental measurements are in reasonable agreement with daytime estimates of visibility. Visibility and MOR should be equal if the observer's contrast threshold is 0.05 (using the criterion of recognition) and the extinction coefficient is the same in the vicinity of both the instrument and the observer.

Middleton (1952) found, from 1 000 measurements, that the mean contrast ratio threshold for a group of 10 young airmen trained as meteorological observers was 0.033 with a range, for individual observations, from less than 0.01 to more than 0.2. Sheppard (1983) has pointed out that when the Middleton data are plotted on a logarithmic scale they show good agreement with a Gaussian distribution. If the Middleton data represent normal observing conditions, we must expect daylight estimates of visibility to average about 14% higher than MOR with a standard deviation of 20% of MOR. These calculations are in excellent agreement with the results from the First WMO Intercomparison of Visibility Measurements (WMO, 1990), where it was found that, during daylight, the observers' estimates of visibility were about 15% higher than instrumental measurements of MOR. The interquartile range of differences between the observer and the instruments was about 30% of the measured MOR. This corresponds to a standard deviation of about 22%, if the distribution is Gaussian.

Accuracy of night-time visual estimates of meteorological optical range

From Table 9.2 in section 9.2.3, it is easy to see how misleading the values of MOR can be if based simply on the distance at which an ordinary light is visible, without making due allowance for the intensity of the light and the viewing conditions. This emphasizes the importance of giving precise, explicit instructions to observers and of providing training for visibility observations.

Note that, in practice, the use of the methods and tables described above for preparing plans of luminous objects is not always easy. The light sources used as objects are not necessarily well located or of stable, known intensity, and are not always point sources. With respect to this last point, the lights may be wide- or narrow-beam, grouped, or even of different colours to which the eye has different sensitivity. Great caution must be exercised in the use of such lights.

The estimation of the visual range of lights can produce reliable estimates of visibility at night only when lights and their background are carefully chosen; when the viewing conditions of the observer are carefully controlled; and when considerable time can be devoted to the observation to ensure that the observer's eyes are fully accommodated to the viewing conditions. Results from the First WMO Intercomparison of Visibility Measurements (WMO, 1990) show that, during the hours of darkness, the observer's estimates of visibility were about 30% higher than instrumental measurements of MOR. The interquartile range of differences between the observer and the instruments was only slightly greater than that found during daylight (about 35% to 40% of the measured MOR).

9.3   INSTRUMENTAL MEASUREMENT OF THE METEOROLOGICAL OPTICAL RANGE

9.3.1   General

The adoption of certain assumptions allows the conversion of instrumental measurements into MOR. It is not always advantageous to use an instrument for daytime measurements if a number of suitable visibility objects can be used for direct observations. However, a visibility-measuring instrument is often useful for night observations or when no visibility objects are available, or for automatic observing systems. Instruments for the measurement of MOR may be classified into one of the following two categories:

(a)   Those measuring the extinction coefficient or transmission factor of a horizontal cylinder of air: Attenuation of the light is due to both scattering and absorption by particles in the air along the path of the light beam;

(b)   Those measuring the scatter coefficient of light from a small volume of air: In natural fog, absorption is often negligible and the scatter coefficient may be considered as being the same as the extinction coefficient.

Both of the above categories include instruments used for visual measurements by an observer and instruments using a light source and an electronic device comprising a photoelectric cell or a photodiode to detect the emitted light beam. The main disadvantage of visual measurements is that substantial errors may occur if observers do not allow sufficient time for their eyes to become accustomed to the conditions (particularly at night).

The main characteristics of these two categories of MOR-measuring instruments are described below.

9.3.2   Instruments measuring the extinction coefficient

Telephotometric instruments

A number of telephotometers have been designed for daytime measurement of the extinction coefficient by comparing the apparent luminance of a distant object with that of the sky background (for example, the Lohle telephotometer), but they are not normally used for routine measurements since, as stated above, it is preferable to use direct visual observations. These instruments may, however, be useful for extrapolating MOR beyond the most distant object.

Visual extinction meters

A very simple instrument for use with a distant light at night takes the form of a graduated neutral filter, which reduces the light in a known proportion and can be adjusted until the light is only just visible. The meter reading gives a measure of the transparency of the air between the light and the observer, and, from this, the extinction coefficient can be calculated. The overall accuracy depends mainly on variations in the sensitivity of the eye and on fluctuations in the radiant intensity of the light source. The error increases in proportion to MOR.

The advantage of this instrument is that it enables MOR values over a range from 100 m to 5 km to be measured with reasonable accuracy, using only three well-spaced lights, whereas without it a more elaborate series of lights would be essential if the same degree of accuracy were to be achieved. However, the method of using such an instrument (determining the point at which a light appears or disappears) considerably affects the accuracy and homogeneity of the measurements.

Transmissometers

The use of a transmissometer is the method most commonly used for measuring the mean extinction coefficient in a horizontal cylinder of air between a transmitter, which provides a modulated flux light source of constant mean power, and a receiver incorporating a photodetector (generally a photodiode at the focal point of a parabolic mirror or a lens). The most frequently used light source is a halogen lamp or xenon pulse discharge tube. Modulation of the light source prevents disturbance from sunlight. The transmission factor is determined from the photodetector output and this allows the extinction coefficient and the MOR to be calculated.

Since transmissometer estimates of MOR are based on the loss of light from a collimated beam, which depends on scatter and absorption, they are closely related to the definition of MOR. A good, well-maintained transmissometer working within its range of highest accuracy provides a very good approximation to the true MOR.

There are two types of transmissometer:

(a)   Those with a transmitter and a receiver in different units and at a known distance from each other, as illustrated in Figure 9.2;

(b)   Those with a transmitter and a receiver in the same unit, with the emitted light being reflected by a remote mirror or retroreflector (the light beam travelling to the reflector and back), as illustrated in Figure 9.3.
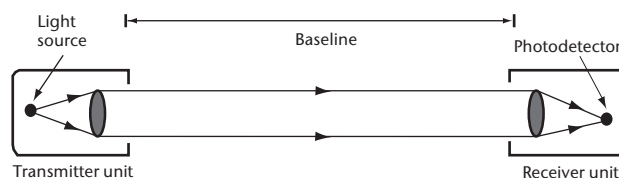
Figure 9.2. Double-ended transmissometer
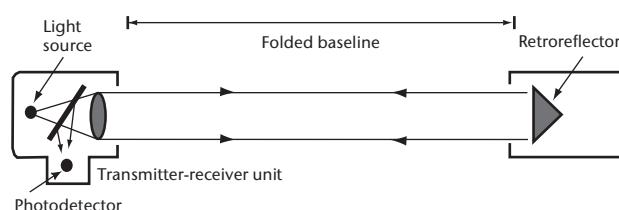
Figure 9.3. Single-ended transmissometer

The distance covered by the light beam between the transmitter and the receiver is commonly referred to as the baseline and may range from a few metres to 150 m (or even 300 m) depending on the range of MOR values to be measured and the applications for which these measurements are to be used.

As seen in the expression for MOR in equation 9.7, the relation:

$$P = a \cdot \ln(0.05)/\ln(T) \tag{9.14}$$

where a is the transmissometer baseline, is the basic formula for transmissometer measurements. Its validity depends on the assumptions that the application of the Koschmieder and Bouguer-Lambert laws is acceptable and that the extinction coefficient along the transmissometer baseline is the same as that in the path between an observer and an object at MOR.

If the measurements are to remain acceptable over a long period, the luminous flux must remain constant during this same period. When halogen light is used, the problem of lamp filament ageing is less critical and the flux remains more constant. However, some transmissometers use feedback systems (by sensing and measuring a small portion of the emitted flux) giving greater homogeneity of the luminous flux with time or compensation for any change.

As will be seen in the section dealing with the accuracy of MOR measurements, the value adopted for the transmissometer baseline determines the MOR measurement range. It is generally accepted that this range is between about 1 and 25 times the baseline length. Modern opto-electronics, however, may provide more accurate results with an extended range (see section 9.3.6 and WMO, 1992b).

A further refinement of the transmissometer measurement principle is to use two receivers or retroreflectors at different distances to extend both the lower limit (short baseline) and the upper limit (long baseline) of the MOR measurement range. These instruments are referred to as "double baseline" instruments.

Many state-of-the-art transmissometers use LEDs as light sources. It is generally recommended that polychromatic light in the visible spectrum be used to obtain a representative extinction coefficient.

Visibility lidars

The lidar (light detection and ranging) technique as described for the laser ceilometer in Part I, Chapter 15, may be used to measure visibility when the beam is directed horizontally. The range-resolved profile of the backscattered signal S depends on the output signal S_0, the distance x, the backscatter coefficient β, and transmission factor T, such that:

$$S(x) \sim S_0 \cdot 1/x^2 \cdot \beta(x) \cdot T^2 \text{ where } T = \int -\sigma(x)\,dx \tag{9.15}$$

Under the condition of horizontal homogeneity of the atmosphere, β and σ are constant and the extinction coefficient σ is determined from only two points of the profile:

$$\ln\left(S(x) \cdot x^2/S_0\right) \sim \ln\beta - 2\,\sigma\,x \tag{9.16}$$

In an inhomogeneous atmosphere the range-dependent quantities of $\beta(x)$ and $\sigma(x)$ may be separated with the Klett Algorithm (Klett, 1985).

As MOR approaches 2 000 m, the accuracy of the lidar method becomes poor.

More information on the requirements for performing visual-range lidar measurements to determine the direction-dependent meteorological optical range can be found in the International Organization for Standardization standard, ISO 28902-1:2012 (ISO, 2012).
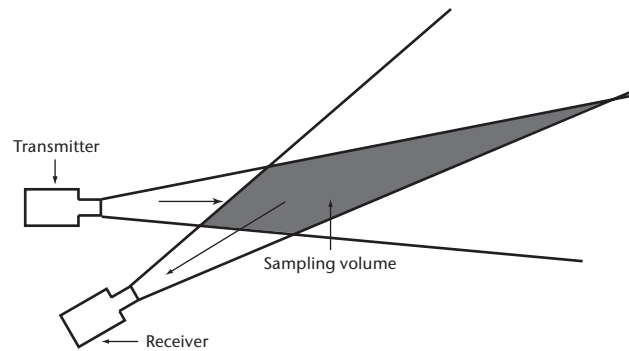
Figure 9.4. Visibility meter measuring backscatter

9.3.3   Instruments measuring the scatter coefficient

The attenuation of light in the atmosphere is due to both scattering and absorption. The presence of pollutants in the vicinity of industrial zones, ice crystals (freezing fog) or dust may make the absorption term significant. However, in general, the absorption factor is negligible and the scatter phenomena due to reflection, refraction, or diffraction on water droplets constitute the main factor reducing visibility. The extinction coefficient may then be considered as equal to the scatter coefficient, and an instrument for measuring the latter can, therefore, be used to estimate MOR.

Measurements are most conveniently taken by concentrating a beam of light on a small volume of air and by determining, through photometric means, the proportion of light scattered in a sufficiently large solid angle and in directions which are not critical. Provided that it is completely screened from interference from other sources of light, or that the light source is modulated, an instrument of this type can be used during both the day and night. The scatter coefficient b is a function that may be written in the following form:

$$b = \frac{2\pi}{\Phi_v} \int_0^\pi I(\phi)\sin(\phi)d\phi \tag{9.17}$$

where Φ_v is the flux entering the volume of air V and $I(\Phi)$ is the intensity of the light scattered in direction Φ with respect to the incident beam.

Note that the accurate determination of b requires the measurement and integration of light scattered out of the beam over all angles. Practical instruments measure the scattered light over a limited angle and rely on a high correlation between the limited integral and the full integral.

Three measurement methods are used in these instruments: backscatter, forward scatter, and scatter integrated over a wide angle.

(a) *Backscatter*: In these instruments (Figure 9.4), a light beam is concentrated on a small volume of air in front of the transmitter, the receiver being located in the same housing and below the light source where it receives the light backscattered by the volume of air sampled. Several researchers have tried to find a relationship between visibility and the coefficient of backscatter, but it is generally accepted that that correlation is not satisfactory.

(b) *Forward scatter*: The profile of light scattered by small particles (aerosols, small droplets) is angular dependent. Moreover, the angular dependency (i.e. the scattered light profile) depends on the chemical composition (e.g. salt concentration), type of nucleus (sand, dust) and size of the particles. As a consequence, a scattering angle should be chosen so that the angular dependency is minimal. Several authors have shown that the best angle is between 20° and 50° (Kneizys et al., 1983; Jia and Lü, 2014; Barteneva, 1960; Van de Hulst, 1957). The instruments, therefore, comprise a transmitter and a receiver, the angle between the beams being 20° to 50°. Another arrangement involves placing either a single diaphragm
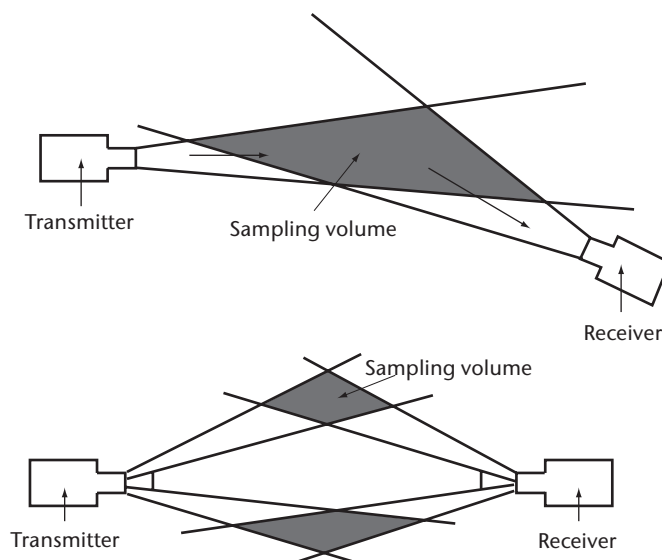
Figure 9.5. Two configurations of visibility meters measuring forward scatter

half-way between a transmitter and a receiver or two diaphragms each a short distance from either a transmitter or a receiver. Figure 9.5 illustrates the two configurations that have been used.

(c) *Scatter over a wide angle*: Such an instrument, illustrated in Figure 9.6, which is usually known as an integrating nephelometer, is based on the principle of measuring scatter over as wide an angle as possible, ideally 0° to 180°, but in practice about 0° to 120°. The receiver is positioned perpendicularly to the axis of the light source which provides light over a wide angle. Although, in theory, such an instrument should give a better estimate of the scatter coefficient than an instrument measuring over a small range of scattering angles, in practice it is more difficult to prevent the presence of the instrument from modifying the extinction coefficient in the air sampled. Integrating nephelometers are not widely used for measuring MOR, but this type of instrument is often used for measuring pollutants.

In all the above instruments, as for most transmissometers, the receivers comprise photodetector cells or photodiodes. The light used is pulsed (for example, high-intensity discharge into xenon).

These types of instruments require only limited space (1 to 2 m in general). They are, therefore, useful when no visibility objects or light sources are available (on board ships, by roadsides, and so forth). Since the measurement relates only to a very small volume of air, the representativeness of measurements for the general state of the atmosphere at the site may be open to question. However, this representativeness can be improved by averaging a number of samples or measurements. In addition, smoothing of the results is sometimes achieved by eliminating extreme values.

The use of these types of instruments has often been limited to specific applications (for example, highway visibility measurements, or to determine whether fog is present) or when less precise MOR measurements are adequate. These instruments are now being used in increasing numbers in automatic meteorological observation systems because of their ability to measure MOR over a wide range and their relatively low susceptibility to pollution compared with transmissometers.
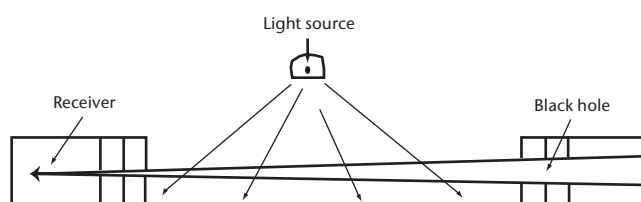
Figure 9.6. Visibility meter measuring scattered light over a wide angle

9.3.4   **Instrument exposure and siting**

Measuring instruments should be located in positions which ensure that the measurements are representative for the intended purpose. Thus, for general synoptic purposes, the instruments should be installed at locations free from local atmospheric pollution, for example, smoke, industrial pollution, dusty roads.

The volume of air in which the extinction coefficient or scatter coefficient is measured should normally be at the eye level of an observer, about 1.5 m above the ground.

It should be borne in mind that transmissometers and instruments measuring the scatter coefficient should be installed in such a way that the sun is not in the optical field at any time of the day, either by mounting with a north-south optical axis (to ±45°) horizontally, for latitudes up to 50°, or by using a system of screens or baffles.

For aeronautical purposes, measurements are to be representative of conditions at the aerodrome. These conditions, which relate more specifically to aerodrome operations, are described in Part II, Chapter 2.

The instruments should be installed in accordance with the directions given by the manufacturers. Particular attention should be paid to the correct alignment of transmissometer transmitters and receivers and to the correct adjustment of the light beam. The poles on which the transmitter/receivers are mounted should be mechanically firm (while remaining frangible when installed at aerodromes) to avoid any misalignment due to ground movement during freezing and, particularly, during thawing. In addition, the mountings must not distort under the thermal stresses to which they are exposed.

9.3.5   **Calibration and maintenance**

In order to obtain satisfactory and reliable observations, instruments for the measurement of MOR should be operated and maintained under the conditions prescribed by the manufacturers, and should be kept continuously in good working order. Regular checks and calibration in accordance with the manufacturer's recommendations should ensure optimum performance.

Calibration in very good visibility (over 10 to 15 km) should be carried out regularly. Atmospheric conditions resulting in erroneous calibration must be avoided. When, for example, there are strong updraughts, or after heavy rain, considerable variations in the extinction coefficient are encountered in the layer of air close to the ground; if several transmissometers are in use on the site (in the case of aerodromes), dispersion is observed in their measurements. Calibration should not be attempted under such conditions.

Note that in the case of most transmissometers, the optical surfaces must be cleaned regularly, and daily servicing must be planned for certain instruments, particularly at aerodromes. The instruments should be cleaned during and/or after major atmospheric disturbances, since rain or violent showers together with strong wind may cover the optical systems with a large number of water droplets and solid particles resulting in major MOR measurement errors. The same is true for snowfall, which could block the optical systems. Heating systems are often placed at the front of the optical systems to improve instrument performance under such conditions. Air-blowing systems are sometimes used to reduce the above problems and the need for frequent cleaning. However, it must be pointed out that these blowing and heating systems may generate air currents warmer than the surrounding air and may adversely affect the measurement of the extinction coefficient of the air mass. In arid zones, sandstorms or blowing sand may block the optical system and even damage it.

9.3.6 Sources of error in the measurement of meteorological optical range and estimates of accuracy

General

All practical operational instruments for the measurement of MOR sample a relatively small region of the atmosphere compared with that scanned by a human observer. Instruments can provide an accurate measurement of MOR only when the volume of air that they sample is representative of the atmosphere around the point of observation out to a radius equal to MOR. It is easy to imagine a situation, with patchy fog or a local rain or snow storm, in which the instrument reading is misleading. However, experience has shown that such situations are not frequent and that the continuous monitoring of MOR using an instrument will often lead to the detection of changes in MOR before they are recognized by an unaided observer. Nevertheless, instrumental measurements of MOR must be interpreted with caution.

Another factor that must be taken into account when discussing representativeness of measurements is the homogeneity of the atmosphere itself. At all MOR values, the extinction coefficient of a small volume of the atmosphere normally fluctuates rapidly and irregularly, and individual measurements of MOR from scatter meters and short baseline transmissometers, which have no in-built smoothing or averaging system, show considerable dispersion. It is, therefore, necessary to take many samples and to smooth or average them to obtain a representative value of MOR. The analysis of the results from the First WMO Intercomparison of Visibility Measurements (WMO, 1990) indicates that, for most instruments, no benefit is gained by averaging over more than 1 min, but for the "noisiest" instruments an averaging time of 2 min is preferable.

Accuracy of telephotometers and visual extinction meters

Visual measurements based on the extinction coefficient are difficult to take. The main source of error is the variability and uncertainty of the performance of the human eye. These errors have been described in the sections dealing with the methods of visual estimation of MOR.

Accuracy of transmissometers

The sources of error in transmissometer measurements may be summarized as follows:

(a) Incorrect alignment of transmitters and receivers;

(b) Insufficient rigidity and stability of transmitter/receiver mountings (freezing and thawing of the ground, thermal stress);

(c) Ageing and incorrect centring of lamps;

(d) Calibrating error (visibility too low or calibration carried out in unstable conditions affecting the extinction coefficient);

(e) Instability of system electronics;

(f) Remote transmission of the extinction coefficient as a low-current signal subject to interference from electromagnetic fields (particularly at aerodromes). It is preferable to digitize the signals;

(g) Disturbance due to rising or setting of the sun, and poor initial orientation of the transmissometers;

(h) Atmospheric pollution dirtying the optical systems;
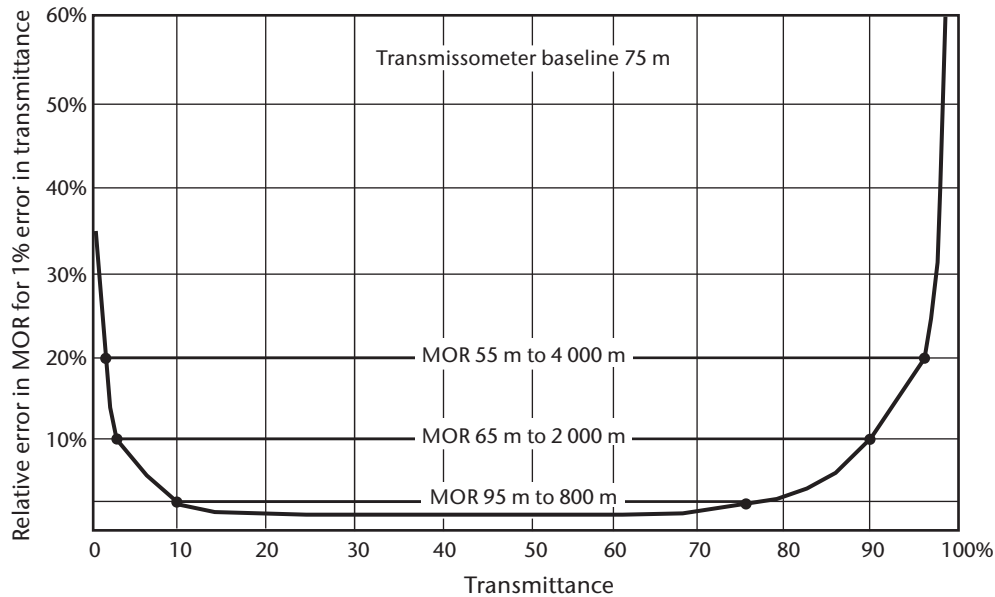
Figure 9.7. Error in measurements of meteorological optical range as a function of a 1% error in transmittance

(i)   Local atmospheric conditions (for example, rain showers and strong winds, snow) giving unrepresentative extinction coefficient readings or diverging from the Koschmieder law (snow, ice crystals, rain, and so forth). Extra absorption by sand and dust affects visibility and its measurement. This is taken into account by the transmissometer measurement principle. (Scatterometer measurements cannot take into account the effect of extra absorption due to the nature of the measurement principle.) Large-particle scattering and reflection creates a small amount of unwanted forward scatter in transmissometer measurements. This may affect the measurement uncertainty of transmissometer measurements, depending on the transmitter divergence and the receiver's field of view.

The use of a transmissometer that has been properly calibrated and well maintained should give good representative MOR measurements if the extinction coefficient in the optical path of the instrument is representative of the extinction coefficient everywhere within the MOR. However, a transmissometer has only a limited range over which it can provide accurate measurements of MOR. A relative error curve for MOR may be plotted by differentiating the basic transmissometer formula (see equation 9.7). Figure 9.7 shows how the relative error varies with transmission, assuming that the measurement accuracy of the transmission factor T is 1%.

This 1% value of transmission error, which may be considered as correct for many older instruments, does not include instrument drift, dirt on optical components, or the scatter of measurements due to the phenomenon itself. If the accuracy drops to around 2% to 3% (taking the other factors into account), the relative error values given on the vertical axis of the graph must be multiplied by the same factor of 2 or 3. Note also that the relative MOR measurement error increases exponentially at each end of the curve, thereby setting both upper and lower limits to the MOR measurement range. The example shown by the curve indicates the limit of the measuring range if an error of 5%, 10% or 20% is accepted at each end of the range measured, with a baseline of 75 m. It may also be deduced that, for MOR measurements between the limits of 1.25 and 10.7 times the baseline length, the relative MOR error should be low and of the order of 5%, assuming that the error of T is 1%. The relative error of MOR exceeds 10% when MOR is less than 0.87 times the baseline length or more than 27 times this length. When the measurement range is extended further, the error increases rapidly and becomes unacceptable. However, since contemporary transmissometers produce transmission errors that are clearly lower than the exemplary 1%, the usable measurement range may be extended accordingly.

Already results from the First WMO Intercomparison of Visibility Measurements (WMO, 1990) show that the best transmissometers, when properly calibrated and maintained, can provide measurements of MOR with a standard error of about 10% when MOR is up to 60 times their baseline.

Accuracy of scatter meters

The principal sources of error in measurements of MOR taken with scatter meters are as follows:

(a)   Calibration error (visibility too low or calibration carried out in unstable conditions affecting the extinction coefficient);

(b)   Lack of repeatability in terms of procedure or materials when using opaque scatterers for calibration;

(c)   Instability of system electronics;

(d)   Remote transmission of the scatter coefficient as a low-current or voltage signal subject to interference from electromagnetic fields (particularly at aerodromes). It is preferable to digitize the signals;

(e)   Disturbance due to rising or setting of the sun, and poor initial orientation of the instrument;

(f)   Atmospheric pollution dirtying the optical systems (these instruments are much less sensitive to dirt on their optics than transmissometers, but heavy soiling does have an effect);

(g)   Atmospheric conditions (for example, rain, snow, ice crystals, sand, local pollution) giving a scatter coefficient that differs from the extinction coefficient.

Results from the First WMO Intercomparison of Visibility Measurements (WMO, 1990) show that scatter meters are generally less accurate than transmissometers at low values of MOR and show greater variability in their readings. There was also evidence that scatter meters, as a class, were more affected by precipitation than transmissometers. However, the best scatter meters showed little or no susceptibility to precipitation and provided estimates of MOR with standard deviation of about 10% over a range of MOR from about 100 m to 50 km. Almost all the scatter meters in the intercomparison exhibited significant systematic error over part of their measurement range. Scatter meters showed very low susceptibility to contamination of their optical systems.

An overview of the differences between scatter meters and transmissometers is given by WMO (1992*b*).

––––––––––––––

REFERENCES AND FURTHER READING

Barteneva, O.D., 1960: Scattering functions of light in the atmospheric boundary layer. *Izv. Akad. Nauk SSR, Ser. Geofiz.* [*Bull. Acad. Sci. USSR, Geophysics Series*], 12:1237–1244.

International Civil Aviation Organization, 2013: *Meteorological Service for International Air Navigation*, Annex 3 to the Convention on International Civil Aviation. Eighteenth edition. Montreal.

International Electrotechnical Commission, 1987: *International Electrotechnical Vocabulary*, Chapter 845: Lighting, IEC 60050-845. Geneva.

International Organization for Standardization, 2012: *Air Quality – Environmental Meteorology – Part 1: Ground-based Remote Sensing of Visual Range by Lidar*, ISO 28902-1:2012. Geneva.

Jia S-J. and D-R. Lü, 2014: Optimal forward-scattering angles of atmospheric aerosols in North China. *Atmospheric and Oceanic Science Letters*, 7(3):236–242.

Klett, J.D., 1985: Lidar inversion with variable backscatter/extinction ratios. *Applied Optics*, 24(11):1638–1643.

Kneizys, F.X., E.P. Shettle, W.O. Gallery, J.H. Chetwynd, L.W. Abreu, J.E.A. Selby, S.A. Clough and R.W. Fenn, 1983: *Atmospheric Transmittance/Radiance: Computer Code LOWTRAN 6*, Appendix D. AFGL-TR-83-0187, Environmental Research Papers No. 846. Air Force Geophysics Laboratory, Massachusetts.

Middleton, W.E.K., 1952: *Vision Through the Atmosphere*. University of Toronto Press, Toronto.

Sheppard, B.E., 1983: Adaptation to MOR. *Preprints of the Fifth Symposium on Meteorological Observations and Instrumentation* (Toronto, 11–15 April 1983), pp. 226–269.

Van de Hulst, H.C., 1957: *Light Scattering by Small Particles*. Wiley & Sons, New York (repr. Dover Books on Physics, 1981).

World Meteorological Organization, 1990: *The First WMO Intercomparison of Visibility Measurements: Final Report* (D.J. Griggs, D.W. Jones, M. Ouldridge and W.R. Sparks). Instruments and Observing Methods Report No. 41 (WMO/TD-No. 401). Geneva.

——, 1992*a*: *International Meteorological Vocabulary* (WMO-No. 182). Geneva.

——, 1992*b*: Visibility measuring instruments: Differences between scatterometers and transmissometers (J.P. van der Meulen). *Papers Presented at the WMO Technical Conference on Instruments and Methods of Observation (TECO-92)* (Vienna, Austria, 11–15 May 1992), Instruments and Observing Methods Report No. 49 (WMO/TD-No. 462). Geneva.

——, 2010*a*: *Manual on the Global Observing System* (WMO-No. 544), Volume I. Geneva.

——, 2010*b*: *Guide to the Global Observing System* (WMO-No. 488). Geneva.

——, 2014: *Guide to Meteorological Observing and Information Distribution Systems for Aviation Weather Services* (WMO-No. 731). Geneva.

CHAPTER CONTENTS

CHAPTER 10. MEASUREMENT OF EVAPORATION

10.1 GENERAL

10.1.1 Definitions

The *International Glossary of Hydrology* (WMO/UNESCO, 2012) and the *International Meteorological Vocabulary* (WMO, 1992) present the following definitions (but note some differences):

(Actual) evaporation: Quantity of water evaporated from an open water surface or from the ground.

Transpiration: Process by which water from vegetation is transferred into the atmosphere in the form of vapour.

(Actual) evapotranspiration (or *effective evapotranspiration*): Quantity of water vapour evaporated from the soil and plants when the ground is at its natural moisture content.

Potential evaporation (or *evaporativity*): Quantity of water vapour which could be emitted by a surface of pure water, per unit surface area and unit time, under existing atmospheric conditions.

Potential evapotranspiration: Maximum quantity of water capable of being evaporated in a given climate from a continuous expanse of vegetation covering the whole ground and well supplied with water. It includes evaporation from the soil and transpiration from the vegetation from a specific region in a specific time interval, expressed as depth of water.

If the term *potential evapotranspiration* is used, the types of evaporation and transpiration occurring must be clearly indicated. For more details on these terms refer to WMO (2008), Volume I.

10.1.2 Units and scales

The rate of evaporation is defined as the amount of water evaporated from a unit surface area per unit of time. It can be expressed as the mass or volume of liquid water evaporated per area in unit of time, usually as the equivalent depth of liquid water evaporated per unit of time from the whole area. The unit of time is normally a day. The amount of evaporation should be read in millimetres (WMO, 2010). Depending on the type of instrument, the usual measuring accuracy is 0.1 to 0.01 mm.

10.1.3 Meteorological requirements

Estimates both of evaporation from free water surfaces and from the ground and of evapotranspiration from vegetation-covered surfaces are of great importance to hydrological modelling and in hydrometeorological and agricultural studies, for example, for the design and operation of reservoirs and irrigation and drainage systems.

Performance requirements are given in Part I, Chapter 1. For daily totals, an extreme outer range is 0 to 100 mm, with a resolution of 0.1 mm. The uncertainty, at the 95% confidence level, should be ±0.1 mm for amounts of less than 5 mm, and ±2% for larger amounts. A figure of 1 mm has been proposed as an achievable accuracy. In principle, the usual instruments could meet these accuracy requirements, but difficulties with exposure and practical operation cause much larger errors (WMO, 1976).

Factors affecting the rate of evaporation from any body or surface can be broadly divided into two groups, meteorological factors and surface factors, either of which may be rate-limiting.

The meteorological factors may, in turn, be subdivided into energy and aerodynamic variables. Energy is needed to change water from the liquid to the vapour phase; in nature, this is largely supplied by solar and terrestrial radiation. Aerodynamic variables, such as wind speed at the surface and vapour pressure difference between the surface and the lower atmosphere, control the rate of transfer of the evaporated water vapour.

It is useful to distinguish between situations where free water is present on the surface and those where it is not. Factors of importance include the amount and state of the water and also those surface characteristics which affect the transfer process to the air or through the body surface. Resistance to moisture transfer to the atmosphere depends, for example, on surface roughness; in arid and semi-arid areas, the size and shape of the evaporating surface is also extremely important. Transpiration from vegetation, in addition to the meteorological and surface factors already noted, is largely determined by plant characteristics and responses. These include, for example, the number and size of stomata (openings in the leaves), and whether these are open or closed. Stomatal resistance to moisture transfer shows a diurnal response but is also considerably dependent upon the availability of soil moisture to the rooting system.

The availability of soil moisture for the roots and for the evaporation from bare soil depends on the capillary supply, namely, on the texture and composition of the soil. Evaporation from lakes and reservoirs is influenced by the heat storage of the water body.

Methods for estimating evaporation and evapotranspiration are generally indirect; either by point measurements by an instrument or gauge, or by calculation using other measured meteorological variables (WMO, 1997).

10.1.4   **Measurement methods**

Direct measurements of evaporation or evapotranspiration from extended natural water or land surfaces are not practicable at present. However, several indirect methods derived from point measurements or other calculations have been developed which provide reasonable results.

The water loss from a standard saturated surface is measured with evaporimeters, which may be classified as atmometers and pan or tank evaporimeters. These instruments do not directly measure either evaporation from natural water surfaces, actual evapotranspiration or potential evapotranspiration. The values obtained cannot, therefore, be used without adjustment to arrive at reliable estimates of lake evaporation or of actual and potential evapotranspiration from natural surfaces.

An evapotranspirometer (lysimeter) is a vessel or container placed below the ground surface and filled with soil, on which vegetation can be cultivated. It is a multi-purpose instrument for the study of several phases of the hydrological cycle under natural conditions. Estimates of evapotranspiration (or evaporation in the case of bare soil) can be made by measuring and balancing all the other water budget components of the container, namely, precipitation, underground water drainage, and change in water storage of the block of soil. Usually, surface runoff is eliminated. Evapotranspirometers can also be used for the estimation of the potential evaporation of the soil or of the potential evapotranspiration of plant-covered soil, if the soil moisture is kept at field capacity.

For reservoirs or lakes, and for plots or small catchments, estimates may be made by water budget, energy budget, aerodynamic and complementarity approaches. The latter techniques are discussed in section 10.5.

It should also be emphasized that different evaporimeters or lysimeters represent physically different measurements. The adjustment factors required for them to represent lake or actual or potential evaporation and evapotranspiration are necessarily different. Such instruments and their exposure should, therefore, always be described very carefully and precisely, in order to understand the measuring conditions as fully as possible.

More details on all methods are found in WMO (2008), Volumes I and II.

10.2 ATMOMETERS

10.2.1 Instrument types

An atmometer is an instrument that measures the loss of water from a wetted, porous surface. The wetted surfaces are either porous ceramic spheres, cylinders, plates, or exposed filter-paper discs saturated with water. The evaporating element of the livingstone atmometer is a ceramic sphere of about 5 cm in diameter, connected to a water reservoir bottle by a glass or metal tube. The atmospheric pressure on the surface of the water in the reservoir keeps the sphere saturated with water. The Bellani atmometer consists of a ceramic disc fixed in the top of a glazed ceramic funnel, into which water is conducted from a burette that acts as a reservoir and measuring device. The evaporating element of the Piche evaporimeter is a disc of filter paper attached to the underside of an inverted graduated cylindrical tube, closed at one end, which supplies water to the disc. Successive measurements of the volume of water remaining in the graduated tube will give the amount lost by evaporation in any given time.

10.2.2 Measurement taken by atmometers

Although atmometers are frequently considered to give a relative measure of evaporation from plant surfaces, their measurements do not, in fact, bear any simple relation to evaporation from natural surfaces.

Readings from Piche evaporimeters with carefully standardized shaded exposures have been used with some success to derive the aerodynamic term, a multiplication of a wind function and the saturation vapour pressure deficit, required for evaporation estimation by, for example, Penman's combination method after local correlations between them were obtained.

While it may be possible to relate the loss from atmometers to that from a natural surface empirically, a different relation may be expected for each type of surface and for differing climates. Atmometers are likely to remain useful in small-scale surveys. Their great advantages are their small size, low cost and small water requirements. Dense networks of atmometers can be installed over a small area for micrometeorological studies. The use of atmometers is not recommended for water resource surveys if other data are available.

10.2.3 Sources of error in atmometers

One of the major problems in the operation of atmometers is keeping the evaporating surfaces clean. Dirty surfaces will affect significantly the rate of evaporation, in a way comparable to the wet bulb in psychrometry.

Furthermore, the effect of differences in their exposure on evaporation measurements is often remarkable. This applies particularly to the exposure to air movement around the evaporating surface when the instrument is shaded.

10.3 EVAPORATION PANS AND TANKS

Evaporation pans or tanks have been made in a variety of shapes and sizes and there are different modes of exposing them. Among the various types of pans in use, the United States Class A pan, the Russian GGI-3000 pan and the Russian 20 m² tank are described in the following subsections. These instruments are now widely used as standard network evaporimeters and their performance has been studied under different climatic conditions over fairly wide ranges of latitude and elevation. The pan data from these instruments possess stable, albeit complicated and climate-zone-dependent, relationships with the meteorological elements determining evaporation, when standard construction and exposure instructions have been carefully followed.

The adoption of the Russian 20 m^2 tank as the international reference evaporimeter has been recommended.

10.3.1   United States Class A pan

The United States Class A pan is of cylindrical design, 25.4 cm deep and 120.7 cm in diameter. The bottom of the pan is supported 3 to 5 cm above the ground level on an open-frame wooden platform, which enables air to circulate under the pan, keeps the bottom of the pan above the level of water on the ground during rainy weather, and enables the base of the pan to be inspected without difficulty. The pan itself is constructed of 0.8 mm thick galvanized iron, copper or monel metal, and is normally left unpainted. The pan is filled to 5 cm below the rim (which is known as the reference level).

The water level is measured by means of either a hookgauge or a fixed-point gauge. The hookgauge consists of a movable scale and vernier fitted with a hook, the point of which touches the water surface when the gauge is correctly set. A stilling well, about 10 cm across and about 30 cm deep, with a small hole at the bottom, breaks any ripples that may be present in the tank, and serves as a support for the hookgauge during an observation. The pan is refilled whenever the water level, as indicated by the gauge, drops by more than 2.5 cm from the reference level.

10.3.2   Russian GGI-3000 pan

The Russian GGI-3000 pan is of cylindrical design, with a surface area of 3 000 cm^2 and a depth of 60 cm. The bottom of the pan is cone-shaped. The pan is set in the soil with its rim 7.5 cm above the ground. In the centre of the tank is a metal index tube upon which a volumetric burette is set when evaporation observations are made. The burette has a valve, which is opened to allow its water level to equalize that in the pan. The valve is then closed and the volume of water in the burette is accurately measured. The height of the water level above the metal index tube is determined from the volume of water in, and the dimensions of, the burette. A needle attached to the metal index tube indicates the height to which the water level in the pan should be adjusted. The water level should be maintained so that it does not fall more than 5 mm or rise more than 10 mm above the needle point. A GGI-3000 raingauge with a collector that has an area of 3 000 cm^2 is usually installed next to the GGI-3000 pan.

10.3.3   Russian 20 m² tank

This tank has a surface of 20 m^2 and a diameter of about 5 m; it is cylindrical with a flat bottom and is 2 m deep. It is made of 4 to 5 mm thick welded iron sheets and is installed in the soil with its rim 7.5 cm above the ground. The inner and exposed outer surfaces of the tank are painted white. The tank is provided with a replenishing vessel and a stilling well with an index pipe upon which the volumetric burette is set when the water level in the tank is measured. Inside the stilling well, near the index pipe, a small rod terminating in a needle point indicates the height to which the water level is to be adjusted. The water level should always be maintained so that it does not fall more than 5 mm below or rise more than 10 mm above the needle point. A graduated glass tube attached laterally to the replenishing tank indicates the amount of water added to the tank and provides a rough check of the burette measurement.

10.3.4   Measurements taken by evaporation pans and tanks

The rate of evaporation from a pan or tank evaporimeter is measured by the change in level of its free water surface. This may be done by such devices as described above for Class A pans and GGI-3000 pans.

Several types of automatic evaporation pans are in use. The water level in such a pan is kept constant by releasing water into the pan from a storage tank or by removing water from the pan

when precipitation occurs. The amount of water added to, or removed from, the pan is recorded. In some tanks or pans, the level of the water is also recorded continuously by means of a float in the stilling well. The float operates a recorder.

Measurements of pan evaporation are the basis of several techniques for estimating evaporation and evapotranspiration from natural surfaces whose water loss is of interest. Measurements taken by evaporation pans are advantageous because they are, in any case, the result of the impact of the total meteorological variables, and because pan data are available immediately and for any period required. Pans are, therefore, frequently used to obtain information about evaporation on a routine basis within a network.

10.3.5 Exposure of evaporation pans and tanks

Three types of exposures are mainly used for pans and tanks as follows:

(a) Sunken, where the main body of the tank is below ground level, the evaporating surface being at or near the level of the surrounding surface;

(b) Above ground, where the whole of the pan and the evaporation surface are at some small height above the ground;

(c) Mounted on moored floating platforms on lakes or other water bodies.

Evaporation stations should be located at sites that are fairly level and free from obstructions such as trees, buildings, shrubs or instrument shelters. Such single obstructions, when small, should not be closer than 5 times their height above the pan; for clustered obstructions, this becomes 10 times. Plots should be sufficiently large to ensure that readings are not influenced by spray drift or by upwind edge effects from a cropped or otherwise different area. Such effects may extend to more than 100 m. The plot should be fenced off to protect the instruments and to prevent animals from interfering with the water level; however, the fence should be constructed in such a way that it does not affect the wind structure over the pan.

The ground cover at the evaporation station should be maintained as similar as possible to the natural cover common to the area. Grass, weeds, and the like should be cut frequently to keep them below the level of the pan rim with regard to sunken pans (7.5 cm). Preferably this same grass height of below 7.5 cm applies also to Class A pans. Under no circumstance should the instrument be placed on a concrete slab or asphalt, or on a layer of crushed rock. This type of evaporimeter should not be shaded from the sun.

10.3.6 Sources of error in evaporation pans and tanks

The mode of pan exposure leads both to various advantages and to sources of measurement errors.

Pans installed above the ground are inexpensive and easy to install and maintain. They stay cleaner than sunken tanks as dirt does not, to any large extent, splash or blow into the water from the surroundings. Any leakage that develops after installation is relatively easy to detect and rectify. However, the amount of water evaporated is greater than that from sunken pans, mainly because of the additional radiant energy intercepted by the sides. Adverse side-wall effects can be largely eliminated by using an insulated pan, but this adds to the cost, would violate standard construction instructions and would change the "stable" relations mentioned in section 10.3.

Sinking the pan into the ground tends to reduce objectionable boundary effects, such as radiation on the side walls and heat exchange between the atmosphere and the pan itself. But the disadvantages are as follows:

(a) More unwanted material collects in the pan, with the result that it is difficult to clean;

(b)   Leaks cannot easily be detected and rectified;

(c)   The height of the vegetation adjacent to the pan is somewhat more critical. Moreover, appreciable heat exchange takes place between the pan and the soil, and this depends on many factors, including soil type, water content and vegetation cover.

A floating pan approximates more closely evaporation from the lake than from an onshore pan exposed either above or at ground level, even though the heat-storage properties of the floating pan are different from those of the lake. It is, however, influenced by the particular lake in which it floats and it is not necessarily a good indicator of evaporation from the lake. Observational difficulties are considerable and, in particular, splashing frequently renders the data unreliable. Such pans are also costly to install and operate.

In all modes of exposure it is most important that the tank should be made of non-corrosive material and that all joints be made in such a way as to minimize the risk of the tank developing leaks.

Heavy rain and very high winds are likely to cause splash-out from pans and may invalidate the measurements.

The level of the water surface in the evaporimeter is important. If the evaporimeter is too full, as much as 10% (or more) of any rain falling may splash out, leading to an overestimate of evaporation. Too low a water level will lead to a reduced evaporation rate (of about 2.5% for each centimetre below the reference level of 5 cm, in temperate regions) due to excessive shading and sheltering by the rim. If the water depth is allowed to become very shallow, the rate of evaporation rises due to increased heating of the water surface.

It is advisable to restrict the permitted water-level range either by automatic methods, by adjusting the level at each reading, or by taking action to remove water when the level reaches an upper-limit mark, and to add water when it reaches a lower-limit mark.

10.3.7   Maintenance of evaporation pans and tanks

An inspection should be carried out at least once a month, with particular attention being paid to the detection of leaks. The pan should be cleaned out as often as necessary to keep it free from litter, sediment, scum and oil films. It is recommended that a small amount of copper sulphate, or of some other suitable algacide, be added to the water to restrain the growth of algae.

If the water freezes, all the ice should be broken away from the sides of the tank and the measurement of the water level should be taken while the ice is floating. Provided that this is done, the fact that some of the water is frozen will not significantly affect the water level. If the ice is too thick to be broken the measurement should be postponed until it can be broken, the evaporation should then be determined for the extended period.

It is often necessary to protect the pan from birds and other small animals, particularly in arid and tropical regions. This may be achieved by the use of the following:

(a)   Chemical repellents: In all cases where such protection is used, care must be taken not to change significantly the physical characteristics of the water in the evaporimeter;

(b)   A wire-mesh screen supported over the pan: Standard screens of this type are in routine use in a number of areas. They prevent water loss caused by birds and animals, but also reduce the evaporation loss by partly shielding the water from solar radiation and by reducing wind movement over the water surface. In order to obtain an estimate of the error introduced by the effect of the wire-mesh screen on the wind field and the thermal characteristics of the pan, it is advisable to compare readings from the protected pan with those of a standard pan at locations where interference does not occur. Tests with a

protective cylinder made of 25 mm hexagonal-mesh steel wire netting supported by an 8 mm steel-bar framework showed a consistent reduction of 10% in the evaporation rate at three different sites over a two-year period.

10.4 EVAPOTRANSPIROMETERS (LYSIMETERS)

Several types of lysimeters have been described in the technical literature. Details of the design of some instruments used in various countries are described in WMO (1966, 2008 (Volume I)).

In general, a lysimeter consists of the soil-filled inner container and retaining walls or an outer container, as well as special devices for measuring percolation and changes in the soil-moisture content.

There is no universal international standard lysimeter for measuring evapotranspiration. The surface area of lysimeters in use varies from 0.05 to some 100 m² and their depth varies from 0.1 to 5 m. According to their method of operation, lysimeters can be classified into non-weighable and weighable instruments. Each of these devices has its special merits and drawbacks, and the choice of any type of lysimeter depends on the problem to be studied.

Non-weighable (percolation-type) lysimeters can be used only for long-term measurements, unless the soil-moisture content can be measured by some independent and reliable technique. Large-area percolation-type lysimeters are used for water budget and evapotranspiration studies of tall, deep-rooting vegetation cover, such as mature trees. Small, simple types of lysimeters in areas with bare soil or grass and crop cover could provide useful results for practical purposes under humid conditions. This type of lysimeter can easily be installed and maintained at a low cost and is, therefore, suitable for network operations.

Weighable lysimeters, unless of a simple microlysimeter-type for soil evaporation, are much more expensive, but their advantage is that they secure reliable and precise estimates of short-term values of evapotranspiration, provided that the necessary design, operation and siting precautions have been taken.

Several weighing techniques using mechanical or hydraulic principles have been developed. The simpler, small lysimeters are usually lifted out of their sockets and transferred to mechanical scales by means of mobile cranes. The container of a lysimeter can be mounted on a permanently installed mechanical scale for continuous recording. The design of the weighing and recording system can be considerably simplified by using load cells with strain gauges of variable electrical resistance. The hydraulic weighing systems use the principle of fluid displacement resulting from the changing buoyancy of a floating container (so-called floating lysimeter), or the principle of fluid pressure changes in hydraulic load cells.

The large weighable and recording lysimeters are recommended for precision measurements in research centres and for standardization and parameterization of other methods of evapotranspiration measurement and the modelling of evapotranspiration. Small weighable types of lysimeters are quite useful and suitable for network operation. Microlysimeters for soil evaporation are a relatively new phenomenon.

10.4.1 Measurements taken by lysimeters

The rate of evapotranspiration may be estimated from the general equation of the water budget for the lysimeter containers. Evapotranspiration equals precipitation/irrigation minus percolation minus change in water storage.

Hence, the observational programme on lysimeter plots includes precipitation/irrigation, percolation and change in soil water storage. It is useful to complete this programme through observations of plant growth and development.

Precipitation – and irrigation, if any – is preferably measured at ground level by standard methods. Percolation is collected in a tank and its volume may be measured at regular intervals or recorded. For precision measurements of the change in water storage, the careful gravimetric techniques described above are used. When weighing, the lysimeter should be sheltered to avoid wind-loading effects.

The application of the volumetric method is quite satisfactory for estimating long-term values of evapotranspiration. With this method, measurements are taken of the amount of precipitation and percolation. It is assumed that a change in water storage tends to zero over the period of observation. Changes in the soil moisture content may be determined by bringing the moisture in the soil up to field capacity at the beginning and at the end of the period.

10.4.2   Exposure of evapotranspirometers

Observations of evapotranspiration should be representative of the plant cover and moisture conditions of the general surroundings of the station (WMO, 2010). In order to simulate representative evapotranspiration rates, the soil and plant cover of the lysimeter should correspond to the soil and vegetation of the surrounding area, and disturbances caused by the existence of the instrument should be minimized. The most important requirements for the exposure of lysimeters are given below.

In order to maintain the same hydromechanical properties of the soil, it is recommended that the lysimeter be placed into the container as an undisturbed block (monolith). In the case of light, rather homogenous soils and a large container, it is sufficient to fill the container layer by layer in the same sequence and with the same density as in the natural profile.

In order to simulate the natural drainage process in the container, restricted drainage at the bottom must be prevented. Depending on the soil texture, it may be necessary to maintain the suction at the bottom artificially by means of a vacuum supply.

Apart from microlysimeters for soil evaporation, a lysimeter should be sufficiently large and deep, and its rim as low as practicable, to make it possible to have a representative, free-growing vegetation cover, without restriction to plant development.

In general, the siting of lysimeters is subject to fetch requirements, such as that of evaporation pans, namely, the plot should be located beyond the zone of influence of buildings, even single trees, meteorological instruments, and so on. In order to minimize the effects of advection, lysimeter plots should be located at a sufficient distance from the upwind edge of the surrounding area, that is, not less than 100 to 150 m. The prevention of advection effects is of special importance for measurements taken at irrigated land surfaces.

10.4.3   Sources of error in lysimeter measurements

Lysimeter measurements are subject to several sources of error caused by the disturbance of the natural conditions by the instrument itself. Some of the major effects are as follows:

(a)   Restricted growth of the rooting system;

(b)   Change of eddy diffusion by discontinuity between the canopy inside the lysimeter and in the surrounding area. Any discontinuity may be caused by the annulus formed by the containing and retaining walls and by discrepancies in the canopy itself;

(c)   Insufficient thermal equivalence of the lysimeter to the surrounding area caused by:

     (i)   Thermal isolation from the subsoil;

     (ii)   Thermal effects of the air rising or descending between the container and the retaining walls;

    (iii)   Alteration of the thermal properties of the soil through alteration of its texture and its moisture conditions;

(d)   Insufficient equivalence of the water budget to that of the surrounding area caused by:

    (i)   Disturbance of soil structure;

    (ii)   Restricted drainage;

    (iii)   Vertical seepage at walls;

    (iv)   Prevention of surface runoff and lateral movement of soil water.

Some suitable arrangements exist to minimize lysimeter measurement errors, for example, regulation of the temperature below the container, reduction of vertical seepage at the walls by flange rings, and so forth. In addition to the careful design of the lysimeter equipment, sufficient representativeness of the plant community and the soil type of the area under study is of great importance. Moreover, the siting of the lysimeter plot must be fully representative of the natural field conditions.

10.4.4   **Lysimeters maintenance**

Several arrangements are necessary to maintain the representativeness of the plant cover inside the lysimeter. All agricultural and other operations (sowing, fertilizing, mowing, and the like) in the container and surrounding area should be carried out in the same way and at the same time. In order to avoid errors due to rainfall catch, the plants near and inside the container should be kept vertical, and broken leaves and stems should not extend over the surface of the lysimeter.

The maintenance of the technical devices is peculiar to each type of instrument and cannot be described here.

It is advisable to test the evapotranspirometer for leaks at least once a year by covering its surface to prevent evapotranspiration and by observing whether, over a period of days, the volume of drainage equals the amount of water added to its surface.

10.5   **ESTIMATION OF EVAPORATION FROM NATURAL SURFACES**

Consideration of the factors which affect evaporation, as outlined in section 10.1.3, indicates that the rate of evaporation from a natural surface will necessarily differ from that of an evaporimeter exposed to the same atmospheric conditions, because the physical characteristics of the two evaporating surfaces are not identical.

In practice, evaporation or evapotranspiration rates from natural surfaces are of interest, for example, reservoir or lake evaporation, crop evaporation, as well as areal amounts from extended land surfaces such as catchment areas.

In particular, accurate areal estimates of evapotranspiration from regions with varied surface characteristics and land-use patterns are very difficult to obtain (WMO, 1966, 1997).

Suitable methods for the estimation of lake or reservoir evaporation are the water budget, energy budget and aerodynamic approaches, the combination method of aerodynamic and energy-balance equations, and the use of a complementarity relationship between actual and potential evaporation. Furthermore, pan evaporation techniques exist which use pan evaporation for the establishment of a lake-to-pan relation. Such relations are specific to each pan type and mode of exposure. They also depend on the climatic conditions (see WMO, 1985, 2008 (Volume I, Chapter 4)).

The water non-limiting point or areal values of evapotranspiration from vegetation-covered land surfaces may be obtained by determining such potential (or reference crop) evapotranspiration with the same methods as those indicated above for lake applications, but adapted to vegetative conditions. Some methods use additional growth stage-dependent coefficients for each type of vegetation, such as crops, and/or an integrated crop stomatal resistance value for the vegetation as a whole.

The Royal Netherlands Meteorological Institute employs the following procedure established by G.F. Makkink (Hooghart, 1971) for calculating the daily (24 h) reference vegetation evaporation from the averaged daily air temperature and the daily amount of global radiation as follows:

Saturation vapour pressure at air temperature T:

$$e_s(T) = 6.107 \cdot 10^{7.5 \cdot \frac{T}{237.3+T}} \qquad \text{hPa}$$

Slope of the curve of saturation water vapour pressure versus temperature at T:

$$\Delta(T) = \frac{7.5 \cdot 237.3}{(237.3+T)^2} \cdot \ln(10) \cdot e_s(T) \qquad \text{hPa/°C}$$

Psychrometric constant:

$$\Delta(T) = 0.646 + 0.0006T \qquad \text{hPa/°C}$$

Specific heat of evaporation of water:

$$\lambda(T) = 1\,000 \cdot (2\,501 - 2.38 \cdot T) \qquad \text{J/kg}$$

Density of water:

$$\rho = 1\,000 \qquad \text{kg/m}^3$$

Global radiation (24 h amount):

$$Q \qquad \text{J/m}^2$$

Air temperature (24 h average):

$$T \qquad \text{°C}$$

Daily reference vegetation evaporation:[1]

$$E_r = \frac{1000 \cdot 0.65 \cdot \delta(T)}{\{\delta(T) + \gamma(T)\} \cdot \rho \cdot \lambda(T)} \cdot Q \qquad \text{mm}$$

By relating the measured rate of actual evapotranspiration to estimates of the water non-limiting potential evapotranspiration and subsequently relating this normalized value to the soil water content, soil water deficits, or the water potential in the root zone, it is possible to devise coefficients with which the actual evapotranspiration rate can be calculated for a given soil water status.

Point values of actual evapotranspiration from land surfaces can be estimated more directly from observations of the changes in soil water content measured by sampling soil moisture on a regular basis. Evapotranspiration can be measured even more accurately using a weighing lysimeter. Further methods make use of turbulence measurements (for example, eddy-correlation method) and profile measurements (for example, in boundary-layer data methods and, at two heights, in the Bowen-ratio energy-balance method). They are much more expensive and require special instruments and sensors for humidity, wind speed and temperature. Such estimates, valid for the type of soil and canopy under study, may be used as reliable independent reference values in the development of empirical relations for evapotranspiration modelling.

The difficulty in determining basin evapotranspiration arises from the discontinuities in surface characteristics which cause variable evapotranspiration rates within the area under

---

[1]   The constant 1 000 is for conversion from metres to millimetres; the constant 0.65 is a typical empirical constant.

consideration. When considering short-term values, it is necessary to estimate evapotranspiration by using empirical relationships. Over a long period (in order to minimize storage effects) the water-budget approach can be used to estimate basin evapotranspiration (see WMO, 1971). One approach, suitable for estimates from extended areas, refers to the atmospheric water balance and derives areal evapotranspiration from radiosonde data. WMO (2008, Volume I, Chapter 4) describes the above-mentioned methods, their advantages and their application limits.

The measurement of evaporation from a snow surface is difficult and probably no more accurate than the computation of evaporation from water.

Evaporimeters made of polyethylene or colourless plastic are used in many countries for the measurement of evaporation from snow-pack surfaces; observations are made only when there is no snowfall.

Estimates of evaporation from snow cover can be made from observations of air humidity and wind speed at one or two levels above the snow surface and at the snow-pack surface, using the turbulent diffusion equation. The estimates are most reliable when evaporation values are computed for periods of five days or more.

_____

REFERENCES AND FURTHER READING

Hooghart, J.C. (ed.), 1971: *Evaporation and Weather*. TNO Committee of Hydrological Research, Technical Meeting 44, Proceedings and Information No. 39, TNO, The Hague.

World Meteorological Organization, 1966: *Measurement and Estimation of Evaporation and Evapotranspiration*. Technical Note No. 83 (WMO-No. 201, TP. 105). Geneva.

——, 1971: *Problems of Evaporation Assessment in the Water Balance* (C.E. Hounam). WMO/IHD Report No. 13 (WMO-No. 285). Geneva.

——, 1973: *Atmospheric Vapour Flux Computations for Hydrological Purposes* (J.P. Peixoto). WMO/IHD Report No. 20 (WMO-No. 357). Geneva.

——, 1976: *The CIMO International Evaporimeter Comparisons* (WMO-No. 449). Geneva.

——, 1977: *Hydrological Application of Atmospheric Vapour-Flux Analyses* (E.M. Rasmusson). Operational Hydrology Report No. 11 (WMO-No. 476). Geneva.

——, 1985: *Casebook on Operational Assessment of Areal Evaporation*. Operational Hydrology Report No. 22 (WMO-No. 635). Geneva.

——, 1992: *International Meteorological Vocabulary* (WMO-No. 182). Geneva.

——, 1997: *Estimation of Areal Evapotranspiration.* Technical Reports in Hydrology and Water Resources No. 56 (WMO/TD-No. 785). Geneva.

——, 2008: *Guide to Hydrological Practices* (WMO-No. 168), Volumes I and II. Geneva.

——, 2010: *Manual on the Global Observing System* (WMO-No. 544), Volume I. Geneva.

World Meteorological Organization/United Nations Educational, Scientific and Cultural Organization, 2012: *International Glossary of Hydrology* (WMO-No. 385). Geneva.

_____

CHAPTER CONTENTS

CHAPTER 11. MEASUREMENT OF SOIL MOISTURE

11.1 GENERAL

Soil moisture is an important component in the atmospheric water cycle, both on a small agricultural scale and in large-scale modelling of land/atmosphere interaction. Vegetation and crops always depend more on the moisture available at root level than on precipitation occurrence. Water budgeting for irrigation planning, as well as the actual scheduling of irrigation action, requires local soil moisture information. Knowledge of the degree of soil wetness helps to understand the initiation of convective events and to forecast the risk of flash floods or the occurrence of fog.

Nevertheless, soil moisture has been seldom observed routinely at meteorological stations. Documentation of soil wetness was usually restricted to the description of the "state of the ground" by means of WMO Code Tables 0901 and 0975, and its measurement was left to hydrologists, agriculturalists and other actively interested parties. Around 1990, the interest of meteorologists in soil moisture measurement increased. This was partly because, after the pioneering work by Deardorff (1978), numerical atmosphere models at various scales became more adept at handling fluxes of sensible and latent heat in soil surface layers. Moreover, newly developed soil moisture measurement techniques are more feasible for meteorological stations than most of the classic methods.

To satisfy the increasing need for determining soil moisture status, the most commonly used methods and instruments will be discussed, including their advantages and disadvantages. Some less common observation techniques are also mentioned. This chapter discusses both in situ and remote-sensing soil moisture measurements. Space-based remote-sensing is also included, complemented by information in Part III of this Guide.

11.1.1 Definitions

Soil moisture determinations measure either the soil water content or the soil water potential.

Soil water content

Soil water content is an expression of the mass or volume of water in the soil, while the soil water potential is an expression of the soil water energy status. The relation between content and potential is not universal and depends on the characteristics of the local soil, such as soil density and soil texture.

Soil water content on the basis of mass is expressed in the gravimetric soil moisture content, θ_g, defined by:

$$\theta_g = M_{water}/M_{soil} \tag{11.1}$$

where M_{water} is the mass of the water in the soil sample and M_{soil} is the mass of dry soil that is contained in the sample. Values of θ_g in meteorology are usually expressed in %.

Because precipitation, evapotranspiration and solute transport variables are commonly expressed in terms of flux, volumetric expressions for water content are often more useful. The volumetric soil moisture content of a soil sample, θ_v, is defined as:

$$\theta_v = V_{water}/V_{sample} \tag{11.2}$$

where V_{water} is the volume of water in the soil sample and V_{sample} is the total volume of dry soil + air + water in the sample. Again, the ratio is usually expressed in %, although many research communities are now adopting volumetric water content (m^3/m^3) as the standard for expressing soil moisture. The relationship between gravimetric and volumetric moisture contents is:

$$\theta_v = \theta_g \left(\rho_b / \rho_w \right) \tag{11.3}$$

where ρ_b is the dry soil bulk density and ρ_w is the soil water density.

The basic technique for measuring soil water content is the gravimetric method, described in section 11.2. Because this method is based on direct measurements, it is the standard with which all other methods are compared. Unfortunately, gravimetric sampling is destructive, rendering repeat measurements on the same soil sample impossible. Because of the difficulties of accurately measuring dry soil and water volumes, volumetric water contents are not usually determined directly.

Soil water potential

Soil water potential describes the energy status of the soil water and is an important parameter for water transport analysis, water storage estimates and soil-plant-water relationships. A difference in water potential between two soil locations indicates a tendency for water flow, from high to low potential. When the soil is drying, the water potential becomes more negative and the work that must be done to extract water from the soil increases. This makes water uptake by plants more difficult, so the water potential in the plant drops, resulting in plant stress and, eventually, severe wilting.

Formally, the water potential is a measure of the ability of soil water to perform work, or, in the case of negative potential, the work required to remove the water from the soil. The total water potential ψ_t, the combined effect of all force fields, is given by:

$$\psi_t = \psi_z + \psi_m + \psi_o + \psi_p \tag{11.4}$$

where ψ_z is the gravitational potential based on elevation above the mean sea level; ψ_m is the matric potential, suction due to attraction of water by the soil matrix; ψ_o is the osmotic potential, due to energy effects of solutes in water; and ψ_p is the pressure potential, the hydrostatic pressure below a water surface.

The potentials which are not related to the composition of water or soil are together called hydraulic potential, ψ_h. In saturated soil, this is expressed as $\psi_h = \psi_z + \psi_p$, while in unsaturated soil, it is expressed as $\psi_h = \psi_z + \psi_m$. When the phrase "water potential" is used in studies, sometimes with the notation ψ_w, it is advisable to check the author's definition because this term has been used for $\psi_m + \psi_z$ as well as for $\psi_m + \psi_o$.

The gradients of the separate potentials will not always be significantly effective in inducing flow. For example, ψ_o requires a semi-permeable membrane to induce flow, and ψ_p will exist in saturated or ponded conditions, but most practical applications are in unsaturated soil.

11.1.2   **Units**

In solving the mass balance or continuity equations for water, it must be remembered that the components of water content parameters are not dimensionless. Gravimetric water content is the weight of soil water contained in a unit weight of soil (kg water/kg dry soil). Likewise, volumetric water content is a volume fraction (m³ water/m³ soil).

The basic unit for expressing water potential is energy (in joules = kg m² s⁻²) per unit mass, J kg⁻¹. Alternatively, energy per unit volume (J m⁻³) is equivalent to pressure, expressed in pascals (Pa = kg m⁻¹ s⁻²). Units encountered in older literature are bar (= 100 kPa), atmosphere (= 101.32 kPa), or pounds per square inch (= 6.895 kPa). A third class of units are those of pressure head in (centi)metres of water or mercury, energy per unit weight. The relation of the three potential unit classes is:

$$\psi \left(J\ kg^{-1} \right) = \gamma \cdot \psi \left(Pa \right) = \left[\psi \left(m \right) \right] \big/ g \tag{11.5}$$

where $\gamma = 10^3$ kg m^{-3} (density of water) and g = 9.81 m s^{-2} (gravity acceleration). Because the soil water potential has a large range, it is often expressed logarithmically, usually in pressure head of water. A common unit for this is called pF, and is equal to the base 10 logarithm of the absolute value of the head of water expressed in centimetres.

11.1.3   **Meteorological requirements**

Soil consists of individual particles and aggregates of mineral and organic materials, separated by spaces or pores which are occupied by water and air. The relative amount of pore space decreases with increasing soil grain size (intuitively one would expect the opposite). The movement of liquid water through soil depends upon the size, shape and generally the geometry of the pore spaces.

If a large quantity of water is added to a block of otherwise "dry" soil, some of it will drain away rapidly by the effects of gravity through any relatively large cracks and channels. The remainder will tend to displace some of the air in the spaces between particles, the larger pore spaces first. Broadly speaking, a well-defined "wetting front" will move downwards into the soil, leaving an increasingly thick layer retaining all the moisture it can hold against gravity. That soil layer is then said to be at "field capacity", a state that for most soils occurs about $\psi_m \approx -33$ J/kg, with a range of values from –1 J/kg for organic soils to –100 J/kg for heavy clay soils. A value of –10 J/kg (pF $\approx$ 2) can be assigned for a loamy sand soil. This state must not be confused with the undesirable situation of "saturated" soil, where all the pore spaces are occupied by water. After a saturation event, such as heavy rain, the soil usually needs at least 24 h to reach field capacity. When moisture content falls below field capacity, the subsequent limited movement of water in the soil is partly liquid, partly in the vapour phase by distillation (related to temperature gradients in the soil), and sometimes by transport in plant roots.

Plant roots within the block will extract liquid water from the water films around the soil particles with which they are in contact. The rate at which this extraction is possible depends on the soil moisture potential. A point is reached at which the forces holding moisture films to soil particles cannot be overcome by root suction, and plants are starved of water and lose turgidity: soil moisture has reached the "wilting point", which in most cases occurs at a soil water potential of –1.5 MPa (pF = 4.2). In agriculture, the soil water available to plants is commonly taken to be the quantity between field capacity and the wilting point, and this varies highly between soils: in sandy soils it may be less than 10 volume per cent, while in soils with much organic matter it can be over 40 volume per cent.

Usually it is desirable to know the soil moisture content and potential as a function of depth. Evapotranspiration models concern mostly a shallow depth (tens of centimetres); agricultural applications need moisture information at root depth (order of a metre); and atmospheric general circulation models incorporate a number of layers down to a few metres. For hydrological and water-balance needs – such as catchment-scale runoff models, as well as for effects upon soil properties such as soil mechanical strength, thermal conductivity and diffusivity – information on deep soil water content is needed. The accuracy needed in water content determinations and the spatial and temporal resolution required vary by application. An often-occurring problem is the inhomogeneity of many soils, meaning that a single observation location cannot provide absolute knowledge of the regional soil moisture, but only relative knowledge of its change.

11.1.4   **Measurement methods**

The methods and instruments available to evaluate soil water status may be classified in three ways. First, a distinction is made between the determination of water content and the determination of water potential. Second, a so-called direct method requires the availability of sizeable representative terrain from which large numbers of soil samples can be taken for destructive evaluation in the laboratory. Indirect methods use an instrument placed in the soil to measure some soil property related to soil moisture. Third, methods can be ranged according to operational applicability, taking into account the regular labour involved, the degree of

dependence on laboratory availability, the complexity of the operation and the reliability of the result. Moreover, the preliminary costs of acquiring instrumentation must be compared with the subsequent costs of local routine observation and data processing.

Reviews such as WMO (1968, 1989, 2001) and Schmugge et al. (1980) are very useful for learning about practical problems, but dielectric measurement methods were only developed well after 1980, so too-early reviews should not be relied on much when choosing an operational method.

There are five operational alternatives for the determination of soil water content. First, there is classic gravimetric moisture determination, which is a simple direct method. Second, there is lysimetry, a non-destructive variant of gravimetric measurement. A container filled with soil is weighed either occasionally or continuously to indicate changes in total mass in the container, which may in part or totally be due to changes in soil moisture (lysimeters are discussed in more detail in Part I, Chapter 10). Third, water content may be determined indirectly by various radiological techniques, such as neutron scattering and gamma absorption. Fourth, water content can be derived from the dielectric properties of soil, for example, by using time-domain reflectometry. Lastly, soil moisture can be inferred on a global scale from remotely sensed measurements of the Earth's thermal or reflective properties.

Soil water potential measurement can be performed by several indirect methods, in particular using tensiometers, resistance blocks and soil psychrometers. None of these instruments is effective at this time over the full range of possible water potential values. For extended study of all methods of various soil moisture measurements, up-to-date handbooks are provided by Klute (1986), Dirksen (1999), Gardner et al. (2001) and Mullins (2001).

11.2   GRAVIMETRIC DIRECT MEASUREMENT OF SOIL WATER CONTENT

The gravimetric soil moisture content θ_g is typically determined directly. Soil samples of about 50 g are removed from the field with the best available tools (shovels, spiral hand augers, bucket augers, perhaps power-driven coring tubes), disturbing the sample soil structure as little as possible (Dirksen, 1999). The soil sample should be placed immediately in a leak-proof, seamless, pre-weighed and identified container. As the samples will be placed in an oven, the container should be able to withstand high temperatures without melting or losing significant mass. The most common soil containers are aluminium cans, but non-metallic containers should be used if the samples are to be dried in microwave ovens in the laboratory. If soil samples are to be transported for a considerable distance, tape should be used to seal the container to avoid moisture loss by evaporation.

The samples and container are weighed in the laboratory both before and after drying, the difference being the mass of water originally in the sample. The drying procedure consists in placing the open container in an electrically heated oven at 105 °C until the mass stabilizes at a constant value. The drying times required usually vary between 16 and 24 h. Note that drying at 105 ± 5 °C is part of the usually accepted definition of "soil water content", originating from the aim to measure only the content of "free" water which is not bound to the soil matrix (Gardner et al., 2001).

If the soil samples contain considerable amounts of organic matter, excessive oxidation may occur at 105 °C and some organic matter will be lost from the sample. Although the specific temperature at which excessive oxidation occurs is difficult to specify, lowering the oven temperature from 105 °C to 70 °C seems to be sufficient to avoid significant loss of organic matter, but this can lead to water content values that are too low. Oven temperatures and drying times should be checked and reported.

Microwave oven drying for the determination of gravimetric water contents may also be used effectively (Gee and Dodson, 1981). In this method, soil water temperature is quickly raised to boiling point, then remains constant for a period due to the consumption of heat in vaporizing water. However, the temperature rapidly rises as soon as the energy absorbed by the soil water

exceeds the energy needed for vaporizing the water. Caution should be used with this method, as temperatures can become high enough to melt plastic containers if stones are present in the soil sample.

Gravimetric soil water contents of air-dry (25 °C) mineral soil are often less than 2%, but, as the soil approaches saturation, the water content may increase to values between 25% and 60%, depending on soil type. Volumetric soil water content, θ_v, may range from less than 10% for air-dry soil to between 40% and 50% for mineral soils approaching saturation. Soil θ_v determination requires measurement of soil density, for example, by coating a soil clod with paraffin and weighing it in air and water, or some other method (Campbell and Henshall, 2001).

Water contents for stony or gravelly soils can be grossly misleading. When rocks occupy an appreciable volume of the soil, they modify direct measurement of soil mass, without making a similar contribution to the soil porosity. For example, gravimetric water content may be 10% for a soil sample with a bulk density of 2 000 kg m^{-3}; however, the water content of the same sample based on finer soil material (stones and gravel excluded) would be 20% if the bulk density of fine soil material was 1 620 kg m^{-3}.

Although the gravimetric water content for the finer soil fraction, $\theta_{g,fines}$, is the value usually used for spatial and temporal comparison, there may also be a need to determine the volumetric water content for a gravelly soil. The latter value may be important in calculating the volume of water in a root zone. The relationship between the gravimetric water content of the fine soil material and the bulk volumetric water content is given by:

$$\theta_{v,stony} = \theta_{g,fines}\left(\rho_b/\rho_w\right)\left(1 + M_{stones}/M_{fines}\right) \tag{11.6}$$

where $\theta_{v,stony}$ is the bulk volumetric water content of soil containing stones or gravel and M_{stones} and M_{fines} are the masses of the stone and fine soil fractions (Klute, 1986).

11.3 SOIL WATER CONTENT: INDIRECT METHODS

The capacity of soil to retain water is a function of soil texture and structure. When removing a soil sample, the soil being evaluated is disturbed, so its water-holding capacity is altered. Indirect methods of measuring soil water are helpful as they allow information to be collected at the same location for many observations without disturbing the soil water system. Moreover, most indirect methods determine the volumetric soil water content without any need for soil density determination.

11.3.1 Radiological methods

Two different radiological methods are available for measuring soil water content. One is the widely used neutron scatter method, which is based on the interaction of high-energy (fast) neutrons and the nuclei of hydrogen atoms in the soil. The other method measures the attenuation of gamma rays as they pass through soil. Both methods use portable equipment for multiple measurements at permanent observation sites and require careful calibration, preferably with the soil in which the equipment is to be used.

When using any radiation-emitting device, some precautions are necessary. The manufacturer will provide a shield that must be used at all times. The only time the probe leaves the shield is when it is lowered into the soil access tube. When the guidelines and regulations regarding radiation hazards stipulated by the manufacturers and health authorities are followed, there is no need to fear exposure to excessive radiation levels, regardless of the frequency of use. Nevertheless, whatever the type of radiation-emitting device used, the operator should wear some type of film badge that will enable personal exposure levels to be evaluated and recorded on a monthly basis.

11.3.1.1   *Neutron scattering method*

In neutron soil moisture detection (Visvalingam and Tandy, 1972; Greacen, 1981), a probe containing a radioactive source emitting high-energy (fast) neutrons and a counter of slow neutrons is lowered into the ground. The hydrogen nuclei, having about the same mass as neutrons, are at least 10 times as effective for slowing down neutrons upon collision as most other nuclei in the soil. Because in any soil most hydrogen is in water molecules, the density of slow "thermalized" neutrons in the vicinity of the neutron probe is nearly proportional to the volumetric soil water content.

Some fraction of the slowed neutrons, after a number of collisions, will again reach the probe and its counter. When the soil water content is large, not many neutrons are able to travel far before being thermalized and ineffective, and then 95% of the counted returning neutrons come from a relatively small soil volume. In wet soil, the "radius of influence" may be only 15 cm, while in dry soil that radius may increase to 50 cm. Therefore, the measured soil volume varies with water content, and thin layers cannot be resolved. This method is hence less suitable to localize water-content discontinuities, and it cannot be used effectively in the top 20 cm of soil on account of the soil air discontinuity.

Several source and detector arrangements are possible in a neutron probe, but it is best to have a probe with a double detector and a central source, typically in a cylindrical container. Such an arrangement allows for a nearly spherical zone of influence and leads to a more linear relation of neutron count to soil water content.

A cable is used to attach a neutron probe to the main instrument electronics, so that the probe can be lowered into a previously installed access tube. The access tube should be seamless and thick enough (at least 1.25 mm) to be rigid, but not so thick that the access tube itself slows neutrons down significantly. The access tube must be made of non-corrosive material, such as stainless steel, aluminium or plastic, although polyvinylchloride should be avoided as it absorbs slow neutrons. Usually, a straight tube with a diameter of 5 cm is sufficient for the probe to be lowered into the tube without a risk of jamming. Care should be taken in installing the access tube to ensure that no air voids exist between the tube and the soil matrix. At least 10 cm of the tube should extend above the soil surface, in order to allow the box containing the electronics to be mounted on top of the access tube. All access tubes should be fitted with a removable cap to keep rainwater from entering the tubes.

In order to enhance experimental reproducibility, the soil water content is not derived directly from the number of slow neutrons detected, but rather from a count ratio (CR), given by:

$$CR = C_{\mathrm{soil}}/C_{\mathrm{background}} \qquad\qquad (11.7)$$

where C_{soil} is the count of thermalized neutrons detected in the soil and $C_{\mathrm{background}}$ is the count of thermalized neutrons in a reference medium. All neutron probe instruments now come with a reference standard for these background calibrations, usually against water. The standard in which the probe is placed should be at least 0.5 m in diameter so as to represent an "infinite" medium. Calibration to determine $C_{\mathrm{background}}$ can be done by a series of ten 1 min readings, to be averaged, or by a single 1 h reading. C_{soil} is determined from averaging several soil readings at a particular depth/location. For calibration purposes, it is best to take three samples around the access tube and to average the water contents corresponding to the average CR calculated for that depth. A minimum of five different water contents should be evaluated for each depth. Although some calibration curves may be similar, a separate calibration for each depth should be conducted. The lifetime of most probes is more than 10 years.

11.3.1.2   *Gamma-ray attenuation*

Whereas the neutron method measures the volumetric water content in a large sphere, gamma-ray absorption scans a thin layer. The dual-probe gamma device is nowadays mainly used in the laboratory since dielectric methods became operational for field use. Another reason for this is that gamma rays are more dangerous to work with than neutron scattering devices, as well as the fact that the operational costs for the gamma rays are relatively high.

Changes in gamma attenuation for a given mass absorption coefficient can be related to changes in total soil density. As the attenuation of gamma rays is due to mass, it is not possible to determine water content unless the attenuation of gamma rays due to the local dry soil density is known and remains unchanged with changing water content. Determining accurately the soil water content from the difference between the total and dry density attenuation values is therefore not simple.

Compared to neutron scattering, gamma-ray attenuation has the advantage of allowing accurate measurements at a few centimetres below the air-surface interface. Although the method has a high degree of resolution, the small soil volume evaluated will exhibit more spatial variation due to soil heterogeneities (Gardner and Calissendorff, 1967).

11.3.2　Soil water dielectrics

When a medium is placed in the electric field of a capacitor or waveguide, its influence on the electric forces in that field is expressed as the ratio between the forces in the medium and the forces which would exist in vacuum. This ratio, called permittivity or "dielectric constant", is for liquid water about 20 times larger than that of average dry soil, because water molecules are permanent dipoles. The dielectric properties of ice, and of water bound to the soil matrix, are comparable to those of dry soil. Therefore, the volumetric content of free soil water can be determined from the dielectric characteristics of wet soil by reliable, fast, non-destructive measurement methods, without the potential hazards associated with radioactive devices. Moreover, such dielectric methods can be fully automated for data acquisition. At present, two methods which evaluate soil water dielectrics are commercially available and used extensively, namely time-domain reflectometry and frequency-domain measurement.

11.3.2.1　*Time-domain reflectometry*

Time-domain reflectometry is a method which determines the dielectric constant of the soil by monitoring the travel of an electromagnetic pulse, which is launched along a waveguide formed by a pair of parallel rods embedded in the soil. The pulse is reflected at the end of the waveguide and its propagation velocity, which is inversely proportional to the square root of the dielectric constant, can be measured well by actual electronics.

The most widely used relation between soil dielectrics and soil water content was experimentally summarized by Topp et al. (1980) as follows:

$$\theta_v = -0.053 + 0.029\,\varepsilon - 5.5{\cdot}10^{-4}\varepsilon^2 + 4.3{\cdot}10^{-6}\varepsilon^3 \tag{11.8}$$

where ε is the dielectric constant of the soil water system. This empirical relationship has proved to be applicable in many soils, roughly independent of texture and gravel content (Drungil et al., 1989). However, soil-specific calibration is desirable for soils with low density or with a high organic content. For complex soil mixtures, the De Loor equation has proved useful (Dirksen and Dasberg, 1993).

Generally, the parallel probes are separated by 5 cm and vary in length from 10 to 50 cm; the rods of the probe can be of any metallic substance. The sampling volume is essentially a cylinder of a few centimetres in radius around the parallel probes (Knight, 1992). The coaxial cable from the probe to the signal-processing unit should not be longer than about 30 m. Soil water profiles can be obtained from a buried set of probes, each placed horizontally at a different depth, linked to a field data logger by a multiplexer.

11.3.2.2　*Frequency-domain measurement*

While time-domain reflectometry uses microwave frequencies in the gigahertz range, frequency-domain sensors measure the dielectric constant at a single microwave megahertz frequency. The microwave dielectric probe utilizes an open-ended coaxial cable and a single reflectometer at the probe tip to measure amplitude and phase at a particular frequency. Soil measurements

are referenced to air, and are typically calibrated with dielectric blocks and/or liquids of known dielectric properties. One advantage of using liquids for calibration is that a perfect electrical contact between the probe tip and the material can be maintained (Jackson, 1990).

As a single, small probe tip is used, only a small volume of soil is ever evaluated, and soil contact is therefore critical. As a result, this method is excellent for laboratory or point measurements, but is likely to be subject to spatial variability problems if used on a field scale (Dirksen, 1999).

11.4   SOIL WATER POTENTIAL INSTRUMENTATION

The basic instruments capable of measuring matric potential are sufficiently inexpensive and reliable to be used in field-scale monitoring programmes. However, each instrument has a limited accessible water potential range. For example, tensiometers work well only in wet soil, while resistance blocks do better in moderately dry soil.

11.4.1   Tensiometers

The most widely used and least expensive water potential measuring device is the tensiometer. Tensiometers are simple instruments, usually consisting of a porous ceramic cup and a sealed plastic cylindrical tube connecting the porous cup to some pressure-recording device at the top of the cylinder. They measure the matric potential, because solutes can move freely through the porous cup.

The tensiometer establishes a quasi-equilibrium condition with the soil water system. The porous ceramic cup acts as a membrane through which water flows, and therefore must remain saturated if it is to function properly. Consequently, all the pores in the ceramic cup and the cylindrical tube are initially filled with de-aerated water. Once in place, the tensiometer will be subject to negative soil water potentials, causing water to move from the tensiometer into the surrounding soil matrix. The water movement from the tensiometer will create a negative potential or suction in the tensiometer cylinder which will register on the recording device. For recording, a simple U-tube filled with water and/or mercury, a Bourdon-type vacuum gauge or a pressure transducer (Marthaler et al., 1983) is suitable.

If the soil water potential increases, water moves from the soil back into the tensiometer, resulting in a less negative water potential reading. This exchange of water between the soil and the tensiometer, as well as the tensiometer's exposure to negative potentials, will cause dissolved gases to be released by the solution, forming air bubbles. The formation of air bubbles will alter the pressure readings in the tensiometer cylinder and will result in faulty readings. Another limitation is that the tensiometer has a practical working limit of $\psi \approx$ –85 kPa. Beyond –100 kPa ($\approx$ 1 atm), water will boil at ambient temperature, forming water vapour bubbles which destroy the vacuum inside the tensiometer cylinder. Consequently, the cylinders occasionally need to be de-aired with a hand-held vacuum pump and then refilled.

Under drought conditions, appreciable amounts of water can move from the tensiometer to the soil. Thus, tensiometers can alter the very condition they were designed to measure. Additional proof of this process is that excavated tensiometers often have accumulated large numbers of roots in the proximity of the ceramic cups. Typically, when the tensiometer acts as an "irrigator", so much water is lost through the ceramic cups that a vacuum in the cylinder cannot be maintained, and the tensiometer gauge will be inoperative.

Before installation, but after the tensiometer has been filled with water and degassed, the ceramic cup must remain wet. Wrapping the ceramic cup in wet rags or inserting it into a container of water will keep the cup wet during transport from the laboratory to the field. In the field, a hole of the appropriate size and depth is prepared. The hole should be large enough to create a snug fit on all sides, and long enough so that the tensiometer extends sufficiently above the soil surface for de-airing and refilling access. Since the ceramic cup must remain in contact with the soil, it may be beneficial in stony soil to prepare a thin slurry of mud from the

excavated site and to pour it into the hole before inserting the tensiometer. Care should also be taken to ensure that the hole is backfilled properly, thus eliminating any depressions that may lead to ponded conditions adjacent to the tensiometer. The latter precaution will minimize any water movement down the cylinder walls, which would produce unrepresentative soil water conditions.

Only a small portion of the tensiometer is exposed to ambient conditions, but its interception of solar radiation may induce thermal expansion of the upper tensiometer cylinder. Similarly, temperature gradients from the soil surface to the ceramic cup may result in thermal expansion or contraction of the lower cylinder. To minimize the risk of temperature-induced false water potential readings, the tensiometer cylinder should be shaded and constructed of non-conducting materials, and readings should be taken at the same time every day, preferably in the early morning.

A new development is the osmotic tensiometer, where the tube of the meter is filled with a polymer solution in order to function better in dry soil. For more information on tensiometers see Dirksen (1999) and Mullins (2001).

11.4.2　　Resistance blocks

Electrical resistance blocks, although insensitive to water potentials in the wet range, are excellent companions to the tensiometer. They consist of electrodes encased in some type of porous material that within about two days will reach a quasi-equilibrium state with the soil. The most common block materials are nylon fabric, fibreglass and gypsum, with a working range of about –50 kPa (for nylon) or –100 kPa (for gypsum) up to –1 500 kPa. Typical block sizes are 4 cm × 4 cm × 1 cm. Gypsum blocks last a few years, but less in very wet or saline soil (Perrier and Marsh, 1958).

This method determines water potential as a function of electrical resistance, measured with an alternating current bridge (usually ≈ 1 000 Hz) because direct current gives polarization effects. However, resistance decreases if soil is saline, falsely indicating a wetter soil. Gypsum blocks are less sensitive to soil saltiness effects because the electrodes are consistently exposed to a saturated solution of calcium sulphate. The output of gypsum blocks must be corrected for temperature (Aggelides and Londra, 1998).

Because resistance blocks do not protrude above the ground, they are excellent for semi-permanent agricultural networks of water potential profiles, if installation is careful and systematic (WMO, 2001). When installing the resistance blocks it is best to dig a small trench for the lead wires before preparing the hole for the blocks, in order to minimize water movement along the wires to the blocks. A possible field problem is that shrinking and swelling soil may break contact with the blocks. On the other hand, resistance blocks do not affect the distribution of plant roots.

Resistance blocks are relatively inexpensive. However, they need to be calibrated individually. This is generally accomplished by saturating the blocks in distilled water and then subjecting them to a predetermined pressure in a pressure-plate apparatus (Wellings et al., 1985), at least at five different pressures before field installation. Unfortunately, the resistance is less on a drying curve than on a wetting curve, thus generating hysteresis errors in the field because resistance blocks are slow to equilibrate with varying soil wetness (Tanner and Hanks, 1952). As resistance-block calibration curves change with time, they need to be calibrated before installation and to be checked regularly afterwards, either in the laboratory or in the field.

11.4.3　　Psychrometers

Psychrometers are used in laboratory research on soil samples as a standard for other techniques (Mullins, 2001), but a field version is also available, called the Spanner psychrometer (Rawlins and Campbell, 1986). This consists of a miniature thermocouple placed within a small chamber with a porous wall. The thermocouple is cooled by the Peltier effect, condensing water on a

wire junction. As water evaporates from the junction, its temperature decreases and a current is produced which is measured by a meter. Such measurements are quick to respond to changes in soil water potential, but are very sensitive to temperature and salinity (Merrill and Rawlins, 1972).

The lowest water potential typically associated with active plant water uptake corresponds to a relative humidity of between 98% and 100%. This implies that, if the water potential in the soil is to be measured accurately to within 10 kPa, the temperature would have to be controlled to better than 0.001 K. This means that the use of field psychrometers is most appropriate for low matric potentials, of less than –300 kPa. In addition, the instrument components differ in heat capacities, so diurnal soil temperature fluctuations can induce temperature gradients in the psychrometer (Brunini and Thurtell, 1982). Therefore, Spanner psychrometers should not be used at depths of less than 0.3 m, and readings should be taken at the same time each day, preferably in the early morning. In summary, soil psychrometry is a difficult and demanding method, even for specialists.

11.5 SITE SELECTION AND SAMPLE SIZE

There is no standard depth or measurement interval at which soil moisture observations are taken, since this strongly depends on the research objectives for which the sensors are installed. The International Soil Moisture Network (ISMN; Dorigo et al., 2011) provides an extensive database with harmonized in situ soil moisture time series of networks all over the world. Here the data are harmonized to a half-hourly measurement interval whenever possible. Most networks and stations in the ISMN measure soil moisture at several depths, from 0.05 m up to 0.50 m or 1 m. As a result, the behaviour of soil moisture at different depths can be compared and used to validate measurements. Measurements of other meteorological parameters are very valuable for determining soil moisture. For example, precipitation data at the measurement site can help validate the soil moisture data.

The representativeness of any soil moisture observation point is limited because there are likely to be significant variations, both horizontally and vertically, in the soil structure (porosity, density, chemical composition), land cover and relief. It is pivotal that soil moisture and its variability be captured on the scale necessary for conducting studies on hydrological processes and for satellite validation. Gravimetric water content determinations or indirect measurements of soil moisture are only reliable at the point of measurement, making it necessary to collect a large number of samples to adequately describe the site's soil moisture status. In order to estimate the number of samples n needed at a local site to determine soil water content at an observed level of accuracy (L), the following equation can be used:

$$n = 4\left(\sigma^2 / L^2\right) \tag{11.9}$$

where σ^2 is the sample variance generated from a preliminary sampling experiment. For example, suppose that a preliminary sample yielded a (typical) σ^2 of 25% and the accuracy level needed to be within 3%, 12 samples would be required from the site (if it can be assumed that water content is normally distributed across the site). A study by Brocca et al. (2007) showed that the minimum number of point samples needed for an area in central Italy with an extent of about 9 to 8 800 m^2 varied between 15 and 35. The higher number of samples was needed for sites with more significant relief. Famiglietti et al. (2008) found that 30 samples are sufficient for a footprint of 50 km, assuming that the data are independent and spatially uncorrelated.

Upscaling the point measurements obtained by gravimetric water content determination or indirect measurements with in situ sensors has been the subject of many studies. Upscaling methods vary from relatively straightforward interpolation and time/rank stability techniques to more complicated techniques such as statistical transformations and land surface modelling. The widely used time/rank stability analysis developed by Vachaud et al. (1985) assesses whether a single soil moisture sensor location can be used to estimate the average over the site. A new method was presented by Friesen et al. (2008) and applied by Bircher et al. (2011), where soil moisture sampling was based on landscape units with internally consistent hydrological behaviour. This method ensures statistically reliable validation via the reduction of the footprint variance and reduces the chance of sampling bias.

11.6 REMOTE-SENSING OF SOIL MOISTURE

As mentioned earlier in this chapter, a single observation location cannot provide absolute knowledge of regional soil moisture. Soil moisture is highly variable in both space and time, rendering it difficult to measure on the continental or global scale needed by researchers (Seneviratne et al., 2010). Space-based remote-sensing of soil moisture accommodates these needs by providing surface soil moisture observations on a global scale every one to two days under a variety of conditions.

In general, remote-sensing aims to measure properties of the Earth's surface by analysing the interactions between the ground and electromagnetic radiation. This can be done by recording the naturally emitted radiation (passive systems) or by illuminating the ground and recording the reflecting signal (active systems). Soil moisture is usually assessed through its effects on the soil's electric or thermal properties. While microwave remote-sensing observations are sensitive to the soil's dielectric constant, infrared remote-sensing systems are sensitive to its thermal conditions. Information about space-based observations can be found in Part III, Chapter 5, 5.6.2 and 5.6.3, where the basic principles of soil moisture observation are included within the context of many observed geophysical variables. In the section here, additional detail and practical information is provided.

Over the last decades, many soil moisture datasets have been developed from various space-borne instruments using different retrieval algorithms (Owe et al., 2001; Njoku et al., 2003; Naeimi et al., 2009). Recently, several of these datasets from both active and passive microwave remote-sensing observations have been combined (Liu et al., 2011), generating a global soil moisture dataset covering the last 30 years (Liu et al., 2012).

Although remote-sensing has proven to be a valuable tool to measure soil moisture on a global scale, in situ measurements are imperative for the calibration and validation of satellite-based soil moisture retrievals. The International Soil Moisture Network, a global in situ soil moisture database, was mainly developed for the validation of satellite products. Many validation efforts have been undertaken to assess the quality of remote-sensing products using in situ measurements (Albergel et al., 2012; Matgen et al., 2012; Pathe et al., 2009; Su et al., 2013; Wagner et al., 2008). In addition, many studies have focused on error characterization of the different soil moisture products (Dorigo et al., 2010; Draper et al., 2013). These studies show that most soil moisture products from remote-sensing are capable of depicting seasonal and short-term soil moisture changes quite well. However, biases in the absolute value and dynamic range may be large when compared to in situ and modelled soil moisture data.

The following paragraphs will give an overview of the theoretical background behind the different remote-sensing techniques, space-borne instruments and algorithms in use.

11.6.1 Microwave remote-sensing

11.6.1.1 *Introduction*

Microwave remote-sensing uses electromagnetic waves with wavelengths of 1 m to 1 cm, which corresponds to frequencies of 0.3 to 300 GHz. An important quality of these microwaves is that they can travel through the Earth's atmosphere undisturbed and thus allow observations to be made independent from cloud coverage. Furthermore, since they are not bound to illumination by the sun, microwave measurements are operable all day long.

When applied to remote-sensing of the Earth's surface, Kirchhoff's radiation law states that the emission of a body is equal to one minus its reflectivity. This means that emission and reflection are complementary, and thus that surfaces that are good scatters are weak emitters and vice versa. As a result, active and passive microwave systems are influenced inversely by the same physical phenomena on the ground. Fresnel's reflection law describes the relationship between the dielectric constant and reflectivity (and thus emissivity), where a higher dielectric constant yields a higher rate of reflection (and smaller emissivity). At microwave lengths, the dielectric constant of water is of an order of magnitude larger than that of dry soils. Therefore, the dielectric
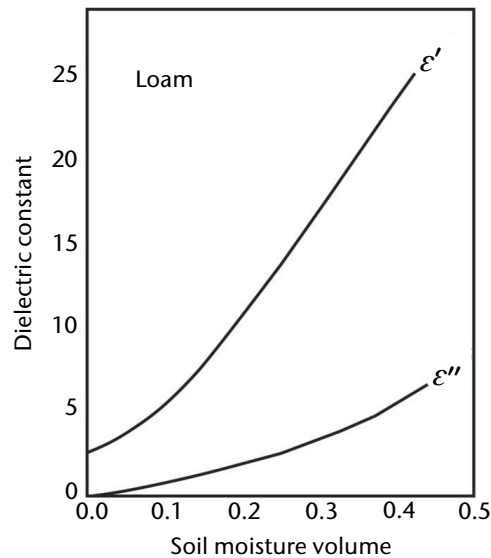
Figure 11.1. The relationship between the complex dielectric constant (ε' and ε'' are magnitudes of the real and imaginary parts, respectively) and volumetric soil moisture for a loamy soil at a frequency of 5 GHz (after Hallikainen et al., 1985)

constant of soils rises with increasing soil moisture (see Figure 11.1). With these physical relations, it is possible to retrieve soil moisture of the Earth's surface from passive as well as from active microwave remote-sensing systems.

Microwave beams are able to interact to some extent with the volumes of targets since their waves are longer and are not reflected immediately at the surface. Thus, information about the inner conditions of vegetation or soils, for example, can be gained. As a rule of thumb, the longer the wavelength, the deeper the radiation penetrates into volumes. In contrast, optical waves only interact with surfaces and tell us about the visible colour and brightness.

When observed from above the canopy, vegetation affects the microwave emission in two ways: first, vegetation absorbs or scatters the radiation emitted from the soil; second, the vegetation also emits its own radiation. Under a sufficiently dense canopy, the emitted soil radiation will become totally masked and the observed radiation will be mostly due to vegetation. Generally, all frequency bands used in microwave remote-sensing of soil moisture are sensitive to vegetation and require some correction in the data for this. Higher-frequency bands are more vulnerable to vegetation influences.

11.6.1.2   *Multi-frequency radiometers*

Passive systems like radiometers record the brightness temperature of the Earth's surface. Brightness temperatures are related to the amount of emissivity (and thus reflection) described by the Rayleigh–Jeans approximation of Planck's law. This law states that brightness temperatures are a function of the physical temperature and emissivity. The amount of emission depends on the dielectric constant of the emitting body as described by Fresnel's reflection law.

Since 1978, instruments have been providing global passive data over land and oceans (Figure 11.2), beginning with the Scanning Multichannel Microwave Radiometer (SMMR, 1978–1987), the Special Sensor Microwave - Imager (SSM/I, since 1987), the Tropical Rainfall Measuring Mission (TRMM, since 1997) and, more recently, the Advanced Microwave Radiometers (AMSR-E, 2002–2011 and AMSR-2 since 2012), the Coriolis WindSat (since 2003) and the Chinese satellites FengYun-3 (since 2010). Initially these instruments were not designed for soil moisture observations but for precipitation, evaporation, sea-surface temperatures and cryospheric parameters. However, in the 1970s studies already showed the potential of retrieving
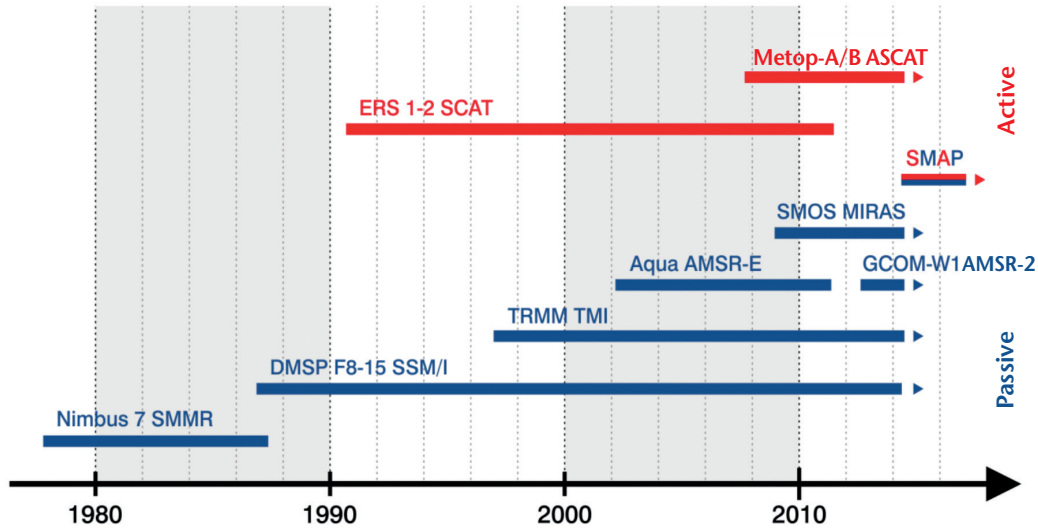
Figure 11.2. Active and passive microwave sensors used for soil moisture retrieval

soil moisture from brightness temperatures at these frequencies (Schmugge, 1976). The big advantage of radiometers is that data are available from multiple multi-frequency microwave radiometers since 1978, providing a long-term dataset to investigate trends and anomalies.

The instruments used for soil moisture remote-sensing have frequencies varying from 6.6 to 10.7 GHz. It has to be taken into account that a higher microwave frequency leads to less accurate estimates of soil moisture since attenuation due to vegetation increases and penetration ability decreases. Therefore, retrievals from SMMR (6.6 GHz), AMSR-E (6.9 GHz), WindSat (6.8 GHz) and AMSR-2 (6.9 GHz) tend to be more accurate. Another advantage of these sensors is that spatial resolution and radiometric accuracy are much improved. The spatial resolution of AMSR-E is 56 km where the soil moisture products are provided at a spatial resolution of 0.25°.

11.6.1.3   *Scatterometers*

A scatterometer is an active microwave instrument that continuously transmits short directional pulses of energy towards the Earth's surface and detects the returned energy. The amount of energy returned to the instrument depends upon geometric and dielectric properties of the surface and is often referred to as normalized radar cross-section or backscatter (sigma nought, σ^0). Sacrificing range and spatial resolution, scatterometers surpass other types of radars in accuracy and stability for measuring the radar cross-section of a target. Space-borne scatterometers were initially developed and designed to derive wind speed and direction over the oceans. Nevertheless, a number of studies acknowledge the capacity of scatterometers for land applications such as soil moisture monitoring (Magagi and Kerr, 1997; Pulliainen et al., 1998; Wagner et al., 1999). Since European scatterometers operate in longer wavelengths (5.3 GHz) than US scatterometers (14 GHz), they are more suitable for soil moisture retrieval.

The unique instrument design of the European scatterometers on board the European Remote-sensing (ERS) satellites and the Meteorological Operational (Metop) satellites enables soil moisture retrieval on a global scale with almost daily coverage. Both scatterometers, the Active Microwave Instrument (AMI) in wind mode on board ERS (Attema, 1991) and the Advanced Scatterometer (ASCAT) on board Metop (Figa-Saldaña et al., 2002), operate in C-band (5.3 GHz) with a wavelength of approximately 5.6 cm. The major differences between these two scatterometers are the number of sideways-looking antennas and the range of the incidence angles observed. The spatial resolution of the AMI is approximately 50 km while the ASCAT product is provided at spatial resolutions of 25 km and 50 km.

11.6.1.4   *Synthetic aperture radars*

Space- or airborne synthetic aperture radars (SAR) are active microwave sensor systems that offer a higher spatial resolution than scatterometers due to advanced signal processing. As side-looking imaging radars, they operate similarly to scatterometers and use the same frequency domain. Besides hydrological applications, SAR systems can be used for the accurate retrieval of three-dimensional geometries, as they enable interferometry.

As a side-looking imaging radar moves along its path on the ground, it accumulates data. The spatial resolution of radars is dependent on the (limited) physical size of its antenna, the aperture. Taking advantage of the along-track motion of the carrier, an SAR system simulates a bigger synthetic aperture as it records amplitude and phase of the ground targets continuously while they are visible to the SAR. These multiple measurements of each target are then summed up coherently. Smaller objects are subsequently resolved on the ground. However, higher energy consumption and a smaller footprint result in a longer revisit time on individual locations and thus the temporal resolution of SARs is inferior to other microwave systems these days.

The higher complexity of soil and surface properties at the scale below 10 km introduces additional error and uncertainty sources. As a consequence, SAR systems are not yet employed in operational soil moisture services but instead are used for pre-operational services and scientific products (Doubkova et al., 2009; Pathe et al., 2009). Nonetheless, upcoming SAR satellite missions such as the European Space Agency (ESA) Sentinel-1 programme (Attema et al., 2007) promise improved temporal and radiometric resolution and a suggestion has been made to use SARs for operational soil moisture services on a local scale (Hornacek et al., 2012).

11.6.1.5   *Dedicated L-band missions*

As stated before, lower frequencies tend to be less sensitive to vegetation interactions and are therefore thought to be more suitable for soil moisture retrieval. Hence, the first two space-borne missions specifically designed for soil moisture retrieval operate in the L-band channel (1.4 GHz). The aim of the Soil Moisture and Ocean Salinity (SMOS) and the Soil Moisture Active Passive (SMAP) missions is to provide absolute soil moisture with a maximum root mean square error of 0.04 m^3/m^3.

The Soil Moisture and Ocean Salinity mission of the European Space Agency was launched successfully on 2 November 2009. The instrument on board the SMOS satellite has a unique design to provide the spatial resolution needed for measuring soil moisture. The so-called Microwave Imaging Radiometer using Aperture Synthesis (MIRAS) is a 2D interferometric radiometer, on which the size of the antenna needed for measuring at the required spatial resolution is simulated through 69 small antennas. MIRAS provides brightness temperatures with a spatial resolution varying between 30 and 50 km. Global coverage is achieved every 2–3 days.

The Soil Moisture Active Passive mission, run by the US National Aeronautics and Space Administration (NASA), is planned for launch on 31 January 2015. Like SMOS, the passive microwave instrument operates in L-band to enhance the sensitivity to soil moisture. However, the instrument design for SMAP is very different from SMOS. SMAP uses a real aperture antenna in the shape of a large (6 m) parabolic reflector that rotates. Measurements are made with a spatial resolution of 40 km. In addition to the passive measurements, SMAP also carries a radar that makes concurrent measurements at a spatial resolution of 1–3 km. By combining active and passive measurements, SMAP provides a soil moisture product with a spatial resolution of 10 km.

11.6.1.6   *Soil moisture retrieval*

For retrieving soil moisture it is necessary to have models that are capable of accounting for vegetation and surface roughness effects on the microwave signal and then to convert accordingly the received intensity to soil moisture values. Again, it should be noted that a shorter wavelength leads to inferior performance due to vegetation scattering and less penetration depth. Soil moisture retrieval is not possible over densely vegetated areas such as

tropical rainforests due to the lack of penetration of the L-band and C-band waves through the vegetation canopy. Additionally, retrieved estimates of soil moisture are only reasonable over snow-free and non-frozen soils.

Passive systems measure the microwave brightness temperature and derive indirectly the emissivity, which is then ingested into a radiative transfer model. Data on soil temperature, roughness, texture and other parameters of the observed area are necessary ancillary information. Data from passive microwave observations are available from AMSR-E using either the VUA–NASA retrieval algorithm developed by Vrije Universiteit Amsterdam (VUA) and NASA and based on the Land Parameter Retrieval Model (LPRM) as described by Owe et al. (2001), the official NASA AMSR-E product (Njoku et al., 2003; Njoku, 2004) or the retrieval algorithm from the University of Montana (Jones et al., 2009; Jones and Kimball, 2010). All of these retrieval algorithms are based on radiative transfer equations. However, the retrieval algorithms vary significantly and generate quite different soil moisture values. The VUA–NASA retrieval algorithm solves for vegetation optical depth and the soil dielectric constant simultaneously. Soil moisture is calculated using the Wang–Schmugge mixing model (Wang and Schmugge, 1980).

The SMOS instrument provides an operational soil moisture product (Kerr et al., 2012). The SMOS retrieval algorithm uses an iterative approach to minimize the cost function between modelled brightness temperatures and the direct measurements. In this way the best set of parameters is found, including the soil moisture and vegetation. SMOS Level 2 soil moisture data can be downloaded via ESA Earthnet Online (https://earth.esa.int/web/guest/-/how-to-obtain-data-7329).

Active instruments measure the backscattered intensity, which is a function of roughness, incidence angle and dielectric properties of the surface. Again, vegetation and other influences contribute to the signal, which is used to determine the backscatter coefficient. Soil moisture retrieval provided as an operational product from the ASCAT instrument and as a scientific product from the AMI in wind mode relies on a semi-empirical change-detection method. This method, the TU Wien change detection algorithm, is tailored to the unique instrument design. Assuming a linear relationship between radar backscatter and soil moisture, in the decibel domain, a relative measure of moisture in the first few centimetres of soil can be obtained, representing the degree of saturation (0%–100%). In very dry regions, particularly over sand deserts, the retrieval approach fails, seemingly due to a complex mechanism of surface, volume and sub-surface scattering. Soil moisture data from the TU Wien change detection algorithm are freely available on the website of the Technische Universität Wien (http://rs.geo.tuwien.ac.at/products/) or the European Organization for the Exploitation of Meteorological Satellites (EUMETSAT; http://www.eumetsat.int/website/home/Data/Products/Land/index.html).

An overview of operational soil moisture products is given in the table below.

Operational soil moisture products and their characteristics

Product reference	SMOS	AMSR-E	ASCAT
Satellite			
Name	SMOS	Aqua	Metop-A/B
Agencies	ESA/CNES[a]/CDTI[b]	NASA	EUMETSAT/ESA
Lifetime	Since 2.11.09	4.5.02 – 4.10.11	Since 19.10.06
Orbit	Polar	Polar	Polar
Altitude	758 km	705 km	837 km
Period	100 min	99 min	100 min
Equator crossing time	6 a.m. (ascending) 6 p.m. (descending)	1.30 p.m. (ascending) 1.30 a.m. (descending)	9.30 p.m. (ascending) 9.30 a.m. (descending)
Type	Research satellite	Research satellite	Operational (3 satellites)

Product reference	SMOS	AMSR-E	ASCAT
Sensor			
Name	MIRAS	AMSR-E	ASCAT
Type	Synthetic aperture radiometer	Multi-frequency real aperture radiometer	Real aperture scatterometer
Swath	1 000 km	1 450 km	2 x 550 km
Scanning principle	Forward looking 2D interferometer	Rotating parabolic reflector	6 side-looking fan beam antennas
Incidence angle range	0°– 55°	55°	25°– 53° (mid beam); 34°– 64° (fore and aft beams)
Frequency	1.4 GHz	6.9, 10.7, 18.7, 23.8, 36.5, and 89 GHz	5.3 GHz
Polarization	H and V (polarimetric mode optional)	H and V	VV
Spatial resolution	30–50 km	75 x 43 km at 6.9 GHz	25/50 km
Daily global coverage	~82%	~90%	~82%
Retrieval			
Model name	L-MEB	LPRM	WARP
Forward model	Radiative transfer model	Radiative transfer model	Semi-empirical change-detection
Model complexity	High	Medium	Low
Inversion approach	Iterative least-square matching	Iterative least-square matching	Direct inversion
Concurrent retrievals	Soil temperature, vegetation optical depth, roughness	Soil temperature, vegetation optical depth	None
Model calibration	None	None	Based on long-term time series
Need for auxiliary data	High	Medium	Low
Error propagation estimates	Not available	Available	Available
Product			
Target quantity	Volumetric soil moisture	Volumetric soil moisture	Degree of saturation
Units	$m^3\,m^{-3}$	$m^3\,m^{-3}$	0–1 or %
Grid	Fixed ISEA4-9 Discrete Global Grid	Regular grid	Swath geometry
Pixel spacing	15 km	0.25°	12.5 km
Data latency	Within a few days after sensing	Irregular updates	Within 130 min after sensing

Notes:

a   National Centre for Space Studies (France)

b   Centro para el Desarrollo Tecnológico Industrial (Spain)

11.6.2 **Thermal infrared remote-sensing**

All bodies with a temperature above absolute zero emit electromagnetic energy in the thermal infrared domain. By detecting the thermal properties of the Earth's surface, soil moisture can be derived based on the distinct differences in thermal properties of soil and water (Idso et al., 1975; Van de Griend et al., 1985). Thermal infrared remote-sensing has been used in an increasing number of studies for the derivation of soil moisture. The advantage of thermal infrared remote-sensing is that it can provide soil moisture information on a spatial resolution down to a few metres. Furthermore, it can provide soil moisture information over dense vegetation, which is one of the limitations of microwave remote-sensing. The disadvantages of thermal infrared remote-sensing are that it is unable to measure soil moisture when cloud cover is present and it is considerably affected by atmospheric phenomena. Therefore, complex noise-removal mechanisms are needed in most cases. Thermal infrared remote-sensing of soil moisture is not as straightforward as microwave remote-sensing since there is no direct link between temperature data and soil moisture. Nevertheless, several approaches exist to indirectly retrieve soil moisture data using thermal infrared observations from the geostationary operational environmental satellite (GOES), advanced very high resolution radiometer (AVHRR), moderate resolution imaging spectroradiometer (MODIS), Landsat and others.

The first approach is called the triangle approach and is based on the empirical relationship between soil moisture, soil temperature and fractional vegetation cover. This relationship was demonstrated by Price (1990) and resulted in a triangular scatterplot of surface temperatures and the remotely sensed normalized difference vegetation index. The triangle approach was later used in several studies to estimate soil moisture, namely by Sandholt et al. (2002) and Carlson et al. (1994) among others.

The second approach makes use of the differences in thermal properties between water and soils. Water differs from many other matters in its relatively large heat capacity and thermal inertia. Thermal inertia is defined as the resistance of an object against its heating for 1 K. The thermal inertia of water is relatively high, which indicates a high resistance to temperature changes. It has been shown that the behaviour of land surface temperature in the morning strongly depends on soil moisture in the soil, since the water will heat up more slowly. One of the approaches that uses this behaviour is the calculation of the apparent thermal inertia (ATI), which can be done when measuring the difference between maximum and minimum temperatures over one day. It is described as:

$$\mathrm{ATI} = (1 - A) / \Delta T \tag{11.10}$$

where A is the albedo of the pixel in the visible band and ΔT the difference between the minimum and maximum temperature. Many studies have already assessed the potential of ATI to describe soil moisture and its spatial and temporal variability (e.g. Verstraeten et al., 2006; Van doninck et al., 2011).

Another method to retrieve soil moisture using thermal infrared remote-sensing is by integrating the data into land surface models. Soil moisture controls latent heat fluxes by way of both evaporation and transpiration, where wet soil conditions lead to increased evaporation and transpiration. The atmosphere–land exchange inversion model (ALEXI) uses the relationship between evaporation, transpiration and soil moisture to derive soil moisture data. All major components, including the latent heat flux, of the energy budget are estimated from net radiation and vegetation parameters retrieved from AVHRR and GOES. Accordingly, soil moisture can be derived from latent heat fluxes by using a soil water stress function (Anderson et al., 1997; Anderson et al., 2007; Hain et al., 2011). An intercomparison of soil moisture retrieved from microwave remote-sensing and ALEXI showed that the two datasets are complementary: ALEXI is better at estimating soil moisture over dense vegetation and microwave remote-sensing shows more reliable results over low to moderate vegetation (Hain et al., 2011).

––––––––––––

REFERENCES AND FURTHER READING

Aggelides, S.M. and P.A. Londra, 1998: Comparison of empirical equations for temperature correction of gypsum sensors. *Agronomy Journal*, 90:441–443.

Albergel, C., P. de Rosnay, C. Gruhier, J. Muñoz-Sabater, S. Hasenauer, L. Isaksen, Y. Kerr and W. Wagner, 2012: Evaluation of remotely sensed and modelled soil moisture products using global ground-based in situ observations. *Remote Sensing of Environment*, 118:215–226.

Anderson, M.C., J.M. Norman, G.R. Diak, W.P. Kustas and J.R. Mecikalski, 1997: A two-source time-integrated model for estimating surface fluxes using thermal infrared remote sensing. *Remote Sensing of Environment*, 60:195–216.

Anderson, M.C., J.M. Norman, J.R. Mecikalski, J.A. Otkin and W.P. Kustas, 2007: A climatological study of evapotranspiration and moisture stress across the continental United States based on thermal remote sensing: 1. Model formulation. *Journal of Geophysical Research: Atmospheres*, 112(D10117).

Attema, E.P.W., 1991: The Active Microwave Instrument on-board the ERS-1 satellite. *Proceedings of the IEEE*, 79(6):791–799.

Attema, E., P. Bargellini, P. Edwards, G. Levrini, S. Lokas, L. Moeller, B. Rosich-Tell, P. Secchi, R. Torres, M. Davidson and P. Snoeij, 2007: Sentinel-1: The radar mission for GMES operational land and sea services. *ESA Bulletin*, 131:10–17.

Bircher, S., N. Skou, K.H. Jensen, J.P. Walker and L. Rasmussen, 2011: A soil moisture and temperature network for SMOS validation in Western Denmark. *Hydrol. Earth Syst. Sci. Discuss.*, 8:9961–10006.

Brocca, L., R. Morbidelli, F. Melone and T. Moramarco, 2007: Soil moisture spatial variability in experimental areas of central Italy. *Journal of Hydrology*, 333(2–4):356–373.

Brunini, O. and G.W. Thurtell, 1982: An improved thermocouple hygrometer for in situ measurements of soil water potential. *Soil Science Society of America Journal*, 46:900–904.

Campbell, D.J. and J.K. Henshall, 2001: Bulk density. In: *Soil and Environmental Analysis: Physical Methods* (K.A. Smith and C.E. Mullins, eds.), Marcel Dekker, New York, pp. 315–348.

Carlson, T.N., R.R. Gillies and E.M. Perry, 1994: A method to make use of thermal infrared temperature and NDVI measurements to infer surface soil water content and fractional vegetation cover. *Remote Sensing Reviews*, 9:161–173.

Deardorff, J.W., 1978: Efficient prediction of ground surface temperature and moisture, with inclusion of a layer of vegetation. *Journal of Geophysical Research*, 83:1889–1904.

De Jeu, R.A.M., 2003: Retrieval of land surface parameters using passive microwave remote sensing. PhD Thesis, VU Amsterdam.

Dirksen, C., 1999: *Soil Physics Measurements*. Catena Verlag, Reiskirchen, Germany.

Dirksen, C. and S. Dasberg, 1993: Improved calibration of time domain reflectometry soil water content measurements. *Soil Science Society of America Journal*, 57:660–667.

Dorigo, W.A., K. Scipal, R.M. Parinussa, Y.Y. Liu, W. Wagner, R.A.M. de Jeu and V. Naeimi, 2010: Error characterisation of global active and passive microwave soil moisture datasets. *Hydrology and Earth System Sciences*, 14:2605–2616.

Dorigo, W.A., W. Wagner, R. Hohensinn, S. Hahn, C. Paulik, A. Xaver, A. Gruber, M. Drusch, S. Mecklenburg, P. van Oevelen, A. Robock and T. Jackson, 2011: The International Soil Moisture Network: a data hosting facility for global in situ soil moisture measurements. *Hydrology and Earth System Sciences*, 15:1675–1698.

Doubkova, M., A. Bartsch, C. Pathe, D. Sabel and W. Wagner, 2009: The medium resolution soil moisture dataset: Overview of the SHARE ESA DUE TIGER project. *2009 IEEE International Geoscience and Remote Sensing Symposium: Proceedings*, I:116–119.

Draper, C., R. Reichle, R. de Jeu, V. Naeimi, R. Parinussa and W. Wagner, 2013: Estimating root mean square errors in remotely sensed soil moisture over continental scale domains. *Remote Sensing of Environment*, 137:288–298.

Drungil, C.E.C., K. Abt and T.J. Gish, 1989: Soil moisture determination in gravelly soils with time domain reflectometry. *Transactions of the American Society of Agricultural Engineering*, 32:177–180.

Famiglietti, J.S., D. Ryu, A.A. Berg, M. Rodell and T.J. Jackson, 2008: Field observations of soil moisture variability across scales. *Water Resources Research*, 44(1).

Figa-Saldaña, J., J.J.W. Wilson, E. Attema, R. Gelsthorpe, M.R. Drinkwater and A. Stoffelen, 2002: The advanced scatterometer (ASCAT) on the meteorological operational (MetOp) platform: A follow on for European wind scatterometers. *Canadian Journal of Remote Sensing*, 28(3):404–412.

Friesen, J., C. Rodgers, P.G. Oguntunde, J.M.H. Hendrickx and N. Van de Giesen, 2008: Hydrotope-based protocol to determine average soil moisture over large areas for satellite calibration and validation – with results from an observation campaign in the Volta Basin, West Africa. *IEEE Transactions on Geoscience and Remote Sensing*, 46(7):1995–2004.

Gardner, C.M.K., D.A. Robinson, K. Blyth and J.D. Cooper, 2001: Soil water content. In: *Soil and Environmental Analysis: Physical Methods* (K.A. Smith and C.E. Mullins, eds.), Marcel Dekker, New York, pp. 1–64.

Gardner, W.H. and C. Calissendorff, 1967: Gamma-ray and neutron attenuation measurement of soil bulk density and water content. *Proceedings of the Symposium on the Use of Isotope and Radiation Techniques in Soil Physics and Irrigation Studies* (Istanbul, 12–16 June 1967). International Atomic Energy Agency, Vienna, pp. 101–112.

Gee, G.W. and M.E. Dodson, 1981: Soil water content by microwave drying: A routine procedure. *Soil Science Society of America Journal*, 45:1234–1237.

Greacen, E.L., 1981: *Soil Water Assessment by the Neutron Method*. CSIRO, Australia.

Hain, C.R., W.T. Crow, J.R. Mecikalski, M.C. Anderson and T. Holmes, 2011: An intercomparison of available soil moisture estimates from thermal infrared and passive microwave remote sensing and land surface modeling. *Journal of Geophysical Research: Atmospheres*, 116(D15107).

Hallikainen, M., F. Ulaby, M. Dobson, M. El-Rayes and L.K. Wu, 1985: Microwave dielectric behavior of wet soil – Part 1: Empirical models and experimental observations. *IEEE Transactions on Geoscience and Remote Sensing*, 23:25–34.

Hasenauer, S., W. Wagner, K. Scipal, V. Naeimi and Z. Bartalis, 2006: Implementation of near real-time soil moisture products in the SAF network based on MetOp ASCAT data. *EUMETSAT Meteorological Satellite Conference*, 12–16 June 2006, Helsinki.

Hornacek, M., W. Wagner, D. Sabel, H.-L. Truong, P. Snoeij, T. Hahmann, E. Diedrich and M. Doubkova, 2012: Potential for high resolution systematic global surface soil moisture retrieval via change detection using Sentinel-1. *IEEE Journal of Selected Topics in Applied Earth Observation and Remote Sensing*, 5(4):1303–1311.

Idso, S.B., R.D. Jackson, R.J. Reginato and T.J. Schmugge, 1975: The utility of surface temperature measurements for the remote sensing of sun for soil water status. *Journal of Geophysical Research*, 80:3044–3049.

Jackson, T.J., 1990: Laboratory evaluation of a field-portable dielectric/soil moisture probe. *IEEE Transactions on Geoscience and Remote Sensing*, 28:241–245.

Jackson, T.J. and T.J. Schmugge, 1989: Passive microwave remote sensing system for soil moisture: Some supporting research. *IEEE Transactions on Geoscience and Remote Sensing*, 27:225–235.

Jones, L.A. and J.S. Kimball, 2010: *Daily Global Land Surface Parameters Derived from AMSR-E*. Boulder, Colorado: NASA National Snow and Ice Data Center Distributed Active Archive Center (available from http://nsidc.org/data/nsidc-0451.html).

Jones, L.A., J.S. Kimball, E. Podest, K.C. McDonald, S.K. Chan and E.G. Njoku, 2009: A method for deriving land surface moisture, vegetation optical depth, and open water fraction from AMSR-E. *2009 IEEE International Geoscience and Remote Sensing Symposium: Proceedings*, III:916–919.

Kerr, Y.H., P. Waldteufel, P. Richaume, J.P. Wigneron, P. Ferrazzoli, A. Mahmoodi, A. Al Bitar, F. Cabot, C. Gruhier, S.E. Juglea, D. Leroux, A. Mialon and S. Delwart, 2012: The SMOS soil moisture retrieval algorithm. *IEEE Transactions on Geoscience and Remote Sensing*, 50(5):1384–1403.

Klute, A. (ed.), 1986: *Methods of Soil Analysis, Part 1: Physical and Mineralogical Methods*. American Society of Agronomy, Madison, Wisconsin, United States.

Knight, J.H., 1992: Sensitivity of time domain reflectometry measurements to lateral variations in soil water content. *Water Resources Research*, 28:2345–2352.

Liu, Y.Y., W.A. Dorigo, R.M. Parinussa, R.A.M. De Jeu, W. Wagner, M.F. McCabe, J.P. Evans and A.I.J.M van Dijk, 2012: Trend-preserving blending of passive and active microwave soil moisture retrievals. *Remote Sensing of Environment*, 123:280–297.

Liu, Y.Y., R.M. Parinussa, W.A. Dorigo, R.A.M. De Jeu, W. Wagner, A.I.J.M van Dijk, M.F. McCabe and J.P. Evans, 2011: Developing an improved soil moisture dataset by blending passive and active microwave satellite-based retrievals. *Hydrology and Earth System Sciences*, 15:425–436.

Magagi, R.D. and Y.H. Kerr, 1997: Retrieval of soil moisture and vegetation characteristics by use of ERS-1 wind scatterometer over arid and semi-arid areas. *Journal of Hydrology*, 188–189:361–384.

Marthaler, H.P., W. Vogelsanger, F. Richard and J.P. Wierenga, 1983: A pressure transducer for field tensiometers. *Soil Science Society of America Journal*, 47:624–627.

Matgen, P., S. Heitz, S. Hasenauer, C. Hissler, L. Brocca, L. Hoffmann, W. Wagner and H.H.G. Savenije, 2012: On the potential of MetOp ASCAT-derived soil wetness indices as a new aperture for hydrological monitoring and prediction: a field evaluation over Luxembourg. *Hydrological Processes*, 26(15):2346–2359.

Merrill, S.D. and S.L. Rawlins, 1972: Field measurement of soil water potential with thermocouple psychrometers. *Soil Science*, 113:102–109.

Mullins, C.E., 2001: Matric potential. In: *Soil and Environmental Analysis: Physical Methods* (K.A. Smith and C.E. Mullins, eds.), Marcel Dekker, New York, pp. 65–93.

Naeimi, V., K. Scipal, Z. Bartalis, S. Hasenauer and W. Wagner, 2009: An improved soil moisture retrieval algorithm for ERS and MetOp scatterometer observations. *IEEE Transactions on Geoscience and Remote Sensing*, 47(7):1999–2013.

Njoku, E.G., 2004: *AMSR-E/Aqua L2B Surface Soil Moisture, Ancillary Parms, & QC EASE-Grids, Version 2*. Boulder, Colorado: NASA National Snow and Ice Data Center Distributed Active Archive Center (available from http://nsidc.org/data/ae_land.html).

Njoku, E.G., T.J. Jackson, V. Lakshmi, T.K. Chan and S.V. Nghiem, 2003: Soil moisture retrieval from AMSR-E. *IEEE Transactions on Geoscience and Remote Sensing*, 41(2):215–229.

Owe, M., R. de Jeu and T. Holmes, 2008: Multisensor historical climatology of satellite-derived global land surface moisture. *Journal of Geophysical Research*, 113(F01002).

Owe, M., R. de Jeu and J. Walker, 2001: A methodology for surface soil moisture and vegetation optical depth retrieval using the microwave polarization difference index. *IEEE Transactions on Geoscience and Remote Sensing*, 39(8):1643–1654.

Pathe, C., W. Wagner, D. Sabel, M. Doubkova and J. B. Basara, 2009: Using ENVISAT ASAR global mode data for surface soil moisture retrieval over Oklahoma, USA. *IEEE Transactions on Geoscience and Remote Sensing*, 47(2):468–480.

Perrier, E.R. and A.W. Marsh, 1958: Performance characteristics of various electrical resistance units and gypsum materials. *Soil Science*, 86:140–147.

Price, J.C., 1990: Using spatial context in satellite data to infer regional scale evapotranspiration. *IEEE Transactions on Geoscience and Remote Sensing*, 28(5):940–948.

Pulliainen, J.T., T. Manninen and M.T. Hallikainen, 1998: Application of ERS-1 wind scatterometer data to soil frost and soil moisture monitoring in boreal forest zone. *IEEE Transactions on Geoscience and Remote Sensing*, 36(3):849–863.

Rawlins, S.L. and G.S. Campbell, 1986: Water potential: Thermocouple psychrometry. In: *Methods of Soil Analysis – Part 1: Physical and Mineralogical Methods* (A. Klute, ed.), American Society of Agronomy, Madison, Wisconsin, United States, pp. 597–618.

Sandholt, I., K. Rasmussen and J. Andersen, 2002: A simple interpretation of the surface temperature/vegetation index space for assessment of surface moisture status. *Remote Sensing of Environment*, 79(2–3):213–224.

Schmugge, T.J., 1976: *Remote Sensing of Soil Moisture*. Doc. X-913-76-118, NASA Goddard Space Flight Center, Greenbelt, Maryland.

Schmugge, T.J., T.J. Jackson and H.L. McKim, 1980: Survey of methods for soil moisture determination. *Water Resources Research*, 16:961–979.

Seneviratne, S.I., T. Corti, E.L. Davin, M. Hirschi, E.B. Jaeger, I. Lehner, B. Orlowsky and A.J. Teuling, 2010: Investigating soil moisture–climate interactions in a changing climate: A review. *Earth-Science Reviews*, 99(3–4):125–161.

Su, C.-H., D. Ryu, R.I. Young, A.W. Western and W. Wagner, 2013: Inter-comparison of microwave satellite soil moisture retrievals over the Murrumbidgee Basin, southeast Australia. *Remote Sensing of Environment*, 134:1–11.

Tanner, C.B. and R.J. Hanks, 1952: Moisture hysteresis in gypsum moisture blocks. *Soil Science Society of America Proceedings*, 16:48–51.

Topp, G.C., J.L. Davis and A.P. Annan, 1980: Electromagnetic determination of soil water content: Measurement in coaxial transmission lines. *Water Resources Research*, 16:574–582.

Ulaby, F.T., R.K. Moore and A.K. Fung, 1986: *Microwave Remote Sensing: Active and Passive*, Volume III. Artech House, Norwood, Massachusetts.

Vachaud, G., A. Passerat De Silans, P. Balabanis and M. Vauclin, 1985: Temporal stability of spatially measured soil water probability density function. *Soil Science Society of America Journal*, 49(4):822–828.

Van de Griend, A.A., P.J. Camillo and R.J. Gurney, 1985: Discrimation of soil physical parameters, thermal inertia and soil moisture from diurnal surface temperature fluctuations. *Water Resources Research*, 21:997–1009.

Van doninck, J., J. Peters, B. De Baets, E. De Clercq, E. Ducheyne and N. Verhoest, 2011: The potential of multitemporal Aqua and Terra MODIS apparent thermal inertia as a soil moisture indicator. *International Journal of Applied Earth Observation and Geoinformation*, 13(6):934–941.

Verstraeten, W.W., F. Veroustraete, C.J. van der Sande, I. Grootaers and J. Feyen, 2006: Soil moisture retrieval using thermal inertia, determined with visible and thermal spaceborne data, validated for European forests. *Remote Sensing of Environment*, 101(3):299–314.

Visvalingam, M. and J.D. Tandy, 1972: The neutron method for measuring soil moisture content: A review. *European Journal of Soil Science*, 23:499–511.

Wagner, W., G. Lemoine and H. Rott, 1999: A method for estimating soil moisture from ERS scatterometer and soil data. *Remote Sensing of Environment*, 70(2):191–207.

Wagner, W., C. Pathe, M. Doubkova, D. Sabel, A. Bartsch, S. Hasenauer, G. Blöschl, K. Scipal, J. Martínez-Fernández and A. Löw, 2008: Temporal stability of soil moisture and radar backscatter observed by the Advanced Synthetic Aperture Radar (ASAR). *Sensors*, 8(2):1174–1197.

Wang, J.R. and T.J. Schmugge, 1980: An empirical model for the complex dielectric permittivity of soils as a function of water content. *IEEE Transactions on Geoscience and Remote Sensing*, GE-18(4): 288–295.

Wellings, S.R., J.P. Bell and R.J. Raynor, 1985: *The Use of Gypsum Resistance Blocks for Measuring Soil Water Potential in the Field.* Report No. 92, Institute of Hydrology, Wallingford, United Kingdom.

World Meteorological Organization, 1968: *Practical Soil Moisture Problems in Agriculture.* Technical Note No. 97 (WMO-No. 235, TP.128). Geneva.

———, 1989: *Land Management in Arid and Semi-arid Areas.* Technical Note No. 186 (WMO-No. 662). Geneva.

———, 2001: *Lecture Notes for Training Agricultural Meteorological Personnel* (J. Wieringa and J. Lomas) (WMO-No. 551). Geneva.

CHAPTER 12. MEASUREMENT OF UPPER-AIR PRESSURE, TEMPERATURE AND HUMIDITY

12.1 GENERAL

12.1.1 Definitions

The following definitions based on WMO (1992, 2010*a*) are relevant to upper-air measurements using a radiosonde:

Radiosonde: Instrument intended to be carried by a balloon through the atmosphere, equipped with devices to measure one or several meteorological variables (pressure, temperature, humidity, etc.), and provided with a radio transmitter for sending this information to the observing station.

Radiosonde observation: An observation of meteorological variables in the upper air, usually atmospheric pressure, temperature, humidity and, often, horizontal wind, by means of a radiosonde.

Note: The radiosonde may be attached to a balloon (or another slow-moving unmanned aircraft), or the design adjusted to be dropped (as a dropsonde) from an aircraft or rocket.

Radiosonde station: A station at which observations of atmospheric pressure, temperature, humidity and usually horizontal wind in the upper air are made by electronic means.

Upper-air observation: A meteorological observation made in the free atmosphere, either directly or indirectly.

Upper-air station, upper air synoptic station, aerological station: A surface location from which upper-air observations are made.

Sounding: Determination of one or several upper-air meteorological variables by means of instruments carried aloft by balloon, aircraft, kite, glider, rocket, and so on.

This chapter deals with radiosonde systems. Measurements using special platforms, specialized equipment, and aircraft, or made indirectly by remote-sensing instruments such as microwave radiometers and Raman water vapour lidars in the boundary layer and troposphere, are discussed in other chapters of Part II of this Guide. Radiosonde systems are normally used to measure pressure, temperature and relative humidity. At most operational sites, the radiosonde system is also used for upper-wind determination (see Part I, Chapter 13). In addition, some radiosondes are flown with sensing systems for atmospheric constituents, such as ozone concentration or radioactivity. These additional measurements are not discussed in any detail in this chapter.

12.1.2 Units used in upper-air measurements

The units of measurement for the meteorological variables of radiosonde observations are hectopascals for pressure, degrees Celsius for temperature, and per cent for relative humidity. Relative humidity is reported relative to saturated vapour pressure over a water surface, even at temperatures less than 0 °C.

The unit of geopotential height used in upper-air observations is the standard geopotential metre (gpm), defined as 0.980 665 dynamic metres. The relationship between geopotential height and geometric height is shown in section 12.3.6.2. Differences in the lower troposphere are not very large but get larger as the height increases.

The values of the physical functions and constants adopted by WMO (2011*a*) should be used in radiosonde computations.

12.1.3 Meteorological requirements

12.1.3.1 *Radiosonde data for meteorological operations*

Upper-air measurements of temperature, relative humidity and wind are three of the basic measurements used in the initialization of the analyses of numerical weather prediction (NWP) models for operational weather forecasting. Radiosondes provide most of the in situ temperature and relative humidity measurements over land, while radiosondes launched from remote islands or ships can, in practice, provide a very limited but important coverage over the oceans. Temperatures with resolution in the vertical similar to radiosondes can be observed by aircraft either during ascent, descent, or at cruise levels. Aircraft observations during ascent and descent are used to supplement radiosonde observations over land and in some cases may be used to replace the radiosondes at a given site. Aircraft observations at cruise level give measurements over both land and oceans. Nadir-viewing satellite observations of temperature and water vapour distribution have lower vertical resolution than radiosonde or aircraft measurements. Satellite observations have a large impact on numerical weather prediction analyses over the oceans and other areas of the globe where radiosonde and aircraft observations are sparse or unavailable.

Accurate measurements of the vertical structure of temperature and water vapour fields in the troposphere are extremely important for all types of forecasting, especially regional and local forecasting and nowcasting. Atmospheric temperature profiles have discontinuities in the vertical, and the changes in relative humidity associated with the temperature discontinuities are usually quite pronounced (see Figure 12.1). The measurements indicate the typical structure of cloud or fog layers in the vertical. This vertical structure of temperature and water vapour determines the stability of the atmosphere and, subsequently, the amount and type of cloud that will be forecast. Radiosonde measurements of the vertical structure can usually be provided with sufficient accuracy to meet most user requirements.

High-resolution measurements of the vertical structure of temperature and relative humidity are important for environmental pollution studies (for instance, identifying the depth of the atmospheric boundary layer). This high vertical resolution is also necessary for computing the effects of atmospheric refraction on the propagation of electromagnetic radiation or sound waves. The time resolution should be as high as possible, for instance 1 s, but not more than 5 s. Besides that, information on the time and position of the radiosonde at each level is required to obtain the correct description of the atmosphere.

Civil aviation, artillery and other ballistic applications, such as space vehicle launches, have operational requirements for detailed measurements of the density of air at given pressures (derived from radiosonde temperature and relative humidity measurements).

Radiosonde observations are also important for studies of upper-air climate change. Hence, it is necessary to keep adequate records of the systems, including the software version and corrections, and consumables used for measurements, as well as the methods of observation (e.g. suspension length from the balloon) used with the systems. Climatologists would prefer that raw data be archived in addition to processed data and made available for subsequent climatological studies. It is essential to record any changes in the methods of observation introduced over time. In this context, it has proved essential to establish the changes in radiosonde instruments and practices that have taken place since radiosondes were used on a regular basis (see for instance WMO, 1993*a*). Climate change studies based on radiosonde measurements require extremely high stability in the systematic errors of the radiosonde measurements. However, the errors in early radiosonde measurements of some meteorological variables, particularly relative humidity and pressure, were too high and complex to generate meaningful corrections at all the heights required for climate change studies. Thus, improvements and changes in radiosonde design were necessary. Furthermore, expenditure limitations on meteorological operations require that radiosonde consumables remain cheap if widespread radiosonde use is to continue.
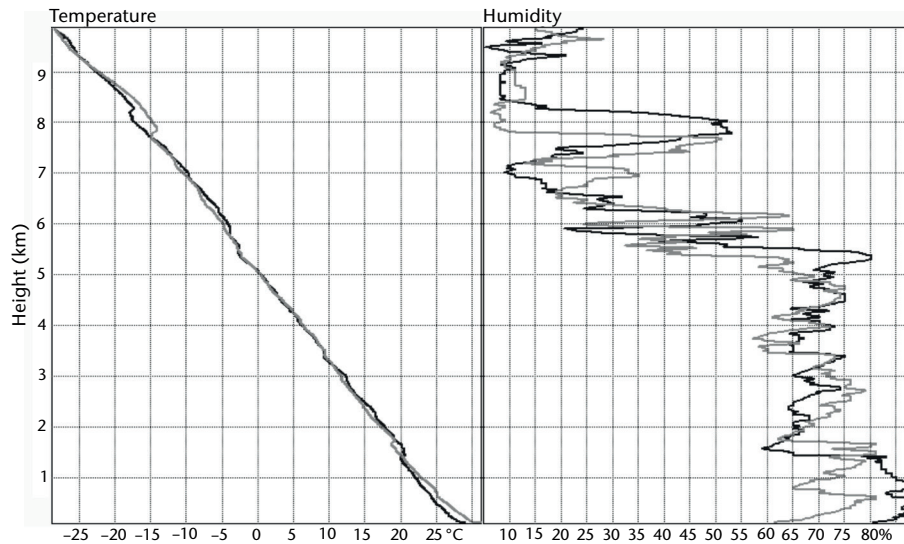
(a) Example of daytime temperature and humidity profiles from the WMO
Intercomparison of High Quality Radiosonde Systems, Yangjiang, China (22°N).
The grey sounding was made 8 h after the black. Relatively small shifts in
the rate of temperature change in the vertical were associated with rapid
drops in relative humidity (near 0.7, 1.6, 3.5, 5.5 and 8 km).
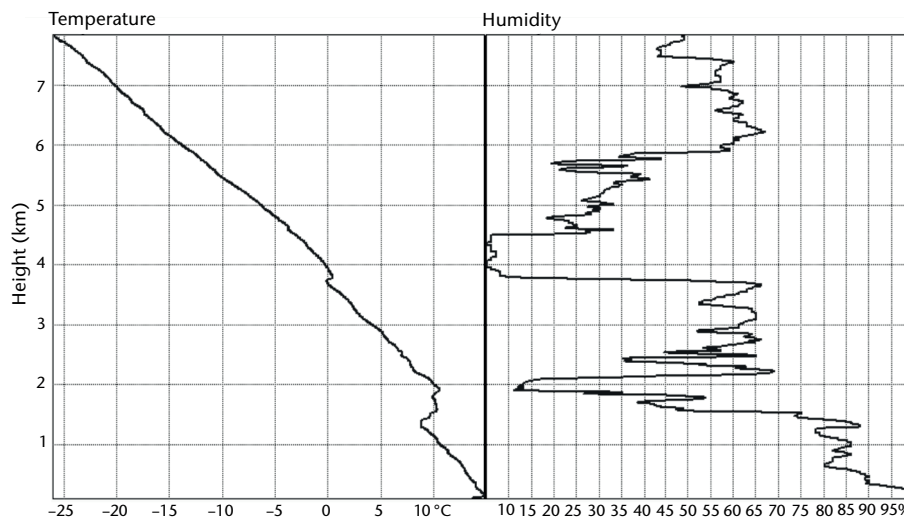
(b) Example of temperature and relative humidity in summer at 0600 UTC in
the United Kingdom (50°N), showing a shallow layer of 100% relative humidity
in fog near the ground and very rapid drops in relative humidity in the
temperature inversion layers between 1.5 and 2 km and at 3.8 km.

**Figure 12.1. Examples of temperature and relative humidity profiles in
the lower and middle troposphere**

When new radiosonde designs are introduced, it is essential that enough testing be conducted
of the performance of the new radiosonde relative to the old, so that time series of observations
at a station can be harmonized based on comparison data. This harmonization should not
result in the degradation of good measurements generated by the improved radiosonde in
order to make them compatible with the poorer measurements of an earlier design. It should
also be recognized that in some cases the errors in the earlier measurements were too large for
use in climatological studies (this is particularly true with respect to recent relative humidity
measurements, see section 12.5.7).

Certain compromises in system measurement accuracy have to be accepted by users, taking into account that radiosonde manufacturers are producing systems that need to operate over an extremely wide range of meteorological conditions:

    1 050 to 5 hPa for pressure
    50 °C to –95 °C for temperature
    100% to 1% for relative humidity
    30 hPa at the surface to 10^{-4} hPa at the tropopause for water vapour pressure in the tropics

Systems also need to be able to sustain continuous reliable operation when operating in heavy rain, in the vicinity of thunderstorms, and in severe icing conditions.

The coldest temperatures are most often encountered near the tropical and subtropical tropopause, although in winter very cold temperatures can also be observed at higher levels in the stratospheric polar vortex. Figure 12.2 shows examples of profiles from the subtropics: example (a) in Yangjiang, China (22°N) in summer, and example (b) at 50°N in summer and winter in the United Kingdom. The colder temperatures near the tropopause in the tropics pose a major challenge for operational relative humidity sensors, because few currently respond very rapidly at temperatures below –70 °C (see sections 12.5.7.6 and 12.5.7.7). Thus, radiosondes that can perform well throughout the troposphere at mid-latitudes may have less reliable relative humidity measurements in the upper troposphere in the tropics.

A radiosonde measurement is close to an instant sample of a given layer of the atmosphere (a radiosonde usually ascends 300 m in 1 min). When short-term fluctuations in atmospheric temperature from gravity waves and turbulence are small, the radiosonde measurement can represent the situation above a location very effectively for many hours. On the other hand, when the atmosphere is very variable (for example, a convective atmospheric boundary layer), the instant sample may not be valid for longer than a minute and may not represent a good average value above the location, even for an hour. In Figure 12.2(a), radiosonde temperatures in the troposphere were more reproducible with time than in the stratosphere because of the larger influence of gravity waves in the stratosphere. These larger differences at upper levels were not the result of instrument error. Similarly, the variation of temperatures in the vertical in the stratosphere in Figure 12.2(b) was not the result of instrument error, as the same structure was measured by two different radiosonde types on the test flights.

12.1.3.2   *Relationships between satellite and radiosonde upper-air measurements*

Nadir-viewing satellite observing systems do not measure vertical structure with the same accuracy or degree of confidence as radiosonde or aircraft systems. The current satellite temperature and water vapour sounding systems either observe upwelling radiances from carbon dioxide or water vapour emissions in the infrared, or alternatively oxygen or water vapour emissions at microwave frequencies (see Part III, Chapter 3). Both infrared and microwave sounding measurements are essential for current operational numerical weather prediction. The radiance observed by a satellite channel is composed of atmospheric emissions from a range of heights in the atmosphere. This range is determined by the distribution of emitting gases in the vertical and the atmospheric absorption at the channel frequencies. Most radiances from a single satellite temperature channel approximate the mean layer temperature of a layer at least 10 km thick. However, much finer vertical resolution has been achieved by the recent Fourier-transform interferometers operating in the infrared, using information from a much larger number of channels with slightly different absorption characteristics. The height distribution (weighting function) of the observed temperature channel radiance will vary with geographical location to some extent. This is because the radiative transfer properties of the atmosphere have a small dependence on temperature. The concentrations of the emitting gas may vary to a small extent with location and cloud; aerosol and volcanic dust may also modify the radiative heat exchange. Hence, basic satellite temperature sounding observations provide good horizontal resolution and spatial coverage worldwide for relatively thick layers in the vertical, but the precise distribution in the vertical of the atmospheric emission observed may be more difficult to specify at any given location.
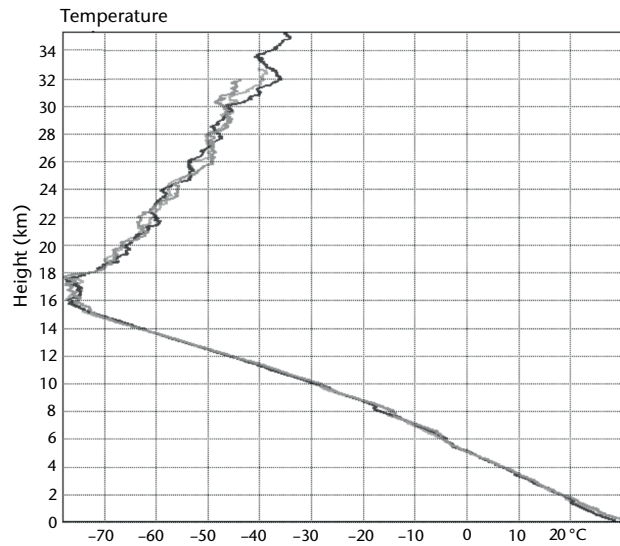
(a) July, Yangjiang, China (3 ascents in 8 h)
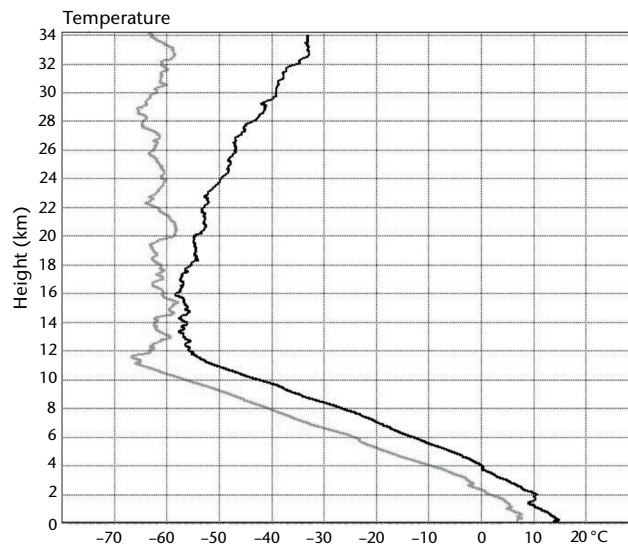
(b) United Kingdom, summer (black) and winter (grey)

Figure 12.2. Examples of complete individual temperature profiles made with large balloons suitable for climate observations

Most radiances observed by nadir-viewing satellite water vapour channels in the troposphere originate from layers of the atmosphere about 4 to 5 km thick. The pressures of the atmospheric layers contributing to the radiances observed by a water vapour channel vary with location to a much larger extent than for the temperature channels. This is because the thickness and central pressure of the layer observed depend heavily on the distribution of water vapour in the vertical. For instance, the layers observed in a given water vapour channel will be lowest when the upper troposphere is very dry. The water vapour channel radiances observed depend on the temperature of the water vapour. Therefore, water vapour distribution in the vertical can be derived only once suitable measurements of vertical temperature structure are available.

Limb-viewing satellite systems can provide measurements of atmospheric structure with higher vertical resolution than nadir-viewing systems; an example of this type of system is temperature and water vapour measurement derived from global positioning system (GPS) radio occultation. In this technique, vertical structure is measured along paths in the horizontal of at least 200 km

(Kursinski et al., 1997). The technique is now in widespread use as it provides improved measurements of vertical temperature structure, particularly around the tropopause where radiosondes are not available.

Thus, the techniques developed for using satellite sounding information in numerical weather prediction models incorporate information from other observing systems, mainly radiosondes and aircraft, or from the numerical weather prediction model fields themselves. The radiosonde information may be contained in an initial estimate of vertical structure at a given location, which is derived from forecast model fields or is found in catalogues of possible vertical structure based on radiosonde measurements typical of the geographical location or air mass type. In addition, radiosonde measurements are used to cross-reference the observations from different satellites or the observations at different view angles from a given satellite channel. The comparisons may be made directly with radiosonde observations or indirectly through the influence from radiosonde measurements on the vertical structure of numerical forecast fields.

Hence, radiosonde and satellite sounding systems, together with aircraft, are complementary observing systems and provide a more reliable global observation system when used together. Radiosonde and aircraft observations improve numerical weather prediction, even given the much larger volume of satellite measurements available.

12.1.3.3   *Maximum height of radiosonde observations*

Radiosonde observations are used regularly for measurements up to heights of about 35 km (see, for example, Figure 12.2). However, many observations worldwide will not be made to heights greater than about 25 km, because of the higher cost of the balloons and gas necessary to lift the equipment to the lowest pressures. Temperature errors tend to increase with height, but the rate of increase with modern radiosondes is not that high and useful measurements can be made up to 35 km, particularly at night.

When planning radiosonde measurements for climate monitoring, it is necessary to ensure that a sufficient number of large balloons are procured to obtain measurements up to 30 km on a regular basis in each region.

The problems associated with the contamination of sensors during flight and very long time-constants of sensor response at low temperatures and pressures currently limit the usefulness of quality radiosonde relative humidity measurements to the troposphere.

12.1.4   **Accuracy requirements**

This section summarizes the requirements for uncertainty (always stated in terms of $k = 2$, see Part I, Chapter 1 of this Guide) of the meteorological variables measured by radiosondes and compares them with typical operational performance. A more detailed discussion of performance and sources of errors is given in detail in the later sections dealing with the individual meteorological variable (see sections 12.3.5, 12.3.7, 12.4.7 and 12.5.7 for pressure, height, temperature and relative humidity, respectively). The definition of uncertainty, systematic bias and so on can be found in Part I, Chapter 1 of this Guide.

Estimates of achievable optimum uncertainty for radiosonde observations, as of 2012, are included in Annex 12.A. This annex was generated following the WMO Intercomparison of High Quality Radiosonde Systems in Yangjiang, China (WMO, 2011*b*). It describes the optimum performance that can currently be obtained from operational radiosondes.

A summary of requirements for uncertainty and vertical resolution limits for radiosonde observations extracted from WMO documents is presented in Annex 12.B. These tables include information from the WMO observing requirements database (OSCAR/Requirements; see WMO, 2014), the observation requirement targets published by WMO (2009) for the Global Climate Observing System (GCOS) Reference Upper-Air Network (GRUAN), and limited information from atmospheric variability studies in WMO (1970).

The WMO observing requirements database includes three limits for most meteorological variables:

(a)   The goal: an ideal requirement;

(b)   The threshold: the minimum requirement to be met to ensure that data are useful;

(c)   A breakthrough: an intermediate level between threshold and goal which, if achieved, would result in a significant improvement for the target application.

Tables 12.B.1, 12.B.2 and 12.B.3 in Annex 12.B are based mainly on the requirements of the high-resolution numerical weather prediction application area, although information on goals derived from atmospheric variability studies are also shown when the goals differ from those established in the WMO observing requirements database. Climate requirements are based on the GRUAN requirements and those in the section of the observing requirements database for AOPC or SPARC activities. Again, when there are significant differences between the goals from the two databases, these are indicated in the tables. Requirements for geopotential height in Table 12.B.4 were derived as described in Annex 12.B.

A radiosonde meeting the less stringent breakthrough requirements, as summarized in Annex 12.A, should provide measurements that give good value for money in terms of national targeted use. However, the less stringent accuracy requirements will not meet the expectations of some users, for instance for primary sites used to detect climate change. Thus, an operational decision has to be made as to the quality of the observation required by the national network, taking into account that the use of such data in forecasts will improve forecast quality across the country if the observation meets the breakthrough targets.

The requirements for spacing between observations in the horizontal from the WMO observing requirements database have not been shown here, but these clearly show that radiosonde observations on their own cannot meet the minimum requirements of the WMO Integrated Global Observing System (WIGOS), and must be supplemented by temperature, relative humidity and wind measurements from other observing systems.

12.1.4.1   *Geopotential height: requirements and performance*

Modern radiosonde systems can have systematic pressure bias a little larger than 1 hPa near the surface, but systematic errors as large as this at pressures lower than 100 hPa are now rare (see Table 12.4). The radiosondes still using the best pressure sensors can measure heights near 10 hPa with a random error ($k = 2$) between 300 and 400 m, that is, with a random error in pressure of about 0.6 hPa.

Thus, the uncertainty goal for height measurements for numerical weather prediction can be met by most radiosondes using a pressure sensor up to 100 hPa. However, it requires a radiosonde measuring height with GPS technology to measure up to 30 km with a random error of only 20 m, which is equivalent to a random error less than or equal to 0.05 hPa in pressure, depending on the uncertainty of the radiosonde temperature measurements.

The uncertainty goal for cloud-base heights in the lower troposphere in Table 12.B.4 of Annex 12.B requires pressure uncertainties ($k = 2$) of only 3 hPa associated with the cloud-base height. Most modern radiosondes can come close to this requirement.

Ozone concentrations in the stratosphere have pronounced gradients in the vertical, and height assignment errors from even relatively small pressure sensor errors introduce significant inaccuracies into the ozonesonde profile reports at all latitudes. This has proved to be one of the limiting factors in these measurements when using the older type of radiosonde with larger pressure errors in the stratosphere.

12.1.4.2 *Temperature: requirements and performance*

Most modern radiosonde systems (introduced since 2000) measure temperature in the troposphere and stratosphere up to a height of about 31 km with an uncertainty ($k = 2$) between 0.4 and 1 K. This is usually close to the optimum performance for numerical weather prediction suggested in Table 12.B.2 of Annex 12.B. However, uncertainty well in excess of 2 K can still be found in some national radiosonde networks in tropical regions. If used, measurements with such large errors damage numerical weather prediction forecasts.

In the stratosphere, radiosonde temperature uncertainties can be close to the goal for numerical weather prediction, but require some improvement in daytime conditions to be optimized for climate requirements.

As the goals for climate temperatures are more demanding than for numerical weather prediction, the GRUAN Lead Centre continues to work with manufacturers and operators to reduce the uncertainty of the current operational measurements in the troposphere and stratosphere. In this case, it is extremely important that systematic bias be as near constant with time as possible, requiring tighter limits on the methods of observation than at standard operational sites. To obtain the most useful performance, operators must take care to prepare and operate the radiosondes according to the instructions, whether from this Guide, the manufacturer or at GRUAN stations, according to the procedures agreed with the GRUAN Lead Centre. In the case of GRUAN, the details of the radiosonde preparation must be noted and archived as part of the metadata associated with the measurement (Immler et al., 2010).

12.1.4.3 *Relative humidity: requirements and performance*

The uncertainties in modern relative humidity sensor measurements at temperatures higher than –50 °C fall mostly within the range of 5% to 14% relative humidity (RH). Thus, the measurements mostly meet the breakthrough limit for numerical weather prediction, but many need improvement to meet the breakthrough limit for climate measurements (see Annex 12.B, Table 12.B.3).

At temperatures lower than –50 °C, the uncertainties increase, with the best operational radiosonde sensors having an uncertainty of about 16% relative humidity at –70 °C, i.e. close to the breakthrough for numerical weather prediction and not meeting the breakthrough for climate requirements. However, most modern sensors have uncertainties of about 24% relative humidity at the lowest temperatures. Several problems were identified in the WMO Intercomparison of High Quality Radiosonde Systems in Yangjiang, China (WMO, 2011*b*). It is expected that the uncertainties in upper troposphere relative humidity will improve with time as these are rectified.

12.1.5 **Methods of measurement**

This section discusses radiosonde methods in general terms. Details of instrumentation and procedures are given in other sections.

12.1.5.1 *Constraints on radiosonde design*

Certain compromises are necessary when designing a radiosonde:

(a) Temperature measurements are found to be most reliable when sensors are exposed unprotected above the top of the radiosonde, but this also leads to direct exposure to solar radiation. In most modern radiosondes, coatings are applied to the temperature sensor to minimize solar heating and heat exchange in the infrared. The radiation corrections work most reliably if the temperature sensor and its supports are designed so that the solar heating does not vary significantly as the radiosonde rotates in flight relative to the sun. Software corrections for the residual solar heating are then applied during data processing.

(b)   Nearly all relative humidity sensors require some protection from rain. A protective cover or duct reduces the ventilation of the sensor and hence the speed of response of the sensing system as a whole. The cover or duct also provides a source of contamination after passing through cloud. However, in practice, the requirement for protection from rain or ice is usually more important than perfect exposure to the ambient air. Thus, protective covers or ducts are used mostly with a relative humidity sensor. One of the alternatives is to have two sensors which alternate: one is heated to drive off contamination while the other reports the relative humidity; then the second sensor is heated while the first reports the relative humidity, and so on. Humidity sensors are often placed close to the temperature sensor since, until recent years, the humidity sensor was assumed to be at the same temperature as the temperature sensor. However, many radiosondes now measure the temperature of the humidity sensor directly, as the humidity sensor's temperature is rarely exactly the same as the air temperature reported by the radiosonde. If this is done, the relative humidity sensor may be given an improved exposure away from contamination from the main temperature sensor and its supports.

(c)   Pressure sensors are usually mounted internally to minimize the temperature changes in the sensor during flight and to avoid conflicts with the exposure of the temperature and relative humidity sensors.

(d)   In many modern radiosondes a pressure sensor is not used, and geometric height is measured using GPS technology and then converted into geopotential height based on knowledge of the gravitational fields at the location.

Other important features required in radiosonde design are reliability, robustness, and light weight and small dimensions to facilitate the launch. With modern electronic multiplexing readily available, it is also important to sample the radiosonde sensors at a high rate. If possible, this rate should be about once per second, corresponding to a minimum sample separation of about 5 m in the vertical. Since radiosondes are generally used only once, or not more than a few times, they must be designed for mass production at low cost. Ease and stability of calibration is very important, since radiosondes must often be stored for long periods (more than a year) prior to use. (Many of the most important Global Climate Observing System stations, for example, in Antarctica, are on sites where radiosondes cannot be delivered more than once per year.)

A radiosonde should be capable of transmitting an intelligible signal to the ground receiver over a slant range of at least 200 km. The voltage of the radiosonde battery varies with both time and temperature. Therefore, the radiosonde must be designed to accept battery variations without a loss of measurement accuracy or an unacceptable drift in the transmitted radio frequency.

12.1.5.2   *Radio frequency used by radiosondes*

The radio frequency spectrum bands currently used for most radiosonde transmissions are shown in Table 12.1. These correspond to the meteorological aids allocations specified by the International Telecommunication Union (ITU) Radiocommunication Sector radio regulations.

The radio frequency actually chosen for radiosonde operations in a given location will depend on various factors. At sites where strong upper winds are common, slant ranges to the radiosonde

Table 12.1. Primary frequencies used by radiosondes in the meteorological aids bands

Radio frequency band (MHz)	Status	ITU Regions
400.15 – 406	Primary	All
1 668.4 – 1 700	Primary	All

Note: Some secondary radar systems manufactured and deployed in the Russian Federation may still operate in a radio frequency band centred at 1 780 MHz.

are usually large and balloon elevations are often very low. Under these circumstances, the 400-MHz band will normally be chosen for use since a good communication link from the radiosonde to the ground system is more readily achieved at 400 MHz than at 1 680 MHz. When upper winds are not so strong, the choice of frequency will, on average, be usually determined by the method of upper-wind measurement used (see Part I, Chapter 13). The frequency band of 400 MHz is usually used when navigational aid windfinding is chosen, and 1 680 MHz when radiotheodolites or a tracking antenna are to be used with the radiosonde system.

The radio frequencies listed in Table 12.1 are allocated on a shared basis with other services. In some countries, the national radiocommunication authority has allocated part of the bands to other users, and the whole of the band is not available for radiosonde operations. In other countries, where large numbers of radiosonde systems are deployed in a dense network, there are stringent specifications on radio frequency drift and bandwidth occupied by an individual flight.

Any organization proposing to fly radiosondes should check that suitable radio frequencies are available for their use and should also check that they will not interfere with the radiosonde operations of the National Meteorological Service.

There are now strong requirements from governments to improve the efficiency of radio frequency use. Therefore, radiosonde operations will have to share with a greater range of users in the future. Wideband radiosonde systems occupying most of the available spectrum of the meteorological aids bands will become impracticable in many countries. Therefore, preparations for the future in most countries should be based on the principle that radiosonde transmitters and receivers will have to work with bandwidths of much less than 1 MHz in order to avoid interfering signals. Transmitter stability will have to be better than ±5 kHz in countries with dense radiosonde networks, and not worse than about ±200 kHz in most of the remaining countries.

National Meteorological Services need to maintain contact with national radiocommunication authorities in order to keep adequate radio frequency allocations and to ensure that their operations are protected from interference. Radiosonde operations will also need to avoid interference with, or from, data collection platforms transmitting to meteorological satellites between 401 and 403 MHz, with the downlinks from meteorological satellites between 1 690 and 1 700 MHz and with the command and data acquisition operations for meteorological satellites at a limited number of sites between 1 670 and 1 690 MHz.

12.1.6　Radiosonde errors: general considerations

12.1.6.1　*Types of error*

This section contains a detailed discussion of the errors encountered with radiosonde sensors.

Measurement errors by radiosondes may be classified into three types (WMO, 1975):

(a)　Systematic errors characteristic of the type of radiosonde in general;

(b)　Sonde error, representing the variation in errors that persist through thick layers in the vertical for a particular type of radiosonde from one flight to the next;

(c)　Random errors in individual observations, producing the scatter superimposed on the sonde error through a given ascent.

However, for many users it is also helpful to take note of the magnitude of the representativeness errors that are associated with a measurement (see Kitchen, 1989, and Part I, Chapter 1 of this Guide). For instance, radiosonde temperature observations are assigned an error in data assimilation schemes, and this has more to do with a representativeness error than the small instrumentation errors identified in section 12.4.7. These errors differ depending on the atmospheric situation and also on the use made of the measurement. For example, as the scales of motion represented in a numerical weather prediction model increase, the radiosonde

representativeness errors ought to decrease because the model represents more of what the radiosonde measures. On the other hand, a climatologist wants measurements that are close to a longer-term average, representing a significant area around the launch site. The structure introduced by localized small-scale fluctuations in the radiosonde measurement is undesirable for this purpose.

12.1.6.2   *Potential references*

High-precision tracking radar measurements or GPS height measurements can allow systematic errors in geopotential height measurements to be quantified. These results can then be used to identify systematic errors in radiosonde pressure sensor measurements, given that errors in temperature measurements are known to be relatively small.

Most newly developed radiosondes measure temperatures at night which fall within a range of ±0.2 K at a height of 30 km (WMO, 2006a, 2011b). Thus, at night, it is possible to identify systematic errors that bias radiosonde measurements away from this consensus.

However, interpreting daytime temperature comparisons with similar uncertainty is still not feasible. For instance, average temperatures in the same tests fall within about ±0.5 K at a height of 30 km. When used in big international tests, the scientific sounding instrumentation has not yet achieved the required performance in daytime to be able to identify correct measurements with the same uncertainty as at night.

Relative humidity measurements can be checked at high humidity when the radiosondes pass through clouds. Here, laser ceilometer and cloud radars can provide better evidence on the cloud observed by the radiosonde during its ascent. The vertical structure in relative humidity reported by radiosondes, including the presence of very dry layers, can be validated by comparison with Raman lidar measurements.

In most radiosonde comparison tests, the results from one radiosonde design are compared with those of another to provide an estimate of their systematic differences. The values of sonde error and random errors can usually be estimated from the appropriate method of computing the standard deviations of the differences between the two radiosonde types. The most extensive series of comparison tests performed since 1984 have been those of the WMO international radiosonde comparisons (WMO, 1987, 1991, 1996a, 2006b) and the tests performed in Brazil (WMO, 2006c), Mauritius (WMO, 2006a) and Yangjiang, China (WMO, 2011b). Results from these and other tests using the same standards in the United Kingdom (see results from the Camborne Met Office (WMO, 2010b)), the United States and Switzerland will sometimes be quoted in the subsequent sections.

There are several national facilities in which the performance of radiosonde sensors can be tested at different pressures and temperatures in the laboratory. The WMO Radiosonde Humidity Sensor Intercomparison (WMO, 2006b) contains results from laboratory comparisons with humidity standards in the Russian Federation. These results can be helpful in identifying some, but not all, of the problems identified when flying in the atmosphere.

12.1.6.3   *Sources of additional error during radiosonde operations*

It is extremely important to perform pre-flight radiosonde checks very carefully, since mistakes in measuring values for control data used to adjust calibrations can produce significant errors in measurement during the ascent. Observation errors in the surface data obtained from a standard screen and then included in the radiosonde message must also be avoided. An error in surface pressure will affect all the computed geopotential heights. For the same reason, it is important that the surface pressure observation should correspond to the official station height.

Random errors in modern radiosonde measurements are now generally small. This is the result of improved radiosonde electronics and multiplexing, providing more reliable data telemetry links between the ground station, and reliable automated data processing in the ground station.

Thus, the random errors are usually less significant than systematic radiosonde errors and flight-to-flight variation in sensor performance and calibration (sonde error). However, random errors may become large if there is a partial radiosonde failure in flight, if interference is caused by another radiosonde using a similar transmission frequency, or if the radiosondes are at long slant ranges and low elevations that are incompatible with the specifications of the ground system receiver and aerials.

Thus, errors in radiosonde measurements may be caused not only by the radiosonde sensor design and problems with calibration in the factory during manufacture, but also by problems in the reception of the radiosonde signal at the ground and the effect on subsequent data processing. When signal reception is poor, data-processing software will often interpolate values between the occasional measurements judged to be valid. Under this circumstance, it is vital that the operator is aware of the amount of data interpolation occurring. Data quality may be so poor that the flight should be terminated and a replacement radiosonde launched.

Software errors in automated systems often occur in special circumstances that are difficult to identify without extensive testing. Usually, the errors result from an inadvertent omission of a routine procedure necessary to deal with a special situation or combination of events normally dealt with instinctively by an expert human operator.

12.2 RADIOSONDE ELECTRONICS

12.2.1 General features

A basic radiosonde design usually comprises three main parts as follows:

(a)   The sensors plus references;

(b)   An electronic transducer, converting the output of the sensors and references into electrical signals;

(c)   The radio transmitter.

In rawinsonde systems (see Part I, Chapter 13), there are also electronics associated with the reception and retransmission of radionavigation signals, or transponder system electronics for use with secondary radars.

Radiosondes are usually required to measure more than one meteorological variable. Reference signals are used to compensate for instability in the conversion between sensor output and transmitted telemetry. Thus, a method of switching between various sensors and references in a predetermined cycle is required. Most modern radiosondes use electronic switches operating at high speed with one measurement cycle lasting typically between 1 and 2 s. This rate of sampling allows the meteorological variables to be sampled at height intervals of between 5 and 10 m at normal rates of ascent.

12.2.2 Power supply for radiosondes

Radiosonde batteries should be of sufficient capacity to power the radiosonde for the required flight time in all atmospheric conditions. For radiosonde ascents to 5 hPa, radiosonde batteries should be of sufficient capacity to supply the required currents for up to three hours, given that the radiosonde launch may often be delayed and that flight times may be as long as two hours. Three hours of operation would be required if descent data from the radiosonde were to be used. Batteries should be as light as practicable and should have a long storage life. They should also be environmentally safe following use. Many modern radiosondes can tolerate significant changes in output voltage during flight. Two types of batteries are in common use, the dry-cell type and water-activated batteries.

The use of dry-cell batteries has increased rapidly as these have the advantages of being widely available at very low cost because of the high volume of production worldwide and of posing less risk in terms of occupational health and safety (and environmental impact). However, they may have the disadvantage of having limited shelf life. Also, their output voltage may vary more during discharge than that of water-activated batteries.

Water-activated batteries usually use a cuprous chloride and sulphur mixture. The batteries can be stored for long periods. The chemical reactions in water-activated batteries generate internal heat, reducing the need for thermal insulation and helping to stabilize the temperature of the radiosonde electronics during flight. These batteries are not manufactured on a large scale for other users. Therefore, they are generally manufactured directly by the radiosonde manufacturers.

Care must be taken to ensure that batteries do not constitute an environmental hazard once the radiosonde falls to the ground after the balloon has burst.

12.2.3   Methods of data transmission

12.2.3.1   *Radio transmitter*

A wide variety of transmitter designs are in use. Solid-state circuitry is mainly used up to 400 MHz and valve (cavity) oscillators may be used at 1 680 MHz. Modern transmitter designs are usually crystal-controlled to ensure a good frequency stability during the sounding. Good frequency stability during handling on the ground prior to launch and during flight are important. At 400 MHz, widely used radiosonde types are expected to have a transmitter power output lower than 250 mW. At 1 680 MHz the most widely used radiosonde type has a power output of about 330 mW. The modulation of the transmitter varies with radiosonde type. It would be preferable in the future if radiosonde manufacturers could agree on a standard method and format for transmission of data from the radiosonde to the ground station, which would allow user interoperability between radiosonde types without the need to modify the ground reception hardware and software each time. In any case, the radiocommunication authorities in many regions of the world will require that radiosonde transmitters meet certain specifications in the future, so that the occupation of the radio-frequency spectrum is minimized and other users can share the nominated meteorological aids radio-frequency bands (see section 12.1.5.2).

12.3   PRESSURE SENSORS (INCLUDING HEIGHT MEASUREMENTS)

12.3.1   General aspects

Radiosonde pressure sensors must sustain accuracy over a very large dynamic range from 3 to 1 000 hPa, with a resolution of 0.1 hPa over most of the range and a resolution of 0.01 hPa for pressures less than 100 hPa. Changes in pressure are usually identified by a small electrical or mechanical change. For instance, the typical maximum deflection of an aneroid capsule is about 5 mm, so that the transducer used with the sensor has to resolve a displacement of about 0.5 μm. Changes in calibration caused by sensor temperature changes during the ascent must also be compensated. These temperature changes may be as large as several tens of degrees, unless the pressure sensor is mounted in a stabilized environment.

Thus, pressure sensors are usually mounted internally within the radiosonde body to minimize the temperature changes that occur. In some cases, the sensor is surrounded by water bags to reduce cooling. When water-activated batteries are used, the heat generated by the chemical reaction in the battery is used to compensate the internal cooling of the radiosonde. However, even in this case, the radiosonde design needs to avoid generating temperature gradients across the sensor and its associated electrical components. If a pressure sensor has an actively controlled temperature environment, the sensor assembly should be mounted in a position on the radiosonde where heat contamination from the pressure sensor assembly cannot interfere with the temperature or relative humidity measurements.

The pressure sensor and its transducer are usually designed so that sensitivity increases as pressure decreases. The time constant of response of radiosonde pressure sensors is generally very small, and errors from sensor lag are not significant.

Historically, when reliable pressure sensors for low pressure were being manufactured, sensors with poor performance were replaced by pressure measurements deduced from radar heights, as in the United Kingdom before 1978. In some countries of the Commonwealth of Independent States, very accurate secondary radars are used to measure geometric heights instead of using a pressure sensor on the radiosonde.

Today, many modern radiosonde systems use GPS navigation signals to locate the position of the radiosonde and have dispensed with the use of a pressure sensor on the radiosonde (to save on consumable costs). As a result, geometric height, and hence geopotential height, is measured directly (see section 12.3.6), with the pressure changes in flight computed from the radiosonde temperature and humidity measurements.

12.3.2   Aneroid capsules

Aneroid capsules have been used as the pressure sensor in the majority of radiosondes. In the older radiosonde designs, the capsules were usually about 50 to 60 mm in diameter. The sensors were made from a metal with an elastic coefficient that is independent of temperature. The measurement of the deflection of the aneroid capsule can be achieved either by an external device requiring a mechanical linkage between the capsule and the radiosonde transducer or by an internal device (see section 12.3.3).

Aneroid sensitivity depends mainly on the effective surface area of the capsule and its elasticity. Capsules can be designed to give a deflection that is linearly proportional to the pressure or to follow some other law, for example, close to a logarithmic dependence on pressure. The long-term stability of the capsule calibration is usually improved by seasoning the capsules. This is achieved by exercising the capsules through their full working range over a large number of cycles in pressure and temperature.

When the aneroid is used with a mechanical linkage to a transducer, the sensor usually suffers from a hysteresis effect of about 1 to 2 hPa. This hysteresis must be taken into account during the sensor calibration. The change in pressure during calibration must be of the same sense as that found in actual sounding conditions. The mechanical linkage to the radiosonde transducer often consists of a system amplifying the movement of the capsule to a pointer operating switch contacts or resistive contacts. A successful operation requires that friction be minimized to avoid both discontinuous movements of the pointer and hysteresis in the sensor system.

12.3.3   Aneroid capsule (capacitive)

Many modern radiosonde designs use aneroid capsules of smaller diameter (30 mm or less in diameter) with the deflection of the capsule directly measured by an internal capacitor. A parallel plate capacitor used for this purpose is formed by two plates each fixed directly to one side of the capsule. The capacitance, C, is then:

$$C = \in \cdot S / e \tag{12.1}$$

where S is the surface area of each plate, e is the distance between the plates and ϵ is the dielectric constant. As e is a direct function of the deflection of the capsule, the capacitance C is a direct electrical measurement of the deflection. In many radiosonde sensors, each capacitor plate is fixed to the opposite side of the capsule by mounts passing through holes in the other plate. With this configuration, e decreases when the pressure lowers. The sensitivity of the capacitive sensor is:

$$- \in \cdot S / e^2 \cdot de / dp \tag{12.2}$$

This will be greatest when e is small and the pressure is smallest. The capacitive sensor described is more complicated to manufacture but is best suited for upper-air measurements, as the sensitivity can be 10 times greater at 10 hPa than at 1 000 hPa. The value of the capacitance is usually close to 6 pF.

Capacitive aneroid capsules are usually connected to a resistance-capacitance electronic oscillator with associated reference capacitors. This arrangement needs to measure very small variations of capacity (for example, 0.1% change in a maximum of 6 pF) without any significant perturbation of the oscillator from changes in temperature, power supply or ageing. Such high stability in an oscillator is difficult to achieve at a low price. However, one solution is to multiplex the input to the oscillator between the pressure sensor and two reference capacitors. A reference capacitor C_1 is connected alone to the oscillator, then in parallel with C_p, the pressure sensor capacitor, and then in parallel with a second reference C_2 to provide a full-scale reference.

The calibration of an aneroid capacitive sensor will usually have significant temperature dependence. This can be compensated either by referencing to an external capacitor which has a temperature coefficient of similar magnitude or during data processing in the ground system using calibration coefficients from factory calibrations. The correction applied during processing will depend on the internal temperature measured close to the pressure sensor. In practice, both of these compensation techniques may be necessary to achieve the required accuracy.

12.3.4   **Silicon sensors**

Following rapid developments in the use of silicon, reliable pressure sensors can now be made with this material. A small cavity is formed from a hole in a thick semiconductor layer. This hole is covered with a very thin layer of silicon, with the cavity held at a very low pressure. The cavity will then perform as a pressure sensor, with atmospheric pressure sensed from the deflection of the thin silicon cover.

A method of detecting the deflection of the silicon is to use a capacitive sensor. In this case, the thin silicon layer across the cavity is coated with a thin metallic layer, and a second metallic layer is used as a reference plate. The deflection of the silicon cover is measured by using the variation in the capacitance between these two layers. This type of sensor has a much lower temperature dependence than the strain gauge sensor and is now in widespread use. Because the sensor is very small, it is possible to avoid the calibration errors of the larger capacitive aneroid sensors introduced by changes in temperature gradients across the aneroid sensor and associated electronics during an ascent.

12.3.5   **Pressure sensor errors**

Systematic errors and the radiosonde error (flight-to-flight variation at $k = 2$) have been estimated from the WMO international radiosonde comparisons for selected radiosonde types. The results are shown in Table 12.2. The range of values of systematic error usually represents the spread of results from several tests.

Aneroid capsules were liable to change calibration unless they had been well seasoned through many pressure cycles over their working range before use. Software corrections applied during data processing, but based on ground control readings before launch, went some way toward reducing these errors. Nevertheless, corrections based on ground checks relied on a fixed error correction pattern across the working range. In practice, the change in pressure sensor calibration was more variable over the working range.

The MRZ secondary radar system was introduced into the Russian Federation in the mid-1980s, with the results shown obtained in 1989. There is no pressure sensor in this system. The pressure is computed from measurements of geometric height which are then converted to geopotential height as shown in section 12.3.6. The quality of the measurements depended on the performance of each individual secondary radar.

The VIZ MKII and Meisei RS2-91 radiosondes had capacitive aneroid sensors, but of differing design. Overall uncertainties ($k = 2$) for the capacitive aneroids were usually lower than 2 hPa at most pressures. However, these capacitive aneroid capsules could have significant systematic errors, particularly when the internal temperature of the radiosonde changed and temperature gradients developed across the sensor and its associated electronics. Systematic errors with capacitive aneroids were usually not larger than ±1 hPa. However, errors could be larger if the pressure sensors experienced very large thermal shock during the launch.

The Vaisala RS92 uses a silicon sensor. The performance of these sensors did not show the effects of thermal shock, and the uncertainties obtained with the systems were even better than with the capacitative aneroids.

The consequences of the pressure errors in Table 12.2 on reported temperatures would be as follows: a 1 hPa pressure error will produce a temperature error, on average, of −0.1 K at 900 hPa, −0.3 K in the upper troposphere (at 200 hPa in the tropics), ±0.5 K at 30 hPa (varying between summer and winter conditions at about 55°N) and up to at least 1 K for most situations at 10 hPa.

12.3.5.1 *Relationship of geopotential height errors to pressure errors*

The error, $\varepsilon_z(t_1)$, in the geopotential height at a given time into flight is given by:

$$\varepsilon_z(t_1) = \frac{R}{g} \int_{p_0}^{p_1} \left[\varepsilon_T(p) - \frac{\delta T}{\delta p} \varepsilon_p(p) \right] \frac{dp}{p} + \frac{R}{g} \int_{p_1}^{p_1 + \varepsilon_p(p_1)} \left[T_v(p) + \varepsilon_T(p) - \frac{\delta T}{\delta p} \varepsilon_p(p) \right] \frac{dp}{p} \tag{12.3}$$

where p_0 is the surface pressure; p_1 is the true pressure at time t_1; $p_1 + \varepsilon_p(p_1)$ is the actual pressure indicated by the radiosonde at time t_1; $\varepsilon_T(p)$ and $\varepsilon_p(p)$ are the errors in the radiosonde temperature and pressure measurements, respectively, as a function of pressure; $T_v(p)$ is the virtual temperature at pressure p; and R and g are the gas and gravitational constants as specified in WMO (2011a).

Table 12.2. Range of systematic error and radiosonde error (flight to flight, $k = 2$) and overall uncertainty in pressure from the WMO international radiosonde comparisons and associated tests

Radiosonde type	Systematic error			Sonde error			Uncertainty		
Pressure level (hPa)	850	100	10	850	100	10	850	100	10
MRZ[a] (Russian Federation)	−1.5 to −0.5	−1.2 to −0.8	0 – 0.2	7	3.5	0.5	8	4	0.7
Meisei RS2-91	0.2 – 1	−0.1 – 0.5	−0.2 – 0.2	1	0.6	0.6	2	1.1	0.8
VIZ MKII	0 – 1	0.7 – 1.1	0.3 – 0.7	1.6	0.6	0.4	2.5	1.6	1
Vaisala RS92, silicon sensor	< 0.5	< 0.3	< 0.2	0.8	0.4	0.2	1	0.6	0.4
MODEM M2K2[a]	−0.8 to −0.4	< 0.1	< 0.05	1.2	0.4	0.03	1.6	0.4	0.05
Vaisala RS92[a]	< 0.5	< 0.1	< 0.05	1.2	0.4	0.03	1.6	0.4	0.05
Lockheed Martin Sippican (LMS),[a] LMG-6	< 0.5	< 0.1	< 0.05	1.2	0.4	0.03	1.2	0.4	0.05

Note:
a Does not use a pressure sensor but computes pressure from geopotential height measurements; see section 12.3.6.

Table 12.3. Systematic errors in geopotential height (gpm) from given pressure and temperature errors

	ε_T,T error (K)	$\varepsilon_{p'}$ P error (hPa)	Latitude	300 hPa	100 hPa	30 hPa	10 hPa
Standard pressure height, T error	0.25	0	All	9	17	26	34
Standard pressure height, p error	0	–1	25°N	3	12	–2	–24
Standard pressure height, p error	0	–1	50°N summer	3	5	1	–20
Standard pressure height, p error	0	–1	50°N winter	3	5	6	–4
Significant level height, p error	0	–1	25°N	27	72	211	650
Significant level height, p error	0	–1	50°N summer	26	72	223	680
Significant level height, p error	0	–1	50°N winter	26	70	213	625

For a specified standard pressure level, p_s, the second term in equation 12.3 disappears because there is no error in p_s, and so the error in the standard pressure level geopotential height is smaller:

$$\varepsilon_z(p_s) = \frac{R}{g} \int_{p_0}^{p_s} \left[\varepsilon_T(p) - \frac{\delta T}{\delta p} \varepsilon_p(p) \right] \frac{dp}{p} \qquad (12.4)$$

And for radiosondes without a pressure sensor using a radar:

$$\varepsilon_z(p_s) = T_v(p_s) \int_{z_0}^{z_{ps}} g / T^2 \left[\varepsilon_T(z) + \varepsilon_z(Range, \theta) \cdot dT_v / dz \right] \qquad (12.5)$$

where Z_{ps} is the geopotential height of the specified pressure level p_s, and the error in geopotential height for a radar is a function of slant range and elevation angle (θ), and will vary from flight to flight according to the wind conditions.

Table 12.3 shows the errors in geopotential height that are caused by radiosonde sensor errors for typical atmospheres. The geopotentials of given pressure levels have small errors, whether caused by a radiosonde temperature or pressure error. The pressure error has a slightly different effect at different latitudes because the typical temperature profile structure varies with latitude. However, the same pressure sensor errors produce much larger errors at the heights of specific structures, such as temperature inversions, including at the tropopause, and cloud tops and bases.

The importance of equations 12.4 and 12.5 is that the errors in standard pressure level geopotentials are primarily related to the temperature errors, and so if geopotential heights are compared against collocated NWP first-guess forecast fields, the height anomalies give an indication of the relative temperature performance at the two sites (see WMO, 2003).

12.3.6 Use of geometric height observations instead of pressure sensor observations

12.3.6.1 *General*

Geometric height observations can now be provided by GPS radiosondes that decode global positioning satellite signals, as opposed to the early GPS radiosondes that did not decode the signals. The geometric height observations have small enough uncertainty (between 10 and 20 m) to be used to compute pressure at a given time into flight, using surface pressure and temperature and relative humidity observations (see equations 12.12 and 12.13). In the stratosphere, the computed pressures are found to have smaller uncertainty than measurements provided by the best radiosonde pressure sensors (see Table 12.2).

The elimination of the pressure sensor from GPS radiosondes provides a considerable saving in terms of the cost of some radiosondes, but it is also necessary to check user requirements for the non-hydrostatic numerical weather prediction models that are being introduced, since direct measurements of pressure and geopotential height in the troposphere may be of some advantage when hydrostatic balance does not represent atmospheric conditions.

12.3.6.2 *Method of calculation*

The conversion from geometric height measured with a GPS radiosonde to geopotential height is purely a function of the gravitational field at a given location and does not depend on the temperature and humidity profile at the location. The gravitational potential energy (Φ_1) of a unit mass of anything is the integral of the normal gravity from mean sea level ($z = 0$) to the height of the radiosonde ($z = z_1$), as given by equation 12.6:

$$\Phi_1 = \int_0^{z_1} \gamma(z, \varphi) \cdot dz \tag{12.6}$$

where $\gamma(z, \varphi)$ is the normal gravity above the geoid. This is a function of geometric altitude, z, and the geodetic latitude φ.

This geopotential is divided by the normal gravity at 45° latitude to give the geopotential height used by WMO, as:

$$Z_1 = \Phi_1 / \gamma_{45°} \tag{12.7}$$

where $\gamma_{45°}$ was taken in the definition as 9.806 65 m s^{-2}. Note that surface gravity is greatest at the poles (9.832 18 m s^{-2}) and least at the Equator (9.780 33 m s^{-2}).

The variation of gravity with height must take into account the ellipsoidal shape of the Earth and the Earth's rotation. However, when the variation of γ with height was taken into account, the geopotential height, Z_1, at geometric height, z_1, was approximated using the Smithsonian meteorological tables (List, 1968) as:

$$Z_1(z_1, \varphi) = \left(\gamma_{\text{SMT}}(\varphi) / \gamma_{45°}\right) \cdot \left(\left(R_{\text{SMT}}(\varphi) \cdot z_1\right) / \left(R_{\text{SMT}}(\varphi) + z_1\right)\right) \tag{12.8}$$

where $R_{\text{SMT}}(\varphi)$ is an effective radius of the Earth for latitude (φ) and is the value in the Smithsonian tables which was chosen to take account of the actual changes with geometric height in the combined gravitational and centrifugal forces. It is not the actual radius of the Earth at the given latitude. This is shown in Figure 12.3, where the Smithsonian radius increases from the Equator to high latitudes, but the actual radius of the Earth's ellipsoid is largest at the Equator and smallest at the poles.

As the values for $R_{\text{SMT}}(\varphi)$ in the Smithsonian tables were obtained around 1949, the International Ellipsoid 1935 was used in the computations rather than the World Geodetic System 1984 (WGS-84) currently used with GPS receivers. Also, the Smithsonian tables used a value for $\gamma_{\text{SMT}}(\varphi)$ of:

$$\gamma_{\text{SMT}}(\varphi) = 9.806\,16 \cdot \left(1 - 0.002\,637\,3 \cdot \cos(2\varphi) + 0.000\,005\,9 \cdot \cos(2\varphi)^2\right) \left[\text{m s}^{-2}\right] \tag{12.9}$$
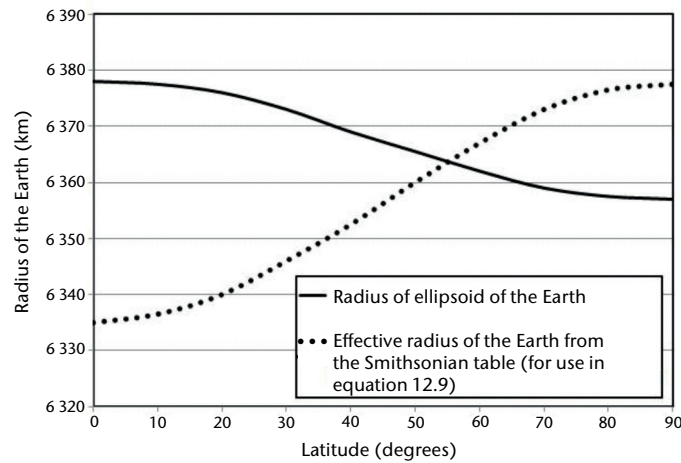
Figure 12.3. Variation of the Earth's radius with latitude compared to the variation of the Smithsonian table radius used in equation 12.8

This formula was not explicitly derived in the published scientific literature, although it was recommended for meteorological use by the International Association of Geodesy in 1949.

An alternative expression for the relationship in equation 12.8 has been proposed by Mahoney (personal communication), based on the WGS-84 geoid. Then, geopotential height for geometric height, z_1, becomes:

$$Z_1\left(z_1,\varphi\right) = \left(\gamma_s\left(\varphi\right)/\gamma_{45°}\right)\cdot\left(\left(R\left(\varphi\right)\cdot z_1\right)/\left(R\left(\varphi\right)+z_1\right)\right) \tag{12.10}$$

where $\gamma_s(\varphi)$ is the normal gravity on the surface of an ellipsoid of revolution, and where:

$$\gamma_s\left(\varphi\right) = 9.780\,325\cdot\left(\left(1+0.001\,931\,85\cdot\sin\left(\varphi\right)^2\right)\middle/\left(1-0.006\,694\,35\cdot\sin\left(\varphi\right)^2\right)^{0.5}\right) \tag{12.11}$$

with the radius $R(\varphi) = 6\,378.137/(1.006\,803 - 0.006\,706 \cdot \sin(\varphi)^2)$, giving results for R similar to the values in the Smithsonian tables.

If the geopotential height for a geometric height of 30 km is computed, it ranges from 29.778 5 km at the Equator to 29.932 km at 80°N, whether equations 12.8 and 12.9 or 12.10 and 12.11 are used. Differences between the geopotential height values obtained by the two methods are less than 1 m, and as such are not critical for meteorologists.

The difference between geometric height and geopotential height increases with height above the Earth's surface. An example of typical differences taken from measurements in the WMO Intercomparison of High Quality Radiosonde Systems in Yangjiang, China, at 22°N is shown in Table 12.4.

Table 12.4. Differences between geopotential and geometric height measured at the WMO Radiosonde Intercomparison in Yangjiang, China, at 22°N

Geopotential height	Geopotential – geometric height
8 000	25
16 000	70
24 000	135
32 000	220

Once the variation of the geopotential heights with respect to temperature and relative humidity has been established, the pressures can be computed integrating upwards from the measured surface pressure, using the hypsometric relationship, in a discrete form:

$$L_n\left(p_{i+1}/p_i\right) = -9.806\,65 \cdot dZ/R^* \cdot T_v \tag{12.12}$$

where p is the pressure in hPa; R^* is the gas constant for dry air; T_v is the mean virtual temperature for the layer in degrees K; dZ is the layer thickness in geopotential height; and i refers to the lower boundary of this layer.

The virtual temperature T_v is computed from:

$$T_v = T\big/\left(1 - \left(U/100\right)\cdot\left(e_s\left(T\right)\big/p\right)\cdot\left(1 - \varepsilon_a\right)\right) \tag{12.13}$$

where U is the relative humidity of the air, e_s is the saturation vapour pressure for water vapour and ε_a the ratio of the molecular weight of wet and dry air, with $\varepsilon_a = 0.622$.

It has to be emphasized again that the radiosonde temperature and relative humidity are used only in the computation of the pressures with systems using GPS geometric height measurements, as the geopotential values come purely from the geometric heights and the Earth's gravitational fields.

The algorithms for computing geometric height from windfinding radar observations of slant range and elevation and for the conversion of geometric heights to geopotential heights are included in WMO (1986). The actual algorithm used with secondary radar systems in the Russian Federation can be found in WMO (1991). If radar height observations are used as a replacement for pressure sensor observations, the heights need to be corrected for the effects of the Earth's curvature and radio-wave refraction before pressure is computed. Corrections for refraction can be made using seasonal averages of atmospheric profiles, but better pressure accuracy might require height corrections for the conditions encountered in individual flights.

12.3.7 Sources of error in direct height measurements

12.3.7.1 *In GPS geometric height measurements*

As long as there is no local interference at GPS navigation signal frequencies, most modern radiosonde systems are able to generate heights with good accuracy relative to the height where GPS lock occurs in flight. However, the software has to be able to interpolate reliably back to the surface (taking into account changes in the balloon rate of ascent just after launch) in order to ensure best performance in GPS measurements. In the WMO Intercomparison of High Quality Radiosondes in Yangjiang, China (WMO, 2011b), some of these interpolation software modules worked better than others, and systematic errors larger than 10 m resulted in the worst cases, persisting throughout the flight of a given radiosonde type.

It is essential to check the height of the local GPS antenna relative to the surface pressure sensor and ensure that this is used correctly in the radiosonde system software computations. Remember that a mismatch (or pressure error) of 1 hPa in the pressure at the antenna relative to the surface pressure sensor at the radiosonde station will result in a 10 m height bias throughout the flight.

In-flight processing must be able to cope with significant variations (positive and negative) in the rates of ascent of the balloons lifting the radiosonde. Errors in temperature and relative humidity will only affect the pressure computation from the geopotential heights (see equations 12.12 and 12.13). The effect of temperature errors on pressure computations can be judged from the values of height errors in Table 12.3 resulting from a 0.25 K temperature error throughout the profile. This temperature error would lead to pressure errors of 0.4, 0.3, 0.13 and 0.05 hPa at nominal pressures of 300, 100, 30 and 10 hPa, respectively.

Thus, in the stratosphere, GPS geometric heights are able to deliver much more reliable height measurements than any other operational height measuring system. Near the surface, GPS

height measurements must be performed with care to be of similar quality to the best pressure sensors. The breakthrough requirements for pressure in Annex 12.A can be achieved with GPS radiosondes at all pressures. However, it is not obvious that all GPS radiosonde systems can achieve the optimum pressure sensor requirements at low levels, while at pressures lower than 100 hPa, optimum requirements could be achieved as long as temperature errors are low.

12.3.7.2 *In radar height measurements*

The effect of radar observational errors upon windfinding is considered in Part I, Chapter 13. However, for radar heights (random and systematic) errors in elevation are much more significant than for winds. Systematic bias in slant range is also more critical for height than for wind measurements. Therefore, radars providing satisfactory wind measurements often have errors in elevation and slant range that prevent best quality height (and hence pressure) measurements.

Small but significant systematic errors in elevation may arise from a variety of sources as follows:

(a) Misalignment of the axes of rotation of azimuth and elevation of the radar during manufacture. If this is to be avoided, the procurement specification must clearly state the accuracy required;

(b) Errors in levelling the radar during installation and in establishing the zero elevation datum in the horizontal;

(c) Differences between the electrical and mechanical axes of the tracking aerials, possibly introduced when electrical components of the radar are repaired or replaced.

Errors may arise from errors introduced by the transducer system measuring the radar elevation angle from the mechanical position of the tracking aerial.

Systematic errors in slant range may arise from the following:

(a) A delay in triggering the range-timing circuit or incorrect compensation for signal delay in the radar detection electronics;

(b) Error in the frequency of the range calibrator.

Thus, radiosonde systems operating without pressure sensors and relying solely on radar height measurements require frequent checks and adjustments of the radars as part of routine station maintenance. These systems are not suitable for use in countries where technical support facilities are limited.

12.4 **TEMPERATURE SENSORS**

12.4.1 **General requirements**

The best modern temperature sensors have a speed of response to changes of temperature which is fast enough to ensure that systematic bias from thermal lag during an ascent, the typical rate of ascent being 5 to 6 m s^{-1}, remains less than 0.1 K through any layer of depth of 1 km in the troposphere and less than 0.2 K through any layer of similar depth in the stratosphere. This is achieved in most locations using a sensor with a time constant of response faster than 1 s in the early part of the ascent. In addition, the temperature sensors should be designed to be as free as possible from radiation errors introduced by direct or backscattered solar radiation. There must be as small a variation as possible in the area of cross-section for solar heating as the sensor rotates relative to the sun during ascent. Heat exchange in the infrared needs to be avoided by using sensor coatings that have low emissivity in the infrared.

Temperature sensors also need to be sufficiently robust to withstand buffeting during launch and sufficiently stable to retain accurate calibration over several years. The main types of temperature sensors in routine use are resistive sensors (for example, thermistors made of ceramic resistive semiconductors or metal resistors), capacitive sensors and thermocouples.

The rate of response of the sensor is usually measured in terms of the time constant of response, τ. This is defined (as in Part I, Chapter 1, 1.6.3) by:

$$dT_e/dt = -1/\tau \cdot (T_e - T)$$ (12.14)

where T_e is the temperature of the sensor and T is the true air temperature.

Thus, the time constant is defined as the time required to respond by 63% to a sudden change of temperature. The time constant of the temperature sensor is proportional to thermal capacity and inversely proportional to the rate of heat transfer by convection/diffusion from the sensor. Thermal capacity depends on the volume and composition of the sensor, whereas the heat transfer from the sensor depends on the sensor surface area, the heat transfer coefficient and the rate of the air mass flow over the sensor. The heat transfer coefficient has a weak dependence on the diameter of the sensor. Thus, the time constants of response of temperature sensors made from a given material are approximately proportional to the ratio of the sensor volume to its surface area. Consequently, thin sensors of large surface area are the most effective for obtaining a fast response. The variation of the time constant of response with the mass rate of airflow can be expressed as:

$$\tau = \tau_0 \cdot (\rho \cdot v)^{-n}$$ (12.15)

where ρ is the air density, v the air speed over the sensor, and n a constant.

The value of n varies between 0.4 and 0.8, depending on the shape of the sensor and on the nature of the airflow (laminar or turbulent). A selection of the time constants of response of both older and modern types of temperature sensors is shown in Table 12.5. These are for pressures of 1 000, 100 and 10 hPa, with a rate of ascent of 5 m s^{-1}. The values were derived from a combination of laboratory testing and comparisons with very fast response sensors during ascent in radiosonde comparison tests.

Modern bead thermistors, wire thermocapacitors and thermocouples have a very fast response, so the systematic errors from thermal lag are expected to be less than 0.05 K in the upper troposphere for the better sensors, and less than 0.1 K in the upper stratosphere.

WMO (2011b) shows examples in which the response speeds of most of the bead thermistors used by radiosondes in the test were similar or slightly faster than those of the chip thermistor included in Table 12.5.

12.4.2   **Thermistors**

Thermistors are usually made of a ceramic material whose resistance changes with temperature. The sensors have a high resistance that decreases with absolute temperature. The relationship between resistance, R, and temperature, T, can be expressed approximately as:

$$R = A \cdot \exp(B/T)$$ (12.16)

where A and B are constants. Sensitivity to temperature changes is very high, but the response to temperature changes is far from linear since the sensitivity decreases roughly with the square of the absolute temperature. As thermistor resistance is very high, typically tens of thousands of ohms, self-heating from the voltage applied to the sensor is negligible. It is possible to manufacture very small thermistors and, thus, fast rates of response can be obtained. Solar heating of a modern chip thermistor is about 1 K at 10 hPa.

Table 12.5. Typical time-constants of response of radiosonde temperature sensors

Temperature sensor	Operational use	τ (1 000 hPa)	τ (100 hPa)	τ (10 hPa)
Chip thermistor,[a] 0.4 x 0.8 x 0.8 mm	2003–	≤ 1	≤ 3	≤ 10
Wire thermocapacitor,[a] diameter 0.1 mm	2002–	0.4	1.1	3
Copper-constantan thermocouple,[a] diameter 0.06 mm	1991–	< 0.3	< 0.8	2
Other modern bead thermistors[a]	2005–	≤ 1	≤ 4	5 – 12

Note:

a   The time constants of response at 10 hPa of the chip thermistors in Yangjiang, China, were larger than those of the Copper-constantan thermocouple by about 4 s. The other small bead thermistors had time constants of response between 3 and 10 s larger than the Copper-constantan thermocouple. The wire thermocapacitor showed time constants of response of at least 4 s, a little larger than the results from the laboratory test cited above. This may be because the diameter of the wire thermocapacitor in the Vaisala RS92 radiosondes had been increased in 2007 by incorporating a quartz support fibre, and may also be a consequence of the software used with the sensor in Yangjiang.

12.4.3   **Thermocapacitors**

Thermocapacitors are usually made of a ceramic material whose permittivity varies with temperature. The ceramic used is usually barium-strontium titanate. This ferro-electric material has a temperature coefficient of permittivity of the order of 10^{-2} per K. The temperature coefficient is positive at temperatures below the Curie point and negative at temperatures above the Curie point. Sensors can now have a diameter of about 0.1 mm. The wire thermocouple measures the change in capacitance between two fine platinum wires separated by a glass ceramic (see Turtiainen et al., 1995). This sensor gives improved speed of response, and solar heating errors are less than 1 K at 10 hPa.

12.4.4   **Thermocouples**

Copper-constantan thermocouple junctions are also used as a temperature sensor in one national radiosonde (WMO, 1989*a*). Wires of 0.05 mm in diameter are used to form the external thermocouple junction and these provide a sensor with a very fast response. The relationship between the thermal electromotive force and the temperature difference between the sensor and its reference is an established physical relationship. The thermocouple reference is mounted internally within the radiosonde in a relatively stable temperature environment. A copper resistor is used to measure this reference temperature. In order to obtain accurate temperatures, stray electromotive force introduced at additional junctions between the sensor and the internal references must also be compensated.

12.4.5   **Scientific sounding instruments**

Two specialized scientific temperature sounding sensors were deployed during the WMO Intercomparison of High Quality Radiosonde Systems in Yangjiang, China (WMO, 2011*b*):

(a)   The MTR temperature sensor uses an ultrathin tungsten wire as a sensor. The wire is 0.01 mm in diameter, 44 cm long and wound into a helical coil with a diameter of 0.2 mm and a pitch of 0.1 mm. The wire is coated with aluminium to improve reflectivity and thus reduce solar heating (see Shimizu and Hasebe, 2010). This sensor has smaller time-constants of response than the Copper-constantan thermocouple;

(b)   The multithermistor radiosonde in Yangjiang was an independent instrument based on the National Aeronautics and Space Administration (NASA) Accurate Temperature Measuring (ATM) multithermistor radiosonde (see Schmidlin et al., 1995; WMO, 2006d). The system made measurements with three aluminized thermistors and one white and one black thermistor. In Yangjiang, the time constants of response were similar to those of the modern bead thermistors. With the measurements from the five sensors and an exact knowledge of the optical properties of the different sensor coatings, a reference temperature is derived as well as estimates of the solar and infrared radiation environments. This estimated temperature does not depend on any assumption about the backscattering from the surface and clouds, unlike other radiosonde temperature correction schemes.

The reliability of the absolute calibration and daytime corrections of these scientific systems did not prove to be better than those of the good operational radiosondes in the Yangjiang test.

12.4.6   Exposure

Radiosonde temperature sensors are best exposed in a position above the main body of the radiosonde (but below the body of a dropsonde). Thus, air heated or cooled by contact with the radiosonde body or sensor supports cannot subsequently flow over the sensor. This is usually achieved by mounting the sensor on an arm or outrigger that holds the sensor in the required position during flight. For long-term stability of operation, this position needs to be reproducible and must not vary from flight to flight. For good exposure at low pressures, the supports and electrical connections to the sensor should be thin enough so that heating or cooling errors from thermal conduction along the connections are negligible.

With this method of exposure, the radiosonde temperature sensors are exposed directly to solar radiation and to the infrared environment in the atmosphere. The sensors receive solar radiation during daytime soundings and will exchange long-wave radiation with the ground and the sky at all times. The magnitude of radiation errors is only weakly dependent on the size and shape of the sensors, since convective heat transfer coefficients are only weakly dependent on sensor size. Thus, small radiation errors may be obtained with small sensors, but only when the sensor coating is chosen to provide low absorption for both solar and long-wave radiation. The required coating can be achieved by the deposition of a suitable thin metallic layer. Many white paints have high absorption in the infrared and are not an ideal coating for a radiosonde sensor.

An additional consequence of exposing the temperature sensor above the radiosonde body is that, when ascending during precipitation or through cloud, the sensor may become coated with water or ice. It is extremely important that the sensor design sheds water and ice efficiently. Evaporation of water or ice from the sensor when emerging from a cloud into drier layers will cool the sensor below true ambient temperature. The absorptivity in the infrared of a temperature sensor that remains coated with ice throughout a flight differs from usual. Thus, an abnormal systematic bias from infrared heat exchange will be introduced into the iced sensor measurements, particularly at low pressures.

12.4.7   Temperature errors

Errors in older radiosonde types widely used in the period 1980–2000 are discussed in more detail in WMO (2015).

12.4.7.1   *Calibration*

Temperature errors related to calibration during an ascent may result from:

(a)   Errors in factory calibration. This can occur from time to time and is one of the reasons the radiosonde measurements should be checked on the ground before launch;

Table 12.6. Systematic error, sonde error and uncertainty ($k = 2$) at night from the WMO international radiosonde comparisons and other associated tests (using the NASA-ATM multithermistor reference as an arbitrary reference for systematic offsets where available)

Temperature sensor	System error (K)				Sonde error		Uncertainty ($k = 2$)		
Pressure (hPa)	300	100	30	10	30	10	100	30	10
Rod thermistor, white paint, MRZ (Russian Federation)	0.2±0.5	0.2±0.5	−0.3±0.7	−0.8±0.7	1	1	1–1.7	1–2	1.1–2.5
Copper-constantan thermocouple, Meteolabor (Switzerland)	0.1±0.1	0±0.1	−0.1±0.2	−0.1±0.2	0.3	0.4	0.3–0.4	0.3–0.6	0.4–0.7
Wire thermo-capacitor, Vaisala RS92 (Finland)	0.05±0.1	0.05±0.1	0.07±0.2	0.07±0.2	0.2	0.3	0.2–0.4	0.2–0.5	0.3–0.6
Chip thermistor, Lockheed Martin Sippican (USA)	0±0.1	−0.05±0.2	−0.07±0.2	−0.07±0.2	0.2	0.3	0.2–0.4	0.2–0.5	0.3–0.6
Bead thermistor, aluminized	0±0.2	0.1±0.2	0.1±0.2	0.2±0.2	0.2	0.4	0.2–0.5	0.2–0.5	0.4–0.8
NASA-ATM multi-thermistors, used by F. Schmidlin	Bias assumed to be within ±0.1 K				0.2	0.2	0.2–0.3	0.2–0.3	0.2–0.3

(b)   Small changes in the sensor, such as the stray capacitance associated with a capacitative sensor or in the electrical connections to the sensor;

(c)   Instabilities in the radiosonde transducer system and references. This is possible during storage or during the ascent. Sensor or transducer drift during storage can usually be partially corrected during data processing, using adjustments based on pre-flight ground checks.

Table 12.6 summarizes the relative performance of temperature sensors at night for different temperature sensors in operation in 2013. The results represent the typical performance averaged over a minimum of at least 15 test flights. The absolute uncertainty of the reference at night was probably better than 0.3 K, with NASA and Sippican multithermistor radiosondes agreeing as well as can be expected from the error analysis.

Where a range of systematic errors has been attributed to a radiosonde type, the range represents the spread in systematic difference found in a number of tests and also takes into account the range of likely performance up to 30 hPa estimated from radiosonde monitoring (WMO, 2003). As modern sensors have aluminized coatings, infrared errors are very small, and any spread in the performance is mainly down to the long-term consistency of factory calibration, small instabilities in the sensors, perhaps depending on the atmospheric structure and internal temperature of the radiosonde electronics, and so on. It is difficult to differentiate between the best systems in Table 12.6 as similar errors have been attributed to the sensors.

The reproducibility of the temperature measurements can be measured relatively easily, but it is not currently possible to ascertain the systematic bias better than the limits shown in the table. Large-scale tests in the tropics have not given the same results for systematic bias as those in Europe, so the values shown are an average between the two conditions with the range of values necessary to encompass both sets of results.

Sonde errors are only quoted for pressures of 30 hPa and 10 hPa in Table 12.6 since, for most modern temperature sensors, sonde errors show little variation between the surface and 30 hPa, although some systems had problems near the tropopause (WMO, 2011b).

The Indian MKIII radiosondes have not performed good-quality temperature measurements for many years, but in this case, the poor reproducibility was not just the result of sensor performance, but also of instability in the radiosonde electronics during the ascent, resulting in effective changes in sensor calibration so that the data were degraded by the radiosonde system itself. Sonde errors for this radiosonde at 100 hPa have been in the range of 2 to 4 K for many years (WMO, 2003), although the uncertainties found from the sensors in Phase II of the WMO Radiosonde Comparison (WMO, 1987) were very much smaller than this.

12.4.7.2 *Thermal lag*

Most modern radiosonde temperature sensors are fast enough to not require significant correction for thermal lag errors in the troposphere and lower stratosphere.

12.4.7.3 *Radiative heat exchange in the infrared*

Most white paints used on radiosonde sensors have relatively high emissivity in the infrared (> 0.8). Heat exchange with the infrared background is then capable of producing significant errors in temperature measurements. For a given vertical temperature structure, the infrared fluxes will also vary significantly from flight to flight depending on the cloud present in the vicinity of the ascent. Luers and Eskridge (1998) provide a good example of users who tried to model the solar and infrared radiation errors on radiosondes in use in the 1990s.

Infrared errors affect both day and night observations. The effects of infrared heat exchange errors at night can be seen in the measurements of the rod thermistors (used on the Russian radiosonde) in Table 12.6. At high pressures, these sensors give temperatures close to the reference, but at low pressures the temperatures reported are much colder than the reference. At pressures lower than 30 hPa, the radiative equilibrium temperature at night was usually significantly lower than the actual atmospheric temperatures. Therefore, the infrared radiation emitted by the temperature sensor exceeded the infrared radiation absorbed by the sensor from the atmospheric environment, and the sensor cooled to a temperature lower than truth. Additional information on the effects of infrared errors in the past can be found in WMO (2015).

The use of white paint on the temperature sensor should be discontinued as soon as possible so that variation in systematic temperature error from infrared errors will then be negligible across the radiosonde network.

12.4.7.4 *Heating by solar radiation*

All radiosonde temperature sensors will have heating errors in daytime caused by incident solar radiation, including backscattered radiation from clouds and the surface. Table 12.7 shows the day–night differences associated with the temperature measurements of the radiosondes considered in Table 12.6. These values were derived mostly from the software corrections used for daytime temperatures by each system for solar elevations between 30° and 80°. Temperature sensors of the Russian radiosonde had relatively poor thermal isolation from supporting structures, which could often be heated more than the sensor itself, and so the Russian radiosondes also had large day–night differences at upper levels.

**Table 12.7. Day–night differences for selected temperature sensors from the WMO
international radiosonde comparisons and other associated tests**

Temperature sensor	Systematic error (K)			
Pressure (hPa)	300	100	30	10
Rod thermistor, white paint, MRZ (Russian Federation)	1	1.8	3.3	5.1
Copper-constantan thermocouple, Meteolabor (Switzerland)	0.5[a] 0.3[b]	0.75[a] 0.5[b]	1.1[a] 0.75[b]	1.8[a] 1[b]
Chip thermistor, Lockheed Martin Sippican (USA)	0.3	0.5	0.8	0.95
Wire thermocapacitor, Vaisala (Finland)	0.15	0.3	0.5	0.8
Bead thermistor,[c] aluminized	0.2 – 0.5	0.3 – 1.1	0.4 – 1.5	0.6 – 2.3

Notes:
a   As used in WMO (2011*b*)
b   As revised in subsequent tests (Philipona et al., 2013)
c   Summary of the range of results from other radiosonde systems using bead thermistors in
      the Yangjiang comparison (WMO, 2011*b*). See WMO (2015) for details of the individual
      radiosonde types at Yangjiang.

In all modern operational radiosonde systems, software corrections are applied during data
processing to compensate for the solar heating (see Table 12.7). These correction schemes are
usually derived from special investigations of day–night differences in temperature (taking
into account real diurnal variation in temperature caused by atmospheric tides) coupled with
solar heating models, and possibly laboratory testing. The correction is then expressed as a
function of solar elevation during the ascent. The correction may also take into account the
actual rates of ascent, since ventilation and heating errors will change if the rate of ascent differs
from the standard test conditions. At low solar elevations (less than 10°) the heating errors
are extremely sensitive to changes in solar elevation. Thus, if the correction software does not
update solar elevation during flight, significant errors will be generated when correcting sunrise
or sunset flights. A simple correction scheme will work effectively only for certain cloud and
surface conditions and cannot provide adequate correction for all flight conditions that might
be encountered. For instance, in many ascents from coastal sites the radiosonde proceeds out
to sea. In clear sky conditions, the low surface albedo of the sea will reduce backscattered solar
radiation by a factor of two or three compared with average atmospheric conditions during
flight. In such circumstances, software corrections based on average conditions will be up to 30%
too large. On the other hand, in ascents over thick upper cloud with very high albedo or over
desert conditions, backscattering may be much larger than usual and the software correction will
underestimate the required correction.

Table 12.8 contains a review of the systematic and sonde errors in most modern radiosonde
types. In the systematic errors derived from the test in Yangjiang, China (WMO, 2011*b*), it was
assumed that zero systematic bias in Yangjiang was halfway between Vaisala/MODEM and LMS/
multithermistor at 30 and 10 hPa. This is because subsequent testing in the United States has not
shown significant errors in the multithermistor system used in Yangjiang, that is to say, there was
some real atmospheric diurnal variation in temperature between 30 and 10 hPa in Yangjiang,
with a probable amplitude of about 0.15 K. In the estimates of the range of systematic error in
Table 12.8, it has been assumed that the standardized software correction schemes produce
a range of possible systematic bias of ±30%. During a particular radiosonde test, the radiative

Table 12.8. Systematic error, sonde error and uncertainty (k = 2) for selected temperature sensors in the day from WMO international radiosonde comparisons and other associated tests, and from operational monitoring as in WMO (2003)

Temperature sensor	Systematic error (K)			Sonde error			Uncertainty (k = 2)		
Pressure (hPa)	100	30	10	100	30	10	100	30	10
Rod thermistor, white paint, MRZ (Russian Federation)	0.7±0.5	0.5±1	−0.7±1.3	1	1.2	1.5	1.2–2.2	1.2–2.7	1.5–3.5
Copper-constantan thermo-couple, Meteolabor (Switzerland)	−0.2[a] −0.05[b]	−0.5[a] −0.2[b]	−0.8[a] 0[b]	0.4	0.4	0.8	0.6	0.9	1.5
Wire thermo-capacitor, Vaisala (Finland)	0±0.2	−0.2±0.2	−0.3±0.3	0.4	0.4	0.4	0.4–0.7	0.4–0.9	0.4–0.9
Chip thermistor, Lockheed Martin Sippican (USA)	−0.1±0.2	0.2±0.2	0.3±0.3	0.3	0.3	0.4	0.3–0.6	0.3–0.8	0.4–1.0
Bead thermistor,[c] aluminized	0.1±0.2	0±0.3	0±0.5	0.4–0.8	0.4–1.3	0.4–1.7	0.5–1.0	0.8–1.6	0.4–2.3
Multi-thermistor	±0.2	±0.2	±0.3	0.3	0.3	0.4	0.3–0.5	0.4–0.6	0.4–0.7

Notes:

a   As used in WMO (2011b)

b   As revised in subsequent tests (Philipona et al., 2013)

c   Summary of the range of results from other radiosonde systems using bead thermistors in the Yangjiang comparison (WMO, 2011b). See WMO (2015) for details of the individual radiosonde types at Yangjiang.

conditions (cloud, surface albedo) do not usually change much, so the illusion is given that the systematic bias obtained has low errors. However, a test performed at another location can give systematic errors that differ by much more than the sonde error found in the individual test.

The sonde errors for all radiosondes are larger in daytime than in night-time conditions (see Tables 12.6 and 12.8). During ascent, radiosondes swing and rotate like a pendulum suspended from the balloon, so the absorption cross-sections of the sensor change as the sensor rotates. Also, air heated by contact with either the sensor supports or the radiosonde body may flow over the external sensor from time to time. If these possibilities have not been prevented in the design (for example, if the temperature sensor is mounted close to the radiosonde body, perhaps halfway between the top and the bottom), much larger sonde errors will result in daytime. Backscattered radiation varies from flight to flight with changing cloud cover and also contributes to the increase in daytime sonde errors.

When a support frame surrounds the temperature sensor, air heated by contact with the frame passes over the sensor in part of the pendulum cycle, producing positive pulses in the reported temperature as the radiosonde moves around in flight. These pulses can be as large as 1 K at 10 hPa. The heating pulses can be readily recognized when flying radiosondes on the rigs used in

WMO radiosonde comparisons since the radiosondes rotate in a very regular fashion during the flight. In this situation, suitable raw data filtering can remove the positive pulses to some extent. Thus, the filtering applied to the basic observations of several systems must also be taken into account when investigating daytime radiosonde temperature errors.

The range of systematic errors in daytime measurements shown in Table 12.8 should be smallest for the radiosonde systems with smallest day–night differences. Given that most of the increase in uncertainty relative to night-time measurements comes from poor sensor position relative to the radiosonde body and from poor design of the sensor supports, it is hoped that most of the modern radiosondes with the larger errors and day–night differences in Table 12.7 will be improved within a few years of the Yangjiang intercomparison. Thus, the results of Yangjiang represent a snapshot of performance at the time, and radiosondes with significant systematic errors in Yangjiang will all have been modified to some extent within a couple of years of completion of the test. For example, the radiation errors of the Swiss radiosonde have been revised through additional testing and the solar heating correction is now reduced as shown. This would eliminate the negative bias seen in the daytime results in WMO (2011*b*) as represented in Table 12.8.

The WMO intercomparison tests were performed with the radiosondes suspended at least 30 m and most commonly 40 m under the balloon. However, many national networks, such as China, Japan and the Russian Federation, have used much shorter suspensions which will produce additional daytime bias and increased sonde errors compared to those quoted in Tables 12.7 and 12.8, especially at pressures lower than 30 hPa.

12.4.7.5 *Deposition of ice or water on the sensor*

Another source of temperature error is the deposition of water or ice on the temperature sensor. This will lead to psychrometric cooling (from the wet-bulb effect) of the temperature sensor, once atmospheric relative humidity drops to less than 100% later in the ascent. If the sensor tends to collect water or ice, rather than rapidly shed the precipitation, large parts of the temperature measurements during the ascent may be corrupted. At night, a coating of ice will cause an aluminized sensor to act like a black sensor in the infrared, leading to large cooling at low pressures in commonly encountered conditions.

Furthermore, if water deposited on the sensor freezes as the sensor moves into colder air, the latent heat released will raise the temperature towards 0 °C. If a sensor becomes coated with ice and then moves into a warmer layer, the temperature will not rise above 0 °C until the ice has melted. Thus, isothermal layers reported close to 0 °C in wet conditions should be treated with some caution.

12.4.7.6 *Representativeness issues*

Representativeness issues are discussed in WMO (2015).

12.5 RELATIVE HUMIDITY SENSORS

12.5.1 General aspects

Operational relative humidity measurements worldwide have a wide range of performance (from good to poor) as all the sensor types listed in Table 12.10 are still in use in some national networks in 2013. The most widely used sensor is the heated twin thin-film capacitor. This sensor is mounted externally, without a cover, on a boom which holds it above the top of the radiosonde body. The other modern thin-film capacitors are usually deployed externally on a boom with an aluminized cover to protect against contamination from precipitation and minimize solar heating of the humidity sensor. Carbon hygristor sensors are usually mounted in some type of protective duct in the radiosonde. The use of carbon hygristors is decreasing. Goldbeater's skin sensors are

Table 12.9. Variation of saturation vapour pressure over a water surface as a function of temperature after Sonntag (1994)

Temperature (°C)	Saturation vapour pressure (hPa)
40	73.9
30	42.5
15	17.1
0	6.1
–15	1.92
–30	0.51
–45	0.112
–60	0.019 5
–75	0.002 5
–90	0.000 23
–100	0.000 036

too inaccurate and limited in coverage in the vertical to meet the requirements of modern users, but are still in use in one national network. The goldbeater's skin is also mounted in some type of protective duct.

A good modern radiosonde relative humidity sensor should be able to measure relative humidity to a useful accuracy at all temperatures from 40 °C down to about –70 °C. Temperatures are lower than this near the tropical and subtropical tropopause, and radiosonde sensors can make useful measurements at these temperatures provided that certain corrections are applied (see below). However, the most reliable practical method of measuring water vapour at these lowest temperatures is with a frost-point hygrometer (see Vömel et al. (2007a) and the results from the WMO Intercomparison of High Quality Radiosonde Systems (WMO, 2011b)). Table 12.9 shows the range of saturated water vapour pressures with respect to a water surface that must be resolved to provide relative humidity measurements at all levels. At temperatures below 0 °C, relative humidity sensors should be calibrated to report relative humidity with respect to a water surface.

The saturation with respect to water cannot be measured much below –50 °C, so manufacturers should use one of the following expressions for calculating saturation vapour pressure relative to water at the lowest temperatures – Wexler (1976, 1977), Hyland and Wexler (1983) or Sonntag (1994) – and not the Goff-Gratch equation recommended in earlier WMO publications. Saturation vapour pressure in ice clouds at the lowest temperatures in the tropical upper troposphere will be about 50% of the saturation vapour pressure with respect to a water surface in Table 12.9.

Satisfactory relative humidity sensor operation becomes extremely difficult at very low temperatures and pressures. The free exchange of water molecules between the sensor and the atmosphere becomes more difficult as the temperature falls. Also, contamination of the sensor from high water vapour concentrations earlier in the ascent may cause substantial systematic bias in sensor measurements at the lowest temperatures. For instance, if a positive systematic bias of 5% relative humidity is caused by contamination at –60 °C, this would become a positive systematic bias of 40% relative humidity at –75 °C unless the contamination is ventilated away.

In the lower stratosphere and upper troposphere, water vapour measurements should be evaluated in terms of mixing ratio as well as relative humidity. Figure 12.4 shows the variation of temperature, relative humidity and mixing ratio with height, measured by four different radiosonde sensors in the WMO Intercomparison of High Quality Radiosonde Systems (WMO,
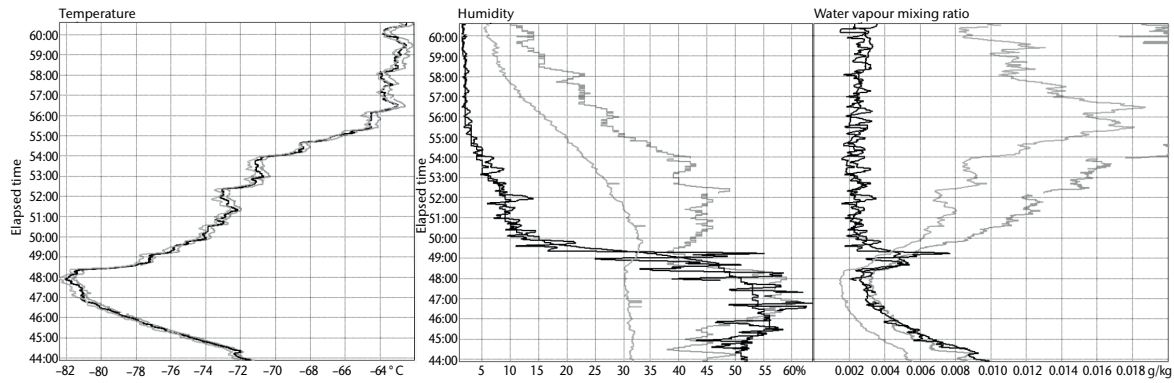
Figure 12.4. Temperature, relative humidity and water vapour mixing ratio presented as a function of time into flight, from flight 56 of the WMO Intercomparison of High Quality Radiosonde Systems. The grey measurements are from radiosondes with capacitative sensors, uncorrected for slow response time. The black measurements are from a heated twin capacitor sensor (corrected for time constant of response) and a frost-point hygrometer. (The frost-point hygrometer shows more variation with time in relative humidity and mixing ratio than the heated twin capacitor.)

2011*b*). Just under the tropopause, relative humidity was slightly higher than saturation, but the water vapour mixing ratio was close to the minimum, having dropped rapidly with temperature, as would be expected from Table 12.9. Where the temperature rises above the tropopause, the two relative humidity sensors with slower response (grey) show much higher water vapour mixing ratio than is realistic. The corrected sensor and the chilled-mirror hygrometer (black) show a short-lived maximum in water vapour mixing ratio immediately above the tropopause. This is unlikely to be real and suggests that the relative humidity reported by the black sensors in this layer between minutes 48.4 and 50 are too high by up to a factor of 2.5. This is probably the result of contamination of the payload or the radiosonde sensing area, and not a calibration issue. Contamination could have occurred earlier in the flight between minutes 33 and 38 after passing through a thick layer of cirrus cloud detected by the cloud radar (not shown in Figure 12.4).

The rate of response of the relative humidity sensors can be defined as:

$$dU_e/dt = -1/\tau \cdot \left(U_e - U\right) \tag{12.17}$$

where U_e is the relative humidity reported by the sensor, U is the actual relative humidity and τ is the time constant of response.

A further complication is that the relative humidity sensor reports relative humidity for the temperature of the sensor itself. If this differs from the true atmospheric temperature, then an additional error is introduced because of the thermal lag of the humidity sensor relative to the air temperature. Modern humidity sensors have become much smaller than in the older radiosonde types to minimize this problem, and the temperature of the sensor is in any case measured directly in many, but not all, widely used modern radiosondes.

The time constant of response of a relative humidity sensor increases much more rapidly during a radiosonde ascent than the time constant of response of a temperature sensor. This can be seen in Table 12.10, where approximate values of the time constant of response of two older and three modern sensor types are shown. In the case of the goldbeater's skin, the time constant of response quoted is for changes between about 70% and 30% relative humidity. The time constants of response of the goldbeater's skin sensors are much larger at a given temperature if measuring high or low relative humidity. The values for the twin thin-film capacitor (Vaisala RS92) in this table differ from those in Miloshevich et al. (2004) and were taken from updated information supplied by the manufacturer.

Table 12.10. Time constants of response τ (in seconds) of relative humidity sensors

Humidity sensor	In use	τ at 20 °C	τ at 0 °C	τ at –20 °C	τ at –40 °C	τ at –70 °C
Heated twin thin-film capacitor, no cap	2004	< 0.15	0.4	2	10	80
Other single thin-film capacitors covered with cap	2000–	0.1 – 0.6	0.6 – 0.9	4 – 6	15 – 20	150 – 300[a]
Carbon hygristor	1960–	0.3	1.5	9	20	Not reliable
Goldbeater's skin	1950–	6	20	100	> 300	Not usable
Frost-point hygrometer, CFH	2003– for science		< 2[b]	< 4[b]		< 25
Chilled-mirror hygrometer, Snow White at night	1996– for science		< 2[b]	< 4[b]		< 25

Notes:
a   Values derived from a comparison with hygrometers, from the WMO Intercomparison of High Quality Radiosonde Systems (WMO, 2011*b*); may include problems with the ventilation of the caps covering the sensor.
b   Value estimated from an in-flight comparison with best quality radiosonde relative humidity sensors, from WMO (2011*b*).

Two profiles of radiosonde temperature and relative humidity are shown in Figures 12.5. and 12.6. Figure 12.5 is an example of a radiosonde ascent in the United Kingdom, where the measurements from two different sensors were combined. Sudden changes in relative humidity with height occur on many flights and were observed here by both radiosonde types. The very dry layers in particular are associated with temperature inversions. The existence of these very dry layers is accepted as correct, but in the past they were considered erroneous because the earlier sensors could not measure them well. In this case, the rate of change of relative humidity with height above the lowest inversion was 6% relative humidity per second. Thus, modern sensors offer advantages to those who need a detailed knowledge of the variation of atmospheric refractive index with height, which is significant for radio propagation. At mid-levels, rates of change of 3% relative humidity per second are often found.

Miloshevich et al. (2004) proposed a method for correcting the slow time-constant of response in humidity measurements based on the equation:

$$U = U_e\left(t_2\right) - U_e\left(t_1\right) \cdot X / \left(1 - X\right) \tag{12.18}$$

where U is the true ambient relative humidity, U_e is the reported relative humidity for times t_1 and t_2, U is assumed not to change significantly between t_1 and t_2 (limiting the size of the time step used), and $X = e^{-\left(t_2 - t_1\right)/\tau}$, where τ is the time constant of response of the relative humidity sensor.

For the algorithm to give satisfactory results, the data used must be as free as possible of anomalous data, noise and so on. Therefore, some form of quality control has to be applied to the basic observations and to other corrections (such as for solar heating of the humidity sensor) before the time constant of response correction is attempted. This correction cannot retrieve exact detail of the vertical profile of relative humidity at a much higher temporal resolution than the time constant of response of the sensor. It generates a smoothed vertical profile, with higher rates of change of relative humidity than in the original measurements, but any detail
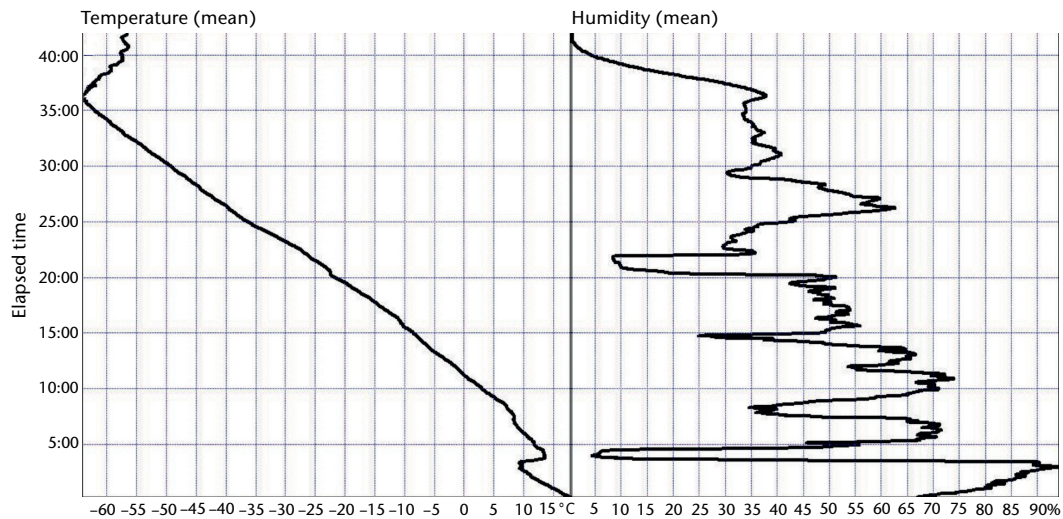
Figure 12.5. Average of simultaneous measurements at first intervals by two radiosondes suspended together under one balloon, with measurements made at night

in the profile at time steps much smaller than the time constant of response should be treated with caution. As seen in Miloshevich et al. (2004), for a given original measurement there are quite a few possible answers, consistent with the known time-constants of response. The type of smoothing applied to the original data influences the retrieved profile, so the smoothing used needs to be well documented and the assumptions made in the use of the algorithm need to be explained to the users.

From the examples seen in Yangjiang (WMO, 2011*b*, Annex D), it was concluded that to report the relative humidity structure near the tropical tropopause, the humidity sensing system should have a time constant of response of 3 min or better, so that the adjustments for a slow time-constant of response are not too large and are not merely amplifying errors from noise in the measurements or from water/ice contamination.

Figure 12.6 illustrates the magnitude of the adjustments in a relative humidity profile for a sensor with a time constant of response of about 80 s at –70 °C and which was observing in the tropical upper troposphere during the WMO Intercomparison of High Quality Radiosonde Systems in Yangjiang, China (WMO, 2011*b*). The corrected profile in Figure 12.6 is clearly much smoother than the relative humidity profiles measured in the upper troposphere by the chilled-mirror hygrometers in Figure 12.4. In Yangjiang, where corrections for slow response were applied, the result looked reasonable in about 65% of the cases and quite wrong the rest of the time. Further testing of this type of adjustment and the type of smoothing applied seems to be justified at this time.

During the Yangjiang test, the highest rates of change observed in the troposphere/stratosphere transition were about 30% relative humidity over about 30 seconds. Thus, at the moment even the fastest operational radiosonde relative humidity sensor cannot define the true height of the rapid drop in humidity at the tropical tropopause without correction. Corrections to the height of the top of the humid layer in Yangjiang were found to be in the range of 200 to 500 m. However, the two scientific sounding instruments in Yangjiang had faster response and could resolve this height better when the instruments were functioning correctly (see Table 12.10).

12.5.2   Thin-film capacitors

Capacitive thin-film sensors are now used in nearly all modern radiosonde designs. These sensors rely on the variation of the dielectric constant of a polymer film with ambient water vapour pressure. The dielectric constant is proportional to the number of water molecules captured at binding sites in the polymer structure. The lower electrode of the capacitor is usually formed by etching a metal-coated glass plate, with dimensions of either 5 by 3 mm or 4 by 1.5 mm and a

thickness of 0.55 or 0.2 mm. There is often a trade-off in thickness, with a thinner film having a faster time-constant of response at low temperatures but perhaps less stability in performance over time. The upper electrode is vacuum-evaporated onto the polymer surface and is permeable to water vapour. Sensor capacitance is usually a nearly linear function of relative humidity, and the temperature dependence of calibration is not large. These sensors are always mounted on a supporting boom which should expose the sensor above the top of the radiosonde or a long way away from the radiosonde body to the side.

The calibration of these relative humidity sensors is temperature dependent. The correction for this dependence must be applied during data processing by the ground system if the accuracy claimed for the sensor at room temperatures in the laboratory is to be obtained throughout most of the troposphere.

Contamination from rain, water drops in clouds or ice accretion has to be driven off if no protective cap is used with the sensor. This can be achieved by heating the sensor well above ambient temperature. Twin sensors are used, with one sensor measuring while the other is heated and then cooled back to normal operation (Paukkunen, 1995). The twin sensors are mounted about 1 cm apart. These particular sensors also have a thin hydrophobic coating to minimize contamination from liquid water. As the sun shines directly on the sensors and their supports, the humidity sensors warm up relative to the correct temperature, particularly in the upper troposphere. This warming effect needs to be compensated in order to achieve accurate humidity measurements. One method is to directly measure the temperature of the humidity sensor and use this information for the compensation. In early versions of this sensor system, the surrounding printed circuit board was not coated with a highly reflective surface, and the humidity sensor was warming too much in the upper troposphere in daytime. So, all the support surfaces were then aluminized, and this was first tested in Mauritius (WMO, 2006a) and then as an operational product in Yangjiang, China (WMO, 2011b). Initially, the manufacturer advised users to use this sensor with correction software for slow time-constants of response at low temperatures and a correction for solar heating of the sensor in the daytime. However, the most recent version of the manufacturer's system software applies these corrections automatically by default.

Four radiosondes in the WMO Intercomparison of High Quality Radiosonde Systems (WMO, 2011b) used another sensor, manufactured by E+E Elektronik. This sensor was always deployed with a protective cap to minimize contamination. This cap usually has a highly reflective coating, so the sensor does not warm up too much in the daytime in the upper troposphere. Also, the sensor supports and the cap must not be hygroscopic, otherwise outgassing from these
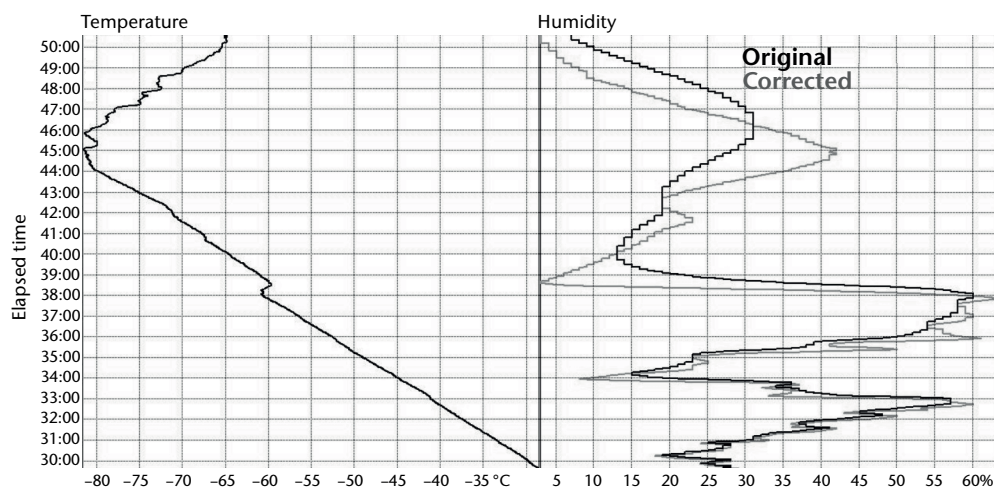
Figure 12.6. Twin thin-film capacitor measurement in the upper troposphere at night in Yangjiang, China, presented as a function of time into flight, showing the humidity profile measured directly by the sensor (black) and then corrected for time constant of response errors (grey)

surfaces will cause significant errors. Some of the manufacturers apply corrections for slow time-constants. With this sensor, the errors from a slow time-constant are larger than with the twin sensor. Most of the radiosondes using this sensor used an additional thermistor to measure the temperature of the humidity sensor directly, rather than assuming the humidity sensor was at the same temperature as the corrected temperature sensor.

12.5.3   **Carbon hygristors**

Carbon hygristor sensors are made by suspending finely divided carbon particles in a hygroscopic film. A modern version of the sensor consists of a polystyrene strip (of approximately 1 mm thick, 60 mm long and 18 mm wide) coated with a thin hygroscopic film containing carbon particles. Electrodes are coated along each side of the sensor. Changes in the ambient relative humidity lead to dimensional changes in the hygroscopic film such that the resistance increases progressively with humidity. The resistance at 90% relative humidity is about 100 times as large as the resistance at 30% relative humidity. Corrections can be applied for temperature dependence during data processing. The sensors are usually mounted on a duct within the radiosonde body to minimize the influence of precipitation wash and to prevent direct solar heating of the sensor.

The implementation of this sensor type requires a manufacturing process that is well controlled so that the temperature dependence of the sensors does not have to be determined individually. The hygristors will normally be subjected to many seasoning cycles over a range of relative humidity at room temperatures in the factory to reduce subsequent hysteresis in the sensor during the radiosonde ascent. The resistance of the sensor can be adjusted to a standard value during manufacture by scratching part of the carbon film. In this case, the variables can be issued with the appropriate standard resistance value for the specified conditions, and the sensors can be made interchangeable between radiosondes without further calibration. The sensor must be kept sealed until just before it is used, and the hygroscopic surface must not be handled during insertion into the sensor mount on the radiosonde.

It should be noted that the sensors do not seem to have stable calibration at high humidity, and the reproducibility of the sensor measurements at lower humidity is often poor. In the WMO Radiosonde Humidity Sensor Intercomparison (WMO, 2006*b*), it was shown that if the sensors (supplied by the main hygristor manufacturer) were kept at a high humidity for several hours, the calibration of the sensor changed irreversibly. Also, the sensors did not measure low humidity (less than 20%) in a reproducible fashion (see Wade, 1995), and measurements from these sensors misled many meteorologists into thinking that relative humidity lower than about 20% did not occur in the lower troposphere.

12.5.4   **Goldbeater's skin sensors**

Goldbeater's skin (beef peritoneum) is still being used. The length of a piece of goldbeater's skin changes by between 5% to 7% for a change in humidity from 0% to 100%. While useful measurements can be obtained at temperatures higher than –20 °C, sensor response becomes extremely slow at temperatures lower than this (see Table 12.10). Goldbeater's skin sensors also suffer from significant hysteresis following exposure to low humidity.

The goldbeater's skin used for humidity variables should be single-ply and unvarnished, with a thickness of about 0.03 mm. The skin should be mounted with a tension of about 20 g cm^{-1} width and should be seasoned for several hours, in a saturated atmosphere, while subjected to this tension. To minimize hysteresis, it is advisable to condition the sensor by keeping it in a saturated atmosphere for 20 min both before calibration and before use. Calibration should be carried out during a relative humidity cycle from damp to dry conditions. The sensor must be protected from rain during flight.

The time constant of response of the sensor is much higher than the values quoted in Table 12.10 at very high and very low humidity (McIlveen and Ludlam, 1969). Thus, it is difficult to avoid large bias in goldbeater's skin measurements during an ascent (low bias at high humidity, high bias at low humidity) even in the lower troposphere.

12.5.5   Scientific sounding instruments

Two specialized scientific water vapour sounding instruments were successfully deployed during the WMO Intercomparison of High Quality Radiosonde Systems in Yangjiang, China (WMO, 2011b). These systems were not as inherently reliable as the operational radiosondes, but when they worked correctly they were extremely useful in identifying the limitations of the operational radiosondes.

(a)   The Cryogenic Frost-point Hygrometer (CFH) (Vömel et al., 2007a) is a chilled-mirror hygrometer. The CFH uses a feedback loop that actively regulates the temperature of a small mirror, which is coated with ice (or dew in the lower troposphere). In the feedback loop, an optical detector senses the amount of ice covering the mirror, and the feedback controller regulates the temperature of the mirror such that the amount of ice remains constant.

When the feedback controller is operating correctly, the mirror temperature is equal to the frost-point temperature, and if there is no internal ice/water contamination, then the frost-point temperature of the atmosphere. The inlet tubes to the CFH are stainless steel and 17 cm long with a diameter of 2.5 cm, mounted directly above and below the hygrometer. This is intended to ensure that contamination from the air passing through the hygrometer is minimal, and the test results in Yangjiang confirmed that the CFH contamination was lower than experienced by the Snow White chilled-mirror hygrometer in the upper troposphere and lower stratosphere.

Time constants of response vary from a few seconds in the lower troposphere and increase with height up to about 20 to 30 s in the stratosphere. Thus, in the lower troposphere, the CFH time constant of response is not distinguishable from the best operational radiosondes. However, in the upper troposphere and lower stratosphere, it is faster in response than the best operational radiosondes. The main measurement uncertainty in CFH measurements is the stability and drift of the feedback controller. Thus, the total measurement uncertainty is estimated to be about 0.5 K in dewpoint or frost-point temperature, corresponding approximately to about 9% relative humidity at the tropical tropopause and 4% relative humidity in the lower troposphere.

The CFH uses a cold liquid at temperatures below –100 °C to cool the mirror during flight. Preparation and handling of this coolant before flight requires training and special handling procedures to avoid personal injury.

Correction schemes (solar heating, time constant) applied to the operational radiosonde relative humidity in the upper troposphere have benefited from comparisons with CFH measurements, for example the unpublished comparisons of the LAPBIAT Upper Troposphere Lower Stratosphere Water Vapour Validation Project (LAUTLOS-WAVVAP) in Sodankyla, Finland (2004), and the Lindenberg Upper-air Methods Intercomparison (LUAMI) in Lindenberg, Germany (2008).

(b)   The Snow White hygrometer also uses the chilled-mirror principle for sensing water vapour (see Fujiwara et al., 2003). However, this uses a Peltier cooler to cool its mirror. There are two versions of the sensing system. The daytime mirror hygrometer was mounted in an internal duct in the sensing system. This configuration did not prevent contamination, thus affecting the accuracy of the measurements below temperatures of about –50 °C, and was only used on a few flights in Yangjiang. In the night-time version, the mirror hygrometer was mounted above the radiosonde body. Thus, the night-time mirror hygrometer had little direct protection against contamination, but a very good exposure to ambient conditions. In Yangjiang, the Snow White night-time system was able to measure dewpoint temperatures down to below –75 °C on 70% of the night-time flights. Two daytime flights

suffered bad contamination near thunderstorms in the afternoon, but night-time Snow White sensing systems were not significantly contaminated in upper cloud because on this occasion ascent conditions were favourable to the Snow White operation. However, contamination around the hygrometer structure limited the use of Snow White to heights less than 18 km, just above the tropical tropopause in Yangjiang. Snow White has the same advantage as CFH in terms of the time constants of response that are much smaller than the operational humidity sensors in the upper troposphere.

It is necessary to have a skilled operator who can recognize when the mirror film changes phase from water to ice (Snow White must also be flown with a good operational humidity sensor). The operator must also be able to detect possible failure modes (such as the mirror losing its ice film) in the middle and upper troposphere. Identifying when contamination has corrupted the hygrometer measurements is a skill required for both Snow White and CFH.

The two chilled-mirror hygrometers have the advantage over operational relative humidity sensors of being sensitive in the upper troposphere and lower stratosphere down to the lowest temperatures, provided that contaminated measurements are recognized and excluded. Their measurements also do not have significant day–night differences in performance. Therefore, as working references, their measurements have proved to be the best method of identifying these differences. Comparison with the chilled-mirror measurements has allowed the development of correction procedures or changes in operational procedures to produce better-quality operational measurements in the middle and upper troposphere.

Sensors in ducts do not provide the best method of observing relative humidity structure through rain and low cloud, so it is unwise to treat the chilled mirrors as more reliable than the best operational radiosonde sensors in the lower troposphere.

12.5.6   **Exposure**

Rapid changes in relative humidity greater than 25% are common during radiosonde ascents. Accurate measurements of these changes are significant for some users. Accurate measurements require that the humidity sensor is well ventilated, but the sensor also needs to be protected as far as possible from the deposition of water or ice onto the surface of the sensor or its supports, and also from solar heating.

Thus, the smaller relative humidity sensors, such as thin-film capacitors, are mounted on an external outrigger. The sensor may be covered by a small protective cap, or the sensors may be heated periodically to drive off contamination from water or ice in cloud or fog. The design of the protective cap may be critical, and it is essential to ensure that the cap design is such that the humidity sensor is well ventilated during the radiosonde ascent.

Larger sensors were usually mounted in an internal duct or a large protective duct on the top or side of the radiosonde body. The duct design should be checked to ensure that airflow into the duct guarantees adequate sensor ventilation during the ascent. The duct should also be designed to shed ice or water, encountered in cloud or heavy precipitation, as quickly as possible. The duct should protect the sensor from incident solar radiation and should not allow significant backscattering of solar radiation onto the sensor. Particular care is required in duct design if contamination in upper cloud is to be avoided.

Protective covers or duct coatings should not be hygroscopic. For examples, see the stainless steel inlet pipes used by CFH or the aluminized sensor mounts of some operational radiosondes.

12.5.7   **Relative humidity errors**

Errors in older radiosonde types widely used between 1980 and 2000 are discussed in more detail in WMO (2015).

12.5.7.1 *General considerations*

Operational relative humidity sensors have improved greatly compared to the sensors in use before the 1980s, especially at low temperatures in the middle and upper troposphere. Relative humidity observations at temperatures lower than –40 °C were not reported in most of the early radiosonde systems, and relative humidity reports at such temperatures were not in significant use until about 2000.

Real-time operational assessment of radiosonde relative humidity measurements by users is not very extensive, and methods need to be developed for providing information to the manufacturers on the calibration performance of the sensors. For example, records could be provided of the relative humidity reported when the radiosonde was known to pass through low cloud, or statistics could be sent of the pre-flight ground checks. When testing radiosondes, it should not be assumed that the uncertainty in the measurements is the same for all relative humidity bands. Non-uniform performance across the relative humidity range was still found for many systems in the WMO Intercomparison of High Quality Radiosonde Systems (WMO, 2011*b*). However, the better systems are now much closer to uniformity at all relative humidity than what was found at the start of the WMO radiosonde comparison series in 1984. During manufacture, calibrations on individual sensors are often performed only at a few (less than three) pre-set relative humidity points, and possibly only at one temperature (see, for example, Wade, 1995). In many cases, the temperature dependence of the sensor calibration is not checked individually, or in batches, but is again assumed to follow curves determined in a limited number of tests. Sensor calibrations have often varied by several per cent in relative humidity from batch to batch, as can be seen from measurements in low-level cloud (Nash et al., 1995). This may be a consequence of faulty calibration procedures during manufacture. For instance, actual sensor performance in a given batch may differ from the standardized calibration curves fitted to the pre-set humidity checks. On the other hand, it could be the result of batch variation in the stability of the sensors during storage. In addition, the thickness of the film in some thin-film capacitors is not always the same, so the thicker sensors are sometimes quite unresponsive to humidity changes at low temperatures, while the majority of the sensors of the same type respond well in the same conditions.

In the following sections, errors are first considered for temperatures greater than –20 °C, where both older and newer sensors were expected to work reliably. Before 1990, most of the radiosondes in use had significant problems with measurements at temperatures lower than –30 °C. Thus, only the errors of the more modern sensor types are considered for the temperature bands between –20 °C and –50 °C, where such sensors work more reliably, and then for temperatures between –50 °C and –70 °C, where only the newest relative humidity sensors could respond quickly enough to make useful measurements. The analysis is then further divided into night-time and daytime performance. Night-time measurements may not necessarily be more reliable than those in the daytime because, in many cases, there seems to be a greater chance of contamination around the sensor at night if its ventilation is poor, while solar heating of the sensor surroundings drives off more of the contamination in the day or produces a compensating low bias in the daytime humidity.

Water vapour pressure is obtained by multiplying the saturation vapour pressure computed from the radiosonde temperature by the radiosonde relative humidity measurement. If the temperature of the relative humidity sensor does not correspond to the temperature reported by the radiosonde, the reported water vapour (and hence any derived dewpoint) will be in error. In a region of the troposphere where temperature is decreasing with height, the humidity sensor temperature will be higher than the air temperature reported. If the humidity sensor temperature is higher than true temperature by 0.5 K at a temperature close to 20 °C, the relative humidity reported by the sensor will be about 97% of the true relative humidity. This will result in an error of –1.5% at a relative humidity of 50%. As temperature decreases to –10 °C and then to –30 °C, the same temperature lag in the sensor causes the reported relative humidity to decrease to 96% and then to 95% of the true value.

Systematic errors in relative humidity measurements may occur because of changes in calibration during storage. This may simply be due to sensor ageing or the build-up of chemical contamination, where contamination occupies sites that normally would be open

for water vapour molecules. The rate of contamination may depend on the chemicals used in manufacturing the radiosonde body or the packaging, and cannot be assumed to be the same when the manufacturing of the radiosonde body or printed circuit boards changes with time. The manufacturer's instructions regarding the storage of the sensors and preparations for use must be applied carefully. For instance, it is essential that the ground check process be performed with the Vaisala RS92 sensor before launch, since this drives off any build-up of chemical contamination and hence low bias early in the ascent.

12.5.7.2 *Relative humidity at night for temperatures above –20 °C*

Table 12.11 summarizes night-time systematic differences in relative humidity at temperatures higher than –20 °C for the most widely used sensors tested during the WMO International Radiosonde Comparison. The results shown in Table 12.11 have been limited to night flights to eliminate complications caused by solar heating. More detailed results on the earlier tests may be found in Nash et al. (1995). From 1984 until 2000, the performance of the Vaisala RS80 A-Humicap was used as an arbitrary reference linking the earlier tests in the WMO Radiosonde Comparison. More recent tests in Brazil and Mauritius have also used the Meteolabor Snow White chilled-mirror hygrometer as a working standard. Both Snow White and CFH measurements were used in the WMO Intercomparison of High Quality Radiosonde Systems in Yangjiang, China, and the systematic error in the reference used in these tests was probably somewhere in the range of ±2% for the temperature range in Table 12.11.

Table 12.11. Systematic differences, sonde error and uncertainty ($k = 2$) of radiosonde relative humidity measurements at night for temperatures higher than –20 °C

Humidity sensor	System bias (% RH)			Sonde error			Uncertainty ($k = 2$)		
Relative humidity (% RH)	80–90	40–60	10–20	80–90	40–60	10–20	80–90	40–60	10–20
Goldbeater's skin, MRZ (Russian Federation) and RS3 (UK)[a]	–8	–1	9	12	18	16	20	19	25
Carbon hygristor, VIZ MKII (USA)	4–10	–4–4	–20–10	10	4–16	6–20	14–20	4–20	6–40
Twin thin-film capacitor, Vaisala RS92 (Finland)	1±2[d]	0±2	0±2	3	5	3	3–6	5–8	3–5
Thin-film capacitor, used in LMS-6[b] (USA)	–1±2	1±3	2±2	3	5	3	4–6	6–9	5–9
Other thin-film capacitors[c]	3±2	6±3	2±2	4	5	3	5–9	8–14	3–7
Snow White, Meteolabor (Switzerland)	–1	–1	–1	4	5	3	5	6	4
CFH (USA/Germany)	4[e]	3[e]	0	8	7	2	13	10	2

Notes:
a   Data from dry conditions only were used in the analysis.
b   Uses E+E Elektronik sensor from Austria.
c   Summary of the range of results from other radiosonde systems without major design faults in the Yangjiang comparison (WMO, 2011*b*). See WMO (2015) for details of the individual radiosonde types at Yangjiang.
d   Uses information from Miloshevich et al. (2009) as well as other WMO and UK tests.
e   CFH seemingly had positive bias at low levels in WMO (2011*b*), similar to the situation in Miloshevich et al. (2009).

In the comparisons in Table 12.11, the time constants of response of most thin-film capacitors and the carbon hygristor were similar and fast enough to avoid significant systematic bias from slow sensor response. Goldbeater's skin is able to respond reasonably well to rapid changes in mid-range relative humidity at these temperatures. Nonetheless, the very slow response of this sensor at high and low humidity contributes to the large systematic differences in Table 12.11, with measurements too low at high relative humidity and too high at low relative humidity.

The results quoted for the VIZ MKII carbon hygristor show very wide ranges in uncertainty, especially at very low humidity. The results were different according to whether the conditions were dry or generally very moist (especially with liquid water present in cloud or rain). This seemed to be because the calibration of this newer hygristor sensor also changed when conditions were very moist (in cloud), giving a significant dry bias at lower humidities. Proposed changes in algorithms, especially at low humidity, did not result in any consistent improvement in the measurement quality. The LMS-6 radiosonde, successor to the VIZ MKII, now uses a capacitor sensor. Carbon hygristors have been in use in India and China in the last decade.

Since 2005, the majority of the modern humidity sensors have shown improved stability and protection against water contamination in cloud (contamination effects normally being short lived and not resulting in permanent offsets during the ascent), and improved reproducibility from batch to batch. Thus, the results from dry and wet conditions can now be combined, apart from in very heavy rain when no system performs reliably. Thus, for the better sensor types, uncertainties ($k = 2$) in the range of 5% to 10% seem achievable across the whole relative humidity range.

12.5.7.3　　*Relative humidity in the day for temperatures above –20 °C*

Table 12.12 contains the summary of daytime systematic differences, sonde error and uncertainty of the radiosonde relative humidity measurements for temperatures higher than –20 °C. This table only includes information on the modern humidity sensor designs.

Comparison with collocated remote-sensing observations (microwave radiometers or GPS water vapour) has confirmed that there is a day–night difference in modern radiosonde relative humidity measurements (for examples, see Turner et al., 2003; and WMO, 2006a, 2011b). The day–night difference can also be estimated independently from comparisons with the Snow White hygrometer, as Snow White measurements are relatively consistent between day and night at temperatures higher than –40 °C.

The situation with the Vaisala RS92 changed in 2006 when significant developments in sensor support designs led to changes in performance in daytime measurements. Early versions had a bare printed circuit board as part of the sensor supports. These supports heated up much more than the aluminized surfaces, and thus led to higher heating of the air passing over the humidity sensors. This was recognized as causing a problem and, by the time the WMO radiosonde comparison in Mauritius (WMO, 2006a) was conducted, the sensor supports had been fully aluminized, with the results corresponding to footnote "d" in Table 12.12. Thus, the measurements reported by Vömel et al. (2007b), performed with the original RS92 version (footnote "c"), show larger dry biases than those observed in Mauritius. This aluminization did not eliminate the solar heating problem, but did reduce the magnitude of the effect. As can be seen, this represents the main step forward in reducing the uncertainty of the Vaisala daytime relative humidity measurements at higher temperatures. In the WMO Intercomparison of High Quality Radiosonde Systems in Yangjiang, China (WMO, 2011b), software was used to correct the daytime negative bias from solar heating.

Thus, the daytime twin thin-film capacitor measurements were optimized only after the software used in the Yangjiang comparison was introduced operationally worldwide, and the uncertainty in the daytime measurements was much worse than in the night-time measurements until the hardware and software modifications were introduced after 2006.

Table 12.12. Systematic differences, sonde error and uncertainty ($k = 2$) of radiosonde relative humidity measurements in the day for temperatures higher than –20 °C

Humidity sensor	System bias (% RH)			Sonde error			Uncertainty ($k = 2$)		
Relative humidity (% RH)	80–90	40–60	10–20	80–90	40–60	10–20	80–90	40–60	10–20
Carbon hygristor, VIZ MKII (USA)	–2±4	–3±6	0±10	7	7	10	7–13	7–16	10–20
Twin thin-film capacitor, Vaisala RS92 (Finland)	–9±2[c]			4	4	2	11–15		
	–3±2[d]	–3±2[d]	–1±2[d]	4	4	2	5–9	5–9	3–5
	1±2[e]	0±2[e]	–1±2[e]	4	4	2	5–7	4–6	3–5
Thin-film capacitor, LMS-6[a] (USA)	–3±2	0±3	0±2	4	4	2	7–9	4–7	2–4
Other thin-film capacitors[b]	1±2	2±2	0±2	4	4	3	4–7	4–8	3–5
Snow White, Meteolabor (Switzerland)	–1	–1	–1	4	8	4	5	9	5
CFH (USA/ Germany)	1	1	0	8	8	2	9	9	2

Notes:

a Uses E+E Elektronik sensor from Austria.

b Summary of the range of results from other radiosonde systems without major design faults in the Yangjiang comparison (WMO, 2011*b*). See WMO (2015) for details of the individual radiosonde types at Yangjiang.

c Vaisala RS92 original with a bare printed board as part of support for relative humidity sensors; values for tropics from Vömel et al. (2007*b*).

d Vaisala RS92 with fully aluminized supports but no correction for solar heating (WMO, 2006*a*).

e Vaisala RS92 with fully aluminized sensor support and correction for solar heating, in the tropics (WMO, 2011*b*).

However, in general, uncertainties ($k = 2$) for the better sensor types in the range of 5% to 10% seem achievable across the whole relative humidity range, and day–night differences in systematic error are not usually large in this temperature range.

12.5.7.4   *Relative humidity at night for temperatures between –20 °C and –50 °C*

Table 12.13 contains a summary of night-time systematic differences, sonde error and uncertainty of the radiosonde relative humidity measurements for temperatures between –20 °C and –50 °C. For most radiosonde systems designed before 2000, the relative humidity sensor performance was usually influenced by the conditions experienced earlier in the flight, so the values obtained in early tests in this temperature range were not very reproducible, even when thick cloud and rainy conditions were excluded and are not considered here.

Whereas the twin thin-film capacitor and LMS capacitor had small systematic errors, this was not true of all the remaining radiosonde types in Yangjiang, where poor ventilation of the sensor under the protective cap gave rise to increased positive bias in the measurements at high and mid-range relative humidity. Not all the humidity sensors in Yangjiang could provide uncertainties ($k = 2$) in the range of 5% to 10% relative humidity in the humid conditions experienced in this temperature range.

Table 12.13. Systematic differences, sonde error and uncertainty ($k = 2$) of radiosonde relative humidity measurements at night for temperatures between –20 °C and –50 °C

Humidity sensor	System bias (% RH)			Sonde error			Uncertainty ($k = 2$)		
Relative humidity (% RH)	60–80	40–60	10–20	60–80	40–60	10–20	60–80	40–60	10–20
Carbon hygristor, VIZ MKII (USA)[a]	–5–0	–10 to –4	–20–10	10	8	7	10–15	12–18	17–27
Twin thin-film capacitor, Vaisala RS92 (Finland)	1±3[d]	0±3	0±2	6	6	4	6–10	6–9	4–6
Thin-film capacitor, used in LMS-6[b] (USA)	–1±2	1±3	2±2	6	6	4	6–9	6–10	4–8
Other thin-film capacitors[c]	3±10	7±8	4±4	6	8	4	6–19	8–23	4–8
Snow White, Meteolabor (Switzerland)	–2	–1	3	6	8	4	8	9	7
CFH (USA/Germany)	2	1	0	5	5	5	7	6	5

Notes:
a   Data from dry conditions only were used in the analysis.
b   Uses E+E Elektronik sensor from Austria.
c   Summary of the range of results from other radiosonde systems with low sonde errors in the Yangjiang comparison (WMO, 2011*b*). See WMO (2015) for details of the individual radiosonde types at Yangjiang.
d   Uses information from Miloshevich et al. (2009) as well as other WMO and UK tests.

12.5.7.5   *Relative humidity in the day for temperatures between –20 °C and –50 °C*

Table 12.14 contains a summary of daytime systematic differences, sonde error and uncertainty of the radiosonde relative humidity measurements for temperatures between –20 °C and –50 °C.

The systematic errors in the twin thin-film capacitor measurements in daytime had larger negative biases than at the higher temperatures in Table 12.12. Thus, it took until about 2011 before the erroneous dry biases were removed from the daytime twin thin-film capacitor measurements and the large uncertainties in these measurements were reduced to the values found at night in Table 12.13.

In the daytime, the other sensors in the Yangjiang test did not have the significant positive biases relative to the LMS capacitor that were seen at night in Table 12.13. However, it was more difficult in this daytime temperature band to ensure that the operational radiosondes were able to measure with an uncertainty ($k = 2$) of between 5% and 10% under all conditions.

Two of the radiosonde systems in Yangjiang had very large sonde errors both day and night because of problems with sensor design, and one more system had large sonde errors in daytime only, because of poor positioning of the humidity sensor. So, obtaining good performance in this band requires significant testing and elimination of design problems that do not necessarily affect the measurements at higher temperatures very much (see WMO, 2015).

12.5.7.6   *Relative humidity at night for temperatures between –50 °C and –70 °C*

Table 12.15 shows the systematic differences, sonde error and uncertainty ($k = 2$) for night-time measurements at temperatures between –50 °C and –70 °C for the modern sensors only. These sensors/sensing systems differ in terms of time constant of response. All have longer than optimum time-constants in the upper troposphere/lower stratosphere in the tropics, with some

Table 12.14. Systematic differences, sonde error and uncertainty ($k = 2$) of radiosonde relative humidity measurements in daytime for temperatures between –20 °C and –50 °C

Humidity sensor	System bias (% RH)			Sonde error			Uncertainty ($k = 2$)		
Relative humidity (% RH)	60–80	40–60	10–20	60–80	40–60	10–20	60–80	40–60	10–20
Carbon hygristor, VIZ MKII (USA)[a]	–8	–9	±10	10	8	7	18	17	7–17
Twin thin-film capacitor, Vaisala RS92 (Finland)	–16±4[d]			6	4	2	16–24		
	–7±2[e]	–5±2[e]	–3±2[e]	6	4	2	11–15	7–11	3–7
	2±2[f]	3±2[f]	–1±2[f]	6	4	2	6–10	5–9	2–5
Thin-film capacitor, used in LMS-6[b] (USA)	–2±2	–3±3	0±2	6	8	2	6–10	8–14	2–6
Other thin-film capacitors[c]	–3±2	0±3	1±3	7	6	4	7–12	6–9	4–8
Snow White, Meteolabor (Switzerland)	0	1	1	6	8	4	8	9	7
CFH (USA/Germany)	2	1	0	5	5	5	7	6	5

Notes:

a   Data from dry conditions only were used in the analysis.

b   Uses E+E Elektronik sensor from Austria.

c   Summary of the range of results from other radiosonde systems with low sonde errors in the Yangjiang comparison (WMO, 2011b). See WMO (2015) for details of the individual radiosonde types at Yangjiang.

d   Vaisala RS92 original with a bare printed board as part of support for relative humidity sensors; values for tropics from Vömel et al. (2007b).

e   Vaisala RS92 with fully aluminized supports but no correction for solar heating (WMO, 2006a).

f   Vaisala RS92 with fully aluminized sensor support and correction for solar heating, in the tropics (WMO, 2011b).

becoming slow at –60 °C and others at –80 °C. The chilled-mirror hygrometers are capable of working reasonably quickly at these low temperatures and have thus provided evidence on the speed of response of the operational sensors.

The sonde errors in Table 12.15 at –60 °C are generally about twice as large as those at temperatures higher than –20 °C in Table 12.11, the exception being the CFH with more reproducible measurements at upper levels than in the lower troposphere. The reference used in Table 12.15 for systematic errors cannot be defined better than ±4%, as all the sensors including CFH (due to possible contamination) have limitations. The time constant of response corrections applied to Vaisala RS92 in 2011 only changed the systematic bias by +0.5% RH in the 40% to 60% relative humidity band and –1.2% RH in the 20% to 40% band. In analysing the results from the WMO Intercomparison of High Quality Radiosonde Systems, some CFH and Snow White flights had to be flagged out because of technical problems. Remember that the systematic errors in Table 12.15 are straightforward difference in relative humidity and are not presented as a percentage ratio of the relative humidity being measured.

Table 12.15 shows that probably only two radiosonde systems were capable of providing relative humidity measurements with uncertainty in the range of 6% to 12% at night and at temperatures between –50 °C and –70 °C, whether cloud was present or not. WMO (2015) showed that another four were capable of providing measurements in the range of 10% to 20%.

At very low humidity in the stratosphere, the expected sonde error of CFH becomes about 2% when measuring 10% relative humidity, and 0.4% when measuring 2% relative humidity, whereas operational radiosonde errors will stay near the values quoted in Table 12.15 and are thus not suitable for stratospheric measurements where fractions of a per cent relative humidity make a significant difference to the water vapour mixing ratio reported.

Table 12.15. Systematic differences, sonde error and uncertainty ($k = 2$) of radiosonde relative humidity measurements at night for temperatures between –50 °C and –70 °C in the troposphere

Humidity sensor	System bias (% RH)		Sonde error		Uncertainty (k = 2)	
Relative humidity (% RH)	40 – 60	20 – 40	40 – 60	20 – 40	40 – 60	20 – 40
Twin thin-film capacitor, Vaisala RS92 (Finland)	0 ± 4[c]	1 ± 3	7	4	7 – 11	4 – 8
Thin-film capacitor, used in LMS-6[a] (USA)	1 ± 4	–1 ± 3	12	14	12 – 17	14 – 18
Other thin-film capacitors[b]	4 ± 6	5 ± 4	12 ± 8	12 ± 8	6 – 30	5 – 29
Snow White, Meteolabor (Switzerland)	–3 ± 3	–2	9	8	9 – 15	10
CFH (USA/Germany)	2	2	5	3	7	5

Notes:

a Uses E+E Elektronik sensor from Austria.

b Summary of the range of results from other radiosonde systems known to be in operational use from the Yangjiang comparison (WMO, 2011b). See WMO (2015) for details of the individual radiosonde types at Yangjiang.

c Uses information from Miloshevich et al. (2009) as well as other WMO and UK tests.

12.5.7.7 *Relative humidity in the day for temperatures between –50 °C and –70 °C*

Table 12.16 shows the systematic biases, sonde errors and uncertainty for daytime humidity measurements centred at a temperature of –60 °C. The daytime sonde errors were similar or slightly smaller than the night-time sonde errors. Thus, any increase in sonde error from solar heating was balanced by a decrease in some of the other sources of error at night, such as contamination. It appeared that the structures in the vertical were similar between day and night, but it is possible that time constant of response errors were bigger in night-time conditions, which may have influenced the difference in the sonde errors between day and night.

The system with the most pronounced negative bias in daytime was the Vaisala RS92 in its original form. The temperature sensors were heated both directly by solar heating of the humidity sensor and by air which is heated by the bare copper surfaces on the supports near the sensor and then passes over the sensor. The other systems mostly have aluminized covers, so direct solar heating is not primarily the problem. However, air heated by passing over the supports and plastic does affect the humidity sensor temperature. Some manufacturers, such as Lockheed Martin Sippican and InterMet, measure the temperature of the humidity sensor with a dedicated sensor. In the most recent tests, the Vaisala RS92 had a software correction for heating, as did the Graw system (see WMO, 2011b, Annex D). Values reported in cloud at very low temperatures for both systems seemed higher in the daytime than at night and much higher than was shown by Snow White or CFH. Thus, at this stage it is probable that the corrections applied to the operational radiosondes may have errors, especially in cloudy conditions, although the corrections probably bring the systematic bias closer to the correct values compared to measurements without the correction (see the Vaisala results).

Table 12.16 shows that in 2011, probably only two radiosonde systems were capable of providing relative humidity measurements with uncertainty in the range of 6% to 12% in daytime at temperatures between –50 °C and –70 °C, whether cloud was present or not (given that the twin thin-film capacitor had the complete set of corrections used in Yangjiang). WMO (2015) shows another four capable of providing measurements in the uncertainty range of 10% to 20%.

Most of the test data used for Tables 12.15 and 12.16 have been obtained in the tropics, where the temperature band centred on –60 °C may be 4 km higher than at higher latitudes

Table 12.16. Systematic differences, sonde error and uncertainty (_k_ = 2) of radiosonde relative humidity measurements in the day for temperatures between –50 °C and –70 °C in the troposphere

Humidity sensor	System bias (% RH)		Sonde error		Uncertainty (k = 2)	
Relative humidity (% RH)	_40 – 60_	_20 – 40_	_40 – 60_	_20 – 40_	_40 – 60_	_20 – 40_
Twin thin-film capacitor, Vaisala RS92 (Finland)	–22 ± 4[c]	–14 ± 4	5	3	23 – 31	13 – 21
	–12 ± 3[d]	–7 ± 3	5	3	14 – 20	7 – 13
	3 ± 3[e]	0 ± 3	5	3	5 – 11	3 – 6
Thin-film capacitor, used in LMS-6[a] (USA)	–4 ± 3	–3 ± 3	8	10	9 – 15	10 – 16
Other thin-film capacitors[b]	–2 ± 6	–1 ± 5	9 ± 3	11 ± 2	6 – 20	9 – 19
CFH (USA/Germany)	2	1	5	5	7	6

Notes:
a   Uses E+E Elektronik sensor from Austria.
b   Summary of the range of results from other radiosonde systems known to be in operational use from the Yangjiang comparison (WMO, 2011_b_). See WMO (2015) for details of the individual radiosonde types at Yangjiang.
c   Vaisala RS92 original with a bare printed board as part of support for relative humidity sensors; values for tropics from Vömel et al. (2007_b_).
d   Vaisala RS92 with fully aluminized supports but no correction for solar heating (WMO, 2006_a_).
e   Vaisala RS92 with fully aluminized sensor support and correction for solar heating (WMO, 2011_b_).

(see Figure 12.2). The systematic biases for heating error for a given temperature can be expected to have a range of values, with the lower negative biases associated with the mid-latitude operation in cloudy conditions at higher pressures and the large negative biases associated with tropical operations in clear situations.

12.5.7.8   _Wetting or icing in cloud_

Modern humidity sensors can get contaminated when passing through cloud, but normally the main effects of positive bias are short-lived and contamination ventilates away or, on the twin thin-film capacitor, is heat-pulsed away in the next heating cycle of the sensor. Icing in cloud can occur at temperatures much lower than –40 °C; this may not ventilate away as quickly as the contamination in the lower troposphere.

12.5.7.9   _Representativeness issues_

Representativeness issues are discussed in WMO (2015).

12.6   **GROUND STATION EQUIPMENT**

12.6.1   **General features**

The detailed design of the ground equipment of a radiosonde station will depend on the type of radiosonde that is used. However, the ground station will always include the following:

(a)   An aerial and radio receiver for receiving the signals from the radiosonde;

(b)   Equipment to decode the radiosonde signals and to convert the signals to meteorological units;

(c)   Equipment to present the meteorological measurements to the operator so that the necessary messages can be transmitted to users, as required.

Other equipment may be added to provide wind measurements when required (for example, radar interface, and LORAN-C or GPS trackers).

The output of the decoder should usually be input to a computer for archiving and subsequent data processing and correction.

Modern ground station systems can be either purchased as an integrated system from a given manufacturer, or may be built up from individual modules supplied from a variety of sources. If maintenance support will mainly be provided by the manufacturer or its agents, and not by the operators, an integrated system may be the preferred choice. A system composed of individual modules may be more readily adapted to different types of radiosonde. This could be achieved by adding relevant decoders, without the extra cost of purchasing the remainder of the integrated ground system offered by each manufacturer. A modular type of system may be the preferred option for operators with their own technical and software support capability, independent of a given radiosonde manufacturer. Systems built from modules have encountered problems in the last 10 years because of the complexity of testing such systems and the problems introduced when adapting manufacturers' standard correction software to non-standard use by another processing system.

Note: The rate of development in modern electronics is such that it will prove difficult for manufacturers to provide in-depth support to particular integrated systems for longer than 10 to 15 years. Thus replacement cycles for integrated ground systems should be taken as about 10 years when planning long-term expenditure.

12.6.2   **Software for data processing**

Satisfactory software for a radiosonde ground system is much more complicated than that needed merely to evaluate, for example, standard level geopotential heights from accurate data. Poor quality measurements need to be rejected and interpolation procedures developed to cope with small amounts of missing data. There is a serious risk that programmers not thoroughly versed in radiosonde work will make apparently valid simplifications that introduce very significant errors under some circumstances. For instance, if reception from the radiosonde is poor, it is counterproductive to allow too much interpolation of data using mathematical techniques that will be quite stable when data quality is generally good, but will become unstable when data quality is generally poor. A good example of an algorithm that can become unstable when signal quality is poor is the time constant of response correction used by some manufacturers for temperature.

In the past, certain problems with signal reception and pressure errors near the launch were sometimes compensated by adjusting the time associated with incoming data. This may not cause significant errors to reported measurements, but can make it almost impossible to check radiosonde sensor performance in radiosonde comparison tests.

Thus, it is essential to use the services of a radiosonde specialist or consultant to provide overall control of the software design.[1] The specialist skills of a professional programmer will usually be necessary to provide efficient software. This software will include the display and interactive facilities for the operator which are required for operational use. The software must be robust and not easily crashed by inexpert operators. In the last decade, most software for commercial radiosonde ground systems has required at least two or three years of development in collaboration with testing by National Meteorological Services. This testing was performed by highly skilled operators and test staff, until the software had become thoroughly reliable in operation. The ground system software was then suitable for use by operators without any significant specialized computing skills.

---

[1]   As recommended by the Commission for Instruments and Methods of Observation at its twelfth session (1998), through Recommendation 2 (CIMO-XII).

The software in the ground system should be well documented and should include clear descriptions of the algorithms in use.[2] The overall system should be designed to allow sounding simulations for testing and comparison purposes. It is proposed that sets of a suitable range of raw pressure, temperature and humidity data records should be used to check the reliability of newly developed software. Software errors are often the limiting factors in the accuracy of data reports from the better radiosonde types.

12.7   RADIOSONDE OPERATIONS

12.7.1   Control corrections immediately before use

It is recommended that radiosonde measurement accuracy should always be checked in a controlled environment before the radiosonde is launched. These control checks should be made when the radiosonde is ready for flight, and should take place a few minutes before release. The aim is to prevent the launch of faulty radiosondes. A further aim is to improve calibration accuracy by adjusting for small changes in calibration that may have occurred when the radiosonde was transported to the launch site and during storage.

These control checks are usually performed indoors. They can be conducted in a ventilated chamber with a reference temperature and relative humidity sensors of suitable accuracy to meet user specifications. Relative humidity can then be checked at ambient humidity and lower and higher humidity, if necessary. If no reference psychrometer is available, known humidity levels can be generated by saturated saline solutions or silica gel.

The differences between the radiosonde measurements and the control readings can be used to adjust the calibration curves of the sensors prior to flight. The sensors used for controlling the radiosonde must be checked regularly in order to avoid long-term drifts in calibration errors. A suitable software adjustment of radiosonde calibration normally improves the reproducibility of the radiosonde measurements in flight to some extent. The type of adjustment required will depend on the reasons for calibration shift following the initial calibration during manufacture and will vary with radiosonde type.

If there are large discrepancies relative to the control measurements, the radiosonde may have to be rejected as falling outside the manufacturer's specification and returned for replacement. Maximum tolerable differences in ground checks need to be agreed upon with the manufacturer when purchasing the radiosondes.

It is also wise to monitor the performance of the radiosonde when it is taken to the launch area. The reports from the radiosonde should be checked for compatibility with the surface observations at the station immediately before launch.

In view of the importance of this stage of the radiosonde operation, the Commission for Instruments and Methods of Observation recommends that:[3]

(a)   The performance of the radiosonde pressure, temperature and relative humidity sensors should be checked in a controlled environment, such as a calibration cabinet or baseline check facility prior to launch;

(b)   The baseline check should be automated as far as possible to eliminate the possibility of operator error;

(c)   The temperature and relative humidity observations should also be checked against the standard surface temperature and relative humidity observations at the station immediately before the launch;

---

[2]   See Recommendation 2 (CIMO-XII).
[3]   As recommended by the Commission for Instruments and Methods of Observation at its eleventh session, held in 1994, through Recommendation 9 (CIMO-XI).

(d)   The sensors used as the reference should be at least as accurate as the radiosonde sensors and be calibrated regularly according to the manufacturer's instructions.

12.7.2   Deployment methods

Radiosondes are usually carried by balloons rising with a rate of ascent of between 5 and 8 m s^{-1}, depending on the specifications and characteristics of the balloon in use (see Part II, Chapter 8). These rates of ascent allow the measurements to be completed in a timely fashion – i.e. about 40 min to reach 16 km and about 90 min to reach heights above 30 km – so that the information can be relayed quickly to the forecast centres. The designs and positioning of the temperature and relative humidity sensors on the radiosonde are usually intended to provide adequate ventilation at an ascent rate of about 6 m s^{-1}. Corrections applied to temperature for solar heating errors will usually only be valid for the specified rates of ascent.

A radiosonde transmits information to a ground station that is usually at a fixed location. However, advances in modern technology mean that fully automated radiosonde ground systems are now very small. Therefore, the ground systems are easily deployed as mobile systems on ships or in small vans or trailers on land.

Dropsondes deployed from research aircraft use parachutes to slow the rate of descent. Temperature sensors are mounted at the bottom of the dropsonde. Rates of descent are often about 12 m s^{-1} to allow the dropsonde measurement to be completed in about 15 min. The high descent rate allows one aircraft to deploy sufficient dropsondes at a suitable spacing in the horizontal for mesoscale research (less than 50 km). The dropsonde transmissions will be received and processed on the aircraft. Systems under development will be able to take and transmit direct readings and operate automatically under programme control. Systems are also under development to use remotely piloted vehicles to deploy dropsondes.

12.7.3   Radiosonde launch procedures

Once a radiosonde is prepared for launch, the meteorological measurements should be checked against surface measurements either in an internal calibration chamber or externally against surface observations in a ventilated screen. This is necessary since the radiosonde may have been damaged during shipment from the factory, manufacture may have been faulty, or sensor calibrations may have drifted during storage. Radiosondes producing measurements with errors larger than the limits specified in the procurement contract should be returned to the manufacturer for replacement.

Radiosondes are usually launched by hand or using a launch aid from a shed or shelter. The complexity of the shed and the launch procedures will depend on the gas used to fill the balloon (see Part II, Chapter 8) and on the strength and direction of the surface winds at the site. Even over the last decade there have been fatal accidents in the global radiosonde network through careless use of hydrogen gas. Managers of radiosonde stations using hydrogen gas must be aware of the dangers of an explosion and must ensure that all staff are properly informed and trained in the use of hydrogen. It is essential that equipment for generating and storing hydrogen is well maintained. Faulty equipment shall not be used. The balloon filling equipment must be grounded to earth to prevent static discharge.

In strong winds the launching procedure is aided by the use of unwinders that allow the suspension cord for the radiosonde to deploy slowly following the launch. Very strong surface winds require unwinders that deploy the suspension cord at rates as low as 0.5 to 1 m s^{-1}.

Automatic launch systems for radiosondes are commercially available. These may offer cost advantages at radiosonde stations where staff are used solely for radiosonde operations. These systems may not be suitable for operations in very exposed conditions where very strong surface winds are common.

If users require accurate vertical structure in the atmospheric boundary layer, the surface observations incorporated in the upper-air report should be obtained from a location close to the radiosonde launch site. The launch site should also be representative of the boundary layer conditions relevant to the surface synoptic network in the area. It is preferable that the operator (or automated system) should make the surface observation immediately after the balloon release rather than prior to the release. The operator should be aware of inserting surface observations into the ground system prior to launch, as meteorological conditions may change before the launch actually takes place when a significant delay in the launch procedure occurs (for instance, a balloon burst prior to launch, or air traffic control delay). It is particularly important to ensure that the surface pressure measurement inserted into the ground system is accurate if the radiosonde system's pressure measurements are GPS-based.

The speed of response of the radiosonde sensors is such that conditioning the radiosonde before launch is less critical than in the past. However, when it is raining, it will be necessary to provide some protection for the radiosonde sensors prior to launch.

12.7.4   **Radiosonde suspension during flight**

The radiosonde must not be suspended too close to the balloon when in flight. This is because the balloon is a source of contamination for the temperature and relative humidity measurements. A wake of air, heated from contact with the balloon surface during the day, and cooled to some extent during the night, is left behind the balloon as it ascends. The balloon wake may also be contaminated with water vapour from the balloon surface after ascent through clouds. The length of suspension needed to prevent the radiosonde measurements from suffering significant contamination from the balloon wake varies with the maximum height of observation. This is because the balloon wake is heated or cooled more strongly at the lowest pressures. A suspension length of 20 m may be sufficient to prevent significant error for balloons ascending only to 20 km. However, for balloons ascending to 30 km or higher, a suspension length of about 40 m is more appropriate (see, for instance, WMO, 1994).

Note: When investigating the influence of the balloon wake on radiosonde measurements, it is vital to ensure that the sensors on the radiosonde used for the investigation are correctly exposed. The sensors must be mounted so that it is impossible for air that has had contact with other surfaces on the radiosonde to flow over the radiosonde sensor during ascent. Possible sources of heat or water vapour contamination from the radiosondes are the internal surfaces of protective ducts, the mounts used for the sensor, or the external surfaces of the radiosonde body.

12.7.5   **Public safety**

The radiosonde design must fall well within existing air traffic safety regulations as to size, weight and density. These should ensure that the radiosonde should not cause significant damage if it collides with an aircraft or if ingested by the aircraft engine. In many countries, the national air traffic authority issues regulations governing the use of free flight balloons. Balloon launch sites must often be registered officially with the air traffic control authorities. Balloon launches may be forbidden or possible only with specific authorization from the air traffic controllers in certain locations. The situation with respect to flight authorization must be checked before new balloon launch locations are established.

In some countries, safety regulations require that a parachute or other means of reducing the rate of descent after a balloon burst must also be attached to the radiosonde suspension. This is to protect the general public from injury. The parachute must reduce the rate of descent near the surface to less than about 6 m s^{-1}. The remains of the balloon following a burst usually limit the rate of descent at lower levels. However, on occasion, most of the balloon will be detached from the flight rig following a burst and the rates of descent will be too high unless a parachute is used.

It is important that radiosondes should be environmentally safe after returning to Earth or after falling in the sea, whether picked up by the public or by an animal, or left to decay.

12.8 COMPARISON, CALIBRATION AND MAINTENANCE

12.8.1 Comparisons

The overall quality of operational measurements of geopotential height by radiosonde (and hence temperature measurements averaged through thick layers) is monitored at particular forecast centres by comparison to geopotential heights at standard pressures with short-term (6 h) forecasts from global numerical weather prediction models for the same location. The statistics are summarized into monthly averages that are used to identify both substandard measurement quality and significant systematic changes in radiosonde performance. The European Centre for Medium-Range Weather Forecasts, in Reading (United Kingdom), is the lead centre currently designated by the Commission for Basic Systems for this work, but other national forecast centres also produce similar statistics.

Random errors in geopotential height (and hence temperature) measurements can also be identified at individual stations from analyses of the changes in the time series of measurements of geopotential height, at 100 hPa or lower pressures, where atmospheric variability is usually small from day to day. Examples of the compatibility between the results from this method and those from comparison with short-term forecast fields are provided in Nash (1984) and WMO (1989*b*, 1993*b*, 1998, 2003).

Statistics of the performance of the relative humidity sensors are also generated by the numerical weather prediction centres, and are also compared with satellite observations.

The performance of radiosondes or radiosonde sensors can be investigated in the laboratory with suitably equipped test chambers, where temperature and pressure can be controlled to simulate radiosonde flight conditions.

Detailed investigations of temperature, pressure and relative humidity sensor performance in flight are best performed using radiosonde comparison tests, where several radiosonde types are flown together on the same balloon ascent. Annex 12.C gives guidelines for organizing radiosonde intercomparisons and for the establishment of test sites. When testing a new radiosonde development, it is advisable to have at least two other types of radiosonde with which to compare the newly developed design. The error characteristics of the other radiosondes should have been established in earlier tests. An ideal comparison test site would have an independent method of measuring the heights of the radiosondes during flight. This can now be achieved by using measurements taken from two different well-tested GPS radiosondes.

12.8.1.1 *Quality evaluation using short-term forecasts*

For the better global numerical weather prediction models, the random error in short-term (6 h) forecasts of 100 hPa geopotential heights is between 10 and 20 m in most areas of the world. These errors correspond to a mean layer temperature error from the surface to 100 hPa of between 0.15 and 0.3 K. Thus, the comparison with the forecast fields provides good sensitivity in detecting sonde errors in temperature, if sonde errors are greater than about 0.3 K. Forecast fields, rather than analysis fields, are used as the reference in this comparison. Forecast fields provide a reference that is less influenced by the systematic errors in geopotential heights of the radiosonde measurements in the area than the meteorological analysis fields. However, 6 h forecast fields will have small systematic errors and should not be considered as an absolute reference. Uncertainty in the systematic error of the forecast field is at least 10 m at 100 hPa. The systematic differences of forecasts from the measurements of a given radiosonde station vary between forecast centres by at least this amount. In addition, systematic errors in forecast fields may also change with time by similar amounts, when forecast models and data assimilation techniques are improved. Nonetheless, comparisons with the forecast fields at the lead centres for operational monitoring give clear indications of those radiosonde stations and radiosonde types where there are large systematic errors in the radiosonde reports. Reference WMO (2003) provides the most recent reported review of radiosonde errors in the global network for heights up to 30 hPa, and subsequent monitoring statistics can be found on the WMO website at http://www.wmo.int/pages/prog/www/IMOP/monitoring.html.

12.8.1.2   *Quality evaluation using atmospheric time series*

Random errors in radiosonde measurements can be estimated from the time series of closely spaced measurements of geopotential heights, at pressure levels where the geopotential heights change only slowly with time. Suitable pressure levels are 100, 50, or 30 hPa. For radiosonde observations made at 12 h intervals, this is achieved by computing the difference between the observation at +12 h, and a linear interpolation in time between the observations at 0 and +24 h. Further differences are subsequently computed by incrementing in steps of 24 h through the time series. An estimate of the random errors in the radiosonde measurements can then be derived from the standard deviation of the differences. For much of the year, the sensitivity of this procedure is similar to the comparison made with forecast fields. One exception may be during winter conditions at middle and high latitudes, when the geopotential heights at 100 and up to 30 hPa will sometimes change very rapidly over a short time.

The average values of the differences from the time series may provide information on the day–night differences in radiosonde temperature measurements. The interpretation of day–night differences must allow for real daily variation in geopotential height caused by diurnal and semidiurnal tides. Real day–night differences at mid-latitudes for 100 hPa geopotential heights can be as large as 30 m between observations at 1800 and 0600 local time (Nash, 1984), whereas real day–night differences between observations at 1200 and 0000 local time will usually be in the range 0 ± 10 m.

It is beneficial if individual radiosonde stations keep records of the variation in the time series of geopotential height measurements at 100 hPa and in the geopotential height increment, 100–30 hPa. This allows the operators to check for large anomalies in measurements as the ascent is in progress.

12.8.1.3   *Comparison of water vapour measurements with remote-sensing*

Given that many radiosonde stations now have collocated GPS water vapour sensors and some scientific sites have collocated microwave radiometers, it is practical to use the integrated water vapour measurements from these two systems to check the quality of the radiosonde water vapour measurements, primarily at low levels. Comparison with GPS measurements was performed during the last two WMO radiosonde comparisons (WMO, 2006*a*, 2011*b*), where the GPS measurements were used to quantify day–night differences in the radiosonde relative humidity measurements. A more extensive global study was performed by Wang and Zhang (2008). The use of microwave radiometers to check day–night differences is illustrated in Turner et al. (2003).

Although identification of day–night differences with integrated water vapour measurements seems relatively reliable, this does not mean that all the differences seen between radiosonde and remotely sensed water vapour are due to errors in the radiosonde water vapour, since both the GPS water vapour and microwave radiometer measurements have errors that are not necessarily constant with time.

12.8.1.4   *Radiosonde comparison tests*

Radiosonde comparison tests allow the performance of the pressure, temperature and relative humidity sensors on the radiosonde to be compared independently as a function of time. However, it is important to design the support rig for the radiosondes so that the motion of the radiosondes under the supports is not too dissimilar from the motion on an individual balloon, and to ensure that in daylight the support rig (including the balloon) does not shed warmer air onto some of the sensors from time to time.

Laboratory tests should be performed in facilities similar to those required for the detailed calibration of the radiosondes by the manufacturer. These tests can be used to check the adequacy of radiosonde calibration, for example, the dependence of calibration on sensor

temperature. However, in the laboratory, it is difficult to simulate real atmospheric conditions for radiative errors and wetting or icing of sensors. Errors from these sources are best examined in comparisons made during actual ascents.

In order to compare measurements taken during actual ascents, the timing of the samples for the different systems must be synchronized as accurately as possible, ideally to better than ±1 s. In recent years, software packages have been developed to support WMO radiosonde comparison tests (WMO, 1996b). These allow all the radiosonde samples to be stored in a comparison database and to be compared by the project scientists immediately following a test flight. It is important that comparison samples are reviewed very quickly during a test. Any problem with the samples caused by test procedures (for example, interference between radiosondes) or faults in the radiosondes can then be identified very quickly and suitable additional investigations initiated. The software also allows the final radiosonde comparison statistics to be generated in a form that is suitable for publication.

Initial tests for new radiosonde designs may not merit large numbers of comparison flights, since the main faults can be discovered in a small number of flights. However, larger-scale investigations can be justified once systems are more fully developed. As the reproducibility of the measurements of most modern radiosondes has improved, it has become possible to obtain useful measurements of systematic bias in temperature and pressure from about 10 to 15 flights for one given flight condition (i.e., one time of day). Since it is unwise to assume that daytime flights at all solar elevations will have the same bias, it is preferable to organize tests that produce at least 10 to 15 comparison flights at a similar solar elevation. The measurements of temperature sensor performance are best linked to other test results by comparisons performed at night. The link should be based on measurements from radiosondes with wire or aluminized sensors and not from sensors with significant infrared heat exchange errors. If a continuous series of comparison flights (alternating between day and night) can be sustained, it is possible to use the atmospheric time-series technique to estimate the magnitude of day–night differences in temperature measurements.

As noted earlier, the most extensive series of comparison tests performed in recent years were those of the WMO International Radiosonde Comparison. Initial results have been published in WMO (1987, 1991, 1996a, 2006a, 2006b, 2006c, 2011b). The results from these tests were the basis of the information provided in Tables 12.2 and 12.6 to 12.8.

The first international comparison of radiosondes was held at Payerne (Switzerland) in 1950. Average systematic differences between radiosonde pressures and temperatures (at pressures higher than 100 hPa) were 4 hPa and 0.7 K, with random errors (two standard deviations) of 14 hPa and 2 K. These values should be compared with the results for modern systems shown in Tables 12.2 and 12.6 to 12.8. The results from a second comparison carried out at the same site in 1956 showed that accuracy needed to be improved by the application of radiation corrections to the temperature readings. The errors in pressure and temperature at the 50-hPa level were quite large for most radiosondes and increased rapidly at higher levels, especially during daylight. In 1973, a regional comparison was held in Trappes (France). This identified significant calibration errors in some radiosondes, with one bimetallic temperature sensor having a radiation error as large as 10 K.

12.8.2   **Calibration**

The calibration methods used by manufacturers should be identified before purchasing radiosondes in large numbers. The quality control procedures used to ensure that measurement accuracy will be sustained in mass production must also be checked for adequacy. Purchasers should bear in mind that certain specified levels of error and product failure may have to be tolerated if the cost of the radiosonde is to remain acceptable. However, the in-flight failure rate of radiosondes from reliable manufacturers should not be higher than 1% or 2%.

Unless radiosonde sensors can be produced in large batches to give the reproducibility and accuracy required by users, it is necessary to calibrate the instruments and sensors individually. Even if the sensors can be produced in large batches to meet an agreed set of standardized

performance checks, it is necessary for representative samples, selected at random, to be checked in more detail. The calibration process should, as far as possible, simulate flight conditions of pressure and temperature. Calibrations should normally be performed with falling pressure and temperature. Relative humidity will probably be checked in a separate facility. The reference sensors used during calibration should be traceable to national standards and checked at suitable intervals in standards laboratories. The references should be capable of performing over the full temperature range required for radiosonde measurements.

The design of the calibration apparatus depends largely on whether the complete radiosonde must be calibrated as a unit or on whether the meteorological units can be tested while separated from the radiosonde transmitter. In the latter case, a much smaller apparatus can be used. The calibration facility should be able to cover the range of pressures and temperatures likely to be encountered in actual soundings. It should be possible to maintain the conditions in the calibration chamber stable at any desired value better than ± 0.2 hPa min^{-1} for pressure, ± 0.25 K min^{-1} for temperature and 1% relative humidity per minute. The conditions in the calibration chamber should be measured with systematic errors less than ± 0.2 hPa for pressure, ± 0.1 K for temperature and ± 1% relative humidity. Reference thermometers should be positioned in the calibration chamber in order to identify the range of temperatures in the space occupied by the sensors under calibration. The range of temperatures should not exceed 0.5 K. Sufficient measurements should be taken to ensure that the calibration curves represent the performance of the sensors to the accuracy required by the users. Pressure sensors which are not fully compensated for temperature variations must be calibrated at more than one temperature. Thus, it may be an advantage if the temperature calibration chamber is also suitable for the evaluation of the pressure units.

Humidity calibration is usually carried out in a separate apparatus. This can take place in a chamber in which a blower rapidly circulates air past a ventilated psychrometer or dewpoint hygrometer and then through one of four vessels containing, respectively, warm water, saturated solutions of sodium nitrate and calcium chloride, and silica gel. Any one of these vessels can be introduced into the circulation system by means of a multiple valve, so that relative humidities of 100%, 70%, 40% and 10% are readily obtained. The standard deviation of the variation in relative humidity should not exceed 1% in the space occupied by the units under calibration.

An alternative arrangement for humidity calibration is a duct or chamber ventilated with a mixture of air from two vessels, one of which is kept saturated with water while the other is dried by silica gel, with the relative humidity of the mixture being manually controlled by a valve which regulates the relative amounts passing into the duct.

Because of the importance of the type or batch calibration of radiosondes, the Commission for Instruments and Methods of Observation urges Members to test, nationally or regionally, selected samples of radiosondes under laboratory conditions in order to ensure that the calibrations supplied by the manufacturer are valid.[4]

12.8.3   **Maintenance**

Failure rates in the ground system should be low for radiosonde systems based on modern electronics, as long as adequate protection is provided against lightning strikes close to the aerials. The manufacturer should be able to advise on a suitable set of spares for the system. A faulty module in the ground system would normally be replaced by a spare module while it is returned to the manufacturer for repair.

The maintenance requirements for radiosonde systems relying on radar height measurements to replace radiosonde pressure measurements are quite different. In this case, local maintenance should be readily available throughout the network from staff with good technical capabilities (both mechanical and electrical). This will be essential if accurate tracking capability is to be retained and if long-term drifts in systematic height errors are to be avoided.

---

[4]   As recommended by the Commission for Instruments and Methods of Observation at its eleventh session held in 1994, through Recommendation 9 (CIMO-XI).

12.9   COMPUTATIONS AND REPORTING

There are no prescribed standardized procedures for the computation of radiosonde observations. The main issue is the selection of levels or the provision of measurements in sufficient detail to reproduce accurately and efficiently the temperature and humidity profile (such as the heights of temperature inversions) against geopotential from the radiosonde data. Guidance is given in WMO (1986) and in the coding procedures agreed by WMO (2011c) (Code FM 35–XI Ext. TEMP). However, the accuracy of this reporting method was suitable for the performance of radiosondes in 1970, but not for today. In order to justify the cost of the radiosonde, it is essential that the radiosonde information be reported more accurately and in more detail than in the TEMP code using relevant BUFR codes. In some cases, the use of BUFR code has involved only retaining the description of the ascent as contained in the TEMP code. This is not the intention of this Guide: a BUFR template should be used allowing a more detailed representation of the vertical structure of the meteorological variables, reported with a resolution that does not generate additional uncertainty in the measurements of these variables.

12.9.1   Radiosonde computations and reporting procedures

Upper-air measurements are usually input into numerical weather forecasts as a series of levels as reported or layer averages, with the thickness of the layers depending on the scales of atmospheric motion relevant to the forecast. The layers will not necessarily be centred at standard pressures or heights, but will often be centred at levels that vary as the surface pressure changes. Thus, the variation in temperature and relative humidity between the standard levels in the upper-air report must be reported to sufficient accuracy to ensure that the layer averages used in numerical forecasts are not degraded in accuracy by the reporting procedure.

Prior to 1980, most radiosonde measurements were processed manually by the operators by using various computational aids. These methods were based on the selection of a limited number of significant levels to represent the radiosonde measurement, possibly about 30 significant levels for a flight up to 30 km. The WMO codes reflected the difficulties of condensing a large amount of information on vertical structure into a short message by manual methods. The coding rules allowed linear interpolations in height between significant levels to differ from the original measurements by up to ±1 K for temperature and up to ±15% for relative humidity in the troposphere and up to ±2 K for temperature in the stratosphere. It was expected that operators would not allow large interpolation errors to persist over deep layers in the vertical.

In modern radiosonde ground systems, the use of cheap but powerful computing systems means that much higher sampling rates can be used for archiving and processing the radiosonde measurements than is possible with manual computations. The manual processing of radiosonde measurements nearly always introduces unnecessary errors in upper-air computations and should be eliminated.

The available algorithms for automated upper-air TEMP message generation often have significant flaws. For instance, when there are few pronounced variations in relative humidity in the vertical, automated systems often allow large temperature interpolation errors to extend over several kilometres in the vertical. Furthermore, the algorithms often allow large systematic bias between the reported relative humidity structure and the original measurements over layers as thick as 500 m. This is unacceptable to users, particularly in the atmospheric boundary layer and when the radiosonde passes through clouds. Interpolation between significant cloud levels must fit close to the maximum relative humidity observed in the cloud.

Therefore, reports from automated systems need to be checked by operators to establish whether reporting procedures are introducing significant systematic bias between the upper-air report and the original radiosonde measurements. Additional significant levels may have to be inserted by the operator to eliminate unnecessary bias. TEMP messages with acceptable systematic errors are often produced more easily by adopting a national practice of reducing the WMO temperature fitting limits to half the magnitude cited above. Today, the advent of

improved meteorological communications should allow the approximation in reporting upper-air observations to be reduced by reporting measurements in detail using the appropriate BUFR code message.

Given the large amount of money spent each year on radiosonde consumables, radiosonde operators should migrate urgently to BUFR (or equivalent) codes, to enable them to report accurately all the information that is measured and is needed by the user community.

12.9.2   **Corrections**

It should be clear from earlier sections that the variation in radiosonde sensor performance caused by the large range of conditions encountered during a radiosonde ascent is too large to be represented by a simple calibration obtained at a given temperature. Modern data processing allows more complex calibration algorithms to be used. These have provided measurements of better accuracy than that achieved with manual systems. It is vital that these algorithms are adequately documented. Users should be informed of any significant improvements or modifications to the algorithms. Records archived in radiosonde stations should include the model numbers of radiosondes in use and an adequate reference to the critical algorithms used for data processing.

All radiosonde temperature measurements have radiation errors. Therefore, it is recommended that a radiation correction (based on expected sensor performance in usual conditions) should always be applied during data processing, if known. The details of this radiation correction should be recorded and kept with the station archive, along with an adequate archive of the original raw radiosonde observations, if required by national practice.

Errors from infrared heat exchange pose a particular problem for correction, since these errors are not independent of atmospheric temperature. Thus, it is preferable to eliminate as soon as possible the use of white paint with high emissivity in the infrared as a sensor coating, rather than to develop very complex correction schemes for infrared heat exchange errors.

Similarly, it is unwise to attempt to correct abnormally high solar radiation heating errors using software, rather than to eliminate the additional sources of heating by positioning the sensor correctly with respect to its supports, connecting leads and radiosonde body.

Relative humidity measurements may have corrections applied for slow time-constants of response and for daytime heating of the humidity sensor system. As with temperature, the records of corrections and changes to the correction procedures need to be known by the user and retained in the station archive of observations, preferably along with a raw data archive. The details of these algorithms need to be clear to those purchasing new systems.

Considering the importance of the ways in which corrections are applied, the Commission for Instruments and Methods of Observation[5] urges Members to:

(a)   To correct and make available the corrected upper-air data from the various Global Observing System upper-air stations;

(b)   To make users of the data aware of changes in the methodology used to correct reports, so that they may be adjusted, if desired;

(c)   To archive both the corrected and uncorrected upper-air observations and produce records for climatological applications of the correction applied. The method used should be determined nationally;

(d)   To inform WMO of the method of correction applied.

_____

[5]   As recommended by the Commission for Instruments and Methods of Observation at its eleventh session, held in 1994, through Recommendation 8 (CIMO-XI).

12.10   **PROCUREMENT ISSUES**

12.10.1   **Use and update of the results from the WMO Intercomparison of High Quality Radiosonde Systems**

The results of the WMO Intercomparison of High Quality Radiosonde Systems (WMO, 2011*b*) were published to provide a snapshot in 2010 of the relative performance of the different systems in tropical conditions. The report includes an assessment of the operational performance of the radiosonde systems (see WMO, 2011*b*, Table 12.1). While many of the systems performed well, some radiosondes had limitations in their measurements, mostly in daytime temperature but also in night-time relative humidity measurements at temperatures higher than –40 °C and in daytime relative humidity measurements in the upper troposphere at temperatures lower than –40 °C.

Table 12.1 of the report is intended to help manufacturers identify where the most critical problems lie. Once these deficiencies have been identified, it is probable that many can and will be improved within a year or two, as was done with the MODEM temperature after non-optimum performance at night was observed in the WMO Radiosonde Comparison in Mauritius (WMO, 2006*a*). Therefore, WMO recommends that manufacturers, especially those with markings below 3 in Table 12.1, arrange for a limited number of independent tests to be conducted to provide evidence to WMO that the performance has been improved once the problem has been rectified. Otherwise, manufacturers with promising products may be rejected inappropriately in the procurement process.

WMO (2015) contains individual radiosonde values for Tables 12.5 to 12.16 from the test in Yangjiang, China, and these can also be used as a guide to the systems with low systematic bias and fast enough time constants of response leading to small sonde error in relative humidity. Low and stable systematic bias is very desirable for radiosonde measurements for climate records.

12.10.2   **Some issues to be considered in procurement**

The first stage in the procurement process should be to determine what quality of radiosonde is necessary for use in a given network. Here, it is recommended that any radiosonde used should be capable of meeting the breakthrough requirements indicated in Annex 12.A in the climate of that country. If the radiosonde station is considered important for climate records, then a radiosonde performing closer to the optimum requirement should be considered. Ideally the procurement should be competitive. This may mean cooperating with other countries in a similar region to procure larger numbers together and to try and set up a system where the radiosondes are procured on a regular basis, for instance each year or every two years. It should be remembered that systems that differ only slightly in their performance would probably come out in a different order if the tests were repeated. Thus, only marked differences in performance should be treated as significant and not small differences in the relative marking.

Experience from consultations in regional training workshops suggests that there are some issues which need to be considered when procuring equipment:

(a)   Equipment must be sustainable over the long term. In other words, in addition to purchasing the hardware and software, arrangements must be made for the long-term support of the system, either by the manufacturer or the local staff, or a mixture of both.

(b)   Make sure that the ground antenna is sufficiently sensitive to receive signals under all conditions at the site, whether upper winds are very weak or very strong. Do not try to save money by buying a cheap antenna which is inadequate in some conditions.

(c)   Decide whether local staff can maintain a secondary radar and thus use cheaper non-GPS radiosondes, or whether a fully automated GPS radiosonde system is more likely to be successful and run successfully in the long term. Note also that the use of radar-

derived wind measurements will result in lower-accuracy wind measurements than those obtained by GPS radiosondes. Therefore, one must also decide whether the reduced wind measurement accuracy is tolerable if opting for non-GPS radiosondes.

(d)   If a GPS radiosonde system is to be procured, check whether there is any source of local radio-frequency interference likely to cause problems.

(e)   Decide what altitude performance is required and determine which sondes and balloon size will suit (if the radiosondes are not to be used at pressures lower than 30 hPa, then there is a wider range of suitable radiosondes available; see Tables 12.5 to 12.8).

(f)   Decide what relative humidity sensor performance is required (for example, a GRUAN or GUAN (GCOS Upper-Air Network) station has a higher standard required than a routine Global Observing System station) basing the requirement on Table 12.1 of WMO (2011*b*) and Tables 12.11 to 12.16 of this Guide.

(g)   If conditions are often wet and cloudy, specify that radiosonde sensors need to have some protection against wetting and contamination, and ask for evidence on how this works.

(h)   Ask for a compensation agreement if too many radiosondes fail in flight.

(i)   Ask for evidence that the manufacturer has reliably supplied radiosondes to other users on the scale that will be used at the station.

(j)   Make sure that the ground equipment can produce messages which allow higher resolution data to be reported compared to the old TEMP message. This message must be suitable for the communications available from the site and meet user requirements for data with good vertical resolution.

(k)   Ensure that the ground equipment computers are compatible with the local telecommunication system (including internet links, if required).

————————

ANNEX 12.A. CURRENT BREAKTHROUGH AND OPTIMUM ACCURACY REQUIREMENTS FOR RADIOSONDE MEASUREMENTS

Note: The requirements are based on current technological capability as assessed in the eighth WMO international radiosonde intercomparison, in Yangjiang, China (WMO, 2011b). They apply to radiosonde measurements in synoptic and climate meteorology.

Variable	Height (km) (temperature (°C) in the case of humidity)	Breakthrough uncertainty requirement[a,b]	Optimum uncertainty requirement[b]
Pressure	1	3 hPa	2 hPa
	10	3 hPa	1 hPa
	16	2 hPa	0.6 hPa
	24	1 hPa	0.2 hPa
	32	0.4 hPa	0.1 hPa
Temperature	0 to 16	1 K	0.4 K
	Above 16	2 K	0.8 K
Relative humidity	0 to 12 (40 °C to –50 °C)[c]	15% RH	6% RH
(Troposphere only)	12 to 17 (–50 °C to –90 °C)[c]	30% RH	10% RH
Mixing ratio, lower stratosphere (specialized systems)	12 to 25	20% ppmv[d]	4% ppmv
Wind direction	0 to 16	10°, speed < 10 m s^{-1} 4° at higher speeds	5°, speed < 10 m s^{-1} 2° at higher speeds
	Above 16	20°, speed < 10 m s^{-1} 8° at higher speeds	5°, speed < 10 m s^{-1} 2° at higher speeds
Wind speed	0 to 16	2 m s^{-1}	1 m s^{-1}
	Above 16	4 m s^{-1}	1 m s^{-1}
Wind components	0 to 16	2 m s^{-1}	1 m s^{-1}
	Above 16	3 m s^{-1}	1 m s^{-1}
Geopotential height of significant level	1	30 gpm	20 gpm
	5	40 gpm	20 gpm
	10	60 gpm	20 gpm
	16	120 gpm	40 gpm
	20	200 gpm	40 gpm
	32	240 gpm	60 gpm

Notes:
a   Values derived for the main targeted applications for radiosondes.
b   Expressed as expanded uncertainties ($k = 2$), which encompass approximately 95% of the variation of results in sounding conditions including all significant sources of uncertainty (e.g. dynamic and radiative conditions).
c   Change in expected relative humidity sensor performance corresponds better with temperature than with altitude in the troposphere.
d   ppmv = parts per million by volume

––––––––––––––––

ANNEX 12.B. ESTIMATES OF GOAL, BREAKTHROUGH AND THRESHOLD LIMITS FOR UPPER WIND, UPPER-AIR TEMPERATURE, RELATIVE HUMIDITY AND GEOPOTENTIAL HEIGHT (DERIVED FROM THE WMO ROLLING REVIEW OF REQUIREMENTS FOR UPPER-AIR OBSERVATIONS)

(a)   The *goal* is an ideal requirement above which further improvements are not necessary.

(b)   The *breakthrough* is an intermediate level between *threshold* and *goal* which, if achieved, would result in a significant improvement for the targeted application. The breakthrough level may be considered as an optimum, from a cost-benefit point of view, when planning or designing observing systems.

(c)   The *threshold* is the minimum requirement to be met to ensure that data are useful.

It is recommended that expenditure on radiosondes be considered as justified when the accuracy and vertical resolution obtained is equal to or better than the threshold and as close to the goal as is affordable.

Table 12.B.1. Summary of WMO/GCOS limits for uncertainty (root-mean-square vector error, $k = 2$) and vertical resolution for upper wind measurements

Layer		Goal for NWP	Goal for climate	Breakthrough for NWP	Breakthrough for climate	Threshold for NWP	Threshold for climate
Lower troposphere	Uncertainty	1^a – 2 m s^{-1}	1.4^b – 4^c m s^{-1}	4 m s^{-1}	6 m s^{-1}	10 m s^{-1}	10 m s^{-1}
Lower troposphere	Vertical resolution	200 m	50^b – 500^c m	300 m	800 m	500 m	2 km
Upper troposphere	Uncertainty	1^b – 2^c m s^{-1}	1.4^b – 4^c m s^{-1}	4 m s^{-1}	6 m s^{-1}	10 m s^{-1}	10 m s^{-1}
Upper troposphere	Vertical resolution	500 m	50^b – 500^c m	700 m	800 m	1 km	2 km
Lower stratosphere	Uncertainty	2 m s^{-1}	1.4^b – 4^c m s^{-1}	4 m s^{-1}	6 m s^{-1}	10 m s^{-1}	10 m s^{-1}
Lower stratosphere	Vertical resolution	1 km	250^b – 500^c m	2 km	800 m	3 km	2 km
Upper stratosphere	Uncertainty	2 m s^{-1}	1.4^b – 4^c m s^{-1}	6 m s^{-1}	8 m s^{-1}	16 m s^{-1}	10 m s^{-1}
Upper stratosphere	Vertical resolution	1 km	250^b – 500^c m	2 km	800 m	3 km	2 km
Long-term stability			0.1 m s^{-1} in 10 years				

Notes:
a   Limit derived from atmospheric variability studies (WMO, 1970).
b   Limit derived from the GCOS Reference Upper-Air Network observation requirements (WMO, 2009).
c   Limit derived from the Commission for Basic Systems (CBS) Rolling Review of Requirements WMO observing requirements database (OSCAR/Requirements; see WMO, 2014), sampled August 2011.

Table 12.B.2. Summary of WMO/GCOS uncertainty (k = 2) and vertical resolution limits for upper-air temperature measurements (Note: These limits are for temperatures at a given height and may be different to those when temperatures are integrated over relatively deep layers, e.g. see Table 12.B.4 for breakthrough limits derived from requirements for 100 hPa geopotential height.)

Layer		Goal for NWP	Goal for climate	Breakthrough for NWP	Breakthrough for climate	Threshold for NWP	Threshold for climate
Lower troposphere	Uncertainty	0.6[a] – 1[c] K	0.2[b] – 1[c] K	1.8 K	1.2 K	6[c] K (extratropics) 3[a] K (tropics)	2 K
Lower troposphere	Vertical resolution	100 m	100 m	200 m	800 m	1 km	2 km
Upper troposphere	Uncertainty	0.6[a] – 1[c] K	0.2[b] – 1[c] K	1.8 K	1.2 K	6[c] K (extratropics) 3[a] K (tropics)	2 K
Upper troposphere	Vertical resolution	300 m	100 m	400 m	800 m	1 km	2 km
Lower stratosphere	Uncertainty	1[c] K	0.4[b] – 1[c] K	1.8 K	1.2 K	6[c] K (extratropics) 3[a] K (tropics)	2 K
Lower stratosphere	Vertical resolution	1 km	100[b] – 500[c] m	1.5 km	800 m	3 km	2 km
Upper stratosphere	Uncertainty	1[c] K	0.4[b] – 1[c] K	2.8 K	1.2 K	6 K	2 K
Upper stratosphere	Vertical resolution	1 km	100[b] – 500[c] m	1.5 km	800 m	3 km	2 km
Long-term stability			0.05 K in 10 years[b]				

Notes:
a   Limit derived from atmospheric variability studies (WMO, 1970).
b   Limit derived from the GCOS Reference Upper-Air Network observation requirements (WMO, 2009).
c   Limit derived from the CBS Rolling Review of Requirements WMO observing requirements database (OSCAR/Requirements; see WMO, 2014), sampled August 2011.

Table 12.B.3. Summary of WMO/GCOS performance limits for aerological instruments measuring humidity

Layer		Goal for NWP	Goal for climate	Breakthrough for NWP	Breakthrough for climate	Threshold for NWP	Threshold for climate
Lower troposphere	Uncertainty	2[a] – 4[c] % RH	4% RH	16% RH	6% RH	40% RH	10% RH
Lower troposphere	Vertical resolution	100 m	50[b] – 500[c] m	200 m	800 m	1 km	2 km
Upper troposphere	Uncertainty	4% RH	4% RH	16% RH	6% RH	40% RH	10% RH

Layer		Goal for NWP	Goal for climate	Breakthrough for NWP	Breakthrough for climate	Threshold for NWP	Threshold for climate
Upper troposphere	Vertical resolution	300 m	100[b] – 500[c] m	500 m	800 m	1 km	2 km
Lower stratosphere	Uncertainty	10% mixing ratio ppmv	4% mixing ratio ppmv	16% mixing ratio ppmv	6% mixing ratio ppmv	40% mixing ratio ppmv	10% mixing ratio ppmv
Lower stratosphere	Vertical resolution	1 km	100[b] – 500[c] m	1.5 km	800 m	3 km	2 km
Upper stratosphere	Uncertainty	Not stated	4% mixing ratio ppmv	Not stated	6% mixing ratio ppmv	Not stated	10% mixing ratio ppmv
Upper stratosphere	Vertical resolution	Not stated	100[b] – 500[c] m	Not stated	800 m	Not stated	2 km
Long-term stability			0.3% in 10 years[b]				

Notes:
a   Limit derived from atmospheric variability studies (WMO, 1970).
b   Limit derived from the GCOS Reference Upper-Air Network observation requirements (WMO, 2009).
c   Limit derived from the CBS Rolling Review of Requirements WMO observing requirements database (OSCAR/Requirements; see WMO, 2014), sampled August 2011.

Note: The Rolling Requirement and GCOS requirement refer to specific humidity, but this leads to far too stringent limits on uncertainty in layers where relative humidity is very low in the lower and middle troposphere. So values are shown as approximately equivalent relative humidity, and mixing ratio should be used at very low temperatures or in the stratosphere.

Table 12.B.4. Summary of uncertainty ($k = 2$) and vertical resolution limits for geopotential heights of 100 hPa and significant levels, consistent with WMO/GCOS limits for upper-air temperature

Layer		Goal for NWP	Goal for climate	Breakthrough for NWP
Surface to 100 hPa	Uncertainty	24 gpm (= to 0.4 K temperature layer)	12 gpm (= to 0.2 K temperature layer)	50 gpm (= to 0.8 K temperature layer)
Lower troposphere	Uncertainty for temperature[a]	40 gpm	16 gpm on average	120 gpm
Lower troposphere	Uncertainty for cloud base[b]	30 gpm		
Upper troposphere	Uncertainty for temperature[a]	40 gpm	14 gpm on average	120 gpm
Lower stratosphere equatorial	Uncertainty for temperature[a]	70 gpm	48 gpm	200 gpm

Layer		Goal for NWP	Goal for climate	Breakthrough for NWP
Lower stratosphere extratropical	Uncertainty for temperature[a]	100 gpm	68 gpm	300 gpm
Upper stratosphere	Uncertainty for temperature[a]	80 gpm	60 gpm	240 gpm
Long-term stability			4 – 8 gpm in 10 years	

Notes:

a   Limit for height error produces a typical temperature error of half the magnitude specified for the limits for temperature in Table 12.B.2.

b   Limit derived to be compatible with measurements from operational laser ceilometers in the lower troposphere.

———————

ANNEX 12.C. GUIDELINES FOR ORGANIZING RADIOSONDE INTERCOMPARISONS AND FOR THE ESTABLISHMENT OF TEST SITES[1]

PART I – GUIDELINES FOR ORGANIZING RADIOSONDE INTERCOMPARISONS

1. Introduction

1.1   These guidelines assume that procedures that may be established by various test facilities are consistent with procedures established by other national and international organizations. They also assume that an Organizing Committee will be formed of participants (Members) interested in comparing radiosondes and that at least one non-participant will be included with ability to provide guidance for conducting the intercomparison. The involvement of an independent non-participant is important in order to avoid bias during the planning of the intercomparison. Consideration must also be given to whether radiosonde manufacturers' personnel should actively participate or whether independent operational personnel of the host should prepare and launch such radiosondes.

1.2   All intercomparisons differ from each other to some extent; therefore, these guidelines are to be construed only as a generalized checklist of tasks needing to be accomplished. Modifications should be made by the Organizing Committee, as required, but the validity of the results and scientific evaluation should not be compromised.

1.3   Final reports of previous intercomparisons and organizational meeting reports of other Organizing Committees may serve as an example of the methods that can be adopted for the intercomparison. These previous reports should be maintained and made available by the WMO Secretariat.

2. Objectives of intercomparisons

2.1   The intercomparison objectives must be clear, must list what is expected from the intercomparisons and identify how results will be disseminated. The Organizing Committee is tasked to examine the achievements to be expected from the radiosonde intercomparison and to identify and anticipate any potential problem. The Organizing Committee's role is to provide guidance, but it must also prepare clear and detailed statements of the main objectives and agree on the criteria to be used in evaluating the results. The Organizing Committee should also determine how best to guarantee the success of the intercomparison by drawing on background knowledge and accumulated experience from previous intercomparisons.

3. Place, date and duration of intercomparison

3.1   The host facility should provide to the Organizing Committee and to the participants a description of the proposed intercomparison site and facilities (locations, etc.), environmental and climatological conditions, and site topography. The host facility should also name a Project Leader or Project Manager who will be responsible for the day-to-day operation and act as the facility point of contact.

3.2   The Organizing Committee should visit the proposed site to determine the suitability of its facilities and to propose changes, as necessary. After the Organizing Committee agrees that the site and facilities are adequate, a site and environmental description should be prepared by

---

[1]   Based on the *Abridged Final Report with Resolutions and Recommendations of the Twelfth Session of the Commission for Instruments and Methods of Observation* (WMO-No. 881), Annex II, and updated thereafter.

the Project Leader for distribution to the participants. The Project Leader, who is familiar with his facility's schedule, must decide the date for the start of the intercomparison, as well as its duration. A copy of this schedule shall be delivered to the Organizing Committee.

3.3   In addition to the starting date of the intercomparisons, the Project Leader should propose a date when his facility will be available for the installation of the participant's equipment and arrange for connections to the data acquisition system. Time should be allowed for all of the participants to check and test equipment prior to starting the intercomparison and to allow additional time to familiarize the operators with the procedures of the host facility.

4.   Participation

4.1   As required, the Project Leader and/or Organizing Committee should invite, through the Secretary-General of WMO, participation of Members. However, once participants are identified, the Project Leader should handle all further contacts.

4.2   The Project Leader should draft a detailed questionnaire to be sent by the Secretary-General to each participant in order to obtain information on each instrument type proposed to be intercompared. Participants are expected to provide information on their space, communication, unique hardware connection requirements, and software characteristics. They also should provide adequate documentation describing their ground and balloon-borne instrumentation.

4.3   It is important that participants provide information about their radiosonde calibration procedures against recognized standards. Although it is expected that operational radiosondes will be intercompared, this may not always be the case; new or research-type radiosondes may be considered for participation with the agreement of all of the participants, the Project Leader, and the Organizing Committee.

5.   Responsibilities

5.1   *Participants*

5.1.1   The participants shall be responsible for the transportation of their own equipment and costs associated with this transportation.

5.1.2   The participants should install and remove their own equipment with the cognizance of the Project Leader. The host facility shall assist with unpacking and packing, as appropriate.

5.1.3   The participants shall provide all necessary accessories, mounting hardware for ground equipment, signal and power cables, spare parts and expendables unique to their system. The participants shall have available (in the event that assistance from the host facility should become necessary) detailed instructions and manuals needed for equipment installation, operation, maintenance and, if applicable, calibration.

5.1.4   The participants should sign the data protocol agreement of the intercomparison.

5.2   *Host facility*

5.2.1   The host facility should assist participants in the unpacking and installation of equipment as necessary, and provide storage capability to house items such as expendables, spare parts and manuals.

5.2.2   The host facility should provide auxiliary equipment as necessary, if available.

5.2.3   The host facility should assist the participants with connections to the host facility's data acquisition equipment, as necessary.

5.2.4   The host shall insure that all legal obligations relating to upper-air measurements (for example, the host country's aviation regulations and frequency utilization) are properly met.

5.2.5   The host facility may provide information on items such as accommodation, local transportation and daily logistics support, but is not obligated to subsidize costs associated with personnel accommodation.

6.   **Rules during the intercomparison**

6.1   The Project Leader shall exercise control of all tests and will keep a record of each balloon launch, together with all the relevant information on the radiosondes used in the flight and the weather conditions.

6.2   Changes in equipment or software will be permitted with the cognizance and concurrence of the Project Leader. Notification to the other participants is necessary. The Project Leader shall maintain a log containing a record of all the equipment participating in the comparison and any changes that occur.

6.3   Minor repairs (for example, fuse replacement, etc.) not affecting instrumentation performance are allowed. The Project Leader should be made aware of these minor repairs and also submit the information to the record log.

6.4   Calibration checks and equipment servicing by participants requiring a specialist or specific equipment will be permitted after notification to the Project Leader.

6.5   Any problem that compromises the intercomparison results or the performance of any equipment shall be addressed by the Project Leader.

7.   **Data acquisition**

7.1   The Organizing Committee should agree on appropriate data acquisition procedures such as measurement frequency, sampling intervals, data averaging, data reduction (this may be limited to an individual participant's capability), data formats, real-time quality control, post-analysis quality control and data reports.

7.2   The initial international Organizing Committee shall decide on the data acquisition hardware and software for the test. This should be well tested before commencement of the intercomparison, and the use of an established processing package such as described in WMO (1996*b*) is to be preferred.

7.3   The time delay between observation and delivery of data to the Project Leader shall be established by the Project Leader and agreed by the participants. One hour after the end of the observation (balloon burst) should be considered adequate.

7.4   The responsibility for checking data prior to analysis, the quality control steps to follow, and delivery of the final data rests with the Project Leader.

7.5   Data storage media shall be the Project Leader's decision after taking into consideration the capability of the host facility, but the media used to return final test data to participants may vary in accordance with each of the participant's computer ability. The Project Leader should be cognizant of these requirements.

7.6   The Project Leader has responsibility for providing final data to all participants and, therefore, the host facility must be able to receive all individual data files from each participant.

8. Data processing and analysis

8.1 *Data analysis*

8.1.1 A framework for data analysis should be encouraged and decided upon even prior to beginning the actual intercomparison. This framework should be included as part of the experimental plan.

8.1.2 There must be agreement among the participants as to methods of data conversion, calibration and correction algorithms, terms and abbreviations, constants, and a comprehensive description of proposed statistical analysis methods. It is essential that the data processing be performed by experienced experts, nominated by WMO.

8.1.3 The Organizing Committee should verify the appropriateness of the analysis procedures selected.

8.1.4 The results of the intercomparisons should be reviewed by the Organizing Committee, who should consider the contents and recommendations given in the final report.

8.2 *Data processing and database availability*

8.2.1 All essential meteorological and environmental data shall be stored in a database for further use and analysis by the participants. The Project Leader shall exercise control of these data.

8.2.2 After completion of the intercomparison, the Project Leader shall provide a complete set of all of the participants' data to each participant.

9. Final report of the intercomparison

9.1 The Project Leader shall prepare the draft final report which shall be submitted to the Organizing Committee and to the participating members for their comments and amendments. A time limit for reply should be specified.

9.2 Comments and amendments should be returned to the Project Leader with copies also going to the Organizing Committee.

9.3 When the amended draft final report is ready, it should be submitted to the Organizing Committee, who may wish to meet for discussions, if necessary, or who may agree to the final document.

9.4 After the Organizing Committee approves the final document for publication, it should be sent to the Secretariat for publication and distribution by WMO.

9.5 Reproduction for commercial purposes of any plots or tables from the final report should not be allowed without specific permission from WMO.

10. Final comments

10.1 The Organizing Committee may agree that intermediate results may be presented only by the Project Leader, and that participants may present limited data at technical conferences, except that their own test data may be used without limitation. Once the WMO Secretariat has scheduled the final report for publication, WMO shall make the data available to all Members who request them. The Members are then free to analyse the data and present the results at meetings and in publications.

PART II – GUIDELINES FOR THE ESTABLISHMENT OF TEST SITES

1. **Introduction**

1.1 In order to support the long-term stability of the global upper-air observing system, it is essential to retain the capability of performing quantitative radiosonde comparisons. Current and new operational radiosonde systems must be checked against references during flight on a regular basis. Members must ensure that a minimum number of test sites with the necessary infrastructure for performing radiosonde comparison tests are retained.

1.2 Experience with the series of WMO Radiosonde Intercomparisons since 1984 has shown that it is necessary to have a range of sites in order to compare the radiosondes over a variety of flight conditions.

1.3 Relative humidity sensor performance is particularly dependent on the conditions during a test, for example, the amount of cloud and rain encountered during ascents, or whether surface humidity is high or low.

1.4 Daytime temperature errors depend on the solar albedo, and hence the surface albedo and cloud cover. Thus, temperature errors found at coastal sites may differ significantly from continental sites. Infrared errors on temperature sensors will not only depend on surface conditions and cloud distribution, but also on atmospheric temperature. Thus, infrared temperature errors in the tropics (for instance near the tropopause) will be quite different from those at mid-latitudes.

1.5 The errors of many upper-wind observing systems depend on the distance the balloon travels from the launch site (and also the elevation of the balloon from the launch site). Thus, comparison tests must cover situations with weak upper winds and also strong upper winds.

2. **Facilities required at locations**

2.1 Locations suitable for testing should have enough buildings/office space to provide work areas to support the operations of at least four different systems.

2.2 The site should have good quality surface measurements of temperature, relative humidity, pressure and wind, measured near the radiosonde launch sites. Additional reference quality measurements of temperature, pressure and relative humidity would be beneficial.

2.3 The test site should have a method of providing absolute measurements of geopotential height during test flights (probably using a Global Positioning System (GPS) radiosonde capable of producing accurate heights).

2.4 The test site should have a well-established surface-based GPS sensor for measuring integrated water vapour, or ground-based radiometers and interferometers.

2.5 Cloud observing systems at the test site, such as laser ceilometers and cloud radars, are desirable.

2.6 Aerosol lidars and relative humidity lidars may also prove useful at the test site.

2.7 The site must be cleared by the national air traffic control authorities for launching larger balloons (3 000 g) with payloads of up to 5 kg. Balloon sheds must be able to cope with launching these large balloons.

3.   **Suggested geographical locations**

3.1   In order to facilitate testing by the main manufacturers, it is suggested that test sites should be retained or established in mid-latitudes in North America, Europe and Asia. Ideally, each of these regions would have a minimum of two sites, one representing coastal (marine) conditions, and another representing conditions in a mid-continent location.

3.2   In addition, it is suggested that a minimum of two test locations should be identified in tropical locations, particularly for tests of relative humidity sensors.

3.3   If the main test sites noted above do not provide adequate samples of extreme conditions for relative humidity sensors (for example, very dry low-level conditions), it may be necessary to identify further test sites in an arid area, or where surface temperatures are very cold (below –30 °C in winter). It is possible that some of these could be selected from established GRUAN sites.

PART III – GUIDELINES FOR PROTOTYPE TESTING

1.   **Introduction**

1.1   The major WMO radiosonde comparisons are organized about every 5 to 6 years, when a large group of manufacturers can benefit from a large-scale test, with systems that have already been through prototype testing. For new designs or for those manufacturers rectifying problems identified in the WMO radiosonde comparisons, there is a need to perform smaller, less expensive tests.

1.2   It is probably best for manufacturers trying to demonstrate that a problem has been resolved to have the tests done at one of the designated CIMO test sites.

1.3   On the other hand, the development and selection of new national radiosonde designs merits prototype testing at suitable national locations.

2.   **Recommended procedures**

2.1   Testing to prove that problems have been rectified needs to be done to similar standards and methods used in the WMO radiosonde comparisons. This requires that any CIMO test site must have staff who are fully conversant with the procedures and techniques of the WMO radiosonde comparisons, and also requires the use of two radiosonde types of known good quality as working references/link radiosondes to the WMO radiosonde comparison results.

2.2   With national prototype testing it is essential to compare measurements with radiosondes flown together under one balloon. Ideally the radiosondes should be suspended in such a way that they are free to rotate in flight, as this is what happens on individual ascents. The radio-frequency performance of the new radiosonde needs to be good enough to ensure that the frequency does not drift and cause interference to the radiosonde with which it is being compared. Comparison of results should be performed as a function of time into flight, since it is unwise to assume that height/pressure assignments to temperature and relative humidity measurements have negligible errors. The number of initial test flights may be quite small since some initial errors are often large and can be quickly identified even by comparison with a lower quality national radiosonde.

2.3   However, once the aim is to improve the new national radiosonde design so that its measurement quality comes close to that of the high-quality radiosondes tested in the WMO Intercomparison of High Quality Radiosonde Systems, then it will be necessary to use one of the better quality radiosondes as a test reference. Always follow the manufacturer's instructions

when preparing the better quality radiosonde for the test flights. Testing must be performed both day and night, since the sonde errors for daytime temperatures need to be identified and at night the errors in relative humidity are often worse than in daytime.

2.4   Final prototype tests need to be performed at a time of year when the variation of relative humidity in the vertical and with time is high at all levels in the troposphere.

3.   **Archiving of results**

3.1   Results of tests at CIMO test centres need to be forwarded to the relevant CIMO expert team for checking and display on the CIMO websites.

3.2   Once a new national development becomes mature, it would also be helpful for the future to forward comparison test results to the relevant CIMO expert team.

_____

REFERENCES AND FURTHER READING

Fujiwara, M., M. Shiotani, F. Hasebe, H. Vömel, S.J. Oltmans, P.W. Ruppert, T. Horinouchi and T. Tsuda, 2003: Performance of the Meteolabor "Snow White" chilled-mirror hygrometer in the tropical troposphere: Comparisons with the Vaisala RS80 A/H-Humicap sensors. *Journal of Atmospheric and Oceanic Technology*, 20:1534–1542.

Hyland, R.W. and A. Wexler, 1983: Formulations for the thermodynamic properties of the saturated phases of H2O from 173.15 K to 473.15 K. *ASHRAE Transactions*, 89(2A):500–519.

Immler, F.J., J. Dykema, T. Gardiner, D.N. Whiteman, P.W. Thorne and H. Vömel, 2010: Reference quality upper-air measurements: guidance for developing GRUAN data products. *Atmospheric Measurement Techniques*, 3:1217–1231.

Kitchen, M., 1989: Representativeness errors for radiosonde observations. *Quarterly Journal of the Royal Meteorological Society*, 115:673–700.

Kursinski, E.R., G.A. Hajj, J.T. Schofield, R.P. Linfield and K.R. Hardy, 1997: Observing Earth's atmosphere with radio occultation measurements using the Global Positioning System. *Journal of Geophysical Research*, 102:23429–23466.

List, R.J., 1968: *Smithsonian Meteorological Tables*. Washington, Smithsonian Institution Press.

Luers, J.K. and R.E. Eskridge, 1998: Use of radiosonde temperature data in climate studies. *Journal of Climate*, 11:1002–1019.

McIlveen, J.F.R. and F.H. Ludlam, 1969: The lag of the humidity sensor in the British radiosonde. *Meteorological Magazine*, 98:233–246.

Miloshevich, L.M., A. Paukkunen, H. Vömel and S.J. Oltmans, 2004: Development and validation of a time-lag correction for Vaisala radiosonde humidity measurements. *Journal of Atmospheric and Oceanic Technology*, 21:1305–1327.

Miloshevich, L.M., H. Vömel, D.N. Whiteman and T. Leblanc, 2009: Accuracy assessment and correction of Vaisala RS92 radiosonde water vapor measurements. *Journal of Geophysical Research: Atmospheres*, 114(D11305).

Nash, J., 1984: *Compatibility of Radiosonde Measurements in the Upper Troposphere and Lower Stratosphere for the Period 1 November 1981 to 31 October 1982*. Meteorological Office, Bracknell, OSM No. 24.

Nash, J., J.B. Elms and T.J. Oakley, 1995: Relative humidity sensor performance observed in recent international radiosonde comparisons. *Ninth AMS Symposium on Meteorological Observations and Instrumentation*, Charlotte, North Carolina, pp. 43–48.

Paukkunen, A., 1995: Sensor heating to enhance reliability of radiosonde humidity measurement. *Ninth AMS Symposium on Meteorological Observations and Instrumentation*, Charlotte, North Carolina, pp. 65–69.

Philipona, R., A. Kräuchi, G. Romanens, G. Levrat, P. Ruppert, E. Brocard, P. Jeannet, D. Ruffieux and B. Calpini, 2013: Solar and thermal radiation errors on upper-air radiosonde temperature measurements. *Journal of Atmospheric and Oceanic Technology*, 30:2382–2393.

Schmidlin, F.J., H. Sang Lee and B. Ranganayakamma, 1995: Deriving the accuracy of different radiosonde types using the three-thermistor radiosonde technique. *Ninth AMS Symposium on Meteorological Observations and Instrumentation*, Charlotte, North Carolina, pp. 27–31.

Shimizu, K. and F. Hasebe, 2010: Fast-response high-resolution temperature sonde aimed at contamination-free profile observations. *Atmospheric Measurement Techniques*, 3:1673–1681.

Sonntag, D., 1994: Advancements in the field of hygrometry. *Zeitschrift für Meteorologie*, 3(2):51–66.

Turner, D.D., B.M. Lesht, S.A. Clough, J.C. Liljegren, H.E. Revercomb and D.C. Tobon, 2003: Dry bias and variability in Vaisala RS80-H radiosondes: The ARM experience. *Journal of Atmospheric and Oceanic Technology*, 20:117–132.

Turtiainen, H., S. Tammela and I. Stuns, 1995: A new radiosonde temperature sensor with fast response time and small radiation error. *Ninth AMS Symposium on Meteorological Observations and Instrumentation*, Charlotte, North Carolina, pp. 60–64.

Vömel, H., D.E. David and K. Smith, 2007a: Accuracy of tropospheric and stratospheric water vapor measurements by the cryogenic frost point hygrometer: Instrument details and observations. *Journal of Geophysical Research*, 112(D08305).

Vömel, H., H. Selkirk, L. Miloshevich, J. Valverde-Canossa, J. Valdés, E. Kyrö, R. Kivi, W. Stolz, G. Peng and J.A. Diaz, 2007b: Radiation dry bias of the Vaisala RS92 humidity sensor. *Journal of Atmospheric and Oceanic Technology*, 24:953–963.

Wade, C.G., 1995: Calibration and data reduction problems affecting national weather service radiosonde humidity measurements. *Ninth AMS Symposium on Meteorological Observations and Instrumentation*, Charlotte, North Carolina, pp. 37–42.

Wang, J. and L. Zhang, 2008: Systematic errors in global radiosonde precipitable water data from comparisons with ground-based GPS measurements. *Journal of Climate*, 21:2218–2238.

Wexler, A., 1976: Vapor pressure formulation for water in range 0 to 100 °C. A revision. *Journal of Research of the National Bureau of Standards – A. Physics and Chemistry*, 80A(5 and 6):775–785.

——, 1977: Vapor pressure formulation for ice. *Journal of Research of the National Bureau of Standards – A. Physics and Chemistry*, 81A(1):5–20.

World Meteorological Organization, 1970: *Performance Requirements of Aerological Instruments: an Assessment Based on Atmospheric Variability* (C.L. Hawson). Technical Note No. 112 (WMO-No. 267, TP. 151). Geneva.

——, 1975: *Upper-Air Sounding Studies* (A.H. Hooper). Technical Note No. 140 (WMO-No. 394), Volume I. Geneva.

——, 1986: *Algorithms for Automatic Aerological Soundings* (A.H. Hooper). Instruments and Observing Methods Report No. 21 (WMO/TD-No. 175). Geneva.

——, 1987: *WMO International Radiosonde Comparison (UK 1984, USA 1985): Final Report* (J. Nash and F.J. Schmidlin). Instruments and Observing Methods Report No. 30 (WMO/TD-No. 195). Geneva.

——, 1989*a*: SRS-400: The new Swiss radiosonde (B. Hoegger, A. Heimo, G. Levrat and J. Rieker). *Papers Presented at the Fourth WMO Technical Conference on Instruments and Methods of Observation (TECIMO-IV)*. Instruments and Observing Methods Report No. 35 (WMO/TD-No. 303). Geneva.

——, 1989*b*: *Compatibility of Radiosonde Geopotential Measurements* (M. Kitchen). Instruments and Observing Methods Report No. 36 (WMO/TD-No. 344). Geneva.

——, 1991: *WMO International Radiosonde Comparison – Phase III, Dzhambul (USSR), 1989: Final Report* (A. Ivanov, A. Kats, S. Kurnosenko, J. Nash and N. Zaitseva). Instruments and Observing Methods Report No. 40 (WMO/TD-No. 451). Geneva.

——, 1992: *International Meteorological Vocabulary.* (WMO-No. 182). Geneva.

——, 1993*a*: *Historical Changes in Radiosonde Instruments and Practices* (D.J. Gaffen). Instruments and Observing Methods Report No. 50 (WMO/TD-No. 541). Geneva.

——, 1993*b*: *Report by the Rapporteur on Radiosonde Compatibility Monitoring.* Part A: WMO Catalogue of Radiosondes and Upper-air Wind Systems in Use by Members (1993), Part B: Compatibility of Radiosonde Geopotential Measurements 1990, 1991 and 1992 (T. Oakley). Instruments and Observing Methods Report No. 56 (WMO/TD-No. 587). Geneva.

——, 1994: The difference in observed temperatures from radiosondes suspended 10 m and 40 m beneath a 1400 g balloon (J.B. Elms, J. Nash and G. Williams). *Papers Presented at the WMO Technical Conference on Instruments and Methods of Observation (TECO-94)*. Instruments and Observing Methods Report No. 57 (WMO/TD-No. 588). Geneva.

——, 1996*a*: *WMO International Radiosonde Comparison – Phase IV, Tsukuba (Japan), 1993: Final Report* (S. Yagi, A. Mita and N. Inoue). Instruments and Observing Methods Report No. 59 (WMO/TD-No. 742). Geneva.

——, 1996*b*: *Description and User Guide for the Radiosonde Comparison and Evaluation Software Package (RSKOMP – Version 3/Version 4)* (S. Kurnosenko and T. Oakley). Instruments and Observing Methods Report No. 60 (WMO/TD-No. 771). Geneva.

——, 1998: *Report by the Rapporteur on Radiosonde Compatibility Monitoring.* Part A: WMO Catalogue of Radiosondes and Upper-air Wind Systems in Use by Members (1998), Part B: Compatibility of Radiosonde Geopotential Measurements 1995, 1996 and 1997 (T. Oakley). Instruments and Observing Methods Report No. 72 (WMO/TD-No. 886). Geneva.

——, 2003: *WMO Catalogue of Radiosondes and Upper-air Wind Systems in Use by Members in 2002 and Compatibility of Radiosonde Geopotential Measurements for Period from 1998 to 2001* (J. Elms). Instruments and Observing Methods Report No. 80 (WMO/TD-No. 1197). Geneva.

——, 2006*a*: *WMO Intercomparison of Radiosonde Systems – Vacoas (Mauritius), 2005* (J. Nash, R. Smout, T. Oakley, B. Pathack and S. Kurnosenko). Instruments and Observing Methods Report No. 83 (WMO/TD-No. 1303). Geneva.

——, 2006*b*: *The WMO Radiosonde Humidity Sensor Intercomparison* (A. Balagurov, A. Kats and N. Krestyannikova (Phase I, Russian Federation) and F. Schmidlin (Phase II, USA)). Instruments and Observing Methods Report No. 85 (WMO/TD-No. 1305). Geneva.

——, 2006*c*: *WMO Intercomparison of GPS Radiosondes – Alcântara (Brazil), 2001* (R. da Silveira, G.F. Fisch, L.A.T. Machado, A.M. Dall'Antonia, L.F. Sapucci, D. Fernandes, R. Marques and J. Nash). Instruments and Observing Methods Report No. 90 (WMO/TD-No. 1314). Geneva.

───, 2006*d*: Recent application of the Accurate Temperature Measuring (ATM) radiosonde (F.J. Schmidlin). *Papers and posters presented at the WMO Technical Conference on Meteorological and Environmental Instruments and Methods of Observation (TECO-2006).* Instruments and Observing Methods Report No. 94 (WMO/TD-No. 1354). Geneva.

───, 2009: *GRUAN Implementation Plan 2009–2013.* GCOS-134 (WMO/TD-No. 1506). Geneva.

───, 2010*a*: *Manual on the Global Observing System* (WMO-No. 544), Volume I. Geneva.

───, 2010*b*: A new operational radiosonde for the UK. Procurement testing at Camborne Met Office, September–October 2009 (J. Nash, M. Smees et al.). *Papers and posters presented at the WMO Technical Conference on Meteorological and Environmental Instruments and Methods of Observation (TECO-2010).* Instruments and Observing Methods Report No. 104 (WMO/TD-No. 1546). Geneva.

───, 2011*a*: *Technical Regulations* (WMO-No. 49), Volume I, Appendix A. Geneva.

───, 2011*b*: *WMO Intercomparison of High Quality Radiosonde Systems – Yangjiang (China), 2010* (J. Nash, T. Oakley, H. Vömel and L. Wei). Instruments and Observing Methods Report No. 107 (WMO/TD-No. 1580). Geneva.

───, 2011*c*: *Manual on Codes* (WMO-No. 306), Volume I.1. Geneva.

───, 2014: Observing Systems Capability Analysis and Review Tool (OSCAR): user requirements for observation, http://www.wmo-sat.info/oscar/observingrequirements.

───, 2015: *Measurement of Upper-air Pressure, Temperature and Humidity* (J. Nash). Instruments and Observing Methods Report No. 121. Geneva.

CHAPTER CONTENTS

CHAPTER 13. MEASUREMENT OF UPPER WIND

13.1 GENERAL

13.1.1 Definitions

The following definitions are taken from the *Manual on the Global Observing System* (WMO, 2010):

Pilot-balloon observation: A determination of upper winds by optical tracking of a free balloon.

Radiowind observation: A determination of upper winds by tracking of a free balloon by electronic means.

Rawinsonde observation: A combined radiosonde and radiowind observation.

Upper-air observation: A meteorological observation made in the free atmosphere either directly or indirectly.

Upper-wind observation: An observation at a given height or the result of a complete sounding of wind direction and speed in the atmosphere.

This chapter will deal primarily with radiowind and pilot-balloon observations. Balloon techniques, and measurements using special platforms, specialized equipment, or made indirectly by remote-sensing methods are discussed in various chapters of Part II. Large numbers of observations are now received from commercial aircraft and also from wind profiler and weather radars. Data from balloons are mainly acquired by using rawinsonde techniques, although pilot-balloon and radiowind observations may be used when additional upper wind data are required without the expense of launching a radiosonde.

13.1.2 Units of measurement of upper wind

The speed of upper winds is usually reported in metres per second or knots, but kilometres per hour are also used. The direction from which the airflow arrives is reported in degrees from north: 90° represents a wind arriving from the east, 180° from the south, 270° from the west and 0/360° from the north. In TEMP reports, the wind direction is rounded to the nearest 5°. Reporting to this resolution degrades the accuracy achievable by the best modern windfinding systems, particularly when upper winds are strong. Data from these systems encoded in BUFR provide more accurate information on the direction and speed of upper wind.

Within 1° latitude of the North or South Pole, surface winds are reported using a direction where the azimuth ring is aligned with its zero coinciding with the Greenwich 0° meridian. This different coordinate system should be used by all fixed and mobile upper-air stations located within 1° latitude of the North or South Pole for wind direction at all levels of the entire sounding, even if the balloon moves farther away than 1° latitude from the pole. The reporting code for these measurements should indicate that a different coordinate system is being used in this upper-air report, in particular if encoded in traditional alphanumeric codes; the location of the station in BUFR automatically indicates usage of this different coordinate system.

The height used in reporting radiowind/rawinsonde measurements is geopotential height so that the wind measurements are at the same heights as the radiosonde measurements of temperature and relative humidity (see Part I, Chapter 12, 12.3.6). The conversion from geometric height, as measured with a GPS radiosonde or radar, to geopotential height is purely a function of the gravitational field at a given location and does not depend on the temperature and humidity profile at the location. The gravitational potential energy (Φ) of a unit mass of anything is the integral of the normal gravity from mean sea level ($z_{geometric} = 0$) to the height of the mass ($z_{geometric} = Z$), as given by equation 13.1.

$$\Phi = \int_0^z \gamma(z_{\text{geometric}}, \varphi) dz_{\text{geometric}} \tag{13.1}$$

where $\gamma(z_{\text{geometric}}, \varphi)$ is the normal gravity above the geoid. This is a function of geometric altitude, $z_{\text{geometric}}$, and the geodetic latitude φ.

This geopotential is divided by the normal gravity at 45° latitude to give the geopotential height used by WMO, as:

$$z\left(z_{\text{geometric}}, \varphi\right) = \Phi\left(z_{\text{geometric}}, \varphi\right)/\gamma_{45°} = (\int_0^z \gamma\left(z_{\text{geometric}}, \varphi\right) dz_{\text{geometric}})/\gamma_{45°} \tag{13.2}$$

where $\gamma_{45°}$ was taken in the definition as 9.806 65 m s^{-2}.

Thus, the unit of height is the standard geopotential metre. In the troposphere, the value of geopotential height is a close approximation to the geometric height expressed in metres (see, for example, Part I, Chapter 12, Table 12.4). The geopotential heights used in upper-wind reports are reckoned from sea level, although in many systems the computations of geopotential height will initially be performed in terms of height above the station level.

The conversion of geometric height to geopotential height is derived in fuller detail in Part I, Chapter 12, with suitable expressions given for the dependence of the gravitational field on height and latitude.

13.1.3 Meteorological requirements

13.1.3.1 *Uses in meteorological operations*

Observations of upper winds are essential for operational weather forecasting on all scales globally, and are often most effective when used in conjunction with simultaneous measurements of mass field (temperature and relative humidity).

(a) In the boundary layer, upper winds providing reliable measurements of vertical wind shear are essential for environmental pollution forecasting;

(b) They are vital to the safety and economy of aircraft operations;

(c) Accurate upper wind and vertical wind shear measurements are critical for the launching of space vehicles and other types of rocket;

(d) Uncertainties in upper winds are the limiting factor in the accuracy of modern artillery, and reliable wind measurements are therefore important for safety in military operations;

(e) Upper winds are one of the essential climate variables.

13.1.3.2 *Improvements in reporting procedures*

Upper winds are normally input into numerical weather forecasts as layer averages, the thickness of the layers depending on the scales of atmospheric motion relevant to the forecast. The values are not usually input at standard pressures or heights, but will usually be centred at pressure heights that vary as the surface pressure changes at the location of the observation. Thus, it is of primary importance that the variation in winds between standard levels is accurately represented in upper-wind reports. This is in addition to ensuring that accurate winds are reported at the standard levels.

In modern radiowind systems, computers have the capability of readily providing all the detailed structure relevant to meteorological operations and scientific research. The upper-wind reports should contain enough information to define the vertical wind shear across the boundaries

between the various layers in the mass fields. For instance, wind shear across temperature inversions or significant wind shear associated with large changes in relative humidity in the vertical should be reported whenever possible.

When upper winds are reported using either the FM 35–XI Ext. TEMP code or the FM 32–XI Ext. PILOT code (WMO, 2011a), wind speeds are allowed to deviate by as much as 5 m s^{-1} from the linear interpolation between significant levels. The use of automated algorithms with this fitting limit can produce errors in reported messages which are much larger than the observational errors. On occasion, the coding procedure may also degrade the accuracy outside the accuracy requirements outlined in Part I, Chapter 12.

This should be prevented, as soon as possible, by submitting reports in a suitable BUFR code that allows reporting of high-resolution vertical wind data in addition to the significant levels to fulfil user requirements. However, until this is achieved, a fitting limit for a wind speed of 3 m s^{-1} instead of 5 m s^{-1} can be implemented as a national practice for TEMP and PILOT messages. The tightening of the fitting limit should lead, on average, to about one significant level wind report per kilometre in the vertical. The TEMP or PILOT report should be visually checked against the detailed upper-wind measurement, and the reported messages should be edited to eliminate unacceptable fitting errors before issue.

In earlier years, upper winds were generally processed manually or with a small calculator, and it was impractical to produce detailed reports of the vertical wind structure – hence the use of significant levels and the relatively crude fitting limits, which are not appropriate for the quality of observation produced by modern rawinsonde systems.

13.1.3.3   *Accuracy requirements*

Accuracy requirements for upper-wind measurements are presented in terms of wind speed and direction and also orthogonal wind components in Part I, Chapter 12, Annex 12.A. Most upper-wind systems should be capable of measuring winds over a range from 0 to 100 m s^{-1}. If systems are designed to provide winds at low levels, they may not need to cope with such a large range. Systematic errors in wind direction must be kept as small as possible and certainly much less than 5°, especially at locations where upper winds are usually strong. In the 1990s, most well-maintained operational windfinding systems provided upper winds with a standard vector error (2σ) that was better than or equal to 3 m s^{-1} in the lower troposphere and 5 to 6 m s^{-1} in the upper troposphere and stratosphere (Nash, 1994). The advent of very reliable GPS windfinding systems means that many modern systems are capable of even better performance than this, with a standard vector error ($k = 2$) less than 1 m s^{-1} with little degradation of the measurement quality in the vertical (see the results of the WMO Intercomparison of High Quality Radiosonde Systems in Yangjiang, China (WMO, 2011b)).

Examples of vertical profiles of horizontal wind from Yangjiang, China, and the United Kingdom are shown in Figure 13.1. These measurements were made with a vertical resolution better than 150 m. Figure 13.1(a) shows two measurements from Yangjiang spaced six hours apart. The fine structure in the vertical is not the result of noise, but is the real structure in the atmosphere also measured by the other rawinsonde systems on the respective flights. During this test, there were very strong easterly winds at upper levels in the stratosphere (associated with the easterly phase of the quasi-biennial oscillation). The stronger northerly winds associated with the jet at about 16 km extend up to about 21 km and thus through the tropopause at 17.5 km. The detailed wind structure in the stratosphere between 22 and 34 km mostly persists over seven hours, illustrating that much of the detailed structure is not transient and thus merits archiving and reporting.

Figure 13.1(b) is from early winter in the United Kingdom, with the tropopause much lower at about 11 km, but again the stronger winds associated with the upper troposphere jet extend up to at least 16 km. The large perturbations in wind caused by the gravity waves immediately above the tropopause would not be resolved at 1 km vertical resolution. On this occasion, there is another jet associated with circulation around the polar vortex at heights above 30 km. Figure 13.1(c) is from UK summertime conditions. In this case there is significant wind shear
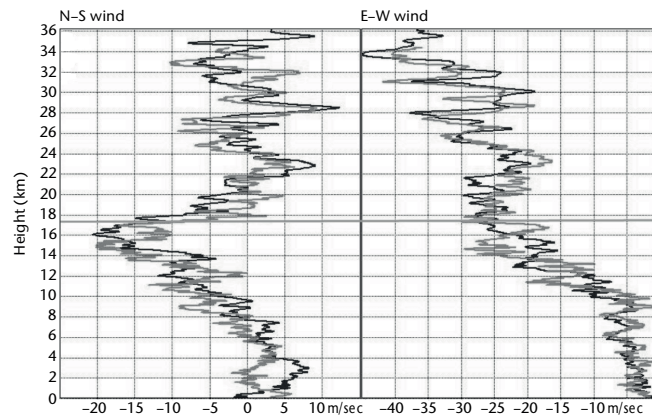
(a) Flight 1 at 0800 hours (black) and flight 3 at 1448 hours (grey) on 14 July 2010, from the WMO Intercomparison of High Quality Radiosonde Systems in Yangjiang, China
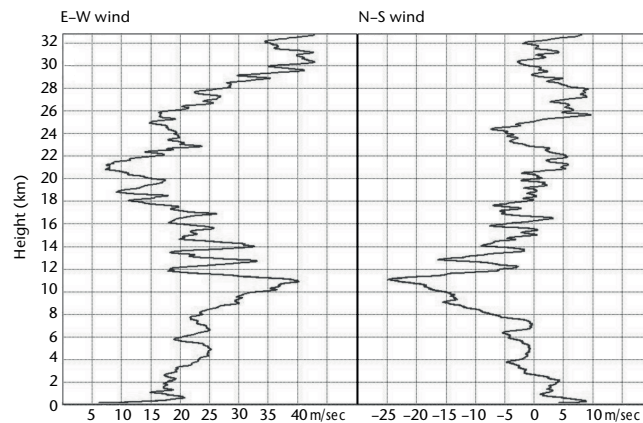
(b) November measurement made at Camborne, United Kingdom; data from two different radiosonde types are superimposed. (Note: In this frame, the zonal and meridional wind components are reversed, i.e. the zonal component is displayed on the left.)
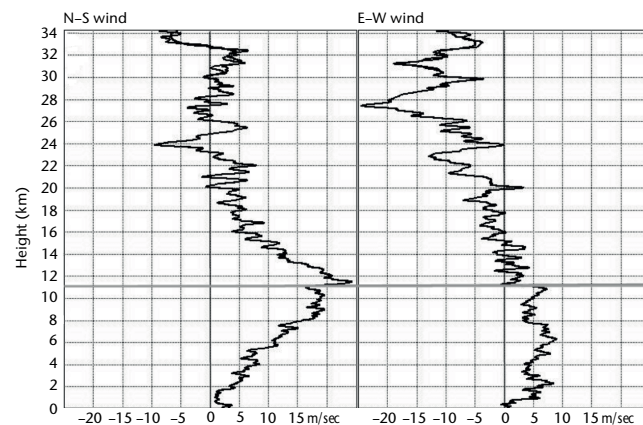
(c) July measurement made at Camborne, United Kingdom; data from two different radiosonde types are superimposed.

Figure 13.1. Examples of vertical profiles of horizontal wind measured at about 150 m vertical resolution in Yangjiang, China, and in early winter and summer in the United Kingdom; horizontal grey line shows tropopause height.

across the tropopause. Easterly winds predominate in the stratosphere above about 16 km, and these are not as strong as the westerly winds in the winter. However, between 20 and 32 km, there are again significant perturbations in the winds in summertime.

Thus, although the user requirement for vertical resolution quoted for upper-wind measurements in Part I, Chapter 12, Annex 12.B, Table 12.B.1 is 200 to 500 m in the troposphere and 1 km in the stratosphere, in practice there is information in the rawinsonde measurement which should

be archived and reported for reasons other than numerical weather prediction analyses. So, it is recommended that, where possible, systems should use the higher resolution now available, with vertical resolution better than or equal to 200 m in the lower troposphere, and better than 300 m in the upper troposphere and lower stratosphere. As can be seen, there are strong shears near the jet maximum, and to resolve these reliably requires a vertical resolution better than the 500 m quoted in Table 12.B.1.

A vertical resolution of 50 to 150 m can prove beneficial for general meteorological operations in the atmospheric boundary layer (up to 2 km above the surface). However, the tracking system used must be able to sustain acceptable wind measurement accuracy at the higher vertical resolution if the increased resolution is to be useful.

Very high-accuracy upper-wind measurements are often specified for range operations such as rocket launches. In this case, special balloons with sculptured surfaces which follow the winds more closely than standard meteorological balloons must be used. The observing schedules required to meet a very high-accuracy specification need careful planning since the observations must be located close to the required site and within a given time frame. The following characteristic of atmospheric variability should be noted. The root-mean-square vector differences between two error-free upper-wind observations at the same height (sampled at the 300 m vertical resolution) will usually be less than 1.5 m s^{-1} if the measurements are simultaneous and separated by less than about 5 km in the horizontal. This will also be the case if the measurements are at the same location, but separated by an interval of less than about 10 min (derived from similar, smaller-scale studies to the representativeness studies of Kitchen (1989)).

13.1.3.4   *Maximum height requirements*

Upper winds measured from balloon-borne equipment, as considered in this chapter, can be required at heights up to and above 35 km at some sites, especially those designated as part of the Global Climate Observing System. The balloons necessary to reach these heights may be more expensive than the cheap, small balloons that will lift the rawinsonde systems to heights between 20 and 25 km.

An ideal upper-wind observing network must adequately sample all scales of motion, from planetary scale to mesoscale, in the troposphere and lower stratosphere. The observing network will also identify significant small-scale wind structures using high temporal resolution remote-sensing systems. However, in the middle and upper stratosphere, the predominant scales of motion observed for meteorological operations are larger, primarily the planetary scale and larger synoptic scales. Thus, all the upper-air observing sites in a national network with network spacing being optimized for tropospheric observations may not need to measure to heights above 25 km. Overall operating costs may be less if a mix of the observing systems described in this chapter with the sensing systems described in Part II is used. If this is the case, national technical infrastructure must be able to provide adequate maintenance for the variety of systems deployed.

13.1.4   **Methods of measurement**

Data on upper winds from balloon-borne systems are mainly acquired by using rawinsonde techniques, although pilot-balloon and radiowind observations may be used when additional upper wind data are required without the expense of launching a radiosonde. Observations from the upper-air stations in the Global Observing System are supplemented over land by measurements from aircraft, wind profilers and Doppler weather radars. In areas with high levels of aircraft operations, the information available from aircraft and radars dominates that available from radiosondes up to heights of about 12 km. Over the sea, upper winds are mainly produced by civilian aircraft at aircraft cruise levels. These are supplemented with vertical profiles from rawinsondes launched from ships or remote islands, and also by tracking clouds or water vapour structures observed from geostationary meteorological satellites. In the future, wind measurements from satellite-borne lidars (light detection and ranging) and radars are expected to improve the global coverage of the current observing systems. Sodars (sound detection

and ranging), lidars and kite anemometers are also used to provide high temporal resolution winds for specific applications. Low-cost pilotless aircraft technology is being developed for meteorological applications.

Rawinsonde methods for measuring the speed and direction of the wind in the upper air generally depend upon the observation of either the movement of a free balloon ascending at a more or less uniform rate or an object falling under gravity, such as a dropsonde on a parachute. Given that the horizontal motion of the air is to be measured, the target being tracked should not have any significant horizontal motion relative to the air under observation. The essential information required from direct tracking systems includes the height of the target and the measurements of its plan position or, alternatively, its horizontal velocity at known time intervals. The accuracy requirements in Part I, Chapter 12, Annex 12.A, include the effect of errors in the height or pressure assigned to the wind measurement. It is unlikely that the usual operational accuracy requirements can be met for levels above the atmospheric boundary layer with any tracking method that needs to assume a rate of ascent for the balloon, rather than using a measurement of height from the tracking system or from the radiosonde attached to the target.

Remote-sensing systems measure the motion of the atmosphere by scattering electromagnetic radiation or sound from one or more of the following targets: hydrometeors, dust, aerosol, or inhomogeneities in the refractive index caused by small-scale atmospheric turbulence or the air molecules themselves.

The direct windfinding methods considered in this chapter use targets whose position can be tracked continuously. While the targets can be tracked by a large number of methods, only two widely used types of methods will be considered here.

13.1.4.1 *Tracking using radionavigation signals*

A radiosonde with the capability of receiving signals from a system of navigational radio transmitters is attached to a target (either an ascending balloon or dropsonde parachute). The most widely used system is to use signals from navigation satellites. In practice, for the moment, this means using the NAVSTAR GPS signals, although other, more recently introduced satellite radionavigation services may be used in the future. The signals from the satellites are received by a dedicated antenna on the radiosonde. The system will also have a GPS antenna on the ground to receive signals for reference. A GPS engine, either on the ground or in the radiosonde, will decode the signals or allow computation of the radiosonde position in three dimensions as a function of time.

Tracking using radionavigation signals was first achieved on a large scale with the surface-based Omega navigation chain, but once this service was closed most of these radiosonde operators changed to GPS windfinding. Surface-based long-range navigation signals were also used from the LORAN system, described in WMO (1985). The coverage offered by LORAN-C coupled with the Russian Chayka system has decreased in recent years, and now operational use is mainly limited to eastern Europe at the times that Chayka is operational.

The use of GPS navaid tracking has increased in routine meteorological operations because of the high degree of automation that can be achieved with this type of windfinding system. The level of maintenance required by navaid ground equipment is also very low. Height measurements from the GPS radiosonde provide the best method for assigning heights for accurate stratospheric temperatures in climate studies.

Early GPS radiosondes all used the meteorological aids (MetAids) frequency band centred at 403 MHz for transmitting data to the ground, but there are a few countries where large-scale civilian radiosonde operation in this band is not feasible, and GPS radiosondes using the higher frequency MetAids band centred at 1 680 MHz have also been developed.

13.1.4.2 *Tracking using a directional aerial*

In many large national networks the higher cost of GPS radiosonde consumables has meant that non-GPS radiosondes continue to be used with a ground system that tracks the target with a directional aerial measuring azimuth, plus any two of the following parameters: elevation angle, slant range, and height. Measurements are mostly achieved using a radiotheodolite or secondary radar (see section 13.2.3.2) to track a radiosonde carried by a balloon. In some cases, an optical theodolite is used to track the balloon. A primary radar (see section 13.2.3.1) can also track a reflecting target carried by the balloon, but although this system was quite widely used in the past, it is not in common use now. The difference between primary and secondary radars is that the primary radar detects pulses reflected from its target, while the secondary radar only transmits pulses and does not look for reflections. With a secondary radar, the radiosonde/transponder attached to the balloon receives the radar pulses and then transmits information on the time of receipt back to the radar ground station. Radar and radiotheodolite systems usually have a tracking accuracy for elevation and azimuth of about 0.1°, while for radar systems, the range error should normally be less than 30 m.

Modern radiotheodolite systems with antenna dimensions of less than 2 m are best suited for upper-wind measurements when balloon elevations stay above 10° to 15°. Secondary radar systems continue to be used in national networks where sufficient radio-frequency spectrum in the meteorological aids bands is available. Successful directional antennas are operated mostly in the 1 680 MHz band, as the antenna size required for directional tracking at 403 MHz is too large for most modern operational practice.

The choice between using a radiotheodolite or GPS radiosonde for upper-wind measurements will be partly influenced by the maximum slant range expected at the observation site. The GPS windfinding system will provide good measurement accuracy at very long ranges. The maximum range varies considerably with latitude, with 70 km being adequate in equatorial and polar regions, but with ranges of up to at least 200 km being possible in some mid-latitude temperate zones. Table 13.1 shows the proportion of occasions when certain slant ranges were exceeded for a balloon at 30 km. The data are for stations located in Europe between 50°N and 60°N. The proportions are given for a whole year, but it should be noted that the soundings which exceeded the limits were centred in the winter season.

13.2 UPPER-WIND SENSORS AND INSTRUMENTS

Radiowind systems were originally introduced to allow measurements of upper wind in the presence of clouds. The systems were also capable of high measurement accuracy at long ranges when balloons were tracked up to heights of 30 km. The use of these systems is now essential to satisfy the majority of modern upper-wind accuracy requirements. The high degree of automation possible with most modern rawinsonde systems has eliminated the need for operator intervention in most of the measurement cycle. This has major advantages in reducing costs for meteorological operations.

13.2.1 Optical theodolite

Optical theodolites may be used for tracking balloons when the expense of radiowind measurements cannot be met, for example at intermediate times between main ascents or at other locations in a country to fill gaps in the network at lower levels (see WMO, 2008).

Table 13.1. Proportion of occasions when certain slant ranges were exceeded (balloon at 30 km altitude)

Slant range exceeded (km)	140	160	175	190
Proportion of occasions (%)	5	2	1	0.5

Operators need significant training and skill if upper-wind measurement errors are not to increase rapidly as the balloon ascends above the boundary layer, but useful periods of observation have been achieved in parts of South America and Africa.

The optical system of the pilot balloon theodolite should be such that the axis of the eyepiece remains horizontal irrespective of the direction in which the telescope is pointed. A pentagonal prism is preferable to a right-angled prism since a slight displacement of the former does not affect the perpendicularity of the two parts of the optical axis.

The focusing eyepiece of the telescope should be fitted with cross-wires or a graticule and should have a magnification of between 20 and 25 times and a field of view of no less than 2°. The mounting of the theodolite should be of robust construction. It should be possible to turn the theodolite rapidly by hand or slowly by friction or worm gearing on the azimuth and elevation circles. These circles should be subdivided into sections no larger than 1° and should be provided with verniers or micrometer hand wheels allowing the angles to be read to 0.05°, with estimation possible to 0.01°. The scales should be arranged and illuminated so that readings can be taken by day and night. Backlash in the gearing of the circles should not exceed 0.025°. Errors in horizontal and vertical collimation should not exceed 0.1°.

The theodolite should be fitted with open sights to facilitate the tracking of a rapidly moving balloon. A secondary telescope with a wide field of view of no less than 8° is also useful for this purpose.

The base of the theodolite should be designed to fit into a standard tripod or other support and should incorporate some means of adjustment to allow accurate levelling. It should be possible to adjust the supports to suit the height of the observer. The theodolite should be of robust construction and should be protected against corrosion.

The system should be used with a suitable computer programme for inputting and checking the observational data for errors.

13.2.2 Radiotheodolite

Radiotheodolite windfinding is best suited to situations where the balloon elevations from the ground station remain high throughout the flight. If the balloon elevations remain above about 16°, most of the upper-wind accuracy requirements in Part I, Chapter 12, can be met with relatively small tracking aerials. At low balloon elevations, the measurement errors with radiotheodolites increase rapidly with decreasing elevation, even with larger tracking aerials (see section 13.5.3). It is extremely difficult to satisfy the accuracy requirements of Part I, Chapter 12, with a radiotheodolite if upper winds are consistently very strong, unless a transponder is used to provide a measurement of the slant range (see section 13.2.3.2).

A radiotheodolite is usually used to track the emissions from a radiosonde suspended beneath a weather balloon. A directional aerial coupled to a radio receiver is rotated around the vertical and horizontal axes to determine maximum signal strength using suitable servo-mechanisms. The radio frequency employed is usually 1 680 MHz. A good aerial design with a diameter of about 2 m should have low sensitivity in its side lobes relative to the main beam; with this size, angular tracking of 0.1° accuracy can be achieved. If this is the case, the radiotheodolite should be able to track at elevations as low as 6° to 10° without interference between signals received directly from the radiosondes and those received by reflection from adjacent surfaces. Interference between direct and reflected signals is termed multipath interference and is usually the limiting factor in radiotheodolite tracking capability at low elevations. The amount of multipath interference depends very critically on the positioning of the antenna relative to adjacent reflecting surfaces, whether the radiotheodolite is positioned on a roof or on the ground.

Detailed descriptions of the radiotheodolite aerial performance, detection system, servo-controls, and data-processing algorithms should be obtained from the manufacturer prior to purchase. Modern portable radiotheodolites with aerial dimensions of less than 2 m can encounter multipath interference problems at elevations as high as 16°. When multipath

interference occurs, the maximum signal will not usually be found in the direction of the balloon. The elevation error varies with time as the multi-path interference conditions change as the radiosonde moves; this can lead to large systematic errors in wind data (greater than 10 m s^{-1}).

While the radiotheodolite is tracking the radiosonde, the observed azimuth and elevation angles are transmitted from the radiotheodolite to the ground system computer. The incoming radiosonde measurements give, with time, the variation of geopotential height corresponding to the observed directions. The rates for the change in the position of the balloon can then be derived. The computer should display the upper-wind measurements in tabular or graphical form. The continuity of winds in the vertical will allow the operator to check for faulty tracking. Once the operator is satisfied that tracking is adequate, a suitable upper-wind report can be issued to users.

Balloons will sometimes reverse direction shortly after launch because of marked wind shear just above the surface. The balloon will fly back over the radiotheodolite even though it is launched so that it should move away from the radiotheodolite. If the radiotheodolite is to sustain accurate automated tracking when this happens, it must be capable of very high scan rates in azimuth and elevation. This leads to a more demanding mechanical specification than is necessary for the majority of the flights when the balloon is at longer ranges. In order to reduce the mechanical specification needed for accurate tracking, several modern radiotheodolite designs incorporate interferometric tracking. In these systems, the interferometer compares the phase of the signals arriving at different sections of its tracking aerial in order to determine the position of the transmitting source relative to the aerial orientation. In practice, the phase data are sampled at a high rate using microprocessors, while a simple servo-mechanism orientates the aerial approximately in the direction of the radiosonde. The approximate orientation of the aerial is necessary to provide a good signal-to-noise ratio for the interferometer and to minimize the reflections received from the ground. The elevation and azimuth are then derived from a combination of aerial positions, while the direction to the source is deduced by the interferometer from the phase measurements. The measurement accuracy achieved is similar to that of the better standard radiotheodolites. The interferometric radiotheodolite systems are often more reliable and cheaper to maintain.

13.2.3 Radar

13.2.3.1 *Primary radars*

The essential feature of the radar-tracking technique compared to the radiotheodolite method is that slant range is measured directly together with azimuth and elevation. A primary radar relies on the detection of pulses of ultra-short radio waves reflected from a suitable target carried by the balloon. With a reliable primary radar, the accuracy requirements for upper winds outlined in Part I, Chapter 12, can be met in almost all circumstances. Very high-accuracy specifications for upper winds can be met with high-precision tracking radars, but in practice these are very expensive to use. For measurement accuracy better than about 1 m s^{-1} it is essential to use balloons with sculptured surfaces (which are also very expensive) rather than standard meteorological balloons.

A radiosonde does not have to be used in order to determine winds with a primary radar, a suitable reflector is enough. Substantial savings from minimizing expenditure on radiosondes might be possible as long as there is a technical support structure to maintain the radar and staff costs are very low. However, the use of primary radar as a windfinding tool to provide cheap operational measurements has not been successful in developing countries, with equipment rarely being maintained; in most countries, GPS radiosondes or radiotheodolites are now used.

13.2.3.2 *Secondary radars*

In secondary radar systems, pulses of energy transmitted from the ground station are received by a responder system carried by the balloon. This can either be a separate transponder package or a feature that is incorporated in the basic radiosonde design. The frequency of the return signal

does not necessarily have to be the same as that of the outgoing signal. The time taken between the transmission of the pulse and the response from the responder allows the slant range to be measured directly. This type of system is still in widespread use in large national networks.

The advantage of this technique over a primary radar is that tracking can be sustained to longer ranges for a given power output from the ground transmitter. This is because the energy transmitted by the responder is independent and usually larger than the energy received from the ground transmitter. Thus, the energy received at the ground receiver is inversely proportional to the square of the slant range of the target. The energy received is inversely proportional to the fourth power of the slant range in the case of a primary radar.

The complexity of the system and the maintenance requirements of a secondary radar system usually fall between that of radiotheodolites and primary radars. The network managers must be able to ensure that the systems are well maintained. For instance, in the Russian Federation some older systems (see Table 13.4) of good tracking performance and which are in widespread use but difficult to maintain are now being replaced by improved ground tracking systems, which are relatively easy to maintain (see WMO, 2005).

13.2.4 Navaid tracking systems

In navaid tracking systems, the radiosonde incorporates an aerial system which receives the signals from a radionavigation system. This radionavigation system will be operated by agencies independent of the national weather Services. The navaid systems currently used operationally for windfinding are the satellite-based GPS giving global coverage, and LORAN systems using ground-based transmitters with very limited area of coverage.

One of the main advantages of navaid systems is the simplicity of the ground system, which does not consist of moving parts and does not need very accurate alignment of tracking aerials. This makes the systems suitable for deployment from aircraft and ships, as well as from land-based sites.

In order to keep the costs of signal processing in the radiosonde to a minimum, the majority of the processing to produce wind measurements from LORAN signals is performed after the radiosonde has relayed the navaid signals back to the ground system. Thus, good reception from the radiosonde is essential for this windfinding system; the siting of the ground system aerials must provide a good line of sight to the radiosondes in all directions. As the cost of GPS engines which process the GPS signals reduces, it is possible to perform much of the processing of the GPS signals on the radiosonde, although some processing on the ground is required to incorporate the information from the GPS reference signals received by a local ground-based antenna. In normal operation, the accuracy of GPS radiosonde position measurements does not reduce significantly with range from the ground stations (see WMO, 2011*b*).

The main operational problems with modern operational GPS radiosondes have been when there are radio transmitters in the vicinity at frequencies which cause interference to the reception of GPS signals by the radiosonde.

Height is assigned to upper-wind measurements using the radiosonde geopotential height measurements. It is vital that time stamping of the processed navaid wind data by the ground system is accurately aligned with the time stamping of the radiosonde height measurements.

13.2.4.1 *Availability of navaid signals in the future*

International navigational operations have mainly moved to navigation using signals from the array of GPS navigational satellites orbiting the Earth. These satellite signals have largely replaced reliance on signals from fixed terrestrial transmitters. The other global satellite navigation service in operation is GLONASS, in the Russian Federation. BeiDou (COMPASS), in China, and Galileo, in Europe, are also in early stages of operation, in preparation for use as global services before 2020. A limited number of countries have chosen to persist with LORAN terrestrial navigational

systems for regional or national navigational networks. Navigation authorities must be consulted as to the future availability of signals before any long-term investment in a given system is considered.

Although the computation of winds using GPS navigation is more complex than with navaid signals from terrestrial transmitters because the satellites move continuously relative to the radiosondes, the development of the GPS radiosonde systems is now mature, and 11 commercial systems were thus able to be tested in Yangjiang, China (see WMO, 2011*b*). Very few designs had any significant problems, with most having adequate signal reception (signals from between five and eight satellites received at a given time) and suitable processing algorithms relating the GPS signals received by the radiosonde to the signals received by a reference antenna at the ground station.

13.2.4.2   *Global positioning system*

GPS radiosondes are now used at about half of the active global radiosonde network stations.

NAVSTAR GPS is a very high-accuracy radionavigation system based on radio signals transmitted from a constellation of 25 satellites orbiting the Earth in six planes. Each of the orbital planes intersects the Equator at a spacing of 60°, with the orbit planes inclined at 55° to the polar axis. An individual satellite orbits during a period of about 11 h and 58 min. The constellation of satellites is configured so that in any location worldwide a minimum of four satellites appear above the horizon at all times, but, in some situations, up to eight satellites may be visible from the ground.

The signals transmitted from the satellites are controlled by atomic frequency standards intended to provide a frequency stability of better than $1 \cdot 10^{-13}$. Each satellite transmits two unique pseudo-random digital ranging codes, along with other information including constellation almanac, ephemeris, UTC time and satellite performance. The ranging codes and system data are transmitted using biphase digital spread spectrum technology. The power level of the ranging code signals is –130 dBm, well below thermal background noise.

The following codes are taken into consideration:

(a)   The coarse acquisition code is transmitted on a carrier at 1 575.42 MHz. This is modulated by a satellite-specific pseudo-random noise code with a chipping rate of 1.023 MHz. This modulation effectively spreads the coarse acquisition spectrum width to 2 MHz;

(b)   The precision code may be replaced by a military controlled Y-code during periods when anti-spoofing is active. The precision code and system data are transmitted coherently on carriers L1 (1 575 MHz) and L2 (1 228 MHz).

The wavelengths of the GPS signals are very much shorter than for LORAN. The much smaller aerial used for receiving the GPS signals is positioned at the top of the radiosonde body and should be free of obstructions in all directions towards the horizon. The small aerial is better protected from the damaging effects of atmospheric electricity than LORAN aerials. Although the siting of the GPS aerial could cause a conflict with siting of the temperature sensor on the radiosonde, this has now been overcome in the designs available.

The GPS signals need to be pre-processed on the radiosonde to reduce the GPS information to signals that can be transmitted to the ground station on the radiosonde carrier frequency (either as analogue information, as used for LORAN, or as a digital data stream). The pre-processing can be carried out by a variety of techniques. Modern GPS radiosondes use the precision code in a differential mode. This requires simultaneous reception of the GPS signals by a receiver at the ground station as well as the receiver on the radiosonde. Accurate wind computations require signals from a minimum of four satellites. In a differential mode, the phase of the signals received at the radiosonde is referenced to those received at the ground station. This is especially

beneficial when the radiosonde is near the ground station, since location errors introduced by propagation delays from the spacecraft to the receivers or by anti-spoofing are similar in both receivers and can be eliminated to a large extent.

GPS tracking systems are able to track accurately at a very high sample rate (rates of a few seconds). Thus, it is possible to measure the modulation of apparent horizontal velocity when the radiosonde swings as a pendulum under the balloon during a period of about 10 to 15 s. Most of the small differences found between GPS radiosonde wind measurements in Yangjiang, China, resulted from the use of different algorithms to filter out the balloon motion, with the algorithm often tuned to suit a particular configuration of radiosonde suspension and not that used in the radiosonde comparison test (WMO, 2011*b*).

One of the practical considerations with GPS radiosondes is the time taken for the GPS tracker on the radiosonde to synchronize with the signals being received from the satellite. It is unwise to launch the radiosonde before this synchronization has been achieved. This may require placing the radiosonde outside for several minutes before launch or, alternatively, a method for transmitting GPS signals to the radiosonde at the location where it is being prepared.

13.2.4.3   *LORAN-C chains*

The LORAN-C system is a relatively long-range navaid operating in the low frequency band centred on 100 kHz (wavelength 3 km). Because its primary purpose was for marine navigation, particularly in coastal and continental shelf areas, LORAN-C coverage was provided only in certain parts of the world. These were mostly in maritime areas of the northern hemisphere. Some of the chains have been refurbished under new ownership to provide regional or national marine navigational networks.

A LORAN-C transmission consists of groups of eight or nine pulses of the 100 kHz carrier, each being some 150 μs in duration. Each chain of transmitters consists of one master station and two or more slaves. In principle, chain coherence is established by reference to the master transmission. Each slave transmits its groups of pulses at fixed intervals after the master, at a rate that is specific to a given chain. Typically this rate is once every 100 μs.

The LORAN-C signals propagate both as ground and sky waves reflected from the ionosphere. The ground waves are relatively stable in propagation. There are only very small phase corrections which are dependent on whether the signals are propagating across land or sea. The rate of change of the phase corrections as the radiosonde position changes is not usually large enough to affect wind measurement accuracy. Sky wave propagation is more variable since it depends on the position of the ionosphere and will change with time of day. Ground wave signals from the transmitter are much stronger than sky waves, but sky waves attenuate much less rapidly than ground waves. Thus, the best situation for LORAN-C windfinding is obtained when the signals received at the radiosonde from all the transmitters are dominated by ground waves. This can be achieved in parts of the LORAN-C service areas, but not at all locations within the theoretical coverage.

The LORAN-C radiosonde receives the signals through its own aerial and then modulates the radiosonde carrier frequency in order to transmit the signals to the radiosonde receiver. The LORAN tracker used to detect the times of arrival of the LORAN pulses should be able to differentiate between ground and sky wave signals to some extent. This is achieved by detecting the time of arrival from the leading sections of the pulses. Modern LORAN trackers are able to operate in cross-chain mode, so that signals from more than one LORAN chain can be used together. This facility is essential for good-quality wind measurements in many parts of the LORAN-C service areas. Winds are computed from the rates of change in the time of arrival differences between pairs of LORAN-C transmitters. The computations use all the reliable LORAN-C signals available, rather than a bare minimum of three.

The use of LORAN navigation for operational radiosondes is now very limited.

13.3 MEASUREMENT METHODS

13.3.1 General considerations concerning data processing

Modern tracking sensors can take readings much more frequently than at the 1 min intervals commonly used with earlier manual systems. The processing of the winds will normally be fully automated using an associated ground system computer. The upper winds will be archived and displayed by the operator for checking before the information is issued to users.

Thus, the sampling of tracking data is optimal at intervals of 10 s or less. Sampling should be at the highest rate considered useful from the tracking system. High sampling rates make it easier to control the quality of the data with automated algorithms. After editing, the tracking data can then be smoothed by statistical means and used to determine the variation in position with time, if required. The smoothing applied will determine the thickness of the atmospheric layer to which the upper-wind measurement applies. The smoothing will often be changed for different parts of the flight to account for the differing user requirements at different heights and the tracking limitations of the upper-wind system used. If measurement accuracy drops too low at higher levels, the vertical resolution of the measurement may have to be reduced below the optimum requirement to keep the wind measurement errors within acceptable limits.

Effective algorithms for editing and smoothing may use low-order polynomials (Acheson, 1970), or cubic splines (de Boor, 1978). Algorithms for computing winds from radar and radiotheodolite observations can be found in WMO (1986). In general, winds may either be derived from differentiating positions derived from the tracking data, or from the rates of change of the smoothed engineering variables from the tracking system (see Passi, 1978). Many modern systems use this latter technique, but the algorithms must then be able to cope with some singularities in the engineering variables, for instance when a balloon transits back over the tracking site at high elevation.

When the winds computed from the tracking data are displayed for checking, it is important to indicate those regions of the flight where tracking data were missing or judged too noisy for use. Some of the algorithms used for interpolation may not be very stable when there are gaps in the tracking data. It is important to differentiate between reliable measurements of vertical wind shear and shears that are artefacts of the automated data processing when tracking data are absent. Tracking data are often of poor quality early in a balloon ascent. If the upper-wind system is unable to produce a valid wind measurement shortly after launch, it is preferable to leave a gap in the reported winds until valid tracking data are obtained. This is because interpolation between the surface and the first levels of valid data often requires interpolation across layers of marked wind shear in the vertical. The automated algorithms rarely function adequately in these circumstances.

13.3.2 Pilot-balloon observations

The accurate levelling and orientation of the optical theodolite with respect to the true north are an essential preliminary to observing the azimuth and elevation of the moving balloon. Readings of azimuth and elevation should be taken at intervals of no less than 1 min. Azimuth angles should be read to the nearest tenth of a degree. In a pilot-balloon ascent, the elevation angles should be read to the nearest tenth of a degree whenever the angles are 15° or greater. It is necessary to measure elevation to the nearest 0.05° whenever the angles are less than 15°.

If a radiosonde ascent is being followed by optical theodolite, a higher upper-wind measurement accuracy can be achieved at lower elevations. Thus, the elevation angles should be read to the nearest tenth of a degree whenever the angles are greater than 20°, to the nearest 0.05° whenever the angles are 20° or less, but greater than 15°, and to the nearest 0.01° whenever the angles are 15° or less. Timing may be accomplished by either using a stop-watch or a single alarm clock which rings at the desired intervals.

In single-theodolite ascents, the evaluation of wind speed and direction involves the trigonometric computation of the minute-to-minute changes in the plane position of the balloon. This is best achieved by using suitable computer software.

If higher accuracy is required, the double-theodolite technique should be used. The baseline between the instruments should be at least 2 km long, preferably in a direction nearly at right angles to that of the wind prevailing at the time. Computations are simplified if the two tracking sites are at the same level. Communication between the two sites by radio or land-line should help to synchronize the observations from the two sites. Synchronization is essential if good measurement accuracy is to be achieved. Recording theodolites, with the readings logged electronically, will be helpful in improving the measurement accuracy achieved.

For multiple-theodolite tracking, alternative evaluation procedures can be used. The redundancy provided by all the tracking data allows improved measurement accuracy, but with the added complication that the calculations must be performed on a personal computer (see Lange, 1988; Passi, 1978).

13.3.3   **Observations using a directional aerial**

Windfinding systems that track using directional aerials require very careful installation and maintenance procedures. Every effort must be made to ensure the accuracy of elevation and azimuth measurements. This requires accurate levelling of the installation and careful maintenance to ensure that the orientation of the electrical axis of the aerial remains close to the mechanical axis. This may be checked by various methods, including tracking the position of local transmitters or targets of known position. Poor alignment of the azimuth has caused additional errors in wind measurement at many upper-air stations in recent years.

The calibration of the slant range of a primary radar may be checked against known stationary targets, if suitable targets exist. The tracking of the radar in general may be checked by comparing radar geopotential heights with simultaneous radiosonde measurements. The corrections to the radar height measurements for tracking errors introduced by atmospheric refraction are discussed in section 13.7.

The comparison of radar height measurements with GPS radiosonde geopotential heights may be used to identify radar tracking which fails to meet the standards. Furthermore, if the radar slant range measurements are known to be reliable, it is possible to identify small systematic biases in elevation by comparing radar heights with radiosonde heights as a function of the cotangent of elevation. The typical errors in GPS radiosonde geopotential heights were established for the most widely used radiosondes by WMO (2011*b*).

Both radar and radiotheodolite systems can encounter difficulties when attempting to follow a target at close ranges. This is because the signal strength received by a side lobe of the aerial may be strong enough to sustain automated tracking at short ranges; however, when tracking on a side lobe, the signal strength received will then drop rapidly after a few minutes and the target will apparently be lost. Following target loss, it may be difficult to recover tracking with some systems when low cloud, rain or fog is present at the launch site. Thus, it is necessary to have a method to check that the target is centred in the main beam early in flight. This check could be performed by the operator using a bore-sight, telescope or video camera aligned with the axis of the aerial. The tracking alignment is more difficult to check with an interferometric radiotheodolite, where the mechanical tracking of the radiotheodolite will not necessarily coincide exactly with the observed direction of travel of the balloon.

13.3.4   **Observations using radionavigation systems**

The development of observations using GPS winds was first reported by Call (WMO, 1994) and Kaisti (1995). These systems did not decode the GPS signals received, but they have now been superseded by GPS radiosondes that do decode the signals.

The geometry for using satellite navigation signals is such that GPS windfinding algorithms seem to work most reliably when signals are received from at least five satellites during the ascent. The GPS almanac can be used to identify times when satellite geometry is weak for windfinding. In practice, this rarely occurs with the current satellite configuration and the good satellite reception antenna used with modern radiosondes.

When making upper-wind measurements with navaid tracking systems, the ground system navaid tracker should be accurately synchronized to the navaid transmissions prior to launch. Synchronization is usually achieved by using signals received by a local aerial connected to the ground system receiver. This aerial should be capable of receiving adequate signals for synchronization in all the weather conditions experienced at the site. The ground system should provide clear indications to the operator of the navaid signals available for windfinding prior to launch and also during the radiosonde flight. Where the GPS radiosonde is being used to make height measurements for the operational ascent, it is essential that the height of the local GPS antenna relative to the surface is accurately determined and entered into the ground station processing software.

Once launched, the navaid windfinding systems are highly automated. However, estimates of the expected measurement errors based on the configuration and quality of the navaid signals received would be helpful to the operators. During flight, the operator must be able to identify faulty radiosondes with poor receiver or transmitter characteristics which are clearly providing below-standard observations. These observations need to be suppressed and a re-flight attempted, where necessary.

Satisfactory upper-wind measurements from LORAN radionavigation systems require the radiosonde to receive signals from at least three LORAN stations. The difference in the time of arrival of the navigation signals received by the radiosonde, after coherent transmission from two locations, defines a locus or line of position (see WMO, 1985). This will have the shape of a hyperbola on a plane (but becomes an ellipse on the surface of a sphere). Thus, navigational systems using this technique are termed hyperbolic systems. Two intersecting lines of position are sufficient to define plan positions. However, there may be a large error in position associated with a small error in time of arrival if the lines of position are close to parallel when they intersect. With LORAN navaid upper-wind systems, it has been clearly demonstrated that all available navaid signals of a given type (usually at least four or five) should be used to improve tracking reliability. One type of algorithm used to exploit all the navaid signals available was outlined in Karhunen (1983).

13.4   **EXPOSURE OF GROUND EQUIPMENT**

An appropriate site for a radiotheodolite or radar is on high ground, with the horizon being as free from obstructions as possible. There should be no extensive obstructions subtending an angle exceeding 6° at the observation point. An ideal site would be a symmetrical hill with a downward slope of about 6° for a distance of 400 m, in a hollow surrounded by hills rising to a 1° or 2° elevation.

The tracking system should be provided with a firm foundation on which the equipment can be mounted. Good reception of signals by a local navaid aerial and by the ground system aerial for the radiosonde is essential if the navaid measurements are to be successful. These aerials should be mounted in positions on the upper-air site where there is a good horizon for reception in all directions.

Upper-wind measurements are usually reported in association with surface-wind measurements. It is preferable that surface wind be obtained from a site close to the balloon launch site. The launch site should be chosen to provide winds that are appropriate to the purpose of the upper-wind measurement. For example, if the upper-wind measurement is required to detect a localized effect influencing an airfield, the optimum location might differ from a site needed to observe mesoscale and synoptic scale motions over a larger area.

13.5   **SOURCES OF ERROR**

13.5.1   **General**

Errors in upper-wind measurements are a combination of the errors resulting from imperfect tracking of the horizontal motion of the target, the errors in the height assigned to the target, and the differences between the movement of the target and the actual atmospheric motion.

13.5.1.1   *Target tracking errors*

The relationship between wind errors and tracking errors differs according to the method of observation. For some systems, such as radiotheodolites, the wind errors vary markedly with range, azimuth and elevation, even when the errors of these tracking parameters remain constant with time. On the other hand, wind errors from systems using navaid tracking do not usually vary too much with range or height.

The uncertainties caused by the manual computation of wind were evaluated in WMO (1975). It was concluded that the risks of introducing significant errors by using manual methods for wind computations (such as plotting tables, slide rules, etc.) were too great, and that upper-wind computations should be automated as far as possible.

The measurement accuracy of all upper-wind systems varies from time to time. This variation may occur for short periods during a given target flight, when tracking temporarily degrades, or during an entire flight, for instance if the transmitted signals from a navaid radiosonde are faulty. At some locations, the accuracy of upper-wind tracking may gradually degrade with time over several months because of either instability in the tracking capability or the set-up of the ground system. In all cases, it would be helpful if estimates of wind measurement accuracy were derived by the upper-wind systems in real time to supplement the reported upper-wind measurements. The reported errors would allow poorer quality measurements to be identified and less weight would be given in numerical analyses. The reporting of errors could be achieved in practice by using the appropriate TEMP or PILOT codes and BUFR tables (WMO, 2011*a*).

When errors in target tracking start to introduce unacceptable wind errors at a given vertical resolution, the situation is usually compensated by computing the winds at a lower vertical resolution.

The practice of reducing the vertical resolution of upper-wind measurements in steps through the upper troposphere and lower stratosphere was mainly adopted to overcome the tracking limitations of radiotheodolites. This practice is not justified by the actual vertical structure observed in the atmosphere. Many of the larger vertical wind shears are found in the upper levels of jet streams at heights between 10 and 18 km (see, for instance, the detailed vertical wind profiles presented in Nash, 1994).

13.5.1.2   *Height assignment errors*

Height assignment errors for rawinsonde winds in the troposphere and lower stratosphere will be the same as those discussed for height measurements in Part I, Chapter 12. These errors will be highest for radiosondes using pressure sensors in the upper stratosphere, and would be most significant for numerical weather prediction or climate studies if there were significant wind shear in the vertical, such as in the polar-night vortex (see Figure 13.1(b)).

For pilot balloons tracked with a single theodolite, height is derived from time into flight, and the rate of ascent for the balloon is assumed. In practice, it is difficult to launch balloons with a precisely determined rate of ascent. Thus, where there is significant vertical shear in the vertical at low levels, possibly associated with significant differences in vertical velocity from thermals, pilot-balloon measurements could be adversely affected by the height assignment errors.

Prototype testing of fully automated upper-wind systems often reveals discrepancies between the times assigned to wind observations and those assigned to the associated radiosonde measurements. In some cases, the wind timing is not initiated at the same time as that of the radiosonde, in others synchronization is lost during flight for a variety of reasons. Times assigned to the reported winds are not always those corresponding to the data sample used to compute the wind, but rather to the time at the beginning or end of the sample. All types of timing error could produce large errors in the heights assigned to wind measurements and need to be eliminated during prototype testing if reliable operations are to be achieved.

13.5.1.3 *Target motion relative to the atmosphere*

The motion of the target relative to the air matters most for systems with the highest tracking accuracy and highest vertical resolution. For instance, the swinging of the GPS radiosonde under a balloon is clearly visible in the GPS tracking measurements and must be filtered out as far as possible.

The balloon motion relative to the atmosphere, introduced by the shedding of vortices by the balloon wake, may result in errors as large as 1 to 2 m s^{-1} (2σ level) when tracking small pilot balloons (50 g weight) at vertical resolutions of 50 m. Balloon motion errors are less significant in routine operational measurements (vertical resolutions of about 300 m) where measurements are obtained by tracking larger balloons (weight exceeding 350 g).

The horizontal slip of the dropsonde parachutes relative to the atmosphere may also be the limiting factor in the accuracy of GPS dropsonde measurements. The descent rates used in dropsonde deployments are usually about twice the ascent rate of operational radiosonde balloons.

13.5.2 **Errors in pilot-balloon observations**

The instrumental errors of a good optical theodolite are not likely to exceed ±0.05°. The errors may vary slowly with azimuth or elevation but are small compared with the errors introduced by the observer. Errors of reading scales should not exceed 0.1°. These errors become increasingly important at long ranges and when working at low elevations.

In single-theodolite ascents, the largest source of error is the uncertainty in the balloon rate of ascent. This uncertainty arises from variations in filling the balloon with gas, in the shape of the balloon, and in the vertical velocity of the atmosphere through which the balloon ascends. A given proportional error in the rate of ascent results in a proportional error in the height of the balloon and, hence, as modified by elevation angle, a proportional error in wind speed.

In double-theodolite ascents, the effect of system errors depends upon the method of evaluation adopted. Error analyses have been provided by Schaefer and Doswell (1978).

13.5.3 **Errors of systems using a directional aerial**

The relationship between vector wind errors and the errors of the actual tracking measurements can be expressed as an approximate function of height and mean wind (or ratio of the latter to the mean rate of ascent of the balloon). The relationships for random errors in primary radar and radiotheodolite wind measurements are as follows:

(a) Primary or secondary radar measuring slant range, azimuth and elevation:

$$\varepsilon_v^2 = 2 \cdot \left[\varepsilon_r^2 \cdot Q^2 \Big/ \left(Q^2 + 1 \right) + \varepsilon_\theta^2 \cdot h^2 + \varepsilon_\varphi^2 \cdot h^2 \cdot Q^2 \right] \Big/ \tau^2 \tag{13.3}$$

(b)   Optical theodolite or radiotheodolite and radiosonde measuring azimuth, elevation angle
       and height:

$$\varepsilon_v{}^2 = 2 \cdot \left[\varepsilon_h{}^2 \cdot Q^2 + \varepsilon_\theta{}^2 \cdot h^2 \cdot \left(Q^2 + 1 \right)^2 + \varepsilon_\varphi{}^2 \cdot h^2 \cdot Q^2 \right] \Big/ \tau^2 \qquad (13.4)$$

where ε_v is the vector error in computed wind; ε_r is the random error in the measurement of slant range; ε_θ is the random error in the measurement of elevation angle; ε_φ is the random error in the measurement of azimuth; ε_h is the random error in height (derived from pressure measurement); Q is the magnitude of mean vector wind up to height h divided by the mean rate of ascent of the balloon up to height h; and τ is the time interval between samples.

Table 13.2 illustrates the differences in vector wind accuracy obtained with these two methods of upper-wind measurement. The mean rate of ascent used in upper-wind measurements will usually be in the range of 5 to 8 m s^{-1}. The vector wind error values are derived from equations 13.3 and 13.4 for various heights and values of Q, for a system tracking with the following characteristics: ε_r 20 m; ε_θ 0.1°; ε_φ 0.1°; ε_h height error equivalent to a pressure error of 1 hPa; τ 1 min.

Table 13.2 demonstrates that measurements with a radio (or optical) theodolite clearly produce less accurate winds for a given tracking accuracy than primary or secondary radars.

In the expressions for vector error in the computed winds in equations 13.3 and 13.4, the first two terms within the square brackets represent the radial error and the error in the winds observed with the same azimuth as the tracking aerial. The third term in the square brackets represents the tangential error, the error in winds observed at right angles to the azimuth of the tracking aerial. With these types of upper-wind systems, the error distribution is not independent of the directions and cannot be adequately represented by a single parameter. Thus, the values in Table 13.2 indicate the size of the errors but not the direction in which they act.

When the tangential and radial errors are very different in size, the error distribution is highly elliptic and the combined errors tend to concentrate either parallel to the axis of the tracking antenna or perpendicular to the axis. Table 13.3 shows the ratio of some of the tangential and radial errors that are combined to give the vector errors in Table 13.2. Values above 3 in Table 13.3 indicate situations where the tangential error component dominates. Thus, in radar windfinding, the tangential errors dominate at longer ranges (high mean winds and hence high Q values, plus largest heights). With radiotheodolite windfinding, the radial errors dominate at longer ranges

Table 13.2. 90% vector error (m s^{-1}) as a function of height and ratio Q of mean wind to rate of ascent

	Radar						Radiotheodolite					
Q	ε_v 5 km	ε_v 10 km	ε_v 15 km	ε_v 20 km	ε_v 25 km	ε_v 30 km	ε_v 5 km	ε_v 10 km	ε_v 15 km	ε_v 20 km	ε_v 25 km	ε_v 30 km
1	1	1	1.5	1.5	2.5	2.5	1	1.5	3	5.5	9	25
2	1	1.5	2.5	3	4	4	5	4	6.5	11	19	49
3	1.5	2.5	3	4	5	6	4	7	11	19	30	76
5	1.5	3	5	6	8	10	9	18	27	42	59	131
7	2.5	5	7	9	11	13	18	34	51	72	100	194
10	3	6.5	10	13	16	19	34	67	100	139	182	310

Notes:
a   This table does not include the additional errors introduced by multipath interference on radiotheodolite observations. Additional errors can be expected from these effects for values of Q between 7 and 10.
b   In practice, radiotheodolite wind observations are smoothed over thicker layers than indicated in these calculations at all heights apart from 5 km. Thus, at heights of 15 km and above, the radiotheodolite errors should be divided by at least a factor of four to correspond to operational practice.

Table 13.3. Ratio of upper-wind error components (α_v = tangential error/radial error α)

	Radar						Radiotheodolite					
Q	α_v 5 km	α_v 10 km	α_v 15 km	α_v 20 km	α_v 25 km	α_v 30 km	α_v 5 km	α_v 10 km	α_v 15 km	α_v 20 km	α_v 25 km	α_v 30 km
1	1/2	1	1	1	1	1	1/3	1/2	1/3	1/4	1/5	1/13
2	1	1	2	2	2	2	1/3	1/3	1/3	1/4	1/6	1/13
3	1	2	2	3	3	3	1/4	1/4	1/4	1/5	1/6	1/13
5	1	3	4	4	5	5	1/5	1/5	1/6	1/6	1/7	1/14
7	3	5	5	6	6	7	1/7	1/7	1/7	1/7	1/9	1/14
10	4	7	8	9	9	9	1/10	1/10	1/10	1/11	1/11	1/16

and the ratios become very much smaller than 1. Errors in elevation angle produce the major contribution to the radiotheodolite radial errors. However, random errors in the radiosonde height make the most significant contribution at high altitudes when values of Q are low.

The results in Tables 13.2 and 13.3 are based on a theoretical evaluation of the errors from the different types of systems. However, it is assumed that winds are computed from a simple difference between two discrete samples of tracking data. The computations take no account of the probable improvements in accuracy from deriving rates of change of position from large samples of tracking information obtained at high temporal resolution. Table 13.4 contains estimates of the actual measurement accuracy achieved by a variety of radars and radiotheodolites in the four phases of the WMO International Radiosonde Comparison (see section 13.6.1.2 for references to the tests).

Table 13.4. Estimates of the typical random vector errors (2σ level, unit: m s⁻¹) in upper-wind measurements obtained during the WMO International Radiosonde Comparison (estimates of typical values of Q and α_v for each of the four phases are included)

System	ε_v 3 km	α_v 3 km	Q 3 km	ε_v 18 km	α_v 18 km	Q 18 km	ε_v 28 km	α_v 28 km	Q 28 km	Test site
Primary radar (United Kingdom)	1.1	1	3.5	2.1	1.3	5	2.7	1.6	5	United Kingdom[a]
Radiotheodolite (United States)	2.1	≈ 1	1.5	4.8	≈ 1	2.5	5.2	≈ 1	1	United Kingdom
Radiotheodolite (United States)	2.8	≈ 1	2.5	10.4	0.4	6	9	0.33	4	United States
Radiotheodolite, portable	1.5	≈ 1	< 1	4.8	≈ 1	3	5.8	≈ 1	1.5	Kazakhstan
Radiotheodolite, portable	2.2	≈ 1	1.5	12	0.31	5.5	9	0.23	4	Japan
Radiotheodolite (Japan)	1.7	≈ 1	1.5	6.4	0.48	5.5	4.7	0.48	4	Japan
Secondary radar (AVK, Russian Federation)	1.5	≈ 1	< 1	2.6	≈ 1	3	2.6	≈ 1	1.5	Kazakhstan
Secondary radar (China)	1.5	≈ 1	< 1	3.8	≈ 1	3	3.4	≈ 1	1.5	Kazakhstan

Note:
a   Data obtained in the United Kingdom test following Phase I of the WMO International Radiosonde Comparison (See Edge et al., 1986)

Of the three radiotheodolites tested in the WMO International Radiosonde Comparison, the Japanese system coped best with high Q situations, but this system applied a large amount of smoothing to elevation measurements and did not measure vertical wind very accurately in the upper layers of the jet streams. The smaller portable radiotheodolite deployed by the United States in Japan had the largest wind errors at high Q because of problems with multipath interference.

The ellipticity of the error distributions for radar and radiotheodolite observations showed the tendencies predicted at high values of Q. However, the ellipticity in the errors was not as high as that shown in Table 13.3, probably because the random errors in the rates of change of the azimuth and elevation were, in practice, smaller than those taken for Table 13.3.

In the WMO Intercomparison of High Quality Radiosonde Systems in Yangjiang, China (WMO, 2011b), China used a modern secondary radar operating at 1 680 MHz with the Daqiao radiosonde system. When winds were strong in the lower troposphere, values of Q at a height of about 4 km were between 2 and 3, range was about 15 km, and the root-mean-square (RMS) vector errors ($k = 2$) in the winds were about 1 to 1.2 m s^{-1} with an ellipticity between 1 and 1.3. Towards the ends of the flights in the stratosphere, Q was again about 2.5 on average, but at the longer ranges of 70 to 100 km, ε_v for $k = 2$ was about 2.7 m s^{-1} and the ellipticity was 2. The reference winds in Yangjiang were GPS winds at a high vertical resolution, better than 150 m, whereas the vertical resolution of the working reference in Kazakhstan was 300 m at the best. Thus, the modern Chinese secondary radar was working well and is an improvement on the previous 403 MHz system.

13.5.4 Errors in the global positioning system windfinding systems

In theory, GPS windfinding systems using coarse acquisition ranging codes in a differential mode should be capable of measuring winds to an uncertainty of 0.2 m s^{-1}. The estimates of accuracy in Table 13.5 were made on the basis of recent WMO tests of GPS radiosondes. The main difference between systems comes from the filtering applied to the winds to remove the motion of the radiosonde relative to the balloon. This motion is partly a regular pendulum of the radiosondes under the balloon, and partly some additional irregular rotation and displacement in reaction to differences between the winds experienced by the balloon and the radiosonde as the balloon ascent progresses.

Examples of simultaneous observations of winds obtained in the upper troposphere from the GPS radiosondes in the WMO Intercomparison of High Quality Radiosonde Systems are shown in Figure 13.2. Only excerpts from the flights are shown because it is only when looking at a short sample of data from the flights that the differences can be seen, as the general agreement is much better than what the standard has been for earlier operational wind measurements.

The extracts in Figure 13.2 show that nearly all the systems agree well in resolving vertical structure with peaks in the wave structures separated by about 90 s, but not to the same extent for fluctuations where the peaks were separated by 40 s or less. Thus, the vertical wavelengths that generally resolved without any ambiguity were 600 m, but those where there was considerable ambiguity corresponded to 200 m or less. One system in Figure 13.2(a) was over-smoothed compared to the others, while one system in Figure 13.2(b) attempted to fit straight lines to the GPS measurements; both behaviours lead to outliers from the correct values on occasion.

These extracts, representing neither the best nor the worst, suggest that the processing of GPS wind measurements is relatively mature and that a large number of manufacturers have achieved satisfactory results. This was confirmed when the statistics from the 60 flights performed with operational GPS radiosondes in Yangjiang were generated (see Table 13.5). In this table, the wind differences (obtained from about 30 comparison flights) were averaged over either 2 min, 30 s or 10 s, and the best performance was attributed to the two systems with the lowest RMS vector differences. The errors found in Table 13.5 are good enough to meet the optimum user requirement for winds stated in Part I, Chapter 12, Annex 12.A.
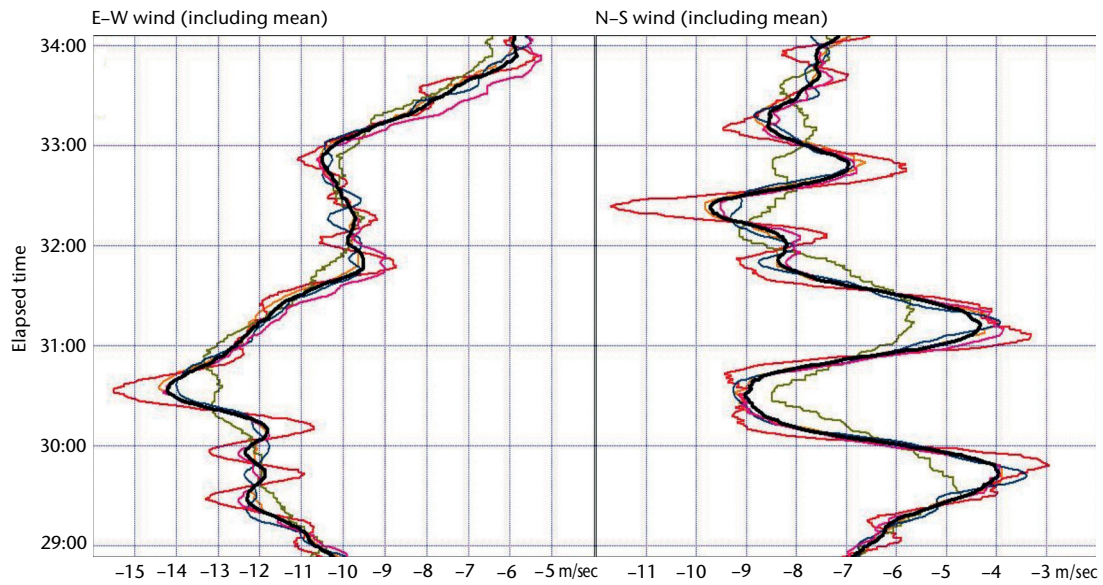
(a)   Flight 33: Jinyang, InterMet, Lockheed Martin Sippican, MODEM and Vaisala
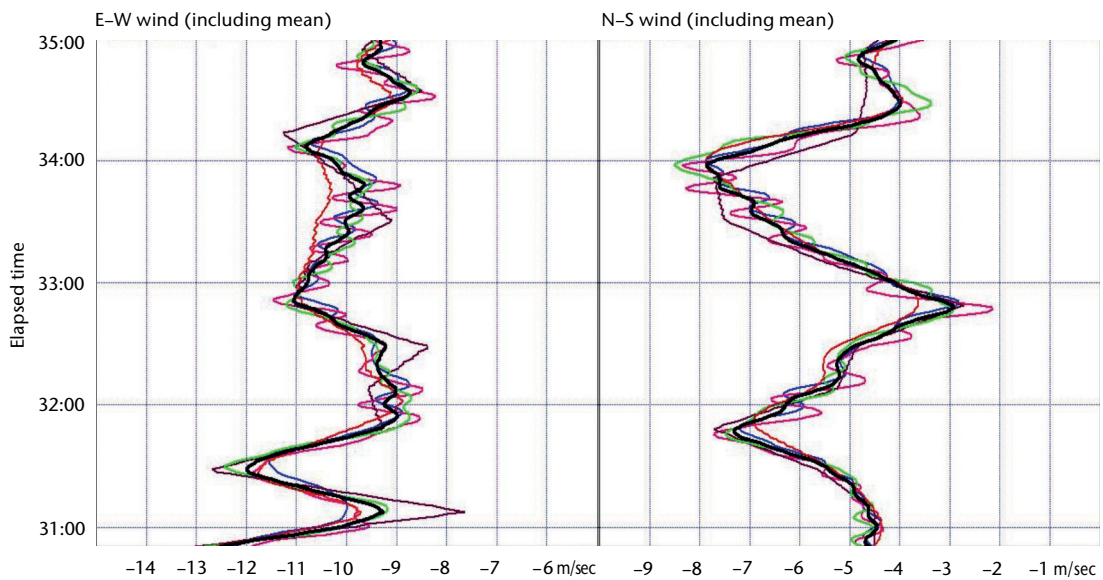
(b)   Flight 34: Changfeng, Graw, Huayun, Meisei and Meteolabor

Figure 13.2. Extracts from intercomparison flights of GPS winds made at Yangjiang, China, during the WMO Intercomparison of High Quality Radiosonde Systems (WMO, 2011*b*)

In time, the differences in the filtering of the GPS position measurements to minimize the effects of the radiosonde measurements relative to the balloon will probably reduce compared to the ranges indicated in Table 13.5. However, the irregular movements (as opposed to the relatively smooth pendulum motion) of the radiosonde relative to the balloon will limit the agreement that can be obtained between two radiosondes in a test flight. For the same reason, the error in an individual radiosonde measurement can be expected to be larger than might be computed given the expected accuracy of radiosonde position that can be obtained with the satellite radionavigation systems.

The external balloon of the double balloons used in China often burst near 16 km, and the resulting perturbations on the stability of the radiosonde motion may have led to the largest RMS vector errors near 16 km in Table 13.5. In UK tests (60 flights), conducted over several seasons in 2009/2010 on GPS radiosondes from two different manufacturers present in Yangjiang, results in the lower troposphere and the stratosphere were similar to those in Table 13.5. However, RMS

vector wind errors in the upper troposphere were in the range 0.3 to 0.6 m s^{-1} at a vertical resolution of 100 m, and 0.2 to 0.5 m s^{-1} at a vertical resolution of 300 m. Thus, for these two systems the fine structure in the wind measurements in the United Kingdom in the upper troposphere agreed more closely than for the systems in Yangjiang.

On occasion, a GPS radiosonde malfunctions and does not report winds throughout a flight when reporting temperature and humidity until the balloon bursts. On some occasions, radio-frequency interference from an external source causes problems, and winds may have larger errors. The processing software needs to be able to inform the operator when problems like these are present, as it is difficult to distinguish between real atmospheric structure and measurements with large random errors (for example, see the wind profile in Figure 13.3).

Unlike the ground-based LORAN-C, the performance of the GPS winds will not vary significantly with conditions in the ionosphere.
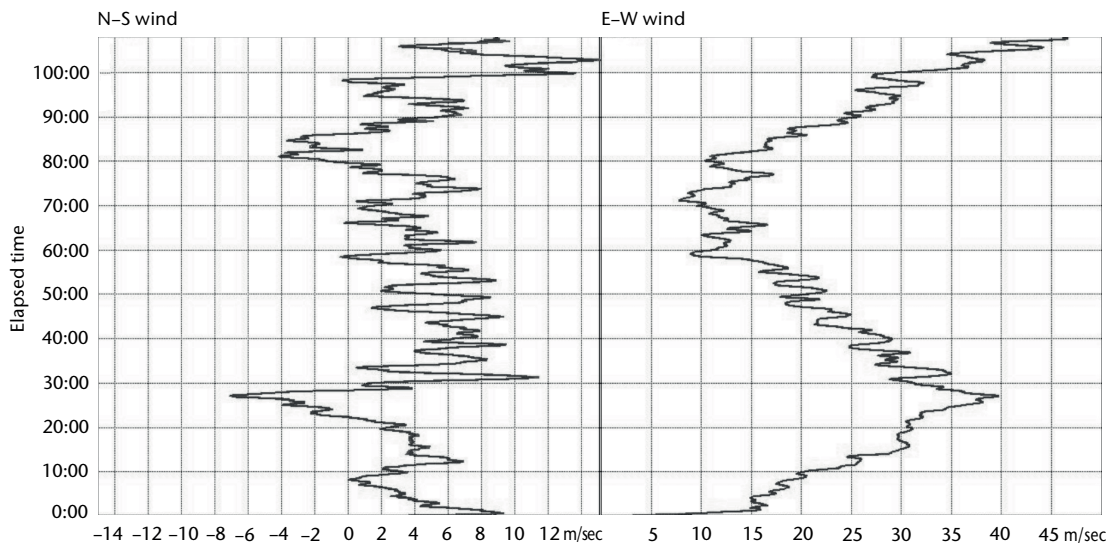
Figure 13.3. Example of a vertical wind profile measured independently by GPS radiosondes from two different manufacturers at Camborne, United Kingdom, and showing the small-scale structure which is present in many correct measurements. The radiosonde processing software needs to indicate which parts of a flight are less reliable when the reception of GPS signals is clearly not as reliable as usual.

Table 13.5. Random vector error ($k = 2$) and systematic bias for good quality GPS navaid windfinding systems during the WMO Intercomparison of High Quality Radiosonde Systems in Yangjiang, China

Height range	Systematic bias (m s^{-1})	RMS vector error at 2 km vertical resolution (m s^{-1})	RMS vector error at 300 m vertical resolution (m s^{-1})	RMS vector error at 100 m vertical resolution (m s^{-1})
Lower troposphere 0–8 km	Up to ±0.05	0.06 – 0.15	0.12 – 0.50	0.3 – 0.7
Upper troposphere 8–17 km	Up to ±0.10	0.1 – 0.4[a]	0.3 – 0.9[a]	0.4 – 1.4[a]
Stratosphere 17–34 km	Up to ±0.15	0.15 – 0.40[b]	0.3 – 0.8[b]	0.4 – 1.1[b]

Notes:
a Poorest performance found at heights near 16 km
b Poorest performance found at heights greater than 28 km

13.5.5 Errors in ground-based LORAN-C radionavigation systems

Navaid system errors depend on the phase stability of navaid signals received at the radiosonde and upon the position of the radiosonde relative to the navaid network transmitters. However, the quality of the telemetry link between the radiosonde and the ground receiver cannot be ignored. In tests where radiosondes have moved out to longer ranges (at least 50 to 100 km), wind errors from the navaid windfinding systems are found to increase at the longer ranges, but usually at a rate similar to or less than the increase with the range for a primary radar. Signal reception from a radiosonde immediately after launch is not always reliable. LORAN-C wind measurements have larger errors immediately after launch than when the radiosonde has settled down to a stable motion several minutes into flight.

LORAN-C navaid wind measurement accuracy is mainly limited by the signal-to-noise ratios in the signals received at the radiosonde. Integration times used in practice to achieve reliable windfinding vary from 30 s to 2 min for LORAN-C signals. Signal strength received at a given location from some LORAN-C transmitters may fluctuate significantly during the day. This is usually because, under some circumstances, the diurnal variations in the height and orientation of the ionospheric layers have a major influence on signal strength. The fluctuations in signal strength and stability can be so large that successful wind measurement with LORAN-C may not be possible at all times of the day.

A second major influence on LORAN-C measurement accuracy is the geometric dilution of precision of the navigation system accuracy, which depends on the location of the radiosonde receiver relative to the navaid transmitters. When the radiosonde is near the centre of the baseline between the two transmitters, a given random error in the time of arrival difference from two transmitters will result in a small random positional error in a direction that is parallel to the baseline between the transmitters. However, the same random error in the time of arrival difference will produce a very large positional error in the same direction if the radiosonde is located on the extension of the baseline beyond either transmitter. The highest accuracy for horizontal wind measurements in two dimensions requires at least two pairs of navaid transmitters with their baselines being approximately at right angles, with the radiosonde located towards the centre of the triangle defined by the three transmitters. In practice, signals from more than two pairs of navaid transmitters are used to improve wind measurement accuracy whenever possible. Techniques using least squares solutions to determine the consistency of the wind measurements obtained prove useful in determining estimates of the wind errors.

Disturbance in the propagation of the signals from the navaid network transmitters is another source of error.

Passi and Morel (1987) performed an early study on LORAN wind errors. Commercially available systems could produce wind data of good quality, as illustrated in Table 13.6. The measurement quality obtained when working with mainly ground-wave signals was derived from installation tests in the British Isles as reported by Nash and Oakley (1992). The measurement quality obtained when working with transmitters at longer ranges, where sky waves are significant, was estimated from the results of Phase IV of the WMO International Radiosonde Comparison in Japan (see WMO, 1996). In the United Kingdom, LORAN-C windfinding was discontinued because of uncertainty about the future of LORAN-C in north-west Europe and was replaced by GPS windfinding at all operational sites.

Table 13.6. Random error ($k = 2$) and systematic bias expected from LORAN-C navaid windfinding systems in areas where the coverage is close to optimum

System	Averaging time (s)	Systematic bias (m s^{-1})	Random error (m s^{-1})
LORAN-C (ground wave)	30 – 60	Up to ±0.2	0.6 – 3
LORAN-C (sky wave)	60 – 120	Up to ±0.2	1.6 – 4

13.5.6   **Representativeness errors**

Most modern radiowind measurements observe small-scale variations in wind in the atmosphere which are not represented in current numerical weather prediction models. Thus, for instance, when GPS wind component profiles are compared directly with numerical model output from global models, the standard deviation of observation/numerical model output ($k = 2$) in mid-latitudes is usually between 4 and 6 m s^{-1} in the lower troposphere, and between 4 and 9 m s^{-1} in the upper troposphere, that is, it is always much larger than the instrumental vector errors quoted in Table 13.5 for a vertical resolution of 300 m. Some of this discrepancy will result from the poor accuracy of the reported winds as noted earlier in section 13.1.3.2.

Root-mean-square vector differences between radiosonde upper-wind measurements 2, 6, 18 and 54 h apart have been computed from the time series of measurements produced in the WMO Intercomparison of High Quality Radiosonde Systems in Yangjiang, China (WMO, 2011b), applying the technique used by Kitchen (1989). The results are shown as a function of height in Figure 13.4.

The RMS vector error in wind can then be expected to relate to time separation using the relationship, after Kitchen (1989):

$$\left(\tau_{\mathrm{v}}\left(\Delta t\right)\right)^2 = \left(b_{\mathrm{v}}\Delta t^{\gamma}\right)^2 + \left(\tau_{\mathrm{v(small\ scale)}}\left(\Delta t\right)\right)^2 \tag{13.5}$$

where $\tau_{\mathrm{v}}(\Delta t)$ is the RMS vector difference between wind measurements separated by the time separation Δt; and $b_{\mathrm{v}}\Delta t^{\gamma}$ is the structure function representing the RMS deviation due to synoptic scale and mesoscale changes with time, with b_{v} a constant and γ a constant. In Yangjiang, γ had a value of between 0.5 and 0.6 for wind measurements in the troposphere at time separations between 6 and 54 h. Finally, $\tau_{\mathrm{v(small\ scale)}}(\Delta t)$ is the RMS vector difference in upper wind from small-scale structures, such as quasi-inertial gravity waves, turbulent layers or cloud-scale structure.

In the troposphere in Yangjiang, the small-scale structure RMS vector difference was about 2 m s^{-1} ± 0.5 m s^{-1}, while the synoptic and mesoscale RMS vector difference was between
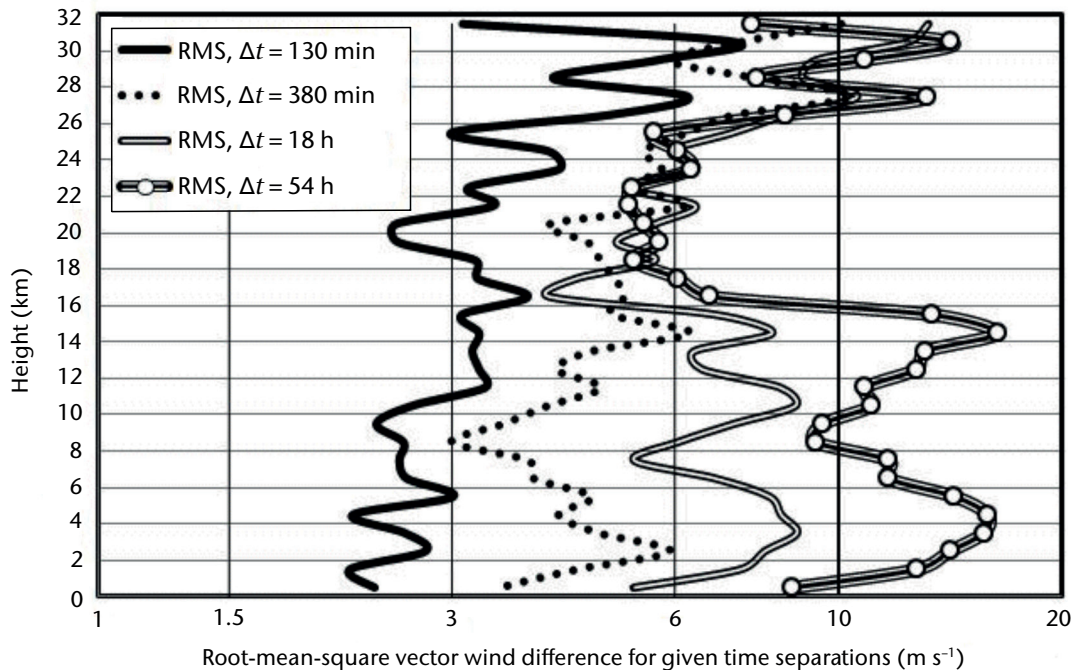
Figure 13.4. Root-mean-square vector wind differences ($k = 1$) for time separations of 2, 6, 18 and 54 h for 11 pairs of observations, with vertical resolution of 1 km, from the WMO Intercomparison of High Quality Radiosonde Systems in Yangjiang, China, in July 2010. The contributions from instrumental error have been removed from the differences.

2 and 3 m s^{-1} at a time separation of 2 h, increasing to about 7 m s^{-1} at a time separation of 18 h. These values are of similar magnitude to the values found by Kitchen (1989) in the lower and middle troposphere in the United Kingdom. The RMS vector differences were higher in the upper troposphere in the United Kingdom because of the synoptic scale variations associated with mid-latitude jet streams. Whereas the synoptic and mesoscale vector difference might be expected to fall to lower than 1 m s^{-1} at a time separation of 40 min in Yangjiang, there is no information on the time separations necessary to reduce the small-scale RMS vector difference to a value less than 1 m s^{-1}. This is why, to get close agreement between wind measurements, or for the measurement to represent the conditions in the atmosphere at a given time with high accuracy, the measurement needs to be performed at a time separation much lower than 20 min, as stated in section 13.1.3.3.

In Yangjiang, the small-scale fluctuations associated with quasi-inertial gravity waves dominate the variation of RMS vector difference with time, and it is not possible to fit a structure function for synoptic and mesoscale variation with time, as was also found in the United Kingdom in summertime conditions by Kitchen. The RMS vector differences at 18-hour time separation in Yangjiang were in the range 5 to 9 m s^{-1}, values of similar magnitude to those found in the United Kingdom.

Thus, representativeness errors in the winds will normally be most influenced by the small-scale variations, with synoptic and mesoscale variations most likely to be significant in association with the structures found with jet streams in the upper troposphere and lower stratosphere. As a result, there will be variation between different sites, and the values discussed here are only a snapshot of one type of location and synoptic condition, which did include measurements with typhoons approaching and leaving the area.

13.6   COMPARISON, CALIBRATION AND MAINTENANCE

13.6.1   Comparison

Upper-wind systems are usually fairly complex, with a number of different failure modes. It is not uncommon for the systems to suffer a partial failure, while still producing a vertical wind structure that appears plausible to the operators. Many of the systems need careful alignment and maintenance to maintain tracking accuracy.

The wind measurement accuracy of operational systems can be checked by reference to observation monitoring statistics produced by numerical weather prediction centres. The monitoring statistics consist of summaries of the differences between the upper-wind measurements from each site and the short-term forecast (background) fields for the same location. With current data assimilation and analysis techniques, observation errors influence the meteorological analysis fields to some extent. Thus, it has been shown that observation errors are detected most reliably by using a short-term forecast from an analysis performed 6 h before the observation time.

The performance of upper-wind systems can also be compared with other systems of known measurement quality in special tests. These tests can allow tracking errors to be evaluated independently of height assignment errors.

Both types of comparisons may be interpreted using the statistical methods proposed in WMO (1989).

13.6.1.1   *Operational monitoring by comparison with forecast fields*

The statistics for daily comparisons between operational wind measurements and short-term forecast fields of numerical weather prediction models can be made available to system operators through the lead centres designated by the WMO Commission for Basic Systems.

Interpretation of the monitoring statistics for upper winds is not straightforward. The random errors in the forecast fields are of similar magnitude or larger than those in the upper-wind system if it is functioning correctly. The forecast errors vary with geographical location, and guidance for their interpretation from the numerical weather prediction centre may be necessary. However, it is relatively easy to identify upper-wind systems where the random errors are much larger than normal. In recent years, about 6% of the upper-wind systems in the global network have been identified as faulty. The system types associated with faulty performance have mainly been radiotheodolites and secondary radar systems.

Summaries of systematic biases between observations and forecast fields over several months or for a whole year are also helpful in identifying systematic biases in wind speed and wind direction for a given system. Small misalignments of the tracking aerials of radiotheodolites or radars are a relatively common fault.

13.6.1.2 *Comparison with other windfinding systems*

Special comparison tests between upper-wind systems have provided a large amount of information on the actual performance of the various upper-wind systems in use worldwide. In these tests, a variety of targets are suspended from a single balloon and tracked simultaneously by a variety of ground systems. The timing of the wind reports from the various ground stations is synchronized to better than 1 s. The wind measurements can then be compared as a function of time into flight, and the heights assigned to the winds can also be compared independently. The interpretation of the comparison results will be more reliable if at least one of the upper-wind systems produces high-accuracy wind measurements with established error characteristics.

A comprehensive series of comparison tests was performed between 1984 and 1993 as part of the WMO International Radiosonde Comparison. Phases I and II of the tests were performed in the United Kingdom and United States, respectively (WMO, 1987). Phase III was performed by the Russian Federation at a site in Kazakhstan (WMO, 1991), and Phase IV was performed in Japan (WMO, 1996). Further tests in Brazil in 2001 (WMO, 2006*a*) were performed specifically to identify problems in GPS windfinding in the tropics, and this led to improved GPS radiosonde systems which were also tested in Mauritius in 2005 (WMO, 2006*b*) and most comprehensively in Yangjiang, China in 2010 (WMO, 2011*b*).

The information in Tables 13.4, 13.5 and 13.6 was primarily based on results from the WMO International Radiosonde Comparison and additional tests performed to the same standard as the WMO tests.

Now that the development of GPS windfinding systems is mature, most of these systems can be used as reliable travelling standards for upper-wind comparison tests in more remote areas of the world.

13.6.2 **Calibration**

The calibration of slant range should be checked for radars using signal returns from a distant object whose location is accurately known. Azimuth should also be checked in a similar fashion.

The orientation of the tracking aerials of radiotheodolites or radars should be checked regularly by comparing the readings taken with an optical theodolite. If the mean differences between the theodolite and radar observations of elevation exceed 0.1°, the adjustment of the tracking aerial should be checked. When checking azimuth using a compass, the conversion from geomagnetic north to geographical north must be performed accurately.

With navaid systems, it is important to check that the ground system location is accurately recorded in the ground system computer. The navaid tracking system needs to be configured correctly according to the manufacturer's instructions and should be in stable operation prior to the radiosonde launch.

13.6.3 **Maintenance**

Radiotheodolites and radars are relatively complex and usually require maintenance by an experienced technician. The technician will need to cope with both electrical and mechanical maintenance and repair tasks. The level of skill and frequency of maintenance required will vary with the system design. Some modern radiotheodolites have been engineered to improve mechanical reliability compared with the earlier types in use. The cost and feasibility of maintenance support must be considered important factors when choosing the type of upper-wind system to be used.

Electrical faults in most modern navaid tracking systems are repaired by the replacement of faulty modules. Such modules would include, for instance, the radiosonde receivers or navaid tracker systems. There are usually no moving parts in the navaid ground system and mechanical maintenance is negligible, though antenna systems, cables and connectors should be regularly inspected for corrosion and other weathering effects. Provided that sufficient spare modules are purchased with the system, maintenance costs can be minimal.

13.7 **CORRECTIONS**

When radiowind observations are produced by a radar system, the radar tracking information is used to compute the height assigned to the wind measurements. These radar heights need to be corrected for the curvature of the Earth using the following:

$$\Delta z_{\text{curvature}} = 0.5 (r_s \cdot \cos\theta)^2 / (R_c + r_s \sin\theta) \tag{13.6}$$

where r_s is the slant range to the target; θ is the elevation angle to the target; and R_c is the radius of the Earth curvature at the ground station.

In addition, the direction of propagation of the radar beam changes since the refractive index of air decreases on average with height, as temperature and water vapour also decrease with height. The changes in refractive index cause the radar wave to curve back towards the Earth. Thus, atmospheric refraction usually causes the elevation angle observed at the radar to be larger than the true geometric elevation of the target.

Typical magnitudes of refraction corrections, $\Delta z_{\text{refraction}}$, are shown in Table 13.7. These were computed by Hooper (1986). With recent increases in available processing power for ground system computers, algorithms for computing refractive index corrections are more readily available for applications with high-precision tracking radars. The corrections in Table 13.7 were computed from five-year climatological averages of temperature and water vapour for a variety of locations. On days when refraction errors are largest, the correction required could be larger than the climatological averages in Table 13.7 by up to 30% at some locations.

Table 13.7. Examples of corrections to radar height observations for Earth curvature and typical refraction

Plan range (km)	Altitude (km)	$\Delta z_{curvature}$	$\Delta z_{refraction}$ 60°N 01°W	$\Delta z_{refraction}$ 36°N 14°E	$\Delta z_{refraction}$ 1°S 73°E
25	10	49	−9	−10	−12
50	15	196	−31	−34	−39
100	20	783	−106	−117	−133
150	25	1 760	−211	−231	−262
200	30	3 126	−334	−363	−427

REFERENCES AND FURTHER READING

Acheson, D.T., 1970: *LORAN-C Windfinding Capabilities: Wallops Island Experiments*. United States Department of Commerce, Weather Bureau. ESSA Technical Memorandum WBTM EDL 11.

de Boor, C., 1978: *A Practical Guide to Splines*. Springer Verlag, New York.

Edge, P., M. Kitchen, J. Harding and J. Stancombe, 1986: *The Reproducibility of RS3 Radiosonde and Cossor WF Mk IV Radar Measurements*. Meteorological Office, Bracknell, OSM No. 35.

Hooper, A.H., 1986: *The Calculation of Radio-wave Refraction, with Special Reference to Data Height-finding Radars*. Meteorological Office, Bracknell, OSM No. 17.

Kaisti, K., 1995: New low-cost GPS solution for upper-air windfinding. *Proceedings of the Ninth Symposium on Meteorological Observations and Instrumentation*, Charlotte, North Carolina (27–31 March 1995). American Meteorological Society, pp. 16–20.

Karhunen, P., 1983: Automated windfinding developments. *Preprints of the Fifth AMS Symposium on Meteorological Observations and Instrumentation* (Toronto, 11–15 April 1983), pp. 110–115.

Kitchen, M., 1989: Representativeness errors for radiosonde observations. *Quarterly Journal of the Royal Meteorological Society*, 115:673–700.

Lange, A.A., 1988: A high-pass filter for optimum calibration of observing systems with applications. In: *Simulation and Optimization of Large Systems* (A.J. Osiadacz, ed.). Clarendon Press, Oxford, pp. 311–327.

Nash, J., 1994: Upper wind observing systems used for meteorological operations. *Annales Geophysicae*, 12:691–710.

Nash, J. and T.J. Oakley, 1992: Experience in the use of LORAN-C windfinding in the United Kingdom. *Proceedings of the Twenty-first Annual Technical Symposium*, Wild Goose Association, Birmingham, England, pp. 81–88.

Passi, R.M., 1978: Overdetermined windfinding systems. *Atmospheric Technology*, 10:65–75.

Passi, R.M. and C. Morel, 1987: Wind errors using the worldwide LORAN network. *Journal of Atmospheric and Oceanic Technology*, 4:690–700.

Schaefer, J.T. and C.A. Doswell, 1978: The inherent position errors in double-theodolite pibal measurements. *Journal of Applied Meteorology*, 17:911–915.

World Meteorological Organization, 1975: *Upper-air Sounding Studies* (R.E. Vockeroth). Technical Note No. 140 (WMO-No. 394), Volume II. Geneva.

———, 1985: *Meteorological Observations Using Navaid Methods* (A.A. Lange). Technical Note No. 185 (WMO-No. 641). Geneva.

———, 1986: *Algorithms for Automatic Aerological Soundings* (A.H. Hooper). Instruments and Observing Methods Report No. 21 (WMO/TD-No. 175). Geneva.

———, 1987: *WMO International Radiosonde Comparison (UK 1984, USA 1985): Final Report* (J. Nash and F.J. Schmidlin). Instruments and Observing Methods Report No. 30 (WMO/TD-No. 195). Geneva.

———, 1989: An algorithmic approach for improving and controlling the quality of upper-air data (A.A. Lange). *Papers Presented at the Fourth WMO Technical Conference on Instruments and Methods of Observation (TECIMO-IV)*. Instruments and Observing Methods Report No. 35 (WMO/TD-No. 303). Geneva.

———, 1991: *WMO International Radiosonde Comparison – Phase III, Dzhambul (USSR), 1989: Final Report* (A. Ivanov, A. Kats, S. Kurnosenko, J. Nash and N. Zaitseva). Instruments and Observing Methods Report No. 40 (WMO/TD-No. 451). Geneva.

———, 1994: A new GPS rawinsonde system (D.B. Call). *Papers Presented at the WMO Technical Conference on Instruments and Methods of Observation (TECO-94)*. Instruments and Observing Methods Report No. 57 (WMO/TD-No. 588). Geneva.

———, 1996: *WMO International Radiosonde Comparison – Phase IV, Tsukuba (Japan), 1993: Final Report* (S. Yagi, A. Mita and N. Inoue). Instruments and Observing Methods Report No. 59 (WMO/TD-No. 742). Geneva.

———, 2005: Studying the accuracy of AFAR-based radar sounding system (A. Ivanov and V. Tseitlin). *Papers and posters presented at the WMO Technical Conference on Meteorological and Environmental Instruments and Methods of Observation (TECO-2005)*. Instruments and Observing Methods Report No. 82 (WMO/TD-No. 1265). Geneva.

———, 2006a: *WMO Intercomparison of GPS Radiosondes – Alcântara (Brazil), 2001* (R. da Silveira, G.F. Fisch, L.A.T. Machado, A.M. Dall'Antonia, L.F. Sapucci, D. Fernandes, R. Marques and J. Nash). Instruments and Observing Methods Report No. 90 (WMO/TD-No. 1314). Geneva.

———, 2006*b*: *WMO Intercomparison of Radiosonde Systems – Vacoas (Mauritius), 2005* (J. Nash, R. Smout, T. Oakley, B. Pathack and S. Kurnosenko). Instruments and Observing Methods Report No. 83 (WMO/TD-No. 1303). Geneva.

———, 2008: Suggestions for upgrading the pilot balloon network in West Africa and elsewhere in the tropics (M. Douglas, J. Mejia, R. Orozco and J. Murillo). *Papers and posters presented at the WMO Technical Conference on Meteorological and Environmental Instruments and Methods of Observation (TECO-2008).* Instruments and Observing Methods Report No. 96 (WMO/TD-No. 1462). Geneva.

———, 2010: *Manual on the Global Observing System* (WMO-No. 544), Volume I. Geneva.

———, 2011*a*: *Manual on Codes* (WMO-No. 306), Volume I. Geneva.

———, 2011*b*: *WMO Intercomparison of High Quality Radiosonde Systems – Yangjiang (China), 2010* (J. Nash, T. Oakley, H. Vömel and L. Wei). Instruments and Observing Methods Report No. 107 (WMO/TD-No. 1580). Geneva.

CHAPTER CONTENTS

CHAPTER 14. OBSERVATION OF PRESENT AND PAST WEATHER; STATE OF THE GROUND

14.1 GENERAL

14.1.1 Definitions

In observational practice the term *weather* is regarded as covering those observations of the state of the atmosphere, and of phenomena associated with it, which were initially not intended to be measured quantitatively. These observations are qualitative descriptions of phenomena observed in the atmosphere or on the Earth's surface, such as precipitation (hydrometeor falling through the atmosphere), suspended or blowing particles (hydrometeors and lithometeors), or other specially designated optical phenomena (photometeor) or electrical manifestations (electrometeor). Detailed descriptions can be found in WMO (1975).

A *hydrometeor* is an ensemble of liquid or solid water particles suspended in, or falling through, the atmosphere, blown by the wind from the Earth's surface, or deposited on objects on the ground or in free air.

A *lithometeor* is an ensemble of particles most of which are solid and non-aqueous. The particles are more or less suspended in the air, or lifted by the wind from the ground.

A *photometeor* is a luminous phenomenon produced by the reflection, refraction, diffraction or interference of light from the sun or the moon.

An *electrometeor* is a visible or audible manifestation of atmospheric electricity.

A special class of weather phenomena are localized weather events. Definitions of such events can be found in WMO (1992). Specific events such as dust whirls and funnel clouds are defined and described in section 14.2.3.

In meteorological observations, weather is reported in two forms. *Present weather* (PW) is a description of the weather phenomena present at the time of observation. *Past weather* is used to describe significant weather events occurring during the previous hour, but not occurring at the time of observation.

This chapter also describes the methods of observing a related item, namely the state of the ground. *State of the ground* refers to the condition of the Earth's surface resulting from the recent climate and weather events, in terms of the amount of moisture or description of any layers of solid, or aqueous or non-aqueous particles covering the normal surface.

14.1.2 Units and scales

At manned stations, the observations identified as present weather, past weather and state of the ground are reported together with quantitative data. Such observations have been standardized on scales that enable the observer to select an appropriate term from a large number of descriptions derived from the perceptions of human observers and laid down in WMO (2011).

Since 1990, the introduction of automated weather stations has created the need to quantify the functions previously performed by observers. In order to accommodate the varying levels of sophistication and effectiveness of automated meteorological stations in observing present and past weather, specific coding directives have been included in WMO (2011). Because of the

complexity of reporting data on present and past weather determined by sophisticated present weather systems, such data should be reported as quantities in binary code format given that the alphanumeric code format suffers from many restrictions in comprehensive reporting.[1]

14.1.3   Meteorological requirements

Present and past weather, as well as the state of the ground, are primarily meant to serve as a qualitative description of weather events. They are required basically because of their impact on human activities and transport safety, as well as for their significance for understanding and forecasting synoptic weather systems. Several other chapters in this Guide deal with related topics. The quantitative measurement of precipitation amounts is described in Part I, Chapter 6, and cloud observations are described in Part I, Chapter 15. Part II addresses topics that are specific to aeronautical and marine observations, automated systems, radar and atmospherics.

In this chapter, weather observations of interest in the determination of present and past weather are categorized into three types, namely precipitation (falling hydrometeors), atmospheric obscurity and suspensoids (lithometeors and suspended or blowing hydrometeors), and other weather events (such as funnel clouds, squalls and lightning). Liquid precipitation or fog which leave frozen deposits on surfaces are included in the appropriate precipitation and suspended hydrometeor category.

Other phenomena, such as those of an optical nature (photometeors) or electrometeors other than lightning, are indicators of particular atmospheric conditions and may be included in the running record maintained at each station of the weather sequence experienced. However, they are of no significance in the determination of present and past weather when coding standard meteorological observations, and are included here only for completeness.

14.1.4   Observation methods

The only current capability for observing all of the different forms of weather are the visual and auditory observations of a trained human observer. However, given the high cost of maintaining a significant staff of trained observers, a number of Meteorological Services are increasing their use of automated observing systems in primary observing networks, as well as continuing their use for supplementing manned networks with automated observations from remote areas.

Basic research (Bespalov et al., 1983) has confirmed the possibility that weather phenomena may be determined by the logical analysis of a group of data variables. No single sensor is currently available which classifies all present weather; rather, data from a variety of sensors are used (such as visibility, temperature, dewpoint, wind speed and the differentiation of rain versus snow) to make such determinations. Automated observing systems have the capability to perform this logical analysis, but they vary in their ability to observe the required weather phenomenon, based on the instrumentation included in the system and the sophistication of the algorithms. While automated systems cannot observe all types of weather event, those of significance can be observed, making such systems cost-effective alternatives to the fully trained human observer.

14.2   OBSERVATION OF PRESENT AND PAST WEATHER

The observations to be recorded under the present weather and past weather headings include the phenomena of precipitation (rain, drizzle, snow, ice pellets, snow grains, diamond dust and hail), atmospheric obscurity and suspensoids (haze, dust, smoke, mist, fog, drifting and blowing snow, dust or sandstorms, dust devils), funnel clouds, squalls and lightning.

---

[1]   Recommendation 3 (CBS-XII) refers to the requirement "to report observed quantities rather than qualitative parameters for present weather in observation from automatic stations in FM 94 BUFR and FM 95 CREX".

When observing present weather, it is necessary to note the various phenomena occurring at the station or in sight of the station at the time of observation. In synoptic reports, if there is no precipitation at the time of observation, account is taken of the conditions during the last hour in selecting the code figure.

14.2.1   Precipitation

14.2.1.1   *Objects of observation*

The *character of precipitation* can be defined as being one of three forms, namely showers, intermittent precipitation and continuous precipitation. Showers are the precipitation events associated with physically separated convective clouds. Observers (or instruments replacing humans) also have to classify precipitation into the three intensity categories, namely light, moderate and heavy, according to the rates of precipitation fall or other related factors (such as visibility).

The *type of precipitation* (rain, drizzle, snow, hail) is the third major observable of precipitation. Observations of rain or drizzle at low temperatures should distinguish whether or not the precipitation is freezing. By definition, frozen rain or drizzle causes glazed frost by freezing on coming into contact with solid objects. Solid precipitation can occur in the form of diamond dust, snow grains, isolated star-like snow crystals, ice pellets and hail, full descriptions of which are given in WMO (1975).

The precipitation character (intermittent, continuous, showery) and type (rain, drizzle, snow, hail) affect the definition of scales of *precipitation intensity*. Several combined Commission for Instruments and Methods of Observation/Commission for Basic Systems expert team meetings have developed tables to obtain a more universal relation between the qualitative and subjective interpretation by an observer and the measured quantities obtained by a present-weather system. For an example of these tables and other relations, see the annex.

14.2.1.2   *Instruments and measuring devices: precipitation type*

One major area of instrumentation involves the identification of the type of precipitation. Systems which are currently under evaluation, or in operational use, generally involve optical methods or radar (van der Meulen, 2003). Field tests (WMO, 1998) have shown that all of these systems are capable of detecting major precipitation types – except for the very lightest snow or drizzle – in over 90% of occurrences compared to a trained observer. The percentage of detection of very light precipitation is usually much lower.[2] Sophisticated algorithms are required to differentiate between several of the precipitation types. For example, wet or melting snow is difficult to distinguish from rain. Sensors detecting precipitation type are listed below.

Forward-scatter/backscatter present weather sensor

A variety of scatter sensors are used to report present weather, in particular precipitation type. In general, scatter of a light source by the precipitation particles is observed under a fixed angle. This gives information on the size of the particles. Additional measurements (such as water content of the particles, fall speed, temperature) help determine the nature of the particles. For example, large particles with small water content will be classified as snow. Some sensors report unidentified precipitation when the precipitation type cannot be properly determined by the system. This mainly occurs at low precipitation intensities and during the start and cessation of precipitation events. Apart from precipitation type, these sensors may (depending on the sensor type) also provide precipitation intensity, precipitation duration (thus able to indicate intermittent precipitation) and visibility.

---

[2]   The threshold for the detection of rain intensity is 0.02 mm h^{-1} (see Part I, Chapter 1, Annex 1.E).

These sensors are widely in use and generally give acceptable results for common precipitation types (rain, snow), with 70%–90% detection rates (WMO, 1998), depending on the exact test set up and the specific instrument. Other precipitation types are not so well observed, particularly mixed precipitation (rain and snow) and hail. Thresholds for light precipitation may vary.

Optical disdrometer

Optical disdrometers are also used to determine precipitation type. These instruments use the extinction of a horizontal (infrared) light sheet to detect hydrometeors. When a particle falls through the light sheet, the receiver intensity is reduced. The amplitude of this reduction correlates with the particle size, and the duration correlates with the particle fall speed. The type of precipitation is determined by comparing the particle fall speed distribution of a series of detected particles against known relationships for different types of liquid, mixed and solid precipitation.

These sensors also generally give acceptable results for common precipitation types. Detection rates compared to human observers are similar to those found for scatter sensors (WMO, 2005*a*). Again, mixed precipitation types and hail are difficult to detect.

Doppler radar

Specific Doppler radars can also be used to determine precipitation type. The (vertically) emitted beam from the radar is backscattered by the falling hydrometeors. From the Doppler shift of the backscattered signal, the particle fall speeds can be determined. Near the ground, these are terminal fall velocities and correspond with the particle sizes. Some instruments have a measuring volume above the sensor; others determine the fall speeds at different altitudes above the sensor to determine precipitation type. Additional measurements (for example, surface temperature) are also used.

Different types of Doppler radar are available for detection of precipitation type. They tend to be insensitive to small particles, like all radar-based detection techniques. Some types show similar results compared with forward-scatter/backscatter sensors and disdrometers, that is, they produce decent results for rain and for snow, but not for mixtures. Hail is not observed.

Impact detector

This type of sensor consists of a piezoelectric material which is capable of detecting the impact of the individual hydrometeors. The difference between the impact of hail and rain differs sufficiently to distinguish these two precipitation types. Other precipitation types are not reported.

Since only rain and hail can be reported, this sensor is not a fully operational present-weather sensor. The hail detection part may, however, be helpful to some users, since this is generally a weak point of other present weather sensors.

Acoustic detector

The acoustic detector senses the sound of the falling hydrometeors. This is related to the precipitation type. The sensor was developed to supplement a forward-scatter/backscatter PW sensor, in particular to improve the detection of hail and ice pellets.

Initial results of the sensor were promising (Wade, 2003; Loeffler-Mang, 2009).

Other methods

Cameras can also be used to monitor precipitation type. An observer/operator can then monitor the various cameras from a central facility. A proper background needs to be selected in order to observe the precipitation. Since this type of measurement requires an observer/operator, it is not an automatic measurement of present/past weather.

A sensor specifically designed to detect freezing rain or glaze is in operational use (Starr and van Cauwenberghe, 1991). It senses the amount of ice accumulation on a probe. The probe vibrates at a frequency that is proportional to the mass of the probe. When ice freezes on the probe, its mass changes and the vibration frequency decreases. A heater is built into the sensor to de-ice the probe when required. The sensor has also been found effective for identifying wet snow.

Icing detectors may be used to identify freezing precipitation. Various methods exist. For instance, the weight of ice on a pole can be measured. Another method uses a probe that vibrates ultrasonically and the frequency of this probe changes when ice is formed on it. An extensive test has recently been performed (Fikke et al., 2007). Results from PW sensors improve by including data from icing detectors, particularly freezing rain (Sheppard and Joe, 2000). Automated Weather Observing Systems (AWOSs) use this technique.

14.2.1.3 *Instruments and measuring devices: precipitation intensity and character*

Present weather reports include an indication for the intensity of precipitation and thus of the precipitation character (that is, showers, intermittent precipitation or continuous precipitation). In many cases, these parameters are measured by the same sensor that determines the precipitation type. But it is also possible to employ a different sensor for this purpose. Measuring intensity also allows for the determination of intermittent precipitation (for example, snow showers). A laboratory and field intercomparison for precipitation intensity measurements has recently been completed (WMO, 2006*a*, 2009). This intercomparison included many different instruments using a variety of measurement techniques for collecting precipitation. Automatic measurement methods to provide an indication of precipitation intensity are listed below.

Forward-scatter/backscatter present weather sensor

The sensor is described in section 14.2.1.2. By combining the particle size distribution, number of particles and precipitation type, the intensity of the precipitation is calculated. The precipitation intensity determined in this manner is usually less accurate than using conventional methods (for example, weighing raingauges, tipping-bucket raingauges). Calibration of the precipitation intensity is also a problem. For a coarse indication of precipitation intensity (light, heavy, etc.), this method is usable. Manufacturers are working on refining the precipitation intensity output.

Optical disdrometer

This sensor type is also described in section 14.2.1.2. By combining the particle size distribution, number of particles and precipitation type, the intensity of the precipitation is calculated. Work is being done to refine the precipitation intensity output (see, for example, WMO, 2006*b*).

Doppler radar

The sensor is described in section 14.2.1.2. By combining the particle size distribution, number of particles and precipitation type, the intensity of the precipitation is calculated. Precipitation intensity results have shown decent correlations ($\rho = 0.9$) with conventional raingauges when 30 min intervals are considered (see Peters et al., 2002).

Raingauge

There are many different types of "conventional" raingauges. These are based on several different measurement methods and described in Part I, Chapter 6. They are generally designed to measure precipitation amount, although some (smaller) instruments are also specifically designed to give (an indication of) precipitation intensity. Those raingauges designed for precipitation amount tend to be less accurate in reporting precipitation intensity. However, an indication of precipitation intensity, which is required for the present weather reporting, is generally satisfactory. Also, many manufacturers are improving these instruments with respect to the precipitation intensity (WMO, 2006*a*, 2009).

14.2.1.4   *Instruments and measuring devices: multi-sensor approach*

To determine present weather characteristics and quantities of precipitation, observing systems use a variety of sensors in combination with algorithms. This multi-sensor approach creates a constraint on the techniques involved. Typical observations also involved are the measurement of precipitation, visibility, air temperature, dewpoint and cloud base. The algorithms are characterized by filtering (for example, liquid precipitation only if the air temperature is above 6 °C). Combining numerous sensors to determine present weather is also used in road-weather systems (see also section 14.3).

14.2.2   **Atmospheric obscurity and suspensoids**

14.2.2.1   *Objects of observation*

In reports taking into account the atmospheric conditions during the last hour, haze should be distinguished from mist or water fog. With haze, the air is relatively dry, whereas with mist or water fog, there is usually evidence of high humidity in the form of water droplets or rime on grass, leaves, etc. If the station is equipped with measuring instruments, it is fairly safe to assume that the obscurity is haze if the relative humidity is less than a certain percentage, for example 80%, and if the visibility is within certain limit values, for example, greater than 1 km in the horizontal, and greater than 2 km in the vertical. Mist is to be reported at high humidity values and at a visibility of 1 km or more. In synoptic reporting, fog is regarded as applying to water or ice fogs, generally reducing the horizontal visibility at the Earth's surface to less than 1 km. Wherever the term "fog" occurs in present weather and past weather codes, it should be read in this sense. In climatological summaries, however, all occasions of visibility of less than 1 km are regarded as fog.

Rime deposit is caused by the solidification into ice of water droplets in fog on coming into contact with solid objects at a temperature below freezing point. The present and past weather codes do not distinguish between different types of rime.

Drifting or blowing snow is snow blown off the ground into the air after it has already fallen. In the present weather code, drifting and blowing snow are distinguished separately, the former referring to snow not raised above the observer's eye level.

Other meteorological phenomena to be identified include widespread dust in suspension in the air, dust or sand raised by wind, a duststorm and sandstorm caused by turbulent winds raising large quantities of dust or sand into the air and reducing visibility severely, dust whirls or sand whirls and, occasionally, funnel clouds.

WMO (1975) should be at the observer's disposal as an auxiliary means.

14.2.2.2   *Instruments and measuring devices for obscurity and suspensoid characteristics*

A possible approach for the identification of obscurity and suspensoid characteristics is the complex processing of measured values which can act as predictors. This approach requires

researching the meteorological quantities that accompany the formation, intensification and disappearance of the phenomenon, as well as determining the limiting conditions. The problem of identifying fog, mist, haze, snowstorms and duststorms is reported in Goskomgidromet (1984) and WMO (1985). The meteorological visual range serves as the most important indicating element. Of the remaining variables, wind velocity, humidity, temperature and dewpoint have proved to be important identifying criteria.

Instruments measuring visibility can be used to determine the meteorological visual range, as described in Part I, Chapter 9, particularly section 9.3. Note that for the determination of fog, mist and haze, however, the range of these instruments can be limited to a few kilometres. Three types of visibility instruments used in the determination of fog, haze and mist are described below.

Transmissometer

Transmissometers measure the extinction of a light source over a known distance. Usually, the light of a flash lamp is detected at a distance of between 10 and 200 m. The visibility is calculated from the extinction of this light. In order to increase the range of detection, two detectors at different distances can be used (a so-called double-baseline transmissometer). Transmissometers are well suited to measure visibility, and are widely in use, particularly at airports. For larger visibilities, the uncertainty in the measurement increases with an increase in visibility (for further details, see Part I, Chapter 9). They are relatively expensive to install and to maintain, as they require regular cleaning. Some transmissometers are capable of maintaining their operational accuracy significantly longer due to automatic calibration and automatic compensation of contamination effects.

Forward-scatter sensor

This sensor is described in section 14.2.1.2. Apart from precipitation type, visibility can also be measured using this instrument. The amount of scatter is related to the optical extinction. This is determined empirically in the calibration process by comparing the output with a transmissometer. Forward-scatter sensors are also well suited for measuring visibility and are being used increasingly. Compared to the transmissometer, the forward-scatter sensor can be generally used for a larger visibility range. One drawback is that its calibration is not trivial and needs attention. The instrument is relatively inexpensive to install and to maintain, as it does not require cleaning as often as transmissometers. Certain sensors can further extend the cleaning interval by automatic compensation of the optical impact of contamination.

Lidar

A relatively small lidar system can also be used to determine the visibility used in the determination of fog. A diode laser emits light pulses, and the light reflected back by the fog/haze particles (if present) is measured. The visibility is determined from the intensity of the reflected light and its time-of-flight. The visibility range measured by a lidar is limited, but for the determination of fog and haze and similar phenomena, a large visibility range is not required.

14.2.3 **Other weather events**

14.2.3.1 *Objects of observation*

One event of critical importance in the protection of life and property is the recognition and observation of funnel clouds.

Funnel cloud (tornado or waterspout): A phenomenon consisting of an often violent whirlwind, revealed by the presence of a cloud column or inverted cloud cone (funnel cloud), protruding from the base of a cumulonimbus. The cloud may extend all the way down to the Earth's surface,

but not necessarily reaching the ground, in which case water, dust, sand or litter may be raised, producing a "bush" around the tip of the funnel. The diameter can vary from a few metres to some hundreds of metres. A funnel cloud is considered well developed if the violent rotating column of air touches the ground or water surface. A well-developed funnel cloud is considered a tornado when over ground, and a waterspout when over water. The most violent tornadoes can have associated wind speeds of up to 150 m s^{-1}.

Dust/sand whirls (dust devils): A rapidly rotating column of air usually over dry and dusty or sandy ground which carries dust and other light material picked up from the ground. Dust or sand whirls are a few metres in diameter. Normally, in the vertical they extend no higher than 60 to 90 m (dust devils). Well-developed dust/sand whirls in very hot desert regions may reach 600 m.

Squall: A strong wind that rises suddenly, lasts for a few minutes, then passes away. Squalls are frequently associated with the passage of cold fronts. In such circumstances, they occur in a line and are typically accompanied by a sharp fall in temperature, veering wind (northern hemisphere) or backing wind (southern hemisphere), a rise in relative humidity, and a roll-shaped cloud with a horizontal axis (line squall).

The definition of a thunderstorm (see WMO, 1992) is an example of deriving the description exclusively from the perception of human observers. The event should be considered as a thunderstorm when thunder is heard (even if lightning is not observed).

14.2.3.2 *Instruments and measuring devices*

The presence of funnel clouds, or tornadoes, can often be determined with the use of weather radar (see Part II, Chapter 7). Modern Doppler weather radars have become quite effective in the recognition of mesocyclones, thus providing more detailed and advanced information about this severe weather phenomenon than visual observation alone.

Squalls can be determined from the discrete succession of measured values of wind velocity. If the output of a wind velocity measuring device is combined with that of a wind direction sensor, a thermometer or a humidity sensor, the identification of a line squall seems to be possible.

Thunderstorms are mainly detected through the use of lightning counters. On the basis of the instructions provided to observers and issued by different Services, a certain number of lightning strokes per interval of time must be selected which can be used in combination with precipitation rates or wind speeds to define slight, moderate and heavy thunderstorms (see Part II, Chapter 6).

14.2.4 **State of the sky**

14.2.4.1 *Objects of observation*

The specifications of the state of the sky are used to describe the progressive changes that have occurred in the sky during a given time. Changes in the total amount of clouds, in the height of the cloud base and in the type of cloud are to be considered likewise.

14.2.4.2 *Instruments and measuring devices*

Cloud amount characteristics (total cloud cover in oktas, height of cloud base, and total cloud cover in various cloud layers) can be approximated from the variation of cloud-base height measured by a cloud-base optical measuring system by the application of statistical methods (see also Part I, Chapter 15). Obviously, this is limited to cloud layers within the vertical range of the cloud-base measuring system (Persin, 1987; US NOAA, 1988; ICEAWS, 1999).

14.3   OBSERVATION OF STATE OF THE GROUND

14.3.1   Objects of observation

State of the ground refers to the condition of the surface resulting from recent weather events in terms of amount of moisture or a description of solid, aqueous or non-aqueous particles covering the natural surface. Observations of the state of the ground (symbolic letters E and E´) should be made in accordance with the specifications given in WMO (2011).

Reporting state of the ground is also a part of present weather reporting, which, until recently, was carried out solely by human observers. Automatic measurement of state of the ground is still relatively new (for example, see Stacheder et al., 2008) and not widely in use. Some meteorological institutes are working on standardizing the surface(s) to be observed.

14.3.2   Instruments and measuring devices

Research has shown that it is possible to discriminate main states of soil by means of reflecting and scattering phenomena (dry, humid, wet, snow-covered, rimed or iced) (Gaumet et al., 1991). Methods in use are briefly described below.

Scatter sensor: These sensors have an optical design that uses the reflecting and scattering properties of the surface. Various light sources may be used. For example, flux from a white light source reflected from a reference tile will depend on the state of this surface. Other (road-) sensors analyse reflection of an infrared light source on a road surface. Here the wavelength of the reflected light depends on the state of the surface. Not all these sensors are suited for meteorological purposes, as they may be designed for surfaces other than natural surfaces. Sensors are currently being improved.

Capacitive sensor: A new, capacitive sensor is currently being developed and tested. A grid mat with conductive strips is placed on the (natural) surface. It is basically a capacitor with the natural ground as the dielectric. The dielectric constant for dry and wet earth differs considerably. The capacitance thus depends on the humidity of surface and, by measuring the absolute values and phase of the emitted signals at two frequencies, the state of the ground can be determined. The first results of the tests look promising, but this sensor is still under development.

Combination of sensors: Particularly for road surfaces, a combination of sensors may be used to determine the surface state. For example, optical detection may determine the surface coverage; a conductivity measurement may determine the presence of chemical substances, surface temperature and ground temperature, and so forth. All these measurements, combined with atmospheric data, can be used in determining road condition. However, state of the ground is defined as the state on the natural surface present; this method thus determines not the exact state of the ground, but a related property.

Cameras (and observer): Cameras are also used to determine state of the ground. They can be pointed at various surfaces and an observer/operator determines the state of the ground. As this method is basically a manual method of observation, it is not analysed here.

14.4   OBSERVATION OF SPECIAL PHENOMENA

14.4.1   Electrical phenomena

Electrometeors either correspond to discontinuous electrical discharges (lightning, thunder) or occur as more or less continuous phenomena (Saint Elmo's fire, polar aurora). Full descriptions of electrometeors are given in WMO (1975).

Special records of lightning should include information regarding its type and intensity, the frequency of flashes and the range of azimuth over which discharges are observed; the lapse of

time between lightning and the corresponding thunder should be noted. Care should be taken to distinguish between the actual lightning flash and its possible reflection on clouds or haze. Automatic detection systems for lightning location are in operational use in many countries. Part II, Chapter 6, contains more information on this topic.

Exceptional polar aurora should be described in detail. Light filters, where available, may be used as a means of increasing the sensitivity of the observations, and theodolites or clinometers (alidades) may be used to increase the accuracy of the angular measurements.

14.4.2 Optical phenomena

A photometeor is a luminous phenomenon produced by the reflection, refraction, diffraction or interference of light from the sun or moon. Photometeors may be observed in more or less clear air (mirage, shimmer, scintillation, green flash, twilight colours), on or inside clouds (halo phenomena, corona, irisation, glory) and on or inside certain hydrometeors or lithometeors (glory, rainbow, fog bow, Bishop's ring, crepuscular rays).

Observers should take careful note of any optical phenomena that occur. A written description should be accompanied by drawings and photographs, if possible. Full descriptions of these phenomena are given in WMO (1975). Concise instructions for observing the more common phenomena are given in some observers' handbooks, for example, the United Kingdom Meteorological Office (1982).

A theodolite is a very suitable instrument for precise measurements. However, when one is not available, a graduated stick held at arm's length is useful; with the occurrence of a mock sun, the position may be determined by noting its relation to fixed landmarks. The diameter of a corona may be estimated by taking the angular diameter of the sun or moon as approximately half a degree.

———————————

ANNEX. CRITERIA FOR LIGHT, MODERATE AND HEAVY PRECIPITATION INTENSITY[1]

(Light, moderate and heavy precipitation defined with respect to the type of precipitation and to intensity, i)[a]

Variable	Range	Intensity
Drizzle	$i < 0.1$ mm h^{-1}	Light
	$0.1 \leq i < 0.5$ mm h^{-1}	Moderate
	$i \geq 0.5$ mm h^{-1}	Heavy
Rain (also showers)	$i < 2.5$ mm h^{-1}	Light
	$2.5 \leq i < 10.0$ mm h^{-1}	Moderate
	$10.0 \leq i < 50.0$ mm h^{-1}	Heavy
	$i \geq 50.0$ mm h^{-1}	Violent[b]
Snow (also showers)	$i < 1.0$ mm h^{-1} (water equivalent)	Light
	$1.0 \leq i < 5.0$ mm h^{-1} (water equivalent)	Moderate
	$i \geq 5.0$ mm h^{-1} (water equivalent)	Heavy

Notes:
a   Intensity values based on a 3 min measurement period.
b   The term "violent", as it pertains to precipitation rate, is inconsistent with the other categories and is confusing. A term such as "intense" or "extreme" may be more appropriate.

Mixed precipitation of rain and snow

The same as for snow (since the rain/snow ratio is not subject to any measurement, a simple choice should be made).

Hail: The same as for rain.

Ice pellets and snow pellets: The same as for snow.

Freezing phenomena: The same as for the non-freezing phenomena.

Guide for approximating the intensity of snow

Light: Snowflakes small and sparse; in the absence of other obscuring phenomena, snow at this intensity generally reduces visibility, but to no less than 1 000 m.

Moderate: Larger, more numerous flakes generally reducing visibility to between 400 and 1 000 m.

Heavy: Numerous flakes of all sizes generally reducing visibility to below 400 m.

Showers or intermittent precipitation

Automated systems should report showers or intermittent precipitation. Intermittent can be defined as no precipitation within 10 min of two consecutive precipitation events, i.e. if there is period of 10 min of no precipitation in a running 10 min average of precipitation within the last hour, it should be reported as intermittent.

---

[1]   Recommended by the WMO Expert Meeting on Automation of Visual and Subjective Observations (Trappes/Paris, France, 14–16 May 1997) and the Working Group on Surface Measurements (Geneva, 27–31 August 2001).

Representativeness of present weather events

A present weather event may be well defined by a 3 min observing period. The highest running 3 min average in the 10 min period should be reported for present weather.

———————————

REFERENCES AND FURTHER READING

Bespalov, S.M. et al., 1983: *Osnovnyje voprosy razrabotki setevoj avtomaticeskoj gidrometeorologiceskoj stancii* [Main aspects of designing a network of automatic hydrometeorological stations]. Trudy GGO, Gidrometeoizdat, Leningrad, 473:3–12.

Bloemink, H.I., 2004: *Precipitation type detection, Present Weather Sensor: Final Report*. KNMI TR259, De Bilt.

De Haij, M.J., 2007: *Automated discrimination of precipitation type using the FD12P present weather sensor: evaluation and opportunities*. KNMI TR297, De Bilt.

Fikke, S., G. Ronsten, A. Heimo, S. Kunz, M. Ostrozlik, P.E. Persson, J. Sabata, B. Wareing, B. Wichura, J. Chum, T. Laakso, K. Säntti and L. Makkonen, 2007: *COST-727: Atmospheric Icing on Structures; Measurements and data collection on icing: State of the Art*, MeteoSwiss, No. 75.

Gaumet, J.L., P. Salomon and R. Paillisse, 1991: Automatic observations of the state of the soil for meteorological applications. *Preprints of the Seventh Symposium on Meteorological Observations and Instrumentation: Special Sessions on Laser Atmospheric Studies*, American Meteorological Society (New Orleans, 14–18 January 1991), pp. J191–J193.

Goskomgidromet, 1984: *Opredelenije atmosfernych javlenij po dannym avtomaticeskich stancij, soveqanije gruppy ekspertov GMS/MS socialisticeskich stran po teme 9.1. KR GMS/MS* [Identification of atmospheric phenomena from the data from automatic weather stations: Meeting of the panel of socialist countries HMS/MS on theme 9.1.], Obninsk, 24–28 August 1984, Moscow.

ICEAWS, 1999: *Second International Conference on Experiences with Automatic Weather Stations* (Vienna, 27–29 September). Österreichische Beiträge zu Meteorologie und Geophysik, No. 20 (available on CD-ROM only), ZAMG, Vienna, Austria.

Loeffler-Mang, M., 2009: *HARE – A New Intelligent Hail Recorder for Networks and Field Campaigns*. Fifth European Conference on Severe Storms, 12–16 October, Landshut, Germany (available from http://www.essl.org/ECSS/2009/preprints/P09-06-loefflermang.pdf).

Persin, S.M., 1987: *Izmerrenije vysoty niznej granicy oblakov i charakteristika oblacnosti kak zadaca paspoznavanija obrazov* [Measuring cloud ceiling and characterizing cloudiness as a task of image identification]. Trudy GGO, Gidrometeoizdat, Leningrad, 512:49–91.

Peters, G., B. Fischer and T. Andersson, 2002: Rain observations with a vertically looking Micro Rain Radar (MRR). *Boreal Environment Research*, 7:353–362.

Sheppard, B.E. and P.I. Joe, 2000: Automated precipitation detection and typing in winter: a two-year study. *Journal of Atmospheric and Oceanic Technology*, 17(11):1493–1507.

Stacheder, M., F. Koeniger, R. Schuhmann, A. Brandelik, G. Schmitt, W. Sommer and R. Fiel, 2008: A new sensor for the automatic detection of the state of the ground. *Near Surface Geophysics*, 6(1):67–70.

Starr, K.M. and R. van Cauwenberghe, 1991: The development of a freezing rain sensor for automated surface observing systems. *Preprints of the Seventh Symposium on Meteorological Observations and Instrumentation: Special Sessions on Laser Atmospheric Studies*, American Meteorological Society (New Orleans, 13–18 January 1991), pp. 338–343.

United Kingdom Meteorological Office, 1982: *Observer's Handbook*. Her Majesty's Stationery Office, London.

United States National Oceanic and Atmospheric Administration (NOAA), 1988: *Federal Standard Algorithms for Automated Weather Observing Systems Used for Aviation Purposes*. Office of the Federal Coordinator for Meteorological Services and Supporting Research, United States Department of Commerce, FCM-S5-1988, Washington DC.

Van der Meulen, J.P., 2003: *Present Weather – Science: Exploratory Actions on Automatic Present Weather Observations*. Final Report, E-PWS-SCI, KNMI, de Bilt, Netherlands, EUMETNET (available from http://www.knmi.nl/samenw/geoss/eumetnet/E-PWS-Sci/report/PWS-SCI_final_report.pdf).

Wade, C.G., 2003: Detecting ice pellets, snow pellets and hail on ASOS using an acoustic sensor. *Twelfth AMS Symposium on Meteorological Observations and Instrumentation*, Long Beach, CA, United States, 8–13 February 2003.

Wauben, W., 2002: Automation of visual observations at KNMI; (I) Comparison of present weather. *Papers presented at the Symposium on Observations, Data Assimilation, and Probabilistic Prediction*. Orlando, Florida, 13–17 January 2002, American Meteorological Society.

World Meteorological Organization, 1975: *International Cloud Atlas: Manual on the Observation of Clouds and Other Meteors* (WMO-No. 407), Volume I. Geneva.

———, 1985: Algorithms for automatic coding of the present and past weather by unmanned meteorological stations (M. Mezösi, A. Simon, P. Hanák and O. Szenn). *Papers Presented at the*

Third WMO Technical Conference on Instruments and Methods of Observation (TECIMO-III) (Ottawa, 8–12 July 1985), Instruments and Observing Methods Report No. 22 (WMO/TD-No. 50). Geneva.

———, 1992: *International Meteorological Vocabulary* (WMO-No. 182). Geneva.

———, 1994: A comparison of two present weather systems with human observations (J.P. van der Meulen). *Papers Presented at the WMO Technical Conference on Instruments and Methods of Observation (TECO-94).* Instruments and Observing Methods Report No. 57 (WMO/TD-No. 588). Geneva.

———, 1998: *WMO Intercomparison of Present Weather Sensors/Systems: Final Report* (Canada and France, 1993–1995) (M. Leroy, C. Bellevaux and J.P. Jacob). Instruments and Observing Methods Report No. 73 (WMO/TD-No. 887). Geneva.

———, 2002: Improvements to automated present weather reporting in the Met Office (S.G. McRobbie, M.J. Molyneux and P.D. Shearn). *Papers Presented at the WMO Technical Conference on Meteorological and Environmental Instruments and Methods of Observation (TECO-2002).* Instruments and Observing Methods Report No. 75 (WMO/TD-No. 1123). Geneva.

———, 2005a: Precipitation type from the Thies disdrometer (H.I. Bloemink and E. Lanzinger). *Paper presented at the WMO Technical Conference on Meteorological and Environmental Instruments and Methods of Observation (TECO-2005).* Instruments and Observing Methods Report No. 82 (WMO/TD-No. 1265). Geneva.

———, 2005b: Piezoelectric precipitation sensor from Vaisala (A. Salmi and J. Ikonen). *Paper presented at the WMO Technical Conference on Meteorological and Environmental Instruments and Methods of Observation (TECO-2005).* Instruments and Observing Methods Report No. 82 (WMO/TD-No. 1265). Geneva.

———, 2006a: *WMO Laboratory Intercomparison of Rainfall Intensity Gauges* (France, Italy, The Netherlands, 2004–2005) (L.G. Lanza, M. Leroy, C. Alexandropoulos, L. Stagi and W. Wauben). Instruments and Observing Methods Report No. 84 (WMO/TD-No. 1304). Geneva.

———, 2006b: Rainfall amount and intensity measured by the Thies laser precipitation monitor (E. Lanzinger, M. Theel and H. Windolph). *Paper presented at the WMO Technical Conference on Meteorological and Environmental Instruments and Methods of Observation (TECO-2006).* Instruments and Observing Methods Report No. 94 (WMO/TD-No. 1354). Geneva.

———, 2008: Results from UK Met Office investigations into new technology present weather sensors (D. Lyth). *Paper presented at the WMO Technical Conference on Meteorological and Environmental Instruments and Methods of Observation (TECO-2008).* Instruments and Observing Methods Report No. 96 (WMO/TD-No. 1462). Geneva.

———, 2009: *WMO Field Intercomparison of Rainfall Intensity Gauges* (Italy, 2007–2009) (E. Vuerich, C. Monesi, L.G. Lanza, L. Stagi and E. Lanzinger). Instruments and Observing Methods Report No. 99 (WMO/TD-No. 1504). Geneva.

———, 2010: Investigations into the improvement of automated precipitation type observations at KNMI (M. de Haij and W. Wauben). *Paper presented at the WMO Technical Conference on Meteorological and Environmental Instruments and Methods of Observation (TECO-2010).* Instruments and Observing Methods Report No. 104 (WMO/TD-No. 1546). Geneva.

———, 2011: *Manual on Codes* (WMO-No. 306), Volume I. Geneva.

———————————

CHAPTER CONTENTS

CHAPTER 15. OBSERVATION OF CLOUDS

15.1 GENERAL

The observation of clouds and the estimation or measurement of the height of their bases above the Earth's surface are important for many purposes, especially for aviation and other operational applications of meteorology. This chapter describes the methods in widespread use. Important further information is to be found in WMO (1975, 1987), which contain scientific descriptions of clouds and illustrations to aid in the identification of cloud types. Information on the practices specific to aeronautical meteorology is given in WMO (2014).

15.1.1 Definitions

Cloud: An aggregate of very small water droplets, ice crystals, or a mixture of both, with its base above the Earth's surface, which is perceivable from the observation location. The limiting liquid particle diameter is of the order of 200 μm; drops larger than this comprise drizzle or rain.

With the exception of certain rare types (for example, nacreous and noctilucent) and the occasional occurrence of cirrus in the lower stratosphere, clouds are confined to the troposphere. They are formed mainly as the result of condensation of water vapour on condensation nuclei in the atmosphere. Cloud formation takes place in the vertical motion of air, in convection, in forced ascent over high ground, or in the large-scale vertical motion associated with depressions and fronts. Clouds may result, in suitable lapse-rate and moisture conditions, from low-level turbulence and from other minor causes. Human activity, such as aviation or industry, can also result in cloud formation, by adding condensation nuclei to the atmosphere.

At temperatures below 0 °C, cloud particles frequently consist entirely of water droplets supercooled down to about –10 °C in the case of layer clouds and to about –25 °C in the case of convective clouds. At temperatures below these very approximate limits and above about –40 °C, many clouds are "mixed", with ice crystals predominating in the lower part of the temperature range.

Cloud amount: The amount of sky estimated to be covered by a specified cloud type (partial cloud amount), or by all cloud types (total cloud amount). In either case, the estimate is made to the nearest okta (eighth) and is reported on a scale which is essentially one of the nearest eighth, except that figures 0 and 8 on the scale signify a completely clear and cloudy sky, respectively, with consequent adjustment to other figures near either end of the scale.

Cloud base: The lowest zone in which the obscuration corresponding to a change from clear air or haze to water droplets or ice crystals causes a significant change in the profile of the backscatter extinction coefficient. In the air below the cloud, the particles causing obscuration show some spectral selectivity, while in the cloud itself, there is virtually no selectivity; the difference is due to the different droplet sizes involved. The height of the cloud base is defined as the height above ground level. For an aeronautical meteorological station, the ground (surface) level is defined as the official aerodrome elevation.

Cloud type (classification): Various methods of cloud classification are used, as follows:

(a) In WMO (1975), division is made into cloud genera with 10 basic characteristic forms, with further subdivision, as required, into:

   (i)   Cloud species (cloud shape and structure);

   (ii) Cloud varieties (cloud arrangement and transparency);

(iii) Supplementary features and accessory clouds (for example, incus, mamma, virga, praecipitatio, arcus, tuba, pileus, velum and pannus);

(iv) Growth of a new cloud genus from a mother-cloud, indicated by the addition of "genitus" to the new cloud and mother-cloud genera – in that order, if a minor part of the mother-cloud is affected – and of "mutatus" if much or all of the mother-cloud is affected, for example, stratocumulus cumulogenitus, or stratus stratocumulomutatus;

(b) A classification is made in terms of the level – high, middle or low – at which the various cloud genera are usually encountered. In temperate regions, the approximate limits are: high, 6–12 km (20 000–40 000 ft); middle, surface–6 km (0–20 000 ft); and low, surface–1.5 km (0–5 000 ft). The high clouds are cirrus, cirrocumulus and cirrostratus; the middle clouds are altocumulus and altostratus (the latter often extending higher) and nimbostratus (usually extending both higher and lower); and the low clouds are stratocumulus, stratus, cumulus and cumulonimbus (the last two often also reaching middle and high levels);

For synoptic purposes, a nine-fold cloud classification is made in each of these three latter divisions of cloud genera, the corresponding codes being designated C_H, C_M and C_L, respectively. The purpose is to report characteristic states of the sky rather than individual cloud types;

(c) Less formal classifications are made as follows:

(i) In terms of the physical processes of cloud formation, notably into heap clouds and layer clouds (or "sheet clouds");

(ii) In terms of cloud composition, namely ice-crystal clouds, water-droplet clouds and mixed clouds.

Most of these forms of cloud are illustrated with photographs in WMO (1987).

Vertical visibility: The maximum distance at which an observer can see and identify an object on the same vertical as him/herself, above or below. Vertical visibility can be calculated from the measured extinction profile, $\sigma(h)$, as stated by WMO (2010). The relationship, however, is less simple than for horizontal visibility, because σ may not be regarded as a constant value. Nevertheless, the $I(h = VV)/I_{I0} = 5\%$ rule can be applied. Taking into account this assumption, the vertical visibility can be expressed in a relation with $\sigma(h)$, in which VV is represented intrinsically, i.e.:

$$\int_{h=0}^{h=VV} \sigma(h)dh = -\ln(5\%) \approx 3$$

(15.1)

See also Part II, Chapter 2, equations 2.6 and 2.7.

15.1.2 **Units and scales**

The unit of measurement of cloud height is the metre or, for some aeronautical applications, the foot. The unit of cloud amount is the okta, which is an eighth of the sky dome covered by cloud.

15.1.3 **Meteorological requirements**

For meteorological purposes, observations are required for cloud amount, cloud type and height of cloud base. For synoptic observations, specific coding requirements are stated in WMO (2011), which is designed to give an optimum description of the cloud conditions from the surface to high levels. From space, observations are made of cloud amount and temperature (from which the height of the cloud top is inferred). Measurements from space can also be used to follow cloud and weather development.

Accuracy requirements are stated in Part I, Chapter 1, Annex 1.E.

15.1.4 Observation and measurement methods

15.1.4.1 *Cloud amount*

Traditionally, measurements of cloud amount were made by visual observation. Instrumental methods are now widely accepted and are used operationally in many applications for determination of cloud amount and height. The cloud amount in each identified layer and the total cloud amount in view of the observation point are determined.

The total cloud amount, or total cloud cover, is the fraction of the celestial dome covered by all clouds visible. The assessment of the total amount of cloud, therefore, consists in estimating how much of the total apparent area of the sky is covered with clouds.

The partial cloud amount is the amount of sky covered by each type or layer of clouds as if it were the only cloud type in the sky. The sum of the partial cloud amounts may exceed both the total cloud amount and eight oktas.

The scale for recording the amount of cloud is that given in Code table 2700 in WMO (2011), which is reproduced below:

Code figure	Meaning	
0	0	0
1	1 okta or less, but not zero	1/10 or less, but not zero
2	2 oktas	2/10–3/10
3	3 oktas	4/10
4	4 oktas	5/10
5	5 oktas	6/10
6	6 oktas	7/10–8/10
7	7 oktas or more, but not 8 oktas	9/10 or more, but not 10/10
8	8 oktas	10/10
9	Sky obscured by fog and/or other meteorological phenomena	
/	Cloud cover is indiscernible for reasons other than fog or other meteorological phenomena, or observation is not made	

15.1.4.2 *Cloud-base height*

The height of the cloud base lends itself to instrumental measurement, which is now widely used at places where cloud height is operationally important. However, the estimation of cloud-base height by human observer is still widespread.

Several types of instruments are in routine operational use, as described in this chapter. An international comparison of several types of instruments was conducted by WMO in 1986, and is reported in WMO (1988). The report contains a useful account of the accuracy of the measurements and the performance of the instruments.

Instrumental measurement of cloud-base height is common and important for aeronautical meteorological services. This is discussed further in Part II, Chapter 2.

15.1.4.3 *Cloud type*

At present, the only method for observing most cloud types is visual. Pictorial guides and coding information are available from many sources, such as WMO (1975, 1987), as well as from publications of National Meteorological Services.

15.2 ESTIMATION AND OBSERVATION OF CLOUD AMOUNT, CLOUD-BASE HEIGHT AND CLOUD TYPE BY HUMAN OBSERVER

15.2.1 Making effective estimations

The site used when estimating cloud variables should be one which commands the widest possible view of the sky, and it should not be affected by fixed lighting which would interfere with observations at night. In making observations at night, it is very important that the observer should allow sufficient time for the eyes to adjust to the darkness.

There are, of course, occasions when it is very difficult to estimate cloud amount, especially at night. The previous observation of cloud development and general knowledge of cloud structure will help the observer to achieve the best possible result. Access to reports from aircraft, if available, can also be of assistance.

15.2.2 Estimation of cloud amount

The observer should give equal emphasis to the areas overhead and those at the lower angular elevations. On occasions when the clouds are very irregularly distributed, it is useful to consider the sky in separate quadrants divided by diameters at right angles to each other. The sum of the estimates for each quadrant is then taken as the total for the whole sky.

Code figure 9 is reported when the sky is invisible owing to fog, falling snow, etc. or when the observer cannot estimate cloud amount owing to darkness or extraneous lighting. During moonless nights, it should usually be possible to estimate the total amount by reference to the proportion of the sky in which the stars are dimmed or completely hidden by clouds, although haze alone may blot out stars near the horizon.

The observer must also estimate the partial cloud amount. There are times, for example, when a higher layer of cloud is partially obscured by lower clouds. In these cases, an estimate of the extent of the upper cloud can be made with comparative assurance in daylight by watching the sky for a short time. Movement of the lower cloud relative to the higher cloud should reveal whether the higher layer is completely covering the sky or has breaks in it.

It should be noted that the estimation of the amount of each different type of cloud is made independently of the estimate of total cloud amount. The sum of separate estimates of partial cloud amounts often exceeds both the total cloud amount, as well as eight eighths.

15.2.3 Estimation of cloud-base height

At stations not provided with measuring equipment, the values of cloud-base height can only be estimated. In mountainous areas, the height of any cloud base which is lower than the tops of the hills of the mountains around the station can be estimated by comparison with the heights of well-marked topographical features as given in a contour map of the district. It is useful to have, for permanent display, a diagram detailing the heights and bearings of hills and the landmarks which might be useful in estimating cloud height. Owing to perspective, the cloud may appear to be resting on distant hills, and the observer must not necessarily assume that this reflects the height of the cloud over the observation site. In all circumstances, the observer must use good judgment, taking into consideration the form and general appearance of the cloud.

The range of cloud-base heights above ground level which are applicable to various genera of clouds in temperate regions is given in the table below and refers to a station level of not more than 150 m (500 ft) above mean sea level. For observing sites at substantially greater heights, or for stations on mountains, the height of the base of the low cloud above the stations will often be less than indicated in the table below.

In other climatic zones, and especially under dry tropical conditions, cloud-base heights may depart substantially from the given ranges. The differences may introduce problems of cloud

classification and increase the difficulty of estimating the height. For instance, when reports on tropical cumulus clouds of an obviously convective origin, with a base well above 2 400 m (8 000 ft) or even as high as 3 600 m (12 000 ft), have been confirmed by aircraft observations. It is noteworthy that, in such cases, surface observers frequently underestimate cloud heights to a very serious degree. These low estimates may be due to two factors, namely either the observer expects the cumulus cloud to be a "low cloud" with its base below 2 000 m (6 500 ft) and usually below 1 500 m (5 000 ft), or the atmospheric conditions and the form of the cloud combine to produce an optical illusion.

When a direct estimate of cloud-base height is made at night, success depends greatly on the correct identification of the form of the cloud. General meteorological knowledge and close observation of the weather are very important in judging whether a cloud base has remained substantially unchanged or has risen or fallen. A most difficult case, calling for great care and skill, occurs when a sheet of altostratus covers the sky during the evening. Any gradual lowering of such a cloud sheet may be very difficult to detect, but, as it descends, the base is rarely quite uniform and small contrasts can often be discerned on all but the darkest nights.

Cloud-base height genera above ground level in temperate regions

Cloud genera	Usual range of height of base[a]		Wider range of height of base sometimes observed, and other remarks	
	(m)	(ft)	(m)	(ft)
Low				
Stratus	Surface–600	Surface–2 000	Surface–1 200	Surface–4 000
Stratocumulus	300–1 350	1 000–4 500	300–2 000	1 000–6 500
Cumulus	300–1 500	1 000–5 000	300–2 000	1 000–6 500
Cumulonimbus	600–1 500	2 000–5 000	300–2 000	1 000–6 500
Middle	(km)			
Nimbostratus	Surface–3	Surface–10 000	Nimbostratus is considered a middle cloud for synoptic purposes, although it can extend to other levels	
Altostratus	2–6	6 500–20 000	Altostratus may thicken with progressive lowering of the base to become nimbostratus	
Altocumulus				
High				
Cirrus			Cirrus from dissipating cumulonimbus may occur well below 6 km (20 000 ft) in winter	
Cirrostratus	6–12	20 000–40 000	Cirrostratus may develop into altostratus	
Cirrocumulus				

Note:
a   For stations over 150 m above sea level, the base of low-level clouds will often be less than indicated.

15.2.4   **Observation of cloud type**

Observation of cloud type is still widely performed by human observers. Pictorial guides and coding information are available from many sources, such as WMO (1975, 1987), as well as from publications of National Meteorological Services.

15.3   **INSTRUMENTAL MEASUREMENTS OF CLOUD AMOUNT**

Multiple types of ground-based operational sensors are available to measure total cloud amount. Measurements from space-borne radiometers in the visible band, supplemented by infrared images, can be used to estimate cloud amounts over wide areas, even though difficulties are often experienced, for example, the inability to distinguish between low stratus and fog. Amounts of low cloud within the range of a ceilometer can be estimated by measuring the proportion of elapsed time occupied by well-identified layers and assuming that these time-averaged results are representative of the spatial conditions around the observing site. For synoptic meteorology, this technique is satisfactory in many cases but for airfield observations it can lead to significant errors in the estimation of cloud amount over the airfield. For automatic weather stations in the United States, a "clustering" technique has been developed using data from ceilometers. Other countries, like Sweden (Larsson and Esbjörn, 1995) and the Netherlands (Wauben, 2002), have introduced similar techniques in their operational observations. Other instruments used to measure cloud amount are pyrometers which may sample in multiple fixed directions and/or scan the sky, and sky cameras that are designed specifically for this purpose.

15.3.1   **Using a laser ceilometer**

Several meteorological services use time series of cloud-base measurements from laser ceilometers (see section 15.4.1) to determine cloud amount. This method has some advantages compared to manual observations. Using a ceilometer gives more consistent results. Also, output can be generated more frequently and there are no problems during night-time. However, there are also some drawbacks and large deviations can occur in situations with high, thin cirrus clouds when the performance of the ceilometer is reduced; when a moist layer is reported as a cloud base by the ceilometer; when a ceilometer detects no cloud base or at the wrong height during precipitation; and when the ceilometer reports a cloud base at the lowest elevation during shallow fog. This method relies on the clouds to move over the field of view of the instrument. Clouds do not always move in that way. Even if clouds do move across the field of view of the ceilometer, these clouds may not be representative of the total sky. Thus, the time series of the cloud base may not always represent the total sky, on which the reporting of cloud cover should be based. Agreements (within 2 okta) between this method and manual observation of total cloud amounts are typically 80%–90%, as found for coastal stations at mid-latitudes (WMO, 2006*a*). However, most differences can be attributed to the limited spatial representativeness of a ceilometer sampling only a small area directly overhead.

Some airports are equipped with several ceilometers and a multiple-ceilometer sky condition algorithm. However, evaluation at an airport has shown only small improvements when using three ceilometers compared to one (Wauben, 2002). This indicates that monitoring three points instead of one is still not sufficient to get a representative value for the entire sky.

In the United States National Weather Service's Automated Surface Observing System (ASOS), the cloud height indicator (laser ceilometer – see section 15.4.1) compiles samples of backscatter return signals every 30 s and determines the height of valid cloud "hits". Every minute, the last 30 min of 30 s data are processed to give double weighting to the last 10 min in order to be more responsive to recent changes in sky condition. The data are then sorted into height "bins".

Each minute, if more than five height bin values have been recorded (during the last 30 min), the cloud heights are clustered into layers using a least-square statistical procedure until there are only five bins remaining (each bin may have many hits in it). These bins, or clusters, are then ordered from lowest to highest height. Following this clustering, the ASOS determines whether clusters can be combined and rounded, depending on height, into meteorologically significant height groups. The resulting bins now are called "layers" and the algorithm selects up to three of these layers to be reported in the METAR/SPECI in accordance with the national cloud layer reporting priority.

The amount of sky cover is determined by adding the total number of hits in each layer and computing the ratio of those hits to the total possible. If there is more than one layer, the hits

in the first layer are added to the second (and third) to obtain overall coverage. For reporting purposes, the ASOS-measured cloud amount for each layer is then converted to a statistical function equivalent to a human observation.

The algorithm also tests for total sky obscuration based on criteria of low surface visibility and a high percentage of "unknown hits" at low levels.

A sky condition algorithm has also been developed for use where cloud formation (or advection) typically occurs in (or from) a known location and results in significant concurrent differences in sky conditions over an airport. This meteorological discontinuity algorithm uses input from two cloud-height indicator sensors. The primary sensor is sited near the touchdown zone of the primary instrument runway. The second sensor is typically sited 3 to 6 km (2 to 4 miles) from the primary sensor, upwind in the most likely direction of the advection, or closer to the fixed source of the unique sky condition. The second cloud-height indicator serves to detect operationally significant differences in sky conditions.

Further details on the ASOS sky condition algorithm and its verification are provided by NOAA (1988) and the United States Government (1999).

15.3.2   **Using a pyrometer**

Pyrometers, or passive infrared radiometers, are basically remote-sensing infrared thermometers (8–14 μm). These can be used to observe elementary solid angles of the sky either by using multiple fixed sensors (for example, four fixed sensors used to sample the whole sky), by scanning the entire sky dome with a single sensor, or by a combination of the two methods (one manufacturer's design has 14 sensors across 180 degrees of elevation from one horizon to the opposite horizon, and a physical mechanism scans the azimuth). The downward thermal emission from the clouds and from the air column between clouds and the instrument is measured and the temperature of each sampled solid angle is derived from a combination of the Planck and the Stefan-Boltzmann laws. The infrared temperature can then be used to provide an indication of cloud presence in each sampled solid angle. The total proportion of sky containing cloud can then be derived and reported as the cloud cover.

Scanning pyrometers avoid the problems of representativeness of the measurement that is present in other methods, depending on the number of points sampled. Also, nocturnal observations are possible. A disadvantage is that fractioned and/or transparent "pixels" are difficult to classify.

15.3.3   **Using a sky camera**

Cameras specifically designed to measure cloud amount exist. They view the total sky using, for example, curved mirrors. The image from the sky is analysed by an algorithm that determines whether a cloud is present in each pixel using the measured colour. The sum of all pixels results in cloud amount.

This method avoids the problems of representativeness of the measurement that can be present in some other methods. Some cameras use daylight and are thus not applicable at night. Cameras measuring in the infrared do not have this disadvantage, but these have a smaller field-of-view and are more expensive. Sky cameras require frequent maintenance in the form of cleaning of the optical surfaces.

15.4 INSTRUMENTAL MEASUREMENT OF CLOUD-BASE HEIGHT

Several methods exist for measuring cloud-base height. They are: using a laser ceilometer, using a rotating beam ceilometer, using a searchlight and using a balloon. The method currently most used is the laser ceilometer. This technique has great advantages over other technologies and should therefore be considered as the most appropriate.

15.4.1 Using a laser ceilometer

15.4.1.1 Measurement method

With the laser ceilometer, the height of the cloud base is determined by measuring the time taken for a pulse of coherent light to travel from a transmitter to the cloud base and to return to a receiver (principle: light detection and ranging, lidar). The output from a laser is directed vertically upwards to where, if there is cloud above the transmitter, the radiation is scattered by the hydrometeors forming the cloud. The major portion of the radiation is scattered upward but some is scattered downward and is focused in the receiver onto a photoelectric detector. The radiant flux backscattered to the receiver decreases with range according to an inverse-square law. The ceilometer (Figure 15.1) generally comprises two units, a transmitter-receiver assembly and a recording unit.

The transmitter and receiver are mounted in a single housing, together with signal detection and processing electronics. The light source is generally a semiconductor laser with a wavelength in the near infrared. The optics of the transmitter are arranged to place the laser source and receiver detector at the focus of a conventional or Newtonian telescope system. The surfaces of the lens are given a suitable quarter-wavelength coating to reduce reflection and to provide high transmission of light. The transmitter aperture is sealed by a glass window that is anti-reflection, coated on its inner surface and angled so that rain will run off it.

The receiver is of similar construction to the transmitter, except that the light source is replaced by a photodiode, and a narrowband optical filter is incorporated. The filter excludes most of the background diffuse solar radiation, thus improving the detection of the scattered laser radiation by day.

The transmitter and receiver can be mounted side-by-side so that the transmitter beam and the receiver field of view begin to overlap at about 5 m above the assembly and are fully overlapped at a few hundred metres. Some systems use the same lens for the transmitted and received radiation, so that this problem is avoided.
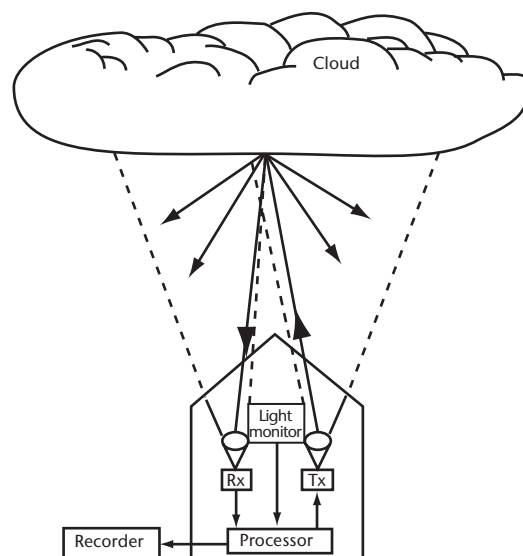
Figure 15.1. Typical laser ceilometer

The housing is provided with heaters to prevent condensation from forming on the optical surfaces, and the humidity within the housing can be reduced by the use of a desiccator. The top of the housing is fitted with a cover hood incorporating optical baffles that exclude direct sunlight.

The output from the detector is separated into sequential "range gates", each range gate representing the minimum detectable height increment. A threshold is incorporated so that the probability of the instrument not "seeing" cloud, or "seeing" non-existent cloud, is remote.

15.4.1.2   *Exposure and installation*

The unit should be mounted on a firm base, with a clear view overhead within a cone of approximately 30° about the vertical. If necessary, a rooftop site can be used with suitable adjustment of reported heights to ground level. Although laser ceilometers in operational use are designed to be "eye safe", care should be taken to prevent the casual observer from looking directly into the transmitted beam.

To reduce the impact of strong reflecting raindrops, the beam with the telescope can be aligned about 5° from the vertical.

15.4.1.3   *Sources of error*

There are four main sources of error as follows:

(a)   Ranging errors: These can occur if the main timing oscillator circuits develop faults, but, in normal operation, errors due to this source can be ignored;

(b)   Verticality of the transmitted/received beams: Provided that the instrument is aligned with the beam at better than 5° from the vertical, errors from this source can be ignored;

(c)   Errors due to the signal-processing system: Because a cloud base is generally diffuse and varies greatly in time and distance, complex algorithms have been developed to estimate a representative cloud-base height from the returned cloud signal. In conditions of fog (with or without cloud above) and during precipitation, serious errors can be generated. Thus, it is important to have an awareness of visibility and precipitation conditions to assess the value of ceilometer information. In conditions of well-defined stratiform cloud (for example, low stratocumulus), measurement errors are controlled solely by the cloud threshold algorithms and can be assumed to be consistent for a particular make of ceilometer;

(d)   Measurement range: Due to the limited power available from the laser, reflected radiation from high altitudes may have such low intensity that it cannot be detected. Therefore, cloud-base height from cirrus clouds may not always be observed.

In operational use and conditions of uniform cloud base, laser ceilometer measurements can be compared routinely with pilot balloon ascents, aircraft measurements and, at night, with cloud searchlight measurements. Intercomparisons of laser ceilometers of different manufacturers have been carried out extensively. During the WMO International Ceilometer Intercomparison (WMO, 1988), for example, several designs of ceilometer were intercompared and comparisons made with rotating-beam ceilometers and pilot-balloon observations. The international intercomparison revealed that, using current technology, laser ceilometers provided the most accurate, reliable and efficient means of measuring cloud-base height from the ground when compared with alternative equipment.

15.4.1.4   *Calibration and maintenance*

Most laser ceilometers are provided with a built-in capability to monitor transmitted output power and guard against serious timing errors. Calibration checks are normally confined
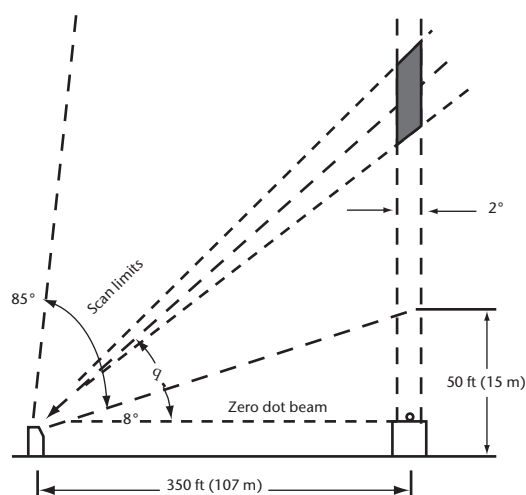
Figure 15.2. A typical rotating-beam ceilometer

to checking both the master oscillator frequency and stability, using external high-quality frequency standards and the output power of the transmitter. Calibration may also be performed by intercomparison (WMO, 1988). Pointing the ceilometer to a target at a known distance (for example, a tower) can be used to confirm the distance measurement of the instrument. Routine maintenance consists typically of cleaning the exposed optics and external covers and of replacing air filters when cooling blowers are provided.

15.4.2 **Using a rotating beam**

15.4.2.1 *Measurement method*

The rotating-beam ceilometer (RBC) involves the measurement of the angle of elevation of a light beam scanning in the vertical plane, at the instant at which a proportion of the light scattered by the base of the cloud is received by a photoelectric cell directed vertically upwards at a known distance from the light source (see Figure 15.2). The equipment comprises a transmitter, a receiver and a recording unit.

The transmitter emits a narrow light beam of a 2° divergence, with most of the emitted radiation on the near infrared wavelengths, that is, from 1 to 3 μm. Thus, the wavelength used is small in comparison with the size of the water droplets in clouds. The light beam is swept in a vertical arc extending typically from 8° to 85° and is modulated at approximately 1 kHz so that, through the use of phase-sensitive detection methods, the signal-to-noise ratio in the receiver is improved.

The receiving unit comprises a photoelectric cell and an angle-of-view restrictor; the restrictor ensures that only light that falls vertically downwards can reach the photoelectric cell. A pen in the recording unit, moving simultaneously with the transmitter beam, records when a cloud signal is received.

15.4.2.2 *Exposure and installation*

The transmitter and receiver should be sited on open, level ground separated by some 100 to 300 m and mounted on firm and stable plinths. It is extremely important that the transmitter scan in the same plane as the receiver. This is achieved by the accurate alignment of the optics and by checking the plane of the transmitter beam in suitable conditions at night.

15.4.2.3 **Sources of error**

Errors in the measurement of cloud-base height using an RBC may be due to the following:

(a) Beamwidth;

(b) Optical misalignment;

(c) Mechanical tolerances in moving parts;

(d) Receiver response.

Since in most designs the volume of intersection of the transmitter and receiver cone is very significant with a cloud height above 500 m, beamwidth-induced errors are generally the most serious. The definition of cloud base given in section 15.1.1 is not an adequate basis for the objective design of ceilometers, thus the algorithms in current use are based on experimental results and comparisons with other methods of estimation. Some RBCs use a "threshold" technique to determine the presence of cloud, while others use a "peak" signal detection scheme. In either case, receiver sensitivity will affect reported cloud heights, giving rise to large errors in excess of stated operational requirements in some circumstances (Douglas and Offiler, 1978). These errors generally increase with indicated height.

Rotating-beam ceilometers are very sensitive to the presence of precipitation. In moderate or heavy precipitation, the instrument can either indicate low cloud erroneously or fail to detect clouds at all. In foggy conditions, the light beam may be dissipated at a low level and the ceilometer can fail to give any useful indication of clouds, even when a low cloud sheet is present.

Comparisons of RBCs and laser ceilometers have been carried out and widely reported (WMO, 1988). These have shown good agreement between the two types of ceilometers at indicated heights up to some 500 m, but the detection efficiency of the RBC in precipitation is markedly inferior.

15.4.2.4 **Calibration and maintenance**

The only maintenance normally undertaken by the user is that of cleaning the transmitter and receiver windows and changing the chart. The outside of the plastic windows of the transmitter and receiver should be cleaned at weekly intervals. A soft, dry cloth should be used and care should be taken not to scratch the window. If the transmitter lamp is replaced, the optical alignment must be checked. The transmitter and receiver levelling should be checked and adjusted, as necessary, at intervals of about one year.

15.4.3 **Using a searchlight**

15.4.3.1 **Measurement method**

Using this method, illustrated in Figure 15.3, the angle of elevation, E, of a patch of light formed on the base of the cloud by a vertically-directed searchlight beam is measured by an alidade from a distant point. If L is the known horizontal distance in metres (feet) between the searchlight and the place of observation, the height, h, in metres (feet) of the cloud base above the point of observation is given as the following:

$$h = L \tan E \qquad (15.2)$$

The optimum distance of separation between the searchlight and the place of observation is about 300 m (1 000 ft). If the distance is much greater than this, then the spot of light may be difficult to see; if it is much less, the accuracy of measuring a height above about 600 m (2 000 ft) suffers. A distance of 250–550 m (800–1 800 ft) is usually acceptable.

15.4.3.2   *Exposure and installation*

It is desirable to have a clear line of sight between the searchlight and the alidade, both of which should be mounted on firm, stable stands. Where there is a difference in the height above the ground between the searchlight and the alidade, a correction must be incorporated in the calculated heights. If a clear line of sight is not possible, any obstruction between the searchlight beam and the alidade should not be higher than 100 feet.

15.4.3.3   *Sources of error*

The largest source of error is due to uncertainty in the measured angle of elevation. Height errors due to small errors of verticality are insignificant.

The absolute error Δh in the derived cloud height due to an error ΔE in the measured elevation is given by the following (L is assumed to be an accurately measured constant):

$$\Delta h = L \cdot \left(1 / \cos^2 E\right) \cdot \Delta E = L \sec^2 E \cdot \Delta E \tag{15.3}$$

with E in radians (1° = π/180 rad). Note that Δh tends to infinity when $E \rightarrow 90°$. If $L = 1\ 000$ ft (300 m) and $\Delta E = 1°$, the value of Δh is 17 ft (6 m) when $h = 1\ 000$ ft (300 m), and Δh is about 450 ft (140 m) when $h = 5\ 000$ ft (1 500 m). The relative error in h is given by:

$$\Delta h / h = 1 / \left(\sin E \cdot \cos E\right) \cdot \Delta E \tag{15.4}$$

with E in radians. $\Delta h/h$ is minimal when $E = 45°$ (or $h = L$).

15.4.3.4   *Calibration and maintenance*

The focusing and verticality of the beam, should, if possible, be checked about once a month because the lamp filament is liable to undergo slight changes in shape with time. When a lamp is replaced, the adjustment for lamp position should be carried out since not all lamps are identical.

The verticality of the beam should be checked during an overcast night with the aid of a theodolite. The check should be made from two positions, one near the alidade and the other at about the same distance away from the searchlight in a direction at right angles to the line joining the searchlight and the alidade (Figure 15.4). The azimuths of the searchlight and of the spot of light on the cloud should be measured as accurately as possible, together with the elevation of the spot of light. If the difference between the azimuth readings is A and the angle of elevation is E, the deviation ϕ of the beam from the vertical is given by:
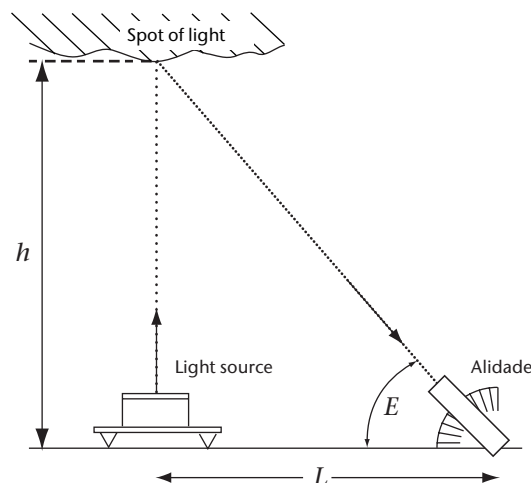
Figure 15.3. Principle of the cloud searchlight method

$$\phi = \arctan\left(\tan A/\tan E\right) \approx A/\tan E$$
$$\left(\text{for } A \approx 1° \text{ or less}\right)$$

(15.5)

If the value of ϕ is more than 1° when viewed from the alidade, or more than 0.5° in the other position, these adjustments should be repeated until the necessary accuracy is obtained.

Focusing can be checked and adjusted on an overcast night by observing the diameter of the light spot on the highest cloud above the instrument. If necessary, the focus should be adjusted to minimize the spot diameter.

15.4.4 Using a balloon

15.4.4.1 *Measurement method*

Cloud height may be measured in daylight by determining the time taken by a small rubber balloon, inflated with hydrogen or helium, to rise from ground level to the base of the cloud. The base of the cloud should be taken as the point at which the balloon appears to enter a misty layer before finally disappearing.

The rate of ascent of the balloon is determined mainly by the free lift of the balloon and can be adjusted by controlling the amount of hydrogen or helium in the balloon. The time of travel between the release of the balloon and its entry into the cloud is measured by means of a stop-watch. If the rate of ascent is n metres per minute and the time of travel is t minutes, the height of the cloud above ground is $n \cdot t$ metres, but this rule must not be strictly followed. Eddies near the launch site may prevent the balloon from rising until some time after it is released. Normally the stop-watch is started on the release of the balloon and, therefore, the elapsed time between when the balloon is released and the moment when it is observed to have left the eddies will need to be subtracted from the total time before determining the cloud height. Apart from eddy effects, the rate of ascent in the lowest 600 m (2 000 ft) or so is very variable.

Although the height of the base of a cloud at middle altitude is sometimes obtained as a by-product of upper wind measurements taken by pilot balloons, the balloon method is mainly applicable to low clouds. Where no optical assistance is available in the form of binoculars, telescope or theodolite, the measurement should not be attempted if the cloud base is judged to be higher than about 900 m (3 000 ft), unless the wind is very light. In strong winds, the balloon may pass beyond the range of unaided vision before it enters the cloud.

Precipitation reduces the rate of ascent of a balloon and measurements of cloud height taken by a pilot balloon should not be attempted in other than light precipitation.
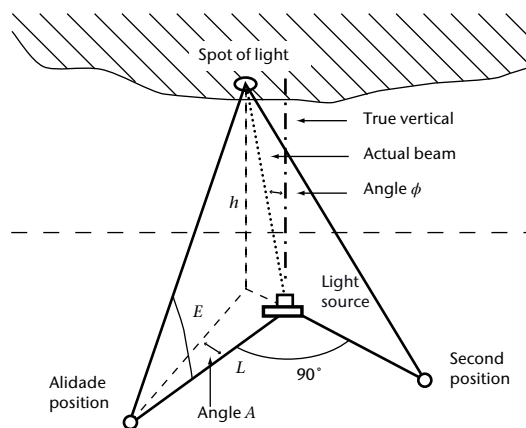
Figure 15.4. Checking the verticality of the searchlight beam

This method can be used at night by attaching an electric light to the balloon. For safety reasons, the use of candle lanterns is strongly discouraged.

15.4.4.2　*Sources of error*

Measurements of cloud-base taken using a height balloon must be used with caution, since the mean rate of ascent of a balloon, especially in the first few hundred metres, may differ appreciably from the assumed rate of ascent (owing to the effects of vertical currents, the shape of the balloon, precipitation and turbulence).

15.5　INSTRUMENTAL MEASUREMENT OF CLOUD TYPE

Observation of cloud type is still generally performed by human observers. Only one automatic method to observe cloud type is known, which is specifically for detecting cumulonimbus/towering cumulus. In this method, data from a precipitation radar and lightning detection network are used. The radar-reflectivity classes and the number of lightning discharges within a certain area are combined to give information on the presence of cumulonimbus and/or towering cumulus.

This is a new method which is used by a few Meteorological Services. The false alarm rate is relatively high (see WMO, 2006*b*).

15.6　OTHER CLOUD-RELATED PROPERTIES

15.6.1　Vertical visibility

Vertical visibility is defined as the maximum distance at which an observer can see and identify an object on the same vertical as him/herself. It can be calculated from the extinction profile of the atmosphere (WMO, 2010). Ceilometers (see sections 15.4.1 and 15.4.2) may provide an estimate of vertical visibility, based on the integrated backscatter energy with range. WMO (1988) showed that this method frequently produces unreliable results. In practice, a vertical visibility report is often given by a ceilometer when the cloud-base requirements are not met, but when reflected light is received from a certain altitude.

_____

REFERENCES AND FURTHER READING

Douglas, H.A. and D. Offiler, 1978: The Mk 3 cloud base recorder: A report on some of the potential accuracy limitations of this instrument. *Meteorological Magazine*, 107:23–32.

Larsson, B. and E. Esbjörn, 1995: *Cloud Cover Algorithm*. SMHI IO-BN 1995-01-11, SMHI, Norrköping, Sweden.

National Oceanic and Atmospheric Administration (NOAA), 1988: *Federal Standard Algorithms for Automated Weather Observing Systems Used for Aviation Purposes*. Office of the Federal Coordinator for Meteorological Services and Supporting Research, United States Department of Commerce, FCM-S5-1988, Silver Spring, MD, United States.

United States Government, 1999: *Automated Surface Observing System*. Air Force Operational Test and Evaluation Center: Final Assessment Report for the Federal Aviation Administration, California, United States.

Wauben, W.M.F., 2002: Automation of visual observations at KNMI: (II) Comparison of automated cloud reports with routine visual observations. In: *Symposium on Observations, Data Assimilation and Probabilistic Prediction*. AMS Annual Meeting, 2002 Report, Orlando, FL, United States.

World Meteorological Organization, 1975: *International Cloud Atlas: Manual on the Observation of Clouds and Other Meteors* (WMO-No. 407), Volume I. Geneva.

———, 1987: *International Cloud Atlas* (WMO-No. 407), Volume II. Geneva.

———, 1988: *WMO International Ceilometer Intercomparison* (D.W. Jones, M. Ouldridge and D.J. Painting). Instruments and Observing Methods Report No. 32 (WMO/TD-No. 217). Geneva.

———, 2006*a*: Status, evaluation and new developments of the automated cloud observations in the Netherlands (W. Wauben, H. Klein Baltink, M. de Haij, N. Maat and H. The). *Paper presented at the WMO Technical Conference on Meteorological and Environmental Instruments and Methods of Observation (TECO-2006)*. Instruments and Observing Methods Report No. 94 (WMO/TD-No. 1354). Geneva.

———, 2006*b*: Status of the automatic observation on aerodrome and ongoing improvements in France (M. Leroy). *Paper presented at the WMO Technical Conference on Meteorological and Environmental Instruments and Methods of Observation (TECO-2006)*. Instruments and Observing Methods Report No. 94 (WMO/TD-No. 1354). Geneva.

———, 2010: *Manual on the Global Observing System* (WMO-No. 544), Volume I. Geneva.

———, 2011: *Manual on Codes* (WMO-No. 306), Volume I.1. Geneva.

———, 2014: *Guide to Meteorological Observing and Information Distribution Systems for Aviation Weather Services* (WMO-No. 731). Geneva.

CHAPTER CONTENTS

CHAPTER 16. MEASUREMENT OF ATMOSPHERIC COMPOSITION

16.1 GENERAL

The main purpose of this chapter is to introduce readers (particularly those who are new to these measurements) to methods and specific techniques used for measuring various components of atmospheric composition and a number of related physical parameters. This is often accompanied by measurements of basic meteorological variables, as introduced in the preceding chapters. Within WMO, the Global Atmosphere Watch (GAW) Programme was established to coordinate atmospheric composition and related physical parameter measurements taken by WMO Member countries. For further practical details on measurement activities, see the GAW reports and other references listed at the end of the chapter.

The need to understand and identify scientifically sound measures to control the increasing influence of human activity on the global atmosphere forms the rationale of the GAW Programme (WMO, 2007*b*). The grand challenges addressed by GAW include:

(a) Stratospheric ozone depletion and the increase of ultraviolet (UV) radiation at the Earth's surface;

(b) Changes in the weather and climate related to human influence on atmospheric composition, particularly greenhouse gases, and the impact on ozone and aerosols, due also to natural processes;

(c) Risk reduction of air pollution on human health and issues involving long-range transport and deposition of air pollution.

In addition, measurements of atmospheric composition are essential for understanding the radiation budget of the atmosphere and improving numerical weather prediction.

The GAW monitoring system focuses on six classes of variables:

(a) Ozone: column (total) ozone and ozone vertical profiles with a focus on the stratosphere and upper troposphere;

(b) Greenhouse gases: carbon dioxide CO_2 (including $\Delta^{14}C$, $\delta^{13}C$ and $\delta^{18}O$ in CO_2, and oxygen/nitrogen (O_2/N_2) ratios), methane CH_4 (including $\delta^{13}C$ and δD in CH_4), nitrous oxide (N_2O) and halogenated compounds (SF_6);

(c) Reactive gases: surface and tropospheric ozone (O_3), carbon monoxide (CO), volatile organic compounds (VOCs), nitrogen oxides (NO_x), sulphur dioxide (SO_2) and molecular hydrogen (H_2);

(d) Atmospheric wet deposition (focused largely on major ions);

(e) Ultraviolet radiation;

(f) Aerosols (including physical properties, size distribution and chemical composition).

A number of ancillary parameters are recommended for measurement at GAW stations:

(a) Solar radiation;

(b) Major meteorological parameters;

(c) Natural radioactivity including krypton-85, radon and some other radionuclides.

Due to the low mixing ratios of atmospheric trace constituents, the instruments and methods used for the quantitative and qualitative determination of atmospheric constituents are complex and sometimes difficult to operate. Small errors, for example in spectral signatures, or cross-sensitivities to other compounds can easily confound the accuracy of atmospheric composition measurements. Therefore, besides correct operation, regular calibration of the equipment, participation in intercomparison exercises, station audits and personnel training are essential for accurate and reliable measurements. Obtaining reliable and high-quality results for most of the measurements described here is not feasible without the close involvement of specialist staff at a professional level. The main principles of the quality assurance of atmospheric composition observations within GAW are described in section 16.1.4.

16.1.1   **Definitions/descriptions**

Depending on the measurement principle and instrument platform, three types of measurements are routinely performed and reported, namely:

(a)   Near-surface atmospheric content (from monitoring stations or mobile platforms such as ships, cars or trains);

(b)   Total atmospheric column content (from surface- or space-based remote-sensing);

(c)   Vertical concentration profiles (from aircraft, balloons, rockets, surface-based remote-sensing or satellite instruments).

Near-surface atmospheric content refers to the results of (continuous or discrete) measurements of a particular component's quantity in an atmospheric layer of a few tens of metres above the surface at a particular location on the Earth's surface. Results of surface measurements are commonly given in units of partial pressure, concentration, mixing ratio or mole fraction. The use of units that are not part of the International System of Units (SI) is strongly discouraged.

Total atmospheric column refers to the total amount of a particular substance contained in a vertical column extending from the Earth's surface to the upper edge of the atmosphere. Commonly used units of total ozone are (i) column thickness of a layer of pure ozone at standard temperature and pressure conditions of 273.15 K and 101.325 kPa, respectively, and (ii) vertical column density (total number of molecules per unit area in an atmospheric column). For the other atmospheric constituents, vertical column density or column-averaged abundances are used. It is also common to report the partial column content of a substance, for example the tropospheric column content of NO_x. Here, the vertical column that is integrated extends from the Earth's surface to the tropopause.

The *vertical concentration profile* expresses the variation of the content of a trace compound in the atmosphere (given in the same units as near-surface content, namely partial pressure, concentration, number density, mixing ratio or mole fraction) as a function of height or ambient pressure.

Observations of atmospheric composition include gaseous composition, aerosol and precipitation chemistry. The characteristics of the precipitation chemical composition are given in section 16.5. The variables describing aerosols (physical and chemical properties) are listed in section 16.6.

16.1.2   **Units and scales**

The following units are used to express the results of atmospheric trace compound observations:

Number of molecules per unit area: represents the column abundance of atmospheric trace compounds. Still widely used is the Dobson unit (DU), which corresponds to the number of

molecules of ozone required to create a layer of pure ozone 10^{-5} m thick at standard temperature and pressure (STP). Expressed another way, 1 DU represents a column of air containing about $2.6868 \cdot 10^{16}$ ozone molecules for every square centimetre of area at the base of the column.

Milliatmosphere centimetre (m-atm-cm): A measure of total ozone equal to a thickness of 10^{-3} cm of pure ozone at STP (1 m-atm-cm is equivalent to 1 DU).

Mole fractions of substances in dry air (dry air includes all gaseous species except water vapour (H_2O):

> μmol/mol = 10^{-6} mole of trace substance per mole of dry air
> nmol/mol = 10^{-9} mole of trace substance per mole of dry air
> pmol/mol = 10^{-12} mole of trace substance per mole of dry air

Dry mole fraction requires either drying air samples prior to measurement or correcting the measurement for water vapour. When drying is impossible or the correction would add substantial uncertainty to the measurement, wet mole fractions can be reported instead. This must be clearly indicated in the metadata of the observational record.

The appropriate unit for expressing amount of substance is dry-air mole fraction, reported as ppm (parts per million, i.e. μmol/mol), ppb (parts per billion, i.e. nmol/mol) or ppt (parts per trillion, i.e. pmol/mol). A "v" has often been appended to these units to indicate mixing ratio by volume. When reporting mole fractions as volume mixing ratios, one assumes the atmosphere to be an ideal gas. Deviations from the ideal under GAW conditions can be large (such as for CO_2), so the use of mole fraction is strongly preferred because it does not require an implicit assumption of ideality of the gases and, more importantly, because it is also applicable to condensed-phase species. In general, the use of SI units is highly recommended.

Isotope or molecular ratios:

Atmospheric molecules can be present in different isotopic configurations.[1] Isotope ratio data are expressed as deviations from an agreed upon reference standard using the delta notation:

$$\delta = \left(R_{\text{sample}} / R_{\text{reference}} - 1 \right), \text{with } R = \left[\text{heavy isotope} \right] / \left[\text{light isotope} \right] \qquad (16.1)$$

δ-Values are expressed in multiples of 1 000 (‰ or per mil).

The international reference scale (i.e. the primary scale) for $\delta^{13}C$ is Vienna Pee Dee Belemnite (VPDB). NBS 19 and LSVEC (Coplen et al., 2006) are the primary international reference materials defining the VPDB scale. For $\delta^{18}O$, multiple scales are in use (VPDB, Vienna Standard Mean Ocean Water (VSMOW), air-O_2).

The delta notation is also used to express relative abundance variations of O_2/N_2 (and argon/nitrogen (Ar/N_2)) ratios in air:

$$\delta \left(O_2 / N_2 \right) = \left(R_{\text{sample}} / R_{\text{standard}} - 1 \right), \text{with } R = O_2 / N_2 \qquad (16.2)$$

The respective international air standard is not yet established. The Scripps Institution of Oceanography (SIO) local O_2/N_2 scale, based on a set of cylinders filled at the Scripps Pier, is the most widely used scale.

$\delta(O_2/N_2)$ values are expressed in multiples of 10^6 or per meg.

Precipitation chemistry observations include measurements of several parameters which are described in more detail in section 16.5. The following units are used:

---

[1] CO_2, for example, mostly consists of $^{12}C^{16}O^{16}O$, while the smaller abundance higher-mass isotopologues from mass 45 up to mass 49 ($^{13}C^{16}O^{16}O$, $^{14}C^{16}O^{16}O$, or $^{12}C^{18}O^{16}O$, the corresponding ^{17}O siblings and the mixed-isotope species) are also found in the atmosphere.

(a)   pH measurements are expressed in units of acidity defined as: pH = –$\log_{10}$ [H$^+$], where [H$^+$] is expressed in mole L^{-1} ;

(b)   Conductivity is expressed in μS cm^{-1} (microsiemens per centimetre), a unit commonly used for measuring electric conductivity;

(c)   Acidity/alkalinity is expressed in μmole L^{-1} (micromole per litre);

(d)   Major ions content is expressed in mg L^{-1} (milligram per litre).

Aerosol observations of volumetric quantities, i.e. the amount of substance in a volume of air, are reported for STP. These may refer to a particle number concentration (cm^{-3}), an area concentration (m^2 m^{-3}, or m^{-1}) or a mass concentration (μg m^{-3}). Aerosol optical depth is a dimensionless quantity.

16.1.3   **Measurement principles and techniques**

The existing techniques for atmospheric chemical composition measurements can be separated into three main groups: passive sampling, active sampling and remote-sensing techniques. Essentially, active techniques draw the air sample through the detector or sampling device by a pump, whereas passive techniques use the diffusion of air to the sampling device. In remote-sensing techniques, the analysed air volume and the detector are at different locations. Total or partial column measurements are possible only with remote-sensing techniques.

In the case of active sampling, measurements can either be done continuously (or at least quasi-continuously with short integration times)[2] or samples can be collected or specially prepared (in glass or stainless steel cylinders, on sorbent substrates or filters) and analysed offline in specialized laboratories. The collection of discrete samples entails the storage of samples. During this time, flask properties may influence the composition of the sample due to chemical or surface effects or permeation through sealing polymers. This demands careful tests of the sampling containers.

The analytical techniques most commonly used (and recommended in the GAW Programme) for detecting and quantifying atmospheric trace constituents can be summarized as follows:

(a)   *Spectroscopic methods* refer to the measurement of changes in radiation intensity due to absorption, emission, photoconductivity or Raman scattering of a molecule or aerosol particle as a function of wavelength. Spectral measurement devices are referred to as spectrometers, spectrophotometers, spectrographs or spectral analysers. Spectral measurements can be performed in different parts of a spectrum depending on the component to be measured, or on several individual wavelengths. As absorption lines are different for molecules with different isotopic composition, and line shapes depend on the bulk composition of the gas, care should be taken to ensure that reference gases have similar properties to the analysed atmospheric air.

(b)   *Gas chromatography* (GC) is a physical method of separation that distributes components to separate between two phases, one stationary (stationary phase), the other (the mobile phase) moving in a definite direction. There are numerous chromatographic techniques and corresponding instruments. To be suitable for GC analysis, a compound must have sufficient volatility and thermal stability. Gas chromatography involves a sample being vapourized and injected onto the head of the chromatographic column. The sample is transported through the column by the flow of inert, gaseous mobile phase. The column itself contains a liquid stationary phase which is adsorbed onto the surface of an inert solid. A chromatography detector is a device used to visualize components of the mixture being eluted off the chromatography column. There are two general types of detectors: destructive and non-destructive. The destructive detectors, such as a flame ionization detector (FID), perform continuous transformation of the column effluent (burning,

---

2   This is, for example, common practice in gas chromatography measurements.

evaporation or mixing with reagents) with subsequent measurement of some physical property of the resulting material (plasma, aerosol or reaction mixture). The non-destructive detectors, such as an electron capture detector (ECD), are directly measuring some property of the column effluent (for example UV absorption) and thus allow for the further analyte recovery.

(c) *Mass spectrometry* (MS) is an analytical technique that produces spectra of the masses of the molecules comprising a sample of material. The spectra are used to determine the elemental composition of a sample, the masses of particles and of molecules, and to elucidate the chemical structures of molecules. Mass spectrometry works by ionizing chemical compounds to generate charged molecules or molecule fragments and measuring their mass-to-charge ratios. In a number of instruments mass spectrometry can be used as a detector method for gas chromatography.

Detection methods of gases and aerosols can be different and based on different physical phenomena. Details on the detection methods applicable to different gases and aerosol properties are summarized in the sections below.

The measurement techniques of the main compounds observed under the GAW Programme are briefly described in this chapter, while comprehensive measurement guidelines can be found in the specialized GAW reports, cited in individual sections. In the cases where GAW measurement guidelines or standard operating procedures are not available, links are provided to the information necessary to carry out the respective measurements. The background for the measurements of individual components can be found in the WMO Global Atmosphere Watch (GAW) Strategic Plan: 2008–2015 (WMO, 2007b) and its addendum (WMO, 2011b).

Satellite remote-sensing of the atmospheric species mentioned below is treated separately in Part III, Chapter 5.

16.1.4 **Quality assurance**

The objectives of the GAW quality assurance (QA) system are to ensure that data reported by stations are consistent, of known and adequate quality, supported by comprehensive metadata, and regionally or globally representative with respect to spatial and temporal distribution.

The principles of the GAW QA system apply to each measured variable and include:

(a) Defined data quality objectives (including tolerable levels of uncertainty in the data, completeness, compatibility requirements, etc.);

(b) Establishment of harmonized recommendations on measurement techniques and quality control (QC) procedures to reach data quality objectives (measurement guidelines and standard operating procedures);

(c) Network-wide use of only one reference standard or scale (primary standard). In consequence, there is only one institution that is responsible for this standard;

(d) Traceability to the primary standard of all measurements made by GAW stations;

(e) Use of detailed logbooks for each parameter containing comprehensive meta information related to the measurements, maintenance, and quality control actions;

(f) Regular independent assessments (including audits and comparison campaigns);

(g) Timely submission of data and associated metadata to the responsible World Data Centre as a means of permitting independent review of data by a wider community.

The following Global Climate Observing System (GCOS) monitoring principles apply also to the GAW observations:

(a)   The impact of new systems or changes to existing systems should be assessed prior to implementation;

(b)   A suitable period of overlap for new and old observing systems should be required;

(c)   Uninterrupted station operations and observing systems should be maintained.

The GAW QA system further recommends the adoption and use of internationally accepted methods and vocabulary to describe uncertainty in measurements.

Five types of central facilities (see the annex) dedicated to the six groups of measurement variables (see section 16.1) are operated by WMO Members and form the basis of the quality assurance and data archiving system. These include:

(a)   Central Calibration Laboratories (CCLs), which host primary standards and scales;

(b)   World/Regional Calibration Centres (WCCs/RCCs), which coordinate intercomparison campaigns, help with instrument calibration and perform station/lab audits;

(c)   Quality Assurance/Science Activity Centres (QA/SACs), which provide technical and scientific support and coordinate cooperation between the central facilities and GAW stations;

(d)   World Data Centres (WDCs), which mainly ensure dissemination and easy access of GAW data and secure the data through appropriate data archiving.

The work of the central facilities on the quality assurance of the GAW observations is supported by respective scientific advisory groups, whose tasks include assisting in the development of measurement procedures and guidelines, data quality objectives and, when applicable, standard operating procedures, reviewing new measurement techniques and making recommendations about their applicability for the GAW observations.

16.2   (STRATOSPHERIC) OZONE MEASUREMENTS

16.2.1   Ozone total column

Measurements of total ozone are possible using remote-sensing techniques only. The most precise information on total ozone and its changes at individual sites can be obtained by measurements from the ground, for example by solar spectroscopy in the wavelength region of 300–340 nm. Within the GAW Programme, Dobson spectrophotometers (designed for manual operation) and Brewer spectrophotometers (designed for automatic operation) are used as the instruments for routine total ozone observations, thus providing two independent networks.

Details of the total ozone measurements with the Dobson spectrometer and their quality assurance are provided in WMO (2008c). Total ozone observations are made with this instrument by measuring the relative intensities of selected pairs of ultraviolet wavelengths, called the A, B*, C, C', and D wavelength pairs, emanating from the sun, moon or zenith sky. The A wavelength pair, for example, consists of the 3 055 Å (Ångström units, 1 Å = 0.1 nm) wavelength that is highly absorbed by ozone, and the more intense 3 254 Å wavelength that is relatively unaffected by ozone. Outside the Earth's atmosphere, the relative intensity of these two wavelengths remains essentially fixed. In passing through the atmosphere to the instrument, however, both wavelengths lose intensity because of scattering of the light by air molecules and dust particles; additionally, the 3 055 Å wavelength is strongly attenuated while passing through the ozone layer whereas the attenuation of the 3 254 Å wavelength is relatively weak. Therefore, the relative intensity of the A wavelength pair as seen by the instrument varies with the amount of

ozone present in the atmosphere since, as the ozone amount increases, the observed intensity of the 3 055 Å wavelength decreases, whereas the intensity of the 3 254 Å wavelength remains practically unaltered. Thus, by measuring the relative intensities of suitably selected pair wavelengths with the Dobson instrument, it is possible to determine how much ozone is present in a vertical column of air extending from ground level to the top of the atmosphere in the neighbourhood of the instrument. The result is expressed in terms of a thickness of a layer of pure ozone at STP.

The measurement principle of the Brewer spectrometer is similar to that of the Dobson instrument. The operating procedures are provided by the producing company at http://www.kippzonen.com/?productgroup/26142/Brewer+Spectrophotometer.aspx. The recommendations for the GAW network are available from the World Ozone and Ultraviolet Radiation Data Centre (WOUDC) at http://woudc.org/archive/Documentation/SOP_Documents/brewerspectrophotometer_sop-june2008.pdf.

Results of comparisons of Brewer and Dobson instruments, as well as recommendations on the operation of the Brewer instruments, are provided in the reports of the biennial WMO consultations on Brewer ozone and UV spectrometer operation, calibration and data processing (for example, see WMO, 2008*a*).

The world (primary) standard instruments of Brewer and Dobson networks are calibrated by the Langley plot method performed at the Mauna Loa Observatory in Hawaii (every 2–4 years); regional standards are calibrated against the primary standard every 2–3 years; and the station instruments are calibrated by side-by-side calibration with the standard instruments every 4 years. An extension of these calibration cycles up to 5–6 years for station instruments is currently in the pipeline. In addition, three successful Langley plot campaigns at the Izaña Atmospheric Observatory on Tenerife with primary and regional standard Dobson instruments have proved the suitability of that location and facility for this absolute calibration method.

Complementary measurements of total ozone are provided by the differential optical absorption spectroscopy (DOAS) type UV/visible spectrometers that also allow detection of various minor trace gases (such as NO_2 and BrO). The French instrument is called Système d'Analyse par Observations Zénithales (SAOZ), but it is based on the same principle as DOAS. These instruments are part of the measurement suites within the Network for the Detection of Atmospheric Composition Change (NDACC, http://www.ndsc.ncep.noaa.gov/instr/). Compared to the more established Brewer/Dobson network, the measurement and analysis procedures for DOAS type instruments are less standardized, but regular comparison campaigns have been carried out. Other instruments providing total ozone measurements from the ground (Russian filter instruments or those of the DOAS/SAOZ type) are not operated under the same data QA/QC programme as Dobson and Brewer instruments. The Russian and other filter instruments are not independently calibrated, but are tied to either Dobson or Brewer instruments. Data quality of all individual total ozone series deposited at WOUDC needs to be documented for the users.

16.2.2   Ozone profile measurements

Measurements of the vertical ozone distribution are possible by both active and remote-sensing methods.

16.2.2.1   *Umkehr method*

Dobson and Brewer spectrometers can be used for the measurement of vertical ozone distribution utilizing the Umkehr method (WMO, 2008*c*). The reduction of the Umkehr measurement to an ozone profile requires a complex algorithm that includes knowledge of the radiative properties of the real atmosphere. As this knowledge changes, the algorithm will change. A standard Umkehr observation consists of a series of C-pair wavelength measurements made on a clear zenith sky during morning or afternoon. The measurements are commenced a few minutes before sunrise and continued until the sun is at an elevation of not less than about 20 degrees, or commenced in the afternoon when the sun is at an elevation of not less than

about 20 degrees and continued until shortly after sunset. The zenith sky must be free from clouds for a period of 30 min to 1 h near sunrise or sunset. This is especially true at low latitude stations where the sun rises or sets rapidly. At other times, it is desirable that the zenith sky be cloudless, but permissible that clouds cross it periodically when measurements are not made. Umkehr observations cannot be made at a polar station or at high latitude stations during summertime when the sun does not sink below the horizon.

To be able to compute the vertical distribution of ozone, it is necessary to know the total amount of ozone present at the time of observation. Several total ozone measurements must, therefore, be made during the morning or afternoon, particularly if the ozone amount is changing fairly rapidly.

The resulting ozone profile derived from reduction of these measurements is quite dependent on the algorithm used. The method of Umkehr data analysis was originally developed by Götz et al. (1934). Later the method was refined by Ramanathan and Dave (1957), Mateer and Dütsch (1964), and Mateer and DeLuisi (1992). The Umkehr algorithm is described by Petropavlovskikh et al. (2005), and updated information is available from http://www.esrl.noaa.gov/gmd/ozwv/umkehr/.

16.2.2.2 *Ozonesonde measurements*

Ozone measurement from light balloons (ozonesondes) is an active method for measuring the ozone vertical distribution in the atmosphere. Other active methods for ozone mole fraction measurements (that are used on aircraft platforms) are described in the section on reactive gases (see section 16.4.1).

Ozonesondes are small, lightweight and compact balloon-borne instruments, developed for measuring the vertical distribution of atmospheric ozone up to an altitude of about 30–35 km. The sensing device is interfaced to a standard meteorological radiosonde for data transmission to the ground station and can be flown on a small rubber balloon. Three major types of ozonesondes – the Brewer-Mast sonde, the electrochemical concentration cell and the carbon iodine cell – are nowadays in use. Each sonde type has its own specific design.

The flight package typically weighs about 1 kg in total and can be flown on small weather balloons. Normally data are taken during ascent, at a rise rate of about 5 m/s, to a balloon burst altitude of 30–35 km. The inherent response time of the ozonesonde is 20–30 s such that the effective height resolution of the measured vertical ozone profile is typically 100–150 m.

The principles of ozonesonde operations and an overview of the different aspects of quality assurance and quality control for ozonesonde measurements in GAW are given in detail in WMO (2014).

16.2.2.3 *Other measurement techniques*

Ozone profile measurements can also be obtained by other instruments operated under the umbrella of NDACC. Lidar and microwave measurements are part of the NDACC suite of measurements and are valuable for assessing ozone trends in the upper stratosphere and for validating satellite measurements in the upper atmosphere. The disadvantage of microwave ozone measurements is the rather poor vertical resolution, but they have a potential to measure up to the mesopause region. The combination of sonde, Umkehr, lidar and microwave data from the ground is important for assessing the quality of the ozone profile measurements from space.

16.2.3 **Aircraft and satellite observations**

Ozone in the atmosphere is also measured by instruments located on board aircraft and space satellites. The airborne observations are usually made by in situ photometers sampling the air in the troposphere and lower stratosphere during a flight. The measurements are used mostly

in research campaigns on atmospheric chemistry, but there have also been long-term projects using commercial aircraft, such as MOZAIC (measurement of ozone, water vapour, carbon monoxide and nitrogen oxides aboard airbus in-service aircraft), CARIBIC (Civil Aircraft for the Regular Investigation of the Atmosphere Based on an Instrument Container, http://www.caribic-atmospheric.com/), and recently IAGOS (In-service Aircraft for a Global Observing System).

Large-scale monitoring of atmospheric ozone is performed by remote-sensing instruments from satellites. These programmes can be divided according to lifetime: the long-term operational monitoring systems that generate large (global) datasets used for trend analyses and for operational mapping of ozone, and the temporary experimental missions.

Satellite observations can be grouped according to the radiation-detection technology used for the instruments and the retrieval schemes applied for the derivation of ozone column density or concentration from the measured radiances. While nadir-viewing instruments are primarily used for column observations and coarse vertical profiling, limb sounding instruments are able to measure vertical profiles of ozone at high vertical resolution by solar, lunar or stellar occultation or by observing limb scatter and emission through the atmospheric limb (Tegtmeier et al., 2013; Sofieva et al., 2013).

16.3 GREENHOUSE GASES

All greenhouse gases are reported in dry mole fractions on the most recent scales summarized in WMO (2012*b*) (status as of 2013) and reviewed every two years at the WMO/IAEA Meetings on Carbon Dioxide, Other Greenhouse Gases and Related Measurement Techniques (GGMT). The primary reference for greenhouse gases is a set of cylinders of natural air with known mole fractions of the studied gases. The primary scale is transferred to station working standards through secondary and tertiary gas standards in cylinders.

16.3.1 Carbon dioxide (including $\Delta^{14}C$, $\delta^{13}C$ and $\delta^{18}O$ in CO_2, and O_2/N_2 ratios)

Carbon dioxide is usually measured by active methods in the atmospheric boundary layer.

Most of historical background atmospheric CO_2 measurements are made with non-dispersive infrared (NDIR) gas analysers, but a few programmes use a gas chromatographic method. The GC method requires separation of CO_2 from other gases in the air sample, reduction of this CO_2 over a catalyst with H_2 to CH_4, and detection of the CO_2-derived CH_4 using a flame ionization detector. Chromatographic peak responses from samples are compared to those from standards with known CO_2 mole fractions to calculate the CO_2 mole fraction in the sample. Gas chromatography techniques are limited to a measurement frequency of one sample every few minutes. Non-dispersive infrared instruments are based on the same principle that makes CO_2 a greenhouse gas: its ability to absorb infrared radiation. They measure the intensity of infrared radiation passing through a sample cell relative to radiation passing through a reference cell. It is not necessary to know the CO_2 mole fraction of the reference cell gas. Sample air, pumped from inlets mounted well away from the measurement building, and standard gas flow alternately through the sample cell. A difference in CO_2 concentration between sample and reference gases (or standard and reference gases) contained in the two cells results in a voltage that is recorded by the data acquisition system.

Most of the new instalments are performing the measurements of CO_2 with laser-based optical spectroscopic methods, like Fourier transform infrared (FTIR) absorption spectroscopy or high-finesse cavity absorption spectroscopy, which includes cavity ring-down spectroscopy (CRDS) and off-axis integrated cavity output spectroscopy (ICOS). Advantageous properties of these techniques are reduced calibration demands due to better linearity and detector response stability.

Carbon dioxide abundances are reported in dry-air mole fraction, μmol mol^{-1}, abbreviated ppm, on the WMO CO_2 Mole Fraction Scale (WMO CO_2 X2007 scale, status as of 2013). Water vapour

affects the measurement of CO_2 in two ways: (i) H_2O also absorbs infrared radiation and can interfere with the measurement of CO_2; (ii) H_2O occupies volume in the sample cell, while standards are dry. At warm, humid sites, 3% of the total volume of air can be H_2O vapour. The impact of water vapour on the CO_2 measurement must therefore be considered. Drying to a dewpoint of –50 °C is sufficient to eliminate interferences. The novel optical spectroscopic methods often allow simultaneous determination of the H_2O vapour content, making it, in principle, possible to correct for dilution due to H_2O and spectroscopic effects. However, current best practice (see WMO, 2012*b*) still recommends sample drying while the determination of dry-air mole fractions without sample drying and the subsequent correction are under review.

An alternative method of CO_2 measurement that is generally applicable to many other trace gases is the collection of discrete air samples in vacuum-tight flasks. These flasks are returned to a central laboratory where CO_2 is determined by a NDIR, GC or other instrument. This method is used where low-frequency sampling (for example, once a week) is adequate to define CO_2 spatial and temporal gradients, and for comparison with in situ measurements as a quality-control step. This sampling strategy has the advantage that many species can be determined from the same sample.

Measurements of O_2/N_2 ratios and stable isotopes of CO_2 ($\delta^{13}C$ and $\delta^{18}O$) help to partition carbon sources and sinks between the ocean and biosphere. Isotopic measurements are often made from the same discrete samples used for CO_2 mole fraction measurements. Isotopic standards are maintained by the International Atomic Energy Agency (IAEA), but measurement sites are part of the GAW CO_2 network.

A measurement method for stable isotope determination is isotope ratio mass spectrometry (IRMS), a specialization of mass spectrometry in which mass spectrometric methods are used to measure the relative abundance of isotopes in a given sample. The measurement set-up is described by the GAW Central Calibration Laboratory for stable isotopes at the Max Planck Institute for Biogeochemistry in Jena, Germany (http://www.bgc-jena.mpg.de/service/iso_gas_lab/pmwiki/pmwiki.php/IsoLab/Co2InAir). In recent years, optical analysers that report mole fractions of individual isotopologues have become increasingly available and are now in routine use. Many of these instruments can provide isotopic ratios with a repeatability of about 0.05‰ for $\delta^{13}C$ of atmospheric CO_2 and are valuable for continuous measurements. Unlike with mass spectrometric techniques, δ values from such instruments are often calculated from the ratio of individual measured mole fractions using tabulated absorption line strengths and are not from direct measurements of a standard material. The reference isotopic abundance is normally taken from a spectral parameter database (typically the high-resolution transmission molecular absorption database, HITRAN) that is used in the analysis, and this does not provide a common scale such as VPDB or the Jena Reference Air Set (JRAS). Some corrections applicable to mass spectrometric methods, such as those for ^{17}O and N_2O, are not required, but other corrections, such as for interference from other atmospheric components and instrument fluctuations, may be required depending on the method used to calculate the isotopic δ values from individual mole fractions. It is important to realize compatibility between the techniques before measurement results are made public.

Measurements of the changes in atmospheric O_2/N_2 ratio are useful for constraining sources and sinks of CO_2 and testing land and ocean biogeochemical models. The relative variations in O_2/N_2 ratio are very small but can now be observed by at least six analytical techniques. These techniques can be grouped into two categories: (i) those which measure O_2/N_2 ratios directly (mass spectrometry and gas chromatography), and (ii) those which effectively measure the O_2 mole fraction in dry air (interferometric, paramagnetic, fuel cell, vacuum-ultraviolet photometric). A convention has emerged to convert the raw measurement signals, regardless of technique, into equivalent changes in mole ratio of O_2 to N_2. For mole-fraction type measurements, this requires accounting for dilution due to variations in CO_2 and possibly other gases. If synthetic air is used as a reference material, corrections may also be needed for differences in Ar/N_2 ratio. There are currently about 10 laboratories measuring O_2/N_2 ratios. The O_2/N_2 reference is typically tied to natural air delivered from high-pressure gas cylinders. As there is no common source of reference material, each laboratory has employed its own

reference. There is currently no CCL for O_2/N_2. Hence it has not been straightforward to report measurements on a common scale, but several laboratories report results on a local implementation of the Scripps scale. There are no named versions yet.

The practice of basing O_2/N_2 measurements on natural air stored in high-pressure cylinders appears acceptable for measuring changes in background air, provided the cylinders are handled according to certain best practices, including orienting cylinders horizontally to minimize thermal and gravitational fractionation. Nevertheless, improved understanding of the source of variability of measured O_2/N_2 ratios delivered from high-pressure cylinders is an important need of the community. An independent need is the development of absolute standards for O_2/N_2 calibration scales to the level of 5 per meg or better.

Atmospheric $^{14}CO_2$ measurements are usually reported in $\Delta^{14}C$ notation, the per mil deviation from the absolute radiocarbon reference standard, corrected for isotopic fractionation and for radioactive decay since the time of collection. For atmospheric measurements of $\Delta^{14}C$ in CO_2, two main sampling techniques are used: high-volume CO_2 absorption in basic solution or by molecular sieve, and whole-air flask sampling (typically 1.5–5 L flasks). Two methods of analysis are used: conventional radioactive counting and accelerator mass spectrometry. The current level of measurement uncertainty for $\Delta^{14}C$ in CO_2 is 2‰–5‰, with a few laboratories at slightly better than 2‰. Recommendations on calibration are provided in WMO (2012*b*).

Recommendations on quality assurance of CO_2 measurements (including $\Delta^{14}C$, $\delta^{13}C$ and $\delta^{18}O$ in CO_2, and O_2/N_2 ratios) are reviewed every two years at the WMO/IAEA Meeting on Carbon Dioxide, Other Greenhouse Gases and Related Measurement Techniques. The report (WMO, 2012*b*) can be used as the most recent reference regarding calibration and measurement quality control.

16.3.2   **Methane**

Methane is usually measured quasi-continuously or from discrete samples by active methods in the atmosphere. Recommendations for CH_4 measurements are provided in WMO (2009*a*).

For CH_4 measurements at GAW stations, GC-FID is typically used. The analytical set-up can vary greatly depending on details such as type (manufacturer) of GC, chromatographic separation scheme used, carrier gas (such as N_2 or helium (He)), data acquisition, system control hardware and software, and peak integration system. Consequently, operating procedures for the individual systems will vary.

New analysers for atmospheric measurements of CH_4 based on optical methods give better repeatability than GC methods, but their long-term reliability is still being assessed. They are also difficult to repair in the field, and they often need to be returned to the factory for repairs. Although these instruments, which also measure water vapour, often come advertised as not needing calibration or sample drying, attendees at the 13th meeting of CO_2 experts (WMO, 2006) strongly recommend that the analysers be calibrated routinely and that air samples be dried to a dewpoint of ≤ –40 °C.

16.3.3   **Nitrous oxide**

Nitrous oxide is usually measured by active methods in the atmospheric boundary layer. Recommendations for N_2O measurements are provided in WMO (2009*a*).

A gas chromatograph equipped with an electron capture detector (GC-ECD) is widely used to separate and detect N_2O in ambient air. This technique offers good repeatability, but it can be difficult to implement. Because the N_2O lifetime is long and its fluxes small, spatial gradients are small; therefore, their quantification requires very precise measurements. The digitized ECD signal is recorded and integrated to quantify peak heights and areas. Collecting discrete samples of air in flasks is an alternative method of monitoring N_2O. Flasks should be returned to a central laboratory for analysis by GC. Typical sampling frequencies are weekly or bi-weekly.

Updated recommendations on the measurement calibration and quality control are provided in WMO (2012*b*).

Very recently, optical analysers including high-finesse cavity absorption spectrometers with near-infrared laser sources, FTIR analysers and off-axis ICOS analysers with mid-infrared laser sources became commercially available for N_2O. These exceed the precision of gas chromatography and should allow the data quality objectives to be reached. First experiments typically show excellent performance; however, no recommendations can be made since the assessment of their long-term applicability is still in progress.

16.3.4   **Halocarbons and SF$_6$**

Halocarbons and SF$_6$ are usually measured quasi-continuously or from discrete air samples by active methods in the atmospheric boundary layer. Measurement guidelines for these species are not formalized yet in the GAW Programme.

SF$_6$ is typically measured using GC-ECD techniques on the same channel as N_2O.

Global measurements of halocarbons are currently performed by the National Oceanic and Atmospheric Administration (NOAA) and Advanced Global Atmospheric Gases Experiment (AGAGE). The measurement histories for both NOAA and AGAGE extend back to the late 1970s. Both groups measure halocarbons using GC-ECD and gas chromatography with mass spectrometry (GC-MS) techniques. Halocarbons measured include chlorofluorocarbons (CFCs), hydrochlorofluorocarbons (HCFCs), chlorinated solvents such as CCl_4 and CH_3CCl_3, halons, hydrofluorocarbons (HFCs), methyl halides and SF$_6$. For many halocarbons, measurement of mole fractions in the background troposphere requires sample pre-concentration. The AGAGE group operates a network of in situ systems, while the NOAA group operates in situ systems (for a limited number of gases) and a flask-based programme. For more information on instrumentation and sampling sites, see: http://agage.eas.gatech.edu, http://www.esrl.noaa.gov/gmd/hats/.

16.3.5   **Remote-sensing of greenhouse gases**

There are several techniques used for remote-sensing of greenhouse gases. The Total Carbon Column Observing Network (TCCON, https://tccon-wiki.caltech.edu/) is a network of surface-based Fourier transform spectrometers recording direct solar spectra in the near-infrared spectral region. From these spectra, column-averaged abundances of CO_2, CH_4, N_2O, HF, CO, H_2O and HDO are retrieved. Observations in the mid-infrared (in the NDACC network, http://www.acom.ucar.edu/irwg/) allow for accurate measurements of column-averaged abundances of CH_4, N_2O and CO.

16.4   **REACTIVE GASES**

The reactive gases considered in the GAW Programme include surface and tropospheric ozone, carbon monoxide, volatile organic compounds, oxidized nitrogen compounds and sulphur dioxide. All of these compounds play a major role in the chemistry of the atmosphere and, as such, are heavily involved in interrelations between atmospheric chemistry and climate, either through control of ozone and the oxidizing capacity of the atmosphere, or through the formation of aerosols. The global measurement base for most of them is entirely unsatisfactory, the only exceptions being surface ozone and carbon monoxide.

Different reference standards and methods are used in the group of reactive gases. For more stable gases, the reference material can be prepared as a cylinder filled with the air/other matrix with known gas mole fraction (for example, for CO, non-methane hydrocarbons and terpenes), while for others (such as ozone or oxidized nitrogen compounds) only reference methods/instruments are possible.

16.4.1   **Tropospheric (surface) ozone**

The detailed measurement guidelines for measuring tropospheric ozone (surface ozone is a part of tropospheric ozone measured at the Earth's surface) are provided in WMO (2013).

The mole fraction most appropriate to the chemical and physical interpretation of ozone measurements is the mole fraction of ozone in dry air. However, ozone measurements are usually made without sample drying, because an efficient system for drying air and leaving the ozone content of the air unchanged has not been developed. It is recommended that ozone measurements be accompanied by measurements of water vapour mole fraction of sufficient precision that the ozone measurements could be converted to mole fractions with respect to dry air without loss of precision.

A number of techniques are used for measurements of ozone in the background atmosphere. These include:

> Ultraviolet absorption techniques
> Chemiluminescence techniques
> Electrochemical techniques
> Cavity ring-down spectroscopy (CRDS) with NO titration
> Differential optical absorption spectroscopy (DOAS)
> Multi-axis differential optical absorption spectroscopy (MAxDOAS)
> Tropospheric ozone lidar

A review of each of these techniques, along with information on their applicability for use at GAW stations, is provided in WMO (2013). Note that only the first four of these techniques (those conducted in situ) can be traceable via a chain of calibrations to the primary standard as recommended by GAW.

16.4.1.1   *In situ techniques*

The main principle of the UV method is based on the absorption of light in the UV region by the ozone molecule. The broad UV spectrum of ozone shows its maximum around 254 nm. This wavelength represents exactly the strongest emission line of an Hg lamp and the highest spectral sensitivity of a UV detector, which is a caesium-telluride vacuum UV diode or UV-sensitive photomultiplier tube (PMT). The instrument measures the relative light attenuation between an air sample which remains unchanged (i.e. containing ozone) and one in which ozone has been removed. The ozone mole fraction is calculated via the Lambert-Beer law. Though UV absorption is an absolute measuring method, calibration is necessary, at least to determine the scrubber efficiency. Details of this measurement technique are given in WMO (2013).

Because of its high accuracy and precision, low detection limit, long-term stability, sufficient time resolution and ease of operation (almost no consumables), the UV absorption technique is recommended for use for routine surface ozone measurements at all GAW stations.

The advantages of the chemiluminescence methods (or chemiluminescence detection – CLD) for ozone measurements are their fast response times and high sensitivity relative to the UV method. This makes the chemiluminescence suitable for ambient air measurements which require high time resolution (such as airborne measurements). Since CLD is not an absolute method, calibrations are necessary. Due to its relative complexity, chemiluminescence is not recommended for routine surface ozone measurements at GAW stations. However, the chemiluminescence method is appropriate for experimental studies of ozone at GAW stations with extended programmes, as backup or for QA/QC reasons, since both instruments produce different artefacts.

All electrochemical techniques use the oxidation of iodide to iodine by O_3:

$$2\,I^- + O_3 + H_2O \rightarrow I_2 + 2\,OH^- + O_2$$
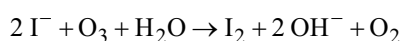
Depending on the approach, the formed iodine is stabilized by former reactions or reduced at the surface of a cathode where the electrical current is measured. Like UV absorption, it is an absolute measuring method in principle. However, due to some sources of error, such as overvoltage or zero current, calibration is necessary.

The cavity ring-down spectroscopy with NO titration is an experimental method with promise for future observations and should be incorporated into experimental studies of ozone measurements at selected GAW stations where appropriate.

16.4.1.2   *Remote-sensing techniques*

Remote-sensing techniques (DOAS, MAxDOAS, lidar) would require a similar traceability chain as in situ measurements, which is theoretically possible via the knowledge of the ozone cross-sections at the particular wavelengths used in the instruments. This issue is currently under consideration by the Absorption Cross Sections of Ozone (ACSO) committee.

Differential optical absorption spectroscopy is a surface-based remote-sensing method suitable for observations of several trace substances. The instrument consists of a light source, a long ambient air open optical path generally between 100 m and several km, a retro-reflector and a spectrometer with a telescope, housed with the light source. The spectrometer observes the light source via the retro-reflector. The DOAS system uses Beer's law to determine the ozone concentration (averaged over the light path). In principle, DOAS should be a sensitive technique, but this is confounded by the inability of the system to regularly measure a definitive zero and determine the contribution of other UV absorbing gases and aerosols to the observed signal. The DOAS may be used as an experimental technique.

Multi-axis differential optical absorption spectroscopy is a surface-based remote-sensing method for observations of several trace substances. While this method is suitable for stratospheric monitoring, it is also possible to apply it for trace gas profile measurements in the upper and lower troposphere. However, since the retrieval procedures, as well as possible tropospheric interferences, are more complicated in the lower troposphere, it needs highly experienced personnel for extracting and calculating the mole fractions for the respective trace gases out of the various spectra. MAxDOAS measurements of ozone, nitrogen dioxide, formaldehyde, bromine monoxide (BrO) and other species are recommended especially for providing a link between surface-based and satellite measurements at selected GAW stations with extended research programmes.

Lidar (light detection and ranging) is a surface-based remote-sensing method for observations of several trace substances. For tropospheric ozone measurements, a lidar typically uses two or more wavelengths between 266 nm and 295 nm. The chosen wavelengths are shorter than the ones used for stratospheric ozone detection (typically between 308 and 353 nm). Compared to in the stratosphere, higher ozone absorption efficiency is necessary in the troposphere in order to get enough sensitivity because of the lower ozone mixing ratios in the troposphere. Too much absorption means that most light is extinguished at lower elevations, making it difficult to collect measurement signals from higher elevations. The extreme dynamic range of the backscattering signal over the troposphere (some decades over a few kilometres of height) is a major technical problem. Lidar tropospheric ozone measurements are recommended especially for providing a link between surface-based and satellite measurements at selected GAW stations with extended research programmes.

16.4.2   **Carbon monoxide**

The detailed measurement guidelines for carbon monoxide measurements are provided in WMO (2010). The carbon monoxide scale is evaluated every two years together with the scales of the major greenhouse gases. For the most recent scale, please consult WMO (2012*b*).

Measurements of CO are possible both in situ and by flask collection with subsequent analysis in the laboratory. In situ continuous observations provide information about CO variability on a timescale ranging from seconds to one hour depending on the measurement technique. In contrast to flask sampling, continuous measurements allow for near-real-time data delivery.

In situ observations can be made using a broad variety of analytical techniques. Non-dispersive infrared radiometry is based on spectral absorption at 4.7 μm. It is frequently used for continuous measurements at remote locations; however, instrument drift, limited precision and long averaging times are factors limiting the achievable data quality. Gas chromatography, when coupled with a number of different detectors (such as flame ionization (GC-FID) or hot mercuric oxide reduction/UV absorption (GC-HgO)) can provide high-precision and adequate detection limits. The HgO-reduction detector tends to have a non-linear response over the range of atmospheric CO, and requires careful, repeated multipoint characterization of the detector response. The GC-FID technique requires catalytic conversion of CO to CH_4. For confidence in the results, the catalytic conversion efficiency must be determined on a regular basis. This type of issue complicates efforts to properly maintain instrument calibration and provide accurate measurements. Gas chromatography measurements are quasi-continuous in nature and therefore may not detect fast changes of mole fractions that can be captured by high-frequency measurements.

Several new measurement techniques have recently become available. The most established technique is based on resonance fluorescence of CO (induced by a high-frequency discharge) in the vacuum ultraviolet (VURF). This method provides low detection limits with excellent precision in the range of atmospheric mixing ratios. A commercially available instrument based on VURF is used in several research laboratories, field sites and on other platforms, for example in the CARIBIC project.

Spectroscopic techniques based on CRDS and cavity-enhanced quantum cascade laser (QCL) spectroscopy have become available. The CRDS technique operates using lasers in the near-infrared and was previously mainly used for measurements of carbon dioxide, methane and ammonia. The QCL technique measures in the mid-infrared, and commercial instruments are available that can determine both CO and N_2O with a single laser. Both CRDS and QCL techniques provide CO measurements with low detection limits and excellent reproducibility. Tests of their long-term applicability for routine measurements at the GAW stations are still ongoing. An additional alternative with similar performance that has recently been commercialized is Fourier transform infrared absorption spectroscopy.

Remote-sensing of CO column from the ground is done in the TCCON network using surface-based Fourier transform spectrometers in the near-infrared spectral region.

16.4.3   **Volatile organic compounds**

The measurement of VOCs is complex due to the many different molecules present in the atmosphere. While systematic surveying of many of these species is important for air quality purposes, the low concentrations of VOCs away from their sources imply that only a few molecules can be measured routinely in the background atmosphere. A core set of molecules recommended for measurement in the GAW Programme with suggested measurement methods is provided in Table 16.1.

The measurement guidelines for VOCs are currently under development in collaboration with the ACTRIS (Aerosols, Clouds and Trace Gases Research Infrastructure) network (http://www.actris.eu). A standard operating procedure for taking air samples with stainless steel canisters is available in WMO (2012a). General recommendations on VOC measurements can be found in WMO (2007a). Regular GAW VOC workshops review the status of VOC measurements in the GAW Programme (http://www.wmo.int/pages/prog/arep/gaw/4VOC_expert_meeting2012.html) and provide further guidance on the development of measurement techniques, quality assurance and gas standards.

Table 16.1. List of the priority VOCs in the GAW Programme

	Molecule	Lifetime (assuming OH concentration is 10^6 cm^{-3})	Importance to GAW	Steel flask[a]	Glass flask	Analysis method[b]
1.	Ethane	1.5 months	– Source of methane – Natural sources – Biomass burning – Fossil fuel – Ocean production (southern hemisphere) – Trend in size of seasonal cycle – Indicator of halogen chemistry	✓	✓	GC-FID
2.	Propane	11 days	– Source of methane – Natural sources – Biomass burning – Fossil fuel – Ocean production (southern hemisphere)	✓	✓	GC-FID
3.	Acetylene	15 days	– Motor vehicle tracer – Biomass burning tracer – Ratios to the other hydrocarbons – Trends	✓	✓	GC-FID
4.	Isoprene	3 hours	– Biosphere product – Sensitive to temperature/land – Used for climate change – O_3 precursor – Oxidizing capacity – Precursor to formaldehyde	?	?	GC-FID PTR-MS
5.	Formaldehyde	1 day	– Indicator of isoprene oxidation – Biomass burning – Comparison with satellites – Trends	–	–	DOAS
6.	Terpenes	1–5 hours	– Precursors to organic aerosols	–	–	GC-MS PTR-MS
7.	Acetonitrile	0.5–1 year	– Biomass burning indicator – Biofuel burning indicator	–	?	GC-MS PTR-MS
8.	Methanol	12 days	– Sources in the biosphere (methane oxidation) – Abundant oxidation product	–	?	GC-FID PTR-MS
9.	Ethanol	4 days	– Tracer of alternative fuel usage	–	?	GC-FID PTR-MS
10.	Acetone	1.7 months	– Abundant oxidation product – Free radical source in the upper troposphere	?	?	GC-FID PTR-MS
11.	Dimethyl sulphide	2 days	– Major natural sulphur source – Sulphate aerosol precursor – Tracer of marine bioproductivity	?	?	GC-FID PTR-MS
12.	Benzene	10 days	– Tracer of combustion – Biomass burning indicator	✓	?	GC-FID GC-MS
13.	Toluene	2 days	– Ratio to benzene used for airmass age – Precursor to particulates	–	?	GC-FID GC-MS
14.	Iso/normal butane	5 days	– Chemical processing indicator – Lifetime/ozone production	✓	✓	GC-FID GC-MS

Molecule	Lifetime (assuming OH concentration is 10^6 cm^{-3})	Importance to GAW	Steel flask[a]	Glass flask	Analysis method[b]
15. Iso/normal pentane	3 days	– Ratio provides impact of NO_3 chemistry	✓	✓	GC-FID GC-MS

Notes:
a   ✓ indicates state of current practice
b   GC-FID = gas chromatography flame ionization detection; GC-MS = gas chromatography mass spectrometry; DOAS = differential optical absorption spectroscopy; PTR-MS = proton transfer reaction mass spectrometry

Measurements of low molecular weight aliphatic and aromatic hydrocarbons (C2–C9) have been made successfully for many years, predominantly in short-term regional experiments. The preferred analytical method for these compounds, which include the molecules 1–4 and 12–15 of Table 16.1, is GC-FID. Air samples, from flasks or in situ, are normally pre-concentrated using cryogenic methods or solid adsorbents. An alternative technique is GC-MS. Although GC-MS is potentially the more sensitive method, it is typically subject to greater analytical uncertainties (changes in instrument response over time, detection of common, low-mass fragments). However, GC-MS may be valuable for the detection of certain hydrocarbons in very remote locations where ambient levels may be below the detection limit of a typical GC-FID.

The recommended analytical technique for monoterpenes is GC-MS. Although it is possible to measure some terpenes using an FID, the complexity of the chromatographic analysis (co-eluting peaks, particularly with aromatics) makes peak identification and quantification difficult. The GC-MS method gives better sensitivity.

Oxygenated hydrocarbons, including the target compounds 8–10 (Table 16.1), can also be measured using GC-FID or GC-MS. Particular care should be taken with sample preparation (including water removal), and inlet systems must be designed to minimize artefacts and component losses commonly encountered with oxygenate analysis. Acetone and methanol can also be measured using proton transfer reaction mass spectrometry (PTR-MS). An advantage of PTR-MS is that it is an online method that does not require the pre-concentration of samples. However, it is less sensitive than GC methods, and there are potential interferences from isobaric compounds, such as O_2H^+ and methanol. As the stability of oxygenated VOCs in grab samples (stainless steel or glass flasks) remains highly uncertain, it is suggested that these species be measured primarily by online methods at a selection of surface-based measurement stations. The successful storage of acetone in certain flasks has been reported, so the possibility of analysing this compound in the glass or stainless steel flask network should be investigated.

Formaldehyde (HCHO) is not stable in flasks and has to be measured in situ. Methods of analysis include the Hantzsch fluorometric (wet chemical) method or DOAS. Both are relatively complex and would require specialist training for potential operators. It is unlikely, therefore, to be able to make measurements at more than a few ground stations. Formaldehyde is routinely detected by satellites. Satellite retrievals yield total vertical column amount, and an important objective of the GAW Programme would be to provide periodic surface-based measurements at selected sites for comparison/calibration purposes (ground truthing).

The feasibility of HCHO measurements with PTR-MS (Wisthaler et al., 2008; Warneke et al., 2011) and QCL (Herndon et al., 2007) was shown during limited measurement campaigns. Their applicability for long-term routine HCHO measurements has not yet been tested.

Acetonitrile is preferably measured with GC-MS, because this compound is relatively insensitive to FID detection. Measurements of acetonitrile have also been reported using various reduced gas and nitrogen-specific detectors. Many recently reported atmospheric measurements of acetonitrile have been made using PTR-MS or atmospheric pressure chemical ionization mass spectrometry (AP-CIMS). The stability of acetonitrile in grab samples is highly uncertain, so grab sampling is not acceptable in the framework of GAW and measurements may be limited to a few selected comprehensive measurement sites.

Dimethyl sulphide (DMS) can be measured by GC-FID, gas chromatography using a flame photometric detector (GC-FPD), GC-MS and PTR-MS. However, as DMS concentrations can be measured routinely as part of a standard non-methane hydrocarbon (NMHC) analysis, GC-FID analysis of the whole air samples would be the simplest choice of measurement strategy. There is evidence in the literature that DMS is stable in some flasks, so its measurement as a component of a flask network is quite feasible. It is also desirable to make in situ measurements of DMS at least in the early stage of operation of the flask network to ensure method compatibility.

16.4.4 **Nitrogen oxide**

The sum of nitric oxide (NO) and nitrogen dioxide (NO_2) has traditionally been called NO_x. The sum of all nitrogen oxides with an oxidation number greater than 1 is called NO_y. Their measurement in the global atmosphere is very important since NO has a large influence on both ozone and the hydroxyl radical (OH). NO_2 is now being measured globally from satellites, and these measurements suggest that substantial concentrations of this gas are present over most of the continents. A large reservoir of fixed nitrogen is present in the atmosphere as NO_y. The influence of the deposition of this reservoir on the biosphere is not well known at present but could be substantial. There are efficient in situ measurement techniques for NO and NO_2, whereas the reliability of NO_y measurement techniques still needs to be improved. The widely used CLD technique with molybdenum (Mo) converters gives a signal between NO_2 and NO_y and should be named $NO_{2(Mo)}$ or NO_{2+} (see below).

Detailed measurement guidelines for reactive nitrogen measurements are currently being developed in collaboration with the ACTRIS network. The focus here is mostly on NO and NO_2 because their measurements are presently more extensive and robust and allow for implementation of a complete quality assurance system. Recommendations on NO and NO_2 measurements can be found in WMO (2011a).

Nitrogen oxide (NO and NO_2) measurements can be done by passive, active and remote-sensing techniques. The active techniques can be divided into integrating and in situ techniques: integrating techniques consist of a sampling step usually involving liquid-phase sample collection and offline analysis, whereas in situ (continuous) measurements directly analyse the sample air. Passive methods are always integrating. Active integrating methods comprise the Saltzman method and related methods like the Griess or sodium iodide method. The latter is being used, for example, in the Cooperative Programme for Monitoring and Evaluation of the Long-range Transmission of Air Pollutants in Europe (EMEP, http://www.emep.int) network. Due to the high reactivity of NO_x, flask sampling is impossible.

Ozone-induced chemiluminescence detection is the most widely used among the in situ techniques. These instruments are typically very sensitive to NO; however, they cannot measure NO_2. Thus, NO_2 must be converted to NO before detection. The instrument makes measurements in an NO mode and then an $NO + NO_2$ mode. The difference, when conversion efficiency is determined carefully, gives the NO_2 mixing ratio. Thus, a high time resolution (< 10 min) is recommended to ensure sampling of the same airmass during subsequent NO and NO_x measurements. The conversion of NO_2 to NO is achieved by photolysis of NO_2 at wavelengths $320 < \lambda < 420$ nm using a photolytic converter (PLC) with an arc lamp or a blue-light converter (BLC) with light-emitting diodes (LEDs). Advantages of LEDs are the substantially longer lifetime and nearly constant conversion efficiencies, the mechanical simplicity and the simple on/off characteristic of the LED (no additional valves/dead volumes). The disadvantage is the small conversion efficiency. However, new LED-based converters provide efficiencies equal to or even greater than traditional arc-lamp systems. The use of UV-LED converters is thus recommended for GAW NO_2 measurements.

The use of molybdenum converters for NO_2 to NO conversion is strictly discouraged, as this conversion technique is not selective of NO_2 but also converts other oxidized nitrogen species in different quantities. Already existing measurements with Mo converters should be marked as $NO_{2(Mo)}$ or NO_{2+}.

The luminol-CLD method measures NO_2 directly and NO indirectly after oxidation. Since the sensitivity depends strongly on the quality of the luminol solution, which decreases during use due to ageing, frequent re-calibration is needed.

In addition to these methods, optical absorption techniques for NO_2 detection have been developed, including tunable diode laser absorption spectroscopy (TDLAS), differential optical absorption spectroscopy, laser-induced fluorescence (LIF), Fourier transform infrared absorption spectroscopy and cavity ring-down spectroscopy. They all measure NO_2 directly. Recent developments in CRDS for the measurement of NO_2 and of NO as NO_2 after oxidation by ozone show some promise, but the measurements still suffer from uncertainties in the zero level.

Recently, the suitability of research-type quantum cascade laser instrumentation for continuous and direct measurements of NO and NO_2 was shown (Tuzson et al., 2013). This technique may become an alternative standard method in the future.

Also recently, a cavity attenuated phase shift (CAPS) monitor has become commercially available. A side-by-side intercomparison experiment at ACTRIS showed excellent results. However, the lower detection limit (LDL) is some 50 ppt. Therefore, the instrument is very good for rural or anthropogenic-influenced sites but not suitable for remote ones with typical NO_2 mole fractions below 50 ppt.

At present, there is no mature technique that can compete with the ozone-induced chemiluminescence detection measurement of NO at remote locations. Passive and active integrating methods are not accepted in the GAW Programme due to their poor selectivity and time resolution.

16.4.5   **Sulphur dioxide**

Measurement guidelines for SO_2 observations are so far not available in the GAW Programme. General recommendations are given in WMO (2001). However, the GAW Scientific Advisory Group for Reactive Gases is planning to establish the same quality assurance system for SO_2 (including measurement guidelines and central facilities) as it is doing at present for nitrogen oxides after that item is solved.

There are various measurement techniques for determining atmospheric SO_2. EMEP is using integrating techniques, such as an alkaline-impregnated filter (pack) or coated annular denuder, both followed by ion chromatography in a central laboratory. These methods yield potentially more accurate results, but with a lower time resolution of usually one sample per day, as is typical for integrative techniques. Additionally, they require frequent attention, and personnel costs for filter analysis are high.

In the group of in situ measurements, the TCM (photometry after reaction of SO_2 with tetrachloromercurate) and the pulse fluorescence methods are widely used. The first one has a high accuracy but high LDL, and the handling of mercury in the laboratory could be harmful. Even though the response of the pulsed-fluorescence sensor is slower, its ease of calibration, dependability, accuracy and SO_2 specificity make it preferable. More sensitive gas chromatographic techniques are also available. However, they require significant technical expertise and regular attention. In order to enhance the sensitivity, some fluorescence analysers are equipped with more selective excitation filters. For example, two mirror assemblies are connected in series and specially selected PMTs are employed. Numerical corrections of interfering substances could be done; however, this is not necessary in rural or remote areas. The typical LDL which can be reached with these provisions is some 50 ppt. A further enhancement of sensitivity may be possible by means of a second channel in which only SO_2 is removed, leading to a highly specific read-out after subtraction of both channels.

Since SO$_2$ has a short atmospheric lifetime, understanding the sulphur cycle requires knowledge of the source and sink terms. This is best accomplished with sampling frequencies of less than 1 h. Therefore, the best technique for long-term monitoring of SO$_2$ today is a combination of the pulsed-fluorescence analyser and filter sampling. Filter samples should be exposed at intervals, but often enough to act as a quality control for the continuous analyser.

More detailed recommendations can be found in EMEP (2014), available at http://www.nilu.no/projects/ccc/manual/index.html.

16.4.6   **Molecular hydrogen**

The detailed measurement guidelines for molecular hydrogen are currently not available in the GAW Programme.

Molecular hydrogen is reported as dry mole fraction on the most recent scale (WMO, 2012*b*). Measurements of H$_2$ are possible both in situ and by flask collection with subsequent analysis in the laboratory. An example of the measurement system set up at the GAW global stations is given in Grant et al. (2010).

Molecular hydrogen measurements are performed with gas chromatography followed by hot mercuric oxide reduction/UV absorption detection. An alternative GC set-up with pulsed-discharge detectors (PDD) has a more linear detector response and provides better repeatability for molecular hydrogen measurements.

Problems with instability of H$_2$ in reference gases have frequently been experienced. Therefore, recommendations on calibration and quality assurance of H$_2$ measurements available in WMO (2012*b*) should be consulted.

16.5   **ATMOSPHERIC WET DEPOSITION**

Atmospheric wet deposition refers to the gases and particles deposited by precipitation on the Earth's surface. These gases and particles have a wide variety of sources and compositions and generally are present in trace amounts in the atmosphere and in precipitation. These trace materials are captured by precipitation as it forms in the atmosphere and falls to the Earth. The deposited materials constitute an important contribution to the mass balance of pollutants associated with long-range transport. These materials not only affect the chemistry of precipitation but also can affect the chemistry of the terrestrial and aquatic surfaces on which they are deposited. The effects can be harmful or beneficial, and they can be direct or indirect. For example, acidic wet deposition is an environmental problem that results from combustion of fossil fuels. It occurs when oxides of sulphur and nitrogen, emitted during combustion, are transformed in the atmosphere and become acidic sulphate and nitrate in precipitation. Other trace materials that occur in wet deposition include sea salt, nutrients, chemicals found in soil particles, toxic organic and inorganic chemicals, organic acids, etc. Research has shown that some wet-deposited chemicals can stimulate marine biotic production, potentially linking atmospheric wet deposition to the carbon cycle and climate change.

Measuring the chemistry of precipitation tells us what trace materials are present in wet deposition and in what amounts. This information can be used to evaluate air quality and to identify and track changes in gaseous and particulate emissions to the atmosphere. In short, precipitation chemistry measurements provide information on the exchange of trace materials between the atmosphere and the land/oceans, and hence are important in furthering our understanding of the chemical cycles of these materials, especially those that can result in damage to terrestrial and aquatic systems or affect our climate.

Special care is required when planning precipitation chemistry measurements to ensure that they are representative. Though the measurements are made at a particular location, on average they should represent measurements in the surrounding region. In general, the sample

collection site should be characteristic of the land use in the region. For example, the site in an area dominated by agricultural activities should have an agricultural setting. This quality of spatial representativeness should extend across seasons and even over years. Ideally, a site would be both spatially and temporally representative. Contamination of localized nature from agricultural, industrial or other human activities must be avoided, as must the local impact of natural sources, such as oceanic shores, volcanoes or fumaroles. Sample collection should not be impacted by trees or other vegetation, and the on-site topography should be level and the exposure relatively unaffected by wind patterns that may result in an unrepresentative catch of rain and snow. Human contact with the sample or contact with anything that might change the sample chemistry must be avoided as well. Ensuring representative precipitation chemistry measurements entails strict adherence to requirements for site location, site conditions, equipment installation and site operational protocols and maintenance. These requirements are documented in WMO (2004b).

Precipitation chemistry monitoring can be divided into sample collection activities and chemical analysis activities.

16.5.1 Sample collection

The primary goal of the GAW Precipitation Chemistry Programme is to collect wet-only deposition samples. This means that the samplers are exposed only during precipitation and trace materials in the samples are deposited only by precipitation. The trace materials from dust or fine particles or gases deposited during dry weather are excluded. This makes it possible to study precipitation chemistry without contamination from dry deposition. More importantly, the equipment and methods for collecting a representative wet deposition sample are inappropriate for collecting a representative dry deposition sample. The physical and chemical processes affecting wet and dry deposition are distinctly different.

The best way to ensure collection of a wet-only sample is to employ an automated sampler that is open only during precipitation. A typical automated, wet-only deposition sampler has the following components: a precipitation sample container (funnel-and-bottle, bucket, etc.), a lid that opens and closes over the sample container orifice, a precipitation sensor, a motorized drive mechanism with associated electronic controls and a support structure to house the components. The containers should have sufficient volume to hold all precipitation collected during the sampling period. A system that can be activated manually for testing, cleaning and routine maintenance is recommended. A modular design that allows removal of individual components, such as the sensor, facilitates rapid repair with a minimum of tools and expertise. An alternative to using an automated sampler is to collect samples by manually exposing a sample container at the very onset of precipitation and closing it as soon as precipitation ceases. This requires diligent round-the-clock observers alert to weather conditions; as a consequence, manual sample collection is very labour-intensive.

To complement the collection of wet-only deposition samples, the GAW Precipitation Chemistry Programme requires every site to measure precipitation depths using the standard precipitation gauge designated by National Meteorological and Hydrological Services or its equivalent (see Part I, Chapter 6 of this Guide). Manual gauges are preferred. Precipitation depths are used to calculate the mass of a chemical deposited by precipitation on an area of the Earth's surface (called the wet deposition flux or loading). Standard precipitation gauges are designed to be the most accurate and representative means of measuring precipitation depths. Thus, each site must operate a precipitation gauge in parallel with its precipitation chemistry sampler. Precipitation chemistry sampler volumes are used to calculate wet deposition fluxes only when the standard gauge fails or is temporarily out of service. The data record should document such cases.

The highest priority of the GAW Precipitation Chemistry Programme is to collect a wet-only sample on a daily (24 h) basis with sample removal set at a fixed time each day, preferably 0900 local time. Should the resources be inadequate to collect and analyse daily samples, multi-day sampling periods up to one week is the next highest priority. Alternative sampling protocols are described in WMO (2004b). Collecting samples daily reduces the potential for the degradation of labile chemical species and for other physical and chemical changes in the sample

while it is held in the field sampler. Not only is the sample integrity less likely to be compromised by a daily sampling protocol but the data have greater value as well. Storm trajectory analyses and source-receptor models are much less complicated when precipitation is more likely to have come from a single event or storm. Multi-day and one-week samples are much more likely to contain precipitation from several storms, each occurring under different meteorological settings. Further, daily data can be integrated mathematically to determine weekly or longer-term averages, but weekly data cannot be differentiated into daily components without making substantial assumptions.

Containers used to collect, store and ship samples should be unbreakable and sealable against leakage of liquids or gases. High-density polyethylene containers are recommended. All sample containers must be cleaned with deionized water of known and assured quality. The report (WMO, 2004b) contains detailed descriptions of the procedures for cleaning containers and ensuring that cleanliness standards are maintained throughout the collection, storage and shipment of samples.

16.5.2   **Chemical analysis**

The following chemical parameters are recommended for analysis in GAW precipitation samples: pH, conductivity, sulphate, nitrate, chloride, ammonium, sodium, potassium, magnesium and calcium. Analyses for formate and acetate are recommended for areas suspected of having high organic acid concentrations. Nitrite, phosphate and fluoride concentrations also may be important in certain areas, although their analyses are not required by GAW at this time. Preferred analytical methods are given in Table 16.2.

Past experience from regional networks and laboratory intercomparisons has shown that measuring pH in precipitation is difficult due mainly to the low ionic strength of the samples. Samples may also degrade due to biological activities and should therefore be kept refrigerated until the time of analysis, when they are brought to room temperature. The pH measurements should be carried out within two days of sample arrival in the laboratory.

Commercial pH meters are available with different specifications and options. A pH meter should have both an intercept and slope adjustment and should be capable of measuring to within

Table 16.2. Chemical parameters required for analysis in the GAW Precipitation Chemistry Programme with recommended analytical methods

Analyte	Status	Preferred methods[a]
pH	Required	Glass electrode
Conductivity	Required	Conductivity cell
Alkalinity	Optional	Titration
Cl^-, NO_3^-, SO_4^{2-}	Required	IC
NH_4^+	Required	IC, AC
Na^+, K^+, Ca^{2+}, Mg^{2+}	Required	IC, ICP, AAS/AES
Organic acids[b]	Optional	IEC, IC
NO_2^-, F^-	Optional	IC
PO_4^{3-}	Optional	IC, AC

Notes:
a   IC = ion chromatography; AC = automated colorimetry; ICP = inductively
    coupled plasma spectrometry; IEC = ion exclusion chromatography;
    AAS = atomic absorption spectrometry; AES = atomic emission spectrometry
b   For areas with high organic acid concentrations, formate and acetate analyses
    are recommended.

±0.01 pH unit. Combination electrodes containing both measuring and reference functions are often preferred since they require smaller amounts of a sample, but a set of two electrodes may also be used with the pH meter. The measuring glass electrode is sensitive to hydrogen ions and the reference electrode can be calomel, or silver/silver chloride. Low ionic strength electrodes are now available commercially. Other reference electrodes can also be used as long as they have a constant potential. When selecting any electrode, confirm its ability to measure low ionic strength solutions by measuring a certified reference material. Response time should be less than 1 min and the addition of potassium chloride (KCl) should not be needed.

The conductivity of a solution is the reciprocal value of its specific resistance and can be directly measured using a conductivity bridge with a measuring cell. Conductivity varies with the temperature of the solution and is proportional to the concentration and the species of free ions present in the solution. Since the conductivity also depends on the electrode area and its spacing, the measuring apparatus has to be calibrated to obtain the cell constant or to adjust the meter. A KCl solution of known concentration and conductivity is used for calibration. Conductivity is measured and expressed in units of microsiemens per centimetre (μS cm^{-1}), corrected to 25 °C. The conductivity range of precipitation samples is 5 to 1 000 μS cm^{-1}. In case of small sample volumes, the aliquot that is used for conductivity measurement can be used for pH determination. If this is done, the conductivity should be measured first to avoid any possible error due to salt contamination from the pH electrode.

The apparatus for conductivity measurements consists of:

(a)   A conductivity meter (with operating range of 0.1 to 1 000 μS cm^{-1}; or, better, 0.01 to 1 000 μS cm^{-1}). Precision has to be within 0.5% of the range and accuracy at 1% of the range;

(b)   A conductivity cell (if the values in precipitation samples are expected to be mainly very low (<20 μS cm^{-1}), use special conductivity cells, with a low cell constant);

(c)   A thermometer (0 °C to 40 °C / 0.1 °C);

(d)   A water bath at 25 °C;

(e)   A polyethylene or glass vessel corresponding to the diameter of the cell used.

Ion chromatography (IC) has been widely used in recent years to analyse major anions and cations in precipitation, mainly in combination with electrochemical detection.

Sulphate, nitrate, chloride as well as other anions in precipitation are separated on an ion exchange column because of their different affinities for the exchange material. The material commonly used for anion separation is a polymer coated with quaternary ammonium active sites. After separation, the anions pass through a suppressor that exchanges all cations for H$^+$ ions. Instead of strong acid cation exchange columns, today micro membrane and self-regenerating suppressors with chemical or electrochemical regeneration are used. As a result of the suppression reaction, corresponding acids of the eluent ions and of chloride, nitrate and sulphate will reach the conductivity detector. A decreased basic conductivity and higher analytical signals now allow the detection of anions also in the lower μg L^{-1} range.

There are several anion exchangers with different properties available on the market. The time for one analysis and the quality of separation of single signals are dependent on the type of column and eluent, and on the concentration and flow rate of the eluent.

Any anions with a retention time similar to that of the main anions in the solution can cause an interference. For example, when NO_2^- is present, it elutes just after Cl$^-$, which can cause the peak to be asymmetric. In rare cases, when the concentration of Cl$^-$ is very high compared with NO_3^-, it can also influence the determination of NO_3^-. The manual should be consulted to see how different integration programmes handle this problem.

With care, up to several thousand analyses can be performed with the same anion separator column. The most effective method of protecting the separator column is to use a pre-column in front of it. Details are provided by the manufacturers in the manuals for the columns.

The principle of cation measurements is the same as that of anion determination except that different column materials are used and the suppressor column is often omitted. The material commonly used for cation separation is a cation exchange resin with active surface groups. Sodium, ammonium, potassium, calcium and magnesium ions are detected by a conductivity detector, without changing the eluent when certain columns are used. In other columns, monovalent cations (Na^+, NH_4^+, K^+) are determined using one eluent and divalent cations (Mg^{2+} and Ca^{2+}) with another eluent (because of their higher affinity to the resin).

Any cation with a retention time similar to that of the main cations may cause interference. For example, in samples with high concentrations of Na^+, the peak of NH_4^+ becomes asymmetrical and often causes significant error. In this case, measurement using more dilute eluent could improve the separation of peaks.

Sodium, potassium, magnesium and calcium in precipitation are often analysed by atomic spectroscopic methods. Both flame (atomic absorption spectrometry (AAS) and atomic emission spectrometry (AES)) and plasma (inductively coupled plasma atomic emission spectrometry (ICP-AES) and inductively coupled plasma mass spectrometry (ICP-MS)) based methods can be used. For these ions, ion chromatography has no special advantage in terms of sensitivity, precision and accuracy over the spectroscopic methods, although analysis of all ions in one sample run is not possible with flame AAS or AES (single element methods).

The ions in the sample solution are transformed to neutral atoms in an air/acetylene flame. Light from a hollow cathode or an electrodeless discharge lamp (EDL) is passed through the flame. In the AAS mode, light absorption of the atoms in the flame is measured by a detector following a monochromator set at the appropriate wavelength. Light absorption is proportional to the ion concentration in the sample. In the AES mode, the light emitted from the atoms excited in the flame is measured. Most commercial instruments can be run in both modes. Atomic emission spectrometry is the preferred mode for sodium measurements.

In atomic absorption spectrometry, both ionization and chemical interferences may occur. These interferences are caused by other ions in the sample, which reduce the number of neutral atoms in the flame. Ionization interference is avoided by adding a relatively high amount of an easily ionized element to the samples and calibration solutions. For the determination of sodium and potassium, caesium is added. For the elimination of chemical interferences from aluminium and phosphate, lanthanum can be added to the samples and calibration solutions for calcium and magnesium.

Formic and acetic acids (HCOOH and CH_3COOH, respectively) are major chemical constituents of precipitation in both continental and marine regions. Available evidence suggests that these compounds originate primarily from natural biogenic sources; both direct emissions (over continents) and emissions of precursor compounds appear to be important. Biomass and fossil fuel combustion also result in the emission of carboxylic acids and/or their precursors to the atmosphere.

Carboxylic acids in precipitation are very unstable and rapidly disappear from unpreserved samples. To generate reliable data, precipitation must be sampled on a daily or event basis and immediately preserved with the addition of a biocide such as chloroform ($CHCl_3$). Typically, 250 ml aliquots of sample (or less for low volume events) are treated with 0.5 ml of $CHCl_3$. Samples are then tightly sealed and refrigerated until analysis.

Carboxylic species can be analysed by both IC (using a dilute eluent) and ion exclusion chromatography (IEC). However, acetate and propionate typically co-elute when analysed by IC and are thus impossible to resolve quantitatively. The IEC method exhibits fewer interferences associated with co-eluting species and is thus preferred for analysis of precipitation samples.

For analysis by IEC, samples are added to a hydrochloric acid (HCl) eluent which then flows through a separator column, a suppressor column and a detector. Resin in the separator column partitions anions using the principle of Donnan exclusion; anions are retained and sequentially separated based on their respective pK_as and van der Waals interactions with the resin. Anions of stronger acids with lower pK_as, such as H_2SO_4, HNO_3 and HCl, are effectively excluded and co-elute early in the chromatogram; those of weaker acids with higher pK_as, such as HCOOH and CH_3COOH, elute later in the chromatogram. The suppressor column incorporates a cation exchange resin with silver added to the exchange sites; H^+ exchanges with the silver; the released silver subsequently reacts with Cl^- in the eluent to form silver chloride (AgCl), which precipitates within the column. Acid analytes exit the suppressor in a stream of deionized water. Detection is by conductivity.

16.6 AEROSOLS

Atmospheric aerosols are important for a diverse range of issues including global climate change, acidification, regional and local scale air quality, and human health. The climate impact of aerosols is a result of direct radiative effects and indirect effects on cloud properties. Regional problems include potential impacts on human health and mortality and environmental impacts such as visibility impairment. Major sources of aerosols include urban/industrial emissions, smoke from biomass burning, secondary formation from gaseous aerosol precursors, sea salt and dust. Outstanding problems include determining the natural sources of aerosols and the organic fraction.

Table 16.3 provides a list of aerosol parameters recommended for measurement in the GAW Programme. Comprehensive measurement guidelines for aerosol measurements are provided in WMO (2003b) and WMO (2011c), which are currently under review.[3]

Table 16.3. List of comprehensive aerosol variables recommended for long-term measurements in the global network

Variable	Frequency of observation
Multiwavelength aerosol optical depth	Continuous
Mass concentration in two size fractions (fine, coarse)	Continuous
Mass concentration of major chemical components in two size fractions	Continuous
Light absorption coefficient at various wavelengths	Continuous
Light scattering and hemispheric backscattering coefficient at various wavelengths	Continuous
Aerosol number concentration	Continuous
Aerosol number size distribution	Continuous
Cloud condensation nuclei number concentration at various supersaturations	Continuous
Vertical distribution of aerosol backscattering and extinction	Continuous
Detailed size fractionated chemical composition	Intermittent
Dependence of aerosol variables on relative humidity, especially aerosol number size distribution and light scattering coefficient	Intermittent

Source: WMO (2011b)

---

[3] For the latest versions, see the GAW publications (available from http://www.wmo.int/pages/prog/arep/gaw/gaw-reports.html).

16.6.1   **Aerosol chemical measurements**

At present, filter collection of ambient aerosol, followed by laboratory analyses, still remains the most commonly used and cost-efficient method for the determination of aerosol chemical composition despite well-documented artefacts. Artefacts are very often linked to the presence of semi-volatile species that can either condense upon sampling (positive artefact) or evaporate from the filter media after sampling (negative artefact). A number of methods have been proposed to limit these artefacts, but none of them will satisfactorily apply to all chemical substances present in aerosol.

The optimal set-up for the characterization of chemical properties of aerosol would be composed of a series of denuders to remove condensable species present in the gas phase (limiting positive artefact) and a filter pack collecting both particles and condensable species re-emitted from the first filter (accounting for negative artefact). Filter packs have been developed, consisting of a sandwich of filters and collection media of various types in series, to collect aerosols and selectively trap gases and aerosol volatilization products. Ideally, sampling for inorganic and carbonaceous species is performed with two different sampling lines since different kinds of denuders and filter media are required for analyses of elemental and organic carbon (EC/OC), and inorganic species. A third line could be implemented for sampling and analysis of elemental aerosol composition.

Clearly, methods for artefact limitation can be rather impractical and are relatively expensive. For GAW purposes, considering remoteness and the availability of resources in a number of sites, the use of denuders should be seen as a simple recommendation and not a requirement. This means, however, that sampling artefacts do exist for a number of semi-volatile species, in particular when temperatures in the sampling system exceed 20 °C. This should be accounted for when reporting data to the World Data Centre for Aerosols.

High-volume and low-volume sampling lines are accepted in the context of GAW. For simplicity, it is suggested that a differencing technique be utilized to separate the coarse fraction from the fine fraction. Specifically, one filter should be run behind the 10 μm aerodynamic diameter cut inlet. A parallel filter should be run behind the inlet suitable for the fine fraction (i.e. 2.5 μm aerodynamic diameter at ambient relative humidity or 1.0 μm in dry air). While the second filter will yield the fine fraction, the difference between the two filters will yield the coarse fraction. For high-volume sampling, use of dichotomous samplers is an interesting alternative to differentiate fine and coarse aerosol fractions.

Low-volume samplers are more easily implemented than high-volume samplers. For the routine long-term aerosol measurements at GAW stations, it is recommended that up to three sets of 47 mm diameter filters be collected in parallel by low-volume samplers. If financial constraints are limiting, the priorities for filter sampling are: (i) Teflon filters for gravimetric and ionic analyses; (ii) quartz-fibre filters for carbonaceous aerosol analyses; and (iii) Teflon filters for elemental analyses. Each set would consist, ideally, of two filters, one for total mass below 10 μm diameter and one for the fine fraction. The separation would be achieved by running the filters behind the size-selective inlets. High-volume samplers are usually more expensive, and running more than one set of sampler in parallel is often unpractical. For that reason, it is recommended that high-volume samplers be operated with quartz fibre filters for both inorganic and EC/OC analyses. It should be noted that denuders for high-volume samplers are not commercially available.

There is no recommendation for determining sampling time as this will highly depend upon the sites. In general, short sampling time (24 to 48 h) provides information that is more easily used in models and should be preferred over week-long sampling, even if discontinuous. Filters should be removed from the sampling unit shortly after collection and stored between 0 °C and 5 °C if analyses cannot be performed immediately. Regular blanks should be performed in order to control for contamination. Ideally, blanks are prepared by mounting filters into the sampling unit with the pump off. We recommend that one blank be performed every 10 samples.

For each GAW aerosol station, a list of core aerosol chemical measurements is strongly recommended: (i) mass; (ii) major ionic species; (iii) carbonaceous components, and (iv) dust aerosols.

The *mass concentration of atmospheric aerosols* is clearly a fundamental parameter in the GAW measurement programme. It is recommended that this be done gravimetrically on Teflon filters. It is expressed in units of μg m^{-3}, where the volume is related to STP. Updated measurement guidelines on mass concentration measurements using gravimetric analysis of Teflon filters are provided in WMO (2011*c*).

The tapered element oscillating microbalance (TEOM) has been widely used for aerosol mass measurements. The instrument provides continuous measurements and can produce high time resolution data. The original TEOM has a recommended temperature setting of 50 °C. There is evidence that semi-volatile components of aerosols are lost from the TEOM measurements at this temperature. The most likely explanation is that semi-volatile organic compounds, nitrates and water are lost from the aerosols during sampling. In newer TEOM models, the operating temperature has been lowered to 30 °C to reduce losses of the semi-volatile components. In addition, sudden changes in ambient relative humidity may cause negative mass readings from the instrument. New modifications have been made to dry the aerosol particles before measurement to reduce the effect of ambient relative humidity.

A different type of instrument for continuous mass measurements, the β-meter, has also been commercialized. It operates on the principle of β-ray attenuation by a layer of aerosol. The β-ray source is usually ^{14}C or ^{85}Kr decay, and the attenuation can be calibrated with a known mass. Sampling can be done with individual filters or filter tapes, and the β-ray that passes through the filter is continuously monitored. The β-meters have the same inherent difficulties concerning volatilization as the TEOM. However, comparison with gravimetric methods usually produces reasonable agreement. Updated guidelines on the mass concentration measurements with beta attenuation (with the Met One Instruments model BAM-1020) are provided in WMO (2011*c*).

The *concentration of major inorganic species* is one of the core pieces of information recommended for the GAW stations. Major ionic species include sulphate, nitrate, chloride, sodium, ammonium, potassium, magnesium and calcium. This selection is based on the fact that analytical procedures for these species have become well established. More importantly, under most atmospheric conditions, this set of ions is expected to account for a major part of the aerosol mass, and the measurements here are an important step towards mass closure of the aerosols. As mentioned above, quantitative measurements of nitrate with a filter technique remain problematic and are associated with high uncertainties.

In the GAW Programme, it is recommended that analyses be done using ion chromatography for the most cost-effective approach. The IC technique has the advantage of chemical speciation and relatively low cost per analysis, and has matured to the degree that the sensitivities for each ionic species, the cost and the maintenance are all reasonably well known. If IC is set up properly, all the recommended ionic species can be analysed in one single sample injection. Alternative analytical techniques exist but their use may introduce systematic differences among GAW stations. It is part of each laboratory's responsibility to document the equivalence of these alternative techniques, such as AAS or ICP-MS, with IC whenever they are used. Calibration of IC instruments is an integral part of every laboratory's standard operating procedures, and each laboratory must implement quality control procedures that guarantee the accuracy of calibrations. Recommendations for GAW are similar to those reported in WMO (2004*b*) for precipitation chemistry. In addition, protocols for filter extraction should be well documented.

Instruments are emerging on the scene for continuous and semi-continuous measurement of sulphate, nitrate, and organic carbon in aerosols. In particular, progress in aerosol mass spectrometry (AMS) has led to the development of instruments that can be used for monitoring purposes, providing quantitative measurements of the total mass and size distribution of non-refractory chemical composition in the submicron-size range. For example, the aerosol chemical speciation monitor (ACSM) is a simple version of AMS that can provide chemically speciated mass loadings and aerosol mass spectra with one-hour time resolution. No standard operating procedures exist yet for ACSM or other AMS instruments, but the method's suitability for long-term monitoring is clear and will undoubtedly bring revision of aerosol chemical speciation procedures in the future.

The *concentration of carbonaceous species* (with both elemental and organic fractions) is also one of the core pieces of information recommended at GAW stations. Carbonaceous species are still the least understood and most difficult to characterize of all aerosol chemical components. Total aerosol carbon mass can be divided into three fractions: inorganic carbonates, organic carbon (OC), and a third fraction ambiguously called elemental carbon (EC), black carbon (BC), soot or refractory carbon in the scientific literature with no clear definition of the terms. Recommendations for proper use of terminology for BC-related species have been proposed by Petzold et al. (2013) to clarify the terms used in atmospheric research; they recommend that the term "black carbon" be used only in a qualitative sense, and that terms related to the measurement technique be used when reporting quantitative results. According to this terminology, thermo-optical methods can be used to derive total carbon (TC) and OC/ EC fraction in atmospheric aerosol filters. When using optical methods, the light-absorbing component is called equivalent black carbon (EBC), even though the optical method is not specific for carbon.

It is recommended that TC, OC and EC be measured in the GAW Programme, leaving out the relatively minor and difficult inorganic carbon component and the more complicated issue of organic carbon speciation. Sampling of aerosol carbonaceous materials is recommended using quartz filters, pre-fired at 350 °C to 400 °C for 2 h, and at the same sampling frequency as the Teflon filters. The quartz filter can be analysed for TC using the thermal evolution technique. The mass concentration of the total carbon is obtained by thermal oxidation of the carbon, usually at 750 °C in the presence of a catalyst, to measurable carbon dioxide. Detection of the evolved carbon dioxide is done in one of two ways: either by reduction to methane in the presence of a catalyst, and then FID, or by direct detection by NDIR detectors.

The measurement of the TC components – OC and EC – is more difficult than the measurement of TC (Schmid et al., 2001). The distinction between the fractions is made by temperature-controlled volatilization/pyrolysis. This is followed by catalysed oxidation to CO_2 and detection by NDIR, or in some instruments, further catalysed reduction of the CO_2 to CH_4 and final detection by FID. There are different temperature-control programmes in use. At present, GAW recommends the use of one of three thermo-optical techniques: the IMPROVE (Interagency Monitoring of Protected Visual Environments) protocol (Chow et al., 1993; Chow et al., 2005), NIOSH (National Institute for Occupational Safety and Health) protocol (Birch and Cary, 1996) and EUSAAR-2 (European Supersites for Atmospheric Aerosol Research) protocol (Cavalli et al., 2010). Relatively good agreement is obtained between the IMPROVE, NIOSH and EUSAAR-2 protocols for TC determination, while they strongly differ for EC determination (Chow et al., 2001). Because EC represents a relatively small fraction of TC, OC determination by the three protocols is also comparable. It is accepted that the IMPROVE and EUSAAR-2 protocols are most suited for non-urban background sites, while the NIOSH is applied to samples from urban sites in the US Environmental Protection Agency (EPA). The use of IMPROVE or EUSAAR-2 may therefore be preferred over NIOSH for global remote GAW stations. Use of the EUSAAR-2 and IMPROVE protocols for EC determination may lead to different results but should be preferred over any alternative techniques. Whenever an alternative approach is used for OC measurements, it is recommended that a periodic determination of OC using one of the thermo-optical methods be conducted so that results can be compared. This is also true for AMS techniques before a standardized protocol is well established.

The use of optical methods for estimating EBC involves measuring the change in optical transmission of a deposit of particles on a filter (absorption) and applying a site-specific and instrument type-specific mass absorption efficiency to derive EBC. Two key assumptions are required to derive the equivalent black carbon mass concentration from light absorption measurements: (i) black carbon is the only species responsible for the aerosol light absorption, and (ii) the sampled black carbon has the same mass absorption efficiency as the standards used in laboratory calibrations of the absorption instrument. These assumptions can be evaluated by experimentally determining the mass absorption efficiency by simultaneously making light absorption measurements and EC measurements as described above. At sites where EC concentrations are not routinely determined on quartz-fibre filters, less frequent filter collections can be used to derive site- and season-specific values of the mass absorption efficiency. Thus, for

GAW measurements of EBC, experimentally derived values of the mass absorption efficiency at a site are essential when estimating black carbon mass concentration from light absorption measurements.

The use of incandescent methods, such as single-particle soot photometers, or volatility techniques, such as volatility scanning mobility particle sizer (SMPS), can provide information on refractory material present in aerosol, but their use in monitoring activities at GAW stations remains problematic given the lack of standardized protocols and of consistent intercomparison with thermo-optical techniques.

Dust aerosols can be sampled relatively easily without the problems posed by more semi-volatile aerosol components such as organics and ammonium nitrate. For GAW stations, it is recommended that a multi-elemental analysis approach be used to determine the mineral dust component. Teflon filters should be analysed for at least four of the major crustal elements, aluminium (Al), silicon (Si), iron (Fe), titanium (Ti) and scandium (Sc), and the related elements, sodium (Na), magnesium (Mg), potassium (K) and calcium (Ca). No specific analytical technique is recommended as there is a good selection available, including proton-induced X-ray emission (PIXE), instrumental neutron activation analysis (INAA), X-ray fluorescence (XRF), AAS and ICP-MS. These techniques usually have high sensitivities for the crustal elements. Not all techniques can provide all the required elements, and depending on availability, a combination of two or more techniques may be necessary.

16.6.2   **In situ measurements of aerosol radiative properties**

The following aerosol radiative properties are needed for climate studies, all at multiple wavelengths across the visible spectrum:

(a)   The aerosol light extinction coefficient (σ_{ep}) and its two components (scattering and absorption).

(b)   The aerosol optical depth (δ, see 16.6.5), defined as the integral over the vertical column of the aerosol light extinction coefficient.

(c)   The aerosol single-scattering albedo (ω_o), defined as $\sigma_{sp}/(\sigma_{ap} + \sigma_{sp})$, describes the relative contributions of scattering and absorption to the total light extinction. Purely scattering aerosols (such as sulphuric acid) have values of 1, while very strong absorbers (such as black carbon) have values of about 0.3.

(d)   Radiative transfer models commonly require one of two integral properties of the angular distribution of scattered light (phase function): the asymmetry factor (g) or the upscatter fraction (β). The asymmetry factor is the cosine-weighted average of the phase function, ranging from a value of –1 for entirely backscattered light to +1 for entirely forward-scattered light. The upscatter fraction gives the fraction of sunlight scattered in the upwards direction (back to space), which depends on the solar zenith angle as well as the size distribution and chemical composition of the particles. It can be estimated from the hemispheric backscatter fraction (b).

(e)   The mass scattering efficiency for species i, (α_{si}), is used in chemical transport models to evaluate the radiative effects of each chemical species forecast by the model. It is often calculated as the slope of the linear regression line relating the aerosol light scattering coefficient (σ_{sp}) and the mass concentration of the chemical species (though multiple linear regression is preferred, to deal with covariance of some chemical species). This parameter has units of $m^2 g^{-1}$.

(f)   The mass absorption efficiency for species i, (α_{ai}), is used in chemical transport models to evaluate the radiative effects of each chemical species forecast by the model. It is often calculated as the slope of the linear regression line relating the aerosol light absorption

coefficient (σ_{ap}) and the mass concentration of the chemical species (though multiple linear regression is preferred, to deal with covariance of some chemical species). This parameter has units of m^2 g^{-1}.

(g) The functional dependence of components of the aerosol light extinction coefficient (σ_{ep}, σ_{sp}, σ_{ap}) on relative humidity, f(RH), expressed as a multiple of the value at a low reference relative humidity (typically < 40%).

The aerosol light scattering coefficient is measured with an integrating nephelometer. Integrating nephelometers have been operated at baseline monitoring stations since the deployment of a four-wavelength instrument at the NOAA Mauna Loa Observatory in 1974. At present, there are about four dozen sites monitoring σ_{sp} routinely around the globe as part of the GAW global network. A few of these are operating single-wavelength units, but most are measuring σ_{sp} at three wavelengths. The multiwavelength integrating nephelometer TSI model 3563 operates at wavelengths of 450, 550 and 700 nm, and has the added feature of being able to measure σ_{sp} over two angular ranges: total scattering (7°–170°) and hemispheric backscattering (90°–170°, denoted as σ_{bsp}). The Aurora 3000 integrating nephelometer, manufactured by Ecotech, makes comparable measurements. While instruments do not exist for direct determination of g or β, the ratio $b = \sigma_{bsp}/\sigma_{sp}$ can be used to estimate either of these parameters (updated measurement guidelines are available in WMO (2011c)). Simpler, less expensive and less sensitive one-wavelength instruments are also commercially available. These instruments can provide useful information on the aerosol light scattering coefficient at regional sites where aerosol loadings allow the use of a less sensitive instrument.

Instruments capable of high time-resolution determination of the aerosol light absorption coefficient are commercially available. They are based on the rate of change of transmission through a fibre filter as particles are deposited on the filter. Calibration of these filter-based methods is difficult but required because the relationship between the change in light transmission and aerosol absorption optical depth on the filter depends on many factors, including the particular filter medium and the light-scattering nature of the particles.

One instrument in common use is the aethalometer. Originally, this instrument was calibrated in terms of an equivalent mass of black carbon rather than the fundamental property that provides the instrumental response: aerosol light absorption. Early models of the aethalometer have a very broad wavelength response, while newer versions offer narrowband measurements at multiple wavelengths.

Another commercial, filter-based instrument for determining σ_{ap} is the particle soot absorption photometer (PSAP) that measures laboratory aerosols with different single-scattering albedos, using a calibration standard based on the difference between σ_{ep}, measured with a long-path extinction cell, and σ_{sp}, measured with an integrating nephelometer. Updated measurement guidelines for PSAP instruments are provided in WMO (2011c).

Yet another filter-based instrument is the multi-angle absorption photometer (MAAP). The MAAP uses a different optical configuration than the aethalometer and PSAP, with measurements of the filter reflectivity at two different angles in addition to the filter transmission measurement. The two reflectivity measurements allow correction for multiple scattering processes involving the deposited particles and the filter matrix. This approach eliminates the need for a correction scheme based on independent measurements of the aerosol light scattering coefficient. The MAAP operates at a wavelength of 670 nm. Updated measurement guidelines for MAAP instruments are provided in WMO (2011c).

Recent improvements in a different approach to determining the aerosol light absorption coefficient, called photoacoustic spectroscopy, offer a promising alternative to filter-based methods. Although not as sensitive, the photoacoustic method allows determination of the aerosol light absorption coefficient while the particles are suspended in air, eliminating the artefacts introduced by depositing the particles on a filter. The photoacoustic method can be used in regions where light absorption levels are moderately high, and as a calibration standard for filter-based instruments.

16.6.3   **Particle number concentration and size distribution**

Condensation nuclei (CN) can be detected after the condensation of water or other condensable vapour (often an alcohol such as butanol) from a supersaturated atmosphere onto the particle. The supersaturation in condensation nuclei counters (CNCs), which are also known as condensation particle counters (CPCs), is typically quite large, about 150%, allowing the detection of particles as small as a few nanometres in diameter.

Optical methods are usually used to detect the resulting droplets. Early counters relied on manual counting, either in situ or after photography. The Nolan-Pollak counter and its derivatives (such as the Gardner counter) rely on determination of the optical extinction of the resulting cloud. Photometric observation of light scattered by the droplets is used in some counters. The most satisfactory method is individual counting of particles condensed in a continuous flow, as employed in the family of CNCs that have developed from the design of Bricard et al. (1976). This procedure is employed in most modern commercial CNCs. It has the advantage of giving a direct determination of CN concentrations up to about 10^5 cm^{-3} (although this limit is not generally reached by simpler, lower-cost counters).

Because of the complexity of the particle number size distribution measurement, it is recommended that number size distribution determinations be undertaken only at GAW stations with more highly developed aerosol programmes. Many commercial instruments are available to do this. They utilize a wide range of physical principles to classify particles according to size. Some of the better-known approaches use the electrical mobility of particles, aerodynamic size, or optical size determined by light scattering. This latter class includes a number of relatively small, low-cost instruments utilizing laser diodes. While any of these measurement approaches has the potential to add useful data to the overall GAW aerosol measurement programme, it is assumed that stations operating such instrumentation will have a highly developed aerosol programme that includes documentation, calibration and quality control measures.

16.6.4   **Cloud condensation nuclei**

Cloud condensation nuclei (CCN) measurements are made to determine the concentration and establish climatologies of those particles that have the potential to produce cloud droplets at supersaturations typical of natural clouds, that is, less than about 1%. Because of the complexity of the measurement, it is recommended that CCN determinations be undertaken at GAW stations with more highly developed aerosol programmes. Past CCN measurements in the GAW Programme have been made predominantly using static thermal-gradient chambers, which are well suited to relatively low-frequency sampling and low-resolution (differential) CCN spectrum determination. Instruments utilizing continuous flow offer another approach, and a commercial instrument using this approach is being deployed at a growing number of GAW stations. Measurement methods that have available droplet growth times comparable to real clouds are preferable.

16.6.5   **Aerosol optical depth**

Aerosol optical depth (AOD) is retrieved from observations of atmospheric spectral transmission. The solar spectral irradiance I at a given wavelength can be expressed as:

$$I = I_0 \exp\left(-m\delta\right) \tag{16.3}$$

with I_0 being the extraterrestrial (top of the atmosphere) irradiance of the sun, m the optical airmass and δ the total optical depth. The optical airmass equals 1 for a vertical path through the atmosphere and is roughly proportional to 1/cos z, with z being the zenith angle of the sun during the observation. The total optical depth δ at a given wavelength is composed of several components, such as scattering by gas molecules δ_R (Rayleigh scattering), extinction by aerosol particles δ_A, absorption of trace gases δ_G (ozone, nitrogen dioxide, etc.), and possible cloud contamination. Thus, the AOD can be obtained from the total optical depth by subtracting modelled estimates of the other components $\delta_A = \delta - \delta_R - \delta_G$.

Because AOD is essentially a difference between two larger numbers, it is sensitive to small calibration errors and, to a minor degree, to the methods chosen to model the other components. A traceable calibration uncertainty of 1.5%, corresponding to an uncertainty of 0.015 optical depths at unit optical airmass, should be maintained for AOD observations (WMO, 2005).

Wavelengths and bandpasses specifically for AOD that are largely free of variable extinction components (water vapour and NO_x) and strong ozone extinction have been recommended in WMO (2003*a*). The Baseline Surface Radiation Network (BSRN) and GAW-PFR (a network of aerosol optical depth observations with precision filter radiometers) are using four AOD channels at 368, 412, 500 and 862 nm. While some other networks have selected different wavelengths based on their specific needs (validation of satellite sensors, modelling efforts), measurements at 500 ±3 nm and 865 ±5 nm are typically available in most networks.

Measurements of the solar spectral irradiance are traditionally taken by sun-pointing radiometers (sun photometers) mounted on a two-axis solar tracker, with a sampling rate of once every minute to allow for objective quality control and cloud filtering algorithms. Homogeneous quality control is more difficult to achieve with handheld sun photometers.

Rotating shadow-band filter radiometers measure global and diffuse spectral irradiance at several wavelength bands. Direct normal irradiance obtained as the difference between global and diffuse radiation, normalized by the solar zenith angle, can be used to retrieve AOD the same way as with sun photometers.

More advanced instruments like sky-scanning radiometers can be used to infer additional column aerosol optical properties, including size distribution, single-scattering albedo or phase function, through sophisticated mathematical inversion models.

Sun photometers and shadow-band and sky-scanning radiometers are commercially available from several manufacturers. Centralized data evaluation and calibration services[4] are offered for standardized instruments by global networks, such as the Aerosol Robotic Network (AERONET), GAW-PFR or SKYNET (WMO, 2005).

16.6.6   **GAW aerosol lidar**

The basic lidar principle is the following: a laser pulse is transmitted into the atmosphere where it encounters gas molecules and particles; a small amount of this energy is backscattered in the direction of the receiver system, typically a telescope, and transferred to a photodetector as a photomultiplier. The resulting electrical signal is proportional to the optical power received, which depends on the presence, range and concentration of atmospheric scatterers and absorbers in the light path volume. Lidar techniques are able to characterize atmospheric aerosols in terms of vertical profiles of extinction and backscatter coefficients, lidar ratio, optical depth and microphysical properties such as shape, refractive index and size distribution, on timescales as short as minutes and vertical scales as short as metres.

Lidar observations are much more powerful if used in coordinated networks. Lidar networks are fundamental to studying aerosols on a large spatial scale and to investigating transport and modification phenomena. There are several research lidar networks that contribute to GAW: the Asian Dust and Aerosol Lidar Observation Network (AD-NET), Latin American Lidar Network (LALINET or ALINE), Commonwealth of Independent States Lidar Network (CIS-LINET), European Aerosol Research Lidar Network (EARLINET), Micro Pulse Lidar Network (MPLNET), NDACC, and the NOAA Cooperative Remote Sensing Science and Technology (CREST) Lidar Network. These networks are coordinated within the GAW Aerosol Lidar Observation Network (GALION; WMO, 2008*b*).

---

[4]   For more details, see the World Optical Depth Research and Calibration Centre website (at http://www.pmodwrc. ch/worcc/index.html).

Several different lidar techniques exist, depending on the specific instrument design and mainly on the specific laser-atmosphere scattering process.

Elastic backscatter lidar

This is the simplest type of aerosol lidar: the backscattered wavelength is identical to the transmitted wavelength, and the magnitude of the received signal at a given range depends on the backscatter cross-section of scatterers along the path to that range. Typical operating wavelengths are 355, 532 and 1 064 nm. The typical product of a backscatter lidar is the vertical profile of the aerosol backscatter coefficient obtained assuming a lidar ratio, i.e. the extinction-to-backscatter ratio, that is mostly constant throughout the profile and usually derived from an existing climatology obtained with measurements from a Raman lidar, described later. In this sense, it is necessary to underline that without an a priori assumption about the lidar ratio, this kind of lidar system cannot provide quantitative aerosol backscatter data.

Depolarization lidar

These are elastic backscatter lidars equipped with channels for the detection of the two parallel and cross-polarized components of the backscattered radiation. This provides quantitative information about particle shape, strongly contributing to aerosol typing as well as to the identification of thin clouds contaminating the profiles. A depolarization channel allows discrimination of volcanic ash and other aerosol particles. Typical operating wavelengths are 355 and 532 nm. Depolarization lidar systems need accurate calibration.

Raman lidar

The Raman lidar technique operates by measuring the inelastic Raman scattering by a specific gas. The Raman backscattered radiation from molecular nitrogen (or oxygen) is typically used for retrieving the vertical profile of the aerosol extinction coefficient that, coupled with the elastic scattering collected at the same emission wavelength, provides also the vertical profile of the aerosol backscatter coefficient without assuming a lidar ratio. Typical operating wavelengths are 355 and 532 nm. Most of the existing Raman lidar instruments are also equipped with a depolarization channel providing data on the particle linear depolarization ratio. Advanced multiwavelength Raman aerosol lidar techniques have been demonstrated to be the only technique capable of providing range-resolved aerosol microphysical properties. Moreover, rotational Raman lidar systems can be designed for optimizing extinction measurements in daytime conditions.

High spectral resolution lidar

The high spectral resolution lidar (HSRL) technique provides calibrated measurements of aerosol optical depth, extinction and backscatter. Measurements are computed from ratios of the particulate scattering to the measured molecular scattering. This provides absolute calibration and makes the calibration insensitive to dirt or precipitation on the output window. A very narrow, angular field-of-view reduces contamination from spurious sources, like multiple scattering contributions. The small field-of-view, coupled with a narrow optical bandwidth, nearly eliminates noise due to scattered sunlight, improving the signal-to-noise ratio also during daytime operations.

Ceilometers

Ceilometers are basically elastic backscatter lidars that employ a diode laser source emitting at infrared wavelengths (typically 905 or 1 064 nm) using a low energy but a high repetition rate (in units of μJ of energy per pulse and kHz for the rate) and that detect the elastic backscattered radiation by clouds and precipitation. Ceilometers are a self-contained, turnkey, surface-based,

active, remote-sensing device designed to measure cloud-base height and potentially the backscatter signals by aerosols. Ceilometers can provide qualitative information about aerosol vertical distribution. Generally, older and typically less powerful instruments are barely able to detect aerosol layers in the atmosphere, while newer instruments are quite useful for volcanic ash/dust detection and ash/dust plume tracking.

All of these lidar techniques can provide data products suitable for monitoring the spatial and temporal distribution of aerosol up to the upper troposphere/lower stratosphere region and can characterize them from a dynamical and microphysical point of view. The main lidar limitation is related to the presence of rain, dense fog and thick clouds (optical depths larger than 2–3) that do not allow monitoring of the atmosphere above the cloud-base region. The altitude range covered by lidars is limited at the bottom by the overlap height (altitude where there is a full overlap between the transmitter and the receiver) that is typically about 250–500 m above the ground level but could be also up to 2 km above the ground depending on the specific design. The maximum altitude range strongly depends on the laser power and optical design, but can be up to 25–30 km for high-power systems. It is difficult to provide general estimates of the accuracy of the different lidar products because these strongly depend on the specific system and on the meteorological conditions. On average, uncertainties for extinction and backscatter coefficient are about 20% (in the case of Raman lidar or HSRL). The retrieval of microphysical properties is possible only if optical data have uncertainties lower than 20%–30%.

Aerosol lidar products (see Table 16.4 for more details):

(a) Geometrical properties:

   (i)   Layer identification (top, bottom and centre of mass);

(b) Profiles of optical properties:

   (i)   Extensive optical parameters: aerosol backscatter coefficient (β_a), aerosol extinction coefficient (α_a);

   (ii) Intensive optical parameters: lidar ratio, particle linear depolarization ratio (δ_a), Ångström backscatter-related exponent ($\mathring{A}_\beta$), Ångström extinction-related exponent ($\mathring{A}_\alpha$);

(c) Optical properties in the identified layer:

   (i)   Integrated backscatter, aerosol optical depth;

   (ii) Mean intensive optical parameters (lidar ratio, particle linear depolarization ratio, Ångström backscatter-related exponent, Ångström extinction-related exponent);

(d) Aerosol typing classification;

(e) Mass concentration estimate;

(f) Microphysical properties retrieved.

Table 16.4. Lidar products related to specific surface-based lidar techniques (note that (d) = daytime only)

Surface-based lidar techniques	Geometrical properties	β_a	α_a	Lidar ratio^a	AOD	$\mathring{A}_\beta$	$\mathring{A}_\alpha$	Type^b	Microphysical properties
Ceilometer^c	✓	✓^{d}							
Ceilometer + sun photometer	✓	✓	✓(d)^f		✓(d)				
Ceilometer + sun photo. + depolarization lidar	✓	✓	✓(d)^f		✓(d)			✓ (limited)	
1-wavelength (1-λ) backscatter lidar	✓	✓							
1-λ backscatter lidar + sun photometer	✓	✓	✓(d)^f		✓(d)				
1-λ backscatter lidar + sun photo. + depolarization lidar	✓	✓	✓(d)^f		✓(d)			✓(d) (limited)	
Multiwavelength (m-λ)^e backscatter lidar	✓	✓					✓		
M-λ^e backscatter lidar + sun photometer	✓	✓	✓(d)^f		✓(d)	✓(d)^f	✓		✓(d)^f
M-λ^e backscatter lidar + sun photo. + depolarization lidar	✓	✓	✓(d)^f		✓(d)	✓(d)^f	✓	✓	✓(d)^f
1-λ Raman lidar/ HSRL	✓	✓	✓^{g}	✓^{g}	✓^{g}			✓^{g} (limited)	
1-λ Raman lidar/ HSRL + sun photometer	✓	✓	✓^{g}	✓^{g}	✓^{g}	✓(d)^f	✓(d)^f	✓ (limited)	✓(d)^f
1-λ Raman lidar/ HSRL + sun photo. + depolarization lidar	✓	✓	✓^{g}	✓^{g}	✓^{g}	✓(d)^f	✓(d)^f	✓	✓(d)^f
M-λ^e Raman lidar	✓	✓	✓^{g}	✓^{g}	✓^{g}	✓^{g}	✓	✓^{g}	✓^{g}
M-λ^e Raman lidar + sun photometer	✓	✓	✓^{g}	✓^{g}	✓^{g}	✓^{g}	✓	✓	✓^{g}
M-λ^e Raman lidar + sun photo. + depolarization lidar	✓	✓	✓^{g}	✓^{g}	✓^{g}	✓^{g}	✓	✓	✓^{g}

Notes:

a   From two independent measurements

b   Identification of scattering type (aerosol particles, cloud droplets, ice crystals, some aerosol type information)

c   A ceilometer is a single-wavelength, low-power lidar, with lower signal-to-noise ratio.

d   If calibrated

e   m > 2

f   Estimate only

g   Most Raman lidar systems operate during night-time. Some 24-h Raman lidar systems exist and their operability has been proved. However, few systems nowadays operate Raman channels also during daytime; HSRL is independent of daytime.

16.7   **NATURAL RADIOACTIVITY**

The global distributions of the source/sink terms of the naturally occurring radionuclides (^{7}Be, ^{10}Be, ^{210}Pb and ^{222}Rn) and the anthropogenic radionuclides (^{85}Kr) are reasonably well known. ^{7}Be and ^{10}Be are produced by cosmic-ray interactions in the upper troposphere and lower stratosphere. ^{222}Rn is exhaled from the Earth's land surface as a result of uranium decay in soil. ^{210}Pb is produced in the lower troposphere from the decay of ^{222}Rn. Most of the ^{85}Kr in the atmosphere is released during nuclear fuel reprocessing. Atoms of ^{7}Be, ^{10}Be and ^{210}Pb attach themselves to submicron-size aerosol particles, and therefore act as aerosol-borne tracers in the atmosphere. ^{222}Rn and ^{85}Kr, which are chemically and physically inert, act as noble gases in the atmosphere.

Measurements of radionuclides are not a priority area within the GAW Programme. Some general recommendations can be found in WMO (2001) and WMO (2004*a*).

————————

ANNEX. GAW CENTRAL FACILITIES

List of GAW central facilities and host institutions as of September 2013; the World Central Facilities have assumed global responsibilities, unless indicated.

Variable	Quality Assurance/Science Activity Centre	Central Calibration Laboratory (host of primary standard)	World Calibration Centre	Regional Calibration Centre	World Data Centre
CO_2	JMA (A/O)[a]	NOAA-ESRL	NOAA-ESRL (round robin) Empa (audits)		JMA
Carbon isotopes		MPI-BGC			JMA
CH_4	Empa (Am, E/A)[a] JMA (A/O)[a]	NOAA-ESRL	Empa (Am, E/A)[a] JMA (A/O)[a]		JMA
N_2O	UBA	NOAA-ESRL	IMK-IFU		JMA
CFCs, HCFCs, HFCs					JMA
SF_6		NOAA-ESRL	KMA		JMA
H_2		MPI-BGC			JMA
Total ozone	JMA (A/O)[a]	NOAA-ESRL,[b] EC[c]	NOAA-ESRL,[b] EC[c]	BoM,[b] NOAA-ESRL,[b] IZO,[c] JMA,[b] MOHp,[b] MGO,[d] OCBA,[b] SAWS,[b] SOO-HK[b]	EC,[f] DLR[g]
Ozonesondes	IEK-8	IEK-8	IEK-8		EC
Surface ozone	Empa	NIST	Empa	OCBA	JMA
Precipitation chemistry	NOAA-ARL	ISWS	ISWS		NOAA-ARL
CO	Empa	NOAA-ESRL	Empa		JMA
VOCs	UBA	NPL, NIST	IMK-IFU		JMA
SO_2					JMA
NO_x	UBA		IEK-8 (NO_x)		JMA
Aerosol	UBA (physical properties)		TROPOS (physical properties)		NILU,[f] DLR[g]
Optical depth		PMOD/WRC[e]	PMOD/WRC		NILU
UV radiation			PMOD/WRC	NOAA-ESRL (Am),[a] EUVC/ PMOD (E)[a]	EC
Solar radiation		PMOD/WRC	PMOD/WRC		MGO

Notes:
a   Am = Americas; E/A = Europe and Africa; A/O = Asia and the South-West Pacific
b   Dobson
c   Brewer
d   Filter instruments
e   Precision filter radiometers
f   Surface-based
g   Space-based

Host institutions

BoM	Bureau of Meteorology, Melbourne, Australia
BSRN	Baseline Surface Radiation Network, Federal Institute of Technology (ETH), Zürich, Switzerland
DLR	German Aerospace Centre, Oberpfaffenhofen, Wessling, Germany
EC	Environment Canada, Toronto, Canada
Empa	Swiss Federal Laboratories for Materials Testing and Research, Dübendorf, Switzerland
EUVC	European Ultraviolet Calibration Centre (see PMOD/WRC)
IEK-8	Institute of Energy and Climate Research: Troposphere (IEK-8), Research Centre Jülich GmbH, Jülich, Germany
TROPOS	Institute for Tropospheric Research, Leipzig, Germany
IMK-IFU	Karlsruhe Institute of Technology (KIT), Institute of Meteorology and Climate Research – Atmospheric Environmental Research, Garmisch-Partenkirchen, Germany
ISWS	Illinois State Water Survey, Champaign, IL, United States
IZO	Izaña Observatory, Tenerife, Spain
JMA	Japan Meteorological Agency, Tokyo, Japan
KMA	Korea Meteorological Administration, Seoul, the Republic of Korea
MGO	A.I. Voeikov Main Geophysical Observatory, Russian Federal Service for Hydrometeorology and Environmental Monitoring, St. Petersburg, the Russian Federation
MPI-BGC	Max Planck Institute for Biogeochemistry, Jena, Germany
MOHp	Meteorologisches Observatorium Hohenpeissenberg, Hohenpeissenberg, Germany
NOAA-ARL	National Oceanic and Atmospheric Administration, Air Resources Laboratory, Silver Spring, MD, United States
NOAA-ESRL	National Oceanic and Atmospheric Administration, Earth System Research Laboratory, Global Monitoring Division, Boulder, CO, United States
NILU	Norwegian Institute for Air Research, Kjeller, Norway
NIST	National Institute of Standards and Technology, Gaithersburg, MD, United States
NPL	National Physical Laboratory, Teddington, Middlesex, United Kingdom
OCBA	Observatorio Central de Buenos Aires, Argentina
PMOD/WRC	Physikalisch-Meteorologisches Observatorium Davos/World Radiation Centre, Davos, Switzerland
SAWS	South African Weather Service, Pretoria, South Africa
SOO-HK	Solar and Ozone Observatory, Hradec Kralove, Czech Republic
UBA	German Environmental Protection Agency, Berlin, Germany

_____

REFERENCES AND FURTHER READING

Birch, M.E. and R.A. Cary, 1996: Elemental carbon-based method for monitoring occupational exposures to particulate diesel exhaust. *Aerosol Science and Technology*, 25:221–241.

Bricard, J., P. Delattre, G. Madelaine and M. Pourprix, 1976: Detection of ultra-fine particles by means of a continuous flux condensation nuclei counter. In: *Fine Particles* (B.Y.H. Liu, ed.), Academic Press, New York.

Cavalli, F., M. Viana, K.E. Yttri, J. Genberg and J.-P. Putaud, 2010: Toward a standardised thermal-optical protocol for measuring atmospheric organic and elemental carbon: the EUSAAR protocol. *Atmospheric Measurement Techniques*, 3:79–89.

Chow, J.C., J.G. Watson, L.-W.A. Chen, G. Paredes-Miranda, M.-C.O. Chang, D. Trimble, K.K. Fung, H. Zhang and J. Zhen Yu, 2005: Refining temperature measures in thermal/optical carbon analysis. *Atmospheric Chemistry and Physics*, 5:2961–2972.

Chow, J.C., J.G. Watson, D. Crow, D.H. Lowenthal and T. Merrifield, 2001: Comparison of IMPROVE and NIOSH carbon measurements. *Aerosol Science and Technology*, 34:23–34.

Chow, J.C., J.G. Watson, L.C. Pritchett, W.R. Pierson, C.A. Frazier and R.G. Purcell, 1993: The DRI thermal/optical reflectance carbon analysis system: Description, evaluation, and applications in U.S. air quality studies. *Atmospheric Environment*, 27A(8):1185–1201.

Cooperative Programme for Monitoring and Evaluation of the Long-range Transmission of Air Pollutants in Europe (EMEP), 2014: *EMEP Manual for Sampling and Chemical Analysis*, Norwegian Institute for Air Research, Kjeller (available from http://www.nilu.no/projects/ccc/manual/index.html).

Coplen, T.B., W.A. Brand, M. Gehre, M. Gröning, H.A.J. Meijer, B. Toman and R.M. Verkouteren, 2006: New Guidelines for $\delta^{13}C$ Measurements. *Analytical Chemistry*, 78(7):2439–2441.

Götz, F.W.P., A.R. Meetham and G.M.B. Dobson, 1934: The vertical distribution of ozone in the atmosphere. *Proceedings of the Royal Society of London*, A145(855):416–446.

Grant, A., C.S. Witham, P.G. Simmonds, A.J. Manning and S. O'Doherty, 2010: A 15 year record of high-frequency, in situ measurements of hydrogen at Mace Head, Ireland. *Atmospheric Chemistry and Physics*, 10:1203–1214 (available from http://www.atmos-chem-phys.net/10/1203/2010/acp-10-1203-2010.pdf).

Heath, D.F., A.J. Krueger and H. Park, 1978: The solar backscatter ultraviolet (SBUV) and total ozone mapping spectrometer (TOMS) experiment. In: *The NIMBUS-7 User's Guide* (C.R. Madrid, ed.), NASA Goddard Space Flight Center, Greenbelt, Maryland.

Herndon, S.C., M.S. Zahniser, D.D. Nelson Jr., J. Shorter, J.B. McManus, R. Jiménez, C. Warneke and J.A. de Gouw, 2007: Airborne measurements of HCHO and HCOOH during the New England Air Quality Study 2004 using a pulsed quantum cascade laser spectrometer. *Journal of Geophysical Research*, 112(D10S03).

International Organization for Standardization/International Electrotechnical Commission, 2008: *Uncertainty of Measurement – Part 3: Guide to the Expression of Uncertainty in Measurement*, ISO/IEC Guide 98-3:2008, Incl. Suppl. 1:2008/Cor 1:2009, Suppl. 1:2008, Suppl. 2:2011. Geneva. (equivalent to: Joint Committee for Guides in Metrology, 2008: *Evaluation of Measurement Data – Guide to the Expression of Uncertainty in Measurement*, JCGM 100:2008, Corrected in 2010).

Jaroslawski, J., 2013: Improvement of the Umkehr ozone profile by the neural network method: analysis of the Belsk (51.80°N, 20.80°E) Umkehr data. *International Journal of Remote Sensing*, 34(15):5541–5550.

Mateer, C.L. and J.J. DeLuisi, 1992: A new Umkehr inversion algorithm. *Journal of Atmospheric and Terrestrial Physics*, 54(5):537–556.

Mateer, C.L. and H.U. Dütsch, 1964: *Uniform Evaluation of Umkehr Observations from the World Ozone Network, Part I – Proposed Standard Evaluation Technique*, NCAR, Boulder, Colorado.

National Institute for Occupational Safety and Health, 2014: Elemental Carbon (Diesel Particulate): Method 5040 (available from http://www.cdc.gov/niosh/docs/2003-154/method-6000.html).

Petropavlovskikh, I., P.K. Bhartia and J. DeLuisi, 2005: New Umkehr ozone profile retrieval algorithm optimized for climatological studies. *Geophysical Research Letters*, 32(L16808).

Petzold, A., J.A. Ogren, M. Fiebig, P. Laj, S.-M. Li, U. Baltensperger, T. Holzer-Popp, S. Kinne, G. Pappalardo, N. Sugimoto, C. Wehrli, A. Wiedensohler and X.-Y. Zhang, 2013: Recommendations for reporting "black carbon" measurements. *Atmospheric Chemistry and Physics*, 13:8365–8379.

Ramanathan, K.R. and J.V. Dave, 1957: The calculation of the vertical distribution of ozone by the Götz Umkehr Effect (method B). *Annals of the International Geophysical Year*, V(1):23–45.

Schmid, H., L. Laskus, H.J. Abraham, U. Baltensperger, V. Lavanchy, M. Bizjak, P. Burba, H. Cachier, D. Crow, J. Chow, T. Gnauk, A. Even, H.M. ten Brink, K.P. Giesen, R. Hitzenberger, C. Hueglin,

W. Maenhaut, C. Pio, A. Carvalho, J.-P. Putaud, D. Toom-Sauntry and H. Puxbaum, 2001: Results of the "carbon conference" international aerosol carbon round robin test stage I. *Atmospheric Environment*, 35(12):2111–2121.

Sofieva, V.F., N. Rahpoe, J. Tamminen, E. Kyrölä, N. Kalakoski, M. Weber, A. Laeng, T. von Clarmann, G. Stiller, S. Lossow, D. Degenstein, A. Bourassa, C. Adams, C. Roth, N. Lloyd, P. Bernath, R.J. Hargreaves, J. Urban, D. Murtagh, A. Hauchecorne, M. van Roozendael, N. Kalb and C. Zehner, 2013: Harmonized dataset of ozone profiles from satellite limb and occultation measurements. *Earth System Science Data Discussions*, 6:189–222.

Tegtmeier, S., M.I. Hegglin, J. Anderson, A. Bourassa, S. Brohede, D. Degenstein, L. Froidevaux, R. Fuller, B. Funke, J. Gille, A. Jones, Y. Kasai, K. Krüger, E. Kyrölä, G. Lingenfelser, J. Lumpe, B. Nardi, J. Neu, D. Pendlebury, E. Remsberg, A. Rozanov, L. Smith, M. Toohey, J. Urban, T. von Clarmann, K.A. Walker, and R. Wang, 2013: SPARC Data Initiative: A comparison of ozone climatologies from international limb satellite sounders. *Journal of Geophysical Research*, 118:12229–12247.

Tuzson, B., K. Zeyer, M. Steinbacher, J.B. McManus, D.D. Nelson, M.S. Zahniser and L. Emmenegger, 2013: Selective measurements of NO, NO_2 and NO_y in the free troposphere using quantum cascade laser spectroscopy. *Atmospheric Measurement Techniques*, 6:927–936.

Van der A, R. J., M.A.F. Allaart and H.J. Eskes, 2010: Multi sensor reanalysis of total ozone. *Atmospheric Chemistry and Physics*, 10:11277–11294.

Warneke, C., P. Veres, J.S. Holloway, J. Stutz, C. Tsai, S. Alvarez, B. Rappenglueck, F.C. Fehsenfeld, M. Graus, J.B. Gilman and J.A. de Gouw, 2011: Airborne formaldehyde measurements using PTR-MS: calibration, humidity dependence, inter-comparison and initial results. *Atmospheric Measurement Techniques*, 4:2345–2358.

Watson, J.G., J.C. Chow, L.-W. A. Chen and N.H. Frank, 2009: Methods to assess carbonaceous aerosol sampling artifacts for IMPROVE and other long-term networks. *Journal of the Air and Waste Management Association*, 59(8):898–911.

Wisthaler, A., E.C. Apel, J. Bossmeyer, A. Hansel, W. Junkermann, R. Koppmann, R. Meier, K. Müller, S.J. Solomon, R. Steinbrecher, R. Tillmann and T. Brauers, 2008: Technical note: Intercomparison of formaldehyde measurements at the atmosphere simulation chamber SAPHIR. *Atmospheric Chemistry and Physics*, 8:2189–2200.

World Meteorological Organization, 2001: *Global Atmosphere Watch Measurements Guide*. Global Atmosphere Watch Report No. 143 (WMO/TD-No. 1073). Geneva.

———, 2003*a*: *Quality Assurance in Monitoring Solar Ultraviolet Radiation: the State of the Art* (A.R. Webb). Global Atmosphere Watch Report No. 146 (WMO/TD-No. 1180). Geneva.

———, 2003*b*: *WMO/GAW Aerosol Measurement Procedures: Guidelines and Recommendations*. Global Atmosphere Watch Report No. 153 (WMO/TD-No. 1178). Geneva.

———, 2004*a*: *1st International Expert Meeting on Sources and Measurements of Natural Radionuclides Applied to Climate and Air Quality Studies* (Gif sur Yvette, France, 3–5 June 2003). Global Atmosphere Watch Report No. 155 (WMO/TD-No. 1201). Geneva.

———, 2004*b*: *Manual for the GAW Precipitation Chemistry Programme (Guidelines, Data Quality Objectives and Standard Operating Procedures)* (M.A. Allan, ed.). Global Atmosphere Watch Report No. 160 (WMO/TD-No. 1251). Geneva.

———, 2005: *WMO/GAW Experts Workshop on a Global Surface-based Network for Long Term Observations of Column Aerosol Optical Properties* (U. Baltensperger, L. Barrie and C. Wehrli, eds.) (Davos, Switzerland, 8–10 March 2004). Global Atmosphere Watch Report No. 162 (WMO/TD-No. 1287). Geneva.

———, 2006: *13th WMO/IAEA Meeting of Experts on Carbon Dioxide Concentration and Related Tracers Measurement Techniques* (J.B. Miller, ed.) (Boulder, Colorado, USA, 19–22 September 2005). Global Atmosphere Watch Report No. 168 (WMO/TD-No. 1359). Geneva.

———, 2007*a*: *A WMO/GAW Expert Workshop on Global Long-Term Measurements of Volatile Organic Compounds (VOCs)* (Geneva, Switzerland, 30 January to 1 February 2006). Global Atmosphere Watch Report No. 171 (WMO/TD-No. 1373). Geneva.

———, 2007*b*: *WMO Global Atmosphere Watch (GAW) Strategic Plan: 2008–2015*. Global Atmosphere Watch Report No. 172 (WMO/TD-No. 1384). Geneva.

———, 2008*a*: *The Tenth Biennial WMO Consultation on Brewer Ozone and UV Spectrophotometer Operation, Calibration and Data Reporting* (C.T. McElroy and E.W. Hare, eds.) (Northwich, United Kingdom, 4–8 June 2007). Global Atmosphere Watch Report No. 176 (WMO/TD-No. 1420). Geneva.

———, 2008*b*: *Plan for the Implementation of the GAW Aerosol Lidar Observation Network GALION* (J. Bösenberg and R. Hoff) (Hamburg, Germany, 27–29 March 2007). Global Atmosphere Watch Report No. 178 (WMO/TD-No. 1443). Geneva.

———, 2008*c*: *Operations Handbook – Ozone Observations with a Dobson Spectrophotometer* (R.D. Evans, rev.). Global Atmosphere Watch Report No. 183 (WMO/TD-No. 1469). Geneva.

———, 2009*a*: *Guidelines for the Measurement of Methane and Nitrous Oxide and their Quality Assurance.* Global Atmosphere Watch Report No. 185 (WMO/TD-No. 1478). Geneva.

———, 2010: *Guidelines for the Measurement of Atmospheric Carbon Monoxide.* Global Atmosphere Watch Report No. 192 (WMO/TD-No. 1551). Geneva.

———, 2011*a*: *WMO/GAW Expert Workshop on Global Long-term Measurements of Nitrogen Oxides and Recommendations for GAW Nitrogen Oxides Network* (S. Penkett, S. Gilge, C. Plass-Duelmer and I. Galbally) (Hohenpeissenberg, Germany, 8–9 October 2009). Global Atmosphere Watch Report No. 195 (WMO/TD-No. 1570). Geneva.

———, 2011*b*: *Addendum for the Period 2012–2015 to the WMO Global Atmosphere Watch (GAW) Strategic Plan 2008–2015* (J. Klausen, ed.). Global Atmosphere Watch Report No. 197. Geneva.

———, 2011*c*: *WMO/GAW Standard Operating Procedures for In-situ Measurements of Aerosol Mass Concentration, Light Scattering and Light Absorption* (J.A. Ogren, ed.). Global Atmosphere Watch Report No. 200. Geneva.

———, 2012*a*: *Standard Operating Procedures (SOPs) for Air Sampling in Stainless Steel Canisters for Non-Methane Hydrocarbons Analysis* (R. Steinbrecher and E. Weiß). Global Atmosphere Watch Report No. 204. Geneva.

———, 2012*b*: *16th WMO/IAEA Meeting on Carbon Dioxide, Other Greenhouse Gases and Related Measurement Techniques (GGMT-2011)* (G. Brailsford, ed.) (Wellington, New Zealand, 25–28 October 2011). Global Atmosphere Watch Report No. 206. Geneva.

———, 2013: *Guidelines for Continuous Measurements of Ozone in the Troposphere* (I.E. Galbally and M.G. Schultz). Global Atmosphere Watch Report No. 209 (WMO-No. 1110). Geneva.

———, 2014: *Quality Assurance and Quality Control for Ozonesonde Measurements in GAW* (H.G.J. Smit and ASOPOS Panel). Global Atmosphere Watch Report No. 201. Geneva.

———————

PART II. OBSERVING SYSTEMS

PART CONTENTS

CHAPTER CONTENTS

CHAPTER 1. MEASUREMENTS AT AUTOMATIC WEATHER STATIONS

1.1 GENERAL

1.1.1 Definition

An automatic weather station (AWS) is defined as a "meteorological station at which observations are made and transmitted automatically" (WMO, 1992*a*).

At an AWS, the instrument measurements are read out or received by a central data-acquisition unit. The collected data from the autonomous measuring devices can be processed locally at the AWS or elsewhere, for example, at the central processor of the network (WMO, 2010*a*). Automatic weather stations may be designed as an integrated concept of various measuring devices in combination with the data-acquisition and processing units. Such a combined system of instruments, interfaces and processing and transmission units is usually called an automated weather observing system (AWOS) or automated surface observing system (ASOS). It has become common practice to refer to such a system as an AWS, although it is not a "station" fully in line with the stated definition. Nevertheless, throughout this chapter, an AWS may refer to just such a system.

1.1.2 Purpose

Automatic weather stations are used for increasing the number and reliability of surface observations. They achieve this by:

(a) Increasing the density of an existing network by providing data from new sites and from sites that are difficult to access and inhospitable;

(b) Supplying, for manned stations, data outside the normal working hours;

(c) Increasing the reliability of measurements by using sophisticated technology and modern, digital measurement techniques;

(d) Ensuring the homogeneity of networks by standardizing the measuring techniques;

(e) Satisfying new observational needs and requirements;

(f) Reducing human errors;

(g) Lowering operational costs by reducing the number of observers;

(h) Measuring and reporting with high frequency or continuously.

1.1.3 Meteorological requirements

The general requirements, types, location and composition, frequency and timing of observations are described in WMO (2010*b*, 2011*c*).

Considering that AWSs are fully accepted as meteorological stations when providing data with accuracy comparable to that of conventional stations, the accuracy requirements given in Part I, Chapter 1 of the Guide may also be applied, as appropriate, to AWSs.

The guidance provided in this chapter must be used in conjunction with the chapters on measurements of the various meteorological variables in Part I and, in particular, with the chapters on quality management (Chapter 1), sampling (Chapter 2) and data reduction (Chapter 3) in Part IV.

The development and installation of AWSs should be the result of a definite, coordinated plan for getting data to users in the format required. To achieve this, negotiations should first be undertaken with the users to draw up a list of all functional requirements and to develop practical means of fulfilling them.

Furthermore, it is not always satisfactory to rely on equipment suppliers to determine operational requirements. The Commission for Instruments and Methods of Observation (CIMO) gives the following advice to Members of WMO and, by inference, to any Service taking meteorological measurements.

When considering the introduction of new AWS instrument systems, Meteorological Services should:

(a)   Introduce into service only those systems that are sufficiently well documented so as to provide adequate knowledge and understanding of their capabilities, characteristics and any algorithms used;[1]

(b)   Retain or develop sufficient technical expertise to enable them to specify system requirements and to assess the appropriateness of the capabilities and characteristics of such systems and algorithms used therein;[2]

(c)   Explore fully user requirements and engage users in system design of AWSs;

(d)   Engage users in validation and evaluation of the new automated systems;

(e)   Engage manufacturers in the system assessment and need for improvements in performance;

(f)   Develop detailed guides and documentation on the systems to support all users;

(g)   Develop adequate programmes for maintenance and calibration support of the AWSs;

(h)   Consult and cooperate with users, such as aeronautical authorities, throughout the process from AWS design, to implementation, to operational use;

(i)   Develop and apply reporting methods for national use to accommodate both observations generated by traditional and automated systems.

With respect to the automation of traditional visual and subjective observations, and future changes in reporting code, Meteorological Services should improve their definition of requirements with respect to:[3]

(a)   Areas of application for which data are no longer required;

(b)   Areas of application for which different or new data are needed;

(c)   Prioritizing the requirements for data to be provided by AWSs.

---

[1]   Recommended by the Commission for Instruments and Methods of Observation at its twelfth session (1998) through Recommendation 2 (CIMO-XII).
[2]   Recommended by the Commission for Instruments and Methods of Observation at its twelfth session (1998) through Recommendation 2 (CIMO-XII).
[3]   Recommended by the Commission for Instruments and Methods of Observation at its twelfth session (1998) through Recommendation 5 (CIMO-XII).

When considering the development and application of algorithms for AWSs, Meteorological Services should:[4]

(a) Encourage instrument and system designers to work closely with relevant users to understand fully user requirements and concerns;

(b) Work together with system designers to publish and disseminate, for widespread use and possible standardization, descriptions of the data-processing algorithms used in their systems to derive meteorological variables;

(c) Test and evaluate thoroughly new algorithms and systems being introduced and disseminate the test results in the form of performance characteristics to users of the observations;

(d) Evaluate thoroughly, through field testing and intercomparison, the relationship of new algorithms and systems to previous methods, and establish transfer functions for use in providing data continuity and homogeneity, and disseminate these data to users.

1.1.4 Climatological requirements[5]

Where a proposed automatic station has a role in providing data for climatological records, it is important for the integrity, homogeneity and utility of the climate datasets that the following areas be considered for action (see WMO, 1993):

(a) In cases where an AWS replaces a manual observing system that has been in operation for a long time, a sufficient overlap in observation systems to facilitate maintaining the homogeneity of the historical record must be assured.[6] The overlap time is dependent on the different measured variables and on the climate region. In tropical regions and islands, the overlap time could be shorter than in extratropical and mountainous regions. The following general guidelines are suggested for a sufficient operational overlap between existing and new automated systems:

   (i)   Wind speed and direction: 12 months

   (ii)   Temperature, humidity, sunshine, evaporation: 24 months

   (iii) Precipitation: 60 months

   (It will often be advantageous to have an ombrometer operated in parallel with the automatic raingauge.)

   A useful compromise would be an overlap period of 24 months (i.e. two seasonal cycles);

(b) Accurate metadata should be maintained for each AWS installation;[7]

(c) Procedures should be standardized for quality assurance and processing of data from AWSs (see section 1.3.2.8);

(d) The existing and future requirements of climate data users should be defined precisely and considered in developing statements of requirement for automated observations by AWSs;[8]

---

[4] Recommended by the Commission for Instruments and Methods of Observation at its twelfth session (1998) through Recommendation 2 (CIMO-XII).

[5] Recommended by the Commission for Instruments and Methods of Observation at its twelfth session (1998) through Recommendation 3 (CIMO-XII).

[6] Note also WMO (2010a), section 3.2.1.4.4.4(c) "one year of parallel measurements does not suffice; preference is given to at least two years, depending on the climatic region".

[7] See Part I, Chapter 1, section 1.1.3.

[8] See Part I, Chapter 1, Annex 1.E.

(e)   Climate users should be trained in the most effective use of AWS data;[9]

(f)   Specifications for a standardized climatological AWS should be developed which would record a basic set of climate variables such as temperature, precipitation, pressure and wind. Standardized water vapour measurements should be included due to the significance of this parameter in climate-change studies. Extreme values of all variables should be accurately and consistently recorded in a way that can be precisely related to older, manually-observed, data.[10]

1.1.5   Types of automatic weather stations

Automatic weather stations are used to satisfy several needs, ranging from a simple aid-to-the-observer at manned stations to complete replacement of observers at fully automatic stations. It is possible to classify AWSs into a number of functional groups; these frequently overlap each other, however, and the classification then begins to break down. A general classification could include stations that provide data in real time and those that record data for non-real-time or off-line analysis. It is not unusual, however, for both of these functions to be discharged by the same AWS.

Real-time AWS: A station providing data to users of meteorological observations in real time, typically at programmed times, but also in emergency conditions or upon external request. Typical real-time use of an AWS is the provision of synoptic data and the monitoring of critical warning states such as storms and river or tide levels.

Off-line AWS: A station recording data on site on internal or external data storage devices possibly combined with a display of actual data. The intervention of an observer is required to send stored data to the remote data user. Typical stations are climatological and simple aid-to-the-observer stations.

Both types of stations can optionally be set up with means both for manual entry and for the editing of visual or subjective observations that cannot yet be made fully automatically. This includes present and past weather or observations that involve high costs, such as cloud height and visibility. Such a station could be described as partially or semi-automated.

Since AWSs can be very expensive, the stations' facilities can also be used to satisfy the common and specific needs and requirements of several applications, such as synoptic, aeronautical and agricultural meteorology, hydrology and climatology. They may also be used for special purposes, such as nuclear power safety, air and water quality, and road meteorology. Some AWSs are, therefore, multipurpose AWSs.

1.1.6   Networking

An AWS usually forms part of a network of meteorological stations, each transmitting its processed data to a central network processing system by various data transmission means. As the tasks to be executed by this central system are strongly related, and often complementary, to the tasks of the AWSs, the functional and technical requirements of both the central system and the AWSs should be very well coordinated.

When planning the installation and operation of a network of AWSs, it is of the utmost importance to consider the various problems associated with maintenance and calibration facilities, their organization and the training and education of technical staff. Network density considerations are beyond the scope of this Guide as they depend on the specific applications. However, the optimum siting and exposure of stations have an important influence on the performance of the stations and must be studied before they are installed.

---

[9]   For example, see WMO (1997), especially Part II – "Implementation and user training considerations".
[10]   Ibid.

1.2 AUTOMATIC WEATHER STATION HARDWARE

An AWS may consist of an integrated AWOS (and data-acquisition system) or a set of autonomous measuring devices connected to a data-collection and transmission unit. The layout of an AWS typically consists of the following:

(a) On a standard observing area, preferably no smaller than 25 m x 25 m (Part I, Chapter 1, and WMO, 2010*a*), a series of automated sensors sited at the recommended positions and interconnected to one or more data collection units using interfaces, or for an AWOS, a set of sensors installed in close combination, but not affecting each other, directly connected to a central processing unit (CPU) by means of shielded cables, fibre optics, or radio links;

(b) A CPU for sensor data-acquisition and conversion into a computer-readable format, proper processing of data by means of a microprocessor-based system in accordance with specified algorithms, the temporary storage of processed data, and their transmission to remote users of meteorological information;

(c) Peripheral equipment such as a stabilized power supply providing power to the various parts of the station, a real-time clock, and built-in test equipment for automatic monitoring of the status of vital parts of the station. For specific applications, local terminals for the manual entry and editing of data, display devices and printers, or recorders are added to the station.

The growing interaction between society and the atmosphere results in changing and growing requirements, such as demands for more stations and more variables to be measured, transmission at more frequent intervals, new formats and better performance. As a consequence, existing AWS hardware and software have to be adapted to new requirements. This can be carried out only if the AWS is well planned on a modular basis. Adaptation processes and tests are often more complicated than expected. A well-planned AWS includes pre-tested options that allow changes in the configuration and the system parameters. Other desirable features include spare power capacity, space in installation frames, spare communication interfaces, spare processing capacity and a flexible software environment. Guidance on preparing a functional specification for the AWS system is available in Part I of WMO (1997).

1.2.1 Sensors

The meteorological requirements for sensors used at AWSs are not very different from those of sensors at manual observation stations. See also the recommendations in the relevant chapters in Part I of this Guide. Because measurements at most AWSs are controlled from long distances, these sensors must be robust, fairly maintenance-free and should have no intrinsic bias or uncertainty in the way in which they sample the variables to be measured. In general, all sensors with an electrical output are suitable. A large number of sensors of varying performance and quality (and price) are suitable for use with automatic data-acquisition systems. There are frequent new developments, some enhancing the performance of existing sensors, while others are often based on new physical principles. Depending on their output characteristics, sensors can be classified as analogue, digital and "intelligent" sensors.

Analogue sensors: Sensor output is commonly in the form of voltage, current, charge, resistance or capacitance. Signal conditioning converts these basic signals into voltage signals.

Digital sensors: Sensors with digital signal outputs with information contained in a bit or group of bits, and sensors with pulse or frequency output.

"Intelligent" sensors/transducers: Sensors including a microprocessor performing basic data-acquisition and processing functions and providing an output in serial digital or parallel form.

With regard to meteorological sensors, Part I of this Guide gives a full description of general aspects, types of sensors, methods of measurement, units, scales, exposure, sources of error, calibration and maintenance. CIMO assists Members through the regular organization of

international instrument intercomparisons. The results can be very valuable for evaluating different measuring approaches. Since 1968, CIMO has been using questionnaires to obtain information on instrument development, and a report, entitled the *Instrument Development Inquiry*, is published every four years. The reports contain information on both instruments under development and instruments put into operational use. Information on new developments and operational experience can be found in the proceedings of national symposiums, magazines and journals, and also in the proceedings of the technical conferences organized regularly by CIMO. These technical conferences are accompanied by an exhibition of meteorological instrumentation where manufacturers present their latest developments. The results of CIMO intercomparisons, the *Instrument Development Inquiry* reports and the proceedings of CIMO technical conferences are published by WMO in the Instruments and Observing Methods reports series. The direct exchange of experience between operators of AWS networks, in particular those operating stations in similar environmental conditions, is recommended as another way of obtaining information.

Some specific considerations concerning AWS sensors are given in the following paragraphs. Achievable operational accuracies are given in Part I, Chapter 1, Annex 1.E[11] of the Guide. As experimental results become available, these estimates will be updated by CIMO, as appropriate. Sensor (laboratory) calibration accuracy should be better by a factor of at least two allowing for transformation to linear response functions. Sensor resolution should be better by a factor of about three than the stated requirement (which includes the performance of the interface).

Atmospheric pressure: A wide variety of devices exists, mostly based upon the use of an aneroid capsule, vibrating wire, or quartz crystal which provide an output in electrical analogue or digital form. For digital sensors, reference is made to WMO (1992*b*). The main problems to be carefully considered by the designer or specifier of an AWS are the adverse effects of temperature, long-term drift, vibration and exposure. Temperature effects are severe and are not always fully compensated by built-in temperature compensation circuits. AWS pressure sensors have an intrinsic long-term drift in accuracy, typically less than 0.2 to 0.3 hPa every six months, and therefore require regular calibration. The effects of vibration and mechanical shocks on the output of pressure sensors are important, especially where marine AWS applications are concerned. Because of the vulnerability of most readily available pressure sensors to the effects of external exposure, it is common practice to house the pressure instrument within a sealed and thermo-stabilized small box inside the CPU enclosure. In some countries, the sensor is connected to the outside of the box via a tube equipped with a static pressure head. For aeronautical applications or at remote stations, where a high degree of accuracy and reliability are required, two or more pressure sensors are incorporated in the station.

Part I, Chapter 3 gives guidelines on the use of digital barometers with AWSs.

Temperature: The most common types of thermometers used in an AWS are pure metal resistance thermometers or thermistors. The platinum resistance thermometer (100 Ω at 0 °C) shows very good long-term stability and can be considered as the preferred type of sensor.

Electrical thermometers usually have a short time-constant and, when sampled by fast electronic circuits, their output reflects high-frequency low amplitude fluctuations of the local temperature. This problem can be avoided by using sensors with a long time-constant, by artificially damping the response with a suitable circuit to increase the time constant of the output signal, or by averaging digitally the sampled outputs in the CPU. Resistance thermometers require linearization. This can be obtained by appropriate circuits in signal conditioning modules, or by software algorithms. It is highly recommended that the thermistor characteristics should be linearized. Of great concern is the proper protection of the sensor against the effects of radiation. Radiation shields adjusted to the size of the sensor are widely used and replace the common naturally ventilated Stevenson screen in an AWS. For accurate measurements, the radiation shields should be artificially ventilated with an air speed of about 3 m s^{-1}, but precautions should be taken to prevent the entry of aerosols and drizzle in order to avoid wet-bulb effects.

---

[11] As specified by the Meeting of Experts on Operational Accuracy Requirements (1991) and approved by the forty-fourth session of the Executive Council (1992) for inclusion in this Guide.

Humidity: A very comprehensive overview of humidity sensors for use in an AWS can be found in WMO (1989*a*).

Although relatively low-cost resistance and capacitive sensors for direct relative humidity measurements are widely employed in AWSs, they are still susceptible to poor performance in the presence of pollutants and require special protection filters. Intercomparisons reveal that additional corrections have to be applied for measurements below 0 °C, even if the sensors incorporate temperature compensation circuits and if hysteresis problems occur when exposed to saturated conditions.

Dewpoint meters, such as the saturated lithium chloride sensor and the chilled-mirror sensor, are also used in an AWS. The major drawback of lithium chloride sensors is their sensitivity to power failures; they require field interventions after a power interruption. The optical dewpoint meter is considered as the most promising technique, but further investigations are required in order to develop a good automatic mirror-cleaning device.

The problems associated with the short time-constant of many humidity sensors are more critical than for temperature sensors. As for temperature measurements, all types of sensors have to be installed in proper radiation shields. Preference should be given to aspirated or well-ventilated radiation shields. Shields may be similar in construction to those used for temperature measurements. Large errors can occur due to aspiration and cleaning problems.

Wind: The use of conventional cup or propeller anemometers with pulse or frequency output is widespread and presents no particular technical problem other than that associated with icing in severe conditions. This complication can be overcome by heating the sensor in moderate icing conditions, but this results in a significant increase in electrical power consumption. It is recommended that, for new cup and propeller anemometers, the response length should be smaller than 5 m and that, in new digital systems, the sampling frequency must be compatible with the filtering applied. In counting devices, this implies that the number of pulses over one counting interval is considered as one sample.

The use of conventional analogue instruments equipped with a potentiometer for wind direction measurements is also widespread in AWSs. Wind-vane devices with digital angle encoders, usually in one or other form of Gray code, are increasingly used. Wind vanes with an undamped natural response length smaller than 10 m and a damping ratio between 0.3 and 0.7 are recommended. For vanes with digital encoders, a minimum resolution of 7 bits is required.

CIMO also recommends that, for new systems, it should be possible to report standard deviations of wind speed and direction with a resolution of 0.1 m s^{-1} and 10°, respectively.

A wind system with a serial digital output and one or more digital displays providing a direct visualization of the operational variables (wind peak, wind averages over two and 10 min, wind direction and extremes) is a typical example of an intelligent sensor.

Precipitation: The most common rainfall-measuring equipment in an AWS is the tipping-bucket raingauge. Gauges are rapidly clogged by debris such as leaves, sand or bird droppings; therefore, care must be taken with AWSs used for long unattended operations. For measurements of rain and snowfall below 0 °C, different parts of the gauge must be heated properly. This can give rise to serious electrical power problems, in particular for battery-operated AWSs. Care should be taken since heated gauges introduce errors due to evaporation losses. An achievable observing accuracy of 5% to 10% is considered to be excellent. Accuracy can be improved by surrounding the raingauge with a proper windshield (for example, a Nipher shield) (see WMO, 1994, for a comparison of precipitation sensors).

Sunshine: A number of sunshine duration recorders with electrical output are available. Reference is made to WMO (1989*b*). WMO has adopted a threshold value of 120 W m^{-2} for bright sunshine of direct solar irradiance, thus solving a long-term problem. A drawback of a sunshine sensor for unattended use over long periods of time is that dirt accumulates on the front aperture which results in apparent changes in threshold.

Radiation: Most of the sensors used for these measurements at conventional stations can, in principle, be connected to an automatic system. The main technical problem is that these sensors are usually analogue devices that produce very small, continuously variable voltages as signal output. These voltages are very vulnerable to electromagnetic interference on the signal cables and adequate measurements have to be taken. The problem of contamination of the front aperture is even more severe for radiation measurements (which are absolute measurements) than for bright sunshine. Dust deposits on uncleaned pyranometer domes are considered to give a 2% loss of accuracy (excluding days with frost and dew). As a result, the effective use of radiation instruments at sites that are unattended for several days is hard to envisage. An achievable observing accuracy (daily mean) is of the order of 5%.

Cloud height: The measurement of cloud height at an AWS is now mostly accomplished with the aid of (laser) ceilometers. Reference is made to WMO (1988) for an evaluation of current systems. Difficulties are still experienced in processing automatically the signals from the sensors in order to produce accurate measurements of cloud-base height under the wide range of conditions encountered in nature, in particular rain and snow. Another difficulty is that the sensors sample the cloud height only over a very small area of sky directly above the detector. When provided to a remote user, such information can present a dangerously incorrect picture of the state or coverage of the sky, especially if the data are to be used for aviation purposes. This may be overcome by the use of algorithms to estimate cloud cover during a 30 min processing interval. In some countries, the role of the ceilometer is, however, that of an aid to the observer who is watching the sky. Ceilometers normally require a significant amount of electrical power and cannot generally be used unless a conventional supply is available. Furthermore, their performance may be reduced or distorted by the accumulation of snow, dust or other forms of contamination on the window of the exit and front apertures of the optical or infrared beam.

Visibility: A wide variety of instruments is readily available for making visibility measurements at AWSs. Refer to WMO (1990).

A distinction can be made between transmissometers and visibility meters. High accuracy transmissometers are mostly used at airports, while lower accuracy (and less expensive) backward, forward or integrated visibility meters are more common for other AWSs. Both types are available in versions which can be battery-powered and which can, therefore, be used at remote sites where primary alternating current or "mains" power is not available. However, they consume a considerable amount of electrical power and, unless supported by an auxiliary power source, it is not normally feasible to operate them for more than a few weeks without battery changes.

1.2.2 Central processing unit

The core of an AWS is its CPU. Its hardware configuration depends on the complexity and magnitude of the functions it has to perform and on whether a unique hardware solution exists. In general, the main functions of the CPU are data acquisition, data processing, data storage and data transmission.

In the majority of existing AWSs, all of these functions are carried out by one microprocessor-based system installed in a weather-proof enclosure as close as possible to the sensors, or at some local indoor location. If the unit is located near the sensors, on-site processing reduces the amount of data which must be transmitted and enables those data to be presented in a form suitable for direct connection to communication channels. In such cases, however, the CPU is vulnerable to power-supply failure and must be protected against the outdoor environment in which it must operate. If the unit can be located indoors, it can usually be connected to a mains supply and operated as if it were located in a normal office environment. However, such a configuration results in an increased number of long signal cables and appropriate signal conditioners.

Depending on local circumstances and requirements, the different functions of the CPU may also be executed by different units. In such cases, each unit has its own microprocessor and relevant software, can be installed at different places in the station, and can communicate with

each other through well-established inter-processor data transfer links and procedures. They operate in a dependency relation, the data-processing unit being the independent unit. An example is the installation of one or more data-acquisition units in the field close to the sensors that are connected to the data processing or transmission unit of the CPU by means of one or more telephone lines using digital data transmission. These units can consist of one sensor (for example, an intelligent sensor such as a laser ceilometer), a number of similar sensors (for example, thermometers), or a number of different sensors.

The rapid technological evolution of modern industrial data-acquisition and process-control systems opens up new possibilities for meteorological applications. The high degree of input/output modulation and flexibility, the drastically increased operating speed of microprocessors and, in particular, the availability of dedicated data-acquisition, process-control and telecommunications software make it possible to develop AWSs which can meet the diverse observation needs and requirements of various users. As a consequence, any description of an AWS can be soon out of date and has to be considered with reservation. With this in mind, the following paragraphs give a general idea of the state of the art.

1.2.2.1 *Data acquisition*

In general, the data-acquisition hardware is composed of:

(a) Signal-conditioning hardware for preventing unwanted external sources of interference from influencing the raw sensor signals, for protecting the CPU electronics, and for adapting signals to make them suitable for further data processing;

(b) Data-acquisition electronics with analogue and digital input channels and ports, scanning equipment and data conversion equipment to enter the signals into the CPU memory.

Signal conditioning

Signal conditioning is a vital function in the data-acquisition process and starts with the proper selection of cables and connectors for connecting the sensor to the data-acquisition electronics. It is further accomplished by means of different hardware modules. Taken over from industrial process control, several conditioning functions are now integrated into one removable module. The most convenient and, hence, most common location for installing these modules is on the terminal panels of sensor cables in the same waterproof enclosure as the data-acquisition electronics. Depending on the sensor and local circumstances, various signal-conditioning techniques are available.

Sensor cables: Electrical signals from the sensors entering a data-acquisition system might include unwanted noise. Whether this noise is troublesome depends upon the signal-to-noise ratio and the specific application. Digital signals are relatively immune to noise because of their discrete (and high-level) nature. In contrast, analogue signals are directly influenced by relatively low-level disturbances. The major noise transfer mechanisms include capacitive and inductive coupling. A method of reducing errors due to capacitive coupling is to employ shielded cables for which a conductive material (at ground potential) is placed between the signal cables and the interference source. The additional use of a pair of wires that are entwined is effective in reducing electromagnetic coupling.

Surge protection: When an AWS could be subject to unintentional high-voltage inputs, the installation of a protection mechanism is indispensable to avoid possible destruction of the equipment. High-voltage input can be induced from magnetic fields, static electricity and, especially, from lightning.

Two-wire transmitters: It is sometimes desirable to pre-amplify low-level signals close to the sensor to maintain a maximum signal-to-noise ratio. One way of performing this kind of signal conditioning is to use a two-wire transmitter. These transmitters not only amplify the input signal, but also provide isolation and conversion to a high-current level (typically 4 to 20 mA). Current transmission allows signals to be sent to a distance of up to about 1 500 m.

Digital isolation: Electrical modules are used to acquire digital input signals while breaking the galvanic connection between the signal source and the measuring equipment. The modules not only isolate, but also convert the inputs into standard voltage levels that can be read by the data-acquisition equipment.

Analogue isolation: Analogue isolation modules are used to protect equipment from contact with high voltages, the breaking of ground loops and the removal of large common-mode signals. Three types of analogue isolation are in wide use today: the low-cost capacitive coupling or "flying capacitor", the good performance and moderate cost optical coupling, and the high-isolation and accurate, but higher-cost, transformer coupling.

Low-pass filtering: Filters are used to separate desired signals from undesirable signals. Undesirable signals are noise, alternating current line frequency pick-up, radio or television station interference, and signal frequencies above half the sampling frequency. Generally, a low-pass filter is employed to control these unwanted sources of error, excluding that portion of the frequency spectrum where desired signals do not exist.

Amplifiers: Analogue sensor signals can vary in amplitude over a wide range. The analogue-to-digital (A/D) converter, however, requires a high-level signal in order to perform best. In many cases, an amplifier module is used to boost possible low-level signals to the desired amplitude. Amplifier modules are also employed to standardize the voltage output of all sensors to a common voltage, for example 0–5 voltage direct current.

Resistances: Special modules are used to convert resistances, such as platinum thermometers, into a linearized output voltage signal and to provide the necessary output current for this conversion. It should be noted that the conversion to a linear signal can introduce inaccuracies, which can be critical for some applications.

Data-acquisition function

The data-acquisition function consists of scanning the output of sensors or sensor-conditioning modules at a predetermined rate, and translating the signals into a computer-readable format.

To accommodate the different types of meteorological sensors, the hardware for this function is composed of different types of input/output channels, covering the possible electrical output characteristics of sensors or signal-conditioning modules. The total number of channels of each type depends on the output characteristics of the sensors and is determined by the type of application.

Analogue inputs: The number of analogue channels is usually between 4 and 32. In general, a basic configuration can be extended by additional modules that provide more input channels. Analogue input channels are of particular significance as most of the commonly used meteorological sensors, such as temperature, pressure and humidity sensors, deliver a voltage signal either directly or indirectly through the sensor-conditioning modules.

The data-acquisition tasks are the scanning of the channels and their A/D conversion. A scanner is simply a switch arrangement that allows many analogue input channels to be served by one A/D converter. Software can control these switches to select any one channel for processing at a given time. The A/D converter transforms the original analogue information into computer readable data (digital, binary code). The A/D resolution is specified in terms of bits. An A/D resolution of 12 bits corresponds to approximately 0.025%, 14 bits to 0.006%, and 16 bit to 0.001 5% of the A/D full range or scale.

Parallel digital input/output: The total number of individual channels is mostly grouped in blocks of 8 out of 16 bits with extension possibilities. They are used for individual bit or status sensing or for input of sensors with parallel digital output (for example, wind vanes with Gray code output).

Pulses and frequencies: The number of channels is generally limited to two or four. Typical sensors are wind speed sensors and (tipping-bucket) raingauges. Use is made of low- and high-speed counters accumulating the pulses in CPU memories. A system that registers pulses or the on-off status of a transducer is known as an event recorder.

Serial digital ports: These are individual asynchronous serial input/output channels for data communication with intelligent sensors. The ports provide conventional inter-device communications over short (RS232, several metres) to long (RS422/485, several kilometres) distances. Different sensors or measuring systems can be on the same line and input port, and each of the sensors is addressed sequentially by means of coded words.

1.2.2.2   *Data processing*

The data-processing hardware is the heart of the CPU and its main functions are to act as the master control of the input/output of data to, and from, the CPU and to carry out the proper processing of all incoming data by means of the relevant software.

The hardware is operated by a microprocessor. Microprocessors do not change the principles of meteorological measurements or observing practices but they do allow the instrument designer to perform technical functions in a new way to make measurements easier, faster and more reliable, and to provide the instrument with higher capabilities, especially in data handling. The adoption of microprocessors considerably reduces hardware costs for some applications. It must be noted, however, that the expanded expectations which may be met by this device will lead very often to a fast-growing and considerably underestimated cost of the development of software.

Existing AWOSs are equipped with 8-bit microprocessors and limited memory (32 to 64 kbytes). New systems using 16- or 32-bit microprocessors surrounded by a considerable amount of solid-state memory (up to 1 Mbyte) are becoming standard. These AWOSs provide more input/output facilities which operate at much higher processing speeds and are capable of performing complex computations. Together with new hardware, sophisticated software is applied which was, some years ago, available only in minicomputer systems. The unit can be equipped with different types of memories such as random access memories (RAM) for data and program storage, non-volatile programmable read-only memories (PROMs) for program storage (programs are entered by means of a PROM programmer), and non-volatile electrically erasable PROMs (EEPROMs) mostly used for the storage of constants which can be modified directly by software. At most stations, the RAM memory is equipped with a battery backup to avoid loss of data during power failures. At non-real-time stations without data transmission facilities, data can be stored in external memories. Mechanical devices with tapes which were used for this purpose for many years are now replaced by memory cards (RAM with battery backup, EEPROMs, etc.), which have a much higher reliability.

1.2.2.3   *Data transmission*

The data transmission part of the CPU forms the link with the "outside world", which may be the local observer or the maintenance personnel, the central network processing system of the National Meteorological and Hydrological Service, or even directly the users of meteorological information. The equipment is interfaced to the CPU by using commonly available serial and parallel input/output ports. The most suitable means of data transmission depends mainly on the site in question and the readily available transmission equipment. No single solution can be regarded as universally superior, and sometimes the transmission chain requires the use of several means (see section 1.3.2.10).

1.2.3   **Peripheral equipment**

Power supply: The design and capability of an AWS depend critically upon the method used to power it. The most important characteristics of an AWS power supply are high stability and

interference-free operation. For safety reasons, and because of the widespread use and common availability of 12 V batteries in motor vehicles, consideration should be given to the use of 12 V direct current power. Where mains power is available, the 12 V batteries could be float-charged from the main supply. Such a system provides the advantage of automatic backup power in the event of a mains power failure. Automatic weather stations deployed at remote sites where no mains power is available must rely upon batteries that may, or may not, be charged by an auxiliary power source, such as a diesel generator, wind- or water-driven generator, or solar cells. However, such low-power systems cannot, in general, support the more complex sensors required for cloud height and visibility measurements, which require large amounts of power. Furthermore, AWSs with auxiliary equipment such as heaters (anemometers, raingauges) and aspirators can also consume considerable power, thus restricting the installation of an AWS to locations where mains power is available. If, because of the need for a versatile and comprehensive system, only the mains can supply sufficient power for full operation, provision should be made for support, from a backup supply, of at least the system clock, the processor and any volatile memory that may contain recent data needed to restart the station automatically.

Real-time clock: An essential part of data processing is a 24 h real-time clock powered by a battery, which ensures that the time is kept even during power outages. Ensuring the accuracy of actual AWS clocks requires special attention to guarantee correct read-outs, sample intervals and time stamps. At some AWSs, devices are used to synchronize the clock with broadcast radio time reference signals or the Global Positioning System.

Built-in test equipment: Vital parts of an AWS often include components whose faulty operation or failure would seriously degrade or render useless the principal output. The inclusion of circuits to monitor automatically these components' status is an effective means of continuously controlling their performance during operation. Examples are: a power-failure detector which restarts the processor and continues the AWS function after a power failure; a "watchdog" timer to monitor the proper operation of microprocessors; and test circuits for monitoring the operation of station subsystems such as battery voltage and charger operation, aspirators (temperature and humidity screens), A/D converters, heaters, etc. Status information can be automatically displayed on site or input into the CPU for quality-control and maintenance purposes.

Local display and terminals: Operational requirements often require observations to be entered or edited manually, for example at semi-automatic weather stations. Depending on the requirements, and on the station designer, different types of local terminals are used for this purpose, including a simple numerical light-emitting diode (LED) display with keyboard forming an integral part of the CPU, a screen with keyboard, or even a small personal computer installed at some distant indoor location. For maintenance purposes, special handheld terminals are sometimes used which can be plugged directly into the station. For particular applications, such as AWSs at airports or simple aid-to-the-observer stations, digital displays are connected for the visualization of data at one or more places at the site. On request, a printer or graphical recorders can be added to the station.

1.3   AUTOMATIC WEATHER STATION SOFTWARE

When designing or specifying an AWS it is a guiding principle that the cost of developing and testing the software will be one of the largest financial elements in the package. Unless great care is exercised in the preliminary design and strong discipline maintained while coding, complex software readily become inflexible and difficult to maintain. Minor changes to the requirements — such as those often induced by the need for a new sensor, code changes, or changes in quality-control criteria — may often result in major and very expensive software revisions.

In general, a distinction can be made between application software consisting of algorithms for the proper processing of data in accordance with user specifications, and system software inherently related to the microprocessor configuration and comprising all software to develop and run application programs.

Advice on the development of algorithms for AWSs is given in section 1.1.3 above. Discussion of the design of algorithms for synoptic AWSs is found in WMO (1987), and for the processing of surface wind data in WMO (1991). Information on the algorithms used by Members can be found in WMO (2003). For detailed information on sampling, data reduction and quality management, the appropriate chapters in Part IV should be consulted.

1.3.1 System software

The software for many existing AWSs is developed by the manufacturer in accordance with user requirements and is put into the CPU memory in a non-readable format for the user (so-called firmware), thus turning the CPU into a sort of black box. The user can execute only predetermined commands and, as a consequence, depends entirely on the manufacturer in the event of malfunctions or modifications.

Fortunately, the increasing demand for data-acquisition systems for industrial process control has opened up new possibilities. Users can now develop their own application software (or leave it to a software company or even the manufacturer of the station) using programming languages like Basic, Pascal or, in particular, C, and using readily available utility packages for data acquisition, statistics, storage and transmission. The result is that the user acquires more insight into, and control over, the different processes and becomes consequently less dependent on the manufacturer of the station.

In recent systems, increasing use is made of well-proven real-time multitasking/multi-user operating systems, which were available only for minicomputers in the past. They are *real-time* because all operations are activated by hardware and software interrupts, *multitasking* because different tasks can be executed quasi-simultaneously following a predetermined priority, and *multi-user* because different users can have quasi-simultaneous access to the system. Software developers can give their full attention to the development of application programs in the language of their choice while leaving the very difficult and complex control and execution of tasks to the operating system.

1.3.2 Application software

The processing functions that must be carried out either by the CPU, the sensor interfaces, or a combination of both, depend to some extent on the type of AWS and on the purpose for which it is employed. Typically, however, some or all of the following operations are required: initialization, sampling of sensor output, conversion of sensor output to meteorological data, linearization, averaging, manual entry of observations, quality control, data reduction, message formatting and checking and data storage, transmission and display. The order in which these functions are arranged is only approximately sequential. Quality-control may be performed at different levels: immediately after sampling, after deriving meteorological variables, or after the manual entry of data and message formatting. If there are no checks on data quality-control and message content, the AWS data are likely to contain undetected errors. While linearization may be inherent in the sensor or signal-conditioning module, it should always be carried out before the calculation of an average value.

The execution of the application software is governed by a schedule that controls when specific tasks must be executed. The overview of AWS application software in the following paragraphs is limited to some practical aspects related to AWSs.

1.3.2.1 *Initialization*

Initialization is the process that prepares all memories, sets all operational parameters and starts running the application software. In order to be able to start normal operations, the software first requires a number of specific parameters, such as, among others, those related to the station (station code number, altitude, latitude and longitude); date and time; physical location of the sensor in the data-acquisition section; type and characteristics of sensor-conditioning modules;

conversion and linearization constants for sensor output conversion into meteorological values; absolute and rate of change limits for quality-control purposes; and data buffering file location. Depending on the station, all or part of these parameters may be locally input or modified by the user through interactive menus on a terminal. In the latest generation of AWSs, initialization may be executed remotely, for instance, by the central network processing system or by a remote personal computer. In addition to full initialization, a partial initialization should be programmed. This automatically restores normal operation, without any loss of stored data, after a temporary interruption caused by real-time clock setting, maintenance, calibration or power failure.

1.3.2.2 *Sampling and filtering*

Sampling can be defined as the process of obtaining a well-spaced sequence of measurements of a variable. To digitally process meteorological sensor signals, the question arises of how often the sensor outputs should be sampled. It is important to ensure that the sequence of samples adequately represents significant changes in the atmospheric variable being measured. A generally accepted rule of thumb is to sample at least once during the time constant of the sensor. However, as some meteorological variables have high frequency components, proper filtering or smoothing should be accomplished first by selecting sensors with a suitable time-constant or by filtering and smoothing techniques in the signal-conditioning modules (see Part IV, Chapter 2).

Considering the need for the interchangeability of sensors and homogeneity of observed data, it is recommended:[12]

(a) That samples taken to compute averages should be obtained at equally spaced time intervals which:

(i) Do not exceed the time constant of the sensor; or

(ii) Do not exceed the time constant of an analogue low-pass filter following the linearized output of a fast response sensor; or

(iii) Are sufficient in number to ensure that the uncertainty of the average of the samples is reduced to an acceptable level, for example, smaller than the required accuracy of the average;

(b) That samples to be used in estimating extremes of fluctuations should be taken at least four times as often as specified in (i) or (ii) above.

1.3.2.3 *Raw-data conversion*

The conversion of raw sensor data consists of the transformation of the electrical output values of sensors or signal-conditioning modules into meteorological units. The process involves the application of conversion algorithms making use of constants and relations obtained during calibration procedures.

An important consideration is that some sensors are inherently non-linear, namely their outputs are not directly proportional to the measured atmospheric variables (for example, a resistance thermometer), that some measurements are influenced by external variables in a non-linear relation (for example, some pressure and humidity sensors are influenced by the temperature) and that, although the sensor itself may be linear or incorporate linearization circuits, the variables measured are not linearly related to the atmospheric variable of interest (for example, the output of a rotating beam ceilometer with photo detector and shaft-angle encoder providing backscattered light intensity as a function of angle is nonlinear in cloud height). As a

---

[12] Recommended by the Commission for Instruments and Methods of Observation at its tenth session (1989) through Recommendation 3 (CIMO-X).

consequence, it is necessary to include corrections for non-linearity in the conversion algorithms as far as this is not already done by signal-conditioning modules. Linearization is of particular importance when mean values must be calculated over a certain time. Indeed, when the sensor signal is not constant throughout the averaging period, the "average then linearize" sequence of operations can produce different results from the "linearize then average" sequence. The correct procedure is to only average linear variables.

1.3.2.4 *Instantaneous meteorological values*

The natural small-scale variability of the atmosphere, the introduction of noise into the measurement process by electronic devices and, in particular, the use of sensors with short time-constants make averaging a most desirable process for reducing the uncertainty of reported data.

In order to standardize averaging algorithms it is recommended:[13]

(a) That atmospheric pressure, air temperature, air humidity, sea-surface temperature, visibility, among others, be reported as 1 to 10 min averages, which are obtained after linearization of the sensor output;

(b) That wind, except wind gusts, be reported as 2 or 10 min averages, which are obtained after linearization of the sensor output.

These averaged values are to be considered as the "instantaneous" values of meteorological variables for use in most operational applications and should not be confused with the raw instantaneous sensor samples or the mean values over longer periods of time required from some applications. One-minute averages, as far as applicable, are suggested for most variables as suitable instantaneous values. Exceptions are wind (see (b) above) and wave measurements (10 or 20 min averages). Considering the discrepancy of observations between the peak gust data obtained from wind measuring systems with different time responses, it is recommended that the filtering characteristics of a wind measuring chain should be such that the reported peak gust should represent a 3 s average. The highest 3 s average should be reported. In practice, this entails sampling the sensor output and calculating the 3 s running mean at least one to four times a second.

Some specific quantities for which data conversion is necessary and averaging is required before conversion are given in Part IV, Chapter 2.

1.3.2.5 *Manual entry of observations*

For some applications, interactive terminal routines have to be developed to allow an observer to enter and edit visual or subjective observations for which no automatic sensors are provided at the station. These typically include present and past weather, state of the ground and other special phenomena.

1.3.2.6 *Data reduction*

Beside instantaneous meteorological data, directly obtained from the sampled data after appropriate conversion, other operational meteorological variables are to be derived and statistical quantities calculated. Most of them are based on stored instantaneous values, while, for others, data are obtained at a higher sampling rate, as for instance is the case for wind gust computations. Examples of data reduction are the calculation of dewpoint temperature values from the original relative humidity and air temperature measurements and the reduction of pressure to mean sea level. Statistical data include data extremes over one or more time periods

---

[13] Recommended by the Commission for Instruments and Methods of Observation at its ninth session (1985) through Recommendation 6 (CIMO-IX).

(for example, temperature), total amounts (for example, rain) over specific periods of time (from minutes to days), means over different time periods (climatological data), and integrated values (radiation). These variables or quantities can be computed at an AWS or at a central network processing system where more processing power is normally available.

CIMO is involved in an extensive programme to survey and standardize algorithms for all variables. The results are published in the WMO (2003).

Formal recommendations exist for the computation of pressure tendency[14] and humidity quantities[15] (Part I, Chapter 4, Annex 4.B).

WMO investigated the methods for pressure reduction used by Members in 1952 (WMO, 1954) and concluded that the "international formula" (using the formula of Laplace or Angot's tables) or some "simplified" methods are in practice (for example, for "low-level" stations[16], see, Part I, Chapter 3). As a result of this inquiry, a study of the standardization of methods of reduction was undertaken and one general equation of pressure reduction was recommended as standard[17] (WMO, 1964). Nevertheless, this recommended method, the "international formula" and methods using simplified formulae are still in common practice (WMO, 1968).

1.3.2.7   *Message coding*

Functional requirements often stipulate the coding of meteorological messages in accordance with WMO (2011*b*). Depending on the type of message and the elements to be coded, the messages can be generated fully or semi-automatically. Generating fully automatic messages implies that all elements to be coded are measurable data, while generating semi-automatic messages involves the intervention of an observer for entering visual or objective observations, such as present and past weather, the state of the ground, and cloud type. Message coding algorithms should not be underestimated and require considerable efforts not only for their development but also for updating when formats are altered by international, regional and national regulations. They also occupy a considerable amount of memory that can be critical for small performance stations. It should be noted that observational data could be transmitted to the central network processing system, where more computer power is normally available for message coding.

1.3.2.8   *Quality control*

The purpose of quality-control at an AWS is to minimize automatically the number of inaccurate observations and the number of missing observations by using appropriate hardware and software routines. Both purposes are served by ensuring that each observation is computed from a reasonably large number of quality-controlled data samples. In this way, samples with large spurious errors can be isolated and excluded and the computation can still proceed, uncontaminated by that sample.

Quality-control achieves assured quality and consistency of data output. It is achieved through a carefully designed set of procedures focused on good maintenance practices, repair, calibration, and data quality checks. Currently, there is no agreed set of procedures or standards for the various AWS platforms. Such a set of procedures should be developed and documented.

In modern AWSs, the results of data quality-control procedures for sensors which reveal the reasons why a measurement is suspect or erroneous, and the results of hardware self-checks

---

[14]   Recommended by the Commission for Instruments and Methods of Observation at its ninth session (1985) through Recommendation 7 (CIMO-IX).

[15]   Recommended by the Commission for Instruments and Methods of Observation at its tenth session (1989) through Recommendation 7 (CIMO-X).

[16]   Recommended by the Commission for Instruments and Methods of Observation at its first session (1953) through Recommendation 13 (CIMO-I) and adopted by EC-IV.

[17]   Based on the recommendations by the CIMO-I Working Committee II on "Reduction of Pressure" (WMO, 1954, Part 2).

by built-in test equipment, are stored in appropriate housekeeping buffers. The visual display of these status indicators forms a very handy tool during field maintenance. The transmission of housekeeping buffers – either as an appendix to the routine observational message, or as a clocked or on-request housekeeping message, from a network of AWSs to a central network processing system – is a valuable possible approach to the maintenance of meteorological equipment.

Real-time procedures for the quality-control of AWS data are highly advisable, and detailed recommendations exist in Part IV, Chapter 1, and as basic quality-control procedures in WMO (1993). The following is a practical elaboration of the recommendations.

Intra-sensor checks

Intra-sensor checks: This is when each sensor sample is checked at the earliest practical point in the processing, taking into account sensor and signal-conditioning response functions, for a plausible value and a plausible rate of change.

Plausible value: This is a gross check that the measured value lies within the absolute limits of variability. These limits are related to the nature of the meteorological variable or phenomena but depend also on the measuring range of selected sensors and data-acquisition hardware. Additional checks against limits which are functions of geographical area, season and time of year could be applied. Suggested limits for these additional checks are presented in Tables 6.3–6.9 in Chapter 6 of WMO (1993). The checks provide information as to whether the values are erroneous or suspect.

Plausible rate of change: This checks for a plausible rate of change from a preceding acceptable level. The effectiveness of the check depends upon the temporal consistency or persistence of the data and is best applied to data of high temporal resolution (high sampling rate) as the correlation between adjacent samples increases with the sampling rate. One obvious difficulty is determining how quickly an atmospheric variable can change taking into account the response characteristics of the sensor in question. Additional time consistency checks using comparisons of data between two consecutive reports can be made. WMO (1993) provides checking tolerances for different time periods on the synoptic scales (1, 2, 3, 6, 12 h) for air temperature, dewpoint, and pressure tendency.

Inter-sensor checks

It is possible to make internal consistency checks of a variable against other variables, based upon established physical and meteorological principles. Some examples are as follows: dewpoint cannot exceed ambient temperature; precipitation without clouds overhead or just after they have passed overhead is very unlikely; non-zero wind-speed and zero wind-direction variance strongly suggest a wind-direction sensor problem; and zero average wind speed and non-zero wind direction (variance) suggest a defective wind-speed sensor.

Observations entered manually

When a manually observed quantity is entered into the AWS, the inter- and intra-sensor checks mentioned above can be conducted. Some special consistency checks are suggested in WMO (1993) concerning present weather with visibility; present weather with cloud cover; cloud cover, weather and cloud information; present weather with air temperature; present weather with dewpoint temperature; height of clouds with types of clouds; and state of the sea with wind speed.

Hardware checks

During operation, the performance of an AWS deteriorates with the ageing of hardware components, exposure to untested situations, improper maintenance, product failure, and so on. Therefore, it is important to implement and execute automatically and periodically internal self-check features using built-in test equipment for AWS hardware and to make the results of these

tests available to appropriate personnel or to store the results in housekeeping buffers. These buffers can be examined, and the information contained in them should be used to classify the measurements as correct, erroneous or suspect.

Message checking

For AWSs equipped with software for coding messages and for transmitting the messages over the Global Telecommunication System, it is of vital importance that all the above checks are executed very carefully. In addition, compliance with regulations concerning character, number, format, and so forth, should be controlled. Proper actions are to be considered in cases of values that are classified as suspect.

1.3.2.9 **Data storage**

Processed and manually observed data, including quality-control status information (housekeeping data) must be buffered or stored for some time in the AWS. This involves a relevant database that must be updated in real time. The number of database cells and memory required is determined as a function of the maximum possible number of sensors, intermediate data, derived quantities and the required autonomy of the station. In general, a circular memory structure is adopted allowing the old data to be overwritten by new incoming data after a predetermined time. The database structure should allow easy and selective access by means of data transfer and transmission algorithms.

Depending on observational requirements and the type of station, the data can be transferred at regular time intervals from the AWS main memory to other kinds of storage devices, such as a removable memory.

1.3.2.10 **Data transmission**

Dictated by operational requirements and data transmission facilities, data transmission between an AWS and either local users or the central network processing system can operate in different modes, as follows:

(a) In response to external commands, as this is the most common basic mode given that it allows more control of the station, such as initialization, setting and resetting of the real-time clock, inhibiting faulty sensors, selective database transfer, and so on. Upon reception and after transmission control of an external command, a task schedule activates the appropriate task or subroutine as requested by the command;

(b) At periodic time intervals controlled by the AWS time scheduler;

(c) In AWS emergency conditions when certain meteorological thresholds are crossed.

In general, readily available data transmission software packages can be used for proper data transfer and control and for transmission protocols. As data transmission means are subject to several interference sources, careful attention must be paid to adequate error coding, such as parity bits and cyclical redundancy codes. A brief review of some telecommunications options for establishing an AWS network follows.

One-way communications

A simple AWS network could use one-way communications where the remote stations operate on a timed cycle to scan the sensor channels, or otherwise when alarm conditions are triggered, to dial up over telephone lines the central control and data-acquisition computer, and having established the link, deliver their data messages. Each AWS might have a serial interface to an analogue modem, and data transmission would be at a rate, of say, 9 600 bits per second (bps) using audio tones. The advantage of this point-to-point communications system is that it uses well-established, simple technology and ordinary voice-grade telephone lines. The cost, which

should be modest, depends on a tariff formula including distance and connection time. The drawbacks are that data security is only moderate; data volumes must be relatively low; no powerful network architectures can be used; and telecommunications companies may restrict future access to analogue data circuits as the technology moves inexorably to broadband digital networks.

Two-way communications

A more powerful network has two-way communications so that the central computer may poll the network stations, not only at the synoptic times, or hourly, but on a random access basis when a forecaster or hydrologist wishes to obtain a current update on weather conditions at a particular site or sites. The remote stations would initiate the procedure for sending their own alarm messages in real time. Two-way communication also enables the remote station to send command messages to change its mode of operation, or to have new operating software downloaded onto its processor.

AWS network communication

The network might use landline or radio communications (especially for very remote sites) or a combination of both. The advantage of using a telecommunications service provider is that all responsibility for maintenance of the network service and probably the communications interfaces lies with the provider, who should respond promptly to the AWS system manager's fault reports. Note the need to be able to determine on which side of the communications interface (AWS or telecommunications circuits) the fault lies, which may be problematical. AWS networks have often used dial-up circuits in the Public Switched Telephone Network (PSTN), with costs related to distance and connect time, depending on the tariffs of the local communications provider. The other option is to have a "private network" network based on dedicated leased lines of defined quality. There is no switching delay in establishing the circuits, higher transmission speeds are available, and there is a high certainty that the circuit will be maintained. The leasing costs depend on the line distances, but not on the volume of data. Costs are higher than for dial-up connections when the volume of data is fairly low.

Integrated services digital network

Many telecommunications authorities offer an integrated services digital network that provides for voice, data and video transmission with pulse-code modulation over upgraded PSTN cables and switches. A basic channel provides for 64 kbps data, which may carry X.25 packet-switch or frame-relay protocols. The digital circuits provide very high data security.

Wide area network communications

With the worldwide increase in data traffic and the use of modern communications protocols, together with the increased computing and data-storage capability at remote terminals, it is now common to view the remote AWS and the central control and data-acquisition computer as nodes of a wide area network (WAN). The data or control message is divided into "packets" according to rules (protocols) such as X.25 or the faster frame relay. Each data packet is routed through the telecommunication provider's switched data network and may arrive at the destination by different routes (making efficient use of the network with other unrelated packets). At the destination, the packets are reassembled under the protocol after variable delays to reform the message. Error detection with the automatic resending of corrupted or lost packets ensures reliable transmission. Note the contrast with ordinary PSTN based on circuit-switching technology, in which a dedicated line is allocated for transmission between two parties. Circuit-switching is ideal when real-time data (like live audio and video) must be transmitted quickly and arrive in the same order in which it was sent. Packet switching is more efficient and robust for data that can withstand some short delay in transmission. Message costs are related to connect time and data volume. There should be a means to terminate the connection reliably when data collection is finished, as a faulty AWS may keep the line open and incur unwanted costs.

Frame relay and asynchronous transfer mode

Frame relay is a packet-switching, networking protocol for connecting devices on a WAN, operating at data speeds from 64 kbps to 2 Mbps or higher, depending on line quality. Unlike a point-to-point private line, network switching occurs between the AWS and the central station. In fact, there is a private line to a node on the frame relay network, and the remote location has a private line to a nearby frame relay node. The user gets a "virtual private network". Costs are decreasing and are independent of the volume of data or the spent time connected. However, frame relay is being replaced in some areas by newer, faster technologies, such as asynchronous transfer mode (ATM). The ATM protocol attempts to combine the best of both worlds – the guaranteed delivery of circuit-switched networks and the robustness and efficiency of packet-switching networks.

Transmission protocol

A de facto standard for transmission between computers over networks is the Transmission Control Protocol/Internet Protocol (TCP/IP). The Internet Protocol (IP) specifies the format of packets, called "datagrams" and the addressing scheme. The higher-level protocol TCP establishes a virtual connection between source and destination so that two-way data streams may be passed for a time and so that datagrams are delivered in the correct sequence with error correction by retransmission. The TCP also handles the movement of data between software applications. The functioning of the Internet is based on TCP/IP protocols, and the IP is also used in WANs, where the nodes have processing capability and high volumes of data are exchanged over the network. The IP enables the AWS data and road condition analyses performed in the central station computer to be shared by national and regional road administrations over a private Intranet.

Switched or dedicated circuits

It is necessary to decide whether to use cheaper switched data circuits where telecommunications network access has to be shared with other users, or to lease much more expensive dedicated circuits that provide reliable, high-speed, real-time communications. The switched network will have some latency where there will be a delay of as much as a few seconds in establishing the circuit, but packet-switch protocols handle this without difficulty. The reliability consideration, the amount of data to be exchanged with each message or special "downloads" to the remote stations, as well as the operational need for actual real-time communications, will help determine the choice. The seasonal factor will also have a bearing on the choice of communications. If the critical use of the road meteorological data is only for a few months of the year, maintaining a year-round dedicated communications network imposes a high overhead cost per message. Actual message costs will depend on the charging formulas of the telecommunications company, and will include factors like data rate, distance of link, connection time and whether the terminal modems are provided by the company. The local telecommunications companies will be ready to offer guidance on the choice of their services.

1.3.2.11 *Maintenance and calibration*

Specific software routines are incorporated in the application software allowing field maintenance and calibration. Such activities generally involve running interactive programs for testing a particular sensor, AWS reconfiguration after the replacement of sensors or models, resetting of system parameters, telecommunication tests, entering new calibration constants, and so on. In general, maintenance and calibration is conducted in an off-line mode of operation, temporarily interrupting the normal station operation.

1.3.2.12 *Data display*

In addition to data display routines for the different functions mentioned in the above paragraphs, operational requirements often specify that selected data should be displayed

locally with periodic updating in real time or, on LED displays, existing terminals, or on special screens. Examples of this are AWSs at airports and at environmental control sites. In some countries, a printout of local data or a graphical display on pen recorders is required.

1.4 AUTOMATIC WEATHER STATION SITING CONSIDERATIONS

The siting of an AWS is a very difficult matter and much research remains to be done in this area. The general principle is that a station should provide measurements that are, and remain, representative of the surrounding area, the size of which depends on the meteorological application. Existing guidelines for conventional stations are also valid for AWSs and are given in Part I as well as in WMO (2010*a*, 2010*b*, 2014).

Some AWSs have to operate unattended for long periods at sites with difficult access both on land and at sea. Construction costs can be high and extra costs can be necessary for servicing. They may have to operate from highly unreliable power supplies or from sites at which no permanent power supply is available. The availability of telecommunication facilities should be considered. Security measures (against lightning, flooding, theft, vandalism, and so forth) are to be taken into account and the stations must, of course, be able to withstand severe meteorological conditions. The cost of providing systems capable of operating under all foreseen circumstances at an automatic station is prohibitive; it is essential that, before specifying or designing an AWS, a thorough understanding of the working environment anticipated for the AWS be obtained. At an early stage of planning, there should be a detailed analysis of the relative importance of the meteorological and technical requirements so that sites can be chosen and approved as suitable before significant installation investment is made.

1.5 CENTRAL NETWORK DATA PROCESSING

An AWS usually forms part of a network of meteorological stations and transmits its processed data or messages to a central network processing system by various data telecommunication means. The specification of the functional and, consequently, the technical requirements of a central system is a complex and often underestimated task. It requires good cooperation between AWS designers, specialists in telecommunication, software specialists, and data users. Decisions have to be taken concerning the tasks that must be executed in the central system and at the AWSs. In fact, depending on the application, certain functions at an AWS could be transferred to the central system where more computer power and memory are available. Examples are long mathematical calculations, such as the reduction of atmospheric pressure and coding of meteorological messages. The AWS data buffers can be reduced to an operational minimum when they are regularly transferred to the central system. It is good practice to first arrange for an agreement on the functional requirements of both the central system and the AWS before specifying their technical requirements.

1.5.1 Composition

The composition of a central network processing system depends considerably not only on the functions to be accomplished, but also on local facilities. Use can be made of powerful personal computers or workstations, operating in a real-time multitasking and multi-user environment. However, existing telecommunication and processing systems are used. Central network processing systems are increasingly integrated into a local area network allowing distribution and execution of tasks at the most convenient place by the most appropriate people.

The main functions of a central network system are data acquisition, including decoding of messages from the AWS network, remote control and housekeeping of AWSs, network monitoring and data quality control, further processing of data to satisfy user requirements,

access to the network database, data display, and data transfer to internal or external users. The latter may include the Global Telecommunication System if the data are exchanged internationally.

1.5.2 **Quality management of network data**

This topic is discussed further in Part IV, Chapter 1. It is recommended that operators of networks:[18]

(a) Establish and test near-real-time measurement monitoring systems in which reported values are regularly tested against analysed fields corresponding to the same measurement location;

(b) Establish effective liaison procedures between the monitoring service and the appropriate maintenance and calibration services to facilitate rapid response to fault or failure reports from the monitoring system.

Automated quality-control procedures at an AWS have their limitations and some errors can go undetected even with the most sophisticated controls, such as long-term drifts in sensors and modules. Data transmission from an AWS adds another source of error. Therefore, it is recommended that additional quality-control procedures should be executed by a network monitoring system forming part of the central network system. Quality-control procedures of prime importance in such a monitoring system include:

(a) Detecting data transmission errors; the required routines depend on the transmission protocol and cyclic redundancy codes used;

(b) Checking the format and content of WMO coded messages (WMO, 1993);

(c) Further processing of data to exclude or otherwise deal with data flagged as erroneous or suspect in the AWS housekeeping files.

Interactive display systems also allow complementary quality-control of incoming data. Time series for one or more variables and for one or more stations can be displayed on colour screens; statistical analysis can be used by trained and experienced personnel to detect short- and long-term anomalies that are not always detected by fully automatic quality-control algorithms.

Monitoring algorithms, by which reported values are regularly tested in space and time against an analysed numerical field, are very powerful ways to identify errors and to establish the need for investigative or remedial action. The low level of turbulent fluctuations in atmospheric pressure and the confidence with which local geographic influences can be removed by normalizing all observations to a common reference level make atmospheric pressure a prime candidate for this type of quality control. By averaging over space or time, observations with other variables should be susceptible to this analysis as well. However, local orographic effects must be carefully considered and taken into account.

1.6 **MAINTENANCE**

The cost of servicing a network of automatic stations on land and, in particular, at sea can greatly exceed the cost of their purchase. It is, therefore, of central importance that AWSs are designed to have the greatest possible reliability and maintainability. Special protection against environmental factors is often justified, even when initial costs are high.

---

[18] Recommended by the Commission for Instruments and Methods of Observation at its ninth session (1985) through Recommendation 5 (CIMO-IX).

It is evident that any complex system requires maintenance support. Corrective maintenance is required for component failures. Hardware components may fail for many reasons; computer programs can also fail because of errors in design that can go undetected for a long time. To minimize corrective maintenance and to increase the performance of an AWS, well-organized preventive maintenance is recommended. Preventive maintenance is required for all system components, not only cleaning and lubricating the mechanical parts. In view of the increasing reliability of the electronic components of an AWS, preventive maintenance, including services and sensor calibration, will become the controlling factor in maintenance.

Adaptive maintenance is required to take into account the rapid changes in technology and the availability of spare parts after a few years. Indeed, costs for repair and components often increase quite rapidly after a system is no longer in active distribution, making it necessary to replace modules by new ones with different technology, as exact replacements are seldom found. Examples include transferring data from one recording medium to another and programs and operating systems from one processor to another, introducing modular changes for system reliability, connecting with new telecommunication systems, and so on. In order to reduce the costs for this kind of maintenance, it is desirable that widely accepted standards on equipment and interfaces, as well as on software, be established and included in AWS technical specifications.

Since the maintenance of a network of automatic stations is often a grossly underestimated task, it is essential to organize maintenance according to a rational plan that details all the functions and arranges them so as to minimize costs without adversely affecting performance. The modular structure of many modern automatic stations allows maintenance to take place in the field, or at regional and national centres.

Field maintenance: In general, it is not advisable to repair AWS sensors or other modules in the field because conditions do not favour effective work. Also, because of high staff costs and relatively low equipment costs, it is more cost-effective to discard faulty modules rather than to repair them. It is recommended that corrective maintenance in the field be carried out by specialized technical personnel from a regional or national centre, depending on the size of the country, and to leave simple preventive maintenance to the local observer (when available). The periodic transmission of self-checking diagnostic information by the AWS is a very desirable practice to ensure rapid response to failures.

Regional centre: At a regional centre, technical personnel should be available to replace or repair modules and sensors which require the detection and elimination of simple defects. The personnel should have good knowledge of the station hardware operation and must be trained in the execution of software maintenance routines. Such regional centres should be equipped with appropriate test equipment and sufficient spare modules and sensors to support the maintenance of the stations in their area. These centres need adequate transportation facilities for conducting field work. Care should be taken to plan and visit periodically the remote sites to check for operational problems, vandalism, site conditions, changes, and so forth. Procedures for emergency visits to the different stations must be established, based on priorities defined at the station.

National centre: A national centre requires more skilled technical personnel, who should be capable of detecting and eliminating complex problems in sensors, modules and data transmission means. The equipment necessary for checking and correcting all parts of an AWS should be available and the work should be performed in the centre. Any recurring defects should be referred to designers or suppliers in charge of correcting the design fault.

As software plays a very important role in each AWS and in the central network processing system, personnel with a profound knowledge of the AWS and central network system software are required. The necessary software development and test facilities should be available. Moreover, the national centre should be able to execute all tasks associated with adaptive maintenance.

With reference to the quality-control of network data, it is desirable to establish effective liaison procedures between the monitoring service and the appropriate maintenance and calibration service in order to facilitate rapid response to fault or failure reports from the monitoring system.

The scheme outlined above is suitable for big countries. For small countries, the tasks of the regional centres could be taken over by the national centre. Developing countries could consider establishing joint maintenance arrangements with neighbouring counties. A common international maintenance centre could be envisaged in order to keep maintenance costs reasonably low. However, such international cooperation would probably require the use of similar equipment. If the Meteorological Service is unable to expand its staff or facilities, contractor services could be used to perform many of the support functions. Such support could, for example, be negotiated as part of the system procurement. However, a maintenance contract should be extremely well prepared and the execution of the contract should be very carefully verified by the appropriate staff.

Suggestions for quality-management techniques are given in Part IV, Chapter 1.

1.7 CALIBRATION

Sensors, in particular AWS sensors with electrical outputs, show accuracy drifts in time and, consequently, need regular inspection and calibration. In principle, the calibration interval is determined by the drift specifications given by the manufacturer and the required accuracy. WMO international instrument intercomparisons also provide some objective indications of sensor accuracy drifts and desirable calibration intervals. As signal conditioning modules and data-acquisition and transmission equipment also form a part of the measuring chain, their stability and correct operation also have to be controlled or calibrated periodically. The summary given below is limited to practical aspects related to AWSs. Refer to the different chapters of Part I and to Part IV, Chapter 4, for more detailed information on calibration techniques and methods.

Initial calibration: It is easy to overlook the requirement that appropriate calibration facilities and instrumentation should be available prior to the procurement and installation of AWSs in order to be able to verify the specifications given by the manufacturer, to test the overall performance of the station and to verify that transportation did not affect the measuring characteristics of the equipment.

Field inspection: The periodic comparison of AWS sensors with travelling standards at the station is an absolute requirement to monitor the performance of the sensors. Travelling standards having similar filtering characteristics to the AWS measuring chain and with a digital read-out are to be preferred. In many countries, two travelling standards of the same type are used to prevent possible accuracy change problems due to transportation. In order to be able to detect small drifts, the travelling standards should have an accuracy that is much better than the relevant station sensor and should be installed during the comparison process in the same environmental conditions as the sensors for a sufficiently long time. As signal conditioning modules and data-acquisition equipment, such as the A/D converter, can also show performance drifts, appropriate electrical reference sources and multimeters should be used to locate anomalies.

Before and after field inspections, the travelling standards and reference sources must be compared with the working standards of the calibration laboratory. The maintenance service must be informed as soon as possible when accuracy deviations are detected.

Laboratory calibration: Instruments at the end of their calibration interval, instruments showing an accuracy deviation beyond allowed limits during a field inspection and instruments repaired by the maintenance service should return to a calibration laboratory prior to their re-use. Sensors should be calibrated in a conditioned environment (environmental chambers) by means of appropriate working standards. These working standards should be compared and calibrated periodically with secondary standards and be traceable to international standards.

Attention should also be paid to the calibration of the different components forming the measuring and telemetry chain, in particular the signal-conditioning modules. This involves appropriate voltage, current, capacitance and resistance standards, transmission test equipment and high-accuracy digital multimeters. Highly accurate instruments or data-acquisition systems are required for calibration. A computer is desirable for calculation of calibration constants. These constants will accompany the sensor or module between calibrations and must be entered in the AWS whenever a sensor or module is replaced or installed in an AWS during field maintenance.

A schedule should be set up to compare periodically the secondary standards of the calibration laboratory with national, international or regional WMO primary standards.

1.8   **TRAINING**

As an AWS is based on the application of technology that differs considerably from the equipment at conventional stations and networks, a comprehensive review of existing training programmes and of the skills of the necessary technical staff is obviously required. Any new training programme should be organized according to a plan that is geared to meeting user needs. It should especially cover the maintenance and calibration outlined above and should be adapted to the system. Requesting existing personnel to take on new functions, even if they have many years of experience with conventional stations, is not always possible and may create serious problems if they have no basic knowledge of electrical sensors, digital and microprocessor techniques or computers. It could be necessary to recruit new personnel who have such knowledge. Personnel competent in the different areas covered by automatic stations should be present well before the installation of a network of AWSs (see WMO, 1997).

It is essential that AWS equipment manufacturers provide very comprehensive operational and technical documentation together with operational and technical training courses. Generally, two sets of documentation are required from the manufacturer: user manuals for operational training and use of the system, and technical manuals with more complex documentation describing in great technical detail the operating characteristics of the system, down to sub-unit and even electronic component level and including maintenance and repair instructions. These manuals can be considered as the basic documentation for training programmes offered by the manufacturer and should be such that they can serve as references after the manufacturer's specialists are no longer available for assistance.

For some countries, it may be advisable to organize common training courses at a training centre that serves neighbouring countries. Such a training centre would work best if it is associated with a designated instrument centre and if the countries served have agreed on the use of similar standardized equipment.

––––––––––––

REFERENCES AND FURTHER READING

World Meteorological Organization, 1954: *Reduction of Atmospheric Pressure.* Technical Note No. 7
(WMO-No. 36, TP. 12). Geneva.

——, 1964: *Note on the Standardization of Pressure Reduction Methods in the International Network of Synoptic
Stations: Report of a Working Group of the Commission for Synoptic Meteorology.* Technical Note
No. 61 (WMO-No. 154, TP. 74). Geneva.

——, 1968: *Methods in Use for the Reduction of Atmospheric Pressure.* Technical Note No. 91 (WMO-No. 226,
TP. 120). Geneva.

——, 1987: *Some General Considerations and Specific Examples in the Design of Algorithms for Synoptic Automatic
Weather Stations* (D.T. Acheson). Instruments and Observing Methods Report No. 19
(WMO/TD-No. 230). Geneva.

——, 1988: *WMO International Ceilometer Intercomparison (United Kingdom, 1986)* (D.W. Jones, M. Ouldridge
and D.J. Painting). Instruments and Observing Methods Report No. 32
(WMO/TD-No. 217). Geneva.

——, 1989*a*: *WMO International Hygrometer Intercomparison* (J. Skaar, K. Hegg, T. Moe and K. Smedstud).
Instruments and Observing Methods Report No. 38 (WMO/TD-No. 316). Geneva.

——, 1989*b*: Preliminary results of the WMO automatic sunshine duration measurement comparison
1988/89 in Hamburg (K. Dehne). *Papers Presented at the Fourth WMO Technical Conference on
Instruments and Methods of Observation (TECIMO-IV).* Instruments and Observing Methods
Report No. 35 (WMO/TD-No. 303). Geneva.

——, 1990: *The First WMO Intercomparison of Visibility Measurements: Final Report (United Kingdom 1988/1989)*
(D.J. Griggs, D.W. Jones, M. Ouldridge and W.R. Sparks). Instruments and Observing Methods
Report No. 41 (WMO/TD-No. 401). Geneva.

——, 1991: *Guidance on the Establishment of Algorithms for Use in Synoptic Automatic Weather Stations:
Processing of Surface Wind Data* (D.J. Painting). Instruments and Observing Methods Report
No. 47 (WMO/TD-No. 452). Geneva.

——, 1992*a*: *International Meteorological Vocabulary* (WMO-No. 182). Geneva.

——, 1992*b*: *The WMO Automatic Digital Barometer Intercomparison: Final Report* (J.P. van der Meulen).
Instruments and Observing Methods Report No. 46 (WMO/TD-No. 474). Geneva.

——, 1993: *Guide on the Global Data-processing System* (WMO-No. 305). Geneva.

——, 1994: WMO solid precipitation measurement intercomparison: Preliminary results (B.E. Goodison,
E. Elomaa, V. Golubev, T. Gunther and B. Sevruk). *Papers Presented at the WMO Technical
Conference on Instruments and Methods of Observation (TECO-94).* Instruments and Observing
Methods Report No. 57 (WMO/TD-No. 588). Geneva.

——, 1997: *Guidance on Automatic Weather Systems and their Implementation.* Instruments and Observing
Methods Report No. 65 (WMO/TD-No. 862). Geneva.

——, 2000: Operation of automated surface observing systems in harsh climatological environments
(M.D. Gifford, G.M. Pearson and K. Hegg). *Papers Presented at the WMO Technical Conference on
Meteorological and Environmental Instruments and Methods of Observation (TECO-2000).*
Instruments and Observing Methods Report No. 74 (WMO/TD-No. 1028). Geneva.

——, 2003: *Algorithms Used in Automatic Weather Stations: Evaluation of Questionnaire* (M.D. Gifford).
Instruments and Observing Methods Report No. 78 (WMO/TD-No. 1160). Geneva.

——, 2010*a*: *Guide to the Global Observing System* (WMO-No. 488). Geneva.

——, 2010*b*: *Manual on the Global Observing System* (WMO-No. 544), Volume I. Geneva.

——, 2011*a*: *Guide to Climatological Practices* (WMO-No. 100). Geneva.

——, 2011*b*: *Manual on Codes* (WMO-No. 306), Volumes I.1 and I.2. Geneva.

——, 2011*c*: *Technical Regulations* (WMO-No. 49), Volume I. Geneva.

——, 2014: *Guide to Meteorological Observing and Information Distribution Systems for Aviation Weather Services*
(WMO-No. 731). Geneva.

_____

CHAPTER CONTENTS

CHAPTER 2. MEASUREMENTS AND OBSERVATIONS AT AERONAUTICAL METEOROLOGICAL STATIONS

2.1 GENERAL

2.1.1 Definitions

This chapter deals with the requirements for observations at aeronautical meteorological stations and the instruments and methods that are used. Synoptic observations measure at one location a representative value for a rather large area, but meteorological observations for aeronautical purposes are often made at several locations at the aerodrome and in the surrounding area, at more frequent intervals, to be representative of rather limited areas, such as the approach, touchdown and take-off areas.

The meteorological measurements to be taken are for the most part essentially the same as those taken for other applications, and described in other chapters in this Guide. The exceptions are runway visual range (RVR), slant visual range and low level wind shear which are unique to this application.

2.1.2 Units

The units for measuring and reporting meteorological quantities for aeronautical purposes are the same as for other applications, except that:

(a) Surface wind speed may be measured and reported in metres per second or knots;[1] and wind direction[2] reported in degrees measured clockwise from geographic north[3] (see section 2.2.1);

(b) Cloud-base height may be measured in metres or feet.

The choice of units is a matter for national practice, depending on the requirements of the aviation regulatory bodies.

2.1.3 Requirements

The formal requirements for aeronautical observations are stated in the *Technical Regulations*, Volume II (WMO, 2013). Detailed guidance on procedures and practices is found in WMO (2014). Useful guidance on observing and monitoring meteorological conditions is contained in WMO (2003). Special attention should be given to aeronautical meteorological stations established on offshore structures in support of helicopter operations (ICAO, 1996).

The requirements for uncertainty, resolution and range, and for currently achievable performance in meteorological measurements are given in Part I, Chapter 1, and the operationally desirable accuracies of some measurements are provided in the *Technical Regulations*, Volume II, Part II, Attachment A.

Despite the excellent performance of modern aircraft, weather factors still have a marked effect on their operation. The reliability and representativeness of aerodrome observations are very

---

[1] The unit of wind speed used is determined by national decision. However, the primary unit prescribed by the *Technical Regulations*, Volume II (WMO, 2013) for wind speed is the metre per second, with the knot permitted for use as a non-SI alternative unit (further information is given in ICAO, 2010).

[2] Direction from which surface wind is blowing.

[3] Because wind direction reported to aircraft for landing or take-off purposes may be converted into degrees magnetic, the display at the air traffic service unit usually presents direction with respect to the magnetic north.

important in ensuring that landings and take-offs are made safely. The wind observation will determine the runway to be used, and the maximum take-off and landing weights. Temperature is also important and affects engine performance. Consequently, the load carried might have to be reduced, or the take-off would require a longer runway, particularly at airports in hot countries.

Routine observations are to be made at aeronautical meteorological stations, at times and frequencies determined by the Member country to meet the needs of national and international air navigation, giving due regard to regional air-navigation arrangements. Special and other non-routine observations are to be made on the same basis. Routine observations at aerodromes should be made at hourly or half-hourly intervals, during all or part of each day, or as necessitated by aircraft operations. Special observations must be made when specified changes occur between routine observations in respect of surface wind, visibility, RVR, present weather and/or cloud. These specified changes are set out in the *Technical Regulations*, Volume II, Part II, Appendix 3, 2.3.2. These observations, in the form of coded reports of the METAR or SPECI types, are exchanged internationally between aeronautical meteorological stations. Other types of reports are intended only for aeronautical operations, and should be prepared in a form defined jointly by the meteorological and airport authorities.

In view of the importance of meteorological observations for aircraft safety, it is essential that observers be correctly trained and have good eyesight. Observer training should include basic courses and regular refresher courses (for further information see the *Technical Regulations*, Volume I, Part II, 4, and WMO, 2012).

Siting, installation and the nature of meteorological systems are specified in the *Technical Regulations*, Volume II, Part I, 4, with technical specifications and detailed criteria in the *Technical Regulations*, Volume II, Part II, Appendix 3. These specifications are summarized below.

Special care is necessary in selecting appropriate sites for making observations, or for the installation of instruments at aeronautical meteorological stations, to ensure that the values are representative of the conditions at or near the aerodrome. In some instances, where information over a large area is required, it may be necessary to provide multiple installations for some instruments to ensure that values reported are representative of the entire area. For example, for long runways or for large aerodromes with several runways, where approach, touchdown and take-off areas may be as much as 2 to 5 km apart, the values of various parameters such as wind, cloud height, RVR, and so forth, measured at one end of a runway may be quite different from the conditions prevailing elsewhere on that runway, or over other areas of the runway complex of interest to aircraft operations.

At all aerodromes, the sites should be such that the measured values of the various meteorological parameters are representative of the aerodrome itself and/or the appropriate area of a particular runway or runway complex. At aerodromes where precision approach and landing operations are not in practice (non-instrument or non-precision approach runways), this criterion on representativeness is less restrictive than with precision approach runways (i.e. with Category I, II or III runways (see WMO, 2014, and ICAO, 2011)).

In selecting locations for instruments at aerodromes, it is particularly important that, while the site and exposure of the instruments meet operational requirements, the instruments or their operation do not present hazards to air navigation; and that the presence or movement of aircraft at the aerodrome (taxiing, take-off runs, landing, parking, etc.) and the various aerodrome installations do not unduly influence the measured values.

The types of instruments to be used, their characteristics and the methods employed for the presentation and reporting of the measured values of the parameters are equally important. Meteorological instruments should be exposed, operated and maintained in accordance with the practices, procedures and specifications promulgated in this Guide. Aeronautical meteorological stations shall be inspected at sufficiently frequent intervals to ensure that a high standard of observations is maintained, that instruments and all their indicators are functioning correctly, and that the exposure of the instruments has not changed significantly (*Technical Regulations*, Volume II, Part I, 4.1.4).

Instrument design should permit remote indication, simultaneously at both the air traffic service (ATS) units and at the meteorological stations and offices, of the appropriate values of surface wind, temperature, dewpoint, atmospheric pressure, present weather, visibility, RVR (if the runways are equipped for take-offs and landings in fog) and cloud height, all of which should be representative of conditions in the touchdown and take-off areas concerned. Automatic instrumental systems for measuring the height of the cloud base and RVR are particularly useful at aeronautical stations.

At aerodromes where precision approaches and, in particular, where Category II, III A and III B operations are affected, and/or at aerodromes with high levels of traffic, it is preferable to use integrated automatic systems for acquisition, processing and dissemination/display in real time of the meteorological parameters affecting landing and take-off operations. These automatic systems should be capable of accepting the manual insertion of meteorological data that cannot be measured by automatic means (*Technical Regulations*, Volume II, Part I, 4.1.7). The requirements for automatic meteorological observing systems are specified in the *Technical Regulations*, Volume II, Part II, Appendix 3.

2.1.4 **Methods**

The methods for taking meteorological measurements at aerodromes are essentially the same as those for other meteorological applications and described in other chapters of this Guide. This chapter describes some siting and sampling requirements, and some algorithms, which are particular to the aeronautical application.

2.2 **SURFACE WIND**

2.2.1 **General**

In aviation, measurements of airflow and low-level wind shear in the vicinity of the landing and take-off areas are of primary interest. The regulations are described in the *Technical Regulations*, Volume II, Part I, 4.1, with details in Part II, Appendix 3. At international aerodromes, ATS units, air traffic control towers, and approach control offices are normally equipped with wind-speed and wind-direction indicators, and air traffic controllers supply arriving and departing aircraft with readings from these indicators. To ensure compatibility, the indicators at the ATS units and the meteorological station should be connected to the same sensors.

The mean direction and speed of the wind are measured as well as gusts and specified significant variations of direction and speed. Wind reports disseminated beyond the aerodrome (*Technical Regulations*, Volume II, Part II, Appendix 3, 4.1.5) have the same content as those in synoptic observations (10 min means, and direction reported with respect to the geographic north),[4] and the values transmitted should be representative of all runways. For local routine and special reports and for wind indicator displays in ATS units (*Technical Regulations*, Volume II, Part II, Appendix 3, 4.1.3.1), the averaging period is 2 min for both speed and direction, and the values should be representative of the runway in use. Although wind direction shall be reported with respect to the geographic north, expressed in "degrees true" (*Technical Regulations*, Volume II, Part I, 4.6.1 and Part II, Appendix 3, 4.1.5.1), it is still common practice that ATS personnel report the aircraft with respect to the magnetic north ("degree magnetic"). Gusts should be determined from 3 s running means. Part I, Chapter 5, and Part IV, Chapter 2, of this Guide should be consulted on the precautions to be taken for sampling the anemometer output to measure the mean, gusts and variability of the wind speed and direction. Vector averaging is to be preferred to scalar averaging.

---

[4] Usually referred to as the "true" north, with the unit "degree true". The word "true" in "true north" or "degree true" should not be confused with the "true wind" (defined by WMO, 1992*a*). "True wind" is represented by the wind vector in relation to the Earth's surface. For a moving object like an aircraft, it is the vector sum of the apparent wind (i.e. the wind vector relative to the moving object) and the velocity of the object.

The wind measurements needed at aerodromes, such as mean value, extreme values, and so forth, should preferably be determined and displayed automatically, particularly when several sensors are used on different runways. When several sensors are required, the indicators shall be clearly marked to identify the runway and the section of runway monitored by each sensor.

2.2.2   Instruments and exposure

Wind-measuring instruments used at aeronautical stations are generally of the same type as those described in Part I, Chapter 5. The lag coefficients of direction and speed sensors should comply with the requirements of that chapter.

Sensors for direction and speed should be exposed approximately 10 m above the runway and should provide measurements that are representative of the conditions at the average lift-off and touchdown areas of the runway.

If wind sensors installed at aerodromes are to be representative of the conditions at take-off or landing areas, any disturbance or turbulence due to the proximity and passage of the aircraft themselves must be avoided (false gust indications due to landings and take-offs). For similar reasons, they must not be placed too close to buildings or hills or located in areas subject to microclimatic conditions (sea breeze, frequent storms, etc.). The preferred standard exposure of wind instruments is in open terrain, defined as an area where the distance between the anemometer and any obstruction is at least 10 times the height of the obstruction.

It is recommended that back-up or standby equipment should be provided in case of failure of the service instrument in order to avoid any interruption in the transmission of data to the ATS units. Where local conditions so warrant, one or more sets of sensors should be installed for each runway concerned. In such cases, the use of digital techniques is recommended since they enable data from a large number of sensors to be transmitted by one or two telephone cable pairs, and allow digital indicators to be used to display wind measurements using light-emitting diodes of different colours. The displays should show the "instantaneous" wind speed and direction (with a distance constant of 2 to 5 m), the average wind speed and direction over 2 or 10 min, and the minimum and maximum wind speeds. It is sometimes possible to select wind readings for different measurement points on the same indicator (thus reducing the number of indicators required).

When installing wind sensors at the aerodrome, particular attention must be paid to protecting them against atmospheric storm discharge (by the use of lightning conductors, earthing of the mast, and shielded or fibre optic cables); electronic data-processing equipment should also be protected.

In order to maintain the required accuracy, wind-measuring instruments should be kept in good order and regularly checked and recalibrated. Sensor performance must sometimes be checked in the wind tunnel, particularly for analogue systems. The use of digital techniques with the built-in testing of certain functions calls for fewer checks, but does not eliminate errors due to friction. Regular checks are to be made to detect defective components and deterioration of certain parts of the sensors.

The sources of error include friction, poor siting and problems with transmission or display equipment. Errors may also be caused by the design of the sensors themselves and are noticed particularly in light winds (rotation threshold too high, excessive inertia) or variable winds (over- or underestimation of wind speed or incorrect direction due to excessive or inadequate damping).

2.3   VISIBILITY

The definition of the meteorological optical range (MOR) and its estimation or instrumental measurement are discussed in Part I, Chapter 9. The measurement of visibility in aviation is

a specific application of MOR. However, the term MOR is not yet commonly used in aviation and the term visibility has been retained in this chapter to describe operational requirements. For aviation purposes, it is common practice to report visual ranges like the RVR and "visibility for aeronautical purposes" (VIS-AERO). Note that the latter is used in reports and indicated as "visibility" only, which differs from the common definition of visibility (see Part I, Chapter 9). Instruments used to measure MOR may also be used to measure RVR (see section 2.4) and VIS-AERO (see section 2.3.1). The *Technical Regulations*, Volume II, Part II, Appendix 3, 4.2 and 4.3 contain the formal descriptions for international aviation.

At international aerodromes, visibility observations made for reports disseminated beyond the aerodrome should be representative of conditions pertaining to the aerodrome and its immediate vicinity. Visibility observations made for reports for landing and take-off and disseminated only within the aerodrome should be representative of the touchdown zone of the runway, remembering that this area may be several kilometres from the observing station.

For aeronautical purposes, the measurement range for visibility is from 25 m to 10 km. Values greater than or equal to 10 km are indicated as 10 km. A sensor must therefore be able to measure values above 10 km or indicate if the measurement is greater than or equal to 10 km. The operationally desirable measurement uncertainty is 50 m up to 600 m, 10% between 600 m and 1 500 m and 20% above 1 500 m (*Technical Regulations*, Volume II, Part II, Attachment A). See Part I, Chapters 1 and 9, for advice on the accuracy of measurements.

In view of the meteorological minima governing the operational decisions on whether an aircraft can or cannot land or take-off, precise, reliable information must be given whenever visibility passes through certain limits, namely whenever visibility drops below or increases beyond the limit values of 800, 1 500 or 3 000 and 5 000 m, in the case, for example, of the beginning, cessation or change in fog or precipitation (*Technical Regulations*, Volume II, Part II, Appendix 3, 2.3.3 (b)).

When there are significant directional variations in visibility, particularly when they affect take-off and landing areas, this additional information should be given with indications of the direction of observation, for example, "VIS 2000 M TO S".

When visibility is less than 800 m it shall be expressed in steps of 50 m in the form VIS 350M; when it is 800 m or more but less than 5 km in steps of 100 m; when it is 5 km or more but less than 10 km, in kilometre steps in the form VIS 7KM; and when it is 10 km or more, it shall be given as 10 km, except when the conditions for the use of CAVOK (Ceiling and Visibility OK) apply (*Technical Regulations*, Volume II, Part II, Appendix 3, 4.2.4.1).

The methods described in Part I, Chapter 9, apply. Meteorological visibility observations are to be made by an observer who has "normal" vision, viewing selected targets of specified characteristics at known distances from the meteorological station. These observations may also be made by using visibility-measuring instruments, such as transmissometers and scatter coefficient meters. The location of the observing sites should be such as to permit continuous viewing of the aerodrome, including all runways.

If a transmissometer is used for visibility measurements, a baseline length of 75 m is suitable for aeronautical operations. However, if the instrument is also to be used for measuring RVR, the baseline length should be chosen after taking into account the operational categories in force at the aerodrome.

2.3.1 Visibility for aeronautical purposes

The *Technical Regulations*, Volume II, Part I, 1.1 defines visibility. VIS-AERO is the greater of:

(a) The greatest distance at which a black object of suitable dimensions, situated near the ground, can be seen and recognized when observed against a bright background;

(b)   The greatest distance at which lights in the vicinity of 1 000 cd can be seen and identified against an unlit background.

This VIS-AERO is in fact a "visual range" like RVR, involving subjective elements such as the virtual performance of a human eye and artificial lights. Nevertheless, the word "visibility" is commonly used without the addition "for aeronautical purposes" and confusion may arise with the official definition of "visibility" as defined by WMO (see Part I, Chapter 9) which is known as the MOR (meteorological optical range). An optical range is purely based on the physical state of the atmosphere and not on human or artificial elements, and is therefore an objective variable. This visibility (for aeronautical purposes) shall be reported, as in METAR. Because an aeronautical meteorological station may be combined with a synoptic station, visibility in SYNOP reports will differ from visibility in METAR, although it is measured by the same equipment.

Visibility for aeronautical purposes can be measured and calculated similarly to RVR (see section 2.4 for details), except that for the intensity of the light source, I, a constant value of 1 000 cd shall be used. Note that this value holds for lights usually used for the assessment of visibility, which are 10 times more intense than lights of moderate intensity (i.e. 100 cd, see Part I, Chapter 9).

2.3.2   Prevailing visibility

Prevailing visibility is defined as the greatest visibility value, observed in accordance with the definition of "visibility (for aeronautical purposes)", which is reached within at least half the horizon circle or within at least half of the surface of the aerodrome. These areas could comprise contiguous or non-contiguous sectors. This value may be assessed by human observation and/or instrumented systems, but when instruments are installed, they are used to obtain the best estimate of the prevailing visibility (*Technical Regulations*, Volume II, Part I, 1.1). Prevailing visibility should be reported in METAR and SPECI code forms.

2.4   RUNWAY VISUAL RANGE

2.4.1   General

RVR is the range over which the pilot of an aircraft on the centre line of a runway can see the runway surface markings or the lights delineating the runway or identifying its centre line. It is discussed in the *Technical Regulations*, Volume II, Part I, 4.6.3 and Part II, Appendix 3, 4.3. Details on observing and reporting RVR are given in ICAO (2005). It is recommended that this measurement be taken during periods when horizontal visibility is less than 1 500 m.

A height of approximately 5 m is regarded as corresponding to the average eye-level of a pilot in an aircraft on the centre line of a runway. Note that for wide-bodied aircraft, the pilot's eye-level may be at least 10 m. In practice, RVR cannot be measured directly from the position of a pilot looking at the runway centre line, but must be an assessment of what he or she would see from this position. Nevertheless, RVR should be assessed at a height of approximately 2.5 m above the runway for instrumented systems or approximately 5 m above the runway by a human observer (*Technical Regulations*, Volume II, Part II, Appendix 3, 4.3.1.1).

The RVR should be reported to the ATS units whenever there is a change in RVR, according to the reporting scale. The transmission of such reports should normally be completed within 15 s of termination of the observation. These reports are to be given in plain language.

2.4.2   Methods of observation

The RVR may be measured indirectly, by observers with or without supplementary equipment, by instrumental equipment such as the transmissometer or sensors measuring scattered light, or by video systems. At aerodromes, where precision approaches and, in particular, where

Category I, II, III A and III B operations are executed, RVR measurements should be made continuously by using appropriate instruments, namely transmissometers or forward-scatter meters (*Technical Regulations*, Volume II, Part II, Appendix 3, 4.3.2.1 for Category II and III, and recommended for Category I in Appendix 3, 4.3.2.2).

The RVR can then be assessed for operational purposes using tables or, preferably, by automatic equipment with digital read-out of RVR. It should be computed separately for each runway in accordance with the *Technical Regulations*, Volume II, Part II, Appendix 3, 4.3.5.

2.4.2.1 *Measurement by observers*

The counting of runway lights visible in fog (or lights specially installed parallel to the runway for that purpose) by observers can provide a simple and convenient method of determining RVR (but for precision instrument landing, only if the instrumented system fails). The difficulty arising with this method is related to the resolution capability of the human eye which, beyond a certain distance (dependent on the observer), does not permit the runway lights to be distinguished and counted.

Since the observer's position when observing runway lights is not identical to that of the pilot, the use of conversion curves to determine the true RVR is essential. Specially designed marker boards, spaced out along the side of the runway, may also be used for RVR assessment during the day.

2.4.2.2 *Measurement by video*

To assess RVR using a video system, use is made of a video camera and receiver to observe markers at known distances consisting of either runway lights, special lights, or markers positioned alongside the runway. Such a system is also beneficial for detecting patchy or shallow fog, which cannot be detected by the instruments.

2.4.2.3 *Measurement by transmissometer*

The instrument most commonly used at present for making an assessment of RVR is the transmissometer, which measures the transmission factor along a finite path through the atmosphere (see Part I, Chapter 9). RVR can be determined as follows:

(a) RVR when runway lights are dominant (RVR based on illumination threshold): The RVR depends on the transmission factor of the air, on the intensity of the runway lights and on the observer's (and pilot's) threshold of illuminance, which itself depends on the background luminance. It can be computed from:

$$E_t = I \, R^{-2} \, T^{R/a} \qquad\qquad (2.1)$$

where E_t is the visual threshold of illuminance of the observer (pilot), which depends on the background luminance L; I is the effective intensity of centre-line or edge lights toward the observer (pilot); T is the transmission factor, measured by the transmissometer; R is the RVR; and a is the transmissometer baseline or optical light path. Note that for the illuminance E of the observer (pilot), it holds that $E = I / R^2$. The requirements for the light intensity characteristics of runway lights are given in ICAO (2013). In fact, it holds for both centre-line and edge light that the illumination of the observer (pilot) is angular dependent and as a consequence I depends on R. Therefore $I = I(R)$ and $E = E(I, R)$. The calculation of R from equation 2.1 can be done only iteratively, which is relatively easy with the help of a simple calculator suitable for numerical mathematics. The value of E_t is determined with the help of a background luminance sensor (see section 2.4.3.3);

(b)   Assessment of RVR by contrast (RVR based on contrast threshold): When markers other than lights are used to give guidance to pilots during landing and take-off, the RVR should be based upon the contrast of specific targets against the background. A contrast threshold of 0.05 should be used as a basis for computations. The formula is:

$$R = a \frac{\ln 0.05}{\ln T} \tag{2.2}$$

where R is RVR by contrast. Because the contrast threshold level is 0.05, RVR by contrast is identical to MOR, namely $R =$ MOR. Note that RVR (based on illumination threshold) will always supersede RVR (based on contrast threshold), or RVR ≥ MOR.

2.4.2.4   *Measurement by forward-scatter or backscatter meters*

Instruments for measuring the forward-scatter or backscatter coefficient (sometimes known as scatterometers) are discussed in Part I, Chapter 9. Because of the physical principles of light scattering by aerosols, the measurement uncertainty of a forward-scatter meter (scatter-angle about 31°–32°) is smaller than with backscatter meters. Therefore, a forward-scatter meter is to be preferred. With these instruments the extinction coefficient σ can be determined, which is the principal variable to calculate RVR. Experience and studies with forward-scatter meters have demonstrated their capability to measure RVR for aeronautical applications (WMO, 1990, 1992*b*).

Since accuracy can vary from one instrument design to another, performance characteristics should be checked before selecting an instrument for assessing RVR. Therefore, the calibration of a forward-scatter meter has to be traceable and verifiable to a transmissometer standard, the accuracy of which has been verified over the intended operational range (*Technical Regulations*, Volume II, Part II, Appendix 3, 4.3.2).

A scatter meter determines, from the received scattered light, the extinction coefficient σ of the atmosphere at the position of the optical volume (see Part I, Chapter 9). Because σ is a direct measure for the visibility, R can be determined relatively easily (from σ or MOR, where MOR $= -\ln 0.05/\sigma \approx 3/$MOR). The RVR can be determined as follows:

(a)   RVR when runway lights are dominant (RVR based on illumination threshold): RVR will be calculated in a similar way as with a transmissometer except that σ is used and not T. It can be computed from:

$$R = \frac{1}{\sigma} \left(\frac{I(R)}{E_t \cdot R^2} \right) \tag{2.3}$$

where R is the runway visual range; σ is the extinction coefficient (or 3/MOR); E_t is the visual threshold of illuminance of the observer (pilot), which depends on the background luminance; and I is the effective intensity of centre-line or edge lights toward the observer (pilot). As with a transmissometer, R should be calculated iteratively;

(b)   Assessment of RVR by contrast (RVR based on contrast threshold): When markers other than lights are used to give guidance to pilots during landing and take-off, the RVR should be based upon the contrast of specific targets against the background. A contrast threshold of 0.05 should be used as a basis for computations. The formula is:

$$R = -\ln 0.05 / \sigma = \text{MOR} \tag{2.4}$$

where R is RVR by contrast. Note that RVR (based on illumination threshold) will always exceed RVR (based on contrast threshold), namely RVR ≥ MOR.

2.4.3   **Instruments and exposure**

Instrumented systems may be based on transmissometers or forward-scatter meters to assess RVR. Runway visual range observations should be carried out at a lateral distance of not more than 120 m from the runway centre line. The site for observations that are representative of the touchdown zone should be located about 300 m along the runway from the threshold.

The sites for observations that are representative of the middle and far sections of the runway should be located at a distance of 1 000 to 1 500 m along the runway from the threshold and at a distance of about 300 m from the other end of the runway (*Technical Regulations*, Volume II, Part II, Appendix 3, 4.3.1.2). The exact position of these sites and, if necessary, additional sites (for long runways), should be determined after considering aeronautical, meteorological and climatological factors, such as swamps and other fog-prone areas. Runway visual range should be observed at a height of approximately 2.5 m above the runway for instrumented systems or approximately 5 m above the runway by a human observer (*Technical Regulations*, Volume II, Part II, Appendix 3, 4.3.1.1).

The units providing air traffic and aeronautical information services for an aerodrome should be informed without delay of changes in the serviceability status of the RVR observing system.

A computer is usually used to compute the RVR at several measurement points and to display the measurements on screen with the time of observation, the transmission factors, the luminance measured at one or more points on the aerodrome and the runway light intensity. The data are sent to display panels at the ATS and meteorological and other units concerned, or to printers for recording.

The runway light intensity should be entered automatically in the computer in accordance with the procedure described in the *Technical Regulations*, Volume II, Part II, Appendix 3, 4.3.5 or as formally agreed upon between the ATS units and the local meteorological unit.

Analogue or digital graphic recorders (with time base) for transmission factors T and background luminance L may also be used. A graphic display of the RVR should also properly show the record of E_t and I (see equation 2.1).

2.4.3.1 *Transmissometers*

A description of transmissometers, their installation on site and their maintenance and sources of error is given in Part I, Chapter 9, with references to other literature.

A transmissometer system consists of a projector that directs a light of known intensity onto a photoelectric receiving device placed at a known distance from the projector. The variations in atmospheric transmission, due to fog or haze, and so on, are continuously measured and recorded. The instrument is calibrated to be direct-reading, giving the transmission factor in per cent.

The transmitter and receiver must be mounted at the same height on rigid, secure and durable stands, which, if possible, are not frangible and in such a way that shifting soil, frost, differential heating of towers, and so forth, do not adversely affect the alignment of the two units. The height of the optical path should not be less than 2.5 m above the level of the runway.

In one type of transmissometer, the transmitter and receiver are incorporated in the same unit (see Part I, Chapter 9). In this case, a reflector (for example, mirror) is installed at the normal receiver location. The light travels out and is reflected back, with the baseline length being twice the distance between the transmitter/receiver and the reflector. The transmissometer may have a single or double base, depending on whether one or two receivers or retro-reflectors, positioned at different distances, are used.

The transmissometer baseline length, namely, the length of the optical path covered by the light beam between transmitter and receiver, determines the RVR measurement range. For an RVR between 50 and 1 500 m, the most commonly used baseline lengths are between 15 and 75 m.

However, for shorter transmissometer baseline lengths, a higher transmission factor measurement accuracy and better system linearity are necessary. If low RVRs must be measured for Category II and III landing requirements, a short base transmissometer should be selected. However, the maximum RVR that can be measured is then relatively low. A compromise must

be found. Double-base transmissometers exist, offering a wider measurement range by the selection of one base or the other, but care must be taken when switching baselines to ensure that the RVR measurements remain consistent with each other.

Higher RVR values can be measured by using longer transmissometer baseline lengths, but greater luminous power is needed for transmission to compensate for light attenuation between the transmitter and receiver in dense fog, and a narrower reception angle is required to avoid scatter disturbance phenomena. The measurement of the weakest signals is also dependent on background noise in the measuring equipment.

Transmissometers are generally aligned parallel to the runway. However, direct (or reflected) sunlight should be avoided as this may cause damage. The optical axis should, therefore, be positioned in an approximate north-south direction horizontally (for latitudes below 50°). Otherwise, a system of baffles should be used.

2.4.3.2   *Forward-scatter meters*

Forward-scatter meters should be sited near the runway in a similar fashion to transmissometers. The positioning of forward-scatter meters requires fewer precautions than for transmissometers. Nevertheless, care should be taken to avoid direct or scattered sunlight which might influence (or damage) the receiver. In particular, sunlight may influence the receiver after scattering by snow cover, or lake or sea surface. Modern instruments compensate for contamination of the optical components.

2.4.3.3   *Background luminance sensor*

The threshold of illuminance E_t must be known when computing the RVR. A background luminance sensor should be placed at the end of the runway along which one or more transmissometers or scatter meters have been installed. One or more luminance sensors may be installed at the airport depending on the number of runways covered.

The background luminance sensor measures the luminance of the horizon or sky in the direction opposite the sun. The illuminance thresholds are introduced in the RVR computation either as a continuous or a step function (two to four steps). The curve for converting background luminance to illumination threshold is given in the *Technical Regulations*, Volume II, Part II, Attachment D, and in ICAO (2005). The recommended relation used for this curve is:

$$\log_{10} E_t = 0.05\left(\log_{10} L\right)^2 + 0.573 \log_{10} L - 6.667 \tag{2.5}$$

where L is the luminance of the horizon sky.

The background luminance sensor consists of a photodiode placed at the focal point of a lens with an angular aperture of about 10° to 20°, aligned in a north-south direction (to avoid direct sunlight) and at an angle of elevation of approximately 30° to 45° to the horizon.

2.4.4   **Instrument checks**

It is essential that regular periodic checks be made on all components of the transmissometer – or scatter meter – RVR system to ensure the proper operation and calibration of the system. In general, the literature provided by the companies manufacturing and developing such equipment will give detailed instructions for making such checks and will indicate the corrective action to be taken when specified instrumental tolerances are not met. For a transmissometer, when the visibility exceeds 10 to 15 km, it is simple to check that the equipment indicates a transmissivity of approximately 100% (see Part I, Chapter 9). For scatter meters, "scatter plates" may be used, which emulate certain extinction values. However, the calibration of a forward-scatter meter should be traceable and verifiable to a transmissometer standard (see section 2.4.2.4).

Correct maintenance and calibration are necessary in order to:

(a)   Prevent dirt from accumulating, on optical surfaces;

(b)   Check variations in the light intensity of the transmitter;

(c)   Avoid drift after calibration;

(d)   Check the alignment of transmitters and receivers.

Frequent maintenance is necessary at heavily polluted sites. Care is to be taken so that not all equipment is taken out of service at the same time during maintenance, and so that this interruption of service is not of long duration, particularly during periods when fog is forecast.

When fog persists for several consecutive days, the projector should be checked to ensure that its light intensity is steady and the equipment should be checked for drift. Checking optical settings is difficult, if not impossible, in very dense fog; it is therefore vital that instruments should be mechanically reliable and optically stable.

2.4.5   **Data display**

The RVR data display for the units concerned is updated according to the local agreements in force: every 15 to 60 s, and even every 2 min on some occasions. Changes in RVR should normally be transmitted within 15 s after termination of the observation.

2.4.6   **Accuracy and reliability of runway visual range measurements**

If scattered light sensors are used, as distinct from transmissometers, the equations for RVR are acceptable in the case of fine water droplets as fog, but not when visibility is reduced by other hydrometeors such as freezing fog, rain, snow or lithometeors (sandstorms). In which case, MOR and RVR measurements must be used with much caution since satisfactory relations for such cases have not yet been accepted.

Divergence between the RVR for a pilot and the measured value may reach 15% to 20%, with an assumed standard deviation of not more than 10%. In the case of observers, there are divergences in visual threshold and in observing conditions that, together, can cause differences in reported visual range amounting to 15% or 20%.

RVR measurements taken using transmissometers or scatter coefficient meters are representative of only a small volume of the atmosphere. In view of the considerable fluctuations of fog density in time, as well as in space, a mean value established over a large number of samples or measurements is essential. Rapid changes in RVR may give rise to difficulties for the ATS units when transmitting the information to aircraft. For these reasons, an averaging period of between 30 s and 1 min is recommended, computed as a mean or a sliding mean.

Operationally desirable accuracies of RVR measurement or observation are specified in the *Technical Regulations*, Volume II, Part II, Attachment A.

2.5   **PRESENT WEATHER**

The observation and reporting of present weather is discussed in Part I, Chapter 14, and the procedures are described in the *Technical Regulations*, Volume II, Part I, 4.6.4 with details in Part II, Appendix 3, 4.4. For aviation, emphasis is placed upon observing and reporting the onset, cessation, intensity and location of phenomena of significance to the safe operation of aircraft, for example, thunderstorms, freezing precipitation and elements that restrict flight visibility.

For take-off and landing, present weather information should be representative, as far as practicable, of the take-off and climb-out area, or the approach and landing area. For information disseminated beyond the aerodrome, the observations of present weather should be representative of the aerodrome and its immediate vicinity.

Most observations relating to present weather are made by visual means. Care should be taken to select observing sites that afford adequate views in all directions from the station. Instruments may be used to support the human observations, especially for measuring the intensity of precipitation.

Detectors used to identify the type of precipitation (rain, snow, drizzle, etc.) or visibility-reducing phenomena other than precipitation (fog, mist, smoke, dust, etc.) can assist the human observer and this can help if done by automation. They are based essentially on the measurement of the extinction coefficient or scintillation, and may also make use of relations between weather phenomena and other quantities, such as humidity. At present, there is no international agreement on the algorithms used for processing data to identify these phenomena. There is no vital need for this equipment in aeronautical meteorology while human observers are required to be present.

Descriptions of phenomena reported in present weather appear in Part I, Chapter 14, as well as in WMO (1975, 1987, 1992a, 2011a) and ICAO (2011).

Specifications for special reports regarding present weather are contained in the *Technical Regulations*, Volume II, Part II, Appendix 3, 4.4.2. The abbreviations and code figures used in METAR or SPECI plain language reports appear in the *Technical Regulations*, Volume II, Part II, Appendix 3, 4.4.2.3–4.4.2.9.

2.6   **CLOUD**

2.6.1   **General**

Observations and measurements of clouds are discussed in Part I, Chapter 15. For aviation applications (see the *Technical Regulations*, Volume II, Part I, 4.6.5 and Part II, Appendix 3, 4.5), cloud information (amount, base height, type) is required to be representative of the aerodrome and its immediate vicinity and, in reports for landing, of the approach area. Where cloud information is supplied to aircraft landing on precision approach runways, it should be representative of conditions at the instrument landing system middle marker site, or, at aerodromes where a middle marker beacon is not used, at a distance of 900 to 1 200 m from the landing threshold at the approach end of the runway (*Technical Regulations*, Volume II, Part II, Appendix 3, 4.5.1).

If the sky is obscured or not visible, the cloud-base height is replaced by a vertical visibility in the local routine (MET REPORT) and local special (SPECIAL) reports (*Technical Regulations*, Volume II, Part I, 4.5.1(i)) and in weather reports METAR and SPECI (WMO, 2011a, FM 15/FM 16, paragraph 15.9). Vertical visibility is defined as the maximum distance at which an observer can see and identify an object on the same vertical as himself or herself, above or below. Vertical visibility can be derived from the optical extinction profile, determined by a LIDAR-based ceilometer. Assuming that the total extinction σ at altitude h can be derived from the backscatter extinction coefficient σ_B at that altitude after appropriate calibration for the whole altitude range, and assuming that a contrast threshold of 5% is applicable similar to MOR, it should hold for the vertical visibility VV that:

$$\int_0^{VV} \sigma(h) \cdot dh = \ln\left(\frac{I(VV)}{I_0}\right) = \ln(0.05) = 3 \qquad (2.6)$$

Because LIDAR-based ceilometers determine the local extinction coefficient for fixed intervals Δh, VV may be derived relatively easily from:

$$\sum_{i=1}^{N} \sigma_i \cdot \Delta h = 3, \text{ with } h_N = VV \qquad (2.7)$$

Typical code words like CAVOK, SKC (sky clear), NCD (no clouds detected) and NSC (nil significant clouds) are used in reports when the state of the atmospheric or weather will not affect the operations of take-off and landing; replacing the quantitative information with simple acronyms is beneficial. Details on the use of these practices are given in the *Technical Regulations*, Volume II, Part II, Appendix 3, 2.2 and 4.5.4.3. For instance, CAVOK shall be used when cloud and present weather is better than the prescribed values or conditions, but if the specified conditions are met. Great care should be taken when using these abbreviations with automated measuring systems, which are not capable of measuring clouds or vertical visibility within the stated requirements.

The height of clouds bases shall be reported above aerodrome elevation. However, when a precision approach runway is in use which has a threshold elevation of 15 m or more below the aerodrome elevation, local arrangements shall be made in order that the height of the clouds reported to arriving aircraft shall refer to the threshold elevation.

2.6.2 Observation methods

The principal methods used for determining the height of the cloud base are:

(a) Cloud-base searchlight;

(b) Rotating-beam ceilometer;

(c) Laser ceilometer;

(d) Ceiling balloon;

(e) Visual estimation;

(f) Aircraft reports.

Cloud-base height should be obtained by measurement whenever possible. At busy or international aerodromes with precision approach systems, cloud-base measurements should be taken automatically so that this information and any changes can be available on a continuous basis.

The ceiling-balloon method is too slow and too prone to errors to be a routine method for measuring cloud-base height at aerodromes, and the visual method is also too prone to error, especially at night, to be used where the observations are critical. Aircraft reports of cloud-base height can provide the observer with useful supplementary information. Care should be taken when interpreting pilots' information due to the fact that the information may be several kilometres from the surface observation point.

2.6.3 Accuracy of cloud-base height measurements

The ragged, diffuse and fluctuating nature of many cloud bases limit the degree of accuracy with which cloud-base heights can be measured. Isolated or infrequent measurements, such as those obtainable by the use of cloud-base height balloons, may be unrepresentative of the cloud conditions as a whole. The best estimate requires the study of a quasi-continuous recording over a period of several minutes provided by one of the instruments mentioned above.

The accuracy of instrumental measurements indicated by manufacturers is usually obtained by using solid or artificial targets. Operational accuracy is, however, more difficult to achieve in view of the fuzzy nature of the cloud base.

2.7   AIR TEMPERATURE

A general discussion of instruments and methods of observation for air temperature may be found in Part I, Chapter 2. For air navigation purposes (see the *Technical Regulations*, Volume II, Part I, 4.1 and 4.5.1(j)), it is necessary to know the air temperature over the runway. Normally, data from well-sited, properly ventilated screens give sufficient approximations of the required values. Rapid fluctuations in air temperature (2 °C to 3 °C per half-hour) should be notified immediately to ATS units, principally in tropical and subtropical areas.

Temperature sensors should be exposed in such a way that they are not affected by moving or parked aircraft, and should yield values that are representative of general conditions over the runways. Thermometers with a time constant of 20 s should preferably be used to avoid excessively small fluctuations in temperature (average wind speed of 5 m s^{-1}), or, in cases of automatic measurements, an appropriate digital averaging or resistance/capacitance filtering should be applied. Remote indicating and recording systems are an advantage. Moreover, aerodromes with runways intended for Category II and III instrument approach and landing operations, require automated measuring equipment and displays at the automatic retrieval system site. Temperature measurements have become more integrated into automatic stations or data acquisition systems, and are displayed in digital form. The displayed temperature should represent an average value over 1 to 10 min, obtained after linearization of the sensor output signal. The value obtained should be rounded off to the nearest whole degree for aeronautical use.

2.8   DEWPOINT

Atmospheric moisture at aeronautical stations is usually expressed in terms of the dewpoint temperature. The reading is rounded off to the nearest whole degree as in the case of air temperature. The procedures are described in the *Technical Regulations*, Volume II, Part I, 4.1 and 4.5.1(j). Observation methods are described in Part I, Chapter 4.

Modern humidity sensors allow the use of remote indicators and recorders. For manual observations the psychrometer is commonly used. A psychrometer of the ventilated type is to be preferred to meet the stated measurement uncertainty. The types of instruments commonly in use are as follows:

(a)   Capacitive sensors based on the measurement of a capacitor's capacitance, in which the value of the polymer dielectric varies as a function of the water vapour content of the ambient air. In practice, the measured capacitance is fairly linear with relative humidity. Dewpoint is calculated using the ambient air temperature (measured separately and at a very short distance) ($t_d = t_d(t, U)$). The appropriate formulae are given in Part I, Chapter 4, Annex 4.B. To avoid condensation, which may last long after $U < 100\%$ and which might be trapped by the filter protecting the sensor, the sensor may be heated. For such a practice, the ambient air temperature should not be used, rather a temperature value should be used that represents the heated air around the sensor. In practice, the appropriate procedure can only be achieved after careful calibration in well-designed climate chambers;

(b)   Dewpoint hygrometers, measuring the temperature at which a very light deposit of dew occurs on a mirror. The mirror is heated or cooled, most frequently by the Peltier effect, to obtain the point of equilibrium at which dew is deposited. The mirror is used with an associated photo-electronic dew-detection system. Although such systems deliver dewpoint temperature directly, pollution and deterioration of the mirror may cause significant biases. In particular, frost may destroy the mirror. At least every six months the mirror should be inspected, but only by skilled personnel. Great care should be taken when cleaning the mirror and the manufacturer's instructions should be followed precisely.

2.9 ATMOSPHERIC PRESSURE

2.9.1 General

A general discussion on the observations of atmospheric pressure may be found in Part I, Chapter 3, and that for aviation purposes is found in the *Technical Regulations*, Volume II, Part I, 4.6.7. Pressure measurements for setting aircraft altimeters are essential at an aeronautical station. They are computed in tenths of hectopascals (0.1 hPa). They are referred to in the Q code as QFE and QNH, where:

(a) QFE (field elevation pressure) is defined as the pressure value at an elevation corresponding to the official elevation of the aerodrome (*Technical Regulations*, Volume II, Part II, Appendix 3, 4.7.2). Aerodrome reference point, elevation and runway elevation are described in ICAO (2013);

(b) QNH (atmospheric pressure at nautical height) is defined as the pressure value at which an aircraft altimeter is set so that it will indicate the official elevation of the aerodrome when the aircraft is on the ground at that location. QNH is calculated using the value for QFE and the pressure altitude relationship of the ICAO standard atmosphere. In fact, the ICAO standard atmosphere is a sub-range of the International Standard Atmosphere, which is documented by the ISO 2533:1975 standard and developed in liaison with the Committee on Space Research, ICAO and WMO. This standard atmosphere is a static atmosphere, with a fixed pressure and temperature at sea level and a fixed temperature gradient. Details of the standard atmosphere and its predefined constants are given in WMO (1966) and ICAO (1993). For the calculation of QNH from QFE, namely the reduction to mean sea level, this virtual atmosphere is used, and not the current true state of the atmosphere. As a consequence, QNH will differ from the reported atmospheric pressure reduced to sea level as described in Part I, Chapter 3, 3.11 and for which the actual temperature is used. The calculation of QNH from QFE is based on a slide rule relationship (for stations below about 3 000 to 4 000 m):

$$QNH = A + B \times QFE \tag{2.8}$$

where A and B depend on the geopotential altitude of the station (for details, see WMO, 1966, Introduction to Table 3.10). To derive QNH, the following three-step procedure should be followed:

(i) Determine the pressure altitude of the station from the QFE (the pressure altitude is calculated from QFE using the formulae of the standard atmosphere);

(ii) Subtract (or add for stations below mean sea level) from this pressure altitude the elevation of the station with respect to mean sea level to give the pressure altitude at mean sea level (may be positive or negative);

(iii) Derive from this pressure altitude the associated pressure value according to the standard atmosphere, which will be QNH.

An example of this procedure to derive QNH from QFE is shown in the figure below. The measured pressure and QNH and/or QFE values should be computed in tenths of a hectopascal. In local reports and reports disseminated beyond the aerodrome, QNH and QFE values should be included and the values should be rounded down to the nearest whole hectopascal. The ATS units, should be notified of rapid major changes in pressure.

The curve represents the standard atmosphere (pressure altitude as a function of pressure).
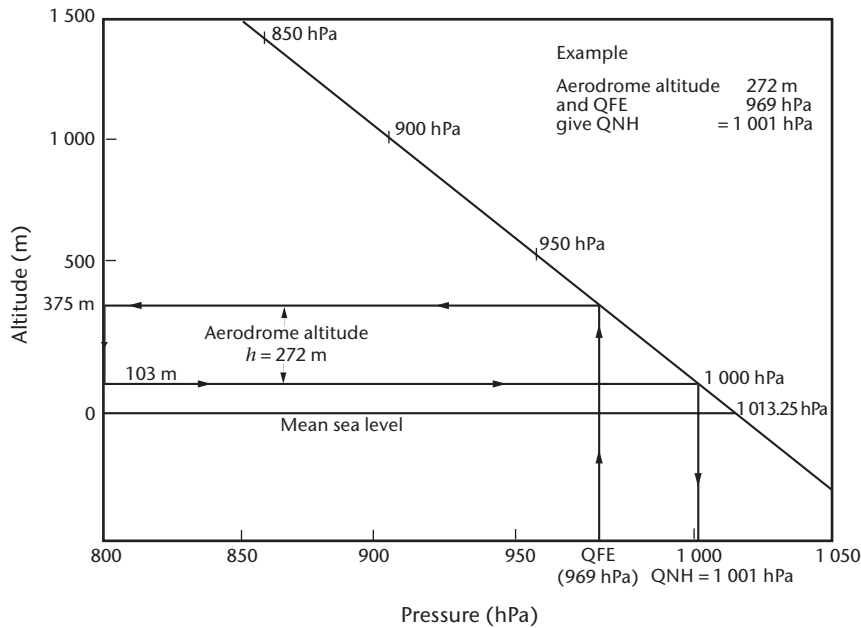
The relation between QFE and QNH

2.9.2   Instruments and exposure

The instrumental equipment used at an aeronautical station for pressure measurement is identical to that at a synoptic station, except that greater use is often made of precision automatic digital barometers for convenience and speed of reading in routine observations. Aeronautical stations should be equipped with one or more well-calibrated barometers traceable to a standard reference. A regular schedule should be maintained for comparing the instruments against this standard instrument. Both manual and automated barometers are suitable, provided that temperature dependence, drift and hysteresis are sufficiently compensated. Details of suitable barometers are given in Part I, Chapter 3.

The exposure of barometers at an aeronautical station is the same as at a synoptic station. If barometers have to be exposed inside a building, sensors should be vented to the outside, using an appropriately located static-tube arrangement. Owing to wind impacts on a building, pressure differences inside and outside the building may be larger than 1 hPa. To prevent such bias, which may extend to about plus or minus 3 hPa with high wind speeds, the static-tube should be placed sufficiently far away from this building. Also, air conditioning may have impacts on pressure measurements, which will be avoided by using such a static tube.

Direct-reading instruments for obtaining QNH values are available and may be used in place of the ordinary aneroid or mercury barometer, which require reference to tables in order to obtain the QNH values. For such devices, correct values of A and B, which are a function of the station geopotential altitude (see equation 2.8), shall be entered. The readings given by these instruments must be compared periodically with QNH values calculated on the basis of measurements obtained using the mercury barometer.

2.9.3   Accuracy of and corrections to pressure measurements

Pressure values used for setting aircraft altimeters should have a measurement uncertainty to 0.5 hPa or better (*Technical Regulations*, Volume II, Part II, Attachment A). All applicable corrections should be applied to mercury barometer readings, and corrections established through regular comparisons between the mercury and aneroid instruments routinely used in observations must be applied to all values obtained from the latter instruments. Where aneroid

altimeters are used in ATS tower positions, corrections different from those used in the observing station must be provided, for proper reduction to official aerodrome or runway level (*Technical Regulations*, Volume II, Part II, Appendix 3, 4.7).

The pressure values used for setting altimeters must refer to the official elevation for the aerodrome. For non-precision approach runways, the thresholds of which are 2 m or more below or above the aerodrome elevation, and for precision approach runways, the QFE, if required, should refer to the relevant threshold elevation.

2.10   OTHER SIGNIFICANT INFORMATION AT AERODROMES

2.10.1   General

Observations made at aeronautical stations should also include any available information on meteorological conditions in the approach and climb-out areas relating to the location of cumulonimbus or thunderstorms, moderate or severe turbulence, horizontal and/or vertical wind shear and significant variations in the wind along the flight path, hail, severe line squalls, moderate or severe icing, freezing precipitation, marked mountain waves, sandstorms, dust storms, blowing snow or funnel clouds (tornadoes or waterspouts), for example, SURFACE WIND 320/10 WIND AT 60M 360/25 IN APCH or MOD TURB AND ICE INC IN CLIMB OUT.

2.10.2   Slant visual range

Despite the development work carried out in various countries, no instrument for measuring the slant visual range has been made operational. The rapid technological development of all-weather landing systems has made it possible to reduce the set landing minima at aerodromes (Categories II, III A and III B) and has gradually resulted in this parameter being considered less important. No recommendation has been established for measuring this parameter.

2.10.3   Wind shear

Wind shear is a spatial change in wind speed and/or direction (including updraughts and downdraughts). Wind shear intensity may be classified into light, moderate, strong or violent according to its effect on aircraft. Low-level wind shear, that may affect landing and take-off operations, may exist as a vertical wind gradient in the lower layers of a thermally stable atmosphere, or it may be due to the effect of obstacles and frontal surfaces on wind flow, the effect of land and sea breezes, and to wind conditions in and around convection clouds, particularly storm clouds. Violent storms are by far the major cause of low-level wind shear, and a cause of fatal accidents for aircraft both on approach and landing, and during take-off.

The preparation and issuing of wind-shear warnings for climb-out and approach paths are described in the *Technical Regulations*, Volume II, Part II, Appendix 3, 4.8.1.4.

The measurement of vertical wind shear based on the information presented in Part I, Chapter 5, may be determined directly by anemometers on tall masts, which must be at a certain distance from the airport. Remote-sensing systems include Doppler Radar, Lidar, Sodar and the wind profiler. The Lidar uses laser light, the Sodar is based on acoustic radiation, and the wind profiler radar employs electromagnetic radiation at a frequency of around 50 MHz, 400 MHz or 1 000 MHz.

Horizontal wind shear is usually detected by a system of anemometers over the entire aerodrome. This system is designated as a low-level wind shear alert system. Computer-processed algorithms enable a wind-shear warning to be given. This system is used particularly in tropical and subtropical regions where frequent, intense storm build-up occurs.

Global coverage of this subject is given in the *ICAO Manual on Low-level Wind Shear* (Doc. 9817), first edition, 2005.

Although wind shear may have a significant impact on aircraft operations, no recommendation or criteria has yet been established. Nevertheless, details on wind-shear warnings are given in ICAO (2011), Chapter 4.

2.10.4   **Marked temperature inversions**

Information on marked temperature inversions exceeding 10 °C between the surface and levels up to 300 m should be provided, if available. Data are usually obtained from balloon-borne radiosondes, remote-sensing, aircraft observations (for example, AMDAR) or by meteorological inference.

2.11   **AUTOMATED METEOROLOGICAL OBSERVING SYSTEMS**

Specially-designed instrument systems have become common practice at aeronautical stations for measuring, processing, remotely indicating and recording values of the various meteorological parameters representative of the approach, landing, take-off and general runway conditions at the airport (*Technical Regulations*, Volume II, Part I, 4.1).

These automated systems comprise the following:

(a)   An acquisition system for converting electrical analogue measurements (volts, milliamperes, resistance, capacitance) to digital values in the appropriate units, and for the direct introduction of digital data;

(b)   A data pre-processing unit (averaging of readings over a time period of 1 to 10 min depending on the parameter measured and minimum, maximum and average values for the various parameters);

(c)   A computer, used, for example, to prepare SYNOP, METAR and SPECI reports, and telecommunication software.

The observer should be able to include in these reports those parameters which are not measured by the automatic station; these may include present weather, past weather, cloud (type and amount) and, sometimes, visibility. For aviation purposes, these stations are, therefore, often only an aid for acquiring meteorological data and cannot operate without observers.

Instruments at the automatic station should be checked and inspected regularly. Quality checks are necessary and recommended in order to avoid major errors and equipment drift. Measurements taken by automatic weather stations are dealt with in detail in Part II, Chapter 1. Quality assurance and other management issues can be found in Part IV, Chapter 1. To guarantee the stated performance of the automated instruments, a detailed evaluation plan should be established with details on maintenance and calibration intervals, and with feedback procedures to improve the observing system.

Recommendations on reporting meteorological information from automatic observing systems are given in the *Technical Regulations*, Volume II, Part II, Appendix 3, 4.

2.12   **RADAR**

At aerodromes with heavy traffic, weather radars have become indispensable since they provide effective, permanent, real-time surveillance by producing additional observations to the usual

meteorological observations for landings and take-offs. A radar can provide information over a wider area of up to 150 to 200 km. It is also an aid to short-range forecasting – within the hour or a few hours following the observation (possible aid in preparing the TREND report).

The echoes received are interpreted to identify the type of precipitation around the station: precipitation from stratus or convective clouds; isolated or line precipitation; or precipitation due to storms and, under certain conditions, detection of precipitation in the form of snow or hail. The image received enables the paths of squall lines or fronts to be followed and their development (intensification or weakening) to be monitored. If the radar is equipped with a Doppler system, the speed and direction of movement of these echoes can be computed.

The most widely used radars operate on wavelengths of 3, 5 or 10 cm. The choice depends on the region of the globe and the intended purpose, but the present general trend is towards the use of a 5 cm wavelength.

In certain regions, centralizing centres collect radar images from a series of radar stations in the country or region and assemble a composite image. Images are also exchanged between the various centres so that radar protection is provided over the largest possible area.

A general discussion on radar observations may be found in Part II, Chapter 7.

2.13   ICE SENSOR

This type of instrument, described in Part I, Chapter 14, is installed at a number of aerodromes to provide information on runway conditions in winter. The temperature at the surface and a few centimetres below the runway, the presence of snow, water, clear ice or white ice and the presence of salts or de-icing products, if any, are measured or detected. These sensors, in the form of a compact unit, are placed at a certain number of points on the runways or taxiways with their number depending on the size of the aerodrome and the number of runways to be protected. Atmospheric sensors are also placed close to the runways for the measurement of air temperature and humidity, wind and precipitation.

A data-acquisition and data-processing system displays the parameters measured and their variations with time. Depending on the type of software used, warning systems alert the airport authority responsible for aerodrome operations to the presence of clear ice or forecasts of dangerous conditions for aircraft.

2.14   LIGHTNING DETECTION

Systems for locating thunderstorms based on the detection of the low-frequency electromagnetic radiation from lightning have been developed in recent years (see Part II, Chapter 6). These systems measure the time taken for the signal to arrive and/or the direction from which it comes. Also, some systems analyse the characteristics of each radio impulse to identify cloud-to-ground lightning strokes. In certain regions, a number of these units are installed to measure and locate these phenomena in an area of 50 to 100 km around the aerodrome.

2.15   OTHER RELEVANT OBSERVATIONS

Additional information should be provided if the atmosphere is affected by dangerous pollution, for example, during volcanic eruptions. Information should also be provided to support rescue operations, especially at off-shore stations. If relevant for aircraft operations during take-off and landing, information on the state of the runway should be reported in METAR and SPECI, provided by the appropriate airport authority.

Volcanic ash should be reported (in SIGMET reports) as part of the supplementary information (*Technical Regulations*, Volume II, Part II, Appendix 3, 4.8). Details on observing volcanic ash, radioactive material and toxic chemical clouds are given in ICAO (2004, 2007).

In METAR and SPECI, information on sea-surface temperature and the state of the sea or the significant wave height should be included from aeronautical meteorological stations established on offshore structures in support of helicopter operations (*Technical Regulations*, Volume II, Part II, Appendix 3, 4.8.1.5).

———————————

REFERENCES AND FURTHER READING

Committee on Low-Altitude Wind Shear and its Hazard to Aviation, 1983: *Low-Altitude Wind Shear and Its Hazard to Aviation.* National Academy Press, Washington DC (available from http://www.nap.edu/books/0309034329/html/).

International Civil Aviation Organization (ICAO), 1993: *Manual of the ICAO Standard Atmosphere: extended to 80 kilometres (262 500 feet).* Third edition, Doc. 7488, Montreal.

———, 1996: *Manual on the Provision of Meteorological Service for International Helicopter Operations.* Doc. 9680, Montreal.

———, 2004: *Handbook on the International Airways Volcano Watch (IAVW).* Second edition, Doc. 9766, Montreal.

———, 2005: *Manual of Runway Visual Range Observing and Reporting Practices.* Third edition, Doc. 9328, Montreal.

———, 2007: *Manual on Volcanic Ash, Radioactive Material and Toxic Chemical Clouds.* Second edition, Doc. 9691, Montreal.

———, 2010: *Units of Measurement to be Used in Air and Ground Operations.* ICAO Annex 5, Fifth edition, Montreal.

———, 2011: *Manual of Aeronautical Meteorological Practice.* Ninth edition, Doc. 8896, Montreal.

———, 2013: *Aerodromes.* ICAO Annex 14, Volume I, Sixth edition, Montreal.

World Meteorological Organization, 1966: *International Meteorological Tables* (S. Letestu, ed.) (1973 amendment). (WMO-No. 188, TP 94). Geneva.

———, 1975: *International Cloud Atlas: Manual on the Observation of Clouds and Other Meteors* (WMO-No. 407), Volume I. Geneva.

———, 1987: *International Cloud Atlas* (WMO-No. 407), Volume II. Geneva.

———, 1990: *The First WMO Intercomparison of Visibility Measurements: Final Report (United Kingdom 1988/1989)* (D.J. Griggs, D.W. Jones, M. Ouldridge and W.R. Sparks). Instruments and Observing Methods Report No. 41 (WMO/TD-No. 401). Geneva.

———, 1992a: *International Meteorological Vocabulary* (WMO-No. 182). Geneva.

———, 1992b: Visibility measuring instruments: Differences between scatterometers and transmissometers (J.P. van der Meulen). *Papers Presented at the WMO Technical Conference on Instruments and Methods of Observation (TECO-92).* Instruments and Observing Methods Report No. 49 (WMO/TD-No. 462). Geneva.

———, 2003: *Guide to Practices for Meteorological Offices Serving Aviation* (WMO-No. 732). Geneva.

———, 2011a: *Manual on Codes* (WMO-No. 306), Volume I.1. Geneva.

———, 2011b: *Technical Regulations* (WMO-No. 49), Volume I. Geneva.

———, 2012: *Manual on the Implementation of Education and Training Standards in Meteorology and Hydrology* (WMO-No. 1083), Volume I. Geneva.

———, 2013: *Technical Regulations* (WMO-No. 49), Volume II. Geneva.

———, 2014: *Guide to Meteorological Observing and Information Distribution Systems for Aviation Weather Services* (WMO-No. 731). Geneva.

———————

CHAPTER CONTENTS

CHAPTER 3. AIRCRAFT-BASED OBSERVATIONS

3.1 GENERAL

3.1.1 Definitions

This chapter describes the methods used for automatic meteorological measurements on modern commercial aircraft, known collectively as aircraft-based observations. The principles described here may be used for data processing on any adequately instrumented aircraft to define and develop aircraft-based observing systems.

The WMO aircraft meteorological data relay (AMDAR) observing system is an aircraft-based observing system that is specified in WMO (2013) so as to meet meteorological requirements for reporting meteorological data from an aircraft platform. The AMDAR system is operated by WMO Members in collaborative agreement with their partner airlines, and the resulting data are transmitted on the WMO Global Telecommunication System. Additional information is available in WMO (2003).

AMDAR and other aircraft-based observing systems are generally implemented on aircraft that are equipped with sophisticated navigation and other sensing systems. There are sensors for measuring airspeed, air temperature and air pressure. Other data relating to aircraft position, acceleration and orientation are available from the aircraft navigation system. The aircraft also carry airborne computers for the flight management and navigation systems, by which navigation and meteorological data are computed continuously and are made available to the aircrew at the flight deck. In aircraft-based observing systems, they are further processed and fed automatically to the aircraft communication system for transmission to the ground, or, alternatively, a dedicated processing package can be used on the aircraft to access raw data from the aircraft systems and derive the meteorological variables independently.

In AMDAR systems, these facilities are used to compile and transmit meteorological reports in real time. Normally, the messages contain wind speed and direction (in the horizontal plane), air temperature, pressure altitude (altitude in the Standard Atmosphere related to a reference pressure level), time of observation, phase of flight and the aircraft position. If the aircraft is properly equipped, it may also report humidity or water vapour mixing ratio and a measure of turbulence.

The source data for meteorological observations require significant correction and complex processing to yield meteorological measurements that are representative of the free air-stream in the aircraft vicinity. A full description of all the processes involved is beyond the scope of this Guide, but an outline of the principles is given here, with references for further reading.

3.1.2 Aircraft meteorological sensors

The basic sensors carried on modern commercial aircraft comprise the pitot-static probe and the total air temperature (TAT) probe. Data from these sensors, together with information from the aircraft navigation system, usually provided by one or a combination of radio navaid systems (Global Positioning System, GPS), distance-measuring equipment (DME), VHF omni-directional radio range (VOR), an instrument landing system and in some cases an inertial navigation system (INS), are processed to give the following meteorological elements:

(a)   Pressure altitude H_p,[1] horizontal position and time (PALT in Figure 3.1);

(b)   Static air temperature T_s (SAT in Figure 3.1);

(c)   Wind speed |V|;

(d)   Wind direction D_w.

On some aircraft, additional processing for measuring turbulence is available or additional sensors are available for measuring ice build-up on the front surfaces and/or for measuring relative humidity or water vapour mixing ratio r.

In order to appreciate the complexity of the processing system, the following description is structured according to the process flow in a typical operational system. It will be noted (Figure 3.1) that the computed variables are highly interdependent.

3.2   PRESSURE AND MACH NUMBER

3.2.1   Pitot-static probe

The pitot-static probe (Figure 3.2) is exposed in the free air-stream beyond the aircraft boundary layer and provides the total pressure (static pressure plus impact or dynamic pressure). Some of these sondes can provide static pressure as well (i.e. free air-stream pressure, ideally the undisturbed ambient pressure), but on most airliners normally in use for AMDAR, the static pressure is provided via orifices on the side of the aircraft body. The pressure values are measured by electronic transducers and passed to a central unit hosting the algorithms for the aerodynamic adjustments (correction for the built-in error) and finally to the air data computer (ADC). The ADC computes pressure altitude, static temperature and Mach number from these two measurements.
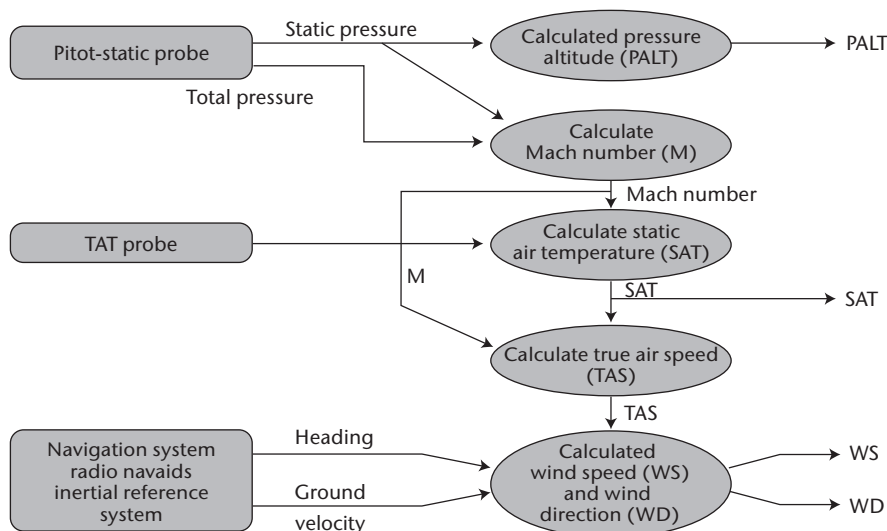
Figure 3.1. AMDAR sensor data processing

---

[1]   Pressure altitude is defined as a measure of height relative to the standard datum plane of 1 013.2 hPa. The variable flight level (FL) equals the pressure altitude for all levels. Pressure altitude and flight level may not be interchanged with indicated aircraft altitude, aircraft altitude, or aircraft height, for which other definitions apply. Because aircraft may fly at pressure levels above 1 013.2 hPa (i.e. below the standard datum plane), pressure altitude (or flight level) may be negative.
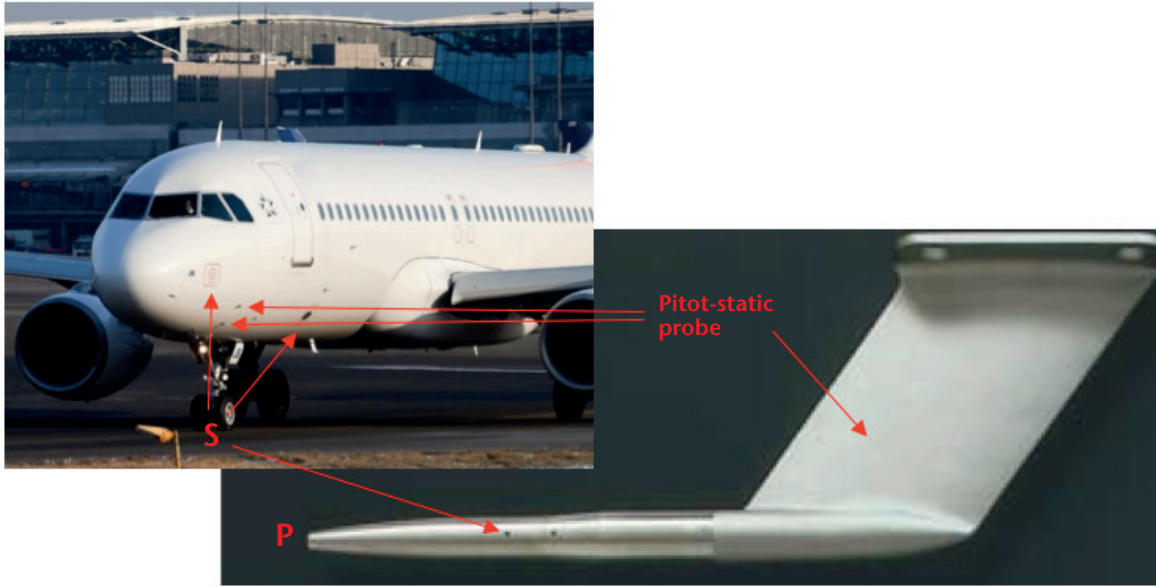
Figure 3.2. Typical configuration for the measurement of static pressure and pitot pressure on aircraft. Static pressure is taken (see the mark "S") either at ports on both sides of the fuselage or at side ports of the pitot-static probe. Total pressure is taken at the forward-headed orifice of the pitot probes or the pitot-static probes (see the mark "P") mounted on the fuselage a few metres behind the nose.

3.2.2 Pressure altitude

The static pressure measurement is not normally reported in AMDAR but is converted in the ADC to the equivalent altitude based on the International Standard Atmosphere (ISO, 2007). The Standard Atmosphere (see Figure 3.3) assumes a linear decrease in temperature with height of 6.5 °C per km up to 11 km or 36 089 ft,[2] and a mean sea-level temperature and pressure of 15 °C and 1 013.25 hPa, respectively. From 11 km to 20 km the temperature is assumed constant at –56.5 °C.
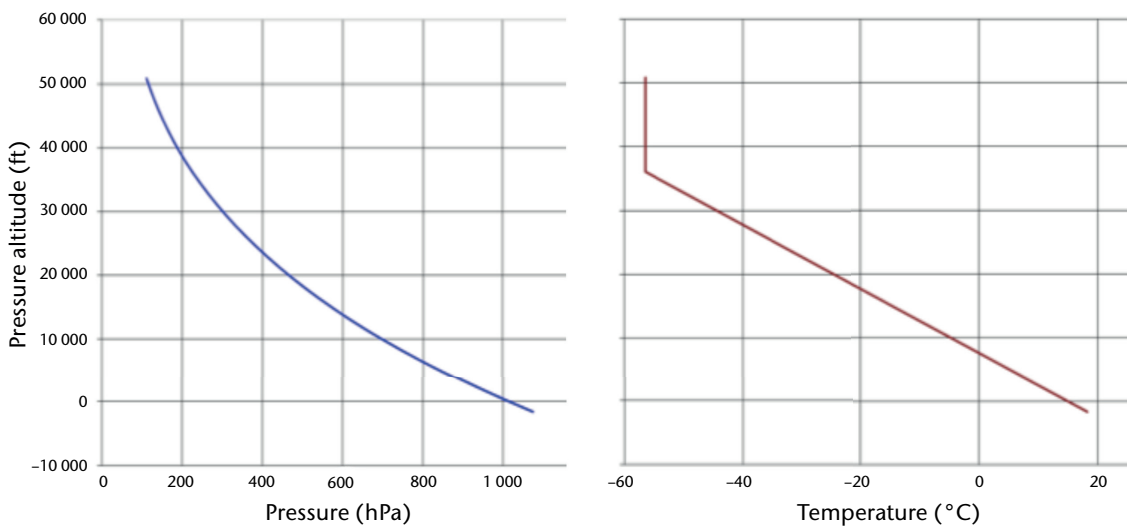
Figure 3.3. International Standard Atmosphere

---

[2]   Despite the general policy to use SI units, feet are used for altitude in this chapter, respecting common practice in the aviation community.

For pressure altitude H_p equal to or less than 36 089 ft, static pressure (p_s) is related to H_p by the following expression:

$$p_s = 1\,013.25 \cdot \left(1 - 6.8756 \cdot 10^{-6} \cdot H_p\right)^{5.2559}$$ (3.1)

with H_p in units of ft and p_s in units of hPa. For example, if H_p is 30 000 ft, p_s = 300.9 hPa.

The above expression (3.1) can be used to calculate the static pressure from the reported pressure altitude, provided that the on-board static pressure value was corrected only for aerodynamically-induced effects (built-in error) and the aircraft altimeter sub-scale (zero-reference) was set to ICAO standard mean sea level pressure (1 013.25 hPa). Navigational procedures also provide for altimeter sub-scale settings at other reference levels. For example, the setting can be aerodrome pressure (field elevation pressure, QFE) or QNH (QFE value reduced to sea level by use of the Standard Atmosphere), which is a pressure reference on the standard atmosphere scale such that aerodrome height is indicated at touchdown on a specific airfield. The pressure altitude reported by the AMDAR on-board software should always be with respect to ICAO mean sea level pressure only.

For use in the cockpit, the indicated altitude H_i (the pressure altitude above mean sea level (MSL)) is given by the pressure altitude (H_p) minus the altitude of the altimeter sub-scale reference on the standard atmosphere scale (H_r) plus the elevation of the reference pressure level above MSL (E_{Ref}). The general expression is:

$$H_i = H_p - H_r + E_{Ref}$$ (3.2)

$$H_r = \left[1 - \left(\frac{p_r}{1\,013.25}\right)^{0.190\,26}\right] \cdot 145\,442$$ (3.3)

with H_r, H_i, and E_{Ref} in units of ft, and p_r in units of hPa; p_r is the altimeter sub-scale setting, such as:

    QNH, then E_{Ref} = 0 ft above mean sea level

or

    QFE, then E_{Ref} = field elevation above mean sea level

Note that H_r = 0 if p_r = 1 013.25 hPa.

For example:

(a)   If the sub-scale setting is a QNH value of 1 000.0 hPa and the indicated altitude is 9 335 ft, H_p = 9 335 ft + 364 ft = 9 699 ft and p_s = 705 hPa;

(b)   If the sub-scale setting is a QFE value of 990 hPa, the aerodrome height is 276 ft and the indicated altitude is 9 058 ft, H_p = H_i + H_r (QFE) – E_{Ref} = 9 058 ft + 641 ft – 276 ft = 9 423 ft and the QNH value would be 1 000 hPa.

However, for the purpose of AMDAR, the altitude parameter should be chosen which is solely based on the aerodynamically clean static pressure without any reference to QNH or QFE.

If H_p is greater than 36 089 ft (11 km), static pressure is given by:

$$p_s = 226.32 \cdot e^{\frac{36\,089 - H_p}{20\,806}}$$

or   (3.4)

$$H_p = 36\,089 - 20\,806 \cdot \ln\left(\frac{p_s}{226.32}\right)$$

with H_p in units of ft, and p_s in units of hPa. For example, if H_p is 40 000 ft, p_s = 187.5 hPa.

3.2.2.1 *Measurement uncertainty*

Sources of uncertainty include:

(a) Calibration uncertainty;

(b) Short-term random instrument error;

(c) Calibration drift;

(d) Exposure uncertainty or static source uncertainty (built-in).

Because aircraft safety separations are critical, these uncertainties are corrected for as much as possible in the ADC. Static source uncertainty, which is a function of probe location, Mach number and aircraft weight, is determined empirically during flight-testing. Uncertainty of pressure is inferred from reported heights.

A possible source of data latency with the AMDAR system is in the radio link between aircraft and ground. This link process is regulated by international standards, such as ARINC 620, AOSFRS (AMDAR Onboard Software Functional Requirements Specification) or AAA, which stands for ACMS (Aircraft Condition Monitoring System) ACARS AMDAR. In earlier versions of these standards, the pressure altitudes were reported in hundreds of feet, equivalent at cruise level to some 1.5 hPa. This represents roughly 0.1% of the full scale pressure measurement. With instrumental accuracy at best of the order of 1 hPa, the uncertainty in static pressure at cruise level derived from converting pressure altitude is about 2 hPa. At zero reference level, the resolution is equivalent to about 3.7 hPa, leading to an uncertainty of some 4 hPa. In recent versions of the AMDAR on-board software, the altitude is reported in tens of feet, in which case the uncertainty due to coding-related error is lower than the remainder of the measurement uncertainty. AMDAR-equipped aircraft meet the rules and requirements of Reduced Vertical Separation Minima (RVSM) as laid down by the approved authorities within Air Traffic Management (ATM). The aircraft are required to maintain an altitude uncertainty of 50 m (160 ft), even in the altitude range of 30 000 to 40 000 ft. Hence, the pressure uncertainty has to be within the range of ±1.5 hPa and the quality control system of the airline must maintain this level of accuracy.

3.2.3 **Mach number**

Mach number (M, the true airspeed divided by the speed of sound in the free air) is an important element for aircraft operations. In AMDAR systems, it is used to correct air-temperature measurements and airspeed measurements. In dry air, the speed of sound is proportional to the square root of absolute (static) temperature T_s. Mach number only depends on two parameters:

(a) The impact pressure q_c measured by the aircraft's pitot tubes; and

(b) The static pressure p_s measured at specific locations on the side of the aircraft fuselage:

$$M^2 = \frac{2}{\kappa - 1} \left[\left(\frac{q_c + p_s}{p_s} \right)^{\frac{\kappa - 1}{\kappa}} - 1 \right]$$

(3.5)

where $q_c + p_s$ is the total pressure, and κ is the ratio of specific heats of dry air (C_p/C_v).

For further details, see the standard texts on aircraft aerodynamics such as Abbott and von Doenhoff (1959) and Dommasch et al. (1958).

3.2.3.1   *Measurement uncertainty*

The measurement uncertainty is determined almost entirely by the uncertainty of the fundamental measurements of pressure. In normal operation, the derived Mach number uncertainty should be lower than 0.2%.

3.3   **AIR TEMPERATURE**

3.3.1   **Total air temperature probe**

The TAT probe is exposed in the free air-stream and used to derive static (free air-stream) temperature. The accurate measurement of air temperature is fundamental to the other derived meteorological elements. For example, it is used in the calculation of true airspeed and thus has an impact on the calculation of the wind velocity components. The ADC corrects the temperature actually measured by the probe using the computed Mach number.

Most commercial aircraft are equipped with TAT probes of the immersion thermometer type. Figure 3.4 shows a typical example. The sensing element is a resistance thermometer. The housing is designed to divert cloud and precipitation hydrometeors from the sensing element, although it has been reported (Lawson and Cooper, 1990) that the sensing element becomes wet in cumulus clouds. However, the main reason for the aerodynamic particle separation is to protect the element against abrasive impacts.

The thermodynamically important part of the housing's design is to achieve for the sampled air a nearly complete adiabatic conversion of its kinetic energy into internal energy. The airspeed has to be reduced to a leftover of a few m/s at the sensor. At this location, the air-stream getting in contact with the sensitive element must have been kept free of heat exchange with the internal walls. That is why all the different kinds of TAT housings are equipped/designed with holes in the walls around the intake flow. These holes produce an aerodynamic sucking effect to curb the
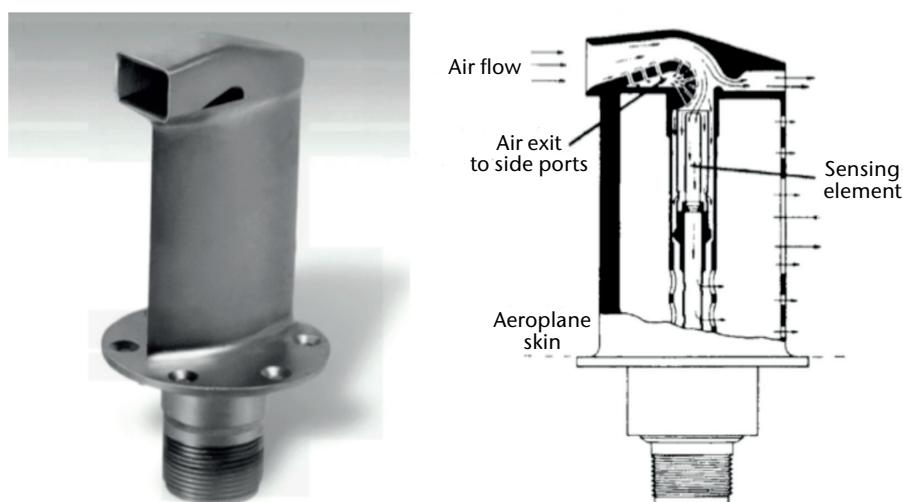
Figure 3.4. Typical example of an aircraft temperature sensor: a total air temperature probe. The internal aerodynamics is designed to make the flow stagnate before touching the sensor. The associated internal boundary-layer is kept small enough and away from the sensor element to enable a pure adiabatic process. The flow's curvature serves for particle separation.

internal boundary layer. As a result, the heat exchange with the wall is kept sufficiently small to maintain accuracy of the measurements. Even if the housing's intake edge is heated for de-icing, the associated increase of the measured temperature is below 0.5 K at $M > 0.3$.

The temperature (T_r) measured by the probe is close to the theoretical value of T_t that would occur with perfect adiabatic compression of the free air-stream at an aerodynamically ideal stagnation point. The static air temperature T_s, which is the temperature of the free air-stream, is related to the measured temperature T_r by the expression (with T as absolute temperature):

$$\frac{T_r}{T_s} = 1 + \lambda \cdot \frac{\kappa - 1}{2} \cdot M^2$$

(3.6)

where λ is the probe recovery factor. Modern TAT probes show typical values of the probe recovery factor around 0.98 for Mach numbers between 0.5 and 0.9. It primarily includes the effect of incomplete stagnation of air and, secondarily, that of a small frictional heat transfer to the flow to be sampled. The value of this coefficient is slightly smaller than 1. It depends on the housing's design but also on the Mach number. At cruise level at Mach 0.85, the probe temperature exceeds the ambient temperature by more than 30 K.

Further details about TAT probes can be found in Stickney et al. (1990).

3.3.1.1 *Measurement uncertainty*

The static temperature is a function of probe temperature and Mach number. As shown above, the Mach number is derived from total pressure and static pressure, themselves independent measurements from the pitot-static head. The uncertainty of measurement is therefore a function of three error sources in addition to calibration uncertainties and other effects (for example, probe de-icing).

The temperature uncertainty is about 0.4 °C at Mach 0.8, reducing to 0.3 °C at low Mach numbers. In the first version of the on-board software standard ARINC 620, the temperature had a resolution of 1 K. Since 1994, it has been specified to be coded in 0.1 K. If the sensor is wetted in cloud, it will be cooled by evaporation leading to additional uncertainties up to 3 °C or so. At very low airspeed (for example prior to take-off) there may be insufficient airflow over the sensor to maintain the accuracy of measurement. Some aircraft employ aspirated sensors to overcome this problem. Normally the on-board software should be configured so that a data transfer does not begin before take-off. Despite the complexity of the data processing involved, operational experience suggests that mean-temperature uncertainty at cruise height is about 1 K.

3.4 **WIND SPEED AND DIRECTION**

The measurement of the three-dimensional wind vector uses data from the aircraft navigation system (the complete combination or a subset of a radio navaid, inertial platform, magnetic compass and GPS system) and the airspeed system (air data computer using pitot-static system plus TAT probe). Using these data, it is possible to calculate to a high degree of accuracy the velocity (V_g) of the aircraft, the ground speed with respect to the Earth and the aircraft velocity with respect to the air (V_a, true airspeed). The wind vector (V), therefore, is given by the vector triangle:

$$\vec{v} = \vec{v}_g - \vec{v}_a$$

(3.7)

The vectors $\vec{v}_g$ and $\vec{v}_a$ must be measured accurately since typical horizontal winds are small

(some 10 m/s) compared with aircraft ground speed and true airspeed (200 to 300 m/s). In early AMDAR systems during long-range navigation the ground speed was derived solely from inertial navigation systems without any support of ground-based navaids or GPS. Sometimes this may have reduced the accuracy of the ground-speed vector and the wind vector by some m/s. This has been improved with modern multi-sensor navigation systems in order to produce operational quality data (Meteorological Service of Canada, 2003). However, the three-dimensional solution of the vector (equation 3.7) needs the measurements of aircraft pitch, roll

X Y Z = Meteorological axes
X' Y' Z' = Aircraft axes

Ψ = Heading
β = Angle of side-slip
α = Angle of attack
θ = Pitch
ϕ = Roll

Air-stream

Air-stream

X, Y Plane

Side

Top

X, Y Plane

Front
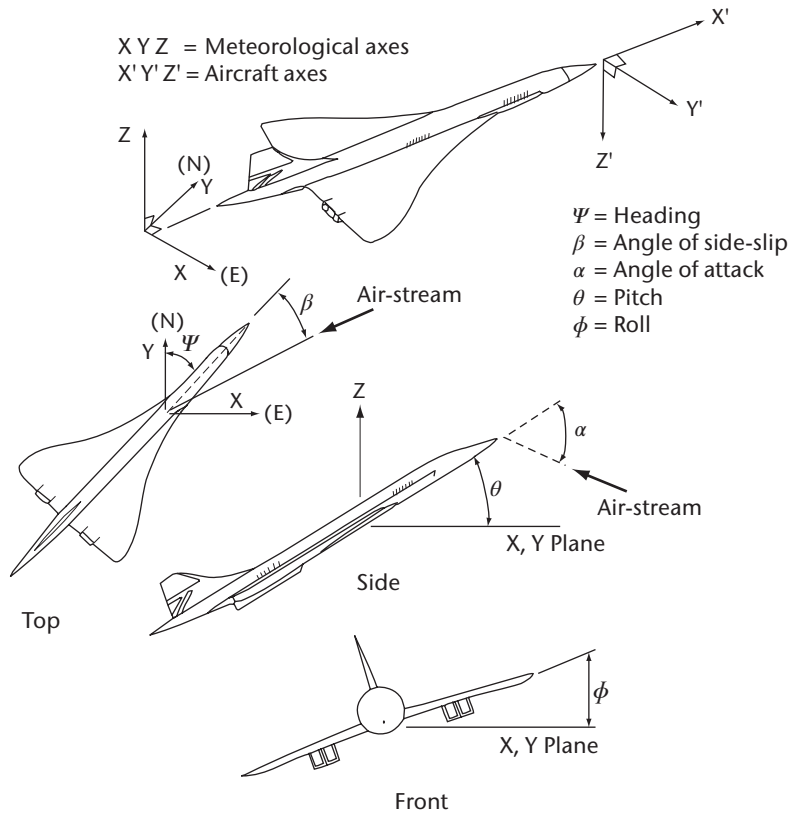
**Figure 3.5. Angles between aircraft and the Earth's coordinate system
as well as the air-stream**

and yaw as well as the angle of attack and side-slip (Figure 3.5). In normal level flight, pitch and roll angle are very small and can be neglected. In the on-board system of a commercial aircraft, the wind vector triangle is only calculated in the X-Y plane of the Earth coordinate system and the angles of attack and side-slip are not measured.

The input data requirement reduces to true airspeed, heading and ground velocity. Heading and ground velocity are taken from the navigation system. True airspeed must be calculated from the Mach number and T_s. The components of the horizontal wind (u, v) are:

$$u = u_g - |\vec{v}_a| \cdot \sin \Psi$$
$$(3.8)$$

$$v = v_g - |\vec{v}_a| \cdot \cos \Psi$$
$$(3.9)$$

where $|\vec{v}_a|$ is the magnitude of the true airspeed; Ψ is the heading relative to true north, positive clockwise; and u_g and v_g are the components of the ground speed.

3.4.1   **Measurement uncertainty**

True airspeed is a function of the Mach number and T_s (SAT in Figure 3.1):

$$|\vec{v}_a| = 38.867 \cdot M \cdot \sqrt{T_s}$$
$$(3.10)$$

$$|\vec{v}_a| = 38.867 \cdot M \cdot \sqrt{\frac{T_r}{1 + 0.194 \cdot M^2}}$$
$$(3.11)$$

Since uncertainties exist in both Mach number and T_s, the total uncertainty of the true airspeed's magnitude is given by:

$$\Delta \left| \vec{v}_a \right| = 38.867 \cdot \Delta M \cdot \sqrt{T_s} + \frac{19.433 \cdot M \cdot \Delta T_s}{\sqrt{T_s}} \tag{3.12}$$

with $\left| \vec{v}_a \right|$ in units of kt; T_s, T_r in units of K; ΔM is the uncertainty of the Mach number; and ΔT_s is the uncertainty of the static temperature.

Note from equation 3.5 that Mach uncertainty depends on the uncertainty of the pressure measurements. Unless gross temperature errors exist, the Mach number uncertainty can be the most significant. For example, with a Mach number uncertainty of 0.2% at cruise level, airspeed uncertainty is some 1 kt (0.5 m/s). Thus, with zero uncertainty from the navigation system, wind vector uncertainty of up to 0.5 m/s is to be expected. Note, however, that gross temperature errors will lead to gross wind errors.

Uncertainty in true airspeed combines with uncertainty from the inertial reference unit. The basic calculations assume perfect alignment of the aircraft with the air-stream (no angle of side-slip) and zero roll and perfect inertial platform alignment. At high roll angles, wind vector uncertainty, which is proportional to true airspeed, can be significant. Roll angles of 10 to 20 degrees imply that the actual angle of attack makes an angular deviation of the true airspeed by a couple of m/s. So, wind data are usually excluded or at least flagged when the roll angle is above a threshold (typically 3 to 5 degrees). At low wind speeds, vector uncertainty can lead to large errors in wind direction. Thus, a more useful indication, considering all of the above uncertainty sources and combining wind speed and direction uncertainty as vector uncertainty, would suggest a typical uncertainty of 4–6 kt (2–3 m/s). These estimates are in line with operational experience (see, e.g., Nash, 1994).

3.5   HUMIDITY

Various sensor principles for the measurement of humidity are in use on research and operational commercial aircraft. The range of technologies covers capacitative-absorption, chilled mirrors and optical methods based on absorption or scattering. The instrument most widely used within AMDAR operations is one based on a tunable diode laser (TDL) (May, 1998; Fleming, 2000, 2003) – the Water Vapor Sensing System (WVSS-II). The TDL absorption spectroscopy technology was originally designed by NASA's Jet Propulsion Laboratory for use on missions to Mars, because it provides high accuracy and extreme stability of measurement over many years. WVSS-II is designed specifically for commercial aviation use in support of AMDAR, using a special relative narrowband absorption method at a suitable infrared line of the water vapour. The intensity of radiation at the detector is related to the emitted radiation by Beer's law such that:

$$I = I_0 \cdot e^{-k\,x\,\rho_w} \tag{3.13}$$

where I is the received signal; I_0 is the emitted signal; k is the mass attenuation coefficient; x is the path length; and ρ_w is the absolute humidity (density of water vapour) in the sensing volume. I_0, k and x are known properties of the system. A local pressure and temperature measurement enables the system to take account of the density of dry air ρ_d. The absorption is scanned over a narrowband of wavelengths around the H_2O line at 1.37 μm. The absolute humidity in the sampling volume is derived by use of the 2f method (May and Webster, 1993). The system's firmware finally converts the raw 2f signal together with coincident temperature and pressure measurements to the proper output parameter, the water vapour mass mixing ratio, m:

$$m = \frac{\rho_w}{\rho_d} \tag{3.14}$$

The sensor system is small enough for a manageable integration on commercial aircraft. Except for during possible phase transitions, m is conserved during the pressure and temperature shift from outside into the sensor probe. The generated value of the mixing ratio is suitable for reporting without knowledge of local pressure and temperature values. This is also convenient in numerical atmospheric models using specific humidity (numerically almost indistinguishable from m) as the input variable.

3.5.1 Measurement uncertainty

Up to 2012, some climate chamber assessments as well as flight tests of this spectrometric humidity measurement system have revealed two features of the instrument's performance: at measurement values above the detection limit of about 4 mg/m³, the relative uncertainty is in the range of ±10%. At an altitude of 200 hPa, the corresponding detection limit in the mixing ratio is 0.02 g/kg (or 30 ppmv). Comparison of this aircraft-based method with contemporary radiosondes (see, e.g., Petersen et al., 2011), shows that the sensor appears to meet WMO observational requirements across all specific humidity and relative humidity ranges, during both ascent and descent.

3.6 TURBULENCE

Turbulence, especially clear-air turbulence (turbulence in the absence of clouds), is an important and potentially dangerous phenomenon in aviation. Although for routine commercial operations flight paths are designed to avoid turbulence, inevitably aircraft will experience unexpected bumpiness and the departure from normal level flight can be measured by the aircraft instrumentation.

3.6.1 Turbulence from vertical acceleration

Vertical acceleration (normal to the aircraft horizontal reference plane) is measured in the inertial reference unit. The data output is referenced and scaled to the acceleration due to gravity and may be categorized as shown in the table. However, the severity of turbulence affecting an aircraft depends principally on airspeed, the mass of the aircraft, the altitude and the nature of the turbulence itself. Hence, reports of turbulence from an aircraft derived from peak acceleration according to the crude relationships given in the table are of limited application and are aircraft-specific because a given gust will have different effects on different aircraft.

Example of coding for the scale of turbulence, defined by peak acceleration

Turbulence category	Peak acceleration[a]	Code
None	Less than 0.15 g	0
Light	0.15 g to, but not including, 0.5 g	1
Moderate	0.5 g to 1.0 g	2
Severe	Greater than 1.0 g	3

a   These accelerations, which may be positive or negative, are departures from the normal acceleration of gravity (1.0 g).

3.6.1.1 *Measurement uncertainty*

There are two main sources of uncertainty in the aircraft instrumentation, namely the "zero", or reference, uncertainty and the output calibration (measurement) uncertainty. For most aircraft, the reference value is nominally +1.0 g, but this can vary typically by 3%. This uncertainty can be virtually eliminated by correction when the aircraft is on the ground, leaving a residual (including measurement) uncertainty of about 3% of measurement (Sherman, 1985).

3.6.2 Derived equivalent vertical gust velocity

An alternative indicator of turbulence is the derived equivalent vertical gust velocity (DEVG), defined as the instantaneous vertical gust velocity, which, superimposed on a steady horizontal wind, would produce the measured acceleration of the aircraft. The effect of a gust on an aircraft

depends on the mass and other characteristics, but these can be taken into account so that a gust velocity can be calculated which is independent of the aircraft. The derived equivalent vertical gust is given (Sherman, 1985) by:

$$U_{de} = \frac{Am\Delta n}{V_c}$$ (3.15)

where U_{de} is the derived equivalent gust velocity; Δn is the modulus of the peak deviation of the aircraft vertical acceleration from 1 g in units of g; m is the total mass; V_c is the calibrated airspeed at the time of the occurrence of the acceleration peak; and A is a parameter that depends on the aircraft type, and weakly on the mass, the altitude and the Mach number.

3.6.2.1 *Measurement uncertainty*

Uncertainties in each of the elements contributing to U_{de} have been estimated. These are typically less than 3% maximum for each element in normal level flight and in the extreme could lead to a total uncertainty of 10% to 12%. Assuming a random distribution of errors, a typical uncertainty would be 3% or 4% of the final value of U_{de}. Aircraft manoeuvres can also lead to large vertical accelerations of an aircraft, and, conversely, active control techniques can dampen the acceleration due to gusts, leading to serious underestimation of vertical gust velocities.

3.6.3 **Eddy dissipation rate**

The eddy dissipation rate, ε, is a parameter that quantifies the turbulence intensity within a fluid. In the context of aircraft turbulence, it is standard practice to refer to $\varepsilon^{1/3}$ as EDR. The advantage of EDR is that it is an aircraft-independent measure of the atmospheric turbulence intensity. There are several ways of estimating EDR (accelerometer-based versus wind-based), and they can be estimated, in principle, along any direction (though usually either vertical or longitudinal (along-track) is used). There are also different spectral models of turbulence that can be used for any of the algorithms:

$$F_v(f) = \frac{9\pi}{55V_t}\,\alpha\,\varepsilon^{2/3}\,L^{5/3}\,\frac{(1+\frac{32}{3}\pi^2 L^2 f^2 / V_t^2)}{(1+4\pi^2 L^2 f^2 / V_t^2)^{11/6}}$$ (3.16)

Equation 3.16 is the von Karman spectral model, where f is the frequency (Hz), V_t is the aircraft true airspeed (m/s), α is an empirical constant (taken here to be 1.6), and L is a length-scale parameter of the turbulence.

$$F_k(f) = \frac{24\pi}{55V_t}\,\alpha\,\varepsilon^{2/3}\left(2\pi f / V_t\right)^{-5/3}$$ (3.17)

Equation 3.17 is the Kolmogorov spectral model, which is just the high-frequency limit of equation 3.16. Both models attempt to describe the frequency power spectrum shape of wind data. The von Karman model better represents the larger scales, especially of the vertical velocity, though it is more complicated and includes the situation-dependent length scale L, in addition to EDR (squared). Research aircraft measurements have shown values of L from about 300 to 2 000 m. For most of the algorithm implementations to date, a mid-range value of 669 m is used.

3.6.3.1 *Vertical accelerometer-based EDR*

This method, described in Cornman et al. (1995), is based on the vertical-acceleration parameter available from the inertial navigation system. For this method, the following relation (Cornman et al., 1995, equation 21) is used:

$$\varepsilon_w^{1/3} = \frac{\hat{\sigma}_{\ddot{z}}}{\left[0.7V_t^{2/3}I(f_l, f_h)\right]^{1/2}}$$ (3.18)

where $\hat{\sigma}_{\ddot{z}}$ is the variance of the bandpass filtered vertical acceleration, I is the integral of the aircraft response bandpass filtered function H, and:

$$I(f_l, f_h) = \int_{f_l}^{f_h} \left| H_{\ddot{z}w}(f) \right|^2 \hat{S}_w(f) df \tag{3.19}$$

where $\hat{S}_w$ is the assumed Kolmogorov spectral model with $\varepsilon = 1$. The von Karman model could be substituted for the Kolmogorov. In the current implementation, f_l (stopband cut-off) and f_h (passband cut-off) are set to 0.1 Hz and 0.8 Hz, respectively. The purpose of the bandpass filter is to remove accelerations that are due to aircraft manoeuvres and wing bending mode frequencies rather than turbulence.

The aircraft response integral is evaluated for a range of flight conditions and stored in look-up tables, thus simplifying and reducing the on-board computation requirement. The algorithm calculates the running root-mean-square of the filtered signal over ten-second windows. At an 8 Hz sampling rate, this provides 480 EDR estimates per minute, from which the median and 90th percentile (referred to as the "peak") of these estimates are used for downlink. The EDR measurement results are converted into reporting numbers by use of tables which are far more detailed than that given in section 3.6.1. Extensive descriptions of these tables are given in the *Aircraft Meteorological Data Relay (AMDAR) Reference Manual* (WMO, 2003).

3.6.3.2 *Vertical wind-based EDR*

This technique is briefly outlined in Cornman et al. (2004). The main idea is to compute the vertical winds directly, and then estimate the EDR from those calculations. This method has the advantage of not requiring the aircraft response function, which is difficult to obtain due to its proprietary nature.

$$w = V_T \left(\sin \alpha_b \cos \theta \cos \varphi - \cos \alpha_b \sin \theta \right) - \dot{Z} \tag{3.20}$$

The above equation is used to compute the vertical winds, where α_b is the body-axis angle of attack, θ is the pitch angle, φ is the roll angle, and $\dot{Z}$ is the inertial vertical velocity. EDR is computed by:

$$\hat{\varepsilon}^{1/3} = \left[\frac{1}{k_h - k_l + 1} \sum_{k=k_l}^{k_h} \frac{S^w(k)}{\hat{S}_w(k)} \right]^{1/2} \tag{3.21}$$

where k_l and k_h are index bounds corresponding to frequency bounds of 0.5 and 3.5 Hz (respectively) for the current 8 Hz implementations, S^w is the power spectrum of w (equation 3.20) after time-series processing, and $\hat{S}_w$ is the assumed von Karman spectral model with $\varepsilon = 1$, modified to account for various signal processing artefacts in S^w.

Nominally, the algorithm calculates EDR ($\varepsilon^{1/3}$) over ten-second windows, every five seconds. This provides 12 EDR estimates per minute, from which the actual mean and peak of these estimates are used for downlink. The mean and peak EDRs, along with quality-control metrics, are converted into reporting numbers by use of encoding (see section 5.3.13.5 in ARINC, 2012). The reported precision of both the mean and peak EDR is 0.02, significantly higher than in the accelerometer-based method.

3.6.3.3 *True airspeed-based EDR*

This technique is similar to the vertical wind-based EDR (section 3.6.3.2) except that the spectral models are slightly different and true airspeed is used in place of w. The advantage of this method is that it is simpler to implement, requiring only one parameter. The disadvantage is that it estimates EDR mainly in the direction along the track, which has much less impact on the aircraft than from turbulence in the vertical direction.

3.6.3.4 *Measurement uncertainty*

As for DEVG, in the EDR there are potentially a large number of sources contributing to measurement uncertainty. Based on the analysis for DEVG, in the accelerometer-based method an uncertainty of some 5% to 10% can be expected for the mean, and somewhat larger for the peak. Based on simulations, similar performance is expected from the other EDR algorithms. A further complication arises over the choices of sampling interval and averaging time. Examination of typical time series of vertical acceleration data often indicates high variability of statistical properties over short distances. Variation of airspeed for a single aircraft alters the sampling distances.

3.6.3.5 *Relationship between EDR and DEVG*

Detailed field comparisons (Stickland, 1998) have been made between the accelerometer-based EDR and DEVG. These have shown a high correlation between peak EDR and DEVG for the same turbulence incidents. This result should be expected since the accelerometer-based EDR is directly proportional to the standard deviation of vertical acceleration over the measurement interval chosen. Hence, for a "normal" distribution, the extreme value will correlate closely with the peak vertical gust (proportional to the peak deviation of vertical acceleration). Clearly, this relationship will not apply to a singular event falling outside the assumed distribution, and the EDR filter cut-off at 0.8 Hz might well unduly attenuate very sharp gust events. For the vertical wind- and true airspeed-based methods, little filtering is applied, and it is not significantly susceptible to this last issue.

3.7 ICING

Several types of sensors may detect ice build-up on the flying surfaces. The following two types are in use:

(a) A thin-film capacitive sensor attached to the airfoil;

(b) A mechanical (vibrating-transducer) sensor exposed to the air-stream in a probe adjacent to the relevant flying surface.

3.7.1 Measurement uncertainty

The output of both sensors is essentially an "ice/no ice" signal, and uncertainty would be described by false-alarm rate. At present, no data are available on false-alarm rates for these sensors.

3.8 AIRCRAFT-BASED OBSERVING SYSTEMS

There are a number of operational aircraft-based observing systems in current operation. AMDAR is currently the major source of aircraft-based observations on the Global Telecommunication System; however, additional observations derived from other aircraft-based observing systems contribute significantly and are expected to provide increased data volumes in the future.

A number of AMDAR-like systems either have or are being developed which will improve global coverage and increase the number of observations in the boundary layer and lower troposphere. Some emphasis is being placed on recruiting smaller regional and general aviation aircraft to install either conventional AMDAR systems or dedicated sensor and communication systems. These aircraft operate from smaller airports that are not normally covered by existing AMDAR-reporting aircraft from airlines participating in national and regional AMDAR programmes.

3.8.1 Aircraft meteorological data relay

The AMDAR observing system should be operated according to WMO specification and standards (WMO, 2013). AMDAR is currently based and relies almost exclusively upon the Aircraft Communications Addressing and Reporting System (ACARS). AMDAR systems report data in profile (ascent/descent) mode as well as during level flight at cruise altitude.

For additional information on the regulatory requirements for establishment and operation of an AMDAR programme and the provision of other aircraft-based observations, consult the WMO *Manual on the Global Observing System*, Part III, 2.5 (WMO, 2010*a*), and the WMO *Guide to the Global Observing System*, Part III, 3.4 (WMO, 2010*b*).

For current information on operational AMDAR programmes and additional resource and guidance material, refer to the WMO AMDAR website: http://www.wmo.int/amdar.

3.8.2 Tropospheric Airborne Meteorological Data Reporting

3.8.2.1 *TAMDAR overview*

Tropospheric Airborne Meteorological Data Reporting (TAMDAR) is a commercially developed, deployed and operated system that derives and sells meteorological data derived from the predominantly aircraft-independent sensing and communications probe. Unlike in the WMO AMDAR observing system, in the TAMDAR system emphasis has been placed on equipping primarily regional carriers, as these flights tend to (i) fly into more remote and diverse locations, and (ii) be of shorter duration, thereby producing more daily vertical profiles and remaining in the boundary layer for longer periods. Although TAMDAR is fully functional and regularly operates above 40 000 ft, the aircraft that typically host the sensor often cruise below 25 000 ft.

TAMDAR collects measurements of relative humidity (RH), pressure, temperature, winds, icing and turbulence, along with the corresponding location, time and geometric altitude from a built-in GPS. These data are relayed via satellite in real time to a ground-based network operations centre, where in-line quality control procedures are performed prior to distribution. The overall humidity and temperature data quality is similar to that of radiosondes (Gao et al., 2012). The wind observations are derived in a similar fashion as typical AMDAR winds, using aircraft heading, true airspeed, and the ground track vector, which is provided by the internal GPS unit.

The TAMDAR sensor samples on a pressure-based interval on ascent and descent, and a time-based interval in cruise, which also varies with altitude from 3 min at lower altitudes to 7 min at higher altitudes. At present, on ascent and descent, the sensor reports every 10 hPa; however, this can be adjusted remotely in real time down to 1 hPa (~30 ft) depending on the rate of ascent and descent. During cruise, if any metric changes above a set threshold, the sensor will send a custom report, so turbulent flights through the cloud tops will generate far more observations than a higher-altitude cruise in clear skies.

3.8.2.2 *Relative humidity and temperature*

TAMDAR uses two capacitive sensing devices for redundancy to measure RH. The fundamental physical parameter that the TAMDAR capacitive sensor technology responds to is the density of H_2O molecules. RH is a derived parameter, which takes into account temperature and pressure. A custom hydrophobic membrane filter has been added to the devices, which significantly increases the reliability and accuracy by preventing direct wetting of the sensor element (see Mulally and Braid, 2009).

The reported RH value is a "consensus" value between the two devices that is determined by an algorithm in the ground processing system described in Anderson (2006). The system considers the value and quality of each sensor output. Typically, if both sensors are reporting similar values,

the consensus value is simply the average of the two. If the sensors disagree by more than 5%, and one is determined to be faulty using methods described in Anderson (2006) and Gao et al. (2012), then the errant sensor's value is flagged and not used in the mean RH calculation.

Certain corrections must be applied to the actual RH that the sensor is reporting. The primary corrections are because of the Mach heating and the difference in air pressure between the ambient conditions and the conditions observed by the sensor. The RH for a parcel of air with a given water vapour concentration is a function of both temperature and pressure. There are four major factors that contribute to the uncertainty of the measurement of true RH as is done in TAMDAR:

(a)   The measurement uncertainty of the RH sensor itself (ΔRH);

(b)   The uncertainty of the TAMDAR probe temperature (T_{probe}) measurement – via a platinum resistance temperature device;

(c)   The measurement uncertainty of the calculated static air temperature (T_{static});

(d)   The measurement uncertainty of the ratio of the static pressure (P_{static}) to the RH sensor pressure (P_{probe}).

The basic calculation necessary for static RH is described by:

$$RH_{static} = RH_{probe} \left(\frac{P_{static}}{P_{probe}} \right) \cdot \left(\frac{e_{s_{probe}}(T_{probe})}{e_{s_{static}}(T_{static})} \right) \qquad (3.22)$$

where RH_{static} is the atmospheric RH, RH_{probe} is the actual RH measurement from the RH sensor in the TAMDAR probe, P_{static} is the static air pressure, P_{probe} is the air pressure at the RH sensor in the probe, T_{probe} is the temperature in the probe sensing cavity, T_{static} is the static air temperature, $e_{s,probe}$ is the probe saturation vapour pressure relative to water, and $e_{s,static}$ is the static saturation vapour pressure relative to water. The saturation pressure ratio is strictly a function of T_{probe} and T_{static} as shown above. The calculation for the pressure ratio (P_{static}/P_{probe}) has been derived from data from extensive wind tunnel testing (see Braid et al., 2011; Smith et al., 2012).

The relationship between T_{probe} (essentially the recovered temperature) and T_{static} is:

$$T_{probe} = T_{static}(1 + \lambda \cdot M^2) \qquad (3.23)$$

where M is the Mach number and λ is a constant approximately equal to 0.17. The actual RH sensor measurement is the true value plus a sensor uncertainty, ΔRH, thus:

$$RH_{probe} = RH_{true} + \Delta RH \qquad (3.24)$$

Substituting equation 3.24 into equation 3.22 illustrates an issue that needs consideration when using the RH method. As the Mach number increases and the temperature decreases, the saturation pressure ratio ($e_{s,probe}/e_{s,static}$) in equation 3.22 increases rapidly, and, as a result, the effect of the sensor uncertainty, ΔRH, is amplified. The ground processing system estimates the error in the RH based on temperature and Mach. This is used along with the known accuracy of the RH sensor and the temperature accuracies to calculate an overall RH uncertainty, which is reported along with the RH.

The range of RH that will be experienced by the RH sensor is also reduced due to the Mach heating. At high speeds, the RH internal to the probe will generally be less than 10% due to the Mach heating of the air. This effect is addressed in TAMDAR by the calibration process. Each RH sensor is characterized over several RH and temperature conditions. Values are specifically chosen at conditions which are error prone, in particular cold, dry conditions. This calibration process results in an RH measurement capability that is useful even at high altitudes. It should be mentioned that one effect of Mach heating is beneficial. Since the response of the capacitive sensor slows down as temperature decreases, the Mach heating effect keeps the RH sensor significantly warmer than ambient, resulting in a response time much faster than otherwise.

3.8.2.3   *TAMDAR icing detection*

The TAMDAR sensor detects icing using two light-emitting diode (LED) and photo detector (PD) pairs, each having an associated analogue-to-digital converted (AtDC) voltage output value. When a TAMDAR sensor encounters conditions where icing is present, ice accumulates on the surface of the foil gap in the area between the LED/PD pairs. As the thickness of the ice increases, the infrared beams become obscured, dropping the AtDC values of the LED/PD pairs below half of the nominal unblocked value, which results in a positive icing indication within the TAMDAR sensor. Once the detection of ice is confirmed via algorithms that verify consistency of the event with current environmental conditions (that is, T and RH), the TAMDAR probe heaters are automatically activated to remove the ice. This process continues until the PD voltage values are greater than half the nominal unblocked value.

All icing events experienced by TAMDAR are tracked in the data stream with the use of icing flags. These flags track the initiation of the icing event, the time at which the heaters were activated, the period of continued icing, the probe cool-down, and when icing is no longer present. The AtDC values of the LED/PD pairs, which are used to detect the presence or absence of icing, are used to calculate TAMDAR liquid water content (LWC). The resulting rate of change in the TAMDAR AtDC voltage output is used to calculate accretion rate, and this is the basis for obtaining LWC values. The temporal drop rate of AtDC values is used to calculate the icing intensity or accretion rate.

3.8.2.4   *TAMDAR turbulence detection*

Turbulence is reported as an eddy dissipation rate and is based on true airspeed (TAS) samples which are calculated from the TAMDAR pitot and static port pressures and the TAMDAR temperature. The report includes the mean and peak EDR, and the time of peak for each one minute period. The EDR turbulence algorithm is independent of aircraft configuration and flight condition. Thus, it does not depend on the type of aircraft or on load and flight capacity.

The TAMDAR methodology utilizes an estimate of the longitudinal wind via the TAS parameter to calculate EDR. TAMDAR can obtain TAS via two sources: (i) from the TAMDAR static and pitot pressure sensor measurements or (ii) from the aircraft's ARINC 429 databus. Once the system takes a measurement of the differential pressure between the pitot and static pressure, the measure is then passed through a filter before TAS is calculated.

The MacCready method is used to estimate the EDR based on the expected –5/3 power spectra slope from the Kolmogorov model of the TAS signal. The filtering of the differential pressure sensor uses a low-pass Butterworth anti-alias filter, with 4th order 5 Hz 3 decibel cut-off frequencies. Windowing is completed prior to fast Fourier transformation (FFT) to make the measurement more spectral (64 point FFT). An EDR is calculated every 3 s using a 6 s block of 10.67 Hz TAS data. EDR values can be averaged if desired for a smoother result; normally a 6 s average is used, but users have the ability to configure this averaging to match their needs. A quality assurance filter is also employed.

3.9   OTHER SYSTEMS AND SOURCES OF AIRCRAFT-BASED OBSERVATIONS

3.9.1   ICAO Automatic Dependent Surveillance

The development of global air navigation systems is closely linked to developments in communication systems. Thus, the Future Air Navigation System (FANS) is coupled with the development of an Automatic Dependent Surveillance (ADS) system which itself is dependent on global satellite aircraft communication. The global aircraft communication system is migrating to an open network under the Aeronautical Telecommunication Network project (Wells et al., 1990). This will link the VHF and Satcom Systems into a common open network.

The successful weather routing of commercial aircraft, especially to provide flight safety, minimize fuel consumption and airframe fatigue, and to ensure passenger comfort, demands greater accuracy in aviation forecasts. Hence, automatic reports of aircraft position for ADS allow for the inclusion of automated meteorological reports. The data to be included in these reports are essentially the same as those of current AMDAR systems including allowance for turbulence and humidity elements.

Data derived from the ICAO ADS contract (ADS-C) system are being transmitted on the WMO Global Telecommunication System. These data are made available through the arrangement established with ICAO as set out in ICAO Annex 3 to the Convention on International Civil Aviation, *Meteorological Service for International Air Navigation*, Chapter 5 and Appendix 4. ICAO regulations stipulate that air traffic management centres are to transmit the ADS-C messages to the World Area Forecast Centres (WAFCs), which are then responsible for transmission of the data on the Global Telecommunication System (see *Procedures for Air Navigation Services – Air Traffic Management*, ICAO Doc. 4444, 4.11.4).

3.9.2   New and developing systems

3.9.2.1   *Mode-S Enhanced Surveillance*

Wind and temperature observations can also be inferred from surveillance data gathered for air traffic control (ATC) purposes using a Mode-S(elective) Enhanced Surveillance (EHS) radar. This radar interrogates every aircraft for specific information at a frequency rate of 4 to 20 s, depending on the ATC purposes of the radar. In designated airspace, all aircraft are obliged to respond to the interrogation by the Mode-S EHS radar. The mandatory registers (BDS4,0, BDS5,0 and BDS6,0) contain information on aircraft identity, flight level, roll angle, magnetic heading, airspeed, Mach number and ground track. Position of the aircraft can be obtained either from the ATC radar or from the Automatic Dependent Surveillance Broadcast (ADS-B) data which are transmitted continuously by the aircraft.

The derivation of wind from Mode-S EHS is similar to AMDAR, except that the true heading has to be determined from the magnetic heading. Besides applying a magnetic variance table, additional aircraft-dependent corrections need to be applied. Heading corrections may change with time due to maintenance of the aircraft. At present these corrections are determined for every aircraft based on comparison with numerical weather prediction (NWP) data. Next to the heading correction, an airspeed correction is applied also based on long-term comparison with NWP data (see de Haan, 2013). After corrections and quality control, the derived wind information is of similar quality as from AMDAR (de Haan, 2011, 2013). The derivation of temperature from Mode-S EHS observations is done by combining the Mach number and the airspeed. The quality of the derived temperature is hampered by the reported resolution of the Mach number and airspeed, and is clearly of less quality than AMDAR temperature (de Haan, 2011, 2013).

3.9.2.2   *Mode-S Meteorological Routine Air Report*

A Mode-S EHS radar can also interrogate non-mandatory registers which may contain meteorological information. An example is the Mode-S EHS BDS4,4 register, called Meteorological Routine Air Report (MRAR). This register contains direct wind and temperature information which is very close to the AMDAR wind and temperature information (Stranjar, 2012). Since the register BDS4,4 is not mandatory, only a fraction (about 5%) of the aircraft respond to the request with valuable meteorological information.

REFERENCES AND FURTHER READING

Abbott, I.H. and A.E. von Doenhoff, 1959: *Theory of Wing Sections*. Dover Publications, Inc., Mineola, New York, 693 pp.

AirDat, 2003: *TAMDAR – Tropospheric Airborne Meteorological Data Reporting Sensor and System Overview; AirDat Infrastructure and Global Capabilities*. Information document, AirDat LLC, Evergreen, Colorado.

Anderson, A.K., 2006: *AirDat system for ensuring TAMDAR data quality*. Tenth Symposium on Integrated Observing and Assimilation Systems for the Atmosphere, Oceans, and Land Surface (IOAS-AOLS), American Meteorological Society, Atlanta, GA.

ARINC, 2012: *620-7 Data Link Ground System Standard and Interface Specification*. Aeronautical Radio, Inc., Annapolis, Maryland.

Benjamin, S.G., B.D. Jamison, W.R. Moninger, S.R. Sahm, B.E. Schwartz and T.W. Schlatter, 2010: Relative short-range forecast impact from aircraft, profiler, radiosonde, VAD, GPS-PW, METAR, and Mesonet observations via the RUC hourly assimilation cycle. *Monthly Weather Review*, 138:1319–1343.

Braid, J., P. Van Wie and J. Rex, 2011: Using the TAMDAR sensor for in-flight ice detection and improved safety of flight. *SAE Technical Paper 2011-38-0051*, International Conference on Aircraft and Engine Icing and Ground Deicing, Society of Automotive Engineers.

Cornman, L.B., G. Meymaris and M. Limber, 2004: *An update on the FAA Aviation Weather Research Program's in situ turbulence measurement and reporting system*. Eleventh Conference on Aviation, Range and Aerospace Meteorology, Hyannis, MA.

Cornman, L.B., C.S. Morse and G. Cunning, 1995: Real-time estimation of atmospheric turbulence severity from in situ aircraft measurements. *Journal of Aircraft*, 32(1):171–177.

Dommasch, D.O., S.S. Sherby and T.F. Connolly, 1958: *Airplane Aerodynamics.* New York, Pitman, 560 pp.

Fleming, R.J., 2000: Water vapor measurements from commercial aircraft: Progress and plans. *Preprints*. Fourth Symposium on Integrated Observing Systems, Long Beach, CA, American Meteorological Society, 30–33.

———, 2003: The WVSS-II and the UCAR air sampler: Purpose, design, status (personal communication). University Corporation for Atmospheric Research, Boulder, Colorado.

Gao, F., X.Y. Zhang, N.A. Jacobs, X.-Y. Huang, X. Zhang and P.P. Childs, 2012: Estimation of TAMDAR observational error and assimilation experiments. *Weather and Forecasting*, 27:856–877.

Haan, S. de, 2011: High-resolution wind and temperature observations from aircraft tracked by Mode-S air traffic control radar. *Journal of Geophysical Research*, 116(D10111).

———, 2013: *An Improved Correction Method for High Quality Wind and Temperature Observations Derived from Mode-S EHS*. KNMI Technical Report No. TR-338, De Bilt.

International Civil Aviation Organization (ICAO), 2007: *Procedures for Air Navigation Services – Air Traffic Management*. Fifteenth edition, Doc 4444, Montreal.

———, 2013: *Meteorological Service for International Air Navigation*. ICAO Annex 3, Eighteenth edition, Amendment 76, Montreal.

International Organization for Standardization (ISO), 2007: *Standard Atmosphere*, ISO 2533:1975 (with two additions in 1985 and 1997, reviewed and confirmed in 2007). Geneva.

Lawson, R.P. and W.A. Cooper, 1990: Performance of some airborne thermometers in clouds. *Journal of Atmospheric and Oceanic Technology*, 7:480–494.

May, R.D., 1998: Open-path, near-infrared tuneable diode laser spectrometer for atmospheric measurements of H_2O. *Journal of Geophysical Research*, 103:19161–19172.

May, R.D. and C.R. Webster, 1993: Data processing and calibration for tuneable diode laser harmonic absorption spectrometers. *Journal of Quantitative Spectroscopy and Radiative Transfer*, 49(4):335–347.

Meteorological Service of Canada, 2003: *The Effect of Pitch and Roll Attitude on the Calculation of Wind* (G. Bruce). Aeromechanical Services Ltd., 1118-1c, Rev. 1.0.

Moninger, W.R., S.G. Benjamin, B.D. Jamison, T.W. Schlatter, T.L. Smith and E.J. Szoke, 2010: Evaluation of regional aircraft observations using TAMDAR. *Weather and Forecasting*, 25:627–645.

Mulally, D.J. and J.T. Braid, 2009: *The TAMDAR Sensor's Relative Humidity Performance on ERJ-145 Commercial Aircraft*. Thirteenth Symposium on Integrated Observing and Assimilation Systems for the Atmosphere, Oceans, and Land Surface (IOAS-AOLS), American Meteorological Society, Phoenix, AZ.

Nash, J., 1994: Upper wind observing systems used for meteorological operations. *Annales Geophysicae*, 12:691–710.

Petersen, R.A., L. Cronce, W. Feltz, E. Olson and D. Helms, 2011: *Validation Studies of WVSS-II Moisture Observations*. Fifteenth Symposium on Integrated Observing and Assimilation Systems for the Atmosphere, Oceans, and Land Surface (IOAS-AOLS), American Meteorological Society, Seattle, WA.

Rodi, A.R. and P.A. Spyer-Duran, 1972: Analysis of time response of airborne temperature sensors. *Journal of Applied Meteorology*, 11:554–556.

Sherman, D.J., 1985: *The Australian Implementation of AMDAR/ACARS and the Use of Derived Equivalent Gust Velocity as a Turbulence Indicator*. Structures Report No. 418, Department of Defence, Defence Science and Technology Organisation, Aeronautical Research Laboratories, Melbourne, Victoria.

Smith, W.L., P. Minnis, C. Fleeger, D. Spangenberg, R. Palikonda and L. Nguyen, 2012: Determining the flight icing threat to aircraft with single-layer cloud parameters derived from operational satellite data. *Journal of Applied Meteorology and Climatology*, 51:1794–1810.

Stickland, J.J., 1998: *An Assessment of Two Algorithms for Automatic Measurement and Reporting of Turbulence from Commercial Public Transport Aircraft*. A report to the ICAO METLINK Study Group. Observations and Engineering Branch, Bureau of Meteorology, Melbourne.

Stickney, T.M., M.W. Shedlov, D.I. Thompson, 1990: *Rosemount Total Temperature Sensors*. Technical Report 5755, Revision B, Rosemount Inc.

Strajnar, B., 2012: Validation of Mode-S Meteorological Routine Air Report aircraft observations. *Journal of Geophysical Research: Atmospheres*, 117(D23).

Wells, V.E. et al., 1990: Migration of ACARS to the Aeronautical Telecommunication Network. *Proceedings of the Aeronautical Telecommunications Symposium on Data Link Integration*, Annapolis, Maryland.

World Meteorological Organization, 2003: *Aircraft Meteorological Data Relay (AMDAR) Reference Manual* (WMO-No. 958). Geneva.

———, 2010*a*: *Manual on the Global Observing System* (WMO-No. 544), Volume I. Geneva.

———, 2010*b*: *Guide to the Global Observing System* (WMO-No. 488). Geneva.

———, 2011: *Manual on Codes* (WMO-No. 306), Volume I.1. Geneva.

———, 2013: *AMDAR Onboard Software Functional Requirements Specification*. Instruments and Observing Methods Report No. 114. Geneva.

————————

CHAPTER CONTENTS

CHAPTER 4. MARINE OBSERVATIONS

4.1 GENERAL

Marine observations in the broadest definition cover any meteorological and related environmental observations at the air–sea interface, below the sea surface and in the air above the sea surface. Observations can be made using fixed or moving platforms, and be in situ or remote, using surface- or space-based techniques. In situ measurements are essentially single-point observations intended to be representative of the surrounding sea area, as for synoptic meteorology. Remote-sensing techniques lead to large area or volume representation, which is particularly appropriate for observations of sea ice.

This chapter discusses observations at the air–sea interface made in situ, which include the usual surface parameters that are also measured over land and discussed in that context in Part I of this Guide. This chapter also considers other observations of importance to marine physics and physical oceanography, including: sea-surface temperature; ocean waves; sea ice, icebergs and ice accretion; and salinity. Upper-air measurements are taken using techniques that are essentially the same over the sea and over land.

Detailed formal requirements for observations from sea stations are given in the *Manual on the Global Observing System* (WMO, 2010, 2011*a*). Advice on requirements and procedures is given in the *Guide to Marine Meteorological Services* (WMO, 2001). In situ marine measurements or observations are made from a variety of platforms. They include ships recruited by WMO Members to participate in the Voluntary Observing Ship (VOS) Scheme, manned and unmanned light vessels, moored buoys, drifting buoys, towers, oil and gas platforms and rigs, island automatic weather stations (AWS), and ship-borne AWS systems. The type of platform generally determines the range of elements measured and reported. Thus, ships of the VOS, using both measured and manual observation techniques, report the full range of observations required for synoptic meteorology. By contrast, the majority of drifting buoys report only up to three parameters, namely, position, atmospheric pressure at sea surface, and sea-surface temperature (SST). Observations from voluntary observing ships are most commonly compiled and transmitted to shore in a nationally agreed ship-to-shore transmission format, and then distributed internationally in appropriate WMO codes (for example, FM 94 BUFR as of approximately 2012). WMO codes are documented in the *Manual on Codes* (WMO, 2011*b*, 2011*c*); general information is found in Volume I.2, Part B, and templates specific to particular types of marine observations, such as the B/C10 template for SHIP reports, are documented in Volume I.2, Part C.[1] Further information can be found in the proceedings of a 2009 meeting on the ocean observing system (Hall et al., 2010), including information on VOS (Kent et al., 2010), research vessels (Smith et al., 2010), ship-based oceanographic measurements (Goni et al., 2010), profiling floats (Freeland et al., 2010), buoys (Meldrum et al., 2010; McPhaden et al., 2010; Send et al., 2010; Dohan et al., 2010; Keeley et al., 2010), and waves and sea-level (Swail et al., 2010*a*; Swail et al., 2010*b*; Merrifield et al., 2010).

On the recommendation of the Joint WMO/IOC Technical Commission for Oceanography and Marine Meteorology (JCOMM), a network of WMO/Intergovernmental Oceanographic Commission (IOC) Regional Marine Instrument Centres (RMICs) has been set up to facilitate adherence of observational data, metadata, and processed observational products to higher level standards for instruments and methods of observation, by providing (i) facilities for the calibration and maintenance of marine instruments and the monitoring of instrument performance; and (ii) assistance for instrument intercomparisons, as well as appropriate training facilities complementing what the manufacturers are also providing. Their terms of reference and locations are given in Annex 4.A.

---

[1] The *Manual on Codes*, Volume I.1 also presently describes the traditional alphanumeric codes (TAC) that have been used to circulate data for many years over the Global Telecommunication System (GTS), principally in the VOS context referring to the FM 13 SHIP code. WMO, however, is in the process of fully discontinuing the TAC for GTS transmission. Therefore, the *Manual on Codes* may in the future be restructured to omit the first volume altogether.

4.2   **OBSERVATIONS FROM SHIPS**

This section contains detailed guidance and advice for taking measurements and making observations on ships. Reference WMO (1991*a*) is another source. Details on surface observations to be carried out within the framework of the WMO VOS Scheme are provided in WMO (2001), Chapter 6. WMO (2001) also includes information on the different classes of VOS. Studies of the quality of observations from ships are given in WMO (1991*b*, 1999), Kent et al. (1993), WMO/IOC (2003*a*, 2003*b*), Kent and Berry (2005), Ingleby (2010), and Kennedy et al. (2012). A discussion of good observing practice from the research community is presented by Bradley and Fairall (2006) and information on sensors used in the marine environment by Weller et al. (2008).

4.2.1   **Operation of the WMO Voluntary Observing Ship Scheme**

The VOS Scheme is operated by National Meteorological and Hydrological Services (NMHSs) under the guidance of the JCOMM Ship Observations Team (SOT) and in particular the SOT VOS Panel (VOSP). Full information on the VOS Scheme is given in WMO (2001). VOS Programme Managers work with Port Meteorological Officers (PMOs) who typically act as the link between the VOS operator and the ship. An essential first step in recruiting VOS is to obtain the permission of the owners and master of the vessel. When permission has been granted and the ship has been identified, PMOs should do the following:

(a)   Install calibrated instruments ensuring best exposure;

(b)   Issue stationery or install electronic logbook software;

(c)   Train observers on instrument care and operation;

(d)   Train observers in all aspects of observing practices;

(e)   Demonstrate use of electronic logbook software and compilation of the observation;

(f)   Record the required ship metadata as required for WMO (1955–);

(g)   Demonstrate methods of report transmission;

(h)   Explain NMHS marine forecast products.

Once a ship has been recruited, the PMO should ideally endeavour to visit it at least every three months (subject to shipping movements and staff resources; if not practicable, less frequent visits can be considered) to check the accuracy of the instruments and renew the supply of forms, documents and so on. Automatic weather stations and digital sensors may allow a longer checking period of one year. The PMO should take the opportunity to foster interest in meteorology and explain the mutual value to seafarers and meteorologists of accurate weather observations.

In some instances, a company (usually oil or gas) operating a ship or platform takes observations/measurements for its own use and makes them available on the GTS without much participation from a PMO. The installation, maintenance and training on the metocean equipment may be done under contract. In cases where the vessel/station was not recruited by a PMO, efforts should be made to ensure that the relevant metadata are made available through the appropriate WMO channels.

4.2.2   **Voluntary Observing Ship observations**

4.2.2.1   *Elements observed*

Ships participating in the VOS[2] Scheme undertaking meteorological observations should ideally observe the following elements:

(a)   Ship position (from ship's navigation system);

(b)   Ship course and speed (from ship's navigation system);

(c)   Wind speed and direction (measured or visually estimated);

(d)   Atmospheric pressure (measured);

(e)   Pressure tendency and its characteristics (measured or estimated from barograph trace);

(f)   Air temperature (measured);

(g)   Humidity (measured);

(h)   Sea-surface temperature (measured);

(i)   Present and past weather, and weather phenomena (visually estimated);

(j)   Cloud amount, type and base height (visually estimated);

(k)   Precipitation (often visually estimated);

(l)   Visibility (visually estimated);

(m)   Ocean wind waves and swell, including height, period and direction (often visually estimated);

(n)   Sea ice (often visually estimated) and/or ice accretion (often visually estimated) on board ship, when appropriate;

(o)   Special phenomena (visually estimated).

Some specially equipped ships, for example research or light vessels, may make instrumentally measured observations and reports of precipitation, radiation, visibility, cloud parameters or wave parameters.

In general, instrumental observations requiring the use of a light at night should be ideally made after non-instrumental ones, so that the observer's eyes can adapt to the darkness without being impaired.

4.2.2.2   *Equipment required*

The following instruments are suitable for use on ships:

(a)   A precision aneroid, dial aneroid or electronic digital barometer (Part I, Chapter 3);

(b)   A barograph, preferably open scale (desirable but not mandated) or a digital barometer that includes a barometric tendency trace (Part I, Chapter 3);

---

[2]   http://www.bom.gov.au/jcomm/vos/resources.html

(c)   A liquid-in-glass (mercury[3] or alcohol) or electrical resistance thermometer (Part I, Chapter 2);

(d)   A hygrometer or psychrometer (Part I, Chapter 4);

(e)   A sea-temperature thermometer and suitable receptacle for obtaining a sample of seawater, or a continuously immersed sensor or hull contact sensor with remote indicator.

The use of anemometers with suitable exposure as an alternative to the visual estimation of wind force is encouraged, provided that such instruments are routinely checked to ensure that they remain within calibration. Precipitation gauges are rarely provided for use on VOS.

The instruments used on ships should conform to the requirements laid down or recommended in other chapters of this Guide, apart from the modifications described in the following sections of this chapter. Instruments supplied to ships should be regularly tested and inspected by the NMHSs concerned.

4.2.2.3   *Automation of ship observations*

Automatic weather stations or partially automated systems are increasingly being used on observing ships for both observation and data transmission purposes. Three basic modes of operation are used, as follows:

(a)   The observation is made manually, typically entered into an electronic logbook[4] on a computer, coded, as necessary, and formatted for automatic or manually initiated report transmission;

(b)   The observation is made automatically using standard AWS techniques, as described in Part II, Chapter 1. The position, course and speed of a ship are taken from its navigation system or computed independently using a satellite navigation system, usually the Global Positioning System (GPS). The transmission of such observations can be either purely automatic or initiated manually according to the communications facilities;

(c)   The observations making up the marine report are a combination of automated and manual observations, namely, automated observations augmented with visual observations entered by the observer before transmission (i.e. adding visibility, weather codes, cloud amounts, types and heights, wave heights, periods and directions, ice parameters and wind speed and direction where not measured using an anemometer).

4.2.2.4   *Times of observation*

When done manually, the observation of elements other than pressure should be made within 10 min preceding the standard time for the synoptic observation. Atmospheric pressure, however, should be read at the exact time or as close as possible to the standard time.

Surface observations on board ships are typically made as follows:

(a)   Synoptic observations from manually reporting observing ships should be made at main standard times: 0000, 0600, 1200 and 1800 UTC. When additional observations are required, they should be made at one or more of the intermediate standard times: 0300, 0900, 1500 and 2100 UTC;

---

[3]   Advice concerning the safe use of mercury is given in Part I, Chapter 3, 3.2.7. A United Nations Environment Programme (UNEP) convention (the Minamata Convention on Mercury) entered into force in October 2013 and will have a significant impact on the use of mercury for meteorological applications.

[4]   http://sot.jcommops.org/vos/resources.html

(b)   Hourly observations should be made when an automated system is used (using manual input, ship observers may in addition provide complete synoptic observations at synoptic times, including the additional visual elements);

(c)   When operational difficulties on board ships make it impracticable to make the synoptic observation at a main standard time, the actual time of observation should be as near as possible to the main standard times;

(d)   Observations should be made more frequently than at the main standard times whenever storm conditions threaten or prevail;

(e)   When sudden and dangerous weather developments are encountered, observations should be made for immediate transmission without regard to the standard times of observation (for example, within 300 nautical miles of a named tropical system);

(f)   Marine observations are just as valuable in coastal zones as in the open ocean and observations should be continued during the whole journey.

4.2.2.5   *Transmission of ship's observations*

Satellite communication systems are now in widespread use for disseminating ship observations. Details are given in WMO (2001), section 6.6. The following four methods are most commonly used:

(a)   The International Data Collection System through the meteorological geosynchronous (GOES, METEOSAT, MTSAT) satellites. This system, funded mainly by NMHSs, allows for purely automatic data communication at predetermined time slots, once an hour. Data transmission is one-way only and error rates can be significant. It is primarily used in connection with moored buoys but is also used for some shipboard AWS systems;

(b)   Commercial satellite systems through the INMARSAT-C system which is carried by most ocean going ships for compliance with the International Convention for the Safety of Life at Sea (SOLAS) and Global Maritime Distress and Safety System (GMDSS) requirements. Weather observations are normally sent to a suitable Land Earth Station (LES) via a special access code (SAC) 41 message which allows the costs of the report to be borne by the NMHS. A list of the acceptable LESs for SAC messages is maintained on the WMO website at http://www.wmo.int/pages/prog/amp/mmop/inmarsat_les.html. INMARSAT-C has near-global coverage, but very high latitudes are not covered. However, other dedicated SACs are now being set up to allow ship-to-shore messages to be sent in a compressed format, thereby allowing National Meteorological Services to reduce the transmission costs of their national observing fleets. The INMARSAT-C data reporting service is also used for sending compressed meteorological data from certain AWS systems. INMARSAT-C is used by a majority of non-automated manually reporting observing ships;

(c)   Commercial satellite services such as Iridium are increasingly being used for shipboard AWS systems. The Iridium Short Burst Data system using binary formatted messages can significantly reduce transmission costs. Iridium has the advantage of providing global satellite coverage and can also improve data timeliness;

(d)   Service Argos: This system is primarily designed for location as well as data transmission and is limited by the number and the orbital characteristics of the polar-orbiting satellites carrying the Argos payload. The Argos system is used both for the communication and for the processing of ship observations onto the GTS (WMO/IOC, 1995) but there can be several hours of delay, depending on the location of the observing station and the land receiving station. Costs can also be significant when compared to other satellite systems. It is typically used for small drifting buoys, although it is increasingly being replaced by Iridium. A few autonomous shipboard AWS systems also use Argos for data transmission.

4.2.2.6   *Wind*

Observations of wind speed and direction may be made either by visual estimates or by means of anemometers or anemographs. Winds should be measured only if using a well-maintained and recently calibrated instrument sited in a well-exposed location away from the influence of the superstructure, mast and spars. Reports of wind speed can be recorded in either knots or m s^{-1}; reporting in knots is preferred if the data are to be transmitted from the ship in a format not allowing the recording of tenths.

4.2.2.6.1   Visual observations

Visual estimates are based on the appearance of the sea surface. The wind speed is obtained by reference to the Beaufort scale (see table below). The Beaufort number obtained by estimation is converted into m s^{-1} or knots by the use of the wind speed equivalent columns of the Beaufort scale, so the wind speed is reported at a specific value in metres per second or knots according to the best estimate of the observer from within those equivalent ranges. National instructions may give guidance on preferred practice. The wind direction is determined by observing the orientation of the crests of wind waves (that is, wind-driven waves, and not swell) or the direction of streaks of foam which are blown in the direction of the wind. The specifications of the Beaufort scale numbers refer to the conditions in the open sea. In practice, wind directions made by visual methods are of good quality.

The wave height in itself is not always a reliable criterion since it depends not only on wind speed, but also on the fetch and duration of the wind, the depth of shallow waters, and the presence of swell running through a sea. The Beaufort scale, therefore, makes use of the relation between the state of the sea and the wind speed. This relation is, however, affected by several other factors which should, in principle, be taken into account in estimating wind speeds. These factors are the lag between the wind increasing and the sea rising, the smoothing or damping down of wind effects on the sea surface by heavy rain, and the effects of strong surface currents (such as tidal currents) on the appearance of the sea. Sea criteria become less reliable in shallow water or when close inshore, owing to the effect of tidal currents and the shelter provided by the land. At these locations, or when the surface of the sea cannot be clearly seen (e.g. at night), the Beaufort force of the relative wind on the ship may be estimated by noting wind effects on sound, on ship-borne objects such as flags, and on funnel smoke. In the latter case, the direction of the relative wind may also be estimated, for example, by observation of the funnel smoke. From these estimates, the speed and direction of the true wind can be computed (United Kingdom Meteorological Office, 1995). If no other means are available to estimate the wind direction, low-level cloud movement can be a helpful tool.

4.2.2.6.2   Measurements with instruments

If instruments for measuring wind are installed on ships, the equipment should give both wind speed and direction and should be capable of minimizing roll effects (suitably designed cup anemometers and damped wind vanes are capable of rendering the effects of pitch and roll insignificant). The marine environment is harsh, so cup or propeller anemometers require regular maintenance and calibration in order to produce reliable wind data. Ultrasonic anemometers have no moving parts, require less maintenance, and are therefore increasingly being used on ships.

Beaufort scale in operational use for WMO reports of estimated wind referenced to 10 m above sea level

Beaufort number (force)	Descriptive term	Mean equivalent wind speed		Wind speed equivalent range		Specifications for observations	Probable height of waves	Probable maximum height of waves
		knots	$m\,s^{-1}$	knots	$m\,s^{-1}$	On board ship (open sea)	m	m
0	Calm	0	0	< 1	0–0.2	Sea like a mirror		
1	Light air	2	0.8	1–3	0.3–1.5	Ripples with the appearance of scales are formed, but without foam crests	0.1	0.1
2	Light breeze	5	2.4	4–6	1.6–3.3	Small wavelets; still short but more pronounced; crests have a glassy appearance and do not break	0.2	0.3
3	Gentle breeze	9	4.3	7–10	3.4–5.4	Large wavelets; crests begin to break; foam of glassy appearance; perhaps scattered white horses	1.6	1.0
4	Moderate breeze	13	6.7	11–16	5.5–7.9	Small waves, becoming longer; fairly frequent white horses	1.0	1.5
5	Fresh breeze	19	9.3	17–21	8.0–10.7	Moderate waves, taking a more pronounced long form; many white horses are formed (chance of some spray)	2.0	2.5
6	Strong breeze	24	12.3	22–27	10.8–13.8	Large waves begin to form; the white foam crests are more extensive everywhere (probably some spray)	3.0	4.0
7	Near gale	30	15.5	28–33	13.9–17.1	Sea heaps up and white foam from breaking waves begins to be blown in streaks along the direction of the wind	4.0	5.5
8	Gale	37	18.9	34–40	17.2–20.7	Moderately high waves of greater length; edges of crests begin to break into the spindrift; the foam is blown in well marked streaks along the direction of the wind	5.5	7.5
9	Strong gale	44	22.6	41–47	20.8–24.4	High waves; dense streaks of foam along the direction of the wind; crests of waves begin to topple, tumble and roll over; spray may affect visibility	7.0	10.0

Beaufort number (force)	Descriptive term	Mean equivalent wind speed		Wind speed equivalent range		Specifications for observations	Probable height of waves	Probable maximum height of waves
		knots	m s⁻¹	knots	m s⁻¹	On board ship (open sea)	m	m
10	Storm	52	26.4	48–55	24.5–28.4	Very high waves with long overhanging crests; the resulting foam, in great patches, is blown in dense white streaks along the direction of the wind; on the whole, the surface of the sea takes a white appearance; the "tumbling" of the sea becomes heavy and shock-like; visibility affected	9.0	12.5
11	Violent storm	60	30.5	56–63	28.5–32.6	Exceptionally high waves (small and medium-sized ships might be for a time lost to view behind the waves); the sea is completely covered with long white patches of foam lying along the direction of the wind; everywhere the edges of the wave crests are blown into froth; visibility affected	11.5	16.0
12	Hurricane	64 and over	32.7 and over	64 and over	32.7 and over	The air is filled with foam and spray; sea completely white with driving spray; visibility very seriously affected	14 and over	–

Note that wave heights are indicated as a guide to show roughly what might be expected in the open sea. These wave heights should never be used for logging or reporting the state of the sea. In enclosed waters, or when near land, with an offshore wind, wave heights will be smaller and the waves steeper.

Source: OMI-CMI (1947)

It is difficult to obtain a good exposure for ship-borne wind instruments (WMO/IOC, 2003*b*; Yelland et al., 2001; Moat et al., 2005; Moat et al., 2006). The local effects produced by the superstructure, mast and spars should be minimized as much as possible by siting the instrument as far forward and as high as practicable. If fitted on a yardarm, it may be preferable that the speed and direction heads should form separate units, as a more even distribution of the weight on the yardarm can be obtained, and it may then be possible to fit the instruments farther outboard. Whether fitted on a yardarm or on a bracket fixed to the foremast, each unit should be mounted in position at a distance of at least 10 mast diameters away from the mast. If this is impracticable, a good technique is to fit two instruments, one on each side of the foremast, and always to use the one which is more freely exposed. The top of the foremast, if available, is generally thought to be the best site for an anemometer. Ultrasonic wind sensors are efficient and provide good accuracy when installed on the top of the main mast.

Various types of portable anemometers are on occasion used at sea (often to assist with ship berthing). Their main disadvantage is that they can hardly be given representative exposure, and, in practice, measurements taken with them show substantial scatter (Kent et al., 1993). Only an observer who understands the nature of the airflow over the ship in different circumstances

would be able to choose the best place for making such observations and thus arrive at satisfactory results. This method may be useful if visual estimates of wind force are difficult or impossible, for example, with light winds at night.

When observations are taken from a moving ship, it is necessary to distinguish between the relative and the true wind; for all meteorological purposes the true wind must be reported (although for VOS Climate (VOSClim) class ships the apparent wind is also reported). The procedure for the calculation of true wind speed and direction from relative wind speed, relative wind direction, ship speed, course and heading is described in detail in WMO/IOC (2003c). It should be noted that the ship's course and the ship's heading may be significantly different particularly at low ship speeds or with large leeway. A simple vector diagram or a table may be used for computing the true wind from observations of the relative wind and ship speed and course (Bowditch, 2002). These additional elements are preferably obtained from a magnetic compass and the ship's speed information. They can also be obtained from the ship movement derived from a GPS receiver, but in that case the drift is not taken into account. In the past, this vector conversion was a frequent source of error in reported winds. However, increasing use of electronic logbook software that computes true wind will have reduced this source of error. For AWS, all of the required information is likely to be directly obtained from the anemometer and ship's navigation system.

The reported wind speed and direction will be the mean speed and direction measured over the 10 min period immediately preceding the observation. However, when the 10 min period includes a discontinuity in the wind characteristics, only data obtained after the discontinuity shall be used for reporting the mean values, and hence the period in these circumstances shall be correspondingly reduced.

The recording of ship metadata for WMO (1955–) is particularly important for wind observations (Yelland et al., 2001). Metadata should be provided to indicate the instrumentation used, how it is installed on board the ship (where on the ship and at what height), as well as details about the type of vessel (Kent et al., 2007). Metadata are used in particular to interpret the data correctly and increase data coherence (e.g. bias correction), and permit traceability to standards.

4.2.2.7 *Atmospheric pressure, pressure tendency and characteristic of pressure tendency*

4.2.2.7.1 **Methods of observation**

Pressure can be measured either by a precision aneroid, a dial aneroid or an electronic digital barometer. The barometer reading shall be taken as close to the observation time as possible. In a manual observation, the barometer will be read last and entered into the observation just prior to completion of the report. Automatic systems should have an averaging period of 1 min (Part I, Chapter 1, Annex 1.E). Most ships should report pressure to one decimal place. However, on VOS Auxiliary ships using coarse scale, uncalibrated ship's barometers where the pressure cannot be read to tenths of a hectopascal (hPa), the pressure should be recorded in whole hPa, ideally with an associated indicator or other coding mechanism to clearly document the reduced precision (for example, in the old FM 13 SHIP code (WMO, 2011b) the tenths position was replaced by a solidus to indicate the lower precision of the observation).

With manned observation, the characteristic and amount of the pressure tendency in the past 3 h are usually obtained from a marine barograph, preferably an open-scale instrument graduated in divisions of 1 hPa. However, digital barometers that include an LCD display of the pressure tendency are increasingly being used.

With AWS, the characteristic and amount of the pressure tendency in the past 3 h are calculated from the four last hourly pressure values.

4.2.2.7.2   Instruments

All barometers should conform to the general requirements given in Part I, Chapter 3, and should be supplied with a certificate giving the corrections (if any) that must be applied to the readings of each individual instrument. Barometers should be capable of being read to 0.1 hPa. The operational measurement uncertainty requirements and instrument performance are stated in Part I, Chapter 1, Annex 1.E. The required measurement uncertainty is better than 0.1 hPa (after reduction to sea level: < 0.2 hPa). The achievable measurement uncertainty should never be worse than 0.3 hPa. Marine barographs should have a built-in damping device, for example, an oil bath containing the aneroid box or a dash pot connected to the lever mechanism, to prevent the wide trace produced by rapid pressure variations caused by gusty winds and movement of the ship. Both the barometer and barograph should also be vented to the outside with a static pressure head so that readings can be taken more accurately and are not affected by sealed bridges or conditions inside. If this is not possible, instructions should be given to ensure that the bridge wing doors are opened prior to taking an observation. This is especially important on newer ships with pressurized accommodation blocks or on vessels that are carrying hazardous cargoes where the wheelhouse may be hermetically sealed.

In general, most (but not all) NMHSs set their precision aneroid and electronic barometers to "station level" pressure, and therefore the observations need to be corrected for the height of the barometer to give a sea-level pressure output. This height correction is calculated automatically with electronic logbook software. Dial aneroid barometers are typically set to indicate sea-level pressure.

4.2.2.7.3   Exposure and management

Digital and aneroid barometers and barographs

Barometers and barographs should be mounted on shock-absorbing material in a position where they are least affected by concussion, vibration or movement of the ship. The best results are generally obtained from a position as close to the centre of flotation as possible. Barographs should be installed with the pen-arm oriented athwart ships (to minimize the risk of the arm swinging off the chart).

4.2.2.7.4   Corrections

Provision should be made for the application of the following corrections:

(a)   Instrument error (bias);

(b)   Reduction to sea level as appropriate;

(c)   Temperature (if applicable and appropriate tables are provided).

Barometers should be adequately compensated for temperature, otherwise the instruments should be provided with a temperature correction table and means should be provided for measuring the temperature. A table for reducing to sea-level pressure should be supplied when barometers are set to the station height, although this is not necessary for ships that use electronic logbooks that are capable of automatically applying the height correction (Bowditch, 2002, Tables 29–34).

4.2.2.7.5   Sources of error

Errors are discussed in Part I, Chapter 3, but on ships in particular appreciable errors may be caused by the effect of the wind on the pressure in the compartment in which the barometer is

placed. Where possible, these should be minimized by enclosing the instrument in a chamber connected to a static pressure head or by connecting the device directly to this static pressure head.

On non-automated barometers, the most frequent (human) errors are due to an absence of reduction to the sea level, a bad appreciation of the barometer height or a non-intentional double correction (correction applied on a barometer which already gives sea-level pressure).

4.2.2.7.6 Checking with standard instruments

Barometers and barographs should be checked, wherever possible, at approximately three-monthly intervals against the standard barometer of a PMO or a Transfer Standard barometer. However, as shipping movements can be highly dynamic this may not always be possible. A report of all comparisons should be logged by the PMO, and a calibration label attached to the barometer showing the barometer check date and the correction to be applied.

Digital barometers have a much better stability and the length of time between calibrations may be as large as two years for some models.

4.2.2.8 *Air temperature and humidity*

Temperature (Part I, Chapter 2) and humidity (Part I, Chapter 4) observations are considered together as they are often measured by psychrometric methods with paired wet- and dry-bulb thermometers. With the increasing use of AWS, however, it is becoming more common for these parameters to be measured independently with a thermometer and separate hygrometer. Whichever method is used, the instruments should have good ventilation and be well exposed in a stream of air, directly from the sea, which has not been in contact with, or passed over, the ship, and should be adequately shielded from radiation, precipitation and spray.

For manned observations, if a louvred screen is to be used, two should be provided, one secured on each side of the vessel, so that the observation can also be made from the windward side. In this way, thermometers in the hygrometer can be completely exposed to the air-stream and are uninfluenced by artificial sources of heat and water vapour. As an alternative, a single portable louvred screen can be used, which is hung on whichever side is windward to gain the same exposure. The muslin wick fitted to a wet-bulb thermometer in a louvred screen should be changed at least once each week, and more often in stormy weather.

Sling or aspirated psychrometers exposed on the windward side of the bridge have been found to be satisfactory. If manually operated psychrometers are used, the thermometers must be read as soon as possible after ventilation has stopped. Handheld hygrometers require several minutes to be acclimated to the open environment if they have been stored indoors before use.

For the general management of psychrometers, the recommendations of Part I, Chapter 4 should be followed. Distilled water should be used for the wet-bulb thermometer. If this is not readily available, water from the condenser will generally be more suitable than ordinary freshwater. Water polluted by traces of seawater should never be used because any traces of salt will affect the wet-bulb temperature significantly.

With AWS or a distant digital display, a manual reading of the instruments inside the screen is no longer necessary and a single screen typically can be installed far enough from the ship's structure to provide good exposure. This means, however, that the filling of wet-bulb reservoirs becomes difficult, and consequently electronic temperature and relative humidity sensors are typically used with AWS. These instruments require calibration at least annually. As noted in Part I, Chapter 4, accuracy for such relative humidity sensors is likely to be lower than for psychrometric sensors, but there has not yet been a systematic assessment of the accuracy of these sensors in the marine environment. The AWS should report both air temperature and humidity as 1-min averages.

Humidity can be represented by several different variables, for example dewpoint temperature, wet-bulb temperature or relative humidity (Part I, Chapter 4) and should be recorded as the variable measured. Any conversion between humidity variables adds uncertainty and will be affected by any errors in other variables used and by truncation to fit transmission formats. For psychrometric measurements, both dry-bulb and wet-bulb temperature should be recorded to 0.1 °C precision. The dewpoint should be calculated using standard tables issued nationally or using standard WMO formulae (Part I, Chapter 4, Annexes 4.A and 4.B) and the psychrometric coefficient appropriate to the instrument being used. Dewpoint temperature should also be reported to 0.1 °C precision. Conversion of measurements of wet-bulb or dewpoint temperature to relative humidity recorded in whole per cent introduces significant uncertainty and should be avoided.

On VOS Auxiliary ships using coarse scale, uncalibrated ship's thermometers where the temperature cannot be read to tenths of a degree, the temperature should be recorded in whole degrees, ideally with an associated indicator or other coding mechanism to clearly document the reduced precision (for example, in the old FM 13 SHIP code the tenths position was replaced by a solidus to indicate the lower precision of the observation). All other ship observations should report temperature to one decimal place.

4.2.2.9   *Sea-surface temperature*

The routine measurement is to take the seawater temperature from near or just below the sea surface. More rarely the radiometric temperature of the surface skin of the ocean is measured.

The sea-surface temperature should be very carefully measured. This is because, among other things, it is used to obtain the difference with air temperature, which provides a measure of the stratification of temperature and humidity and of other characteristics of the lower layers of maritime airmasses. The temperature of the seawater thermometer should be read to 0.1 °C.

It has not been possible to adopt a standard device for observing sea-surface temperatures on account of the great diversity in ship size and speed and because of cost, ease of operation and maintenance considerations.

The SST may be observed by:

(a)   Taking a sample of the sea-surface water with a specially designed sea bucket;

(b)   Reading the temperature of the condenser intake water;

(c)   Exposing an electrical thermometer to sea-water temperature either directly or through the hull (for example, using an internally mounted hull contact sensor);

(d)   Using an infrared radiometer mounted on the ship to look down on the sea surface;

(e)   Using an expendable bathythermograph.[5]

The principal methods used for many years have been (a) and (b). Studies of the difference in temperature provided by the two methods have been made (WMO, 1972) in which it is reported that intake temperatures average 0.3 °C greater than those measured by sea-bucket samples. More recent studies suggest that this warm bias has reduced over time (Kent and Taylor, 2006). This study reported that the details of the intake temperature installation have a significant impact on the quality of observation. In recent years, as the speed and height of ships have increased, method (c), which gives the most consistent results, has been more widely used (WMO, 1991*b*; Kent et al., 1993). The use of radiometers is rarely encountered on VOS but may be used on some research vessels or on offshore platforms. Of all these methods, the condenser intake technique is the least desirable because of the great care needed to obtain good results.

---

[5]   Not currently supported by WMO (1955–)

4.2.2.9.1   Sea buckets

A sea bucket is lowered over the side of the ship to obtain a sample of seawater. The bucket is hauled back on board and a thermometer is then used to measure the temperature of the water. The sample should be taken from the leeward side of the ship, and well forward of all outlets. The thermometer should be read as soon as possible after it has attained the temperature of the water sample, ensuring that it is read out of the direct sunlight. When not in use, the bucket should be hung in the shade to drain.

A sea bucket should be designed to ensure that seawater can circulate through it during collection and that the heat exchange due to radiation and evaporation is minimized. The associated thermometer should have a quick response and be easy to read and should preferably be fixed permanently in the bucket. If the thermometer must be withdrawn for reading, it should have a small heat capacity and should be provided with a cistern around the bulb such that the temperature of the water withdrawn with it does not vary appreciably during the reading. The design of the bucket should be deemed adequate for its purpose by the organization recruiting the ship for observations.

Measurements from sea buckets of good design can be expected to agree well over an extensive range of conditions. However, sea buckets are less convenient to use than instruments attached to the ship and their use is sometimes restricted by weather conditions or by the size or speed of the ship.

4.2.2.9.2   Intake and tank thermometers

The thermometer provided within the intake pipe when the ship is built is normally not suitable for the measurement of SST to the required accuracy. Thus, the organization recruiting the ship should ideally, with the permission of the shipping company concerned, install an appropriate thermometer. The thermometer should preferably be mounted in a special tube providing adequate heat conductivity between the thermometer bulb and surrounding seawater, and positioned close to the water intake, although this may not always be practical.

When a direct-reading thermometer is installed in cramped conditions, the observer should be warned of the possibility of reading errors due to parallax. A distant reading system with the display elsewhere (for example, in the engine room or on the bridge) overcomes this problem. The observer should also be aware that, for ships of deep draught, or when a marked temperature gradient exists within the sea-surface layer, intake temperature readings usually differ considerably from those close to the sea surface, and will vary according to the ship's load or ballast condition. Lastly, of course, the intake temperature should not be recorded when the ship is stationary, otherwise the cooling water is not circulating. It should be noted that the installation of retrofit intake, or hull contact SST sensor can often be time-consuming and complicated, often forcing PMOs or technicians to work in a difficult environment (interior of ships, with limited access, etc.).

The sea chest in the bottom of a ship is a cavity in which the intake pipes may terminate and which may be used to observe the intake temperature. It is a favoured position for the sensor of a distant-reading thermometer. The limitations already mentioned apply to such installations.

Although the majority of intake thermometers will only provide instantaneous temperature readouts, some ships may be equipped with temperature probes that can sample the measurements at a given frequency and average them over a period of time. In that case, and in order to provide for measurements that are more representative of the SST, a modal filtration algorithm may be used to exclude the extreme readings from the computed average.

4.2.2.9.3   Hull-attached thermometers

Hull-attached thermometers provide a very convenient and accurate means of measuring SST. They are necessarily distant-reading devices, the sensor being mounted either externally in direct

contact with the sea using a "through-the-hull" connection, or internally (the "limpet" type) attached to the inside of the hull, except if the hull is a twin hull. Both types show very good mutual agreement, with the "through-the-hull" type showing a slightly quicker response.

The sensors must be located forward of all discharges at a depth of 1 to 2 m below the water line. When large changes of draught can occur, more than one sensor may be needed. There can be considerable problems of fitting and wiring, which is best done when the ship is being built. For subsequent fitting, the limpet-type thermometer avoids the need for drydocking the ship.

4.2.2.9.4 Trailing thermometers

Several means have been devised for trailing the sensor of a distant-reading thermometer in the sea at a point from which a sea bucket would take its sample. The differences concern the way in which the connecting cable is brought on board and the arrangement for exposing the sensor to the sea. These devices provide readings that are in good agreement with those of an accurate sea bucket and can be used readily. However, since experience is limited, no information is available on their possible fouling by weeds, and so on. Thus, streaming and recovery may be necessary on each occasion as for a sea bucket. Trailing thermistors are rarely used by the VOS but are more common for research applications (Fairall et al., 1997; Bradley and Fairall, 2006; Weller et al., 2008).

4.2.2.9.5 Radiometers

Because of its temperature, any substance gives off heat energy as infrared radiation. The amount of energy and the wavelength of the radiation depend upon the temperature of the substance and its emissivity. Thus, radiometers which respond to infrared radiation can be used to measure the temperature of a substance. When directed at the sea surface, a radiometer measures the temperature of only the uppermost 1 mm or so, because the emissivity of water is near unity. This uppermost layer is often called the ocean skin. Large temperature gradients, with the coolest temperature at the top, may exist in the first few centimetres of the ocean, especially in relatively calm conditions.

Radiometers can be handheld (pointing forward and downward), mounted on the bow or on a boom extending over the water. Radiometer measurements represent the evaporative surface-skin temperature and are used on only a few ships (Barton et al., 2004; Donlon et al., 2008).

4.2.2.10 *Clouds and weather*

4.2.2.10.1 Amount of cloud and cloud type

Visual cloud observations should follow the same rules as those applicable to a land station (see Part I, Chapter 15). Detailed instructions should be provided by the PMO. Pictorial guides and coding information are available from many sources, such as WMO (1975, 1987), as well as from publications of NMHSs. Most electronic logbook software include extensive pictures of clouds to assist with cloud type identification. Additionally, the template for reporting SHIP observations (B/C10 in the *Manual on Codes*, Volume I.2, Part C (WMO, 2011c)) provides specific information on how to make and code VOS cloud reports.

The assessment of the total amount of cloud consists in estimating how much of the total sky area is covered with cloud and should be reported in oktas. National instructions should provide guidance on the conversion of observations in oktas to per cent (%) as required for transmission in FM 94 BUFR. The assessment of low cloud amount is performed in a similar way and reported in oktas for both ship-to-shore transmission and onward transmission in FM 94 BUFR. If no low cloud is present, the amount of medium cloud is reported instead. The type of low, middle and high cloud shall be determined as specified in the *International Cloud Atlas*, Volume I (WMO, 1975), or by identifying the appropriate cloud type from the photographs displayed in the electronic logbook software.

4.2.2.10.2　Cloud-base height

The cloud-base height is normally estimated by the VOS. In order to improve their ability to do this, observers should be encouraged to take every opportunity to check their estimates against known heights, for example, when a cloud base is seen to intercept a mountainous coast, although in such circumstances the cloud base may be lower at the mountain than out at sea.

Some specialized ships may have instruments installed to measure cloud-base height. The cloud-base searchlight is of limited value on a ship because of the short baseline. An instrument which does not require a baseline is to be preferred, such as a laser ceilometer (see Part I, Chapter 15). It should be installed so that it can be operated and read by the officer on watch on the navigation bridge.

4.2.2.10.3　Present and past weather

Present and past weather are primarily meant to serve as a qualitative description of weather events. Most VOS reports of present and past weather are made by visual and auditory observations and follow the same rules as those applicable to a land station (see Part I, Chapter 14). There are 100 categories of present weather for VOS manual observations (the first 100 codes in FM 94 BUFR code table 0 20 003). Past weather is reported in 10 categories (the first 10 codes in FM 94 BUFR code table 0 20 004 and 0 20 005). Two past weather categories should be reported which have been selected to give as complete a description of conditions over the reporting interval as possible. As for clouds, detailed instructions should be provided by the PMO. Template B/C10 (WMO, 2011c) provides specific information on how to make and code VOS weather reports. For observers using electronic logbook software, further guidance is likely to be available from the software.

Measurements, rather than manual observations, of present and past weather are rare at sea. However, it is possible to use similar instrumentation as over land (Part I, Chapter 14), and the categories available for the report are different to the manual observations because of the different nature of the observation (WMO, 2011c). Some instrumental measurements of present and past weather may be made by fixed platforms under programmes which are not actively coordinated at present by WMO.

4.2.2.11　*Visibility*

At sea, the absence of suitable objects makes it impossible to estimate visibility as accurately as at land stations. On a large ship, it is possible to make use of objects aboard the ship (e.g. the foremast) for estimation when the visibility is very low, but it should be recognized that these estimates may be in error since the ship may affect the air. For the higher ranges, the appearance of the land when near the coast is a useful guide, and, if fixes can be obtained, the distance of landmarks, just as when they are appearing or disappearing, may be measured from the chart. Similarly, in open sea, when other ships are sighted and their distances known, for example, by radar, the visibility may be estimated. In the absence of other objects, the appearance of the horizon, as observed from different levels, may be used as a basis for the estimation. Although abnormal refraction may introduce errors into such methods of estimation, these methods are the only ones available in some circumstances. At night, the appearance of navigation lights can give a useful indication of the visibility.

When the visibility is not uniform in all directions it should be estimated or measured in the direction of least visibility and a suitable entry should be made in the log (excluding reduction of visibility due to the ship's exhaust).

Information about visibility meters is given in Part I, Chapter 9. Only those types of visibility meters which can be used with a baseline or light-path short enough to be practicable on a ship are suitable. This is the case of forward-scatter meters. Unfortunately, the heating effect of the ship, and its exhaust, may lead to unrepresentative measurements.

4.2.2.12   *Precipitation*

The VOS do not normally report information on precipitation within coded reports on weather types (section 4.2.2.10). However, precipitation measurements can be reported from fixed stations or vessels equipped with a precipitation gauge. The measurement of precipitation at sea is discussed in WMO (1962, 1981) and in the context of observations from research vessels by Bradley and Fairall (2006) and Weller et al. (2008), who also describe newer measurement systems, such as optical raingauges, not typically used for routine observations. As an aid to observers on ships, descriptions of precipitation at sea, for use in reporting present weather, are given in Annex 4.B.

The complete measurement comprises the determination of both the amount and the duration of precipitation. The amount of precipitation should be measured with a raingauge adapted for use aboard a ship.

It is difficult to obtain reliable measurements of precipitation on board a ship, owing to the aerodynamic effect of the superstructure of the ship, the influence of roll and pitch, the capture of spray, and the changes in ship position. The equipment used on ships for the measurement of precipitation should be constructed and exposed in such a manner that the first three effects mentioned above are avoided or minimized as far as possible. For a shipboard raingauge, placing the instrument as far forward and as high as practicable seems to be most effective. However, other exposures may be found in particular cases to provide for easier management.

Precipitation measurements from moored or fixed stations (lightships, large buoys, towers, etc.) are particularly valuable because the effect of ship speed is eliminated and the data can, thus, be included in climatological analyses without reduction. However, any problems of platform motion and salt contamination must still be considered.

Gimbal-mounted raingauge

The most common instrument used on board ships for the measurement of precipitation is the gimbal-mounted raingauge, an arrangement that is not very effective, especially during bad weather, as it is not able to keep the gauge horizontal at all times. An efficient gimbal arrangement is very complicated and expensive and is used only aboard special ships. Generally, when a raingauge is used, a fixed installation with a remote measurement arrangement seems to be a better option.

Conical marine raingauge

The conical marine raingauge is normally fixed high up on a mast. A plastic tube leads the water to a remotely placed collector on the deck, or in the wheelhouse. This can be a useful device for measuring precipitation, provided that the installation precautions are taken into account. The raingauge orifice should be fixed in a plane parallel to the ship's deck.

Recording raingauge

Several types of recording raingauges have been developed for use at sea. In one type, the collector is installed in the open while the recorder is mounted indoors. The rainwater is channelled along a pipe from the collector to a reservoir near the recorder. A pen linked to a float in the reservoir records the change of water level therein on a chart on a rotating drum. The reservoir is emptied automatically by a siphon when the total collected corresponds to 20 mm of rainfall.

In the electrical contact type of raingauge, the connection between the gauge and the recorder is made by electrical means. The rainwater caught by the collector is stored temporarily in a reservoir. After an amount corresponding to 0.5 mm of rainfall has been received, the rising surface touches a needle to close an electric circuit. A motor then closes the inlet valve and simultaneously opens a drain valve. After the water has drained away, the valves revert to their original state and a single pulse is sent to the recorder. Errors occur when the motion of the ship or buoy causes the water level to fluctuate rather than to rise steadily. This limitation can be

overcome by using a peristaltic pump. This device drains a fixed quantity of water (rather than all the water available) each time the contact is made and, therefore, is less sensitive to fluctuations in water level; there are also no valves to maintain.

The observation of precipitation by radar requires the use of narrow radar beams and calibrating raingauges together with the addition of specialized equipment to monitor the state of the radar and to apply corrections. Radars provided on board ships for other purposes do not have these features and their use for the quantitative observation of precipitation is not normal practice.

A third type of recording raingauge is a specifically designed ship raingauge that uses a horizontal and a vertical omnidirectional collector to allow for rainfall measurements at high wind speeds (Hasse et al., 1998). By measuring the amount of water that is collected by the vertical collector surface, a correction for the wind effect is possible by using the wind speed measured simultaneously at the site of the instrument. Rainfall intensities and amounts are measured and calculated separately for the top and the side collectors and corrected rainfall values are obtained as a wind-speed-dependent weighted average.

4.2.2.13   *Ocean waves*

The main topics of this section are the definitions and behaviour of waves and the visual methods of observing them. Automated methods are briefly mentioned in section 4.3 on moored buoys, although they are applied on other types of platforms.

4.2.2.13.1   **Definitions and descriptions of waves**

Fetch: Distance along a large water surface trajectory over which a wind of almost uniform direction and speed blows.

Wind wave or wind sea: Waves raised by the wind blowing in the immediate neighbourhood of an observation site at the time of observation.

Swell: Any system of water waves which has left its generating area (or observed when the wind field that generated the waves no longer exists).

Wave length: Horizontal distance between successive crests or troughs. It is equal to the wave period multiplied by the wave speed.

Wave height: Vertical distance between the trough and crest of a wave.

Wave period: Time between the passage of two successive wave crests past a fixed point. It is equal to the wave length divided by the wave speed.

Wave speed: The distance travelled by a wave in a unit of time. It is equal to the wave length divided by the wave period.

The observation should include the measurement or estimation of the following characteristics of the wave motion of the sea surface in respect of each distinguishable system of waves, namely, sea and swell (principal and secondary):

(a)   Direction (from which the waves come) on the scale 01–36 as for wind direction;

(b)   Period in seconds;

(c)   Height.

The following methods of observing wave characteristics of separate wave systems should be used as a guide.
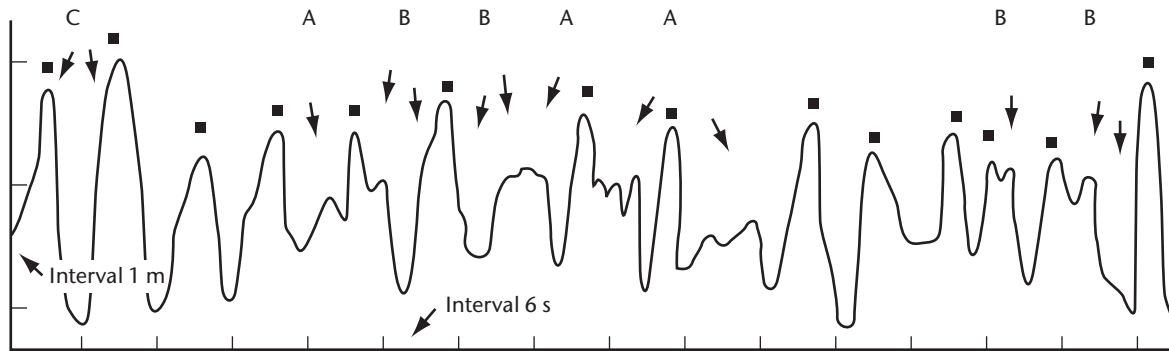
Figure 4.1. Typical sea and swell waves as shown by a wave-height recorder

Wind-generated ocean waves occur in large systems which are defined in connection with the wind field that produced the waves and also with the relative position of the point of observation. Bearing in mind the distinction between sea and swell, the observer should differentiate between the recognizable wave systems on the basis of direction, appearance and period of the waves.

Figure 4.1 shows a typical record drawn by a wave-height recorder. It shows the height of the sea surface above a fixed point against time, namely, it represents the up-and-down movement of a floating body on the sea surface as it is seen by the observer. It gives a representation of the sea surface in its normal appearance when it is stirred by the wind to form a wind wave.

Waves invariably travel in irregular groups with areas of slight wave development of two or more wave lengths between the groups. The irregularity is greater in the wind wave than in a swell. Furthermore, and this cannot be shown by a wave record, groups consisting of two or more well-formed waves in the sea can be seen to travel in directions which may differ as much as 20° or 30° from each other; as a result of interference of crossing waves, the crests of sea waves are rather short. Swell waves have a more regular appearance. These waves travel in a rather regular succession and well-defined direction with generally long and smooth crests. Undisturbed typical swell waves may be observed in areas where there has been little or no wind over a period of several hours to a day or more. In most areas, sea and swell are intermixed.

4.2.2.13.2 Visual observations from merchant ships

In trying to observe the wave characteristics of each of the recognizable wave systems (sea and swell) separately, the observer should be aware of the fact that the higher components of a wind wave resemble swell waves by their comparatively long crests and large periods. It may seem possible to split the assembly of waves of different heights, periods and directions (together forming the system of a wind wave) into two different waves systems and consider the smaller waves as wind waves and the larger waves as swell, but this may not be correct.

The distinction between wind waves and swell should be made on the basis of one of the following criteria:

Wave direction: If the mean direction of all waves of more or less similar characteristics (in particular, height and length) differs by 30° or more from the mean direction of waves of different appearance (in particular, height and/or length), the two sets of waves should be considered to belong to separate wave systems.

Appearance and period: When typical swell waves, characterized by their regular appearance and long crestedness, arrive approximately, namely, within 20°, from the direction of the wind, they should be considered as a separate wave system if their period is at least 4 s greater than the period of the larger waves of the existing wind wave.

For measuring the mean period and height of a wave system, significant waves should be considered only; these are the higher waves in the centre of each group of well-formed waves (Figure 4.1). The flat and badly formed waves (A) in the area between the groups must be omitted from the record.

The mean period and the mean height of about 15 to 20 well-formed waves from the centres of the groups is actually required; of course, these waves cannot be consecutive. The smaller wave-like disturbances (B) which can be seen clearly to be forming under the action of the wind on top of the larger waves are also to be omitted from the record.

Occasionally, waves may be encountered which literally stand out above the environmental waves (C). Such waves may occur singly or in a group of two or three. The observer should not concentrate on these maximum waves only; in order to arrive at a measure for the mean period and mean height of about 15 to 20 waves, he or she should also consider groups of well-formed waves of medium height. Consequently, the reported wave height will be smaller than the maximum height obtained by the observed waves. On average, the actual height of 1 out of about 10 waves will exceed the height to be reported. It is common practice to define the significant wave height measured by wave height recorders as the average height of the highest one third of the waves; it should approximate the wave height, which would be estimated by a manual observer.

The observer must bear in mind that only measurements or quite good estimates are to be recorded. Rough guesses have little value. The quality of the observations must have priority over their quantity. If only two, or even only one, of the three elements (direction, period, height) could be measured, or really well estimated, for example, at night, the report would still be of value.

The above considerations must be taken into account in all methods of observation described below. More details on waves are provided in WMO (1998), sections 4.4.1 and 4.4.2 of WMO (2001), and sections 4.3.4 to 4.3.6 of this chapter.

The direction from which the waves are coming is most easily found by sighting along the wave crests and then turning 90° to face the advancing waves. The observer is then facing the direction in which the waves are coming.

The recommended procedures for the reporting of swell by manually reporting ships are found in Annex 4.C.

Wave period

This is the only element that can actually be measured on board moving merchant ships. If a stop-watch is available, only one observer is necessary; otherwise, two observers and a watch with a second hand are required. The observer notes some small object floating on the water at some distance from the ship: if nothing is available, a distinctive patch of foam can usually be found which remains identifiable for the few minutes required for the observations. The watch is started when the object appears at the crest of the wave. As the crest passes, the object disappears into the trough, then reappears on the next crest, and so forth. The time at which the object appears to be at the top of each crest is noted. The observations are continued for as long as possible; they will usually terminate when the object becomes too distant to identify, on account of the ship's motion. Obviously, the longest period of observation will be obtained by choosing an object initially on the bow as far off as it can be clearly seen.

Another method is to observe two or more distinct consecutive periods from an individual group while the watch is running continuously; with the passage of the last distinct crest of a group or the anticipated disappearance of the object, the watch is stopped, then restarted with the passage of the first distinct crest of a new group. The observer keeps count of the total number of periods until it reaches at least 15 or 20.

Observations can also be made by watching the pitch and roll of the ship's bow. The observer picks the point which is at the highest or lowest in the cycle and starts the timer from there.
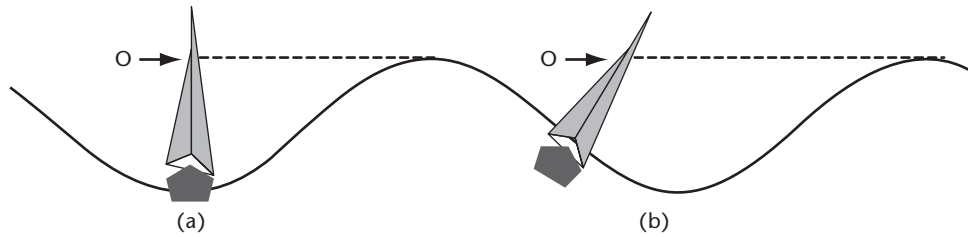
Figure 4.2. The effect of the ship's roll on the estimation of wave height

When it returns to the same point, the observer records the time. By repeating this process several times, a reliable observation can be determined. This also works during night-time observation for which the observer feels the rise and fall within his or her body.

With observations of a period less than 5 s and low wind velocity, the above observation may not be easily made, but such waves are less interesting than those with longer periods.

Wave height

With some experience, fairly reliable wave height estimates can be made. For estimating the height of waves having wave lengths much shorter than the ship, the observer should take up a position as low down in the ship as possible, preferably amidships where the pitching is least, and on the side of the ship from which the waves are coming. Use should be made of the intervals which occur every now and then, when the rolling of the ship temporarily ceases.

In cases of waves longer than the ship, the preceding method fails because the ship as a whole rises over the wave. Under these circumstances, the best results are obtained when the observer moves up or down in the ship until, when the ship is in the wave trough and upright, the oncoming waves appear just level with the horizon (Figure 4.2). The wave height is then equal to the height of the observer above the level of the water beneath him or her (a). If the ship is rolling, care should be taken to ensure that the approaching wave is in line with the horizon at the instant when the ship is upright, otherwise the height estimate will be too large (b).

By far the most difficult case is that in which the wave length exceeds the length of the ship, but the wave height is small. The best estimate of height can be obtained by going as near to the water as possible, but even then the observation can be only a rough estimate.

4.2.2.13.3   Observations from ocean station vessels and other special ships

Ocean station vessels are normally provided with suitable recording instruments. However, if visual observations are made, the above procedure should be followed; in addition, the ship should heave with the waves coming directly from ahead. For measuring wave period, an object can be thrown over the side of the vessel. For measuring wave height, marks should be painted amidships on the ship's side (half a metre apart).

Length can best be observed by streaming a buoy for such a distance astern that the crests of two successive waves simultaneously pass the buoy and the observer. The distance between the two is the wave length.

The velocity can be obtained by noting the time of the passage of a wave from the stern to the buoy, with allowance being made for the ship's speed.

4.2.2.13.4 Waves in coastal waters

The following are additional definitions applying to sea surface in coastal waters:

Breaker: The collapse of a whole wave resulting from its running into very shallow water, of a depth of the order of twice the wave height.

Surf: The broken water between the shoreline and the outermost line of the breakers.

Breaking sea: The partial collapse of the crest of a wave caused by the action of the wind; steepening of waves due to their encountering a contrary current or tidal stream; or steepening of waves due to their running into shoal water not shallow enough to cause a breaker.

Wave observations made from a coastal station cannot be expected to be representative of conditions in the open sea. This is because the waves are affected by the depth of the water, by tidal influence and by reflection from objects such as steep rocks and jetties. In addition, the location may be sheltered by headlands or, less obviously, by shoals, both of which may affect the height and direction of travel. An extensive account of these phenomena is given in WMO (1991*b*).

When observations are to be made despite these difficulties, the waves should be chosen in the same way as at sea. If they are required for wave research, the exact mean depth of water at the time of observation and the time itself should both be stated.

4.2.2.13.5 Terminology for sea and swell waves

The following terminology is recommended for uses other than the inclusion in coded messages, such as supplying weather information and forecasts for shipping, publications, pilots, and so on:

For the length of swell waves:	
Short	0–100 m
Average	100–200 m
Long	over 200 m
For the height of swell waves:	
Low	0–2 m
Moderate	2–4 m
Heavy	over 4 m
For the height of sea waves:	
Calm (glassy)	0 m
Calm (rippled)	0–0.1 m
Smooth (wavelets)	0.1–0.5 m
Slight	0.5–1.25 m
Moderate	1.25–2.5 m
Rough	2.5–4 m
Very rough	4–6 m
High	6–9 m
Very high	9–14 m
Phenomenal	over 14 m

In all cases, the exact bounding length or height is included in the lower category, namely, a sea of 4 m is described as rough. When the state of the sea surface is so confused that none of the above descriptive terms can be considered appropriate, the term "confused" should be used.

4.2.2.14 *Ice*

Several forms of floating ice may be encountered at sea. The most common is that which results from the freezing of the sea surface, namely sea ice. The reporting of sea ice is discussed in WMO (1970).

The other forms are river ice and ice of land origin. River ice is encountered in harbours and estuaries where it is kept in motion by tidal streams and normally presents only a temporary hindrance to shipping. Ice of land origin in the form of icebergs is discussed separately below.

Both icebergs and sea ice can be dangerous to shipping and always have an effect on navigation. Sea ice also affects the normal processes of energy exchange between the sea and the air above it. The extent of sea-ice cover can vary significantly from year to year and has a great effect both on adjacent ocean areas and on the weather over large areas of the world. Its distribution is therefore of considerable interest to meteorologists and oceanographers. Broad-scale observations of the extent of sea-ice cover have been revolutionized by satellite photography, but observations from shore stations, ships and aircraft are still of great importance for detailed observations and for establishing the ground truth of satellite observations.

At present, observations of floating ice depend almost entirely on visual estimation. The only instrumental observations of floating ice are carried out by conventional radar and new techniques, such as passive microwave sensors or sideways-looking airborne radar. However, icebergs are poor reflectors of radar energy and cannot always be detected by this means.

4.2.2.14.1   Observations of ice accretion

Ice accretion can be extremely hazardous because of its effects on small ships, particularly on vessels of less than about 1 000 gross tonnage. Even on larger ships, it can cause radio and radar failures due to the icing of aerials. Visibility from the bridge may also be affected. Problems have occurred due to icing on the deck cargoes of large container ships. Apart from its possible effect on stability, it may cause difficulty in unloading cargo at the port of destination when containers and their lashings are frozen solidly to the deck. Fishing vessels are particularly vulnerable to ice accretion. Further information is given in WMO (1991*b*), while a detailed consideration of the meteorological aspects appears in WMO (1974).

There are two main types of icing at sea: icing from seawater and icing from freshwater. Icing from seawater may be due either to spray and seawater thrown up by the interaction between the ship or installation and the waves, or to spray blown from the crests of the waves, or both. Icing from freshwater may be due to freezing rain and/or drizzle, or occasionally when the occurrence of wet snow is followed by a drop in temperature, or it may be due to freezing fog. Both types may occur simultaneously.

The most important meteorological elements governing ice accretion at sea are wind speed and air temperature. The higher the wind speed relative to the ship and the lower the air temperature, the greater the rate of ice accretion. There appears to be no limiting air temperature below which the icing risk decreases.

Provision is made in the WMO code form for ships (WMO, 2011*b*, 2011*c*), used for radio weather reports from ships at sea, for the inclusion of reports of ice accretion. This may be done either in code or in plain language. The coded form, in a single five-figure group, provides for reports of the cause of icing, the ice thickness and the rate of accretion. Plain-language reports must be preceded by the word ICING and are particularly encouraged for indicating features of the icing which are dangerous to vessels.

4.2.2.14.2   Formation and development of sea ice

Ice less than 30 cm thick

The first indication of ice formation is the appearance of small ice spicules or plates in the top few centimetres of the water. These spicules, known as frazil ice, form in large quantities and give the sea an oily appearance. As cooling continues the frazil ice coalesces to form grease ice, which has a matt appearance. Under near-freezing, but as yet ice-free, conditions, snow falling on the surface may result in the sea surface becoming covered by a layer of slush. These forms may be regrouped by the action of wind and waves to form shuga and all are classified as new

ice. With further cooling, sheets of ice rind or nilas are formed, depending on the rate of cooling and on the salinity of the water. Ice rind is formed when water of low salinity freezes into a thin layer of brittle ice which is almost free of salt, whereas when water of high salinity freezes, especially if the process is rapid and the wind is very light, the ice has an elastic property which is characteristic of nilas. The latter form of ice is subdivided, according to its thickness, into dark and light nilas; the second, more advanced form reaches a maximum thickness of 10 cm.

The action of wind and waves may break up ice rind or nilas into pancake ice, which can later freeze and thicken into grey ice and grey-white ice, the latter attaining a thickness of up to 30 cm. These forms of ice are referred to collectively as young ice. In rough conditions this ice may be broken up into ice cakes or floes of various sizes.

Ice 30 cm to 2 m thick

The next stage of development is known as first-year ice and is subdivided into thin, medium and thick categories. Thin first-year ice has a thickness of 30 to 70 cm. Medium first-year ice has a range of thickness from 70 to 120 cm. In polar areas, thick first-year ice may attain a thickness of approximately 2 m at the end of the winter.

Old ice

Thick first-year ice may survive the summer melt season and is then classified as old ice. This category is subdivided into second-year ice or multi-year ice, depending on whether the floes have survived one or more summers. The thickness of old ice is normally in the range of 1.2 to 3 m or more before the onset of the melt season. Towards the end of the summer melt season, old ice may be considerably reduced in thickness. Old ice may often be recognized by a bluish surface, in contrast to the greenish tint of first-year ice.

Snow cover

During winter, ice is usually covered with snow which insulates it from the air above and tends to slow down its rate of growth. The thickness of the snow cover varies considerably from region to region as a result of differing climatic conditions. Its depth may also vary considerably within very short distances in response to variable winds and to ice topography.

Decay of sea ice

While the snow cover persists, almost 90% of the incoming radiation is reflected back into space. Eventually, however, the snow begins to melt as air temperatures rise above 0 °C in early summer, and the resulting freshwater forms puddles on the surface. These puddles absorb about 90% of the incoming radiation and rapidly enlarge as they melt the surrounding snow or ice. Eventually, the puddles penetrate to the bottom surface of the floes and are known as thaw holes. This slow decay process is characteristic of ice in the Arctic Ocean and seas where movement is restricted by the coastline or islands. Where ice is free to drift into warmer waters (for example, the Antarctic, East Greenland and the Labrador Sea), decay is accelerated in response to wave erosion as well as warmer air and sea temperatures.

Movement of sea ice

Sea ice is divided into two main types according to its mobility. One type is drift ice, which is continually in motion under the action of the wind and current; the other is fast ice, attached to the coast or islands, which does not move. When ice concentration is high, namely seven tenths or more, drift ice may be replaced by the term pack ice.

Wind stress in the drift ice causes the floes to move in an approximately downwind direction. The deflecting force due to the Earth's rotation (Coriolis force) causes the floes to deviate about 30° to the right of the surface wind direction in the northern hemisphere. Since the surface wind is itself deviated by a similar amount but in the opposite sense from the geostrophic wind (measured directly from isobars), the direction of movement of the ice floes, due to the wind drift alone, can be considered to be parallel to the isobars.

The rate of movement due to wind drift varies not only with the wind speed, but also with the concentration of the drift ice and the extent of deformation (see subsection below). In very open ice (1/10–3/10) there is much more freedom to respond to the wind than in close ice (7/10–8/10), where free space is limited. Two per cent of the wind speed is a reasonable average for the rate of ice drift caused by the wind in close ice, but much higher rates of ice drift may be encountered in open ice. Since it is afloat, a force is exerted on drift ice by currents that are present in the upper layers of the water, whether these are tidal in nature or have a more consistent direction due to other forces. It is usually very difficult to differentiate between wind- and current-induced ice drift, but in any case, where both are present, the resultant motion is always the vector sum of the two. Wind stress normally predominates, particularly in offshore areas.

Deformation of sea ice

Where the ice is subject to pressure, its surface becomes deformed. On new and young ice, this may result in rafting as one ice floe overrides its neighbour; in thicker ice, it leads to the formation of ridges and hummocks according to the pattern of the convergent forces causing the pressure. During the process of ridging and hummocking, when pieces of ice are piled up above the general ice level, large quantities of ice are also forced downward to support the weight of the ice in the ridge or hummock. The draught of a ridge can be three to five times as great as its height, and these deformations are major impediments to navigation. Freshly formed ridges are normally less difficult to navigate than older weathered and consolidated ridges.

4.2.2.14.3 Icebergs

Icebergs are large masses of floating ice derived from glaciers, including ice shelves. The depth of a berg under water, compared with its height above, varies widely with different shapes of bergs. The underwater mass of an Antarctic iceberg derived from a floating ice shelf is usually less than the underwater mass of icebergs derived from Greenland glaciers. A typical Antarctic tabular berg, of which the uppermost 10 to 20 m is composed of old snow, will show one part of its mass above the water to five parts below. However, the ratio for an Arctic berg, composed almost wholly of ice with much less snow, is typically 1:8.

Icebergs diminish in size in three different ways: by calving, melting and wave erosion. A berg is said to calve when a piece breaks off; this disturbs its equilibrium and as a result it may drift at a different angle or capsize. Large underwater projections, which may be difficult to observe, are a usual feature of icebergs. In cold water, melting takes place mainly on the water-line, while, in warm water, a berg melts mainly from below and calves frequently. It is particularly dangerous to approach a berg melting in warm water for it is unstable and may fragment or overturn at any time. There are likely to be many growlers and bergy bits around rapidly disintegrating icebergs, thus forming a particular hazard to navigation.

Bergs are poor reflectors of radar energy and cannot always be detected by this means. Their breakdown fragments (bergy bits and growlers) are even more difficult to detect with a ship's radar since they are often obscured by the background clutter from waves and swell. These smaller fragments are especially dangerous to shipping. Despite their low profile, they contain sufficient mass to damage a vessel which comes into contact with them at normal cruising speed. Some growlers consisting of pure ice hardly break the sea surface and are extremely difficult to detect.

4.2.2.14.4 Observations of sea ice and icebergs

The key to good ice observing lies in familiarity with the nomenclature and experience. WMO (1970), with its illustrations, is the best guide to the mariner for ice identification.

The four important features of sea ice which affect navigation are as follows:

(a) Thickness: the stage of development (i.e. new ice, young ice, first-year ice or old ice and their subdivisions);

(b)　Amount: concentration (estimated according to the tenths of the sea surface covered by ice);

(c)　The form of the ice, whether it is fast or drift ice and the size of the constituent floes;

(d)　Movement: particularly with regard to its effect on deformation.

Since icebergs represent such a hazard to navigation, particularly at night or in poor visibility, it is also important to report the number in sight at the time of the observation, especially in waters where they are less frequently observed.

Sea ice can be reported in plain language or by the use of codes. WMO has adopted two sea-ice codes for international use. The simplest is the ICE group appended to the SHIP code format. The ICEAN code has been developed for specialist use for the transmission of sea-ice analysis and prognoses.

There are two basic rules for observation from ships and shore stations:

(a)　Obtain a large field of view by making the observation from the highest convenient point above the sea surface (for example, the top of a lighthouse, the bridge or crow's nest of a ship);

(b)　Do not attempt to report sea-ice conditions beyond a radius of more than half the distance between the point of observation and the horizon.

WMO has developed a set of symbols for use on maps depicting actual or forecast sea-ice conditions. These symbols are intended for the international exchange of sea-ice information and for radio-facsimile transmission of ice data.

4.2.2.15　*Observations of special phenomena*

Marine observers can make reports of natural phenomena using either traditional or some electronic logbooks. However, such special observations cannot normally be circulated over the GTS owing to international format limitations. The observations can take the form of written descriptions, sketches or photographs, or a combination. A wide range of phenomena can be reported, including:

(a)　Astronomical phenomena (e.g. eclipses, comets, zodiacal light, sunspots and novae);

(b)　Phenomena of the high atmosphere (e.g. high-frequency radio fadeouts or blackouts, magnetic disturbances and storms, airglow, aurorae, meteors and fireballs, and noctilucent clouds);

(c)　Phenomena of the lower atmosphere (e.g. abnormal refraction and mirages, glory or brocken spectres, coloured suns and moons, coronae, St Elmo's Fire, crepuscular rays, dust fall, the green flash, halo phenomena, iridescent cloud, lightning, rainbows, scintillation, unusual sky colouration and waterspouts). Note that when describing waterspouts, the direction of rotation should always be given as if seen from above;

(d)　Sightings of marine mammals, birds, fish, invertebrates and mass plankton effects such as bioluminescence, red tides and discoloured water;

(e)　Other marine phenomena (e.g. abnormal occurrences of compass deviations, changes in sea level or waves).

National publications, or information provided with electronic logbooks, provide information about the kinds of phenomena that are of interest and the information that is required for reporting particular types of phenomena.

4.3   **MOORED BUOYS**

Moored buoys come in a wide variety of configurations (e.g. in terms of mooring design, sensor types, sampling schemes, mounting techniques and telemetry) serving a wide variety of operational and research applications and disciplines. This section, which does not reflect the wide variety of possibilities used in currently functioning systems, is focusing on requirements for marine meteorological measurements from operational meteorological moored buoys. Information regarding other systems addressing the requirements for research applications can be found in other publications and websites, for example:

- ATLAS tropical moored buoys: http://www.pmel.noaa.gov/tao/proj_over/mooring.shtml

- Ocean Climate Stations: http://www.pmel.noaa.gov/OCS/

- TRITON tropical western Pacific moored buoys: http://www.jamstec.go.jp/jamstec/ TRITON/real_time/php/top.php

- More recent Indian Ocean m-TRITON moored buoys: http://www.jamstec.go.jp/iorgc/ iomics/index.html

- NOAA guide to making climate quality meteorological and flux measurements at sea (Bradley and Fairall, 2006)

A typical moored buoy designed for deep ocean operation is equipped with sensors to measure the following variables:

(a)   Wind speed;

(b)   Wind direction;

(c)   Atmospheric pressure;

(d)   Sea-surface temperature;

(e)   Wave height and period;

(f)   Air temperature;

(g)   Dewpoint temperature or relative humidity.

Additional elements measured by some moored buoys are as follows:

(a)   Maximum wind gust;

(b)   Wave spectra (directional or non-directional);

(c)   Solar radiation (downward short-wave radiation);

(d)   Surface current or current profiles;

(e)   Surface salinity;

(f)   Subsurface temperature and salinity down to 500 m or 750 m;

(g)   Atmospheric visibility;

(h)   Precipitation;

(i)   Surface CO_2 concentration.

For waves, the following variables are generally measured or estimated using the following definitions (see also section 4.2.2.13 to complement these definitions):

Significant wave height: Estimate of the average height of the one-third highest waves;

Maximum wave height: The maximum single wave height which is observed in a certain time period;

Mean zero crossing wave period: The wave period corresponding to the number downward zero-crossing of the surface elevation. It can also be estimated from the second frequency moment of the wave energy spectrum;

Peak height: The wave height corresponding to the peak of the wave energy spectrum (the part of the spectrum with the highest wave energy);

Peak period: The wave period corresponding to the peak height of the wave energy spectrum;

Spectral wave period: The wave period corresponding to the mean frequency of the spectrum.

In addition to the meteorological and oceanographic measurements, it is necessary to monitor buoy location and various housekeeping parameters to aid data quality control and maintenance. Moored-buoy technology has matured to the extent that it is expected to obtain six months to as long as two years of unattended operation even in the most severe conditions. Operational life is largely determined by the life of the sensors, with sensor exchanges often carried out at 12 to 18 month intervals.

The observations from moored buoys are now considered to be better quality than ship observations with regard to the accuracy and reliability of measurements (Wilkerson and Earle, 1990; Ingleby, 2010). Indeed, moored buoys are generally regarded as providing the highest quality observations of a wide range of marine meteorological variables and, in addition to their use by forecasters and assimilation into numerical weather prediction models, the data are also used to provide information on the climatology of oceanic areas, "ground truth" reference data for satellite calibration/validation and estimates of surface fluxes (e.g. Bourras, 2006).

Typical measurement uncertainties obtained from operational buoys are as follows:

Wind speed	1 m s^{-1} or 5% above 20 m s^{-1}
Wind direction	10°
Air temperature	0.2 °C
Sea-level pressure	0.2 hPa
Sea-surface temperature	0.2 °C
Dewpoint temperature	0.5°
Significant wave height	10% or 0.2 m
Wave direction	10°
Wave period	1 s

The standard suite of sensors on moored buoys samples wind speed, peak gust (e.g. 3 to 5 second gust depending on national requirements); wind direction; barometric pressure; air temperature; water temperature; and non-directional ocean wave energy spectra, from which significant wave height and peak (or average) wave period are determined. For tsunameters, water-column height is the standard measurement.

4.3.1   **Atmospheric pressure**

Atmospheric pressure and its variability in both time and space are crucially important for numerical weather prediction and for analysis and forecasting. Most buoys measure atmospheric pressure by means of digital aneroid barometers. Pressure is found from the electrical capacitance across parallel pressure-sensitive plates. The capacitance between the plates increases as pressure increases. The following pressure measurements are made:

(a)   Station pressure is the actual measurement made by the barometer at the station elevation in hPa. In some cases two barometers may be used and their values averaged.

(b)   Sea-level pressure is the pressure reduced to sea level from the station pressure in units of hPa. For buoys deployed at sea this is very close to the station pressure. A large difference is observed between sea-level pressure and station pressure from buoys deployed in lakes at high elevations. The conversion to sea-level pressure is made using the procedures described in WBAN (United States Weather Bureau, 1963).

Many buoys that are deployed in regions subject to hurricanes or intense low-pressure systems have the capability of measuring supplemental 1 min average pressure data. These data are recorded after the hourly pressure data fall below a predetermined threshold (e.g. 1 008 hPa in the tropics). Supplemental pressure data are identified as follows:

(a)   The minimum 1 min barometric pressure in hPa from the primary (and secondary if one is installed) barometer is the minimum 1 min mean barometric pressure for the entire hour;

(b)   The time is the minute within the hour that the minimum pressure occurred.

4.3.2   **Wind measurements**

Wind measurements are one of the most important measurements made from moored buoys. They are essential for the marine weather forecaster.

Definitions:

Wind direction is the direction from which the wind is blowing in degrees clockwise from true north. It is a unit vector average of the record of wind direction;

Wind speed is the scalar average of the wind speed over the sampling interval (usually 10 min);

Wind speed maximum is the highest wind speed in the wind record. Gusts are determined from the highest running mean of the record over a short time interval (for example, 5 s).

The wind measurements are generally made by a propeller-vane or a cup anemometer and a wind wane. To avoid mechanical wear, ultrasonic wind speed and direction sensors with no moving parts are starting to be used on moored buoys. Wind direction measurement is normally associated with a compass so the buoy relative wind direction can be corrected to True.

Some Members typically use four-blade, impeller-driven, wind-vane sensor on their meteorological moorings. The final measurements are statistical estimates of the wind from time series of instantaneous wind samples taken at a minimum rate of 1 Hertz (Hz) over a particular length of time. The sampling rate is a function of the payload. Most moored buoys use an 8 min acquisition period. The following standard wind measurements are produced each hour.

Some Members have their meteorological moored buoys perform statistical processing at the end of an acquisition period, and the output message is updated with the new statistics and six 10 min segments. Statistical processing includes the calculation of the mean for both direction and speed and the standard deviation of the speed. The hour's data do not represent data from minute 0 to min 59. Rather, these represent the latest, complete six 10 min segments before the end of the last acquisition. The 10 min segments are, however, bounded by minutes 0, 10, 20, etc.

For the moored buoys of some Members, wind speeds at 10 m above site elevation and 20 m above site elevation are derived from an algorithm (Liu et al., 1979) that uses the height of the anemometer, the wind speed, a constant relative humidity of 85%, a constant sea-level pressure of 1 013.25 hPa, and the air and water temperature. If either the air or water temperature is unavailable, then the neutral stability is assumed, taking into account that neutral stability can introduce an error of up to 5%. If both are missing then neither 10 nor 20 m wind speeds are made.

The United Kingdom, French and Irish K-series moored buoys have traditionally used a cup anemometer and a self-referencing wind vane to measure the speed and direction over a 10 min acquisition period each hour. However, during operation, salt water permeates the seals and eventually failure of the instruments occurs when salt crystals form in the lubricant leading to mechanical failure of the moving parts. These moored buoys have dual wind systems to provide increased resilience in the event of anemometer failure. To further improve reliability, some Members are replacing these with a new wind system utilizing a sonic anemometer and electronic compass.

4.3.3 Temperature

Temperature is one of the basic meteorological measurements. Electronic thermistors are generally used to make all temperature measurements which are provided in degrees Celsius (°C). Temperature measurements can also be used for deriving sea-level pressure and standard-height wind speed from non-standard height atmospheric pressure and wind measurements, respectively.

4.3.3.1 *Air temperature*

Air temperature measurements are generally very reliable; however, it is important to note that the physical position of temperature sensors can adversely affect measurements. Air temperature housings can lead to non-representative readings in low wind conditions. Air temperature is sampled at some rate during the sampling period (typically 1 Hz or 0.1 Hz).

4.3.3.2 *Water temperature*

While there are generally few problems with water temperature measurements, it should be noted that the depth of water temperature sensors varies with buoy hull, and that the temperature probes on buoys are attached to the inside of the hull. Since buoy hulls are highly thermally conducting, the temperatures measured may reflect the average temperature of the water around the submerged hull rather than the temperature of the water nearest the probe. In highly stratified water, especially during afternoon hours in calm wind conditions, the water temperature reported from a buoy may be 2 °C to 3 °C below the skin temperature of the water.

4.3.4 Ocean wave estimates

Sea-state estimates are probably the most complex measurements made from moored buoys and are extremely important to marine forecasters, mariners, ocean engineers and scientists. On a buoy, all of the basic wave measurements are derived in some way from the time series of the buoy's motion. NDBC (2003, 2009) provide for complete details on wave measurements made by the United States National Data Buoy Center (NDBC).

Sea state is a description of the properties of sea-surface waves at a given time and place. This might be given in terms of the wave spectrum, or more simply in terms of the significant wave height and some measure of the wave period (AMS, 2000). Many moored buoys provide a measurement of the spectral variance density (Frigaard et al., 1997), which will be referred to as spectral wave density. Most buoys derive all non-directional wave parameters, heights and periods, steepness, and so on, from spectral wave densities. Furthermore, many buoys measure the directional wave spectrum and from that derive mean and principal wave directions, and first and second normalized polar coordinates from the Fourier coefficients that centres disseminate through the WMO FM-65 WAVEOB alphanumeric codes (WMO, 2011*b*, 2011*c*).

4.3.5   **Non-directional ocean wave estimates**

Most buoys use accelerometers to measure buoy heave motion. Accelerometers, fixed to remain vertical relative to the hull or stabilized parallel to the earth vertical, are used in buoys and make the vast majority of ocean wave measurements. Vertical stabilization, when used, is achieved through use of heave, pitch and roll sensor which reference plane is mounted on a gravity-stabilized platform and provides for a natural period in the order of 40 s. This type of equipment is expensive, and has a built-in mechanical system for keeping the accelerometer vertical as the buoy and sensor tilt.

Operational non-directional wave measurement systems report estimates of acceleration or displacement spectra. If not directly reported, displacement spectra are derived from acceleration spectra as part of the calculations involved in the shore-side processing of the wave data. From these spectra, average wave period, dominant wave period, significant wave height, and steepness are calculated. These non-directional wave parameters are defined as follows.

Average wave period, in seconds, can be computed in different ways. It can be such that it corresponds to the wave frequency that divides the wave spectrum into equal areas or it can be based on the second frequency moment of the non-directional spectral density. It can also be estimated using a zero crossing method.

Dominant wave period or peak wave period, in seconds, is the wave period corresponding to the centre frequency of the frequency band with the maximum non-directional spectral density.

Significant wave height, H_{m0}, is estimated from the variance of the wave displacement record obtained from the displacement spectrum according to following equation:

$$H_{m0} = 4 \left[\int_{f_1}^{f_u} S(f) df \right]^{\frac{1}{2}}$$

where $S(f)$ is the spectral density of displacement; df is the width of the frequency band; f_u is the upper frequency limit; and f_1 is the lower frequency limit.

4.3.6   **Directional ocean wave estimates**

Directional wave measurement systems require, in addition to the measurement of vertical acceleration or heave (displacement), buoy azimuth, pitch and roll. These allow east-west slope and north-south slope to be computed. Most buoys use several different methods and sensor suites for the measurement of these angles.

It is recommended (Swail et al., 2010a; Swail et al., 2010b) that in order to serve the full range of users, directional spectral wave measuring systems should reliably estimate the so-called "First 5" standard. Technically, this refers to five defining variables at a particular wave frequency (or wave period). The first variable is the wave energy, which is related to the wave height, and the other four are the first four coefficients of the Fourier series that defines the directional distribution of that energy. At each frequency band, not only is the wave direction defined but also the spread (second moment), skewness (third moment) and kurtosis (the fourth moment). The skewness resolves how the directional distribution is concentrated (to the left or right of the mean) and the kurtosis defines the peakedness of the distribution. Obtaining these three additional parameters (spread, skewness and kurtosis) for each frequency band yields an improved representation of the wave field.

Wave measurements from moored buoys are also used to validate wave measurements derived from high-frequency radar instruments.

4.3.7   **Water-column height for tsunami detection**

Most buoy tsunameters report water level (actually water-column height) based on pressure and temperature measurements made at the sea floor and converted to a water-column height by multiplying the pressure by a constant 670 mm per pound per square inch absolute.

4.3.8   **Relative humidity**

Humidity sensors used by buoys employ a circuit that measures humidity through the change in capacitance of a thin polymer as it is exposed to variations in water vapour. A gas-permeable membrane protects the electronic parts from spray and particulate matter but allows air to enter the instrument housing. The sensor is temperature-sensitive and incorporates a temperature probe to provide a temperature correction in the calculation of relative humidity. The sensor is sampled at some rate during the sampling period (e.g. 1 Hz for the United States and Canadian meteorological moored buoys). For the United Kingdom, French and Irish K-series buoys, an instantaneous value is taken from the electric hygrometric circuit element at the observing time.

4.3.9   **Ocean sensors**

In order to understand and predict the ocean, its properties must be monitored. Many buoys help to monitor the ocean by also measuring surface currents, ocean current profiles, near-surface temperature and water quality parameters. Included in the water quality parameters can be turbidity, redox potential (Eh), pH, chlorophyll-a, and dissolved oxygen. Buoy data are quality controlled in real time and where possible these data are distributed over the Global Telecommunication System.

4.3.10   **Surface ocean currents**

Surface currents are collected to support commerce, safety of operation, search and rescue, oil spill response, and currents near harbour entrances that have an impact on ocean transportation. Surface currents measured from buoys are also used to validate surface currents derived from high-frequency radar instruments. Most buoys acquire these measurements using buoy-mounted acoustic Doppler samplers.

4.3.11   **Ocean current profiles**

Ocean current profiles provide the motion of the ocean at different levels in the water column. This information is essential for assessing oil spill dispersal, search and rescue, stresses on offshore platforms, and validation for ocean models. These data are currently acquired from downward-looking, buoy- or cage-mounted systems. On offshore oil platforms, the current profiles may be downward looking from a number of levels in the water column, or upward-looking from a bottom-mounted system.

Most buoys use Doppler profiler technology as the primary sensor for collection of ocean current profile data. They emit short-duration, high-frequency pulses of acoustic energy along narrow beams. Scatterers (assumed to be passive nekton and plankton) within the water column return the backscattered energy and the instruments resolve the along-beam Doppler frequency shifts into orthogonal earth coordinates to obtain ocean currents at various levels in the water column.

4.3.12   **Salinity**

Salinity is required to initialize ocean models that provide ocean forecasts and predict ocean circulations (which are largely density driven). Salinity is usually derived from measurements of the conductivity of seawater. Some instruments provide the salinity directly (through internal calculations) and others provide the conductivity, temperature and depth required

to calculate the salinity. Salinity measurements are based on the practical salinity scale using the empirical relationship between the salinity and conductivity of seawater (although a new international thermodynamic equation of seawater-2010 (TEOS-10) was recently endorsed by the Intergovernmental Oceanographic Commission of UNESCO through its Assembly Resolution XXV-7). The salinity units are reported in practical salinity units.

4.3.13   **Precipitation**

Siphon raingauges have been installed on some moored buoys.

4.3.14   **Solar radiation measurements**

Solar radiation is an important influence on physical, biological and chemical processes near the air–sea interface, and is therefore of interest to scientists and engineers. Solar radiation measurements taken at the surface have been used to calibrate visible range radiometers aboard satellites. The sensor is placed as high as possible on the platform to avoid shadows. Solar radiative flux is measured in watts per square metre and photosynthetically active radiation is measured in micromols per square metre per second.

4.3.15   **Visibility**

Visibility sensors have been placed on some stations where visibility is a critical concern for safe navigation. The sensor measures the extinction of light across a small volume of air between an emitter and a collector. It is important to note that these are measurements at a single point, and that there are several similar but different definitions.

4.4   **UNMANNED LIGHT VESSELS**

In most respects, these platforms are similar to moored buoys. However, because of their larger dimensions and the feasibility of carrying a large instrument payload, it is more straightforward to deploy additional sensors, such as visibility sensors. In severe weather, such sensors can be affected by sea spray generated by the vessel itself. However, in most conditions, performance is equal to that of instruments deployed on land-based automatic weather stations.

4.5   **TOWERS AND PLATFORMS**

On towers (usually in relatively shallow waters close to shore), and on platforms in more remote areas, it is possible to operate standard automatic weather stations, similar in design to land automatic weather stations (see Part II, Chapter 1). Additional sensors are often deployed, for example, wave sensors and sensors for measuring mean water level above a reference point, ceilometers and visiometers. Fixed platforms can include large gravity based structures, and mobile jack-up rigs and semi-submersible rigs. Jack-up and semi-submersibles rigs, and drill ships, could be considered stationary platforms as they are moored or dynamically positioned to remain in one place while in operation. On manned platforms and rigs, measured data can be supplemented by visual observations of cloud, visibility and weather, thus allowing full synoptic reporting. Visual observations from oil/gas platforms should be made according to the procedures recommended under section 4.2. However, there are cases where different procedures apply. For example, a platform may include wave data from a nearby moored wave buoy, and sea-surface temperature from a nearby supply vessel.

Some manned fixed or stationary (offshore oil and gas) platforms may include significant wave height and some measure of wave period in their weather report (using the same parts of the FM 13 SHIP code as the moored buoys), using output from a nearby wave buoy or from an on-board wave radar.

Platforms and towers make convenient structures for mounting meteorological sensors. Installation and maintenance can be less complicated and more economical than for a moored buoy making data frequency and reliability better. Data quality is unaffected by ship or buoy motion and is less susceptible to errors from sensors damaged by wave action.

However, temperature and humidity sensors need very careful positioning as often there are heat and exhaust sources that will modify the local environment making values unrepresentative of environmental conditions. Wind measurements might be taken at heights in excess of 100 m above mean sea level and require correction to the equivalent 10 m surface wind (note that ideally it would be best to also have the actual observation and its height). In the case of towers close inshore, tide height can significantly alter the effective height of the wind sensor.

In conclusion, therefore, fixed towers and offshore platforms can provide a cost-effective source of data-releasing moored buoys to be used in more remote areas where there are no alternatives.

4.6   **DRIFTING BUOYS**

Drifting buoys have been used for many years in oceanography, principally for the measurement of sea-surface currents. However, the development of reliable satellite tracking and data relay systems (WMO/IOC, 1995) has led to a dramatic increase in the numbers of ocean drifting buoys deployed, and significant development has taken place in the sensor capabilities of drifters for meteorological and oceanographic purposes.

A description of drifting buoy systems and operations is given in UNESCO (1988). More recently, the WMO/IOC Data Buoy Cooperation Panel (DBCP) published the *Global Drifter Programme Barometer Drifter Design Reference* (WMO/IOC, 2009*a*). See also the annual reports and workshop proceedings of the DBCP, such as WMO/IOC (2004*a*, 2004*b*).

The evolution of drifting buoy technology has been driven by the needs of oceanographic research, on the one hand, and operational meteorology, on the other. Thus, three main distinct types of buoys can be characterized as follows:

(a) For oceanographic research, and especially for the World Ocean Circulation Experiment (Surface Velocity Programme, SVP, 1988–1993), a surface-current-following drifter equipped also to measure sea-surface temperature has been developed and deployed in large numbers over the world's oceans;

(b) For operational meteorology, a drifting buoy design has evolved based on those developed for the First Global Atmospheric Research Programme Global Experiment. These buoys primarily measure air pressure, sea-surface temperature and air temperature;

(c) For polar applications, different ice floats have been designed to measure traditional atmospheric variables as well as ice and snow conditions (ice/snow temperature and temperature profiles in the ice, ice thickness, ice stress, water conditions below ice). By tracking the buoy position on the ice it is possible to estimate ice motion. Efforts have been made to develop buoys that meet the combined requirements of oceanographic research and operational meteorology, which has resulted in the development of:

   (i) The SVP-B drifter, which is essentially a surface-current-following drifter with an air pressure sensor added;

(ii)   The SVP-BW drifter (or Minimet), which is essentially an SVP-B drifter with wind-measuring capability using Wind Observation Through Ambient Noise (WOTAN) technology;

(iii)   The wind and temperature profile buoy, which is basically a meteorological drifter with added wind speed sensor and subsurface thermistor chain for the measurement of temperature profile to depths of 100 m or so. Wind direction is measured on these buoys by orienting the whole buoy into the wind using a profiled mast or fixed wind vane;

(iv)   The addition of salinity sensors to SVP drifters.

Drifting buoys are expendable devices, thus performance is a compromise between the requirements and the cost of ownership. As well as hardware costs, it should be noted that the cost of data processing and dissemination throughout the Argos satellite system is significant and can be a limiting factor, although the more recent use of an Iridium satellite data telecommunication system is helping to resolve this problem. However, the performance of drifting buoy sensors is adequate for the purposes of synoptic meteorology and oceanography, as appropriate. Note that the quality of wind speed observations is questionable, resulting in their non-use by operational centres (Ingleby, 2010).

The typical measurement uncertainties of operational systems are as follows:

Sea-surface temperature	0.21 °C[a]
Air pressure	0.84 hPa[b]
Wind speed	3.5 m s^{-1} or 10%[abc]
Wind direction	18.5°[b]
Subsurface temperature	0.1 °C

Notes:
a   *Source*: O'Carroll et al. (2008).
b   *Source*: buoy monitoring statistics, European Centre for Medium-Range Weather Forecasts, January 2012.
c   Because of the low sensor height (approximately 1 m above sea level) these uncertainties apply to low wind speed and low sea states only.

ANNEX 4.A. WMO/IOC REGIONAL MARINE INSTRUMENT CENTRES

1.   Considering the need for high-quality marine meteorology and oceanographic measurements from the world oceans to address the requirements of WMO and UNESCO/IOC programmes and co-sponsored programmes, the need for facilities for the regular calibration and maintenance of marine instruments and the monitoring of instrument performance, on a regional basis in order to address adherence of ocean observations and associated metadata to high level standards for instruments and methods of observation, the need for documenting methods of measurements, for understanding biases introduced by each type of instrumentation, and for developing methods to correct such biases, in order to achieve delivery and use of coherent datasets, it has been recommended that:[1]

Regional Marine Instrument Centres (RMICs) should have the following capabilities to carry out their corresponding functions:

Capabilities:

(a)   An RMIC must have, or have access to, the necessary facilities and laboratory equipment to perform the functions necessary for the calibration of meteorological and related oceanographic instruments deployed to address the common requirements of WMO and UNESCO/IOC marine-related programmes and co-sponsored programmes;[2]

(b)   An RMIC must maintain a set of meteorological and oceanographic standard instruments or references and establish the traceability of its own measurement standards and measuring instruments to the International System of Units (SI);

(c)   An RMIC must have qualified managerial and technical staff with the necessary experience to fulfil its functions;

(d)   An RMIC must develop its individual technical procedures for the calibration of meteorological and related oceanographic instruments using its own calibration equipment;

(e)   An RMIC must develop its individual quality assurance procedures;

(f)   An RMIC must participate in, or organize, inter-laboratory comparisons of standard calibration instruments and methods;

(g)   An RMIC must utilize the resources and capabilities of its region of interest according to the region's best interests, when appropriate;

(h)   An RMIC must apply international standards applicable for calibration laboratories, such as ISO/IEC 17025, to the extent possible;

(i)   A recognized authority[3] must assess an RMIC, at least every five years, to verify its capabilities and performance.

Corresponding functions:

(a)   An RMIC must assist Members/Member States of its region in calibrating their national meteorological standards and related oceanographic monitoring instruments according to the RMIC capabilities;

---

[1]   Recommended by the Joint WMO/IOC Technical Commission for Oceanography and Marine Meteorology at its third session, held in 2009.
[2]   Basically in situ geophysical instruments deployed in the surface marine environment or subsurface.
[3]   JCOMM is the body that formally proposes new RMICs and proposes any authority to do evaluations.

(b)   An RMIC must participate in, or organize, JCOMM and/or regional instrument intercomparisons, following relevant JCOMM recommendations;

(c)   An RMIC must make a positive contribution to Members/Member States regarding the quality of measurements;

(d)   An RMIC must advise Members/Member States on enquiries regarding instrument performance, maintenance and the availability of relevant guidance materials;

(e)   An RMIC must actively participate, or assist, in the organization of regional workshops on meteorological and related oceanographic instruments and measurements;

(f)   The RMIC must cooperate with other RMICs in the standardization of meteorological and related oceanographic measurements and sensors;

(g)   An RMIC must regularly inform Members/Member States and report, on an annual basis, to the JCOMM Management Committee on the services offered to Members/Member States and the activities carried out. JCOMM in turn should keep the Executive Councils of WMO and UNESCO/IOC informed on the status and activities of the RMICs, and propose changes, as required.

2.   The mechanism for formal WMO and UNESCO/IOC designation of RMICs implies the following:

(a)   Governance for defining the functions and adoption of an RMIC is proposed by JCOMM and endorsed by the WMO and UNESCO/IOC Executive Councils;

(b)   A candidate RMIC is required to produce a statement of compliance, list capabilities of the proposed centre, state the suite of instrument expertise offered, state the formal commitment to voluntarily host the centre, and demonstrate capability to JCOMM;

(c)   The establishment of RMICs is initiated by JCOMM, and the designation process is coordinated by JCOMM and the WMO/IOC Secretariats according to the process endorsed by JCOMM and documented in JCOMM Technical Report No. 53;

(d)   Where more than one RMIC is established within a WMO and/or IOC Region, there should be coordination amongst the Centres.

3.   The following centres have been designated as RMICs:

Region	Centre	Location
Asia-Pacific	National Center of Ocean Standards and Metrology	Tianjin, China
North America, Central America and the Caribbean	United States National Data Buoy Center	Stennis Space Center, Mississippi, United States

———————

ANNEX 4.B. DESCRIPTIONS OF PRECIPITATION FOR USE BY SHIP-BORNE OBSERVERS OF PRESENT WEATHER

Precipitation occurs either in a more or less uniform manner (intermittent or continuous) or in showers.

All precipitation other than showers must be reported as intermittent or continuous.

Non-showery precipitation usually falls from stratiform clouds (mainly altostratus and nimbostratus). Showers fall from large convective clouds (mainly cumulonimbus or cumulus of moderate or strong vertical development) and are usually characterized by their abrupt beginning and ending and by variations in the intensity of the precipitation. Drops and solid particles in a shower are generally larger than those occurring in non-showery precipitation.

The drops of precipitation can be supercooled (i.e. the temperature of the drops is below 0 °C). On impact with a surface, drops of supercooled rain form a mixture of water and ice having a temperature near 0 °C.

Forms of precipitation

The descriptions given below are compatible with the definitions given in the *International Cloud Atlas*, Volume I, Part III.2 (WMO, 1975):

Drizzle: Fairly uniform precipitation in the form of very small drops of water. The diameter of the drops is normally less than 0.5 mm. The drops appear almost to float, thus making visible even slight movements of the air. Drizzle falls from a continuous and fairly dense layer of stratiform cloud, which is usually low, sometimes touching the surface (fog). For coding purposes, drizzle must be classified as slight, moderate or heavy, which are defined as follows:

(a)   *Slight drizzle* can be readily detected on the face of wheel-house windows, but produces very little runoff from deck, roofs, and so on;

(b)   *Moderate drizzle* causes windows, decks and superstructures to stream with moisture;

(c)   *Heavy drizzle*: same as for moderate drizzle. It also reduces visibility to below 1 000 m.

Rain: Precipitation of drops of water, which falls from a cloud. The diameter and concentration of raindrops vary considerably according to the intensity, and especially the nature, of the precipitation (continuous rain, rain shower, downpour, etc.). Continuous rain usually falls from a more or less uniform layer or layers of thick stratiform cloud. For coding purposes, rain must be classified as slight, moderate or heavy. These terms are defined as follows:

(a)   *Slight rain* may consist of scattered large drops or numerous smaller drops. The rate of accumulation on a deck is low and puddles form very slowly;

(b)   *Moderate rain*: Individual drops are not clearly identifiable. Rain spray is observable. Puddles form rapidly. Sounds from roofs range from swishing to a gentle roar;

(c)   *Heavy rain*: A downpour which makes a roaring noise on awnings and deckheads and forms a misty spray of fine droplets by splashing on deck surfaces.

Snow: Precipitation of ice crystals, separately or agglomerated, which falls from a cloud. The form, size and concentration of snow crystals vary considerably according to the conditions prevailing at the time of the snowfall. The intensity is coded as slight, moderate or heavy.

Showers: These are characterized by their abrupt beginning and end, and by the generally rapid and sometimes violent variations in the intensity of the precipitation. Drops and solid particles

falling in a shower are generally larger than those falling in non-showery precipitation. Whether the precipitation (rain or snow) occurs as showers or not depends on the clouds in which it originates. Showers fall from large convection clouds and are defined as follows:

(a)   *Rain and snow showers* must be classified for coding purposes with regard to intensity as either slight, moderate or heavy. The description is the same as for slight, moderate or heavy rain or snow. It must be remembered, however, that the visibility in showery weather shows a much greater variability than for the same category of continuous rain;

(b)   *Violent showers* are exceptionally heavy or torrential rain showers. Such showers occur mostly in tropical regions.

Snow pellets: Precipitation of white and opaque ice particles which falls from a cloud. These particles are generally conical or rounded. Their diameter may attain 5 mm. These grains, having a snow-like structure, are brittle and easily crushed; when they fall on a hard surface they bounce and often break up. In most cases, snow pellets fall as showers, often together with snowflakes, normally when temperatures near the surface are close to 0 °C. For recording purposes, the intensity of snow pellets, when they occur alone, is determined according to the visibility in the same manner as for snow.

Hail: Precipitation of transparent, or partly or completely opaque, particles of ice (hailstones), which are usually spherical, conical or irregular in form and have a diameter generally between 5 and 50 mm (smaller particles of similar origin may be classified either as small hail or ice pellets), and fall either separately or agglomerated into irregular lumps. Hail always occurs in the forms of showers and is generally observed during heavy thunderstorms. For coding purposes, hail must be classified as either slight, moderate or heavy. The intensity is determined by the rate of accumulation of stones as follows:

(a)   *Slight hail*: Few stones falling, no appreciable accumulation on flat surfaces;

(b)   *Moderate hail*: Slow accumulation of stones. Fall sufficient to whiten the decks;

(c)   *Heavy hail*: Rapid accumulation of stones. Rarely experienced in temperate latitudes at sea.

Small hail: Precipitation of translucent ice particles which falls from a cloud. These particles are almost spherical and sometimes have conical tips. Their diameter may attain and even exceed 5 mm. Usually, small hail is not easily crushable and when it falls on a hard surface it bounces with an audible sound on impact. Small hail always occurs in showers. For coding purposes, small hail must be classified as either slight, moderate or heavy. The intensity is determined by using the accumulation rate given for hail.

Ice pellets: Precipitation of transparent ice particles which falls from a cloud. These particles are usually spherical or irregular, rarely conical. Their diameter is less than 5 mm. Usually, ice pellets are not easily crushable, and when they fall on hard surfaces they generally bounce with an audible sound on impact. Precipitation in the form of ice pellets generally falls from altostratus or nimbostratus. The intensity of ice pellets is determined in the same manner as for hail.

Snow grains: Precipitation of very small opaque white particles of ice which falls from a cloud. These particles are fairly flat or elongated; their diameter is generally less than 1 mm. When the grains hit a hard surface they do not bounce. They usually fall in small quantities, mostly from stratus or from fog and never in the form of a shower. This precipitation corresponds to drizzle and occurs when the temperature is approximately between 0 °C and –10 °C. As there is only one code specification which refers to snow grains, it is not necessary to classify intensity.

_____

ANNEX 4.C. RECOMMENDED PROCEDURES FOR THE REPORTING OF SWELL BY MANUALLY REPORTING SHIPS

The recommended procedures for the reporting of swell by manually reporting ships, as agreed at the fifth session of the Ship Observations Team (SOT-V) in 2009 (WMO/IOC, 2009*b*), and implemented with the agreement of the Expert Team on Marine Climatology (ETMC; WMO/IOC, 2010), are given below:

(a)   When swell is not determined, meaning no observation has been attempted, the swell groups will be omitted from the observation;

(b)   When no swell is observed owing to a calm sea, the direction of the main swell and the direction of the secondary swell will be reported as calm. The period and height of the main swell and secondary swell can then be omitted, because if a calm sea is reported it is inferred that these elements will also be calm, in which case they provide no additional information;

(c)   When the swell direction is indeterminate, confused swell is reported. When the period and height of the swell are also confused, this will be included in the observation. The period and height of the secondary swell can be omitted;

(d)   When the swell is confused but the period and height can be estimated, the swell direction is reported as confused, and the period and height of the primary swell is included in the report. The period and height of the secondary swell can be omitted;

(e)   When only one swell is observed, the direction, period and height of this swell is reported. The period and height of the secondary swell can be omitted;

(f)   When two swells are observed, both the swell direction and the period and height of each are included in the observation.

_____

REFERENCES AND FURTHER READING

American Meteorological Society (AMS), 2000: *Glossary of Meteorology*. Second edition, American Meteorological Society (available from http://glossary.ametsoc.org/wiki/Main_Page).

Barton, I.J., P.J. Minnett, K.A. Maillet, C.J. Donlon, S.J. Hook, A.T. Jessup and T.J. Nightingale, 2004: The Miami2001 infrared radiometer calibration and intercomparison. Part II: shipboard results. *Journal of Atmospheric and Oceanic Technology*, 21(2):268–283.

Bourras, D., 2006: Comparison of five satellite-derived latent heat flux products to moored buoy data. *Journal of Climate*, 19(24):6291–6313.

Bowditch, N., 2002: *The American Practical Navigator: An Epitome of Navigation*. 2002 Bicentennial edition, NIMA Pub. No. 9. National Imagery and Mapping Agency, Bethesda.

Bradley, F. and C. Fairall, 2006: *A Guide to Making Climate Quality Meteorological and Flux Measurements at Sea*. NOAA Technical Memorandum OAR PSD-311, NOAA/ESRL/PSD, Boulder, CO.

Dohan, K., F. Bonjean, L. Centurioni, M. Cronin, G. Lagerloef, D.-K. Lee, R. Lumpkin, N. Maximenko, P. Niiler and H. Uchida, 2010: Measuring the global ocean surface circulation with satellite and in situ observations. *Proceedings of OceanObs'09: Sustained Ocean Observations and Information for Society (Vol. 2)*. (J. Hall, D.E. Harrison and D. Stammer, eds.) (Venice, 21–25 September 2009). ESA Publication WPP-306.

Donlon, C., I.S. Robinson, W. Wimmer, G. Fisher, M. Reynolds, R. Edwards and T.J. Nightingale, 2008: An infrared sea surface temperature autonomous radiometer (ISAR) for deployment aboard Volunteer Observing Ships (VOS). *Journal of Atmospheric and Oceanic Technology*, 25(1):93–113.

Fairall, C.W., A.B. White, J.B. Edson and J.E. Hare, 1997: Integrated shipboard measurements of the marine boundary layer. *Journal of Atmospheric and Oceanic Technology*, 14(3):338–359.

Freeland, H., D. Roemmich, S. Garzoli, P.-Y. Le Traon, M. Ravichandran, S. Riser, V. Thierry, S. Wijffels, M. Belbéoch, J. Gould, F. Grant, M. Ignazewski, B. King, B. Klein, K. Mork, B. Owens, S. Pouliquen, A. Sterl, T. Suga, M. Suk, P. Sutton, A. Troisi, P. Vélez-Belchi and J. Xu, 2010: Argo – A decade of progress. *Proceedings of OceanObs'09: Sustained Ocean Observations and Information for Society (Vol. 2)*. (J. Hall, D.E. Harrison and D. Stammer, eds.) (Venice, 21–25 September 2009). ESA Publication WPP-306.

Frigaard, P.B., J. Helm-Petersen, G. Klopman, C.T. Standsberg, M. Benoit, M.J. Briggs, M. Miles, J. Santas, H.A. Schäffer and P.J. Hawkes, 1997: IAHR list of sea parameters. *Proceedings of the Twenty-seventh IAHR Congress* (San Francisco, 10–15 August 1997).

Goni, G., D. Roemmich, R. Molinari, G. Meyers, C. Sun, T. Boyer, M. Baringer, V. Gouretski, P. DiNezio, F. Reseghetti, G. Vissa, S. Swart, R. Keeley, S. Garzoli, T. Rossby, C. Maes and G. Reverdin, 2010: The Ship of Opportunity Program. *Proceedings of OceanObs'09: Sustained Ocean Observations and Information for Society (Vol. 2)*. (J. Hall, D.E. Harrison and D. Stammer, eds.) (Venice, 21–25 September 2009). ESA Publication WPP-306.

Hall, J., D.E. Harrison and D. Stammer (eds.), 2010: *Proceedings of OceanObs'09: Sustained Ocean Observations and Information for Society*. (Venice, 21–25 September 2009). ESA Publication WPP-306.

Hasse, L., M. Grossklaus, K. Uhlig and P. Timm, 1998: A ship rain gauge for use in high wind speeds. *Journal of Atmospheric and Oceanic Technology*, 15(2):380–386.

Ingleby, B., 2010: Factors affecting ship and buoy data quality: a data assimilation perspective. *Journal of Atmospheric and Oceanic Technology*, 27:1476–1489.

Keeley, R., M. Pazos and B. Bradshaw, 2010: Data management system for surface drifters. *Proceedings of OceanObs'09: Sustained Ocean Observations and Information for Society (Vol. 2)*. (J. Hall, D.E. Harrison and D. Stammer, eds.) (Venice, 21–25 September 2009). ESA Publication WPP-306.

Kennedy, J.J., R.O. Smith and N.A. Rayner, 2012: Using AATSR data to assess the quality of in situ sea-surface temperature observations for climate studies. *Remote Sensing of Environment*, 116:79–92.

Kent, E.C., G. Ball, D. Berry, J. Fletcher, A. Hall, S. North and S. Woodruff, 2010: The Voluntary Observing Ship (VOS) Scheme. *Proceedings of OceanObs'09: Sustained Ocean Observations and Information for Society (Vol. 2)*. (J. Hall, D.E. Harrison and D. Stammer, eds.) (Venice, 21–25 September 2009). ESA Publication WPP-306.

Kent, E.C. and D.I. Berry, 2005: Quantifying random measurement errors in Voluntary Observing Ships' meteorological observations. In: *Advances in the Applications of Marine Climatology – The Dynamic Part of the WMO Guide to the Applications of Marine Climatology*, JCOMM TR No. 13, REV. 1 (WMO/TD-No. 1081), John Wiley & Sons (available from http://www.wmo.int/pages/prog/amp/mmop/jcomm_reports.html).

Kent, E.C. and P.K. Taylor, 2006: Toward estimating climatic trends in SST, Part I: methods of measurement. *Journal of Atmospheric and Oceanic Technology*, 23(3):464–475.

Kent, E.C., P.K. Taylor, B.S. Truscott and J.S. Hopkins, 1993: The accuracy of Voluntary Observing Ships' meteorological observations – Results of the VSOP-NA. *Journal of Atmospheric and Oceanic Technology*, 10(4):591–608.

Kent, E.C., S.D. Woodruff and D.I. Berry, 2007: Metadata from WMO publication no. 47 and an assessment of Voluntary Observing Ship observation heights in ICOADS. *Journal of Atmospheric and Oceanic Technology* 24(2):214–234.

Liu, W.T., K.B. Katsaros and J.A. Businger, 1979: Bulk parameterization of air–sea exchanges of heat and water vapor including the molecular constraints at the interface. *Journal of Atmospheric Sciences*, 36:1722–1735.

McPhaden, M.J., K. Ando, B. Bourlès, H.P. Freitag, R. Lumpkin, Y. Masumoto, V.S.N. Murty, P. Nobre, M. Ravichandran, J. Vialard, D. Vousden and W. Yu, 2010: The Global Tropical Moored Buoy Array. *Proceedings of OceanObs'09: Sustained Ocean Observations and Information for Society (Vol. 2)*. (J. Hall, D.E. Harrison and D. Stammer, eds.) (Venice, 21–25 September 2009). ESA Publication WPP-306.

Meldrum, D., E. Charpentier, M. Fedak, B. Lee, R. Lumpkin, P. Niiler and H. Viola, 2010: Data buoy observations: the status quo and anticipated developments over the next decade. *Proceedings of OceanObs'09: Sustained Ocean Observations and Information for Society (Vol. 2)*. (J. Hall, D.E. Harrison and D. Stammer, eds.) (Venice, 21–25 September 2009). ESA Publication WPP-306.

Merrifield, M., T. Aarup, A. Allen, A. Aman, P. Caldwell, E. Bradshaw, R.M.S. Fernandes, H. Hayashibara, F. Hernandez, B. Kilonsky, B. Martin Miguez, G. Mitchum, B. Pérez Gómez, L. Rickards, D. Rosen, T. Schöne, M. Szabados, L. Testut, P. Woodworth, G. Wöppelmann and J. Zavala, 2010: The Global Sea Level Observing System (GLOSS). *Proceedings of OceanObs'09: Sustained Ocean Observations and Information for Society (Vol. 2)*. (J. Hall, D.E. Harrison and D. Stammer, eds.) (Venice, 21–25 September 2009). ESA Publication WPP-306.

Moat, B.I., M.J. Yelland and A.F. Molland, 2006: Quantifying the airflow distortion over merchant ships, part II: application of the model results. *Journal of Atmospheric and Oceanic Technology*, 23(3):351–360.

Moat, B.I., M.J. Yelland, R.W. Pascal and A.F. Molland, 2005: An overview of the airflow distortion at anemometer sites on ships. *International Journal of Climatology*, 25(7):997–1006.

National Data Buoy Center, 2003: *Nondirectional and Directional Wave Data Analysis Procedures*. NDBC Technical Document 03-01, National Data Buoy Center, Stennis Space Center, Mississippi (available from http://www.ndbc.noaa.gov/wavemeas.pdf).

———, 2009: *Handbook of Automated Data Quality Control Checks and Procedures*. NDBC Technical Document 09-02, National Data Buoy Center, Stennis Space Center, Mississippi (available from http://www.ndbc.noaa.gov/NDBCHandbookofAutomatedDataQualityControl2009.pdf).

O'Carroll, A.G., J.R. Eyre and R.W. Saunders, 2008: Three-way error analysis between AATSR, AMSR-E, and in situ sea surface temperature observations. *Journal of Atmospheric and Oceanic Technology*, 25(7):1197–1207.

Organisation Météorologique Internationale – Comité Météorologique International (OMI-CMI), 1947: *Procès-Verbaux de la Session de Paris, 1946*. Publication No. 55, 105–106. Lausanne, La Concorde.

Send, U., R.A. Weller, D. Wallace, F. Chavez, R. Lampitt, T. Dickey, M. Honda, K. Nittis, R. Lukas, M. McPhaden and R. Feely, 2010: OceanSITES. *Proceedings of OceanObs'09: Sustained Ocean Observations and Information for Society (Vol. 2)*. (J. Hall, D.E. Harrison and D. Stammer, eds.) (Venice, 21–25 September 2009). ESA Publication WPP-306.

Smith, S.R., M.A. Bourassa, E.F. Bradley, C. Cosca, C.W. Fairall, G.J. Goni, J.T. Gunn, M. Hoo, D.L. Jackson, E.C. Kent, G. Lagerloef, P. McGillivary, L. Petit de la Villéon, R.T. Pinker, E. Schulz, J. Sprintall, D. Stammer, A. Weill, G.A. Wick and M.J. Yelland, 2010: Automated underway oceanic and atmospheric measurements from ships. *Proceedings of OceanObs'09: Sustained Ocean Observations and Information for Society (Vol. 2)*. (J. Hall, D.E. Harrison and D. Stammer, eds.) (Venice, 21–25 September 2009). ESA Publication WPP-306.

Swail, V., R.E. Jensen, B. Lee, J. Turton, J. Thomas, S. Gulev, M. Yelland, P. Etala, D. Meldrum, W. Birkemeier, W. Burnett and G. Warren, 2010*a*: Wave measurements, needs and developments for the next decade. *Proceedings of OceanObs'09: Sustained Ocean Observations and Information for Society (Vol. 2)*. (J. Hall, D.E. Harrison and D. Stammer, eds.) (Venice, 21–25 September 2009). ESA Publication WPP-306.

Swail, V., B. Lee, A. Soares, D. Resio, K. Horsburgh, T. Murty, S. Dube, M. Entel and J. Flowerdew, 2010*b*: Storm Surge. *Proceedings of OceanObs'09: Sustained Ocean Observations and Information for Society (Vol. 2)*. (J. Hall, D.E. Harrison and D. Stammer, eds.) (Venice, 21–25 September 2009). ESA Publication WPP-306.

United Kingdom Meteorological Office, 1995: *Marine Observers Handbook*. Eleventh edition, UK Met Office No. 1016, London.

United Nations Educational, Scientific and Cultural Organization (UNESCO), 1988: *Guide to Drifting Data Buoys*. WMO/IOC Manuals and Guides 20.

United States Weather Bureau, 1963: *Manual of Barometry (WBAN)*. Volume I, first edition, US Government Printing Office, Washington, DC (available from http://babel.hathitrust.org/cgi/pt?id=uc1.31822010663441;seq=7;view=1up;num=i).

Weller, R.A., E.F. Bradley, J.B. Edson, C.W. Fairall, I. Brooks, M.J. Yelland and P.W. Pascal, 2008: Sensors for physical fluxes at the sea surface: energy, heat, water, salt. *Ocean Science*, 4(4):247–263.

Wilkerson, J.C. and M.D. Earle, 1990: A study of differences between environmental reports by ships in the voluntary observing program and measurements from NOAA buoys. *Journal of Geophysical Research*, 95(C3):3373–3385.

World Meteorological Organization, 1955–: *International List of Selected, Supplementary and Auxiliary Ships* (WMO-No. 47). Geneva. (Serial publication; recently annual. Editions prior to 1966 were entitled *International List of Selected and Supplementary Ships*; future editions will be known as *International List of Selected, VOSClim, Supplementary and Auxiliary Ships*) (available from http://www.wmo.int/pages/prog/www/ois/pub47/pub47-home.htm).

———, 1962: *Precipitation Measurements at Sea*. Technical Note No. 47 (WMO-No. 124, TP. 55). Geneva.

———, 1970: *WMO Sea-ice Nomenclature* (WMO-No. 259, TP. 145), Volumes I and III. Geneva.

———, 1972: *Comparative Sea-surface Temperature Measurements* (R.W. James and P.T. Fox). Report on Marine Science Affairs No. 5 (WMO-No. 336). Geneva.

———, 1974: *The Meteorological Aspects of Ice Accretion on Ships* (H.C. Shellard). Report on Marine Science Affairs No. 10 (WMO-No. 397). Geneva.

———, 1975: *International Cloud Atlas: Manual on the Observation of Clouds and Other Meteors* (WMO-No. 407), Volume I. Geneva.

———, 1981: *Precipitation Measurement at Sea* (G. Olbrück). Marine Meteorology and Related Oceanographic Activities Report No. 1. Geneva.

———, 1987: *International Cloud Atlas* (WMO-No. 407), Volume II. Geneva.

———, 1989: *Wind Measurements Reduction to a Standard Level* (R.J. Shearman and A.A. Zelenko). Marine Meteorology and Related Oceanographic Activities Report No. 22 (WMO/TD-No. 311). Geneva.

———, 1991*a*: *Compendium of Lecture Notes in Marine Meteorology for Class III and Class IV Personnel* (J.M. Walker). (WMO-No. 434). Geneva.

———, 1991*b*: *The Accuracy of Ship's Meteorological Observations: Results of the VSOP-NA* (E.C. Kent, B.S. Truscott, P.K. Taylor and J.S. Hopkins). Marine Meteorology and Related Oceanographic Activities Report No. 26 (WMO/TD-No. 455). Geneva.

———, 1998: *Guide to Wave Analysis and Forecasting* (WMO-No. 702). Geneva.

———, 1999: The accuracy of meteorological observations from Voluntary Observing Ships: Present status and future requirements (P.K. Taylor and E.C. Kent). *Final Report of the First Session of the Commission for Marine Meteorology Working Group on Marine Observing Systems Subgroup on Voluntary Observing Ships* (Athens 1999), WMO TC CMM 1999 (available from http://eprints.soton.ac.uk/347754/).

———, 2001: *Guide to Marine Meteorological Services* (WMO-No. 471). Geneva.

———, 2010: *Manual on the Global Observing System* (WMO-No. 544), Volume I. Geneva.

———, 2011*a*: *Manual on the Global Observing System* (WMO-No. 544), Volume II. Geneva.

———, 2011*b*: *Manual on Codes* (WMO-No. 306), Volume I.1. Geneva.

———, 2011*c*: *Manual on Codes* (WMO-No. 306), Volume I.2. Geneva.

World Meteorological Organization/Intergovernmental Oceanographic Commission, 1995: *Guide to Data Collection and Location Services using Service Argos*. Data Buoy Cooperation Panel Technical Document No. 3. Geneva and Paris.

———, 1996: *Guide to Moored Buoys and Other Ocean Data Acquisition Systems* (E.A. Meindl). Data Buoy Cooperation Panel Technical Document No. 8. Geneva and Paris.

———, 2003*a*: Improving global flux climatology: the role of metadata (E.C. Kent, P.K. Taylor and S.A. Josey). *Advances in the Applications of Marine Climatology – The Dynamic Part of the WMO Guide to the Applications of Marine Meteorology* (WMO/TD-No. 1081). Geneva and Paris.

——, 2003*b*: The accuracy of marine surface winds from ships and buoys (P.K. Taylor, E.C. Kent, M.J. Yelland and B.I. Moat). *Advances in the Applications of Marine Climatology – The Dynamic Part of the WMO Guide to the Applications of Marine Meteorology* (WMO/TD-No. 1081). Geneva and Paris.

——, 2003*c*: Establishing more truth in true winds (S.R. Smith, M.A. Bourassa and R.J. Sharp). *Advances in the Applications of Marine Climatology – The Dynamic Part of the WMO Guide to the Applications of Marine Meteorology* (WMO/TD-No. 1081). Geneva and Paris.

——, 2004*a*: *Data Buoy Cooperation Panel: Annual Report for 2003*. Data Buoy Cooperation Panel Technical Document No. 25. Geneva and Paris (available from http://www.jcommops.org/dbcp/doc/dbcp-25/DBCP25.pdf).

——, 2004*b*: *Research, Applications and Developments involving Data Buoys*. Presentations at the Data Buoy Cooperation Panel Technical Workshop (Angra Dos Reis, Brazil, October 2003). Data Buoy Cooperation Panel Technical Document No. 24. Geneva and Paris.

——, 2009*a*: *Global Drifter Programme Barometer Drifter Design Reference* (A.L. Sybrandy, P.P. Niiler, C. Martin, W. Scuba, E. Charpentier and D.T. Meldrum). Data Buoy Cooperation Panel Report No. 4, revision 2.2. Geneva and Paris (available from http://www.jcommops.org/doc/DBCP/SVPB_design_manual.pdf).

——, 2009*b*: *Final Report of the Fifth Session of the JCOMM Ship Observations Team* (Geneva, 18–22 May 2009), JCOMM Meeting Report No. 63 (available from http://www.jcomm.info/index.php?option=com_oe&task=viewDocumentRecord&docID=3830).

——, 2010: *Final Report of the Third Session of the JCOMM Expert Team on Marine Climatology* (Melbourne, Australia, 8–12 February 2010), JCOMM Meeting Report No. 70 (available from http://www.jcomm.info/index.php?option=com_oe&task=viewDocumentRecord&docID=4950).

Yelland, M.J., B.I. Moat and P.K. Taylor, 2001: Air flow distortion over merchant ships. *Progress Report to the Atmospheric Environment Service*, Canada (available from http://eprints.soton.ac.uk/67256).

———————

CHAPTER CONTENTS

CHAPTER 5. SPECIAL PROFILING TECHNIQUES FOR THE BOUNDARY LAYER AND THE TROPOSPHERE

5.1 GENERAL

Special profiling techniques have been developed to obtain data at high temporal and spatial resolution which is needed for analysis, forecasting and research on the smaller meteorological scales and for various special applications. This chapter gives a general overview of current surface-based systems that can be used for these purposes. It is divided into two main parts: remote-sensing and in situ direct measuring techniques. Some of these techniques can be used for measurements over the whole troposphere, and others are used in the lower troposphere, in particular in the planetary boundary layer.

Remote-sensing techniques are based on the interaction of electromagnetic or acoustic energy with the atmosphere. The measuring instrument and the variable to be measured are spatially separated, as opposed to on-site (in situ) sensing. For atmospheric applications, the technique can be divided into passive and active techniques. Passive techniques make use of naturally occurring radiation in the atmosphere (microwave radiometers). Active systems (sodars, windprofilers, RASSs – radio acoustic sounding systems – and lidars) are characterized by the injection of specific artificial radiation into the atmosphere. These surface-based profiling techniques are described in section 5.2. Other remote-sensing techniques relevant to this chapter are discussed in Part II, Chapter 7, and Part III.

Section 5.3 describes in situ techniques with instruments located on various platforms to obtain measurements directly in the boundary layer (balloons, boundary layer radiosondes, instrumented towers and masts, instrumented tethered balloons). Chapters 12 and 13 in Part I describe the more widely used techniques using balloons to obtain profile measurements.

The literature on profiling techniques is substantial. For general discussions and comparisons see Derr (1972), WMO (1980), Martner et al. (1993) and the special issue of the *Journal of Atmospheric and Oceanic Technology* (Volume 11, No. 1, 1994; see http://journals.ametsoc.org/toc/atot/11/1).

5.2 SURFACE-BASED REMOTE-SENSING TECHNIQUES

5.2.1 Acoustic sounders (sodars)

Sodars (sound detection and ranging) operate on the principle of the scattering of acoustic waves by the atmosphere. According to the theory of the scattering of sound, a sound pulse emitted into the atmosphere is scattered by refractive index variations caused by small-scale turbulent temperature and velocity fluctuations, which occur naturally in the air and are particularly associated with strong temperature and humidity gradients present in inversions. In the case of backscattering (180°), only temperature fluctuations with a scale of one half of the transmitting acoustic wavelength determine the returned echo, while, in other directions, the returned echo is caused by both temperature and velocity fluctuations, except at an angle of 90°, where there is no scattering.

Useful references to acoustic sounding include Brown and Hall (1978), Neff and Coulter (1986), Gaynor et al. (1990) and Singal (1990).

A number of different types of acoustic sounders have been developed, but the two most common types considered for operational use are the monostatic sodar and the monostatic Doppler sodar.

A monostatic sodar consists of a vertically pointed pulsed sound source and a collocated receiver. A small portion of each sound pulse is scattered back to the receiver by the thermal fluctuations which occur naturally in the air. The receiver measures the intensity of the returned sound. As in a conventional radar, the time delay between transmitting and receiving an echo is indicative of the target's range. In a bistatic sodar, the receiver is located some distance away from the sound source to receive signals caused by velocity fluctuations.

As well as measuring the intensity of the return signal, a monostatic Doppler sodar also analyses the frequency spectrum of the transmitted and received signals to determine the Doppler frequency shift between transmitted and backscattered sound. This difference arises because of the motion of the temperature fluctuations with the air, and provides a measure of the radial wind speed of the air. A Doppler sodar typically uses three beams, one directed vertically and two tilted from the vertical to determine wind components in three directions. The vertical and horizontal winds are calculated from these components. The vector wind may be displayed on a time-height plot at height intervals of about 30 to 50 m.

The maximum height that can be reached by acoustic sounders is dependent on system parameters, but also varies with the atmospheric conditions. Economical systems can routinely reach heights of 600 m or more with height resolutions of a few tens of metres.

A sodar might have the following characteristics:

Parameter	*Typical value*
Pulse frequency	1 500 Hz
Pulse duration	0.05 to 0.2 s
Pulse repetition period	2 to 5 s
Beam width	15°
Acoustic power	100 W

Monostatic sodars normally produce a time-height plot of the strength of the backscattered echo signal. Such plots contain a wealth of detail on the internal structure of the boundary layer and can, in principle, be used to monitor inversion heights, the depth of the mixing layer – changes in boundary stability – and the depth of fog. The correct interpretation of the plots, however, requires considerable skill and background knowledge, and preferably additional information from in situ measurements and for the general weather situation.

Monostatic Doppler sodar systems provide measurements of wind profiles as well as intensity information. Such systems are a cost-effective method of obtaining boundary layer winds and are particularly suited to the continuous monitoring of inversions and winds near industrial plants where pollution is a potential problem.

The main limitation of sodar systems, other than the restricted height coverage, is their sensitivity to interfering noise. This can arise from traffic or as a result of precipitation or strong winds. This limitation precludes their use as an all weather system. Sodars produce sound, the nature and level of which is likely to cause annoyance in the near vicinity, and this may preclude their use in otherwise suitable environments.

Some systems rely upon absorbent foam to reduce the effect of external noise sources and to reduce any annoyance caused to humans. The physical condition of such foam deteriorates with time and must be periodically replaced in order to prevent deterioration in instrument performance.

5.2.2   **Wind profiler radars**

Wind profilers are very-high and ultra-high-frequency Doppler radars designed for measuring wind profiles in all weather conditions. These radars detect signals backscattered from radio refractive index irregularities associated with turbulent eddies with scales of one half of the radar wavelength (the Bragg condition). As the turbulent eddies drift with the mean wind, their translational velocity provides a direct measure of the mean wind vector. Unlike conventional

weather radars, they are able to operate in the absence of precipitation and clouds. Profilers typically measure the radial velocity of the air in three or more directions — vertically and 15° off-vertical in the north and east direction — and from these components they determine the horizontal and vertical wind components. Simpler systems may only measure the radial velocity in two off-vertical directions and, by assuming that the vertical air velocity is negligible, determine the horizontal wind velocity. The four-beam profiler wind measurement technique is more practical than the three-beam profiler technique in that its measurement is not affected significantly by vertical wind (Adachi et al., 2005).

For further discussion see Gossard and Strauch (1983), Hogg et al. (1983), Weber et al. (1990), Weber and Wuertz (1990) and WMO (1994).

The nature of the scattering mechanism requires wind profiler radars to function between 40 and 1 300 MHz. Performance deteriorates significantly at frequencies over 1 300 MHz. The choice of operating frequency is influenced by the required altitude coverage and resolution. In practice, systems are built for three frequency bands (around 50 MHz, 400 MHz and 1 000 MHz) and these systems operate in low mode (shorter pulse: lower altitude) and high mode (longer pulse: higher altitude) which trade vertical range for resolution. Typical characteristics are summarized in the table below.

Profiler parameter	Stratosphere	Troposphere	Lower troposphere	Boundary layer
Frequency (MHz)	50	400	400	1 000
Peak power (kW)	500	40	2	1
Operating height range (km)	3–30	1–16	0.6–5	0.3–2
Vertical resolution (m)	150	150	150	50–100
Antenna type	Yagi-array	Yagi-array or Coco	Yagi-array or Coco	Dish or phased array
Typical antenna size (m)	100×100	10×10	6×6	3×3
Effect of rain or snow	Small	Small in light rain	Small in light rain	Great

Profilers are able to operate unattended and to make continuous measurements of the wind almost directly above the site. These features are the principal advantages that profilers have over wind-measuring systems which rely on tracking balloons.

Any given profiler has both minimum and maximum ranges below and above which it cannot take measurements. The minimum range depends on the length of the transmitted pulse, the recovery time of the radar receiver and the strength of ground returns received from nearby objects. Thus, care must be taken in siting profilers so as to minimize ground returns. Sites in valleys or pits may be chosen so that only the ground at very short range is visible. These considerations are most important for stratospheric profilers. The extent of the ground clutter effects on higher frequency radars can be reduced by suitable shielding.

The signal received by profilers generally decreases with increasing height. This ultimately limits the height to which a given profiler can take measurements. This maximum range is dependent on the characteristics of the radar and increases with the product of the mean transmitter power and the antenna aperture, but is subject to an absolute limit determined by the radar frequency used. These factors mean that the large high-powered stratospheric profilers are able to take measurements at the greatest heights. For a given profiler, however, the maximum height varies considerably with the meteorological conditions; on occasions there may be gaps in the coverage at lower heights.

Because it is important to take measurements at the maximum height possible, profilers gather data for several minutes in order to integrate the weak signals obtained. Typically, a profiler may take 6 or 12 min to make the three sets of observations required to measure the wind velocity. In many systems, a set of such observations is combined to give an hourly measurement.

Because profilers are made to be sensitive to the very weak returns from atmospheric inhomogeneities, they can also detect signals from aircraft, birds and insects. In general, such signals confuse the profilers and may lead to erroneous winds being output. In these circumstances, a number of independent measurements will be compared or combined to give either an indication of the consistency of the measurements or reject spurious measurements.

In the 1 000 and 400 MHz bands, precipitation is likely to present a larger target than the refractive index inhomogeneities. Consequently, the measured vertical velocity is reflectivity-weighted and is not operationally useful.

Large stratospheric profilers are expensive and require large antenna arrays, typically 100 m x 100 m, and relatively high power transmitters. Because they are large, it can be difficult to find suitable sites for them, and their height resolution and minimum heights are not good enough for certain applications. They have the advantage of being able to take routinely wind measurements to above 20 km in height, and the measurements are unaffected by all but the heaviest of rainfall rates.

Tropospheric profilers operating in the 400–500 MHz frequency band are likely to be the most appropriate for synoptic and mesoscale measurements. They are of modest size and are relatively unaffected by rain.

Boundary layer profilers are less expensive and use small antennas. Vertical velocity cannot be measured in rain, but raindrops increase the radar cross-section and actually increase the useful vertical range for the measurement of horizontal wind.

Profilers are active devices and obtaining the necessary frequency clearances is a serious problem in many countries. However, national and international allocation of profiler frequencies is actively being pursued.

5.2.3   Radio acoustic sounding systems

A radio acoustic sounding system is used to measure the virtual temperature profile in the lower troposphere. The technique consists in tracking a short high-intensity acoustic pulse that is transmitted vertically into the atmosphere by means of a collocated microwave Doppler radar. The measuring technique is based on the fact that acoustic waves are longitudinal waves that create density variations of the ambient air. These variations cause corresponding variations in the local index of refraction of the atmosphere which, in turn, causes a backscattering of the electromagnetic energy emitted by the microwave Doppler radar as it propagates through the acoustic pulse. The microwave radar measures the propagation speed of these refractive index perturbations as they ascend at the local speed of sound. The acoustic wavelength is matched to one half of the microwave wavelength (the Bragg condition), so that the energy backscattered from several acoustic waves adds coherently at the receiver, thus greatly increasing the return signal strength. By measuring the acoustic pulse propagation speed, the virtual temperature can be calculated as this is proportional to the square of the pulse propagation speed minus the vertical air speed.

The extensive literature on this technique includes May et al. (1990), Lataitis (1992*a*, 1992*b*) and Angevine et al. (1994).

A variety of experimental techniques have been developed to sweep the acoustic frequency and then to obtain a virtual temperature profile. A number of RASSs have been developed by adding an acoustic source and suitable processing to existing profiler radars of the type mentioned above. For radar frequencies of 50, 400 and 1 000 MHz, acoustic frequencies of about 110, 900 and 2 000 Hz are required. At 2 000 Hz, acoustic attenuation generally limits the height coverage to 1 to 2 km. At 900 Hz, practical systems can reach 2 to 4 km. At 110 Hz, by using large 50 MHz profilers, maximum heights in the range of 4 to 8 km can be achieved under favourable conditions.

Comparisons with radiosondes show that, under good conditions, virtual temperatures can be measured to an accuracy of about 0.3 °C with height resolutions of 100 to 300 m. However, the measurements are likely to be compromised in strong winds and precipitation.

The RASS technique is a promising method of obtaining virtual temperature profiles, but further investigation is required before it can be used operationally with confidence over a height range, resolution and accuracy that respond to user requirements.

5.2.4 Microwave radiometers

Thermal radiation from the atmosphere at microwave frequencies originates primarily from molecular oxygen, water vapour and liquid water and is dependent on their temperature and spatial distribution. For a gas such as oxygen, whose density as a function of height is well known, given the surface pressure, the radiation contains information primarily on the atmospheric temperature. Vertical temperature profiles of the lower atmosphere can be obtained by surface-based passive microwave radiometers measuring the microwave thermal emission by oxygen in a spectral band near 60 GHz. Spectral measurements in the 22–30 GHz upper wing of the pressure broadened water vapour absorption band provide information on the integrated amount of water vapour and liquid water, and the vertical distribution of water vapour. In addition, spectral measurements in both bands, combined with infrared cloud-base temperature measurements, provide information on the integrated amount and the vertical distribution of liquid water. For further information, see Hogg et al. (1983), Westwater et al. (1990), Solheim et al. (1998), Ware et al. (2003) and Westwater et al. (2005).

Individual downward-looking radiometers operating at different frequencies are maximally sensitive to temperature at particular ranges of atmospheric pressure. The sensitivity as a function of pressure follows a bell-shaped curve (the weighting function). The frequencies of the radiometers are chosen so that the peaks in the weighting functions are optimally spread over the heights of interest. Temperature profiles above the boundary layer are calculated by means of numerical inversion techniques using measured radiations and weighting functions. The relatively broad width of the weighting function curves, and radiation from the terrestrial surface, precludes accurate temperature profiles from being obtained near the surface and in the boundary layer when using space-based radiometer soundings.

The principles of upward-looking radiometric temperature and humidity sounding from the terrestrial surface are well established. The temperature weighting functions of upward-looking profiling radiometers have narrow peaks near the surface that decrease with height. In addition, sensitivity to oxygen and water vapour emissions is not degraded by radiation from the terrestrial surface. This allows accurate temperature and humidity profile retrievals with relatively high resolution in the boundary layer and lower troposphere. Inversion techniques for upward-looking radiometers are based on temperature and humidity climatology for the site that is typically derived from radiosonde soundings. The scanning configuration of microwave temperature profilers provides the highest resolution in the first few hundred metres. A multichannel system with fixed angle gives a better response at height greater than 1 km, but with a much coarser resolution (Cadeddu et al., 2002).

Surface-based and space-based radiometers are highly complementary. Space-based measurements provide coarse temporal and spatial resolution in the upper troposphere, and surface-based measurements provide high temporal and spatial resolution in the boundary layer and lower troposphere. Retrieved profiles from surface-based radiometers can be assimilated into numerical weather models to improve short term (1–12 h) forecasting by providing upper-air data in the interval between radiosonde soundings. Alternatively, raw brightness temperature from terrestrial radiometers can be assimilated directly into numerical weather models. This approach improves results by avoiding errors inherent in the profile retrieval process. A similar method, which assimilates raw satellite radiometer radiances directly into weather models, demonstrated improved results years ago and is now widely used.

The main advantages of surface-based radiometers are their ability to produce continuous measurements in time, and their ability to measure cloud liquid. Continuous upper-air

temperature, humidity and cloud liquid measurements can be used to improve nowcasting and short-term precipitation forecasting. These continuous measurements can be also used to detect the development or time of arrival of well-defined temperature changes (for studies of gas emissions, air pollution, urban heat islands, severe weather forecasting and warnings) (Kadygrov et al., 2003).

Profiling radiometer reliability and accuracy have been widely demonstrated during long-term arctic, mid-latitude and tropical operations (Güldner and Spänkuch, 2001; Liljegren et al., 2005). The result of the 13-month operation of the Radiometrics MP3000 (Gaffard and Hewison, 2003) shows that the root mean square value of the difference between the temperature observed by the radiosonde and that retrieved by the microwave radiometer ranges from 0.5 K (near the surface) to 1.8 K (at a height of 5 km). Güldner and Spänkuch (2001), who operated the Radiometrics TP/WVP-3000 for 18 months and compared retrievals with four radiosonde soundings daily, also shows a similar root mean square value from 0.6 K (near the surface) to 1.6 K (at a height of 7 km in summer and 4 km in winter). The root mean square value of water vapour profile is not more than 1 g m^{-3} in all altitudes (Gaffard and Hewison, 2003; Güldner and Spänkuch, 2001).

Terrestrial profiling radiometers demonstrate significant economic and practical advantage whenever lower tropospheric temperature, humidity and cloud liquid measurements with high temporal resolution are required, and where moderate vertical resolution is acceptable. Commercial profiling radiometer prices have dropped significantly over the past several years, and are now less than the typical annual cost of labour and materials for twice daily radiosonde soundings.

5.2.5   Laser radars (lidars)

Electromagnetic energy at optical and near-optical wavelengths (from ultraviolet through visible to infrared) generated by lasers is scattered by atmospheric gas molecules and suspended particles. Such scattering is sufficient to permit the application of the radar principle to make observations of the atmosphere by means of lidar (light detection and ranging). Optical scattering can generally be divided into inelastic and elastic. When the wavelength of the laser energy, scattered by atmospheric constituents, differs in wavelength from the incident laser wavelength, the process is called inelastic scattering. The most widely used inelastic scattering process used in experimental atmospheric lidar systems is Raman scattering, which results from an exchange of energy between incident photons and the molecular rotational and vibrational states of the scattering molecules. In elastic scattering processes, the incident and the scattered wavelengths are the same. This scattering may be Rayleigh or Mie scattering and depends on the species and size of particles with respect to the incident laser wavelength (see Part II, Chapter 7). Both of these major scattering processes can occur simultaneously in the atmosphere.

For further reference see Hinkley (1976), WMO (1982), Thomas (1991) and Syed and Browell (1994).

The majority of lidars are operated in a monostatic mode, whereby the receiver is collocated with the laser transmitter. A typical lidar system uses a pulsed laser to transmit pulses of coherent light into the atmosphere. The average power of the laser used varies from a few milliwatts to tens of watts. An optical telescope mounted adjacent to the laser is used to capture the backscattered energy. The light collected by the telescope is focused onto a photomultiplier or photoconductive diode. The received information is normally made available on a display for real-time monitoring and is transferred to a computer for more detailed analysis.

The strength of the return signal is dependent both on the amount of scattering from the target and on the two-way attenuation between the lidar and the target — this attenuation depends on the proportion of the beam's energy scattered from its path and on the absorption by atmospheric gases. The scattering and absorption processes are exploited in different lidars to provide a variety of measurements.

Lidars based on elastic scattering (called Rayleigh or Mie lidars, or simply lidars), are mostly used for studies on clouds and particulate matter. The measurement of cloud-base height by a lidar is very straightforward; the rapid increase in the signal that marks the backscattered return from the cloud base can be readily distinguished; the height of the cloud base is determined by measuring the time taken for a laser pulse to travel from the transmitter to the cloud base and back to the receiver (see Part I, Chapter 15).

Lidars are also used to detect the suspended particles present in relatively clear air and to map certain structural features such as thermal stability and the height of inversions. Natural atmospheric particulate levels are sufficiently high in the lower atmosphere to allow lidars to measure air velocities continuously in the absence of precipitation, like weather radars. For the measurement of atmospheric wind, the most commonly used methods include pulsed and continuous-wave coherent Doppler wind lidar, direct-detection Doppler wind lidar and resonance Doppler wind lidar. The annex to this chapter discusses the requirements and performance test procedures for heterodyne pulsed Doppler lidar techniques.

Lidars can also be used to map and measure the concentration of man-made particulates, such as those originating from industrial stacks. Lidar observations have made very extensive and the best-documented contributions to the study of stratospheric aerosol particulate concentration, which is strongly influenced by major volcanic eruptions and is an important factor in the global radiation balance.

It is much more difficult to obtain quantitative data on clouds, because of the variations in shape and distribution of droplets, water content, discrimination between water, ice and mixed phases, and the properties of suspended particles and aerosols. Indeed, such measurements require complex multiparameter research systems making several measurements simultaneously, using hypotheses concerning the optical properties of the medium, and complex mathematical data-reduction methods.

Differential absorption lidars (DIALs) work on the principle that the absorption coefficient of atmospheric gases varies greatly with wavelength. A DIAL system normally uses a laser that can be tuned between two closely-spaced frequencies, one which is strongly absorbed by a particular gas, and one which is not. The differences in the measurements as a function of range can be used to estimate the concentration of the gas under study. This is a most promising remote-sensing technique for the measurement of atmospheric composition and has been successfully used to measure concentrations of water, sulphur dioxide, nitrogen dioxide and, in particular, ozone.

The application of Raman scattering is of particular interest because the scattered radiation is frequency shifted by an amount which depends on the molecular species (Stokes lines). The strength of the backscattered signal is related to the species concentration. Raman lidars do not require a particular wavelength or tuned laser; laser wavelengths can be selected in a spectral region free from atmospheric absorption. By measuring the Raman spectrum, spatially resolved measurements can be taken of preselected atmospheric constituents, which have been used to obtain tropospheric profiles of water vapour, molecular nitrogen and oxygen, and minor atmospheric constituents. The main disadvantages are the lack of sensitivity over long ranges owing to the small scattering cross-sections and the requirement for high power lasers, which can lead to eye-safety problems in practical applications.

Lidar systems have provided a great deal of useful information for research studies but have had limited impact as operational tools. This is because they are relatively expensive and require very skilled staff in order to be developed, set up and operated. In addition, certain lidars are able to operate only under restricted conditions, such as in darkness or in the absence of precipitation.

5.2.6 Global Navigation Satellite System

The main purpose of the Global Navigation Satellite System (GNSS) is positioning, but since an atmospheric term influences the accuracy of the position estimate, meteorological content can

be inferred from the estimated error. The time delay experienced by a signal originating from a satellite and measured by a receiver on Earth is related to the refractivity along the signal path, and thus also to the temperature and humidity along this path.

Meteorological information inferred from ground-based GNSS requires a surface network of GNSS receivers, a data connection and a processing facility. In general, a GNSS network of receivers is installed for land surveying purposes, and as a result close collaboration with national surveying institutes has been established in several countries. The collaboration is generally based on sharing sites and/or sharing information.

Additional information on processing techniques is available in WMO (2006b).

5.2.6.1 *Description of the Global Navigation Satellite System*

The GNSS consists of three segments: the space, the ground and the user segment. The space segment comprises a number of satellites in orbit. Currently four systems are deployed or are being deployed: GPS (United States), GLONASS (Russian Federation), Galileo (European Union) and Compass (China). GNSS satellites transmit time coded signals in a number of carrier wave frequencies which differ for different satellite systems.

The principle of GNSS is the same for all four systems. On-board atomic clocks control all signal components in the satellites. The ground segment controls the satellites for orbit adjustment and provides the broadcast ephemerides, which are disseminated to the user segment via the navigation message of the GNSS signal. A GNSS antenna and receiver (surface-based or space-borne) form the user segment. The receiver compares the time coded signal from the GNSS satellites with its own internal clock, from which the receiver can compute the pseudo ranges (P) to each satellite in view. When at least four pseudo ranges are observed the receiver can compute its position and its clock error. The standard positioning technique using the time coded signals has an accuracy of about 3–5 m.

The GNSS main observables are pseudo range (P) and carrier phase (L). For example, the GPS signals are broadcast at two different frequencies: namely L1 (1 575.42 MHz) and L2 (1 227.60 MHz). Both frequencies transmit P and L observables. Thus, for a dual-frequency receiver, four observables are available per epoch. Equations 5.1 and 5.2 present both P and L expressed as a sum of all error contributions forming the GNSS measurement, that is:

$$P = \rho + c\left(dt_{\mathrm{rec}} - dt_{\mathrm{sat}}\right) + \delta_{\mathrm{rel}} + L_{\mathrm{atm}} + I + K + M + \delta_{\mathrm{tide}} + \varepsilon_P \tag{5.1}$$

$$L = \rho + c\left(dt_{\mathrm{rec}} - dt_{\mathrm{sat}}\right) + \delta_{\mathrm{rel}} + L_{\mathrm{atm}} - I + N\,\omega_L + K + M + \delta_{\mathrm{tide}} + \varepsilon_L \tag{5.2}$$

where c is the speed of light, ρ is the geometric distance between the satellite phase centre and the receiver phase centre, dt_{sat} is the satellite clock offset, dt_{rec} is the receiver clock offset, L_{atm} is the tropospheric delay, or slant total delay, due to the refractive nature of the atmosphere, I is the ionospheric delay along the ray path, δ_{rel} is the relativistic error, K is the receiver instrumental error, M is the multipath effect, δ_{tide} is the receiver position error due to polar tide, solid Earth tide and ocean loading, N is the ambiguity term (only relevant for carrier phase measurements, equation 5.2), ω_L is one wavelength contribution due to circular polarization of the signal and ε is the unmodelled noise error.

The observables have different uncertainty levels and different characteristics. In particular, phase measurements have a noise level of a few millimetres and are very accurate in comparison to pseudo range, which has an uncertainty of a few metres. Carrier phase is the primary and most important observable for low uncertainty parameter estimation, but pseudo-range observables are better suited for the observation and removal of specific receiver-related errors (multipath, etc.). Linear combination of the same kind of observable (P or L) measured at the two different frequencies is used to remove the first order of the ionosphere effect. Other techniques, such as double differencing, can remove the satellite and receiver clock error. However, this requires careful processing of the GNSS data.

5.2.6.2 *Tropospheric Global Navigation Satellite System signal*

The atmospheric excess path is caused by refraction and bending of the signal due to gradients in refractive index n. According to Fermat's principle, this excess path is:

$$L_{\text{atm}} = {}_s\!\int n\ ds - D + \Delta S \approx {}_s\!\int (n-1)\ ds \tag{5.3}$$

where $D\ (={}_s\!\int ds)$ is the geometric distance and ΔS the excess path due to bending; the latter can be neglected for elevations larger than 10 degrees. The refractivity N is defined as $N = 106\ (n-1)$ and, according to Smith and Weintraub (1953) and Thompson et al. (1986),

$$\begin{aligned} N &= k_1\, \rho\, R_d + \left(k_2 R_v - k_1 R_d + R_v / T\, k_3\right) \rho_w \\ &= N_h + N_w \end{aligned} \tag{5.4}$$

for the neutral atmosphere. Here, ρ is air density (kg m^{-3}), ρ_w is water vapour density (kg m^{-3}), T is temperature (K) and $R_d = 287.05$ J kg^{-1} K^{-1} and $R_v = 461.51$ J kg^{-1} K^{-1} are the gas constants for dry air and water vapour. The empirical constants are $k_1 = 77.6$ K hPa^{-1}, $k_2 = 70.4$ K hPa^{-1} and $k_3 = 373\ 900$ K^2 hPa^{-1} (Thayer, 1974). The first term in equation 5.4 is the hydrostatic refractivity, N_h, and the second term is called the wet refractivity, N_w.

Within a so-called network solution of GNSS data, the tropospheric delay is mapped to the zenith for all elevation and azimuth angles. In this way the number of unknowns is reduced and the position of the receiver can be estimated accurately. The mapped slant total delay to the zenith is called the zenith total delay (ZTD). When the precise position is estimated, an estimate of the atmospheric part of the signal can be retrieved. The ZTD can be considered as the sum of the zenith hydrostatic delay (ZHD) and the zenith wet delay (ZWD) (or, better, zenith non-hydrostatic delay). The integrals in the zenith direction of the hydrostatic and wet refractivity (expressed in metres) are:

$$\text{ZHD} = 10^{-6}\ {}_z\!\int N_h\ dz \tag{5.5}$$

$$\text{ZWD} = 10^{-6}\ {}_z\!\int N_w dz \tag{5.6}$$

5.2.6.3 *Integrated water vapour*

Zenith hydrostatic delay is related to the dry part of the atmosphere and, due to its stationary nature, can be estimated very accurately using the surface pressure measurements (p_s) and the location of the receiver (height h and latitude φ), using for example the Saastamoinen (1972) approximation, that is:

$$\text{ZHD}_{\text{saas}}\left(p_s, h, \varphi\right) = 2.2768 \cdot 10^{-5}\, p_s \left(1 - 2.66 \cdot 10^{-3} \cos\left(2\varphi\right) - 2.8 \cdot 10^{-7} h\right)^{-1} \tag{5.7}$$

The ZHD represents approximately 90% of the entire tropospheric path delay. On the other hand, the ZWD cannot be sufficiently well modelled by surface data acquisition due to the irregular distribution of water vapour in the atmosphere. The ZWD can be rewritten as (following Davis et al., 1985):

$$\text{ZWD} = 10^{-6} \left[k_2 R_v - k_1 R_d + k_3 R_v \left({}_z\!\int \rho_w\ T^{-1}\ dz \right) \left({}_z\!\int \rho_w\ dz \right)^{-1} \right] {}_z\!\int \rho_w\ dz \tag{5.8}$$

and by defining the weighted mean temperature as:

$$T_m = \left({}_z\!\int \rho_w\ dz \right) \left({}_z\!\int \rho_w\ T^{-1}\ dz \right)^{-1} \tag{5.9}$$

then:

$$\text{ZWD} = k'\left(T_m\right) {}_z\!\int \rho_w\ dz = k'\left(T_m\right) \text{IWV} \tag{5.10}$$

where IWV is the vertically integrated column of water vapour overlying the GPS receiver. Based on, for example, radiosonde observations, the weighted mean temperature can be estimated

by the surface temperature (T_s), that is $k'(T_m) \approx k(T_s)$ (Bevis et al., 1994). Thus, the IWV can be estimated using the estimated ZTD, surface pressure (p_s), antenna height (h) and latitude (φ) of the receiver:

$$\text{IWV} = k\left(T_s\right)^{-1}\left(\text{ZTD} - \text{ZHD}_{\text{saas}}\left(p_s, h, \varphi\right)\right) \tag{5.11}$$

The value of $k(T_s)$ is approximately 6.5 kg m^{-3}.

5.2.6.4   *Measurement uncertainties*

Since ZTD is estimated, its accuracy depends on the method used, the accuracy of a priori information used, the stability of the receiver position and many other things. For example, the accuracy of the position of the satellite orbits will in general be higher after approximately 14 days when the so-called final orbits are available. Therefore, a distinction has to be made between near-real-time and post-processed estimates of ZTD. The accuracy of IWV is obviously closely related to the accuracy of the ZTD estimate.

The measurement uncertainty of near-real-time estimates is about 10 mm. For post-processed estimates, this value is about 5 to 7 mm. The measurement uncertainty of IWV is dependent on the total amount of water vapour and is of the order of 5%–10% (Elgered et al., 2004). The mean values have a clear seasonal signature: at mid latitudes very low values can be observed in winter (below 5 kg m^{-2}) and values of 40 kg m^{-2} can be seen during summer. In the tropics, values higher than 50 kg m^{-2} are not uncommon.

5.3   IN SITU MEASUREMENTS

5.3.1   Balloon tracking

Balloon tracking is frequently used to obtain boundary layer winds and is usually performed by optical theodolites or a tracking radar. Part I, Chapter 13, gives a more general account of windfinding.

When making lower tropospheric soundings, it is desirable to use a slow rate of balloon ascent in order to give high vertical resolution. The reduced rate of ascent may be achieved either by means of a brake parachute or by a reduced free lift.

For radar tracking, a small radar reflector is suspended below the balloon. For lower tropospheric soundings, the radar should be able to provide data at ranges as short as 100 m, and ideally the launch point must be farther away in a downwind direction than this minimum range.

A basic wind measurement can be taken using a single optical theodolite, but, in order to obtain reasonably accurate winds, a two-theodolite system is required. The baseline between the theodolites should exceed 1 km. In order to facilitate the sounding procedure and to ensure height accuracy, the theodolites should be equipped with computer interfaces so that the data can be logged and the necessary calculations performed in a timely manner. Under good conditions, wind profiles can be obtained up to an altitude of 3 000 m. However, the technique fails in adverse conditions such as precipitation, low cloud or fog.

It is, of course, possible to obtain additional wind data in the lower atmosphere using conventional radiosondes by taking more frequent tracking measurements in the first few minutes of a normal full sounding, for example, between 2 and 10 per minute.

5.3.2   Boundary layer radiosondes

Conventional radiosonde systems are described in detail in Part I, Chapter 12. Special radiosondes have been designed specifically to make detailed observations of the boundary

layer and lower troposphere. They differ from conventional radiosondes in that the sensors have greater sensitivity and faster response rates. Such radiosondes are used to measure temperature, humidity and wind profiles in the layer from the surface to elevations of typically 3 to 5 km.

The vertical ascent rate of these radiosondes is usually arranged to be between 150 and 200 m min^{-1}, which is rather slower than conventional radiosondes. The slower rate of ascent allows more detailed vertical profiles to be produced. The rate of ascent is normally determined by selecting an appropriately sized balloon, but may be modified by the use of a trailing brake parachute.

Because these instruments are required only to reach a limited height, they can normally be carried by a pilot balloon. In other respects, the sounding procedures and data processing are similar to those employed by standard radiosondes.

For soundings to an altitude of no more than 2 000 m, the pressure sensor is sometimes dispensed with, which results in a simpler and less expensive radiosonde. Even simpler systems are available which measure temperature only.

The basic requirements for boundary layer radiosondes are as follows:

Variable	Operating range	Resolution
Pressure	1 050 to 500 hPa	±0.5 hPa
Temperature	+40 °C to –40 °C	±0.1 K
Humidity	100% to 20 (or 10)%	±2%
Wind speed	0.5 to 60 m s^{-1}	±0.5 m s^{-1}
Wind direction	0° to 360°	±5°

Measurements are typically taken at least every 30 s to give a vertical resolution of 50 to 100 m.

5.3.3   Instrumented towers and masts

Special instrumented towers and masts are used for many purposes, especially for the estimation of the diffusion of atmospheric pollution. A discussion is provided by Panofsky (1973).

For some purposes, the height of the tower must be up to 100 m, and for air-pollution monitoring and control projects it should exceed the height of the important sources of pollution by at least 50 m.

Measurements of temperature, humidity and wind should be made at several (at least two or three) levels, the lowest of which should be at the level of standard meteorological screen, close to the tower or mast. The number of measuring levels depends upon both the task and the height of the tower or mast. The use of just two levels provides no information on the shape of the vertical profile of meteorological variables and is, thus, very limiting. The number of measuring levels is usually greater for research projects than for routine use.

Usually, the data are processed and presented automatically together with differences between the levels that are provided to characterize the meteorological conditions. If the data are to be used directly by non-meteorological staff – such as those concerned with keeping concentrations of air pollutants within safe limits – they are often processed further by computer to provide derived data which are easily applied to the task in hand.

The sensors most commonly used for measurements on towers or masts are as follows:

(a)   Temperature: electrical resistance or thermocouple thermometers in screens, with or without aspiration;

(b)   Humidity: psychrometers, electrochemical or electromechanical sensors in screens;

(c)   Wind: cup and vane, propeller, sonic or hot-wire devices.

All sensors should have linear or linearized characteristics and their time constants should be small enough to ensure that the data gathered will adequately reflect local changes in the meteorological variables.

It is important that the structure of the tower or mast should not affect the sensors and their measurements appreciably. For open structures, booms – whether stationary or retractable – should be at least 2 m long, and preferably long enough to keep the sensors at least 10 tower diameters removed from the tower or mast. For solid structures, or where the required booms would not be practicable, a double system is required at each level, with booms on opposite sides of the tower or mast extending for at least three times the structure diameter. Measurements at a given time are then taken from the sensors exposed to the undisturbed wind.

Sometimes, in special situations, towers can be used to gather meteorological profile data without the direct mounting of fixed sensors; rather, a simplified method of sounding is used. A pulley is fastened at the highest possible point and a closed loop of rope extending to ground level is used to carry a radiosonde up and down the levels required by means of a hand- or motor-operated winch. The radiosonde, which is modified to include wind sensors, transmits its data to an appropriate receiving system at ground level. Much more vertical detail is possible than that provided by a boom installation, and the altitudes of significant features can be determined. However, sustained observation is possible at only a single level.

For an accurate definition of the extent of pollution dispersion in certain weather conditions, the tower height may be too limited. In such circumstances, unless a radiosonde station is within about 50 km, a special radiosonde is provided at the site of the tower or mast for making local soundings up to an altitude of about 3 000 m. In addition to their main purpose, the data obtained can be treated as complementary to those of the basic aerological network, and can also be used in more detailed investigations of local weather phenomena.

Tower measuring equipment requires periodical checking by highly qualified instrument maintenance staff who should pay special attention to the state and performance of sensors and recorders and the connecting cables, sockets and plugs exposed to outdoor weather conditions.

5.3.4   **Instrumented tethered balloons**

Typical applications of instrumented tethered balloons include the measurement of temperature, humidity and wind profiles (and their short-period changes) from the surface to an altitude of about 1 500 m, and longer-period investigation of the meteorological conditions at one or more selected levels. The sensors are suspended in one or more packages beneath the balloon, or clamped to the tethering cable. The sensor's response is normally telemetered to the ground either by radio, or by conductors incorporated into the tethering cable. The techniques are discussed by Thompson (1980).

Tethered-balloon systems tend to use either large (~600 m³) or small (~10 to 100 m³) balloons. The small balloons are normally used to obtain profiles, and the larger ones to obtain measurements at multiple levels. Tethered balloons should be designed for low drag and to ride steadily. They are usually inflated with helium. Larger balloons should be able to carry a load of up to 50 kg (in addition to the tethering cable) to an altitude of 1 500 m. The balloon should be capable of operation at wind speeds of up to 5 m s^{-1} at the surface and 15 m s^{-1} at altitudes within the operational range. The tethering cable of a large balloon should be able to withstand a force of 2 000 to 3 000 kg to avoid a breakaway (200 to 300 kg for smaller balloons).

Tethered-balloon flying is subject to national rules concerning aviation safety. For this reason and for the convenience of the operating staff, the use of balloons which have distinct colours and night-warning lights is highly recommended. An automatic device for the rapid deflation of the balloon is mandatory, while a metallized radar target suspended below the balloon is optional.

The main factors limiting tethered-balloon operation are strong wind speed aloft, turbulence near the surface and lightning risk.

The winch used to control the balloon may be operated electrically or by hand. At least two speeds (e.g. 1 and 2 m s⁻¹) should be provided for the cable run. In addition, the winch should be equipped with a hand-brake, a cable-length counter and a tension gauge. The winch should be electrically earthed, whether electrically operated or not, as protection against atmospheric discharges.

The use of conductors to convey the sensor signals back to the ground is undesirable for a number of reasons. In general, it is preferable to use special radiosondes. Such radiosondes will have better resolution than those normally employed for free flights. The temperature and humidity sensors must have a horizontal shield to provide protection against solar radiation and rainfall, while allowing for adequate ventilation. Extra sensors are needed for wind speed and direction.

The basic requirements are the following:

Variable	Operating range	Resolution
Pressure	1 050 to 850 hPa	±0.5 hPa
Temperature	+40 °C to –20 °C	±0.1 K
Humidity	100% to 20 (or 10)%	±2%
Wind speed	0.5 to 15 m s⁻¹	±0.5 m s⁻¹
Wind direction	0° to 360°	±1°

For telemetry, one of the standard radiosonde frequencies may be used; the 400 MHz allocation is a frequent choice. The maximum weight, including the battery, should be within the load capability of the balloon; a limit of 5 kg is reasonable. The radiosonde should be suspended at least three balloon diameters below the balloon in a stable condition so that adequate shielding and ventilation are maintained.

A major problem encountered in the measurement of turbulent, rather than mean, quantities is the effect of cable vibration and balloon motion on the measurements. Special techniques have to be used for such measurements.

The ground-based equipment must include a receiver and recorder. The data are usually processed with the aid of a small computer.

Soundings can be performed during the ascent and descent of the balloon, either continuously or with pauses at selected levels. For the lower levels, height can be estimated from the length of the cable paid out, but at higher levels this method is no more than an approximation and an alternative is necessary. This takes the form of a calculation by means of the hydrostatic equation, using the observed distribution of pressure, temperature and humidity. Thus, the increment in geopotential metres from level n to level n+1 is given by:

$$29.27 \, T_v \ln\left(p_n / p_{n+1} \right) \tag{5.12}$$

where T_v is the mean of the virtual temperatures at levels n and n+1; and p_n and p_{n+1} are the two associated pressures. If conversion from geopotential to geometric height is required, this is readily done by using the Smithsonian meteorological tables; however, this is unlikely to be necessary. The height of the station barometer is taken as the datum for these calculations.

If the meteorological variables are observed using the level-by-level method, a few measuring cycles should be taken at each level, with the time required for stabilization being 2 to 3 min. In this way, the whole sounding sequence could take from a half to one whole hour. As for all radiosondes, a baseline check in a control screen should be made just before use, to establish the differences with a barometer and an aspirated psychrometer. A similar check should also be

made just after the sounding is completed. Again, as for regular radiosonde ascents, the station-level data should be obtained not from the radiosonde data, but from conventional instruments in a standard station screen.

For the sounding data, pressure, temperature and humidity should be averaged at each level. For wind speed, the average should be calculated for a period of 100 or 120 s. If wind direction is not measured directly, it can be roughly estimated from the orientation of the balloon's longitudinal axis with respect to the north. The uncertainty of this method is ±30°.

It should be stressed that operators must advise air traffic authorities of their plans and obtain permission for each sounding or series of soundings using tethered balloons.

———————————

ANNEX. GROUND-BASED REMOTE-SENSING OF WIND BY HETERODYNE PULSED DOPPLER LIDAR

(The text of the common ISO/WMO standard 28902-2:2017(E))

INTRODUCTION

Lidars (light detection and ranging), standing for atmospheric lidars in the scope of this annex, have proven to be valuable systems for remote-sensing of atmospheric pollutants, of various meteorological parameters such as clouds, aerosols, gases and (where Doppler technology is available) wind. The measurements can be carried out without direct contact and in any direction as electromagnetic radiation is used for sensing the targets. Lidar systems, therefore, supplement the conventional in situ measurement technology. They are suited for a large number of applications that cannot be adequately performed by using in situ or point measurement methods.

There are several methods by which lidar can be used to measure atmospheric wind. The four most commonly used methods are pulsed and continuous-wave coherent Doppler wind lidar, direct-detection Doppler wind lidar and resonance Doppler wind lidar (commonly used for mesospheric sodium layer measurements). For further reading, refer to references [1] and [2].

This annex[1] describes the use of heterodyne pulsed Doppler lidar systems. Some general information on continuous-wave Doppler lidar can be found in Attachment A. An International Standard on this method is in preparation.

1.   SCOPE

This annex specifies the requirements and performance test procedures for heterodyne pulsed Doppler lidar techniques and presents their advantages and limitations. The term "Doppler lidar" used in this annex applies solely to heterodyne pulsed lidar systems retrieving wind measurements from the scattering of laser light onto aerosols in the atmosphere. Their performances and limits are described based on standard atmospheric conditions.

This annex describes the determination of the line-of-sight wind velocity (radial wind velocity).

Note: Derivation of wind vector from individual line-of-sight measurements is not described in this annex since it is highly specific to a particular wind lidar configuration. One example of the retrieval of the wind vector can be found in Attachment B.

This annex does not address the retrieval of the wind vector.

This annex may be used for the following application areas:

(a)   Meteorological briefing for, e.g. aviation, airport safety, marine applications and oil platforms;

(b)   Wind power production, e.g. site assessment and power curve determination;

(c)   Routine measurements of wind profiles at meteorological stations;

(d)   Air pollution dispersion monitoring;

---

[1]   Whereas this is referred to as an annex in the *Guide to Meteorological Instruments and Methods of Observation* (WMO-No. 8), it is referred to as a standard in the ISO document.

(e)   Industrial risk management (direct data monitoring or by assimilation into micro-scale flow models);

(f)   Exchange processes (greenhouse gas emissions).

This annex addresses manufacturers of heterodyne pulsed Doppler wind lidars, as well as bodies testing and certifying their conformity. Also, this annex provides recommendations for the users to make adequate use of these instruments.

2.   **NORMATIVE REFERENCES**

There are no normative references in this annex.

3.   **TERMS AND DEFINITIONS**

For the purposes of this annex, the following terms and definitions apply.

Data availability: Ratio between the actual considered measurement data with a predefined data quality and the number of expected measurement data for a given *measurement period*;

Displayed range resolution: Constant spatial interval between the centres of two successive *range gates*;

Note: The displayed range resolution is also the size of a range gate on the display. It is determined by the range gate length and the overlap between successive gates.

Effective range resolution: Application-related variable describing an integrated range interval for which the target variable is delivered with a defined uncertainty;

  Source: ISO 28902-1:2012, term 3.14

Effective temporal resolution: Application-related variable describing an integrated time interval for which the target variable is delivered with a defined uncertainty;

  Source: ISO 28902-1:2012, term 3.12, modified

Extinction coefficient, α: Measure of the atmospheric opacity, expressed by the natural logarithm of the ratio of incident light intensity to transmitted light intensity, per unit light path length;

  Source: ISO 28902-1:2012, term 3.10

Integration time: Time spent in order to derive the line-of-sight velocity;

Maximum acquisition range, R_{MaxA}: Maximum distance to which the lidar signal is recorded and processed;

Note: It depends on the number of acquisition points and the sampling frequency.

Maximum operational range, R_{MaxO}: Maximum distance to which a confident wind speed can be derived from the lidar signal;

Notes:
1.   The maximum operational range is less than or equal to the maximum acquisition range.
2.   The maximum operational range is defined along an axis corresponding to the application. It is measured vertically for vertical wind profiler. It is measured horizontally for scanning lidars able to measure in the full hemisphere.

3.   The maximum operational range can be increased by increasing the measurement period and/or by downgrading the range resolution.
4.   The maximum operational range depends on lidar parameters but also on atmospheric conditions.

Measurement period: Interval of time between the first and last measurements;

Minimum acquisition range, R_{MinA}: Minimum distance from which the lidar signal is recorded and processed;

Note: If the minimum acquisition range is not given, it is assumed to be zero. It can be different from zero, when the reception is blind during the pulse emission.

Minimum operational range, R_{MinO}: Minimum distance where a confident wind speed can be derived from the lidar signal;

Notes:
1.   The minimum operational range is also called blind range.
2.   In pulsed lidars, the minimum operational range is limited by the stray light in the lidar during pulse emission, by the depth of focus, or by the detector transmitter/receiver switch time. It can depend on pulse duration (T_p) and range gate width.

Physical range resolution: Width (FWHM) of the *range weighting function*;

Range gate: Width (FWHM) of the weighting function selecting the points in the time series for spectral processing and wind speed computation;

Notes:
1.   The range gate is centred on the measurement distance.
2.   The range gate is defined in number of bins or equivalent distance range gate.

Range resolution: Equipment-related variable describing the shortest range interval from which independent signal information can be obtained;

    Source: ISO 28902-1:2012, term 3.13

Range weighting function: Weighting function of the radial wind speed along the line of sight;

Temporal resolution: Equipment-related variable describing the shortest time interval from which independent signal information can be obtained;

    Source: ISO 28902-1:2012, term 3.11

Velocity bias: Maximum instrumental offset on the velocity measurement;

Note: The velocity bias has to be minimized with adequate calibration, for example, on a fixed target.

Velocity range: Range determined by the minimum measurable wind speed, the maximum measurable wind speed and the ability to measure the velocity sign, without ambiguity;

Note: Depending on the lidar application, velocity range can be defined on the radial wind velocity (scanning lidars) or on horizontal wind velocities (wind profilers).

Velocity resolution: Instrumental velocity standard deviation;

Note: The velocity resolution depends on the pulse duration, the carrier-to-noise ratio and integration time.

Wind shear: Variation of wind speed across a plane perpendicular to the wind direction.

4.   **FUNDAMENTALS OF HETERODYNE PULSED DOPPLER LIDAR**

4.1   **Overview**

A pulsed Doppler lidar emits a laser pulse in a narrow laser beam (see Figure 5.A.1). As it propagates in the atmosphere, the laser radiation is scattered in all directions by aerosols and molecules. Part of the scattered radiation propagates back to the lidar; it is captured by a telescope, detected and analysed. Since the aerosols and molecules move with the atmosphere, a Doppler shift results in the frequency of the scattered laser light.

At the wavelengths (and thus frequencies) relevant to heterodyne (coherent) Doppler lidar, it is the aerosol signal that provides the principal target for measurement of the backscattered signal.

The analysis aims at measuring the difference, Δf, between the frequencies of the emitted laser pulse, f_t, and of the backscattered light, f_r. According to the Doppler's equation, this difference is proportional to the line-of-sight wind component, as shown in formula 5.A.1:

$$\Delta f = f_r - f_t = -2v_r / \lambda \tag{5.A.1}$$

where:

λ is the laser wavelength;

v_r is the line-of-sight wind component (component of the wind vector, $\vec{v}$, along the axis of laser beam, counted positive when the wind is blowing away from the lidar).
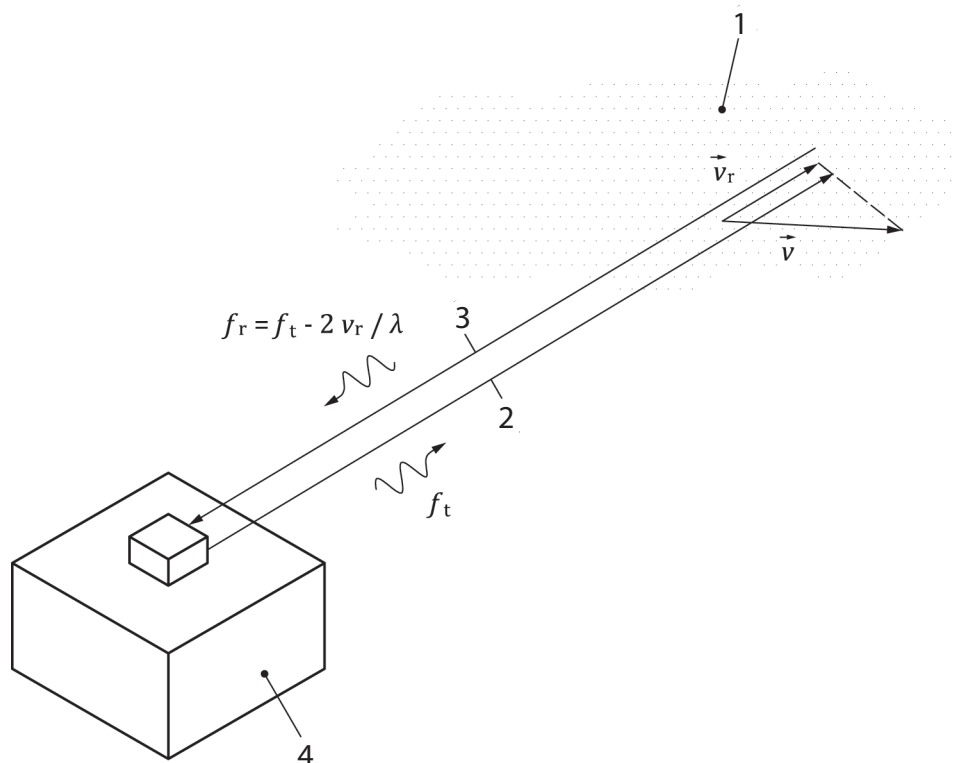
Key
1   Scattering particles moving with the wind
2   Optical path of the emitted laser pulse (laser beam)
3   Optical axis of the receiver
4   Lidar instrument

Figure 5.A.1. Measurement principle of a heterodyne Doppler lidar
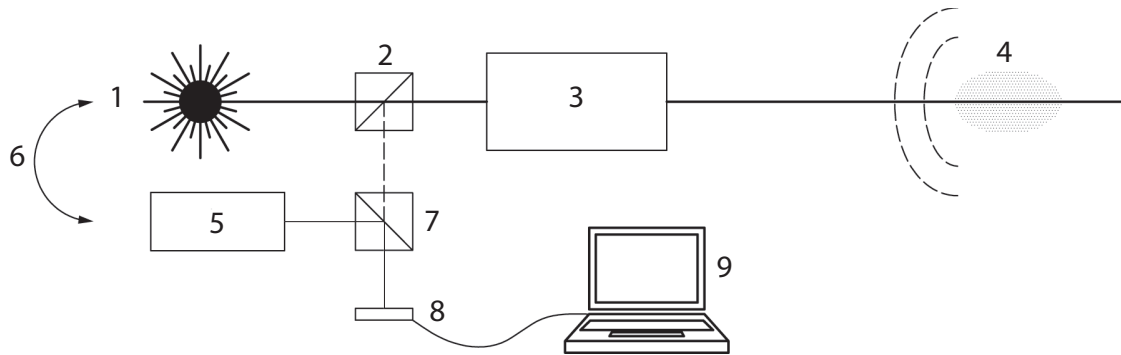
Key

1	Pulsed laser
2	Optical element separating the received and emitted lights
3	Telescope (used for transmitting and receiving)
4	Scatterers
5	Local oscillator laser (continuous-wave laser)
6	Frequency control loop (this device sets the difference, $f_t - f_{lo}$)
7	Optical element aligning the beam of the local oscillator along the optical axis of the received light beam and mixing them together
8	Quadratic detector
9	Analogue-to-digital converter and digital signal processing unit

Figure 5.A.2. Principle of the heterodyne detection

The measurement is range resolved as the backscattered radiation, received at time t after the emission of the laser pulse, has travelled from the lidar to the aerosols at range x and back to the lidar at the speed of light, c. Formula 5.A.2 shows the linear relationship between range and time.

$$x = c \cdot \frac{t}{2} \tag{5.A.2}$$

4.2 Heterodyne detection

In a heterodyne lidar, the detection of the light captured by the receiving telescope (at frequency $f_r = f_t + \Delta f$) is described schematically in Figure 5.A.2. The received light is mixed with the beam of a highly stable, continuous-wave laser called the local oscillator. The sum of the two electromagnetic waves – backscattered and local oscillator – is converted into an electrical signal by a quadratic detector (producing an electrical current proportional to the power of the electromagnetic wave illuminating its sensitive surface). An analogue high-pass filter is then applied for eliminating the low-frequency components of the signal.

The result is a current, $i(t)$, beating at the radio frequency, $f_t + \Delta f - f_{lo}$:

$$i(t) = \underbrace{2 \cdot \frac{\eta \cdot e}{h \cdot f_t} \cdot K \cdot \xi(t) \cdot \sqrt{\gamma(t) \cdot P_r(t) \cdot P_{lo}} \cdot \cos\left[2\pi\left(\Delta f + f_t - f_{lo}\right) \cdot t + \varphi(t)\right]}_{i_{het}(t)} + n(t) \tag{5.A.3}$$

where:

t is the time;

h is the Planck constant;

η is the detector quantum efficiency;

e is the electrical charge of an electron;

K is the instrumental constant taking into account transmission losses through the receiver;

$\xi(t)$ is the random modulation of the signal amplitude by speckles effect (see section 4.5.4);

$\gamma(t)$ is the heterodyne efficiency;

$P_r(t)$ is the power of the backscattered light;

P_{lo} is the power of the local oscillator;

f_{lo} is the frequency of the local oscillator;

$\varphi(t)$ is the random phase;

$n(t)$ is the white detection noise;

$i_{het}(t)$ is the heterodyne signal.

The heterodyne efficiency, $\gamma(t)$, is a measure for the quality of the optical mixing of the backscattered and the local oscillator wave fields on the surface of the detector. It cannot exceed 1. A good heterodyne efficiency requires a careful sizing and alignment of the local oscillator relative to the backscattered wave. Optimal mixing conditions are discussed in reference [3]. The heterodyne efficiency is not a purely instrumental function; it also depends on the refractive index turbulence (Cn^2) along the laser beam (see reference [4]). Under conditions of strong atmospheric turbulence, the effect on varying the refractive index degrades the heterodyne efficiency. This can happen when the lidar is operated close to the ground during a hot sunny day.

In formula 5.A.4, $P_r(t)$ is the instantaneous power of the backscattered light. It is given by the lidar equation (see reference [3]):

$$P_r(t) = A \cdot \int_0^{+\infty} x^{-2} \cdot G(x) \cdot g\left(t - \frac{2x}{c}\right) \cdot \beta(x) \cdot \tau^2(x)\, dx \qquad (5.A.4)$$

with

$$\tau(x) = \exp\left[-\int_0^x \alpha(\zeta)\, d\zeta\right]$$

where:

x is the distance to the lidar;

A is the collecting surface of the receiving telescope;

$G(x)$ is the range-dependent sensitivity function ($0 \le G(x) \le 1$) taking into account, for example, the attenuation of the receiver efficiency at short range to avoid the saturation of the detector;

$g(t)$ is the envelope of the laser pulse power ($\int g(t)\, dt = E_0$, with E_0 as the energy of the laser pulse);

$\beta(x)$ is the backscatter coefficient of the probed atmospheric target;

$\tau(x)$ is the atmospheric transmission as a function of the extinction coefficient, α.

4.3   Spectral analysis

The retrieval of the radial velocity measurement from heterodyne signals requires a frequency analysis. This is done in the digital domain after analogue-to-digital conversion of the heterodyne signals. An overview of the processing is given in Figure 5.A.3. The frequency analysis is applied to a time window ($t, t + \Delta t$) and is repeated for a number, N, of lidar pulses. The window defines a range gate ($x, x + \Delta x$) with $x = c \cdot t / 2$ and $\Delta x = c \cdot \Delta t / 2$. N is linked to the integration time,

$t_{int} = 1/f_{PRF}$, of the measurement (f_{PRF} is the pulse repetition frequency). The signal analysis consists in averaging the power density functions of the range gated signals. A frequency estimator is then used for estimating the central frequency of the signal peak. It is an estimate, $\hat{f}_{het}$, for the frequency, $f_{het} = \Delta f + f_t - f_{lo}$, of the heterodyne signal (see Figure 5.A.3).

Due to the analogue-to-digital conversion, the frequency interval resolved by the frequency analysis is limited to $(0, +F_s/2)$ or $(-F_s/2, +F_s/2)$ for complex valued signals. This limits the minimum and maximum values of $\hat{f}_{het}$ and thus the interval of measurable radial velocities. As shown in reference [5], formula 5.A.5 estimates a range-gate average of the true wind radial velocity:

$$\hat{v}_r = -\frac{\lambda}{2}\left(\hat{f}_{het} - f_t + f_{lo} \right)$$

(5.A.5)

For instance, in the case the signal is real valued (no complex-demodulation), the frequency offset $f_t - f_{lo}$ is set to about $F_s / 4$, so $|\hat{v}_r| \leq \lambda F_s / 8$. Alternatively, a system specification requiring the possibility to measure radial winds up to v_{max} commands $F_s \geq 8 v_{max} / \lambda$.

The averaging kernel is the convolution function between the pulse profile and the range-gate profile. Its length is a function of the pulse footprint in the atmosphere, Δr (see formula 5.A.6), of the range gate, Δx, and of the weighting factor, κ, where κ is the ratio between the gate full width at half maximum (FWHM) and Δx.

$$\Delta r = \frac{c \cdot T_p}{2}$$

(5.A.6)

where:

T_p is the FWHM duration of the laser pulse instantaneous intensity, $g(t)$.

The range resolution, ΔR, is defined as the FWHM of the averaging kernel. For a Gaussian pulse and an unweighted range gate, ΔR is calculated according to formula 5.A.7[6]:

$$\Delta R = \frac{c}{2} \cdot \frac{\Delta t}{\text{erf}\left(\frac{\sqrt{\pi} \cdot \Delta t}{2T_p} \right)} = \frac{\Delta x}{\text{erf}\left(\frac{\sqrt{\pi} \cdot \Delta x}{2\Delta r} \right)}$$

(5.A.7)

For a Gaussian pulse and a Gaussian weighted range gate, ΔR is equal to formula 5.A.8:

$$\Delta R = \frac{c}{2} \cdot \sqrt{T_p^2 + \left(\kappa \cdot \Delta t \right)^2} = \sqrt{\Delta r^2 + \left(\kappa \cdot \Delta x \right)^2}$$

(5.A.8)

As shown in Figure 5.A.3, several signals are considered and range gated. The average spectrum is computed and a frequency estimator is applied.

Successive range gates can be partially overlapping (then successive radial velocity measurements are partially correlated), adjacent or disjoint (then there is a "hole" in the line-of-sight profile of the radial velocity).

Several possible frequency estimators are presented in reference [6] with a first analysis of their performances. Their performances are further discussed in reference [7]. Whatever the estimator, the probability density function of the estimates is the sum of a uniform distribution of "bad" estimates (gross errors) spread across the entire band $[-f_{max}, f_{max}]$ and a relatively narrow distribution of good estimates often modelled by a Gaussian distribution, as shown in formula 5.A.9:

$$p\left(\hat{f}_{het} \right) = \begin{cases} \dfrac{b}{2f_{max}} + \dfrac{1-b}{\sqrt{2\pi}\sigma_f} \exp\left(-\dfrac{\left(\hat{f}_{het} - \overline{f}_{het} \right)^2}{2\sigma_f^2} \right), & \text{for } \hat{f}_r \in \left[-f_{max}, f_{max} \right] \\ 0 & \text{otherwise} \end{cases}$$

(5.A.9)

Key
t	Time elapsed since the emission of the laser pulse
Δt	Duration of the spectral analysis time window (it sets the size of the range gate)
N	Signal number
1	Pulses
2	Time series
3	Spectra
4	Doppler frequency
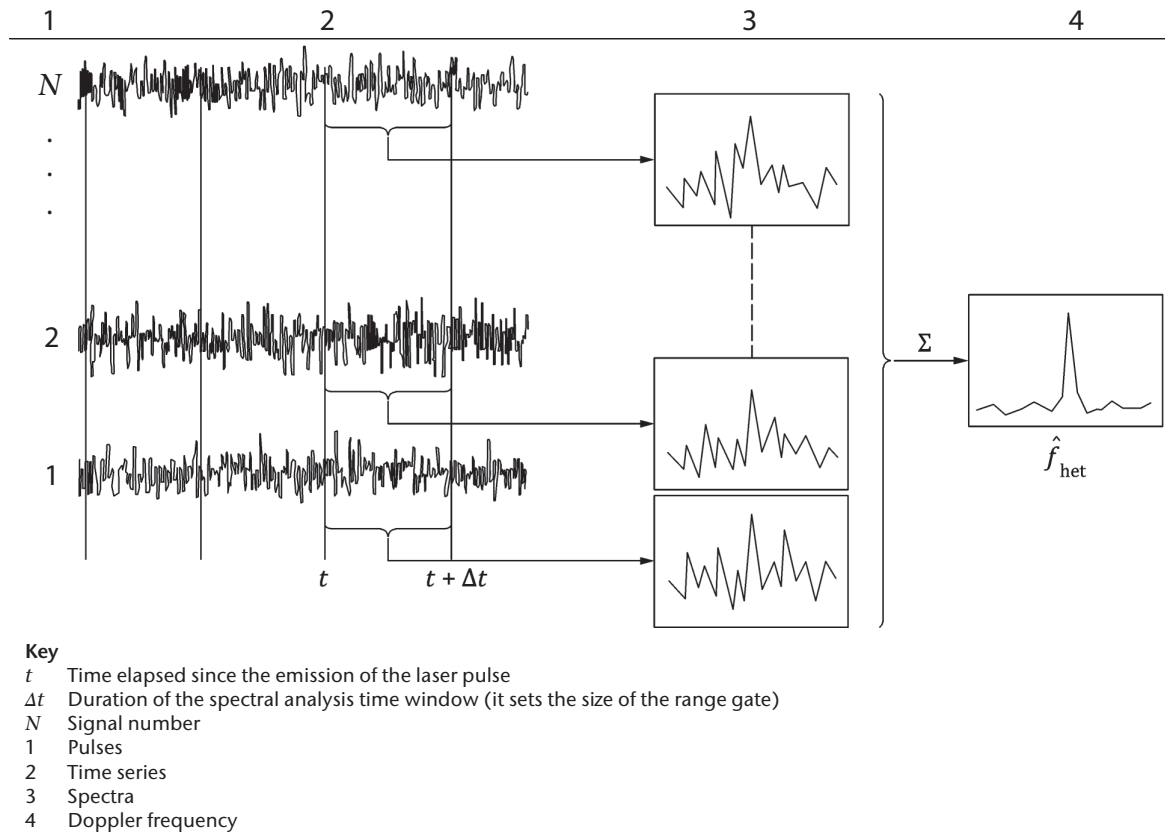
Figure 5.A.3. Diagram showing how the frequency analysis is conducted

In principle, the mean frequency, $\overline{f}_{het}$, can be different from the "true" heterodyne signal frequency, f_{het}. This can happen for instance when the frequency drifts during the laser pulse (chirp, see reference [8]). However, these conditions are rarely met and a good heterodyne Doppler lidar produces in practice unbiased measurements of Doppler shifts.

The parameter σ_f characterizes the frequency precision of the estimator. The corresponding radial velocity precision is $\sigma_v = \lambda \cdot \sigma_f / 2$. In a heterodyne system, it is typically of the order of several to several tens of centimetres per second. It degrades with the level of noise (power of $n(t)$ in formula 5.A.3) and improves with the number of accumulated signals, N. In practice the improvement is limited as the accumulation of a large number of signals results in a long integration time during which the natural variability (turbulence) of the wind increases.

Reference [9] discusses the presence of gross errors (also called outliers[1]) and proposes a model for the parameter b as a function of the several instrument characteristics and the level of detection noise. An outlier happens when the signal processor detects a noise peak instead of a signal peak. The parameter b is a decreasing function of the carrier-to-noise ratio. Quality checks must be implemented in heterodyne lidar systems so gross errors are filtered out and ignored as missing data. The presence of gross errors sets the maximum range of the lidar.

4.4   Target variables

The aim of heterodyne Doppler wind lidar measurements is to characterize the wind field. In each range interval, the evaluation of the measured variable leads to the radial velocity; see formula 5.A.5.

There are additional target values like the variability of the radial velocity that are not discussed in this annex.

The target variables can be used as input to different retrieval methods to derive meteorological products like the wind vector at a point or on a line (profile), in an arbitrary plane or in space as a whole. This also includes the measurement of wind shears, aircraft wake vortices (see figure in Attachment C), updraft and downdraft regions of the wind. An additional aim of the Doppler wind lidar measurements is to determine kinematic properties and parameters of inhomogeneous wind fields such as divergence and rotation. See examples of applications in Attachment C.

4.5   Sources of noise and uncertainties

4.5.1   *Local oscillator shot noise*

The shot noise is denoted $n(t)$ in formula 5.A.3. Its variance is proportional to the local oscillator power, as shown in formula 5.A.10:

$$\left\langle n^2{}_{SN} \right\rangle = 2eSP_{\mathrm{lo}}B \qquad \text{(5.A.10)}$$

where:

S is the detector sensitivity, $S = \dfrac{\eta e}{hf_{\mathrm{t}}}$, where η is the detector quantum efficiency;

B is the detection bandwidth.

It causes gross errors and limits the maximum range of the signal. If no other noise source prevails, the strength of the heterodyne signal relative to the level of noise is measured by the carrier-to-noise ratio (CNR), as shown in formula 5.A.11[6]:

$$\mathrm{CNR} = \frac{\eta \cdot K \cdot \gamma(t)}{h \cdot f_t \cdot B} P_{\mathrm{r}}(t) \qquad \text{(5.A.11)}$$

Note: Some authors sometimes call "signal-to-noise ratio" what is defined here as the "carrier-to-noise ratio".

4.5.2   *Detector noise*

Additional technical sources of noise can affect the signal-to-noise ratio. As the shot noise, their spectral density is constant along the detection bandwidth (white noise).

(a)   Dark noise is created by the fluctuations of the detector dark current, i_D, as shown in formula 5.A.12:

$$\left\langle n^2{}_{DN} \right\rangle = 2e\, i_D B \qquad \text{(5.A.12)}$$

(b)   Thermal noise (Johnson/Nyquist noise) is the electronic noise generated by the thermal agitation of the electrons inside the load resistor, R_L, at temperature T, as shown in formula 5.A.13:

$$\left\langle n^2{}_{TN} \right\rangle = \frac{4k_{\mathrm{B}}T}{R_{\mathrm{L}}} B \qquad \text{(5.A.13)}$$

where:

k_{B} is the Boltzmann constant.

4.5.3   *Relative intensity noise*

The relative intensity noise (dB/Hz) is the local oscillator power noise normalized to the average power level. The relative intensity noise (RIN) typically peaks at the relaxation oscillation frequency of the laser then falls off at higher frequencies until it converges to the shot noise level (pink noise). The RIN current increases with the square of the local oscillator power.

$$n^2{}_{\mathrm{RIN}} = \left(SP_{\mathrm{lo}}\right)^2 10^{0.1\mathrm{RIN}}B \tag{5.A.14}$$

In a good lidar system, i_D, RIN, $1/R_L$ are low enough so that the local oscillator shot noise is the prevailing source of noise. In that case only, formula 5.A.14 is applicable.

4.5.4   *Speckles*

The heterodyne signal for a coherent Doppler wind lidar is the sum of many waves backscattered by individual aerosol particles. As the particles are randomly distributed along the beam in volumes much longer than the laser wavelength, the backscattered waves have a random phase when they reach the sensitive surface of the detector. They, thus, add randomly. As a result, the heterodyne signal has a random phase and amplitude. The phenomenon is called speckles (see reference [10]). It limits the precision of the frequency estimates.

4.5.5   *Laser frequency*

A precise measurement of the radial velocity requires an accurate knowledge of $f_{\mathrm{r}} - f_{\mathrm{lo}}$. Any uncertainty in this value results in a bias in $\hat{f}_{\mathrm{r}}$. If the laser frequency, f_{t}, is not stable, it should either be measured or locked to f_{lo}.

4.6   **Range assignment**

The range assignment of Doppler measurements is based on the time elapsed since the emission of the laser pulse. This time must be measured with a good accuracy (the error, ε_t, must be smaller than or equal to $2\delta \cdot x \,/\, c$, where $\delta \cdot x$ is the required precision on the range assignment). This requires, in particular, that the time of the laser pulse emission is determined with at least this precision.

4.7   **Known limitations**

Doppler lidars rely on aerosol backscatter. Aerosols are mostly generated at ground and lifted up to higher altitudes by convection or turbulence. They are, therefore, in great quantities in the planetary boundary layer (typically 1 000 m thick during the day in tempered areas, 3 000 m in tropical regions), but in much lower concentrations above. It follows Doppler lidars hardly measure winds above the planetary boundary layer except in the presence of higher altitude aerosol layers like desert dusts or volcanic plumes.

Laser beams are strongly attenuated in fogs or in clouds. It follows the maximum range of Doppler lidars is strongly limited in fogs (a few hundreds of metres at best) and they cannot measure winds inside or beyond a cloud. They are able to penetrate into subvisible clouds as cirrus clouds. Therefore, wind information at high altitude (8 to 12 km) can be retrieved from crystal particle backscattering.

Doppler lidars detect cloud water droplets or ice crystals when they are present in the atmosphere. As they are efficient scatterers, they may dominate the return from the atmosphere, in case of heavy precipitation, for example, in which case the Doppler lidar measures the radial velocity of hydrometeors rather than the radial wind.

Rain downwashes the atmosphere, bringing aerosols to the ground. The range of a Doppler lidar is generally significantly reduced after a rain, before the aerosols are lifted again.

The presence of rainwater on the window of a Doppler lidar strongly attenuates its transmission. Unless a lidar is equipped with a wiper or a blower, its window should be wiped manually.

As explained in section 4.2, the efficiency of heterodyne detection is degraded by the presence of refractive index turbulence along the beam. Refractive index turbulence is mostly present near the surface during sunny days. The maximum range of Doppler lidar looking horizontally close to the surface may thus be substantially degraded in such conditions.

5. SYSTEM SPECIFICATIONS AND TESTS

5.1 System specifications

5.1.1 *Transmitter characteristics*

5.1.1.1 Laser wavelength

The laser wavelength depends mainly on the technology used to build the laser source. Most of the existing techniques use near-infrared wavelengths between 1.5 and 2.1 μm, even though other wavelengths up to 10.6 μm may be used. The choice of the wavelength takes into account the expected power parameters but also the atmospheric transmission and the laser safety (see references [11] and [12]). In fact, the choice of the window between 1.5 and 2.1 μm is a compromise between technology and safety considerations (> 1.4 μm to ensure eye safety).

5.1.1.2 Pulse duration

The laser pulse duration, T_p, is the FWHM of the laser pulse envelope, $g(t)$. T_p defines the atmosphere probed length, R_p, contributing to the instantaneous lidar signal, as shown in formula 5.A.15:

$$R_p = \frac{c \cdot T_p}{2} \tag{5.A.15}$$

As an example, a pulse duration of 200 ns corresponds to a probed length of approximately 30 m.

5.1.1.3 Velocity precision and range resolution vs. pulse duration

There is a critical relationship between the pulse duration and two performance-related features. A long pulse duration of several hundreds of nanoseconds leads to a potentially narrow FWHM of the laser pulse spectrum (if "chirping" can be avoided), (see the Fourier transform of the overall pulse in the time domain). This can lead to a very accurate wind measurement even for a very low signal-to-noise ratio provided that outliers can be avoided (see section 4.3). There is an adverse impact from high performance on range resolution. A pulse duration of 1 μs limits the effective range resolution to approximately 150 m (see formula 5.A.6).

5.1.1.4 Pulse repetition frequency

The pulse repetition frequency, f_{PRF}, is the laser pulse emission frequency. f_{PRF} determines the number of pulses sent and averaged per line of sight in the measurement time. It also determines the maximum unambiguous range where the information of two consecutive sent laser pulses will not overlap. The maximum unambiguous range, R_{MaxO}, corresponds to f_{PRF} as in formula 5.A.16:

$$R_{MaxO} = \frac{c}{2 f_{PRF_{max}}} \tag{5.A.16}$$

For example, for a maximum operational range of 15 km, the maximum f_{PRF} is 10 kHz.

As for radars, however, specific types of modulation (carrier frequency, repetition frequency, etc.) can overcome the range ambiguity beyond R_{MaxO}.

5.1.2   *Transmitter/receiver characteristics*

The transmitter/receiver is defined at least by the parameters given in Table 5.A.1.

Table 5.A.1. Transmitter/receiver characteristics

Transmitter/receiver characteristics	Remarks
Aperture diameter	Physical size of the instrument's aperture that limits transmitted and received beams.
Laser beam diameter and truncation factor	For a Gaussian beam, the laser beam diameter is defined as the diameter measured at $1/e^2$ in power at the lidar aperture. The laser beam diameter defines the illuminance level and so the eye safety. The truncation factor is the ratio between the diameter measured at $1/e^2$ and the physical size of the instrument's aperture.
Focus point	Usually, pulsed lidars use collimated beams. For some applications, the beam can be partially focused at a given point to maximize the intensity on the beam laser within the measurement range. The intensity of the signal, and thus the velocity accuracy, will be optimized at this specific point.

In principle, pulsed systems are monostatic systems. For continuous-wave systems, bistatic setups are also available.

5.1.3   *Signal sampling parameters*

The sampling of the pulsed lidar signal in range is determined by the parameters given in Table 5.A.2.

Table 5.A.2. Signal sampling parameters

Signal sampling parameters	Remarks
Range gating	The range gate positions can be defined along the line of sight.
Range gate width	Given by the sampling points or the sampling frequency of the digitizer. Should be chosen close to the pulse length.
Number of range gates	For real-time processing, spectral estimation of all range gates must be computed in a time less than the integration time.
Radial window velocity measurement range	Wind velocities as low as 0.1 m/s can be measured with the aid of Doppler wind lidar systems. The measurement range is restricted towards the upper limit only by the technical design, mainly by the detection bandwidth. A radial wind velocity range of more than 70 m/s can be measured.
Resolution of the radial velocity	The wind velocity resolution is the minimum detectable difference of the wind velocity in a time and range interval. A resolution of 0.1 m/s or better can be achieved by averaging.

5.1.4 *Pointing system characteristics*

The pointing system characteristics are given in Table 5.A.3.

Table 5.A.3. Pointing system characteristics

Pointing system characteristics	*Remarks*
Azimuth range	When using a pointing device, a lidar has the capability to point its laser beam at various azimuth angles with a maximum angular capability of 2π. For endless steering equipment, a permanent steering along the vertical axis is allowed. Other scanning scenarios should be followed for non-endless rotation gear.
Elevation range	The pointing device can be equipped with a rotation capability around the horizontal axis. Potential 360° rotation can be addressed. Typical elevation angles are set from 0° to 180° in order to observe the semi-hemispherical part of the atmosphere above the lidar. Anyhow, a nadir pointing can be used for resting position of the equipment.
Angular velocity	The angular velocity is the speed at which a pointing device is rotating. A measurement can be performed during this rotation. In this case, the wind velocity information will be a mean of the various lines of sights in the probed area, between a starting angle and a stopping angle. Other scenarios of measurement can use a so-called step and stare strategy, with a fixed position during the measurement.
Angular acceleration	Defines how fast the angular velocity can change. To be defined for complex trajectories with fast changes in direction. Angle overshoots can be observed at high angular acceleration.
Pointing accuracy	The relative pointing accuracy is the standard deviation of the angular difference between the actual line-of-sight position (azimuth and elevation) and the position of the target (system of reference of the instrument). The absolute pointing accuracy needs prior calibration by angular sensors (pitch, roll, heading) (system of geographical reference).
Angular resolution	Minimum angle step that the line of sight can move. It can be limited by a motor reduction factor, position, encoder or mechanical friction.

5.2 Relationship between system characteristics and performance

5.2.1 *Figure of merit*

A figure of merit (FOM) helps to compare range performance of different lidars with different parameters. The example shown in Figure 5.A.4 allows the classification of pulsed lidar sensitivities, independently of atmospheric parameters. FOM is derived from the lidar equation (see formula 5.A.4) and is proportional to velocity spectrum, CNR, which is defined on the averaged spectral density as the Doppler peak intensity divided by the spectral noise standard deviation, assumed to be constant (white noise). N is the number of averaged pulses.

FOM is defined for a set of lidar parameters as in formula 5.A.17:

$$\text{FOM} = \eta_{\text{all}} \cdot E \cdot T_{\text{p}} \cdot D^2 \cdot \sqrt{t_i \cdot f_{\text{PRF}}} \tag{5.A.17}$$

where:

η_{all} is the overall efficiency, taking into account beam and image quality, overall transmission and truncation factor;

E is the laser energy at the laser output (received energy is proportional to peak power and laser footprint);

T_p is the pulse duration (this term comes from narrow bandwidth, inversely proportional to T_p);

D is the collecting telescope diameter (for typical long-range applications, the optimum is 100 to 150 mm in size for near-infrared wavelengths);

t_i is the integration time for one line of sight;

f_{PRF} is the pulse repetition frequency.

The FOM is proportional to the square root of number N of accumulated spectra: $N = t_i \cdot f_{PRF}$.

When comparing two lidars at two different wavelengths, spectral dependence of atmospheric parameters should be considered. The FOM must be calculated with an integration time less than or equal to 1 s to avoid that wind or turbulence may fluctuate more than the Doppler spectral width.

A lidar may increase its FOM with a longer accumulation time within this 1 s time limit.

Considering state-of-the-art low aberration optical components, η_{all} can be estimated by the product of the emitting path transmission and the receiving path transmission.

It has to be noted that the FOM for a pulsed Doppler lidar may not be increased indefinitely by increasing the collecting area, D^2, since phase distortion across the beam due to refractive index turbulence degrades the heterodyne efficiency[3]. A practical limit is in the vicinity of a $D = 125$ mm useable diameter for long-range lidars.

Since the velocity spectrum CNR is inversely proportional to the squared range, the maximum operational range is approximately proportional to the square root of FOM, when atmospheric absorption can be neglected. When FOM is expressed in mJ ns m^2, the maximum operational range, expressed in km, is almost the square root of FOM.
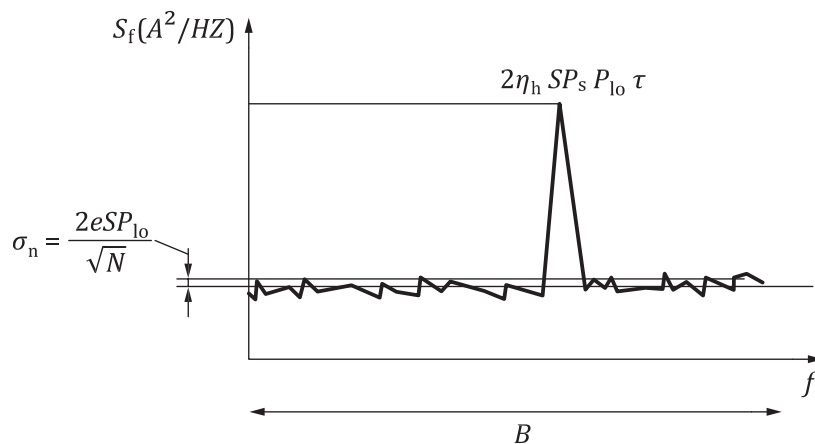
Figure 5.A.4. Example of a figure of merit

Table 5.A.4 computes the FOM for typical lidar figures and their corresponding typical measurement range.

Table 5.A.4. Figure of merit for typical lidar figures and their corresponding typical measurement range

η	E (mJ)	T_p (ns)	D(m)	f_{PRF} (Hz)	t_i(s)	FOM (mJ ns m²)	Typical measurement range (km)
0.5	0.2	800	0.12	10 000	1	115	10
0.5	0.1	400	0.06	20 000	1	10	3
0.5	2	300	0.12	750	1	118	10

5.2.2 *Time-bandwidth trade-offs*

A good practice is to match the pulse duration with the desired range gate (see section 4.6) so that the spatial resolution depends equally on these two parameters. With this assumption, spatial resolution is proportional to pulse duration. The shorter the pulse, the better the resolution. Velocity resolution is proportional to spectrum width and is larger when the spectrum is narrow. Because the spectrum width is inversely proportional to the pulse duration, range resolution and velocity resolution are also inversely proportional.

5.3 Precision and availability of measurements

5.3.1 *Radial velocity measurement accuracy*

Radial velocity measurement accuracy is defined (according to ISO 5725-1) in terms of:

(a) Trueness (or bias) as the statistical mean difference between a large number of measurements and the true value;

(b) Precision (or uncertainty) as the statistical standard deviation of a series of independent measurements. It does not relate to the true value.

Lidar data of good quality are obtained when the precision of the radial velocity measurements is higher than a target value (for example 1 m/s) with a predefined probability of occurrence (for example 95%).

An error value (1σ) of 0.5 m/s can be regarded as adequate for typical meteorological applications and for wind measurements to determine the statistics of dispersion categories for air pollution modelling[13]. For wind energy applications, the requirements may be higher (0.2 m/s).

5.3.2 *Data availability*

Data availability is defined as the ratio of data with precision, P, to the total number of data during a measurement period.

The availability of measurement data, that is, the determinability of the wind profile, is a function mainly of the aerosol concentration and the clouds. Other filtering criteria may be applied, depending on the required data accuracy. For example, data that exhibit significantly non-uniform flow around the scan disk should be rejected.

5.3.3   *Maximum operational range*

Assuming the lidar line of sight remains within the planetary boundary layer (that is, no significant change of signal along the line of sight), Figure 5.A.5 shows a typical pulsed lidar data availability versus range plot.

In this case, the range for 80% data availability (P_{80}) is 7 500 m.

The performance shown in this diagram is based on a standard atmosphere:

(a)   No clouds along the line of sight;

(b)   No precipitation;

(c)   Visibility over 10 km (clear air).

This performance will vary significantly with relevant local climatic and operational conditions. Data from greater ranges should be treated with caution, depending on the application.

Measurement range must be defined with a given availability criteria. A recent study about this link is described in reference [14].

For example, R_{50} corresponds to the maximum range with availability over 50%.

If the availability is not mentioned, the maximum operational range is supposed to be R_{80}, that is, the maximum distance where the availability is over 80%.

For a given availability, a change in velocity precision leads to a change in maximum operational range.

Key
X   Range in metres
Y   Availability in per cent
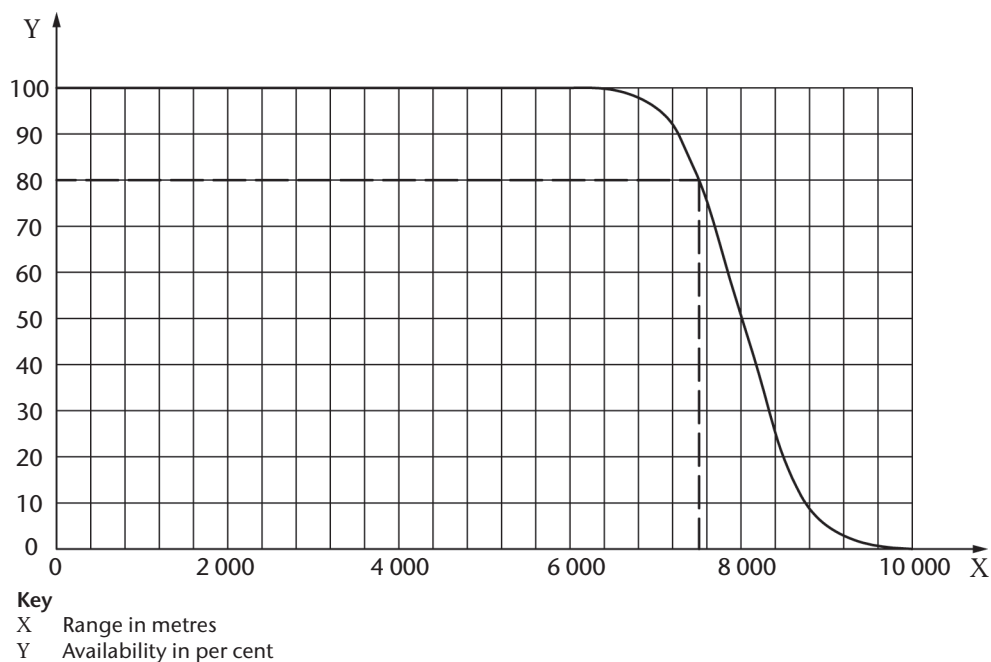
Figure 5.A.5. Example for maximum operational range

5.4 Testing procedures

5.4.1 *General*

In order to accurately assess for the accuracy of the target variables, the manufacturer should perform a set of validation tests for the range and velocity. Some can be performed under laboratory conditions. Certain other validation tests can only be performed by a comparison with other reference instruments, such as cup or sonic anemometers.

5.4.2 *Radial velocity measurement validation*

5.4.2.1 General

This section describes how the quality of radial velocity measurements can be checked and assessed.

5.4.2.2 Hard target return

This test consists in acquiring wind measurements with the beam directed to a stationary (unmoving) hard target (any building within lidar range) and checking the radial velocity measurement returned by the lidar is 0 m/s.

This test checks that the frequency difference, $f_t - f_{lo}$, between emitted laser pulses and the local oscillator is known or determined with a sufficient accuracy (see section 4.5.3).

The range gate length should be close to the length of the laser pulse, and the distances of the range gates should be set so that the hard target is exactly at the centre of one range gate, otherwise, a velocity bias can occur in case of frequency drift within the pulse.

Hard target velocity measurements should be acquired during at least 10 min. The test is successful if the time sequence of hard target radial velocities is centred at about 0 m/s.

5.4.2.3 Self-assessment of radial velocity precision

In this test, the pulsed lidar beam is vertical and radial velocity measurements are acquired during at least 20 min at the rate of at least one profile of radial velocities every second. Let us denote by $v_r(x,k)$, $k = 1,\ldots,K$ the time sequence of radial velocities measured at distance x. The test consists in forming the power spectrum of the time sequence, as shown in formula 5.A.18:

$$V(x,f) = \frac{1}{K}\left|\sum_{k=1}^{K} v_r(x,k)\exp(-2j\pi fk\delta t)\right|^2 \tag{5.A.18}$$

where:

δt is the constant time lag between successive $v_r(x,k)$ measurements.

On average, the power spectrum $V(x,f)$ should look like Figure 5.A.6. At low frequencies, the power spectrum is dominated by natural wind fluctuations and will follow a $f^{-5/3}$ law. At high frequencies, the power spectrum is dominated by the flat level of measurement errors (white noise). The level of this flat part directly gives the variance of these measurements $\sigma_e^2(x)$.

Note: The test must be carried out at night when the natural variability of the wind is weak, that is, when the wind is considered to be calm. It may then happen that measurement errors are much larger than natural wind fluctuations so the $f^{-5/3}$ part of the power spectrum is hidden.
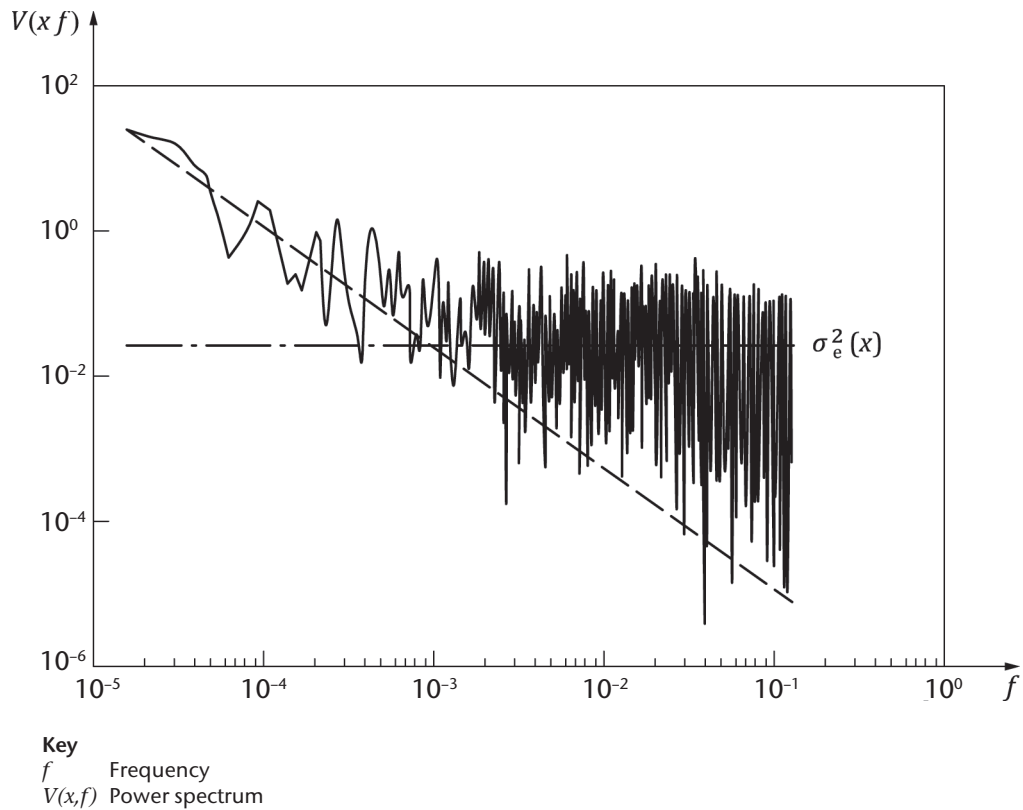
Figure 5.A.6. Power spectrum of radial velocity measurements

Fully described in reference [15], this technique allows for the estimation of the measurement precision of the lidar without any ancillary data.

In Figure 5.A.6, the line is $V(f)$. At low frequencies, $V(f)$ should be proportional to $f^{5/3}$ (spectral behaviour of natural wind variability; see dashes). At high frequencies, the spectrum becomes flat (dash-dot line) at a level directly equal to the variance of measurement errors, $\sigma_e^2(x)$.

5.4.3   *Assessment of accuracy by intercomparison with other instrumentation*

5.4.3.1   Sonic anemometer

The last test consists of directing the lidar beam very close to a sonic anemometer on a mast or platform without vibration and comparing lidar radial velocities with the projection of the three-dimensional wind vectors acquired by the sonic anemometer on the beam direction.

Lidar and sonic anemometer data must be averaged over a minute.

The direction of the lidar beam must be determined with a good accuracy (of the order 1° or better) and as close as possible to the horizontal plane. The lidar beam must be at the height of the sonic anemometer (height difference of the order of 1 m or less).

The root mean square of the differences between lidar and sonic anemometer data must be less than 0.1 m/s.

The mast will most likely cause wind flow perturbations downstream. Winds coming from directions such that the sonic anemometer is in the perturbed zone must be removed from the statistics.

5.4.3.2 Performance test against masts

The mast must be equipped with at least three-cup anemometers mounted horizontally.

5.4.3.3 Comparison with Doppler weather radars

The possibility for intercomparison between Doppler lidars and Doppler weather radars can be an option where the two systems are collocated. The details about this class of intercomparison are just becoming known as the deployment of systems integrating both sensors for all-weather remote-sensing of the wind field at airports, especially for wind shear detection, is just getting under way. Studies have recently been conducted[16;17;18]. Both sensors should be collocated and should probe the same atmospheric volume in order to be certain of representative intercomparisons.

In addition to the siting requirement, it is very important that weather situations be selected in which the tracer targets of both sensors actually represent the flow of air. In conditions of dry weather, the Doppler lidar works best, while under such conditions of clear air, the radar measures only the returns due to scattering by insects. These scattered signals from insects provide no accurate indication of the actual air movement. Comparison with data from Doppler lidars typically shows differences of up to several metres per second. Therefore, echo classification in terms of radar targets has to be enabled in order to be able to reject insect returns. This means that the radar has to be capable of measuring at two orthogonal linear polarizations. During precipitation events, however, conditions are optimal for the radar, whereas the lidar may have significantly reduced range coverage. In weather situations with light rain or drizzle from stratiform cloud, both radar and lidar sensors are expected to obtain high-quality data. Such situations are thus best suited for this validation procedure. Appropriate filtering of radar data on the basis of target classification using dual-polarization moments needs to be conducted in order to get rid of any non-meteorological returns.

If these requirements are fulfilled, cross-comparison of Doppler weather radar and Doppler lidar can be performed on the basis of profiles of horizontal wind as obtained, for example, with velocity volume processing or velocity azimuth display methods. In this case, the scan geometry has to be considered. Ideally, the scan geometry for the radar and lidar should be the same with respect to elevation angles. Another option yet to be evaluated could be to compare the actual radial wind velocities on a range gate by range gate basis between the radar and lidar systems.

5.4.3.4 Comparison with radar wind profilers

Comparison with radar wind profilers may be performed if the two systems are collocated. The weather conditions under which both sensors work optimally are not exclusive of each other (sufficient aerosol tracers for lidar and sufficient turbulent eddies as targets for Bragg scattering for the wind profiler). Care must be taken that both sensors face optimal atmospheric conditions. Additionally, attention has to be paid to the scan mode used to derive the vertical wind profile so that the volume probed by the lidar matches the volume probed by the wind profiler.

5.4.4 *Maximum operational range validation*

In clear sky conditions, the atmosphere can be described by the visibility, V, the aerosol concentration and the aerosol type, where the last two can be properly described by the two optical lidar parameters extinction and backscatter coefficients. The visibility (see, for example, ISO 28902-1) and humidity are measured by standard ground-based meteorological local sensors, whereas the aerosol type and its size distribution are not. To simplify, atmosphere types can be sorted in a few categories associated with their lidar ratio. Lidar ratio values in the near infrared typically are limited in the range of 30 to 50 steradians. R_{MaxO} will not be too dependent on the aerosol variability on site except for conditions with local pollution sources.

Visibility is an important parameter for lidar range. The lidar equation (see formula 5.A.4) indicates that the received power is proportional to the backscatter coefficient and decreases exponentially with extinction, thus increases with visibility. Since $\alpha\,(x)$ and $\beta\,(x)$ are proportional, there is a maximum to the function $P_r(t)$ (see lidar equation in formula 5.A.4, and Figure 5.A.7), and so for R_{MaxO}.

To discard unfavourable visibility conditions for coherent Doppler wind lidars (fog and very clear), only haze and clear visibility conditions are selected for range measurements. Current lidars can work in precipitating conditions, but are subject to error in their determination of the vertical wind component; the horizontal component has been shown to be very accurate (see reference [18]).

Key
X   Visibility in km
Y   Maximum range in metres
1–5 Different figure of merit values (see Table 5.A.5)
A   Fog
B   Haze
C   Clear
D   Very clear
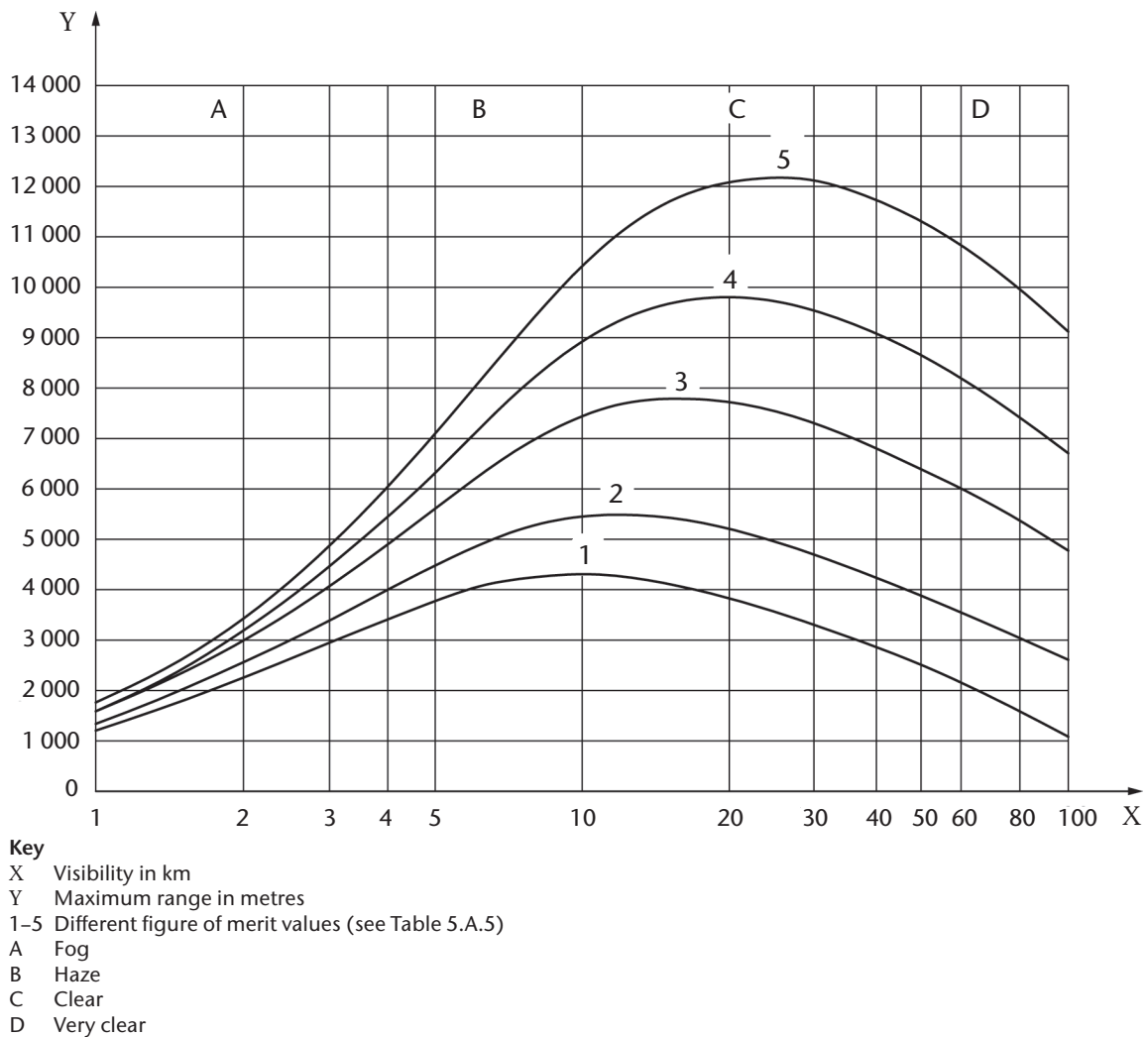
Figure 5.A.7. Dependency of the maximum operational range of the heterodyne Doppler signal to the visibility conditions

Table 5.A.5. Plot numbers

Plot number	1	2	3	4	5
Typical FOM for 1 s integration time (mJ ns m²)	20	30	60	100	150

Because backscatter changes rapidly for high relative-humidity values, data corresponding to relative humidity > 70% should be filtered out the measurement dataset. So, precipitation conditions (rain, snow) are not considered.

Moreover, index turbulence, Cn^2 (depends on temperature and altitude), can modify R_{MaxO} by altering the beam wave front. Strong turbulent conditions must be removed from datasets (sunny days around noon), and experimental protocol must be followed up.

So the validation must be conducted under the following conditions:

(a) The lidar is operated in operational conditions (vertical for profilers, low elevation for scanning lidars);

(b) The full measurement range remains in the boundary layer;

(c) 10 km < visibility < 50 km (at visible wavelength, dependency with wavelength is given in ISO 28902-1);

(d) No precipitation;

(e) No cloud on the line of sight;

(f) $Cn^2 < 10^{-14}$ m$^{-2/3}$ (1 m above ground level).

Data not corresponding to these conditions should be filtered out for assessing the maximum operational range.

(a) Context conditions are recorded simultaneously (temperature, Cn^2, visibility, relative humidity);

(b) Datasets are created following the above-mentioned atmospheric conditions. 100 h of filtered data are required as a minimum for a good statistical dataset. It represents around four days of cumulated measurements with 1 s accumulation time. Depending on the atmospheric conditions, the evaluation period can last from four days and up to one month.

6. MEASUREMENT PLANNING AND INSTALLATION INSTRUCTIONS

6.1 Site requirements

The selection of the measurement site is essentially determined by the measurement task. Careful selection of the measurement site is necessary, in particular, for stationary systems or for the quasi-stationary use of mobile systems during long-term measurement campaigns. The following points must be taken into account when selecting the measurement site:

(a) Unobstructed view: Unrestricted visibility can be limited by built-up areas, trees and buildings near the installation site of the lidar. If the view is limited by buildings, it is

possible to avoid the limitation of the horizontal view by selecting a larger elevation angle. In the case of a velocity azimuth display scan, the measurement signals originating not from the free atmosphere but from obstacles must be excluded from the evaluation;

(b)   Electromagnetic radiation: Doppler wind lidar systems should be shielded properly against interferences by electromagnetic radiation (for example by radar, mobile radio or cellular phone networks).

Early inspection of the envisaged measurement site with the participation of experts (such as meteorologists) is recommended.

For optimal operational range retrieval, the lidar should be installed on a short grass-covered ground with no nearby structures, which would cause atmospheric turbulence affecting the lidar's operation and performance. The lidar should be installed at least at 3 m above the ground, especially when not located on a grass ground, like concrete, asphalt or a plain metallic platform, in order to avoid effects from turbulence nearby the optical output that will destroy the coherency of the atmosphere and thus drastically diminish the detection.

6.2   Limiting conditions for general operation

Interference factors regarding Doppler wind lidar measurements are:

(a)   Optically thick clouds;

(b)   Precipitation of any type (rain, hail, snow);

(c)   Blocking effects (such as from buildings).

6.3   Maintenance and operational test

6.3.1   General

To ensure the system functions as specified and to rule out deviations and technical errors such as maladjustments[19], maintenance and operational tests must be performed in regular intervals. In addition to the information given here, typical application ranges and corresponding requirements can be found in Attachment D.

6.3.2   Maintenance

Maintenance such as regular cleaning of the optical components, calibration, etc. must be performed as a basic requirement of quality assurance. Maintenance procedures may be conducted by on-site personnel, using an automatic software detection of the decrease of the signal due to, for example, dust deposits, and making appropriate corrections to the data, or a combination of the two. Typical maintenance intervals are three months depending on the environmental conditions.

6.3.3   Operational test

Operational tests should be performed every 6 to 36 months. The tests depend on the individual system design. The manufacturer must specify the testing procedures and provide the necessary testing tools.

(a)   Output power and frequency of the laser source should be measured at the periodicity indicated by the manufacturer;

(b)   Signal output of the data acquisition system reacting to a defined light pulse or defined target should be measured at the periodicity indicated by the manufacturer;

(c)   For scanning or steering systems, an alignment test using a calibrated instrument (for example a compass or inclination meter) should be performed.

6.3.4   *Uncertainty*

Table 5.A.6 compiles uncertainty contributions to the measurement variables and the line-of-sight wind velocity. The uncertainty contributions of the measurement variables influence the quality of the data produced by the system. The dominant uncertainties result from:

(a)   The initial calibration process of the system by the manufacturer;

(b)   The prevailing environmental conditions.

Table 5.A.6. Effects leading to uncertainty

Measurement variables	*Effects leading to uncertainty*
Signal-to-noise ratio	(a) Noise including detector noise (b) Speckle effect (when only a few pulses are averaged during the measurement time) (c) Laser power or pulse width fluctuations (d) Refractive index (temperature) turbulence (e) Lag angle at fast rotation speeds
Frequency shift, Δf	(a) Bias and fluctuations of emitted pulse frequency compared to local oscillator frequency (b) Pulse length (c) Signal-to-noise ratio (d) Number of averaged pulses (e) Quality of estimator
Target variable	*Uncertainty contribution*
Line-of-sight wind velocity (radial wind velocity)	(a) Wind turbulence (b) Wind gradient along the line of sight (c) Hard targets close to the range gate (d) Range ambiguities (e) Pointing accuracy

ATTACHMENT A. CONTINUOUS-WAVE DOPPLER WIND LIDAR

(informative)

As stated in this annex, there are several methods by which lidar can be used to measure atmospheric wind. The four most commonly used methods are pulsed and continuous-wave coherent Doppler wind lidar, direct-detection Doppler wind lidar and resonance Doppler wind lidar (most commonly used for mesospheric sodium layer measurements).

This annex describes the use of heterodyne (coherent) pulsed lidar systems. It should be noted that there is also ISO 28902-3 currently in preparation, which describes the use of continuous-wave coherent Doppler wind lidar for the measurement of atmospheric wind. ISO 28902-3 will specify the requirements and performance test procedures for continuous-wave Doppler lidar techniques and present their advantages and limitations. The term "continuous-wave Doppler lidar" or "continuous-wave Doppler wind lidar" is used in this annex to apply to continuous-wave lidar systems making measurements of wind characteristics from the scattering of laser light by aerosols in the atmosphere within the low-altitude boundary layer. A description is provided of typical measurement geometries, signal-processing options, performance requirements, and limits based on standard atmospheric conditions. The applications for continuous-wave lidar are, among others:

(a)   Wind energy;

(b)   Wind resource assessment;

(c)   Power curve verification;

(d)   Loss factor in the wind farm operation;

(e)   Wind hazards monitoring for aviation weather applications;

(f)   Wind shear;

(g)   Requirements for the detection of wake vortices behind aircraft.

ISO 28902-3 will address manufacturers of continuous-wave Doppler wind lidars, as well as those bodies concerned with testing and certifying their conformity. It will also provide recommendations for users to make adequate appropriate use of these instruments. A comprehensive bibliography of independent publications will be provided.

———————

ATTACHMENT B. RETRIEVAL OF THE WIND VECTOR

(informative)

B.1   **General**

The wind is a three-dimensional vector quantity, with the wind field being generally a function of space and time. The measurement of the instantaneous wind at a particular position therefore always requires the determination of three vector components. A single Doppler lidar is only able to measure the component (or projection) of the wind vector along the line of sight of the laser beam. Three separated lidar systems would therefore be required to perform an exact local measurement at any fixed time. Under certain assumptions, it is possible to estimate the full wind vector from a single "monostatic" Doppler lidar. This process is called wind retrieval since the accuracy of the wind vector estimate depends on the validity of the assumptions regarding the wind field.

B.2   **Coordinate system**

The figure below shows the wind vector $\vec{u}(\vec{r},t)$ in the Cartesian coordinate system with the unit vectors $\vec{i},\vec{j},\vec{k}$. The components u_x, u_y, u_z are scalar functions of position, and time, $\vec{r} = \vec{r}(x,y,z,t)$, is the position or radius vector of an air parcel.

$$\vec{u} = \frac{d\vec{r}}{dt} = \begin{pmatrix} u_x \\ u_y \\ u_z \end{pmatrix} \tag{B.1}$$

or

$$\vec{u} = \left(u_x \cdot \vec{i} + u_y \cdot \vec{j} + u_z \cdot \vec{k} \right) \tag{B.2}$$

The coordinate system in the figure points to the east (E) with the positive x-direction $(\vec{i})$, to the north (N) with the positive y-direction $(\vec{j})$ and to the zenith with the positive z-direction $(\vec{k})$.
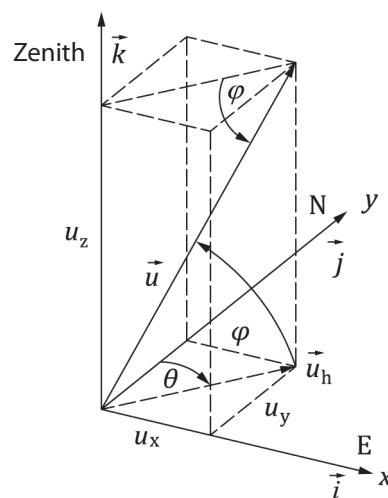
Coordinate system and wind vectors

With θ and ϕ, the components in Cartesian coordinates are:

$$u_x = U \cdot \cos\phi \cdot \sin\theta$$
$$u_y = U \cdot \cos\phi \cdot \cos\theta \qquad \text{(B.3)}$$
$$u_z = U \cdot \sin\phi$$

and the three-dimensional wind vector becomes:

$$\vec{u} = \begin{pmatrix} U \cdot \cos\phi \cdot \sin\theta \\ U \cdot \cos\phi \cdot \cos\theta \\ U \cdot \sin\phi \end{pmatrix} \qquad \text{(B.4)}$$

Example: Horizontal west wind: $\theta = 90°$, $\varphi = 0°$

$$\Rightarrow u_x = U, u_y = u_z = 0 \ \vec{u} = (U, 0, 0)$$

B.3   **Horizontal wind vector**

The horizontal wind vector, $\vec{u}_h$, and the horizontal projection of the three-dimensional wind vector, $\vec{u}$, in the figure becomes:

$$\vec{u}_h = \begin{pmatrix} u_x \\ u_y \end{pmatrix} = \begin{pmatrix} u_h \cdot \sin\theta \\ u_h \cdot \cos\theta \end{pmatrix} \qquad \text{(B.5)}$$

or, in component notation:

$$u_h = |\vec{u}_h| = U \cdot \cos\phi = \sqrt{u_x^2 + u_y^2} \qquad \text{(B.6)}$$

The value u_h is denoted as horizontal wind velocity or colloquially as wind velocity. According to the meteorological convention, the wind direction is defined as the direction opposite to the wind vector, $\vec{u}_h$. It is oriented clockwise from north via east, south and west (see figure above).

For the case of a lidar scanning in a disk at fixed elevation angle in uniform wind flow, the individual line-of-sight velocity points follow a cosine form as a function of azimuth angle. The peaks of the function correspond to the azimuth angle aligned parallel or anti-parallel to the wind direction. The function passes through zero when the azimuth angle is perpendicular to wind bearing since there is no component of velocity along the line of sight. The data are also conveniently displayed on a polar plot, which provides information at a glance on the speed, direction and vertical wind component. A standard least-squares fitting routine provides the best estimates of the values of the three unknown parameters (either u, v and w, or alternatively, horizontal speed, vertical speed and wind bearing).

B.4   **Radial velocity**

In lidar measurements, the component v_r of the local wind vector $\vec{u}(\vec{r}, t)$ in the beam direction of the laser, i.e. the radial velocity at any arbitrary position $\vec{r}$, is the direct measurand determined from the Doppler frequency shift (see Figure 5.A.5). If the wind vector $\vec{u}(\vec{r})$ is written in a spherical coordinate system $(\vec{e}_r, \vec{e}_\theta, \vec{e}_\phi)$ instead of a Cartesian $(\vec{i}, \vec{j}, \vec{k})$ coordinate system, the radial velocity, v_r, is easily defined (compare formula B.2)[20]:

$$\vec{u}(\vec{r}) = \vec{u}(r, \theta, \phi) = (u_r \cdot \vec{e}_r + u_\theta \cdot \vec{e}_\theta + u_\phi \cdot \vec{e}_\phi) \qquad \text{(B.7)}$$

where:

$\vec{e}_r$ is the unit vector in the beam direction;

$\vec{e}_\theta, \vec{e}_\phi$ are the unit vectors in the azimuth and elevation direction;

u_r, u_θ, u_ϕ are the orthogonal wind vector components of the coordinate system carried along during the scanning operation.

The projection of the wind vector $\vec{u}(\vec{r})$ onto the beam direction, i.e. the scalar product ($\circ$), can be derived with formula B.8:

$$\vec{u}(\vec{r}) \circ \vec{e}_r = u_r \equiv v_r \equiv -v_{LOS} \tag{B.8}$$

v_{LOS} is equal by convention to the negative radial component v_r of the local wind vector at the position $\vec{r}$. The negative sign of v_{LOS} corresponds to the convention that in lidar systems the wind velocity is regarded as positive towards the laser.

With the known transformation relation between spherical and Cartesian coordinates[19], v_r can be expressed by the Cartesian wind components u_x, u_y, u_z the result being:

$$v_{LOS} = -v_r = -\left(u_x \cdot \cos\phi \cdot \sin\theta + u_y \cdot \cos\phi \cdot \cos\theta + u_z \cdot \sin\phi\right) \tag{B.9}$$

B.5   **Retrieval of the wind vector**

The atmosphere should be sensed at different angles in order to detect the (Cartesian) components u_x, u_y, u_z of the wind vector with the Doppler wind lidar.

Note: The wind components u_x, u_y, u_z are frequently also called u, v, w.

However, all wind components are usually subject to spatial and temporal fluctuations since the wind field in general cannot be regarded as homogeneous and stationary due to a variety of small-scale atmospheric processes like gravity waves, convection, turbulence or orographically induced flow effects. Homogeneity assumptions should therefore be made in order to retrieve an estimate of the wind vector from the radial components. The better this assumption holds, the more does the estimate represent the actual wind field. The problem has been extensively discussed in the literature and is explained in textbooks for both radar and lidar, see, for example, references [21] and [22].

Therefore, assuring that the wind field can be regarded as stationary over the measurement period and horizontally homogeneous over the sampled volume, that is, if the wind field is only a function of the vertical coordinate z, then the radial wind measurements for a fixed geometrical height are given by formula B.10, the simple matrix equation:

$$A \cdot u = v_r \tag{B.10}$$

The rows of this (n x 3) matrix A are comprised of the unit directional vectors describing the pointing of the n beams. The vector v_r is also of dimension n and contains the radial winds obtained in the n pointing directions. This is nothing more than a compact notation for the n scalar (inner) products as given in formula B.8. For $n = 3$, the inverse A^{-1} exists if A has rank 3 (for example, all row vectors are linearly independent) and the wind vector can be directly obtained through formula B.11:

$$u = A^{-1} \cdot v_r \tag{B.11}$$

For $n > 3$ and rank(A) = 3, the linear system is overdetermined and has usually either one solution or no (exact solution) at all. However, an approximate solution can be found which minimizes $A \cdot u - v_r{}^2$. This least-square solution can be expressed by the Pseudoinverse $(A^T A)^{-1} \cdot A^T$ of matrix A as shown in formula B.12:

$$u = \left(A^T A\right)^{-1} \cdot A^T \cdot v_r \tag{B.12}$$

A^T denotes the transpose of matrix A. Formula B.12 is sufficiently general and describes all possible scanning configurations with n discrete beam pointing directions. Care must be taken in the practical use of this formula to obtain numerically stable implementations.

The Doppler beam swinging technique or the velocity azimuth display scanning methods are two frequently used scan schemes for Doppler lidars.

In the case of the Doppler beam swinging technique, measurements are performed in at least three linearly independent directions. This method allows for a very fast scanning, but it may yield biased measurements if the wind field is non-homogeneous. The validity of the retrieval assumptions (homogeneity, stationarity) can be tested to some extent if more than three directions are used. An explicit example of the Doppler beam swinging method with $n = 3$ and $n = 4$ can be found in reference [23].

In the case of the velocity azimuth display scan, the beam direction azimuth is varied in a continuous scanning operation. The variation of the azimuth angle during the measurement series yields a set of different projections of the local wind vector onto these measurement directions. The elevation angle remains constant in the process. Originally, the velocity azimuth display method was proposed for a horizontally homogeneous wind field[24]. Later discussions were extended to allow for an additional linear variation of the vector components[25]. In the case of a homogeneous wind field, the result is a sinusoidal profile of the measured velocity v_{LOS}.

If the lidar is powerful enough to provide several azimuth scans at different elevations in reasonable time, these can be combined in order to compile a full volume scan. This makes it feasible to use a more elaborate model of the wind field that can be fitted to the vector of observations of v_{r}. That is, analogous to formula B.10, one can further expand the Taylor series incorporating also shearing of the wind, i.e. the first spatial derivatives. For Doppler radars, this procedure is standard and is commonly known as velocity volume processing. It has been originally published in reference [26]. This analysis then leads to formula B.13 instead of formula B.10:

$$
\begin{aligned}
v_{\mathrm{r}} = {}& \sin\theta \cdot \cos\phi \cdot u_0 + \cos\theta \cdot \cos\phi \cdot v_0 + \sin\phi \cdot w_0 \\
&+ r \cdot \sin^2\theta \cdot \cos^2\phi \cdot u'_{\mathrm{x}} \\
&+ r \cdot \cos^2\theta \cdot \cos^2\phi \cdot v'_{\mathrm{y}} \\
&+ r \cdot \cos\theta \cdot \sin\theta \cdot \cos^2\phi \cdot \left(u'_{\mathrm{y}} + v'_{\mathrm{x}} \right) \\
&+ \sin\phi \cdot \left(r \cdot \sin\phi - z_0 \right) \cdot w'_{\mathrm{z}} \\
&+ \sin\theta \cdot \cos\phi \cdot \left(r \cdot \sin\phi - z_0 \right) \cdot \left(u'_{\mathrm{z}} + w'_{\mathrm{x}} \right) \\
&+ \cos\theta \cdot \cos\phi \cdot \left(r \cdot \sin\phi - z_0 \right) \cdot \left(v'_{\mathrm{z}} + w'_{\mathrm{y}} \right)
\end{aligned}
\tag{B.13}
$$

It should be noted that this model does not allow to extract any information about horizontal vorticity since u'_{y} and v'_{x} only appear as a sum in formula B.13. This method has been applied to lidar data and compared with Doppler weather radar data in reference [16].

ATTACHMENT C. APPLICATIONS

(informative)

C.1   **Wind energy**

C.1.1   *General*

One of the main challenges in the wind energy market today is the optimal estimation of the future electrical output of a wind farm. Today, the procedure to estimate this is to have the best evaluation possible of the wind potential at a given site, the best evaluation of what a wind turbine can produce with the free wind that it receives and to properly evaluate the total production loss that can occur during the wind farm operation. Some of these losses can be due to the wakes, to the power performance loss of a wind turbine, downtime due to operation and maintenance of the wind farm and other parameters that can affect the global wind farm operation. Today, the ground-based coherent Doppler lidar is a suitable tool to be used during all the phases of the operation of a wind farm, from the development phase, to the commissioning, operation and repowering of old wind farms.

C.1.2   *Wind resource assessment*

Today the ground-based vertical-profiler lidar (both pulsed and continuous-wave types) is widely used in the wind energy market by all major developers in order to provide highly accurate wind speed data and reduce the horizontal and vertical uncertainty during the wind resource assessment campaign. Today ground-based coherent Doppler lidar can be used without any mast during the campaign and these data are considered as bankable. Considering the size of the wind turbine and the height that it can reach, the lidar allows a proper evaluation of the vertical wind profile that is critical for the design of a wind turbine. The vertical wind shear (change in wind speed along the vertical axis) and the vertical wind veer (change in wind direction along the vertical axis) are two key elements to be considered that can affect the annual energy production of a wind farm.

The wind farms are moving more and more offshore, and today the ground-based pulsed-scanning lidar can be used for wind resource assessment campaign scanning offshore from the shore. This allows to decrease the horizontal uncertainty in the wind resource assessment campaign at a much reduced cost than the standard offshore met mast. In addition to this, the correlation of the wind measured with the scanning lidar can be used to validate some wind models for the wind transition offshore to the shore.

C.1.3   *Power curve verification*

C.1.3.1   **General**

Today, the International Electrotechnical Commission (IEC) standard 61400-12-1[27] mentions that a met mast is to be used for the power curve verification of a wind turbine. Considering the maturity of the ground-based lidar for the wind resource assessment application, IEC 61400-12-1 is in the process of evolving and will be including the ground-based lidar vertical profiler for power curve verification.

The power curve verification standard is also including a new measurement method by applying the rotor equivalent power curve. In this case, the entire wind profile of the rotor diameter is considered and used, in order to estimate the total incoming wind along a plane rather than only the wind coming at hub height.

In addition to the vertical profiler, when a wind turbine cannot be reached within the 2.5D distance of the free wind of the wind turbine (where D is the rotor diameter), the scanning ground-based lidar can also be used to perform some power curve verification, by scanning from the ground to the front of the wind turbine.

C.1.3.2   Loss factor in the wind farm operation

When globally looking at a wind farm, there are some loss coefficients that wind farm developers apply to their annual electrical production output calculation, and the more accurate this information, the better the project and ease of financing.

The ground-based lidar is being used in a variety of programmes for the validation of the wake loss deficit coefficient. Major wind farm developers/owners have their own wind flow modelling tool to optimize the wind farm design and layout, and today the ground-based lidar is the appropriate tool used to validate their model, thanks to data generated by the lidar. In terms of optimization of the wind farm operation, the nacelle-based lidar is also widely used, for turbine control, yaw misalignment or nacelle anemometer calibration.

C.2   Wind hazards monitoring for aviation weather applications

C.2.1   *General*

According to the state of the art and the growth of the worldwide air traffic, several projects are going on worldwide in order to renew and optimize the regulations of air traffic management (ATM), such as the Single European Sky ATM Research project in Europe[28] and the NextGen project in the United States of America. In the field of aviation weather, two major applications have been highlighted: the measurements of wind shears and wake vortices. For these two applications, coherent Doppler lidars are now considered as well adapted and powerful sensors to improve the wind observations in order to increase safety and optimize the air traffic.

C.2.2   *Wind shear*

Wind shears are defined as significant changes of head- or tail-winds along the takeoff path and the approach that can affect aircrafts[29]. These rapid changes in air speed cannot be balanced by acceleration or deceleration due to inertial effects. Thus, lift and drag, and therefore the resultant flight path, change. The effects of wind shear as mentioned above are particularly dangerous if they happen near the ground, i.e. during takeoff or landing, where they can lead to severe accidents. This is why since the conference of Chicago, the International Civil Aviation Organization (ICAO) standards have taken care of the wind shear threats to civil air traffic by mentioning wind shears in Annex 3 to the Convention on International Civil Aviation – *Meteorological Service for International Air Navigation*[29] and by providing the ICAO *Manual on Low-level Wind Shear* (Doc 9817)[30]. The ICAO Annex 3 distinguishes two aspects of wind shears: the wind shear alerts and wind shear warnings.

(a)   Wind shear alerts consist in providing automatic alerts of wind shear intensity observed by ground-based remote sensors. The alerts are created once wind shears are above 15 kn (7.5 m/s) in terms of headwind/tailwind changes. As detailed in reference [30], the danger of wind shears is mainly due to the strong horizontal winds that induce strong headwind and tailwind changes for the aircrafts;

(b)   Wind shear warnings must give concise information on the observed or expected existence of wind shears which could adversely affect aircraft. They are focusing below 500 m and along the takeoff path and approach. They are prepared by the meteorological office in charge of the met observations at a given airport. The wind shear warnings will be prepared "manually", thanks to all the observations (ground-based, aircrafts) and weather forecasts available.

According to the best practices, described in reference [30], coherent Doppler lidars are a good candidate technology for providing wind shear alerts and/or warnings since:

(a)   The areas of interest are the takeoff path and the approach that can be probed by a scanning coherent Doppler lidar with plan position indicator (typically with a 3° of elevation) or glide-path[31] scans or lines of sights along the glide path;

(b)   The probing area for alerting wind shears is two extensions of 3 nautical miles of the runways, that is to say a measurement range of 7 km at least. Measurement range should be 7 km at least in appropriate atmospheric conditions (described in section 5);

(c)   The wind shear alerts are provided on the three boxes (of 1 nautical mile) that compose the extensions of each side of the runways, commonly called the ARENA (Area Noted for Attention). To compute differences of headwind or tailwind, two points are needed at a minimum. This corresponds to a theoretical required resolution better than 1.852 km. But, in order to get accurate wind shear alerts and to be able to monitor all the types of wind shears and especially the smallest ones which are the microbursts (size > 1.5 km), a range resolution of 200 m is commonly used with lidars and radars;

(d)   ICAO documents mention the typical alert frequency suitable for the wind shears detection. In worldwide best practices, this frequency varies from 1 to 3 min;

(e)   Above all, it is important to notice that the configurations (such as accumulation time, scanning speed, alert frequency, probing area shape, probing range) of an equipment like a lidar dedicated to wind shear alerts or warnings should be adapted to the local requirements (typical local wind shear phenomena and the needs of users, such as the air traffic controllers).

Moreover, Doppler lidar systems compliant with requirements in Attachment D should be considered as a valuable supplement to Doppler weather radar observations, since they have complementary performance with respect to precipitation. Doppler lidars perform best in clear air conditions when Doppler radar receives only weak signals, and vice versa, when precipitation limits Doppler lidar observations, Doppler radar performs optimally. An example describing the setup at Hong Kong International Airport including a Doppler lidar can be found in reference [31].

C.2.3   *Requirements for wake vortices detection behind aircrafts*

There is strong interest of the air traffic control stakeholders for studying wake vortices because their strength (commonly characterized by their circulation) determines the minimum separation distance between aircrafts in order to ensure safety. Wake vortices consist of two strong horizontal rotational flows that trail from each wingtip. They are generated by the lift of the aircraft which induces air flow from below the wings around the wingtips into the region above the wings. The wake vortices are very stable compared to turbulence and they can last up to 3 min with stable atmospheric conditions. Their circulation is determined by the aircraft weight and air speed and by the wingspan. Their size is about 20 m but they can be very dangerous especially in the takeoff and landing phases of flight.

That is why, since the 1960s, regulations have been created by ICAO to fix the separation distances between three categories. With the increase of worldwide air traffic and the development of super heavy aircrafts, several projects aim at renewing the air traffic control regulations and especially the separation distances. Thus, plenty of wake vortices studies have been launched since the 1990s in using computational fluid dynamic models and coherent Doppler lidar technology in order to optimize the separation distances while ensuring safety[32;33]. Scanning coherent Doppler lidars are particularly adapted to measure wake vortices since they allow to measure at high resolution below 10 m and at high frequency up to 5 s wake vortices generated by the aircraft below 500 m, for monitoring out-of-ground effects and in-ground
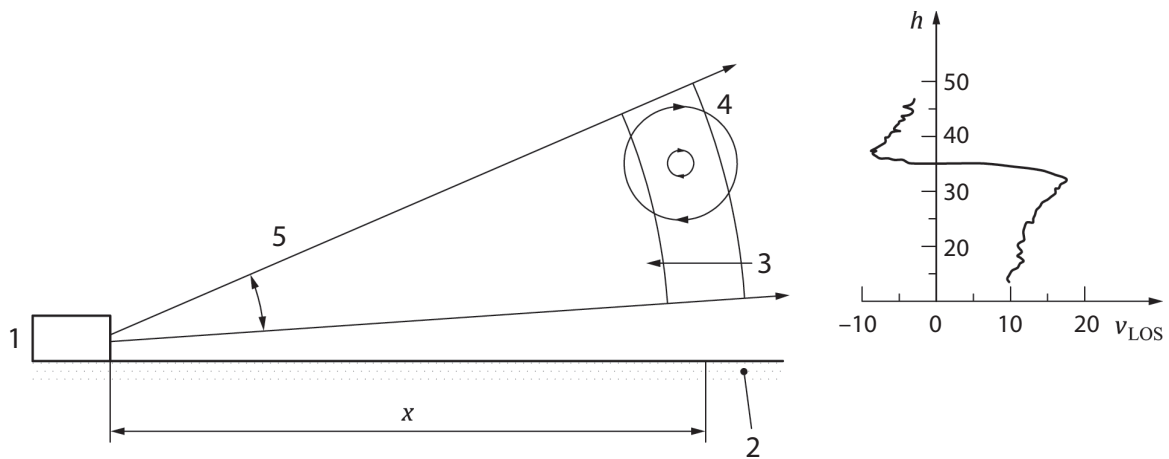
Key
1   Lidar
2   Runway
3   Crosswind
4   Vortex
5   Elevation scan

Measurement principle for determining aircraft wake vortices with Doppler wind lidar

effect wake vortex behaviour. Usually, wake vortices measurements are performed close to the runways with range height indicator scans with narrow angles of typically 10° to 40° to map vertically the motion of the wake vortices.

Lidar measurements can besides be post-processed to calculate wake vortices characteristics like the probability of detection, the localization of their cores and their circulation (strength)[34;35].

C.2.4   *Siting constraints*

Since the Doppler lidar delivers only the radial wind speed, siting of the instrument is a crucial point, because runway-oriented wind has to have a significant projection onto the line of sight of the lidar. In general, the magnitude, and therefore the quality, of the runway-oriented wind component projected onto the line of sight deteriorates as $\cos^2 \theta$, θ being the angle between the line of sight and the runway[6].

Another point is that, ideally, the 3° glide slope is to be scanned. This can be ideally done with one plan position indicator scan, if the lidar is located at the runway threshold. If more than one runway threshold is to be monitored with one instrument, following exactly the 3° glide is not possible, and the above-mentioned timing constraints usually do not allow scanning of more than one elevation. However, a 3° scan centred at the actual location of the lidar still outperforms an anemometer-based low-level wind shear alert system in terms of glide slope wind shear detection.

———————

ATTACHMENT D. TYPICAL APPLICATION RANGES AND CORRESPONDING REQUIREMENTS

(informative)

Accordingly to the needs for the main applications (see table below), three accuracy classes for the wind velocity are being defined. These classes are related to a defined spatial and temporal resolution. The wind velocity accuracy must be ensured in all ranges of interest.

(a) Class A: $x \leq 0.1$ m/s (e.g. for wind energy purposes);

(b) Class B: $0.1 < x \leq 0.5$ m/s (e.g. for meteorological applications)[13];

(c) Class C: $0.5 < x \leq 1.0$ m/s (e.g. for nowcasting)[13].

Typical application ranges and corresponding requirements

Application	Parameter to be provided	Reference	Typical probing range (m)	Range resolution (m)	Time resolution (min)	Velocity measurement accuracy (m/s)	Wind direction accuracy (°)	Minimum data availability (%)
Radial velocity mapping	Line-of-sight radial velocity	Formula 5.A.5	200–10 000	25–100	1–10	0.5	Not applicable	50–99[a]
Wind energy, e.g. site assessment, power curve, wind profile	Profile of the horizontal wind vector along the vertical axis	e.g. [36]	40–200	25	10	0.5	2	85
High-resolution numerical weather prediction	Profile of the horizontal wind vector along the vertical axis	[13]	> 50	25	10	0.5	2	80
Air pollution, e.g. dispersion modelling, risk management	Profile of the horizontal wind vector along the vertical axis	–	40–200	25	10	0.5	–	90
Aviation: wind shear	Radial wind along takeoff path, approach and runways	[29;36]	7 000–8 000 (5 500 + half the runway)	200	1	0.5	5	80
Aviation: vortex monitoring (ground-based systems)	Radial wind speed in perpendicular planes to the runway	–	Distance to runway + 300–500 on each side	25 (5 with overlap)	0.1	1	–	< 50
Met applications, e.g. nowcasting	Profile of the horizontal wind vector along the vertical axis	[13]	0–4 000	100	15	1	5	80

a   Depending on application

BIBLIOGRAPHY

[1]   Henderson, S.W., P. Gatt, D. Rees and R.M.N. Huffaker, 2005: Wind lidar. In: *Laser Remote Sensing* (T. Fujii and T. Fukuchi, eds.). 469–722, CRC Press, ISBN-10: 8247-4256-7.

[2]   Measures, R.M., 1992: *Laser Remote Sensing: Fundamentals and Applications*. Krieger Publishing, 524 pp., ISBN-10: 8946-4619-2.

[3]   Frehlich, R. and M. Kavaya, 1991: Coherent laser radar performance for general atmospheric refractive turbulence. *Appl. Opt.*, 30:5325–5352.

[4]   Belmonte, A., 2003: Analyzing the efficiency of a practical heterodyne lidar in the turbulent atmosphere: telescope parameters. *Opt. Express.*, 11:2041–2046.

[5]   Frehlich, R., S. Hannon and S. Henderson, 1997: Coherent Doppler lidar measurements of winds in the weak signal regime. *Appl. Opt.*, 36:3491–3499.

[6]   Banakh, V.A. and I.N. Smalikho, 1997: Estimation of the turbulence eddy dissipation rate from the pulsed Doppler lidar data. *Atmos. Oceanic Opt.*, 10(12).

[7]   Frehlich, R., 1996: Simulation of coherent Doppler lidar performance in the weak signal regime. *J. Atmos. Ocean. Technol.*, 13:646–658.

[8]   Dabas, A., P. Drobinski and P. Flamant, 2000: Velocity biases of adaptive filters in heterodyne doppler lidar measurements. *J. Atmos. Ocean. Technol.*, 17:1189–1202.

[9]   Dabas, A., 1999: Semi empirical model for the reliability of a matched filter frequency estimator for Doppler lidar. *J. Atmos. Ocean. Technol.*, 16:19–28.

[10]   Goodman, J.W., 1975: Statistical properties of laser speckle patterns. In: *Laser Speckle* (J.C. Dainty, ed.). Springer.

[11]   American National Standards Institute (ANSI) Z136.1-2014: *American National Standard for Safe Use of Lasers*. ISBN: 978-1-940168-00-5.

[12]   IEC 60825-1:2014: *Safety of Laser Products – Part 1: Equipment Classification and Requirement*.

[13]   World Meteorological Organization: http://www.wmo-sat.info/oscar/requirements.

[14]   Boquet, M., P. Royer, J.P. Cariou, M. Machta and M. Valla, 2016: Simulation of doppler lidar measurement range and data availability. *J. Atmos. Ocean. Technol.*, paper accepted, DOI: 10.1175/JTECH-D-15-0057.1.

[15]   Frehlich, R., 2001: Estimation of velocity error for doppler lidar measurements. *J. Atmos. Ocean. Technol.*, 18:1628–1639.

[16]   Ernsdorf, T., B. Stiller, B.R. Beckmann, A. Weipert, S. Kauczok and R. Hannesen, 2014: Inter-comparison of X-band radar and lidar low-level wind measurement for air traffic control (ATC). Eighth Europ. Conf. on Radar in Meteorol. and Hydrol., Garmisch-Partenkirchen, Germany.

[17]   Hannesen, R., S. Kauczok and A. Weipert, 2014: Quality of clear-air radar radial velocity data: do insects matter? Eighth Europ. Conf. on Radar in Meteorol. and Hydrol., Garmisch-Partenkirchen, Germany.

[18]   Weipert, A., S. Kauczok, R. Hannesen, T. Ernsdorf and B. Stiller, 2014: Wind shear detection using radar and lidar at Frankfurt and Munich airports. Eighth Europ. Conf. on Radar in Meteorol. and Hydrol., Garmisch-Partenkirchen, Germany.

[19]   Jörgensen, H., T. Mikkelsen, J. Streicher, H. Herrmann, C. Werner and E. Lyck, 1997: Lidar calibration experiment. *Appl. Phys. B.*, 64:355–361.

[20]   Bronstein, I.N., K.A. Semendjajew, G. Musiol and H. Mühlig, 1993: *Taschenbuch der Mathematik*. Harri Deutsch.

[21]   Fukao, S. and K. Hamazu, 2013: *Radar for Meteorological and Atmospheric Observations*. Springer.

[22]   Banakh, V.A. and I.N. Smalikho, 2013: *Coherent Doppler Wind Lidars in a Turbulent Atmosphere.* Artech House.

[23]   Srinivaso, R.I., V.K. Anandan and R.R. Narasimha, 2008: Evaluation of DBS wind measurement technique in different beam configurations for a VHF wind profiler. *J. Atmos. Ocean. Technol.*, 25(12):2304–2312.

[24]   Lhermite, R.M., 1962: Note on wind variability with Doppler radar. *J. Atmos. Sci.*, 19(4):343–346.

[25]   Browning, K.A. and R. Wexler, 1968: The determination of kinematic properties of a wind field using Doppler radar. *J. Appl. Meteorol.*, 7(1):105–113.

[26]   Waldteufel, P. and H. Corbin, 1979: On the analysis of single Doppler radar data. *J. Appl. Meteor.*, 18:532–542.

[27]   IEC 61400-12-1:2005: *Wind Turbines – Part 12-1: Power Performance Measurements of Electricity Producing Wind Turbines*.

[28]   European ATM Master Plan, 2009: https://www.atmmasterplan.eu/.

[29]   International Civil Aviation Organization, 2007: *Meteorological Service for International Air Navigation*, Annex 3 to the Convention on International Civil Aviation.

[30]   International Civil Aviation Organization, 2005: *Manual on Low-level Wind Shear*, Doc 9817 AN/449.

[31]   Shun, C.M. and P.W. Chan, 2008: Applications of an infrared doppler lidar in detection of wind shear. *J. Atmos. Ocean. Technol.*, 25(5):637–655.

[32]   Wakenet-Eu: http://www.wakenet.eu/.

[33]   Lang, S. and W. Bryant, 2006: *Vortex Research in the USA (WakeNet-USA)*. Air Traffic Organization, Federal Aviation Administration.

[34]   Holzäpfel, F., T. Gerz, F. Köpp, E. Stumpf, M. Harris, R.I. Young and A. Dolfi-Bouteyre, 2003: Strategies for circulation evaluation of aircraft wake vortices measured by lidar. *J. Atmos. Ocean. Technol.*, 20(8):1183–1195.

[35]   Dolfi-Bouteyre, A., B. Augere, M. Valla, D. Goular, D. Fleury and G. Canat, 2009: 1,55 μm pulsed fiber lidar for wake vortex detection (axial or transverse). Wakenet-Eu Workshop.

[36]   Hasager, C.B., D. Stein, M. Courtney, A. Pena, T. Mikkelsen, M. Stickland and A. Oldroyd, 2013: Hub height ocean winds over the North Sea observed by the NORSEWInD lidar array: measuring techniques, quality control and data management. *Remote Sens.*, 5:4280–4303.

[37]   ISO 28902-1: *Air Quality – Environmental Meteorology – Part 1: Ground-based Remote Sensing of Visual Range by Lidar*.

[38]   ISO 28902-3:[1] *Air Quality – Environmental Meteorology – Part 3: Ground-based Remote Sensing of Wind by Continuous-wave Doppler Lidar*.

----

[1]   Under preparation

REFERENCES AND FURTHER READING

Adachi, A., T. Kobayashi, K.S. Gage, D.A. Carter, L.M. Hartten, W.L. Clark and M. Fukuda, 2005: Evaluation of three-beam and four-beam profiler wind measurement techniques using a five-beam wind profiler and collocated meteorological tower. *Journal of Atmospheric and Oceanic Technology*, 22:1167–1180.

Angevine, W.M., W.L. Ecklund, D.A. Carter, K.S. Gage and K.P. Moran, 1994: Improved radio acoustic sounding techniques. *Journal of Atmospheric and Oceanic Technology*, 11(1):42–49.

Bevis, M., S. Businger, S. Chiswell, T.A. Herring, R.A. Anthes, C. Rocken and R.H. Ware, 1994: GPS meteorology: Mapping zenith wet delays onto precipitable water. *Journal of Applied Meteorology*, 33:379–386.

Brown, E.H. and F.F. Hall, 1978: Advances in atmospheric acoustics. *Reviews of Geophysics and Space Physics*, 16:47–109.

Cadeddu, M.P., G.E. Peckham and C. Gaffard, 2002: The vertical resolution of ground-based microwave radiometers analyzed through a multiresolution wavelet technique. *IEEE Transactions on Geoscience and Remote Sensing*, 40(3):531–540.

Candlish, L.M., R.L. Raddatz, M.G. Asplin and D.G. Barber, 2012: Atmospheric temperature and absolute humidity profiles over the Beaufort Sea and Amundsen Gulf from a microwave radiometer. *Journal of Atmospheric and Oceanic Technology*, 29:1182–1201.

Davis, J.L., T.A. Herring, I.I. Shapiro, A.E.E. Rogers and G. Elgered, 1985: Geodesy by radio interferometry: Effects of atmospheric modeling errors on estimates of baseline length. *Radio Science*, 20(6):1593–1607.

Derr, V.E., 1972: *Remote Sensing of the Troposphere*. United States National Oceanic and Atmospheric Administration, WPL, Boulder, Colorado.

Elgered, G., H.-P. Plag, S. Barlag and J. Nash, 2004: *COST716 Final Report*, European Union.

Gaffard, C. and T. Hewison, 2003: Radiometrics MP3000 microwave radiometer trial report. *Technical Report –TR26*, Met Office, Workingham, Berkshire, UK.

Gaynor, J.E., C.B. Baker and J.C. Kaimal, 1990: The international sodar intercomparison experiment. *Proceedings of the Fifth International Symposium on Acoustic Remote Sensing*. McGraw-Hill, New York, pp. 67–74.

Gossard, E.E. and R.G. Strauch, 1983: *Radar Observations of Clear Air and Clouds*. Elsevier, Scientific Publishing Co., Amsterdam.

Güldner, J. and D. Spänkuch, 2001: Remote sensing of the thermodynamic state of the atmospheric boundary layer by ground-based microwave radiometry. *Journal of Atmospheric and Oceanic Technology*, 18:925–933.

Hinkley, E.D., 1976: *Laser Monitoring of the Atmosphere: Topics in Applied Physics*. Volume 14, Springer Verlag, New York.

Hogg, D.C., M.T. Decker, F.O. Guiraud, K.B. Earnshaw, D.A. Merritt, K.P. Moran, W.B. Sweezy, R.G. Strauch, E.R. Westwater and C.G. Little, 1983: An automatic profiler of the temperature, wind and humidity in the troposphere. *Journal of Climate and Applied Meteorology*, 22:807–831.

Kadygrov, E.N., E.A. Miller and A.V. Troitsky, 2013: Study of atmospheric boundary layer thermodynamics during total solar eclipses. *IEEE Transactions on Geoscience and Remote Sensing*, 51(9):4672–4677.

Kadygrov, E.N. and D.R. Pick, 1998: The potential for temperature retrieval from an angular-scanning single-channel microwave radiometer and some comparisons with in situ observations. *Meteorological Applications*, 5:393–404.

Kadygrov, E.N., G.N. Shur and A.S. Viazankin, 2003: Investigation of atmospheric boundary layer temperature, turbulence, and wind parameters on the basis of passive microwave remote sensing. *Radio Science*, 38(3):13.1–13.12.

Lataitis, R.J., 1992a: Signal power for radio acoustic sounding of temperature: The effects of horizontal winds, turbulence and vertical temperature gradients. *Radio Science*, 27:369–385.

———, 1992b: *Theory and Application of a Radio-acoustic Sounding System*. NOAA Technical Memorandum ERL WPL-230.

Liljegren, J.C., S.A. Boukabara, K. Cady-Pereira and S.A. Clough, 2005: The Effect of the half-width of the 22-GHz water vapor line on retrievals of temperature and water vapor profiles with a 12-channel radiometer. *IEEE Transactions on Geoscience and Remote Sensing*, 43(5):1102–1108.

Madhulatha, A., M. Rajeevan, M.V. Ratnam, J. Bhate and C.V. Naidu, 2013: Nowcasting severe convective activity over southeast India using ground-based microwave radiometer observations. *Journal of Geophysical Research: Atmospheres*, 118(1):1–13.

Martner, B.E., D.B. Wuertz, B.B. Stankov, R.G. Strauch, E.R. Westwater, K.S. Gage, W.L. Ecklund, C.L. Martin and W.F. Dabberdt, 1993: An evaluation of wind profiler, RASS and microwave radiometer performance. *Bulletin of the American Meteorological Society*, 74(4):599–613.

May, P.T., R.G. Strauch, K.P. Moran and W.L. Eckund, 1990: Temperature sounding by RASS, with wind profiler radars: A preliminary study. *IEEE Transactions on Geoscience and Remote Sensing*, 28(1):19–28.

Navas-Guzman, F., O. Stahli and N. Kampfer, 2013: Study of cloud effect on the tropospheric temperature retrievals. In: *URSI Commission F Microwave Signatures 2013: Specialist Symposium on Microwave Remote Sensing of the Earth, Oceans, and Atmosphere*, October 2013, Finland, p.136.

Neff, W.D. and R.L. Coulter, 1986: Acoustic remote sounding. In: *Probing the Atmospheric Boundary Layer* (Lenschow, D.H., ed.). American Meteorological Society, 201–236.

Panofsky, H.A., 1973: Tower micrometeorology. In: *Workshop on Micrometeorology* (Haugen, D.A., ed.), Chapter 4, American Meteorological Society.

Saastamoinen, J., 1972: Atmospheric correction for the troposphere and stratosphere in radio ranging of satellites. *Geophysical Monograph Series: The Use of Artificial Satellites for Geodesy*, 15:247–251.

Singal, S.P., 1990: Current status of air quality related boundary layer meteorological studies using sodar. *Proceedings of the Fifth International Symposium on Acoustic Remote Sensing*, McGraw-Hill, New York, 453–476.

Smith, E.K. and S. Weintraub, 1953: The constants in the equation for atmospheric refractive index at radio frequencies. *Proceedings of the IRE*, 41(8):1035–1037.

Solheim, F., J.R. Godwin, E.R. Westwater, Y. Han, S.J. Keihm, K. Marsh, R. Ware, 1998: Radiometric profiling of temperature, water vapor, and cloud liquid water using various inversion methods. *Radio Science*, 33:393–404.

Syed, I. and E.V. Browell, 1994: Recent Lidar technology developments and their influence on measurements of tropospheric water vapor. *Journal of Atmospheric and Oceanic Technology*, 11(1):76–84.

Thayer, G.D., 1974: An improved equation for the radio refractive index of air. *Radio Science*, 9(10):803–807.

Thomas, L., 1991: Lidar probing of the atmosphere. *Indian Journal of Radio and Space Physics*, 20:368–380.

Thompson, A.R., J.M. Moran and G.W. Swenson, 1986: *Interferometry and Synthesis in Radio Astronomy*. John Wiley and Sons, New York.

Thompson, N., 1980: Tethered balloons. In: *Air-sea Interaction: Instruments and Methods* (F. Dobson, L. Hasse and R. Davis, eds.) Chapter 31, Plenum Press, New York.

Ware, R., R. Carpenter, J. Güldner, J. Liljegren, T. Nehrkorn, F. Solheim and F. Vandenberghe, 2003: A multi-channel radiometric profiler of temperature, humidity and cloud liquid. *Radio Science*, 38:8079–8092.

Ware, R., D. Cimini, E. Campos, G. Giuliani, S. Albers, M. Nelson, S.E. Koch, P. Joe and S. Cober, 2013: Thermodynamic and liquid profiling during the 2010 Winter Olympics. *Atmospheric Research*, 132–133:278–290.

Weber, B.L. and D.B. Wuertz, 1990: Comparison of rawinsonde and wind profiler radar measurements. *Journal of Atmospheric and Oceanic Technology*, 7(1):157–174.

Weber, B.L., D.B. Wuertz, R.G. Strauch, D.A. Merritt, K.P. Moran, D.C. Law, D. van de Kamp, R.B. Chadwick, M.H. Ackley, M.F. Barth, N.L. Abshire, P.A. Miller and T.W. Schlatter, 1990: Preliminary evaluation of the first NOAA demonstration network wind profiler. *Journal of Atmospheric and Oceanic Technology*, 7(6):909–918.

Westwater, E., S. Crewell, C. Mätzler and D. Cimini, 2005: Principles of Surface-based Microwave and Millimeter Wave Radiometric Remote Sensing of the Troposphere. *Quaderni Della Società Italiana di Elettromagnetismo*, 1(3).

Westwater, E.R., Y. Han, V.G. Irisov, V. Leuskiy, E.N. Kadygrov and S.A. Viazankin, 1999: Remote sensing of boundary layer temperature profiles by a scanning 5-mm microwave radiometer and RASS: Comparison experiments. *Journal of Atmospheric and Oceanic Technology*, 16:805–818.

Westwater, E.R., J.B. Snider and M.J. Falls, 1990: Ground-based radiometric observations of atmospheric emission and attenuation at 20.6, 31.65, and 90.0 GHz: A comparison of measurements and theory. *IEEE Transactions on Antennas and Propagation*, 38(10):1569–1580.

World Meteorological Organization, 1980: *Lower Tropospheric Data Compatibility: Low-level Intercomparison Experiment* (Boulder, United States, 1979). Instruments and Observing Methods Report No. 3. Geneva.

———, 1982: *Indirect Sensing: Meteorological Observations by Laser Indirect Sensing Techniques* (A.O. Van Gysegem). Instruments and Observing Methods Report No. 12. Geneva.

———, 1994: Comparison of windprofiler and rawinsonde measurements (J. Neisser, V. Görsdorf and H. Steinhagen). *Papers Presented at the WMO Technical Conference on Instruments and Methods of Observation (TECO-94)*. Instruments and Observing Methods Report No. 57 (WMO/TD-No. 588). Geneva.

———, 2006*a*: *Operational Aspects of Different Ground-Based Remote Sensing Observing Techniques for Vertical Profiling of Temperature, Wind, Humidity and Cloud Structure: A Review* (E.N. Kadygrov). Instruments and Observing Methods Report No. 89 (WMO/TD-No. 1309). Geneva.

———, 2006*b*: *National/Regional Operational Procedures of GPS Water Vapour Networks and Agreed International Procedures* (S. de Haan). Instruments and Observing Methods Report No. 92 (WMO/TD-No. 1340). Geneva.

CHAPTER CONTENTS

CHAPTER 6. ELECTROMAGNETIC METHODS OF LIGHTNING DETECTION

6.1   INTRODUCTION

There are many individual physical processes in cloud and ground lightning flashes. Each of these processes is associated with characteristic electric and magnetic fields. Lightning is known to emit significant electromagnetic energy in the radio-frequency range from below 1 Hz to near 300 MHz, with a peak in the frequency spectrum near 5 to 10 kHz for lightning at distances beyond 50 km or so. Further, electromagnetic radiation from lightning is detectable at even higher frequencies, for example, in the microwave (300 MHz to 300 GHz) and, obviously, in visible light (roughly 10^{14} to 10^{15} Hz). At frequencies higher than that of the spectrum peak, the spectral amplitude varies roughly inversely proportional to the frequency up to 10 MHz or so and inversely proportional to the square root of frequency from about 10 MHz to 10 GHz. Also, lightning is known to produce X-rays (up to 10^{20} Hz or more), although at ground level they are usually not detectable beyond a kilometre or so from the source. In general, any observable electromagnetic signal from a lightning source can be used to detect and locate the lightning process that produced it. In addition to electromagnetic radiation, lightning produces the acoustic radiation that can be also used for lightning location. The acoustic locating techniques, acoustic signal time of arrival and acoustic ray tracing are not further discussed here.

6.2   LIGHTNING DISCHARGE

Lightning can be defined as a transient, high-current (typically tens of kiloamperes) electric discharge in air whose length is measured in kilometres. As for any discharge in air, lightning channel is composed of ionized gas, that is, of plasma, whose peak temperature is typically 30 000 K, about five times higher than the temperature of the surface of the Sun. Lightning was present on Earth long before human life evolved, and it may even have played a crucial role in the evolution of life on our planet. The global lightning flash rate is some tens to a hundred per second or so. Each year, some 25 million cloud-to-ground lightning discharges (note that, on average, about three quarters of lightning discharges are confined to the cloud, that is, do not involve ground) occur in the United States alone, killing more people than tornadoes and hurricanes. Lightning initiates many forest fires, and over 30% of all electric power line failures are lightning related. Each commercial aircraft is struck by lightning on average once a year. A lightning strike to an unprotected object or system can be catastrophic.

6.2.1   Lightning types, processes and parameters

About 90% or more of global cloud-to-ground lightning is accounted for by negative (negative charge is effectively transported to the ground) downward (the initial process begins in the cloud and develops in a downward direction) lightning. Other types of cloud-to-ground lightning include positive downward, negative upward, and positive upward discharges. There are also bipolar lightning discharges sequentially transferring both positive and negative charges during the same flash. The basic elements of the negative downward lightning discharge are termed component strokes or just strokes. Each discharge (or flash) typically contains 3 to 5 strokes, the observed range being 1 to 26. Roughly half of all lightning discharges to Earth strike ground at more than one point, with the spatial separation between the channel terminations being up to many kilometres. The two major lightning processes comprising a stroke are termed the leader and the return stroke, which occur as a sequence with the leader preceding the return stroke. The following discussion considers lightning discharges in more detail. Rakov and Uman (2003) and references therein contain more details.

Two photographs of a negative cloud-to-ground discharge are shown in Figures 6.1(a) and 6.1(b). The image in Figure 6.1(a) was obtained using a stationary camera, while the image in Figure 6.1(b) was captured with a separate camera that was moved horizontally during the
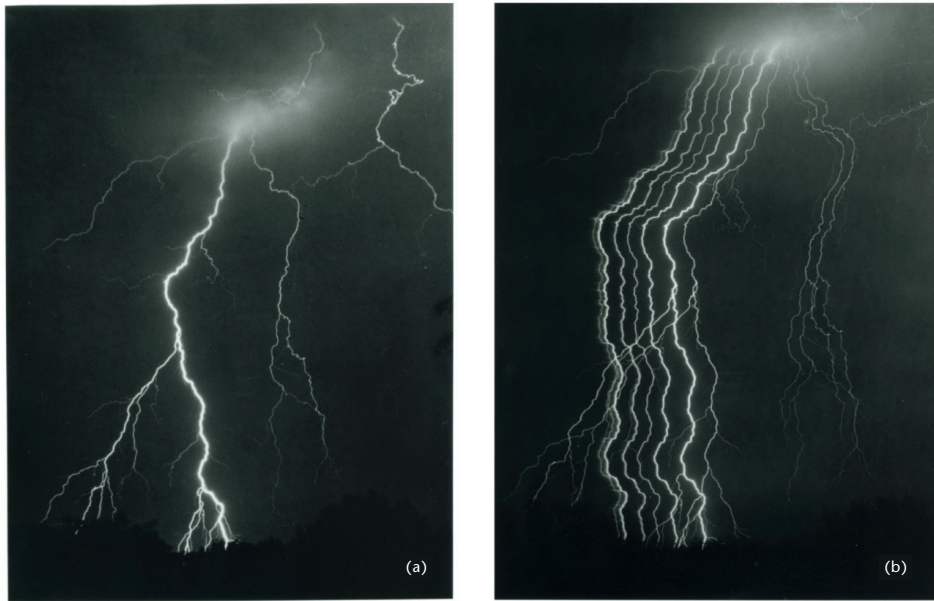
Figure 6.1. Lightning flash which appears to have at least 7 (perhaps as many as 10) separate ground strike points. Image (a) is a still photograph and image (b) a streaked photograph. Some of the strike points are associated with the same stroke having separate branches touching ground, while others are associated with different strokes taking different paths to ground. Adapted from Hendry (1993)

time of the flash. As a result, the latter image is time resolved showing seven distinct luminous channels between the cloud and ground. The dark intervals between these channels are typically of the order of tens of milliseconds and explain why lightning often appears to the human eye to flicker. Each luminous channel corresponds to an individual stroke, the first stroke being on the far right (time advances from right to left). The first two strokes are branched, and the downward direction of branches indicates that this is a downward lightning flash.

Sketches of still and time-resolved images of the three-stroke lightning flash are shown in Figures 6.2(a) and 6.2(b), respectively. A sketch of the corresponding current at the channel base is shown in Figure 6.2(c). In Figure 6.2(b), time advances from left to right, and the timescale is not continuous. Each of the three strokes in Figure 6.2(b), represented by its luminosity as a function of height above ground and time, is composed of a downward-moving process, termed a leader, and an upward-moving process, termed a return stroke (RS). The leader creates a conducting path between the cloud charge source region and ground and distributes negative charge from the cloud source region along this path. The return stroke traverses that path moving from ground toward the cloud charge source region and neutralizes the negative leader charge. Thus, both leader and return-stroke processes serve to effectively transport negative charge from the cloud to ground. As seen in Figure 6.2(b), the leader initiating the first return stroke differs from the leaders initiating the two subsequent strokes (all strokes other than the first are termed subsequent strokes). In particular, the first-stroke leader appears optically to be an intermittent process, hence the term stepped leader (SL), while the tip of a subsequent-stroke leader appears to move continuously. The continuously moving subsequent-stroke leader tip appears on streak photographs as a downward-moving dart, hence the term dart leader (DL). The apparent difference between the two types of leaders is related to the fact that the stepped leader develops in virgin air, while the dart leader follows the pre-conditioned path of the preceding stroke or strokes. Sometimes a subsequent leader exhibits stepping while propagating along a previously formed channel; in which case it is referred to as a dart-stepped leader. There are also so-called chaotic subsequent-stroke leaders. All types of leaders produce bursts of X-ray emission with energies typically up to 250 keV (twice the energy of a chest X-ray) (Dwyer, 2005).
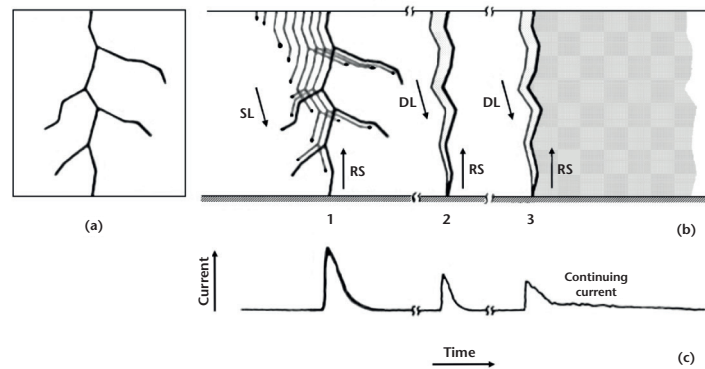
Figure 6.2. Drawing showing the luminosity of a three-stroke ground flash and the corresponding current at the channel base. Figure (a) is a still-camera image, (b) a streak-camera image, and (c) a channel-base current.

The electric potential difference between a downward-moving stepped-leader tip and ground is probably some tens of megavolts, comparable to or a considerable fraction of that between the cloud charge source and ground. The magnitude of the potential difference between two points, one at the cloud charge source and the other on ground, is the line integral of electric field intensity between those points. The upper and lower limits for the potential difference between the lower boundary of the main negative charge region and ground can be estimated by multiplying, respectively, the typical observed electric field in the cloud, 10^5 V/m, and the expected electric field at ground under a thundercloud immediately prior to the initiation of lightning, 10^4 V/m, by the height of the lower boundary of the negative charge centre above ground, 5 km or so. The resultant range is 50 to 500 MV.

When the descending stepped leader attaches to the ground, the first return stroke begins. The first return-stroke current measured at ground rises to an initial peak of about 30 kA in some microseconds and decays to half-peak value in some tens of microseconds. The return stroke effectively lowers to ground the several coulombs of charge originally deposited on the stepped-leader channel including all the branches, as well as any additional cloud charge that may enter the return-stroke channel.

Once the bottom of the dart-leader channel is connected to the ground, the second (or any subsequent) return-stroke wave is launched upward, which again serves to neutralize the leader charge. The subsequent return-stroke current at ground typically rises to a peak value of 10 to 15 kA in less than a microsecond and decays to half-peak value in a few tens of microseconds.

The high-current return-stroke wave rapidly heats the channel to a peak temperature near or above 30 000 K and creates a channel pressure of 1 MPa or more, resulting in channel expansion, intense optical radiation and an outward propagating shock wave that eventually becomes the thunder (sound wave) we hear at a distance.

The impulsive component of the current in a return stroke (usually subsequent) is often followed by a continuing current which has a magnitude of tens to hundreds of amperes and a duration of up to hundreds of milliseconds. Continuing currents with a duration in excess of 40 ms are traditionally termed long continuing currents. Between 30% and 50% of all negative cloud-to-ground flashes contain long continuing currents. Current pulses superimposed on continuing currents, as well as the corresponding enhancements in luminosity of the lightning channel, are referred to as M-components.

There is a special type of lightning that is thought to be the most intense natural producer of HF-VHF (3–300 MHz) radiation on Earth. It is referred to as compact intracloud discharge (CID). Compact intracloud discharges were first reported by Le Vine (1980) and received their name (Smith et al., 1999) due to their relatively small (hundreds of metres) spatial extent. They tend to occur at high altitudes (mostly above 10 km), appear to be associated with strong convection (however, even the strongest convection does not always produce CIDs), tend to produce less

light than other types of lightning discharges, and produce single bipolar electric field pulses (narrow bipolar pulses or NBPs) having typical full widths of 10 to 30 μs and amplitudes of the order of 10 V/m at 100 km, which is comparable to or higher than for return strokes in cloud-to-ground flashes. As an illustration of intensity of wideband electromagnetic signature of CIDs, 48 CIDs examined in detail by Nag et al. (2010) were recorded by 4 to 22 (11 on average) stations of the US National Lightning Detection Network (NLDN), whose average baseline is 300–350 km.

6.2.2   **Lightning electromagnetic signatures**

Both cloud-to-ground and cloud lightning discharges involve a number of processes that produce characteristic electromagnetic field signatures. Salient characteristics of measured electric and magnetic fields generated by various lightning processes at distances ranging from tens to hundreds of kilometres are briefly reviewed below. The emphasis is put on those processes which produce substantial microsecond- and submicrosecond-scale field variations.

The table below summarizes essentially all identifiable lightning radiation field signatures as recorded at ground. Note that apparently there is no characteristic microsecond-scale field signature associated with lightning K- and M- processes. Besides return strokes (the first row) and compact intracloud discharges (the last row), the pulses produced by lightning processes represented in the table occur in sequences with submillisecond-interpulse intervals. Leader pulses (second and third rows) are presumably emitted by the lower portion of the channel to ground just prior to the initiation of a return stroke, while both initial breakdown pulses (fourth and fifth rows) and regular pulse bursts (sixth row) are produced by lightning processes occurring inside the cloud. Characterization given below concerns both the overall pulse sequences and individual pulses.

Negative ground flashes

The typical microsecond-scale pulse structure of naturally occurring negative ground discharges, as observed at ground, includes an initial sequence of pulses (usually called initial or preliminary breakdown pulses) followed, typically some milliseconds to some tens of milliseconds later, by 3 to 5 relatively large return-stroke pulses spaced several tens of milliseconds apart. The duration of the initial sequence of pulses is typically a few milliseconds. Individual pulse waveforms characteristic of the preliminary breakdown in negative ground flashes are shown in Figure 6.3(a). The initial polarity of the preliminary breakdown pulses is usually the same as that of the following return-stroke pulse. The initial breakdown pulses can have amplitudes comparable to or even exceeding that of the corresponding return-stroke pulses. Just prior to the first return-stroke pulse and prior to some subsequent return-stroke pulses there are pulse sequences, in the former case associated with the stepped-leader process and in the latter case with dart-stepped (regular pulse train) or chaotic (irregular pulse train) leader processes. These pulse sequences have been observed to last for some tens of hundreds of microseconds, and the pulse amplitudes are one to two orders of magnitude smaller than the corresponding return-stroke pulse amplitude. The stepped-leader pulses are seen just prior to the return-stroke pulse in Figure 6.4(a), before $t = 0$. A rather irregular pulse train, indicative of chaotic leader, is seen prior to the subsequent return-stroke pulse (before $t = 0$) in Figure 6.4(b). Usually there is a relatively quiet millisecond-scale gap between the preliminary breakdown pulse sequence and the beginning of pronounced stepped-leader pulses. The intervals between the return-stroke pulses, and the interval of some tens of milliseconds following the last return-stroke pulse, contain regular pulse bursts of relatively small amplitude and some other, usually irregular, pulse activity. Pulse peaks in regular pulse bursts are approximately two orders of magnitude smaller than return-stroke initial field peaks in the same flash. As seen in the table, the regular pulse bursts are very similar in their characteristics to the pulse sequences associated with dart-stepped leaders. The geometric mean initial electric field peak normalized to 100 km for negative first strokes, about 6 V/m, is about a factor of two larger than for negative subsequent strokes, about 3 V/m. The geometric mean time interval between return-stroke pulses is 60 ms.

Characterization of microsecond-scale electric field pulses associated with various lightning processes (adapted from Rakov, 1999)

Type of pulses	Dominant polarity (atmospheric electricity sign convention)	Typical total pulse duration (μs)	Typical time interval between pulses (μs)	Comments
Return stroke in negative ground flashes	Positive	30–90 (zero-crossing time)	60×10^3	3–5 pulses per flash
Stepped leader in negative ground flashes	Positive	1–2	15–25	Within 200 μs just prior to a return stroke
Dart-stepped leader in negative ground flashes	Positive	1–2	6–8	Within 200 μs just prior to a return stroke
Initial breakdown in negative ground flashes	Positive	20–40	70–130	Some milliseconds to some tens of milliseconds before the first return stroke
Initial breakdown in cloud flashes	Negative	50–80	600–800	The largest pulses in a flash
Regular pulse burst in both cloud and negative ground flashes	Both polarities are about equally probable	1–2	5–7	Occur later in a flash; 20–40 pulses per burst
Compact intracloud discharge (narrow bipolar event)	Both polarities occur, with negative being more frequent	10–30	–	Typically not preceded or followed by any other lightning process within hundreds of milliseconds

Notes:
a   Polarity refers to the polarity of the initial half cycle in the case of bipolar pulses.
b   According to the atmospheric electricity sign convention, a downward-directed electric field vector is assumed to be positive.

Positive ground flashes

Positive flashes usually contain a single return stroke (although up to four strokes per flash have been observed) whose microsecond-scale electric and magnetic field waveforms are similar to those characteristic of negative first return strokes, except for the initial polarity. An example of positive return-stroke electric field waveform is given in Figure 6.4(c). Small pulses seen before $t = 0$ in Figure 6.4(c) are indicative of a stepped-leader process. As opposed to negative first strokes, these pulses are detected only in about one third of field waveforms. The mean initial electric field peak normalized to 100 km for positive first strokes is about a factor of two larger than for negative first strokes. Positive strokes to ground can be initiated in a way similar to how negative lightning flashes are initiated (see above) or they can be by-products of extensive cloud discharges.

Cloud flashes

The typical pulse structure that is observed in naturally occurring cloud discharges includes an initial sequence (or sequences) of pulses of relatively large amplitude, spaced some hundreds of microseconds apart and occurring within the first several to a few tens of milliseconds, followed by a number of regular pulse bursts of significantly smaller amplitude. Pulses within the burst
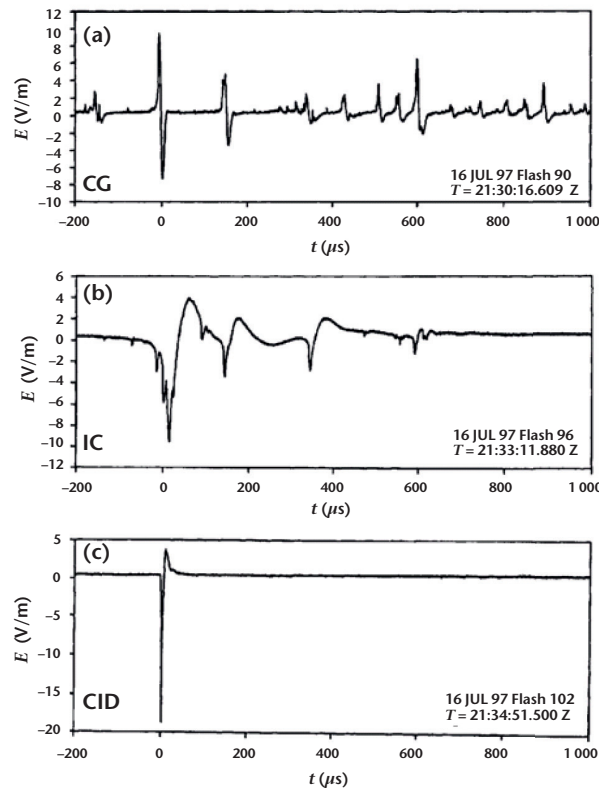
Figure 6.3. Examples of electric field (E) pulse waveforms characteristic of (a) the initial breakdown in negative ground (CG) flashes, (b) the initial breakdown in cloud (IC) flashes, and (c) compact intracloud discharges (CIDs). Positive electric field (atmospheric electricity sign convention) deflects upward. (Adapted from Rakov, 1999)

are several microseconds apart, with each burst lasting for some hundreds of microseconds. Individual pulse waveforms characteristic of the initial breakdown in cloud flashes are shown in Figure 6.3(b). The initial polarity of these pulses tends to be opposite to that of the initial breakdown pulses in negative ground flashes. There are also microsecond-scale pulses, with amplitudes appreciably lower than those of the initial breakdown pulses, which are dispersed, as opposed to clustering in bursts, throughout the flash. Some of these smaller and often irregular pulses are associated with step-like K changes (field signatures of K-processes). K changes typically occur in the late stage of the cloud flash and are separated by many tens of milliseconds.

Compact intracloud discharges

An example of electric field signature of compact intracloud discharges (also called narrow bipolar events) is given in Figure 6.3(c). These pulses have peaks and peak time derivatives comparable to those of return strokes in ground flashes.

6.2.3 Glossary of terms

Atmospheric electricity sign convention: Electric field sign convention according to which a downward-directed field vector is defined as positive.

Bipolar lightning: Lightning discharges sequentially transferring both positive and negative charges to ground during the same flash.

Cloud flash: Flash that does not contact the ground.
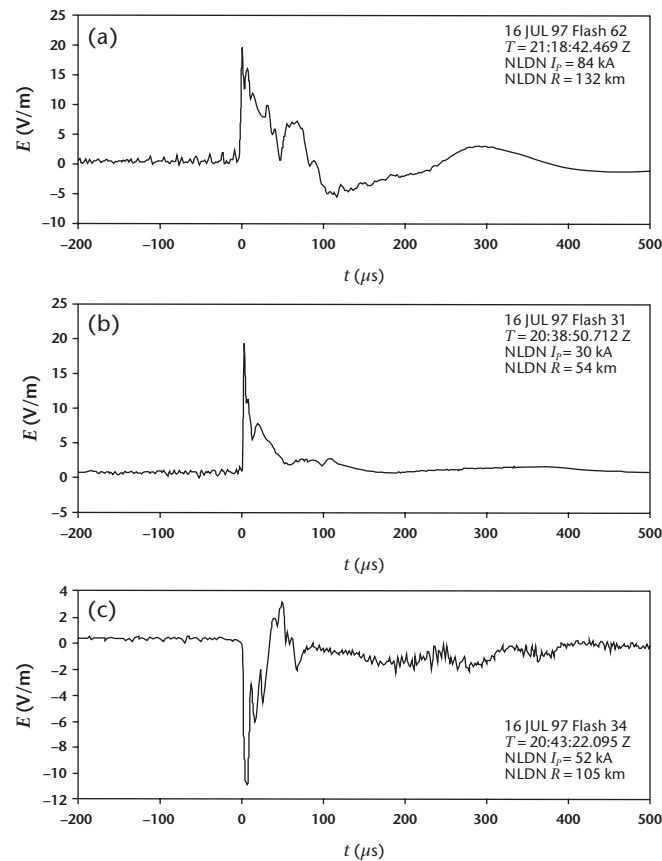
Figure 6.4. Examples of electric field pulse waveforms for (a) the negative first stroke, (b) the negative subsequent stroke, and (c) the positive first stroke. All three events have been detected by the US National Lightning Detection Network (NLDN), and their NLDN-reported characteristics (estimated peak current I_p, and distance R) are given on the plots. See also caption of Figure 6.3. (Adapted from Rakov, 1999)

Cloud-to-ground (CG) flash, ground flash: Flash that contains at least one return stroke.

Cloud lightning: Lightning discharges that do not involve ground.

Compact intracloud discharge (CID): A small-spatial-scale (typically hundreds of metres) lightning discharge in the cloud that is thought to be the most intense natural producer of HF-VHF (3–300 MHz) radiation on Earth.

Continuing current: A steady current immediately following some return-stroke current pulses.

Discharge: Often used synonymously with *flash*.

Downward cloud-to-ground lightning: Lightning discharges to ground initiated by descending leaders from the cloud.

Event: Specific part of a flash, typically any isolated signal measured during a flash.

Flash, lightning flash: Complete neutralization process that involves many events (leaders, strokes, K-processes, continuing currents, etc.) within a time interval of typically about 1 s; refers to a cloud flash or a ground flash.

Ground flash density: The number of ground flashes per unit area per unit of time (usually per square kilometre per year).

K-processes: Transient processes occurring in a previously conditioned lightning channel that is not connected (or lost its connection) to ground. They can occur in both ground and cloud flashes.

Leader: Lightning process that creates a conducting path between the cloud charge source region and ground (in the case of downward cloud-to-ground lightning) and distributes charge from the cloud source region along this path.

Lightning or *lightning flash*: It can be defined as a transient, high-current (typically tens of kiloamperes) electric discharge in air whose length is typically measured in kilometres.

M-components: Transient processes occurring in a grounded lightning channel while it carries continuing current.

Negative lightning: Lightning discharges that effectively lower negative charge from the cloud to ground.

Positive lightning: Lightning discharges that effectively lower positive charge from the cloud to ground.

Return stroke, cloud-to-ground stroke, strike: Lightning process that traverses the previously created leader channel, moving from ground towards the cloud charge source region, and neutralizes the leader charge.

Rocket-triggered lightning: Lightning discharges artificially initiated from natural thunderclouds using the rocket-and-wire technique.

Sferic, or *atmospheric*: Signal from a lightning stroke that travels over long distances.

Strike, stroke: see *return stroke.*

Thunderstorm cell: A unit of convection, typically some kilometres in diameter, characterized by relatively strong updraughts (>10 m/s). The lifetime of an ordinary cell is of the order of 1 h.

Upward cloud-to-ground lightning: Lightning discharges to ground initiated by ascending leaders from grounded objects.

6.3   PRINCIPLES OF LIGHTNING LOCATION

6.3.1   General

For the three most common multistation electromagnetic radio-frequency locating techniques – magnetic direction finding (MDF), time of arrival (TOA) and interferometry – the type of locating information obtained depends on the frequency f (or on the wavelength $\lambda = c/f$, where c is the speed of light) of the radiation detected (Rakov and Uman, 2003). For detected signals whose wavelengths are very short compared to the length of a radiating lightning channel, for example, the very high-frequency (VHF) range where f = 30 to 300 MHz and λ = 10 to 1 m, the whole lightning channel can, in principle, be imaged in two or three dimensions. For wavelengths that exceed or are a significant fraction of the lightning channel length, for example, the very low-frequency (VLF) range where f = 3 to 30 kHz and λ = 100 to 10 km and the low-frequency (LF) range where f = 30 to 300 kHz and λ = 10 to 1 km, generally only one or a few locations can be usefully obtained for each lightning channel. In the case of a single location for a cloud-to-ground return stroke, it is usually interpreted as some approximation to the ground strike point. The best electromagnetic channel imaging methods at VHF and the best ground-strike-point locating techniques at VLF and LF have accuracies (actually location errors or uncertainties) of the order of 100 m. On the other end of the accuracy scale, long-range VLF systems which operate

in a narrow frequency band, usually somewhere between 5 and 10 kHz, and detect lightning at distances up to thousands of kilometres have uncertainties in locating individual lightning flashes of the order of 10 km or more. These latter systems are often called thunderstorm locators.

For those electromagnetic locating techniques involving the measurement of field change amplitudes at multiple stations, the bandwidth of the measurement is not directly related to the locating accuracy. It is only necessary to have a measurement system that can faithfully reproduce the field changes of the process of interest. Hence, for example, from measuring the electrostatic field change in the frequency range from a fraction of a hertz to a few hertz at multiple stations, one can locate an average position for the charge source of a complete cloud-to-ground flash. And with a system bandwidth from a few hertz to a few kilohertz, so as to be able to resolve electrostatic field changes on a millisecond timescale, one can locate the charge sources for individual strokes in the flash as well as for continuing current. Lightning location using the return-stroke electric or magnetic radiation field peaks, similar to using the electrostatic field change, only requires that the system faithfully reproduces those peaks. The electric and magnetic field amplitude lightning locating techniques are not further discussed here.

Accurate lightning locating systems, whether they image the whole lightning channel or locate only the ground strike points or the cloud-charge centres, necessarily employ multiple sensors. Single station surface-based sensors, such as the lightning flash counters, detect the occurrence of lightning, but cannot be used to locate it on an individual flash basis. Nor are they designed to do so because of the wide range of amplitudes and wave shapes associated with individual events. Nevertheless, with single-station sensors one can assign groups of flashes to rough distance ranges if data are accumulated and averaged for some period of time. There are many relatively simple, commercially available single-station devices that purport to locate lightning. Most operate like AM radios, with the amplitude of the radio static being used to gauge the distance to the individual lightning flashes – a technique inherently characterized by large errors. In addition to field amplitude detectors, some commercial single-station devices employ optical detectors, magnetic direction finders and/or characteristics of lightning waveforms to allow estimates of the distance of cloud-to-ground return strokes from the sensor.

Single-station optical sensors on Earth-orbiting satellites detect the light scattered by the volume of cloud that produces the lightning and hence cannot locate to an accuracy better than about 10 km – about the diameter of a small cloud. Additionally, satellite-based sensors cannot distinguish between cloud and ground discharges. The next-generation series of Geostationary Operational Environmental Satellites (GOES-R) is planned to carry a Geostationary Lightning Mapper (GLM), which will monitor lightning continuously over a wide field of view. The launch of the first GOES-R series satellite is scheduled for 2015.

The following subsections discuss how individual sensors measuring various properties of the lightning electromagnetic radiation have been combined into systems to provide practical lightning locating. More details can be found in the reviews by Rakov and Uman (2003) and Cummins and Murphy (2009) and in the references therein.

6.3.2   **Magnetic field direction finding**

Two vertical and orthogonal loops with planes oriented north-south and east-west, each measuring the magnetic field from a given vertical radiator, can be used to obtain the direction to the source. This is because the output voltage of a given loop, by Faraday's law, is proportional to the cosine of the angle between the magnetic field vector and the normal vector to the plane of the loop. For a vertical radiator the magnetic field lines are circles that are coaxial with respect to the source. Hence, for example, the loop whose plane is oriented north-south receives a maximum signal if the source is north or south of the antenna, while the orthogonal east-west loop receives no signal. In general, the ratio of the two signals from the loops is proportional to the tangent of the angle between north and the source as viewed from the antenna.

Crossed-loop magnetic direction finders (DFs) used for lightning detection can be divided into two general types: narrowband (tuned) DFs and gated wideband DFs. In both cases the

direction-finding technique involves an implicit assumption that the radiated electric field is oriented vertically and the associated magnetic field is oriented horizontally and perpendicular to the propagation path.

Narrowband DFs have been used to detect distant lightning since the 1920s. They generally operate in a narrow frequency band with the centre frequency in the range of 5 to 10 kHz, where attenuation in the Earth-ionosphere waveguide is relatively low and where the lightning signal energy is relatively high. Before the development of weather radars in the 1940s, lightning locating systems were the primary means of identifying and mapping thunderstorms at medium and long ranges.

A major disadvantage of narrowband DFs is that for lightning at ranges less than about 200 km, those DFs have inherent azimuthal errors, called polarization errors, of the order of 10°. These errors are caused by the detection of magnetic field components from non-vertical channel sections, whose magnetic field lines form circles in a plane perpendicular to the non-vertical channel section, and also by ionospheric reflections – skywaves – whose magnetic fields are similarly improperly oriented for direction finding of the ground strike point.

To overcome the problem of large polarization errors at short ranges inherent in the operation of narrowband DFs, gated wideband DFs were developed in the early 1970s. Direction finding is accomplished by sampling (gating on) the north-south and east-west components of the initial peak of the return-stroke magnetic field, that peak being radiated from the bottom hundred metres or so of the channel in the first microseconds of the return stroke. Since the bottom of the channel tends to be straight and vertical, the magnetic field is essentially horizontal. Additionally, a gated DF does not record ionospheric reflections since those reflections arrive long after the initial peak magnetic field is sampled. The operating bandwidth of the gated wideband DF is typically from a few kilohertz to about 500 kHz. Interestingly, although an upper-frequency response of many megahertz is needed to assure accurate reproduction of the incoming radiation field peak, particularly if the propagation is over saltwater, practical DFs only need an upper-frequency response of a few hundred kilohertz in order to obtain an azimuthal error of about 1°. This is because the ratio of the peak signals in the two loops is insensitive to the identical distortion produced by the identical associated electronic circuits of the two loops. Similarly, with proper calibration and correction for propagation effects, practical DFs only need an upper-frequency response of a few hundred kilohertz in order to obtain a peak current estimation error of 15%–20%. Thus, the gated wideband DF can operate at frequencies below the AM radio band and below the frequencies of some aircraft navigational transmitters, either of which could otherwise cause unwanted directional noise.

Gated wideband DFs, as well as narrowband DFs, are susceptible to site errors. Site errors are a systematic function of direction but generally are time-invariant. These errors are caused by the presence of unwanted magnetic fields due to non-flat terrain and nearby conducting objects, such as underground and overhead power lines and structures, being excited to radiate by the incoming lightning fields. In order to eliminate site errors completely, the area surrounding a DF must be flat and uniform, and without significant conducting objects, including buried ones, nearby. These requirements are usually difficult to satisfy, so it is often easier to measure the DF site errors and to compensate for any that are found rather than to find a location characterized by tolerably small site errors. Once corrections are made, the residual errors have been reported (using independent optical data) to be usually less than 2° to 3°.

Since it is not known a priori whether a stroke to ground lowers positive or negative charge, there is a 180° ambiguity in stroke azimuth from the measurement of only the orthogonal magnetic fields. That ambiguity is resolved in all wideband DF systems by the measurement of the associated electric field whose polarity indicates the sign of the charge transferred to ground.

6.3.3   Time-of-arrival technique

A single time-of-arrival sensor provides the time at which some portion of the lightning electromagnetic field signal arrives at the sensing antenna. Time-of-arrival systems for locating lightning can be divided into three general types: (i) very short baseline (tens to hundreds of

metres), (ii) short baseline (tens of kilometres), and (iii) long baseline (hundreds to thousands of kilometres). Very short- and short-baseline systems generally operate at VHF, that is, at frequencies from 30 to about 300 MHz, while long-baseline systems generally operate at VLF and LF, 3 to 300 kHz. It is generally thought that VHF radiation is associated with air breakdown processes, while VLF signals are due to current flow in conducting lightning channels. Short-baseline systems are usually intended to provide images of lightning channels and to study the spatial and temporal development of discharges. Long-baseline systems are usually used to identify the ground strike point, cloud lightning events in predominantly vertical channels, or the average location of the flash.

A very short-baseline (tens to hundreds of metres) system is composed of two or more VHF time-of-arrival receivers whose spacing is such that the time difference between the arrival of an individual VHF pulse from lightning at those receivers is short compared to the time between pulses, which is some microseconds to hundreds of microseconds. The locus of all source points capable of producing a given time difference between two receivers is, in general, a hyperboloid, but if the receivers are very closely spaced, the hyperboloid degenerates, in the limit, into a plane on which the source is found. Two time differences from three very closely spaced receivers yield two planes whose intersection gives the direction to the source, that is, its azimuth and elevation. To find source location, as opposed to determining the direction to the source, two or more sets of three closely spaced receivers, the sets being separated by tens of kilometres or more, must be used. Each set of receivers is basically a TOA direction finder, and the intersection of two or more direction vectors yields the location.

Short-baseline TOA systems are typically networks of 5 to 15 stations that make use of time-of-arrival information for three-dimensional (3D) mapping of lightning channels. A portable version of such system has been developed by researchers at the New Mexico Institute of Mining and Technology. This system is presently referred to as the Lightning Mapping Array (LMA) and has recently become a major tool for both lightning research and operational applications. The short-baseline VHF TOA systems provide electromagnetic images of the developing channels of any type of lightning flash.

The first long-baseline (hundreds to thousands of kilometres) TOA systems operated at VLF/LF. For example, one of them employed a pair of receiving stations in Massachusetts with a bandwidth of 4 to 45 kHz and separated by over 100 km (the overall network was composed of four stations) to compare differences in the times of arrival of the signals at each station and hence determine directions to the causative lightning discharge in western Europe. The two-station system was basically a direction finder similar to the very short-baseline systems described above, but operating at lower frequencies and with a longer baseline. The resultant directions compared favourably with the locations reported by the UK Met Office's narrowband DF network which was operational at that time. Spherical geometry was used to account for propagation over the Earth's surface in finding the locus of points for a constant measured arrival time difference between receivers.

Another long-baseline TOA system, called the Lightning Position and Tracking System (LPATS), was developed in the 1980s. The LPATS, operating at LF/VLF, used electric field whip antennas at stations 200 to 400 km apart to determine locations via the measured differences between signal arrival times at the stations. In the frequency band used, return-stroke waveforms were generally the largest and hence most easily identified. In principle, responses from four stations (three time differences) are needed to produce a unique location since the hyperbolae on the Earth's surface from only two time differences can, in general, intersect at two different points. For cloud-to-ground lightning near or within the network, there is often only one solution, in which case the three-station approach suffices.

6.3.4 Interferometry

In addition to radiating isolated pulses, lightning also produces noise-like bursts of electromagnetic radiation lasting tens to hundreds of microseconds. These bursts are hard to locate using TOA techniques due to the difficulty in identifying the individual pulses. In the case of interferometry, no identification of individual pulses is needed, since the interferometer

measures phase difference between narrowband signals corresponding to these noise-like bursts received by two or more closely spaced sensors. The simplest lightning interferometer consists of two antennas some metres apart, each antenna being connected via a narrowband filter to a receiver. The antennas, filters and receivers are identical. The outputs of the two receivers are sent to a phase detector that produces a voltage that is proportional to the difference in phase between the two quasi-sinusoidal signals. The phase difference defines, as does the time difference in very short-baseline TOA systems, a plane on which the source is located, that is, one direction angle to the VHF source. To find the azimuth and elevation of a source, three receiving antennas with two orthogonal baselines are needed at minimum. To locate the source in three dimensions, two or more synchronized interferometers are needed, each effectively acting as a direction finder and separated by a distance of the order of 10 km or more. The principles of interferometric lightning location are described in detail by Lojou et al. (2008).

Most interferometric systems operate over very narrow frequency bands (a few hundred kilohertz to a few megahertz in the VHF/UHF bands), since this allows the system to have high sensitivity in a specific "quiet" band of operation. However, it also makes the system performance subject to local broadband interference, it may not provide the highest possible signal-to-noise ratio and it places a specific limitation in the spacing of the antenna array elements to avoid arrival-time (phase) ambiguity. There is a recent trend toward using broadband interferometry (Shao et al., 1996; Mardiana and Kawasaki, 2000; Morimoto et al., 2004). This trend is made possible by the advent of affordable broadband radio frequency and digital signal processing electronics.

6.4   PERFORMANCE CHARACTERISTICS

Generally, a modern VLF-MF lightning locating system is expected to record (in separate categories) and locate over a certain area all cloud-to-ground strokes of either polarity, as well as cloud discharges. Also expected for each discharge is a measure of its intensity, usually in the form of peak current inferred from measured electric or magnetic fields. Accordingly, the system's performance can be evaluated using the following characteristics:

(a)   Cloud-to-ground flash detection efficiency;

(b)   Cloud-to-ground stroke detection efficiency;

(c)   Cloud flash detection efficiency;

(d)   Percentage of misclassified events (particularly cloud discharges assigned to the positive or negative CG stroke category);

(e)   Location accuracy (or location error);

(f)   Peak current estimation error.

In general, the detection efficiency is the fraction (usually expressed in per cent) of the total events occurred that are detected by the system and is ideally equal to 100%. While the CG stroke detection efficiency can be readily defined (since these strokes involve a unique and observable feature – the luminous channel to ground – and the total number of occurred events can be determined), the cloud flash detection efficiency concept is rather uncertain. Indeed, there are many cloud discharge processes (some of them poorly understood) occurring on different spatial scales and timescales and apparently exhibiting no unique and readily observable features. As a result, the total number of occurred events is generally unknown. In practice, if all cloud discharge events are accepted as counts, the number of detected cloud discharges may be largely determined by the local noise level and the system's signal transmission rate limit.

In defining the CG flash detection efficiency, which is probably the most important performance characteristic for lightning locating systems used for determining ground flash density, a flash is

considered to be detected if at least one stroke of the flash is detected. A similar approach could be applied to cloud flashes, although one would need to decide if a single count constitutes a flash and how to assign multiple counts to individual flashes.

The location error is the distance between the actual location and that reported by the system. In general, the location error consists of random and systematic components. The latter in some cases can be accounted for (e.g. site errors in MDF systems).

The peak current estimation error is the difference between the actual peak current value and that reported by the system, and is usually expressed in per cent of the actual peak current. Peak currents are estimated by lightning locating systems using either an empirical or model-based field-to-current conversion equation. There are reasonable field-to-current conversion equations for CG strokes, but not for cloud discharge processes.

In order to evaluate the performance characteristics listed above, independent (ground-truth) data are needed. For example, discharges occurring at a precisely known location equipped with a current-measuring device (tall tower or lightning-triggering facility) can be used for estimating the location accuracy and peak current estimation error. Detection efficiencies and percentage of misclassified events are usually estimated based on time-resolved optical recordings. Sometimes lightning-related damage to various objects (buildings, trees, etc.) is used in estimating location errors, although identification of the causative lightning event in this approach is uncertain due to insufficient accuracy of timing information (usually not known within better than a minute). Less definitive evaluations of lightning locating systems' performance characteristics are possible via modelling or comparison with a more accurate system operating in the same area. As of today, only a limited number of ground-truth studies have been performed, particularly for first strokes in negative CG flashes, positive CG flashes and cloud discharges.

In some applications (e.g. tracking of thunderstorm cells), the tracking ability may be more important than detection of individual lightning discharges. Performance of the systems intended primarily for such applications is often tested against radar or infrared satellite imagery, with a good correspondence between detected lightning and regions of high radar reflectivity or low cloud-top temperatures being viewed as the system's output validity criteria. For early warning, the ability to detect the first lightning is probably the most important performance characteristic.

It is not clear how to define the performance characteristics for VHF lightning channel imaging systems. Surely, they cannot locate all the VHF sources in the cloud. Limitations in sensitivity prevent these systems from regularly detecting and mapping positive leaders. Thus, the resultant VHF images are necessarily partial. Further, supplementary information about return strokes is usually needed to reliably distinguish between cloud and CG flashes, because the VHF radiation directly associated with subsequent return strokes is limited and difficult to detect. Also, no peak current estimates are possible. Nevertheless, VHF lightning channel imaging systems represent a very valuable tool for studying detailed lightning morphology and evolution, particularly inside the cloud, and are often used in testing other types of lightning locating systems.

6.5　　**EXAMPLES OF MODERN LIGHTNING LOCATING SYSTEMS**

One VHF lightning channel imaging system (LMA), three VLF/LF (NLDN, LINET and USPLN), one ELF/VLF/LF/MF/HF (ENTLN), and three VLF (WWLLN, GLD360 and ATDnet) systems are briefly reviewed here as representative examples of modern lightning locating systems. The systems have been chosen because they are good examples of each type of system, but their inclusion should not be taken to imply that they are better than others or are recommended over the use of other systems not discussed here. Information about these and other systems can be found in Rakov and Uman (2003), Cummins and Murphy (2009), Betz et al. (2009) and references therein. There are more than 60 lightning locating networks worldwide that operate in the VLF/LF range.

Besides a general characterization of each system, the available information on its performance characteristics is given with emphasis on those based on formal ground-truth studies published in the peer-reviewed literature. Generally, the amount of such information for older systems is greater than for more recent ones.

6.5.1   Lightning Mapping Array, 60–66 MHz

Lightning Mapping Array networks typically consist of 10–15 stations separated by 15–20 km and connected by wireless communication links to a central location (Thomas et al., 2004). Each station receives the lightning signals (from both cloud and CG flashes) in a locally unused television channel (usually TV channel 3, 60–66 MHz). A typical time resolution (the measurement time window) is 80–100 μs. A larger time window, typically 400 μs, is used for real-time processing and display.

The location accuracy of the New Mexico LMA has been investigated experimentally using a sounding balloon carrying a VHF transmitter, airplane tracks, and observations of distant storms (Thomas et al., 2004). Simple geometric models for estimating the location uncertainty of sources both over and outside the network have also been developed. The model results were found to be a good estimator of the observed errors. Sources over the network at altitudes ranging from 6 to 12 km were located with an uncertainty of 6–12 m rms in the horizontal and 20–30 m rms in the vertical, resulting in less than a 100-metre 3D error for most located sources. Outside the network the location uncertainties increase with distance.

6.5.2   US National Lightning Detection Network, 400 Hz–400 kHz

The National Lightning Detection Network consists of more than 100 stations separated typically by 300–350 km and covering the contiguous United States (see Cummins and Murphy, 2009). A combination of TOA and MDF locating techniques is employed. Both cloud and CG lightning discharges are reported. Classification is accomplished by applying field waveform criteria. Peak currents are estimated from measured fields using an empirical formula based on rocket-triggered lightning data, with the field peaks being adjusted to account for propagation effects (stronger than the inverse proportionality distance dependence). Further information on the evolution of the NLDN, its enabling methodology and applications of NLDN data can be found in Rakov and Uman (2003, Chapter 17), Orville (2008), Cummins and Murphy (2009) and references therein.

Cloud-to-ground stroke and flash detection efficiencies have been investigated, using video cameras, in southern Arizona, Oklahoma and Texas (Biagi et al., 2007). The stroke detection efficiency in southern Arizona was estimated to be 76% ($N = 3\,620$), and in Texas/Oklahoma it was 85% ($N = 885$). The corresponding flash detection efficiencies were 93% ($N = 1\,097$) and 92% ($N = 367$). Additionally, classification of lightning events as cloud or CG discharges was examined in this study, as well as in a similar study (but additionally using independent electric field waveform measurements) in the Colorado/Kansas/Nebraska region (Fleenor et al., 2009).

Cloud-to-ground stroke and flash detection efficiencies have been also investigated, using rocket-triggered lightning as the ground truth, in the Florida region (Jerauld et al., 2005; Nag et al., 2011). From the latest study (2004–2009), the CG stroke and flash detection efficiencies were found to be 76% ($N = 139$) and 92% ($N = 37$), respectively. Strokes in rocket-triggered flashes are similar to regular subsequent strokes (following previously formed channels) in natural lightning, and hence the 76% stroke detection efficiency is applicable only to regular negative subsequent strokes in natural lightning. The flash detection efficiency derived using rocket-triggered lightning is expected to be an underestimate of the true value for natural negative lightning flashes, since first strokes typically have larger peak currents than subsequent ones.

Nag and Rakov (2012) examined electric field waveforms produced by 45 positive flashes containing 53 strokes. Out of these 53 strokes, the NLDN located 51 (96%), of which 48 (91%) were correctly identified and 3 return strokes were misclassified as cloud discharges.

According to Cummins and Murphy (2009), the NLDN cloud flash detection efficiency (a flash was considered detected if at least one VLF/LF pulse produced by that flash was detected) is in the range of 10% to 20%, depending on local differences in distances between stations. Nag et al. (2010) examined wideband electric fields, electric and magnetic field derivatives, and narrowband VHF (36 MHz) radiation bursts produced by 157 compact intracloud discharges. The NLDN located 150 (96%) of those CIDs, and correctly identified 149 (95%) of them as cloud discharges.

Nag et al. (2011) estimated, from comparison of NLDN-reported locations with the precisely known locations of the rocket launchers which were taken as the accurate ground strike points, the median absolute location error to be 308 m, with the largest error being 4.2 km ($N = 105$). Peak current estimation errors have been estimated from comparison of NLDN-reported peak currents with directly measured currents at the triggered-lightning channel base. The median absolute value of current estimation error was 13% ($N = 96$). The current estimation errors never exceeded 129% in absolute value (60% if two outliers are excluded). These results are applicable only to regular negative subsequent strokes in natural lightning.

6.5.3   Lightning Detection Network, 1–200 kHz

The basic location method used in the Lightning Detection Network (LINET) is TOA, although the magnetic field sensors provide arrival-angle information that is employed as a plausibility check on computed locations. Height information derived from the arrival time at the nearest reporting sensor is employed to assist in classification of processes in cloud flashes and of in-cloud processes (e.g. preliminary breakdown) in CG flashes on the one hand and CG strokes on the other (near-ground locations are assumed to be associated with CG strokes and elevated ones with all the other processes). It is stated that the reliable separation of return strokes and cloud pulses can be achieved as long as the closest sensor is within 100 km of the lightning discharge, which requires baselines of 200–250 km or less. Emphasis is placed on detection of low-amplitude signals of both cloud and CG lightning. Peak currents for processes in cloud flashes and for in-cloud processes (e.g. preliminary breakdown) in CG flashes and CG strokes are estimated assuming direct proportionality between the peak current and peak magnetic (or electric) field and inverse distance dependence of field peak. More information about LINET can be found in Betz et al. (2009) and references therein.

Like for VHF channel imaging systems, it is not clear how to define the detection efficiency for LINET, which in a sense also maps the evolution of lightning channels, although with a considerably smaller number of located sources per flash. Additionally, in-cloud processes (e.g. preliminary breakdown) in CG flashes are assigned to the cloud lightning category, which is apparently inconsistent with the traditional definitions of cloud flash as a lightning discharge without CG strokes and of CG flash as a lightning discharge that consists of both in-cloud processes and CG strokes. This is probably immaterial for a number of applications, such as cell tracking and detection of severe weather.

The random location error is claimed to be approximately 150 m, but the existence of systematic errors is acknowledged. Betz et al. (2009) showed an example of 58 located strokes apparently terminated on an instrumented tower with an average location error of less than ~100 m, after compensating systematic errors that caused a location bias of ~200 m.

Peak current estimation errors for LINET are unknown (no comparison with ground-truth data has been performed to date).

6.5.4   US Precision Lightning Network, 1.5–400 kHz

The US Precision Lightning Network (USPLN) employs the VLF/LF TOA technique and consists of 100 electric field sensors covering the continental United States and other parts of North America. No formal performance testing studies regarding this system have been reported, but the operators of the system claim, apparently from the network simulation analysis, 95% stroke detection efficiency and 250-metre typical location error throughout most of North

America (>80% detection efficiency and <1 km location error in key deployment areas elsewhere in the world). Differentiation between cloud and CG processes is apparently accomplished by examining the frequency content and amplitude of the received signals. The field-to-current conversion procedure has not been formally described, nor is any information available about testing its validity.

6.5.5 Earth Networks Total Lightning Network, 1 Hz–12 MHz

The Earth Networks Total Lightning Network (ENTLN) sensors operate in a frequency range from 1 Hz to 12 MHz (spanning the ELF, VLF, LF, MF and HF ranges). The TOA method has been employed by this network of more than 700 sensors since 2013. Both cloud and CG lightning discharges are reported.

According to Heckman and Liu (2010), the whole electric field waveforms are transmitted from the sensor to the data-processing unit and used in both locating the lightning events and differentiating between cloud and CG processes. Strokes (or individual cloud events) are clustered into a flash if they are within 700 ms and 10 km of the first detected stroke (or cloud event). A flash that contains at least one return stroke is classified as a CG flash, otherwise it is classified as a cloud flash. In cell tracking and thunderstorm alert generation, only flashes (which are less likely than strokes to be missed by the system) are used.

No formal performance testing studies regarding this system have been reported in the peer-reviewed literature, but the operators of the system claim that performance testing studies conclude that ENTLN achieves 40%–50% cloud flash detection efficiency across much of the United States and up to 95% in the US Midwest and East (Heckman and Liu, 2010). Maximizing the detection efficiency for cloud flashes appears to be the primary focus of this system. By extending the frequency range of detection into the MF and HF spectra, the ENTLN aims to detect and report weaker pulses at longer distances than other VLF/LF systems with similar baselines.

The field-to-current conversion procedure has not been formally described to date, nor is any information yet available about testing its validity.

6.5.6 World Wide Lightning Location Network, 6–18 kHz

The World Wide Lightning Location Network (WWLLN) utilizes a time-of-group-arrival (TOGA) method to locate lightning strikes. This method is based on the fact that lightning VLF signals (sferics) propagating in the Earth-ionosphere waveguide experience dispersion, in that the higher-frequency components arrive earlier than the lower-frequency components. The TOGA, a quantity that can be derived from the measured sferic waveform, is related to the distance travelled by the sferic. As of March 2012, the WWLLN employed 57 sensors located on all continents, although, according to Dowden et al. (2002), global coverage could be in principle provided by as few as 10 sensors. Distances between the sensors are of the order of thousands of kilometres. Presently, only those lightning events that triggered at least five sensors and that had residuals (uncertainties in the stroke timing) less than or equal to 30 μs are regarded as located with acceptable accuracy.

In the latest study of WWLLN performance characteristics, Abarca et al. (2010) used NLDN data as the ground truth and found that the CG flash detection efficiency increased from about 3.9% in 2006–2007 to 10.3% in 2008–2009, as the number of sensors increased from 28 in 2006 to 38 in 2009. For events with NLDN-reported peak currents of 130 kA or higher, the detection efficiency was 35%. The average location error was estimated to be 4–5 km.

Interaction of lightning signals with the ionosphere spectrally distorts the received waveform, so that it is not straightforward to infer the peak current and even polarity of lightning. Nevertheless, Hutchins et al. (2012) developed a method to convert the stroke radiated power in the 6–18 kHz band to peak current. Errors involved in such conversion are presently unknown.

6.5.7   **Global Lightning Dataset, VLF**

The Global Lightning Dataset (GLD360), also referred to as the Global Lightning Detection Network (GLDN), employs an unspecified number of VLF sensors strategically placed around the world. Locations are obtained using both TOA and MDF methods in conjunction with a lightning waveform recognition algorithm. The latter relies on a bank of canonical waveforms corresponding to propagation distances of the order of thousands of kilometres (Said et al., 2010).

According to the network operators, the expected CG flash detection efficiency is 60%–70% and the median location error is 5 to 10 km. Demetriades et al. (2010) evaluated the GLD360 performance characteristics using NLDN data as the ground truth and found that the CG flash detection efficiency was 86% to 92%, and the median location error was 10.8 km. From a similar study, but using the Brazilian lightning detection network, Naccarato et al. (2010) reported a CG flash detection efficiency of 16% and a mean location error of 12.5 km. Using synchronized electric field and high-speed video camera measurements of cloud-to-ground lightning in Belgium as ground truth, Poelman et al. (2013) found the CG flash and stroke detection efficiencies for the GLD360 to be 96% and 70%, respectively, with a median location error of 900 m. Using NLDN data as ground truth, Said et al. (2013) reported a CG flash detection efficiency of 57% and a median location accuracy of 2.5 km.

The GLD360 also reports the peak current and polarity. Relative to the NLDN, Said et al. (2013) found the arithmetic and geometric mean peak current magnitude error for the GLD360 to be 21% and 6%, respectively. GLD360 reported the same polarity for 96% of the matched strokes as the NLDN.

6.5.8   **Arrival Time Difference network**

The Arrival Time Difference network (ATDnet) long-range lightning location system (LLS) is the latest version of the UK Met Office VLF LLS that has been in place since 1987. The network currently consists of 10 sensors across Europe that contribute to the main network, with additional sensors within Europe and beyond for development and testing. The network is designed for lightning location in Europe, but is capable of regularly detecting lightning in Africa and South America. The sensors, referred to as outstations, detect VLF (sferic) signal waveforms and transmit waveform data to a central processor at the UK Met Office, where a waveform correlation technique is used to determine the arrival time differences of the waveforms across the network. These arrival time difference data are used to locate lightning.

Poelman et al. (2013) found the random location error of ATDnet to be on the order of 1 km, with a CG flash detection efficiency of 88%. The actual median location uncertainty of CG flashes across Europe is likely to be on the order of 2 to 5 km, although this requires verification in peer-reviewed literature. ATDnet does not currently provide information on stroke polarity, type (CG/IC) or power/peak current.

6.6   **UTILIZATION OF LIGHTNING LOCATION SYSTEMS BY METEOROLOGICAL SERVICES**

Lightning data have utility in different areas of importance to public and private meteorological service organizations. Typically, national meteorological agencies use LLS data to help accomplish their national duties to protect life and property, and commercial entities use lightning data to provide improved severe weather warnings, forecasts and guidance to clients for specialized applications including aviation, agriculture, energy and mass media.

6.6.1 Storm recognition and alarms for severe weather

One of the important duties of the meteorological services is to provide reliable warnings for severe weather conditions. As a rule, the best severe weather forecast skill and lowest false alarm rates are achieved when several data sources are exploited, but since thunderstorms are typically accompanied by an increase of IC, LLS data alone can usually serve as a very clear indicator of the strength and extent of storm cells. This points to the importance of total lightning networks, such as those that detect in the LF/MF/HF ranges, since CG detection alone will not suffice for this application.

Although an alarm can be issued as soon as a stroke occurs in the vicinity of an instrumented area, a more reliable procedure involves the definition of a storm cell and tracking it as it moves inside or towards an area of interest. Some LLS allow for short-term extrapolation (nowcasting) of cell displacements on the order of 1 h or so. Monitoring the total flash rates and the rate changes makes it possible to identify lightning cells with the potential to produce severe weather. When a cell is identified and the total lightning rate exceeds a given threshold, an alert can be generated.

Except for certain storms generated along frontal boundaries, forecasting over longer durations with acceptable skill requires the use of numerical weather prediction models. Finally, it may be pointed out that lightning, in combination with cell tracking, not only indicates the initiation of heavy thunderstorm activity but also signals the end of a threat in a given area.

Although storm reports from spotters on the ground or in the air are an invaluable source of information during severe weather, information derived from remote-sensing techniques (including lightning detection) is becoming more important all the time. One can now use radar reflectivity, cloud images, passive microwave brightness temperatures and lightning data (alone or in combination) to identify thunderstorm activity with high accuracy and reliability even in remote regions. Of all these techniques, global and/or local networks of LLS systems and stand-alone detectors on the ground or in aircraft are clearly the most definitive when it comes to identifying significant thunderstorm activity for the reasons discussed above. While the simple detection of a thunderstorm is feasible with any LLS, more complete measurements require advanced systems and techniques that are capable of providing early detection and identification of thunderstorm activity while at the same time reducing false alarms to an acceptable level.

6.6.2 Nowcasting, forecasting and derived products

Nowcasting is a widely used technique for very short-range weather forecasting. A nowcast starts with information about the current (weather) state of the atmosphere as expressed by one or more observed parameters, and then uses an estimate of their movement to predict their location and extent a short time in the future. Nowcast accuracy depends on the validity of the assumption that the weather associated with the observed parameter(s) will persist during that period without significant change. Of course, certain lightning parameters are indicative of the phase of a storm's life cycle and this may also be exploited for nowcasting. The above assumption is reasonable for short (~1 h) periods, but its validity diminishes with time. As a consequence, extrapolations over periods longer than about 1 h require the use of data assimilation and numerical weather prediction techniques.

Qualitative evaluations of LLS data commonly involve the display of lightning data on maps (with or without other information) in real or near real time. These products can be used for many purposes, such as localizing or limiting an area likely to be effected by a storm and aiding in the decision to issue an alarm. Beyond qualitative evaluation, high-quality LLS data are highly amenable to quantitative treatment including statistical evaluations of stroke rates to estimate storm intensity, which can greatly enhance their utility.

A number of projects are underway that are aimed at developing automated procedures for thunderstorm cell tracking and the evaluation of lightning parameters in these areas.

Refined interpretations, analysis and animations of results from cell tracking should greatly enhance the nowcasting potential of LLS data. The combination of cell tracking involving both lightning and radar represents another type of potentially useful derived product.

Finally, lightning data, as well as other observations such as radar reflectivity, can be used to generate model output statistics for objective forecasting (Glahn and Lowry, 1972; Knüpffer, 1996) that are appropriate for use in probabilistic post-processing techniques like those described for the hourly Rapid Refresh NWP model developed by the NOAA Earth System Research Laboratory (Weygandt et al., 2008).

6.6.3   **Lightning and climate**

Recent climate studies have noted the connection between lighting and climate change (Williams, 2005; Price, 2006, 2009). As surface and lower tropospheric temperatures rise, lightning rates are predicted to increase in the range of 10%–100% for every one degree of surface warming, depending on the model and assumptions used. There is also a clear relationship between temperature, water vapour and lightning activity; thunderstorms carry large amounts of water vapour into the upper troposphere and lower stratosphere, and this in turn influences the greenhouse effect on the Earth's climate. Further, lightning discharges produce nitrogen oxides that influence the production of the greenhouse gas ozone. It must be recognized, however, that even though the underlying mechanisms linking global climate change to lightning are well understood, different processes may dominate in unanticipated ways. For example, climate simulations by Grewe (2008) suggest that global warming can actually lead to the worldwide occurrence of fewer but more intense convective events. As such, lightning decreases in total flash frequency, but individual storms are predicted to produce more lightning.

In any case, lightning activity is one of the factors that should be taken into account in any detailed climate model or predictions of climate change. Consequently, it is important to monitor lightning activity at different scales over large areas and establish or extend the database of lightning events over long time periods. Relationships are also studied on short timescales, ranging from daily and diurnal variations, five-day waves, intra-seasonal, semi-annual and annual to longer periods. To achieve this goal, local high-precision LLS should be expanded, global LLS must be completed and standards for lightning detection must be introduced and implemented.

6.6.4   **Verification of lightning-induced ground damage**

An early motivation for the development of LLS was to have an objective way to verify the cause of lightning-induced damage in legal disputes, and most insurance companies use lightning data to verify or reject lightning damage claims. To be useful in this regard, LLS must exhibit both excellent detection efficiency and location accuracy at all thresholds. Location accuracy should be better than ~1 km so that a reliable correlation between lightning and damage can be demonstrated, and relatively weak strokes must be detected because even a 5 kA stroke can produce significant damage or over-voltage. Even higher location accuracy is needed for the power industry to determine if the interruption of a high-voltage transmission line could have been caused by a lightning stroke. Since heavy storms can produce high stroke rates and lightning flashes may be composed of many strokes with differing strike points, an accuracy of 100–200 m is desired for the establishment of a reliable spatial correlation. Of course, this requirement is relaxed when precise event timing of both the power failure and the strokes are available, and tools for automatic recognition of these incidents are now available commercially.

––––––––––––

REFERENCES AND FURTHER READING

Abarca, S.F., K.L. Corbosiero and T.J. Galarneau Jr., 2010: An evaluation of the Worldwide Lightning Location Network (WWLLN) using the National Lightning Detection Network (NLDN) as ground truth. *Journal of Geophysical Research: Atmospheres*, 115(D18).

Betz, H.D., K. Schmidt and W.P. Oettinger, 2009: LINET – An international VLF/LF lightning detection network in Europe. In: *Lightning: Principles, Instruments and Applications* (H.D. Betz, U. Schumann and P. Laroche, eds.). Dordrecht, NL, Springer-Verlag.

Biagi, C.J., K.L. Cummins, K.E. Kehoe and E.P. Krider, 2007: National Lightning Detection Network (NLDN) performance in southern Arizona, Texas and Oklahoma in 2003–2004. *Journal of Geophysical Research: Atmospheres*, 112(D5).

Cummins, K.L. and M.J. Murphy, 2009: An overview of lightning locating systems: History, techniques, and data uses, with an in-depth look at the U.S. NLDN. *IEEE Transactions on Electromagnetic Compatibility*, 51(3):499–518.

Demetriades, N.W.S., M.J. Murphy and J.A. Cramer, 2010: Validation of Vaisala's Global Lightning Dataset (GLD360) over the continental United States. *Preprints*, Twenty-ninth Conference on Hurricanes and Tropical Meteorology (10–14 May 2010), Tucson, AZ.

Dowden, R.L., J.B. Brundell and C.J. Rodger, 2002: VLF lightning location by time of group arrival (TOGA) at multiple sites. *Journal of Atmospheric and Solar-Terrestrial Physics*, 64(7):817–830.

Dwyer, J.R., 2005: A bolt out of the blue. *Scientific American*, 292(5):64–71.

Fleenor, S.A., C.J. Biagi, K.L. Cummins, E.P. Krider and X.-M. Shao, 2009: Characteristics of cloud-to-ground lightning in warm-season thunderstorms in the Central Great Plains. *Atmospheric Research*, 91:333–352.

Glahn, H.R., and D.A. Lowry, 1972: The use of model output statistics (MOS) in objective weather forecasting. *Journal of Applied Meteorology*, 11:1203–1211.

Grewe, V., 2008: Impact of lightning on air chemistry and climate. In: *Lightning: Principles, Instruments and Applications* (H.D. Betz, U. Schumann and P. Laroche, eds.). Dordrecht, NL, Springer-Verlag.

Heckman, S. and C. Liu, 2010: The application of total lightning detection and cell tracking for severe weather prediction. In: *Proceedings of the International Conference on Grounding and Earthing (GROUND'2010) and Fourth International Conference on Lightning Physics and Effects (LPE)* (November 2010), Salvador, Brazil.

Hendry, J., 1993: Panning for lightning (including comments on the photos by M.A. Uman). *Weatherwise*, 45(6):19.

Hutchins, M.L., R.H. Holzworth, C.J. Rodger and J.B. Brundell, 2012: Far-field power of lightning strokes as measured by the World Wide Lightning Location Network. *Journal of Atmospheric and Oceanic Technology*, 29:1102–1110.

Jerauld, J., V.A. Rakov, M.A. Uman, K.J. Rambo, D.M. Jordan, K.L. Cummins and J.A. Cramer, 2005: An evaluation of the performance characteristics of the U.S. National Lightning Detection Network in Florida using rocket-triggered lightning. *Journal of Geophysical Research: Atmospheres*, 110(D19).

Knüpffer, K., 1996: Methodical and predictability aspects of MOS systems. *Preprints of the Thirteenth Conference on Probability and Statistics in the Atmospheric Sciences* (21–23 February 1996), San Francisco, CA. American Meteorological Society, 190–197.

Le Vine, D.M., 1980: Sources of the strongest RF radiation from lightning, *Journal of Geophysical Research: Oceans*, 85(C7):4091–4095.

Lojou, J.-Y., M.J. Murphy, R.L. Holle and N.W.S. Demetriades, 2008: Nowcasting of thunderstorms using VHF measurements. In: *Lightning: Principles, Instruments and Applications* (H.D. Betz, U. Schumann and P. Laroche, eds.). Dordrecht, NL, Springer-Verlag.

Mardiana, R. and Z-I. Kawasaki, 2000: Broadband radio interferometer utilizing a sequential triggering technique for locating fast-moving electromagnetic sources emitted from lightning. *IEEE Transactions on Instrumentation and Measurement*, 49(2):376–381.

Morimoto, T., A. Hirata, Z. Kawasaki, T. Ushio, A. Matsumoto and J.H. Lee, 2004: An operational VHF broadband digital interferometer for lightning monitoring, *IEEJ Transactions on Fundamentals and Materials*, 124(12):1232–1238.

Naccarato, K.P., O. Pinto Jr., S.A.M. Garcia, M. Murphy, N. Demetriades and J. Cramer, 2010: *Validation of the new GLD360 dataset in Brazil: First results*. Twenty-first International Lightning Detection Conference (19–22 July 2010), Orlando, Florida.

Nag, A., S. Mallick, V.A. Rakov, J.S. Howard, C.J. Biagi, J.D. Hill, M.A. Uman, D.M. Jordan, K.J. Rambo, J.E. Jerauld, B.A. DeCarlo, K.L. Cummins and J.A. Cramer, 2011: Evaluation of U.S. National Lightning Detection Network performance characteristics using rocket-triggered lightning data acquired in 2004–2009. *Journal of Geophysical Research: Atmospheres*, 116(D2).

Nag, A. and V.A. Rakov, 2012: Positive lightning: An overview, new observations, and inferences. *Journal of Geophysical Research: Atmospheres*, 117(D8).

Nag, A., V.A. Rakov, D. Tsalikis and J.A. Cramer, 2010: On phenomenology of compact intracloud lightning discharges. *Journal of Geophysical Research: Atmospheres*, 115(D14).

Orville, R.E., 2008: Development of the National Lightning Detection Network, *Bulletin of the American Meteorological Society*, 89(2):180–190.

Poelman, D.R., W. Schulz and C. Vergeiner, 2013: Performance characteristics of distinct lightning detection networks covering Belgium. *Journal of Atmospheric and Oceanic Technology*, 30(5):942–951.

Price, C., 2006: Global thunderstorm activity. In: *Sprites, Elves and Intense Lightning Discharges* (M. Fullekrug, E. Mareev and M. Rycroft, eds.). Springer, Amsterdam, 85–99.

Price, C., 2009: Will a drier climate result in more lightning? *Atmospheric Research*, 91(2):479–484.

Rakov, V.A., 1999: Lightning electric and magnetic fields. In: *Proceedings of the Thirteenth International Zurich Symposium on Electromagnetic Compatibility* (16–18 February 1999), Zurich, Switzerland.

Rakov, V.A. and M.A. Uman, 2003: *Lightning: Physics and Effects*, Cambridge University Press.

Said, R.K., M.B. Cohen and U.S. Inan, 2013: Highly intense lightning over the oceans: Estimated peak currents from global GLD360 observations. *Journal of Geophysical Research: Atmospheres*, 118(13) (available from http://onlinelibrary.wiley.com/doi/10.1002/jgrd.50508/pdf).

Said, R.K., U.S. Inan and K.L. Cummins, 2010: Long-range lightning geolocation using a VLF radio atmospheric waveform bank. *Journal of Geophysical Research: Atmospheres*, 115(D23).

Shao, X.M., D.N. Holden and P.R. Krehbiel, 1996: Broadband radio interferometry for lightning observation. *Geophysical Research Letters*, 23:1917–1920.

Smith, D.A., X.M. Shao, D.N. Holden, C.T. Rhodes, M. Brook, P.R. Krehbiel, M. Stanley, W. Rison and R.J. Thomas, 1999: A distinct class of isolated intracloud discharges and their associated radio emissions. *Journal of Geophysical Research: Atmospheres*, 104(D4): 4189–4212.

Thomas, R.J., P.R. Krehbiel, W. Rison, S.J. Hunyady, W.P. Winn, T. Hamlin and J. Harlin, 2004: Accuracy of the Lightning Mapping Array. *Journal of Geophysical Research: Atmospheres*, 109(D14).

Weygandt, S.S., M. Hu, S.G. Benjamin, T.G. Smirnova, K.J. Brundage and J.M. Brown, 2008: *Assimilation of lightning data using a diabatic digital filter within the Rapid Update Cycle*. Twentieth International Lightning Detection Conference (21–23 April 2008), Tucson, AZ.

Williams, E., 2005: Lightning and climate: A review. *Atmospheric Research*, 76:272–287.

———————————

CHAPTER CONTENTS

CHAPTER 7. RADAR MEASUREMENTS

7.1 GENERAL

This chapter is a basic discussion of weather radars. It places particular emphasis on the technical and operational characteristics that must be considered when planning, developing and operating individual radars and radar networks in support of Meteorological and Hydrological Services. This is related to the use and application of weather radar data. Radars used for vertical wind profiling are discussed in Part II, Chapter 5.

7.1.1 The weather radar

Meteorological radars are primarily designed for detecting precipitation and associated weather phenomena. However, other objects, such as insects, birds, planes, sand and dust, ground clutter and even fluctuations in the refractive index in the atmosphere generated by local variations in temperature or humidity, can be detected by the weather radar.

This chapter deals with radars in common operational or near-operational use around the world. The meteorological radars having characteristics best suited for atmospheric observation and investigation transmit electromagnetic pulses in the 3–10 GHz frequency range (10–3 cm wavelength, respectively). Primarily, they are designed for detecting and mapping areas of precipitation, measuring their intensity and motion, and their type. Radar echoes due to birds, insects or Bragg scattering (the turbulent fluctuations) can also produce radial wind data with Doppler radar. Their intensity patterns can reveal the location of atmospheric boundaries that are indicative of areas of low-level convergence where thunderstorms may initiate or develop.

Higher frequencies (35 and 94 GHz) are used to detect smaller hydrometeors, such as cloud, fog, drizzle, light snow and precipitation, and are becoming prevalent in the research community. These frequencies are generally not used in operational forecasting because of excessive attenuation of the radar signal by the intervening medium and their relatively short range, particularly in Doppler mode.

At lower frequencies (915–1 440 MHz, ~400–440 MHz and ~50 MHz), radars are capable of detecting variations in the refractive index of clear air, and are used for wind profiling. Although they may detect precipitation, their scanning capabilities are limited by the size and type of the antenna, and they generally point in the vertical or near-vertical.

The returned signal from the transmitted pulse encountering any target, called an echo, has an amplitude, a phase and a polarization. Amplitude is related to the size distribution and number of particles in the (pulse) volume illuminated by the radar beam. The amplitude is used to determine the reflectivity factor (Z), which is used to estimate the intensity of precipitation through the use of empirical relations. A primary application is to detect, map and estimate the precipitation at ground level instantaneously, nearly continuously, and over large areas.

Doppler radars have the capability of determining the phase difference between the transmitted and received pulse which is a measure of the mean radial velocity of the particles. This is the reflectivity weighted average of the radial components of the displacement velocities of the hydrometeors within the pulse volume. The Doppler spectrum width is a measurement of the spatial variability of the Doppler velocities and provides a measure of the variation in the radial velocity that is interpreted in terms of wind shear and turbulence. An important feature of Doppler is the ability to filter out echoes due to ground targets in the signal processing.

The current generation of radars has polarization capability. Operationally, pulses are transmitted simultaneously with horizontal and vertical polarizations. In the past, the pulses were transmitted in sequence but required a high-power polarization switch that was prone to failure. Two receivers (physical or virtual) are used to measure the horizontal and vertical

components of the returned signal. The main benefits are improved data quality through the ability to identify characteristics of the target (birds, bugs, precipitation and its type, clutter), hydrometeor classification and precipitation estimation. For forecast applications, the dual-polarization capability can identify hail and the rain–snow boundary. High precipitation rates affect the horizontal and vertical phase of the transmitted and received pulses, and this can be exploited for precipitation estimation even with partially blocked beams or attenuated signals. Dual polarization can be calibrated through self-consistent relationships between parameters.

Weather radars no longer operate in isolation. Given current telecommunication capabilities, data are exchanged, resulting in networks of weather radars. This has made it possible to extend their use in local applications (e.g. severe weather warnings and nowcasting), regional (e.g. data assimilation, precipitation estimation) and global applications (e.g. climate change detection).

Modern weather radars should have characteristics optimized to produce the best data for operational requirements. They are the most complex of all the weather sensors used in operations and require special training and extensive knowledge of the instrument. The location of the radar is critical to meet the surveillance and detection requirements. There are a variety of configuration options to set up the radar, and components should be adequately installed and monitored for degradation and failure. Hence, a maintenance and support programme is needed to keep this instrument useful.

7.1.2 Radar characteristics, terms and units

The meteorological applications govern the selection of the characteristics of the radar (Tables 7.1, 7.2 and 7.3).

7.1.3 Radar accuracy requirements

Quantitative use of radar data in end-user applications relies on the accuracy and precision of the radar observations. Appropriately installed, calibrated and maintained modern radars are relatively stable and do not produce significant measurement errors due to the stability of the hardware. However, the maintenance and calibration of the radar is still a considerable challenge and requires highly qualified personnel. Measurement error still exists and requires engineering and scientific expertise to monitor, diagnose and mitigate the biases.

External physical factors, such as ground clutter effects, anomalous propagation, attenuation and propagation effects, beam effects, target composition, particularly with variations and changes in the vertical, rain rate-reflectivity relationship inadequacies and the meteorological

Table 7.1. Radar frequency bands

Radar band	Frequency	Wavelength	Nominal
UHF	300–1 000 MHz	1–0.3 m	70 cm
L	1 000–2 000 MHz	0.3–0.15 m	20 cm
S	2 000–4 000 MHz	15–7.5 cm	10 cm
C	4 000–8 000 MHz	7.5–3.75 cm	5 cm
X	8 000–12 500 MHz	3.75–2.4 cm	3 cm
K_u	12.5–18 GHz	2.4–1.66 cm	1.50 cm
K	18–26.5 GHz	1.66–1.13 cm	1.25 cm
K_a	26.5–40 GHz	1.13–0.75 cm	0.86 cm
W	94 GHz	0.30 cm	0.30 cm

Table 7.2. Some meteorological radar parameters and units

Symbol	Parameter	Units
Z_e	Equivalent or effective radar reflectivity factor	$mm^6\ m^{-3}$ or dBZ
V_r	Mean radial velocity	$m\ s^{-1}$
σ_v	Spectrum width	$m\ s^{-1}$
Z_{DR}	Differential reflectivity	dB
K_{DP}, φ_{DP}	Specific differential phase, Differential phase	Degree km^{-1}, Degree
ρ_{HV}	Correlation coefficient	
LDR	Linear depolarization ratio	dB

Table 7.3. Physical radar parameters and units

Symbol	Parameter	Units
c	Speed of light	$m\ s^{-1}$
f	Transmitted frequency	Hz
f_d	Doppler frequency shift	Hz
P_r	Received power	mW or dBm
P_t	Transmitted power	kW
PRF	Pulse repetition frequency	Hz
T	Pulse repetition time (=1/PRF)	ms
Ω	Antenna rotation rate	Degree s^{-1} or rpm
λ	Transmitted wavelength	cm
φ	Azimuth angle	Degree
θ	Beam width between half power points	Degree
τ	Pulse width	μs
γ	Elevation angle	Degree

situation, create artefacts in the data that must be removed during scientific data processing for use in quantitative applications. By considering only errors attributable to the radar system, the measurable radar parameters can be determined with an acceptable accuracy (Table 7.4).

7.2   RADAR PRINCIPLES

7.2.1   Pulse radars

The principles of radar and the observation of weather phenomena were established in the 1940s. Since then, great strides have been made in improving equipment, signal and data processing and data interpretation. The interested reader should consult some of the relevant texts for greater detail. Good references include Skolnik (1970, 1990) for engineering and equipment aspects; Battan (1973) for meteorological phenomena and applications;

Table 7.4. Accuracy requirements

Parameter	Definition	Acceptable accuracy[a]
φ	Azimuth angle	0.1°
γ	Elevation angle	0.1°
V_r	Mean Doppler velocity	1.0 m s^{-1}
Z	Reflectivity factor	1 dBZ
σ_v	Doppler spectrum width	1 m s^{-1}
Z_{DR}	Differential reflectivity	0.2 dB
K_{DP}	Specific differential phase	< 0.5 degree km^{-1}
ρ_{HV}	Cross-polar correlation	0.001

Note:

a   These figures are relative to a normal Gaussian spectrum with a standard deviation smaller than 4 m s^{-1}. Velocity accuracy deteriorates when the spectrum width grows, while reflectivity accuracy improves.

Atlas (1964, 1990), Sauvageot (1982) and WMO (1985) for a general review; Rinehart (2004) for a meteorologist's perspective; Doviak and Zrnić (1993) for Doppler radar principles and applications; and Bringi and Chandrasekar (2001) and Meischner (2003) for dual polarization. Considerable insight on radar quality, maintenance, hardware monitoring and calibration can be gleaned from the RADCAL 2000 (Joe, 2001), RADCAL 2013 (Chandrasekar and Baldini, 2013) and the RADMON 2010 (Joe, 2010) workshops. A brief summary of the principles follows.

Figure 7.1 shows a typical radar and radar site. The antenna (2–8.5 m) is inside the radome on top of the tower, which is of the order of 10–30 m or more in height. A tower is used to elevate the antenna above local obstructions. When determining the height of the tower, the growth of nearby trees should be taken into account. Too tall a tower will result in considerably more ground clutter due to the side of the main lobe and the side lobes. One of the buildings contains the radar electronics (transmitter/receiver and computers) and the other contains the uninterruptible power supply (UPS) and diesel generator. Radars are often located in rural locations and well-conditioned power is often not the norm. The UPS plays a critical role in removing power spikes and other anomalies in the power and is key to maintaining operations. The diesel or other kind of generator is capable of 2–3 days of operation but should be specified according to the needs. Note the lightning rod, on top of the radome, that is connected to grounding cables (not shown). This is critical as lightning can cause serious and long-term damage to the radar components. Power fluctuations due to lightning can exceed the capability of the UPS. Note also the red signal lights on top of the radome for warning aviators.

Electromagnetic waves at fixed preferred frequencies are transmitted from a directional antenna into the atmosphere in a rapid succession of short pulses. The pulse length and range processing determines the range resolution of the radar data. One emerging technology in operational radars is the use of low-power transmitters (solid state, travelling-wave tubes) that exploit a technique called pulse compression using a combination of long pulses at low power, frequency modulation and advanced signal-processing to achieve high-range resolution and high sensitivity that rival traditional pulse systems. Phased array antennas are an emerging technology that forms the beam by electronic phase shifting. They have the ability to point to different locations in an agile and non-sequential fashion. However, they all use a directional beam that can resolve targets in range, azimuth and elevation.

Figure 7.2 shows a directional radar antenna emitting a pulsed-shaped beam of electromagnetic energy over the Earth's surface and illuminating various targets, including non-meteorological targets. Many of the physical limitations and constraints of the observation technique are immediately apparent from the figure. For example, (i) there is a limit to the minimum altitude that can be observed at far ranges due to the curvature of the Earth, (ii) there are non-

Figure 7.1. A typical weather radar within the Canadian network showing the major physical components of a radar system. The tower is about 30 m high, with a radome fitted with hazard lights and a lightning rod.

meteorological targets, (iii) there are other emitters (Radio Local Area Networks, the Sun), (iv) there is anomalous propagation of the beam, (v) there is blockage and partial blockage due to mountains, (vi) there is precipitation of different types, and (vii) there are electromagnetic–precipitation interactions resulting in enhanced returns (bright band), etc.

A parabolic reflector in the antenna system concentrates the electromagnetic energy in a conical-shaped beam that is highly directional. The width of the beam increases with range, for example, a nominal 1° beam spreads to 0.9, 1.7 and 3.5 km at ranges of 50, 100 and 200 km, respectively.

For a pulse radar, the short bursts of electromagnetic energy are absorbed and scattered by the illuminated meteorological and non-meteorological targets. Some of the scattered energy is reflected back to the radar antenna and receiver. Since the electromagnetic wave travels at the speed of light (that is, 2.99×10^8 m s^{-1}), the range of the target can be determined by measuring
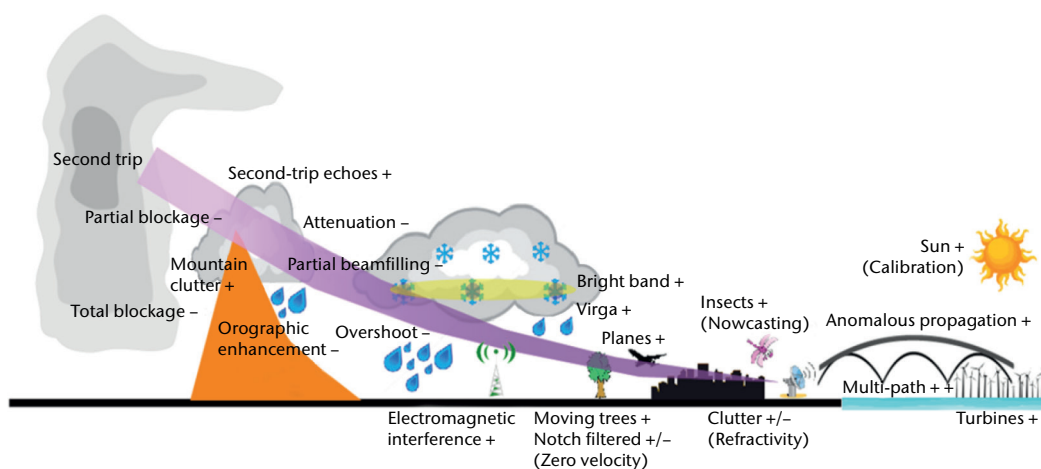
Figure 7.2. The weather radar can detect many things besides weather targets. This schematic illustrates many of these features. The + or – signs indicate whether the radar reflectivity is augmented or diminished by the feature. These artefacts need to be removed for quantitative applications.

the time between the transmission of the pulse and its return. Between the transmissions of successive pulses, the receiver listens for any return of the wave. The return signal from the target is commonly referred to as the radar echo. The time between consecutive pulses determines the maximum unambiguous range of the radar. Echoes can still be received from targets beyond this maximum range and are known as multiple-trip echoes.

For a pulse compression radar with frequency modulation, the range to target is determined by the frequency within the long pulse. However, the maximum unambiguous range is still determined by the time between consecutive pulses. With the transmission of long pulses, the radar receiver is protected from the high power of the transmit pulse, and a long blind zone (10–30 km, depending on the pulse length) is created. In this type of radar, short pulses (with corresponding short blind zones, < 2 km) are transmitted to detect objects that are within this blind zone.

The radar range equation relates the power returned from the target to the radar characteristics. The power returned provides an estimate of the amount of precipitation in the resolution volume. This estimate depends on the assumption of the type of precipitation particles and their size distribution in the resolution volume.

The power measurements are determined by the total power backscattered by the target within a volume being sampled at any one instant in time. This volume is called the pulse volume or sample volume. The pulse volume dimensions (which determine the resolution of the radar) are dependent on the radar pulse length in space (h) and the antenna beam widths in the vertical (ϕ_b) and the horizontal (θ_b). The beam width, and therefore the pulse volume, increases with range. Since the power that arrives back at the radar is involved in a two-way path, the pulse-volume length is only one half the pulse length in space ($h/2$) and is invariant with range. The location of the pulse volume in space is determined by the position of the antenna in azimuth, the elevation, the range to the target and also by the non-linear propagation path of the radar beam away from the radar. For a pulse compression radar, the pulse volume is primarily determined by the resolution of the frequency modulation and the capability of the receiving system to resolve changes in frequency.

Particles within the pulse volume are continuously shuffling relative to one another. This results in intensity fluctuations about the mean target intensity. Little significance can be attached to a single echo intensity measurement from a weather target. At least 25 to 30 pulses must be integrated to obtain a reasonable estimation of mean intensity, though this will depend on the level of data quality considered as acceptable (Smith, 1995). This was formerly carried out by an electronic integrator circuit but is now done in a digital signal processor. Further averaging of pulses in range, azimuth and time is often conducted to increase the sampling size and accuracy of the estimate at the expense of coarser spatial resolution. An important difference with non-meteorological radars is that the signal processing and the interpretation of the data are based on the premise that the backscatter is from a distributed target and not from a point target (such as an aeroplane). This requires processing for quantitative measurements (not just detection) and a different range dependency of the return power (different radar equation) compared to point target detection radars (such as for air traffic control).

Doppler radars have circuitry to measure the phase shift difference from successive pulses from the same radar pulse volume. The phase shift is proportional to the radar wavelength and therefore to the distance in the time between pulses. This phase shift is used to estimate the radial or Doppler velocity.

Dual-polarization radar can be of several types. The polarization can be circular and, though there have been very excellent research radars with this feature, it is not generally used in weather operations. Linear dual-polarization radars can send pulses at horizontal and vertical polarization in alternating or simultaneous fashion. In the former case, a fast high-power switch (switches every pulse) is required, but it has proved to be problematic and so few exist in operations. The simultaneous transmit and receive (STAR mode) technique transmits equal powers in both the horizontal and vertical polarizations and the signal is received separately at horizontal and vertical polarizations. This has proved to be the solution for operations as the high-power, high failure fast switch is avoided. There are variations to these methods of creating

the dual-polarization signal. The major advantage of the alternating dual-polarization mode is that it can measure the cross-polarization backscatter of the target (Linear Depolarization Ratio – LDR), and this is particularly useful for bright band detection. The major disadvantage of the STAR mode is this loss of LDR (as there is cross-polarization already in the transmitted pulse), a 3 dB loss of signal strength in both channels (due to power splitting), and cross-coupling artefacts, particularly in the ice phase of storms.

7.2.2 **Propagation radar signals**

Electromagnetic waves propagate in straight lines in a homogeneous medium. However, the atmosphere is vertically stratified and the rays change direction depending on the changes in the refractive index (which is a function of temperature and moisture). When the waves encounter precipitation and clouds, part of the energy is absorbed and part is scattered in all directions, including back to the radar site.

The amount of bending of electromagnetic waves can be predicted by using the vertical profile of temperature, moisture and pressure (Bean and Dutton, 1966). Under normal atmospheric conditions, the waves travel in a curve bending slightly earthward (Figure 7.3). The representation is drawn in physical space (the Earth is drawn with a radius of 6 371 km) and the figure shows that the beam bends downward, but still rises with range with respect to the Earth's surface. In a four-thirds (4/3) Earth model, where the Earth's surface is drawn with a radius of 8 975 km (4/3 x 6 371 km), the beams are straight lines (Figure 7.4).

This 4/3 model is most often used, but some radars (mountain top) use a 5/4 model. The height above the radar is given by the following equation:

$$h = \left[r^2 + \left(k_e a \right)^2 + 2 r k_e a \sin \theta_e \right]^{1/2} - k_e a \qquad (7.1)$$

where h is the height above the radar antenna, r is the range along the beam, a is the Earth's radius, e is the elevation angle above the horizon and $k_e a$ is the effective Earth radius.

The ray path can bend either upwards (sub-refraction) or more earthward (super-refraction). In either case, the altitude of the beam will be in error using the standard atmosphere assumption. This is known as anomalous propagation. From a precipitation measurement standpoint, the
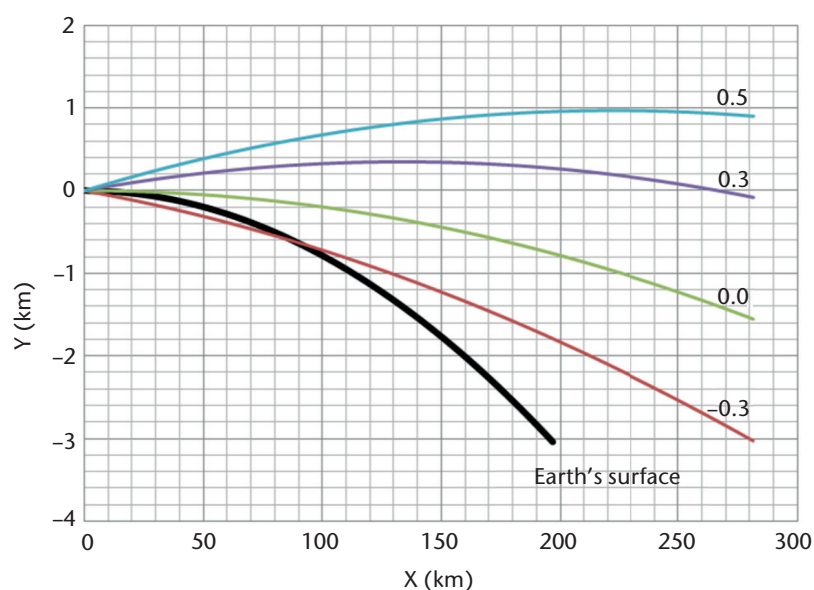
Figure 7.3. Schematic of beam height for selected elevation angles (–0.3, 0, 0.3 and 0.5) above the Earth's surface, for a standard index of refraction profile in the atmosphere plotted in physical space with an Earth curvature equivalent to the Earth radius
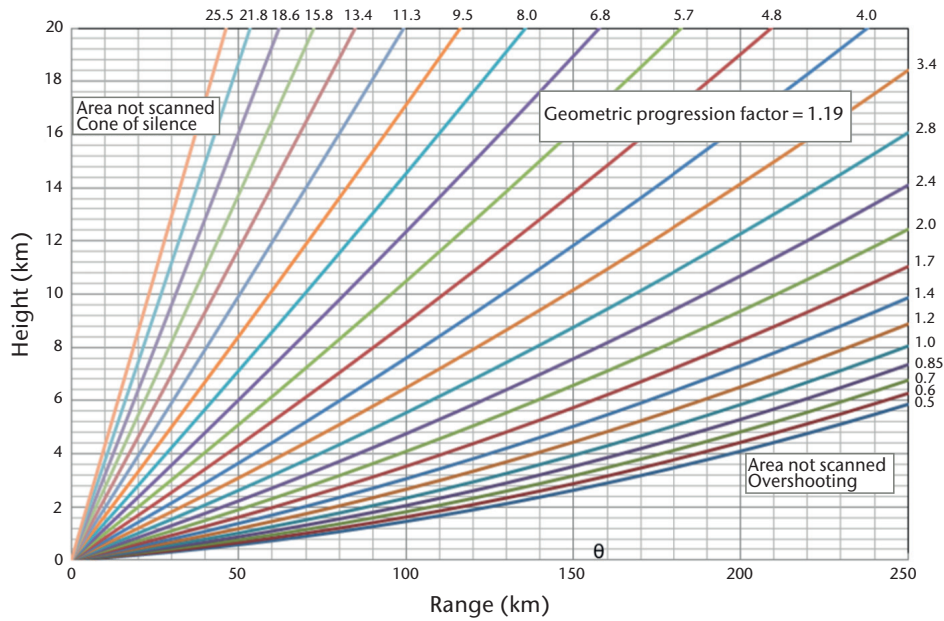
Figure 7.4. The beam height diagram is a useful tool for the interpretation of radar products. The beam height is plotted against a flat Earth, which is a more traditional presentation. The elevation angle sequence is one proposed by Marshall and Ballantyne (1978) to produce optimal horizontal products (CAPPIs, echo tops).

greatest problem occurs under super-refractive or "ducting" conditions, where the ray can bend sufficiently to strike the Earth and cause ground echoes not normally encountered. The phenomenon occurs when the index of refraction decreases rapidly with height. This occurs when there is an increase in temperature and a decrease in moisture with height. These echoes must be eliminated when producing a precipitation map. The sub-refraction situation, where the beam doesn't beam as much as normal or bends in the upward direction, is not evident to identify and thus is also a problem. In actual practice, the vertical profile of the index of refraction is not known, so that the precise location of the beam is not known.

Some "clear air" echoes are due to turbulent fluctuations in the refractive index. This is found in areas of turbulence, layers of enhanced stability, wind shear cells, or strong inversions (Bragg scattering). These echoes usually occur in patterns, mostly recognizable, but must be eliminated as precipitation fields (Gossard and Strauch, 1983).

7.2.3   **Attenuation in the atmosphere**

Microwaves are subject to attenuation owing to atmospheric gases, clouds and precipitation by absorption and scattering.

Attenuation by gases

Gases attenuate microwaves in the 3–10 cm bands. Absorption by atmospheric gases is due mainly to water vapour and oxygen molecules. Attenuation by water vapour is directly proportional to the pressure and absolute humidity and increases almost linearly with decreasing temperature. The concentration of oxygen, to altitudes of 20 km, is relatively uniform.

Attenuation by gases varies slightly with the climate and the season. It is significant at weather radar wavelengths over the longer ranges and can amount to 2 to 3 dB at the longer wavelengths and 3 to 4 dB at the shorter wavelengths, over a range of 200 km. Compensation can be quite easily accomplished automatically.

Table 7.5. One-way attenuation relationships

Wavelength (cm)	Relation (dB km^{-1})
10	0.000 343 $R^{0.97}$
5	0.00 18 $R^{1.05}$
3.2	0.01 $R^{1.21}$

Note: After Burrows and Attwood (1949).
One-way specific attenuations at 18 °C.
R is in units of mm hr^{-1}.

Attenuation by hydrometeors

Attenuation by hydrometeors can result from both absorption and scattering. It is the most significant source of attenuation. It is dependent on the shape, size, number and composition of the particles. This dependence has made attenuation very difficult to overcome in any quantitative way using radar observations alone, though great progress has been made using dual-polarization radar techniques.

Attenuation is dependent on wavelength. At 10 cm wavelengths, the attenuation exists but is rather small, while at 3 cm it is quite significant. At 5 cm, the attenuation may be acceptable for many climates, particularly in the high mid-latitudes. Wavelengths below 5 cm are not recommended for good precipitation measurement except for short-range applications (Table 7.5). Total attenuation of the signal can occur at 3 and 5 cm. Smaller wavelength radars are more sensitive to attenuation and attenuation correction, and quantitative precipitation estimation based on dual-polarization specific differential phase measurements has more impact on resulting data. These techniques are effective starting at lower precipitation rates for smaller wavelengths.

For precipitation estimates by radar, some general statements can be made with regard to the magnitude of attenuation. Attenuation is dependent on the water mass of the target, thus heavier rains attenuate more; clouds, with much smaller mass, attenuate less. Ice particles attenuate much less than liquid particles. Clouds and ice clouds cause little attenuation and can usually be ignored. Snow or ice particles (or hailstones) can grow much larger than raindrops. They become wet as they begin to melt and result in a large increase in reflectivity and, therefore, in attenuation properties. This can distort precipitation estimates.

7.2.4   Scattering by clouds and precipitation

The echo power detected is backscattered by the targets in the resolution volume (hydrometeors, ground, trees, etc.). The backscattering cross-section (σ_b) is defined as the area of an isotropic scatterer that would return to the emitting source by the same amount of power as the actual target. The backscattering cross-section of spherical particles was first determined by Mie (1908). Rayleigh found that if the ratio of the particle diameter to the wavelength was equal to or less than 0.06, a simpler expression could be used to determine the backscatter cross-section:

$$\sigma_b = \frac{\pi^5 |K|^2 D^6}{\lambda^4} \tag{7.2}$$

which is the justification for equation 7.3. $|K|^2$, the refractive index factor, is equal to 0.93 for liquid water and 0.197 for ice.

The radar power measurements are used to derive the scattering intensity of the target by using equation 7.2 in the form:

$$z = \frac{C \bar{P}_r r^2}{|K|^2} \tag{7.3}$$

Table 7.6. Typical backscatter cross-sections for various targets

Object	σ_b (m²)
Aircraft	10 to 1 000
Human	0.14 to 1.05
Weather balloon	0.01
Birds	0.001 to 0.01
Bees, dragonflies, moths	3×10^{-6} to 10^{-5}
2 mm water drop	1.8×10^{-10}

The method and problems of interpreting the reflectivity factor in terms of precipitation rate (R) are discussed in section 7.10.

7.2.5　Scattering in clear air

In regions without precipitating clouds, it has been found that echoes are mostly due to insects or to strong gradients of refractive index in the atmosphere (Bragg scatter). The echoes are of low intensity and are detected by most modern radars unless discarded via thresholding of the data. Equivalent Z_e values for clear air phenomena generally appear in the range of –55 to –5 dBZ, although these are not true Z parameters as the physical process generating the echoes is entirely different. For precipitation measurement, these echoes are "noise" in the signal. However, they can usually be associated with some meteorological phenomenon such as a sea breeze or thunderstorm outflows and therefore are useful to identify areas of potential convective initiation. Clear air echoes can also be associated with birds and insects in very low concentrations. Echo strengths of 5 to 35 dBZ are not unusual, especially during migrations (Table 7.6).

Although normal radar processing would interpret the signal in terms of Z, the scattering properties of the fluctuations of the index of refraction are quite different from that of hydrometeors. It is also known as Bragg scattering. The scattering is most often expressed in terms of the structure parameter of refractive index, Cn^2. This is a measure of the mean-square fluctuations of the refractive index as a function of distance (Gossard and Strauch, 1983).

7.3　THE RADAR EQUATION FOR PRECIPITATION TARGETS

Meteorological targets consist of ice and/or water particles randomly distributed in space. The power backscattered from the target volume is dependent on the number, size, composition, relative position, shape and orientation of the scattering particles. The total power backscattered is the sum of the power backscattered by each of the scattering particles.

Using this target model and electromagnetic theory, Probert-Jones (1962) developed an equation relating the echo power received by the radar to the parameters of the radar and the targets' range and scattering characteristics. It is generally accepted as being a reliable relationship to provide quantitative reflectivity measurements with good accuracy, bearing in mind the generally realistic assumptions made in the derivation:

$$\bar{P}_r = \frac{\pi^3}{1\,024 \ln 2} \cdot \frac{P_t h G^2 \theta_b \phi_b}{\lambda^2} \cdot \frac{|K|^2 10^{-18} Z}{r^2} \tag{7.4}$$

where $\bar{P}_r$ is the power received back at the radar, averaged over several pulses, in watts; P_t is the peak power of the pulse transmitted by the radar in watts; h is the pulse length in space, in metres ($h = c\tau/2$, where c is the speed of light and τ is the pulse duration); G is the gain of the antenna over an isotropic radiator; θ_b and ϕ_b are the horizontal and vertical beam widths,

respectively, of the antenna radiation pattern at the –3 dB level of one-way transmission, in radians; λ is the wavelength of the transmitted wave, in metres; $|K|^2$ is the refractive index factor of the target; r is the slant range from the radar to the target, in metres; and Z is the radar reflectivity factor (usually taken as the equivalent reflectivity factor Z_e when the target characteristics are not well known), in $mm^6\ m^{-3}$.

The second term in the equation contains the radar parameters, and in the third term the parameters depend on the range and characteristics of the target. The radar parameters are relatively fixed, and, if the transmitter is operated and maintained at a constant output (as it should be), the equation can be simplified to:

$$\bar{P}_r = \frac{C|K|^2 Z}{r^2} \tag{7.5}$$

where C is the radar constant.

There are a number of basic assumptions inherent in the development of the equation which have varying importance in the application and interpretation of the results. Although they are reasonably realistic, the conditions are not always met exactly and, under particular conditions, will affect the measurements (Aoyagi and Kodaira, 1995).

These assumptions are summarized as follows:

(a) The scattering precipitation particles in the target volume are homogeneous dielectric spheres whose diameters are small compared to the wavelength, that is $D < 0.06\ \lambda$ for strict application of Rayleigh scattering approximations;

(b) The pulse volume is completely filled with randomly located precipitation particles;

(c) The reflectivity factor Z is uniform throughout the sampled pulse volume and approximately constant during the sampling interval;

(d) The particles are all water drops or all ice particles, that is, all particles have the same refractive index factor $|K|^2$, and the power scattering by the particles is isotropic;

(e) Multiple scattering (among particles) is negligible;

(f) There is no attenuation in the intervening medium between the radar and the target volume;

(g) The radar uses linear polarizations (typically H or V);

(h) The main lobe of the antenna radiation pattern is Gaussian in shape;

(i) The gain of the antenna is known or can be calculated with sufficient accuracy;

(j) The contribution of the side lobes to the received power is negligible;

(k) Blockage of the transmitted signal by ground clutter in the beam is negligible;

(l) The peak power transmitted (P_t) is the actual power transmitted at the antenna, that is, all waveguide losses, and so on, and attenuation in the radar dome, are considered;

(m) The average power measured (P_r) is averaged over a sufficient number of pulses or independent samples to be representative of the average over the target pulse volume.

This simplified expression relates the echo power measured by the radar to the radar reflectivity factor Z, which is in turn related to the rainfall rate. These factors and their relationship are crucial for interpreting the power returned from the target and estimating precipitation amounts from

radar measurements. Despite the many assumptions, the expression provides a reasonable estimate of the precipitation mass. This estimate can be improved by further consideration of factors in the assumptions.

7.4 BASIC WEATHER RADAR SYSTEM AND DATA

The basic weather radar consists of the following:

(a)   An antenna to focus the transmitted microwaves into a narrow beam and receive the returning power;

(b)   A tower to elevate the antenna above immediate obstructions;

(c)   A transmitter to produce power at microwave frequency and a modulator to create the pulses and pulse rates;

(d)   A receiver to detect, amplify and convert the microwave signal into a low-frequency signal;

(e)   A signal processor to extract the desired information from the received signal;

(f)   A system to control the radar and process the data into radar variables;

(g)   A data display to visualize the information in an intelligible form;

(h)   A recording system to archive the data for training, study and records.

A basic weather radar may be non-coherent (e.g. a magnetron or power oscillator type transmitter), that is, the phase of successive transmitted pulses is random. Doppler measurements can be made if the phase of the transmitted pulse is measured and the return signal processed with reference to this phase. This is known as a coherent-on-receive Doppler radar. A coherent-on-transmit radar (e.g. a klystron, power amplifier, solid state or travelling-wave tube type transmitter) transmits the same phase with each pulse. Power transmitted by a weather radar is typically several hundreds of kilowatts to a megawatt of peak power concentrated in a pulse of a microsecond in width, whereas the average power is typically a few hundred watts. Solid state or travelling-wave tube type transmitters send a pulse of much lower power but rely on long pulses to compensate.

7.4.1 Reflectivity

The backscattered power measured by a typical radar is of the order of 10^{-8} to 10^{-15} W, covering a range of about 70 dB from the strongest to the weakest targets detectable. Compared to the transmit power, this is over 20 orders of magnitude smaller. To measure the weakest and strongest signals simultaneously, receivers with large dynamic ranges (> 90 dB) are required and are now commonly available (Heiss et al., 1990; Keeler et al., 1995). In the past, logarithmic receivers with a dynamic range of 90 dB were used for reflectivity measurements. Linear receivers (that maintain phase linearity) are needed for Doppler measurements. In the past, these had limited dynamic range (40 to 50 dB), requiring automatic gain control.

The reflectivity factor is the most important parameter for radar interpretation. The factor derives from the Rayleigh scattering model and is defined theoretically as the sum of particle (drops) diameters to the sixth power in the sample volume:

$$Z = \Sigma_{\text{vol}} N(D)\, D^6 \qquad\qquad (7.6)$$

where the unit of Z is mm^6 m^{-3}. In many cases, the number of particles and their composition and shape are not known and an equivalent or effective reflectivity factor Z_e is defined. For example, snow and ice particles must refer to an equivalent Z_e which represents Z, assuming the backscattering particles were all spherical drops of density ρ.

Rainfall rate is given by:

$$R = \sum\nolimits_{vol} N(D) V_T \rho \; \pi \, / \, 6 \; D^3 \tag{7.7}$$

However, $N(D)$ is not known, and empirical relationships between Z and R have been developed; the most famous being the one commonly known as the Marshall-Palmer relationship:

$$Z = 200 R^{1.6} \tag{7.8}$$

In order to cover the range of values, a common practice is to work in a logarithmic scale or dBZ units which are numerically defined as $dBZ_e = 10 \log_{10} Z_e$.

Volumetric observations of the atmosphere are normally made by scanning the antenna at a fixed elevation angle and subsequently incrementing the elevation angle in steps at each revolution. An important consideration is the resolution of the targets. Parabolic reflector and phased array (through phase shifting) antennas are used to focus the waves into a pencil shaped or Gaussian shaped beam. Larger reflectors create narrower beams, greater resolution and sensitivity at increasing costs. The beam width, often defined by the half power points, is one half that at the axis, is dependent on the wavelength, and may be approximated by:

$$\theta_e = \frac{70\lambda}{d} \tag{7.9}$$

where the units of θ_e are degrees; and d is the antenna diameter in the same units as λ. Good surveillance weather radars have beam widths of 0.5° to 1°. However, broader beams are useful for short-range applications.

The useful range of weather radars is dependent on the application and nature of the weather. Depending on the time interval between pulses (characterized by the pulse repetition frequency (PRF), say 300 s^{-1}), the maximum unambiguous range of the radar can be hundreds of kilometres (e.g. 500 km). However, given the beam propagation and the curvature of the Earth, the beam, and therefore the pulse volume, is high and big (e.g. at 250 km, a 1° beam width radar pointing at an elevation angle of 1° is 9 km high and 6 km wide, Figure 7.4). The beam may overshoot the weather, the pulse volume may not be filled and the sensitivity of the radar may not be sufficient to measure the precipitation intensity accurately. However, if echoes are observed, they will indicate very intense and hazardous thunderstorms or weather. Typical weather radars operate with a maximum range of the order of 250 to 600 km.

For good quantitative precipitation measurements, a 1° beam width radar has an effective range of about 80 km. The smaller the beam width of the radar, the greater the effective range (e.g. a 0.65° beam has an effective range of about 120 km). At longer ranges, the data must be extrapolated to the ground. The beam spreads and under-filling results in under-reporting of the precipitation intensity. This is weather regime dependent, and the results discussed are for mid-latitudes.

7.4.2 Doppler velocity

The development of Doppler weather radars and their introduction to weather surveillance provided a new dimension to the observations (Heiss et al., 1990). Doppler radar provides a measure of the targets' velocity along a radial from the radar. So it provides a measurement of the velocity component of the wind in the direction either towards or away from the radar.

The typical speeds of meteorological targets are less than 50 m s^{-1}, except in the case of tornadoes/hurricanes. As discussed earlier, pulse-to-pulse phase changes are used to estimate the Doppler velocity. If the phase changes by more than ±180°, the velocity estimate is ambiguous. In order to unambiguously and accurately measure the Doppler velocity of meteorological targets, the pulse repetition frequency must be high (smaller time interval between pulses) such that the maximum unambiguous range is reduced from that of a typical radar, measuring reflectivity only. At higher speeds, additional processing steps are required to retrieve the correct velocity. The maximum unambiguous Doppler velocity depends on the radar wavelength (λ) and the PRF, and can be expressed as:

$$V_{max} = \pm \frac{PRF \cdot \lambda}{4} \tag{7.10}$$

The maximum unambiguous range can be expressed as:

$$r_{max} = \frac{c}{PRF \cdot 2} \tag{7.11}$$

Thus, V_{max} and r_{max} are related by the equation:

$$V_{max} r_{max} = \pm \frac{\lambda c}{8} \tag{7.12}$$

These relationships show the limits imposed by the selection of the wavelength and PRF (see Figure 7.5). A high PRF is desirable to increase the unambiguous velocity; a low PRF is desirable to increase the radar range. Unfortunately, these limits fall within the desired measurement space of a weather radar, and compromises in the radar operating conditions are required. This is known as the Doppler dilemma and is further discussed in the signal and data processing section of this chapter. The maximum unambiguous velocity or range is often referred to as the Nyquist velocity or Nyquist range.

One of the significant consequences of the high PRFs is that there are often still detectable echoes beyond the Nyquist range. These echoes are referred to as second- (or multiple-) trip echoes since they are received from pulses transmitted previously. If the targets are strong enough, the power of these targets can still be received by the radar. However, the targets will be located incorrectly in the first trip since the radar cannot determine whether the echo was a result of the current or previous pulse, given that the timing or range of the echo is based on the most recent transmitted pulse.

Some Doppler radars are fully coherent; their transmitters are oscillators and generate the same phase from pulse to pulse. These coherent radars typically employ klystrons, solid state or similar transmitters. Since these types of radars transmit the same phase for every pulse, the velocity of the second echoes will produce discernible mean radial velocities. This kind of radar cannot (without advanced processing) separate the range or the velocity of the multiple-trip echoes.
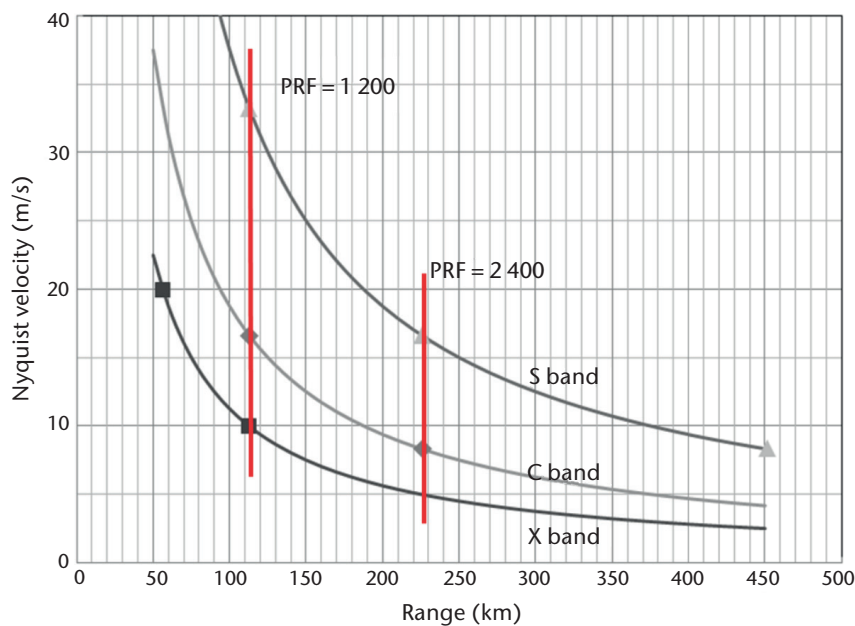
Figure 7.5. This illustrates the Doppler dilemma for the three common radar bands (X, C, S). The dilemma arises because one parameter, the pulse repetition frequency, which is the time between transmitted pulses, controls the maximum unambiguous velocity and the maximum unambiguous range in opposite ways. The markers and red lines indicate commonly used settings.
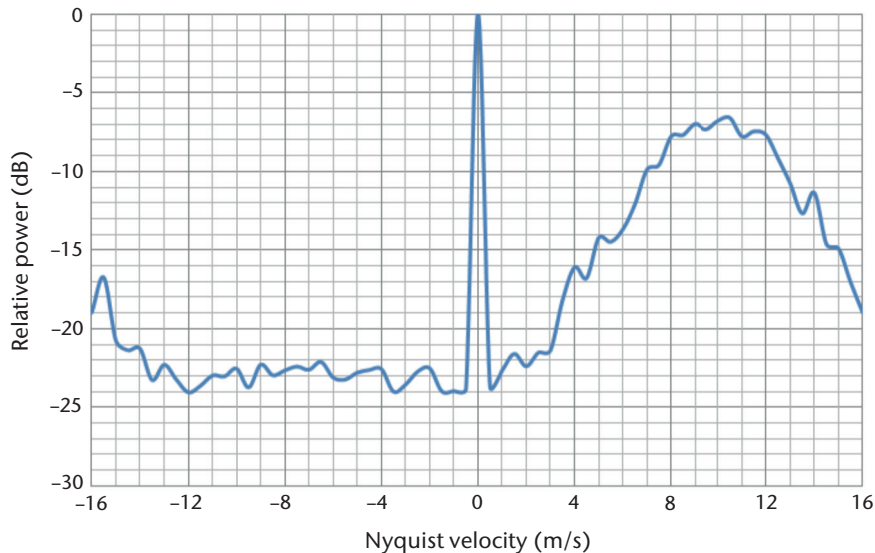
Figure 7.6. This Doppler spectrum shows the distribution of power within a single radar pulse volume as a function of the Doppler velocity.

For coherent-on-receive Doppler radars, such as one with a magnetron amplifier transmitter, the phase from pulse to pulse is random. In this kind of radar, the phase of the most recently transmitted pulse is measured and the phases of all echoes are referenced to it. Therefore, the series of phases from the second-trip echo that referenced to the most recent phase will be random and will appear as noise in the Doppler spectrum. Figure 7.6 is a simulated example of a typical C band radar set-up. The sharp spike at zero velocity is due to stationary ground echoes and has a narrow power distribution. The broad peak on the right is the weather echo. It is broader than the ground clutter peak since it originates from a distribution of drops that are shuffling. Note that the tail of the weather contribution on the right is aliased and appears on the left edge of the graph. The signal fluctuates about the noise floor due to thermal noise in the system, and also about the weather spectrum due to the shuffling of the precipitation targets. A dynamic estimation of the noise power makes it possible to subtract the noise power from the overall power to produce a cleaner estimate of the first-trip power (Figure 7.7). This is an example showing (a) how stationary ground clutter can be filtered using a zero velocity notch filter, and (b) how second-trip echoes can be filtered using a noise type filter (signal quality index).

Two signal-processing systems of different complexity are used to process the Doppler parameters. The simpler pulse pair processing (PPP) system uses the comparison of successive pulses in the time domain to extract mean velocity and spectrum width. The second and more complex system uses fast Fourier transform (FFT) processing to produce a full spectrum of velocities in each sample volume. The PPP system is faster, less computationally intensive and better at low signal-to-noise ratios, but has poorer clutter rejection characteristics than the FFT system.

7.4.3   **Dual polarization**

There are several basic radar polarization techniques in current usage. One system transmits a circularly polarized wave, and the co-polar and orthogonal polarization powers are measured. Another system alternately or simultaneously transmits pulses with horizontal (H) then vertical (V) polarization utilizing a high-power switch. Simultaneous H and V radars do not require a fast switch. The complexity of unravelling the microphysical characteristics of the echo is still a challenge, and manufacturing a high-quality circular polarization system can be more costly. The linear polarization system is generally preferred since the retrieval of meteorological information is less calculation intensive, and conventional radars can be converted to dual polarization
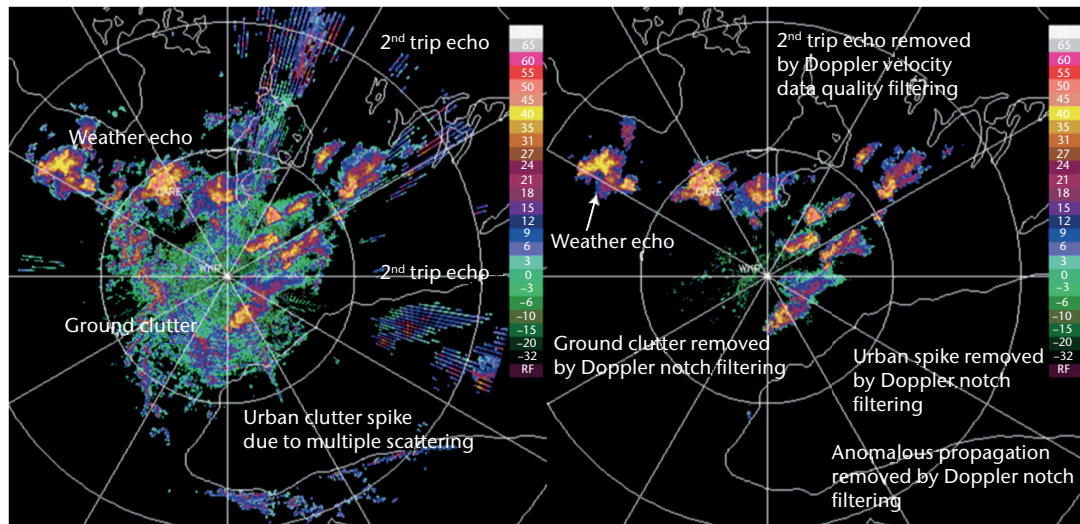
Figure 7.7. Modern Doppler radars can filter bad data or ground clutter in the signal-processing phase of the processing chain. The left image shows the raw data and the right image shows the filtering capability of Doppler signal and data processing. Polarization diversity capability for data quality is shown in Figure 7.29.

more easily. Except in a few situations, the high-power switch has proved to be problematic for alternating polarization, and as a result the simultaneous transmit and receive system is common in operational radars.

In general, the polarization technique is based on micro-differences in the scattering particles. Raindrops are elliptically shaped with the major axis in the horizontal plane when falling freely in the atmosphere. The oblateness of the drop is related to drop size. The power backscattered from an oblate spheroid is larger for a horizontally polarized wave than for a vertically polarized wave assuming Rayleigh scattering. This is also true for other targets such as insects, birds and ground clutter.

Table 7.2 describes the most common polarization diversity parameters. The differential reflectivity, called Z_{DR}, is defined as 10 times the logarithm of the ratio of the horizontally polarized reflectivity Z_H and the vertically polarized reflectivity Z_V. Comparisons of the equivalent reflectivity factor Z_e and the differential reflectivity Z_{DR} suggest that the precipitation may be separated as hail, rain, drizzle or snow (Seliga and Bringi, 1976).

As an electromagnetic wave propagates through a medium with oblate particles, the phase of the incident beam is altered due to attenuation differences (resulting in propagation speed differences) in the vertical and horizontal. The effect on the vertical and horizontal phase components depends on the oblateness and is embodied in an integral parameter termed the differential phase (φ_{DP}). If an appropriate range derivative can be computed, the specific differential phase (K_{DP}) can also be estimated. For heavy rainfall measurements, K_{DP} has certain advantages (Zrnić and Ryzhkov, 1995). English et al. (1991) demonstrated that the use of K_{DP} for rainfall estimation is much better than Z for rainfall rates greater than about 20 mm h^{-1} at the S band. Since this is a phase measurement and can be localized or specific to the range bin, this parameter can be used to overcome issues of power calibration and partial beam blockage. With greater attenuation (shorter wavelengths), the effectiveness of this technique increases at lower reflectivities or precipitation rates.

The correlation of the vertical and horizontal time-series data provides a statistical measure of the dissimilarity of the H and V scattering cross-sections of the hydrometeors. It should be noted that this is a statistical measure, and so rain and snow, though on an individual particle basis appear to have quite different scattering characteristics, actually have high correlation in the statistical sense. Bebbington (1992) designed a parameter for a circularly polarized radar,

termed the degree of polarization, which is insensitive to propagation effects (linear correlation is independent of propagation effects also). This parameter is similar to linear correlation for linearly polarized radars and appears to have value in target discrimination. For example, extremely low values are indicative of scatterers that are randomly oriented such as those caused by airborne grass or ground clutter (Holt et al., 1993).

7.5 SIGNAL AND DATA PROCESSING

7.5.1 The Doppler spectrum

The radar detects an electromagnetic wave returned from the target. This wave is a result of all the scatterers in the radar volume. Mathematically, a wave is characterized by an amplitude and phase or equivalently in complex numbers as the real or imaginary parts of a phasor. This is also called the in-phase or quadrature (I, Q) signals. The wave is measured several times and the results are a time series of I, Q samples. If a Fourier transform is applied to the data, then the magnitude of the Fourier transform coefficients constitutes the Doppler spectrum. The Doppler spectrum is a representation of the auto-correlation of the I, Q time series in frequency space (Wiener, 1964). The more time samples, the finer the resolution in the frequency domain. Processing in time domain is equivalent to that in the frequency domain. Figure 7.6 shows a typical Doppler spectrum and is useful to characterize the various aspects of the information within a single radar volume. The noise level (integrated over the entire spectrum) represents the minimum signal level or minimum detected signal of this range bin. The peak at zero frequency or zero velocity is the contribution of stationary echoes or ground clutter. The broader peak is due to the weather target. Note that the peak at zero velocity is broadened by the antenna motion, poor phase stability of the radar system and a fewer number of samples. The width of the ground clutter spectrum is generally smaller than the width of the weather spectrum and can, in most cases, be used to separate the ground from the weather echo. The area under the weather echo and above the noise level is the power of the weather echo. The area under the ground clutter spectrum is the power due to ground clutter.

7.5.2 Power parameter estimation

The hydrometeors are distributed within the pulse volume and shuffle relative to each other and produce a fluctuating signal. Averaging is required to reduce the variance of the measurements to within acceptable uncertainty. Generally, 30 independent pulses are required to estimate reflectivity (Doviak and Zrnić, 1993). This implies that the pulses need to be sampled at time intervals greater than the de-correlation time of the pulse volume, sampled in different locations in range or using some other technique (frequency shuffling).

Operationally, this is done in various ways depending on the application and processing philosophy. The antenna could slowly scan and the reflectivity could be estimated within one degree of azimuth and within one pulse volume, or it could rotate more quickly and range averaging could be employed in the signal or data processor. Additionally, poorer data quality could be acceptable and data smoothing could be applied at a later stage.

7.5.3 Ground clutter and point targets

Clutter can be the result of a variety of targets, including buildings, hills, mountains, aircraft and chaff, to name just a few. Good radar siting is the first line of defence against ground clutter effects. However, clutter is always present to some extent since the sides of the main beam and the side lobes interact with the nearby terrain (Figure 7.8). The radar beam is not perfectly conical but radiates in all directions, though the main power is along the bore sight. The beam width is often defined as the half power points (–3 dB of the power along the bore sight). This radiation pattern is determined by the geometry of the feed horn, the distance from the focal point, the parabolic dish and the struts holding the feed horn. The height of the first side lobe
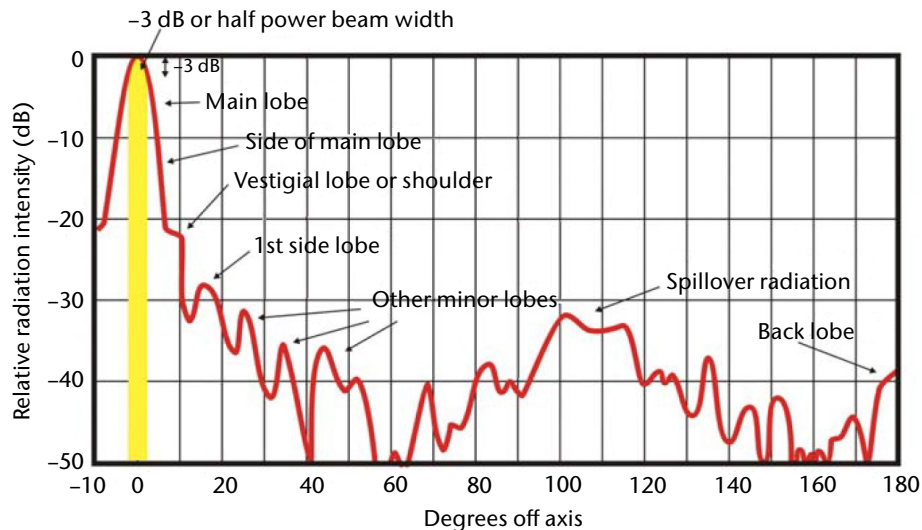
Figure 7.8. A generic antenna radiation pattern. Note that the antenna beam width is typically defined at the half power (50% or –3 dB) points. If the target is highly reflective, power is emitted and received on the side of the main lobe and the other side lobes.

(marked) is more or less determined by these factors and often used as a measure of the quality of the antenna. Reducing or moving this side lobe in azimuth by shifting the feed horn results in either a broader main beam or power loss.

The intensity of ground clutter is inversely proportional to wavelength (Skolnik, 1970, 1990), whereas backscatter from rain is inversely proportional to the fourth power of wavelength. Therefore, shorter wavelength radars are less affected by ground clutter. Ground clutter echoes should be eliminated for precipitation estimation; however, clutter echo can be used for humidity measurements (Fabry, 2004). Point targets, like aircraft, can be eliminated, if they are isolated, by removing echoes that occupy a single radar resolution volume. Weather targets are distributed over several radar resolution volumes. Point targets can be eliminated during the data-processing phase. Point targets, like aircraft echoes, embedded within precipitation echoes may not be eliminated with this technique depending on their relative strength.

To remove ground clutter, a conceptually attractive idea is to use clutter maps. The patterns of radar echoes in non-precipitating conditions are used to generate a clutter map that is subtracted from the radar pattern collected in precipitating conditions. The problem with this technique is that the pattern of ground clutter changes over time. These changes are primarily due to changes in meteorological conditions; a prime example is anomalous propagation echoes that typically last several hours and then disappear. Micro-changes to the environment cause small fluctuations in the pattern of ground echoes which confound the use of clutter maps. Adaptive techniques (Joss and Lee, 1993) attempt to determine dynamically the clutter pattern to account for the short-term fluctuations, but they are not good enough to be used exclusively.

Doppler processing techniques attempt to remove the clutter from the weather echo from a signal-processing perspective. The basic assumption is that the clutter echo is narrow in spectral width and that the clutter is stationary. However, to meet these first criteria, a sufficient number of pulses must be acquired and processed in order to have sufficient spectral resolution to resolve the weather from the clutter echo. A relatively large Nyquist interval is also needed so that the weather echo can be resolved (see Figure 7.6). The spectral widths of ground clutter and weather echo are generally much less than 0.5 m s^{-1} and generally greater than 1 m s^{-1}, respectively. Therefore, Nyquist intervals of about 8 m s^{-1} are needed. Clutter is generally stationary and is identified as a narrow spike at zero velocity in the spectral representation (Figure 7.6). The spike has finite width because the ground echo targets, such as swaying trees, have some associated motion.
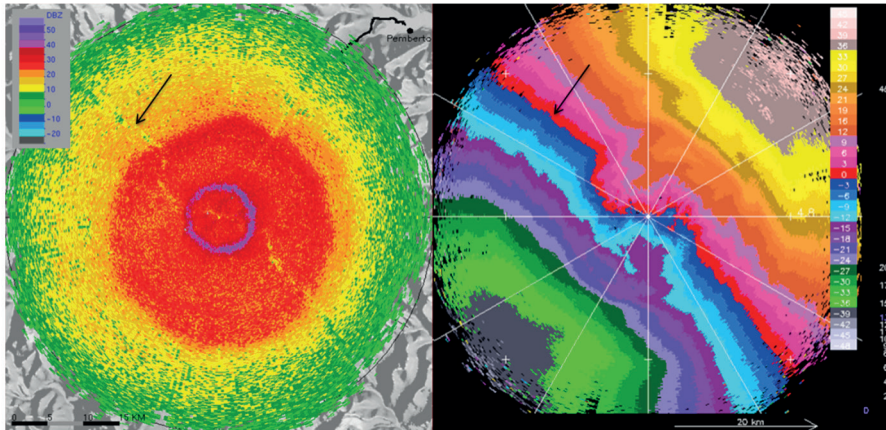
Figure 7.9. Doppler notch filtering can remove too much echo when the Doppler spectrum of the weather echo is narrow and near the zero Doppler velocity (see arrow). This problem is minor compared to other artefacts illustrated in Figure 7.2.

Time domain processing to remove the zero velocity component of a finite sequence is done with a high-pass digital filter. A width and depth of the digital filter to match the clutter must be assumed for the whole scanning domain, and mismatches are inevitable as the clutter varies (Zrnić and Hamidi, 1981). Adaptive spectral (Fourier transform) processing identifies the ground clutter echo, heuristically determines the clutter echo and removes the ground clutter power from the total power, thereby separating ground clutter from the weather echoes even if they are overlapped (Passarelli et al., 1981; Crozier et al., 1991; Figure 7.7). It can be difficult to separate the weather from the clutter echo when the weather echo is narrow (as in light snow situations) and the mean Doppler velocity is near zero. In this situation, too much weather echo can be removed. When the weather echo spectrum is narrow as in the case of snow or drizzle, the zero notch filter cannot distinguish the weather from the ground clutter. This is particularly true when the antenna spins fast, causing the ground echo spectrum to broaden, and when the mean radial velocity of the weather is near zero. Too much power is removed and results in an anomalous depression in reflectivity (Figure 7.9, left image). The arrow shows where the depressed echo corresponds to the zero line in the radial velocity image (Figure 7.9, right image). This is a minor drawback to Doppler notch filtering.

Improvements to the clutter echo identification include better techniques to identify the clutter echo (Gaussian model adaptive processing) and techniques to use texture of the data (variance of the reflectivity) associated with clutter before applying the clutter filters (Hubbert et al., 2009*a*; Hubbert et al., 2009*b*). Systems without Doppler could employ these texture techniques to remove ground clutter and anomalous propagation echoes.

An alternative approach, called micro-clutter removal, takes advantage of the observation that structures contributing to ground clutter are very small in scale (less than, for example, 100 m). Range sampling is carried out at a very fine resolution (less than 100 m) and clutter is identified using reflectivity and Doppler signal processing. Range averaging (to a final resolution of 1 km) is performed with clutter-free range bins. The philosophy is to detect and ignore range bins with clutter, rather than to correct for the clutter (Joss and Lee, 1993; Lee et al., 1995). This is radically different from the previously discussed techniques and it remains to be seen whether the technique will be effective in all situations, in particular in anomalous propagation situations where the clutter is widespread.

Polarization radars can also identify ground clutter since the ground clutter has different polarimetric features as compared to precipitation. In addition, other kinds of clutter targets can be identified.

Clutter can be reduced by careful site selection (see below). Radars used for long-range surveillance, such as for tropical cyclones or in a widely scattered network, are usually placed on

hilltops to extend the useful range, and are therefore likely to see many clutter echoes. A simple suppression technique is to scan automatically at several elevations, and to discard the data at the shorter ranges from the lower elevations, where most of the clutter exists. By processing the radar data into constant altitude plan position indicator (CAPPI) products, low elevation data are rejected automatically at short ranges (Marshall and Ballantyne, 1978). Figure 7.4 shows a geometric scan sequence proposed by Marshall and Ballantyne (1978) that is optimized to produce constant height products such as the CAPPI and echo top.

7.5.4   **Overcoming the Doppler dilemma**

The Nyquist interval and sampling govern the quality of the Doppler velocity estimates. The Nyquist interval (±180°) must be sufficiently large to span the spectrum of the weather echo. Typically, the weather echo usually has a 4–6 m s^{-1} width and so the Nyquist interval must be at least twice as wide. The tails of the spectrum may be aliased, but if the signal is strong the mean velocity can still be estimated.

In order to provide a statistically stable velocity estimate about 20–30 samples are required. These samples need to be correlated, so they need to be made quickly. Note that this is fewer than for reflectivity, and in theory, it is possible to recover velocity at lower signal-to-noise ratios (weaker signal strength) than reflectivity and in a shorter period of time.

To detect returns at various ranges from the radar, the echoes should be sampled periodically, usually about every 1 μs, to obtain information about every 150 m in range. This sampling can continue until it is time to transmit the next pulse (at about every 1 ms). A sample point in time (corresponding to a distance from the radar) is called a range gate. The interval between transmit pulses governs the maximum unambiguous range. The wavelength combined with the transmit interval governs the maximum unambiguous velocity. For weather radar wavelengths and weather scenarios, these maxima are in conflict and this is called the Doppler dilemma, as increasing one results in reducing the other. This is shown in Figure 7.5. So, a fundamental problem with the use of any pulse Doppler radar is to mitigate the impacts of limited range and velocity.

Common techniques to mitigate the velocity limitation or to de-alias the velocities include multiple PRF techniques (Doviak and Zrnić, 1993; Crozier et al., 1991) or continuity techniques (Eilts and Smith, 1990). In the former, radial velocity estimates are collected at two or more different PRFs with different maximum unambiguous velocities and are combined to yield a new estimate of the radial velocity with an extended unambiguous velocity. For example, a C band radar using PRFs of 1 200 and 900 Hz has nominal unambiguous velocities of 16 and 12 m s^{-1}, respectively. The amount of aliasing can be deduced from the difference between the two velocity estimates to de-alias the velocity to an extended Nyquist velocity range of ±48 m s^{-1}. Figure 7.10 shows how the dual-PRF technique is able to extend the unambiguous velocity. The top graph shows what the Doppler radar is able to measure as a function of true radial velocity (–48 to 48 m s^{-1}). In this example, the PRFs are in 4:3 ratio; other ratios such as 7:5 and 3:2 are possible. The bottom graph represents the unique difference in the measured Doppler velocities as a function of true radial velocity. From this difference, the fold number can be determined and the true velocity can be retrieved. The limit of the retrieval is determined by the unambiguous Nyquist velocities and their ratio. This limit is called the extended Nyquist velocity and is 48 m s^{-1} in this case. Figure 7.11 shows an example of the results of this technique.

Combinations of PRF ratios commonly in use are 5:4, 4:3 or 3:2. The maximum unambiguous velocity commonly used is 16 m s^{-1}, though it is not a strict requirement. Lower velocities would result in larger maximum ranges. The difference in the use of the various ratios is that the variance in the mean velocity results in the uniform velocity assumption being violated and dual-PRF errors arising (Joe and May, 2003).

Continuity techniques rely on having sufficient echo to discern that there are aliased velocities and correcting them by assuming velocity continuity (no discontinuities of greater than $2V_{max}$).
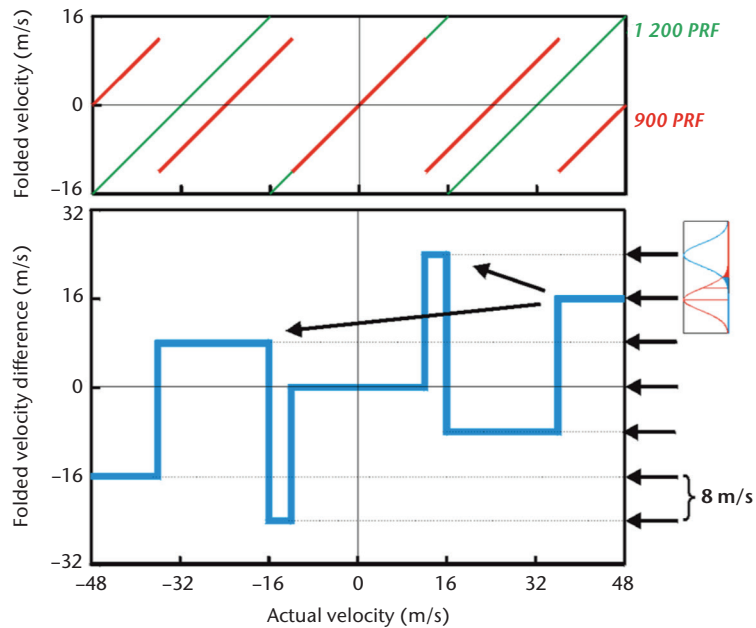
Figure 7.10. This is an example of a C band radar pulsing at 900 and 1 200 s⁻¹ with unambiguous Nyquist velocities of 12 and 16 m s⁻¹, respectively. The technique relies on the difference between measured radial velocities (ordinate on the bottom image) to determine the fold number (abscissa on the bottom image) and then use that with the corresponding measured radial velocity to estimate the true radial velocity.

Fold numbers are determined starting at the zero line, and whenever a discontinuity of a Nyquist interval is encountered, the fold number is increased or decreased and the Nyquist interval is added or subtracted.

The second fundamental problem is the range limitation imposed by the use of high PRFs (greater than about 1 000 Hz). Echoes beyond the maximum range will be aliased back into the primary range. For radars with coherent transmitters (e.g. klystron or solid state), the echoes will appear within the primary range. For coherent-on-receive systems, the second-trip echoes will appear as noise (Joe et al., 1995; Passarelli et al., 1981; Figure 7.12). For the latter system, the noise
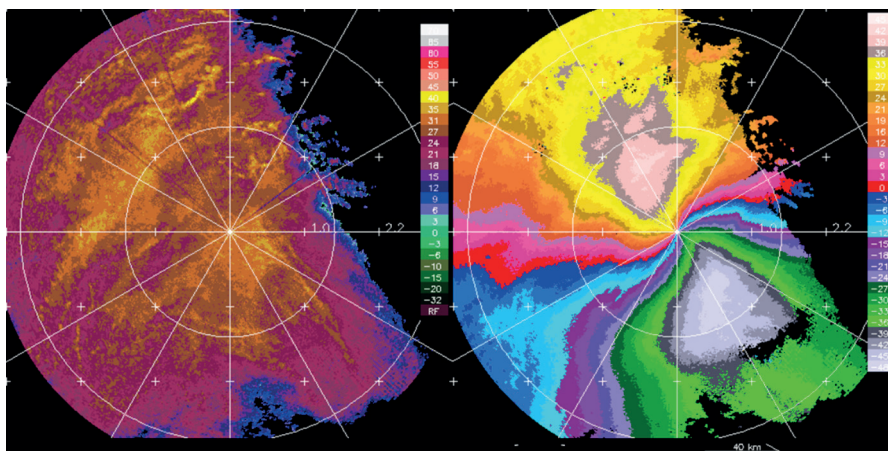
Figure 7.11. This figure illustrates the necessity and ability of a C band radar to extend the velocity out to at least 48 m s⁻¹. This is a case of a hurricane/extratropical transition passage and velocities are near 48 m s⁻¹. In this situation, the assumptions of the dual-PRF technique (the two measured estimates at different PRFs are from the same radial velocity) are satisfied and the result has little noise (right image, compare with Figure 7.20).
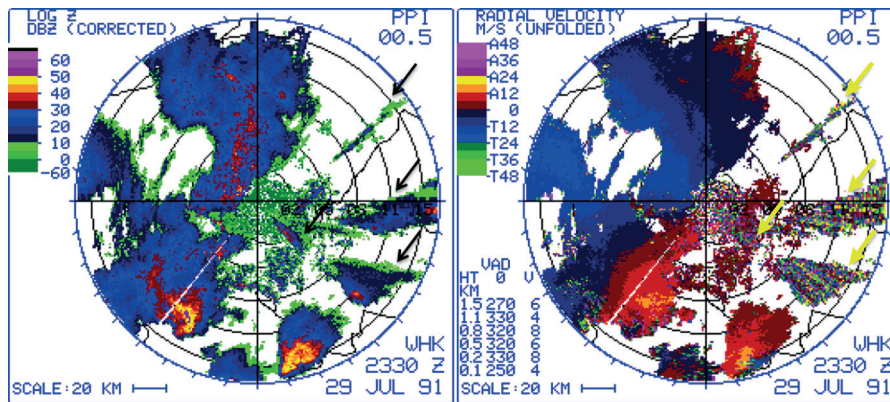
Figure 7.12. An example of second-trip echoes in reflectivity (left) and radial velocity (right) for a magnetron radar

is a result of the randomly transmitted phases. Doppler radars with their short Nyquist range are contaminated with second-trip echoes, regardless of whether they are coherent-on-receive (magnetron) or coherent-on-transmit (klystron) type. In Figure 7.12, from a C band magnetron radar, the second trip reveals itself as wedge-shaped echoes in reflectivity (black arrows) and this can be used to identify them. In the radial velocity field, the data are noisy (yellow arrows) and this can be used in the signal-processing stage to eliminate them as their Doppler spectrum is very broad, elevating the noise level. If these data were taken with a klystron radar, the radial velocity would appear as coherent data.

Phase coding techniques have been developed to distinguish the second-trip echoes for coherent Doppler radars. Processing can be done with respect to the current pulse for the first-trip echo and the previous pulse for the second-trip echo. This is called random phase processing. It is effective if the sensitivity of the radar is good (low) so that the second-trip echo can be detected above noise and if the phase stability is good (low) so that the phase or velocity can be recovered at long ranges. For coherent transmitters, a pseudo-random sequence can be generated. Better still is to modulate the phase in a known way to precisely separate the first from the second trip. Frush et al. (2002) developed this technique for klystron systems.

In a coherent-on-receive (e.g. magnetron) system, the phase variation is implicitly random. In a coherent-on-transmit (e.g. klystron) system, the phase variation is imposed by the modulator in a controlled fashion. An example is the SZ-2 phase modulation used in the US WSR-88D system. The two examples in Figure 7.13 (a–d, e–h) are shown to illustrate the benefits and limitations of the random phase technique. Images 7.13(a) and 7.13(e) are taken with low PRF and represent the "truth". Images 7.13(b) and 7.13(f) are retrieved from the random phase technique. The demarcation of the first–second trip boundary is indicated by the white arrow. The gap is because the receiver is turned off while the pulse is being transmitted. In images 7.13(a–d), a squall line has not reached the radar. The echoes near the radar are weak relative to those at far ranges and the technique works well as most of the second trip is recovered (compare 7.13(a) with 7.13(b)). In images 7.13(e–h), part of the precipitation system has reached the radar and so there are relatively strong echoes near the radar relative to those at far ranges. The technique works less well as there are significant amounts of the second trip that are not recovered (compare 7.13(e) with 7.13(f)). In this implementation of the technique, only single PRF data is possible and the Nyquist is 16 m s^{-1} (images 7.13(c) and 7.13(g)). The dual-PRF data with an extended Nyquist range of 48 m s^{-1} are shown in images 7.13(d) and 7.13(h). While aliased, the single PRF data can still be interpreted and effectively used by a well-trained analyst. For example, a "bookend vortex" can be observed in image 7.13(c) (white and black arrows). The corresponding reflectivity images are the inner (first trip) portions of images 7.13(b) and 7.13(f). An important aspect of random phase processing is that the first trip will have higher data quality as the impacts of the second-trip echo are filtered.
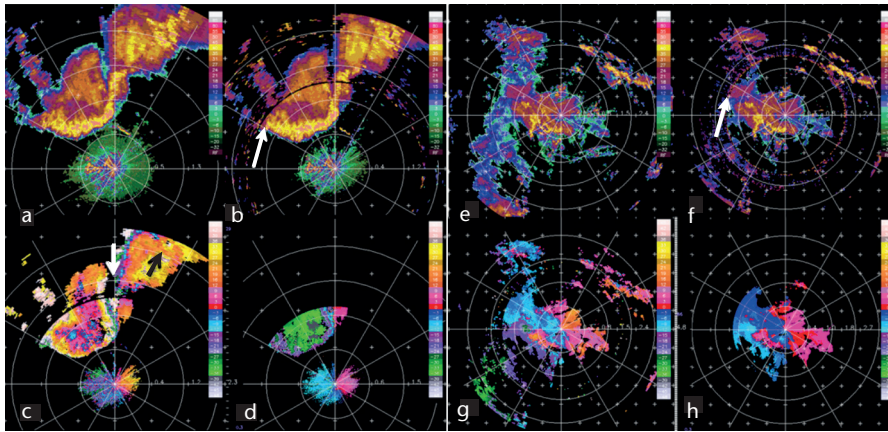
Figure 7.13. Example of random phase range extension: the example on the left (a–d) shows a situation where the first-trip echo is weak and much of the second-trip echo is recoverable. In the example on the right (e–h), there is significant first-trip echo which precludes recovering the second-trip echo.

An earlier technique uses a surveillance scan with low PRF to determine the location of the reflectivity echo. Then when overlapping echoes are encountered in the shorter range Doppler mode, the echo power and velocity are assigned to the location with the greater power (Figure 7.14). This works if the power is significantly different (> 5 dB). A long-range surveillance scan is used to locate the reflectivity echo. A short-range Doppler scan is used to measure the Doppler or radial velocity. The radial velocity is assigned to the reflectivity echo with the greatest power. If the powers are within 5 dB of each other, the technique does not work well and the radial velocity data are not recovered and are designated as range folded. They are marked as white in Figure 7.14. Some colour schemes are employed that mark these echoes as purple and so this is often called purple haze.

A combination of multiple PRF and phase diversity techniques can be used to mitigate both problems simultaneously (WMO, 2012; Yamauchi et al., 2013).
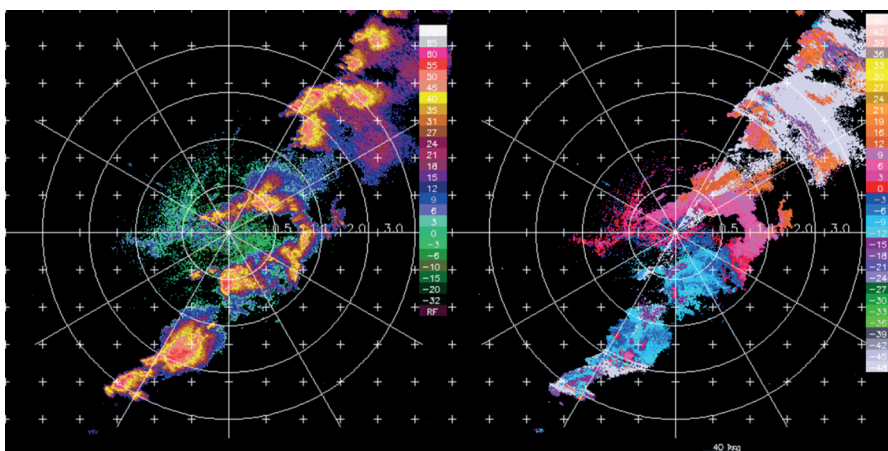
Figure 7.14. Without the advanced phase coded signal processing, multiple PRF techniques are used to recover the second trip. Low PRF scans with long-range capability are used to locate the reflectivity echo. High PRF but short-range scans are used to measure radial velocity. The radial velocity is assigned to the range bin with the highest power.

7.6   **OPTIMIZING RADAR CHARACTERISTICS**

7.6.1   **Selecting a radar**

A radar is a highly effective observation system. However, the application, the climatology, the local environment (blockage) and the network design determine the effectiveness of any particular radar or radar system. Everything about radar is a trade-off. No single radar can be designed to be the most effective for all applications. Characteristics can be selected to maximize the proficiency to best suit a few applications, such as tornado detection or snow squall detection, but not all applications (compared with long-range surveillance). Cost is a significant consideration. Much of the interdependence can be referenced to the radar range equation.

An important consideration is the radar network design and the application. Networks of X band radars are being proposed for a variety of local applications where the range requirement is of the order of 50 km or less and where low-level coverage is critical – as in low-level snow squall, tornado detection, microburst detection, complex terrain (mountainous), urban hydrology and perhaps wind turbine mitigation. The original intention of these networks was for adaptive sensing of the atmosphere for multiple applications – from weather to air traffic control. This is accomplished in conjunction with phased array antennas that have pointing agility and can scan in a cooperative fashion (McLaughlin et al., 2009). An innovation of this technology is the low requirements in terms of infrastructure of the phased array antenna that can be mounted on a side of a building or on an existing tower.

7.6.2   **Wavelength and beam width**

The larger the wavelength, the greater the cost of the radar system, particularly antenna costs for comparable beam widths (i.e. resolution). This is due both to an increase in the amount of material and to the difficulty in meeting tolerances over a greater size. Within the bands of interest for weather radars (S, C and X), the sensitivity of the radar or its ability to detect a target is strongly dependent on the wavelength. However, this dependence is pragmatically mitigated by transmit power. It is also significantly related to antenna size, which impacts gain, beam width and beam filling. Smaller wavelength radars (35 GHz and 94 GHz) are becoming available for specialized applications, such as fog or cloud detection, or used from space-based platforms for cloud or precipitation measurements (e.g. Tropical Rainfall Measuring Mission (TRMM); Global Precipitation Measurement (GPM); CloudSat; and Earth Clouds, Aerosols and Radiation Explorer (EarthCARE)).

Considerations of Doppler range within a radar network have a great impact on the wavelength chosen. For the same Nyquist velocity, an S band will have twice the Nyquist range compared to a C band radar and hence have a significant impact on unambiguous coverage. This may be mitigated with the velocity and range extension techniques discussed earlier.

Radar rays are attenuated most significantly in rain, less in snow and ice, and even less in clouds and atmospheric gases. In broad terms, attenuation at the S band is relatively small. The S band radar, despite its cost, is essential for penetrating the very high reflectivities in mid-latitude and subtropical severe storms with wet hail. X band radars can be subject to severe attenuation over short distances.

The great disadvantage is that smaller wavelengths have much larger attenuation. It remains to be seen whether the dual-polarization K_{DP} techniques can compensate for the attenuation until total attenuation occurs (which is very infrequent) and whether ignoring attenuation at S band is justified. If K_{DP} techniques prove to be superior for precipitation estimation than reflectivity techniques, the smaller wavelength is more sensitive to attenuation and so may be more effective.

The radar signal may be totally lost at C and X band, particularly if the radome is wet. While this may seem disastrous, the key question is whether the loss of signal (typically for tens of minutes

for propagating storms) results in actual missed severe storm warnings or missed flash flooding. Experience indicates that warnings will have usually been already issued and the loss of one or two data points for hydrological purpose is not a devastating situation.

7.6.3 Transmitters and transmit power

Target detectability is directly related to the peak power output of the radar pulse. However, there are practical limits to the amount of power output that is dictated by power tube technology. Unlimited increases in power are not the most effective means of increasing the target detectability. For example, doubling the power only increases the system sensitivity by 3 dB. Technically, the maximum possible power output increases with wavelength and pulse width. Improvements in sampling, receiver sensitivity, antenna gain, pulse width or choice of wavelength may be better means of increasing detection capability.

Magnetrons and klystrons are common power sources. Magnetrons cost less but are power oscillators and so they are less stable in frequency. Many Doppler radars today are based on magnetrons, and with co-axial magnetrons and digital technology, the phase noise of these systems can be comparable to that of klystron systems. Smaller phase noise results in greater capability for clutter rejection (Figure 7.15). Phase noise of less than 0.5° is a minimum performance level of modern radars. At normal operating wavelengths, conventional radars should detect rainfall intensities of the order of 0.1 mm h^{-1} at 200 km and have peak power outputs of the order of 250 kW and 1 000 kW or greater in the C band and S band, respectively.

Solid state transmitters have recently been deployed operationally. They have the promise of reduced maintenance with the high reliability of solid state technology, excellent phase stability and electronic stability for dual-polarization measurements. Solid state transmitters are typically low power and require multiple long pulse lengths and pulse compression to attain the required sensitivities. They are a combination of pulse and frequency-modulated continuous wave radars. Range side lobes are an issue with pulse compression modulation schemes and it remains to be seen whether they are significant in the weather application.

7.6.4 Pulse length

The pulse length determines the target resolving power of the radar in range. The range resolution or the ability of the radar to distinguish between two discrete targets is proportional
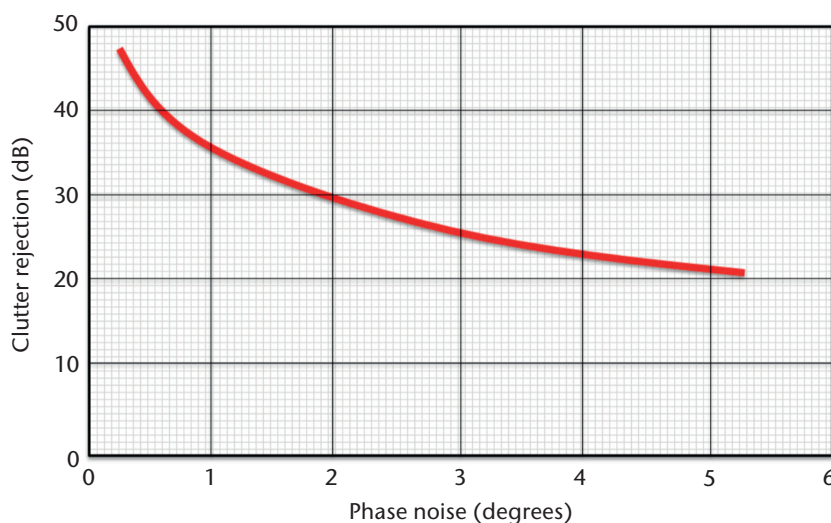
Figure 7.15. Coherency (phase noise) is a measure of the quality of a Doppler radar and is directly related to the ability to remove ground clutter and retrieve second-trip echoes using phase coding techniques.

to the half pulse length in space. For most klystrons and magnetrons, the maximum ratio of pulse width to PRF is about 0.001. Common pulse lengths are in the range of 0.3 to 4 μs. A pulse length of 2 μs has a resolving power of 300 m, and a pulse of 0.5 μs can resolve 75 m.

Assuming that the pulse volume is filled with target, doubling the pulse length increases the radar sensitivity by 6 dB with receiver-matched filtering but decreases the resolution; decreasing the pulse length decreases the sensitivity while increasing the resolution. Shorter pulse lengths allow more independent samples of the target to be acquired in range and the potential for increased accuracy of estimate.

7.6.5　　Pulse repetition frequency

The PRF should be as high as practical to obtain the maximum number of target measurements per unit time. A primary limitation of the PRF is the unwanted detection of second-trip echoes. Most reflectivity-only radars have unambiguous ranges beyond the useful range of weather observation by the radar. An important limit on weather target useful range is the substantial height of the beam above the Earth even at ranges of 250 km.

For Doppler radar systems, high PRFs (~1 200 s^{-1}) are used to increase the Doppler unambiguous velocity measurement limit. This results in the Doppler dilemma, where there is a trade-off between maximum range and maximum velocity. The PRF factor is not a significant cost consideration but has a strong bearing on system performance. Briefly, high PRFs are desirable to increase the number of samples measured, to increase the maximum unambiguous velocity that can be measured, and to allow higher permissible scan rates. Low PRFs (~300 s^{-1}) are desirable to increase the maximum unambiguous range that can be measured, and to provide a lower duty cycle.

7.6.6　　The antenna subsystem

Weather radars normally use a horn fed antenna with a parabolic reflector to produce a focused narrow conical beam. Three important considerations are the beam width (angular resolution), the antenna gain and the side lobes. For common weather radars, the size of the antenna increases with wavelength for a fixed beam width and with the narrowness of the beam required. A common target for weather radar antenna beam width is 1°, though there is inherently nothing special about this number.

Phased array antenna technologies are being explored in research and are now commercially available at X band at an affordable price. These antennas consist of phase controllable radiating elements that form the beam. Adaptable target specific or dependent scan strategies can be developed such that rapid scan or high-quality data requirements can be simultaneously satisfied in theory, but this is still to be demonstrated in operations. Ground clutter rejection may be superior as these systems do not scan but essentially momentarily stare at each radial and so the beam smearing of the ground clutter echo does not occur.

Antenna size and beam width

Weather radars normally have beam widths in the range of 0.5° to 2.0°. For a 0.5° and 1.0° beam at a C band wavelength, the antenna reflector diameter is at least 7.1 and 3.6 m, respectively; at S band it is 14.3 and 7.2 m. The cost of the antenna system and pedestal increases more than linearly with reflector size. There is also an engineering and cost limit. The tower must also be appropriately chosen to support the weight of the antenna.

The desirability of having a narrow beam to maximize the resolution and enhance the possibility of having the beam filled with target is particularly critical for the longer ranges. For a 0.5° beam, the azimuthal (and vertical) cross-beam widths at 50, 100 and 200 km range are 0.4, 0.9 and 1.7 km, respectively. For a 1.0° beam, the widths are 0.9, 1.7 and 3.5 km. Even with these relatively narrow beams, the beam width at the longer ranges is substantially large.

The gain of the antenna is also inversely proportional to the beam width and thus the narrower beams also enhance system sensitivity by a factor equal to differential gain. The estimates of reflectivity and precipitation require a nominal minimal number of target hits to provide an acceptable measurement accuracy. The beam must therefore have a reasonable dwell time on the target in a rotating scanning mode of operation. Thus, there are limits to the antenna rotation speed. Scanning cycles cannot be decreased without consequences. For meaningful measurements of distributed targets, the particles must have sufficient time to change their position before an independent estimate can be made. Systems generally scan at the speed range of about 0.5 to 6 rpm.

Most single polarization weather radars are linearly polarized, with the direction of the electric field vector transmitted being horizontal and sometimes vertical. Reasons for favouring horizontal polarization include: (a) sea and ground echoes are generally less with horizontal polarization; (b) lesser side lobes in the horizontal provide more accurate measurements in the vertical; and (c) there is greater backscatter from rain due to the drop ellipticity. However, at low elevation angles, better reflection of horizontally polarized waves from plane ground surfaces may produce an unwanted range-dependent effect.

Most if not all operational dual-polarization radar employ the STAR mode of transmission, with equal amount of power at two orthogonal linear polarizations (typically horizontal and vertical). This eliminates the need for a high-power, high failure polarization switch.

7.6.7 Illumination

Side lobes are an inherent property of any antenna. Side lobes also include the sides of the main lobe. The beam width is usually defined as the half power points of the main beam and there is power at angular distances away from the main beam. A major contributor to the side lobes is the feed horn and the struts supporting the feed horn. Side lobes may be mitigated by over-illuminating the dish; however, this results in a broader beam and less sensitivity.

In summary, a narrow beam width affects system sensitivity, detectability, horizontal and vertical resolution, effective range and measurement accuracy. The drawback of small beam width is mainly cost. For these reasons, the smallest affordable beam width has proven to improve greatly the utility of the radar (Crozier et al., 1991).

7.6.8 Typical weather radar characteristics

The characteristics of typical radars used in general weather applications are given in Table 7.7.

As discussed, the radar characteristics and parameters are interdependent. The technical limits on the radar components and the availability of manufactured components are important considerations in the design of radar systems.

The Z-only radars are non-coherent pulsed radars that have been in use for decades. The Doppler radars are de rigueur and add a new dimension to the observations. They provide estimates of radial velocity. Specialized Doppler radars have been developed for better detection of small-scale microbursts and tornadoes over very limited areas, such as for air-terminal protection. Dual-polarization radars are deployed and applications for data quality, target classification and quantitative precipitation estimation are finding their way into operations – including in hydrology, numerical weather prediction, and climate change studies.

Table 7.7. Specifications of typical meteorological radars

Type	S	S	S	S	C	C	C	C	C	X
Frequency (GHz)	2 800–3 000	2 700–3 000	2 700–3 000	2 700–3 000	5 400–5 900	5 600–5 650	5 600–5 650	5 500–5 700	5 300–5 850	9 300–9 500
Wavelength (cm)	10.7	10.7	10.7	10.7	5.3	5.3	5.3	5.3	5.3	3
Peak power (kW) per channel	475	850	750	20	500	1 000	250	250	12	75
Pulse lengths (μs)	1.57, 4.5	0.2–2.0	0.4–4.5	0.5–200	0.2–3.0	0.4–4.5	0.4–4.5		0.5–200	0.3–3.3
PRF (/s)	318–1 403, 318–452	200–2 400	250–2 000	100–20 000	200–2 400	200–2 400	250–2 000		100–20 000	250–3 000
Min dBZ at 50 km	–28.7	–15.5		–5.5	–17.5	–19.5		–15	–5	
MDS (dBm)	–113	–114	–114	–114	–114	–114	–114	–115	–114	–113
Receiver dynamic range (dB)		105	115	110	105	105	115	99	110	90
Antenna diameter (m)	8.53	8.5	8.5	8.5	4.2	4.2	4.2	4.5	4.2	2.4
Beam width (degrees)	1	0.95	1	0.95	0.95	0.95	1	1	0.95	1.05
Gain (dB)	45	45	44.5	45	45	45	44.5	45	45	44.5
Polarization	Horizontal	STAR	STAR	STAR	Dual linear	Dual linear	Dual linear	Dual linear	STAR	Dual linear
Max rotation rate (rpm)	6	10	6	6	10	10	8	6.7	6	6
Transmitter type	Klystron	Co-axial magnetron	Klystron	Solid state	Co-axial magnetron	Klystron	Klystron	Co-axial magnetron	Solid state	Co-axial magnetron
Clutter suppression	50	46	55	55	46	46	55	55	55	

7.6.9 Radar volume scan strategy

Most modern radars automatically perform a volume scan consisting of a number of full azimuth rotations of the antenna at several elevation angles. This is called the scan strategy and there are a variety of strategies for different purposes (Marshall and Ballantyne, 1978; Brown et al., 2005; Crum and Alberty, 1993; Germann et al., 2006a, Seltmann et al., 2013).

Long-range scans of 500 km or more (that result in limited Nyquist velocity) are needed for long-range surveillance. Rapid update of the order of 5 min is required to capture the evolving morphology of the convective thunderstorm. In aviation downburst applications, even shorter cycle times are required (Michelson et al., 1990). Research radars scan limited areas or sectors with 1 min or less cycle times (Wurman et al., 1996). Slow low-level scans with long pulse lengths are needed to maximize the capture of clear air echoes. Slow scanning will optimize the Doppler filtering of ground echoes. Multiple PRF techniques require the assumption of uniformity of radial velocity and can be implemented on a ray by ray or scan by scan basis.

Scans as low in elevation as possible are needed for optimizing the retrieval of quantitative precipitation estimates and also to optimize the detection of low-level and shallow weather. A geometric sequence of elevation angles are required to generate optimal CAPPI or echo top products (Marshall and Ballantyne, 1978). The emerging X band phased array radar networks, such as that of the Collaborative Adaptive Sensing of the Atmosphere (CASA) project or the Multifunction Phased Array Radar (MPAR) project, are revolutionizing the scan strategy concept as the electronic scanning can adapt to the weather or application (McLaughlin et al., 2009; Weber et al., 2007), or weaknesses may be mitigated with data from neighbouring radars.

The trade-off is the quality of the data. For example, slow scans for high spectral resolution for ground clutter mitigation or low data variance preclude scan strategies with very many elevation angles and hence result in poor vertical resolution. Data quality is a nebulous concept as it qualitatively refers to trade-offs in timeliness or temporal resolution (cycle time), spatial resolution (azimuth, range, elevation), data bias (velocity or reflectivity bias) and data variance. This is difficult to objectively optimize as the success metrics are quite diverse and setting the number of elevation angle sequence is not an exact science.

Of prime consideration is the nature of the weather and the location that requires the coverage. For example, the scan sequence for a radar located in a valley used for local and short-range application will or can be quite different from a radar that is used for long-range surveillance for land-falling hurricanes (Joe et al., 2014).

While it is attractive conceptually to set the elevation angle changes equal to the beam width, small changes in the elevation angle of even 0.1° degrees can produce significant views of the data, due to the stratified nature of the precipitation (snow, bright band, rain profiles) and the wind profile.

Raw polar data are stored in a three (range, azimuth, elevation) or multiple (radar parameter) dimensional array, commonly called the volume scan. This serves as the data source for further data processing and archiving. There can be several versions of raw data due to different data quality processing.

7.6.10 Radar performance

Minimum detectable signal

The minimum detectable signal (MDS) is a performance measure of the aggregate of the transmit power, antenna size, beam width or gain, pulse length, wavelength and other factors. This is often described in power units or system noise temperature. However, for a radar analyst, reflectivity at a fixed range provides a more intuitive measure of the performance of a radar. High sensitivity is highly desired in order to detect clear air echoes and light precipitation and to enhance the retrieval of second-trip echoes. Table 7.8 shows some MDS of typical high-performance radars.

Phase stability

Phase stability or phase jitter is a measure of the average change of phase from pulse to pulse. Some radar test software can provide this measurement using an acoustic delay line or from external targets. The advantage of the latter is that it tests the stability at different ranges or time delays and the entire processing change. Good phase stability (< 0.5°) results in better velocity estimation, ground clutter rejection and better second-trip retrieval with magnetron systems.

Cross-polar correlation and *ZDR*

A measure of the quality of a dual-polarization radar is the cross-polar correlation (ρ_{HV}). If the radar is pointed at light rain or drizzle that is generally uniformly round, the correlation should be very close to 1.0. Good radars report values typically of 0.995 or better. This indicates that the dual polarization is very good and well configured.

If vertical scans are performed during stratiform conditions, the Z_{DR} values should be 0 and have no azimuthal dependence.

7.7 MAINTENANCE AND CALIBRATION

Radar is arguably the most complex of instruments that a meteorological service or service provider must service and maintain. It requires a very high level of training and skill development. Maintenance is critical to keeping the radar operating, and calibration is critical to the quality of the data. Both should follow the manufacturer's prescribed procedures. The following is an outline.

7.7.1 Maintenance

Modern radars, if properly installed and operated, should not be subject to frequent failures. Some manufacturers claim that their radars have a mean time between failures (MTBF) of the order of a year. However, these claims are often optimistic and the realization of the MTBF requires scheduled preventive maintenance. A routine maintenance plan and sufficient technical staff are necessary in order to minimize repair time. Mechanical and electronic failures are the most prevalent (Sireci et al., 2010; Figure 7.16).

It should be noted that factors external to the radar can result in data not reaching the users. These include failures or poor quality of the main power, or there may be too many spikes or fluctuations in the power. The power grid may fail due to lightning or other reasons. Telecommunications may fail. Air conditioning systems may fail and result in the shutdown of sensitive electronic systems.

Table 7.8. Minimum detectable signal of typical high-performance radars

Radar	MDS at 50 km
Z9110	–8.0 dBZ (few days in August) –10.0 dBZ (2 months)
Z9220	–1.0 dBZ
King City CONVOL (2 μs)	–11.0 dBZ
King City DOPVOL (0.5 μs)	–5.0 dBZ
Twin Lakes, OK	–7.5 dBZ
Lake Charles, LA	–8.5 dBZ
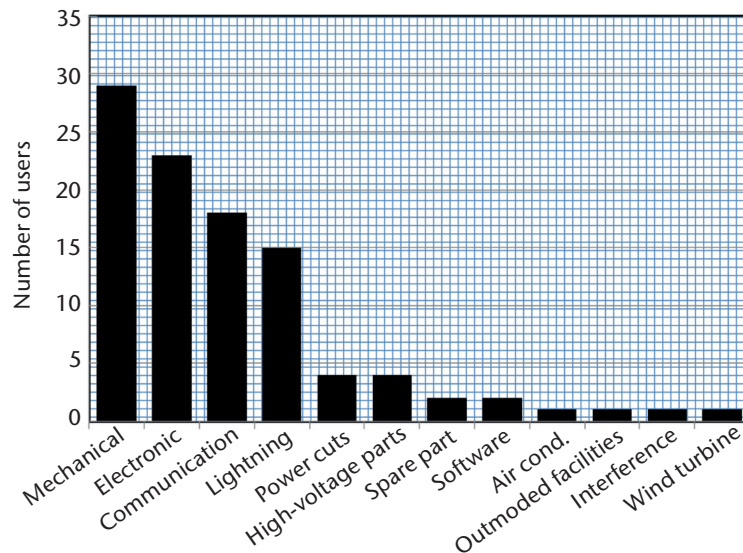
Figure 7.16. Results from the WMO weather radar survey showing the main failure modes of a radar (Sireci et al, 2010); figure courtesy of Oguzhan Sireci of the Turkish State Meteorological Service.

Preventive maintenance should include at least a quarterly check of all radar parts subject to wear, such as gears, motors, fans and infrastructures. The results of the checks should be written in a radar logbook by local maintenance staff and, when appropriate, sent to the central maintenance facility. When there are many radars, there might be a centralized logistic supply facility and a repair workshop. The latter receives failed parts from the radars, repairs them and passes them on to logistics for storage as stock parts, to be used as needed in the field. Basic record keeping is a must.

For corrective maintenance, the Service should be sufficiently equipped with the following:

(a) Spare parts for all of the most sensitive and long lead item components, such as tubes, solid state components, boards, chassis, motors, gears, power supplies and so forth. Experience shows that it is desirable to have 30% of the initial radar investment in critical spare parts on the site. If there are many radars, this percentage may be lowered to about 20%, with a suitable distribution between central and local maintenance;

(b) Test equipment, including the calibration equipment mentioned above. Typically, this would amount to approximately 15% of the radar value;

(c) Well-trained personnel capable of identifying problems and making repairs rapidly and efficiently are critical.

Competent maintenance organization should result in radar availability 96% of the time on a yearly basis, with standard equipment. Better performances are possible at a higher cost.

Recommended minimum equipment for calibration and maintenance includes the following:

(a) Microwave signal generator;

(b) Microwave power meter;

(c) MHz oscilloscope;

(d) Microwave frequency meter;

(e) Standard gain horns;

(f)　　Intermediate frequency signal generator;

(g)　　Microwave components, including loads, couplers, attenuators, connectors, cables, adapters, and so on;

(h)　　Versatile microwave spectrum analyser at the central facility;

(i)　　Standard electrical and mechanical tools and equipment.

7.7.2　　Calibration

Ideally, the complete calibration of reflectivity uses an external target of known radar reflectivity factor, such as a metal-coated sphere. The concept is to check if the antenna and waveguides have their nominal characteristics. However, this method is very rarely used because of the practical difficulties in flying a sphere and multiple ground reflections, as well as the time and skill required (Brunkow, 2001).

A standard procedure is to use the sun as a calibration source for power and pointing accuracy. The sun is a microwave source and appears as a disk of about 0.5 degrees (Tapping, 2001). However, by maximizing the power, greater precision can be achieved. Beam propagation effects may affect low elevation angles and so higher angles are often used for solar calibration. Repeated measurements will statistically improve the precision of the results. It should be noted that antenna elevation pointing accuracy and precision may be a function of angle and so a variety of angles should be measured.

Routine electronic calibration generally ignores the antenna but includes the waveguide and transmitter receiver system. Typically, the following actions are prescribed:

(a)　　Measurement of emitted power and waveform in the proper frequency band;

(b)　　Verification of transmitted frequency and frequency spectrum, out-of-band power should be filtered;

(c)　　Injection of a known microwave signal before the receiver stage, in order to check if the levels of reflectivity indicated by the radar are correctly related to the power of the input;

(d)　　Measurement of the signal-to-noise ratio, which should be within the nominal range according to radar specifications.

If any of these calibration checks indicate any changes or biases, corrective adjustments need to be made.

Doppler calibration includes: the verification and adjustment of phase stability using fixed targets or artificial signals; the scaling of the real and imaginary parts of the complex video; and the testing of the signal processor with known artificially generated signals.

Levelling and elevation are best checked by tracking the position of the sun in receive-only mode and by using available sun location information; otherwise, mechanical levels on the antenna are needed. The presence or absence of echoes from fixed ground targets may also serve as a crude check of azimuthal antenna pointing and transmitter or receiver performance.

Although modern radars are usually equipped with very stable electronic components, calibrations must be performed often enough to guarantee the reliability and accuracy of the data. Calibration must be carried out either by qualified personnel, or by automatic techniques such as online diagnostic and test equipment. In the first case, which requires manpower, calibration should optimally be conducted at least every six months. Emerging systems may be designed to perform this automatically. Simple comparative checks on echo strength and location can be made frequently, using two or more overlapping radars viewing an appropriate target (Zhang et al., 2005).
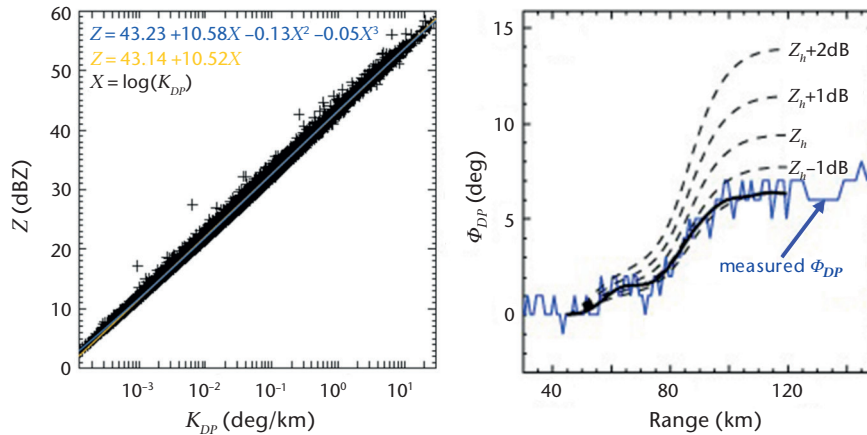
Figure 7.17. There is a close relationship between reflectivity and specific differential phase (Z and K_{DP}). The left figure shows the relationship from disdrometer measurements. The right figure shows one radial of data with significant differential phase. By adjusting the reflectivity and recomputing the differential phase, the radar can be calibrated in a self-consistent manner (figures courtesy of Isztar Zawadzki).

Data techniques such as reflectivity accumulations, probability distributions of reflectivity as a function of range for the minimum detectable signal, transmit–receive cell monitoring, and checking readback and command elevation angles can be used to monitor the health of the radar. Biases in radial velocity accumulations may reveal clutter filtering issues – generally under-filtering which results in biases in radial velocity towards zero (Joe, 2010).

Dual-polarization radars require two receivers that must be matched. Tolerances for all the components need to be tighter since small values are measured. Then, self-consistency and birdbath scans for Z_{DR} nulling can be used to check this. Self-consistency calibration refers to computing Z from K_{DP} using an empirical relationship derived from disdrometer measurements (Figure 7.17) and computed from theoretical formulae. Then, the reflectivity (calibration bias) is adjusted until the K_{DP} derived reflectivity matches the adjusted reflectivity. Given the quality (tightness of the scatter) of the Z–K_{DP} relationship, one could consider using K_{DP} as the dependent parameter for rainfall estimation. If the radar is pointed vertically (the antenna dish appears like a birdbath) in stratiform rain conditions, the Z_{DR} should be zero, and adjustments are needed if it is not. Monitoring the maximum reported ρ_{HV} will provide a check on the overall system performance – good radars should report 0.995 or better.

An innovative technique is the use of the TRMM or GPM space-borne radar for the calibration of ground-based weather radars. It is a single and stable downward-looking instrument that overflies the ground-based weather radars. Comparisons of echo top height, at a fixed and moderately low sensitivity, where attenuation is not significant, are used as the success metric for consistency in cross-radar calibration (Anagnostou et al., 2001).

7.8 RADAR INSTALLATION

7.8.1 Optimum site selection

Optimum site selection for installing a weather radar depends on the intended use. When there is a definite zone that requires storm warnings, the best compromise is usually to locate the equipment at a distance of between 20 and 50 km from the area of interest, and generally upwind of it according to the main storm track. It is recommended that the radar be installed slightly away from the main storm track in order to avoid measurement problems when the storms pass over the radar. At the same time, this should lead to good resolution over the area of interest and permit better advance warning of the coming storms (Leone et al., 1989).
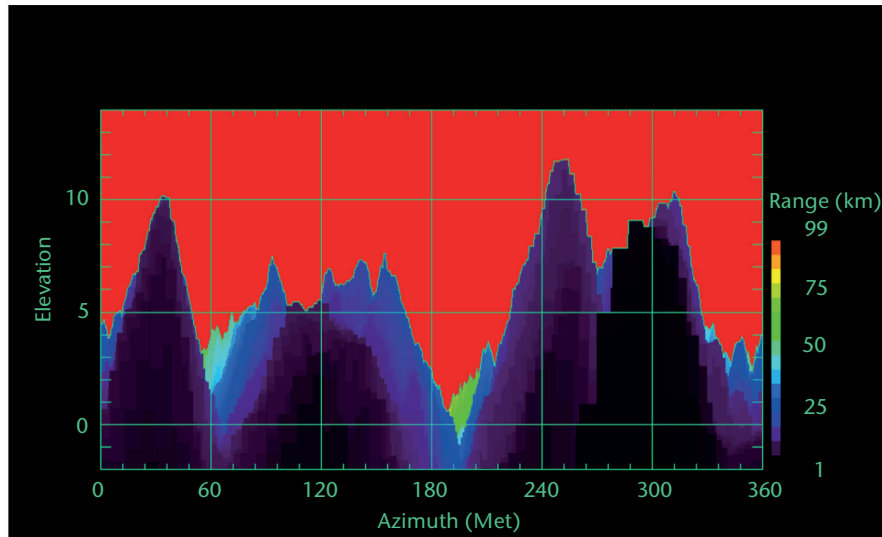
Figure 7.18. Global digital elevation model data are available and sufficiently accurate to be used to assess and help determine the siting of a weather radar. Given an azimuth and elevation, the image indicates the distance in which useful data can be collected.

In the case of a radar network intended primarily for synoptic applications, radars at mid-latitudes should be located at a distance of approximately 150 to 200 km from each other. The distance may be increased at latitudes closer to the Equator, if the radar echoes of interest frequently reach high altitudes. In all cases, narrow-beam radars will yield the best accuracy for precipitation measurements.

The adequacy and availability of digital elevation datasets such as GTOPO30 (https://lta.cr.usgs.gov/GTOPO30), SRTM30 and SRTM03 (http://www2.jpl.nasa.gov/srtm/) have resulted in software applications to help select a site. The basic product is a radar horizon plot where the elevation angle of the horizon, taking into account atmospheric beam propagation, is plotted against radar azimuth angle (Figure 7.18). In this figure, the range to terrain is colour coded as a function of azimuth and elevation angle. The colour indicates the range to which a radar beam (in this case, a 4/3 Earth model is assumed) will collect usable data. This is particularly useful in complex terrain where a radar located in the valley must provide coverage at low levels (in the valley) but with limited range as precipitation changes considerably from mountain crest to mountain valley. For example, the radar can see to 50 or 60 km along the 190° azimuth at elevations of 1° or 2°. This analysis cannot account for trees or artificial towers.

With this plot, the scan angles can be specified for optimal surveillance of the required critical areas. The datasets cannot take into account local blockage due to trees, buildings or towers.

The choice of radar site is influenced by many economic and technical factors as follows:

(a)   The existence of roads for reaching the radar;

(b)   The availability of power and telecommunication links. It is frequently necessary to add commercially available lightning protection devices;

(c)   The cost of land;

(d)   The proximity to a monitoring and maintenance facility;

(e)   Beam blockage obstacles must be avoided. No obstacle should be present at an angle greater than a half beam width above the horizon, or with a horizontal width greater than a half beam width;

(f)   Ground clutter must be avoided as much as possible. For a radar to be used for applications at relatively short range, it is sometimes possible to find, after a careful site inspection and examination of detailed topographic maps, a relatively flat area in a shallow depression, the edges of which would serve as a natural clutter fence for the antenna pattern side lobes with minimum blockage of the main beam. In all cases, the site survey should include a camera and optical theodolite check for potential obstacles. In certain cases, it is useful to employ a mobile radar system for confirming the suitability of the site. On some modern radars, software and hardware are available to greatly suppress ground clutter with minimum rejection of weather echoes (Heiss et al., 1990);

(g)   When the radar is required for long-range surveillance, as may be the case for tropical cyclones or other applications on the coast, it will usually be placed on a hilltop. It will see a great deal of clutter, which may not be so important at long ranges (see section 7.5.3 for clutter suppression);

(h)   Every survey on potential sites should include a careful check for electromagnetic interference, in order to avoid as much as possible interference with other communication systems such as television, microwave links or other radars. There should also be confirmation that microwave radiation does not constitute a health hazard to populations living near the proposed radar site (Skolnik, 1970, 1990; Leone et al., 1989).

7.8.2   **Data exchange, networking, database and processing**

Advancements in telecommunications and computer technology allow the transmission of radar data from a large number of sites to a central site for processing and visualization with common computer systems. Given current internet, cell phone and even satellite data rates and costs, global data exchange of at least limited but useful and usable radar data is conceivable – though the details of telecommunication networks need to be investigated. It should be kept in mind that radars are often located at remote sites where advanced telecommunication systems are not available or the initial capital investments are needed to minimize operating and maintenance costs.

In some countries, multiple radar networks exist to address different applications – weather, aviation hazards at airports, hydrological resource management, air traffic control and even customs and immigration. Data exchange is conceivable given the caveat that the applications are very specific resulting in very specific data collection methodologies and perhaps even technologies. In some locales, this is operational but requires substantial effort to integrate and interpret.

WMO has existing standards for a few radar products. Anticipating the need for radar data for regional and global numerical weather prediction, WMO has initiated a WMO radar data exchange project to define standards for raw radar data (Michelson et al., 2013). In addition, a WMO radar database has been created that attempts to provide basic metadata information about radars and radar networks on a global basis (Sireci et al., 2010).

Radar products are exchanged to generate multi-radar composite or mosaic products that are generally intended to represent surface precipitation over a vast area for long-range weather surveillance. This is common within but also between countries. The OPERA (European Operational Programme for the Exchange of Weather Radar Information) consortium is a centralized networking and processing multinational model (Dupuy et al., 2010). The BALTRAD consortium (http://baltrad.eu) is another networking and processing model for handling heterogeneous radar networks that is open source with a peer-to-peer data exchange and processing software concept that allows individual members to receive or send data, and configure and process the software as they choose (Michelson et al., 2010). A particular challenge is the compositing of heterogeneous radars consisting of products derived from different geographical projection, spatial and temporal resolution and processing. This has led to the concept of exchanging the polar raw radar data to mitigate these issues. However,

depending on the radar and the configuration, various processing steps have already been applied to the raw data to different degrees. These issues also apply to radar data exchange within a country as radars may be of different generations.

In terms of processing, there are many choices these days. Each manufacturer provides their own radar data processing and visualization systems usually with various features, such as networking capability included or for licence. There are also systems such as TITAN (Thunderstorm Identification, Tracking, Analysis and Nowcasting), which is a popular and freely available software used in many research and several meteorological services (Dixon and Wiener, 1993). It initially started as a tool for weather modification activities but has evolved to be multi-purpose. There are many sophisticated commercial systems that are radar system independent and that specialize in advance severe weather applications, such as Warning Decision Support System – Integrated Information (WDSS II) (Lakshmanan et al., 2007; http://www.wdssii.org/). One could build a radar system using tools provided by BALTRAD, or the NASA Radar Software Library (Wolff and Kelley, 2009). One could potentially negotiate or collaborate with an NMHS or a government agency for their system. Functionality varies from very basic decoders, to those generating basic products, to those with sophisticated data quality or automated severe storm detection and classification capability. The system to adopt should be based not only on the functionality, but also on the application and the available scientific and technical support and maintenance capacity.

7.9   SOURCES OF ERROR

Errors in the radar data need to be viewed within the context of the application. Precipitation estimation has often been the objective, and stringent data quality procedures need to be applied to remove and correct for the artefacts. There are different levels of data quality control. Hydrological applications require estimates even when the data are poor quality, whereas data assimilation is tolerant of missing data but not of poor data quality. Many of the issues of poor quality radar data are due to the external environment and not to the radar itself (Figure 7.2). It should be noted that these quantitative applications of weather radar are still in development, whereas the qualitative use of radar data for understanding and detecting severe storms is mature, which fully justifies the existence of radar networks.

The radar equation is developed with many assumptions. Whenever these assumptions are not satisfied, the reflectivity may be considered in error. For example, if the target is not uniform or completely filled or is mixed, the equation is not appropriate. Also, if the parameters in the equation, such as antenna gain, waveguide loss or pulse length, are incorrect then the radar constant will be in error and this will result in systematic biases in the conversion from power to reflectivity. In the following, various sources of error are discussed with respect to qualitative and quantitative applications.

Radar beam filling

In many cases, and especially at long ranges from the radar, the pulse width is large and the pulse volume is not completely filled with homogeneous precipitation, i.e. it can be only partially filled. This is particularly true with shallow weather systems (< 1 km in height, as in lake effect snow storms), where the beam completely overshoots the precipitation and no precipitation echoes can be seen beyond about 50 km. At long ranges, the pulse volume is very large, and considerable smoothing naturally occurs as the radar beam is convolved with the target. In this situation, the beam is also very high above the Earth's surface and does not quantitatively reflect the surface precipitation very well. With taller systems (say 15 km), the radar will be able to detect these systems at long range (> 250 km) and has considerable value to the forecaster as these systems will be very intense. In general, the radar measurements may be quantitatively useful for ranges of less than about 80 km for a 1° beam width radar and about 110 km for a 0.65° beam width radar without additional adjustments to the data (see Figure 7.33).

Non-uniformity of the vertical distribution of precipitation

Related to radar beam filling is the non-uniformity of the precipitation intensity as a function of height. The first parameter of interest when taking radar measurements is usually precipitation at ground level. As with horizontal variability, the vertical variability or profile plays a significant role in the estimation of surface precipitation. Because of the effects of beam width, beam tilting and the Earth's curvature, radar measurements of precipitation at long ranges or equivalently in height are lower than at the surface (see section 7.10.4.1).

Attenuation by intervening precipitation

Attenuation by rain may be significant, especially at the shorter radar wavelengths (5 and 3 cm). Attenuation by snow is less than that of rain but may still be significant over long path lengths. Contrary to common thought, attenuation at S band radar exists, but it is more difficult to identify. Dual-polarization techniques use the specific differential phase (K_{DP}) parameter, which is independent of attenuation and more effective at the shorter wavelengths. K_{DP} is a noisy parameter and the techniques are still being refined (see section 7.10.4.4).

Beam blocking

Depending on the radar installation, the radar beam may be partly or completely occulted by the topography or obstacles located between the radar and the target. This results in underestimates of reflectivity and, hence, of rainfall rate. The K_{DP} is a local parameter; it is a measure of the differential attenuation (revealed in phase) within a radar volume, and so it is independent of beam blocking. In the case of narrow blockage, data interpolation may be sufficient for quantitative application. For qualitative usage, beam blockage is a nuisance that the analyst can overcome. When the beam is totally blocked, vertical adjustments using the profile of reflectivity may be used to a degree of success.

Attenuation due to a wet radome

Most radar antennas are protected from wind and rain by a radome, usually made of fibreglass. The radome is engineered to cause little loss in the radiated energy. For instance, the two-way loss due to this device can be easily kept to less than 1 dB at the C band, under normal conditions. However, under intense rainfall, the surface of the radome can become coated with a thin film of water or ice, resulting in a strong azimuth-dependent attenuation.

Combined with precipitation attenuation and at short wavelengths, the radar echoes may be totally suppressed. While this may seem disastrous, pragmatically, it occurs for a limited time (about 10 min), and for qualitative use, warnings will likely already have been issued. For data assimilation, dual-polarization data (K_{DP}) will be available that indicate that severe attenuation has occurred and data beyond will be unusable. For hydrological applications that operate on timescales of hours or days, short-term loss of data for flood forecasting is not significant. Depending on the weather regime, flash flooding prediction may be affected.

Electromagnetic interference

Electromagnetic interference from other radars or devices, such as Radio Local Area Networks (RLANs), is becoming increasingly significant, requiring substantial diligence to protect against it. Interference among adjacent radars is mitigated through the use of slightly different frequencies (but still in the same band) with appropriate filters on the transmitter and receiver. There may be occasional interference from airborne and ground-based C band radars using the same frequency.

Use of the electromagnetic spectrum is determined by agreement and managed through the International Telecommunication Union. At the World Radiocommunication Conference 2003,

following demand for spectrum by the wireless community, the C band frequencies were opened up to the telecommunication industry on a regulated secondary non-interfering non-licensed basis to be shared with the meteorological community. In order to be non-interfering, the RLAN devices are supposed to implement Dynamic Frequency Selection, which is designed to vacate a C band channel if a weather radar is detected. However, the algorithms used to detect the weather radar are not sufficient to prevent interference before they vacate the channel. The Doppler spectra of RLAN signals appear as white noise and can be removed with adaptive noise techniques. However, they increase the noise level and reduce the sensitivity of the weather radar where the RLAN is detected. WMO has issued guidance statements relating to the co-use of the C band frequencies. Figure 7.19 shows some examples of this interference for sources at different ranges. Interference patterns like these are increasingly being observed. The image on the left shows a total reflectivity (no Doppler ground clutter filtering) plan position indicator (PPI) image at 0.42° elevation angle from a controlled study where the C band radar with an RLAN was specifically located at 6.4 km at about 40° azimuth. The RLAN is observed at 7°–10° of azimuth. Nearer (or farther) positioning of the RLAN would result in broader (or narrower) patterns. In the experiment, an RLAN could be observed as far away as 16.7 km (maximum value in a vertical column within the volume scan). The image on the right is a "max reflectivity" product from the operational Ezeiza radar in Argentina and shows a pattern of perhaps 12 RLANs that are within 5 km of the radar. This is an extreme interference example. Also, if nearby, the interference can affect the three-dimensional radar data.

Extreme diligence is needed as these systems will be deployed massively and on a non-licensed basis where violations will be difficult to control. Cooperation and collaboration is expected, required and encouraged. Interference also occurs at S band due to wireless 4G technology and also other S band radars (air traffic control). WMO has prepared guidelines or statements on spectrum sharing with these new technologies (see Annex 7.A).

Ground clutter

The contamination of rain echoes by ground clutter may cause very large errors in precipitation and wind estimation. Most modern radar antennas have standard side lobe performance that is difficult to improve as it is a geometric issue. Side lobes can be improved or moved to different angular locations, but moving the feed horn away from the focal point results in poorer antenna gain or beam width. The primary method to minimize ground clutter is a good choice of radar location. Ideally, the radar should be located in a slight depression or there should be trees to absorb and scatter the side lobes without blocking the main lobe. Signal and data suppression techniques have been extensively discussed.
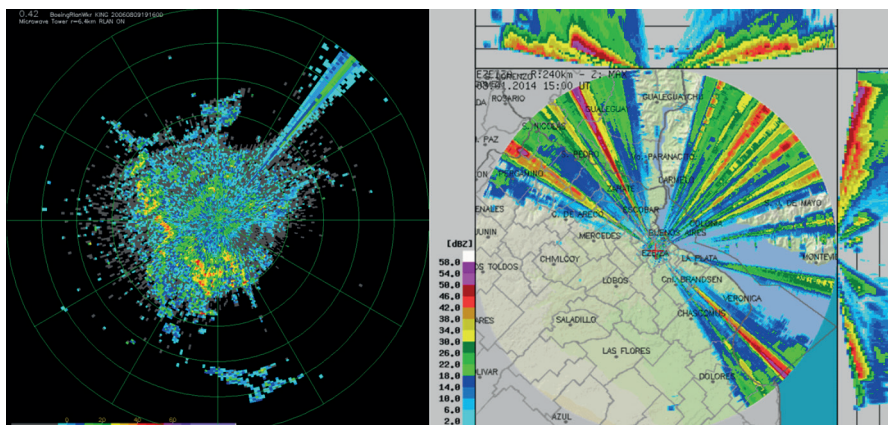
Figure 7.19. The image on the left demonstrates the type of expected interference from a Radio Local Area Network located 6.4 km away at 0.42° elevation angle. The image on the right is from an operational weather radar, courtesy of Claudia Campetella of the Servicio Meteorológico Nacional (Argentina).

Anomalous propagation

Anomalous propagation distorts the radar beam path and has the effect of increasing ground clutter by refracting the beam towards the ground. It may also cause the radar to detect storms located far beyond the usual range, making errors in their range determination because of range aliasing. Anomalous propagation is frequent in some regions, when the atmosphere is subject to strong decreases in humidity and/or increases in temperature with height. Clutter returns owing to anomalous propagation may be very misleading to untrained human observers. These echoes are eliminated in the same manner as ground clutter.

It should be noted that in general the location of the beam is not known since the atmospheric profile of the index of refraction is an idealization (Joe, 1999). Assimilation of radar volume data with the typical number of elevation angles (10–24) is problematic since the numerical weather prediction models now typically have 50–80 model levels. The lack of precise knowledge of the beam location and the mismatch between the number of radar data and model levels preclude the use of the data for assimilation beyond about 100 km.

Antenna accuracy

The antenna position may be known within 0.1° with a well-engineered system. However, positioning errors may arise due to a tilted antenna platform or instability in the feedback loop or mechanism due to wear and tear. This is particularly important at low elevation angles as small changes in elevation angle can result in large changes in coverage of shallow weather.

Electronics stability

Modern electronic systems are subject to small variations with time and have significantly improved since the early days of weather radar where receiver calibrations needed to be done daily. A well-engineered radar can be stable (< 1 dB variation) for months. The addition of a built-in test equipment monitoring system can activate an alarm or issue an e-mail when a fault is detected, and minimize the downtime for weather radars.

Variations in the Z–R relationship

To convert reflectivity to precipitation rate, an empirical relationship between Z and R is needed. The most famous and most frequent relationship used in operational radars is that of Marshall-Palmer (1948, actually reported in Marshall and Gunn, 1952). The uncertainty of this relationship was reported to be a factor of two. It also applies to snow. Reflectivity is a function of the drop size distribution, and different drop size distributions can produce the same Z. Hence, a variety of Z–R relationships have been formulated for different precipitation types – convective, stratiform and snow – with varying degrees of success (see section 7.10.4.2). With dual-polarization radar, techniques have now been developed using the K_{DP} dual-polarization parameter. It remains to be seen whether vertical profile adjustment can rival the K_{DP} technique in partially blocked situations.

Radial velocity

The velocities measured by the Doppler radar are in the radial direction only, which can cause ambiguities. Automated interpretation is still an active area of research, but interpretations are possible in certain situations – large-scale synoptic flows and small-scale convective flows – with knowledgeable and well-trained analysts.

The velocities are reflectivity weighted estimates of the precipitation/target motion. If the radial components of the vertical motions are negligible (e.g. low elevation angles), they can represent the precipitation motion which can often be interpreted as wind. However, care should be taken to not interpret the velocity as motion of the precipitation echo or system itself. In the example

of a lenticular flow over a mountain peak, the echo motion (as indicated by reflectivity) may be stationary but the precipitation particles move through the feature and the echo will have non-zero Doppler. Insects and birds may bias the radial velocities. In general, the biases are relatively small (Wilson et al., 1994) if the birds or insects are not migrating. Ground clutter can also bias the radial velocities towards zero velocity (underestimation) if not enough of the ground echo is removed.

If the wind within a radar volume is not uniform and highly sheared, inaccurate estimates of the radial velocity will result. Consider the extreme case of a tornado that is totally or partially encompassed by radar volume. In the former case, a mean radial velocity of zero with very high spectral width is expected. In the latter case, a non-zero velocity may be expected if the Nyquist velocity is sufficiently high. If the Nyquist is relatively small, the mean velocity may be aliased several times and any velocity may be produced (Fabry et al., 2013). In addition, the weather spectrum may also be aliased, confounding retrieval of both the mean velocity and its spectral width. Dual-PRF techniques also fail in this instant as the uniformity assumption of the two dual-PRF estimates is violated. The antenna rotates as well and so this assumption can be violated in high shear areas, where the two velocity samples at the different PRFs are made at different azimuthal locations and where the velocity has large variance or spectral width. In the latter situation, the error in the technique is determined by this variance and the difference in the unambiguous Nyquist velocities (hence, the ratio of the PRFs). Correction techniques can alleviate the situation of high Doppler variance (Joe and May, 2003). Figure 7.20 shows a simulation. The top image shows a prescribed simulated field with a step in the velocity field. The middle figure shows what a C band Doppler radar would measure. The bottom figure shows the results of the mitigation technique.

Side lobe contamination

When strong reflectivity gradients are present, as in the case of thunderstorms with large wet hail, the side lobes can produce an echo while the main lobe is pointing at a significantly low or no reflectivity target. The side lobes are typically 25 dB or more lower (one way, or 50 dB two
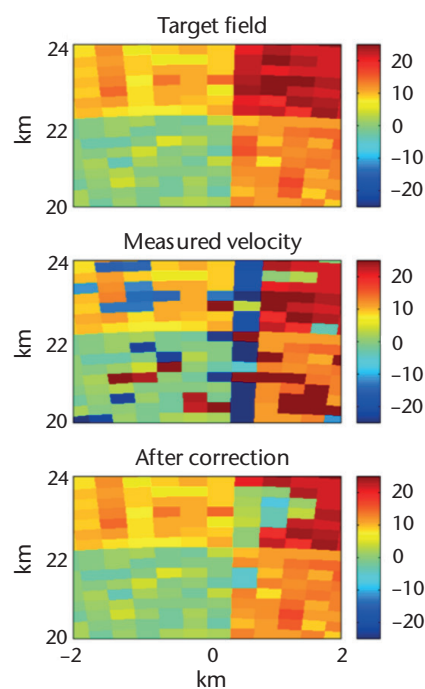
Figure 7.20. The dual-PRF technique assumes that the measurements are made from a volume with the same radial velocity. The images show the prescribed field, the measured and the corrected data. (Figure adapted from Joe and May, 2003)
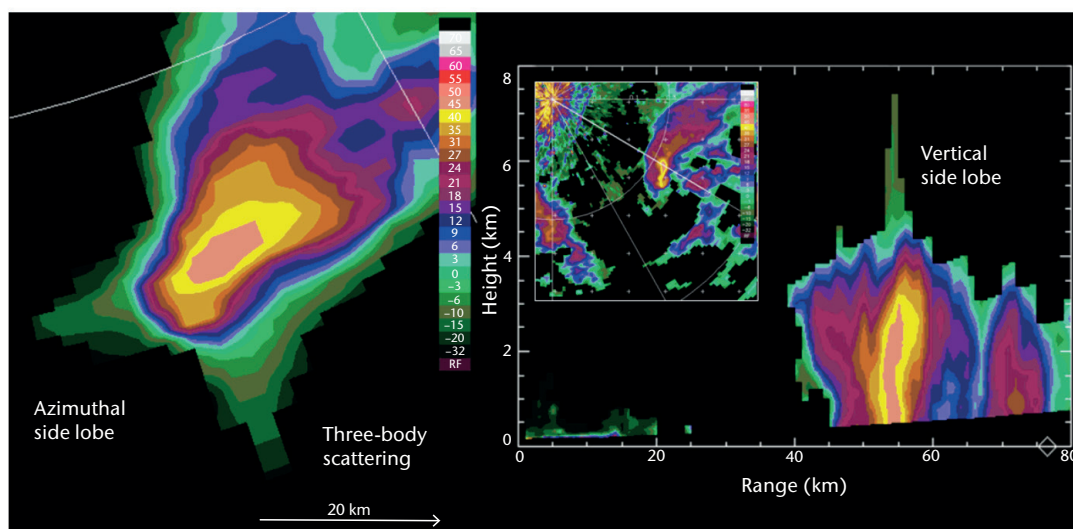
Figure 7.21. Side lobe and multiple scattering effects result in somewhat similar looking artefacts. Side lobe artefacts are at constant range, whereas multiple scattering is at constant azimuth.

way) than the main beam (Figure 7.8). So if the side lobe is pointing at a target that is 60 dBZ in strength, as in the case of wet hail, and the main beam is pointing at a target that is 10 dBZ or lower, the radar will report an echo with reflectivity, radial velocity and dual-polarization characteristics assuming that the power originated in the main beam. Side lobe echoes appear as annular artefacts both in azimuth and elevation at constant range. This can appear as "wings" or "high echo top spikes" near areas of high reflectivities (left and right images in Figure 7.21, respectively). Multiple scattering effects appear as radial artefacts at constant azimuth but with increasing range. These are caused by high reflectivity zones plus reflection effects from a highly reflective surface (ground wetted by rain, for example) and are used as hail indicators in S band radars. Note that in the figure on the right there may have been azimuthal side lobe and/or three-body scattering but this would likely have been obscured by the stronger weather echoes. This is not evident within the thunderstorm area itself as the reflectivity will be dominated by the echo in the main lobe. However, it can be evident in the vertical and result in falsely high echo tops that have been called the hail spike and can be used to qualitatively diagnose hail in a thunderstorm (see Figure 7.21). This type of echo could also occur in the weak echo region that abuts the hail curtain of a thunderstorm, which can confound the interpretation of rotation signatures indicative of the presence of a mesocyclone.

Multiple scattering

The radar beam may be reflected multiple times due to the propagation conditions (see Figure 7.22). It may also be multiply scattered within a highly reflective thunderstorm (wet hail), to a wet underlying surface and back to the radar. This has been called three-body scattering and it results in an elongated echo in range beyond the strong reflectivity core (Zrnić et al., 2010). At S band radars, this is used as a hail signature, which is called the hail flare to distinguish it from the side lobe hail signature (Lemon, 1998). Multiple scattering is more prevalent as the wavelength decreases and the signature could occur in heavy rain at C or X band.

Second/multiple-trip echo

With the high PRFs used in Doppler radars, multiple-trip echoes may occur. This has already been discussed earlier and the differences between coherent-on-transmit and coherent-on-receive
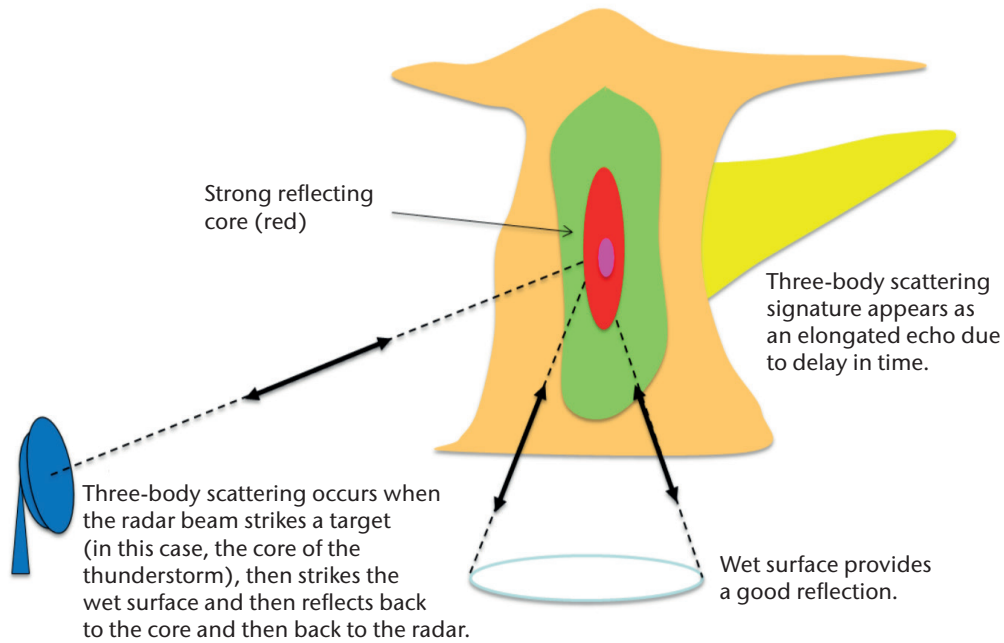
Figure 7.22. This schematic describes how three-body scattering occurs. The echo extending to the right (bright yellow) is an artefact due to the three-body scattering.

radars were highlighted. Figure 7.7 shows an example of second-trip echoes in reflectivity and radial velocity for a coherent-on-receive radar. In a coherent-on-transmit radar, the second-trip echo algorithm paints the overlapping echoes as range folded.

Wind turbines

An increasing issue is the proliferation of wind turbines and its impact on weather radar. Wind turbines are a source of natural power and sited in remote windy areas. These targets appear in the ground echo (and hence at the lower beams), but the turbine blades provide a moving target and hence generate a varying Doppler signature, and so are difficult to remove. In addition, the turbines are deployed in clusters of 100 or more, creating wind farms. Thus, significant areas will be affected. Figure 7.23 shows two different impacts of wind turbines. If the turbines are located close to the radar, they can create blocked sectors (left image). They may appear as somewhat isolated echoes (not shown). Multiple scattering may be observed (right image). In this example, the wind turbines are about 80–100 km from the radar. WMO has developed guidelines for mutual proximal operation.

Clutter maps may be one technique to remove the echoes. However, this removes the weather echo as well and therefore will require other mitigation strategies to infill the missing data (Figure 7.23). These may include interpolation from the sides or from above or with the use of gap filling data sources. As wind farms are proliferating, ongoing modification or adaptive strategies need to be developed to be able to maintain the data quality for weather applications. If the wind turbines are situated very near the radar, they can be an obstruction to the radar beam not only in the lower beams but also in the higher elevation beams through direct blockage and also due to multipath. WMO has developed guidelines regarding their deployment (see Annex 7.B).
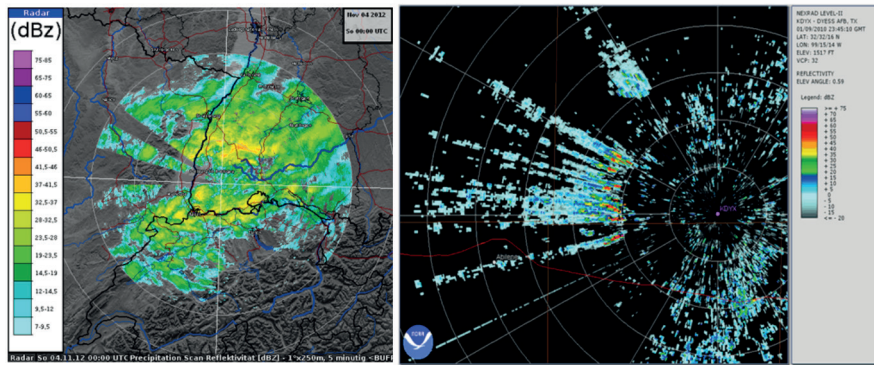
Figure 7.23. The image on the left (courtesy of Deutscher Wetterdienst) shows blocking (west of the radar) by wind turbines, and the image on the right shows interference and multiple scattering effects of the turbines (courtesy of the National Oceanic and Atmospheric Administration).

7.10 OVERVIEW OF METEOROLOGICAL APPLICATIONS

Radar observations have been found most useful for the following:

(a) Surveillance of synoptic and mesoscale weather systems;

(b) Severe weather detection, tracking and warning, including severe wind hazard detection;

(c) Nowcasting;

(d) Estimation of precipitation intensity, echo classification;

(e) Wind profiling and wind mapping;

(f) Initiation of numerical weather prediction models;

(g) Humidity estimation.

7.10.1 General weather surveillance

Radars can provide a nearly continuous monitoring of weather related to synoptic and mesoscale storms over a large area (say a range of 220 km and an area of 125 000 km^2) if unimpeded by buildings, hills, mountains, etc. Generally, only a single low-level sweep of the radar scanning at approximately 10–30 min is required. Owing to the Earth's curvature and the propagation of the radar beam, the maximum practical range for weather observation is about 250 to 350 km, as the radar will overshoot the weather at longer ranges. While radars have sufficient sensitivity to detect to farther ranges, the limit of modern radars is due to the beam height location. A radar with a 1° beam width antenna pointed at 0.5° elevation angle above the horizon is approximately 10 km above the Earth's surface at a range of 350 km. In addition, the beam width at that range is about 7 km wide. Shorter storms would not be detected or would be distorted in their representation. So storms must be substantial in size to be detected at that range. Pragmatically, scans of even 500 km or more are operationally used, particularly at the edges of radar networks. If echoes are detected, the forecaster will be provided with substantial information of a large and intense storm. Satellites and lightning detection networks may provide information on the clouds and the electric activity that produce or are associated with the precipitation. Exchange of radar data to create a radar network is de rigueur and mandatory to create mosaic products for surveillance.

Another surveillance application is the detection of shallow weather (< 1 km), such as lake effect snow squalls, drizzle or even duststorms. Narrower beam widths provide better resolution

and greater effectiveness at longer ranges as they can scan at lower elevation angles without additional ground clutter effects, can provide a filled beam to longer ranges and have greater sensitivity due to greater gain. Networks of low maintenance, low infrastructure and low cost X band radars are emerging which can fill this low-level scanning gap of large S and C band radars.

The cooperative exchange of weather radar data among various operators is now important in radar applications. It can achieve broader views of large-scale precipitation systems, such as synoptic scale fronts and typhoons. Standard radar data formats would enable and facilitate the efficient development of inter-network products. A leading example is that done in the OPERA consortium.

Radar networks employing adaptive and collaborative scanning strategies are emerging (McLaughlin et al., 2009; Weber et al., 2007). Phased array radars with electronic steering capability are being developed that can scan in non-contiguous azimuthal and elevation directions to provide high temporal sampling of rapidly changing weather phenomena, such as tornadoes and downbursts, and even other targets such as aeroplanes. Adjacent radars may also fill low-level gaps in coverage due to beam propagation effects at long range and perhaps the "cone of silence" due to limited elevation scanning.

7.10.2   **Severe weather detection and warning**

A radar is the only realistic means of monitoring severe weather over a wide area (hundreds of kilometres of range) due to the temporal resolution (minute), spatial resolution (kilometres) and detected weather elements (reflectivity from precipitation). Radar echo intensities, area and patterns are used to identify areas of severe weather, including thunderstorms with probable hail and damaging winds. Doppler radars can identify and provide a measurement of intense winds associated with gust fronts, downbursts and tornadoes to add an additional dimension (Lemon, 1978). Dual-polarization radars have the capability to separate echoes due to different types of scatterers and can distinguish hail from heavy rain and rain from snow (Zrnić et al., 2001). The nominal range of coverage of a single radar is about 250 km, which is sufficient for local short-range forecasting of about 1–2 h lead time and warning. Radar networks extend the coverage and lead time (Germann et al., 2006*b*). Effective warnings require effective interpretation performed by alert and well-trained personnel.

Technique for thunderstorm warning by radar

The technique for using radar for the provision of warnings is attributed to Lemon (1978), who outlined the reflectivity features to identify for the provision of severe thunderstorm warnings that include tornadoes, strong wind, heavy rain, flash flooding and hail. Since then, Doppler and dual-polarization features as well as additional reflectivity features have been added to the list of criteria. Figure 7.24 lists (on the left) and provides an example (on the right) of the severe weather features (Lemon, 1978; Lemon et al., 1978). These features include strong reflectivities aloft, high echo tops, weak echo regions aloft indicative of strong updraughts, strong low-level reflectivity gradients and low-level hook patterns. A set of the multi-panel images (shown on the right in Figure 7.24) is called a cell view and is automatically created once a cell has been identified in radar data-processing software. The sub-images are derived radar products that a severe weather analyst would use to decide on the storm severity, its stage in the life cycle and whether to issue a warning. Given the location of various features of the thunderstorm (e.g. location of the echo top, location of the storm centroid or location of the bounded weak echo region), cross-section lines can be configured and vertical cross-sections can be automatically created.

The temporal and three-dimensional spatial relationship is important to diagnose the life cycle phase of the storm for anticipating its evolution and hence for its warnings. This is a challenging problem and not every thunderstorm produces weather reaching the severity threshold for warnings (see Table 7.9). The original technique, that is still used today, was applied by examining various radar products and interrogating the data in various ways (Figure 7.24).

1. Large cell with strong elevated reflectivity (MAX R > 45 dBZ)
2. Tall (high echo top)
3. Weak echo region
4. Hook/kidney beam shape
5. Echo top over the updraught/low-level reflectivity gradient
6. Rotation mesocyclones
7. Downdraughts
8. Hail
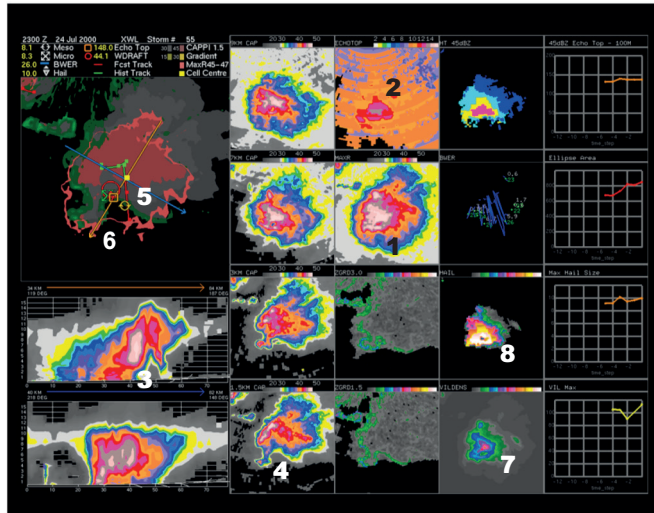
Figure 7.24. The severe storm features are listed on the left (Lemon, 1978). The cell-view product is an image centred on the automatically detected thunderstorm cell and shows relevant products for decision-making (number in cell view matches the list number).

The application of Doppler radar to real-time detection and tracking of severe thunderstorms began in the early 1970s. Donaldson (1970) was probably the first to identify a vortex flow feature in a severe thunderstorm. Quasi-operational experiments have demonstrated that a very high percentage of these single-Doppler vortex signatures are accompanied by damaging hail, strong straight wind or tornadoes (Ray et al., 1980; JDOP, 1979). This vortex is known as a mesocyclone, which is a vertical column of rising rotating air typically 2 to 10 km in diameter. The mesocyclone signature is a small anomalous Doppler velocity pattern and is first observed in the mid-levels of a storm that descends to cloud base and may be coincident with the presence of severe weather (Markowski, 2002; Burgess, 1976; Burgess and Lemon, 1990; Figure 7.25). Mesocyclonic rotation in severe storms indicates a strong and long-lived storm deserving of a severe weather warning. This is identified as small quasi-circular areas of away and toward radial velocities aligned approximately at constant range in an azimuthal direction, as can be seen in Figure 7.25. It should be noted that storm motion should be removed to easily see the away/toward couplet. In the northern hemisphere, the rotation is generally (but not always) counter-clockwise and vice versa in the southern hemisphere. This behaviour has led to improved severe storm and tornado warning lead times of 20 min or longer during quasi-operational experiments in Oklahoma (JDOP, 1979). During these experiments, roughly 50% of all mesocyclones produced verified tornadoes; also, all storms with violent tornadoes formed in environments with strong shear and possessed strong mesocyclones (Burgess and Lemon, 1990).

Table 7.9. Thunderstorm characteristics for different warning thresholds

Thresholds	Rank weight	Rank (0–8)	Bounded weak echo region (BWER) count	Mesoscale shear (m/s/km)	Hail size (cm)	Downdraught (m/s)	VIL density (kg m²/km)	Max Z (dBZ)	45 dBZ echo top height (km)
Minimum	1	0–2	5–11	4	0.5	10	2.2	30	5.5
Weak	2	3–4	12–17	6	1.3	15	3.0	45	8.5
Moderate	3	5–6	18–21	8	2.3	20	3.5	50	10.5
Severe	4	7+	22–26	10	5.0	25	4.0	60	12.5
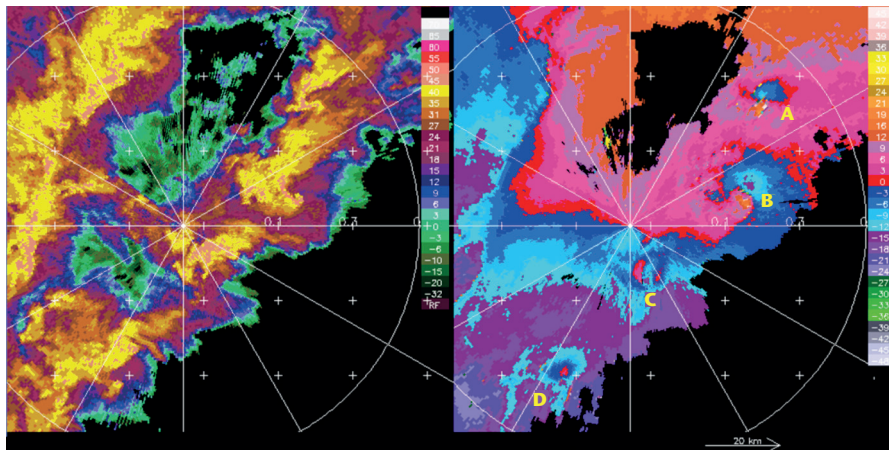
Figure 7.25. Multiple mesocyclones (A–D) are observed along a squall line and are identified as couplets of relative away and toward velocities at constant range. Symmetric velocity signatures observed in the storm are not evident or have been removed.

A tornado is approximately 200–500 m in diameter. This is often at the resolution of the radar data and so difficult to consistently detect unless a high zoom magnification is employed. When detected, it is observed as a large difference in radial velocity in adjacent radar data volumes and called the tornado vortex signature, and this is embedded within the mesocyclone (Figure 7.26). In some cases, the tornado vortex signature has been detected aloft nearly half an hour or more before a tornado touched the ground. Several years of experience with the tornado vortex signature have demonstrated its great utility for determining tornado location, usually within ±1 km. It is estimated that 50% to 70% of the tornadoes east of the Rocky Mountain high plains in the United States can be detected (Brown and Lemon, 1976). Large Doppler spectrum widths (second moment) have been identified with tornado location. However, large values of spectrum width have also been well correlated with large values during storm turbulence. In the reflectivity image (Figure 7.26, left image), a classic hook echo is observed and is indicative of precipitation associated with a strong downdraught in the rear of the strong thunderstorm.

Divergence calculated from the radial velocity data appears to be a good measure of the total divergence. Estimations of storm-summit radial divergence match those of the echo top height, which is an updraught strength indicator. Quasi-operational Doppler experiments have shown that an increase in divergence magnitude is likely to be the earliest indicator that a storm is becoming severe. Moreover, large divergence values near the storm top were found to be a
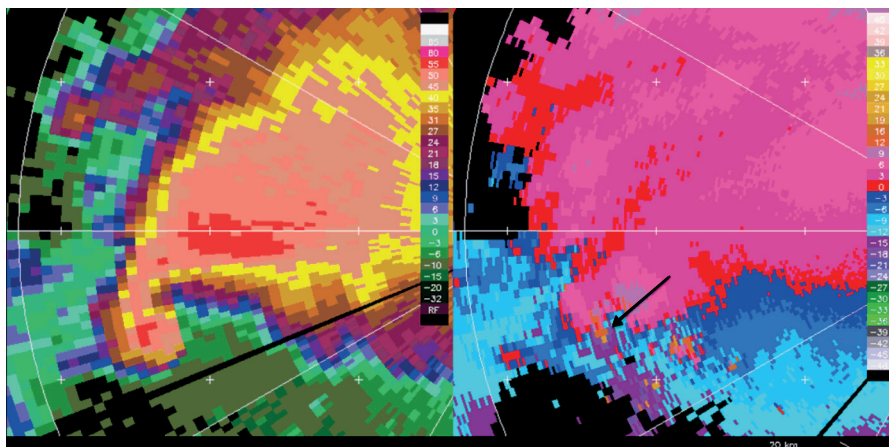
Figure 7.26. A tornado vortex signature is identified as an away/toward couplet on adjacent range bins (see arrow on right image), embedded within a mesocyclone. The image on the left shows a classic hook echo.
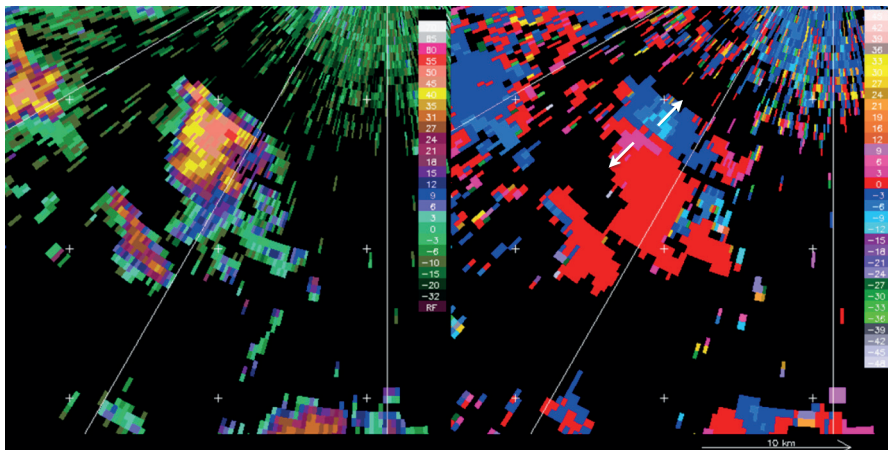
Figure 7.27. A downburst (micro or macro) is observed as a couplet of away and toward radial velocities aligned along a radial (see arrows on the right image). This is a rapidly evolving feature of thunderstorms, and can emanate from very ordinary and small thunderstorms.

useful hail indicator. Low-level divergence signatures of downbursts have been routinely made with terminal Doppler weather radars for the protection of aircraft during take-off and landing. These radars are specially built for limited area surveillance and repeated rapid scanning of the air space around the airport terminals. The microburst has a life cycle of between 10 to 20 min, which requires specialized radar systems for effective detection (see Figure 7.27). This is an example of a wet downdraught and has a strong associated reflectivity. Dry downdraughts may not be identifiable in the radar data if the precipitation evaporates and if there are no other targets for the radar to detect. In this case, a highly sensitive radar is required or a Doppler lidar or anemometer network. In this application, the radar computer system automatically provides warnings to the air-traffic control tower (Michelson et al., 1990). Mesoscale winds (40–50 km in scale) are difficult to interpret with Doppler radar as the orientation of the flows confounds the assumption of uniformity. Assumptions have to be made of the wind direction based on research studies and conceptual models of the airflow within these systems (Smull and Houze, 1987). Fortunately, in some cases, the flows and the reflectivity structure are distinctive and strong winds can be identified and warnings provided. Figure 7.28 shows a system moving to the east, and hence the full strength of the straight line winds (also known as a derecho) is evident in the away (orange) radial velocities (marked A). In this case, the away velocities are moving into toward velocities. This is also shown in the bowing of the reflectivity echo (left image). At other azimuths, the radial wind is not perpendicular to the system motion (marked B) and the analyst must take this into account.
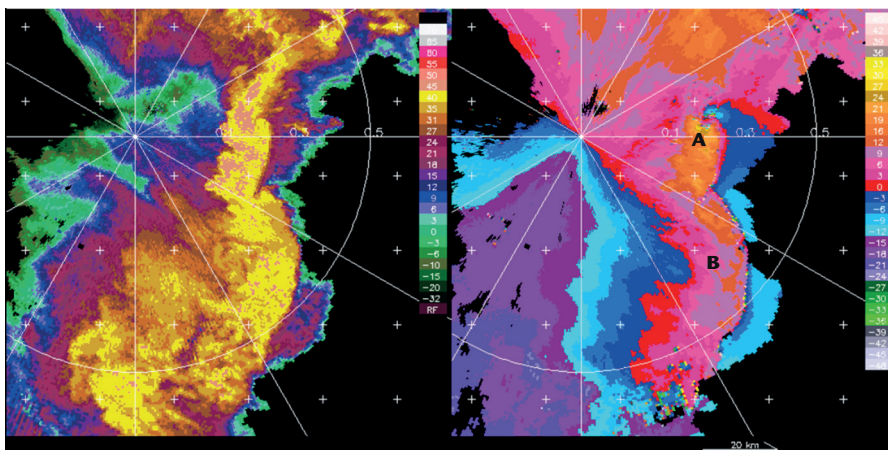
Figure 7.28. Another signature of strong intense hazardous winds can be observed as a linear or curvilinear feature in the reflectivity (left) or radial velocity data (right).
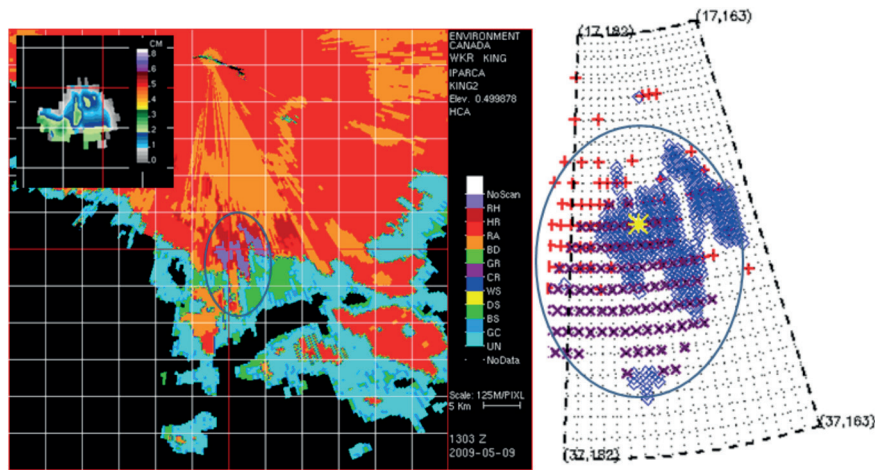
Figure 7.29. The inset figure is a reflectivity-based hail size product and the large image is a polarization diversity product to identify precipitation type, including hail. The image on the right provides detailed analysis of this example. Figure is courtesy of Sudesh Boodoo of Environment Canada.

The best method for measuring winds inside precipitation is the multiple Doppler method, which has been deployed since the mid-1970s for scientific research field programmes of limited duration. However, real-time operational use of dual- or triple-Doppler analyses is not anticipated because of the need of relatively closely spaced radars (~40 km). An exception may be the limited area requirements of airports, where a network of X band radars may be useful (McLaughlin et al., 2009; Wurman et al., 1995).

Many techniques have been proposed for identifying hail with 10 cm conventional radar, such as the presence of 50 dBZ echo at 3 or 8 km heights (Dennis et al., 1970; Lemon et al., 1978). Empirical but limited studies have shown the ability to predict hail size (Treloar, 1998; Joe et al., 2004; Witt et al., 1998). Federer et al. (1978) found that the height of the 45 dBZ contour must exceed the height of the zero degree level by more than 1.4 km for hail to be likely. An extension of this method has been verified at the Royal Netherlands Meteorological Institute and is being used operationally (Holleman et al., 2000; Holleman, 2001). A different approach towards improved hail detection involves the application of dual-wavelength radars – usually X and S bands (Eccles and Atlas, 1973). The physics of what the radar sees at these various wavelengths is crucial for understanding the strengths and limitations of these techniques (hydrometeor cross-section changes or intensity distribution).

Studies of polarization diversity show some promise of improved hail detection and heavy rainfall estimation based upon differential reflectivity (Z_{DR}) as measured by a dual-polarization Doppler radar (Seliga and Bringi, 1976; Figure 7.29). The image on the left shows a classification of the radar echo using dual-polarization signatures of a hail situation. Fuzzy logic techniques are commonly used to combine various dual-polarization parameters such as Z, Z_{DR}, ρ_{HV} and K_{DP} to identify the nature of the radar echo. In this case, the classification scheme is indicated in the left image and includes (from top to bottom): hail, heavy rain, rain, big drops, graupel, ice crystals, wet snow, dry snow, biological scatters and ground clutter. The inset image is a hail size estimate based on combining vertically integrated liquid (VIL), MAX reflectivity and freezing level (Treloar, 1998; Joe et al, 2004). A maximum hail size of 3.2 cm is indicated. The image on the right compares, in detail, the dual-polarization hail detection using data at two different resolutions (plus signs for 1 km resolution and diamond symbols for 250 m resolution) and slightly different times compared to the older reflectivity only technique (crosses). The blue ellipse corresponds to the blue ellipse in the left image. All three algorithms verified with the 3+ cm hail reported at the airport (yellow mark, middle of the red grid lines).

Recent advances include the automated detection and classification of thunderstorms through advanced processing techniques (Lakshmanan et al., 2007; Joe et al., 2002; Joe et al., 2012).

Thunderstorms evolve on a temporal scale of minutes and precipitation initiates aloft. So, radar features both aloft and near the surface are used for identification of severe weather. Hence, the radar should scan in multiple elevation angles with a cycle time of the order of 5 min.

Doppler radars are particularly useful for monitoring tropical cyclones and providing data on their eye, eye wall and spiral-band dynamic evolution, as well as the location and intensity of hurricane-force winds (Ruggiero and Donaldson, 1987; Baynton, 1979).

7.10.3   **Nowcasting**

A strict definition of nowcasting is that it is a prediction in the 0–2 h timescale and, traditionally, it refers to automated linear extrapolation of the current situation as revealed by observations. The original nowcasting system was based on doing a cross-correlation analysis of two radar images (CAPPI) for the echo motion (Bellon and Austin, 1978). The motion analysis was done in nine sectors of the image and used to extrapolate the echoes up to 90 min into the future. Points were identified for the nowcasts and a meteogram was created that indicated the most likely and probable values (Figure 7.30). The figure on the left is a single image of weather, presented as a CAPPI, that is moving to the north-east. The figure on the right shows the nowcast (the most likely, left column, and the most probable reflectivity, right column) for various points. Only two points are indicated in this example for clarity of presentation. This is a meteogram presented as an image (current time is at the top, and future time increments are presented downward in 10 min steps). An inherent assumption in this nowcast is that the precipitation system persists for the next 90 min. This illustrates the specificity characteristic of nowcasts and their precision in terms of time, space and weather element. The skill of this nowcast is very high for the first 20–30 min and it is used as a call to action or warning service. No evolution is assumed.

Using continental composite of radar data and a scaling approach to filter out the high-frequency or small-scale reflectivity patterns, nowcasts of the large-scale patterns have skill out to six or more hours that exceeds the skill of the numerical weather prediction models at this time. This is compared to the 2 to 3 h for the smaller scales. However, the skill levels are not capable of providing the precision needed for call-to-action type warning services.

Doppler radar studies of the role of boundary layer convergence lines in new thunderstorm formations support earlier satellite cloud-arc studies. There are indications that mesoscale boundary-layer convergence lines (including intersecting gust fronts from prior convection) play a major role in determining where and when storms will form. Wilson and Schreiber (1986) have documented and explained several cases of tornado genesis by non-precipitation induced wind shear lines, as observed by Doppler radar (Mueller and Carbone, 1987).
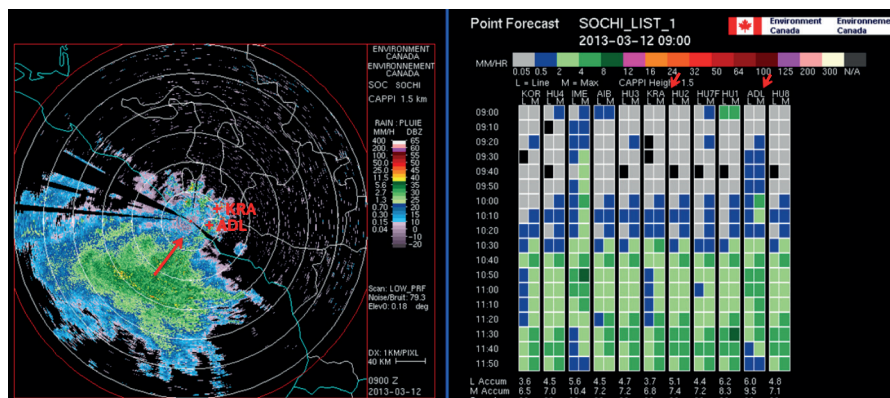
Figure 7.30. An example of a cross-correlation nowcast; the weather is moving from the south-west (left image) and the meteogram on the right shows the most likely and most probable precipitation intensities at different locations (only KRA and ADL are shown on the left, which are the sixth and tenth sites on the right image).
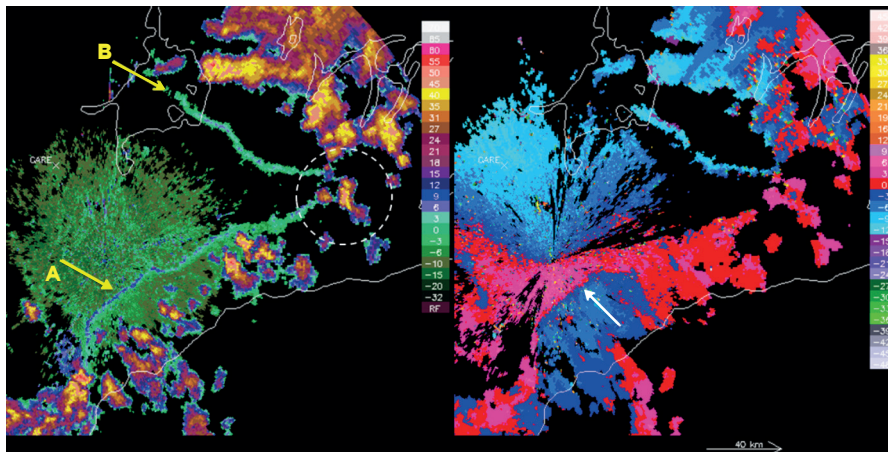
Figure 7.31. Modern radars are sensitive enough to see lake breeze and thunderstorm outflows (A, B, respectively, left image). The intersection is a location of enhanced lift and therefore a location of potential convective initiation (see the storm forming within the dashed white circle).

An important nowcasting application is the analysis of the radar fields for the initiation of convection. Recent scientific studies have shown that airmass thunderstorms, which were previously thought to be random and unpredictable, actually form on small-scale atmospheric boundaries (Wilson et al., 1998). These boundaries can be detected in both the reflectivity and radial velocity fields in the clear air echoes as line features or convergence lines (Figure 7.31). The boundaries are formed by a variety of mechanisms including lake breezes (A), thunderstorm outflows (B), drainage flows from mountain valleys, dry lines and others. Enhanced lift occurring at the intersection of these boundaries can initiate thunderstorms. Note the distinctive convergence signature in the radial velocity image (white arrow, right image).

The source of the clear air echoes can be turbulent fluctuations or insects. Polarization radar studies indicate that insects are the primary source of these radar returns. Extensions to the traditional nowcasting systems include the prediction of convective initiation and dissipation, modelling the life cycle of thunderstorms, and using numerical weather prediction models in the analysis (Wilson et al., 1998; Sun et al., 2013). In addition to the radar data, associated model fields, such as temperature and humidity, are also extrapolated (Crook and Sun, 2002; Sun et al., 2013). Increasing the cycle time (rapid update to 1 h or better), reducing the spin up and improving the physics of high-resolution models are improvements that are anticipated (Sun et al., 2013). Another emerging nowcasting application is the development of ensemble precipitation nowcasts where the small scales are both filtered and re-created using a family of statistically consistent estimates (Seed, 2003).

7.10.4   **Precipitation estimation**

Radars have a long history in estimating the distribution, the intensity and thereby the amount of precipitation with a good resolution in time and space. Most studies have been associated with rainfall, but snow measurements can also be taken with appropriate allowances for target composition. The retrieval of precipitation intensity is mainly based on empirical relationships from the returned power or reflectivity (Marshall and Palmer, 1948; Marshall and Gunn, 1952; Wilson and Brandes, 1979; Chandrasekar et al., 2003). Dual-polarization radars use additional information based on the shift in the phase of the attenuated propagating wave and on the differential scatter due to the large non-spherical particles. Comprehensive hail studies are rare due to difficulty in gathering ground truth information. Readers should consult reviews by Joss and Waldvogel (1990), and Smith (1990) for a comprehensive discussion of the problems and pitfalls, and the effectiveness and accuracy. Emerging radar processing systems are able to remove ground clutter (including anomalous propagation) in a variety of ways, and mitigate the vertical profile of reflectivity problem by adjustment with gauges or disdrometers in quasi-real-time.

7.10.4.1   *Vertical profile of reflectivity*

At long ranges, errors caused by the inability to observe the precipitation close to the ground and the lack of beam filling are usually dominant. Because of growth or evaporation of precipitation, air motion and change of phase (ice and water in the melting layer, or bright band), highly variable vertical reflectivity profiles are observed, both within a given storm and from storm to storm. In convective rainfall, experience shows that there is less difficulty with the vertical profile problem. However, in stratiform rain or snow, the vertical profile becomes more important. With increasing range, the beam becomes wider and higher above the ground. Therefore, the differences between estimates of rainfall by radar and the rain measured at the ground also increase. Reflectivity usually decreases with height; therefore, rain is underestimated by radar for stratiform or snow conditions. Figure 7.32 shows three idealized vertical profiles of reflectivity for different weather situations. They are shown at zero range. These profiles are increasingly smoothed with range due to the broadening of the beam. The beam propagation effect also occurs, and the lower part of the profile no longer contributes to the measured value. At long ranges, for low-level storms, and especially when low antenna elevations are blocked by obstacles such as mountains, the underestimate may be severe. This type of error often tends to dominate all others. This is easily overlooked when observing storms at close ranges only, or when analysing storms that are all located at roughly the same range. The effective range for quantitative precipitation estimation is about 80 km for a 1° beam width radar (Figure 7.33) and longer for smaller beam width radars (120 km for 0.65° beam width radar) without adjustment.

In shallow weather that is prevalent in winter conditions, the beam smoothing effect (illustrated in Figure 7.32) reduces the reflectivity with range. This results in accumulations (radar reflectivity or derived precipitation rate) that take on an annular pattern shown in the left image of Figure 7.33. Non-uniform filling of the radar volume with range also contributes to the rapid reduction in the reflectivity. Comparisons with values measured with gauges over a season are shown on the right (ratio of the radar versus in situ gauge measurements), illustrating this degradation in measured precipitation amounts. In this particular location, with this 1° beam width radar and this weather regime (Finland in winter), the effective range (the flat part of the
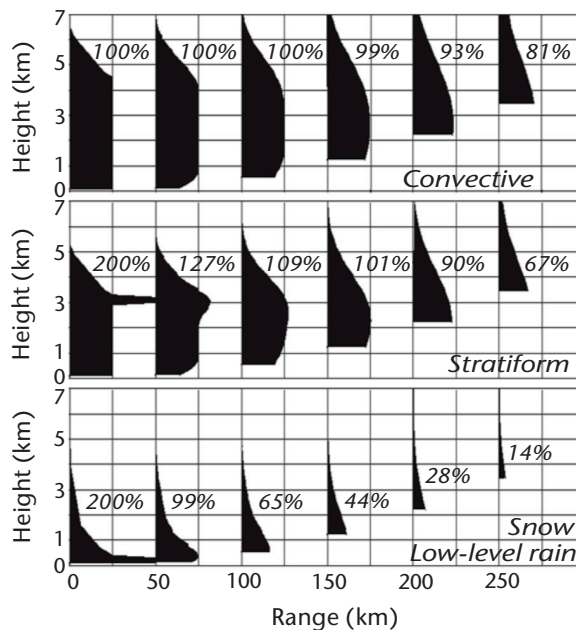
Figure 7.32. Beam smoothing and beam propagation modify the appearance of the vertical profile of reflectivity with range. Three situations are depicted with the maximum reflectivity in the column as a percentage of the surface precipitation taking into account the bright band (adapted from Joss and Waldvogel, 1990).
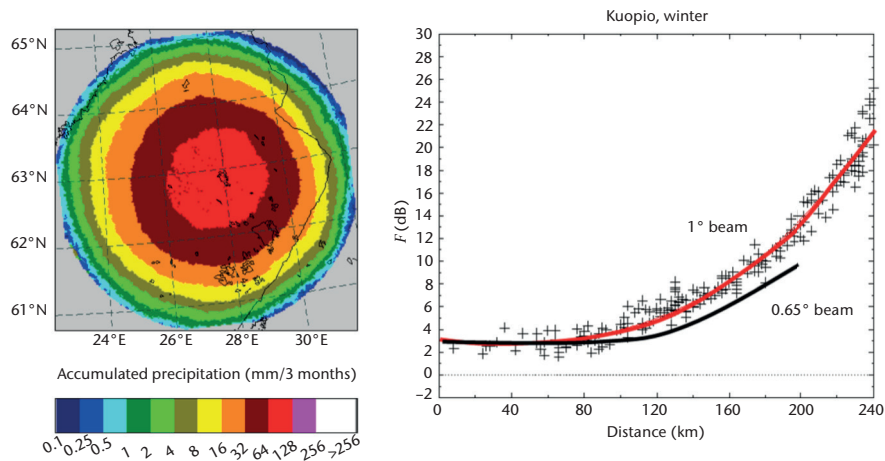
Figure 7.33. This shows an accumulation of radar-derived precipitation over a winter season. The annular pattern is primarily due to the lack of beam filling at long ranges for shallow winter weather systems. The right image shows how this is reflected as a range bias with the radar–gauge comparisons (figure courtesy of Daniel Michelson of the Swedish Meteorological and Hydrological Institute using data from the Finnish Meteorological Institute).

curve) is about 80 km for direct precipitation estimates. Since the effect is geometric, a smaller beam width would extend this effective range. This is illustrated for a 0.65° beam width, where the effective range is extended to about 110–120 km.

No one method of compensating for the effects of the vertical reflectivity profile in real time is widely accepted. However, three compensation methods can be identified:

(a)   Range-dependent correction: The effect of the vertical profile is associated with the combination of increasing height of the beam axis and spreading of the beam with range. Consequently, a climatological mean range-dependent factor can be applied to obtain a first-order correction. Different factors may be appropriate for different storm categories, for example, convective versus stratiform;

(b)   Spatially varying adjustment: In situations where the precipitation characteristics vary systematically over the surveillance area, or where the radar coverage is non-uniform because of topography or local obstructions, corrections varying with both azimuth and range may be useful. If sufficient background information is available, mean adjustment factors can be incorporated in suitable look-up tables. Otherwise, the corrections have to be deduced from the reflectivity data themselves or from comparisons with gauge data;

(c)   Full vertical profiles: The vertical profiles in storms vary with location and time, and the lowest level visible to the radar usually varies because of irregularities in the radar horizon. Consequently, a point-by-point correction process using a representative vertical profile for each zone of concern may be needed to obtain the best results. Representative profiles can be obtained from the radar volume scan data themselves, from climatological summaries or from storm models. This is the most complex approach but can be implemented with modern data systems (Joss and Lee, 1993).

Figure 7.34 shows an example of the latter method of correcting for the vertical profile of reflectivity with range effect, which is now routinely used on a radar network basis. The figure on the left shows a 24 h accumulation of radar-derived precipitation rate during a stationary front passage. The pattern would be expected to be broadly uniform. The figure on the right is created with an adjustment for the vertical profile effect at long ranges, and hence the accumulations at the edges are enhanced. The difference in the images also illustrates the benefits of a network approach to generating precipitation products, as the vertical profile effect of the individual radars is not so evident in the interior of the network.
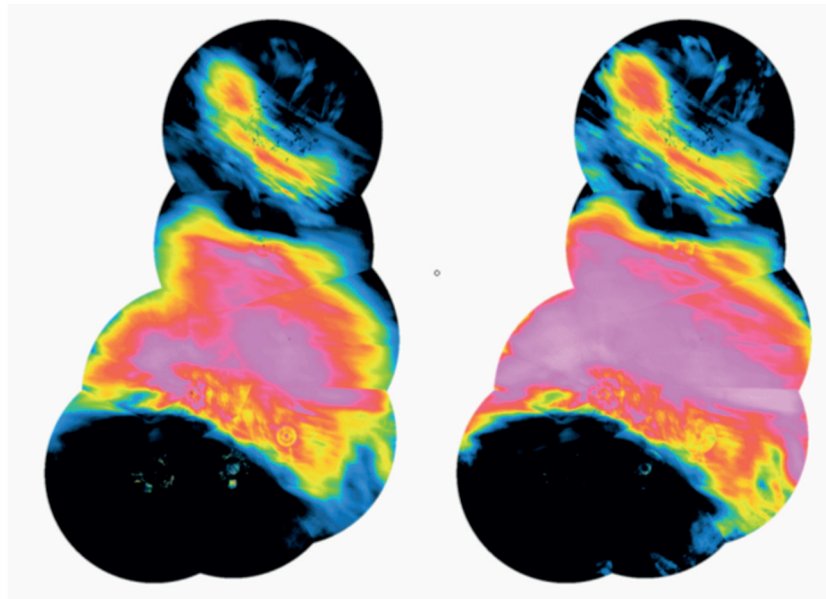
Figure 7.34. This shows the case of an east-west stationary front. The image on the left shows the fall off with range (see Figure 7.33). The image on the right shows the range adjustment made to the data (figure courtesy of Jarmo Koistinen, Finnish Meteorological Institute).

Improvements in digital radar data processing and real-time integration with gauge networks have led to the development of new quantitative, radar-based products for hydrometeorological applications. A number of European countries and Japan are using such radar products with numerical models for operational flood forecasting and control (Berenguer et al., 2012; Cluckie and Owens, 1987). The synthesis of radar data with raingauge data provides a powerful nowcasting product for monitoring rainfall. Radar-AMeDAS Precipitation Analysis is one of the products provided in Japan (Makihara, 2000). Echo intensity obtained from a radar network is converted into precipitation rate using a Z–R relationship, and 1 h precipitation amount is estimated from the precipitation rate. The estimated amounts are then calibrated using raingauge precipitation amounts to provide a map of 1 h precipitation amount with high accuracy.

7.10.4.2 *The Z–R relation*

In ideal conditions (close to the radar, no artefacts), precipitation is usually estimated by using the Z–R relation:

$$Z = A R^b \tag{7.13}$$

where A and b are constants. The relationship is not unique and many empirical relations have been developed for various climates or localities and storm types. Nominal and typical values for the index and exponent are $A = 200$, $b = 1.60$ (Marshall and Palmer, 1948; Marshall and Gunn, 1952). This can be applied to an accuracy of a factor of two for both rain and snow. The equation is developed under a number of assumptions that may not always be completely valid. Nevertheless, history and experience have shown that the relationship in most instances provides a good estimate of precipitation at the ground unless there are obvious anomalies (Figure 7.35). A survey of the Z–R relationships in worldwide use indicated that the Marshall-Palmer relationship is used in 80% of the operational weather radars – a remarkable achievement considering the very few data points used to form the original relationship (Sireci et al., 2010). The red line in Figure 7.35 represents the original Marshall-Palmer relationship (reported in Marshall and Gunn, 1952, and Marshall and Palmer, 1948). Attempts at improvements have been made throughout the years and the black lines represent these other relationships (Battan, 1973). It is remarkable that the original relationship, made with few measurements and in a specific weather regime, has stood the test of time.
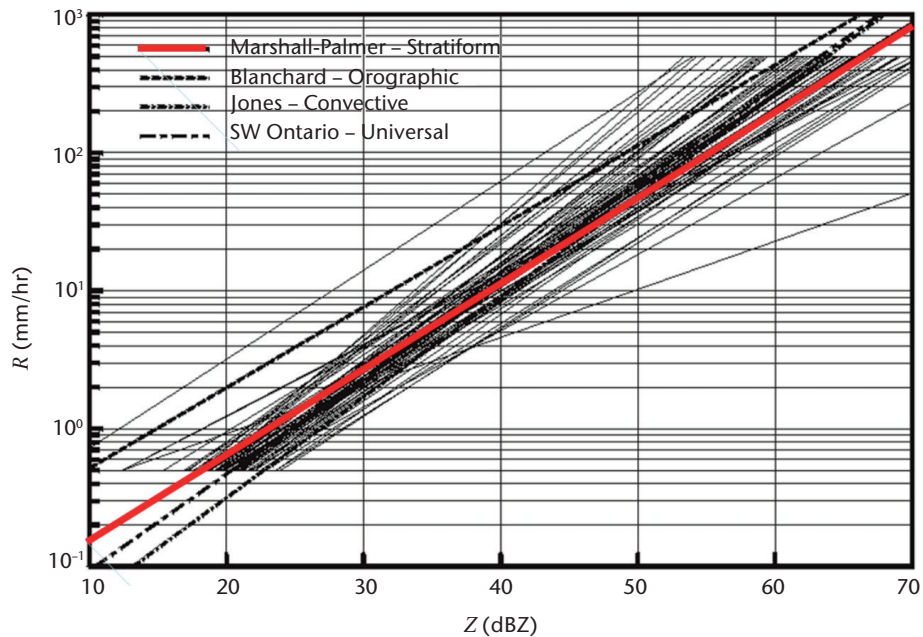
Figure 7.35. A plot of a plethora of Z–R relationships from Battan (1973)

There are some generalities that can be stated. At 5 and 10 cm wavelengths, the Rayleigh approximation is valid for most practical purposes unless hailstones are present ($Z > 57$ dBZ is often taken as the boundary between rain and hail). Large concentrations of ice mixed with liquid can cause anomalies, particularly near the melting level. By taking into account the refractive index factor for ice (i.e. $|K|^2 = 0.208$) and by choosing an appropriate relation between the reflectivity factor and precipitation rate (Z against R), precipitation amounts can be estimated reasonably well in snow conditions (the value of 0.208, instead of 0.197 for ice, accounts for the change in particle diameter for water and ice particles of equal mass). However, snowfall gauge measurements are problematic and there are few comprehensive studies of radar–snowfall relationships.

The rainfall rate (R) is a product of the mass content and the fall velocity in a radar volume. It is roughly proportional to the fourth power of the particle diameters. Therefore, there is no unique relationship between radar reflectivity and the precipitation rate since the relationship depends on the particle size distribution. Thus, the natural variability in drop size distributions is an important source of uncertainty in radar precipitation measurements when other factors are taken into account.

Empirical Z–R relations and the variations from storm to storm and within individual storms have been the subject of many studies over the past forty years, particularly for storm event studies. A Z–R relation can be obtained by calculating values of Z and R from measured drop size distributions produced by an instrument known as a disdrometer. An alternative is to compare Z measured aloft by the radar (in which case it is called the equivalent radar reflectivity factor and labelled Z_e) with R measured at the ground. The latter approach attempts to reflect any differences between the precipitation aloft and that which reaches the ground. It may also include errors in the radar calibration, so that the result is not strictly a Z–R relationship. Disdrometers are now being deployed in operational networks for determining the Z–R relationship for climatology, storm studies and real-time adjustment, and are very sensitive and can detect very light precipitation.

The possibility of accounting for part of the variability of the Z–R relation by stratifying storms according to rain type (such as convective, non-cellular, orographic) has received a good deal of attention. Although variations in the drop size distribution are certainly important, their relative

importance is frequently overemphasized. After some averaging over time and/or space, the errors associated with these variations will rarely exceed a factor of two in rain rate. They are the main sources of the variations in well-defined experiments at near ranges.

7.10.4.3   *Gauge adjustment*

There is general agreement that comparisons with gauges should be made routinely as a check on radar performance, and that appropriate adjustments should be made if a radar bias is clearly indicated. However, this needs to be done judiciously as tuning the adjustment for one situation may create problems in other situations. In situations where radar estimates are far from the mark due to radar calibration or other problems, such adjustments can bring about significant improvements.

Ground level precipitation estimates from radar systems are made for areas of typically 1–4 km^2 spatial resolution and successively for 5–15 min periods using low elevation (elevation angles of < 1°) plan position indicator scans, constant altitude PPI synthetic products or even more sophisticated products. The radar estimates have been found to compare with spot precipitation gauge measurements within a factor of two. The gauge samples an extremely small area (100 cm^2, 200 cm^2), while the radar integrates over a volume, on a much larger scale (1–4 km^2). This difference accounts for a considerable amount of the discrepancy. There are indications that the gauge accuracy may, for some purposes, be far inferior to what is commonly assumed, especially if the estimates come from a relatively small number of raingauges (Neff, 1977). An important consideration is the success metric. Seasonal averages may be acceptable in some applications and a single $Z–R$ relationship may be sufficient. However, for flash flood warnings, real-time adjustments may be required.

Note that these adjustments do not automatically ensure improvements in radar estimates, and sometimes the adjusted estimates are poorer than the original ones. This is especially true for convective rainfall where the vertical extent of echo mitigates the difficulties associated with the vertical profile, and the gauge data are suspect because of unrepresentative sampling. Also, the spatial decorrelation distance may be small, and the gauge–radar comparison becomes increasingly inaccurate with distance from the gauge. A general guideline is that the adjustments will produce consistent improvements only when the systematic differences (i.e. the bias) between the gauge and radar rainfall estimates are larger than the standard deviation of the random scatter of the gauge versus radar comparisons. This guideline makes it possible to judge whether gauge data should be used to make adjustments and leads to the idea that the available data should be tested before any adjustment is actually applied. Various methods for accomplishing this have been explored, but at this time there is no widely accepted approach.

7.10.4.4   *Dual-polarization precipitation techniques*

Various techniques for using polarization diversity radar to improve rainfall measurements have been proposed. In particular, it has been suggested that the difference between reflectivities measured at horizontal and vertical polarization (Z_{DR}) or the phase shift (ϕ_{DP} or K_{DP}) can provide useful information about drop size distributions (Seliga and Bringi, 1976). These methods depend on the hydrodynamic distortions of the shapes of large raindrops, with more intense rainfalls with larger drops giving a stronger polarization signature. The attenuation must be first corrected and again dual-polarization techniques are applicable here. There is still considerable research on whether this technique has promise for operational use for precipitation measurement (English et al., 1991). At long wavelengths, the rain rate thresholds where K_{DP} techniques are effective are higher (for example, at S band it is about 20 mm h^{-1}, and at X band it is about 4 mm h^{-1}).

At close ranges (with high spatial resolution), polarization diversity radars may give valuable information about precipitation particle distributions and other parameters pertinent to cloud physics. At longer ranges, it is impossible to be sure that the radar beam is filled with a homogeneous distribution of hydrometeors. Consequently, the empirical relationship of the polarimetric signature to the drop size distribution increases uncertainty. Of course, knowing
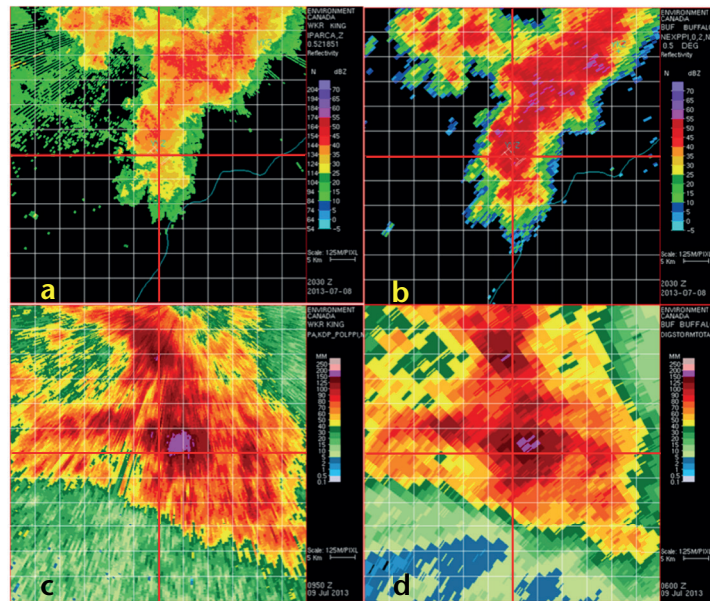
Figure 7.36. The top figures show attenuation of a C band dual-polarization radar (a) compared to an S band radar (b) at one instant. The bottom figures are precipitation accumulations over the period of the event and show remarkable similarities after correction using polarization diversity capability (see also Figure 7.37; figure courtesy of Sudesh Boodoo of Environment Canada).

more about Z–R will help, but, even if multi-parameter techniques worked perfectly well, the error caused by Z–R could be reduced only from 33% to 17%, as shown by Ulbrich and Atlas (1984). For short-range hydrological applications, the corrections for other biases (already discussed) are usually much greater, perhaps by an order of magnitude or more.

Dual-polarization radars can overcome attenuation, partial beam filling and partially blocked beams. Figure 7.36 shows a C band radar where the polarization technique is used to correct for attenuation. The dual-polarization parameters are sensitive to the size and shape of the large particles, and the smaller the wavelength, the more sensitive the radar. In this example, a precipitation system that caused localized flooding was observed by a C band radar and an S band radar. The C band (King City with a 0.65° beam) was about 40 km from the flooding and the S band (Buffalo with a 1° beam) was about 100 km away. Images (a) and (b) show one instance of the low-level radar reflectivity from both radars. The red grid lines are reference lines. The location of the raingauge is about 7 km to the south-west. The C band radar data are attenuated compared to the S band data (image (b) is more intense than image (a)). During the event, the C band radar experienced a wet radome which also strongly attenuated the signal. Images (c) and (d) are accumulations based on their respective dual-polarization-derived precipitation products from over the 8 h period of the event (see also Figure 7.37). The resolution difference is evident, but the accumulation patterns are very similar. This illustrates the great potential for a dual-polarized C band radar to overcome significant attenuation. Interestingly, the dual-polarization precipitation estimate from the S band radar was actually lower and closer to the raingauge value (not shown) than using the traditional Z–R relationship, as the particle classification of hail versus rain was used to prevent the overestimation.

Figure 7.37 shows the comparison of various rainfall estimates from C and S band radars and a raingauge. The bottom (C1) and top (S1) lines are accumulations based on traditional simple reflectivity converted to rain rate ($Z = 300\ R^{1.4}$) from the King City C band (40 km from the gauge site) and the Buffalo S band (100 km from the gauge site) radars. Both radars are well calibrated and only Doppler ground clutter rejection has been applied to the data. The Z_{AC}–R line (C2) is a Z_{DR}-only attenuation corrected reflectivity converted to rain rate and accumulated. The dashed (S2) and dark blue (C3) lines are the precipitation estimates using a mix of dual-polarization techniques from the S band radar (S2) and from the K_{DP}–R technique from the C band radar
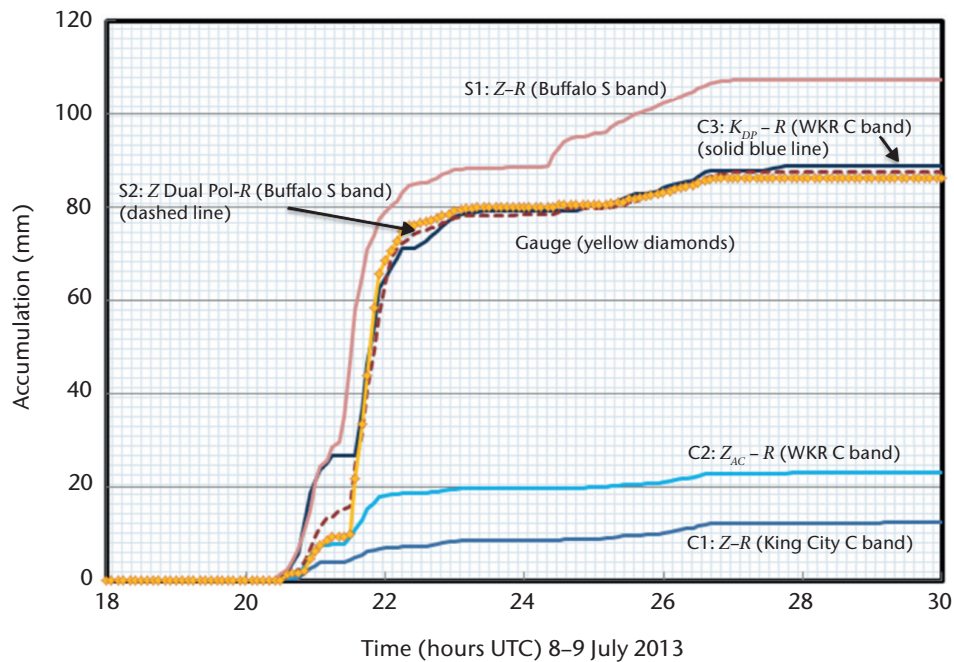
Figure 7.37. A meteogram of accumulated rain from a gauge (yellow line with symbols) and three C band (C1, C2, C3) and two S band (S1, S2) estimates of the precipitation accumulation using a variety of polarization diversity techniques for one gauge site; point is about 7 km south-west of the centre (see also Figure 7.36; figure courtesy of Sudesh Boodoo of Environment Canada).

(C3), respectively. The improved Buffalo S band results are attributed to removing the hail bias using the dual-polarization particle classification technique. The specific differential phase (K_{DP}) technique, which is insensitive to attenuation, partial beam blockage and partial beam filling, improves the King City C band estimates. This illustrates the impact of dual polarization on the quantitative use of both S and C band radars. It also illustrates the larger impact of dual polarization on C band radars.

Rain/snow/hail discrimination and other target classification

With conventional or reflectivity-only radars, the pattern and intensity of the echo were used to roughly estimate the nature of the target. In summer, reflectivities less than about 12 dBZ were considered to be non-precipitating echoes, light rain was up to about 30 dBZ and heavy rain up to about 50 dBZ or so. Reflectivities above 57 dBZ were considered to be hail. Snow is not generally separable with these kinds of radars in the horizontal. In the vertical, the bright band (a region of enhanced reflectivity due to large wet snow aggregates) delineated snow aloft from rain below. Dual-polarization radars characterize the target using reflectivity information from orthogonal channels, their cross-polar signal and changes in propagation phase. Surface temperature and humidity and soundings from numerical weather prediction models are also used. Fuzzy logic techniques use independent estimates from a variety of dual-polarization parameters to classify the echo type into a variety of categories including: ground clutter, rain, snow, hail, biological scatters and even big and small drops (Figure 7.29).

Aeroplanes were identified as isolated point anomalies and ground echoes were identified as stationary or permanent echoes at short range around the radar. The reflectivities of aeroplanes and ground echoes can vary greatly because small changes in aspect angle result in substantial changes in backscatter.

Doppler radars can identify non-moving targets, such as ground clutter and anomalous propagation echoes, even in the presence of weather phenomena. These ground targets can be effectively filtered out in signal processing to produce "corrected (for ground clutter)

reflectivity". Most if not all modern radars have Doppler and thus have this capability. Before Doppler radars, a variety of techniques were used to remove ground clutter including: (i) CAPPI, (ii) ground clutter maps, and (iii) the statistical fluctuation of the reflectivity statistics.

7.10.5 Wind estimation/wind mapping

Doppler velocities are radial velocities, and a family of true velocities can create the same radial velocity. Hence, radial velocities alone are ambiguous and require simplifying assumptions to interpret. On typical colour displays, velocities between $\pm V_{max}$ are generally assigned warm/ cool colours to indicate away/toward motions. Velocities extending beyond the Nyquist (unambiguous or extended) velocity enter the scale of colours at the opposite end. This process may be repeated if the velocities are aliased more than one Nyquist interval.

7.10.5.1 *Wind profiling*

Doppler radar can be used to derive vertical profiles of synoptic scale horizontal winds. When the radar's antenna is tilted above the horizontal, increasing range implies increasing height. A profile of wind with height can be obtained by sinusoidal curve-fitting to the observed data (termed velocity azimuth display (VAD) after Lhermitte and Atlas, 1961) if the wind is assumed to be relatively uniform or linear over the area of the scan. The winds at zero radial velocity bins are perpendicular to the radar beam axis. The colour display may be used to easily interpret VAD data obtained from large-scale precipitation systems. Typical elevated conical scan patterns in widespread precipitation reveal an S-shaped zero radial velocity contour as the mean wind veers with height (Wood and Brown, 1986). On other occasions, closed contours representing jets are evident. See Figure 7.12 for a sample of synoptic Doppler wind fields.

If uniformity can be assumed, then divergence estimates can also be obtained using the VAD technique by fitting a curve with a constant term to the equation. This technique cannot be accurately applied during periods of convective precipitation around the radar as the uniformity assumption is not satisfied. Doppler radars have successfully obtained VAD wind profiles and divergence estimates in the optically clear boundary layer during all but the coldest months, up to heights of 3 to 5 km above ground level. The VAD technique seems well suited for winds from precipitation systems associated with extratropical and tropical cyclones. In the radar's clear-air mode, a time series of measurements of divergence and derived vertical velocity is particularly useful in nowcasting the probability of deep convection.

7.10.5.2 *Convective wind features*

In the case of convection, small-scale wind features are due to divergence, convergence and rotation as observed in gust fronts, downbursts, mesocyclones, etc. These appear as small anomalies of one kilometre to tens of kilometres in scale embedded in mean flows of hundred kilometre scales. Taking into account assumptions about the flow, and in combination with conceptual models and an understanding of the thunderstorm or mesoscale convective system wind flows, colour displays of single-Doppler radial velocity patterns can aid in the real-time interpretation and diagnosis of thunderstorm severity (Burgess and Lemon, 1990). Lemon (1978) listed the features and diagnostic procedure to identify severe thunderstorms (see section 7.10.2). Convective wind features confound the interpretation of radial velocity fields in particular when there are mesoscale flows on the scale of 40 to 100 km and three-dimensional regimes, as in complex mountainous terrain.

7.10.5.3 *Wind mapping*

Since the mid-1970s, experiments have been made for measuring three-dimensional wind fields using multiple Doppler arrays. Measurements taken at a given location inside a precipitation area may be combined, by using a proper geometrical transformation, in order to obtain the three wind components. Such estimations are also possible with only two radars, using the

continuity equation. Kinematic analysis of a wind field is described in Browning and Wexler (1968). However, for accurate velocity estimation, the radars must be relatively close together (40–80 km) and the target area must be in two lobes perpendicular to the radar baselines. Operationally, it is unusual to find radars situated so close to one another.

7.10.6   Initiation and numerical weather prediction models

A variety of radar data and products are used for data assimilation in some numerical weather prediction centres. Not all models use the same products. Precipitation is a derived parameter in numerical weather prediction models, and so it is difficult to directly assimilate precipitation or reflectivity fields. Winds are direct model variables and radial velocities may be assimilated with less contrivance. These include VAD wind profiles, composited radar-derived surface precipitation fields in global models and, in some cases, three-dimensional reflectivity and radial velocity fields for local area or small-scale models in polar coordinates. Lopez (2011) has demonstrated the value of assimilating the US Stage IV surface precipitation product on the weather in Europe and Asia. These and other applications (typhoon tracking) are prime drivers for the global weather radar data exchange initiative.

7.10.7   Humidity estimation

An emerging innovation is the retrieval of humidity from beam propagation differences of echoes from the omnipresent ground targets (Fabry, 2004). This innovation is counter-intuitive to the siting of weather radars since they are sited to minimize ground clutter. Index of refraction fluctuations cause beam propagation path length changes which can be detected as changes in the phase of the signal or the Doppler shift. By comparing the shift in dry versus moist conditions and accounting for range ambiguities, the path length change can be estimated and then related to the index of refraction change using Snell's law. The index of refraction is dependent on temperature, pressure and humidity but primarily on the latter, and hence the humidity can be retrieved very near the radar. Several research radars have this capability and some operational systems (in France and the UK) are prototyping this for operational deployment.

7.11   METEOROLOGICAL PRODUCTS

The radar data can be processed to provide a variety of meteorological products to support various applications. The quality of these products depends on the type of radar, the scan strategy, its signal processing characteristics and the associated radar control and data analysis/ production system. These products include grids of raw or derived radar parameters, vertical wind profiles, location and characteristics of analysed thunderstorm cells, their historical tracks, nowcasts, etc. Polar coordinate data are converted to two- or three-dimensional Cartesian coordinates using interpolation techniques onto grids with different geographical projections. Several of the products listed below are illustrated in Figure 7.24. A list of typical radar products is presented in Table 7.10.

The following is a list of common generated products:

(a) The plan position indicator: A polar format display of a variable, obtained from a single full antenna rotation at one selected elevation. It is the classic radar display, used for weather surveillance. This is the most basic of products. Note that it is made at constant elevation angle, and so increasing range means that the data are taken at increasing height. Any parameter can be displayed in this format.

(b) The constant altitude plan position indicator: A horizontal cross-section display of a variable at a specified altitude, produced by interpolation from the volume data. It is used for surveillance and for identification of severe storms. It is also useful for monitoring the weather at specific flight levels for air traffic applications. One of the rationales for the CAPPI is that by judicious selection of the altitude, a near clutter-free product can be produced in the absence of the Doppler zero velocity notch filter.

(c) The pseudo range–height indicator (RHI): A display of a variable obtained from a volume scan where the data from the same azimuth are extracted and collated to provide vertical information on the structure of the weather. Classically, this was done with an antenna doing a physical vertical sweep, typically from 0° to 90°, at one azimuth. Manual intervention was required to select the azimuth and decide when to do the scan. The advantage of this classic technique is that the density of information is much higher. Typically, very fine elevation angle changes (~0.1°) can be used. The quality of the pseudo RHI technique depends on the scan strategy, but it has the great advantage of flexibility. It is used for identifying severe storms, hail and the bright band.

(d) Vertical cross-section: A display of a variable above a user-defined surface vector (not necessarily through the radar). It is produced by interpolation from the volume data.

(e) The column maximum: A display, in horizontal plane, of the maximum value of a variable (usually reflectivity) above each point of the area being observed. This is useful to identify the maximum reflectivity in a storm to assess its severity or to estimate the maximum precipitation that could be expected. In some cases, due to radar siting issues, where the low levels could not be observed (mountainous terrain), this was used to estimate surface precipitation. Sometimes, there is a minimum altitude threshold to the data, so that the high reflectivities in the bright band do not overly influence the use of this product. A variation is to limit the altitude of the data to quickly provide insight into the vertical structure of the storm.

(f) Vertically integrated liquid: An indicator of the intensity of severe storms. It can be displayed, in horizontal plane, for any specified layer of the atmosphere. As this is dominated by the highest reflectivities, it is very similar to the maximum reflectivity product in pattern but in different units.

Table 7.10. List of typical radar products

Plan position indicator of basic parameters (low level)	Cell identification and tracking
Maximum reflectivity in a column	Mesocyclone, tornado vortex signature
Echo top	Downburst, microburst
Derived thunderstorm severity products	Gust front, convergence
Surface precipitation rate	Nowcast
Surface accumulation products	Hail probability, size
Basin products	Bounded weak echo region
Hydrometeor classification – hail, rain, snow, etc.	Velocity azimuth display wind profiles
Arbitrary cross-sections of various parameters	Mosaics of multiple radar

(g) Echo tops: A display, in horizontal plane, of the height of the highest occurrence of a selectable reflectivity contour, obtained by searching in the volume data. It is an indicator of the strength of the updraught and therefore an indicator of severe weather and hail.

(h) Often the reflectivity products are converted to precipitation products by an empirical relationship between Z and R. These precipitation products are aggregated into accumulation products of varying time duration.

(i) Modern computing systems have significant processing capabilities. Techniques or algorithms have been developed to search the three-dimensional data to locate and quantify the characteristics of contiguous areas of high reflectivity which are related to severe weather thunderstorms for the analyst (Figure 7.24).

In addition to these standard or basic displays, other products can be generated to meet the particular requirements of various users (hydrology, nowcasting or aviation):

(a) Precipitation accumulation: An estimate of the precipitation accumulated over time at each point in the area observed;

(b) Precipitation sub-catchment totals: Area-integrated accumulated precipitation;

(c) Velocity azimuth display: An estimate of the vertical profile of wind above the radar. It is computed from a single antenna rotation at a fixed elevation angle;

(d) Velocity volume processing, which uses three-dimensional volume data;

(e) Storm tracking: A product from complex software to determine the tracks of storm cells and predict future locations of storm centroids;

(f) Wind shear: An estimate of the radial and tangential wind shear at a height specified by the user;

(g) Divergence profile: An estimation of divergence from the radial velocity data given some assumptions;

(h) Mesocyclone: A product from sophisticated pattern-recognition software that identifies rotation signatures within the three-dimensional base velocity data that are on the scale of the parent mesocyclonic circulation often associated with tornadoes;

(i) Tornado vortex signature: A product from sophisticated pattern-recognition software that identifies gate-to-gate shear signatures within the three-dimensional base velocity data that are on the scale of tornadic vortex circulations;

(j) Particle type: The echo is classified according to precipitation type and derived from dual-polarization data.

In addition, radar network processing results in a radar mosaic. The products mentioned above apply on a network basis; in fact, this is standard practice. Considerations for radar products include: (i) projections are used for visualization of the data; (ii) for areas of overlapping radar coverage, various algorithms are used – based either on the nearest radar, the maximum value or a sophisticated estimation of data quality. If the overlap is significant, a neighbouring radar may fill the void in the "cone of silence". The development of networked radar products needs also to consider intra-network and inter-network homogenization of the data. This includes temporal and spatial harmonization, mutual calibration of the radar data, and examination of the radar sensitivities which can result in discontinuities in the network products.

———————

ANNEX 7.A. WMO GUIDANCE STATEMENT ON WEATHER RADAR/RADIO FREQUENCY SHARED SPECTRUM USE

WMO expresses concern over increasing pressure on weather radar related radio-frequency bands and stresses the need for adequate protection and mitigation efforts against the loss and shared use of this spectrum. WMO addresses its concern to policymakers, to national radio-frequency administration agencies, to national hydrological and meteorological societies, to commercial vendors of telecommunication equipment and to the meteorological community.

Protection of traditional weather radar related radio frequencies is critical to the continued function and improvement of weather sensing, monitoring, forecasting, and warning, and is therefore in the best interests of public safety and security. The meteorological community increasingly relies on remote-sensing technologies for both routine and experimental observations of weather and climate. These activities require global access to the radio-frequency spectrum by not only radars but also wind profilers, microwave radiometers, and telemetry systems, as well as satellite-based passive and active sensors. The progress in weather warning services and other meteorological predictions made in recent years is largely attributable to these technologies.

Weather prediction models and localized operational forecasts increasingly depend on national networks of ground-based Doppler radars for severe weather warnings such as tornadoes, flash flooding, land-falling hurricanes, precipitation (rain, snow, hail) forecasts, aircraft icing and air traffic/weather avoidance. Worldwide, Doppler radar networks are now contending with increasing pressures on shared spectrum usage with unlicensed broadband wireless applications. As already experienced in Europe, the impacts of radio-frequency interference by wireless communications can render weather radars blind in particular directions or even over large portions of their coverage. The situation is exacerbated by the ubiquitous and unlicensed nature of these wireless applications that could lead to a total loss of the related spectrum for weather radars.

Development of new radar technologies, including adaptive scanning strategies, shorter pulses, polarization, pulse compression, frequency and phase agility is ongoing. Current and planned satellite radar systems measure clouds and precipitation, which is important for weather forecasting and global climate change research and assessment. Varieties of other space-based and ground-based radio technologies are currently in experimental use and may require future radio spectrum allocations.

New communication applications make the radio-frequency spectrum an extremely valuable commodity, and so the frequency bands used for operational meteorology and research are in increasing jeopardy. WMO and the meteorological community rely on and support mandated international and national radio-frequency agencies and promote cooperation with the telecommunication authorities and industries to continue to protect or to appropriately share these radio frequencies. WMO is intensively working with these agencies, through the International Telecommunication Union (ITU), to establish appropriate mechanisms to protect meteorological uses of the radio-frequency spectrum. WMO encourages the development of a clear definition of interference, permissible or otherwise, and a remedial process or solution if shared use becomes a problem. WMO encourages funding and implementation of studies to determine the impact of the total or partial loss of one or more frequency bands used by current operational observing systems and by planned systems. Further, WMO recommends that the results of these studies be made available to ITU radiocommunication groups and to national radio-frequency agencies and the telecommunications industry to encourage dialogue between active and passive users of the spectrum. Vigilance is necessary, as degradations of meteorological data due to intrusions or shared usage will evolve over time. Cooperation with national radio-frequency agencies, the telecommunications industry, and with other spectrum users is encouraged both to advocate support for critically important meteorological use of radio spectrum and to mitigate potential problems.

It is in all nations' best interests to protect radio frequencies essential for meteorological activities that are critical to the accurate forecasting of adverse weather. Global solutions are sought and should be advocated. WMO is actively participating in international frequency management activities, through a group of experts with global representation, to protect current frequency bands used in meteorology, climatology and Earth observations, as well as to obtain new bands required for research and operations.

Further information is available in a guide entitled *Use of Radio Spectrum for Meteorology: Weather, Water and Climate Monitoring and Prediction*, produced jointly by WMO and ITU.

———————

ANNEX 7.B. WMO GUIDANCE STATEMENT ON WEATHER RADAR/WIND TURBINE SITING

WMO expresses concern over increasing deployment of wind turbine farms and stresses the need for adequate consultation, protection and mitigation efforts. WMO addresses its concern to policymakers, to national radio administration agencies, to national hydrological and meteorological societies, to wind turbine farm developers, to commercial vendors of wind turbine equipment and to the meteorological community.

Protection of weather radar data is critical to the continued function and improvement of weather sensing, monitoring, forecasting, and warning, and is therefore in the best interests of public safety and security. Weather prediction models and localized operational forecasts increasingly depend on national networks of ground-based Doppler weather radars and wind profilers for severe weather warnings such as tornadoes, flash flooding, land-falling hurricanes, precipitation (rain, snow, hail) forecasts, aircraft icing and air traffic/weather avoidance. Worldwide, Doppler radar and wind profile networks are now contending with increasing pressures by wind farms.

Wind farms have already had an impact on operational weather radar networks, creating confounding ground echoes that create a significant loss of data or create false precipitation for hydrological applications. The rotating blades can create velocities which could potentially be mistaken to be severe weather such as a tornado. While weather radars have been voluntarily moved by the wind farm developers, generally, the meteorological community has no jurisdiction on the location of the wind farms and relies on cooperative "good neighbour" policies for mitigation.

Development of new radar and wind profiler networks and wind farms will require strategic planning for mitigation by the meteorological and wind farm communities. WMO and the meteorological community rely on and support mandated international and national radio agencies and will proactively encourage and support these agencies' efforts to promote and to protect the meteorological use of unobstructed space. WMO encourages national radio agencies to develop acceptable obstruction criteria and to provide tools to help the wind farm developer on site selection.

The range between wind turbines and the weather radar can be used to generally describe the impact on radar quality and also used to provide a mitigation strategy for cooperative siting of weather radars and wind turbines. Below are the general guidelines for typical radars and flat terrain situations, which may require modifications for specific situations and for particular radars. Higher powered radars such as S band (10 cm wavelength) radars with less attenuation may necessitate increasing the range limits in the table.

WMO encourages funding and implementation of studies to develop technologies to mitigate the impact. Weather radar signal processing techniques or use of other materials to construct wind turbines may be able to mitigate clutter at long ranges. Further, WMO recommends that the results of these studies be made available to commercial weather radar and wind turbine manufacturers.

It is in all nations' best interests to protect unobstructed space for weather radars and wind profilers that are essential and critical to the accurate forecasting of adverse weather. Local, national and technological solutions are sought. WMO will support and provide guidance material and tools to protect unobstructed space for weather radars and wind profilers.

Range	Potential impact	Guideline
0–5 km	The wind turbine may completely or partially block the radar and can result in significant loss of data that cannot be recovered.	Definite impact zone: Wind turbines should not be installed in this zone.
5–20 km	Multiple reflection and multi-path scattering can create false echoes and multiple elevations. Doppler velocity measurements may be compromised by rotating blades.	Moderate impact zone: Terrain effects will be a factor. Analysis and consultation is recommended. Reorientation or resiting of individual turbines may reduce or mitigate the impact.
20–45 km	Generally visible on the lowest elevation scan groundlike echoes will be observed in reflectivity Doppler velocities may be compromised by rotating blades.	Low impact zone: Notification is recommended.
> 45 km	Generally not observed in the data but can be visible due to propagation conditions.	Intermittent impact zone: Notification is recommended.

REFERENCES AND FURTHER READING

Ahnert, P.R., M. Hudlow, E. Johnson, D. Greene and M. Dias, 1983: Proposed on-site processing system for NEXRAD. *Preprints of the Twenty-first Conference on Radar Meteorology* (Edmonton, Canada), American Meteorological Society, Boston, 378–385.

Anagnostou, E.N., C.A. Morales and T. Dinku, 2001: The use of TRMM precipitation radar observations in determining ground radar calibration biases. *Journal of Atmospheric and Oceanic Technology*, 18(4):616–628.

Aoyagi, J., 1983: A study on the MTI weather radar system for rejecting ground clutter. *Papers in Meteorology and Geophysics*, 33(4):187–243.

Aoyagi, J. and N. Kodaira, 1995: The reflection mechanism of radar rain echoes. *Preprints of the Twenty-seventh Conference on Radar Meteorology* (Vail, Colorado), American Meteorological Society, Boston, 246–248.

Atlas, D., 1964: Advances in radar meteorology. In: *Advances in Geophysics* (H.E. Landsberg and J. Van Meighem, eds.). Academic Press, New York, 10:317–479.

——— (ed.), 1990: *Radar in Meteorology*. American Meteorological Society, Boston.

Atlas, D., R.C. Srivastava and R.S. Sekhon, 1973: Doppler radar characteristics of precipitation at vertical incidence. *Reviews of Geophysics and Space Physics*, 11(1):1–35.

Battan, L.J., 1973: *Radar Observation of the Atmosphere*. University of Chicago Press, Chicago.

Baynton, H.W., 1979: The case for Doppler radars along our hurricane affected coasts. *Bulletin of the American Meteorological Society*, 60(9):1014–1023.

Bean, B.R. and E.J. Dutton, 1966: *Radio Meteorology*. US Government Printing Office, Washington DC.

Bebbington, D.H.O., 1992: Degree of polarization as a radar parameter and its susceptibility to coherent propagation effects. *Preprints from URSI Commission F Symposium on Wave Propagation and Remote Sensing* (Ravenscar, United Kingdom), 431–436.

Bellon, A. and G.L. Austin, 1978: The evaluation of two years of real-time operation of a Short-Term Precipitation Forecasting Procedure (SHARP). *Journal of Applied Meteorology*, 17(12):1778–1787.

Berenguer, M., S. Park, D. Sempere-Torres, J. Didszun, M. Pool and M. Pfeifer, 2012: RAINSCANNER@Barcelona: an experiment to assess the hydrological value of a portable X-band radar. Preprints, *Seventh European Conference on Radar in Meteorology and Hydrology* (ERAD 2012), Toulouse, France.

Bringi, V.N. and V. Chandrasekar, 2001: *Polarimetric Doppler Weather Radar*, Cambridge University Press.

Bringi, V.N. and A. Hendry, 1990: Technology of polarization diversity radars for meteorology. In: *Radar in Meteorology* (D. Atlas, ed.). American Meteorological Society, Boston, 153–190.

Brown, R.A. and L.R. Lemon, 1976: Single Doppler radar vortex recognition: Part II – Tornadic vortex signatures. *Preprints of the Seventeenth Conference on Radar Meteorology* (Seattle, Washington), American Meteorological Society, Boston, 104–109.

Brown, R.A., V.T. Wood, R.M. Steadham, R.R. Lee, B.A. Flickinger and D. Sirmans, 2005: New WSR-88D Volume Coverage Pattern 12: Results of field tests. *Weather and Forecasting*, 20:385–393.

Browning, K.A. and C.G. Collier, 1982: An integrated radar-satellite nowcasting system in the United Kingdom. In: *Nowcasting* (K.A. Browning, ed.). Academic Press, London, 47–61.

Browning, K.A., C.G. Collier, P.R. Larke, P. Menmuir, G.A. Monk and R.G. Owens, 1982: On the forecasting of frontal rain using a weather radar network. *Monthly Weather Review*, 110:534–552.

Browning, K.A. and R. Wexler, 1968: The determination of kinematic properties of a wind field using Doppler radar. *Journal of Applied Meteorology*, 7:105–113.

Brunkow, D., 2001: *Sphere Calibrations, The Most Hated Experiment in Radar Meteorology*, RADCAL 2000 Workshop, AMS Short Course, Albuquerque, NM.

Burgess, D.W., 1976: Single Doppler radar vortex recognition: Part I – Mesocyclone signatures. *Preprints of the Seventeenth Conference on Radar Meteorology* (Seattle, Washington), American Meteorological Society, Boston, 97–103.

Burgess, D.W. and L.R. Lemon, 1990: Severe thunderstorm detection by radar. In: *Radar in Meteorology* (D. Atlas, ed.). American Meteorological Society, Boston, 619–647.

Burrows, C.R. and S.S. Attwood, 1949: *Radio Wave Propagation*. Academic Press, New York.

Byers, H.R., 1948: The use of radar in determining the amount of rain falling over a small area. *Transactions of the American Geophysical Union*, 187–196.

Chandrasekar, V. and L. Baldini, 2013: *RADCAL 2013*, AMS Short Course, Fort Collins, CO.

Chandrasekar, V., R. Meneghini and I. Zawadzki, 2003: Global and local precipitation measurements by radar. *Meteorological Monographs*, 30(52):215–215.

Cluckie, I.D. and M.E. Owens, 1987: Real-time rainfall run-off models and use of weather radar information. In: *Weather Radar and Flood Forecasting* (V.K. Collinge and C. Kirby, eds.). John Wiley and Sons, New York.

Collier, C.G., 1989: *Applications of Weather Radar Systems: A Guide to Uses of Radar Data in Meteorology and Hydrology.* John Wiley and Sons, Chichester, England.

Commission of the European Communities, 1990: *Une revue du programme ARAMIS* (J.L. Cheze). Seminar on Cost Project 73: Weather Radar Networking (Brussels, 5–8 September 1989), 80–85.

Crook, N.A. and J. Sun, 2002: Assimilating radar, surface, and profiler data for the Sydney 2000 Forecast Demonstration Project. *Journal of Atmospheric and Oceanic Technology*, 19:888–898.

Crozier, C.L., P. Joe, J. Scott, H. Herscovitch and T. Nichols, 1991: The King City operational Doppler radar: Development, all-season applications and forecasting. *Atmosphere-Ocean*, 29:479–516.

Crum, T.D. and R.L. Alberty, 1993: The WSR-88D and the WSR-88D Operational Support Facility. *Bulletin of the American Meteorological Society*, 74(9):1669–1687.

Dennis, A.S., C.A. Schock and A. Koscielski, 1970: Characteristics of hailstorms of western South Dakota. *Journal of Applied Meteorology*, 9:127–135.

Dexter, P.E., M.L. Heron and J.F. Ward, 1982: Remote sensing of the sea-air interface using HF radars. *Australian Meteorological Magazine*, 30:31–41.

Dixon, M. and G. Wiener, 1993: TITAN: Thunderstorm identification, tracking, analysis, and nowcasting – A radar-based methodology. *Journal of Atmospheric and Oceanic Technology*, 10(6):785–797.

Donaldson, R.J., Jr., 1970: Vortex signature recognition by a Doppler radar. *Journal of Applied Meteorology*, 9:661–670.

Doneaud, A.A., S. Ionescu-Niscov, D.L. Priegnitz and P.L. Smith, 1984: The area-time integral as an indicator for convective rain volumes. *Journal of Climate and Applied Meteorology*, 23:555–561.

Doneaud, A.A., J.R. Miller Jr., L.R. Johnson, T.H. Vonder Haar and P. Laybe, 1987: The area-time integral technique to estimate convective rain volumes over areas applied to satellite data: A preliminary investigation. *Journal of Climate and Applied Meteorology*, 26:156–169.

Doviak, R.J. and D.S. Zrnić, 1993: *Doppler Radar and Weather Observations*. Second edition, Academic Press, San Diego.

Dupuy, P., S. Matthews, N. Gaussia, R. Scovel and A. Kergomard, 2010: Developing a European Radar Data Centre. Preprints, *Sixth European Conference on Radar in Meteorology and Hydrology* (ERAD 2010), Sibiu, Romania.

Eccles, P.J. and D. Atlas, 1973: A dual-wavelength radar hail detector. *Journal of Applied Meteorology*, 12:847–854.

Eilts, M.D. and S.D. Smith, 1990: Efficient dealiasing of Doppler velocities using local environment constraints. *Journal of Atmospheric and Oceanic Technology*, 7:118–128.

English, M.E., B. Kochtubajda, F.D. Barlow, A.R. Holt and R. McGuiness, 1991: Radar measurement of rainfall by differential propagation phase: A pilot experiment. *Atmosphere-Ocean*, 29:357–380.

Fabry, F., 2004: Meteorological value of ground target measurements by radar. *Journal of Atmospheric and Oceanic Technology*, 21:560–573.

Fabry, F., C. Augros and A. Bellon, 2013: The case of sharp velocity transitions in high vertical wind shear when measuring Doppler velocities with narrow Nyquist intervals. *Journal of Atmospheric and Oceanic Technology*, 30:389–394.

Federer, B., A. Waldvogel, W. Schmid, F. Hampel, Rosini, D. Vento and P. Admirat, 1978: Grossversuch IV: Design of a randomized hail suppression experiment using the Soviet method. *Pure and Applied Geophysics*, 117:548–571.

Frush, C., R.J. Doviak, M. Sachidananda and D.S. Zrnić, 2002: Application of the SZ phase code to mitigate range – Velocity ambiguities in weather radars. *Journal of Atmospheric and Oceanic Technology*, 19:413–430.

Germann, U., G. Galli, M. Boscacci and M. Bolliger, 2006a: Radar precipitation measurement in a mountainous region. *Quarterly Journal of the Royal Meteorological Society*, 132:1669–1692.

Germann, U., I. Zawadzki and B. Turner, 2006b: Predictability of precipitation from continental radar images. Part IV: Limits to prediction. *Journal of the Atmospheric Sciences*, 63:2092–2108.

Gossard, E.E. and R.G. Strauch, 1983: *Radar Observations of Clear Air and Clouds*. Elsevier Scientific Publication, Amsterdam.

Harlan, J.A. and T.M. Georges, 1994: An empirical relation between ocean-surface wind direction and the Bragg line ratio of HF radar sea echo spectra. *Journal of Geophysical Research: Oceans*, 99(C4):7971–7978.

Heiss, W.H., D.L. McGrew and D. Sirmans, 1990: NEXRAD: Next generation weather radar (WSR-88D). *Microwave Journal*, 33(1):79–98.

Holleman, I., 2001: *Hail Detection Using Single-polarization Radar.* Scientific Report, Royal Netherlands Meteorological Institute (KNMI), WR-2001-01, De Bilt.

Holleman, I., H.R.A. Wessels, J.R.A. Onvlee and S.J.M. Barlag, 2000: Development of a hail-detection product. *Physics and Chemistry of the Earth*, Part B, 25:1293–1297.

Holt, A.R., M. Chandra and S.J. Wood, 1995: Polarisation diversity radar observations of storms at C-band. *Preprints of the Twenty-seventh Conference on Radar Meteorology* (Vail, Colorado), American Meteorological Society, Boston, 188–189.

Holt, A.R., P.I. Joe, R. McGuinness and E. Torlaschi, 1993: Some examples of the use of degree of polarization in interpreting weather radar data. *Proceedings of the Twenty-sixth International Conference on Radar Meteorology*, American Meteorological Society, 748–750.

Hubbert, J.C., M. Dixon, S.M. Ellis and G. Meymaris, 2009*a*: Weather radar ground clutter. Part I: Identification, modeling, and simulation. *Journal of Atmospheric and Oceanic Technology*, 26:1165–1180.

Hubbert, J.C., M. Dixon and S.M. Ellis, 2009*b*: Weather radar ground clutter. Part II: Real-time identification and filtering. *Journal of Atmospheric and Oceanic Technology*, 26:1181–1197.

Joe, P., 1999: Beamheight Statistics for Low Elevation Scans. Paper, *Twenty-ninth AMS Radar Conference*, Montreal, American Meteorological Society, Boston, 922–925.

———, 2001: RADCAL 2000 Workshop, AMS Short Course, Albuquerque, NM.

———, 2010: RADMON Workshop, *Sixth European Conference on Radar in Meteorology and Hydrology* (ERAD 2010), Sibiu, Romania.

Joe, P., D. Burgess, R. Potts, T. Keenan, G. Stumpf and A. Treloar, 2004: The S2K severe weather detection algorithms and their performance. *Weather and Forecasting*, 19:43–63.

Joe, P., S. Dance, V. Lakshmanan, D. Heizenrehder, P. James, P. Lang, T. Hengstebeck, Y. Feng, P.W. Li, H.Y. Yeung, O. Suzuki, K. Doi and J. Dai, 2012: Automated processing of Doppler radar data for severe weather forecasting. In: *Doppler Radar Observations, Weather Radar, Wind Profiler, Ionospheric Radar and other Advanced Applications* (J. Bech and J.L. Chau, eds.), Intech.

Joe, P., M. Falla, P. Van Rijn, L. Stamadianos, T. Falla, D. Magosse, L. Ing and J. Dobson, 2002: Radar data processing for severe weather in the national radar project of Canada. Preprints, *Twenty-first Conference on Severe Local Storms*, San Antonio, 12–16 August 2002, 221–224.

Joe, P. and P.T. May, 2003: Correction of dual PRF velocity errors for operational Doppler weather radars. *Journal of Atmospheric and Oceanic Technology*, 20(4):429–442.

Joe, P., R.E. Passarelli and A.D. Siggia, 1995: Second trip unfolding by phase diversity processing. *Preprints of the Twenty-seventh Conference on Radar Meteorology* (Vail, Colorado), American Meteorological Society, Boston, 770–772.

Joe, P., B. Scott, C. Doyle, G. Isaac, I. Gultepe, D. Forsyth, S. Cober, E. Campos, I. Heckman, N. Donaldson, D. Hudak, R. Rasmussen, R. Stewart, J.M. Thériault, H. Carmichael, M. Bailey and F. Boudala, 2014: The monitoring network of the Vancouver 2010 Olympics. *Pure and Applied Geophysics*, 171(1):25–58.

Joint Doppler Operational Project (JDOP), 1979: *Final Report on the Joint Doppler Operational Project.* NOAA Technical Memorandum, ERL NSSL-86, Norman, Oklahoma, National Severe Storms Laboratory.

Joss, J. and R.W. Lee, 1993: Scan strategy, clutter suppression calibration and vertical profile corrections. *Preprints of the Twenty-sixth Conference on Radar Meteorology* (Norman, Oklahoma), American Meteorological Society, Boston, 390–392.

Joss, J. and A. Waldvogel, 1990: Precipitation measurement and hydrology. In: *Radar in Meteorology* (D. Atlas, ed.). American Meteorological Society, Boston, 577–606.

Keeler, R.J., C.A. Hwang and E. Loew, 1995: Pulse compression weather radar waveforms. *Preprints of the Twenty-seventh Conference on Radar Meteorology* (Vail, Colorado), American Meteorological Society, Boston, 767–769.

Keenan, T.D. and S.J. Anderson, 1987: Some examples of surface wind field analysis based on Jindalee skywave radar data. *Australian Meteorological Magazine*, 35:153–161.

Lakshmanan, V., T. Smith, G. Stumpf and K. Hondl, 2007: The Warning Decision Support System–Integrated Information. *Weather and Forecasting*, 22:596–612.

Leber, G.W., C.J. Merrit and J.P. Robertson, 1961: WSR-57 analysis of heavy rains. *Preprints of the Ninth Weather Radar Conference*, American Meteorological Society, Boston, 102–105.

Lee, R., G. Della Bruna and J. Joss, 1995: Intensity of ground clutter and of echoes of anomalous propagation and its elimination. *Preprints of the Twenty-seventh Conference on Radar Meteorology* (Vail, Colorado), American Meteorological Society, Boston, 651–652.

Lemon, L.R., 1978: *New Severe Thunderstorm Radar Identification Techniques and Warning Criteria: A Preliminary Report*. NOAA Technical Memorandum, NWS NSSFC-1, Kansas City, National Severe Storms Forecast Center.

——, 1998: The radar "three-body scatter spike": An operational large-hail signature. *Weather and Forecasting*, 13:327–340.

Lemon, L.R., D.W. Burgess and R.A. Brown, 1978: Tornadic storm airflow and morphology derived from single-Doppler radar measurements. *Monthly Weather Review*, 106:48–61.

Leone, D.A., R.M. Endlich, J. Petriceks, R.T.H. Collis and J.R. Porter, 1989: Meteorological considerations used in planning the NEXRAD network. *Bulletin of the American Meteorological Society*, 70:4–13.

Lhermitte, R. and D. Atlas, 1961: Precipitation motion by pulse Doppler radar. *Preprints of the Ninth Weather Radar Conference*, American Meteorological Society, Boston, 218–233.

Lopez, P., 2011: Direct 4D-Var assimilation of NCEP stage IV radar and gauge precipitation data at ECMWF. *Monthly Weather Review*, 139:2098–2116.

Makihara, Y., 2000: Algorithms for precipitation nowcasting focused on detailed analysis using radar and raingauge data. *Technical Report of the Meteorological Research Institute*, Japan Meteorological Agency, 39:63–111.

Markowski, P.M., 2002: Hook echoes and rear-flank downdrafts: A review. *Monthly Weather Review*, 130:852–876.

Marshall, J.S. and E.H. Ballantyne, 1978: Weather Surveillance Radar. *Journal of Applied Meteorology*, 14(7):1317–1338.

Marshall, J.S. and K.L.S. Gunn, 1952: Measurement of snow parameters by radar. *Journal of Meteorology*, 9:322–327.

Marshall, J.S. and W.M. Palmer, 1948: The distribution of raindrops with size. *Journal of Meteorology*, 5:165–166.

McLaughlin, D., D. Pepyne, B. Philips, J. Kurose, M. Zink, D. Westbrook, E. Lyons, E. Knapp, A. Hopf, A. Defonzo, R. Contreras, T. Djaferis, E. Insanic, S. Frasier, V. Chandrasekar, F. Junyent, N. Bharadwaj, Y. Wang, Y. Liu, B. Dolan, K. Droegemeier, J. Brotzge, M. Xue, K. Kloesel, K. Brewster, F. Carr, S. Cruz-Pol, K. Hondl and P. Kollias, 2009: Short-wavelength technology and the potential for distributed networks of small radar systems. *Bulletin of the American Meteorological Society*, 90(12):1797–1817.

Meischner, P. (ed.), 2003: *Weather Radar: Principles and Advanced Applications*, Springer, Berlin.

Melnikov, V., D.S. Zrnić, R.J. Dovink and J.K. Carter, 2002: Status of the dual polarization upgrade on the NOAA's research and development WSR-88D. *Preprints of the Eighteenth International Conference on Interactive Information Processing Systems* (Orlando, Florida), American Meteorological Society, Boston, 124–126.

Michelson, D., R. Gill, M. Peura and J. Szturc, 2010: Community-based weather radar networking with BALTRAD. Preprints, *Sixth European Conference on Radar in Meteorology and Hydrology* (ERAD 2010), Sibiu, Romania.

Michelson, D.B., P.I. Joe, D. Lockett, S. Goldstraw, L. Bai, A. Becker, K.P. Georgakakos, S. Foreman, E. Fucile, R. Giraud, N. Gaussiat, T. Hohmann, A. Kamilliddin, M. Kitchen, E. Kyte, J.F. Mahfouf, S. Matthews, J.M. de Rezende, O. Sireci, M.A. de Barros Teixeira and E. Wattrelot, 2013: WMO initiative for the global exchange of radar data. Manuscript, *Thirty-sixth AMS Radar Meteorology Conference*, Breckenridge, CO, American Meteorological Society.

Michelson, M., W.W. Schrader and J.G. Wilson, 1990: Terminal Doppler weather radar. *Microwave Journal*, 33(2):139–148.

Mie, G., 1908: Beiträge zur Optik träber Medien, speziell kolloidaler Metalläsungen. *Annalen der Physik*, 25:377–445.

Mueller, C.K. and R.E. Carbone, 1987: Dynamics of a thunderstorm outflow. *Journal of the Atmospheric Sciences*, 44:1879–1898.

Mueller, E.A., S.A. Rutledge, V.N. Bringi, D. Brunkow, P.C. Kennedy, K. Pattison, R. Bowie and V. Chandrasekar, 1995: CSU-CHILL radar upgrades. *Preprints of the Twenty-seventh Conference on Radar Meteorology* (Vail, Colorado), American Meteorological Society, Boston, 703–706.

Neff, E.L., 1977: How much rain does a rain gauge gage? *Journal of Hydrology*, 35:213–220.

Passarelli, R.E., Jr., P. Romanik, S.G. Geotis and A.D. Siggia, 1981: Ground clutter rejection in the frequency domain. *Preprints of the Twentieth Conference on Radar Meteorology* (Boston, Massachusetts), American Meteorological Society, Boston, 295–300.

Probert-Jones, J.R., 1962: The radar equation in meteorology. *Quarterly Journal of the Royal Meteorological Society*, 88:485–495.

Ray, P.S., C.L. Ziegler, W. Bumgarner and R.J. Serafin, 1980: Single- and multiple-Doppler radar observations of tornadic storms. *Monthly Weather Review*, 108:1607–1625.

Rinehart, R.E., 2004: *Radar for Meteorologists*. 4th Edition, Rinehart Publishing.

Ruggiero, F.H. and R.J. Donaldson, Jr., 1987: Wind field derivatives: A new diagnostic tool for analysis of hurricanes by a single Doppler radar. *Preprints of the Seventeenth Conference on Hurricanes and Tropical Meteorology* (Miami, Florida), American Meteorological Society, Boston, 178–181.

Sauvageot, H., 1982: *Radarmétéorologie*. Eyrolles, Paris.

——, 1994: Rainfall measurement by radar: A review. *Atmospheric Research*, 35:27–54.

Seed, A.W., 2003: A dynamic and spatial scaling approach to advection forecasting. *Journal of Applied Meteorology*, 42(3):381–388.

Seliga, T.A. and V.N. Bringi, 1976: Potential use of radar differential reflectivity measurements at orthogonal polarizations for measuring precipitation. *Journal of Applied Meteorology*, 15:69–76.

Seltmann, J.E.E., T. Hohmann, M. Frech and P. Tracksdorf, 2013: DWD's new operational scan strategy. *Thirty-sixth AMS Radar Meteorology Conference*, 16–20 September 2013, Breckenridge, CO, poster 329.

Shearman, E.D.R., 1983: Radio science and oceanography. *Radio Science*, 18(3):299–320.

Sireci, O., P. Joe, S. Eminoglu and K. Akylidiz, 2010: A comprehensive worldwide web-based weather radar database. Preprints, *Sixth European Conference on Radar in Meteorology and Hydrology* (ERAD 2010), Sibiu, Romania.

Skolnik, M.I. (ed.), 1970: *Radar Handbook*. McGraw-Hill, New York.

—— (ed.), 1990: *Radar Handbook*. Second edition, McGraw-Hill, New York.

Smith, P.L., 1990: Precipitation measurement and hydrology: Panel report. In: *Radar in Meteorology* (D. Atlas, ed.). American Meteorological Society, Boston, 607–618.

——, 1995: Dwell time considerations for weather radars. *Preprints of the Twenty-seventh Conference on Radar Meteorology* (Vail, Colorado), American Meteorological Society, Boston, 760–762.

Smull, B.S. and R.A. Houze Jr., 1987: Rear inflow in squall lines with trailing stratiform precipitation. *Monthly Weather Review*, 115(12):2869–2889.

Strauch, R.G., 1981: Comparison of meteorological Doppler radars with magnetron and klystron transmitters. *Preprints of the Twentieth Conference on Radar Meteorology* (Boston, Massachusetts), American Meteorological Society, Boston, 211–214.

Sun, J., M. Xue, J.W. Wilson, I. Zawadzki, S.P. Ballard, J. Onvlee-Hooimeyer, P. Joe, D. Barker, P.W. Li, B. Golding, M. Xu and J. Pinto, 2013: Use of NWP for nowcasting convective precipitation: Recent progress and challenges. *Bulletin of the American Meteorological Society*, 95:409–426.. *Bulletin of the American Meteorological Society*, 95:409–426.

Tapping, K., 2001: Antenna Calibration using 10.7cm Solar Flux, RADCAL 2000, AMS Short Course, Albuquerque, NM.

Treloar, A., 1998: Vertically integrated radar reflectivity as an indicator of hail size in the greater Sydney region of Australia. *Preprints of the Nineteenth Conference on Severe Local Storms*, Minneapolis, MN, American Meteorological Society, 48–51.

Turner, B.J., I. Zawadzki and U. Germann, 2004: Predictability of precipitation from continental radar images. Part III: Operational nowcasting implementation (MAPLE). *Journal of Applied Meteorology*, 43:231–248.

Ulbrich, C.W. and D. Atlas, 1984: Assessment of the contribution of differential polarization to improve rainfall measurements. *Radio Science*, 19(1):49–57.

Weber, M.E., J.Y.N. Cho, J.S. Herd, J.M. Flavin, W.E. Benner and G.S. Torok, 2007: The next-generation multimission U.S. surveillance radar network. *Bulletin of the American Meteorological Society*, 88(11):1739–1751.

Wiener, N., 1964: *Time Series*. M.I.T. Press, Cambridge, Massachusetts.

Wilson, J.W. and E.A. Brandes, 1979: Radar measurement of rainfall – A summary. *Bulletin of the American Meteorological Society*, 60(9):1048–1058.

Wilson, J.W., N.A. Crook, C.K. Mueller, J. Sun and M. Dixon, 1998: Nowcasting thunderstorms: A status report. *Bulletin of the American Meteorological Society*, 79(10):2079–2099.

Wilson, J.W. and W.E. Schreiber, 1986: Initiation of convective storms at radar-observed boundary-layer convergence lines. *Monthly Weather Review*, 114:2516–2536.

Wilson, J.W., T.M. Weckwerth, J. Vivekanandan, R.M. Wakimoto, R.W. Russell, 1994: Origin of echoes and accuracy of derived winds. *Journal of Atmospheric and Oceanic Technology*, 11(5):1184–1206.

Witt, A., M. Eilts, G. Stumpf, J. Johnson, D. Mitchell and K. Thomas, 1998: An enhanced hail detection algorithm for the WSR-88D. *Weather and Forecasting*, 13:286–303.

Wolff, D.B. and B.L. Kelley, 2009: NASA's Radar Software Library (RSL) and RSL in IDL. Paper, *Thirty-fourth AMS Radar Conference*, Breckenridge, CO.. Paper, *Thirty-fourth AMS Radar Conference*, Breckenridge, CO.

Wood, V.T. and R.A. Brown, 1986: Single Doppler velocity signature interpretation of nondivergent environmental winds. *Journal of Atmospheric and Oceanic Technology*, 3:114–128.

World Meteorological Organization, 1985: *Use of Radar in Meteorology* (G.A. Clift). Technical Note No. 181 (WMO-No. 625). Geneva.

———, 2012: Operational use of dual-polarisation: lessons learned at Météo France after 8 years of experience at all wavelengths (S/C/X) (P. Tabary). *Papers Presented at the WMO Technical Conference on Meteorological and Environmental Instruments and Methods of Observation (TECO-2012)*. Instruments and Observing Methods Report No. 109. Geneva.

Wurman, J., M. Randall and C. Burghart, 1995: Real-time vector winds from a bistatic Doppler radar network. *Preprints of the Twenty-seventh Conference on Radar Meteorology* (Vail, Colorado), American Meteorological Society, Boston, 725–728.

Wurman, J., J.M. Straka and E.N. Rasmussen, 1996 : Fine-scale Doppler radar observations of tornadoes. *Science*, 272:1774–1777.

Xue, M., K. Kloesel, K. Brewster, F. Carr, S. Cruz-Pol, K. Hondl and P. Kollias, 2009: Short-wavelength technology and the potential for distributed networks of small radar systems. *Bulletin of the American Meteorological Society*, 90(12):1797–1817.

Yamauchi, H., A. Adachi, O. Suzuki and T. Kobayashi, 2013: Precipitation estimate of a heavy rain event using a C-band solid-state polarimetric radar. Preprints, *Seventh European Conference on Radar in Meteorology and Hydrology* (ERAD 2012), Toulouse, France.

Zhang, J., K. Howard and J.J. Gourley, 2005: Constructing three-dimensional multiple-radar reflectivity mosaics: Examples of convective storms and stratiform rain echoes. *Journal of Atmospheric and Oceanic Technology*, 22:30–42.

Zrnić, D.S. and S. Hamidi, 1981: *Considerations for the Design of Ground Clutter Cancelers for Weather Radar*. Report DOT/FAA/RD-81/72, NTIS.

Zrnić, D.S. and A.V. Ryzhkov, 1995: Advantages of rain measurements using specific differential phase. *Preprints of the Twenty-seventh Conference on Radar Meteorology* (Vail, Colorado), American Meteorological Society, Boston, 35–37.

Zrnić, D.S., A. Ryzhkov, J. Straka, Y. Liu and J. Vivekanandan, 2001: Testing a procedure for automatic classification of hydrometeor types. *Journal of Atmospheric and Oceanic Technology*, 18:892–913.

Zrnić, D.S., G. Zhang, V. Melnikov and J. Andric, 2010: Three-body scattering and hail size. *Journal of Applied Meteorology and Climatology*, 49:687–700.

_____

CHAPTER CONTENTS

CHAPTER 8. BALLOON TECHNIQUES

8.1 BALLOONS

8.1.1 Main types of balloons

Two main categories of balloons are used in meteorology, as follows:

(a) Pilot balloons, which are used for the visual measurement of upper wind, and ceiling balloons for the measurement of cloud-base height. Usually they do not carry an appreciable load and are therefore considerably smaller than radiosonde balloons. They are almost invariably of the spherical extensible type and their chief requirement, apart from the ability to reach satisfactory heights, is that they should keep a good spherical shape while rising;

(b) Balloons which are used for carrying recording or transmitting instruments for routine upper-air observations are usually of the extensible type and spherical in shape. They are usually known as radiosonde or sounding balloons. They should be of sufficient size and quality to enable the required load (usually 200 g to 1 kg) to be carried up to heights as great as 35 km at a rate of ascent sufficiently rapid to enable reasonable ventilation of the measuring elements. For the measurement of upper winds by radar methods, large pilot balloons (100 g) or radiosonde balloons are used depending on the weight and drag of the airborne equipment.

Other types of balloons used for special purposes are not described in this chapter. Constant-level balloons that rise to, and float at, a pre-determined level are made of inextensible material. Large constant-level balloons are partly filled at release. Super-pressure constant-level balloons are filled to extend fully the balloon at release. Tetroons are small super-pressure constant-level balloons, tetrahedral in shape, used for trajectory studies. The use of tethered balloons for profiling is discussed in Part II, Chapter 5.

8.1.2 Balloon materials and properties

The best basic materials for extensible balloons are high-quality natural rubber latex and a synthetic latex based upon polychloroprene. Natural latex holds its shape better than polychloroprene – which is stronger and can be made with a thicker film for a given performance. It is less affected by temperature, but more affected by the ozone and ultraviolet radiation at high altitudes, and has a shorter storage life. Both materials may be compounded with various additives to improve their storage life, strength and performance at low temperatures both during storage and during flight, and to resist ozone and ultraviolet radiation. As one of the precautions against explosion, an antistatic agent may also be added during the manufacture of balloons intended to be filled with hydrogen.

There are two main processes for the production of extensible balloons. A balloon may be made by dipping a form into latex emulsion, or by forming it on the inner surface of a hollow mould. Moulded balloons can be made with more uniform thickness, which is desirable for achieving high altitudes as the balloon expands, and the neck can be made in one piece with the body, which avoids the formation of a possible weak point.

Polyethylene is the inextensible material used for constant-level balloons.

8.1.3 Balloon specifications

The finished balloons should be free from foreign matter, pinholes or other defects and must be homogeneous and of uniform thickness. They should be provided with necks of

between 1 and 5 cm in diameter and 10 to 20 cm long, depending on the size of the balloon. In the case of sounding balloons, the necks should be capable of withstanding a force of 200 N without damage. In order to reduce the possibility of the neck being pulled off, it is important that the thickness of the envelope should increase gradually towards the neck; a sudden discontinuity of thickness forms a weak spot.

Balloons are distinguished in size by their nominal weights in grams. The actual weight of individual balloons should not differ from the specified nominal weight by more than 10%, or preferably 5%. They should be capable of expanding to at least four times, and preferably five or six times, their unstretched diameter and of maintaining this expansion for at least 1 h. When inflated, balloons should be spherical or pear-shaped.

The question of specified shelf life of balloons is important, especially in tropical conditions. Artificial ageing tests exist but they are not reliable guides. One such test is to keep sample balloons in an oven at a temperature of 80 °C for four days, this being reckoned as roughly equivalent to four years in the tropics, after which the samples should still be capable of meeting the minimum expansion requirement. Careful packing of the balloons so that they are not exposed to light (especially sunlight), fresh air or extremes of temperature is essential if rapid deterioration is to be prevented.

Balloons manufactured from synthetic latex incorporate a plasticizer to resist the stiffening or freezing of the film at the low temperatures encountered near and above the tropopause. Some manufacturers offer alternative balloons for daytime and night-time use, the amount of plasticizer being different.

8.2   BALLOON BEHAVIOUR

8.2.1   Rate of ascent

From the principle of buoyancy, the total lift of a balloon is given by the buoyancy of the volume of gas in it, as follows:

$$T = V\left(\rho - \rho_g\right) = 0.523\, D^3\left(\rho - \rho_g\right) \tag{8.1}$$

where T is the total lift; V is the volume of the balloon; ρ is the density of the air; ρ_g is the density of the gas; and D is the diameter of the balloon, which is assumed to be spherical.

All units are in the International System of Units. For hydrogen at ground level, the buoyancy $(\rho - \rho_g)$ is about 1.2 kg m^{-3}. All the quantities in equation 8.1 change with height.

The free lift L of a balloon is the amount by which the total lift exceeds the combined weight W of the balloon and its load (if any):

$$L = T - W \tag{8.2}$$

namely, it is the net buoyancy or the additional weight which the balloon, with its attachments, will just support without rising or falling.

It can be shown by the principle of dynamic similarity that the rate of ascent V of a balloon in still air can be expressed by a general formula:

$$V = \frac{qL^n}{\left(L + W\right)^{1/3}} \tag{8.3}$$

in which q and n depend on the drag coefficient, and therefore on the Reynolds number, $v\rho D/\mu$ (μ being the viscosity of the air). Unfortunately, a large number of meteorological balloons, at some stages of flight, have Reynolds numbers within the critical region of $1 \cdot 10^5$ to $3 \cdot 10^5$, where a rapid change of drag coefficient occurs, and they may not be perfectly spherical. Therefore, it is impracticable to use a simple formula which is valid for balloons of different sizes and different free lifts. The values of q and n in the above equation must, therefore, be derived

by experiment; they are typically, very approximately, about 150 and about 0.5, respectively, if the ascent rate is expressed in m min^{-1}. Other factors, such as the change of air density and gas leakage, can also affect the rate of ascent and can cause appreciable variation with height.

In conducting soundings during precipitation or in icing conditions, a free lift increase of up to about 75%, depending on the severity of the conditions, may be required. An assumed rate of ascent should not be used in any conditions other than light precipitation. A precise knowledge of the rate of ascent is not usually necessary except in the case of pilot- and ceiling-balloon observations, where there is no other means of determining the height. The rate of ascent depends largely on the free lift and air resistance acting on the balloon and train. Drag can be more important, especially in the case of non-spherical balloons. Maximum height depends mainly on the total lift and on the size and quality of the balloon.

8.2.2 Balloon performance

The table in this section lists typical figures for the performance of various sizes of balloons. They are very approximate. If precise knowledge of the performance of a particular balloon and train is necessary, it must be obtained by analysing actual flights. Balloons can carry payloads greater than those listed in the table if the total lift is increased. This is achieved by using more gas and by increasing the volume of the balloon, which will affect the rate of ascent and the maximum height.

Typical balloon performance

Weight (g)	10	30	100	200	350	600	1 000	1 500	3 000
Diameter at release (cm)	30	50	90	120	130	140	160	180	210
Payload (g)	0	0	0	250	250	250	250	1 000	1 000
Free lift (g)	5	60	300	500	600	900	1 100	1 300	1 700
Rate of ascent (m min^{-1})	60	150	250	300	300	300	300	300	300
Maximum height (km)	12	13	20	21	26	31	34	34	38

The choice of a balloon for meteorological purposes is dictated by the load, if any, to be carried, the rate of ascent, the altitude required, whether the balloon is to be used for visual tracking, and by the cloud cover with regard to its colour. Usually, a rate of ascent between 300 and 400 m min^{-1} is desirable in order to minimize the time required for observation; it may also be necessary in order to provide sufficient ventilation for the radiosonde sensors. In choosing a balloon, it is also necessary to bear in mind that the altitude attained is usually less when the temperature at release is very low.

For balloons used in regular operations, it is beneficial to determine the free lift that produces optimum burst heights. For instance, it has been found that a reduction in the average rate of ascent from 390 to 310 m min^{-1} with some mid-size balloons by reducing the amount of gas for inflation may give an increase of 2 km, on average, in the burst height. Burst height records should be kept and reviewed to ensure that optimum practice is sustained.

Daytime visual observations are facilitated by using uncoloured balloons on clear sunny days, and dark-coloured ones on cloudy days.

The performance of a balloon is best gauged by the maximum linear extension it will withstand before bursting and is conveniently expressed as the ratio of the diameter (or circumference) at burst to that of the unstretched balloon. The performance of a balloon in flight, however, is not necessarily the same as that indicated by a bursting test on the ground. Performance can be affected by rough handling when the balloon is filled and by stresses induced during launches

in gale conditions. In flight, the extension of the balloon may be affected by the loss of elasticity at low temperatures, by the chemical action of oxygen, ozone and ultraviolet radiation, and by manufacture faults such as pinholes or weak spots. A balloon of satisfactory quality should, however, give at least a fourfold extension in an actual sounding. The thickness of the film at release is usually in the range of 0.1 to 0.2 mm.

There is always a small excess of pressure p_1 within the balloon during ascent, amounting to a few hPa, owing to the tension of the rubber. This sets a limit to the external pressure that can be reached. It can be shown that, if the temperature is the same inside and outside the balloon, this limiting pressure p is given by:

$$p = \left(\frac{1.07W}{L_0} + 0.075 \right) p_1 \cong \frac{Wp_1}{L_0} \tag{8.4}$$

where W is the weight of the balloon and apparatus; and L_0 is the free lift at the ground, both expressed in grams. If the balloon is capable of reaching the height corresponding with p, it will float at this height.

8.3 HANDLING BALLOONS

8.3.1 Storage

It is very important that radiosonde balloons should be correctly stored if their best performance is still to be obtained after several months. It is advisable to restrict balloon stocks to the safe minimum allowed by operational needs. Frequent deliveries, wherever possible, are preferable to purchasing in large quantities with consequent long periods of storage. To avoid the possibility of using balloons that have been in storage for a long period, balloons should always be used in the order of their date of manufacture.

It is generally possible to obtain the optimum performance up to about 18 months after manufacture, provided that the storage conditions are carefully chosen. Instructions are issued by many manufacturers for their own balloons and these should be observed meticulously. The following general instructions are applicable to most types of radiosondes balloons.

Balloons should be stored away from direct sunlight and, if possible, in the dark. At no time should they be stored adjacent to any source of heat or ozone. Balloons made of either polychloroprene or a mixture, or polychloroprene and natural rubber may deteriorate if exposed to the ozone emitted by large electric generators or motors. All balloons should be kept in their original packing until required for preflight preparations. Care should be taken to see that they do not come into contact with oil or any other substance that may penetrate the wrapping and damage the balloons.

Wherever possible, balloons should be stored in a room at temperatures of 15 to 25 °C; some manufacturers give specific guidance on this point and such instructions should always be followed.

8.3.2 Conditioning

Balloons made from natural rubber do not require special heat treatment before use, as natural rubber does not freeze at the temperatures normally experienced in buildings used for human occupation. It is, however, preferable for balloons that have been stored for a long period at temperatures below 10 °C to be brought to room temperature for some weeks before use.

Polychloroprene balloons suffer a partial loss of elasticity during prolonged storage at temperatures below 10 °C. For the best results, this loss should be restored prior to inflation by conditioning the balloon. The manufacturer's recommendations should be followed.

It is common practice to place the balloon in a thermally insulated chamber with forced air circulation, maintained at suitable temperature and humidity for some days before inflation, or alternatively to use a warm water bath.

At polar stations during periods of extremely low temperatures, the balloons to be used should have special characteristics that enable them to maintain strength and elasticity in such conditions.

8.3.3 Inflation

If a balloon launcher is not used, a special room, preferably isolated from other buildings, should be provided for filling balloons. It should be well ventilated (e.g. NFPA, 1999). If hydrogen gas is to be used, special safety precautions are essential (see section 8.6). The building should be free from any source of sparks, and all electric switches and fittings should be spark-proof; other necessary details are given in section 8.6.2. If helium gas is to be used, provision may be made for heating the building during cold weather. The walls, doors and floor should have a smooth finish and should be kept free from dust and grit. Heating hydrogen-inflation areas can be accomplished by steam, hot water or any other indirect means; however, electric heating, if any, shall be in compliance with national electrical codes (e.g. NFPA 50A for Class I, Division 2, locations).

Protective clothing (see section 8.6.4) should be worn during inflation. The operator should not stay in a closed room with a balloon containing hydrogen. The hydrogen supply should be controlled and the filling operation observed, from outside the filling room if the doors are shut, and the doors should be open when the operator is in the room with the balloon.

Balloons should be inflated slowly because sudden expansion may cause weak spots in the balloon film. It is desirable to provide a fine adjustment valve for regulating the gas flow. The desired amount of inflation (free lift) can be determined by using either a filling nozzle of the required weight or one which forms one arm of a balance on which the balloon lift can be weighed. The latter is less convenient, unless it is desirable to allow for variations in the weights of balloons, which is hardly necessary for routine work. It is useful to have a valve fitted to the weight type of the filler, and a further refinement, used in some services, is to have a valve that can be adjusted to close automatically at the required lift.

8.3.4 Launching

The balloon should be kept under a shelter until everything is ready for its launch. Prolonged exposure to bright sunshine should be avoided as this may cause a rapid deterioration of the balloon fabric and may even result in its bursting before leaving the ground. Protective clothing should be worn during manual launches.

No special difficulties arise when launching radiosonde balloons in light winds. Care should always be taken to see that there is no risk of the balloon and instruments striking obstructions before they rise clear of trees and buildings in the vicinity of the station. Release problems can be avoided to a large extent by carefully planning the release area. It should be selected to have a minimum of obstructions that may interfere with launching; the station buildings should be designed and sited considering the prevailing wind, likely gust effects on the release area and, in cold climates, drifting snow.

It is also advisable in high winds to keep the suspension of the instrument below the balloon as short as possible during launching, by using some form of suspension release or unwinder. A convenient device consists of a reel on which the suspension cord is wound and a spindle to which is attached an air brake or escapement mechanism that allows the suspension cord to unwind slowly after the balloon is released.

Mechanical balloon launchers have the great advantage that they can be designed to offer almost fool-proof safety, by separating the operator from the balloon during filling and

launching. They can be automated to various degrees, even to the point where the whole radiosonde operation requires no operator to be present. They might not be effective at wind speeds above 20 m s^{-1}. Provision should be made for adequate ventilation of the radiosonde sensors before release, and the construction should desirably be such that the structure will not be damaged by fire or explosion.

8.4 ACCESSORIES FOR BALLOON ASCENTS

8.4.1 Illumination for night ascents

The light source in general use for night-time pilot-balloon ascents is a lamp powered by a small electric battery. A battery of two 1.5 V cells, or a water-activated type used with a 2.5 V 0.3 A bulb, is usually suitable. Alternatively, a device providing light by means of chemical fluorescence may be used. For high-altitude soundings, however, a more powerful system of 2 to 3 W, together with a simple reflector, is necessary.

If the rate of ascent is to remain unchanged when a lighting unit is to be used, a small increase in free lift is theoretically required; that is to say, the total lift must be increased by more than the extra weight carried (see equation 8.3). In practice, however, the increase required is probably less than that calculated since the load improves the aerodynamic shape and the stability of the balloon.

At one time, night ascents were carried with a small candle in a translucent paper lantern suspended some 2 m or so below the balloon. However, there is a risk of flash or explosion if the candle is brought near the balloon or the source of hydrogen, and there is a risk of starting a forest fire or other serious fires upon return to the Earth. Thus, the use of candles is strongly discouraged.

8.4.2 Parachutes

In order to reduce the risk of damage caused by a falling sounding instrument, it is usual practice to attach a simple type of parachute. The main requirements are that it should be reliable when opening and should reduce the speed of descent to a rate not exceeding about 5 m s^{-1} near the ground. It should also be water-resistant. For instruments weighing up to 2 kg, a parachute made from waterproof paper or plastic film of about 2 m diameter and with strings about 3 m long is satisfactory. In order to reduce the tendency for the strings to twist together in flight it is advisable to attach them to a light hoop of wood, plastic or metal of about 40 cm in diameter just above the point where they are joined together.

When a radar reflector for wind-finding is part of the train it can be incorporated into the parachute and can serve to keep the strings apart. The strings and attachments must be able to withstand the opening of the parachute. If light-weight radiosondes are used (less than about 250 g), the radar reflector alone may provide sufficient drag during descent.

8.5 GASES FOR INFLATION

8.5.1 General

The two gases most suitable for meteorological balloons are helium and hydrogen. The former is much to be preferred on account of the fact that it is free from risk of explosion and fire. However, since the use of helium is limited mainly to the few countries which have an abundant natural supply, hydrogen is more generally used (see WMO, 1982). The buoyancy (total lift) of helium is 1.115 kg m^{-3}, at a pressure of 1 013 hPa and a temperature of 15 °C. The corresponding figure for pure hydrogen is 1.203 kg m^{-3} and for commercial hydrogen the figure is slightly lower than this.

It should be noted that the use of hydrogen aboard ships is no longer permitted under the general conditions imposed for marine insurance. The extra cost of using helium has to be reckoned against the life-threatening hazards to and the extra cost of insurance, if such insurance can be arranged.

Apart from the cost and trouble of transportation, the supply of compressed gas in cylinders affords the most convenient way of providing gas at meteorological stations. However, at places where the cost or difficulty of supplying cylinders is prohibitive, the use of an on-station hydrogen generator (see section 8.5.3) should present no great difficulties.

8.5.2 Gas cylinders

For general use, steel gas cylinders, capable of holding 6 m^3 of gas compressed to a pressure of 18 MPa (10 MPa in the tropics), are probably the most convenient size. However, where the consumption of gas is large, as at radiosonde stations, larger capacity cylinders or banks of standard cylinders all linked to the same outlet valve can be useful. Such arrangements will minimize handling by staff. In order to avoid the risk of confusion with other gases, hydrogen cylinders should be painted a distinctive colour (red is used in many countries) and otherwise marked according to national regulations. Their outlet valves should have left-handed threads to distinguish them from cylinders of non-combustible gases. Cylinders should be provided with a cap to protect the valves in transit.

Gas cylinders should be tested at regular intervals ranging from two to five years, depending on the national regulations in force. This should be performed by subjecting them to an internal pressure of at least 50% greater than their normal working pressure. Hydrogen cylinders should not be exposed to heat and, in tropical climates, they should be protected from direct sunshine. Preferably, they should be stored in a well-ventilated shed which allows any hydrogen leaks to escape to the open air.

8.5.3 Hydrogen generators

Hydrogen can be produced on site using various kinds of hydrogen generators. All generator plants and hydrogen storage facilities shall be legibly marked and with adequate warnings according to national regulations (e.g. "This unit contains hydrogen"; "Hydrogen – Flammable gas – No smoking – No open flames"). The following have proven to be the most suitable processes for generating hydrogen for meteorological purposes:

(a)   Ferro-silicon and caustic soda with water;

(b)   Aluminium and caustic soda with water;

(c)   Calcium hydride and water;

(d)   Magnesium-iron pellets and water;

(e)   Liquid ammonia with hot platinum catalyst;

(f)   Methanol and water with a hot catalyst;

(g)   Electrolysis of water.

Most of the chemicals used in these methods are hazardous, and the relevant national standards and codes of practice should be scrupulously followed, including correct markings and warnings. They require special transportation, storage, handling and disposal. Many of them are corrosive, as is the residue after use. If the reactions are not carefully controlled, they may produce excess heat and pressure. Methanol, being a poisonous alcohol, can be deadly if ingested, as it may be by substance abusers.

In particular, caustic soda, which is widely used, requires considerable care on the part of the operator, who should have adequate protection, especially for the eyes, from contact not only with the solution, but also with the fine dust which is liable to arise when the solid material is being put into the generator. An eye-wash bottle and a neutralizing agent, such as vinegar, should be kept at hand in case of an accident.

Some of the chemical methods operate at high pressure, with a consequential greater risk of an accident. High-pressure generators should be tested every two years to a pressure at least twice that of the working pressure. They should be provided with a safety device to relieve excess pressure. This is usually a bursting disc, and it is very important that the operational instructions should be strictly followed with regard to the material, size and form of the discs, and the frequency of their replacement. Even if a safety device is efficient, its operation is very liable to be accompanied by the ejection of hot solution. High-pressure generators must be carefully cleaned out before recharging since remains of the previous charge may considerably reduce the available volume of the generator and, thus, increase the working pressure beyond the design limit.

Unfortunately, calcium hydride and magnesium-iron, which have the advantage of avoiding the use of caustic soda, are expensive to produce and are, therefore, likely to be acceptable only for special purposes. Since these two materials produce hydrogen from water, it is essential that they be stored in containers which are completely damp-proof. In the processes using catalysts, care must be taken to avoid catalyst contamination.

All systems produce gas at sufficient pressure for filling balloons. However, the production rates of some systems (electrolysis in particular) are too low, and the gas must be produced and stored before it is needed, either in compressed form or in a gasholder.

The processes using the electrolysis of water or the catalytic cracking of methanol are attractive because of their relative safety and moderate recurrent cost, and because of the non-corrosive nature of the materials used. These two processes, as well as the liquid ammonia process, require electric power. The equipment is rather complex and must be carefully maintained and subjected to detailed daily check procedures to ensure that the safety control systems are effective. Water for electrolysis must have low mineral content.

8.6 USE OF HYDROGEN AND SAFETY PRECAUTIONS

8.6.1 General

Hydrogen can easily be ignited by a small spark and burns with a nearly invisible flame. It can burn when mixed with air over a wide range of concentrations, from 4% to 74% by volume (NFPA, 1999), and can explode in concentrations between 18% and 59%. In either case, a nearby operator can receive severe burns over the entire surface of any exposed skin, and an explosion can throw the operator against a wall or the ground, causing serious injury.

It is possible to eliminate the risk of an accident by using very carefully designed procedures and equipment, provided that they are diligently observed and maintained (Gremia, 1977; Ludtke and Saraduke, 1992; NASA, 1968). The provision of adequate safety features for the buildings in which hydrogen is generated and stored, or for the areas in which balloons are filled or released, does not always receive adequate attention (see the following section). In particular, there must be comprehensive training and continual meticulous monitoring and inspection to ensure that operators follow the procedures.

The advantages of automatic balloon launchers (see section 8.3.4) are that they can be made practically fool-proof and operator injuries can be prevented by completely separating the operator from the hydrogen.

An essential starting point for the consideration of safety precautions is to follow the various national standards and codes of practice concerned with the risks presented by explosive

atmospheres in general. Additional information on the precautions that should be followed will be found in publications dealing with explosion hazards, such as in hospitals and other industrial situations where similar problems exist. The operator should never be in a closed room with an inflated balloon. Other advice on safety matters can be found throughout the chapter.

8.6.2   **Building design**

Provisions should be made to avoid the accumulation of free hydrogen and of static charges as well as the occurrence of sparks in any room where hydrogen is generated, stored or used. The accumulation of hydrogen must be avoided even when a balloon bursts within the shelter during the course of inflation (WMO, 1982).

Safety provisions must be part of the structural design of hydrogen buildings (NFPA, 1999; SAA, 1985). Climatic conditions and national standards and codes are constraints within which it is possible to adopt many designs and materials suitable for safe hydrogen buildings. Codes are advisory and are used as a basis of good practice. Standards are published in the form of specifications for materials, products and safe practices. They should deal with topics such as flame-proof electric-light fittings, electrical apparatus in explosive atmospheres, the ventilation of rooms with explosive atmospheres, and the use of plastic windows, bursting discs, and so on (WMO, 1982).

Both codes and standards should contain information that is helpful and relevant to the design of hydrogen buildings. Furthermore, it should be consistent with recommended national practice. Guidance should be sought from national standards authorities when hydrogen buildings are designed or when the safety of existing buildings is reviewed, in particular for aspects such as the following:

(a)   The preferred location for hydrogen systems;

(b)   The fire resistance of proposed materials, as related to the fire-resistance ratings that must be respected;

(c)   Ventilation requirements, including a roof of light construction to ensure that hydrogen and products of an explosion are vented from the highest point of the building;

(d)   Suitable electrical equipment and wiring;

(e)   Fire protection (extinguishers and alarms);

(f)   Provision for the operator to control the inflation of the balloon from outside the filling room.

Measures should be taken to minimize the possibility of sparks being produced in rooms where hydrogen is handled. Thus, any electrical system (switches, fittings, wiring) should be kept outside these rooms; otherwise, special spark-proof switches, pressurized to prevent the ingress of hydrogen, and similarly suitable wiring, should be provided. It is also advisable to illuminate the rooms using exterior lights which shine in through windows. For the same reasons, any tools used should not produce sparks. The observer's shoes should not be capable of emitting sparks, and adequate lightning protection should be provided.

If sprinkler systems are used in any part of the building, consideration should be given to the possible hazard of hydrogen escaping after the fire has been extinguished. Hydrogen detection systems exist and may be used, for instance, to switch off power to the hydrogen generator at 20% of the lower explosive limit and should activate an alarm, and then activate another alarm at 40% of the lower explosive limit.

A hazard zone should be designated around the generator, storage and balloon area into which entry is permitted only when protective clothing is worn (see section 8.6.4).

Balloon launchers (see section 8.3.4) typically avoid the need for a special balloon-filling room, and greatly simplify the design of hydrogen facilities.

8.6.3 Static charges

The hazards of balloon inflation and balloon release can be considerably reduced by preventing static charges in the balloon-filling room, on the observer's clothing, and on the balloon itself. Loeb (1958) provides information on the static electrification process. Static charge control is effected by good earthing provisions for hydrogen equipment and filling-room fittings. Static discharge grips for observers can remove charges generated on clothing (WMO, 1982).

Charges on balloons are more difficult to deal with. Balloon fabrics, especially pure latex, are very good insulators. Static charges are generated when two insulating materials in contact with each are separated. A single brief contact with the observer's clothing or hair can generate a 20 kV charge, which is more than sufficient to ignite a mixture of air and hydrogen if it is discharged through an efficient spark. Charges on a balloon may take many hours to dissipate through the fabric to earth or naturally into the surrounding air. Also, it has been established that, when a balloon bursts, the separation of the film along a split in the fabric can generate sparks energetic enough to cause ignition.

Electrostatic charges can be prevented or removed by spraying water onto the balloon during inflation, by dipping balloons into antistatic solution (with or without drying them off before use), by using balloons with an antistatic additive in the latex, or by blowing ionized air over the balloon. Merely earthing the neck of the balloon is not sufficient.

The maximum electrostatic potential that can be generated or held on a balloon surface decreases with increasing humidity, but the magnitude of the effect is not well established. Some tests carried out on inflated 20 g balloons indicated that spark energies sufficient to ignite hydrogen-oxygen mixtures are unlikely to be reached when the relative humidity of the air is greater than 60%. Other studies have suggested relative humidities from 50% to 76% as safe limits, yet others indicate that energetic sparks may occur at even higher relative humidity. It may be said that static discharge is unlikely when the relative humidity exceeds 70%, but this should not be relied upon (see Cleves et al., 1971).

It is strongly recommended that fine water sprays be used on the balloon because the wetting and earthing of the balloon will remove most of the static charges from the wetted portions. The sprays should be designed to wet as large an area of the balloon as possible and to cause continuous streams of water to run from the balloon to the floor. If the doors are kept shut, the relative humidity inside the filling room can rise to 75% or higher, thus reducing the probability of sparks energetic enough to cause ignition. Balloon release should proceed promptly once the sprays are turned off and the filling-shed doors opened.

Other measures for reducing the build-up of static charge include the following (WMO, 1982):

(a) The building should be provided with a complete earthing (grounding) system, with all fittings, hydrogen equipment and the lightning conductor separately connected to a single earth, which itself must comply with national specifications for earth electrodes. Provision should be made to drain electrical charges from the floor;

(b) Static discharge points should be provided for the observers;

(c) The windows should be regularly coated with an antistatic solution;

(d) Operators should be encouraged not to wear synthetic clothing or insulating shoes. It is good practice to provide operators with partially conducting footwear;

(e) Any contact between the observer and the balloon should be minimized; this can be facilitated by locating the balloon filler at a height of 1 m or more above the floor.

8.6.4   **Protective clothing and first-aid facilities**

Proper protective clothing should be worn whenever hydrogen is being used, during all parts of the operations, including generation procedures, when handling cylinders, and during balloon inflation and release. The clothing should include a light-weight flame-proof coat with a hood made of non-synthetic, antistatic material and a covering for the lower face, glasses or goggles, cotton gloves, and any locally recommended anti-flash clothing (see Hoschke et al., 1979).

First-aid facilities appropriate to the installation should be provided. These should include initial remedies for flash burns and broken limbs. When chemicals are used, suitable neutralizing solutions should be on hand, for example, citric acid for caustic soda burns. An eye-wash apparatus ready for instant use should be available (WMO, 1982).

_____

REFERENCES AND FURTHER READING

Atmospheric Environment Service (Canada), 1978: *The Use of Hydrogen for Meteorological Purposes in the Canadian Atmospheric Environment Service*, Toronto.

Cleves, A.C., J.F. Sumner and R.M.H. Wyatt, 1971: The Effect of Temperature and Relative Humidity on the Accumulation of Electrostatic Charges on Fabrics and Primary Explosives. *Proceedings of the Third Conference on Static Electrification*, (London).

Gremia, J.O., 1977: *A Safety Study of Hydrogen Balloon Inflation Operations and Facilities of the National Weather Service*. Trident Engineering Associates, Annapolis, Maryland.

Hoschke, B.N. et al., 1979: *Report to the Bureau of Meteorology on Protection Against the Burn Hazard from Exploding Hydrogen-filled Meteorological Balloons*. CSIRO Division of Textile Physics and the Department of Housing and Construction, Australia.

Loeb, L.B., 1958: *Static Electrification*, Springer-Verlag, Berlin.

Ludtke, P. and G. Saraduke, 1992: *Hydrogen Gas Safety Study Conducted at the National Weather Service Forecast Office*. Norman, Oklahoma.

National Aeronautics and Space Administration, 1968: *Hydrogen Safety Manual*. NASA Technical Memorandum TM-X-52454, NASA Lewis Research Center, United States.

National Fire Protection Association, 1999: *NFPA 50A: Standard for Gaseous Hydrogen Systems at Consumer Sites*. National Fire Protection Association, Quincy, Maryland.

———, 2002: *NFPA 68: Guide for Venting of Deflagrations*. National Fire Protection Association, Batterymarch Park, Quincy, Maryland.

———, 2005: *NFPA 70, National Electrical Code*. National Fire Protection Association, Quincy, Maryland.

———, 2006: *NFPA 220, Standard on Types of Building Construction*. National Fire Protection Association, Quincy, Maryland.

Rosen, B., V.H. Dayan and R.L. Proffit, 1970: *Hydrogen Leak and Fire Detection: A Survey*. NASA SP-5092.

Standards Association of Australia, 1970: AS C99: *Electrical equipment for explosive atmospheres – Flameproof electric lightning fittings*.

———, 1980: AS 1829: *Intrinsically safe electrical apparatus for explosive atmospheres*.

———, 1985: AS 1482: *Electrical equipment for explosive atmospheres – Protection by ventilation – Type of protection V*.

———, 1995: ASNZS 1020: *The control of undesirable static electricity*.

———, 2004: AS 1358: *Bursting discs and bursting disc devices – Application selection and installation*.

World Meteorological Organization, 1982: *Meteorological Balloons: The Use of Hydrogen for Inflation of Meteorological Balloons*. Instruments and Observing Methods Report No. 13. Geneva.

———————

CHAPTER CONTENTS

CHAPTER 9. URBAN OBSERVATIONS

9.1 GENERAL

There is a growing need for meteorological observations conducted in urban areas. Urban populations continue to expand, and Meteorological Services are increasingly required to supply meteorological data in support of detailed forecasts for citizens, building and urban design, energy conservation, transportation and communications, air quality and health, storm water and wind engineering, and insurance and emergency measures. At the same time, Meteorological Services have difficulty in making urban observations that are not severely compromised. This is because most developed sites make it impossible to conform to the standard guidelines for site selection and instrument exposure given in Part I of this Guide owing to obstruction of air-flow and radiation exchange by buildings and trees, unnatural surface cover and waste heat and water vapour from human activities.

This chapter provides information to enable the selection of sites, the installation of a meteorological station and the interpretation of data from an urban area. In particular, it deals with the case of what is commonly called a "standard" climate station. Despite the complexity and inhomogeneity of urban environments, useful and repeatable observations can be obtained. Every site presents a unique challenge. To ensure that meaningful observations are obtained requires careful attention to certain principles and concepts that are virtually unique to urban areas. It also requires the person establishing and running the station to apply those principles and concepts in an intelligent and flexible way that is sensitive to the realities of the specific environment involved. Rigid "rules" have little utility. The need for flexibility runs slightly counter to the general notion of standardization that is promoted as WMO observing practice. In urban areas, it is sometimes necessary to accept exposure over non-standard surfaces at non-standard heights, to split observations between two or more locations, or to be closer than usual to buildings or waste heat exhausts.

The units of measurement and the instruments used in urban areas are the same as those for other environments. Therefore, only those aspects that are unique to urban areas, or that are made difficult to handle because of the nature of cities, such as the choice of site, instrument exposure and the documentation of metadata, are covered in this chapter.

The timing and frequency of observations and the coding of reports should follow appropriate standards (WMO, 2006, 2010, 2011*a*, 2011*b*, 2011*c*).

With regard to automated stations and the requirements for message coding and transmission, quality control, maintenance (noting any special demands of the urban environment) and calibration, the recommendations of Part II, Chapter 1, should be followed.

9.1.1 Definitions and concepts

9.1.1.1 *Station rationale*

The clarity of the reason for establishing an urban station is essential to its success. Two of the most usual reasons are the wish to represent the meteorological environment at a place for general climatological purposes and the wish to provide data in support of the needs of a particular user. In both cases, the spatial and temporal scales of interest must be defined, and, as outlined below, the siting of the station and the exposure of the instruments in each case may have to be very different.

9.1.1.2　　　*Horizontal scales*

There is no more important an input to the success of an urban station than an appreciation of the concept of scale. There are three scales of interest (Oke, 1984; Figure 9.1):

(a)　Microscale: Every surface and object has its own microclimate on it and in its immediate vicinity. Surface and air temperatures may vary by several degrees in very short distances, even millimetres, and air-flow can be greatly perturbed by even small objects. Typical scales of urban microclimates relate to the dimensions of individual buildings, trees, roads, streets, courtyards, gardens, and so forth. Typical scales extend from less than 1 m to hundreds of metres. The formulation of the guidelines in Part I of this Guide specifically aims to avoid microclimatic effects. The climate station recommendations are designed to standardize all sites, as far as practical. This explains the use of a standard height of measurement, a single surface cover, minimum distances to obstacles and little horizon obstruction. The aim is to achieve climate observations that are free of extraneous microclimate signals and hence characterize local climates. With even more stringent standards, first order stations may be able to represent conditions at synoptic space and timescales. The data may be used to assess climate trends at even larger scales. Unless the objectives are very specialized, urban stations should also avoid microclimate influences; however, this is hard to achieve;

(b)　Local scale: This is the scale that standard climate stations are designed to monitor. It includes landscape features such as topography, but excludes microscale effects. In urban areas this translates to mean the climate of neighbourhoods with similar types of urban development (surface cover, size and spacing of buildings, activity). The signal is the integration of a characteristic mix of microclimatic effects arising from the source area in the vicinity of the site. The source area is the portion of the surface upstream that contributes the main properties of the flux or meteorological concentration being measured (Schmid, 2002). Typical scales are one to several kilometres;

(c)　Mesoscale: A city influences weather and climate at the scale of the whole city, typically tens of kilometres in extent. A single station is not able to represent this scale.
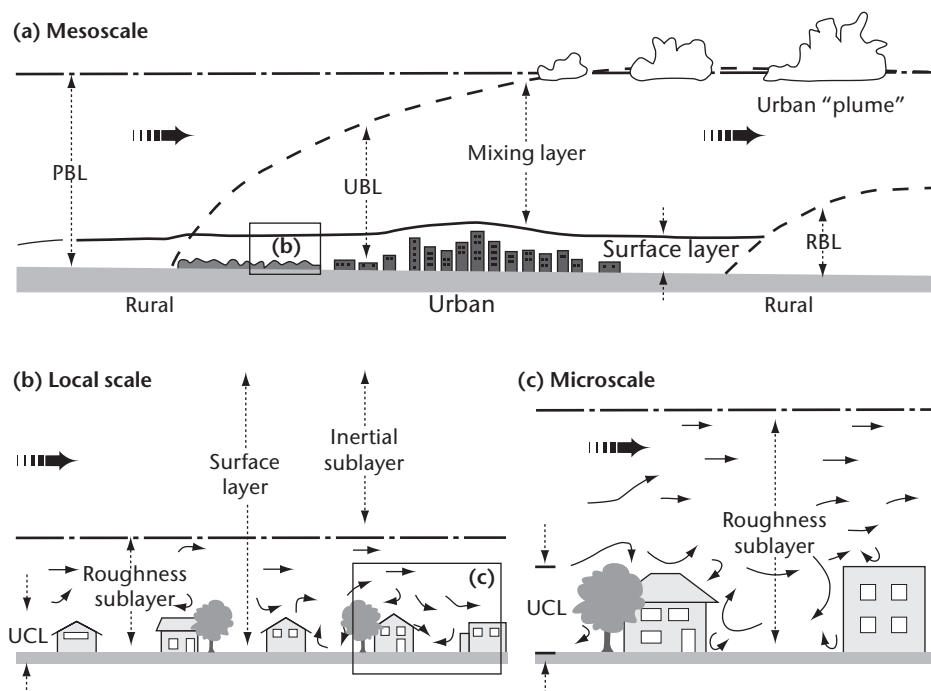
Figure 9.1. Schematic of climatic scales and vertical layers found in urban areas: planetary boundary layer (PBL), urban boundary layer (UBL), urban canopy layer (UCL), rural boundary layer (RBL) (modified from Oke, 1997).

9.1.1.3 *Vertical scales*

An essential difference between the climate of urban areas and that of rural or airport locations is that in cities the vertical exchanges of momentum, heat and moisture do not occur at a (nearly) plane surface, but in a layer of significant thickness, called the urban canopy layer (UCL) (Figure 9.1). The height of the UCL is approximately equivalent to that of the mean height of the main roughness elements (buildings and trees), z_H (see Figure 9.4 for parameter definitions). The microclimatic effects of individual surfaces and obstacles persist for a short distance away from their source and are then mixed and muted by the action of turbulent eddies. The distance required before the effect is obliterated depends on the magnitude of the effect, wind speed and stability (namely, stable, neutral or unstable). This blending occurs both in the horizontal and the vertical. As noted, horizontal effects may persist up to a few hundred metres. In the vertical, the effects of individual features are discernible in the roughness sublayer (RSL), which extends from ground level to the blending height z_r, where the blending action is complete. Rule-of-thumb estimates and field measurements indicate that z_r can be as low as 1.5 z_H at densely built (closely spaced) and homogeneous sites, but greater than 4 z_H in low density areas (Grimmond and Oke, 1999; Rotach, 1999; Christen, 2003). An instrument placed below z_r may register microclimate anomalies, but, above that, it "sees" a blended, spatially averaged signal that is representative of the local scale.

There is another height restriction to consider. This arises because each local scale surface type generates an internal boundary layer, in which the flow structure and thermodynamic properties are adapted to that surface type. The height of the layer grows with increasing fetch (the distance upwind to the edge where the transition to a distinctly different surface type occurs). The rate at which the internal boundary layer grows with fetch distance depends on the roughness and stability. In rural conditions, the height to fetch ratios might vary from as small as 1:10 in unstable conditions to as large as 1:500 in stable cases, and the ratio decreases as the roughness increases (Garratt, 1992; Wieringa, 1993). Urban areas tend towards neutral stability owing to the enhanced thermal and mechanical turbulence associated with the heat island and their large roughness. Therefore, a height to fetch ratio of about 1:100 is considered typical. The internal boundary layer height is taken above the displacement height z_d, which is the reference level for flow above the blending height. (For an explanation of z_d, see Figure 9.4 and Note b in Table 9.2.)

For example, take a hypothetical densely built district with z_H of 10 m. This means that z_r is at least 15 m. If this height is chosen to be the measurement level, the fetch requirement over similar urban terrain is likely to be at least 0.8 km, since fetch = 100 ($z_r - z_d$), and z_d will be about 7 m. This can be a significant site restriction because the implication is that, if the urban terrain is not similar out to at least this distance around the station site, observations will not be representative of the local surface type. At less densely developed sites, where heat island and roughness effects are less, the fetch requirements are likely to be greater.

At heights above the blending height, but within the local internal boundary layer, measurements are within an inertial sublayer (Figure 9.1), where standard boundary layer theory applies. Such theory governs the form of the mean vertical profiles of meteorological variables (including air temperature, humidity and wind speed) and the behaviour of turbulent fluxes, spectra and statistics. This provides a basis for:

(a) The calculation of the source area (or "footprint", see below) from which the turbulent flux or the concentration of a meteorological variable originates; hence, this defines the distance upstream for the minimum acceptable fetch;

(b) The extrapolation of a given flux or property through the inertial layer and also downwards into the RSL (and, although it is less reliable, into the UCL). In the inertial layer, fluxes are constant with height and the mean value of meteorological properties are invariant horizontally. Hence, observations of fluxes and standard variables possess significant utility and are able to characterize the underlying local scale environment. Extrapolation into the RSL is less prescribed.
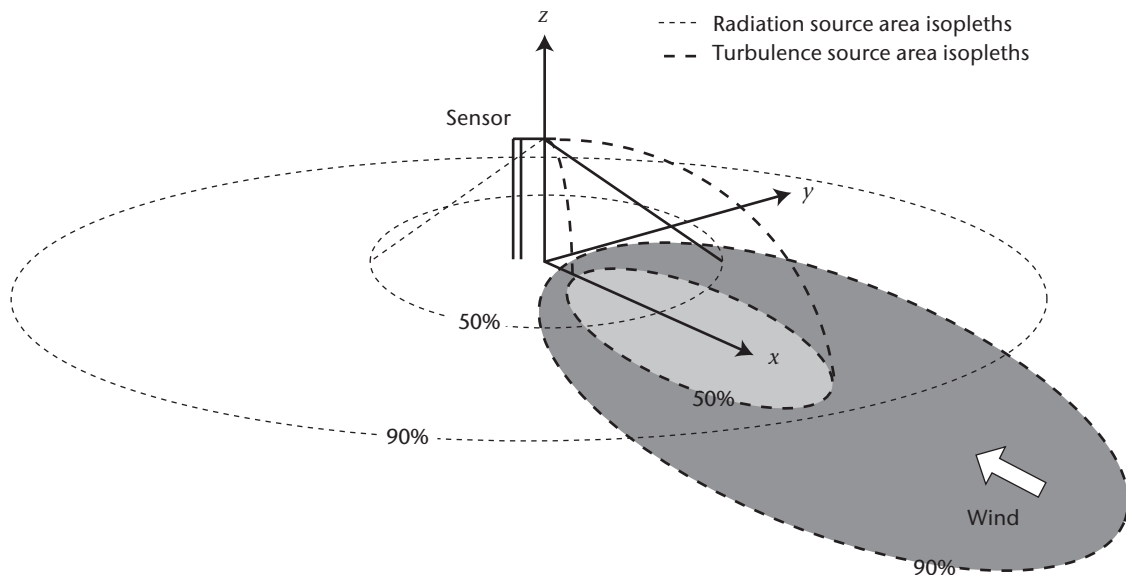
Figure 9.2. Conceptual representation of source areas contributing to sensors for radiation and turbulent fluxes of concentrations. If the sensor is a radiometer 50% or 90% of the flux originates from the area inside the perspective circle. If the sensor is responding to a property of turbulent transport, 50% or 90% of the signal comes from the area inside the respective ellipses. These are dynamic in the sense that they are oriented into the wind and hence move with wind direction and stability.

9.1.1.4 *Source areas ("footprints")*

A sensor placed above a surface "sees" only a portion of its surroundings. This is called the "source area" of the instrument which depends on its height and the characteristics of the process transporting the surface property to the sensor. For upwelling radiation signals (short- and long-wave radiation and surface temperature viewed by an infrared thermometer) the field of view of the instrument and the geometry of the underlying surface set what is seen. By analogy, sensors such as thermometers, hygrometers, gas analysers and anemometers "see" properties such as temperature, humidity, atmospheric gases and wind speed and direction which are carried from the surface to the sensor by turbulent transport. A conceptual illustration of these source areas is given in Figure 9.2.

The source area of a down-facing radiometer with its sensing element parallel to the ground is a circular patch with the instrument at its centre (Figure 9.2). The radius (r) of the circular source area contributing to the radiometer signal at height (z_1) is given in Schmid et al. (1991):

$$r = z_1 \left(\frac{1}{F} - 1 \right)^{-0.5}$$

(9.1)

where F is the view factor, namely the proportion of the measured flux at the sensor for which that area is responsible. Depending on its field of view, a radiometer may see only a limited circle, or it may extend to the horizon. In the latter case, the instrument usually has a cosine response, so that towards the horizon it becomes increasingly difficult to define the actual source area seen. Hence, the use of the view factor which defines the area contributing a set proportion (often selected as 50%, 90%, 95%, 99% or 99.5%) of the instrument's signal.

The source area of a sensor that derives its signal via turbulent transport is not symmetrically distributed around the sensor location. It is elliptical in shape and is aligned in the upwind direction from the tower (Figure 9.2). If there is a wind, the effect of the surface area at the base of the mast is effectively zero, because turbulence cannot transport the influence up to the sensor level. At some distance in the upwind direction the source starts to affect the sensor; this effect rises to a peak, thereafter decaying at greater distances (for the shape in both the x and y directions see Kljun et al., 2002; Schmid, 2002). The distance upwind to the first surface

area contributing to the signal, to the point of peak influence, to the furthest upwind surface influencing the measurement, and the area of the so-called "footprint" vary considerably over time. They depend on the height of measurement (larger at greater heights), surface roughness, atmospheric stability (increasing from unstable to stable) and whether a turbulent flux or a meteorological concentration is being measured (larger for the concentration) (Kljun et al., 2002). Methods to calculate the dimensions of flux and concentration "footprints" are available (Schmid, 2002; Kljun et al., 2004).

Although the situation illustrated in Figure 9.2 is general, it applies best to instruments placed in the inertial sublayer, well above the complications of the RSL and the complex geometry of the three-dimensional urban surface. Within the UCL, the way in which the effects of radiation and turbulent source areas decay with distance has not yet been reliably evaluated. It can be surmised that they depend on the same properties and resemble the overall forms of those in Figure 9.2. However, obvious complications arise due to the complex radiation geometry, and the blockage and channelling of flow, which are characteristic of the UCL. Undoubtedly, the immediate environment of the station is by far the most critical and the extent of the source area of convective effects grows with stability and the height of the sensor. The distance influencing screen-level (~1.5 m) sensors may be a few tens of metres in neutral conditions, less when they are unstable and perhaps more than 100 m when they are stable. At a height of 3 m, the equivalent distances probably extend up to about 300 m in the stable case. The circle of influence on a screen-level temperature or humidity sensor is thought to have a radius of about 0.5 km typically, but this is likely to depend upon the building density.

9.1.1.5   *Measurement approaches*

It follows from the preceding discussion that, if the objective of an instrumented urban site is to monitor the local-scale climate near the surface, there are two viable approaches as follows:

(a)   Locate the site in the UCL at a location surrounded by average or "typical" conditions for the urban terrain, and place the sensors at heights similar to those used at non-urban sites. This assumes that the mixing induced by flow around obstacles is sufficient to blend properties to form a UCL average at the local scale;

(b)   Mount the sensors on a tall tower above the RSL and obtain blended values that can be extrapolated down into the UCL.

In general, approach (a) works best for air temperature and humidity, and approach (b) for wind speed and direction and precipitation. For radiation, the only significant requirement is for an unobstructed horizon. Urban stations, therefore, often consist of instruments deployed both below and above roof level; this requires that site assessment and description include the scales relevant to both contexts.

9.1.1.6   *Urban site description*

The magnitude of each urban scale does not agree precisely with those commonly given in textbooks. The scales are conferred by the dimensions of the morphometric features that make up an urban landscape. This places emphasis on the need to adequately describe properties of urban areas which affect the atmosphere. The most important basic features are the urban structure (dimensions of the buildings and the spaces between them, the street widths and street spacing), the urban cover (built-up, paved and vegetated areas, bare soil, water), the urban fabric (construction and natural materials) and the urban metabolism (heat, water and pollutants due to human activity). Hence, the characterization of the sites of urban climate stations must take account of these descriptors, use them in selecting potential sites, and incorporate them in metadata that accurately describe the setting of the station.

These four basic features of cities tend to cluster to form characteristic urban classes. For example, most central areas of cities have relatively tall buildings that are densely packed together, so the ground is largely covered with buildings or paved surfaces made of durable

materials such as stone, concrete, brick and asphalt and where there are large releases from furnaces, air conditioners, chimneys and vehicles. Near the other end of the spectrum there are districts with low density housing of one- or two-storey buildings of relatively light construction and considerable garden or vegetated areas with low heat releases, but perhaps large irrigation inputs.

No universally accepted scheme of urban classification for climatic purposes exists. A good approach to the built components is that of Ellefsen (1991) who developed a set of urban terrain zone (UTZ) types. He initially differentiates according to 3 types of building contiguity (attached (row), detached but close-set, detached and open-set). These are further divided into a total of 17 sub-types by function, location in the city, and building height, construction and age. Application of the scheme requires only aerial photography, which is generally available, and the scheme has been applied in several cities around the world and seems to possess generality.

Ellefsen's scheme can be used to describe urban structure for roughness, airflow, radiation access and screening. It can be argued that the scheme indirectly includes aspects of urban cover, fabric and metabolism because a given structure carries with it the type of cover, materials and degree of human activity. Ellefsen's scheme is less useful, however, when built features are scarce and there are large areas of vegetation (urban forest, low plant cover, grassland, scrub, crops), bare ground (soil or rock) and water (lakes, swamps, rivers). A simpler scheme of urban climate zones (UCZs) is illustrated in Table 9.1. It incorporates groups of Ellefsen's zones, plus a measure of the structure, z_H/W (see Table 9.1, Note c) shown to be closely related to both flow, solar shading and the heat island, and also a measure of the surface cover (% built) that is related to the degree of surface permeability.

The importance of UCZs is not their absolute accuracy to describe the site, but their ability to classify areas of a settlement into districts, which are similar in their capacity to modify the local climate, and to identify potential transitions to different UCZs. Such a classification is crucial when beginning to set up an urban station, so that the spatial homogeneity criteria are met approximately for a station in the UCL or above the RSL. In what follows, it is assumed that the morphometry of the urban area, or a portion of it, has been assessed using detailed maps, and/ or aerial photographs, satellite imagery (visible and/or thermal), planning documents or at least a visual survey conducted from a vehicle and/or on foot. Although land-use maps can be helpful, it should be appreciated that they depict the *function* and not necessarily the *physical form* of the settlement. The task of urban description should result in a map with areas of UCZs delineated.

Herein, the UCZs as illustrated in Table 9.1 are used. The categories may have to be adapted to accommodate special urban forms characteristic of some ancient cities or of unplanned urban development found in some less-developed countries. For example, many towns and cities in Africa and Asia do not have as large a fraction of the surface covered by impervious materials and roads may not be paved.

9.2   CHOOSING A LOCATION AND SITE FOR AN URBAN STATION

9.2.1   Location

First, it is necessary to establish clearly the purpose of the station. If there is to be only one station inside the urban area it must be decided if the aim is to monitor the greatest impact of the city, or of a more representative or typical district, or if it is to characterize a particular site (where there may be perceived to be climate problems or where future development is planned). Areas where there is the highest probability of finding maximum effects can be judged initially by reference to the ranked list of UCZ types in Table 9.1. Similarly, the likelihood that a station will be typical can be assessed using the ideas behind Table 9.1 and choosing extensive areas of similar urban development for closer investigation.

Table 9.1. Simplified classification of distinct urban forms arranged in approximate decreasing order of their ability to have an impact on local climate (Oke, 2004 unpublished)

Urban climate zone [a]	Image	Roughness class[b]	Aspect ratio[c]	% built (impermeable)[d]
1. Intensely developed urban with detached close-set high-rise buildings with cladding, e.g. downtown towers		8	> 2	> 90
2. Intensely high density urban with 2–5 storey, attached or very-close set buildings often of bricks or stone, e.g. old city core		7	1.0–2.5	> 85
3. Highly developed, medium density urban with row or detached but close-set houses, stores and apartments, e.g. urban housing		7	0.5–1.5	70–85
4. Highly developed, low or medium density urban with large low buildings and paved parking, e.g. shopping malls, warehouses		5	0.05–0.2	70–95
5. Medium development, low density suburban with 1 or 2 storey houses, e.g. suburban houses		6	0.2–0.6, up to > 1 with trees	35–65
6. Mixed use with large buildings in open landscape, e.g. institutions such as hospitals, universities, airports		5	0.1–0.5, depends on trees	< 40
7. Semi-rural development, scattered houses in natural or agricultural areas, e.g. farms, estates		4	> 0.05, depends on trees	< 10

☐ Buildings; 🌳 Vegetation
▬ Impervious ground; ⋯ Pervious ground

Notes:

a   A simplified set of classes that includes aspects of the schemes of Auer (1978) and Ellefsen (1991) plus physical
measures relating to wind, and thermal and moisture control (columns on the right). Approximate correspondence
between UCZ and Ellefsen's urban terrain zones is: 1 (Dc1, Dc8), 2 (A1–A4, Dc2), 3 (A5, Dc3–5, Do2), 4 (Do1, Do4,
Do5), 5 (Do3), 6 (Do6), 7 (none).

b   Effective terrain roughness according to the Davenport classification (Davenport et al., 2000); see Table 9.2.

c   Aspect ratio $= z_h/W$ is the average height of the main roughness elements (buildings, trees) divided by their average
spacing; in the city centre this is the street canyon height/width. This measurement is known to be related to flow
regime types (Oke, 1987) and thermal controls (solar shading and longwave screening) (Oke, 1981). Tall trees
increase this measure significantly.

d   Average proportion of ground plan covered by built features (buildings, roads and paved and other impervious
areas); the rest of the area is occupied by pervious cover (green space, water and other natural surfaces).
Permeability affects the moisture status of the ground and hence humidification and evaporative cooling potential.

The search can be usefully refined in the case of air temperature and humidity by conducting
spatial surveys, wherein the sensor is carried on foot, or mounted on a bicycle or a car and taken
through areas of interest. After several repetitions, cross-sections or isoline maps may be drawn
(see Figure 9.3), revealing where areas of thermal or moisture anomaly or interest lie. Usually, the
best time to do this is a few hours after sunset or before sunrise on nights with relatively calm
air-flow and cloudless skies. This maximizes the potential for the differentiation of microclimate
and local climate differences. It is not advisable to conduct such surveys close to sunrise or sunset
because weather variables change so rapidly at these times that meaningful spatial comparisons
are difficult.

If the station is to be part of a network to characterize spatial features of the urban climate, a
broader view is needed. This consideration should be informed by thinking about the typical
spatial form of urban climate distributions. For example, the isolines of urban heat and moisture
"islands" indeed look like the contours of their topographic namesakes (Figure 9.3). They
have relatively sharp "cliffs", often a "plateau" over much of the urban area interspersed with
localized "mounds" and "basins" of warmth/coolness and moistness/dryness. These features are
co-located with patches of greater or lesser development such as clusters of apartments, shops,
factories or parks, open areas or water. Therefore, a decision must be made: is the aim to make a
representative sample of the UCZ diversity, or is it to faithfully reflect the spatial structure?

In most cases the latter is too ambitious with a fixed-station network in the UCL. This is because
it will require many stations to depict the gradients near the periphery, the plateau region,
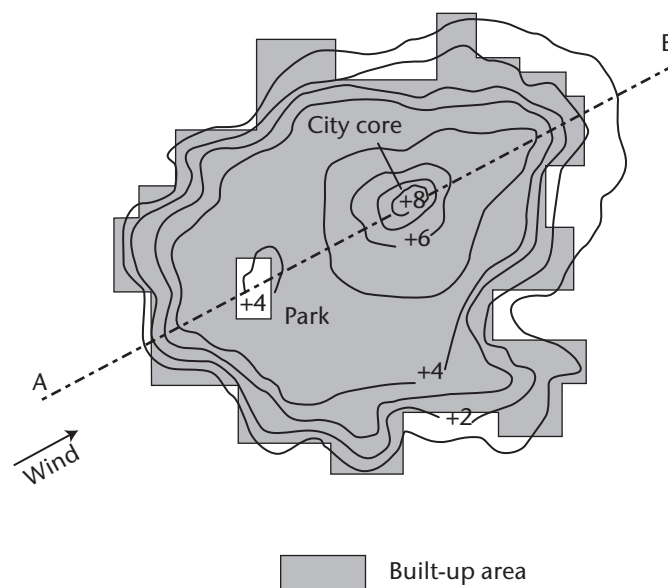
**Figure 9.3. Typical spatial pattern of isotherms in a large city at night with calm, clear weather
illustrating the heat island effect (after Oke, 1982)**

and the highs and lows of the nodes of weaker and stronger than average urban development. If measurements are to be taken from a tower, with sensors above the RSL, the blending action produces more muted spatial patterns and the question of distance of fetch to the nearest border between UCZs, and the urban-rural fringe, becomes relevant. Whereas a distance to a change in UCZ of 0.5 to 1 km may be acceptable inside the UCL, for a tower-mounted sensor the requirement is likely to be more like a few kilometres of fetch.

Since the aim is to monitor local climate attributable to an urban area, it is necessary to avoid extraneous microclimatic influences or other local or mesoscale climatic phenomena that will complicate the urban record. Therefore, unless there is specific interest in topographically generated climate patterns, such as the effects of cold air drainage down valleys and slopes into the urban area, or the speed-up or sheltering of winds by hills and escarpments, or fog in river valleys or adjacent to water bodies, or geographically locked cloud patterns, and so on, it is sensible to avoid locations subject to such local and mesoscale effects. On the other hand, if a benefit or hazard is derived from such events, it may be relevant to design the network specifically to sample its effects on the urban climate, such as the amelioration of an overly hot city by sea or lake breezes.

9.2.2   **Siting**

Once a choice of UCZ type and its general location inside the urban area is made, the next step is to inspect the map, imagery and photographic evidence to narrow down candidate locations within a UCZ. Areas of reasonably homogeneous urban development without large patches of anomalous structure, cover or material are sought. The precise definition of "reasonably" however is not possible; almost every real urban district has its own idiosyncrasies that reduce its homogeneity at some scale. Although a complete list is therefore not possible, the following are examples of what to avoid: unusually wet patches in an otherwise dry area, individual buildings that jut up by more than half the average building height, a large paved car park in an area of irrigated gardens, a large, concentrated heat source like a heating plant or a tunnel exhaust vent. Proximity to transition zones between different UCZ types should be avoided, as should sites where there are plans for or the likelihood of major urban redevelopment. The level of concern about anomalous features decreases with distance away from the site itself, as discussed in relation to source areas.

In practice, for each candidate site a "footprint" should be estimated for radiation (for example, equation 9.1) and for turbulent properties. Then, key surface properties such as the mean height and density of the obstacles and characteristics of the surface cover and materials should be documented within these footprints. Their homogeneity should then be judged, either visually or using statistical methods. Once target areas of acceptable homogeneity for a screen-level or high-level (above-RSL) station are selected, it is helpful to identify potential "friendly" site owners who could host it. If a government agency is seeking a site, it may already own land in the area which is used for other purposes or have good relations with other agencies or businesses (offices, work yards, spare land, rights of way) including schools, universities, utility facilities (electricity, telephone, pipelines) and transport arteries (roads, railways). These are good sites, because access may be permitted and also because they also often have security against vandalism and may have electrical power connections.

Building roofs have often been used as the site for meteorological observations. This may often have been based on the mistaken belief that at this elevation the instrument shelter is free from the complications of the UCL. In fact, rooftops have their own very distinctly anomalous microclimates that lead to erroneous results. Airflow over a building creates strong perturbations in speed, direction and gustiness which are quite unlike the flow at the same elevation away from the building or near the ground (Figure 9.5). Flat-topped buildings may actually create flows on their roofs that are counter to the main external flow, and speeds vary from extreme jetting to a near calm. Roofs are also constructed of materials that are thermally rather extreme. In light winds and cloudless skies they can become very hot by day and cold by night. Hence, there is often a sharp gradient of air temperature near the roof. Furthermore, roofs are designed to be waterproof and to shed water rapidly. This, together with their openness to solar radiation and

the wind, makes them anomalously dry. In general, therefore, roofs are very poor locations for air temperature, humidity, wind and precipitation observations, unless the instruments are placed on very tall masts. They can, however, be good for observing incoming radiation components.

Once the site has been chosen, it is essential that the details of the site characteristics (metadata) be fully documented (see section 9.4).

9.3 INSTRUMENT EXPOSURE

9.3.1 Modifications to standard practice

In many respects, the generally accepted standards for the exposure of meteorological instruments set out in Part I of this Guide apply to urban sites. However, there will be many occasions when it is impossible or makes no sense to conform. This section recommends some principles that will assist in such circumstances; however, all eventualities cannot be anticipated. The recommendations here remain in agreement with general objectives set out in Part I, Chapter 1.

Many urban stations have been placed over short grass in open locations (parks, playing fields) and as a result they are actually monitoring modified rural-type conditions, not representative urban ones. This leads to the curious finding that some rural-urban pairs of stations show no urban effect on temperature (Peterson, 2003).

The guiding principle for the exposure of sensors in the UCL should be to locate them in such a manner that they monitor conditions that are representative of the environment of the selected UCZ. In cities and towns it is inappropriate to use sites similar to those which are standard in open rural areas. Instead, it is recommended that urban stations should be sited over surfaces that, within a microscale radius, are representative of the local scale urban environment. The % built category (Table 9.1) is a crude guide to the recommended underlying surface.

The requirement that most obviously cannot be met at many urban sites is the distance from obstacles — the site should be located well away from trees, buildings, walls or other obstructions (Part I, Chapter 1). Rather, it is recommended that the urban station be centred in an open space where the surrounding aspect ratio (z_H/W) is approximately representative of the locality.

When installing instruments at urban sites it is especially important to use shielded cables because of the ubiquity of power lines and other sources of electrical noise at such locations.

9.3.2 Temperature

9.3.2.1 *Air temperature*

The sensors in general use to measure air temperature (including their accuracy and response characteristics) are appropriate in urban areas. Careful attention to radiation shielding and ventilation is especially recommended. In the UCL, a sensor assembly might be relatively close to warm surfaces, such as a sunlit wall, a road or a vehicle with a hot engine, or it might receive reflected heat from glassed surfaces. Therefore, the shields used should block radiation effectively. Similarly, because an assembly placed in the lower UCL might be too well sheltered, forced ventilation of the sensor is recommended. If a network includes a mixture of sensor assemblies with/without shields and ventilation, this might contribute to inter-site differences. Practices should therefore be uniform.

The surface over which air temperature is measured and the exposure of the sensor assembly should follow the recommendations given in the previous section, namely, the surface should be typical of the UCZ and the thermometer screen or shield should be centred in a space with approximately average z_H/W. In very densely built-up UCZ this might mean that it is located

only 5 to 10 m from buildings that are 20 to 30 m high. If the site is a street canyon, z_H/W only applies to the cross-section normal to the axis of the street. The orientation of the street axis may also be relevant because of systematic sun-shade patterns. If continuous monitoring is planned, north-south oriented streets are favoured over east-west ones because there is less phase distortion, although daytime course of temperature may be rather peaked.

At non-urban stations recommended screen height is between 1.25 and 2 m above ground level. While this is also acceptable for urban sites, it may be better to relax this requirement to allow greater heights. This should not lead to significant error in most cases, especially in densely built-up areas, because observations in canyons show very slight air temperature gradients through most of the UCL, provided that the location is more than 1 m from a surface (Nakamura and Oke, 1988). Measurements at heights of 3 or 5 m are not very different from those at the standard height, have slightly greater source areas and place the sensor beyond easy reach, thus preventing damage, and away from the path of vehicles. They also ensure greater dilution of vehicle exhaust heat and reduce contamination from dust.

Air temperatures measured above the UCL, using sensors mounted on a tower, are influenced by air exchanged with the UCL plus the effects of the roofs. Roofs have much more thermic variability than most surfaces within the UCL. Most roofs are designed to insulate and hence to minimize heat exchange with the interior of the building. As a result, roof-surface temperatures often become very hot by day, whereas the partially shaded and better conducting canyon walls and floor are cooler. At night circumstances are reversed with the roofs being relatively cold and canyon surfaces warmer as they release their daytime heat uptake. There may also be complications due to the release of heat from roof exhaust vents. Therefore, while there is little variation of temperature with height in the UCL, there is a discontinuity near roof level both horizontally and vertically. Hence, if a meaningful spatial average is sought, sensors should be well above mean roof level, $> 1.5\,z_H$ if possible, so that the mixing of roof and canyon air is accomplished. In dealing with air temperature data from an elevated sensor, it is difficult to extrapolate these levels down towards screen level because currently no standard methods are available. Similarly, there is no simple, general scheme for extrapolating air temperatures horizontally inside the UCL. Statistical models work, but they require a large archive of existing observations over a dense network, which is not usually available.

9.3.2.2   *Surface temperature*

Surface temperature is not commonly measured at urban stations, but it can be a very useful variable to use as input in models to calculate fluxes. A representative surface temperature requires the averaging of an adequate sample of the many surfaces, vertical as well as horizontal, that make up an urban area. This is possible only using infrared remote sensing either from a scanner mounted on an aircraft or satellite, or a downward-facing pyrgeometer, or one or more radiation thermometers of which the combined field of view covers a representative sample of the urban district. Hence, to obtain accurate results, the target must be sampled appropriately and its average emissivity known.

9.3.2.3   *Soil and road temperature*

It is desirable to measure soil temperature in urban areas. The heat island effect extends down beneath a city and this may be of significance to engineering design for water pipes or road construction. In practice, the measurement of this variable may be difficult at more heavily developed urban sites. Bare ground may not be available, the soil profile is often highly disturbed, and at depth there may be obstructions or anomalously warm or cool artefacts (for example, empty, full or leaky water pipes, sewers, heat conduits). In urban areas, the measurement of grass minimum temperature has almost no practical utility.

Temperature sensors are often embedded in road pavements, especially in areas subject to freezing. They are usually part of a monitoring station for highway weather. It is often helpful to have sensors beneath both the tire track area and the centre of the lane.

9.3.3   **Atmospheric pressure**

At the scale of urban areas it will probably not be necessary to monitor atmospheric pressure if there is already a synoptic station in the region. If pressure sensors are included, the recommendations of Part I, Chapter 3, apply. In rooms and elsewhere in the vicinity of buildings there is the probability of pressure "pumping" due to gusts. Also, interior-exterior pressure differences may exist if the sensor is located in an air-conditioned room. Both difficulties can be alleviated if a static pressure head is installed (see Part I, Chapter 3, 3.8).

9.3.4   **Humidity**

The instruments normally used for humidity (Part I, Chapter 4) are applicable to urban areas. The guidelines given in section 9.3.2.1 for the siting and exposure of temperature sensors in the UCL, and above the RSL, apply equally to humidity sensors.

Urban environments are notoriously dirty (dust, oils, pollutants). Several hygrometers are subject to degradation or require increased maintenance in urban environments. Hence, if psychrometric methods are used, the wet-bulb sleeve must be replaced more frequently than normal and close attention should be given to ensuring that the distilled water remains uncontaminated. The hair strands of a hair hygrometer can be destroyed by polluted urban air; hence, their use is not recommended for extended periods. The mirror of dewpoint hygrometers and the windows of ultraviolet and infrared absorption hygrometers need to be cleaned frequently. Some instruments degrade to such an extent that the sensors have to be completely replaced fairly regularly. Because of shelter from wind in the UCL, forced ventilation at the rate recommended in Part I, Chapter 4, 4.2 is essential, as is the provision of shielding from extraneous sources of solar and long-wave radiation.

9.3.5   **Wind speed and direction**

The measurement of wind speed and direction is highly sensitive to flow distortion by obstacles. Obstacles create alterations in the average wind flow and turbulence. Such effects apply at all scales of concern, including the effects of local relief due to hills, valleys and cliffs, sharp changes in roughness or in the effective surface elevation (z_d, see below), perturbation of flow around clumps of trees and buildings, individual trees and buildings and even disturbance induced by the physical bulk of the tower or mounting arm to which the instruments are attached.

9.3.5.1   *Mean wind profile*

However, if a site is on reasonably level ground, has sufficient fetch downstream of major changes of roughness and is in a single UCZ without anomalously tall buildings, a mean wind profile such as that in Figure 9.4 should exist. The mean is both spatial and temporal. Within the UCL no one site can be expected to possess such a profile. Individual locations experience highly variable speed and direction shifts as the air-stream interacts with individual building arrangements, streets, courtyards and trees. In street canyons, the shape of the profile is different for along-canyon versus across-canyon flow (Christen et al., 2002) and depends on position across and along the street (DePaul and Shieh, 1986). Wind speed gradients in the UCL are small until quite close to the surface. As a first approximation the profile in the UCL can be described by an exponential form (Britter and Hanna, 2003) merging with the log profile near the roof level (Figure 9.4).

In the inertial sublayer, the Monin-Obukhov similarity theory applies, including the logarithmic law:

$$\bar{u}_z = \left(u_* / k \right) \{ \ln \left[\left(z - z_d \right) / z_0 \right] + \Psi_M \left(\frac{z}{L} \right) \} \tag{9.2}$$

where u_* is the friction velocity; k is von Karman's constant (0.40); z_0 is the surface roughness length; z_d is the zero-plane displacement height (Figure 9.4); L is the Obukhov stability length
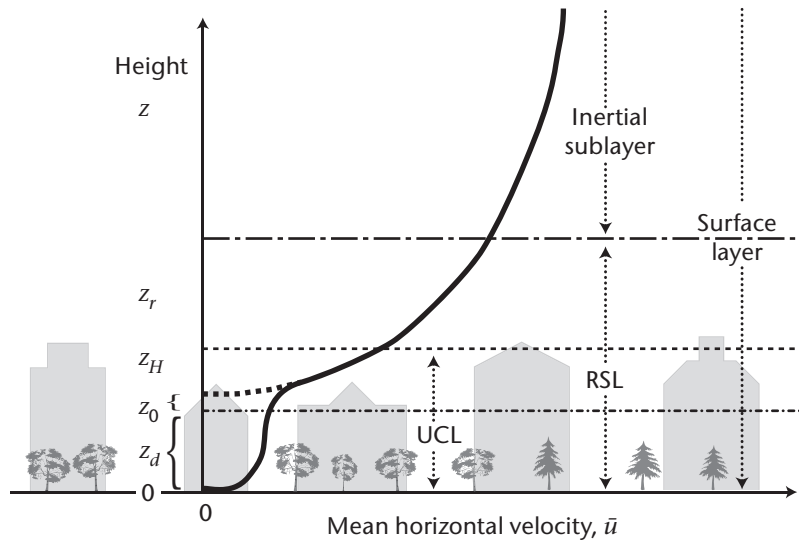
Figure 9.4. Generalized mean (spatial and temporal) wind velocity ($\bar{u}$) profile in a densely developed urban area including the location of sublayers of the surface layer. The measures on the height scale are the mean height of the roughness elements (z_H) the roughness sublayer (z_r, or the blending height), the roughness length (z_0) and zero-plane displacement length (z_d). The dashed line represents the profile extrapolated from the inertial sublayer, the solid line represents the actual profile.

($= -u_*^3/[k(g/\theta_v)Q_H]$), where g is the gravitational acceleration, θ_v the virtual potential temperature and Q_H the turbulent sensible heat flux; and Ψ_M is a dimensionless function that accounts for the change in curvature of the wind profile away from the neutral profile with greater stability or instability.[1] In the neutral case (typically with strong winds and cloud) when Ψ_M is unity, equation 9.2 reduces to:

$$\bar{u}_z = (u_* / k)\ln\left[(z - z_d)/z_0\right] \tag{9.3}$$

The wind profile parameters can be measured using a vertical array of anemometers, or measurements of momentum flux or gustiness from fast-response anemometry in the inertial layer, but estimates vary with wind direction and are sensitive to errors (Wieringa, 1996; Verkaik, 2000). Methods to parameterize the wind profile parameters z_0 and z_d for urban terrain are also available (for reviews, see Grimmond and Oke, 1999; Britter and Hanna, 2003). The simplest methods involve general descriptions of the land use and obstacles (see Tables 9.1 and 9.2 as well as Davenport et al., 2000; Grimmond and Oke, 1999), or a detailed description of the roughness element heights and their spacing from either a geographic information system of the building and street dimensions, or maps and aerial oblique photographs, or airborne/satellite imagery and the application of one of several empirical formulae (for recommendations, see Grimmond and Oke, 1999).

It is important to incorporate the displacement height z_d into urban wind-profile assessments. Effectively, this is equivalent to setting a base for the logarithmic wind profile that recognizes the physical bulk of the urban canopy. It is like setting a new "ground surface" aloft, where the mean momentum sink for the flow is located (Figure 9.4).

Depending on the building and tree density, this could set the base of the profile at a height of between 0.5 and 0.8 z_H (Grimmond and Oke, 1999). Hence, failure to incorporate it in calculations causes large errors. First estimates can be made using the fractions of z_H given in Table 9.2 (Note b).

---

[1]   For more details on L and the form of the ψ_M function, see a standard micrometeorology text, for example, Stull, 1988; Garratt, 1992; or Arya, 2001. Note that u_* and Q_H should be evaluated in the inertial layer above the RSL.

Table 9.2. Davenport classification of effective terrain roughness[a]

Class	z_0 (m)	Landscape description
4 Roughly open	0.10	Moderately open country with occasional obstacles (e.g. isolated low buildings or trees) at relative horizontal separations of at least 20 obstacle heights
5 Rough	0.25	Scattered obstacles (buildings) at relative distances of 8 to 12 obstacle heights for low solid objects (e.g. buildings) (analysis may need z_d)[b]
6 Very rough	0.5	Area moderately covered by low buildings at relative separations of 3 to 7 obstacle heights and no high trees (analysis requires z_d)[b]
7 Skimming	1.0	Densely built-up area without much building height variation (analysis requires z_d)[b]
8 Chaotic	2.0	City centres with mix of low and high-rise buildings (analysis by wind tunnel advised)

Notes:

a   Abridged version (revised 2000, for urban roughness only) of Davenport et al. (2000); for classes 1 to 3 and for rural classes 4 to 8, see Part I, Chapter 5, annex to this Guide and WMO (2003).

b   First order values of z_d are given as fractions of average obstacle height, i.e.: 0.5 z_H, 0.6 z_H and 0.7 z_H for Davenport classes 5, 6 and 7, respectively.

9.3.5.2   *Height of measurement and exposure*

The choice of height at which wind measurements should be taken in urban areas is a challenge. However, if some basic principles are applied, meaningful results can be attained. The poor placement of wind sensors in cities is the source of considerable wasted resources and effort and leads to potentially erroneous calculations of pollutant dispersion. Of course, this is even a source of difficulty in open terrain due to obstacles and topographic effects. This is the reason why the standard height for rural wind observations is set at 10 m above ground, not at screen level, and why there the anemometer should not be at a horizontal distance from obstructions of less than 10 obstacle heights (Part I, Chapter 5, 5.9.2). In typical urban districts it is not possible to find such locations, for example, in a UCZ with 10 m high buildings and trees it would require a patch that is at least 100 m in radius. If such a site exists it is almost certainly not representative of the zone. It has already been noted that the roughness sublayer, in which the effects of individual roughness elements persist, extends to a height of about 1.5 z_H in a densely built-up area and perhaps higher in less densely developed sites. Hence, in the example district the minimum acceptable anemometer height is at least 15 m, not the standard 10 m. When buildings are much taller, an anemometer at the standard 10 m height would be well down in the UCL, and, given the heterogeneity of urban form and therefore of wind structure, there is little merit in placing a wind sensor beneath, or even at about, roof level.

It is well known from wind tunnel and field observations that flow over an isolated solid obstacle, like a tall building, is greatly perturbed both immediately over and around it. These perturbations include modifications to the streamlines, the presence of recirculation zones on the roof and in the so-called "bubble" or cavity behind it, and wake effects that persist in the downstream flow for tens of building height multiples that affect a large part of the neighbourhood (Figure 9.5).

There are many examples of poorly exposed anemometer-vane systems in cities. The data registered by such instruments are erroneous, misleading, potentially harmful if used to obtain wind input for wind load or dispersion applications, and wasteful of resources. The inappropriateness of placing anemometers and vanes on short masts on the top of buildings cannot be over-emphasized. Speed and directions vary hugely in short distances, both horizontally and vertically. Results from instruments deployed in this manner bear little resemblance to the general flow and are entirely dependent on the specific features of the building itself, the mast location on the structure, and the angle-of-attack of the flow to the building. The circulating and vortex flows seen in Figure 9.5 mean that, if the mast is placed ahead of, on top of, or in the cavity zone behind a building, direction measurements could
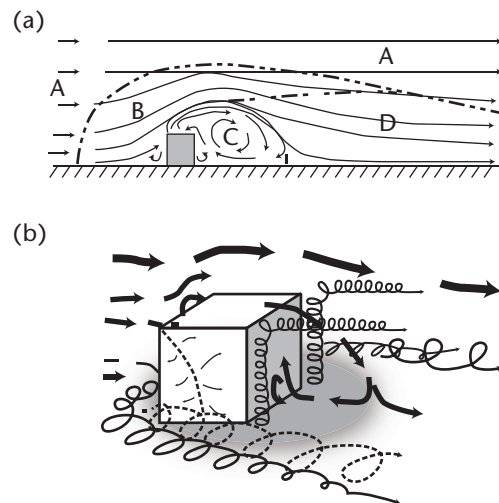
Figure 9.5. Typical two-dimensional flow around a building with flow normal to the upwind face (a): streamlines and flow zones; A represents undisturbed, B represents displacement, C represents cavity, D represents wake (after Halitsky, 1963), and (b): flow, and vortex structures (simplified after Hunt et al., 1978).

well be counter to those prevailing in the flow outside the influence of the building's own wind climate (namely, in zone A of Figure 9.5(a)), and speeds are highly variable. To get outside the perturbed zone, wind instruments must be mounted at a considerable height. For example, it has been proposed that such sensors should be at a height greater than the maximum horizontal dimension of the major roof (Wieringa, 1996). This implies an expensive mast system, perhaps with guys that subtend a large area and perhaps difficulties in obtaining permission to install. Nevertheless, this is the only acceptable approach if meaningful data are to be measured.

Faced with such realities, sensors should be mounted so that their signal is not overly compromised by their support structure. The following recommendations are made:

(a) In urban districts with low element height and density (UCZ 6 and 7), it may be possible to use a site where the "open country" standard exposure guidelines can be met. To use the 10 m height, the closest obstacles should be at least 10 times their height distant from the anemometer and not be more than about 6 m tall on average;

(b) In more densely built-up districts, with relatively uniform element height and density (buildings and trees), wind speed and direction measurements should be taken with the anemometer mounted on a mast of open construction at a minimum height of 1.5 times the mean height of the elements;

(c) In urban districts with scattered tall buildings the recommendations are as in (b), but with special attention to avoid the wake zone of the tall structures;

(d) It is not recommended that measurements be taken of wind speed or direction in densely built areas with multiple high-rise structures unless a very tall tower is used.

Anemometers on towers with open construction should be mounted on booms (cross-arms) that are long enough to keep the sensors at least two (preferable three) tower diameters' distance from the side of the mast (Gill et al., 1967). Sensors should be mounted so that the least frequent flow direction passes through the tower. If this is not possible, or if the tower construction is not very open, two or three booms with duplicate sensors may have to be installed to avoid wake effects and upwind stagnation produced by the tower itself.

If anemometer masts are to be mounted on tall or isolated buildings, the effects of the dimensions of that structure on the flow must be considered (see Part II, Chapter 5, 5.3.3).

This is likely to require analysis using wind tunnel, water flume or computational fluid dynamics models specifically tailored to the building of interest, and including its surrounding terrain and structures.

The objective is to ensure that all wind measurements are taken at heights where they are representative of the upstream surface roughness at the local scale and are as free as possible of confounding influences from microscale or local scale surface anomalies. Hence the emphasis on gaining accurate measurements at whatever height is necessary to reduce error rather than measuring at a standard height. This may require splitting the wind site from the location of the other measurement systems. It may also result in wind observations at several different heights in the same settlement. That will necessitate extrapolation of the measured values to a common height, if spatial differences are sought or if the data are to form input to a mesoscale model. Such extrapolation is easily achieved by applying the logarithmic profile (equation 9.2) to two heights:

$$\bar{u}_1 / \bar{u}_{ref} = \ln\left(z_1/z_0\right) \Big/ \ln\left(z_{ref}/z_0\right)$$ (9.4)

where z_{ref} is the chosen reference height; z_1 is the height of the site anemometer; and z_0 is the roughness length of the UCZ. In urban terrain it is correct to define the reference height to include the zero-plane displacement height, namely, both z_1 and z_{ref} have the form $(z_x - z_d)$, where the subscript x stands for "1" or "ref". A suitable reference height could be 50 m above displacement height.

Other exposure corrections for flow distortion, topography and roughness effects can be made as recommended in Part I, Chapter 5 (see 5.9.4: Exposure correction). It may well be that suitable wind observations cannot be arranged for a given urban site. In that case, it is still possible to calculate the wind at the reference height using wind observations at another urban station or the airport using the "logarithmic transformation" model of Wieringa (1986):

$$\bar{u}_{zA} = \bar{u}_{zB} \left[\frac{\ln\left(z_r/z_{0B}\right) \cdot \ln\left(z_A/z_{0A}\right)}{\ln\left(z_B/z_{0B}\right) \cdot \ln\left(z_r/z_{0A}\right)} \right]$$ (9.5)

where the subscripts A and B refer to the site of interest where winds are wanted and the site where standard wind measurements are available, respectively. The blending height z_r should either be taken as 4 z_H (section 9.1.1.3) or be given a standard value of 60 m; the method is not very sensitive to this term. Again, if either site has dense, tall roughness elements, the corresponding height scale should incorporate z_d.

9.3.5.3   *Wind sensor considerations*

Instruments used to measure wind speed and direction, gustiness and other characteristics of the flow in non-urban environments are applicable to urban areas. In cities, wind direction should always be measured, as well as speed, in order to allow azimuth-dependent corrections of tower influence to be made. If mechanical cup anemometers are used, because of the dirtiness of the atmosphere maintenance should be more frequent and close attention should be given to bearings and corrosion. If measurements are taken in the UCL, gustiness may increase the problem of cup over-speeding, and too much shelter may cause anemometers to operate near or below their threshold minimum speed. This must be dealt with through heightened maintenance and perhaps by using fast-response anemometers, propeller-type anemometers or sonic anemometers. Propeller anemometers are less prone to over-speeding, and sonic anemometers, having no moving parts, are practically maintenance-free. However, they are expensive and require sophisticated electronic logging and processing and not all models work when it is raining.

9.3.6   **Precipitation**

The instruments and methods for the measurement of precipitation given in Part I, Chapter 6 are also relevant to urban areas. The measurement of precipitation as rain or snow is always

susceptible to errors associated with the exposure of the gauge, especially in relation to the wind field in its vicinity. Given the urban context and the highly variable wind field in the UCL and the RSL, concerns arise from four main sources as follows:

(a)   The interception of precipitation during its trajectory to the ground by nearby collecting surfaces such as trees and buildings;

(b)   Hard surfaces near the gauge which may cause splash-in into the gauge, and over-hanging objects which may drip precipitation into the gauge;

(c)   The spatial complexity of the wind field around obstacles in the UCL causes very localized concentration or absence of rain- or snow-bearing airflow;

(d)   The gustiness of the wind in combination with the physical presence of the gauge itself causes anomalous turbulence around it which leads to under- or over-catch.

In open country, standard exposure requires that obstacles should be no closer than two times their height. In some ways, this is less restrictive than for temperature, humidity or wind measurements. However, in the UCL the turbulent activity created by flow around sharp-edged buildings is more severe than that around natural obstacles and may last for greater distances in their wake. Again, the highly variable wind speeds and directions encountered on the roof of a building make these sites to be avoided.

On the other hand, unlike temperature, humidity and wind measurements, the object of precipitation measurements is often not for the analysis of local effects, except perhaps in the case of rainfall rate. Some urban effects on precipitation may be initiated at the local scale (for example, by a major industrial facility), but may not show up until well downwind of the city. Distinct patterns within an urban area are more likely to be due to relief or coastal topographic effects.

Selecting an extensive open site in the city, where normal exposure standards can be met, may be acceptable, but it almost certainly will mean that the gauge will not be co-located with the air temperature, humidity and wind sensors. While the latter sensors need to be representative of the local scale urban structure, cover, fabric and metabolism of a specific UCZ, this is not the case for precipitation.

However, the local environment of the gauge is important if the station is to be used to investigate intra-urban patterns of precipitation type. For example, the urban heat island has an influence on the survival of different forms of precipitation, for example, snow or sleet at the cloud base may melt in the warmer urban atmosphere and fall as rain at the ground. This may result in snow at rural and suburban sites when the city centre registers rain.

With regard to precipitation gauges in urban areas, it is recommended that:

(a)   Gauges should be located in open sites within the city where the standard exposure criteria can be met (for example, playing fields, open parkland with a low density of trees, urban airports);

(b)   Gauges should be located in conjunction with wind instruments if a representative exposure for them is found. In other than low density built-up sites, this probably entails mounting the gauge above roof level on a mast. This means that the gauge will be subject to greater than normal wind speed and hence the error of estimation will be greater than near the surface, and the gauge output will have to be corrected. Such correction is feasible if wind is measured on the same mast. It also means that automatic recording is favoured, and the gauge must be checked regularly to ensure that it is level and that the orifice is free of debris;

(c)   Gauges should not be located on the roofs of buildings unless they are exposed at a sufficient height to avoid the wind envelope of the building;

(d) The measurement of snowfall depth should be taken at an open site or, if made at developed sites, that a large spatial sample should be obtained to account for the inevitable drifting around obstacles. Such sampling should include streets oriented in different directions.

Urban hydrologists are interested in rainfall rates, especially during major storm events. Hence, tipping-bucket raingauges or weighing gauges have utility. The measurement of rain and snowfall in urban areas stands to benefit from the development of techniques such as optical raingauges and radar.

Dew, ice and fog precipitation also occurs in cities and can be of significance to the water budget, especially for certain surfaces, and may be relevant to applications such as plant diseases, insect activity, road safety and finding a supplementary source of water resources. The methods outlined in Part I, Chapter 6 are appropriate for urban sites.

9.3.7   Radiation

At present, there is a paucity of radiation flux measurements conducted in urban areas. For example, there are almost none in the Global Energy Balance Archive of the World Climate Programme and the Atmospheric Radiation Measurement Program of the US Department of Energy. Radiation measurement sites are often located in rural or remote locations specifically to avoid the aerosol and gaseous pollutants of cities which "contaminate" their records. Even when a station has the name of a city, the metadata usually reveal they are actually located well outside the urban limits. If stations are located in the built-up area, only incoming solar (global) radiation is likely to be measured; neither incoming long-wave radiation nor any fluxes with outgoing components are monitored. For the most part, short-term experimental projects focusing specifically on urban effects measure both the receipt and loss of radiation in cities. All short- and long-wave fluxes are affected by the special properties of the atmosphere and surface of cities, and the same is true for the net all-wave radiation balance that effectively drives the urban energy balance (Oke, 1988*a*).

All of the instruments, calibrations and corrections, and most of the field methods outlined in relation to the measurement of radiation at open country sites in Part I, Chapter 7, apply to urban areas. Only differences, or specific urban needs or difficulties, are mentioned here.

9.3.7.1   *Incoming fluxes*

Incoming solar radiation is such a fundamental forcing variable of urban climate that its measurement should be given a high priority when a station is established or upgraded. Knowledge of this term, together with standard observations of air temperature, humidity and wind speed, plus simple measures of the site structure and cover, allows a meteorological pre-processor scheme (namely, methods and algorithms used to convert standard observation fields into the variables required as input by models, but not measured, for example, fluxes, stability, mixing height, dispersion coefficients, and so on) such as the Hybrid Plume Dispersion Model (Hanna and Chang, 1992) or the Local-scale Urban Meteorological Parameterization Scheme (Grimmond and Oke, 2002) to be used to calculate much more sophisticated measurements such as atmospheric stability, turbulent statistics, the fluxes of momentum, heat and water vapour. These in turn make it possible to predict the mixing height and pollutant dispersion (COST 710, 1998; COST 715, 2001). Furthermore, solar radiation can be used as a surrogate for daytime cloud activity, and is the basis of applications in solar energy, daylight levels in buildings, pedestrian comfort, legislated rights to solar exposure and many other fields. At automatic stations, the addition of solar radiation measurement is simple and relatively inexpensive.

The exposure requirements for pyranometers and other incoming flux sensors are relatively easily met in cities. The fundamental needs are for the sensor to be level, free of vibration and free of any obstruction above the plane of the sensing element including both fixed features (buildings, masts, trees and hills) and ephemeral ones (clouds generated from exhaust vents or pollutant

plumes). Therefore, a high, stable and accessible platform like the roof of a tall building is often ideal. It may be impossible to avoid the short-term obstruction of direct-beam solar radiation impinging on an up-facing radiometer by masts, antennas, flag poles and similar structures. If this occurs, the location of the obstruction and the typical duration of its impact on the sensing element should be fully documented (see section 9.4). Methods to correct for such interference are mentioned in Part I, Chapter 7. It is also important to ensure that there is no excessive reflection from very light-coloured walls that may extend above the local horizon. It is essential to clean the upper domes at regular intervals. In heavily polluted environments this may mean on a daily basis.

Other incoming radiation fluxes are also desirable but their inclusion depends on the nature of the city, the potential applications and the cost of the sensors. These radiation fluxes (and their instruments) are the following: incoming direct solar beam (pyrheliometer), diffuse sky solar (pyranometer fitted with a shade ring or a shade disc on an equatorial mount), solar ultraviolet (broadband and narrowband sensors, and spectrometers) and long-wave (pyrgeometer). All of these radiation fluxes have useful applications: beam (pollution extinction coefficients), diffuse (interior daylighting, solar panels), ultraviolet (depletion by ozone and damage to humans, plants and materials) and long-wave (monitoring nocturnal cloud and enhancement of the flux by pollutants and the heat island effect).

9.3.7.2   *Outgoing and net fluxes*

The reflection of solar radiation and the emission and reflection of long-wave radiation from the underlying surface, and the net result of short-, long- and all-wave radiant fluxes, are currently seldom monitored at urban stations. This means that significant properties of the urban climate system remain unexplored. The albedo, which decides if solar radiation is absorbed by the fabric or is lost back to the atmosphere and space, will remain unknown. The opportunity to invert the Stefan-Boltzmann relation and solve for the surface radiant temperature is lost. The critical net radiation that supports warming/cooling of the fabric, and the exchanges of water and heat between the surface and the urban boundary layer, is missing. Of these, net all-wave radiation data lack the most. Results from a well-maintained net radiometer are invaluable to drive a pre-processor scheme and as a surrogate measurement of cloud.

The main difficulty in measuring outgoing radiation terms accurately is the exposure of the down-facing radiometer to view a representative area of the underlying urban surface. The radiative source area (equation 9.1 and Figure 9.2) should ideally "see" a representative sample of the main surfaces contributing to the flux. In the standard exposure cases, defined in the relevant sections of Part I, Chapter 7, a sensor height of 2 m is deemed appropriate over a short grass surface. At that height, 90% of the flux originates from a circle with a diameter of 12 m on the surface. Clearly, a much greater height is necessary over an urban area in order to sample an area that contains a sufficient population of surface facets to be representative of that UCZ. Considering the case of a radiometer at a height of 20 m (at the top of a 10 m high mast mounted on a 10 m high building) in a densely developed district, the 90% source area has a diameter of 120 m at ground level. This might seem sufficient to "see" several buildings and roads, but it must also be considered that the system is three-dimensional, not quasi-flat like grass. At the level of the roofs in the example, the source area is now only 60 m in diameter, and relatively few buildings may be viewed.

The question becomes whether the sensor can "see" an appropriate mix of climatically active surfaces. This means that the sensor must not only see an adequate set of plan-view surface types, but also sample appropriate fractions of roof, wall and ground surfaces, including the correct fractions of each that are in the sun or shade. This is a non-trivial task that depends on the surface structure and the positions of both the sensor and the sun in space above the array. Soux et al. (2004) developed a model to calculate these fractions for relatively simple urban-like geometric arrays. However, more work is needed before guidelines specific to individual UCZ types are available. It seems likely that the sensor height has to be *greater* than that for turbulence measurements. The non-linear nature of radiative source area effects is clear from equation 9.1 (see Figure 9.2). The greater weighting of surfaces closer to the mast location means that the immediate surroundings are most significant. In the previous example of the radiometer at a

height of 20 m on a 10 m high building, 50% of the signal at the roof-level comes from a circle of only 20 m in diameter (perhaps only a single building). If the roof of that building, or any other surface on which the mast is mounted, has anomalous radioactive properties (albedo, emissivity or temperature), it disproportionately affects the flux, which is supposed to be representative of a larger area. Hence, roofs with large areas of glass or metal, or with an unusually dark or light colour, or those designed to hold standing water, should be avoided.

The problems associated with down-facing radiometers at large heights include: (a) the difficulty of ensuring that the plane of the sensing element is level; (b) ensuring that at large zenith angles the sensing element does not "see" direct beam solar radiation or incoming long-wave radiation from the sky; (c) considering whether there is need to correct results to account for radiative flux divergence in the air layer between the instrument height and the surface of interest. To eliminate extraneous solar or long-wave radiation near the horizon, it may be necessary to install a narrow collar that restricts the field of view to a few degrees less than 2π. This will necessitate a small correction applied to readings to account for the missing diffuse solar input (see Part I, Chapter 7, Annex 7.E for the case of a shading ring) or the extra long-wave input from the collar.

Inverted sensors may be subject to error because their back is exposed to solar heating. This should be avoided by using some form of shielding and insulation. Maintaining the cleanliness of the instrument domes and wiping away deposits of water or ice may also be more difficult. The inability to observe the rate and effectiveness of instrument ventilation at a certain height means that instruments that do not need aspiration should be preferred. The ability to lower the mast to attend to cleaning, the replacement of desiccant or polyethylene domes and levelling is an advantage.

It is recommended that:

(a)   Down-facing radiometers be placed at a height at least equal to that of a turbulence sensor (namely, a minimum of $2\,z_H$ is advisable) and preferably higher;

(b)   The radiative properties of the immediate surroundings of the radiation mast should be representative of the urban district of interest.

9.3.8   Sunshine duration

The polluted atmospheres of urban areas cause a reduction in sunshine hours compared with their surroundings or pre-urban values (Landsberg, 1981). The instruments, methods and exposure recommendations given in Part I, Chapter 8 are applicable to an urban station.

9.3.9   Visibility and meteorological optical range

The effects of urban areas upon visibility and meteorological optical range (MOR) are complex because, while pollutants tend to reduce visibility and MOR through their impact on the attenuation of light and the enhancement of certain types of fog, urban heat and humidity island effects often act to diminish the frequency and severity of fog and low cloud. There is considerable practical value in having urban visibility and MOR information for fields such as aviation, road and river transportation and optical communications, and thus to include these observations at urban stations.

The visual perception of visibility is hampered in cities. While there are many objects and lights that can serve as range targets, it may be difficult to obtain a sufficiently uninterrupted line of sight at the recommended height of 1.5 m. The use of a raised platform or the upper level of buildings is considered non-standard and is not recommended. Observations near roof level may also be affected by scintillation from heated roofs, or the "steaming" of water from wet roofs during drying, or pollutants and water clouds released from chimneys and other vents.

Instruments to measure MOR, such as transmissometers and scatter meters, generally work well in urban areas. They require relatively short paths and will give good results if the optics

are maintained in a clean state. Naturally, the instrument must be exposed at a location that is representative of the atmosphere in the vicinity, but the requirements are no more stringent than for other instruments placed in the UCL. It may be that, for certain applications, knowledge of the height variation of MOR is valuable, for example, the position of the fog top or the cloud base.

9.3.10 Evaporation and other fluxes

Urban development usually leads to a reduction in evaporation primarily due to the fact that built features seal the surface and that vegetation has been removed. Nonetheless, in some naturally dry regions, an increase may occur if water is imported from elsewhere and used to irrigate urban vegetation.

Very few evaporation measurement stations exist in urban areas. This is understandable because it is almost impossible to interpret evaporation measurements conducted in the UCL using atmometers, evaporation pans or lysimeters. As detailed in Part I, Chapter 10, such measurements must be at a site that is representative of the area; not closer to obstacles than 5 times their height, or 10 times if they are clustered; not placed on concrete or asphalt; not unduly shaded; and free of hard surfaces that may cause splash-in. In addition to these concerns, the surfaces of the instruments are assumed to act as surrogates for vegetation or open water systems. Such surfaces are probably not representative of the surroundings at an urban site. Hence, they are in receipt of micro-advection that is likely to force evaporation at unrealistically high rates.

Consider the case of an evaporation pan installed over a long period which starts out at a semi-arid site that converts to irrigated agricultural uses and is then encroached upon by suburban development and is later in the core of a heavily developed urban area. Its record of evaporation starts out very high, because it is an open water surface in hot, dry surroundings. Therefore, although actual evaporation in the area is very low, advection forces the loss from the pan to be large. Because the introduction of irrigation makes conditions cooler and more humid, the pan readings drop, but actual evaporation is large. Inasmuch as urban development largely reverses the environmental changes and reduces the wind speed near the ground, pan losses increase but the actual evaporation probably drops. Hence, throughout this sequence pan evaporation and actual evaporation are probably in anti-phase. During the agricultural period a pan coefficient might have been applied to convert the pan readings to those typical of short grass or crops. No such coefficients are available to convert pan to urban evaporation, even if the readings are not corrupted by the complexity of the UCL environment. In summary, the use of standard evaporation instruments in the UCL is not recommended.

The dimensions and heterogeneity of urban areas renders the use of full-scale lysimeters impractical (for example, the requirement to be not less than 100 to 150 m from a change in surroundings). Micro-lysimeters can give the evaporation from individual surfaces, but they are still specific to their surroundings. Such lysimeters need careful attention, including soil monolith renewal to prevent drying out, and are not suitable for routine long-term observations.

Spatially averaged evaporation and other turbulent fluxes (momentum, sensible heat, carbon dioxide) information can be obtained from observations above the RSL. Several of these fluxes are of greater practical interest in urban areas than in many open country areas. For example, the vertical flux of horizontal momentum and the integral wind statistics and spectra are needed to determine wind loading on structures and the dispersion of air pollutants. The sensible heat flux is an essential input to calculate atmospheric stability (for example, the flux Richardson number and the Obukhov length) and the depth of the urban mixing layer. Fast response eddy covariance or standard deviation methods are recommended, rather than profile gradient methods. Appropriate instruments include sonic anemometers, infrared hygrometers and gas analysers and scintillometers. The sensors should be exposed in the same manner as wind sensors: above the RSL but below the internal boundary layer of the UCZ of interest. Again, such measurements rely on the flux "footprint" being large enough to be representative of the local area of interest.

If such flux measurements are beyond the financial and technical resources available, a meteorological pre-processor scheme such as the Ozone Limiting Method, the Hybrid Plume Dispersion Method or the Local-scale Urban Meteorological Parameterization Scheme (see section 9.3.7) can be an acceptable method to obtain aerially representative values of urban evaporation and heat flux. Such schemes require only spatially representative observations of incoming solar radiation, air temperature, humidity and wind speed and general estimates of average surface properties such as albedo, emissivity, roughness length and the fractions of the urban district that are vegetated or built-up or irrigated. Clearly, the wind speed observations must conform to the recommendations in section 9.3.5. Ideally air temperature and humidity should also be observed above the RSL; however, if only UCL values are available, this is usually acceptable because such schemes are not very sensitive to these variables.

9.3.11 Soil moisture

Knowledge of urban soil moisture can be useful, for example, to gardeners and in the calculation of evaporation. Its thermal significance in urban landscapes is demonstrated by the remarkably distinct patterns in remotely sensed thermal imagery. By day, any patch with active vegetation or irrigated land is noticeably cooler than land that is built on, paved or bare. However, the task of sampling to obtain representative values of soil moisture is daunting.

Some of the challenges presented include the fact that large fractions of urban surfaces are completely sealed over by paved and built features; much of the exposed soil has been highly disturbed in the past during construction activity or following abandonment after urban use; the "soil" may actually be largely formed from the rubble of old buildings and paving materials or have been imported as soil or fill material from distant sites; or the soil moisture may be affected by seepage from localized sources such as broken water pipes or sewers or be the result of irrigation. All of these elements lead to a very patchy urban soil moisture field that may have totally dry plots situated immediately adjacent to over-watered lawns. Hence, while some idea of local-scale soil moisture may be possible in areas with very low urban development, or where the semi-natural landscape has been preserved, it is almost impossible to characterize in most urban districts. Again, in this case it may be better to use rural values that give a regional background value rather than to have no estimate of soil moisture availability.

9.3.12 Present weather

If human observers or the usual instrumentation are available, the observation of present weather events and phenomena such as rime, surface ice, fog, dust and sand storms, funnel clouds and thunder and lightning can be valuable, especially those with practical implications for the efficiency or safety of urban activities, for example transportation. If archiving facilities are available, the images provided by webcams can provide very helpful evidence of clouds, short-term changes in cloud associated with fronts, fog banks that ebb and flow, low cloud that rises and falls, and the arrival of dust and sand storm fronts.

9.3.13 Cloud

Although cloud cover observation is rare in large urban areas, this information is very useful. All of the methods and instruments outlined in Part I, Chapter 15 are applicable to urban areas. The large number and intensity of light sources in cities, combined with a hazy, sometimes polluted, atmosphere, make visual observation more difficult. Where possible, the observational site should avoid areas with particularly bright lighting.

9.3.14 Atmospheric composition

The monitoring of atmospheric pollution in the urban environment is increasingly important. However, this is another specialist discipline and will not be dealt with in this chapter. Part I, Chapter 16 deals with the subject in the broader context of the Global Atmosphere Watch.

9.3.15   Profiling techniques for the urban boundary layer

Because urban influences extend throughout the planetary boundary layer (Figure 9.1), it is necessary to use towers and masts to obtain observations above the RSL to probe higher. Of special interest are effects on the wind field and the vertical temperature structure including the depth of the mixing layer and their combined role in affecting pollutant dispersion.

All of the special profiling techniques outlined in Part II, Chapter 5 are relevant to urban areas. Acoustic sounders (sodars) are potentially very useful; nonetheless, it must be recognized that they suffer from two disadvantages: first, their signals are often interfered with by various urban sources of noise (traffic, aircraft, construction activity, and even lawnmowers); and second, they may not be allowed to operate if they cause annoyance to residents. Wind profiler radars, radio-acoustic sounding systems, microwave radiometers, microwave temperature profilers, laser radars (lidars) and modified ceilometers are all suitable systems to monitor the urban atmosphere if interference from ground clutter can be avoided. Similarly, balloons for wind tracking, boundary layer radiosondes (minisondes) and instrumented tethered balloons can all be used with good success rates as long as air traffic authorities grant permission for their use. Instrumented towers and masts can provide an excellent means of placing sensors above roof level and into the inertial sublayer, and very tall structures may permit measurements into the mixing layer above. However, it is necessary to emphasize the precautions given in Part II, Chapter 5, 5.3.3 regarding the potential interference with atmospheric properties by the support structure. Although tall buildings may appear to provide a way to reach higher into the urban boundary layer, unless obstacle interference effects are fully assessed and measures instituted to avoid them, the deployment of sensors can be unfruitful and probably misleading.

9.3.16   Satellite observations

Remote sensing by satellite with adequate resolution in the infrared may be relevant to extended urban areas. A description of these techniques is available in Part III, and a review of their use in the study of urban climates is given in Voogt and Oke (2003).

9.4   METADATA

The full and accurate documentation of station metadata (see Part I, Chapter 1) is absolutely essential for any station "to ensure that the final data user has no doubt about the conditions in which data have been recorded, gathered and transmitted, in order to extract accurate conclusions from their analysis" (WMO, 2003). It can be argued that this is even more critical for an urban station, because urban sites possess both an unusually high degree of complexity and a greater propensity to change. The complexity makes every site truly unique, whereas good open country sites conform to a relatively standard template. Change means that site controls are dynamic, meaning that documentation must be updated frequently. In Figure 9.6 it is assumed that the minimum requirements for station metadata set by WMO (2003) are all met and that hopefully some or all of the best practices they recommend are implemented. Here, emphasis is placed on special urban characteristics that need to be included in the metadata, in particular under the categories of "local environment" and "historical events".

9.4.1   Local environment

As explained in section 9.1.1, urban stations involve the exposure of instruments both within and above the urban canopy. Hence, the description of the surroundings must include both the microscale and the local scale. Following WMO (2003), with adaptations to characterize the urban environment, it is recommended that the following descriptive information be recorded for the station:

(a)   A map at the local scale to mesoscale (~1:50 000) as in Figure 9.6(a), updated as necessary to describe large-scale urban development changes (for example, conversion of open land
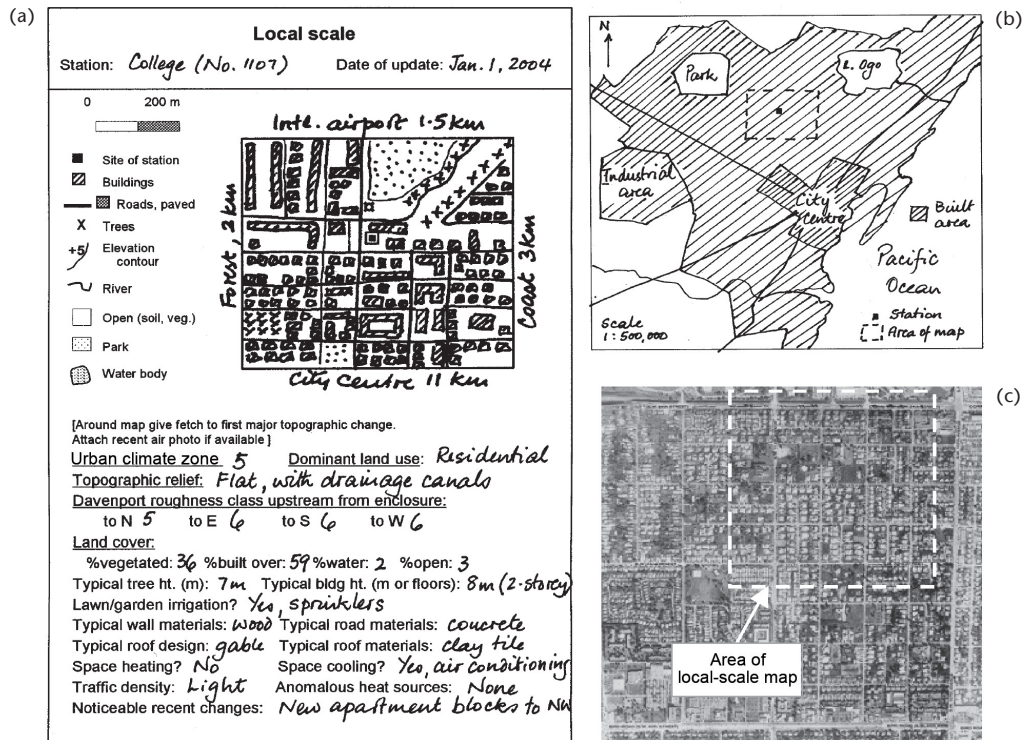
Figure 9.6. Minimum information necessary to describe the local-scale environment of an urban station, consisting of (a) a template to document the local setting; (b) a sketch map to situate the station in the larger urban region; and (c) an aerial photograph.

to housing, construction of a shopping centre or airport, construction of new tall buildings, cutting of a forest patch, drainage of a lake, creation of a detention pond). Ideally, an aerial photograph of the area should also be provided and a simple sketch map (at 1:500 000 or 1:1 000 000) to indicate the location of the station relative to the rest of the urbanized region (Figures 9.6(b) and (c)) and any major geographic features such as large water bodies, mountains and valleys or change in ecosystem type (desert, swamp, forest). An aerial oblique photograph can be especially illuminating because the height of buildings and trees can also be appreciated. If available, aerial or satellite infrared imagery may be instructive regarding important controls on microclimate. For example, relatively cool surfaces by day usually indicate the availability of moisture or materials with anomalous surface emissivity. Hotter than normal areas may be very dry, or have a low albedo or very good insulation. At night, relative coolness indicates good insulation, and relative warmth the opposite, or it could be a material with high thermal admittance that is releasing stored daytime heat or there could be an anomalous source of anthropogenic heat. UCZ and Davenport roughness classes can be judged using Tables 9.1 or 9.2;

(b)   A microscale sketch map (~1:5 000), according to metadata guidelines, updated each year (Figure 9.7(a));

(c)   Horizon mapping using a clinometer and compass survey in a circle around the screen (as shown in the diagram at the base of the template, Figure 9.7(a), and a fisheye lens photograph taken looking vertically at the zenith with the camera's back placed on the ground near the screen, but not such that any of the sky is blocked by it (Figure 9.7(b)). If a fisheye lens is not available, a simpler approach is to take a photograph of a hemispheric reflector (Figure 9.7(c)). This should be updated every year or more frequently if there are marked changes in horizon obstruction, such as the construction or demolition of a new building nearby, or the removal of trees;
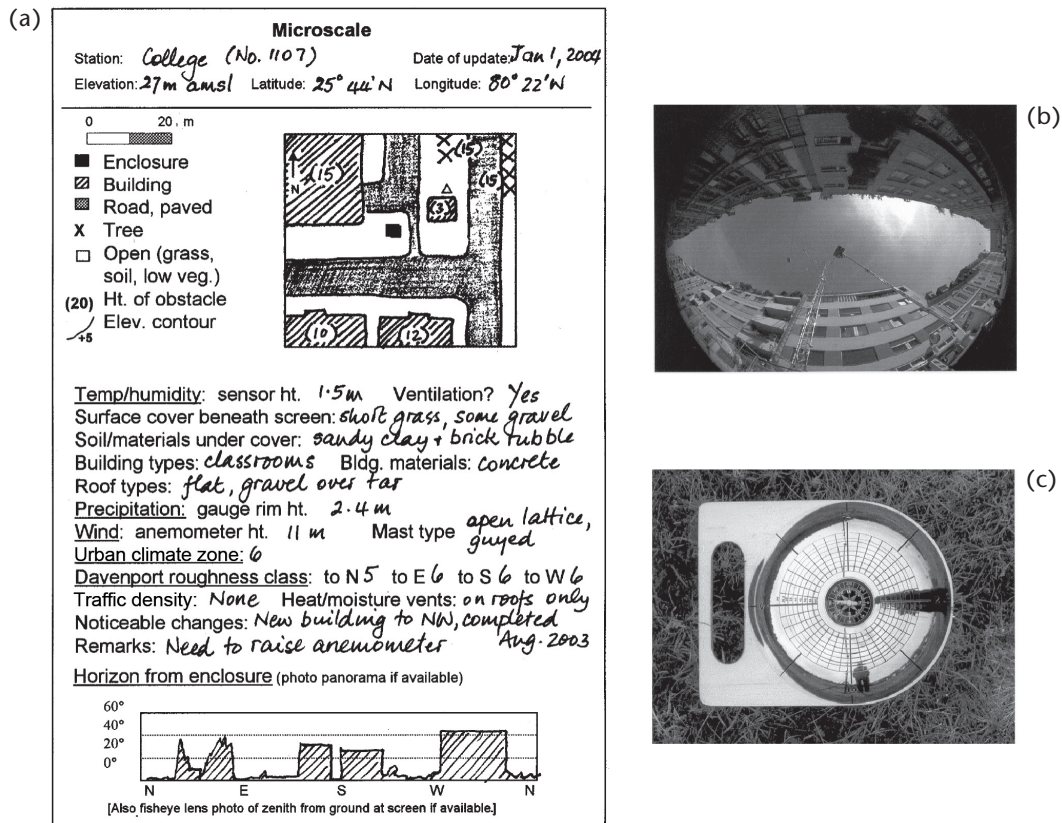
Figure 9.7. Information required to describe the microscale surroundings of an urban climate station; (a) a template for a metadata file; (b) an example of a fisheye lens photograph of a street canyon illustrating horizon obstruction; and (c) a UK Met Office hemispheric reflector placed on a raingauge.

(d)   Photographs taken from cardinal directions of the instrument enclosure and of other instrument locations and towers;

(e)   A microscale sketch of the instrument enclosure, updated when instruments are relocated or other significant changes occur;

(f)   If some of the station's measurements (wind, radiation) are made away from the enclosure (on masts, rooftops, more open locations) repeat steps (b) to (d) above for each site.

9.4.2   Historical events

Urban districts are subject to many forces of change, including new municipal legislation that may change the types of land uses allowed in the area, or the height of buildings, or acceptable materials and construction techniques, or environmental, irrigation or traffic laws and regulations. Quite drastic alterations to an area may result from central planning initiatives for urban renewal. More organic alterations to the nature of a district also arise because of in- or out-migrations of groups of people, or when an area comes into, or goes out of, favour or style as a place to live or work. The urban area may be a centre of conflict and destruction. Such events should be documented so that later users of the data understand some of the context of changes that might appear in the urban climate.

9.4.3 Observance of other WMO recommendations

All other WMO recommendations regarding the documentation of metadata, including station identifiers, geographical data, instrument exposure, types of instruments, instrument mounting and sheltering, data recording and transmission, observing practices, metadata storage and access and data processing should be observed at urban stations.

9.5 ASSESSMENT OF URBAN EFFECTS

The study of urban weather and climate possesses a perspective that is almost unique. People are curious about the role of humans in modifying the urban atmosphere. Therefore, unlike other environments of interest, where it is sufficient to study the atmosphere for its own sake or value, in urban areas there is interest in knowing about urban effects. This means assessing possible changes to meteorological variables as an urban area develops over time, compared to what would have happened had the settlement not been built. This question that is essentially unanswerable when a settlement has been built, and, even if the settlement had not been built, the landscape may well have evolved into a different state compared with the pre-existing one (for example, owing to other human activity such as agriculture or forestry). The assessment of urban effects is therefore fraught with methodological difficulties and no "truth" is possible, only surrogate approximations. If an urban station is being established alone, or as part of a network, to assess urban effects on weather and climate, it is recommended that careful consideration be given to the analysis given in Lowry (1977), and Lowry and Lowry (2001).

9.6 SUMMARY OF KEY POINTS FOR URBAN STATIONS

9.6.1 Working principles

When establishing an urban station, the rigid guidelines for climate stations are often inappropriate. It is necessary to apply guiding principles rather than rules, and to retain a flexible approach. This often means different solutions for individual atmospheric properties and may mean that not all observations at a "site" are made at the same place.

Because the environment of urban stations changes often as development proceeds, frequently updated metadata are as important as the meteorological data gathered. Without good station descriptions it is impossible to link measurements to the surrounding terrain.

9.6.2 Site selection

An essential first step in selecting urban station sites is to evaluate the physical nature of the urban terrain, using a climate zone classification. This will reveal areas of homogeneity.

Several urban terrain types make up an urban area. In order to build a picture of the climate of a settlement, multiple stations are required. Sites should be selected that are likely to sample air drawn across relatively homogenous urban terrain and are thus representative of a single climate zone. Care must be taken to ensure that microclimatic effects do not interfere with the objective of measuring the local-scale climate.

9.6.3　　　**Measurements**

With regard to measurements, the following key points should be taken into account:

(a)　　Air temperature and humidity measurements taken within the UCL can be locally representative if the site is carefully selected. If these variables are observed above roof level, including above the RSL, there is no established link between them and those within the UCL;

(b)　　Wind and turbulent flux measurements should be taken above the RSL but within the internal boundary layer of the selected UCZ. Such measurements must establish that the surface "footprint" contributing to the observations is representative of the climate zone. For wind, it is possible to link the flow at this level and that experienced within the canopy;

(c)　　Precipitation observations can be conducted either near the ground at an unobstructed site, or above the RSL, corrected according to parallel wind measurements;

(d)　　With the exception of incoming solar radiation measurements, rooftop sites are to be avoided, unless instruments are exposed on a tall mast;

(e)　　Measurements of the net and upwelling radiation fluxes must be taken at heights that make it possible to sample adequately the range of surface types and orientations typical of the terrain zone.

_____

REFERENCES AND FURTHER READING

Arya, P.S., 2001: *Introduction to Micrometeorology*. Academic Press, New York.

Auer, A.H. Jr., 1978: Correlation of land use and cover with meteorological anomalies. *Journal of Applied Meteorology*, 17(5):636–643.

Britter, R.E. and S.R. Hanna, 2003: Flow and dispersion in urban areas. *Annual Review of Fluid Mechanics*, 35:469–496.

Christen, A., 2003: (personal communication). Institute of Meteorology, Climatology and Remote Sensing, University of Basel.

Christen, A., R. Vogt, M.W. Rotach and E. Parlow, 2002: *First results from BUBBLE I: Profiles of fluxes in the urban roughness sublayer. Proceedings of the Fourth Symposium on Urban Environment*, (Norfolk, Virginia), American Meteorological Society, Boston, pp. 105-106.

COST 710, 1998: *Final Report*: *Harmonisation of the Pre-processing of Meteorological Data for Atmospheric Dispersion Models*. European Commission. EUR 18195 EN.

COST 715, 2001: *Preparation of Meteorological Input Data for Urban Site Studies*. European Commission, EUR 19446 EN.

Davenport, A.G., C.S.B. Grimmond, T.R. Oke and J. Wieringa, 2000: *Estimating the roughness of cities and sheltered country. Proceedings of the Twelfth Conference on Applied Climatology* (Asheville, North Carolina), American Meteorological Society, Boston, pp. 96–99.

DePaul, F.T. and C.M. Shieh, 1986: Measurements of wind velocity in a street canyon. *Atmospheric Environment*, 20:455–459.

Ellefsen, R., 1991: Mapping and measuring buildings in the canopy boundary layer in ten US cities. *Energy and Buildings*, 16:1025–1049.

Garratt, J.R., 1992: *The Atmospheric Boundary Layer*. Cambridge University Press, Cambridge.

Gill, G.C., L.E. Olsson, J. Sela and M. Suda, 1967: Accuracy of wind measurements on towers or stacks. *Bulletin of the American Meteorological Society*, 48:665–674.

Grimmond, C.S.B. and T.R. Oke, 1999: Aerodynamic properties of urban areas derived from analysis of surface form. *Journal of Applied Meteorology*, 38(9):1262–1292.

——, 2002: Turbulent heat fluxes in urban areas: Observations and a local-scale urban meteorological parameterization scheme (LUMPS). *Journal of Applied Meteorology*, 41(7):792–810.

Halitsky, J., 1963: Gas diffusion near buildings. *Transactions of the American Society of Heating, Refrigerating and Air-conditioning Engineers*, 69:464–485.

Hanna, S.R. and J. C. Chang, 1992: Boundary-layer parameterizations for applied dispersion modeling over urban areas. *Boundary-Layer Meteorology*, 58:229–259.

Hunt, J.C.R., C.J. Abell, J.A. Peterka and H.Woo, 1978: Kinematical studies of the flow around free or surface-mounted obstacles: Applying topology to flow visualization. *Journal of Fluid Mechanics,* 86:179–200.

Kljun, N., P. Calanca, M.W. Rotach, H.P. Schmid, 2004: A simple parameterization for flux footprint predictions. *Boundary-Layer Meteorology*, 112:503–523.

Kljun, N., M. Rotach and H.P. Schmid, 2002: A three-dimensional backward Lagrangian footprint model for a wide range of boundary-layer stratifications. *Boundary-Layer Meteorology*, 103(2):205–226.

Landsberg, H.E., 1981: *The Urban Climate*. Academic Press, New York.

Lowry, W.P., 1977: Empirical estimation of urban effects on climate: A problem analysis. *Journal of Applied Meteorology*, 16(2):129–135.

Lowry, W.P. and P.P. Lowry, 2001: *Fundamentals of Biometeorology: Volume 2 – The Biological Environment*. Chapter 17, Peavine Publications, St Louis, Missouri, pp. 496–575.

Nakamura, Y. and T.R. Oke, 1988: Wind, temperature and stability conditions in an east-west oriented urban canyon. *Atmospheric Environment*, 22:2691–2700.

Oke, T.R., 1981: Canyon geometry and the nocturnal heat island: Comparison of scale model and field observations. *Journal of Climatology*, 1(3):237–254.

——, 1982: The energetic basis of the urban heat island. *Quarterly Journal of the Royal Meteorological Society*, 108(455):1–24.

——, 1984: Methods in urban climatology. In: *Applied Climatology* (W. Kirchofer, A. Ohmura and W. Wanner, eds.). Zürcher Geographische Schriften, 14:19–29.

——, 1987: *Boundary Layer Climates*. Chapter 8, second edition, Routledge, pp. 262–303.

——, 1988*a*: The urban energy balance. *Progress in Physical Geography*, 12:471–508.

——, 1988*b*: Street design and urban canopy layer climate. *Energy and Buildings*, 11:103–113.

——, 1997: Urban environments. In: *The Surface Climates of Canada* (W.G. Bailey, T.R. Oke and W.R. Rouse, eds.). McGill-Queen's University Press, Montreal, pp. 303–327.

Peterson, T.C., 2003: Assessment of urban versus rural in situ surface temperatures in the contiguous United States: No difference found. *Journal of Climate*, 16:2941–2959.

Rotach, M.W., 1999: On the influence of the urban roughness sublayer on turbulence and dispersion. *Atmospheric Environment*, 33:4001–4008.

Schmid, H.P., 2002: Footprint modeling for vegetation atmosphere exchange studies: A review and perspective. *Agricultural and Forest Meteorology*, 113(1):159–183.

Schmid, H.P., H.A. Cleugh, C.S.B. Grimmond and T.R. Oke, 1991: Spatial variability of energy fluxes in suburban terrain. *Boundary-Layer Meteorology*, 54(3):249–276.

Soux, A., J.A. Voogt and T.R. Oke, 2004: A model to calculate what a remote sensor 'sees' of an urban surface. *Boundary-Layer Meteorology*, 111:109–132.

Stull, R.B., 1988: *An Introduction to Boundary Layer Meteorology.* Kluwer Academic Publishers, Dordrecht.

Verkaik, J.W., 2000: Evaluation of two gustiness models for exposure correction calculations. *Journal of Applied Meteorology*, 39(9):1613–1626.

Voogt, J.A. and T.R. Oke, 2003: Thermal remote sensing of urban climates. *Remote Sensing of Environment*, 86(3):370–384.

Wieringa, J., 1986: Roughness-dependent geographical interpolation of surface wind speed averages. *Quarterly Journal of the Royal Meteorological Society,* 112(473):867–889.

——, 1993: Representative roughness parameters for homogeneous terrain. *Boundary-Layer Meteorology*, 63(4):323–363.

——, 1996: Does representative wind information exist? *Journal of Wind Engineering and Industrial Aerodynamics*, 65(1):1–12.

World Meteorological Organization, 2003: *Guidelines on Climate Metadata and Homogenization* (E. Aguilar, I. Auer, M. Brunet, T.C. Peterson and J. Wieringa). World Climate Data and Monitoring Programme No. 53 (WMO/TD-No. 1186). Geneva.

——, 2006: *Initial Guidance to Obtain Representative Meteorological Observations at Urban Sites* (T.R. Oke). Instruments and Observing Methods Report No. 81 (WMO/TD-No. 1250). Geneva.

——, 2010: *Manual on the Global Observing System* (WMO-No. 544), Volume I. Geneva.

——, 2011*a*: *Guide to Climatological Practices* (WMO-No. 100). Geneva.

——, 2011*b*: *Technical Regulations* (WMO-No. 49), Volume I. Geneva.

——, 2011*c*: *Manual on Codes* (WMO-No. 306), Volume I.1 and I.2. Geneva.

———————

CHAPTER CONTENTS

CHAPTER 10. ROAD METEOROLOGICAL MEASUREMENTS

10.1 GENERAL

10.1.1 Definition

Road meteorological measurements are of particular value in countries where the serviceability of the transport infrastructure in winter exerts a great influence on the national economy. In some countries there will be other road hazards such as dust storms or volcanic eruptions. Safe and efficient road transport is adversely affected by the following conditions which affect speed, following distance, tyre adhesion and braking efficiency: poor visibility (heavy precipitation, fog, smoke, sand storm), high winds, surface flooding, land subsidence, snow, freezing precipitation and ice.

10.1.2 Purpose

The role of a road network manager is to ensure the optimal, safe, free flow of traffic on arterial routes. Operational decisions on the issuing of road weather information and on initiating de-icing and snow clearing operations are dependent on road meteorological observations that are increasingly made by special-purpose automatic weather stations (AWSs). While these stations should conform as far as practicable to the sensor exposure and measurement standards of conventional AWSs (see Part II, Chapter 1) they will have characteristics specific to their function, location and measurement requirements.

The reliability of road meteorological measurement stations which supply data to a transport decision support system is critical: Each station will relate to the immediate environment of important high-density transport routes and may be responsible for feeding data to road meteorology forecast routines and for generating automatic alarms. Thus, equipment reliability and maintenance, power supply, communications continuity and data integrity are all important elements in the selection, implementation and management of the weather measurement network. These concerns point to the benefits of an effective collaboration between road management services and the National Meteorological and Hydrological Service (NMHS).

10.1.3 Road meteorological requirements

This chapter should assist in standardizing road meteorological measurements with a method that adheres to WMO common standards as closely as possible. However, those users who may wish to employ road measurements in other meteorological applications will be advised of important deviations, in sensor exposure, for example.

The needs of road network managers focus in four main areas (WMO 1997, 2003):

(a) *Real-time observation of road meteorology*: The practical objective, on the one hand, is to inform road users of the risks (forecast or real-time) that they are likely to face on designated routes; and on the other hand, to launch a series of actions aimed at increasing road safety, such as scraping snow or spreading chemical melting agents;

(b) *Improvement of pavement surface temperature forecasting*: The measurements of road AWSs are the important input data for the temperature and pavement condition forecasting programmes which may be run by the NMHS. This authority has the capability of ensuring continuity and timeliness in the observations and in the forecast service. In practice, two tools are available to forecasters. The first tool is a computer model for the transposition of a weather forecast of atmospheric conditions to a pavement surface temperature

forecast, taking account of the physical characteristics of each station. The second tool is the application of an algorithm based on a specific climatological study of the pavement surface;

(c)   *Road climate database*: The establishment of a road climatological database is important because in many situations an assessment of current events at a well-instrumented location enables experienced road network managers to transpose the data using the climate model to other locations they know well. In some cases, thermal fingerprints can be taken in order to model this spatial relationship. The recording of road weather data will be useful for analysing previous winter disturbances and for carrying out specific road-dedicated climatology studies. National Meteorological and Hydrological Services can fill the data gaps and compare and provide quality assurance for measurements coming from different sources;

(d)   *Reliable data*: Road managers do not need exceedingly accurate measurements (with the exception of road-surface temperature). Rather, they want the data to be as reliable as possible. That is to say the data must be a consistent reflection of the real situation, and the measuring devices must be robust. Communication and power supply continuity are often of prime importance.

10.2   ESTABLISHMENT OF A ROAD METEOROLOGICAL STATION

10.2.1   Standardized representative measurements

The general requirements for meteorological stations, their siting and the type and frequency of measurements are defined in WMO (2003, 2011*a*). It is recommended that these standards and other relevant material in this Guide should be adhered to closely when establishing road meteorological stations in order to make standardized, representative measurements that can be related to those from other road stations in the network and also to data from standard synoptic or climatological stations, except where the unique measurements for road meteorology demand other standards, for example, for the exposure of sensors. Advice on the optimum placement and density of stations may be obtained from the local branch office of the NHMS which will be able to access climatological data for the region.

A meteorological station site is chosen so that it will properly represent a particular geographic region. A road meteorological station will be sited to best represent part of the road network or a particular stretch of important roadway that is known to suffer from weather-related or other hazards. The station must therefore be adjacent to the roadway so that road-surface sensors may be installed, and therefore some compromise on "ideal" meteorological siting and exposure may occur. The sensors are installed so that their exposure enables the best representation in space and time of the variable being measured, without undue interference from secondary influences. In general, the immediate site adjacent to the roadway should be level, with short grass, and not shaded by buildings or trees.

10.2.2   Station metadata

In every case it is important that the location and characteristics of the site and the specification of equipment and sensors are fully documented, including site plans and photographs. These metadata (Part I, Chapter 1 and Part IV, Chapter 1) are invaluable for the management of the station and for comparing the quality of the measurements with those from other sites.

10.3 OBSERVED VARIABLES

10.3.1 Road meteorological measurements

The important measurements at road weather stations for forecasting roadway conditions include air temperature and humidity, wind speed and direction, precipitation amount and type, visibility, global and long-wave radiation, road-surface temperature and road-surface condition. Some of the measurements, for example, temperature and humidity, will be used to forecast conditions of concern to road users, while others (wind and visibility) may indicate impending or real-time hazards; yet others (meteorological radiation, road-surface temperature and condition) are specific to predicting the performance of the road surface.

The sensors will be selected for their accuracy, stability, ease of maintenance and calibration, and for having electrical outputs suitable for connecting with the automatic data-acquisition system. The choice of sensors and their exposure should conform to standard WMO practice and recommendations (see the relevant chapters in Part I of this Guide), except when these are incompatible with the specific requirements of road meteorology. Measurement accuracy should generally conform to the performances quoted in Part I, Chapter 1, Annex 1.E. Note also the recommendations on the measurements at AWSs in Part II, Chapter 1.

10.3.1.1 *Air temperature*

The sensor may be an electrical resistance thermometer (platinum or stable thermistor). The air-temperature sensor, its radiation shield or screen and exposure should conform to the guidelines of Part I, Chapter 2, with the shield mounted at a height of 1.25 to 2 m over short grass or natural soil.

Measurement issues: The sensor and screen should not be mounted above concrete or asphalt surfaces that could inflate the measured temperature. The placement of the shield should ensure that it is not subject to water spray from the wheels of passing traffic, which might cause significant sensing errors.

10.3.1.2 *Relative humidity*

The hygrometric sensor may be one of the thin-film electrical conductive or capacitive types (Part I, Chapter 4). A wet-bulb psychrometer is not recommended on account of the continual contamination of the wick by hydrocarbons. The sensor may be combined with or co-located with the air-temperature sensor in its radiation shield as long as the sensor thermal output (self-heating) is very low, so as not to influence the temperature measurement.

Measurement issues: Note the same water spray hazard as for the temperature sensor. Humidity-sensor performance is subject to the effects of contamination by atmospheric and vehicle pollution. Functional checks should be made regularly as part of the data-acquisition quality control, and calibration should be checked at least every six months, particularly before the winter season. A sensor that is not responding correctly must be replaced immediately.

10.3.1.3 *Wind speed and direction*

These variables are usually measured by either a pair of cup and vane sensors or by a propeller anemometer (Part I, Chapter 5) with pulse or frequency output. The sensors must be mounted at the standard height of 10 m above the ground surface and in a representative open area in order to carry out measurements not influenced by airmass flow disturbances due to traffic and local obstacles.

Measurement issues: The freezing of moving parts, water ingress and corrosion and lightning strike are potential hazards.

10.3.1.4 *Precipitation*

(a) *Accumulated precipitation*: The tipping-bucket recording gauge (Part I, Chapter 6) where increments of usually 0.2 mm of precipitation are summed, is commonly used at automatic stations. Heated gauges may be employed to measure snow or other solid precipitation. A rate of precipitation may be estimated by registering the number of counts in a fixed time interval.

  Measurement issues: The gauge must be kept level and the funnel and buckets clean and free from obstruction. The tipping-bucket gauge is not satisfactory for indicating the onset of very light rain, or in prolonged periods of freezing weather. Totals will be lower than the true values because of wind effects around the gauge orifice, evaporation from the buckets between showers, and loss between tips of the buckets in heavy rain;

(b) *Precipitation occurrence and type*: Sensors are available which use electronic means (including heated grids, conductance and capacitance measurement) to estimate the character of precipitation (drizzle, rain or snow) falling on them. Optical sensors that determine the precipitation characteristic (size, density and motion of particles) by the scattering of a semiconductor laser beam offer better discrimination at much greater expense.

  Measurement issues: These sensing functions are highly desirable at all stations, but existing types of sensors are lacking in discrimination and stable reproducibility. Provisions must be made (heating cycles) to remove accumulated snow from the surface. The regular cleaning of sensitive elements and optical surfaces is required.

  Only sensors that are well documented and that can be calibrated against an appropriate reference should be installed. If any system uses an algorithm to derive a variable indirectly, the algorithm should also be documented.

10.3.1.5 *Meteorological radiation*

(a) *Global radiation*: The solar radiation (direct and diffuse) received from a solid angle of 2π sr on a horizontal surface should be measured by a pyranometer using thermoelectric or photoelectric sensing elements (Part I, Chapter 7). The sensor should be located to have no significant nearby obstructions above the plane of the instrument and with no shadows or light reflections cast on the sensor. Although the location should be such as to avoid accidental damage to the sensor, it should be accessible for inspection and cleaning. Global radiation measured "on site" is particularly relevant to the road manager. It expresses the quantity of energy received by the road during the day. The relationship of incoming radiation to surface temperature and road inertia will depend on the constituent materials and dimensions of the pavement mass.

  Measurement issues: Obstructed sensor horizon, sensor not level, surface dirt, snow or frost obscuring the glass dome or sensing surface, and water condensation inside the glass dome;

(b) *Long-wave radiation*: A pyrgeometer may be used which measures radiation in the infrared by means of a thermopile, filtering out the visible spectrum. Mounted with the sensor facing upwards and a sufficiently unobstructed horizon, it determines the long-wave radiation received from the atmosphere, in particular at night, and gives an indication of cloud cover and therefore of roadway radiative cooling. A sensor sensitive to a spectrum from 5 to 50 μm, with a maximum sensitivity of 15 μV/Wm^{-2} and a response time lower than 5 s is adequate for road weather forecasting purposes.

  Measurement issues: See those for global radiation.

10.3.1.6 *Visibility*

Transmissometers and forward-scatter meters may be applicable (Part I, Chapter 9).

Measurement issues: Road managers are interested in visibilities below 200 m (the danger threshold). Maintaining sensor windows and lenses clean is important. Some systems will compensate for a degree of window contamination. An appropriate calibration procedure should be carried out during routine maintenance.

10.3.1.7 *Road-surface temperature*

Active sensors based on a 100 ohm platinum resistance and providing serial digital transmission are available, and may be imbedded in the road surface. The manufacturer's instructions for the installation of the sensor and cabling and bonding to the road surface should be followed. The sensor has to be positioned out of the line of tyre tracks, otherwise the sensor surface will be soiled and measurements affected by friction heating. The sensor must lie in the road surface plane with no depression where water could gather and affect the measurement. The sensor's correct position must be checked on a regular basis.

Measurement issues: The thermal lag (time constant) of the sensor and the imbedding material should match that of the road-surface composition. The sensor should have a surface finish with low absorptance in the infrared to minimize radiation error. For long connecting cable lengths (over 20 m), cable resistance compensation is recommended.

10.3.1.8 *Road-pavement temperature*

Temperatures of the pavement at 5, 10 and 20 cm below the road surface may be determined by sinking appropriately sheathed electrical resistance sensors at corresponding depths and using suitable bonding material.

Measurement issues: See those for road-surface temperature.

10.3.1.9 *Road-surface condition and freezing temperature*

This sensor estimates the road-surface condition (dry, wet, frost, ice) and the freezing temperature of residual surface water. The sensor control circuit heats the sensor before cooling it, using the Peltier effect. The rate of cooling is a function of the surface condition and freezing temperature. See also Part I, Chapter 6, regarding ice on pavements. The sensor output should give road managers an indication of the chemical de-icing agent's persistence at the specific location and enable them to optimize chemical spreading operations.

Measurement issues: The sensor must not be covered by foreign matter or when road re-surfacing. The sensor requires regular cleaning. It is difficult to ensure a sensor response that is representative of the true road-surface condition because of the small sample size, the location on road surface and variable imbedding practices. Measurement depends on traffic density and is otherwise not very stable with time. This sensor, of which there are few alternative makes, may be difficult to obtain. The remote sensing of road-surface temperature by thermal infrared sensors is generally not practical because of the interference caused by water spray from vehicle tyres. Road-surface frost risk estimation may be improved through better measurement of temperature, air humidity and temperature in and on the road surface, namely, improved sensor exposure and reduction of systematic and random errors.

10.3.1.10 *Video surveillance*

Video surveillance is a component of what have come to be called intelligent transport systems. They are principally used for road-incident detection, but also give a useful indication of present weather for transport management. Image processing algorithms will aid the discrimination between different weather conditions.

10.4 CHOOSING THE ROAD WEATHER STATION EQUIPMENT

Part II, Chapter 1, gives information that may be applied to road meteorological measurement applications. In what follows, attention is drawn to the particular issues and concerns from the experience of road network managers, in particular the need for high performance where public safety is a primary issue.

10.4.1 The road environment

A road weather station is subject to considerable stress due to the vicinity of the roadway: vibration, vehicle ignition interference, exhaust pollution, corrosion from salt spray, and unwelcome attention from members of the public. In some respects the station may be considered to operate in an industrial environment, with all that that implies for the robustness of the design and concern for data integrity. Frequently met problems are: lack of protection against over-voltage on sensor interface circuits; inadequate electrical isolation between sensors, sensor cables and the data-acquisition unit; variable connector contact resistance causing calibration drift; measurement failure; and extended maintenance attention.

10.4.2 Remote-station processing capability

There is a move in AWS design to include increased data-processing capacity and storage at the remote data-acquisition unit in order to employ processing algorithms that act on several sensor signals to give complex outputs; to provide for some level of quality assurance on the data; to provide two-way communications between the control centre and remote units for diagnostics of both the sensor and unit performance; and to provide for downloading new algorithms and software updates to the remote units. On the other hand, a network of remote stations which are not more complex than necessary for reliable data acquisition, and a central control and data-acquisition computer where the more complex algorithms, quality assurance and code translation is carried out as well as the higher level processing for road management decisions, may provide a more reliable and less costly overall system. Those planning for the implementation of a road meteorological measurement network are encouraged to consider flexible and extendable equipment solutions with powerful programming options for sensor data processing and system control.

The station data processing may include: control of the measurement cycle (initiation, frequency, time and date); complex sensor management (power on/off, sampling regime); sensor signal processing (filtering, conversion to scientific units, algorithms); data quality checks; alarm generation (variables outside pre-set limits, partial system failure, station integrity breached); data storage (short-term storage and archiving); output message generation (code form, communications protocol); communications management; and station housekeeping (power supply, sensor checks, communications).

10.4.3 Network configuration and equipment options

The selection of station equipment, communications and network control (the network infrastructure) should reflect the particular demands of road meteorology and the road network management decision-making. These choices will be materially affected by the relationship between the road network authority and the local NMHS. For example, the road network

authority might contract the NMHS to provide road meteorology forecasting services and specified road data, to which the road network managers apply their physical criteria to make operational decisions. In this case, it would be logical for the road network stations to be an extension of the NMHS AWS network employing common station hardware, communications and maintenance service, with particular attention to network reliability, and including the special sensors, algorithms and software for the road meteorological task. However, if such close integration is impractical, the road authority may still wish to adopt some commonality with NMHS systems to take advantage of operational experience and the supply of hardware and spare parts.

If an entirely new or separate network is required, the following guidelines are recommended for the choice of data-acquisition equipment and communications. Rather than develop new hardware and software for road meteorological measurement, it is wise to employ existing proven systems from reputable manufacturers and sources, with only necessary adaptation to the road network application, and taking advantage of the experience and advice of other road network administrations. The equipment and its software should be modular to allow for future added sensors and changes in sensor specifications. To facilitate the extension of the network after a few years it is most helpful if the hardware is sourced from standardized designs from a sound manufacturing base where later versions are likely to maintain technical compatibility with earlier generations.

10.4.4   **Design for reliability**

Data-processing modules should be of industry-standard architecture with robust standard operating systems with a well-managed upgrade process. Application software should be written in a standard language and well documented. To achieve the desired reliability, special industrialized components and modules may be selected. A cheaper alternative may be to use standard commercial designs with redundant parallel or back-up systems to ensure system reliability. The design of the remote-unit power supply needs particular attention. An uninterruptible power supply may be recommended, but it should be recognized that communications systems will also depend on a functioning local power supply.

Whatever the system design, housing the electronics in a robust, corrosion-resistant, secure, even temperature, dust- and moisture-free enclosure will add much to its reliability. Connectors carrying the sensor signals should be of high-quality industrial or military grade and well protected against cable strain, water ingress and corrosion. Sensor cabling should have an earth shield and a robust, waterproof insulating sheath and be laid in conduit.

Special attention should be given to obviating the effect of electrical noise or interference introduced into the data-acquisition system through sensor cables, the power supply or communications lines. These unwanted electrical signals may cause sensor signal errors and corrupt data, and cause electronic failure, particularly in sensitive interface circuits. Great care needs to be given to: the design of sensor and communication line isolation and over-voltage protection, including an appropriate level of protection from atmospheric electricity; the adequate earthing or grounding of sensors, power supplies, communications modems and equipment cabinets; and to earth shielding all parts of the measurement chain, avoiding earth current loops which will cause measurement errors.

Good standardized installation and maintenance practices will contribute much to system reliability. System reliability is also related to the "mean time to repair", which involves the call-out and travel time of maintenance staff to make equipment replacement from whole unit and module stock.

10.5 **MESSAGE CODING**

10.5.1 **Coding functions**

The message transmitted from the remote road meteorological station will contain a station identifier, the message time and date, sensor channel data, including channel identification, and some "housekeeping" data which may include information on station security, power supply, calibration and other data quality checks. This message will be contained in the code envelope relating to the communications channel with an address header, control information and redundancy check characters to provide for error detection. The road meteorological data part of the message may be coded in any efficient, unambiguous way that enables the central control and data-acquisition computer to decode and process before delivering intelligible guidance information to the network managers for their decision-making.

10.5.2 **WMO standard coding**

Designers of road meteorology measurement networks should also consider the value of WMO standard message coding (see WMO, 2011*b*) which enables other users like NMHSs to receive the data by some arrangement and employ it in other meteorological applications. This message coding may be carried out at the remote AWS, which places demands on station software and processing, or, as is more likely, in the central control and data-acquisition computer after the completion of any quality assurance operations on the data.

10.6 **CENTRAL CONTROL AND DATA-ACQUISITION COMPUTER**

The functions of the central computer (or computers) have already been mentioned. The functions are to manage the network by controlling communications (see below), receive reports (road meteorological messages, AWS housekeeping messages and quality information), and process the road measurement data to give the road network managers the operational information and decision-making tools that they require. The network architecture may be designed to enable the central computer to act as an Intranet or Web server to enable ready access to this information by regional managers and other users of the meteorological data.

A separate computer will probably be allocated to manage the road network climate database and to produce and distribute analyses and statistical summaries. In a sophisticated network the central computer will manage certain maintenance and calibration operations, change AWS operating modes and update AWS software.

10.7 **COMMUNICATIONS CONSIDERATIONS**

A reliable telecommunications service that enables the network of stations to be effectively managed while it delivers the requisite data on time is vital. Since communications charges will make up a large proportion of the annual operating cost, the analysis of communications options is important, so that the cost per message can be optimized with respect to the level of service required. A detailed review of telecommunications options for the data collection and management of the road AWS is beyond the scope of this chapter (see Part II, Chapter 1, for guidance on data transmission). The communications solution selected will depend on the management objectives of the road meteorological measurement network and the services offered by the telecommunications providers of the country, with their attendant tariffs.

10.8   **SENSOR SIGNAL PROCESSING AND ALARM GENERATION**

10.8.1   **Signal processing algorithms**

The raw signal data from sensors must be processed or filtered to produce representative average values. This is either done in some active sensors, in the sensor interface in the data-acquisition unit, or in the higher level data processing of the station. The specifications for averaging the sensor outputs may be found in Part I, Chapter 1, Annex 1.E.

Algorithms which are applied to sensor outputs (or groups of outputs) either at the remote station or in the central computer should be from authoritative sources, rigorously tested and preferably published in the open literature. Any in-house algorithms adopted by the road network management should be well defined and recorded in the station metadata or network manuals.

10.8.2   **Alarm generation**

Alarm indications may be generated from sensor outputs when values exceed preset limits to initiate alarm messages from the AWS. The choice of alarms and limit tests will depend on national or regional practice. Some examples of alarms from road AWS follow. Note the use of the logical "and" and "or" combinations in the algorithms.

Examples of alarms include:

Alarm 1: t(air) OR t(road surface) 3 °C
               AND
               t(extrapolated road surface)[a] ≤ 1 °C
Alarm 2: t(air) ≤ 0 °C
Alarm 3:   First condition
               t(road surface) ≤ 1 °C
               OR t(extrapolated road surface) ≤ 0 °C
               OR t(pavement at –5 cm) ≤ 0 °C
               OR t(pavement at –10 cm) ≤ –1 °C
               OR t(pavement at –20 cm) ≤ –2 °C
               AND
               Second condition
               Carriage-way is not dry
               OR at least one precipitation count in the past hour
               OR relative humidity ≥ 95%
               OR t(road surface) – t(dewpoint) ≤ 1 °C
Alarm 4: t(road surface) ≤ 0 °C
               AND
               detected state: frost or black ice
Alarm 5:   First condition
               Detected precipitation = snow or hail
               AND
               Second condition
               t(air) ≤ 2 °C
               OR t(road surface) ≤ 0 °C
Alarm 6:   Wind average ≥ 11 m s^{-1}
               AND
               Wind direction referred to road azimuth,
               between 45° to 135° OR 225° to 315°
Alarm 7:   Visibility ≤ 200 m

a   Extrapolated road-surface temperature is calculated with an algorithm that takes account of the last measures and creates a quadratic equation. This can be used to calculate estimates of temperatures over the next 3 h.

Other alarms may be set if faults are detected in sensors, message formats, power supplies or communications.

10.9 MEASUREMENT QUALITY CONTROL

Good decision-making for road management is dependent on reliable measurements so that, when sensors, their cabling or their interfaces in the AWS develop a fault, the defective unit is detected and repaired without undue delay. It is very difficult for a road manager to detect erroneous measurements. Reference should be made to the guidance on quality control provided in Part II, Chapter 1 and in Part IV, Chapter 1. Gross sensor faults may be detected by the AWS system software, which should then generate an alarm condition.

10.9.1 Checking for spurious values

Measurements that fall outside the expected operating range for the sensor may be rejected by setting limits for each variable. For example, wind directions may be confined to the range of 0° to 359°. Where there has been a faulty zero output, a rapid drift or step change in sensor response, invalid measurements may be rejected by software that performs statistical analysis of measurements over time, either in the AWS if it has sufficient processing power, or in the central data acquisition computer. In some of the examples that follow, the standard deviation of the last n values is compared with a parameterized threshold.

Examples of check algorithms (only for road meteorological measurements) include the following:

(a)   *Test for all temperatures*: Accept data only if standard deviation of the last 30 values is ≥ 0.2 °C;

(b)   *Test for wind speed*: Accept data only if standard deviation of the last 20 values is ≥ 1 km hr^{-1};

(c)   *Test for wind direction*: Accept data only if standard deviation of the last 30 values is ≥ 10°;

(d)   *Test for liquid precipitation*: Check for consistency of amount with previous day's count;

(e)   *Test for snow precipitation*: Check data if t(air) > 4 °C;

(f)   *Test for atmospheric long-wave radiation (AR) (related to cloud cover)*: Refuse data if AR > 130 W m^{-2}, if relative humidity > 97% and AR > 10 W m^{-2}, and if relative humidity ≥ 90% and AR > 10 W m^{-2}, for four successive hours.

10.10 ROAD WEATHER STATION MAINTENANCE

10.10.1 The road environment

Reference should be made to Part I, Chapter 1 and Part II, Chapter 1 for the sections on inspection, maintenance and calibration. The chapters of Part I include advice on the maintenance and calibration of specific sensors. Note, however, that the road AWS exists in an environment with peculiar problems: vulnerability of the AWS and its sensors to accidental or intentional damage; exposure to severe vehicle exhaust pollution; electrical interference from vehicle ignition and nearby high-tension power lines; corrosion from salt spray; and vibration (affecting connections between sensors and cables).

10.10.2   Maintenance plans and documentation

Because operational decisions affecting road safety may critically depend on reliable AWS data, there are stringent requirements for maintenance of specific stations at particular times of the year. These considerations are outlined in the maintenance management plan for the network, which should include scheduled routine preventive maintenance as well as effective response to known fault conditions.

The road network administration should have its own maintenance manual for its road meteorological stations, based on the manufacturer's recommendations, information gleaned from this Guide and from its own experience. A good manual contains checklists to aid inspection and the performance of maintenance tasks. The administration may decide to contract out inspection and maintenance work to the local NMHS, which should have experience with this kind of instrumentation.

10.10.3   Inspections and work programmes

Each station should undergo a complete maintenance programme twice a year, consisting of site maintenance (cutting grass and vegetation which could affect sensor exposure); checking enclosures for water ingress and replacing desiccants; treating and painting weathered and corroded enclosures, screens and supports; checking cable and connector integrity; cleaning and levelling sensors (noting the measurement issues referred to previously); and calibrating or replacing sensors and the AWS measurement chain.

Road managers should maintain a physical inspection programme to check for the integrity and proper operation of their stations once a month in winter and once every two months in the summer. When conducting any work on the road surface, the regulation warning signs must be set out and approved safety clothing must be worn.

10.11   TRAINING

To manage, operate and maintain a network of road meteorological stations in order to obtain a continuous flow of reliable data and to interpret that data to give fully meaningful information requires personnel with specific training in the necessary disciplines. Some of these areas of expertise are: the roadway environment and operational decision-making for the safe and efficient movement of traffic; remote data acquisition, telecommunications and computing; the selection, application and maintenance of meteorological sensors and their signal processing; and the interpretation of meteorological and other data for the operational context. The administration responsible for the road network should collaborate with other agencies as necessary in order to ensure that the optimum mix of knowledge and training is maintained to ensure the successful operation of the road meteorological measurement network.

REFERENCES AND FURTHER READING

World Road Association (PIARC), 2002: *Proceedings of the Eleventh PIARC International Winter Road Congress* (Sapporo, Japan).

World Meteorological Organization, 1997: *Road Meteorological Observations* (R.E.W. Pettifer and J. Terpstra). Instruments and Observing Methods Report No. 61 (WMO/TD-No. 842). Geneva.

———, 2003: *Road Managers and Meteorologists over Road Meteorological Observations: The Result of Questionnaires* (J.M. Terpstra and T. Ledent). Instruments and Observing Methods Report No. 77 (WMO/TD-No. 1159). Geneva.

———, 2010: *Manual on the Global Observing System* (WMO-No. 544), Volume I. Geneva.

———, 2011*a*: Technical Regulations (WMO-No. 49), Volume I. Geneva.

———, 2011*b*: *Manual on Codes* (WMO-No. 306), Volumes I.1 and I.2. Geneva.

———————

PART III. SPACE-BASED OBSERVATIONS

PART CONTENTS

CHAPTER CONTENTS

CHAPTER 1. INTRODUCTION

1.1 HISTORICAL PERSPECTIVE

On 1 April 1960, a new era started for meteorology with the launch of the Television and Infrared Observation Satellite – 1 (TIROS-1). Weather systems, which had only been depicted until then by synoptic maps and aircraft observations, could be visualized at a glance. Their rapidly evolving nature became more evident with geostationary imagery from the Applications Technology Satellite – 1 (ATS-1), launched on 6 December 1966. The term "nowcasting" emerged, becoming the first application of meteorological satellites.

Initially, satellite data were nearly exclusively used for nowcasting. They were first applied to the field of numerical weather prediction, starting with Nimbus-3 (13 April 1969), by using data from experimental instruments to derive vertical profiles of atmospheric temperature and humidity and by deriving cloud-motion winds from geostationary image sequences.

The First Global Atmospheric Research Programme (GARP) Global Experiment (FGGE, 1979–1980) was able to assemble, for the first time, a composite system of four geostationary satellites and two near-polar satellites, which delivered global sounding and imaging coverage four times a day and imagery at low and mid latitudes every half hour. It is important to note that since their early days, in addition to supporting operational applications, meteorological satellites have enabled advances in the understanding of atmospheric dynamics and climate.

Driven by the high economic value of earth resource exploration and vegetation cycle monitoring, new satellite programmes emerged with a focus on land surface observation. Landsat-1, launched on 23 July 1972, led the first series of high-resolution land observation satellites, and coverage from the Satellite pour l'Observation de la Terre (SPOT) series, beginning on 22 February 1986 with SPOT-1, provided imagery at a spatial resolution of 10 to 20 metres.

Exploration of the ocean began with the launch of SeaSat on 27 June 1978, which marked the advent of all-weather microwave sensing, both active and passive. Almost simultaneously, on 24 October 1978, Nimbus-7 used passive microwave sensing with the addition of ocean colour monitoring. After the SeaSat altimetry, scatterometry and synthetic aperture radar imagery missions, no active sensing mission was operated until the launch of the European Remote-sensing Satellite – 1 (ERS-1) on 17 July 1991. The retrieval of information on atmospheric radiation and chemistry was initially explored by several Nimbus missions. A milestone for Earth radiation study was the Earth Radiation Budget Satellite (ERBS), launched on 5 October 1984. For atmospheric chemistry, a major milestone was the Upper Atmosphere Research Satellite (UARS), launched on 12 September 1991.

1.2 SPATIAL AND TEMPORAL SCALES

The concept of the Global Observing System was totally revised with the advent of satellites, taking advantage of the complementary nature of surface-based and space-based observations. The space-based component offers the unique opportunity of uninterrupted global coverage and frequent observing cycles. A striking advantage is the capability of vertical atmospheric sounding over the oceans, alleviating a great limitation of observations for global numerical weather prediction. Over continental areas, observing networks are biased towards populated areas, whereas the vast majority of land surfaces are relatively unpopulated and hence undersampled; furthermore, some local observations available from the ground (e.g. cloud type) are hard to integrate spatially.

One important difference between satellite and surface measurements is the integration in space and time. Satellite measurements integrate the incoming signal over an instantaneous field of view determined by the need to collect sufficient radiant energy to provide the required signal-

to-noise ratio. Surface measurements are usually point-related, although, depending on the observed variable, the measurement may be representative of a larger or smaller area. In the time dimension, the situation is reversed: satellite measurements are nearly instantaneous depending on the satellite motion or the time available to acquire a picture element (pixel) when scanning an image; surface measurements usually integrate over a certain time interval in order to average instantaneous fluctuations. These differences make it more difficult to compare or combine satellite and surface measurements.

1.3 COMPLEMENTARY NATURE OF SPACE-BASED AND SURFACE-BASED MEASUREMENTS

It is acknowledged that satellites are unable to perform all needed observations with the required measurement quality. For certain geophysical variables, no remote-sensing principle exists. For others, the required measurement quality is only achievable with ancillary information from accurate surface-based observing systems. In addition, since satellite measurements are often of indirect nature (the primary observed quantity being radiation), surface-based measurements play a key role for the validation of satellite-derived products.

There are still areas where exclusively surface-based systems can provide measurements of acceptable quality. However, even in those cases, satellites can be useful in spatially extending local and sparse ground measurements. In particular, the practice of assimilation makes it possible to transfer information across geophysical variables measured using different techniques: this means that satellite observations may contribute to the knowledge of geophysical variables even when not directly observed from satellite, provided that there is a strong physical relationship between these variables. Synergistic use of surface-based and space-based observations is fundamental to the WMO Integrated Global Observing System.

Note: Detailed descriptions of satellite programmes and instruments are available in the WMO online database of space-based observation capabilities: http://www.wmo.int/oscar.

CHAPTER CONTENTS

Page

CHAPTER 2. PRINCIPLES OF EARTH OBSERVATION FROM SPACE

This chapter provides an overview of Earth observation from space, including its potential benefits and limitations. It describes basic concepts of orbits and the characteristics of Earth viewing from space. It also introduces the principles of remote-sensing.

2.1 ORBITS AND EARTH VIEWING FROM SPACE

The Earth can be observed from space from different orbits under various viewing conditions. The following issues are considered in this section:

(a) Satellite instrument field of view;

(b) Orbital period, geostationary orbit, observing cycle and repeat cycle;

(c) Orbital precession, Sun-synchronous orbits and drifting orbits;

(d) Elliptical orbits;

(e) Launchers and injection into orbit.

2.1.1 Satellite instrument field of view

The greatest advantage of observing from a satellite platform, rather than from the ground or a balloon, is the wide potential field of view (FOV). Satellite observing platforms usually orbit at a minimum height of 400 km. Often, they orbit much higher, some as far as the geostationary orbit (35 786 km). The FOV depends on the orbital height, the instrument configuration and the intended application. Those may limit the useful range of zenith angles (ζ) under which the Earth can be viewed. If the satellite FOV is characterized as the maximum ground distance potentially viewed from satellite height under a given zenith angle, the relationship set out in Figure 2.1 can be expressed as:

$$\mathrm{FOV} = 2\,R\,\delta\,\pi/180 \qquad \sin\left(\zeta - \delta\right) = \frac{R}{H + R}\sin\zeta \tag{2.1}$$

where $R = 6\,371$ km (Earth's radius), $H =$ orbital height in km, and $\delta =$ geocentric angle in degrees.

Table 2.1 presents values of the satellite FOV (in km) as a function of orbital height for typical values of zenith angle ζ. The corresponding geocentric angle δ is also shown.

The potential satellite FOV may not be entirely covered by a single instrument. Either the sensing principle or the technological features of an instrument may set an upper limit to its FOV. For instance, radar altimeters can only operate in a nadir geometry. They therefore have
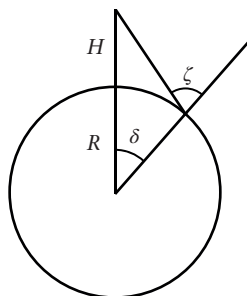
Figure 2.1. Field of view versus zenith angle ζ

Table 2.1. Potential satellite field of view and corresponding geocentric angle, as functions of satellite height and zenith angle, under which the Earth's spot is viewed

Zenith angle for various applications	H = 400 km		H = 600 km		H = 800 km		H = 35 786 km	
	FOV	δ	FOV	δ	FOV	δ	FOV	δ
ζ = 90° (horizon-to-horizon)	4 401 km	19.79°	5 326 km	23.95°	6 076 km	27.32°	18 082 km	81.31°
ζ = 85° (telecommunications)	3 423 km	15.39°	4 322 km	19.43°	5 057 km	22.74°	16 978 km	76.34°
ζ = 70° (qualitative use)	1 746 km	7.85°	2 405 km	10.82°	2 980 km	13.40°	13 752 km	61.84°
ζ = 60° (quantitative use)	1 207 km	5.43°	1 707 km	7.68°	2 157 km	9.70°	11 671 km	52.48°

no proper FOV, except for the broadening of the beam due to diffraction. Very high-resolution imagers usually have an FOV within a range of several tens of kilometres, as do synthetic aperture radars (SARs).

The satellite motion enables the instrument to cover successive FOVs along the orbit. These constitute a strip of observed Earth surface called a swath. The swath may be centred along the sub-satellite track, or be parallel to it for side-looking instruments (e.g. SARs). For several purposes (steerable pointing for emergencies, stereoscopy in association with successive orbits, etc.), certain instruments with limited swath may tilt the swath to the side of the track within what is called a field of regard. The swath width is a cross-track component of the actual FOV of the instrument. The swath is not defined for instruments in geostationary orbit.

2.1.2 Orbital period, geostationary orbit, observing cycle and repeat cycle

The orbital height H determines the orbital period T. The relationship is:

$$T = a\ (1 + \frac{H}{R})^{\frac{3}{2}} \tag{2.2}$$

where a = 84.47 min (T resulting in minutes).

The height, which corresponds to one sidereal day (23 h 56 min 04 s) is 35 786 km. A satellite orbiting at this height is called geosynchronous. The orbit is called geostationary if the orbit lies in the equatorial plane and is run eastward: the satellite appears steady compared to the Earth's surface on the nadir of the equatorial sub-satellite point.

For an inclined orbit with respect to the equatorial plane, the satellite will cross the Equator at a certain longitude. After T minutes, there will be another equatorial crossing at a longitude displaced westward by the number of degrees that corresponds to the Earth's rotation during the orbital period. The difference of longitude (or space distance) between two successive equatorial crossings in the same phase (descending or ascending) is called decalage. Together with the instrument swath, decalage determines the time needed for a full Earth surface observation (observing coverage) (Figure 2.2).

If the instrument swath is at least as large as the decalage, the coverage provided by the two contiguous orbits is continuous. Therefore, the time needed for global coverage (observing cycle) depends on the ratio between instrument swath and decalage.

Table 2.2 shows the period and corresponding decalage for the orbital height examples in Table 2.1. In addition, observing cycles corresponding to several instrument swaths are presented. Those swaths are associated with qualitative and quantitative use; that is with 70° and
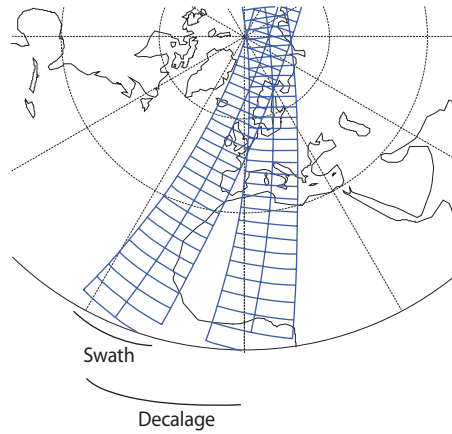
Figure 2.2. Decalage between two successive orbits, and instrument swath

60° zenith angles, respectively. Observing time is halved for instruments capable of observation during the day and night. The decalage and observing cycle are not quoted for $H = 35\ 786$ km (geostationary altitude).

For a geostationary satellite, which continuously views the same area of the Earth's surface, the observing cycle is only determined by instrument characteristics and may take a few minutes or less to complete, depending on the area scanned. Within the satellite's area of coverage, geostationary observation is perfectly suited for continuous monitoring. For example, such monitoring is needed to detect instantaneous events like lightning strokes, or for high-frequency temporal sampling of rapidly evolving situations, such as active convection. However, the coverage excludes very high latitudes or any locations too far from the sub-satellite point. Table 2.1 shows that $\delta = 81.31°$ is the maximum geocentric angle.

For a non-geostationary satellite, the orbit is said to have a repeat cycle if it overpasses the same track exactly after a given number of revolutions. During the timespan of a repeat cycle, the satellite track may shift from day to day, following a determined pattern that may exhibit certain periodicities called sub-cycles. Some sub-cycles may be of interest because distinct areas, relatively close to each other, are visited within short time intervals; other sub-cycles may be of interest because the areas covered are spatially adjacent.

If the orbit is Sun-synchronous (see section 2.1.3), the existence of a repeat cycle means that a whole number of revolutions can be completed in exactly a whole number of days. The orbital period determines N, the number of orbits that the satellite runs in 24 h. This is normally not an integer. In order to obtain a repeat cycle of m days, the orbital period is adjusted to ensure that N multiplied by m is an integer. N can then be expressed in the following form, where n and ℓ are, respectively, the quotient and remainder of the integer division of "$N \cdot m$" by m:

$$N = n + \ell/m \tag{2.3}$$

where n, ℓ and m are integers ($\ell < m$).

Table 2.2. Period, decalage and observing cycle for the orbits indicated in Table 2.1

Orbital parameter	H = 400 km	H = 600 km	H = 800 km	H = 35 786 km
Period T	92.6 min	96.7 min	100.9 min	23 h 56 min 4 s
Decalage	2 570 km	2 690 km	2 800 km	0 km
Observing cycle for $\zeta = 70°$ (day only)	35 h	27 h	23 h	From instrument
Observing cycle for $\zeta = 60°$ (day only)	51 h	38 h	31 h	From instrument
Observing cycle for $\zeta = 70°$ (day and night)	18 h	13 h	11 h	From instrument
Observing cycle for $\zeta = 60°$ (day and night)	26 h	19 h	16 h	From instrument

Table 2.3. Repeat cycles and main sub-cycles for a number of orbits

Orbital height	Sun-synchronous orbits					Non-Sun-synchronous orbit
	909 km (e.g. Landsat 1–3)	705 km (e.g. Landsat 4–8)	832 km (e.g. SPOT)	791 km (e.g. Envisat)	820 km (e.g. Metop)	1 336 km (e.g. JASON)
Period	103.2 min	98.9 min	101.5 min	100.6 min	101.3 min	112.4 min
No. of orbits/day	13 + 17/18	14 + 9/16	14 + 5/26	14 + 11/35	14 + 6/29	12 + 7/10[a]
Cycle	18 days	16 days	26 days	35 days	29 days	10 days[a]
Revolutions/cycle	251	233	369	501	413	127
Main sub-cycle(s)	1 day	7 days, 2 days	5 days	16 days, 3 days	5 days	3 days[a]

Note:
a   In the case of the Joint Altimetry Satellite Oceanography Network (JASON), which is not Sun-synchronous, the figures refer to a day of 23 h 48 min in duration, i.e. 0.99156 of the duration of a solar day.

Equation 2.3 also applies to non-Sun-synchronous orbits. However, in such cases, the repeat cycle m is no longer expressed in solar days of 24 h but must account for a slight correction due to the drift of the orbit. Table 2.3 provides examples of repeat cycles and main sub-cycles for a number of orbits.
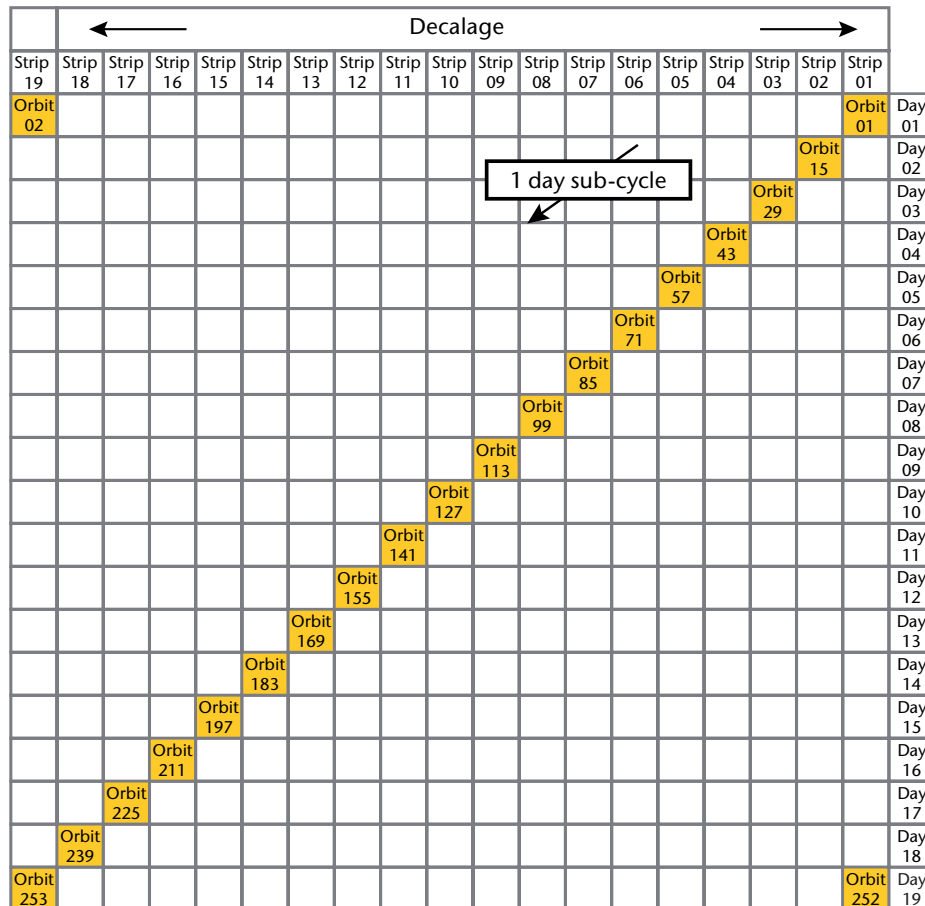
Figure 2.3. Schematic evolution of the orbital track of early Landsat over a repeat cycle (N = 13 + 17/18, repeat cycle: 18 days, 251 revolutions/cycle)

An orbit with a repeat cycle is a necessary feature if a certain location needs to be viewed at fixed intervals under identical conditions. This is true of altimetric measurements for geodetic application, or of high-resolution land observation imagers, used to detect local variations.

Repeat cycles may be useful when the instrument swath is substantially narrower than the decalage and global coverage cannot be achieved in a single day. In that case, the sequence of coverage over successive days can be arranged to follow a certain logic if requested. That logic might be to provide regular progression, or to avoid biases due to unsuitable sampling.

Figure 2.3 shows the pattern evolution of orbital passes for an orbit with a one-day sub-cycle (such as for early Landsat). As Figure 2.3 shows, the one-day sub-cycle ensures that each day, the covered strip is adjacent to the one that was observed on the previous day. The width of the covered strip can be tuned to the instrument swath so as to avoid any gaps. The drawback is that, after the first few daily visits over or close to the target area, the next sequence of visits occurs only after the completion of the repeat cycle.

With the current Landsat, the temporal evolution of the orbit tracks during the repeat cycle (16 days) results in two main sub-cycles, as shown in Figure 2.4. The two-day sub-cycle ensures a shorter temporal gap, but the seven-day sub-cycle provides a closer geographical match.

Although the concept of repeat cycles and sub-cycles stems from the requirements placed on the use of narrow-swath instruments, including those with nadir-only viewing, orbits with sub-cycles may also be useful for relatively wide-swath instruments. For example, sounding instruments may have a swath as wide as several thousand kilometres. (For example, the Advanced
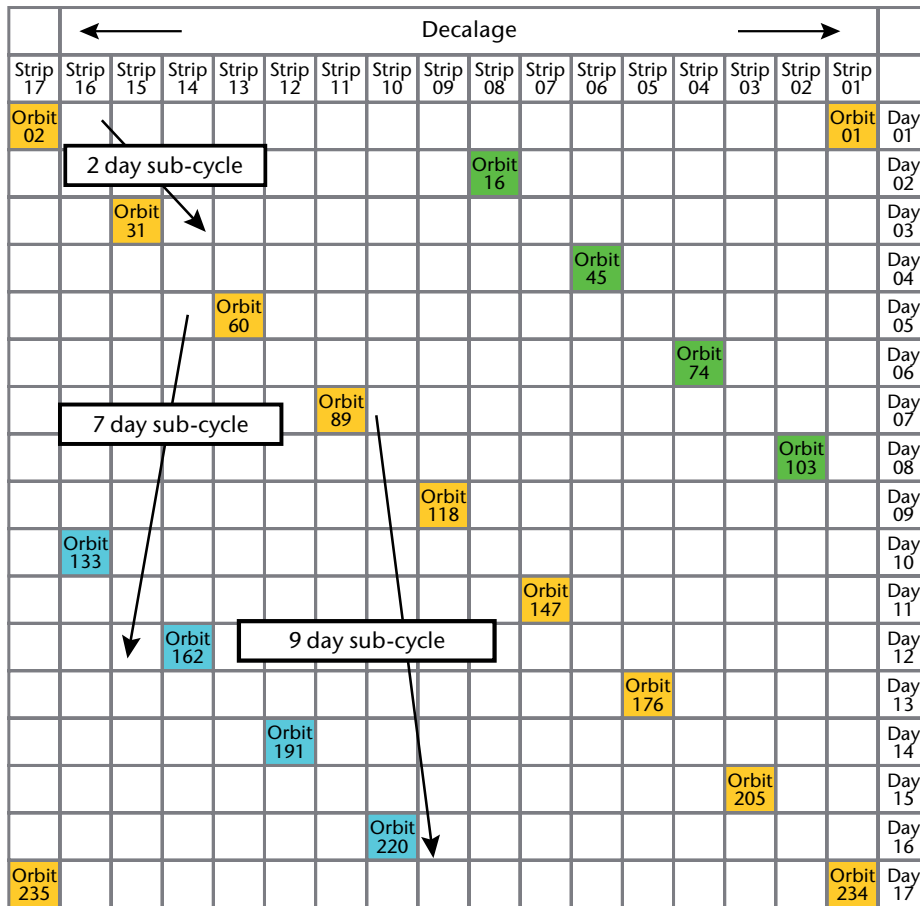
Figure 2.4. Schematic evolution of the orbital track of current Landsat over a repeat cycle
($N = 14 + 9/16$, repeat cycle: 16 days, 233 revolutions/cycle). Three sub-cycles are shown:
seven days (westbound), the main one, providing the closest observations in space; two days
(eastbound), for closer observations in time; and nine days (eastbound), of marginal interest,
the sum of the first two sub-cycles.
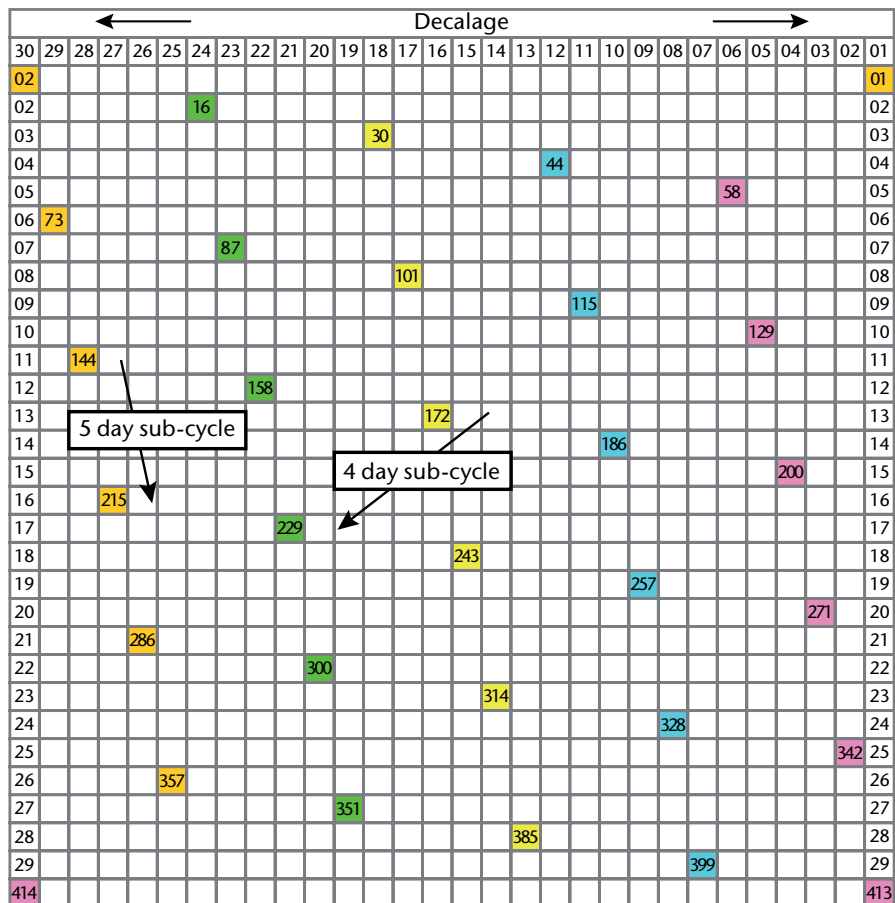
Figure 2.5. Schematic evolution of the orbital track of Metop ($N = 14 + 6/29$, repeat cycle: 29 days, 412 revolutions/cycle). Two sub-cycles are shown: five days (eastbound), the main one, providing the closest observations in space; and four days (westbound), for marginally closer observations in time.

Microwave Sounding Unit (AMSU) or the Infrared Atmospheric Sounding Interferometer (IASI) have swaths of over 2 200 km). However, the quality of the products retrieved is higher when closer to the nadir sub-track. Therefore, there is an interest in ensuring that the coverage provides a fair blend of higher and lower quality data. Orbits for the National Oceanic and Atmospheric Administration (NOAA) satellites and Meteorological Operational (Metop) satellites have a five-day sub-cycle, as shown in Figure 2.5 for Metop.

Repeat cycles and sub-cycles are convenient for several reasons, but a few drawbacks should also be noted:

(a)   If the instrument swath is too narrow with respect to the decalage and the number of orbital passes during the repeat cycle, some areas will never be observed. An extreme case is a nadir-only viewing instrument such as an altimeter.

(b)   The day-to-day sequence of observations from a repeat-cycle orbit may introduce sampling biases in the observations (a spurious wavelength corresponding to a repeat cycle or sub-cycles).

(c)   Maintenance of the repeat cycle/sub-cycles requires costly satellite orbit control systems.

Therefore, if all instruments on board have a sufficiently wide swath, a repeat cycle or sub-cycle is generally not carried out.
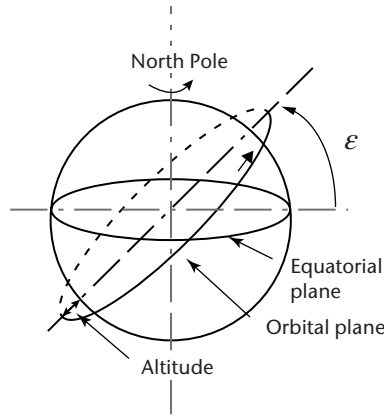
Figure 2.6. Definition of inclined orbit

2.1.3 Orbital precession, Sun-synchronous orbits and drifting orbits

The orbital plane can lie in the Earth's equatorial plane or be inclined by ε degrees (see Figure 2.6).

For $\varepsilon = 90°$, the satellite follows a meridian line and the orbit is polar. This is very convenient for observing the Earth's surface pole-to-pole.

The gravity field acting on the satellite is perpendicular to the geopotential surface at satellite altitude, which is slightly ellipsoid like the geoid. Where $\varepsilon \neq 90°$, the effect of these forces is a precession of the orbital plane around the polar axis. The precession rate α is computed as:

$$\alpha = -10.02 \cos \varepsilon \ (1 + \frac{H}{R})^{-\frac{7}{2}} \quad (\text{degree/day}) \tag{2.4}$$

For a purely polar orbit ($\varepsilon = 90°$), the precession rate is thus zero. The orbital plane has an invariant orientation with respect to the fixed stars. However, as the Earth rotates around the Sun over one year, the illumination conditions of the surface, as viewed by the satellite, change every day by 360/365 degrees; that is 59 min. An area viewed in daylight at noon on day t_0 will be viewed in dawn conditions on day $t = t_0 + 3$ months (Figure 2.7, left panel). For measurements in daylight, this would mean different observing conditions day after day, with seasonally-dependent observation times. In particular, when the Earth–Sun direction becomes perpendicular to the orbital plane, the illumination in dawn–dusk conditions makes many measurements impossible.

The orbital inclination ε can be set in such a way that the precession rate exactly matches the yearly revolution of the Earth around the Sun. By imposing the value $\alpha = 360/365$ (degree/day) in equation 2.4, it is found that the inclination ε_0 must satisfy:
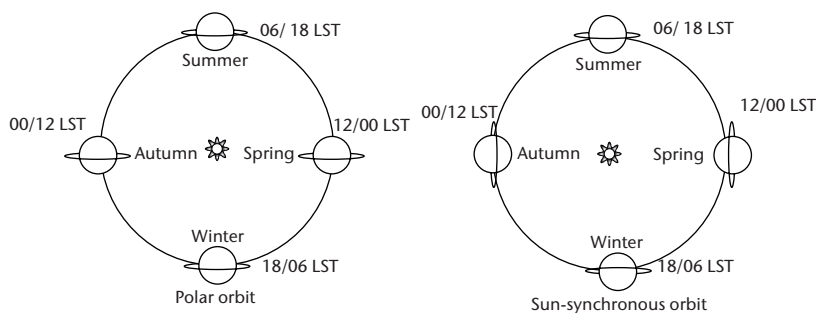
Figure 2.7. Left: Pure polar orbit with changing local solar time (LST) throughout the year; right: Sun-synchronous orbit with fixed LST throughout the year

$$\cos \varepsilon_0 = -0.0988 \ (1+\frac{H}{R})^{\frac{7}{2}}$$ (2.5)

An orbit that satisfies that condition is called Sun-synchronous. The negative value of ε_0 indicates that the orbit is retrograde with respect to the Earth's rotation. The local solar time of the areas overflown by the satellite at a given latitude is constant across the whole year (see Figure 2.7, right panel). Table 2.4 presents the ε_0 values of a number of Sun-synchronous orbits as a function of orbital height.

Table 2.4. Inclination values of Sun-synchronous orbits as a function of orbital height

400 km	600 km	800 km	1 000 km	1 200 km	1 400 km
97.02°	97.78°	98.60°	99.47°	100.41°	101.42°

Note that the deviation from the polar axis increases with orbital height. This is a drawback for high Sun-synchronous orbits: the poles might not be observed unless the instrument swath is wide enough. However, for relatively low orbital heights, the orbital plane is near-polar.

The most important feature of a Sun-synchronous orbit – the fixed local solar time – may be a disadvantage for certain types of measurements. Diurnally-varying phenomena (e.g. convective clouds, precipitation, radiation budget, sea level affected by astronomical tides) display biased sampling if observed from a Sun-synchronous satellite (i.e. at a fixed local solar time).

In general, satellites for operational meteorology, land observation and oceanography, with the exception of geodetic-quality altimetry, use a Sun-synchronous orbit. Scientific missions focused on processes affected by diurnal variation, which require unbiased sampling, may favour non-Sun-synchronous (drifting) orbits.

2.1.4 Elliptical orbits

The previous sections are applicable to circular orbits, which are by far the most widely used in Earth observation, particularly for Sun-synchronous and geostationary orbits. However, both near-polar low Earth orbits (LEO) and geostationary Earth orbits (GEO) have several limitations.

A near-polar LEO satellite provides global but infrequent coverage. Even if the instrument swath is as large as the decalage, thus providing contiguous coverage by consecutive orbits, one satellite can cover the whole of the Earth's surface twice a day at most (or even once a day if sensing can be performed either in daylight only or only in night-time conditions). If more frequent global coverage is needed, additional satellites in complementary orbital planes are necessary (see Table 2.5).

It is clear from Table 2.5 that any observing cycle shorter than, for instance, three hours, would be extremely demanding, as it would require a constellation of LEO satellites in coordinated orbits.

Table 2.5. Number of LEO satellites needed to achieve a required observing cycle (assumed height: H = 800 km)

Instrument swath	Observing capability	Required observing cycle						
		24 h	12 h	8 h	6 h	3 h	2 h	1 h
2 800 km	Only in daylight	1 sat	2 sat	3 sat	4 sat	8 sat	12 sat	24 sat
	Night and day	0.5 sat	1 sat	1.5 sat	2 sat	4 sat	6 sat	12 sat
1 400 km	Only in daylight	2 sat	4 sat	6 sat	8 sat	16 sat	24 sat	48 sat
	Night and day	1 sat	2 sat	3 sat	4 sat	8 sat	12 sat	24 sat

Figure 2.8. The Molniya orbit

The coverage improves substantially for high latitudes (see Figure 2.2). For example, coverage is twice as frequent at 60° latitude than at the Equator. In polar regions, the frequency of coverage becomes close to the orbital period T (i.e. ~100 min) or sub-hourly with more satellites.

A shorter observing cycle may be obtained by leaving aside the Sun-synchronous feature and adopting a lower inclination, but the coverage is then no longer global. Low-inclination orbits are used for monitoring the intertropical zones.

The GEO orbit provides observations at a rate that is limited only by the instrument. However, a constellation of about six satellites around the Equator is needed to cover all longitude sectors up to a latitude of at least 55°; the highest latitudes cannot be covered.

Some of these limitations can be mitigated by adopting an elliptical orbit. On an elliptical orbit, the satellite speed changes along the orbit; it is minimal around the apogee allowing more time for acquiring measurements from the overflown area. Elliptical orbits are usually optimized for specific purposes, particularly for space science, such as to collect in situ measurements up to very high altitudes by physically passing through the ionosphere and plasmasphere.

One problem of elliptical orbits is that, since the argument of the perigee is affected by the secular perturbation, the apogee occurs at latitudes that change with time. The secular perturbation can be compensated for if the orbital inclination is $\varepsilon = \sin^{-1}(4/5)^{1/2} \approx 63.4°$. In this case, the apogee region where the satellite dwells for most of the time is stable. In that position, measurements can be taken very frequently, in a quasi-geostationary fashion.

Two orbits of this kind have been used for telecommunication satellites and are planned to be used for Earth observation: Molniya (Figure 2.8), which has a 12 h period and an apogee at 39 800 km; and Tundra, which has a 24 h period and an apogee at 48 300 km. In the Molniya orbit, the satellite is nearly geostationary for about 8 h of the 12 h period. In the Tundra orbit, it is nearly geostationary for about 16 h of the 24 h period.

The Molniya and Tundra orbits only serve one hemisphere. In addition, the 8 h or 12 h quasi-geostationary observing area is centred on a specific local solar time. If all latitudes above 60° have to be covered 24 h a day, three Molniya satellites or two Tundra satellites are required. An interesting variant is the three-apogee orbit with a 16 h period and an apogee at 43 500 km. Table 2.6 presents the main features of Molniya and Tundra orbits. In the apogee position, which is useful for frequent sampling, the height of the satellite exceeds GEO height.

2.1.5 Launchers and injection into orbit

Satellites are injected into orbit by a launcher, which has to perform the following functions:

(a) To host the satellite in the fairing, where vital functions for the satellite are ensured. When in the fairing, the satellite is stowed in a compact configuration to minimize volume occupancy and to be protected against the effects of acceleration.

(b) To bring the satellite to orbit. In order to minimize the total mass brought to high altitudes, the launcher is generally structured by stages. The first stage, which is the heaviest since it has to provide the maximum thrust for lift-off, is separated early. The fairing is released at an appropriate altitude. A further one or two stages are fired and separated in sequence.

(c) To release the satellite. For satellites in LEO circular orbits, the launcher releases the satellite directly on the final orbit. For elliptical orbits, the launcher releases the satellite at the perigee and provides it with a last acceleration to acquire the energy corresponding to the intended orbit.

When in orbit, the satellite deploys its solar panels and starts autonomous operations. One of the operations is to reach final orbit by activating its propulsion system. In the case of a geostationary orbit, the satellite is released at a perigee in an elliptical orbit whose apogee is 35 786 km, and is equipped with an apogee boost motor. The motor, which uses solid, hybrid or more often, liquid propellant (a liquid apogee motor), is fired at the apogee to provide the acceleration necessary to circularize the orbit (see Figure 2.9).
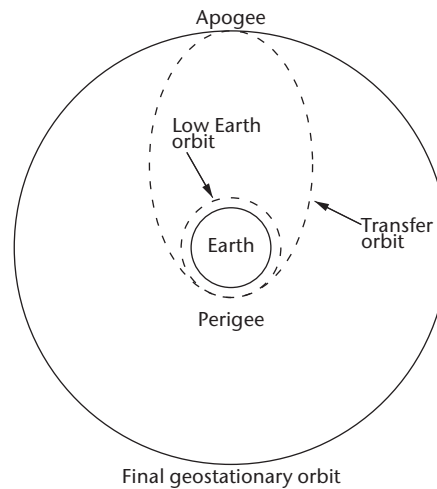
Figure 2.9. Achievement of GEO

**Table 2.6. Main features of Molniya and Tundra orbits
(apogee and perigee heights can be slightly adapted to need)**

Orbit type	Inclination	Period	Apogee	Perigee	Coverage (from one satellite)	Sats for hemispheric coverage
Molniya	63.4°	12 h	~39 800 km	~1 000 km	Visible over 2 positions for ~8 h	3
Tundra	63.4°	24 h	~48 300 km	~24 000 km	Visible over 1 position for ~16 h	2

Launching a satellite is a complicated and costly exercise. In order to optimize cost-effectiveness, a launch is often shared by several satellites. In this case, the task of the last stage is extended to release the various satellites at different times to separate the orbits. The respective platform propulsion systems will thereafter achieve the transfer to the final orbits.

Constellations of minisatellites, whose individual launches would be extremely uneconomical, are a good example of the usefulness of multiple launches. One effective launching strategy is known as the Walker Delta Pattern. The orbital inclination ε of all satellites must be the same. Either the launcher releases the satellites at different altitudes, or the satellite propulsion systems spread them into different altitudes. Therefore, each orbit will have a different precession rate, according to equation 2.4, and the orbital phases will differentiate as time elapses. When the orbits of all the satellites are appropriately spaced, the platform propulsion systems will bring each of the satellites to the desired altitude H. Equation 2.4 shows that, in practice, the strategy works well for relatively low inclinations and relatively low altitudes, otherwise the time needed to deploy the constellation becomes too long. For example, the Constellation Observing System for Meteorology, Ionosphere and Climate (COSMIC) (six satellites, $H = 800$ km, $\varepsilon = 71°$) took one year to deploy.

2.2 PRINCIPLES OF REMOTE-SENSING

Earth observation from space is mainly performed by exploiting electromagnetic radiation. The few exceptions are in situ measurements at platform level (of gravity field, magnetic field, electric field and charged particle density in the solar wind). This section deals with remote-sensing of the Earth and focuses on:

(a)   The electromagnetic spectrum and the ranges used for remote-sensing;

(b)   The basic laws of interaction between electromagnetic radiation and matter;

(c)   Observations in the atmospheric windows;

(d)   Observations in absorption bands;

(e)   Limb sounding and radio occultation;

(f)   Active sensing.

2.2.1 The electromagnetic spectrum and the ranges used for remote-sensing

The spectrum of electromagnetic radiation as observed from space (with nadir viewing) is shown in Figure 2.10. The displayed range (0.2 μm to 3 cm (or 10 GHz)) includes all that is used for remote-sensing from space. The variation in wavelength is due to the interposed atmosphere, with transmissivity ranging from 1 (atmospheric window) to 0 (full opacity due to total atmospheric absorption).
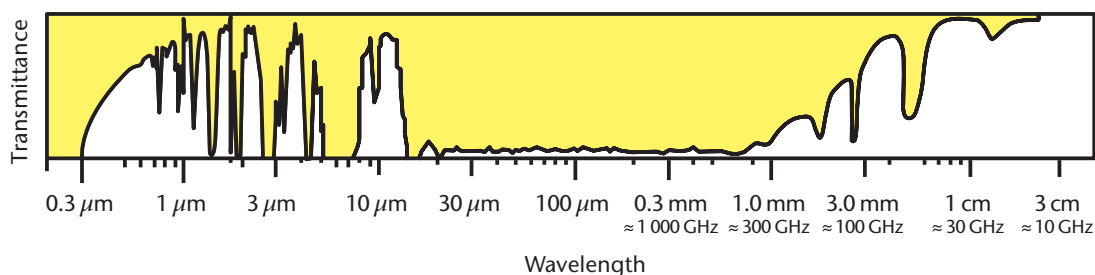
Figure 2.10. Spectrum (transmissivity) of electromagnetic radiation as observed from space with nadir viewing; range: 0.2 μm to 3 cm

Table 2.7. Bands of the electromagnetic spectrum exploited for remote-sensing

	Spectrum subdivision	Wavelength λ	Wave number $\nu^* = 1/\lambda$	Frequency $\nu = c/\lambda$
UV	Ultraviolet	0.01–0.38 μm	26 320–1 000 000 cm^{-1}	
B	Blue	0.436 μm	22 935 cm^{-1}	
G	Green	0.546 μm	18 315 cm^{-1}	
R	Red	0.700 μm	14 285 cm^{-1}	
VIS	Visible	0.38–0.78 μm	12 820–26 320 cm^{-1}	
NIR	Near infrared	0.78–1.30 μm	7 690–12 820 cm^{-1}	
VNIR	Visible and near infrared (VIS + NIR)	0.38–1.3 μm	7 690–26 320 cm^{-1}	
SWIR	Short-wave infrared	1.3–3.0 μm	3 330–7 690 cm^{-1}	
SW	Short wave	0.2–4.0 μm	2 500–50 000 cm^{-1}	
LW	Long wave	4–100 μm	100–2 500 cm^{-1}	
MWIR	Medium-wave infrared	3.0–6.0 μm	1 665–3 330 cm^{-1}	
TIR	Thermal infrared	6.0–15.0 μm	665–1 665 cm^{-1}	
IR	Infrared (MWIR + TIR)	3–15 μm	665–3 330 cm^{-1}	
FIR	Far infrared	15 μm–1 mm	10–665 cm^{-1}	300–20 000 GHz
Sub-mm	Submillimetre wave (part of FIR)	0.1–1 mm	10–100 cm^{-1}	300–3 000 GHz
Mm	Millimetre wave (part of MW)	1–10 mm	1–10 cm^{-1}	30–300 GHz
MW	Microwave	0.1–30 cm	0.033–10 cm^{-1}	1–300 GHz

Table 2.7 presents definitions of the subdivisions of the spectrum that are generally accepted, though not standardized. In addition to the commonly used wavelength λ and frequency ν, the wave number ν^*, mostly used in spectroscopy, is also quoted.

A finer subdivision of the MW range and nearby FIR, used for radar but also by extension, for passive radiometry, is provided in Table 2.8.

The overall spectrum shown in Figure 2.10 comprises five distinct regions, each with rather different features.

Table 2.8. Bands used in radar technology (according to the American Society for Photogrammetry and Remote-sensing)

Band	Frequency range	Wavelength range
P	220–390 MHz	77–136 cm
UHF	300–1 000 MHz	30–100 cm
L	1–2 GHz	15–30 cm
S	2–4 GHz	7.5–15 cm
C	4–8 GHz	3.75–7.5 cm
X	8–12.5 GHz	2.4–3.75 cm
K_u	12.5–18 GHz	1.67–2.4 cm
K	18–26.5 GHz	1.1–1.67 cm
K_a	26.5–40 GHz	0.75–1.18 cm
V	40–75 GHz	4.0–7.5 mm
W	75–110 GHz	2.75–4.0 mm
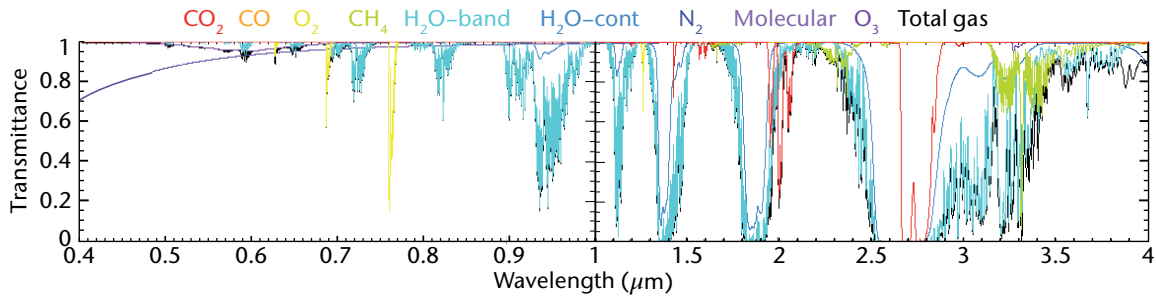
Figure 2.11. Atmospheric spectrum in the range 0.4 to 4.0 μm. It includes several windows and absorption bands from carbon monoxide (CO, about 2.3 μm), carbon dioxide (CO_2, about 1.6, 2.1 and 2.8 μm), methane (CH_4, about 2.3 and 3.4 μm), several oxygen bands (O_2, mainly about 0.77 μm), some nitrogen (N_2) and ozone (O_3) bands, and many important bands of water vapour (H_2O, mainly 0.94, 1.13, 1.37, 1.8 and 2.7 μm). Also shown is the molecular continuum, which prevents using UV for Earth surface and low atmosphere sensing from space.

In the UV region, atmospheric absorption is strong, mainly due to the major air constituents (nitrogen (N_2) and oxygen (O_2)) and trace gases (the most important being ozone (O_3)). The Earth's surface cannot be observed in that spectral region. The radiation source for remote-sensing consists of reflected solar radiation.

The VIS, NIR and SWIR regions, from 0.4 to 3 μm and, in some cases, up to 4 μm, can be sensed by means of reflected solar radiation. This range includes several transparent regions (windows) and many absorption bands (see Figure 2.11).

In the MWIR and TIR regions, from 4 to 15 μm, the radiation source consists of the thermal emission from the Earth's surface and the atmosphere, which is mainly driven by water vapour and carbon dioxide absorption/emission. These are important contributors to the greenhouse effect. This thermal emission combined with the main atmospheric window enables the planet's thermal equilibrium to be maintained at agreeable values (see Figure 2.12).
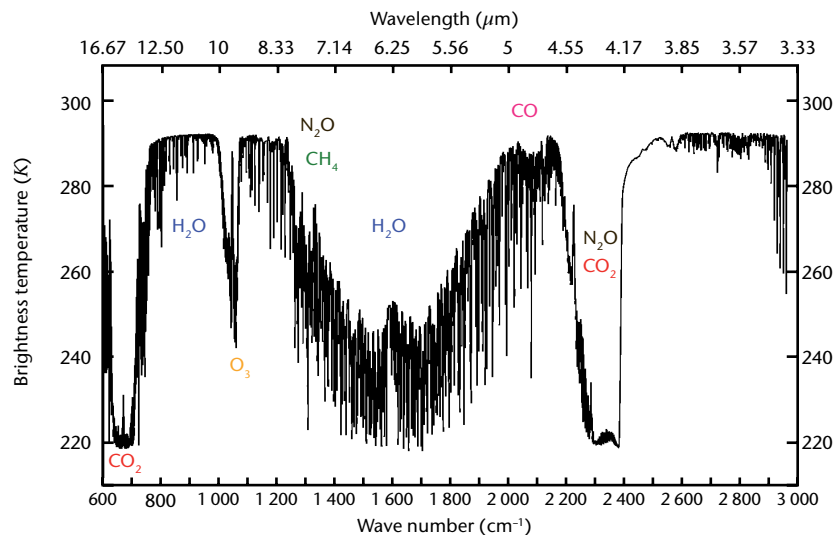
Figure 2.12. Atmospheric spectrum in the range 3.33 to 16.67 μm. The main atmospheric windows are in the ranges 3.7 to 4.0 μm and 10 to 12 μm. There are large absorption bands from water vapour (H_2O) and carbon dioxide (CO_2). Other species are: ozone (O_3, about 9.7 μm), methane (CH_4, about 7.7 μm), carbon monoxide (CO, about 4.6 μm) and nitrous oxide (N_2O, about 4.5 and 7.7 μm).

(A) Summer low latitude
(B) Annual midlatitude
(C) Winter high latitude
(D) Annual midlatitude (dry) with ozone
(E) Annual midlatitude: nitrogen only
(F) Annual midlatitude: oxygen only
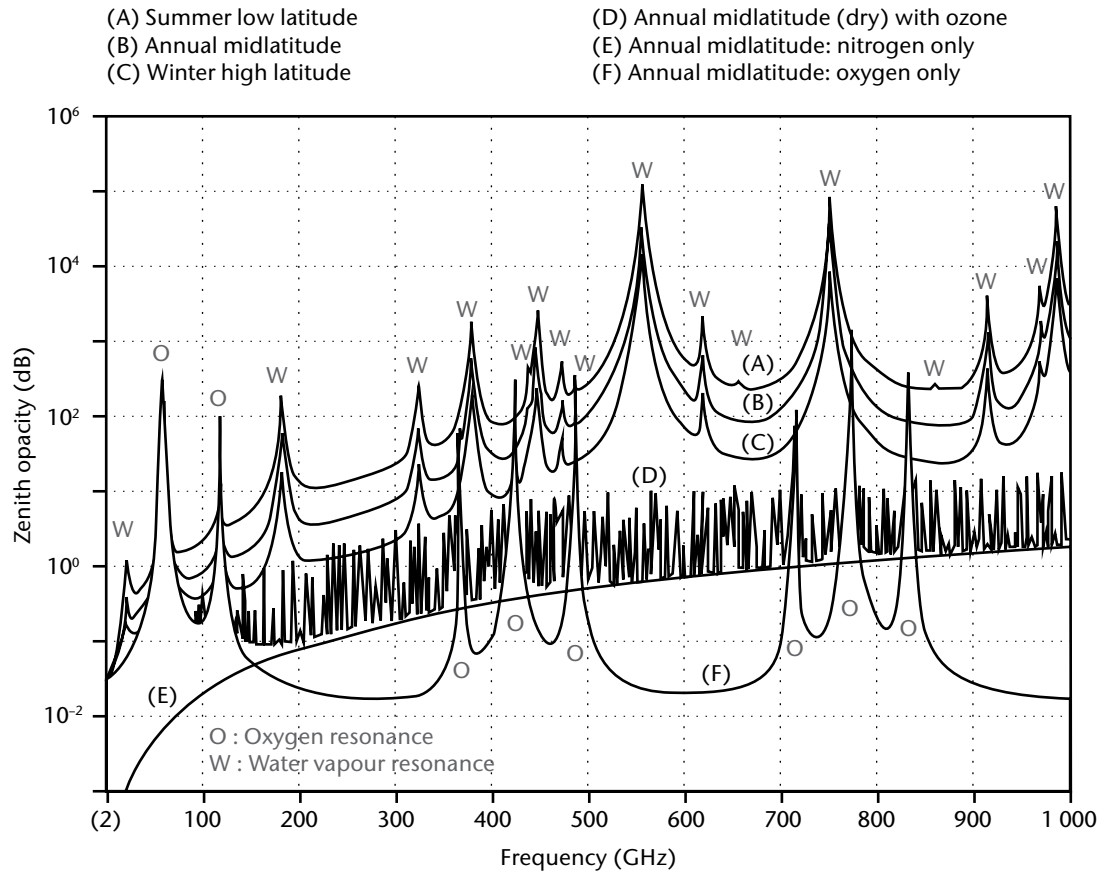
Figure 2.13. Atmospheric spectrum in the range 2 to 1 000 GHz. The dominant feature is the water vapour continuum that grows in opacity as frequency increases into the FIR range. This prevents viewing the Earth's surface at high frequencies from space. Invasive lines of ozone also dominate the spectrum. The most useful features are the oxygen bands (about 57, 118, 388, 424, 487 GHz and above), used to infer atmospheric temperature, and the water vapour bands (about 22, 183, 325, 380, 448 GHz and above).

Source: Klein, M., and A.J. Gasiewski, 2000: Nadir sensitivity of passive millimeter and submillimeter wave channels to clear air temperature and water vapor variations. *Journal of Geophysical Research*, 105(D13):17481–17511.

The next spectral region, the Far IR, ranges from 15 μm to 1 mm (or 300 GHz). It is fully opaque because of the water vapour continuum. In that region, which is difficult to explore because of the lack of efficient detection techniques, there are absorption lines of several important species, such as hydroxil radical (OH), known as a "cleaner" of the atmosphere, and hydrogen chloride (HCl), a reservoir species that releases ozone-aggressive chlorine. Hydroxil radical and hydrogen chloride are only observable in the FIR (e.g. about 120 μm ≈ 2 500 GHz and 480 μm ≈ 625 GHz, respectively).

In the MW range, from 1 to 300 GHz, the radiation source consists of the thermal emission from the Earth's surface and the atmosphere. The atmospheric spectrum, starting from 2 GHz and extending to submillimetre frequencies up to 1 000 GHz, is shown in Figure 2.13.

In the portion of the MW range where the atmosphere is more transparent, (i.e. at frequencies below about 100 GHz), the wavelengths exceed 3 mm and so are much larger than cloud drop size, except for precipitating clouds. Therefore, the MW range is used for observing the Earth's surface or atmospheric properties in nearly all weather conditions.

Active sensing is conditioned by technology and, in the case of MW, by radio-frequency spectrum regulations. Radar makes use of MW, while lidar makes use of optical wavelengths where suitable sources (crystals) are available. Table 2.9 presents a few commonly used radar

Table 2.9. Spectrum utilization from active instruments (radar and lidar) and radio occultation

	Observation	Instrument	Frequency or wavelength
Radar	Sea-surface wind	Scatterometer	C band (~5.3 GHz) or K_u band (~13.4 GHz)
	Ocean topography	Altimeter	C band (~5.3 GHz) + K_u band (~13.6 GHz)
	Cloud and precipitation	Rain radar, cloud radar	K_u band (~13.6 GHz) and/or K_a band (~35.5 GHz) or W band (~94 GHz)
	Imagery	Synthetic aperture radar	L band (~1.3 GHz) or C band (~5.4 GHz) or X band (~9.6 GHz)
Lidar	Clear-air wind	Doppler lidar	UV-lidar (355 nm)
	Aerosol, cloud top	Backscatter lidar	UV-lidar (355 nm), VNIR-lidar (532 + 1 064 nm)
	Ice-sheet topography	Altimeter	VNIR-lidar (532 + 1 064 nm)
Radio occultation	Atmospheric refraction	GNSS + Receiver in LEO	L band: ~1 580 + ~1 250 + ~1 180 GHz (GPS, GLONASS and Galileo)

frequencies and lidar wavelengths. As a comparison, the table also lists frequencies used by the global navigation satellite system (GNSS) and associated radio-occultation sensing of the atmosphere (see Part III, Chapter 3, 3.2.7).

2.2.2 Basic laws of interaction between electromagnetic radiation and matter

The macroscopic properties of a condensed body at thermodynamic equilibrium that is not affected by chemical or nuclear reactions are summarized in terms of electromagnetic radiation by three coefficients linked by the following equation:

$$\rho\left(\lambda,T,\zeta,\varphi\right)+\tau\left(\lambda,T,\zeta,\varphi\right)+\varepsilon\left(\lambda,T,\zeta,\varphi\right)=1 \tag{2.6}$$

In this equation, $\rho(\lambda,T,\zeta,\varphi)$ denotes reflectivity that is the ratio of the backscattered radiation $I(\lambda,T,\zeta,\varphi)$ to the incident radiation $I(\lambda)$; $\tau(\lambda,T,\zeta,\varphi)$ denotes transmissivity, or the fraction of $I(\lambda)$ that crosses the body; and $\varepsilon(\lambda,T,\zeta,\varphi)$ is the fraction of $I(\lambda)$ that is absorbed by the body – it is called emissivity for reasons explained below. The three coefficients depend on the radiation wavelength λ, the body temperature T, and the observing geometry ζ, φ (zenith and azimuth angles, respectively).

A body that is not reflecting and is totally opaque to radiation on any wavelength (where $\rho = \tau = 0$, and thus $\varepsilon = 1$) is called a black body. It radiates at any temperature, T and over the full λ or ν spectrum, according to Planck's law:

$$B(\lambda,T) \;=\; \frac{2\pi hc^2}{\lambda^5}\frac{1}{e^{\frac{hc}{\lambda kT}}-1} \quad \text{or} \quad B(\nu,T) \;=\; \frac{2\pi\nu^3}{c^2}\frac{h}{e^{\frac{h\nu}{kT}}-1} \tag{2.7}$$

where:
$h = 6.6256 \cdot 10^{-34}$ J s (which is the Planck constant);
$c = 2.99793 \cdot 10^8$ m s^{-1} (which is the speed of light in a vacuum); and
$k = 1.38044 \cdot 10^{-23}$ J K^{-1} (which is the Boltzmann constant).

$B(\lambda,T)$ (or $B(\nu,T)$) is the radiative power per unit surface over the hemisphere per unit of wavelength (or frequency). The power radiated per unit of solid angle is B/π. The Planck function for temperatures of 6 000 K and 273.16 K, which are representative of the Sun and the Earth's surfaces respectively, is shown in Figure 2.14.
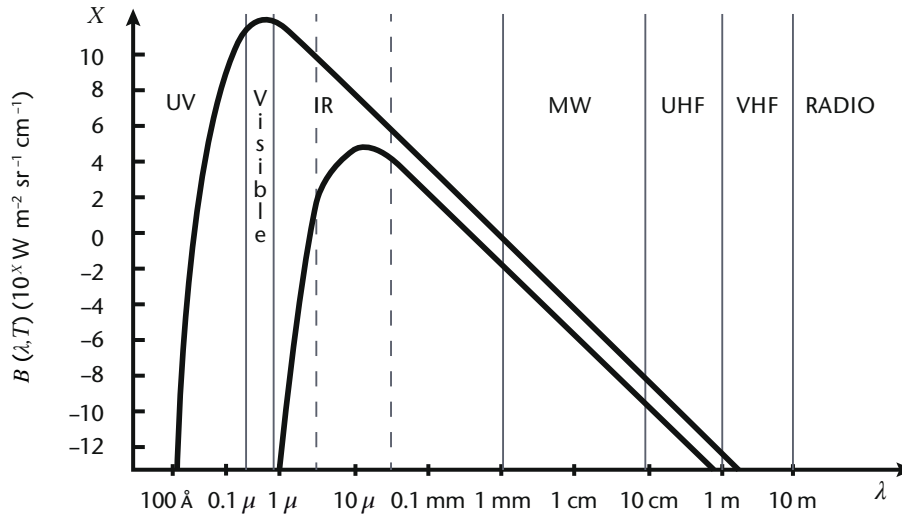
Figure 2.14. The Planck function for $T = 6\,000$ K, representative of the Sun (higher curve), and $T = 273.16$ K, representative of the Earth (lower curve); X values in ordinate are to the power of 10.

The power radiated over the full spectrum is:

$$W(T) = \int_0^\infty B(\lambda, T) \cdot d\lambda = \sigma \cdot T^4 \qquad \text{Stefan-Boltzmann law} \tag{2.8}$$

where $\sigma = 5.6681 \cdot 10^{-8}$ W m^{-2} K^{-4}.

The two curves in Figure 2.14 illustrate that the Sun's and Earth's surfaces have very different radiative powers. However, after scaling down the Sun curve by the square of the distance between the Sun and Earth, the two integrated areas become comparable, which reflects the Earth's radiative balance. If the upper curve in the figure is scaled, it is easy to see that the solar radiation on Earth is very small for $\lambda > 4$ μm, while Earth radiation is negligible for $\lambda < 3$ μm. There are significant amounts of solar and Earth radiation in the narrow interval between 3 and 4 μm.

A major difference between the two curves in Figure 2.14, after scaling, is the wavelength λ_{max} where the maximum emission occurs. This is given by:

$$\lambda_{max} = \frac{b}{T} \quad \text{with } b = 0.0028981 \text{ m K} \quad \text{Wien law} \tag{2.9}$$

Because of the double-logarithmic scale in Figure 2.14, it is difficult to appreciate how sharp the Planck function is around λ_{max}. In the case of solar radiation ($T = 6\,000$ K) the peak emission occurs around $\lambda_{max} = 0.5$ μm and most of that power lies in the 0.2–3.0 μm range. In the case of terrestrial radiation ($T = 273.16$ K, i.e. $T = 0°$C) the peak is around $\lambda_{max} = 10$ μm and most of the power lies in the 3–50 μm range.

Another interesting feature of the Planck function is that, when moving from λ_{max} to shorter wavelengths, radiative power dramatically decreases, whereas when moving to longer wavelengths, the decrease is more gradual (approximately two thirds of power occurs at wavelengths longer than λ_{max}). For very long wavelengths, or low frequencies, such as those in the MW range, where the argument of the exponential in the Planck function is $h\nu/kT \ll 1$, the term $e^{h\nu/kT}$ becomes $\approx 1 + h\nu/kT$ and the Planck function thus reduces to:

$$B(\nu, T) = \frac{2\pi k \nu^2}{c^2} T \qquad \text{Rayleigh-Jeans law} \tag{2.10}$$

Because of this relationship, radiation measurements in the MW range can be considered as temperature measurements and can be expressed as a brightness temperature (T_B) in temperature units. While the total radiative power changes with temperature in proportion to T^4 according to the Stefan-Boltzmann law (equation 2.8), that power changes in a linear way in the MW portion of the spectrum. Conversely, when moving towards shorter wavelengths, the Planck

function is increasingly dependent on temperature. Terrestrial radiation varies approximately with T^5 in the main TIR window around 11 μm and with T^{12} in the window around 3.7 μm. This is an interesting feature for remote-sensing, since it means that sensitivity to high temperatures is higher at 3.7 μm. Conversely, these shorter wavelengths are less sensitive to low temperatures.

For example:

(a) For a body at 220 K (such as a cloud top in the upper troposphere), the radiation at 11 μm is ~1 200 times greater than at 3.7 μm; but at 300 K (surface), it is only ~130 times;

(b) The sensitivity to temperature changes, (i.e. $(\partial B/\partial T)/B$) is three times higher at 3.7 μm than at 11 μm.

As a consequence, 3.7 μm is well suited for surface observations, is optimal for fire detection, and is less useful for high clouds.

The relationship represented by equations 2.7–2.10 is only valid for a black body ($\varepsilon = 1$). For a common body, the relationship can be established through the following conceptual experiment. If a number of bodies in an isolated system only exchange radiation among themselves, it could be assumed that, after a transient time, each of them would reach thermodynamic equilibrium, where the radiation each absorbs according to its absorption coefficient $\varepsilon(\lambda,T)$ is equal to the power it radiates $P(\lambda,T)$. That is, $P(\lambda,T)/\varepsilon(\lambda,T) = $ constant. Assuming that one of the bodies is a perfect black body, this yields:

$$P(\lambda,T) \;=\; \varepsilon(\lambda,T)\cdot B(\lambda,T) \qquad \text{Kirchhoff principle} \qquad (2.11)$$

This shows that the absorption coefficient introduced in equation 2.5 also controls the body's emission properties, hence the name emissivity. Equation 2.11 indicates two important consequences:

(a) At any wavelength and temperature, a body cannot radiate more than a black body at the same wavelength and temperature;

(b) A body can radiate only at wavelengths at which it can also absorb.

Emissivity ε is a function of wavelength and, to a lesser extent, temperature. For certain bodies, ε may be constant over large portions of the spectrum. If it is constant over the whole spectrum, the body is called grey. The shape of the radiated power $P(\lambda,T)$ is then exactly like $B(\lambda,T)$, although it is damped by a factor ε. The Wien law (equation 2.9) applies unchanged. The Stefan-Boltzmann law becomes $W(T) = \varepsilon \cdot \sigma \cdot T^4$.

The Kirchhoff principle also applies to gaseous materials. Therefore, spectral lines of atmospheric gases are generally (but not always) relevant to both absorption and emission.

2.2.3 Observations in the atmospheric windows

2.2.3.1 *Emerging radiation*

Atmospheric windows are spectral regions where the atmosphere is nearly transparent. There is no region where the atmosphere is fully transparent. All regions have some residual disturbance from species that have a continuum, the most common of which is water vapour in the IR, MW and, to some extent, the SW ranges. Another factor, particularly in SW, is scattering from dry air molecules (mostly N_2 and O_2) and aerosols. Ultimately, the most transparent windows are:

(a) In the SW (Figure 2.11): 0.5–0.9 μm, 1.6–1.7 μm and 2.0–2.3 μm;

(b) In the IR (Figure 2.12): 3.5–4.0 μm and 10–12 μm;

(c) In the MW (Figure 2.13): 80–100 GHz, 25–50 GHz and below 20 GHz.

$\tau(\lambda, T) \cdot I_\tau(\lambda) \quad \mathcal{E}(\lambda, T) \cdot B(\lambda, T) \quad \rho(\lambda, T) \cdot I_\rho(\lambda)$

$I_\rho(\lambda, \theta)$

$I_\tau(\lambda)$
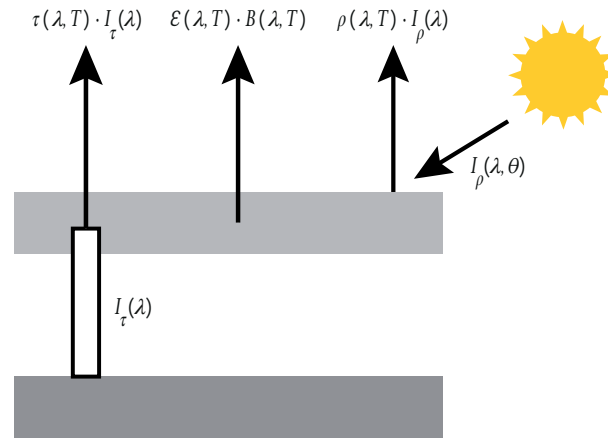
Figure 2.15. The three components of irradiance in space

Equation 2.5 indicates that the coefficients ρ (reflectivity), τ (transmissivity) and ε (emissivity) not only depend on radiation wavelength λ and body temperature T, but also on the geometric condition (zenith angle ζ and azimuth angle φ) of the satellite platform with respect to the body.

In order to simplify the discussion, the following conditions are assumed: vertical viewing from the satellite (Figure 2.15), flat surfaces and radiation towards the zenith (irradiance).

One component, $\tau(\lambda, T) \cdot I_\tau(\lambda)$, is transmitted radiation through the body. It can be found where the body is not totally opaque and where there is a radiation source below it in the opposite hemisphere compared to the satellite.

The component $\varepsilon(\lambda, T) \cdot B(\lambda, T)$ is emitted radiation, expressed through the Kirchhoff principle (equation 2.11). It is always present unless the body is at absolute thermal zero. It is not present in spectral regions, where the body does not absorb.

The component $\rho(\lambda, T) \cdot I_\rho(\lambda, \theta)$ is reflected radiation. It is found where there is a radiation source in the same hemisphere as the satellite. Figure 2.15 indicates the Sun but, in the MW range, where solar radiation is virtually zero, the full hemispheric sky radiates as a black body, at temperature $T = 2.725$ K, where the maximum power occurs at $\lambda_{\max} = 1.9$ mm (160 GHz). The notation $I_\rho(\lambda, \theta)$ indicates that the power of the incoming radiation depends on the angle of incidence θ. Normally for the Sun, $I_\rho(\lambda, \theta) = S(\lambda) \cdot \cos \zeta$, where $S(\lambda)$ denotes incoming power with the Sun at its zenith.

Taking account of all components, the radiation reaching the instrument on the satellite can be expressed as:

$$I(\lambda, T) = \tau(\lambda, T) \cdot I_\tau(\lambda) + \varepsilon(\lambda, T) \cdot B(\lambda, T) + \rho(\lambda, T) \cdot I_\rho(\lambda, \theta) \qquad (2.12)$$

There is considerable variation along the spectrum, so that the significance of the measurement is reasonably stable only within narrow bandwidths around a specific wavelength (channels). However, some general information is also contained in a wider range of wavelengths (VIS + NIR + SWIR; MWIR + TIR; MW).

2.2.3.2 *Measurements in the visible, near-infrared and short-wave infrared range*

In this range, there is no thermal emission from the Earth ($B = 0$). Focusing first on the Earth's surface (land and ocean), the transmitted radiation is zero, since there is no source below the Earth's surface. Also when considering that reflectivity is nearly independent of body temperature, equation 2.12 reduces to:

$$I_{\text{sw}}(\lambda) = \rho(\lambda) \cdot S(\lambda) \cdot \cos \zeta \qquad (2.13)$$

Since the solar spectrum and observing geometry are known, the information carried by a measurement in a SW channel is uniquely associated to surface reflectivity. Many geophysical variables (vegetation parameters, ocean colour, texture of land) may be estimated by measuring reflectivity at several wavelengths. However, clouds are the objects that are most in evidence in SW. Equation 2.13 is not strictly correct for a cloud surface, since radiation from the underlying surface can transmit through them. However, this effect has a limited impact given:

(a)   The total transmissivity through (downward and upward) the atmosphere;

(b)   That the cloud is low;

(c)   The originating radiation source (the Sun) is stronger than any surface below the cloud;

(d)   The reflectivity of the underlying surface is low (except for sand desert, snow and ice);

(e)   The reflectivity of clouds ρ is generally higher than any other terrestrial surface.

Therefore, equation 2.13 is an approximation applicable to most clouds, the exceptions being thin clouds such as cirrus, especially on the bright background of sand deserts, ice and snow.

Using SW-reflected radiation for quantitative purposes is not an easy exercise, since reflectivity is generally anisotropic. The simplest case occurs when the body, whatever the direction of the incoming radiation, and for any azimuth, homogeneously redistributes the reflected radiation from the zenith according to a cosine-law. This is called Lambertian reflection. Fortunately, most Earth surfaces observed from space at relatively large scale appear rather flat and rough, so that Lambertian diffusion may be a good approximation. In many cases, however, the body exhibits a bidirectional reflectance distribution function that should be measured a priori by observations under different viewing directions and for different directions of the incoming radiation. The final computation of the irradiance towards space requires hemispheric integration.

Using SW for Earth observation in atmospheric windows requires spectral sampling at several wavelengths (channels) since at any one wavelength, several bodies may have signatures, and one body may have a signature at several wavelengths. A multichannel capability is therefore necessary to distinguish and simultaneously retrieve the different properties of different bodies. For instance, clouds and snow have identical reflectance in VIS at 0.65 μm, but very different reflectance at 1.6 μm. In addition, channel bandwidths must be appropriate to their purpose. The most stringent are for ocean colour ($\Delta\lambda \approx 10$ nm), and then vegetation ($\Delta\lambda \approx 20$ nm), whereas for other surface features and for clouds, bandwidths of several tens of nanometres are sufficient.

Another feature that affects the quantitative use of VIS + NIR + SWIR is polarization: specular reflection tends to be privileged, with damping of the vertical component of the electric field. The Stokes vector, which in the SW range consists of three components (polarization in three directions with phase differences of 120°), fully describes the electric field, and so provides important information about the body's properties. Multipolarization is important for the observation of those bodies that do not have strong multispectral signatures. Typical examples would be aerosols and cirrus clouds (elongated ice crystals).

2.2.3.3   *Measurements in the medium-wave infrared and thermal infrared range*

In the 4–15 μm range, solar radiation is virtually zero. On the Earth's surface (land and ocean), transmitted radiation is also zero. Furthermore, considering that emissivity is nearly independent from body temperature, equation 2.12 reduces to:

$$I_{IR}\left(\lambda, T\right) = \varepsilon\left(\lambda\right) \cdot B\left(\lambda, T\right) \qquad\qquad (2.14)$$

Equation 2.14 is also approximately valid for clouds, since the transmissivity of clouds in IR is rather low (with the exception of thin cirrus).

The emissivity of most land surfaces, and certainly the ocean, is close to 1, with small variance. Therefore the information acquired by a measurement in an IR channel is closely associated with the Planck function (equation 2.7) or for a given wavelength, with the body's temperature.

At a specified wavelength λ or for a narrow channel $\Delta\lambda$ around λ, the Planck function (equation 2.7) may be easily inverted to retrieve the temperature, T:

$$T(\lambda) = \frac{hc}{\lambda k \ \ln\left[1 + \dfrac{2\pi hc^2}{\lambda^5 B(\lambda)}\right]} \tag{2.15}$$

However, T will not be the body's true temperature unless $\varepsilon = 1$. If the body's emissivity is known, and the channel bandwidth $\Delta\lambda$ is sufficiently narrow to enable ε to be considered as constant, an emissivity correction can be applied to the measured quantity (by inverting $B(\lambda,T) = I_{IR}(\lambda,T)/\varepsilon(\lambda)$), and the body's temperature can be measured. Otherwise, by inverting the measured quantity $B(\lambda,T) = I_{IR}(\lambda,T)$, a temperature T_{BB} (equivalent black-body temperature) is obtained that is lower than the body's true temperature.

For a large variety of bodies where ε is close to 1, radiance observation in a TIR atmospheric window enables rather accurate temperature measurement. It is particularly accurate in the case of the sea, whose emissivity is close to 0.98. However, emissivity is not the only effect that needs to be corrected. As previously mentioned, the atmospheric windows are not perfectly transparent. For instance, the main window in TIR, 10–12 μm, is contaminated by the water vapour continuum, particularly on the long-wave side. One way to reduce this disturbance is to split the window into two channels, generally 10.3–11.3 μm and 11.5–12.5 μm. Differential absorption is then used to estimate a correction (total column water vapour can also be estimated as a by-product).

As a result of those effects, equation 2.15 indicates a dependence of the retrieved temperature on the wavelength (although as there is only one body temperature, that dependence should not exist). The spread of values with wavelength implies how certain information might be explained. For instance, by comparing T_{BB} measured at 3.7 μm and 11 μm it is possible to explain the difference in terms of different emissivity, or in terms of different contamination of the measurement from clouds.

It is important to note that the 3.7 μm window behaves very differently in daylight and at night. In daylight, it is strongly contaminated by reflected solar radiation, which needs to be subtracted before using the channel for quantitative thermal emission estimates. As previously noted, the 3.7 μm window is much more sensitive to high temperatures than the 11 μm window. However, the 3.7 μm window is of little use for low temperatures, such as those found in cloud tops in the upper troposphere. The differential response to the temperatures of the 3.7 and 11 μm windows can also be used for detecting fog at night.

As regards clouds, equation 2.14 is still approximately valid. However, with the exception of very thick clouds (such as cumulus or nimbus-stratus), emissivity is substantially lower than unity. Equivalent black-body temperature substantially underestimates true temperature, and a correction must be applied to account for low emissivity. The usual method is to couple the window channel with a channel that is strongly sensitive to water vapour. The difference between the two T_{BB} values indicates the cloud emissivity: the larger the difference, the lower the emissivity.

The penetration of infrared radiation in clouds is very low. Measured temperature refers to the top surface, and information about the interior of clouds is poor, especially for dense clouds. However, the temperature of cloud tops that is in equilibrium with air temperature at the same level is very important, because it indicates the altitude of the cloud in the troposphere, and therefore the cloud type.

Information derived from black-body temperature about the cloud-top level is often inaccurate. With thin clouds, such as thin cirrus, the background surface is much warmer than the air at
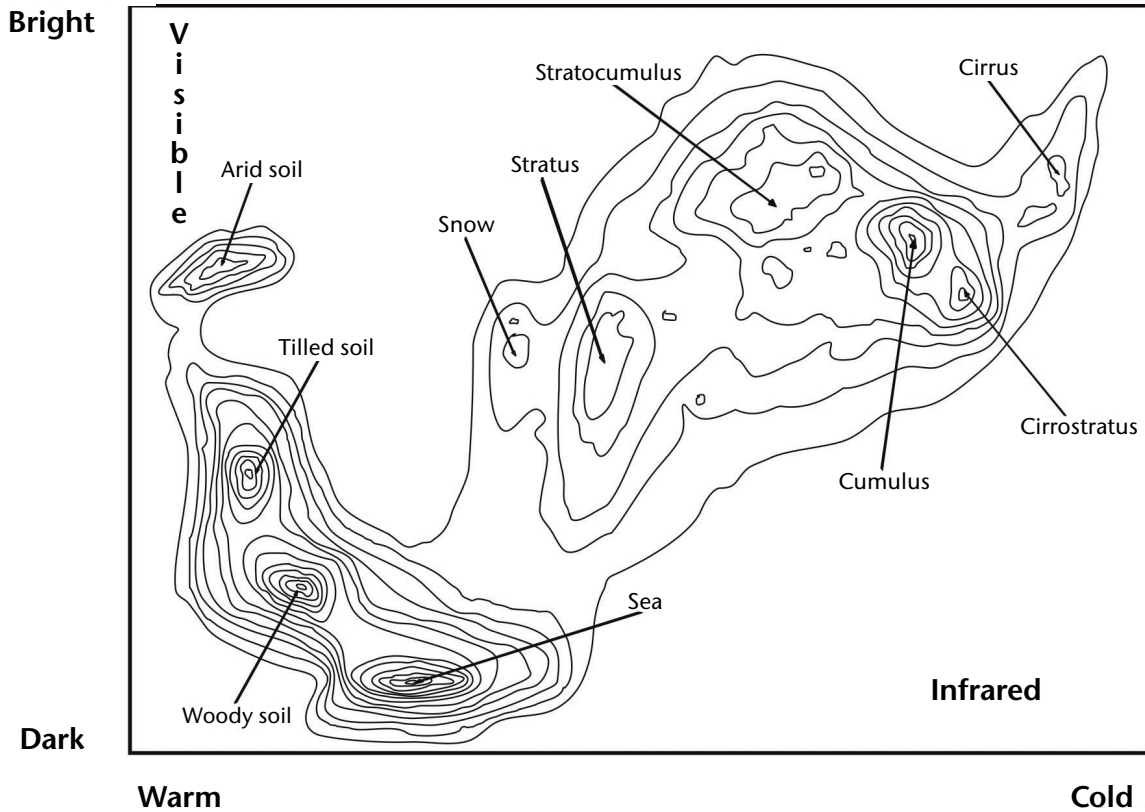
Figure 2.16. Scatterplot of VIS (0.65 μm) versus IR (11.5 μm), enabling the classification of 10 bodies. If projected onto one of either two axes, several clusters would be unresolved.

Source: Bizzarri, B. and C. Tomassini, 1976: Retrieval of information from high-resolution images. *Proceedings of the Symposium on Meteorological Observation from Space*, Committee on Space Research, Philadelphia, 140–144.

cloud level. As a result, surface radiation transmitted through the cloud adds to the cloud emission, the cloud appears warmer, and the assigned level is underestimated. Conversely, thick cirrus with high emissivity are observed as very cold, and may be confused with cumulonimbus.

In order to resolve such ambiguities, it is useful to plot VIS brightness and IR temperatures as bi-dimensional histograms (Figure 2.16). By using only one band (the projection of the 2D pattern on one axis), several clusters would be unresolved. By contrast, this example shows that 10 different objects can be identified through multi-band analysis. This is a simple example using an old instrument (a very high resolution radiometer (VHRR)) and only two channels in VIS and IR. Current multi-band analysis techniques can operate with many more channels.

2.2.3.4   *Measurements in the microwave range*

In the MW range, solar radiation is virtually zero, but there is a diffuse source of incoming radiation: the sky. Transmitted radiance is zero with regard to the Earth's surface, including land and sea. There are only two contributions: thermal emission and reflected radiation. Those are controlled by emissivity and reflectivity coefficients which, since $\tau = 0$, are linked by the condition $\varepsilon + \rho = 1$ (i.e. $\rho = 1 - \varepsilon$). By expressing radiative power in units of temperature according to the Rayleigh-Jeans equation (2.10), observed brightness temperature, T_B, can be rendered:

$$T_B(v) = \varepsilon(v) \cdot T + \left[1 - \varepsilon(v)\right] \cdot T_{\text{sky}}(v) \tag{2.16}$$

$T_{\text{sky}}(v)$, sky brightness temperature, is composed of background cosmic radiation and the contribution of precipitating clouds; it changes with frequency. In the main window and under non-precipitating conditions, where $v \sim 40$ GHz, $T_{\text{sky}}(v)$ may be ~140 K. Under heavy precipitation conditions, T_{sky} may reach values as large as ~250 K.

The impact of $T_{sky}(\nu)$ strongly depends on the value of the emissivity, ε. Sea and land have substantially different ε values.

The emissivity of the sea in the MW range is very low: $\varepsilon \approx 0.5$. As a result, the two components in equation 2.16 have equal weight. In the absence of precipitating clouds, T_{sky} is low and known: the measurement can therefore be associated with sea-surface temperature. The optimal frequency for sea-surface temperature is about 5 GHz (see Figure 2.17) where T_{sky} is much smaller than that at 40 GHz. The measurement is rather accurate and is also applicable in all weather, since the wavelength ($\lambda = 6$ cm) is much longer than any rain droplet. The 5 GHz sea-surface signal intensity is representative of the temperature of a few millimetres of the deep-water layer (sub-skin); that should be compared to a few tens of micrometres in the case of IR (skin temperature). At higher frequencies, T_{sky} strongly increases, especially in the presence of heavy precipitation. The high reflectivity value $(1 - \varepsilon)$ is such that the observation is mainly an indicator of precipitation.

Over land, emissivity is close to unity. The second component in equation 2.16 is therefore ineffective, and precipitation is poorly detected. At higher frequencies (~90 GHz ($\lambda = 3$ mm)), radiation welling up from the surface is scattered by large droplets, and even more so by ice crystals in clouds. As a result, radiation reaching the satellite is decreased.

Polarization can also be used for measuring precipitation. Radiation reflected from the sea is strongly polarized: when crossing a precipitating cloud, it undergoes depolarization that can be measured to infer precipitation. The differential polarization can also be exploited over land, since the emerging radiation scattered from droplets and ice crystals is polarized.

Observation under several polarizations may also be useful, regardless of the objective of precipitation measurement. Differential polarization is sensitive to surface roughness – an effect which must be taken into account when measuring sea-surface temperature. This can also be used to infer wind speed over the sea, as indicated in Figure 2.17.

Figure 2.17 also indicates that MW radiation is sensitive to ocean salinity, but only at very low frequencies, typically about 1.4 GHz (L band). The figure also shows that in order to measure ocean salinity, it is necessary to account for sea-surface temperature and wind speed (or roughness). Similarly to salinity, there is a water vapour absorption band that contaminates the observation of temperature, wind and liquid cloud (precipitation). That band can also be used to infer total column water vapour (precipitable water) over the sea. In summary, different variables may have different signatures on various channels in the MW as well as the optical fields: multi-channel analysis is therefore needed.
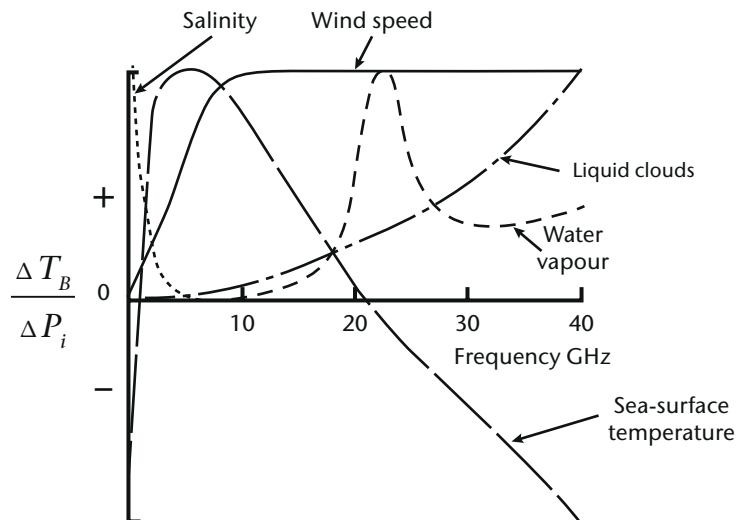
Figure 2.17. Sensitivity (defined as $\Delta T_B/\Delta P_i$) of MW frequencies to several geophysical variables (P).

Due to the totally different emissivity values of sea and land surfaces, the most obvious feature in a MW image is the land/sea boundary. Since the emissivity of ice is close to unity, sea ice is also an obvious observable in all weather conditions. MW images are particularly useful for geographical regions that are often overcast. In cases where emissivity is close to unity over land, a decrease in emissivity indicates the presence of water on the surface. This is because the emissivity of a body is controlled by its dielectric constant: water on land is a salt solution, which increases conductivity and thus decreases emissivity. This effect can be exploited to measure surface soil moisture and snow properties.

Soil moisture measurements can be rather accurate on bare soil, but can decrease in accuracy as vegetation increases. In order to penetrate vegetation, and to measure soil moisture at root level, very low frequencies must be used, either in L or P band. At higher frequencies (above 10 GHz), sensitivity to soil moisture is only significant if disturbance by vegetation is accounted for.

Two properties of snow are detectable in the MW range: surface melting conditions and, in the case of shallow snowpack, water equivalent. In the latter case, relatively high frequencies are preferred, as snow tends to be transparent at low frequencies. However, saturation can occur at very high frequency signals in the upper layers of the snowpack. Several frequencies with different penetration depths are therefore needed.

2.2.4 Observations in absorption bands

2.2.4.1 *The radiative transfer equation*

In an atmospheric absorption band, each layer of thickness dz absorbs radiation coming from below and re-emits it. Assuming zero reflectivity of the atmosphere in IR, the atmospheric transmittance from a height z to a satellite altitude H is given by:

$$\tau(\lambda, z) = e^{-\int_z^H \varepsilon(\lambda, z) \cdot N(z) \cdot dz} \tag{2.17}$$

where $N(z)$ is the concentration of the absorbing gas.

The radiative contribution of an atmospheric layer of thickness dz, at height z and associated with a transmittance change of $d\tau$ (I,z), is: $dI(\lambda, z) = B[\lambda, T(z)] \cdot d\tau(\lambda, z)$.

The radiation from the total atmospheric column to the satellite is:

$$I(\lambda) \;=\; \int_{\tau(\lambda, z_s)}^{1} B[\lambda, T(z)] \cdot d\tau(\lambda, z) \tag{2.18}$$

where z_s is the height of the Earth's surface.

A terrestrial contribution should be added, attenuated by the total atmospheric transmittance. In addition, the weighting function can be defined as:

$$K(\lambda, z) \;=\; \frac{d\tau(\lambda, z)}{dz} \tag{2.19}$$

The combined radiation reaching the satellite is given by the radiative transfer equation:

$$I(\lambda) = B(\lambda, T_s) \cdot \tau(\lambda, z_s) \;+\; \int_{z_s}^{H} B[\lambda, T(z)] \cdot K(\lambda, z) \cdot dz \tag{2.20}$$

Figure 2.18 shows that the transmittance (equation 2.17) tends to 1 as height z increases (i.e. as the thickness of the atmospheric layer between height z and satellite altitude H decreases). This is accompanied by a decrease in emissivity ε and a decrease in concentration N of the absorbing gas. The weighting functions have peak values that correspond to the inflection point of the transmittance function. A simple way to read equation 2.20 is that each atmospheric layer of thickness dz contributes to the radiation reaching the satellite according both to its temperature (through the Planck function), and also to its effectiveness to contribute, as quantified by the weighting function. The weighting function depends on the concentration of the absorbing gas and the strength of absorption/emission (ε). The shape is such that low atmospheric layers are
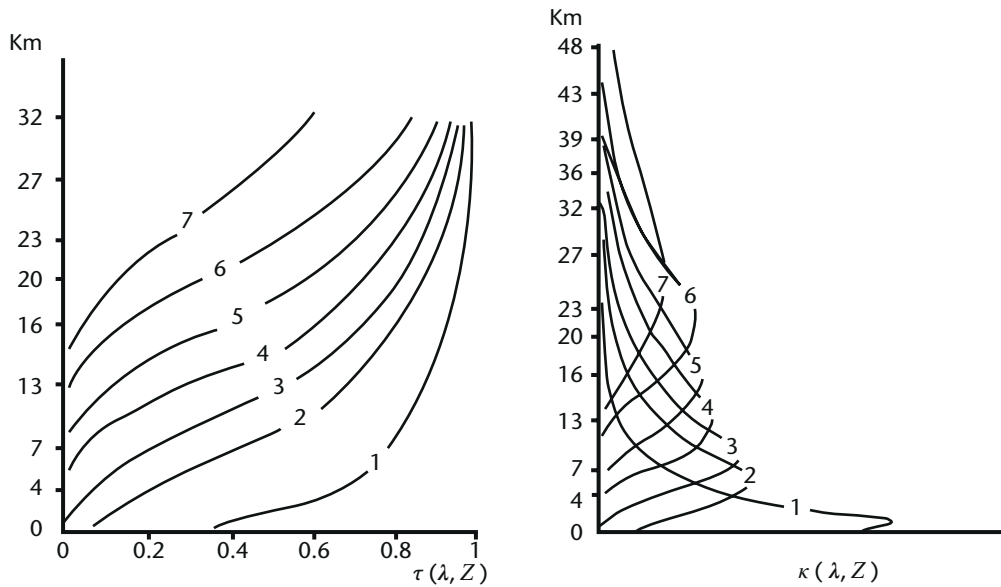
**Figure 2.18. Transmissivity (left) and corresponding weighting
functions (right) for seven channels in the CO_2 14 μm band**

penalized because of absorption by the upper layers, and high layers are penalized because of their low concentration of the absorbing gas. The atmospheric layer that exhibits the greatest change in transmittance is usually the layer that contributes the most.

2.2.4.2   *Profile retrieval*

The inversion of equation 2.20 is not a trivial matter. It is a Fredholm equation of the second kind, for which the existence or the uniqueness of the solution are not mathematically guaranteed. In the present case, the existence is granted by nature. To ensure uniqueness of the solution it is necessary to add constraints to it, since the problem is ill-conditioned. Many methods have been developed since profile sounding from space began. Some are statistical and linear, others are physical and non-linear, while others are a combination of both.

The primary objective is to invert equation 2.20 in order to retrieve an atmospheric temperature profile. This is only possible if the transmittance function is known in advance, which implies working in the absorption bands of a gas that has a known and stable concentration profile. In the IR range, CO_2 has such a profile in the bands around 4.3 and 15 μm (see Figure 2.12). As previously noted, the 4.3 μm band is more sensitive to high temperature, and is thus representative of the lower troposphere. However, that band may be contaminated by radiation from other species, and in daytime, the tail of the solar black-body curve (> 4 μm) cannot be disregarded. The 15 μm band is spectrally more pure, but is somewhat contaminated by the water vapour continuum. The transmittances therefore need to be corrected, either a priori by using external information, or a posteriori, by iterating after the water vapour profile has been retrieved.

The next step is to retrieve the water vapour profile. Once CO_2 absorption band channels have been used to retrieve the temperature profile, H_2O absorption band channels are used. The main band is centred around 6.3 μm, and responds well to high temperature (in the low- to mid- troposphere). For climate monitoring, it is important to measure water vapour in the upper troposphere. But that requires using an 18 μm band, which is technologically difficult to construct due to a lack of efficient detectors in the FIR range.

It is not easy to retrieve a water vapour profile or, more generally, to retrieve the concentration profile of an absorbing gas. The weighting functions of the absorbing gas peak at varying altitudes in the atmosphere, depending on concentration and remote-sensing frequency.

In addition, retrieval is intrinsically inaccurate because the transmittance function to be inverted (equation 2.17) defines the content of a thin layer at altitude z as the difference between the respective content of two very thick layers: H to z and H to $(z - \Delta z)$. In other words, a small number is derived by calculating the difference between two large numbers.

Further difficulties arise where clouds are present. If the instantaneous field of view (IFOV) is entirely filled by a cloud with uniform features, a profile may still be retrieved by the same method, although it will only cover the atmosphere above the cloud. If only a fraction η of the IFOV is filled by a cloud of emissivity ε_{cloud}, the transfer equation becomes:

$$I(\lambda) = (1 - \varepsilon_{cloud} \cdot \eta)\, I_{clear}(\lambda) + \varepsilon_{cloud} \cdot \eta \cdot I_{cloud}(\lambda) \tag{2.21}$$

where $\varepsilon_{cloud} \cdot \eta$ is the effective cover.

Several methods deal with the effects of clouds. One starts the retrieval process by using the channels with weighting functions that peak above the cloud-top level to achieve a first-guess profile. The first guess is then iterated by changing effective cover values, until the measurements in all other channels fit best. Another method compares a number of nearby IFOVs on the assumption that the signals differ only because of the different fractional covers η, and then extrapolates to zero η.

In any event, it is acknowledged that, when cloud cover in the IFOV exceeds approximately 20%, no attempt should be made to retrieve profiles in IR. The IFOV of sounding instruments used to be several tens of kilometres. Fortunately, that has now been reduced to the order of 10 km, so that the probability of finding a substantial number of cloud-free IFOVs in a given area is much higher.

The problem of clouds is greatly alleviated in the MW range, where sounding is possible for all weather conditions except heavy rain. The species of well-known and constant concentration used for temperature profile retrieval is O_2, with absorption bands in the 50–70 GHz range and at about 118 GHz (not yet used from a satellite). For water vapour, the 183 GHz band can be used effectively. The 22 GHz band provides a weak signal that can provide total column-integrated amount over the sea. There are other absorption bands for temperature and water vapour at higher frequencies, but the radiative effect of the water vapour continuum makes it impossible to observe the troposphere using those spectral bands.

The transfer equation in the MW range is essentially a simpler version of the IR equation (2.20): instead of the Planck function (equation 2.7), it is possible to use the Rayleigh-Jeans approximation with linear temperature dependence (equation 2.10).

The question may arise as to why the MW band is not exclusively used for temperature and humidity sounding, as it performs in nearly all weather conditions. This is because vertical resolution requires a high sensitivity to temperature variations (with height). Vertical resolution is best in the 4.3 μm band, where the Planck function varies roughly in relation to T^{12}. In the 15 μm band, there is less sensitivity because the Planck function varies in relation to T^5. In the MW range, since B is a linear function of T (see equation 2.10), sensitivity $(\partial B/\partial T)/B$ varies in relation to T^{-1} (it decreases as temperature increases). One interesting feature of the various bands is that, whereas the 4.3 μm band is well suited to the lower troposphere, and the 15 μm band is well suited to the middle and high troposphere, the MW band at 57 GHz is better suited to the stratosphere.

Vertical resolution is crucial to temperature and humidity sounding. Figure 2.18 shows an example in which the weighting functions are rather broad. That implies that the degrees of freedom (the number of independent pieces of information) are limited. Weighting functions become narrower when the spectral resolution of the instrument improves. Figure 2.18 relates to a radiometer with only seven channels and a low resolving power ($\lambda/\Delta\lambda \approx 100$); its vertical resolution is ~1.5–2 km in the mid-troposphere. Current sounding instruments (spectrometers) have thousands of channels and a higher resolving power ($\lambda/\Delta\lambda \approx 1\,000$); their vertical resolution is less than 1 km in the mid-troposphere. Further increasing the resolving power to $\lambda/\Delta\lambda \approx 10\,000$ would not improve the vertical resolution of temperature and humidity profiles, but would enable single lines of trace gases to be observed for atmospheric chemistry purposes.

Current instruments for the MW range have already reached maximum vertical resolution performance: it cannot improve beyond ~1.5 km in the mid-troposphere, and will be worse in the lower troposphere because of strong contamination from the ground.

In the short-wave range (UV, VIS, NIR, SWIR) absorption band measurements are mostly used for atmospheric chemistry through spectroscopic methods. The radiative transfer equation is more complicated than equation 2.20. Instead of thermal radiation as described by Planck's law, the more complex process of scattering is used. Retrieving geophysical variables relies on modelling rather than explicit equations. As well as being used in atmospheric chemistry, the analysis of absorption bands is used for other purposes (see the spectrum in Figure 2.11), such as deriving:

(a)   Atmospheric pressure at the Earth's surface: this is derived from estimates of the total column of oxygen in the band around 0.77 μm compared with nearby windows. It is one of the very few approaches available to measure surface pressure from space. Accuracy is limited by the scattering effect of aerosols, implying that the measurement also provides information on aerosols.

(b)   Cloud-top height: this is derived from a deficit that arises when the total column of oxygen is measured; the deficit itself is the result of cloud masking the lower part of the column. In principle, this is more accurate than calculating the cloud-top height from the equivalent black-body temperature in IR, correcting for cloud emissivity, and transforming temperature into height using a temperature profile.

(c)   Lightning: a very narrow bandwidth channel at 0.774 μm is used. Strong absorption from oxygen obscures the Earth's surface and enables flashes to be detected even in daylight. The intensity and number of flashes in a given period over a given area are representative of convection, and so serve as a proxy for precipitation. In addition, lightning activity causes NO_x to be generated in the atmosphere, and reflects the Earth's electric field.

(d)   Total column water vapour: the signal in one or more of the water vapour bands (about 0.94 or 1.37 μm) is compared with a signal from nearby windows. This can be more accurate than using IR or MW profiling.

2.2.4.3   *Limb sounding*

Figure 2.18 shows how weighting functions become broader as height increases. This indicates that the vertical resolution of temperature and humidity profiles using passive IR or MW radiometry degrades with increasing altitude. The resolution obtained from using spectrometers is currently considered adequate (~1 km) in the mid-troposphere; but it becomes marginal (~2 km) at tropopause level, where much better resolution is required. In the stratosphere, the vertical resolution degrades further and rapidly becomes unusable. Two techniques offer help: limb sounding (including through occultation of the Sun, moon or stars) and radio occultation.

In cross-nadir sensing mode, vertical resolution is determined by the sharpness of the weighting functions, which is in turn controlled by spectral resolution. In limb mode, vertical resolution is determined by mechanical scanning, i.e. by the instrument IFOV across the atmosphere when viewed transversally in the Earth's limb region (Figure 2.19). Vertical resolution depends on the step change rate, which is tuned to the instrument viewing aperture and to the intensity of available radiation. It is generally set to between one and three kilometres. Horizontal resolution is relatively inaccurate, since the measurement is integrated over a large optical path, as shown in Figure 2.19. The total optical path may be thousands of kilometres long, but the effective path, once weighted by atmospheric density, extends to some 300–500 km around the tangent point.

The sources of radiation are solar radiation reflected from the atmosphere, or atmospheric thermal radiation in the IR or MW ranges. In general, limb observations address not only temperature and humidity profiles, but also trace gases for atmospheric chemistry purposes.

In the short-wave range (UV, VIS, NIR, SWIR), the atmosphere can be scanned by directly pointing to the Sun while the Sun is setting or rising (occultation). Observation is conducted
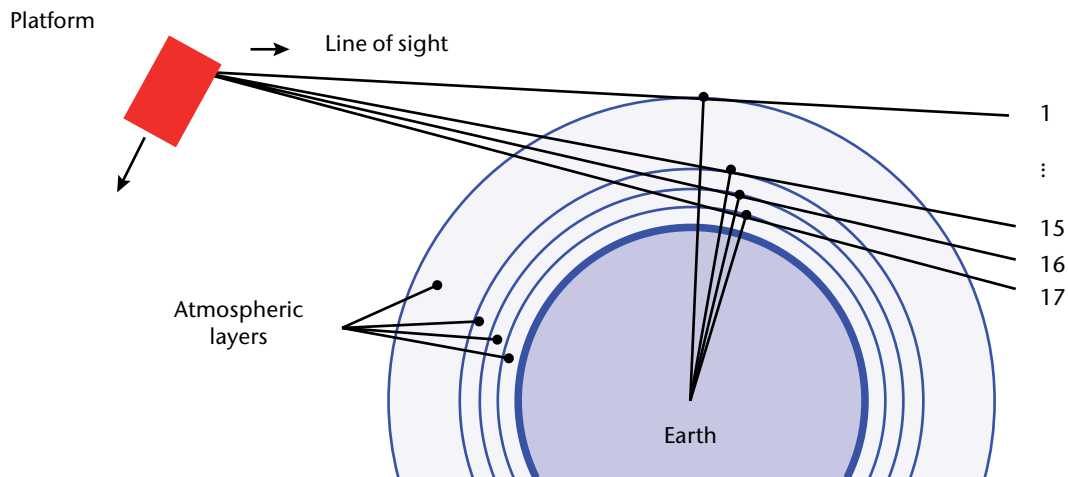
Figure 2.19. Geometry of limb scanning

by measuring the damping of spectral lines in the solar spectrum. Sun occultation has the great advantage of avoiding any mechanical movement of the instrument telescope, and any calibration. That is because the spectra measured during occultation are compared to the solar spectrum measured shortly before (or after) occultation under the same conditions. One disadvantage is that, at least for polar-orbiting satellites, coverage is limited to high latitudes, where a satellite can observe sunrise or sunset as it enters or leaves the night arc of its orbit. More extended coverage is possible by using moon occultation, while all latitudes can be covered through occultation of the stars. However, less radiation is available in those cases.

2.2.5 **Active sensing**

The sensing methods described above assume that the sources for remote-sensing are reflected solar radiation and the Earth's emitted thermal radiation (plus other minor sources, such as background sky radiation in MW and the moon or stars in occultation). These natural sources enable passive sensing, for which observation wavelengths are largely determined by natural targets. In active sensing, the source is artificial and the sensing wavelength is not entirely driven by the physical properties of the target. Instead, the wavelength can be chosen, while also taking account of signal generation and propagation constraints. The following active sensing principles are considered:

(a)   Radio occultation (for high vertical resolution profiles of temperature and humidity);

(b)   Radar (for altimetry, scatterometry, cloud and precipitation, and imagery);

(c)   Lidar (for clouds and aerosols, air motion, altimetry, and atmospheric chemistry).

2.2.5.1 *Radio occultation*

Radio occultation is one of a number of limb-sounding techniques. It has a totally different approach compared to passive radiometric techniques. An artificial source (in this case, the signal from a navigation satellite: GPS, GLONASS, Galileo or Compass) is tracked by a receiver on a satellite in LEO (Figure 2.20).

The change of propagation direction due to refraction by the crossed atmosphere (bending angle α) is converted into a phase shift. The shift is accurately measured and then converted into a refractivity profile during the occultation process, which lasts approximately 90 s.

a = an impact parameter
r = distance from centre of curvature to tangent point
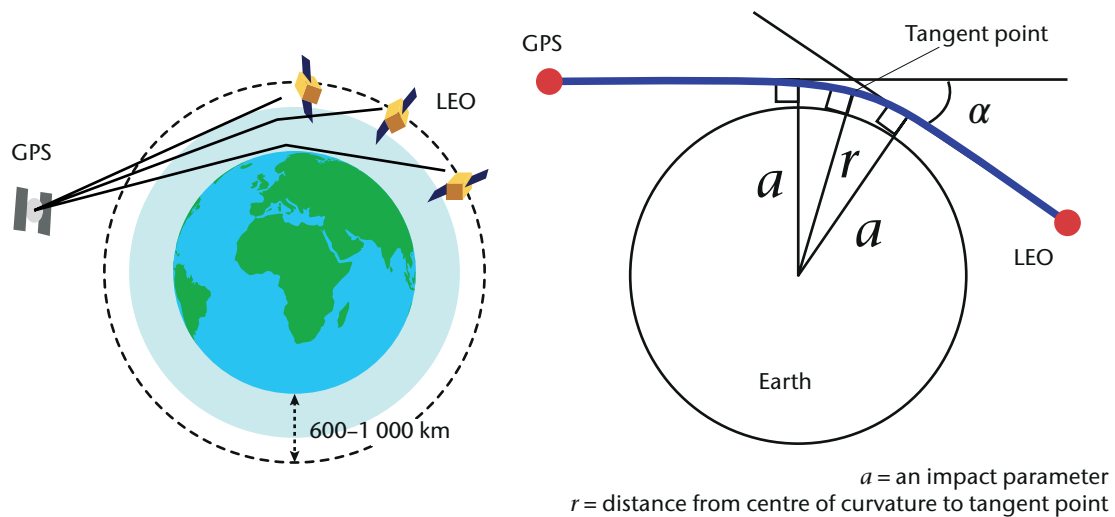
Figure 2.20. Principle of radio-occultation sounding. During the setting or rising of the GPS satellite over the horizon of the LEO satellite, the refraction induced by the crossed atmosphere changes the direction of propagation by a bending angle α.

The refractivity is linked to the atmospheric variables as follows:

$$N = (n-1) \cdot 10^6 = 77.6 \cdot p/T + 3.75 \cdot 10^5 \cdot p_w/T^2 \tag{2.22}$$

where N is refractivity, n is refractive index, p is dry-air pressure, p_w is water vapour partial pressure, and T is temperature. The coefficients for p and p_w are given in hPa, and in kelvin for T.

The phase shift is ultimately a time measurement, one of the most accurate measurements in physics. The other measurement is the distance between satellites. Since time and distance are fundamental metric quantities, radio occultation provides absolute measurements (not requiring calibration): this is a very attractive feature in terms of climate monitoring. In fact, long-term observations of radio occultation are considered a benchmark among methods of detecting climate change.

Radio occultation data are difficult to process for two reasons: first, the position of the tangent point (see Figure 2.20, right hand panel) moves during the profile measurements; and second, pressure, temperature and humidity are not measured independently. Therefore, 4D assimilation into a numerical weather prediction model is needed. It is less complex to retrieve temperatures from the upper troposphere and stratosphere, since water vapour content is very low. Temperature retrieval is similarly straightforward in the lower troposphere, where water vapour is responsible for most variance.

The vertical resolution of radio occultation profiles in the upper troposphere and stratosphere, (approximately 0.5–1.0 km) cannot be matched by cross-nadir viewing IR or MW measurements (1.5–2 km). In addition, the frequencies used (L band: see Table 2.9) are insensitive to clouds, even if precipitating. As a result, although essentially performed in limb mode, the measurement can be extended down to the Earth's surface, in order to observe, for example, atmospheric discontinuities such as the top of the planetary boundary layer. Furthermore, radio occultation is one of the few methods that can infer surface pressure: this is done by correlating the height of the tropopause and the air pressure at ground level.

In order to account for the signal rotation induced by the ionosphere, transmissions from navigation satellites exploit at least two nearby frequencies. As by-products of the correction process, information relevant to space weather is obtained, such as total electron content and electron density profile.

2.2.5.2 *Radar*

Radars (radio detection and ranging) transmit pulsed signals to the object to be observed, and collect the backscattered signal. In essence, radars measure distance (or range) and the backscattered power resulting from the radar reflectivity or radar cross-section of the body.

The radar equation may be written in different forms. The easiest to understand is:

$$P_s = \frac{P_t \cdot G}{4\pi \cdot r^2} \cdot \sigma \cdot \frac{1}{4\pi \cdot r^2} \cdot A_{\text{eff}} \tag{2.23}$$

where P_s is the power backscattered to the antenna, P_t is the power transmitted by the antenna, G is the antenna gain, A_{eff} is the effective area of the radar receiving antenna, r is the distance, and σ is the radar cross-section. Therefore:

$P_t G/4\pi r^2$ is the power hitting the target at distance r;
$P_t G/4\pi r^2 \cdot \sigma$ is the power reflected by the target;
$P_t G/4\pi r^2 \cdot \sigma/4\pi r^2$ is the fraction of (isotropically) reflected power reaching back the antenna.

The antenna gain may be expressed as $G = 4\pi \cdot A_{\text{eff}}/\lambda^2$ (a relation that derives directly from the diffraction law). Expressing the effective area of the radar's receiving antenna A_{eff} from this alternative expression and inserting it into equation 2.23 yields:

$$P_s = \frac{P_t \cdot G^2 \cdot \lambda^2}{64\pi^3 \cdot r^4} \cdot \sigma \tag{2.24}$$

Different types of radar favour the measurement of either range accuracy (altimeters) or reflectivity/cross-section accuracy (scatterometers). Radar for clouds and precipitation focus on both range (for vertical profiling) and reflectivity. One feature that can be emphasized is image resolution by synthetic aperture radar.

Radar altimetry

The main purpose of altimetry is to measure the sea level and to map it so as to determine ocean dynamic topography. The radar characteristics are optimized to enhance range measurement as much as possible. Sea level is measured in terms of the time taken for a radar pulse to reach the sea surface and return to the satellite. Because sea level is computed as distance from the satellite, the satellite needs to be located with extreme accuracy. One or more of the following systems is used to ensure precise orbits:

(a) Laser tracking of the satellite by ground stations and laser-reflecting mirrors on the satellite;

(b) Radio positioning based on networks of ground transmitting-receiving stations and a transponder on the satellite;

(c) A GPS receiver aboard the satellite.

One drawback of radar altimetry is that viewing must be limited to nadir-only; otherwise echoes from surrounding areas interfere with time analysis. As a result, the observing cycle is very long. Corrections to the signal are requested to account for: ionospheric rotation (the two frequencies used are: ~13.6 GHz (main) and ~5.3 GHz (support)); and water vapour (a co-aligned MW radiometer is used at ~23 GHz (main) and ~35 GHz and/or ~19 GHz (support)).

In addition to measuring the range, an altimeter also records and analyses fluctuations and measures the intensity of the echo. The observations provided are:

(a) Significant wave height: derived from analysis of the spread in time of the collected echoes;

(b) Sea level: derived from filtering wave-related fluctuations and considering the instantaneous satellite altitude with respect to the geoid;

(c)   Wind speed: derived from analysis of the fluctuation of the intensity of the echoes;

(d)   Improved knowledge of the geoid: derived from long-term statistics of observed sea levels;

(e)   Total electron content: derived as a by-product of the correction for ionospheric rotation.

Radar scatterometry

Unlike radar altimetry, where the focus is on range measurement, radar scatterometry optimizes the accuracy of the measured radar cross-section σ (see equation 2.24), which is often normalized and called σ^0 (sigma-naught). While the ranging subsystem may be absent from the instrument, calibration must be extremely accurate.

The radar cross-section is a function of the target's dielectric property, the viewing geometry and the incident radiation (wavelength, polarization). Scatterometers are mainly used to derive sea-surface wind. The target is capillary waves, which are closely associated with wind stress. Sigma-naught changes with wind speed, relative wind direction and sight line. By measuring σ^0 under several azimuth angles, both speed and direction can be determined.

The relationship between σ^0 and wind is complicated: the practical solution is empirical or semi-empirical. Furthermore, it is not a unique relationship in terms of direction: with two viewing angles, several ambiguities remain (fewer ambiguities remain with three angles). When σ^0 values are directly assimilated into a numerical weather prediction model that accounts for wave–atmosphere interaction, ambiguities are solved by the model.

The differences between wind measurements taken with scatterometers and those taken with passive MW radiometers can be summarized as follows: (i) passive MW generally provides information on wind speed only; information on direction can only be acquired if several radiometric channels are equipped with full polarization capability; (ii) information from scatterometry is generally better quality, especially for low wind speeds (less than ~3 m/s); however, for high speeds (more than ~20 m/s) passive MW may perform better.

Primarily designed for sea-surface wind, scatterometers provide several kinds of observation:

(a)   Sea-surface wind in all weather conditions (C band) or nearly all weather conditions (K_u band);

(b)   Air pressure over the sea surface (achieved by applying geostrophic relations to wind maps);

(c)   Soil moisture in scarcely vegetated areas (using C band, and occasionally K_u band);

(d)   Leaf area index or total biomass in dense vegetation (forest);

(e)   Ice type (age, roughness) at the polar caps;

(f)   Snow water equivalent (for which K_u band is preferred).

Cloud and precipitation radar

While the radar altimeter focuses on ranging and the radar scatterometer focuses on the radar cross-section, cloud and precipitation radar emphasizes both. Ranging is necessary to measure the vertical profile of cloud particles, while σ is required to infer the concentration and size of reflecting particles. However, the accuracy required for ranging in order to obtain a precipitation profile is of the order of 100 m, instead of 1 cm for altimetry.

For rain droplets, provided that their diameter D is less than $\lambda/10$ (i.e. in Rayleigh-scattering conditions), the radar cross-section is:

$$\sigma = \frac{\pi^5}{\lambda^4} \cdot K^2 \cdot D^6 \qquad \text{where } K \text{ is the dielectric constant} \qquad (2.25)$$

The total backscattered radiation received by the radar is the sum of all reflectors of all diameters in the IFOV. Assuming a Marshall-Palmer distribution ($N_0 \cdot e^{-\Lambda D}$) for the particle diameters, total reflectivity can be expressed as:

$$Z = \frac{\pi^5}{\lambda^4} \cdot \int_0^{D_{max}} K^2 \cdot N_0 \cdot e^{-\Lambda D} \cdot D^6 \cdot dD \qquad \text{(valid for } D \ll \lambda) \qquad (2.26)$$

Equations 2.25 and 2.26 are generally applicable to ground-based meteorological radar that use S band (~10 cm) or C band (~5 cm). They are to be compared with $D \sim 0.5$ cm, which is typical of precipitating clouds. Those frequencies are not used from space, as the corresponding IFOV on the ground that has a reasonably-sized antenna is too coarse. Due to frequency regulations, the frequencies that can be exploited by a spaceborne radar are ~14 GHz (~2 cm), ~35 GHz (~0.9 cm) and ~94 GHz (~0.3 cm). Therefore, equations 2.25 and 2.26 are not fully applicable, but must be corrected in a complex way to account for Mie scattering conditions.

Once the reflectivity Z is measured, there are several ways to convert Z into precipitation rate R. First, it is necessary to infer the precipitation rate at the surface. That cannot be directly measured from space, but must instead be derived from measured properties in the vertical column associated with the precipitation profile.

Cloud and precipitation radar is the only technique that can provide measurements of the cloud base, an important variable for aeronautical meteorology and for climate. The accuracy and reliability of the measurement depends on the radar frequency; the radar must also penetrate the full cloud thickness. From an operational viewpoint, cloud and precipitation radars have several disadvantages, particularly their limited swath, which prevents frequent observing cycles. And so, although passive MW imagery continues to be used as the basis for frequent precipitation observation, the accuracy of precipitation data from passive MW radiometry still needs to be improved. The continuing availability of at least one radar in space is necessary for "calibrating" the system of passive MW radiometers, along the lines of the concept for the Global Precipitation Measurement mission.

Synthetic aperture radar

In the MW range, spatial resolution is limited by diffraction. For a side-looking radar that views $\theta°$ off nadir, at orbital height H, with an antenna diameter L, and assuming a flat surface, the IFOV is:

$$\text{IFOV} = 1.24 \cdot \frac{H \cdot c}{\cos \theta \cdot L \cdot v} \qquad (2.27)$$

Table 2.10 shows the IFOV and L relationship for radar in several bands, assuming that $\theta = 23°$ and $H = 700$ km (parameters of the SAR on SeaSat, Figure 2.21). It illustrates that the requirements for IFOV = 1 km would be very difficult to meet, and requirements for IFOV = 100 m or below would be impossible with a real-aperture antenna concept.

Table 2.10. Examples of corresponding resolutions and antenna sizes for typical frequencies used in SAR

	L band (~1.3 GHz)	C band (~5.4 GHz)	X band (~9.6 GHz)
IFOV for $L = 1$ m	220 km	60 km	30 km
Required L for IFOV = 1 km	220 m	52 m	30 m
Required L for IFOV = 100 m	2 200 m	520 m	300 m
Required L for IFOV = 10 m	22 000 m	5 200 m	3 000 m
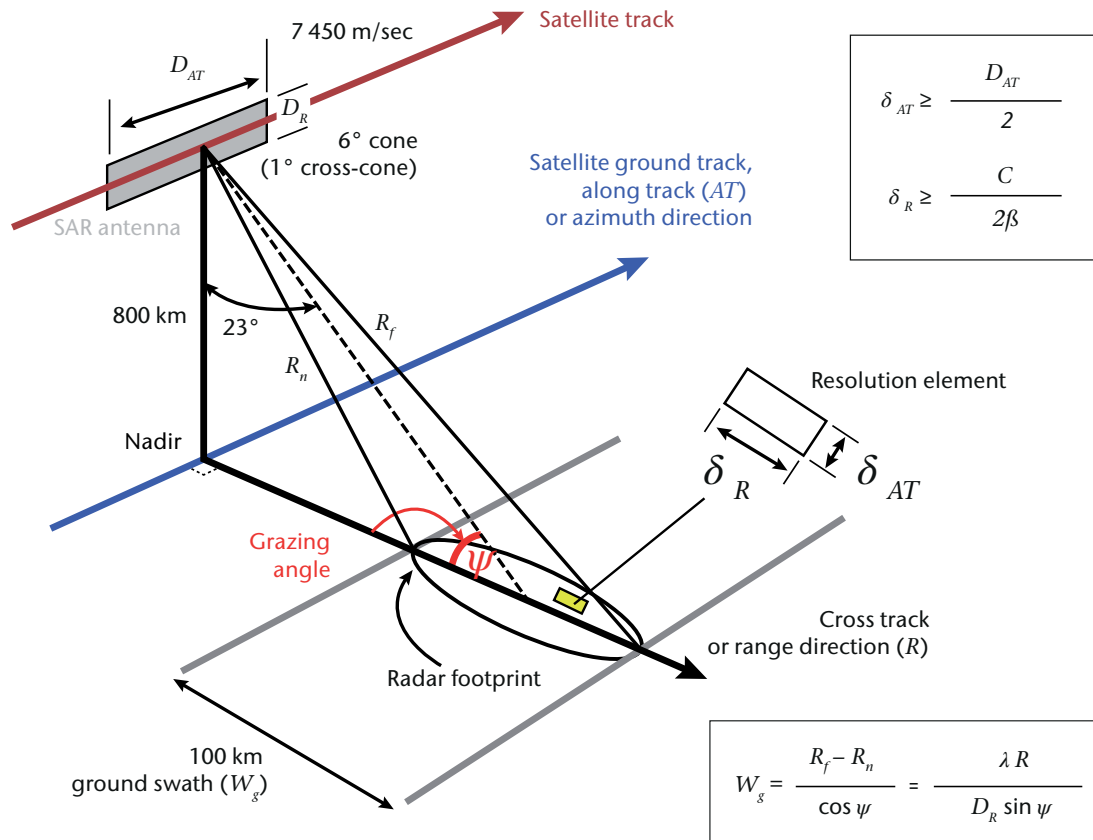
Figure 2.21. Principle of SAR

In the SAR concept (Figure 2.21) the antenna is elongated along the satellite motion. Its narrow dimensions determine the swath and are parallel to the sub-satellite track. The longer side determines the area where signals are to be analysed. The radar footprint corresponds to that of a real-aperture antenna, while the situation is varied for the resolution elements in the field (pixels). The pixels across the swath are at different distances from the satellite. The satellite can locate them due to its ability to distinguish small-range changes. The echoes from the pixels ahead of the sub-satellite cross-track line are affected by a positive Doppler shift (where a frequency is higher than the one transmitted); the echoes from the pixels behind that line undergo a negative Doppler shift. By capturing the moment of shift inversion, the pixels can be assigned to a location along the satellite track.

SAR may be used in different operating modes, depending on the trade-off between resolution and swath, and on the combination of transmitted and received polarizations. One operating mode is designed for wave spectra. A small part of the image (a vignette) is sampled at intervals. With Envisat, for example, the vignette is 5 km x 5 km at the best spatial resolution of 30 m, and sampled at 100 km intervals along the track. The echoes in the vignette are analysed to plot the power spectra, from which it is possible to determine the dominant wave direction, the dominant wave length/period and power associated with significant wave height.

The list of SAR applications is long, although not all bands are suitable for all applications:

(a)   Ocean circulation features (eddies) and waves (preferably L band);

(b)   Ocean pollution and oil spills (preferably C band);

(c)   Sea-ice cover and type (age) (any band);

(d)   Land-ice cover (glaciers) (any band);

(e)   Snow melting conditions and snow water equivalent (preferably X band);

(f)   Surface soil moisture (preferably L band, especially for the areas around plant roots);

(g)   Vegetation type (preferably C band) and total biomass (preferably P band);

(h)   Land use and urbanization (preferably C band);

(i)   Geological structure detection (preferably X band);

(j)   Disaster monitoring and damage inventories (preferably X band);

(k)   Ship traffic surveillance and military surveillance (preferably X band).

Other important applications are possible through interferometry because the phase control of the SAR signal is extremely accurate. Signals from different orbits of the same satellite or different satellites can be accurately co-registered in order to implement interferometry. This enables, for instance, land surface topography to be obtained for an improved digital elevation model, and iceberg heights to be measured.

By using interferometry between passes of the same satellite in an orbit with a repeat cycle, it is possible to measure changes such as iceberg drift, variations of glacier cover and lake extent, volcanic surface topography changes and bradyseisms, coastal erosion and urbanization.

2.2.5.3   *Lidar*

While the principle of lidar (light detection and ranging) is the same as that of radar, the electromagnetic range is different: MW is used for radar, while SW is used for lidar. Most lidars make use of wavelengths in the UV (e.g. 355 nm), VIS (e.g. 532 nm), NIR (e.g. 1 064 nm) or SWIR (e.g. 1 550 nm) ranges; longer wavelengths (e.g. 10.6 μm) may also be used. The source is a laser (light amplification by stimulated emission of radiation). It is extremely directional, but the large distance between the satellite and the Earth means that significant electric power is needed and that large telescopes are required to collect the backscattered signal. The use of lidar in space therefore presupposes considerable resources. Although in principle, lidar could be used to scan an area for imaging purposes, lidar systems in space have so far only been nadir-pointing or monodirectional. The following missions are lidar-based:

(a)   Backscatter lidar for aerosol and cloud-top height;

(b)   Doppler lidar for wind profile in clear air;

(c)   Lidar altimeter specifically for sea ice;

(d)   Differential absorption lidar (DIAL) for atmospheric chemistry.

Backscatter lidar

Backscatter lidar primarily deals with the observation of aerosols. This implies the use of wavelengths that are similar in size to very small aerosols (~1 μm). In order to capture more aerosol properties (size, phase, absorption/scattering ratio, and ultimately, type), more concepts have been developed. Some are based on the use of two wavelengths, while other are based on high spectral resolution laser in order to distinguish Mie and Rayleigh scattering components. In any case, a backscatter lidar is a very large instrument (the telescope may have ~1 m aperture). The footprint may be as small as a few tens of metres, but more decorrelated echoes are included

to increase signal-to-noise ratio. Such echoes will help to ensure that the final resolution is in the range of a few hundred metres. The vertical resolution determined by the lidar ranging system is set to a few hundred metres.

Designed primarily for aerosols (the most demanding mission), the backscatter lidar enables different kinds of observations to be made, including:

(a)   Aerosol profile and aerosol properties (size, phase, absorption/scattering ratio, type);

(b)   Cloud-top height (much more accurately than with passive NIR and IR techniques);

(c)   Optical thickness of thin clouds (cirrus) and cloud base of semi-transparent clouds;

(d)   Polar stratospheric clouds;

(e)   Atmospheric discontinuities such as tropopause and top of the planetary boundary layer, as revealed by the change of refractivity index.

Doppler lidar

Doppler lidar deals primarily with the observation of wind profiles, a key variable for weather forecasting.

The current operational technique available for observing wind profile consists of tracking the movement of clouds or water vapour patches in frequent images, either from geostationary satellites, or from polar orbiting satellites in polar areas with frequent satellite overpasses. This limits the opportunity to take measurements only at altitudes where tracers are present (generally one layer, sometimes two). Hyperspectral IR sounding in GEO is expected soon: when it becomes available, frequent water vapour profiles will be available, and water vapour patterns will be tracked at several heights. However, vertical resolution and accuracy are expected to be limited, and coverage will not include high latitudes.

Cloud-motion tracking is the only technique available for cloudy areas, while the Doppler lidar enables tracking to be conducted in clear air. The tracer consists of eddies of the turbulent atmosphere, of aerosols and of molecular scattering.

Exploitation of the Doppler shift due to the wind implies oblique viewing. The laser pulse repetition frequency is such that the corresponding IFOV may be less than 100 m. However, as with any radar or lidar, a number of decorrelated echoes need to be averaged to improve signal-to-noise ratio: the final resolution is an IFOV as large as several tens of kilometres. Because of the limited availability of electric power, the instrument has a limited duty cycle; for instance it may sample at 200 km intervals along a line parallel to the sub-satellite track. The vertical resolution of the wind data collected depends on the time sampling rate of the return echo. This is adjusted for a vertical resolution of about 1 km in the mid-troposphere, less than 1 km in the planetary boundary layer, and more than 1 km in the stratosphere. No technique based on cloud and water vapour tracking from GEO can compete with this performance. The anticipated accuracy of the wind horizontal component is less than 2 m/s.

A Doppler lidar is a very large instrument (the telescope may have a 1.5 m aperture). It requires a dedicated satellite in an orbit lower than that usually used for meteorological satellites.

For wind lidar, coverage is a major limitation. Since one instrument only covers a line parallel to the sub-satellite track, a constellation of satellites would be required to provide frequent coverage. As long as the sustainability of such a constellation cannot be achieved, the baseline system for wind profile will continue to be imagery and hyperspectral sounding from GEO, with Doppler lidar providing support for calibration of the overall system.

Another difficulty with wind lidar is that measurement can only be along-sight (1D). That means that, in order to retrieve the required 2D horizontal component, assimilation into a numerical weather prediction model is necessary.

The Doppler lidar is primarily designed for wind, which is the most demanding mission. It provides several kinds of observations, including wind profile in clear air or in the presence of thin cirrus, aerosol profile (from echo intensity) and cloud-top height.

Lidar altimeter

Radar altimeters can provide measurements as accurate as a few centimetres. However, at above 20 km, their horizontal resolution is quite coarse. By implementing SAR processing of the along-track signal, the resolution can be brought to ~300 m, which is still insufficient for accurately detecting boundaries. Another limitation of radar altimeters is their unsuitability for observing surfaces with high emissivity (and thus low reflectivity) in the MW range, such as land and ice.

Lidar does not have those limitations. The horizontal resolution can be a few tens of metres and the vertical resolution less than 10 cm. That fine resolution makes it possible to capture the border between sea water and polar ice and (after successive passes) to profile the height along-track in order to map ice thickness.

In order to operate over the sea, even though reflectance in the VNIR range is very low, a lidar altimeter must have a large telescope (aperture ~1 m). For improved cost-effectiveness, a sensor using a second wavelength is usually added to observe the atmosphere (for example, 1 064 nm is used for surface and 532 nm is used for atmosphere). In this case, a lidar altimeter operates as an ordinary backscatter lidar.

As with any other altimeter, the lidar altimeter requires extremely accurate orbit determination, since the basic ranging measurement provides the distance of the object from the satellite in orbit. Precise orbit determination is achieved by a GPS receiver, and laser ranging from a network of ground stations with an array of retroreflectors on the satellite.

Lidar altimeter applications include:

(a) Sea-ice thickness and polar cap topography;

(b) Sea level and ocean-dynamic topography;

(c) Contribution to improved knowledge of the geoid;

(d) Land-surface topography, including glaciers and lakes;

(e) Aerosol profile and aerosol properties;

(f) Cloud-top height, optical thickness of thin clouds and cloud base of semi-transparent clouds;

(g) Polar stratospheric clouds;

(h) Atmospheric discontinuities such as tropopause and top of the planetary boundary layer.

Differential absorption lidar

The principle of differential absorption is to perform complementary observations of a target species at an absorption peak and in a nearby atmospheric window. Using lidar for this purpose is the only way to achieve high vertical resolution profiles in the planetary boundary layer, where such resolution is most important. (The profile is also observed in higher layers, including the stratosphere).

The conditions for DIAL to be applicable are: that the species is relatively abundant; that the absorption line is strong and lies in a spectroscopically "clean" region; and that there is a nearby "clean" atmospheric window. Examples of possible applications are:

(a) CO_2 by exploiting lines at 1.57 μm in the 1.6–1.7 μm window or 2.05 μm in the 2.0–2.3 μm window;

(b) H_2O by exploiting lines at 935 nm, with windows on both sides;

(c) O_3 by exploiting lines and windows in the 305–320 nm region.

Missions exploiting DIAL are only at the stage of proposal or feasibility study. Since the spectral bandwidth (and thus the energy available for the observation) is very narrow and the reflector (a gas) is very weak, the instrument has to be very large and overall measurement is technologically challenging.

2.3   SPACE AND GROUND SEGMENTS

Earth observation from space implies a complex system composed of (i) a space segment to perform observations, and (ii) a ground segment to manage the space segment and process observation data.

2.3.1   Space segment

The space segment of a satellite system includes:

(a)   The platform (also referred to as the bus);

(b)   The instruments installed on board;

(c)   The communication tools to receive commands and convey the instrument output to the ground.

The size and/or mass of satellites for Earth observation can range over two orders of magnitude:

(a)   Nanosat: < 10 kg (actually unlikely to be used for operational Earth observation);

(b)   Microsat: 10–100 kg;

(c)   Minisat: 100–500 kg;

(d)   Smallsat: 500–1 000 kg;

(e)   Mediumsat: 1–2 tons;

(f)   Large facility: > 2 tons.

2.3.1.1   *Platform services*

The satellite platform hosts the instruments and provides several services:

(a)   Power supply for instruments, telecommunications, and all other satellite subsystems;

(b)   Navigation facilities for geographical referencing of observations;

(c)   Attitude control for correct pointing of instruments and stabilization;

(d)   Thermal control to keep the instruments within specified operating conditions;

(e)   Housekeeping devices to monitor and control the status of all satellite subsystems;

(f)   Propulsion for orbit keeping and, if needed, orbit change;

(g)   Processing capability to administrate the various platform subsystems;

(h)   Processing capability to handle instrument data and format data streams to be transmitted;

(i)   Storage device for on-board global data recording;

(j)   Communication facilities to receive commands from the ground;

(k)   Communication facilities to transmit observational and housekeeping data to the ground;

(l)   Other communication services, where the platform has a data relay function only.

2.3.1.2   *Navigation and positioning systems*

Navigation and positioning systems are necessary for geolocation of observed data, both during viewing, and afterwards for ground processing. The following systems are used:

(a)   Laser retroreflectors;

(b)   GNSS receivers;

(c)   Radio-positioning systems;

(d)   Star trackers.

Laser retroreflectors

These are mirrors which tend to be corner cubes. They reflect laser beams sent to the satellite by laser-equipped ground sites during positioning sessions. Laser retroreflectors are used on many satellites for a posteriori precise orbit determination. This is achieved by post-processing a number of measurements in night-time and clear sky only. The analysis involves a full network of coordinated ground stations. The results are sparse and only available after a certain delay. However, they are so accurate that they can be used for space geodesy applications.

Radio-positioning systems

These systems are specifically designed to support altimetry missions. They comprise radio links between the satellite on the one hand, and ground transmitting and/or receiving stations on the other. Positioning is performed in near real time and, with improved accuracy, after post-processing. Two examples of such systems are:

(a)   Doppler Orbitography and Radiopositioning Integrated by Satellite (DORIS), which measures the Doppler shift of signals from ground stations;

(b)   Precise Range and Range-rate Equipment (PRARE), which measures differential signals from a network of ground stations.

GNSS receivers

These systems make use of the phase difference of signals from several satellites in the GNSS. The GNSS includes the navigation satellite constellations of the United States of America (GPS), the Russian Federation (GLONASS), the European Union (Galileo), and China (Compass, known as Beidou in Chinese). A large number of satellites currently use GNSS receivers to support their navigation. Positioning is performed in real time.

Star trackers

These are charge-coupled device imagers that track bright stars, recognize their pattern, and send information to a satellite's attitude control system. Star trackers provide continuous monitoring of satellite attitude much more accurately than systems based on horizon-sensing. This is necessary for instruments that require accurate pointing information (such as limb sounders), both for active attitude control during flight and for subsequent instrument data processing. An increasing number of satellites are now being equipped with star trackers.

2.3.1.3   *Orientation and stabilization*

The orientation and stabilization systems are primary platform features that determine instrument pointing capability.

The side of the platform on which the sensors are placed should ideally be kept facing the Earth's surface, unless the satellite mission has a different purpose (such as monitoring the Sun). Since the platform tends to keep a steady orientation in relation to the stars during its orbital motion, a stabilization mechanism is required.

The stabilization mechanism known as spinning is most straightforward, as it is passive and inertial. The spin axis tends to have a constant orientation in relation to the stars, and therefore does not fulfil the Earth orientation requirement. For GEO satellites, if the spin axis is set parallel to the Earth's rotational axis, the Earth's surface is scanned for a small amount of time (about 5% of the satellite's orbiting time) during each satellite rotation. For low orbiters, the orientation of the spin axis may be set specifically to enable instruments to be pointed towards the Earth's surface for a fraction of time. In any event, spin stabilization is only suitable when an instrument's radiometric budget is sufficient to carry out the measurements for which the instrument was designed, in spite of the small fraction of useful observing time. In addition, spin stabilization can only be implemented for one instrument, or very few instruments, on one platform.

Three-axis stabilization is much more suitable for maintaining a constant orientation towards the Earth and also supports more instruments on one platform. This allows for active control of the satellite attitude with respect to rotations around: the axis perpendicular to the orbital plane (pitch), the axis tangent to instantaneous motion in orbit (roll), and the nadir direction (yaw).

Active control is critical, because it implies accurate attitude determination (by, for example, horizon detection, star trackers or GNSS receivers) and efficient actuators (such as micropropulsion devices, gyros, very fine-angle change detectors and efficient control electronics). A loss of active control is among the primary causes of mission failure. Active control may affect data quality because of limited accuracy, particularly in the case of high-resolution instruments and high orbits (GEO), and mechanical perturbation of instrument pointing associated with turning on the actuators.

In addition to the main orientation and stabilization systems (spinning and three-axis control), smart attitude control systems are also in use, especially with small satellites. For instance, the gravity-gradient system uses a long boom that tends to the nadir direction, and thus keeps one side of the platform pointing towards the Earth's surface.

2.3.1.4   *Housekeeping system*

A basic trade-off for satellite design lies between the capabilities that are implemented on board and those that can be achieved on the ground if sufficient information regarding on-board features is available. Hardware implementation on board may be expensive, prone to irrecoverable failure, and provide limited performance. Therefore, it is advisable to reserve hardware implementation to cases where it is absolutely indispensable and reasonably safe. Moreover, the housekeeping system provides all the ancillary information necessary to accurately process data on the ground.

The housekeeping system manages both the platform (deformations, temperature of radiant surfaces, attitude, status of power generators and all other subsystems) and the instruments (status and temperatures of the various parts, control signals for electronics, etc.). In general, instrument housekeeping is at least partially implemented inside the instrument itself.

The amount and completeness of housekeeping constitutes a discriminating factor for the class of a satellite. Operational satellites are equipped with plenty of housekeeping devices for subsystem monitoring and the possible activation of recovery manoeuvres, such as by switching to redundant units. Housekeeping information is also a basic element of accurate instrument calibration and data georeferencing.

Notwithstanding the importance of a good housekeeping system, there are limitations to the accuracy of what can be achieved by such software processing. The residual errors of software corrections or reconstructions may exceed what is allowed by the application. Therefore, certain corrections need to rely on on-board hardware.

2.3.1.5   *Data transmission*

The platform must transmit to the ground the observation results from the various instruments. Whatever the satellite height over the Earth's surface, radio transmission to the Earth will have to cross the ionosphere and plasmasphere, which block the propagation of electromagnetic waves with frequencies lower than the critical plasma frequency (~25 MHz). Direct visibility is needed between the transmitters and the receivers both on the satellite and the ground station.

The simplest method of collecting observed data from a satellite is by direct broadcast in real time. For a LEO satellite, a ground station will acquire all the data that a satellite transmits when passing within the acquisition range. The size of the acquisition range is the same as a satellite's FOV for zenith angle $\zeta = 90°$ (in principle), or $\zeta = 85°$ (with a reduced risk of interferences from ground sources or occlusion from orography). Table 2.1 shows that, for a satellite height of 800 km for instance, the acquisition range is a circle with a diameter of 5 000 km (for $\zeta = 85°$ or elevation = 5°).

Where the satellite velocity is in the region of 400 km/min and the satellite pass is centred over the acquisition station, the acquisition session lasts 15 min at most, and is reduced to a few minutes for peripheral passes.

This type of acquisition is the most convenient because it provides the observed data to the user in real time for immediate processing. However, only data observed and transmitted during the satellite pass inside the acquisition range can be acquired by the local receiving station. For GEO, direct broadcast can be continuously received by a station located within the FOV.

An alternative way for a LEO satellite to receive data is to store the observed data on board and transmit them on command, when the satellite overflies a central acquisition station. The central station, also used to send commands to the satellite, has the same acquisition range as any local station; if it is placed at a high latitude, it can collect data from many orbits. Table 2.4 shows that most Sun-synchronous orbits pass less than 10° from the pole, so that a central station placed at a latitude of, for instance, 80° will intercept all orbits and provide global data acquisition. The store-and-dump acquisition method has the advantage of enabling data recovery for the whole globe, but also has several drawbacks:

(a)   Access to data is slower, since the delay includes the time needed to: run the whole orbit (up to 100 min), receive at the central station (about 10 min), relay to the central processing facility (about 10 min) and redistribute to the users (about 10 min). The total delay in the availability of data is therefore 2–3 h.

(b)   The satellite has to transmit the data accumulated in one orbit (about 100 min) during the time it spends within the acquisition range of the central station (about 10 min). Therefore data rate and bandwidth need to be one order of magnitude higher than for direct read-out, which heavily impacts on the cost, size and complexity of the station. This acquisition mode is suitable for a satellite operator but generally not suitable for an individual user.

(c)   There are instruments with data rates so high that they cannot be fully stored on board: selection of data to be stored may be needed, either by reducing the resolution or by prior selection of frames (e.g. the local area coverage (LAC) mode of NOAA Polar-orbiting Operational Environmental Satellites (POES)).

If not acquired locally in real time, the data gathered in a central processing facility need to be retransmitted to the users, generally after preprocessing. In the case of GEO satellites, a transponder on the same satellite can be used for data retransmission to local user stations.

For LEO satellites, between the two extreme cases (direct read-out providing data over a limited area in real time, or store-and-dump of global data with 2–3 hours' delay), there are alternative or complementary data recovery schemes, which can use:

(a)   Several downlink stations spread over the globe, including, for instance, one near each polar region; this reduces the length of time that data need to be stored on board the spacecraft;

(b)   A network of direct read-out stations spread over the globe; each one acquires data on limited areas and retransmits them to data centres; this reduces the delay in the availability of data to a few tens of minutes, but does not necessarily achieve global coverage; or

(c)   A data relay satellite that receives data in real time from observing platforms and relays them to a central processing facility; this reduces the delay in the availability of data to a few minutes.

Data recovery timeliness is a critical issue for operational satellites; that is particularly the case for meteorology, because of the coexisting requirements for timeliness and global coverage. For research and development applications, the timeliness requirement is less stringent, and the store-and-dump method tends to be used in conjunction with an effective archiving and retrieving facility, which provides advanced data stewardship.

2.3.1.6   *Data relay services*

In addition to providing Earth observation data from a platform in orbit, satellites can support other services, and so act as a telecommunications relay. The most common forms of such relays are:

(a)   Data collection from in situ platforms located on the ground, on aircraft, on balloons, on buoys, on ships and even on migrating animals. The data collection platform (DCP) may transmit all the time, at fixed intervals, or upon interrogation from the satellite. Mobile platforms may be located from the satellite if in LEO. GEO satellites serve either DCPs within their line of sight (regional) or DCPs carried on mobile platforms (ships, aircraft, etc.) that migrate among the views of different GEO satellites (international).

(b)   Search and rescue distress signals are detected from small pieces of transmitting equipment carried by those in distress. The request for help is then relayed to one of the centres of a worldwide search and rescue network. Search and rescue missions are conducted

cooperatively by several operational meteorological satellites in LEO and GEO. The service from LEO is called the Search and Rescue Satellite-aided Tracking System (SARSAT), while the GEO-based service is known as Geostationary Search and Rescue (GEOSAR).

(c)   Relay of meteorological information from meteorological centres to end users as a broadcast, or to selected centres within view of a GEO satellite. The central facility of the system may perform the uplink or delegate it to auxiliary stations close to the information production centre that are equipped to uplink the satellite.

2.3.2   **Ground segment**

The ground segment of a satellite system includes:

(a)   The central station for satellite command and global data acquisition;

(b)   Peripheral stations for data acquisition;

(c)   Mission and operation control centres;

(d)   Data processing and archiving centres;

(e)   Data and product distribution systems.

2.3.2.1   *Central station for satellite command and global data acquisition*

This element of the ground segment may be generically termed the command and data acquisition station (CDA). Typical tasks of a CDA are:

(a)   To collect command sequences from the mission and operation control centre and uplink commands to the satellite (for payload configuration, satellite configuration, orbit control, etc.);

(b)   To acquire satellite telemetry data (for attitude and orbit determination, satellite and payload status, etc.) and immediately deliver it to the mission and operation control centre(s);

(c)   To acquire geophysical and ancillary data (housekeeping, calibration, etc.) and deliver it to the data processing and archiving centres;

(d)   To index the acquired data streams with accurate time and orbital elements.

It is possible to have only one CDA for geostationary satellites. For near-polar satellite systems, it is possible to avoid blind orbits by placing the CDA at a very high latitude (such as Svalbard at 78°N). In order to improve the timeliness of the availability of observed data, auxiliary stations may be used (such as an Antarctic station). For low-inclination orbits, a network of CDAs is necessary, with one acting as the main CDA.

CDAs use S-band frequencies (about 2 100 MHz) to command the satellite. S band is nearly insensitive to weather and less critical to pointing accuracy. For geophysical data acquisition, the L band is used (about 1 700 MHz) if the data rate is below 10 Mbps; otherwise either the X band is used (about 8 GHz) for data rates of up to some 100 Mbps; or the K_a band (about 26 GHz) is used for data rates of several hundreds of Mbps.

2.3.2.2   *Mission and operation control centres*

These elements may be generically termed the operation control centre (OCC). Their tasks are:

(a) To collect information on satellite, payload, and orbit status from the CDA and (in the case of the orbit only) from other ranging stations;

(b) To collect requirements for elements including payload configuration and measurement sequence planning from data processing and archiving centres, and from other users entitled to input requirements into the mission plan;

(c) To analyse the information on satellite, payload, and orbit status, and on payload or mission configuration requirements; to generate instrument performance monitoring reports; to elaborate the operations plan and deliver commands to the CDA for uplinking the satellite;

(d) To provide data processing and archiving centres with ancillary information, which is relevant for data processing and results from activities relating to operations, payload or mission control (including accurate orbit determination, satellite attitude behaviour and payload status).

Mission control centres are closely connected with users, application centres and scientific teams. OCCs are closely connected with CDAs and the units responsible for satellite development. OCCs also have full knowledge of satellite design features. The two centres are often co-located, although this is not compulsory, and should preferably be secured by a back-up centre.

2.3.2.3   *Data processing and archiving centres*

These elements are responsible for:

(a) Acquiring geophysical, calibration and selected auxiliary data from CDAs;

(b) Acquiring auxiliary data on orbit, satellite and payload from OCCs;

(c) Monitoring instrument calibration and performing inter-calibration as appropriate;

(d) Generating and controlling the quality of various products;

(e) Archiving all products;

(f) Distributing a selection of products;

(g) Analysing mission status, payload status and requirements for mission planning;

(h) Delivering requirements for payload and mission control to OCCs.

Core products are normally generated by the satellite operator at a central facility. External specialized centres may supplement those by processing other specific products.

Satellite data archiving requires the maintenance of high levels of hardware availability for data ingest and storage, as well as discovery and retrieval services, with provision for long-term data preservation over decades. Data must be associated with metadata that contain all the information necessary to use and evaluate the data. Comprehensive, standardized metadata, and standardized globally interoperable catalogue systems enable data discovery to be extended to a worldwide scale within the WMO Information System.

2.3.2.4   *Data and products distribution*

Depending on data volumes and timeliness requirements, several methods of accessing data and products are available:

(a)   Direct read-out from the satellite (when available; particularly prevalent among LEO satellites). This provides the best timeliness but presupposes the capability to receive raw data on an appropriate receiving station and to preprocess that data with an adequate software package.

(b)   Near-real-time satellite retransmission of data after on-ground preprocessing or full processing. For GEO satellites, retransmission may be performed through the same satellite. Currently, retransmission is best achieved via commercial telecommunications satellite channels, such as the GEONETCast system, which consists of three coordinated services: EUMETCast (of the European Organization for the Exploitation of Meteorological Satellites), CMACast (of the China Meteorological Administration), and GEONETCast-Americas (of NOAA). Using this approach, onward dissemination services can be optimized within the ground segment, while taking into account the various missions and product sources available independently of the design constraints of any particular satellite.

(c)   Near-real-time retransmission of data via specialized networks such as the WMO Global Telecommunication System.

(d)   Active FTP retrieval from data centres for off-line data, specifically from archives.

Data and product distribution may be subject to conditions, depending on the status and data policy of the space agency running the programme (operational, research and development, commercial) and what the programme will be used for. Access to data retransmission services is generally controlled by encryption and subject to registration, even if no charges are levied.

2.3.2.5   *User receiving stations*

User stations are installed to make use of real-time or near-real-time data transmission from the satellite. Depending on the satellite access modality and the user requirement, there may be:

(a)   High-data-rate acquisition stations for full reception of the data available either by open access or by agreement with the satellite owner;

(b)   Low-data-rate acquisition stations for a data selection of either reduced volume or quality;

(c)   Receiving terminals of commercial telecommunication satellites used for data dissemination after preprocessing or processing in the data-processing and archiving centre.

Frequencies used by the high-data-rate acquisition stations are in the L band (about 1 700 MHz) if the data rate is below approximately 5 Mbps; otherwise the X band (about 8 GHz) is used for data rates of up to approximately 100 Mbps. The low-data-rate acquisition stations make use of relatively low frequencies (L band: about 1 700 MHz for GEO, and very high frequency (VHF): about 137 MHz for LEO) that can be used on mobile stations, such as ships. Commercial telecommunication satellite terminals use K_u band (about 11 GHz) or C band (about 3.8 GHz).

2.3.2.6   *Product processing levels*

Satellite observations are retrieved from the raw data acquired from the instruments though a processing chain. Different processing levels are usually referred to, the detailed definitions of which depend on the instrument in question. Table 2.11 provides a generic description of these processing levels.

Table 2.11. Generic description of processing levels (to be adapted to each instrument)

Level	Description		
0	Instrument and auxiliary data reconstructed from satellite raw data after removing communications artefacts.		
1	Instrument data extracted, at full original resolution, with geolocation and calibration information.	1a (for LEO) or 1.0 (for GEO): calibration and geolocation attached but not applied.	
		1b (for LEO) or 1.5 (for GEO): calibration and geolocation applied.	
		1c, 1d, etc: optional for specific instruments.	
2	Geophysical product retrieved from a single instrument in the original projection.		
3	Geophysical product retrieved from a single instrument, mapped on uniform space and time grid scales, possibly on a multi-orbital (for LEO) or multi-temporal (for GEO) basis. Irreversible process due to resampling.		
4	Composite multi-sensor and/or multi-satellite products; or result of model analysis.		

Level 0 data are processed from the raw data stream by removing communication artefacts (such as synchronization frames and communication headers) and appending all necessary auxiliary data, including housekeeping and station-added information on timing and tracking. Level 0 data should be archived permanently to enable reprocessing with an updated instrument model (such as improved calibration or georeferencing).

Level 1a or 1.0 data consist of instrument files (counts) in the original instrument projection, with an appended (but not applied) deformation matrix or algorithm for georeferencing and calibration coefficients. The process from Level 0 to Level 1a/1.0 is fully reversible. Level 1a/1.0 data are normally permanently archived, although in principle they could be reproduced if Level 0 data have been archived.

Level 1b or 1.5 data consist of calibrated, co-registered and geolocated data in physical units (generally radiances), still in the original instrument projection. The process from Level 1a/1.0 to Level 1b/1.5 is not reversible because of truncation, discretization and resampling operations. Although Level 1b/1.5 may in any case be reprocessed from Level 1a/1.0 or Level 0, the processing effort is such that, in general, Level 1b/1.5 data are permanently archived.

Level 1c data are processed from the Level 1b data of certain instruments in order to enable end users to make use of that data. The process may be fully reversible (for example, spectra from interferograms by Fourier transform) but equally may not be (such as with apodized spectra). In general, these data are permanently archived. For certain instruments, further Level 1 steps (1d, 1e, etc.) may be defined (the addition of a cloud flag, for instance).

Level 0 and Level 1 processing is performed by the satellite operator. Where there is a direct readout, the satellite operator generally ensures the availability of Level 0 and Level 1 preprocessing software to local data users.

Level 2 products are generated from Level 1 data by applying algorithms that make limited use of external information. Data quality information is appended. These products are generated in the original instrument projection and tend to be permanently archived.

Level 3 products are generated by compositing a sequence of Level 2 products from successive orbits (with LEO) or at successive times (with GEO). Possible gaps in the sequence may be filled by interpolation. Due to the resampling operations implied by mapping on uniform space and time grids, Level 3 is an irreversible process. Products are generated offline by the satellite operators or by end users; they tend to be permanently archived.

Level 4 products are generated by blending data from different instruments on the same or different satellites, either with other data sources, or by assimilation in a model. In Level 4 products, the contribution of a specific satellite instrument may be hardly recognizable.

———————

CHAPTER CONTENTS

CHAPTER 3. REMOTE-SENSING INSTRUMENTS

This chapter provides an overview of basic instrument concepts. It introduces the high-level technical features of representative types of Earth observation instruments.

3.1 INSTRUMENT BASIC CHARACTERISTICS

A large variety of instruments and sensing principles are used in Earth observation. The key instrument features introduced here are:

(a) Scanning, swath and observing cycle;

(b) Spectral range and resolution;

(c) Spatial resolution (IFOV, pixel, MTF);

(d) Radiometric resolution.

3.1.1 Scanning, swath and observing cycle

The most characteristic feature of an instrument is the way in which it scans the scene to acquire the necessary observations. That depends on the type of orbit (low Earth orbit or geostationary Earth orbit), on the platform attitude control (spinning, three-axis stabilized), and sometimes on the specific type of measurement being taken. Only the most common scanning techniques will be described in this chapter.

A driving requirement for scanning is whether the scene should be observed with continuity (imagery) or can be sampled (sounding). A similar scanning mode may be used in both cases. However, imagery requires continuous scene coverage, while sounding can accommodate sampling with gaps.

In low Earth orbit (LEO) spacecraft, a 2D Earth scene scanning can use satellite motion for an along-track dimension. A cross-track scan can then be provided by a rotating scan mirror (Figure 3.1). Rotation speed is synchronized with satellite motion so that the cross-track image lines come out contiguously.
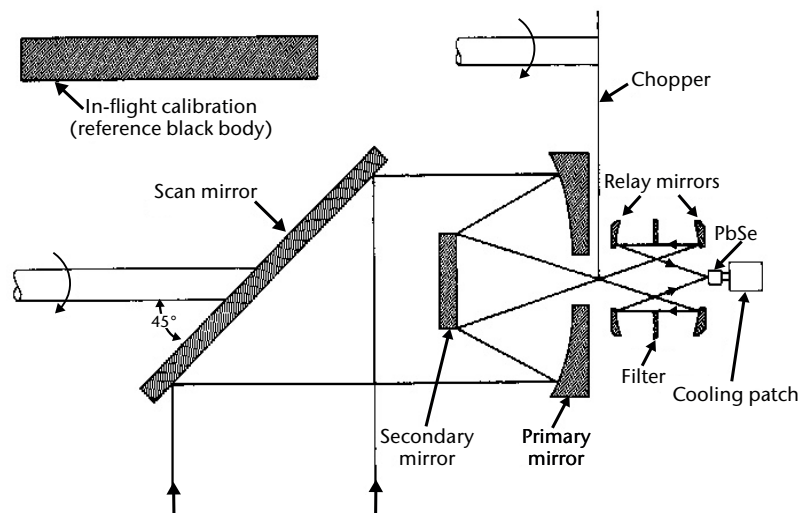
Figure 3.1. Typical scheme of a scanning radiometer in LEO
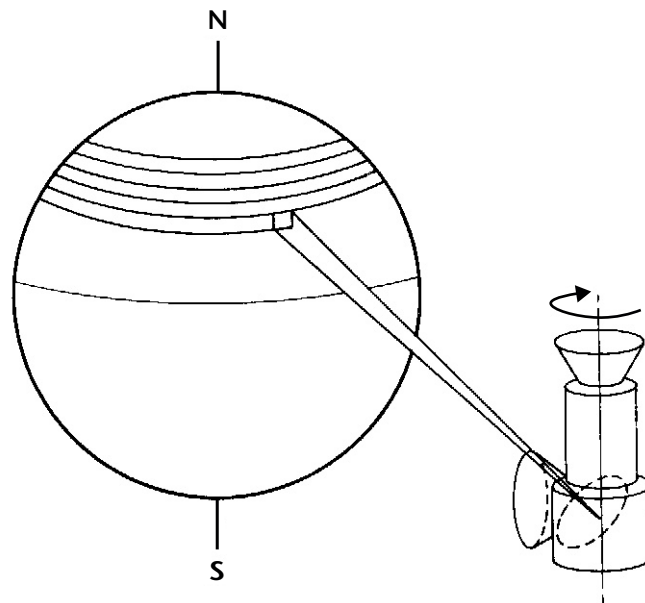
Figure 3.2. Schematic scanning from a spin-stabilized GEO

In the case of geostationary Earth orbit (GEO), there is no satellite motion with respect to the Earth's surface. The two scanning dimensions must therefore be generated either by the instrument or by satellite rotation. In Figure 3.2, it is assumed that the satellite is spin-stabilized: the west–east scan is provided by the satellite rotation, while the north–south scan is obtained by a step motor. For a three-axis stabilized platform, the instrument must generate both west–east and north–south scans.

The advent of array detectors has led to additional scanning possibilities. With LEO, a linear array can be placed orthogonally to the satellite track, and can scan the scene without any mechanical movement (pushbroom scanning). Under another scheme, the linear array can be placed parallel to the track; cross-track mechanical scanning will then scan several lines in parallel (whiskbroom scanning). With GEO, whiskbroom scanning is now the rule. For instance, SEVIRI on Meteosat Second Generation scans three lines in parallel for the infrared (IR) channels, and nine lines for the high-resolution visible spectrum (VIS) channel.

A very convenient scanning mechanism for polarization-sensitive measurements is conical scanning (Figure 3.3). In this geometry, the incidence angle is constant. Therefore the effect of polarization does not change along the scan line (an arc). By contrast, the incidence angle for cross-track scanning changes along the scan line, when moving from the nadir to the image edge. This invariance of the polarization effect across the image is very important for microwave (MW) measurement in window channels, where radiation reflected from elements such as the sea surface is strongly polarized. The measurement of the differential polarization constitutes important information that would be very difficult to use if the incidence angle changed across the scene. Another interesting feature of conical scanning is that the resolution remains constant across the whole image.

A disadvantage of conical scanning is that, with the selected incidence angle, the field of view does not normally reach the horizon. For example, the swath from an 800 km orbital height is ~1 600 km for a typical zenith angle of 53°, which is optimal for enhancing differential polarization information in MW. By contrast, the swath for a cross-track scanning instrument is close to 3 000 km, assuming a ± 70° zenith angle range, as shown in Part III, Chapter 2, Table 2.1.

The swath is an important feature of an instrument in LEO since it determines the observing cycle. Part III, Chapter 2, Table 2.2 outlines that, for a Sun-synchronous orbit at 800 km, one instrument with a swath of at least 2 800 km provides one global coverage per day for
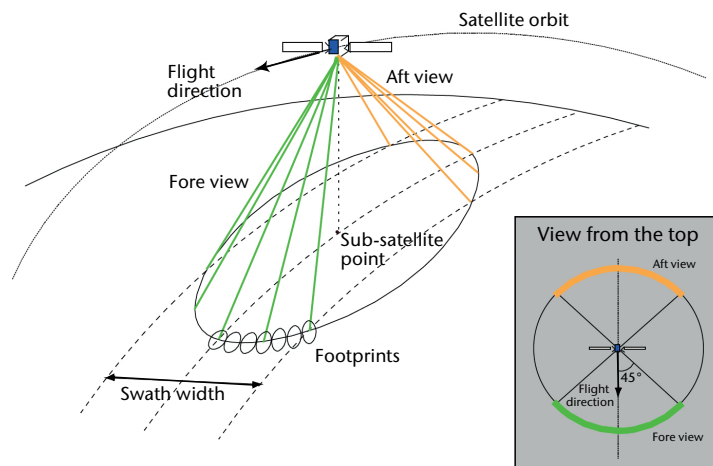
Figure 3.3. Geometry of conical scanning

measurements operated in daytime only (e.g. short-wave (SW) sensors), or two global coverages per day for measurements operated day and night (e.g. IR or MW sensors). MW conical scanning instruments generally provide one global coverage per day.

Estimating the observing cycle

The order of magnitude of the observing cycle (Δt, in days) for a given swath can be estimated by a simple calculation. Considering the Equator's length (~40 000 km), the number of orbits per day (~14.2) and assuming that there is no significant overlap between adjacent swaths at the Equator, the calculation is as follows:

(a) For day and night sensors (IR or MW) operating on both ascending and descending passes: $\Delta t = 1\,400$/swath (e.g. for a MW conical scanner with 1 400 km swath: $\Delta t = 1$ day);

(b) For daytime only sensors (SW) operating on only one pass per orbital period: $\Delta t = 2\,800$/swath (e.g. for VIS land observation with 180 km swath: $\Delta t = 16$ days).

The concept of swath is not applicable for instruments with no cross-track scanning, such as altimeters or cloud radars. Where that is the case, the cross-track sampling interval Δx at the Equator replaces "swath" in the relationship above. It is also useful to estimate the global average of this sampling interval. The interval is given by a slightly different relationship because of shorter orbit spacing at higher latitudes:

(a) At an average cross-track sampling interval Δx, the typical time needed for global coverage is:

   (i) $\Delta t = 900/\Delta x$ for day and night sensors (e.g. the Environmental Satellite (Envisat) Radar Altimeter – 2 (RA-2): $\Delta x = 26$ km, $\Delta t = 35$ days);

   (ii) $\Delta t = 1\,800/\Delta x$ for daytime only (e.g. the National Oceanic and Atmospheric Administration (NOAA) Solar Backscatter Ultraviolet (SBUV) instrument: $\Delta x = 170$ km, $\Delta t = 11$ days).

(b)   Reciprocally, in a time interval Δt (e.g. the orbit repeat cycle or a main sub-cycle) the average cross-track sampling interval obtained is:

   (i) $\Delta x = 900/\Delta t$ for day and night sensors (e.g. the Joint Altimetry Satellite Oceanography Network (JASON) altimeter: $\Delta t = 10$ days, $\Delta x = 90$ km);

   (ii) $\Delta x = 1\,800/\Delta t$ for daytime only (e.g. NOAA SBUV: $\Delta t = 5$ days, $\Delta x = 360$ km).

Limb sounders are generally considered as non-scanning instruments in the cross-track direction. Assuming a cross-track sampling interval $\Delta x = 300$ km which is equal to the horizontal resolution of the measurements, the relationships above yield the following observing cycles:

(a) $\Delta t \approx 3$ days for day and night sensors (e.g. MIPAS on Envisat: 3 days = 1 orbit sub-cycle);

(b) $\Delta t \approx 6$ days for daytime sensors (e.g. SCIAMACHY-limb on Envisat: 6 days = 2 orbit sub-cycles).

For instruments providing sparse but well-distributed observations, the coverage cycle or the average sampling can be estimated by comparing the number of events and their resolution with the Earth's surface to be covered. In the example of radio occultation using GPS and GLONASS, each satellite is able to provide about 1 000 observations per day, with a typical measurement resolution of 300 km for a total Earth's surface of 510 million km². Therefore:

(a)   Time required with one satellite providing 1 000 observations/day:
       $\Delta t = 510\,000\,000/300/300/1\,000 = 5.7$ days;

(b)   Number of satellites required for an observing cycle Δt: $N = 5.7/\Delta t$ (e.g. for $\Delta t = 0.5$ days, the number of satellites is close to 12).

Sun-, moon- or star-occultation instruments are an extreme case. Sun or moon occultation provides very few measurements per day, and only at the high altitudes of the day/night terminator in the case of the Sun, or at somewhat lower latitudes for the moon. Star occultation may provide several tens of measurements per day (e.g. 40 for the Envisat Global Ozone Monitoring by Occultation of Stars (GOMOS)), evenly distributed by latitude.

3.1.2   Spectral range: radiometers and spectrometers

Another major characteristic feature of an instrument is the spectral range over which it operates. As discussed in Part III, Chapter 2, 2.2, the spectral range determines which of the body's properties can be observed including reflectance, temperature and dielectric properties. Within the spectral range, there may be window regions and absorption bands, which mainly address condensed or gaseous bodies, respectively.

A spectral range may be more or less narrow, depending on the effects to be enhanced, or on the disrupting factors that need to be eliminated. The sub-divisions of a band or a window covered by an instrument are called channels. The number of channels depends on the number of pieces of independent information which have to be extracted from one band. If a limited number of well-separated channels are sufficient for the purpose, the instrument may only include those channels, and it is called a radiometer. If the information content rapidly changes with the frequency along the spectral range to the extent that channels must be contiguous, the instrument is called a spectrometer.

The technique adopted for channel separation, or for spectrometer subrange separation, is a major characteristic of the instrument. There are essentially two possible ways to physically separate two channels towards individual detectors (or detector arrays) and associated filter systems. First, the beam could be focused on a field stop and split into two bands by a dichroic mirror. The advantage is that co-registration is ensured, as the two channels look at the same field of view (which could comprise an array of instantaneous fields of view (IFOVs)). However, if the two wavelengths are too close to each other (e.g. a split window), a dichroic mirror cannot
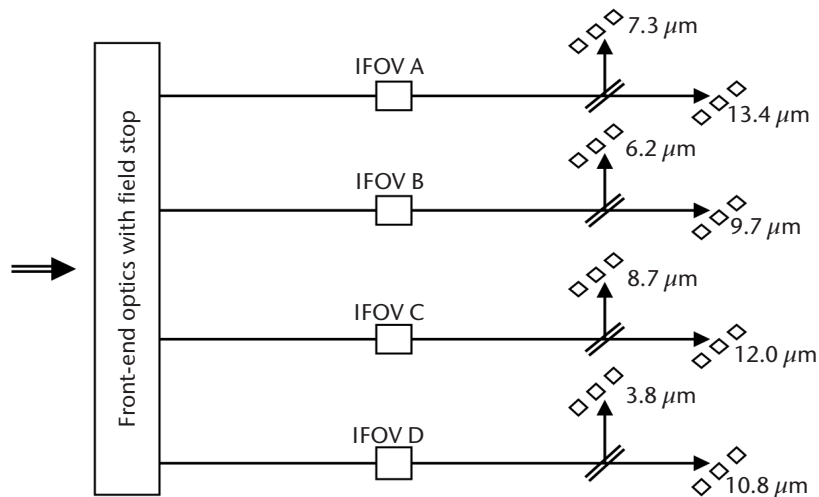
Figure 3.4. Channel separation scheme in SEVIRI on Meteosat Second Generation

separate them sharply enough. The second solution is to let the full beam produce the image in the focal plane and set detectors (or detector arrays) with different filters (thus identifying different channels) in different parts of the focal plane (in-field separation). It is a much simpler solution, but as each channel looks at a different IFOV, co-registration problems can occur. Combined solutions are possible: Figure 3.4 illustrates the solution implemented in the Meteosat Second Generation SEVIRI to separate the eight IR channels. Each channel is viewed by three detectors. Current detector arrays are much larger than they have been in the past, which makes in-field separation more convenient.

Spectrometers provide continuous spectral sampling within the spectral range or in a number of spectral subranges. (These subranges are sometimes called channels and should not be confused with the channels of a radiometer). There are several types of spectrometer, the simplest of which is the prism. Others include grating spectrometers and interferometers; the most common interferometers are the Michelson and the Fabry-Pérot. Figure 3.5 shows the scheme of a Michelson interferometer.
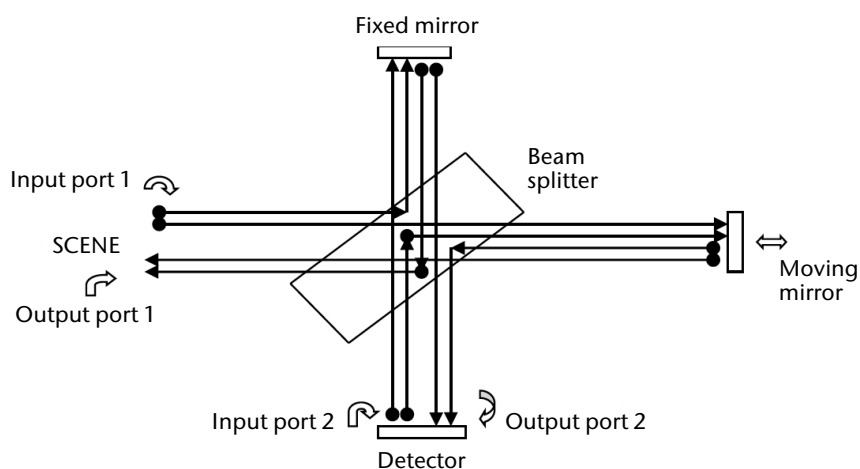
Figure 3.5. Scheme of a Michelson interferometer emphasizing the two input and output ports

The spectral resolution of a spectrometer is an important feature. The resolution of a Michelson interferometer is determined by the maximum length of the optical path difference (OPD) between the rays reflected by the fixed and moving mirrors. Referring to the unapodized resolution, the formula is:

$$\Delta v = 1/\text{OPD}_{max} \tag{3.1}$$

For example, in IASI, an instrument mounted on the Meteorological Operational (Metop) satellite, the excursion of the moving mirror is ± 2 cm. Therefore, $\text{OPD}_{max} = 4$ cm and $\Delta v = 0.25$ cm^{-1}. If fine analysis of the spectrum is needed (for instance, to detect trace gas lines), apodization that implies a factor ~2 is required. The apodized resolution is therefore $\Delta v = 0.5$ cm^{-1}.

For a grating spectrometer, the resolution is determined by the number of grooves, N, and the chosen order of diffraction, m. The resolving power $\lambda/\Delta\lambda$ is given by:

$$\lambda/\Delta\lambda = m \cdot N \tag{3.2}$$

For a Michelson interferometer, the spectral resolution is constant with a variable wavelength. For a grating spectrometer, however, it is the resolving power that is constant, and the spectral resolution that changes with wavelength. If a grating spectrometer is to cover a wide spectral range, that range should be subdivided into subranges that use different orders of diffraction, m. Resolving power may thus change based on subrange.

For a radiometer, the number of channels and their bandwidths play an equivalent role to spectral resolution for a spectrometer.

3.1.3 Spatial resolution (instantaneous field of view, pixel, and the modulation transfer function)

Colloquially, spatial resolution means the association of different features.

The IFOV is probably the closest to what is commonly meant by resolution. In optical instruments (i.e. SW and IR instruments), it is determined by the beamwidth of the optics and the size of the detector. In MW it is determined by the size of the antenna.

In optical systems, the size of the IFOV is designed primarily on the basis of energy considerations (see section 3.1.4). The IFOV may be determined by the shape of the detector; and although that may be square, the contour of an IFOV is not unduly sharp. In fact, the image of a point is a diffraction figure called point spread function (Figure 3.6). The IFOV is the convolution of the point spread function and the spatial response of the detector.
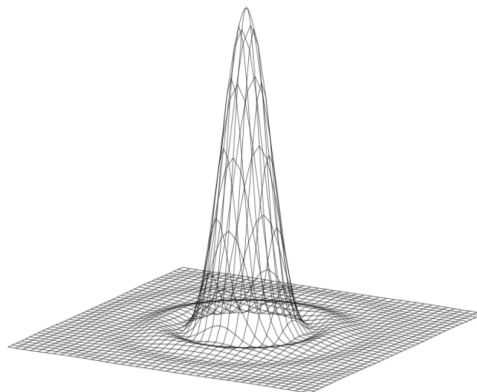
Figure 3.6. Shape of the point spread function

The energy entering the detector is also determined by the integration time between successive signal readings. During image scanning, the position of the line of sight will change by an amount called sampling distance. When plotted in a rasterized 2D pattern, a pixel (picture element) appears as a series of rectangular elements. In the x-direction, they correspond to the sampling distance and in the y-direction, to the satellite motion during the time distance from one line to the next (or the step motion in the north–south direction from GEO). The pixel is often confused with the resolution. That is because users can directly perceive the size of the picture element, whereas the IFOV is an engineering parameter that the user cannot see. Nevertheless, it is wrong to think that resolution can be improved by reducing the integration time, since the integration time must be suitable to ensure an appropriate radiometric accuracy (see section 3.1.4).

There is a balance between the size of the IFOV and the size of the pixel. When using a "perfect" imager, sampling is performed so that the sampling distance is equal to the IFOV size. That means that the IFOVs are continuous and contiguous across the image. Otherwise the image may be oversampled (pixel < IFOV, i.e. there is overlap between successive IFOVs) or undersampled (pixel > IFOV, i.e. there are gaps between successive IFOVs). Oversampling is useful to reduce aliasing effects (undue enhancement of high spatial frequencies because of reflection from the border). Undersampling may be necessary when more energy must be collected in order to ensure the required radiometric accuracy. Examples of relationships between IFOV and pixel are:

(a)   AVHRR – IFOV: 1.1 km; pixel: 1.1 km along-track, 0.80 km along-scan (oversampled);

(b)   SEVIRI – IFOV: 4.8 km; pixel: 3.0 km across-scan and along-scan (oversampled).

The modulation transfer function (MTF) is closely linked to the concept of IFOV and pixel. It is even more directly linked to the size "L" of an instrument's primary optics. The MTF represents the capability of the instrument to correctly manage the response to amplitude variation at the scene. It is the ratio between the observed amplitude, and the true signal amplitude from the scene, figured as sinusoidal. The observed amplitude is damped due to factors such as the diffraction from the optical aperture, the "window" introduced by the detector and smearing from integrating electronics. The effect of integrating the radiation over the (squared) detector introduces a contribution to the MTF:

$$\mathrm{MTF}_{\mathrm{window}}(f) \;=\; \mathrm{sinc}(\pi \cdot \mathrm{IFOV} \cdot f), \text{ with } f = 1/(2\,\Delta x)\left(\mathrm{km}^{-1}\right) \text{ and sinc } y \;=\; \frac{\sin y}{y} \qquad (3.3)$$

This shows that, for Δx = IFOV, MTF = sinc ($\pi/2$) = $2/\pi$. Therefore, even for a "perfect" imager, MTF is lower than unity. The value $2/\pi \approx 0.64$ corresponds to the area of a half sinusoid inscribed in a square. The concept of MTF must be seen as closely associated with radiometric accuracy: it specifies at which spatial wavelength two features are actually resolved if their radiation differs by just the detectable minimum. Two features whose radiation differs by substantially more than the detectable minimum can be resolved, even if they are substantially smaller. However, if they are as small as IFOV/2, then MTF = 0, and they can in no way be resolved (f = 1/IFOV is called the cut-off frequency).

It is interesting to note how MTF$_{\mathrm{window}}$ changes at different spatial wavelengths measured in terms of IFOV (where spatial wavelength is 2 Δx). Table 3.1 can be derived from equation 3.3:

Table 3.1. Variation of the MTF$_{\mathrm{window}}$ function of the ratio Δx/IFOV

Δx/IFOV	1/2	2/3	1	2	3	4	5	6
MTF$_{\mathrm{window}}$	0	0.30	0.64	0.90	0.95	0.97	0.98	0.99

This shows that features as small as two thirds of the IFOV can be resolved, but only if their radiances differ by more than three times the detectable minimum. It also shows that features twice as large as the IFOV can be resolved if their radiance difference exceeds the minimum by 10%.

The other major contribution to the MTF is diffraction. The relation is:

$$\mathrm{MTF}_{\mathrm{diffraction}} = \frac{2}{\pi}\left[\cos^{-1}(\frac{f}{f_d}) - \frac{f}{f_d}\sqrt{1-(\frac{f}{f_d})^2}\right] \tag{3.4}$$

where $f = 1/(2\,\vartheta\,H)$ (with H = satellite height); ϑ = angular resolution (i.e. IFOV/H); $f_d = L/(\lambda\,H)$; L = aperture of the primary optics; and thus $f/f_d = \lambda/(2\,\vartheta\,L)$.

Diffraction is dominant when the wavelength λ is relatively large (as with microwaves), when the optics aperture is relatively small, or when the satellite altitude is relatively large (as with GEO). The value $\mathrm{MTF}_{\mathrm{diffraction}} = 0.5$ occurs for $f/f_d = 0.404$, that is:

$$\vartheta = 1.24\frac{\lambda}{L} \tag{3.5}$$

which is the classical law of diffraction.

In summary, what is commonly meant by the term "resolution" involves at least three parameters. Although they should be considered in context, each one is more closely associated with a different perception:

(a)   IFOV: not visible to the user; controls the radiometric budget of the image;

(b)   Pixel: provides direct perception of the degree of detail in the image;

(c)   MTF: by monitoring the amplitude restitution, provides the perception of contrast.

3.1.4   **Radiometric resolution**

Although scarcely visible to the user, radiometric resolution is a defining element of instrument design. Scanning mechanisms, spectral resolution, spatial resolution, integration time and optics apertures are all designed to fulfil radiometric resolution requirements. Radiometric resolution is the minimum radiance difference necessary to distinguish two objects in two adjacent IFOVs. The observed difference is a combination of the true radiance difference between two bodies (signal) and the difference observed even when the contents of the IFOVs are identical (noise). The signal-to-noise ratio (SNR) is one way of expressing radiometric resolution.

Noise is a function of several factors, as set out in the radiometric performance formula:

$$\mathrm{NESR} = \frac{2\,F}{D^*{\cdot}\Delta v{\cdot}\tau{\cdot}\sqrt{\pi\cdot t\cdot\Delta\Omega}} \tag{3.6}$$

where:
NESR = noise equivalent spectral radiance (unit: W m^{-2} sr^{-1} [cm^{-1}]$^{-1}$, i.e. per unit of wave number);
$F = f/L$, F-number (f = system focal length, L = telescope aperture);
D^* = detectivity (strongly depending on v);
Δv = spectral resolution (expressed in terms of wave number $v = 1/\lambda$);
τ = instrument transmissivity;
t = integration time;
$\Delta\Omega$ = system throughput, given by the product of ($\pi{\cdot}L^2/4$) by (IFOV^2/H^2); where:
$\pi{\cdot}L^2/4$ = areal aperture of the telescope;
H = satellite altitude;
IFOV^2/H^2 = solid angle subtended by the IFOV.

In general, when defining $I(v)$ = spectral radiance at instrument input (unit: W m^{-2} sr^{-1} [cm^{-1}]$^{-1}$), this leads to:

$$\mathrm{SNR} = I(v)\big/\mathrm{NESR} \tag{3.7}$$

For SW, the input radiance is the solar spectral radiance corrected for the incidence angle and reflected according to body reflectivity (or albedo, if the body can be approximated as a Lambertian diffuser). Equations 3.6 and 3.7 lead to:

$$\frac{SNR}{IFOV\sqrt{\Delta\nu \cdot t}} \propto L \quad \text{(at a specific input radiance } I(\nu) \text{ or albedo } \rho\text{)} \tag{3.8}$$

That relationship explicitly links user-oriented parameters such as SNR, spectral resolution $\Delta\nu$, IFOV and integration time t to the size of the primary optics L.

In the case of narrowband IR channels, radiometric resolution is usually quoted as:

$$NE\Delta T = \frac{NESR}{dB/dT} \tag{3.9}$$

where B = Planck function, and $NE\Delta T$ = noise equivalent differential temperature at a specific temperature T.

With $NE\Delta T$, the performance formula 3.6 can be rewritten as follows:

$$NE\Delta T \cdot \Delta\nu \cdot IFOV \cdot \sqrt{t} = \frac{4H}{\pi \cdot dB/dT} \cdot \frac{F}{L \cdot D* \cdot \tau} \tag{3.10}$$

The left-hand side of formula 3.10 shows user-oriented parameters (radiometric, spectral, horizontal and time resolutions), while the right-hand side shows instrument sizing parameters (F-number, optics aperture, detectivity and transmissivity). This formula is not valid in all circumstances, but is instructive for a rough analysis in many instances. Cases where the formula is not valid mainly occur when the detector itself constitutes the dominant noise source, or when the detector response time is not short enough in comparison with the available integration time. This is normally the case in the far infrared (FIR) range. But it may also be the case with shorter wavelengths if, for instance, microbolometers or thermal detectors are used in order to operate at room temperature. In other words, $D*$, which obviously depends on ν, may be heavily dependent on the available integration time.

In the case of broadband channels, the concept of NESR, as expressed in equation 3.6, must be redefined in terms of integrated noise over the full spectral range of each channel. In that case, it is also possible to obtain a relationship similar to formula 3.10:

$$NE\Delta R \cdot IFOV \cdot \sqrt{t} \propto \frac{1}{L} \tag{3.11}$$

where $NE\Delta R$ = noise equivalent differential radiance (unit: W m^{-2} sr^{-1}).

The situation is different in the microwave range for two reasons. First, the need to limit the antenna size means that diffraction law establishes a link between the IFOV and the optics aperture L:

$$IFOV = \frac{1.24 \cdot H \cdot c}{L \cdot \nu*} \tag{3.12}$$

where $\nu*$ = frequency = c/λ; and c = speed of light.

Thus, there is less latitude for trade-off parameters. Second, the detection mechanism is based on comparing the scene temperature with the "system temperature", which increases with the bandwidth. The final outcome is that the equivalent of equations 3.8, 3.10 and 3.11 in the MW range is:

$$NE\Delta T \cdot \sqrt{\Delta\nu* \cdot t} = T_{sys} \tag{3.13}$$

where T_{sys} = system temperature.

The system temperature depends on many technological factors, and increases sharply as frequency increases. On the one hand, equation 3.13 shows that, in the case of MW, radiometric resolution can only marginally be improved by increasing bandwidth and integration time, since the benefit only grows with the square root. On the other hand, because of the diffraction-

limited regime, the usual way to increase SNR by increasing optics aperture is not applicable. That is because, if the antenna diameter is increased, the IFOV is reduced commensurately (see equation 3.12).

This short review highlights the direct impact of user and mission requirements on instrument sizing. In addition, it shows how important it is to formulate requirements in a way that leaves room for optimization, without necessarily compromising the overall required performance. For instance with reference to equation 3.10, it is possible to draw a number of conclusions.

(a)   For a given set of instrument parameters (L, F, τ and D^*), some user-driven parameters (NEΔT, $\Delta\nu$, IFOV and t) can be enhanced at the expense of others. In certain cases, this can be done at the software level during data processing on the ground. However, if all user requirements become more demanding and no compromises are made, a larger instrument will be necessary.

(b)   The effect of NEΔT, $\Delta\nu$ and IFOV on instrument size is linear in relation to the optics diameter L. The effect of t (the integration time, driven by the requirement to cover a given area in a given time) is damped by the square root. Therefore, requirements for increased coverage and/or more frequent observation have a lesser impact than requirements for improved spatial, spectral and radiometric resolution.

(c)   Increasing the optics aperture L has a significant impact on instrument size. Since it is very difficult to implement optical systems with F-number $= f/L < 1$, an increase in L implies an increased focal length, and therefore a volumetric growth of overall instrument optics. For example, a reduction in the IFOV from three to two kilometres would double the instrument mass.

3.2   INSTRUMENT CLASSIFICATION

In this section, Earth observation instruments are classified according to their main technical features. The following instrument types are considered:

(a)   Moderate-resolution optical imager

(b)   High-resolution optical imager

(c)   Cross-nadir scanning short-wave sounder

(d)   Cross-nadir scanning infrared sounder

(e)   Microwave-imaging radiometer or microwave-sounding radiometer

(f)   Limb sounder

(g)   Global navigation satellite system radio-occultation sounder

(h)   Broadband radiometer

(i)   Solar irradiance monitor

(j)   Lightning imager

(k)   Cloud radar and precipitation radar

(l)   Radar scatterometer

(m)   Radar altimeter

(n) Imaging radar (synthetic aperture radar)

(o) Space lidar

(p) Gravity sensor

(q) Solar activity, solar wind or deep space monitor

(r) Space environment monitor

(s) Magnetosphere or ionosphere sounder

Most instrument types are subdivided into more detailed categories. Examples are provided to illustrate how instrumental features can be suited to particular applications. A comprehensive list of satellite Earth observation instruments, with their detailed descriptions, is available through the WMO online database of space-based capabilities, available from the WMO Space Programme website.

3.2.1 Moderate-resolution optical imager

This instrument has the following main characteristics:

(a) Operates in the VIS, near infrared (NIR), short-wave infrared (SWIR), medium-wave infrared (MWIR) and thermal infrared (TIR) bands (i.e. from 0.4 to 15 μm);

(b) Discrete channels, from a few to several tens, separated by dichroics, filters or spectrometers, with bandwidths from ~10 nm to ~1 μm;

(c) Imaging capability: continuous and contiguous sampling, with spatial resolution in the order of one kilometre, covering a swath of several hundred to a few thousand kilometres;

(d) Scanning: generally cross-track, but sometimes multiangle, and sometimes under several polarizations;

(e) Applicable in both LEO and GEO.

Depending on the spectral bands, number and bandwidth of channels, and radiometric resolution, the application fields may include:

(a) Multi-purpose VIS/IR imagery for cloud analysis, aerosol load, sea-surface temperature, sea-ice cover, land-surface radiative parameters, vegetation indexes, fires, and snow cover. The extent of the spectral range is a critical instrument feature;

(b) Ocean-colour imagery, aerosol observation and vegetation classification. The number of channels with narrow bandwidth in VIS and NIR is a critical instrument feature;

(c) Imagery with special viewing geometry, for the best observation of aerosol and cirrus, accurate sea-surface temperature, land-surface radiative parameters including bidirectional reflectance distribution function. The critical instrument features are the number of viewing angles and, when available, polarizations.

Tables 3.2–3.6 describe three examples of multi-purpose VIS/IR imagers (AVHRR/3 in LEO, MODIS in LEO and SEVIRI in GEO), one example of an ocean-colour imager (MERIS) and one example of an imager with special viewing geometry (POLDER). MODIS is an experimental sensor and plays a particular role as a wide scope multi-purpose VIS/IR imager. It is largely used to help define the specifications of follow-on operational instruments. The main uses of its various groups of channels are highlighted in Table 3.3.

Table 3.2. Example of multi-purpose VIS/IR imager operating in LEO:
AVHRR/3 on NOAA and Metop

AVHRR/3	*Advanced Very High Resolution Radiometer 3*
Satellites	NOAA-15, NOAA-16, NOAA-17, NOAA-18, NOAA-19, Metop-A, Metop-B, Metop-C
Mission	Multi-purpose VIS/IR imagery for cloud analysis, aerosol load, sea-surface temperature, sea-ice cover, land-surface radiative parameters, normalized difference vegetation index, fires, snow cover, etc.
Main features	6 channels (channel 1.6 and 3.7 are alternative), balanced VIS, NIR, SWIR, MWIR and TIR
Scanning technique	Cross-track: 2 048 pixels of 800 m SSP (sub-satellite point) with a swath of 2 900 km Along-track: six 1.1 km lines a second
Coverage/cycle	Global coverage twice a day (LW (long-wave) channels) or once a day (SW channels)
Resolution (SSP)	1.1 km IFOV
Resources	Mass: 33 kg Power: 27 W Data rate: 621.3 kbps

Central wavelength	*Spectral interval*	*NEΔT or SNR at specified input spectral radiance*
0.630 μm	0.58–0.68 μm	9 at 0.5% albedo
0.862 μm	0.725–1.00 μm	9 at 0.5% albedo
1.61 μm	1.58–1.64 μm	20 at 0.5% albedo
3.74 μm	3.55–3.93 μm	0.12 K at 300 K
10.80 μm	10.3–11.3 μm	0.12 K at 300 K
12.00 μm	11.5–12.5 μm	0.12 K at 300 K

Table 3.3. Example of multi-purpose VIS/IR imager operating in LEO:
MODIS on EOS-Terra and EOS-Aqua

MODIS	*Moderate-resolution Imaging Spectroradiometer*
Satellites	EOS-Terra and EOS-Aqua
Mission	Multi-purpose VIS/IR imagery for cloud analysis, aerosol properties, sea- and land-surface temperature, sea-ice cover, ocean colour, land-surface radiative parameters, vegetation indexes, fires, snow cover, total ozone, cloud motion winds in polar regions, etc.
Main features	36-channel VIS, NIR, SWIR, MWIR and TIR spectroradiometer
Scanning technique	Whiskbroom: a 19.7 km-wide strip of along-track is cross-track scanned every 2.956 s. The strip includes 16 parallel lines sampled by 2 048 pixels of 1 000 m SSP, or 32 parallel lines sampled by 4 096 pixels of 500 m SSP, or 64 parallel lines sampled by 8 192 pixels of 250 m SSP, with a swath of 2 330 km.
Coverage/cycle	Global coverage nearly twice a day (LW channels) or once a day (SW channels)
Resolution (SSP)	IFOV: 250 m (two channels), 500 m (5 channels), 1 000 m (29 channels)
Resources	Mass: 229 kg Power: 225 W Data rate: 11 Mbps (daytime); 6.2 Mbps (average)

Central wavelength	Spectral interval	NEΔT or SNR at specified input spectral radiance	IFOV at SSP	Primary use
0.645 μm	0.62–0.67 μm	128 at 21.8 W m^{-2} sr^{-1} μm^{-1}	250 m	Land/Cloud/
0.858 μm	0.841–0.876 μm	201 at 24.7 W m^{-2} sr^{-1} μm^{-1}	250 m	Aerosol boundaries
0.469 μm	0.459–0.479 μm	243 at 35.3 W m^{-2} sr^{-1} μm^{-1}	500 m	Land/Cloud/
0.555 μm	0.545–0.565 μm	228 at 29.0 W m^{-2} sr^{-1} μm^{-1}	500 m	Aerosol properties
1.240 μm	1.230–1.250 μm	74 at 5.4 W m^{-2} sr^{-1} μm^{-1}	500 m	
1.640 μm	1.628–1.652 μm	275 at 7.3 W m^{-2} sr^{-1} μm^{-1}	500 m	
2.130 μm	2.105–2.155 μm	110 at 1.0 W m^{-2} sr^{-1} μm^{-1}	500 m	
0.418 μm	0.405–0.420 μm	880 at 44.9 W m^{-2} sr^{-1} μm^{-1}	1 000 m	Ocean colour,
0.443 μm	0.438–0.448 μm	838 at 41.9 W m^{-2} sr^{-1} μm^{-1}	1 000 m	Phytoplankton,
0.488 μm	0.483–0.493 μm	802 at 32.1 W m^{-2} sr^{-1} μm^{-1}	1 000 m	Biogeochemistry
0.531 μm	0.526–0.536 μm	754 at 27.9 W m^{-2} sr^{-1} μm^{-1}	1 000 m	
0.551 μm	0.546–0.556 μm	750 at 21.0 W m^{-2} sr^{-1} μm^{-1}	1 000 m	
0.667 μm	0.662–0.672 μm	910 at 9.5 W m^{-2} sr^{-1} μm^{-1}	1 000 m	
0.678 μm	0.673–0.683 μm	1 087 at 8.7 W m^{-2} sr^{-1} μm^{-1}	1 000 m	
0.748 μm	0.743–0.753 μm	586 at 10.2 W m^{-2} sr^{-1} μm^{-1}	1 000 m	
0.870 μm	0.862–0.877 μm	516 at 6.2 W m^{-2} sr^{-1} μm^{-1}	1 000 m	
0.905 μm	0.890–0.920 μm	167 at 10.0 W m^{-2} sr^{-1} μm^{-1}	1 000 m	Atmospheric
0.936 μm	0.931–0.941 μm	57 at 3.6 W m^{-2} sr^{-1} μm^{-1}	1 000 m	water vapour
0.940 μm	0.915–0.965 μm	250 at 15.0 W m^{-2} sr^{-1} μm^{-1}	1 000 m	
3.75 μm	3.660–3.840 μm	0.05 K at 0.45 W m^{-2} sr^{-1} μm^{-1}	1 000 m	Surface/Cloud
3.96 μm	3.929–3.989 μm	2.00 K at 2.38 W m^{-2} sr^{-1} μm^{-1}	1 000 m	temperature
3.96 μm	3.929–3.989 μm	0.07 K at 0.67 W m^{-2} sr^{-1} μm^{-1}	1 000 m	
4.06 μm	4.020–4.080 μm	0.07 K at 0.79 W m^{-2} sr^{-1} μm^{-1}	1 000 m	
4.47 μm	4.433–4.498 μm	0.25 K at 0.17 W m^{-2} sr^{-1} μm^{-1}	1 000 m	Atmospheric
4.55 μm	4.482–4.549 μm	0.25 K at 0.59 W m^{-2} sr^{-1} μm^{-1}	1 000 m	temperature
1.375 μm	1.360–1.390 μm	150 at 6.0 W m^{-2} sr^{-1} μm^{-1}	1 000 m	Cirrus clouds,
6.77 μm	6.535–6.895 μm	0.25 K at 1.16 W m^{-2} sr^{-1} μm^{-1}	1 000 m	Water vapour
7.33 μm	7.175–7.475 μm	0.25 K at 2.18 W m^{-2} sr^{-1} μm^{-1}	1 000 m	
8.55 μm	8.400–8.700 μm	0.25 K at 9.58 W m^{-2} sr^{-1} μm^{-1}	1 000 m	Cloud properties
9.73 μm	9.580–9.880 μm	0.25 K at 3.69 W m^{-2} sr^{-1} μm^{-1}	1 000 m	Ozone
11.01 μm	10.780–11.280 μm	0.05 K at 9.55 W m^{-2} sr^{-1} μm^{-1}	1 000 m	Surface/Cloud
12.03 μm	11.770–12.270 μm	0.05 K at 8.94 W m^{-2} sr^{-1} μm^{-1}	1 000 m	temperature
13.34 μm	13.185–13.485 μm	0.25 K at 4.52 W m^{-2} sr^{-1} μm^{-1}	1 000 m	Cloud-top
13.64 μm	13.485–13.785 μm	0.25 K at 3.76 W m^{-2} sr^{-1} μm^{-1}	1 000 m	temperature
13.94 μm	13.785–14.085 μm	0.25 K at 3.11 W m^{-2} sr^{-1} μm^{-1}	1 000 m	
14.24 μm	14.085–14.385 μm	0.35 K at 2.08 W m^{-2} sr^{-1} μm^{-1}	1 000 m	

**Table 3.4. Example of multi-purpose VIS/IR imager operating in GEO:
SEVIRI on Meteosat Second Generation**

SEVIRI	*Spinning Enhanced Visible Infrared Imager*
Satellites	Meteosat-8, Meteosat-9, Meteosat-10, Meteosat-11
Mission	Multi-purpose VIS/IR imagery for cloud analysis, aerosol load, sea-surface temperature, land-surface radiative parameters, normalized difference vegetation index, fires, snow cover, wind from cloud motion tracking, etc.
Main features	12 channels, balanced VIS, NIR, SWIR, MWIR and TIR
Scanning technique	Mechanical Spinning satellite E–W continuous S–N stepping
Coverage/cycle	Full disk every 15 min Limited areas in correspondingly shorter time intervals
Resolution (SSP)	4.8 km IFOV, 3 km sampling for 11 narrow channels 1.6 km IFOV, 1 km sampling for 1 broad VIS channel
Resources	Mass: 260 kg Power: 150 W Data rate: 3.26 Mbps

Central wavelength	*Spectral interval (99% encircled energy)*	*SNR or NEΔT at specified input radiance*
Not applicable (broad bandwidth channel)	0.6–0.9 μm	4.3 at 1% albedo
0.635 μm	0.56–0.71 μm	10.1 at 1% albedo
0.81 μm	0.74–0.88 μm	7.28 at 1% albedo
1.64 μm	1.50–1.78 μm	3 at 1% albedo
3.92 μm	3.48–4.36 μm	0.35 K at 300 K
6.25 μm	5.35–7.15 μm	0.75 K at 250 K
7.35 μm	6.85–7.85 μm	0.75 K at 250 K
8.70 μm	8.30–9.10 μm	0.28 K at 300 K
9.66 μm	9.38–9.94 μm	1.50 K at 255 K
10.8 μm	9.80–11.8 μm	0.25 K at 300 K
12.0 μm	11.0–13.0 μm	0.37 K at 300 K
13.4 μm	12.4–14.4 μm	1.80 K at 270 K

Table 3.5. Example of ocean-colour imager operating in LEO: MERIS on Envisat

MERIS	Medium Resolution Imaging Spectrometer
Satellite	Envisat
Mission	Ocean-colour imagery, aerosol properties, vegetation indexes, etc.
Main features	15 very narrow-bandwidth VIS and NIR channels
Scanning technique	Pushbroom 3 700 pixel/line (split into 5 parallel optical systems) Total swath: 1 150 km
Coverage/cycle	Global coverage in 3 days in daylight
Resolution (SSP)	Basic IFOV 300 m Reduced resolution for global data recording: 1 200 m
Resources	Mass: 200 kg Power: 175 W Data rate: 24 Mbps

Central wavelength	Bandwidth	SNR at specified input spectral radiance
412.5 nm	10 nm	1 871 at 47.9 W m^{-2} sr^{-1} μm^{-1}
442.5 nm	10 nm	1 650 at 41.9 W m^{-2} sr^{-1} μm^{-1}
490 nm	10 nm	1 418 at 31.2 W m^{-2} sr^{-1} μm^{-1}
510 nm	10 nm	1 222 at 23.7 W m^{-2} sr^{-1} μm^{-1}
560 nm	10 nm	1 156 at 18.5 W m^{-2} sr^{-1} μm^{-1}
620 nm	10 nm	863 at 12.0 W m^{-2} sr^{-1} μm^{-1}
665 nm	10 nm	708 at 9.2 W m^{-2} sr^{-1} μm^{-1}
681.25 nm	7.5 nm	589 at 8.3 W m^{-2} sr^{-1} μm^{-1}
708.75 nm	10 nm	631 at 6.9 W m^{-2} sr^{-1} μm^{-1}
753.75 nm	7.5 nm	486 at 5.6 W m^{-2} sr^{-1} μm^{-1}
760.625 nm	3.75 nm	205 at 3.4 W m^{-2} sr^{-1} μm^{-1}
778.75 nm	15 nm	628 at 4.9 W m^{-2} sr^{-1} μm^{-1}
865 nm	20 nm	457at 3.2 W m^{-2} sr^{-1} μm^{-1}
885 nm	10 nm	271 at 3.1 W m^{-2} sr^{-1} μm^{-1}
900 nm	10 nm	211 at 2.4 W m^{-2} sr^{-1} μm^{-1}

Table 3.6. Example of imager with special viewing geometry: POLDER on PARASOL

POLDER	Polarization and Directionality of the Earth's Reflectances
Satellite	Polarisation et anisotropie des réflectances au sommet de l'atmosphère, couplées avec un satellite d'observation emportant un lidar (PARASOL)
Mission	Imagery with special viewing geometry, for best observation of aerosol and cirrus, land–surface radiative parameters including bidirectional reflectance distribution function, etc.
Main features	Bidirectional viewing Multipolarization 9 narrow-bandwidth VIS and NIR channels
Scanning technique	242 x 274 charge-coupled device (CCD) arrays Swath: 2 400 km Each Earth's spot viewed from more directions as satellite moves
Coverage/cycle	Near-global coverage every day in daylight
Resolution (SSP)	6.5 km IFOV
Resources	Mass: 32 kg Power: 50 W Data rate: 883 kbps

Central wavelength	Bandwidth	No. of polarizations	SNR at specified input spectral radiance
443.5 nm	13.4 nm	–	200 at 61.9 W m^{-2} sr^{-1} μm^{-1}
490.9 nm	16.3 nm	3	200 at 63.2 W m^{-2} sr^{-1} μm^{-1}
563.8 nm	15.4 nm	–	200 at 58.1 W m^{-2} sr^{-1} μm^{-1}
669.9 nm	15.1 nm	–	200 at 48.7 W m^{-2} sr^{-1} μm^{-1}
762.9 nm	10.9 nm	3	200 at 38.9 W m^{-2} sr^{-1} μm^{-1}
762.7 nm	38.1 nm	–	200 at 38.9 W m^{-2} sr^{-1} μm^{-1}
863.7 nm	33.7 nm	–	200 at 30.8 W m^{-2} sr^{-1} μm^{-1}
907.1 nm	21.1 nm	3	200 at 27.5 W m^{-2} sr^{-1} μm^{-1}
1 019.6 nm	17.1 nm	–	200 at 22.6 W m^{-2} sr^{-1} μm^{-1}

3.2.2 High-resolution optical imager

This instrument has the following main characteristics:

(a) Spatial resolution in the range of less than one metre to several tens of metres;

(b) Wavelengths in the VIS, NIR and SWIR bands (0.4 to 3 μm) with possible extension to MWIR and TIR;

(c) Variable number of channels and bandwidths:

    (i) Single channel (panchromatic) with around 400 nm bandwidth (e.g. 500–900 nm);

    (ii) 3–10 multispectral channels with around 100 nm bandwidth;

    (iii) Continuous spectral range (hyperspectral); typically has 100 channels with around 10 nm bandwidth;

(d)   Imaging capability: continuous and contiguous sampling, covering a swath ranging from a few tens of kilometres to approximately 100 km, often addressable within a field of regard of several hundreds of kilometres;

(e)   Applicable in LEO. GEO is not excluded but not yet in use.

High-resolution optical imagers may perform a number of missions, depending on the spectral bands, the number and bandwidth of channels, and steerable pointing capability. Those missions include:

(a)   Panchromatic imagers: surveillance, recognition, stereoscopy for digital elevation model, etc. Critical instrument features are the resolution and the steerable pointing capability;

(b)   Multispectral imagers: land observation for land use, land cover, ground water, vegetation classification, disaster monitoring, etc. Critical instrument features are the number of channels and the spectral coverage;

(c)   Hyperspectral imagers: land observation, especially for vegetation process study, carbon cycle, etc. Critical instrument features are the spectral resolution and the spectral coverage.

Tables 3.7–3.9 describe an example of a panchromatic imager (WV60), a multispectral imager (ETM+) and a hyperspectral imager (Hyperion).

Table 3.7. Example of panchromatic high-resolution imager: WV60 on WorldView-1

WV60	World View 60 camera
Satellite	WorldView – 1
Mission	Surveillance, recognition, stereoscopy for digital elevation model, etc.
Main features	Panchromatic Resolution: 0.5 m Steering capability 60 cm telescope aperture
Scanning technique	Pushbroom 35 000 detector array Swath: 17.6 km, addressable by tilting the satellite in a variety of operating modes Stereo capability both along-track and cross-orbits
Coverage/cycle	Global coverage in 6 months in daylight Global coverage in a few days (down to 3) by strategic pointing
Resolution (SSP)	0.50 m
Resources	Mass: 380 kg Power: 250 W Data rate: 800 Mbps

Table 3.8. Example of multispectral high-resolution imager: ETM+ on Landsat-7

ETM+	Enhanced Thematic Mapper +
Satellite	Landsat-7
Mission	Land observation for land use, land cover, ground water, vegetation classification, disaster monitoring, etc.
Main features	8 channels: 1 panchromatic, 6 VIS, NIR and SWIR, 1 TIR Resolution: 15 m, 30 m and 60 m

ETM+	Enhanced Thematic Mapper +
Scanning technique	Whiskbroom 6 000 pixel/line (narrowband) 12 000 pixel/line (panchromatic) 3 000 pixel/line (TIR) Swath: 185 km
Coverage/cycle	Global coverage in 16 days in daylight
Resolution (SSP)	30 m (6 narrowband channels), 15 m (panchromatic), 60 m (TIR)
Resources	Mass: 441 kg Power: 590 W Data rate: 150 Mbps

Central wavelength	Spectral interval	SNR at specified input spectral radiance or NEΔT	
		Low signal	High signal
Panchromatic	0.50–0.90 μm	14 at 22.9 W m^{-2} sr^{-1} μm^{-1}	80 at 156.3 W m^{-2} sr^{-1} μm^{-1}
0.48 μm	0.45–0.52 μm	36 at 40 W m^{-2} sr^{-1} μm^{-1}	130 at 190 W m^{-2} sr^{-1} μm^{-1}
0.56 μm	0.53–0.61 μm	37 at 30 W m^{-2} sr^{-1} μm^{-1}	167 at 193.7 W m^{-2} sr^{-1} μm^{-1}
0.66 μm	0.63–0.69 μm	24 at 21.7 W m^{-2} sr^{-1} μm^{-1}	127 at 149.6 W m^{-2} sr^{-1} μm^{-1}
0.83 μm	0.78–0.90 μm	33 at 13.6 W m^{-2} sr^{-1} μm^{-1}	226 at 149.6 W m^{-2} sr^{-1} μm^{-1}
1.65 μm	1.55–1.75 μm	34 at 4.0 W m^{-2} sr^{-1} μm^{-1}	176 at 31.5 W m^{-2} sr^{-1} μm^{-1}
2.20 μm	2.09–2.35 μm	27 at 1.7 W m^{-2} sr^{-1} μm^{-1}	130 at 11.1 W m^{-2} sr^{-1} μm^{-1}
11.45 μm	10.4–12.5 μm	0.2 K at 300 K	0.2 K at 320 K

Table 3.9. Example of hyperspectral high-resolution imager: Hyperion on NMP EO-1

Hyperion	
Satellite	New Millennium Program Earth Observing – 1 (NMP EO-1)
Mission	Land observation, especially for vegetation process study, carbon cycle, etc.
Main features	VIS/NIR/SWIR grating spectrometer with 220 channels (hyperspectral) in two groups, covering the ranges 0.4–1.0 μm and 0.9–2.5 μm respectively Channel bandwidth: 10 nm Resolution: 30 m
Scanning technique	Pushbroom 250 pixel/line Swath: 7.5 km
Coverage/cycle	Global coverage in one year in daylight
Resolution (SSP)	30 m
Resources	Mass: 49 kg Power: 51 W Data rate: 105 Mbps

3.2.3 Cross-nadir scanning short-wave sounder

This spectrometer has the following main characteristics:

(a) Operates in the ultraviolet (UV), VIS, NIR and SWIR bands (0.2 to 3 μm);

(b) Spectral resolution ranging from a fraction of a nanometre to a few nanometres;

(c) Spatial resolution in the order of 10 km;

(d) Horizontal sampling not necessarily continuous and contiguous;

(e) Scanning capability can be from nadir-only pointing to a swath of a few thousand kilometres;

(f) Applicable both in LEO and GEO.

Depending on spectral bands and resolution, cross-nadir scanning SW sounders may be used in atmospheric chemistry for monitoring a number of species, mostly determined by the spectral bands used:

(a) UV only: ozone profile;

(b) UV and VIS: ozone profile and total column or gross profile of a small number of other species, such as BrO, NO_2, OClO, SO_2 and aerosol;

(c) UV, VIS and NIR: ozone profile and total column or gross profile of several other species, such as BrO, ClO, H_2O, HCHO, NO, NO_2, NO_3, O_2, O_4, OClO, SO_2 and aerosol;

(d) UV, VIS, NIR and SWIR: ozone profile and total column or gross profile of many other species, such as BrO, CH_4, ClO, CO, CO_2, H_2O, HCHO, N_2O, NO, NO_2, NO_3, O_2, O_4, OClO, SO_2 and aerosol;

(e) NIR and SWIR, possibly complemented by MWIR and TIR: total column or gross profile of selected species, such as CH_4, CO, CO_2, H_2O and O_2.

Tables 3.10 and 3.11 describe one example with full spectral coverage (SCIAMACHY-nadir in LEO) and another with reduced spectral coverage (UVN in GEO).

**Table 3.10. Example of cross-nadir scanning SW sounder in LEO:
SCIAMACHY-nadir on Envisat**

SCIAMACHY-nadir	*Scanning Imaging Absorption Spectrometer for Atmospheric Cartography – nadir scanning unit*
Satellite	Envisat
Mission	Atmospheric chemistry Tracked species: BrO, CH_4, ClO, CO, CO_2, H_2O, HCHO, N_2O, NO, NO_2, NO_3, O_2, O_3, O_4, OClO, SO_2 and aerosol
Main features	Spectral range: UV/VIS/NIR/SWIR Imaging capability: grating spectrometer covering eight bands, 8 192 channels, with 7 polarization channels
Scanning technique	Mechanical, cross-track IFOV: 25 km along-track x 0.6 km across-track at the SSP Time integration is performed across track to achieve the required SNR Swath: 960 km; one scan line in 4.5 seconds The cross-nadir mode alternates with the limb mode and the solar/lunar occultation mode
Coverage/cycle	Cross-track mode: global coverage every 3 days in daylight, if used full time

SCIAMACHY-nadir	*Scanning Imaging Absorption Spectrometer for Atmospheric Cartography – nadir scanning unit*		
Resolution (SSP)	Typical resolution is 30 km along-track x 60 km across-track at the SSP		
Resources	Mass: 198 kg Power: 122 W Data rate: 400 kbps		
Spectral range	*No. of channels*	*Spectral resolution*	*SNR at specified input spectral radiance*
214–334 nm	1 024	0.24 nm	200 at 0.5 W m^{-2} sr^{-1} μm^{-1}
300–412 nm	1 024	0.26 nm	2 300 at 58 W m^{-2} sr^{-1} μm^{-1}
383–628 nm	1 024	0.44 nm	2 600 at 90 W m^{-2} sr^{-1} μm^{-1}
595–812 nm	1 024	0.48 nm	2 800 at 61 W m^{-2} sr^{-1} μm^{-1}
773–1 063 nm	1 024	0.54 nm	1 900 at 40 W m^{-2} sr^{-1} μm^{-1}
971–1 773 nm	1 024	1.48 nm	1 500 at 25 W m^{-2} sr^{-1} μm^{-1}
1 934–2 044 nm	1 024	0.22 nm	100 at 3.4 W m^{-2} sr^{-1} μm^{-1}
2 259–2 386 nm	1 024	0.26 nm	320 at 2.2 W m^{-2} sr^{-1} μm^{-1}
310–2 380 nm	7	67–137 nm	Not applicable

Table 3.11. Example of cross-nadir scanning SW sounder in GEO: UVN on Meteosat Third Generation (MTG)

UVN	*Ultraviolet, Visible and Near-infrared sounder* *Also known as Sentinel 4*		
Satellites	MTG-S1 MTG-S2		
Mission	Atmospheric chemistry Tracked species: BrO, ClO, H_2O, HCHO, NO, NO_2, NO_3, O_2, O_3, O_4, OClO, SO_2 and aerosol		
Main features	Spectral range: UV/VIS/NIR Imaging capability: grating spectrometer covering 3 bands, 1 470 channels		
Scanning technique	Mechanical 3-axis stabilized satellite E–W continuous S–N stepping		
Coverage/cycle	European area (lat. 30°N–65°N, long. 15°W–50°E) in 60 minutes (30 minutes is also possible)		
Resolution	Defined at 45°N 0°: < 8 km in both N–S and E–W directions		
Resources	Mass: 150 kg Power: 100 W Data rate: 25 Mbps		
Spectral ranges	*No. of channels*	*Spectral resolution*	*SNR at specified input spectral radiance*
305–400 nm	570	0.5 nm	200–1 400 at 40–120 W m^{-2} sr^{-1} μm^{-1}
400–500 nm	600	0.5 nm	1 400 at 140 W m^{-2} sr^{-1} μm^{-1}
755–775 nm	300	0.2 nm	1 200 at 60 W m^{-2} sr^{-1} μm^{-1}

3.2.4 Cross-nadir scanning infrared sounder

These radiometers or spectrometers have the following main characteristics:

(a) Wavelengths in the MWIR and TIR bands (3–15 μm) with a possible extension to FIR (up to 50 μm) and auxiliary channels in the VIS/NIR bands;

(b) Spectral resolution in the order of 0.1 cm^{-1} (very high resolution), 0.5 cm^{-1} (hyperspectral) or 10 cm^{-1} (radiometer);

(c) Spatial resolution in the order of 10 km;

(d) Horizontal sampling not necessarily continuous or contiguous;

(e) Scanning capability can be from nadir-only pointing to a swath of a few thousand kilometres;

(f) Applicable both in LEO and GEO.

Depending on their spectral bands and resolution, cross-nadir scanning IR sounders may be used for atmospheric temperature and humidity profiling, and/or in atmospheric chemistry for a number of species:

(a) Radiometers provide coarse-vertical-resolution temperature and humidity profiles;

(b) Spectrometers provide high-vertical-resolution temperature and humidity profiles, coarse ozone profiles, total column and gross profile of a small number of other species, such as CH_4, CO, CO_2, HNO_3, NO_2, SO_2 and aerosol;

(c) Very high-resolution spectrometers that are specifically for atmospheric chemistry provide profiles or total columns of C_2H_2, C_2H_6, CFC-11, CFC-12, CH_4, $ClONO_2$, CO, CO_2, COS, H_2O, HNO_3, N_2O, N_2O_5, NO, NO_2, O_3, PAN, SF_6, SO_2 and aerosol.

Tables 3.12–3.14 set out three examples: a radiometer in GEO (Sounder on Geostationary Operational Environmental Satellite (GOES)); a hyperspectral sounder in LEO (IASI on Metop) and a very high-resolution spectrometer in LEO (TES-nadir on EOS-Aura).

Table 3.12. Example of radiometric cross-nadir scanning infrared sounder in GEO: Sounder on GOES

GOES Sounder	
Satellites	GOES-8, GOES-9, GOES-10, GOES-11, GOES-12, GOES-13, GOES-14, GOES-15
Mission	Coarse-vertical-resolution temperature and humidity profiles
Main features	Radiometer: 18 narrow-bandwidth channels in MWIR/TIR + 1 VIS
Scanning technique	Mechanical Biaxial 3-axis stabilized satellite Step-and-dwell
Coverage/cycle	Full disk in 8 h 3 000 x 3 000 km^2 in 42 minutes 1 000 x 1 000 km^2 in 5 minutes
Resolution (SSP)	8.0 km
Resources	Mass: 152 kg Power: 93 W Data rate: 40 kbps

Wavelength	Wave number	Bandwidth	SNR or NEΔT at specified input
14.71 μm	680 cm^{-1}	13 cm^{-1}	1.24 K at 290 K
14.37 μm	696 cm^{-1}	13 cm^{-1}	0.79 K at 290 K
14.06 μm	711 cm^{-1}	13 cm^{-1}	0.68 K at 290 K
13.64 μm	733 cm^{-1}	16 cm^{-1}	0.55 K at 290 K
13.37 μm	748 cm^{-1}	16 cm^{-1}	0.49 K at 290 K
12.66 μm	790 cm^{-1}	30 cm^{-1}	0.23 K at 290 K
12.02 μm	832 cm^{-1}	50 cm^{-1}	0.14 K at 290 K
11.03 μm	907 cm^{-1}	50 cm^{-1}	0.10 K at 290 K
9.71 μm	1 030 cm^{-1}	25 cm^{-1}	0.12 K at 290 K
7.43 μm	1 345 cm^{-1}	55 cm^{-1}	0.06 K at 290 K
7.02 μm	1 425 cm^{-1}	80 cm^{-1}	0.06 K at 290 K
6.51 μm	1 535 cm^{-1}	60 cm^{-1}	0.15 K at 290 K
4.57 μm	2 188 cm^{-1}	23 cm^{-1}	0.20 K at 290 K
4.52 μm	2 210 cm^{-1}	23 cm^{-1}	0.17 K at 290 K
4.45 μm	2 248 cm^{-1}	23 cm^{-1}	0.20 K at 290 K
4.13 μm	2 420 cm^{-1}	40 cm^{-1}	0.14 K at 290 K
3.98 μm	2 513 cm^{-1}	40 cm^{-1}	0.22 K at 290 K
3.74 μm	2 671 cm^{-1}	100 cm^{-1}	0.14 K at 290 K
0.70 μm	Not applicable	0.05 μm	1 000 at 100% albedo

**Table 3.13. Example of hyperspectral cross-nadir scanning
infrared sounder in LEO: IASI on Metop**

IASI	Infrared Atmospheric Sounding Interferometer
Satellites	Metop-A, Metop-B, Metop-C
Mission	High vertical-resolution temperature and humidity profile Coarse ozone profile Total column or gross profile of a number of other species, such as CH_4, CO, CO_2, HNO_3, NO_2, SO_2 and aerosol
Main features	Spectrometer: spectral resolution 0.25 cm^{-1} (unapodized) MWIR/TIR spectral range Interferometer with 8 461 channels and a one-channel embedded TIR imager
Scanning technique	Cross-track: 30 steps of 48 km SSP Swath: 2 130 km Along-track: one 48 km line every 8 seconds
Coverage/cycle	Near-global coverage twice a day
Resolution (SSP)	4 x 12 km IFOV close to the centre of a 48 x 48 km^2 cell (average sampling distance: 24 km)
Resources	Mass: 236 kg Power: 210 W Data rate: 1.5 Mbps (after onboard processing)

Spectral range (μm)	Spectral range (cm⁻¹)	Spectral resolution (unapodized)	NEΔT at specified scene temperature
8.26–15.50 μm	645–1210 cm⁻¹	0.25 cm⁻¹	0.2–0.3 K at 280 K
5.00–8.26 μm	1 210–2 000 cm⁻¹	0.25 cm⁻¹	0.2–0.5 K at 280 K
3.62–5.00 μm	2 000–2 760 cm⁻¹	0.25 cm⁻¹	0.5–2.0 K at 280 K
10.3–12.5 μm	Not applicable	Not applicable	0.8 K at 280 K

Table 3.14. Example of very high-resolution cross-nadir scanning infrared sounder in LEO: TES-nadir on EOS-Aura

TES-nadir	Tropospheric Emission Spectrometer – nadir scanning unit
Satellite	EOS-Aura
Mission	Atmospheric chemistry: profiles or total columns of C_2H_2, C_2H_6, CFC-11, CFC-12, CH_4, $ClONO_2$, CO, CO_2, COS, H_2O, HNO_3, N_2O, N_2O_5, NO, NO_2, O_3, PAN, SF_6, SO_2 and aerosol
Main features	Spectrometer Spectral resolution: 0.059 cm⁻¹ (unapodized) MWIR/TIR spectral range Imaging interferometer: four bands; 40 540 channels
Scanning technique	Cross-track mode: array of 16 detectors with a 0.53 km² x 0.53 km² nadir footprint moving in 10 steps to cover a 5.3 km² x 8.5 km² field of view that can be pointed everywhere within a 45°-aperture cone or an 885 km swath. The cross-nadir mode is alternative to the limb mode.
Coverage/cycle	Cross-track mode: if used full time with strategic pointing, global coverage could be obtained for cells of ~80 km wide in 16 days (the orbital repeat cycle)
Resolution (SSP)	0.53 km sampling
Resources	Mass: 385 kg Power: 334 W Data rate: 4.5 Mbps

Spectral range (μm)	Spectral range (cm⁻¹)	Spectral resolution (unapodized)	NEΔT at specified scene temperature
11.11–15.38 μm	650–900 cm⁻¹	0.059 cm⁻¹	< 1 K at 280 K
8.70–12.20 μm	820–1 150 cm⁻¹	0.059 cm⁻¹	< 1 K at 280 K
5.13–9.09 μm	1 100–1 950 cm⁻¹	0.059 cm⁻¹	< 1 K at 280 K
3.28–5.26 μm	1 900–3 050 cm⁻¹	0.059 cm⁻¹	< 2 K at 280 K

3.2.5 Microwave radiometers

These radiometers have the following main characteristics:

(a) Frequencies from 1 to 3 000 GHz (wavelengths from 0.1 mm to 30 cm);

(b) Channel bandwidths from a few MHz to several GHz;

(c) Spatial resolution from a few kilometres to approximately 100 kilometres, determined by antenna size and frequency;

(d) Horizontal sampling not necessarily continuous or contiguous;
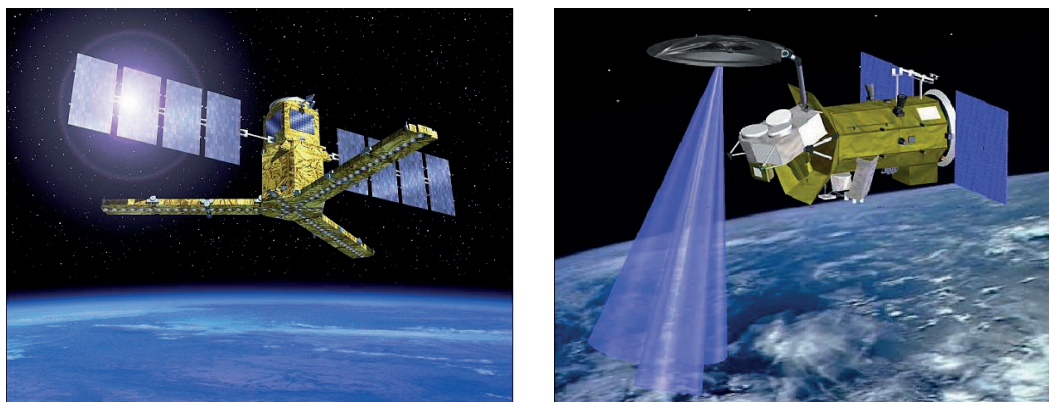
Figure 3.7. Sketch view of SMOS with MIRAS (left) and the satélite de aplicaciones científicas – D (SAC-D) with Aquarius (right). The Aquarius real aperture antenna measures 2.5 m in diameter. The MIRAS synthetic aperture antenna is inscribed in a circle that measures 4 m in diameter.

(e)   Scanning: cross-track (swath in the order of 2 000 km), conical (swath in the order of 1 500 km, possibly providing single or dual polarization) or nadir-only;

(f)   Applicable in LEO.

Depending on their frequency, spatial resolution, and scanning mode, MW radiometers may perform a number of missions:

(a)   Multi-purpose MW imagery for precipitation, cloud liquid water and ice, precipitable water, sea-surface temperature, sea-surface wind speed (and direction if multipolarization is used), sea-ice cover, surface soil moisture, snow status, water equivalent, etc. Critical instrument features are: the extension of the spectral range, from 19 GHz as a minimum (possibly 10 GHz, or ideally 6–7 GHz) to at least 90 GHz; and conical scanning to make use of differential polarization under conditions of a constant incidence angle;

(b)   Nearly-all-weather temperature and humidity sounding, which is also relevant for precipitation. Critical instrument features are the channels in absorption bands: O_2 for temperature (main frequency: 57 GHz) and H_2O for humidity (main frequency: 183 GHz);

(c)   Sea-surface salinity and volumetric soil moisture. One critical instrument feature is the low frequency in the L band (main frequency: 1.4 GHz); this implies the use of very large antennas (see Figure 3.7);

(d)   Atmospheric correction in support of altimetry missions. Critical instrument features are the frequency of the water-vapour 23 GHz band and its nearby windows; and the nadir viewing, co-centred with an altimeter.

Tables 3.15–3.18 describe a multi-purpose radiometer (AMSR-E), a temperature and humidity sounder (ATMS), a low-frequency radiometer (MIRAS) and a nadir-viewing radiometer (AMR).

Table 3.15. Example of multi-purpose MW imager: AMSR-E on EOS-Aqua

AMSR-E	Advanced Microwave Scanning Radiometer for Earth Observation System (EOS)
Satellite	EOS-Aqua
Mission	Multi-purpose MW imagery for precipitation, cloud liquid water and ice, precipitable water, sea-surface temperature, sea-surface wind speed, sea-ice cover, surface soil moisture, snow status, water equivalent, etc.
Main features	Spectral range: 6.9–89 GHz 6 frequencies, 12 channels, mostly windows Conical scanning
Scanning technique	Conical: 55° zenith angle Swath: 1 450 km Scan rate: 40 scan/min = 10 km/scan
Coverage/cycle	Global coverage once a day
Resolution (SSP)	Changes with frequency Consistent with an antenna diameter of 1.6 m
Resources	Mass: 314 kg Power: 350 W Data rate: 87.4 kbps

Central frequency (GHz)	Bandwidth (MHz)	Polarizations	NEΔT	IFOV	Pixel
6.925	350	Vertical (V), Horizontal (H)	0.3 K	43 x 75 km	10 x 10 km
10.65	100	V, H	0.6 K	29 x 51 km	10 x 10 km
18.7	200	V, H	0.6 K	16 x 27 km	10 x 10 km
23.8	400	V, H	0.6 K	14 x 21 km	10 x 10 km
36.5	1 000	V, H	0.6 K	9 x 14 km	10 x 10 km
89.0	3 000	V, H	1.1 K	4 x 6 km	5 x 5 km

Table 3.16. Example of MW temperature/humidity sounder: ATMS on Suomi National Polar-orbiting Partnership (NPP) and Joint Polar Satellite System (JPSS)

ATMS	Advanced Technology Microwave Sounder
Satellites	Suomi-NPP, JPSS-1 and JPSS-2
Mission	Nearly-all-weather temperature and humidity sounding; also relevant for precipitation
Main features	Spectral range: 23–183 GHz 22 channels, including the 57 and 183 GHz bands Cross-track scanning
Scanning technique	Cross-track: 96 steps of 16 km SSP Swath: 2 200 km Along-track: one 16 km line every 8/3 seconds
Coverage/cycle	Near-global coverage twice a day
Resolution (SSP)	16 km for channels at 165–183 GHz 32 km for channels at 50–90 GHz 75 km for channels at 23–32 GHz
Resources	Mass: 75.4 kg Power: 93 W Data rate: 20 kbps

Central frequency (GHz)	Bandwidth (MHz)	Quasi-polarization	NEΔT
23.800	270	Quasi-vertical (QV)	0.90 K
31.400	180	QV	0.90 K
50.300	180	Quasi-horizontal (QH)	1.20 K
51.760	400	QH	0.75 K
52.800	400	QH	0.75 K
53.596 ± 0.115	170	QH	0.75 K
54.400	400	QH	0.75 K
54.940	400	QH	0.75 K
55.500	330	QH	0.75 K
f0 = 57.290344	330	QH	0.75 K
f0 ± 0.217	78	QH	1.20 K
f0 ± 0.3222 ± 0.048	36	QH	1.20 K
f0 ± 0.3222 ± 0.022	16	QH	1.50 K
f0 ± 0.3222 ± 0.010	8	QH	2.40 K
f0 ± 0.3222 ± 0.0045	3	QH	3.60 K
89.5	5 000	QV	0.50 K
165.5	3 000	QH	0.60 K
183.31 ± 7.0	2 000	QH	0.80 K
183.31 ± 4.5	2 000	QH	0.80 K
183.31 ± 3.0	1 000	QH	0.80 K
183.31 ± 1.8	1 000	QH	0.80 K
183.31 ± 1.0	500	QH	0.90 K

Table 3.17. Example of L-band MW radiometer: MIRAS on SMOS

MIRAS	Microwave Imaging Radiometer using Aperture Synthesis
Satellite	Soil Moisture and Ocean Salinity (SMOS)
Mission	Sea-surface salinity, volumetric soil moisture
Main features	Very large synthetic aperture antenna Single L-band frequency (1.413 GHz) Several polarimetric modes
Scanning technique	Pushbroom: correlation interferometry is implemented among receiver arrays deployed on the three arms of a Y-shaped antenna Swath: 1 000 km
Coverage/ cycle	Global coverage in 3 days (soil moisture) Depending on the desired accuracy for salinity measurements, average figures measured over a number of weeks may be needed
Resolution (SSP)	50 km basic; may be degraded, depending on the desired accuracy for salinity measurements
Resources	Mass: 355 kg Power: 511 W Data rate: 89 kbps

**Table 3.18. Example of non-scanning MW radiometer designed
to support altimetry: AMR on JASON**

AMR	Advanced Microwave Radiometer
Satellites	JASON-2, JASON-3
Mission	Atmospheric correction in support of the altimeters of JASON-1 and JASON-2
Main features	3 frequencies: 18.7 GHz, 23.8 GHz and 34 GHz
Scanning technique	Nadir-only viewing, associated with the Poseidon-3 and Poseidon-3B radar altimeters
Coverage/cycle	Global coverage in 1 month for 30 km average spacing, or in 10 days for 100 km average spacing
Resolution (SSP)	25 km
Resources	Mass: 27 kg Power: 31 W Data rate: 100 bps

3.2.6 Limb sounders

This family of instruments has the following main characteristics:

(a) Scanning of the Earth's limb: this determines vertical resolution (in the range 1–3 km), the observed atmospheric layer (in the range 10–80 km), and spatial resolution (about 300 km along-view);

(b) Spectrometers using the UV/VIS/NIR/SWIR (200–3 000 nm) bands, the MWIR/TIR (3–16 μm) bands, or the high-frequency range of MW (100–3 000 GHz);

(c) Spatial resolution, from a few tens of kilometres to a few hundreds of kilometres in the transverse direction;

(d) Horizontal sampling, limited to one or a few azimuth directions;

(e) Applicable only in LEO.

Limb sounders can observe the high troposphere, stratosphere and mesosphere with high vertical resolution, and are mainly used for atmospheric chemistry. Depending on their spectral bands, limb sounders may track different species:

(a) SW spectrometers for a number of species, depending on the part of the spectrum covered; for the full range (UV/VIS/NIR/SWIR), the main species are: BrO, CH_4, ClO, CO, CO_2, H_2O, HCHO, N_2O, NO, NO_2, NO_3, O_2, O_3, O_4, OClO, SO_2 and aerosol;

(b) IR spectrometers for a number of species, depending on the part of the spectrum covered; for the full range (MWIR/TIR), the main species are: C_2H_2, C_2H_6, CFCs (CCl_4, CF_4, F11, F12, F22), CH_4, $ClONO_2$, CO, COF_2, H_2O, HNO_3, HNO_4, HOCl, N_2O, N_2O_5, NO, NO_2, O_3, OCS, SF_6 and aerosol;

(c) MW spectrometers for a number of species, depending on the part of the spectrum covered; for the range 100–3 000 GHz, the main species are: BrO, ClO, CO, H_2O, HCl, HCN, HNO_3, HO_2, HOCl, N_2O, O_3, OH and SO_2;

(d) Occultation sounders, tracking the Sun, the moon or the stars, for a number of species, depending on the part of the spectrum covered; for the full range (UV/VIS/NIR/SWIR) the main species are: H_2O, NO_2, NO_3, O_3, OClO and aerosol.

Tables 3.19–3.22 show limb sounders that use SW (SCIAMACHY-limb), IR (MIPAS), MW (MLS) and occultation in SW (SAGE-III ISS).

Table 3.19. Example of limb sounder using SW: SCIAMACHY-limb on Envisat

SCIAMACHY-limb	Scanning Imaging Absorption Spectrometer for Atmospheric Cartography – limb scanning unit
Satellite	Envisat
Mission	Chemistry of the high atmosphere. Tracked species: BrO, CH_4, ClO, CO, CO_2, H_2O, HCHO, N_2O, NO, NO_2, NO_3, O_2, O_3, O_4, OClO, SO_2 and aerosol
Main features	UV/VIS/NIR/SWIR grating spectrometer Eight bands 8 192 channels, with 7 polarization channels
Scanning technique	Limb scanning of ± 500 km horizontal sector Solar and lunar occultation: the instrument is self-calibrating in this mode (principle of differential optical absorption spectroscopy) The limb mode, solar/lunar occultation mode and cross-nadir mode are alternatives to each other.
Coverage/cycle	If used full time, the limb mode would provide global coverage every 3 days in daylight. Not applicable for solar and lunar occultation
Resolution (SSP)	Vertical: 3 km, in the altitude range 10–100 km Horizontal: effective resolution: ~300 km (limb geometry) Solar and lunar occultation: vertical 1 km, in the altitude range 10–100 km; horizontal ~300 km
Resources	Mass: 198 kg Power: 122 W Data rate: 400 kbps

Spectral range	No. of channels	Spectral resolution	SNR at specified input spectral radiance
214–334 nm	1 024	0.24 nm	500 at 1.5 W m^{-2} sr^{-1} μm^{-1}
300–412 nm	1 024	0.26 nm	4 000 at 130 W m^{-2} sr^{-1} μm^{-1}
383–628 nm	1 024	0.44 nm	4 500 at 170 W m^{-2} sr^{-1} μm^{-1}
595–812 nm	1 024	0.48 nm	3 000 at 49 W m^{-2} sr^{-1} μm^{-1}
773–1 063 nm	1 024	0.54 nm	2 500 at 24 W m^{-2} sr^{-1} μm^{-1}
971–1 773 nm	1 024	1.48 nm	1 000 at 8.2 W m^{-2} sr^{-1} μm^{-1}
1 934–2 044 nm	1 024	0.22 nm	10 at 0.2 W m^{-2} sr^{-1} μm^{-1}
2 259–2 386 nm	1 024	0.26 nm	7 at 0.1 W m^{-2} sr^{-1} μm^{-1}
310–2 380 nm	7	67–137 nm	Not applicable

Table 3.20. Example of limb sounder using IR: MIPAS on Envisat

MIPAS	*Michelson Interferometer for Passive Atmospheric Sounding*
Satellite	Envisat
Mission	Chemistry of the high atmosphere Tracked species: C_2H_2, C_2H_6, CFCs (CCl_4, CF_4, F11, F12, F22), CH_4, $ClONO_2$, CO, COF_2, H_2O, HNO_3, HNO_4, HOCl, N_2O, N_2O_5, NO, NO_2, O_3, OCS, SF_6 and aerosol
Main features	IR spectrometer: Michelson interferometer Range 685–2 410 cm^{-1} (4.15–14.6 μm) Spectral resolution 0.035 cm^{-1} (unapodized) 60 000 channels/spectrum NESR: 50 nW cm^{-2} sr^{-1} cm at 685 cm^{-1}, 4.2 nW cm^{-2} sr^{-1} cm at 2 410 cm^{-1}
Scanning technique	Limb scanning, forward and side 75 seconds for one vertical scan; 80 scans per orbit; 1 145 profiles per day
Coverage/cycle	Global coverage every 3 days for one measurement in every 300 km^2 x 300 km^2 cell
Resolution (SSP)	Vertical: 3 km, in the altitude range 5–150 km Horizontal effective resolution: ~300 km (limb geometry)
Resources	Mass: 320 kg Power: 210 W Data rate: 8 Mbps

Table 3.21. Example of limb sounder using MW: MLS on EOS-Aura

MLS	*Microwave Limb Sounder*
Satellite	EOS-Aura
Mission	Chemistry of the high atmosphere Tracked species: BrO, ClO, CO, H_2O, HCl, HCN, HNO_3, HO_2, HOCl, N_2O, O_3, OH and SO_2
Main features	MW spectrometer: 5-band, 36 sub-bands, 1 000 channels, Millimetre-submillimetre heterodyne radiometer at frequencies of 118 GHz (9 bands), 190 GHz (6 bands), 240 GHz (7 bands), 640 GHz (9 bands) and 2 500 GHz (5 bands)
Scanning technique	Limb scanning
Coverage/cycle	Global coverage every 3 days for 300 km wide cells
Resolution (SSP)	Vertical: 1.5 km, in the altitude range 5–120 km Horizontal effective resolution: ~300 km (limb geometry)
Resources	Mass: 490 kg Power: 550 W Data rate: 100 kbps

Table 3.22. Example of limb sounder using SW in occultation: SAGE-III on ISS

SAGE-III ISS	Stratospheric Aerosol and Gas Experiment – III for the ISS
Satellite	International Space Station (ISS)
Mission	Atmospheric chemistry in the stratosphere Tracked species: H_2O, NO_2, NO_3, O_3, OClO and aerosol
Main features	UV/VIS/NIR/SWIR (290–1 550 nm) 9-band solar and lunar occultation grating spectrometer
Scanning technique	Sun and moon tracking during occultation phase, 1 km step from ~10 km to ~85 km
Coverage/cycle	A few tens of events per day, limited to latitudes below ~52° (orbital inclination of the ISS)
Resolution (SSP)	300 km (horizontal), 1–2 km (vertical)
Resources	Mass: 76 kg Power: 80 W Data rate: 115 kbps

3.2.7 Global navigation satellite system radio-occultation sounders

These instruments have the following main characteristics:

(a) Global navigation satellite system (GNSS) receivers using at least two L-band frequencies around 1 180 GHz, 1 250 GHz and 1 580 GHz;

(b) Earth's limb observation, from surface to satellite altitude during the occultation phase of satellites from the GNSS constellations (such as GPS, GLONASS, Galileo and Compass/Beidou);
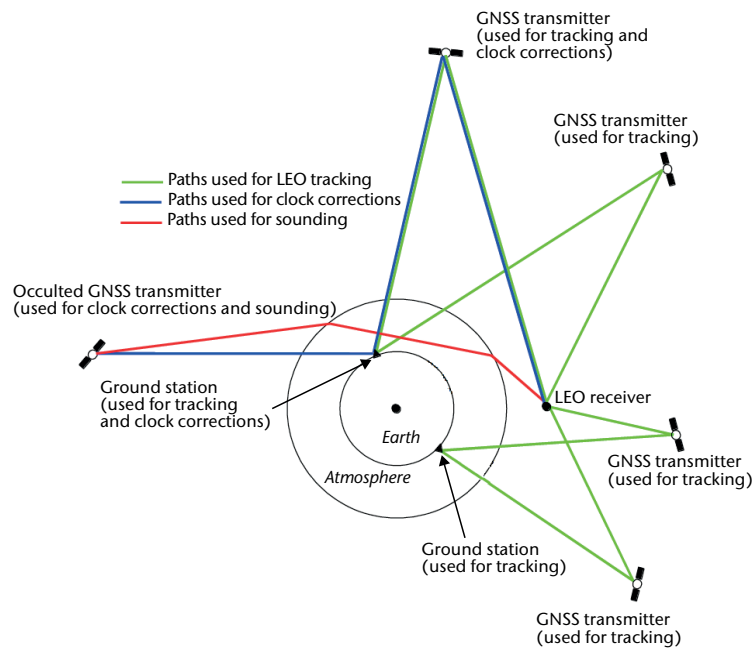
Figure 3.8. The overall system for radio occultation

(c) Directional antennas: aft-looking (for setting GNSS), forward-looking (for rising GNSS), and toroidal (for navigation);

(d) Effective spatial resolution at around 300 km along the direction from the LEO satellite to the occulting GNSS satellite; a few tens of kilometres in the transverse direction;

(e) Horizontal sampling limited by the daily number of occultation events: from 250 to 1 500 events by satellite, depending on the number of GNSS systems received, and on the aft-looking/forward-looking tracking capability;

(f) Supported by a complex system of ground stations (see Figure 3.8);

(g) Applicable in LEO only.

Depending on their detailed features, GNSS radio-occultation sounders can provide different types of information:

(a) The signal-sampling time interval determines the vertical resolution of temperature, humidity and density profiles;

(b) Measurement sensitivity to the low atmospheric layers is determined by the size of the occultation antennas and the time-sampling technique;

(c) The number of frequencies that are used affects the accuracy of two ionospheric measurements: total electron content and electron density profile;

(d) The number of occultation events per day depends on the number of GNSS constellations used (GPS, GLONASS, Galileo, Beidou), the number of receiving channels for simultaneous tracking of further GNSS satellites, and the antenna accommodation feature: only aft-looking, only forward-looking, or both.

Table 3.23 sets out the main features of an example of a radio-occultation sounder (GRAS).

Table 3.23. Example of radio-occultation sounder: GRAS on Metop

GRAS	*GNSS Receiver for Atmospheric Sounding*
Satellites	Metop-A, Metop-B, Metop-C
Mission	High-vertical-resolution temperature, humidity and density profiles
Main features	Measuring the phase delay due to refraction during occultation between a navigation satellite and the LEO satellite GNSS constellation: GPS Frequencies: L1 = 1 575.42 MHz and L2 = 1 227.6 MHz 8 receiving channels: 4 for occultation, 8 for navigation
Scanning technique	Limb scanning from 80 km to close-to-surface by time sampling Azimuth: 90° sectors fore and aft
Coverage/cycle	1 constellation tracked About 650 soundings/day Average spacing 880 km Global coverage (300 km spacing) in 8.5 days
Resolution (SSP)	About 300 km horizontal, 0.5 km vertical
Resources	Mass: 30 kg Power: 30 W Data rate: 27 kbps

3.2.8   **Broadband radiometers**

These instruments have the following main characteristics:

(a)   Wavelengths in the bands of total radiation emerging from the Earth and the atmosphere (0.2–300 μm) as well as from the fraction represented by reflected solar radiation (0.2–4.0 μm);

(b)   One broadband channel, integrating over each of the two bands, and optional narrow-bandwidth channels in VIS and/or TIR to collect information on clouds within the IFOV;

(c)   Cross-track scanning with continuous and contiguous sampling, to cover a swath of a few thousand kilometres with a spatial resolution of the order of 10 km;

(d)   Applicable in LEO and GEO; observation from the L1 Lagrange libration point also is possible.

Broadband radiometers are designed to measure the Earth radiation budget – upward LW and SW irradiance at the top of the atmosphere (TOA). Accuracy depends on their detailed features:

(a)   The greatest possible extension of the SW end of the spectrum into the UV range, and of the LW end of the spectrum into the FIR range, with a maximally flat response inside those ranges;

(b)   Built-in multiviewing capability to convert radiance into irradiance;

(c)   Supportive narrowband channels to collect information on clouds within the IFOV.

Tables 3.24 and 3.25 set out an example of a broadband radiometer in LEO (CERES) and one in GEO (GERB).

Table 3.24. Example of broadband radiometer in LEO: CERES on TRMM, EOS-Terra/Aqua, Suomi-NPP and JPSS

CERES	*Clouds and the Earth's Radiant Energy System*
Satellites	TRMM, EOS-Terra, EOS-Aqua, Suomi-NPP, JPSS-1
Mission	Earth radiation budget: upward LW and SW irradiance at TOA
Main features	Two broadband channels and one narrowband channel Either: two units, one for cross-track scanning, one for biaxial scanning for irradiance computation Or: one unit operating in alternative modes
Scanning technique	Cross-track: 80 steps of 20 km SSP Swath: 3 000 km; along-track: one 20 km line every 3 seconds Biaxial scanning by rotating azimuth while cross-nadir scanning
Coverage/cycle	Global coverage twice a day (IR and total radiance) or once a day (SW)
Resolution (SSP)	20 km
Resources	Double unit configuration: Mass: 114 kg Power: 100 W Data rate: 21 kbps

Channel	Spectral interval	Noise equivalent radiance	Absolute accuracy	SNR
SW	0.3–5.0 μm	0.3 W m^{-2} sr^{-1}	0.8 W m^{-2} sr^{-1}	225
Total radiance	0.3–100 μm	0.3 W m^{-2} sr^{-1}	0.6 W m^{-2} sr^{-1}	750
Narrowband	8–12 μm	0.3 W m^{-2} sr^{-1}	0.3 W m^{-2} sr^{-1}	750

Table 3.25. Example of broadband radiometer in GEO: GERB on Meteosat Second Generation

GERB	Geostationary Earth Radiation Budget
Satellites	Meteosat-8, Meteosat-9, Meteosat-10, Meteosat-11
Mission	Earth radiation budget: upward LW and SW irradiance at TOA
Main features	Two broadband channels
Scanning technique	N–S direction: pushbroom by a linear array of 256 detectors E–W provided by the spinning satellite Integration over 5 minutes to comply with SNR requirements and over 15 minutes to synchronize with SEVIRI
Coverage/cycle	Full disk every 15 minutes
Resolution (SSP)	42 km
Resources	Mass: 25 kg Power: 35 W Data rate: 50.6 kbps

Channel	Spectral interval	Noise equivalent radiance	Absolute accuracy	SNR
SW	0.32–4.0 μm	0.8 W m^{-2} sr^{-1}	2.4 W m^{-2} sr^{-1}	1 250
Total radiance	0.32–100 μm	0.15 W m^{-2} sr^{-1}	0.4 W m^{-2} sr^{-1}	400

3.2.9 Solar irradiance monitors

These instruments have the following main characteristics:

(a) Wavelengths in the solar radiation range 0.15–50 μm;

(b) Integration over the full range (total solar irradiance) and/or spectroscopy in the 0.15–3.00 μm range;

(c) Total solar irradiance is measured by absolute techniques, such as active cavity radiometers pointing at the Sun;

(d) Applicable both in LEO and in GEO.

Solar irradiance monitors complement broadband radiometers in order to measure the Earth radiation budget. They also contribute to solar activity monitoring for the purpose of space weather observation. Detailed features that affect their performance are:

(a) Extending their sensitivity to within the solar radiation range;

(b) Their capability to provide spectral information in context in the UV/VIS/NIR/SWIR ranges.

Table 3.26 sets out the main features of an example of a solar irradiance monitor in LEO (TSIS).

Table 3.26. Example of solar irradiance monitor in LEO:
TSIS on JPSS – Free Flyer (FF)

TSIS	Total and Spectral Solar Irradiance Sensor
Satellite	JPSS-FF (to be confirmed)
Mission	Solar irradiance monitoring (total and spectrally resolved)
Main features	Assemblage of: Four active cavity radiometers for total irradiance (total irradiance monitor: range of 0.2–10 μm), Prism spectrometer for spectral irradiance (spectral irradiance monitor: range of 0.2–2.0 μm; spectral resolution: 0.25–33 nm)
Scanning technique	Sun pointing during orbital movement; data sampled every two minutes
Coverage/cycle	100 minutes: one measurement after integration on all data taken during the diurnal orbit arc
Resolution (SSP)	Not applicable (Sun pointing)
Resources	Total irradiance monitor: Mass 7.9 kg; power 14 W; data rate 0.53 kbps Spectral irradiance monitor: Mass 22 kg; power 25.3 W; data rate 4.84 kbps

3.2.10 Lightning imagers

These instruments have the following main characteristics:

(a) Detector matrix (CCD): continuous Earth observation in a very narrow O_2 band at 777.4 nm;

(b) Measurement of flash rate and intensity in the IFOV;

(c) Spatial resolution of 5–10 km;

(d) Continuous and contiguous horizontal sampling; swath of several hundred kilometres from LEO, and full disk from GEO;

(e) Applicable in LEO and GEO.

Lightning imagery is useful as a proxy for convective precipitation and turbulence, in order to monitor the Earth's electric field, and as a proxy for NO_x generation. Different sampling is applicable from LEO and GEO:

(a) From LEO, the measurement is available for the interval during satellite motion in which one Earth's spot is visible within the field of view of the CCD matrix (about 90 seconds);

(b) From GEO, monitoring is continuous.

Tables 3.27 and 3.28 set out an example of a lightning imager in LEO (LIS) and one in GEO (GLM).

Table 3.27. Example of lightning imager in LEO: LIS on TRMM

LIS	Lightning Imaging Sensor
Satellite	Tropical Rainfall Measuring Mission (TRMM)
Mission	Proxy for convective precipitation and turbulence Proxy for NO_x generation Study of the Earth electric field
Main features	CCD camera operating at 777.4 nm (O_2) to count flashes and measure their intensity
Scanning technique	Pushbroom: matrix array of 128 x 128 detectors; swath of 600 km Each Earth location is observed continuously (every 2 milliseconds) for about 90 seconds
Coverage/cycle	Intertropical coverage: several sequences of passes at ~100 min intervals; longer gaps as latitude increases; more regular coverage at 15°N and 15°S
Resolution (SSP)	4 km
Resources	Mass: 21 kg Power: 33 W Data rate: 6 kbps

Table 3.28. Example of lightning imager in GEO: GLM on GOES

GLM	Geostationary Lightning Mapper
Satellites	GOES-R, GOES-S, GOES-T, GOES-U
Mission	Proxy for convective precipitation and turbulence Proxy for NO_x generation Study of the Earth electric field
Main features	CCD camera operating at 777.4 nm (O_2) to count flashes and measure their intensity
Scanning technique	Pushbroom: matrix array of 1 372 x 1 300 detectors; time resolution of 2 milliseconds
Coverage/cycle	Large fraction of the disk is continuously observed
Resolution (SSP)	8 km
Resources	Mass: 35 kg Power: 110 W Data rate: 77 Mbps

3.2.11 Cloud radar and precipitation radar

These instruments have the following main characteristics:

(a) Operating frequencies in K_u (~14 GHz), K_a (~35 GHz) or W (~94 GHz) bands;

(b) Pulse repetition rate that results in a vertical resolution of a few hundred metres;

(c) Spatial resolution of 2–5 km;

(d)   Continuous and contiguous horizontal sampling; swath from nadir-only to several hundreds of kilometres;

(e)   Only applicable in LEO.

The operating frequency determines possible applications:

(a) K_u band is suitable for heavy rain (liquid, with droplets that may exceed 1 cm). Non-precipitating clouds (droplets of less than 0.1 mm) are totally transparent, and light precipitation can hardly be detected. At these relatively low frequencies, electronic switching, which is necessary to avoid mechanical movements of large antennas, is relatively easy. Relatively wide swaths (several hundreds of kilometres) can therefore be implemented.

(b) K_a band is suitable for light rain (from stratiform clouds) and snowfall. Electronic switching is still possible, and swaths of a few hundreds of kilometres can be implemented.

(c)   W band is suitable for non-precipitating clouds (droplets of less than 0.1 mm). Several studies have also reported that this can be applied to the observation of precipitating cloud systems, specifically on the edges of precipitation or in cases of no precipitation, including the eye of tropical cyclones.

Tables 3.29 and 3.30 set out an example of a dual-frequency (K_u and K_a) precipitation radar (DPR) and an example of a W-band cloud radar (CPR on CloudSat).

Table 3.29. Example of precipitation radar: DPR on GPM Core Observatory

DPR	Dual-frequency Precipitation Radar
Satellite	Global Precipitation Measurement (GPM) Core Observatory
Mission	Vertical profile of heavy rain (liquid), light rain and snowfall
Main features	Dual-frequency imaging radar Frequencies: 13.6 GHz and 35.55 GHz Sensitivity: 0.5 mm/h at 13.6 GHz; 0.2 mm/h at 35.55 GHz
Scanning technique	Electronic scanning Planar array of 148 elements Swath: 245 km at 13.6 GHz; 125 km at 35.55 GHz
Coverage/cycle	Nearly global in 5 days High latitudes (> 65°) not covered
Resolution (SSP)	Horizontal: 5 km Vertical: 250 m (blind to the lowest ~150 m)
Resources	Mass: 780 kg Power: 710 W Data rate: 190 kbps

Table 3.30. Example of cloud radar: CPR on CloudSat

CPR	Cloud Profiling Radar
Satellite	CloudSat
Mission	Vertical profile of non-precipitating cloud water (liquid and ice)
Main features	Frequency: 94.05 GHz Sensitivity: 30 dBZ
Scanning technique	None. Along-track sampling at 2 km intervals

CPR	Cloud Profiling Radar
Coverage/ cycle	Global coverage in 1 month for 30 km average spacing, or in 10 days for 100 km average spacing
Resolution (SSP)	Horizontal: 1.4 km (cross-track) x 3.5 km (along-track) Vertical: 500 m
Resources	Mass: 230 kg Power: 270 W Data rate: 15 kbps

3.2.12 Radar scatterometers

These instruments have the following main characteristics:

(a) Operating frequencies in C (~5 GHz) or K_u (~14 GHz) bands;

(b) Very accurate calibration in order to measure backscatter coefficients (σ^0) from sea capillary waves;

(c) Spatial resolution: 10–50 km;

(d) Continuous and contiguous horizontal sampling; swath of approximately 1 000 km;

(e) Only applicable in LEO.

There are two concepts, mainly differing by the scanning principle (see Figure 3.9):

(a) Electronic scanning: side-looking, generally uses C band and provides three azimuth views for differential σ^0. It is more accurate for low-intensity sea-surface wind and for soil moisture.

(b) Conical scanning: generally uses K_u band, with two beams and two polarizations. It provides four azimuth views for differential σ^0.
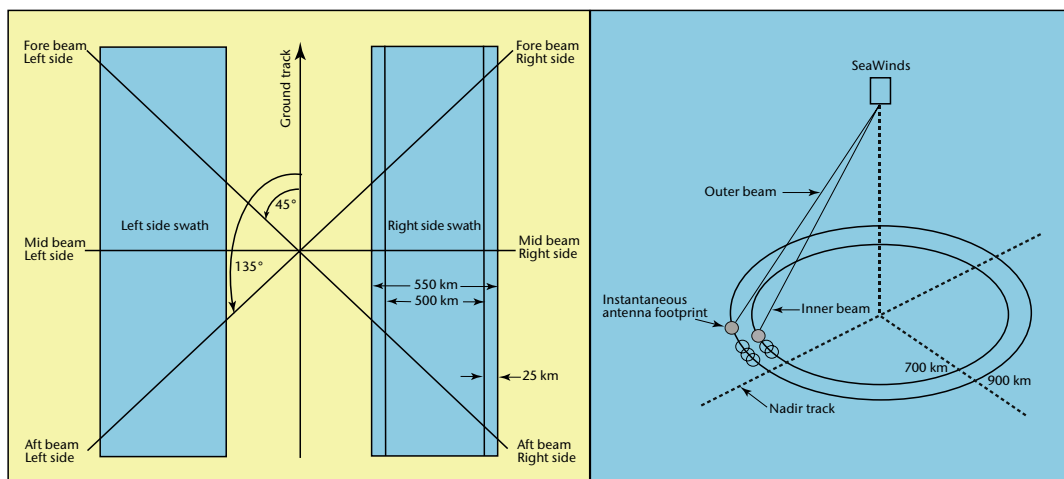
Figure 3.9. Two concepts for multiviewing scatterometers. Left: six antennas for three $\sigma = s$ under azimuth angles, 45°, 90° and 135° respectively, on both the left and right side of the sub-satellite track (ASCAT on Metop). Right: conical scanning of an antenna with two beams and two polarizations, for $\sigma = s$ under four azimuth angles for areas in the inner circle (SeaWinds on QuikSCAT). The ASCAT concept leaves an uncovered strip of ~700 km around the sub-satellite track. In the SeaWinds concept, there appears to be no gap, but accuracy is poor in the inner part of the swath around the sub-satellite track.

Tables 3.31 and 3.32 describe radar scatterometers using pushbroom scanning (ASCAT) and conical scanning (SeaWinds).

Table 3.31. Example of pushbroom radar scatterometer: ASCAT on Metop

ASCAT	Advanced Scatterometer
Satellites	Metop-A, Metop-B, Metop-C
Mission	Sea-surface wind vector; large-scale soil moisture
Main features	C band (5.255 GHz) Left and right side-looking 3 antennas on each side
Scanning technique	Two 550 km swaths, separated by a 700 km along-track gap 3 looks each pixel (45°, 90° and 135° azimuth)
Coverage/cycle	Global coverage in 1.5 days
Resolution (SSP)	Best quality: 50 km Standard quality: 25 km Basic sampling: 12.5 km
Resources	Mass: 260 kg Power: 215 W Data rate: 42 kbps

Table 3.32. Example of conical-scanning radar scatterometer: SeaWinds on QuikSCAT

SeaWinds	
Satellite	Quick Scatterometer (QuikSCAT) mission
Mission	Sea-surface wind vector
Main features	K_u band (13.4 GHz) Conical scanning 2 beams 2 polarizations
Scanning technique	Conical scanning: 2 beams to provide four views of each spot from different angles Swath: 1 800 km
Coverage/cycle	Global coverage every day
Resolution (SSP)	Best quality: 50 km Standard quality: 25 km Basic sampling: 12.5 km
Resources	Mass: 200 kg Power: 220 W Data rate: 40 kbps

3.2.13 Radar altimeters

These instruments have the following main characteristics:

(a)   Operating frequencies in K_u band (~14 GHz), with auxiliary C band (~5 GHz), or K_a band (~35 GHz);

(b)   Very accurate ranging measurement between the satellite and the Earth's surface;

(c)   Spatial resolution in the range of 20 km;
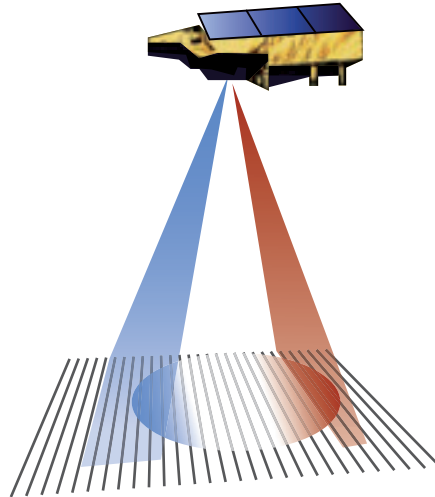
Figure 3.10. Enhancing along-track altimeter resolution by SAR-like signal processing

(d)   Exclusively nadir-pointing;

(e)   Only applicable in LEO.

Radar altimeters generally operate in K_u band, using C band for correction of the signal rotation induced by the ionosphere. They are linked to a nadir-pointing MW radiometer for water vapour correction. Their accurate ranging is used for ocean topography: the echo spread provides information on significant wave height, while the echo intensity provides information on wind speed.

Depending on the detailed features of the instrument and of the satellite orbit, altimeters may be optimized for different applications:

(a)   Relatively high, non-Sun-synchronous orbit (e.g. 1 336 km), where inclination provides high stability to the orbit (e.g. 66°); especially suited to solid Earth (geoid) and ocean circulation;

(b)   SAR-like processing of the return echoes to synthesize higher spatial resolution along the sub-satellite track (see Figure 3.10);

(c)   Parallel antennas to implement wide-swath altimetry by interferometry; particularly useful for land use including on inland waters, such as lakes;

(d)   Dual frequency (C and K_u bands), which provides information on the total electron content between a satellite and the Earth's surface.

Table 3.33 sets out the main features of a radar altimeter with data of geodetic quality (Poseidon-3).

Table 3.33. Example of radar altimeter: Poseidon-3 on JASON-2

Poseidon-3	*Solid-state radar altimeter – 3*
Satellite	JASON-2
Mission	Ocean topography, the geoid, significant wave height, wind speed, total electron content
Main features	2 frequencies: 5.3 GHz; 13.58 GHz

Poseidon-3	*Solid-state radar altimeter – 3*
Scanning technique	Nadir-only viewing Sampling at 30 km intervals along track
Coverage/cycle	Global coverage in 1 month for 30 km average spacing, or in 10 days for 100 km average spacing
Resolution (SSP)	30 km IFOV
Resources	Mass: 70 kg Power: 78 W Data rate: 22.5 kbps

3.2.14   **Imaging radar (synthetic aperture radar)**

This wide range of instruments has the following main characteristics:

(a)   Operating frequencies in P (~0.4 GHz), L (~1.3 GHz), S (~2.7 GHz), C (~5.3 GHz), X (~9.6 GHz), or K_u (~17.2 GHz) bands. The L, C and X bands are most commonly used;

(b)   Several combinations of polarizations in transmission and reception: HH, VV, VV/HH, HH/HV and VV/VH;

(c)   There is a trade-off between spatial resolution and swath: a 1–30 m resolution is associated with a swath of 30–100 km; but a 100–1 000 m resolution is associated with a swath of 300–500 km;

(d)   Side looking, generally on one side, maintaining high resolution within a field of regard of several hundreds of kilometres;

(e)   Applicable in LEO only.

Figure 3.11 illustrates the operating modes of one C-band SAR (ASAR).

The operating frequency is a critical feature, optimized for the purposes for which a synthetic aperture radar (SAR) is designed:

(a)   P band is most suited to biomass monitoring and hydrological mapping;

(b)   L band is best suited to wave observation and volumetric soil moisture;

(c)   S band is best suited to volumetric soil moisture;

(d)   C band covers a wide range of applications: sea ice, wave parameters by spectral analysis of image segments, surface soil moisture, snow parameters, glaciers, ground water, etc. However, each individual parameter can be optimally observed at other frequencies;

(e)   X band provides the best spatial resolution, and is therefore best suited to surveillance;

(f) K_a band is specifically suited to snow, which is transparent at lower frequencies;

(g)   Interferometry of the signals from one SAR at different times or two SARs flying in tandem enables the measurement of the digital elevation model and the detection of contour changes (such as coastlines and lakes) and elevation (e.g. volcano top surface).
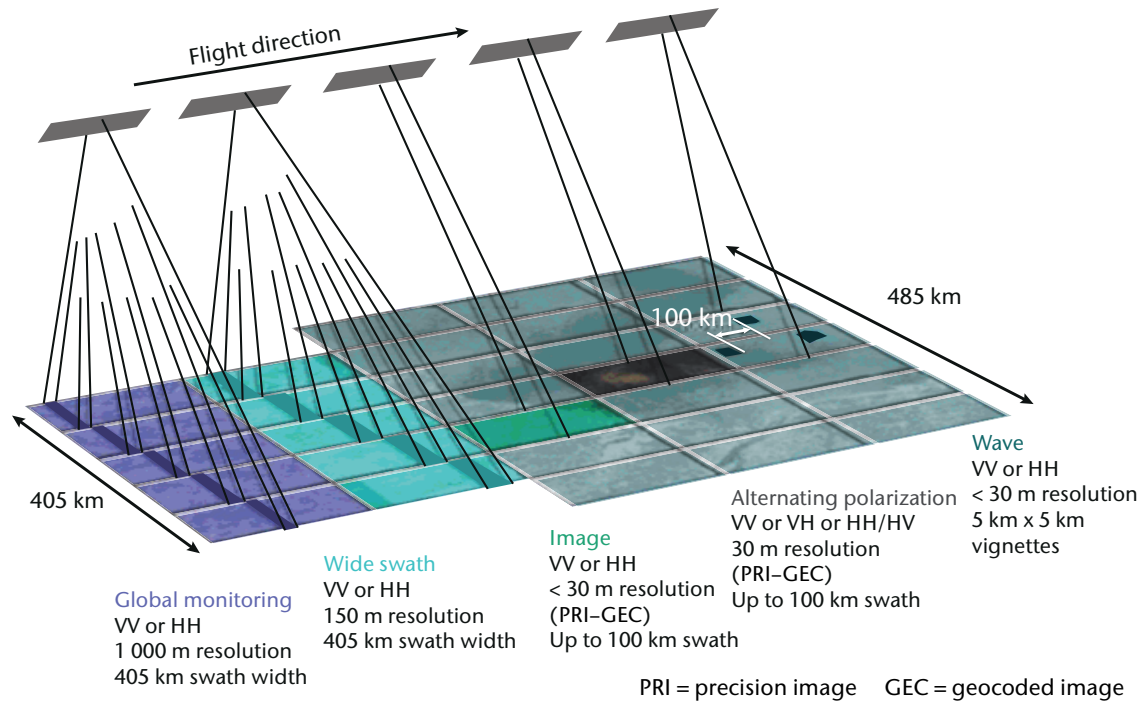
Figure 3.11. Operating modes of ASAR on Envisat. In the global monitoring and wide swath modes, the swath is 405 km and is linked to either a 1 000 m or 150 m resolution. In the image and alternating polarization modes, a 100 km swath with a 30 m resolution can be pointed to one of seven positions within a field of regard of 485 km. In the wave mode, vignettes of 5 km x 5 km with 30 m resolution are sampled at every 100 km along track.

Table 3.34 records the main features of a C-band SAR (ASAR).

Table 3.34. Example of C-band SAR: ASAR on Envisat

ASAR	Advanced Synthetic Aperture Radar
Satellite	Envisat
Mission	Sea ice, wave parameters by spectral analysis of image segments, surface soil moisture, snow parameters, glaciers, ground water, etc.
Main features	C-band SAR Frequency: 5.331 GHz Multipolarization and variable pointing/resolution
Scanning technique	Side-looking; 15°–45° off-nadir Swath: 100–405 km, depending on operation mode (see lower part of table)
Coverage/cycle	Global coverage in 5 day in global monitoring mode (if used for 70% of the time) Longer periods (up to 3 months) for other operation modes
Resolution (SSP)	30 m to 1 km, depending on operation mode (see lower part of the table)
Resources	Mass: 832 kg Power: 1 400 W Data rate: 100 Mbps

Operation mode	Resolution	Swath	Field of regard	Polarization
Stripmap	30 m	100 km	485 km	HH or VV
ScanSAR alternating pol	30 m	100 km	485 km	VV/HH, HH/HV, VV/VH
ScanSAR wide swath	150 m	405 km	405 km	HH or VV
ScanSAR wide swath	150 m	405 km	405 km	HH or VV
ScanSAR global monitoring	1 km	405 km	405 km	HH or VV
Wave	30 m	5 x 5 km² imagettes sampled at 100 km intervals		HH or VV

3.2.15   Lidar-based instruments

This group of instruments has the following main characteristics:

(a)   Operating wavelengths in the UV (e.g. 355 nm), VIS (e.g. 532 nm), NIR (e.g. 1 064 nm), or SWIR (e.g. 1 600 nm) bands;

(b)   Possible dual wavelength, two receivers (for Mie and Rayleigh scattering); polarimetry;

(c)   Horizontal resolution within a 100 m range, often degraded by up to 50 km in order to collect enough de-correlated samples;

(d)   Vertical resolution within a 100 m range (approximately 10 cm for lidar altimeters);

(e)   Non-scanning: either nadir-viewing or oblique.

A space lidar is a voluminous instrument that needs to be optimized for specific applications:

(a)   Doppler lidars generally operate in UV, for both Mie and Rayleigh scattering, in order to track aerosol and air molecules; oblique view is used to measure radial wind in clear air and aerosol;

(b)   Backscatter lidars operate at one (on UV) or two (VIS and NIR) wavelengths, often with more polarizations; nadir view is used for obtaining aerosol profiles, cloud-top height and atmospheric discontinuities, such as the height of the top of the planetary boundary layer and of the tropopause;

(c)   Lidar altimeters usually operate at two wavelengths (VIS and NIR); nadir view is used, as is very high-vertical resolution (for sea-ice elevation) and horizontal resolution (for ice boundaries);

(d)   Differential absorption lidar operate at one wavelength centred on the absorption peak of one trace gas, in UV, VIS, NIR or SWIR, and nearby windows; nadir view is used for high-vertical-resolution observation of, for example, O_3, H_2O and CO_2.

Tables 3.35–3.38 give details of a Doppler lidar (ALADIN), a backscatter lidar (CALIOP), a lidar altimeter (GLAS) and a differential absorption lidar (CO_2 lidar).

Table 3.35. Example of Doppler lidar: ALADIN on ADM-Aeolus

ALADIN	Atmospheric Laser Doppler Instrument
Satellite	Atmospheric Dynamics Mission (ADM) – Aeolus
Mission	Wind profile in clear air, aerosol profile, cloud-top height
Main features	Single-wavelength (355 nm), side-looking; 35° off-nadir High spectral resolution laser for distinguishing aerosol types
Scanning technique	No scanning Pulse echoes averaged over a 50 km field of view Field of view sampled at 200 km intervals
Coverage/cycle	Global coverage in 1 month for 30 km average spacing, or in 10 days for 100 km average spacing
Resolution (SSP)	Horizontal: 50 km field of view sampled at 200 km intervals Vertical: from 250 m in the planetary boundary layer to 2 km at ~20 km
Resources	Mass: 500 kg Power: 840 W Data rate: 11 kbps

Table 3.36. Example of backscatter lidar: CALIOP on CALIPSO

CALIOP	Cloud–Aerosol Lidar with Orthogonal Polarization
Satellite	Cloud–Aerosol Lidar and Infrared Pathfinder Satellite Observations (CALIPSO)
Mission	Aerosol profile, cloud-top height and atmospheric discontinuities (height of the top of the planetary boundary layer and of the tropopause)
Main features	Two wavelengths (532 and 1 064 nm) Measurements at two orthogonal polarizations
Scanning technique	Nadir-only viewing Sampling at 330 m intervals along track Near-continuous profiling
Coverage/cycle	Global coverage in 1 month for 30 km average spacing, or in 10 days for 100 km average spacing
Resolution (SSP)	Horizontal: 70 m IFOV sampled at 333 m intervals along track Vertical: 30 m
Resources	Mass: 156 kg Power: 124 W Data rate: 332 kbps

Table 3.37. Example of lidar altimeter: GLAS on ICESat

GLAS	Geoscience Laser Altimeter System
Satellite	Ice, Cloud and Land Elevation Satellite (ICESat)
Mission	Polar ice sheet thickness and topography, cloud-top height, aerosol
Main features	Dual-wavelength lidar (532 and 1 064 nm)

GLAS	Geoscience Laser Altimeter System
Scanning technique	Nadir-only viewing Sampling at 170 m intervals along track Near-continuous profiling
Coverage/ cycle	Global coverage in 183 days (orbit repeat cycle) Leaves cross-track 2.5 km gaps at 80° latitude (15 km at the Equator)
Resolution (SSP)	Horizontal: 66 m IFOV sampled at 170 m intervals along track Vertical: 10 cm surface, 200 m cloud top
Resources	Mass: 298 kg Power: 300 W Data rate: 450 bps

Table 3.38. Example of differential absorption lidar: CO_2 lidar on ASCENDS

CO_2 lidar	
Satellite	Active Sensing of CO_2 Emissions over Nights, Days, and Seasons (ASCENDS)
Mission	Monitoring CO_2 with unprecedented accuracy by using lidar
Main features	Wavelength: 1.572 μm for CO_2 Option for O_2 at 1 260 or 765 nm also considered
Scanning technique	Nadir-only viewing
Coverage/cycle	Global coverage in one month for 30 km average spacing, or in 10 days for 100 km average spacing
Resolution (SSP)	Horizontal: 125 m Vertical: total column
Resources	Mass: 420 kg Power: 920 W Data rate: 1.9 Mbps

3.2.16 **Gradiometers/accelerometers**

Knowledge of the gravity field is crucial for modelling the solid Earth. Several space techniques address this subject.

(a) The long-wave components of the gravity field are measured through radar or lidar altimetry, or through precise orbitography (e.g. with laser ranging, radio positioning, GNSS, star tracking).

(b) Short-wave components (anomalies and perturbations of the gravity field) are observed at satellite altitude by accelerometers or gradiometers, in association with satellite-to-satellite ranging systems. An accelerometer measures the variation of the gravity field along the satellite trajectory. A gradiometer comprises a network of accelerometers, which measures the gravity-gradient tensor. Satellite-to-satellite ranging systems are transmitter-receiver systems, usually in K band (24 GHz) and K_a band (32 GHz). They are designed to accurately measure the distance and its variations between satellites flying in coordinated orbits. The same measurements are possible through the simultaneous reception of signals from tens of GNSS satellites: that determines positioning changes highly accurately.

Tables 3.39 and 3.40 describe a gradiometer/accelerometer (EGG) and a satellite-to-satellite ranging system (HAIRS).

Table 3.39. Example of accelerometer/gradiometer: EGG on GOCE

EGG	Three-axis Electrostatic Gravity Gradiometer
Satellite	Gravity Field and Steady-state Ocean Circulation Explorer (GOCE)
Mission	Solid Earth Observation of the Earth's gravity field along the orbit
Main features	Three pairs of 3-axis accelerometers, specially assembled to measure the gravity-gradient tensor Accuracy: 10^{-12} m s^{-2} Resolution: 2 10^{-12} m s^{-2} Hz$^{-1/2}$

Table 3.40. Example of satellite-to-satellite ranging system: HAIRS on Gravity Recovery and Climate Experiment (GRACE)

HAIRS	High Accuracy Inter-satellite Ranging System
Satellites	GRACE (2 satellites flying in tandem, 220 km apart)
Mission	Solid Earth Observation of the Earth's gravity field along the orbit
Main features	Dual-frequency ranging, in K band (24 GHz) and K$_a$ band (32 GHz) Accuracy: 10 μm

3.2.17   Solar activity monitors

Solar activity is monitored either by remote-sensing or in situ in the solar wind, from deep space and Earth's orbit. Several measurement approaches are possible:

(a)   Electromagnetic radiation: measured by radiometers, spectrometers and polarimeters for γ-rays (less than 0.001 nm), X-ray (0.001–10 nm), extreme UV (10–120 nm), UV (120–380 nm), VIS (380–780 nm) and longer wavelengths including radio waves (more than 1 m);

(b)   Energetic particles (electrons, protons, α-particles, ions, cosmic rays, neutrons): the energy range is generally broken down into high-, medium- and low-energy; the boundaries of the ranges depend on the type of charged particle; measurements can be integrated over the full energy range, or over partial ranges; spectroscopy within a range may also be performed;

(c)   Magnetic and electric fields, directly measured in the solar wind, and inferred in the photosphere; those fields are inferred from measurements in the solar wind or from spectroscopy of VIS solar images using the Zeeman effect, Doppler analysis or multipolarization;

(d)   Measurements can be performed by: integrating over the full solar disk; imaging the solar disk; or imaging the corona only by occulting the disk (a coronagraph);

(e)   A specific observation is that of solar irradiance, either total or spectrally resolved (see section 3.2.9).

An example of an instrument package for solar activity monitoring from the L1 Lagrange libration point, SOHO, is described in Table 3.41.

3.2.18 Space environment monitors

Space environment monitoring at platform level provides information used for monitoring and making predictions about overall space weather conditions, as well as for platform safety. The instrumentation generally includes:

(a) Charged particle detectors, designed for specific ranges of energy, either integrated or spectrally resolved;

(b) Magnetometers and electrometers.

An example of an instrument package for in situ space environment monitoring, GGAK-M, is described in Table 3.42.

3.2.19 Magnetometers and electric field sensors

Magnetic and electric fields in the magnetosphere can be measured in situ as the satellite moves along its orbit. If the orbit is highly eccentric, it crosses the magnetosphere at different altitudes, thus providing 3D profiles. Gradients of the fields are better observed when more satellites are flown together in coordinated orbits. Usual instruments are:

(a) Either scalar or vector magnetometers;

(b) Electron fluxometers (used to compute the electric field).

An example of an instrument package, Cluster, for 3D observation of the magnetosphere, which uses four satellites, is described in Table 3.43.

Table 3.41. Example of solar activity monitoring package: SOHO instrumentation

SOHO instrumentation	
Satellite	Solar and Heliospheric Observatory (SOHO)
Mission	Sun monitoring from the L1 Lagrange point
Main features	Solar atmosphere remote-sensing instrument package:
	Solar UV Measurement of Emitted Radiation (SUMER)
	Coronal Diagnostic Spectrometer (CDS)
	Extreme UV Imaging Telescope (EIT)
	UV Coronagraph and Spectrometer (UVCS)
	Large Angle and Spectrometric Coronagraph (LASCO)
	Solar Wind Anisotropies (SWAN)
	Solar wind "in situ particle" instrument package:
	Charge, Element and Isotope Analysis System (CELIAS)
	Comprehensive Suprathermal and Energetic Particle Analyzer (COSTEP)
	Energetic and Relativistic Nuclei and Electron Experiment (ERNE)
	Helio-seismology instrument package (study of the Sun's interior):
	Global Oscillations at Low Frequencies (GOLF)
	Variability of Solar Irradiance and Gravity Oscillations (VIRGO)
	Michelson Doppler Imager (MDI)
Scanning technique	Sun pointing
Coverage/cycle	Continuous from the L1 Lagrange point
Resources (of the satellite)	Mass: 1 850 kg
	Power: 1.5 kW
	Data rate: 200 kbps

Table 3.42. Example of space environment monitoring package: GGAK-M on Meteor-M

GGAK-M	Geophysical Monitoring System Complex
Satellites	Meteor-M N1, Meteor-M N2, Meteor-M N2-1, Meteor-M N2-2
Mission	Space environment monitoring at platform level
Main features	Spectrometer for Geoactive Measurements (MSGI-MKA) package: Electron fluxes in the energy range 0.1–15 keV (high-sensitivity channel) Ion (proton) fluxes in the energy range 0.1–15 keV (high-sensitivity channel) Electron fluxes in the energy range 0.1–15 keV (low-sensitivity channel) Monitoring of integral electron fluxes with a threshold energy of 40 keV Radiation Monitoring System (KGI-4C) package: Total proton flux threshold energy of: 5, 15, 25, 30 and 40 MeV Total electron flux threshold energy of: 0.17, 0.7, 1.7, 2.0 and 3.2 MeV Proton fluxes with threshold energies of: 25 and 90 MeV
Resources	Mass: 17 kg Power: 13.6 W Data rate: 16 kbps

Table 3.43. Example of magnetosphere monitoring package: Cluster instrumentation

Cluster instrumentation	
Satellites	Cluster A, B, C and D (four satellites flying together in coordinated orbits)
Mission	Monitoring of the 3D magnetosphere
Main features	Package of the following instruments: Fluxgate Magnetometer (FGM) Spatio-temporal Analysis of Field Fluctuations (STAFF) Electric Fields and Waves (EFW) Waves of High Frequency and Sounder for Probing of Density by Relaxation (WHISPER) Wide Band Data (WBD) Digital Wave Processor (DWP) Electron Drift Instrument (EDI) Cluster Ion Spectrometry (CIS) experiment Plasma Electron and Current Analyzer (PEACE) Research with Adaptive Particle Imaging Detectors (RAPID) Active Spacecraft Potential Control (ASPOC)
Scanning technique	4 satellites travelling across the magnetosphere in highly elliptical orbits
Coverage/cycle	Continuous; in situ along the orbit
Resources (of one satellite)	Mass: 1 200 kg Power: 224 W Data rate: 16.9 kbps

CHAPTER CONTENTS

CHAPTER 4. SATELLITE PROGRAMMES

The measurements described in Part III, Chapter 2 are performed within satellite programmes[1] implemented by space agencies with either an operational mandate to serve particular user communities, or a priority mandate for research and development. In addition to the core meteorological constellations in geostationary and near-polar Sun-synchronous orbits, these programmes include environmental missions focusing on specific atmospheric parameters, ocean and ice, land observation, solid Earth or space weather. Many of these environmental missions are designed and operated in a research or demonstration context, but some of them have reached operational maturity, and contribute to the sustained observation of environmental components, especially when they have been extended over time and/or they give way to an operational follow-on. Further information on measurement principles and uncertainties for geophysical variables can be found in Part III, Chapter 5.

For each type of application, satellite missions may be seen as constituent parts of constellations of spacecraft that, in many cases, will deliver their full benefit only when implemented in a coordinated fashion, ensuring synergy among the different sensors. International coordination among satellite operators is achieved within the Coordination Group for Meteorological Satellites, the primary goal of which is to maintain the operational meteorological and climate monitoring constellations, and the Committee on Earth Observation Satellites, which has initiated "virtual constellations" with thematic objectives (ocean surface topography, precipitation, atmospheric composition, land surface imaging, ocean surface vector wind, ocean colour radiometry and sea-surface temperature).

The following mission categories are considered:

(a)   Operational meteorological satellites;

(b)   Specialized atmospheric missions;

(c)   Missions on ocean and sea ice;

(d)   Land-observation missions;

(e)   Missions on solid Earth;

(f)   Missions on space weather.

4.1   OPERATIONAL METEOROLOGICAL SATELLITES

The system of operational meteorological satellites constitutes the backbone of the space-based Global Observing System. It is split into two components, according to the orbital characteristics:

(a)   Constellation in geostationary or highly elliptical orbit;

(b)   Constellation in Sun-synchronous orbits.

4.1.1   Satellite constellation in geostationary or highly elliptical orbit

The geostationary orbit is particularly suited for operational meteorology because it enables very frequent sampling (at sub-hourly or minute rates) as necessary for rapidly evolving phenomena (daily weather) or detecting events such as lightning, as long as no very high spatial resolution is required (order of 1 km). The primary observations from the geostationary orbit are:

---

[1]   Details on these programmes are available in the WMO online database on space-based capabilities, which is updated on a regular basis.

(a)   Cloud evolution (detection, cover, top height and temperature, type, water phase at cloud top, particle size);

(b)   Frequent profile of temperature and humidity to monitor atmospheric stability;

(c)   Winds by tracking clouds and water-vapour patterns (including wind profile from water-vapour profile tracking);

(d)   Convective precipitation (in combination with microwave (MW) data from low Earth orbit (LEO) satellites and lightning detection);

(e)   Rapidly changing surface variables (sea-surface temperature in coastal zones, fires);

(f)   Ozone and other trace gases affected by diurnal variation or arising from changing sources.

One drawback of the geostationary orbit is the poor visibility at high latitudes, beyond about 60° for quantitative measurements and 70° for qualitative. This limitation can be overcome by using high-eccentricity inclined orbits (Molniya, Tundra or three-apogee orbits) instead of the geostationary orbit (see Part III, Chapter 2, 2.1.4). Additionally, the diffraction limit due to the small angles subtended by the large distance poses challenges for very high-resolution optical imagery and MW radiometry. MW observation for all-weather temperature and humidity sounding and quantitative precipitation measurement from geostationary Earth orbit (GEO) should be feasible by using high frequencies, as the technology becomes available.

The requirement for global non-polar frequent observations from the geostationary satellites calls for six regularly-spaced spacecraft (Figure 4.1). In an operational constellation, backup satellites are required to provide redundancy above this minimum.

Table 4.1 lists the operational programmes that agreed to contribute to the constellation of meteorological geostationary satellites in 2012, and their nominal positions. Other positions may be used on a temporary basis, for instance in contingency situations.
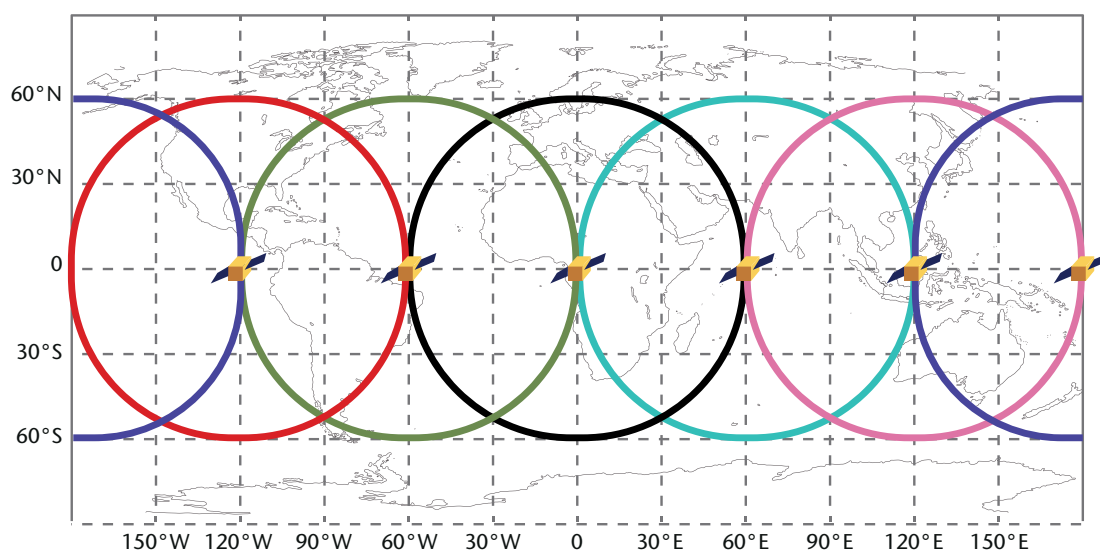
Figure 4.1. Coverage from six regularly-spaced geostationary satellites. The circles subtend a geocentric angle of 60°, considered the practical limit for quantitative observations (for qualitative use, images actually extend beyond). All latitudes between 55°S and 55°N are covered.

**Table 4.1. Present and planned satellite programmes
of the operational meteorological system in GEO**

Acronym	Full name	Responsible	Nominal position(s)
GOES	Geostationary Operational Environmental Satellite	NOAA	75°W and 135°W
Meteosat	Meteorological Satellite	EUMETSAT	0°
Electro/GOMS	Electro/Geostationary Operational Meteorological Satellite	RosHydroMet	76°E, 14.5°W and 166°E
INSAT and Kalpana	Indian National Satellite and Kalpana	ISRO	74°E and 93.5°E
FY-2 and FY-4	Feng-Yun-2 and follow-on Feng-Yun-4	CMA	86.5°E and 105°E
COMS and GEO-KOMPSAT	Communication, Oceanography and Meteorology Satellite and follow-on Geostationary Korea Multi-purpose Satellite	KMA	128.2°E or 116.2°E
Himawari/ MTSAT	Himawari, including Multifunctional Transport Satellite	Japan Meteorological Agency	140°E

4.1.2   Satellite constellation in Sun-synchronous orbits

The Sun-synchronous orbit provides global coverage necessary for applications such as global numerical weather prediction (NWP), polar meteorology, and climatology. For these applications, very frequent sampling is less critical than global coverage and high accuracy. The primary contributions from Sun-synchronous orbits are:

(a)   Profile of temperature and humidity as primary input to NWP;

(b)   Cloud observations at high latitudes complementing GEO;

(c)   Precipitation observations by MW radiometry;

(d)   Surface variables (sea and land surface temperatures, vegetation and soil-moisture indexes);

(e)   Ice cover, snow, hydrological variables;

(f)   Surface radiative parameters (irradiance, albedo, photosynthetically active radiation, fraction of absorbed photosynthetically active radiation);

(g)   Ozone and other trace gases for environment and climate monitoring.

Additional advantages of Sun-synchronous and other low Earth orbits are the capability to perform active sensing in the MW (radar) and optical (lidar) ranges and limb measurements of the higher atmosphere.

Global coverage at roughly four-hour intervals can be achieved by three Sun-synchronous satellites in coordinated orbital planes crossing the equator at, for instance, 05:30, 09:30 and 13:30 local solar time, provided that the instrument swath is sufficiently wide and the measurement can be performed by both day and night (see Figure 4.2).

Table 4.2 lists the operational programmes contributing now or in the future to the constellation of meteorological Sun-synchronous satellites as of 2012.

VIS/IR imagery with
cross-track scanning
– swath 2 900 km

IR/MW sounding with
cross-track scanning
– swath 2 200 km

Microwave radiometer with
conical scanning
– swath 1 700 km
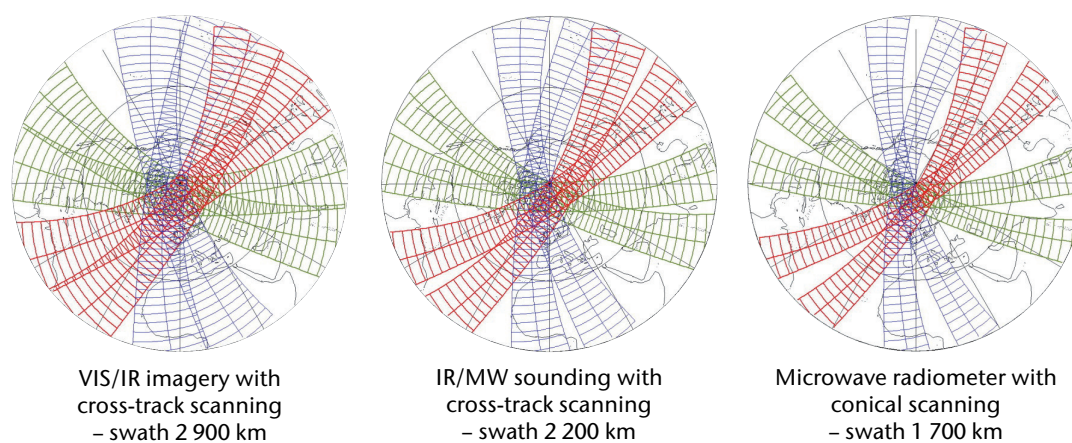
Figure 4.2. Coverage from three Sun-synchronous satellites of height 833 km and equatorial crossing time (ECT) regularly spaced at 05:30 d, 09:30 d and 13:30 a. For the purpose of this schematic diagram, all satellites are assumed to cross the equator at 1200 universal coordinated time (UTC). The figure refers to a time window of 3 h and 23 min (to capture two full orbits of each satellite) centred on 1200 UTC. Three typical swaths are considered. Nearly three-hour global coverage is provided for the VIS/IR imagery mission, whereas for the IR/MW sounding mission coverage is nearly complete at latitudes above 30 degrees. For microwave conical scanners, global coverage in three hours would require eight satellites.

4.2 SPECIALIZED ATMOSPHERIC MISSIONS

4.2.1 Precipitation

Precipitation is a basic meteorological variable, but its measurement requires the exploitation of the microwave spectral range at a resolution consistent with the scale of the phenomenon and at relatively low frequencies; this implies large instruments. Moreover, the relation between passive MW sensing and precipitation is not explicit. Only total-column precipitation is measured, and only in a few channels. The retrieval problem is strongly ill-conditioned and requires modelling of the vertical cloud structure, which can only be observed by radar. The Tropical

**Table 4.2. Present and planned satellite programmes
of the operational meteorological system in LEO**

Acronym	Full name	Responsible	Height	Nominal ECT
NOAA	National Oceanic and Atmospheric Administration	NOAA	833 km	13:30 a
Suomi-NPP	Suomi National Polar-orbiting Partnership	NOAA	833 km	13:30 a
JPSS	Joint Polar Satellite System	NOAA	833 km	13:30 a
DMSP	Defense Meteorological Satellite Program	DoD	833 km	05:30 d
Metop	Meteorological Operational Satellite	EUMETSAT	817 km	09:30 d
Metop-SG	Meteorological Operational Satellite – Second Generation	EUMETSAT	817 km	09:30 d
FY-3	Feng-Yun-3	CMA	836 km	10:00 d and 14:00 a
Meteor-M	Meteor, series "M"	RosHydroMet	830 km	09:30 d and 15:30 a
Meteor-MP	Meteor, series "MP"	RosHydroMet	830 km	09:30 d and 15:30 a

Figure 4.3. Concept of the Global Precipitation Measurement mission

Rainfall Measuring Mission (TRMM; launched in 1997), that carries associated passive and active MW sensors, has enabled algorithms to be developed that allow much better use of passive measurements.

The TRMM mission has enabled the concept of a Global Precipitation Measurement mission to be developed that is being implemented in an international context. Its objective is to provide global coverage of precipitation measurements at three-hour intervals. Since the baseline instrument is an MW conical scanning radiometer with limited swath, the three-hour frequency requires eight satellites in regularly distributed near-polar orbits (Figure 4.3). In addition to those "constellation satellites", a "Core Observatory" in inclined orbit equipped with precipitation radar enables all other measurements from passive MW radiometers to be "calibrated" when constellation and core-satellite orbits cross one another. Beyond the missions specifically tailored for precipitation observation, any operational mission equipped with MW radiometers can contribute to the composite system.

4.2.2 Radio occultation

Radio occultation of GNSS satellites is a powerful technique for providing temperature and humidity profiles with a vertical resolution that is unachievable by nadir-viewing instruments. However, the implementation of operational systems is proceeding slowly. One difficulty is that the payload, although of low mass, power and data rate (see, for instance, the description of the GNSS Receiver for Atmospheric Sounding (GRAS) in Part III, Chapter 3, 3.2.7, Table 3.23), places volumetric constraints on the platform (two large antennas, say 0.5 m^2 each, requiring unobstructed view fore and aft). Another difficulty is that the technique requires a significant number of satellites in different orbits.

The radio occultation concept was demonstrated in space in 1995 by the Global Positioning System/Meteorology (GPS/MET) on MicroLab-1. Since then, establishing a constellation of radio occultation receivers has been advocated, initially for climatological purposes to provide "absolute" measurements that can be compared at any time intervals to detect climate trends, then also for NWP high vertical resolution soundings and for the absolute reference measurements correcting the biases of other sounding systems.

Radio occultation is an infrequent event. By exploiting one GNSS constellation and tracking both rising and setting occultations, about 500 occultation events per day may be captured. In addition to the long-standing GPS and GLONASS, a third constellation, Compass (named

Beidou in Chinese), is now operated by China, and a fourth constellation, Galileo, is being implemented by the European Commission (EC) and the European Space Agency (ESA). The number of occultations per day per satellite rises to 1 000 by exploiting two constellations and 1 500 with three constellations if received in both fore and aft views. It has been estimated that, in order to provide global coverage with an average sampling of 300 km every 12 h, it is necessary to deploy at least 12 satellites on properly distributed orbital planes. One very effective approach is to use clusters of small dedicated satellites placed in orbit by a single launch. The Constellation Observing System for Meteorology, Ionosphere and Climate (COSMIC) includes six micro-satellites launched at once and thereafter separated into regularly-spaced orbits. Several meteorological satellites are also carrying individual GNSS radio-occultation receivers.

4.2.3   **Atmospheric radiation**

A limitation of NWP and general circulation models is the representation of the radiative processes in the atmosphere. Aerosols, cloud interior (particularly ice), radiation fluxes within the 3D atmosphere in addition to the top of the atmosphere (TOA) and the Earth surface, are their main factors. Some of these variables require large observing instruments (lidar, cloud radar, etc.) that are not feasible for multi-purpose operational meteorological satellites, thus the observation of atmospheric radiation relies on a suite of instruments flown either in operational programmes or on dedicated missions.

Atmospheric radiation was the first observation performed from space in October 1959 on Explorer VII. At the time of the first Television and Infrared Observation Satellite (TIROS) flights the Earth's planetary albedo was poorly known. Instruments exploiting multi-viewing, multi-polarization and multi-spectral sensing have been developed, the first one being the Polarization and Directionality of the Earth's Reflectances (POLDER) on the Advanced Earth Observing Satellite – 1 (ADEOS-1; 1996–1997).

Observing atmospheric radiation requires contributing factors to be observed in parallel. Since the radiation budget is a small difference between large quantities, errors of spatial and time co-registration have a high impact on accuracy. Since it is impossible to embark all instruments on a single platform, the concept of formation flying has been implemented, such as the A-Train (Figure 4.4). In this concept, several satellites are flying on nearly the same Sun-synchronous orbit, at 705 km altitude, ECT ~13:30 ascending node, following each other along the same ground track within a few seconds.
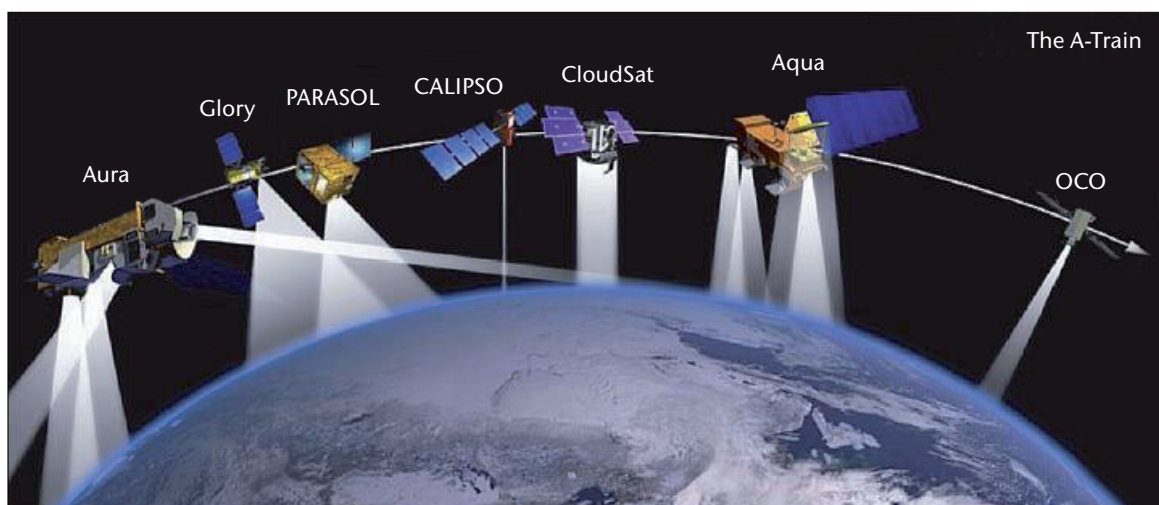
Figure 4.4. The spread of equatorial crossing times across the satellites addressing atmospheric radiation (Glory, PARASOL, CALIPSO, CloudSat and EOS-Aqua) is about two minutes. Note that there may be some changes in the satellites participating in the A-Train; for instance PARASOL was removed after five years, EOS-Aura has been added, Glory failed at launch, OCO, lost at launch, will be replaced by OCO-2, and GCOM-W1 has been added.

4.2.4   **Atmospheric chemistry**

Atmospheric chemistry has grown in importance over time. Attention was focused initially on ozone monitoring, especially after the discovery of the ozone hole; then on the greenhouse effect as a driver of global warming; and finally on air quality, for its impact on living conditions in the biosphere. Depending on the objective, the instrumentation may be quite simple (such as for total column of one or few species) or very complicated (such as for vertical profiles of families of species).

It is noted that:

(a)   On meteorological satellites, infrared (IR) hyperspectral sounders primarily designed for temperature and humidity sounding do contribute to atmospheric chemistry observation, but their performance for chemistry is limited to total columns of a few greenhouse species. The short-wave (SW) instruments are primarily designed for ozone and a few species in the ultraviolet (UV) and visible (VIS) ranges;

(b)   Some atmospheric-chemistry missions are hosted on large multi-purpose facilities, or on dedicated atmospheric-chemistry satellites.

The first comprehensive mission for atmospheric chemistry, the Upper Atmosphere Research Satellite (UARS) was exploiting limb sounding. When launched, in 1991, it was by far the largest Earth observation satellite ever in orbit (mass at launch: 6 540 kg). Table 4.3 provides a list of satellites either substantially addressing, or fully dedicated to, atmospheric chemistry.

The lack of limb sounding on future satellites jeopardizes the observation of the higher atmosphere.

Table 4.3. Satellite programmes with strong or exclusive focus on atmospheric chemistry

Acronym	Full name	Responsible	Measurements
Envisat	Environmental Satellite	ESA	IR limb, SW nadir and limb, UV/VIS star occultation
EOS-Aura	Earth Observation System – Aura	NASA	IR limb, IR nadir and limb, UV/VIS nadir, MW limb
GOSAT	Greenhouse Gas Observing Satellite	JAXA	NIR/SWIR/MWIR/TIR nadir
Odin	Odin	SNSB	UV/VIS/NIR limb, MW limb
OCO-2	Orbiting Carbon Observatory	NASA	NIR/SWIR nadir
SCISAT	Scientific Satellite	CSA	UV/VIS/NIR and SWIR/MWIR/TIR Sun occultation
Sentinel-4	Sentinel-4 on Meteosat Third Generation	ESA, EUMETSAT, EC	UV/VIS/NIR nadir
Sentinel-5P	Sentinel-5 precursor	ESA, EC	UV/VIS/NIR/SWIR nadir
Sentinel-5	Sentinel-5 on Metop Second Generation	ESA, EUMETSAT, EC	SW nadir

Note:
SNSB = Swedish National Space Board
CSA = Canadian Space Agency
NIR = near infrared
SWIR = short-wave infrared
MWIR = medium-wave infrared
TIR = thermal infrared

4.2.5   Atmospheric dynamics

The study of atmospheric dynamics involves missions measuring the 3D wind field, a difficult issue since the wind per se does not have a signature in the electromagnetic spectrum. Nevertheless, considerable effort has been devoted and continues to be devoted to the subject, since wind is a primary observation for NWP and general circulation models.

Deriving wind characteristics from the motion of clouds or other atmospheric patterns has been an early application of geostationary satellites. Still today, it is the operational practice providing thousands of wind vectors every day. Tracking clouds or water vapour patterns, however, determines the wind at one level only. The level depends on the tracer and is measured with limited accuracy. For large areas, all tracers tend to be in the same altitude range, thus limiting the vertical resolution in practice to one or two levels. With the future advent of hyperspectral sounders in GEO, frequent water vapour profiles, with their patterns, will be available at additional heights, and a broad vertical resolution will be achieved in clear air. Atmospheric motion winds are also derived over polar areas from polar-orbiting satellites, taking advantage of the frequent overpasses.

Experiments have been conducted to demonstrate the tracking of atmospheric eddies, aerosol and molecules by Doppler lidar, capable of very high vertical resolution in clear air. This is the scope of the Atmospheric Dynamics Mission (ADM) – Aeolus mission with the Atmospheric Laser Doppler Instrument (ALADIN).

Winds are also of interest in the stratosphere and mesosphere, where clouds and water vapour have no characteristic pattern, and there are no turbulence eddies or dense aerosols either. The technique applicable here is measurement of the Doppler shift of narrow lines in the oxygen band around 760 nm. Demonstrated by UARS, the technique is exploited by TIMED with TIDI (TIMED Doppler Interferometer).

4.3   MISSIONS ON OCEAN AND SEA ICE

Certain observations of ocean and sea ice have been provided by meteorological satellites since the very beginning of the space era. VIS imagery, the very first application of meteorological satellites, is capable of sea-ice mapping. IR imagery added the capability to measure sea-surface temperature. MW imagery extended the observing capability to measure sea-surface temperature and ice cover to all-weather conditions, and added the capability to sea-surface wind speed. Radar scatterometry started in 1978. These observations of sea-surface temperature, sea-surface wind, and ice cover are still provided by operational meteorological satellites. Further measurements, including altimetry, ocean colour, salinity, and waves, are performed in the framework of non-meteorological programmes, sometimes dedicated to ocean and sea ice.

Table 4.4 lists satellite programmes addressing ocean and sea ice.

Table 4.4. Satellite programmes addressing missions on ocean and sea ice

Acronym	Full name	Responsible	Oceanographic missions
COMS	Communication, Oceanography and Meteorology Satellite	KMA	Ocean colour from GEO
Coriolis	Coriolis	DoD, NASA	Surface wind by MW polarimetry
CryoSat	Cryosphere Satellite	ESA	Radar altimetry for ice
Envisat	Environmental Satellite	ESA	Ocean colour Radar altimetry
EOS-Aqua	Earth Observation System – Aqua	NASA	Multi-purpose MW imagery (large antenna) Ocean colour

Acronym	Full name	Responsible	Oceanographic missions
EOS-Terra	Earth Observation System – Terra	NASA	Ocean colour
FY-3	Feng-Yun-3	CMA	Ocean colour Surface wind by C- and K_u-band scatterometer
GCOM-C	Global Change Observation Mission for Climate	JAXA	Ocean colour
GCOM-W	Global Change Observation Mission for Water	JAXA	Multi-purpose MW imagery (large antenna)
GEO-KOMPSAT	Geostationary Korea Multi-purpose Satellite	KMA	Ocean colour from GEO
HY-1	Hai Yang-1	NSOAS, CAST	Ocean colour
HY-2	Hai Yang-2	NSOAS, CAST	Radar altimetry Surface wind by K_u-band scatterometer
ICESat	Ice, Cloud and Land Elevation Satellite	NASA	Lidar altimetry for ice
JASON	Joint Altimetry Satellite Oceanography Network	NASA, CNES, EUMETSAT, NOAA	Radar altimetry, geoid
JPSS	Joint Polar Satellite System	NOAA	Ocean colour
Meteor M/MP N3	Meteor-M and Meteor-MP, flight units N3	RosHydroMet	Ocean colour Surface wind by K_u-band scatterometer
Metop and Metop-SG	Meteorological Operational satellite and follow-on Metop Second Generation	EUMETSAT	Surface wind by C-band scatterometer
OceanSat	Satellite for the Ocean	ISRO	Ocean colour Surface wind by K_u-band scatterometer
SAC-D/ Aquarius	Satélite de aplicaciones científicas – D	NASA, CONAE	Ocean salinity (real-aperture antenna)
SARAL	Satellite with Argos and Altika	CNES, ISRO	Radar altimetry
Sentinel-3	Sentinel-3	ESA, EC, EUMETSAT	Ocean colour Radar altimetry
SMOS	Soil Moisture and Ocean Salinity	ESA	Ocean salinity (synthetic aperture antenna)
Suomi-NPP	Suomi National Polar-orbiting Partnership	NASA, NOAA, DoD	Ocean colour

Note:
KMA = Korea Meteorological Administration
DoD = Department of Defense (United States)
CMA = China Meteorological Administration
JAXA = Japan Aerospace Exploration Agency
NSOAS = National Satellite Ocean Application Service (China)

Note *(cont.)*:
CAST = China Academy of Space Technology
CNES = National Centre for Space Studies (France)
EUMETSAT = European Organization for the Exploitation of Meteorological Satellites
ISRO = Indian Space Research Organisation
CONAE = Argentine Space Agency

4.3.1   **Ocean topography**

Ocean surface topography is a primary mission for oceanography, since it provides insight into the large-scale ocean circulation that is a major oceanographic feature and a basic component of the climate system. Reconstruction of ocean topography also implies accurate determination of the geoid, an insight into the solid Earth domain.

Radar altimetry is the only observing technique for ocean topography. Altimeters are carried by different satellites, some multi-purpose platforms to provide global coverage, and some (since the Topography Experiment (TOPEX) – Poseidon in 1992–2006) dedicated satellites in specially stable orbits to provide accurate reference measurements. Some altimeters are specifically designed for polar-ice topography, in one case exploiting lidar for more accurate boundary detection and vertical resolution (see Table 4.4).

4.3.2   **Ocean colour**

Ocean colour is a very informative observation to infer the state of health of the ocean, its productivity and its capacity to interact with the atmosphere, as a CO_2 sink, for example. Therefore, it is a basic observation for operations in open ocean and in coastal zones, and for climatology.

Several satellites address ocean colour observation. Some of them belong to the operational meteorology framework; one is in geostationary orbit (see Table 4.4).

4.3.3   **Sea-surface wind**

Wind over the sea surface is a basic measurement for oceanography since it drives atmospheric forcing, hence surface currents, and the intensity of air–sea interaction. Of course, it is also an important geophysical variable for weather prediction, enabling derivation of surface pressure that cannot be directly measured from space. Therefore, several wind-observing instruments are part of the operational meteorological mission. Table 4.4 records the missions addressing sea-surface winds that are able to provide both speed and direction (radar scatterometer either in the C band operated in the pushbroom manner, which involves scanning a swath straight down, or in the K_u band with conical scanning; and polarimetric MW passive radiometers). Other passive MW radiometers, that can contribute to wind-speed observation, are mentioned only for multi-purpose MW imagers with large antennas.

4.3.4   **Sea-surface salinity**

Salinity is a basic measurement for oceanography since, with temperature, it controls water density, hence the vertical motion in the thermo-haline layer. Furthermore, it controls the ocean's ability to remove trace gases from the atmosphere. Measuring salinity from space is possible only by low-frequency MW radiometry (L band around 1.4 GHz), which requires large antennas. Missions addressing sea-surface salinity are based either on a synthetic-aperture antenna, or on a real-aperture antenna (see Table 4.4).

4.3.5 **Waves**

The observation of waves is important for ocean operations, in the open ocean and even more so in coastal zones. It is also important for coastal-zone climatology. Unfortunately, waves are difficult to observe from space, since the direct measurement from the radar altimeter provides only the significant wave height, and only along the satellite track. The altimeter missions are listed in Table 4.4.

The 2D wave field can be observed by spectral analysis of SAR imagery. In principle, any vignette from a SAR image could be processed to provide the dominant wave direction and period, as well as the directional energy frequency spectrum. In practice, the vignettes are sampled at intervals during the whole orbit, and stored on board since the associated data rate is rather low. The Envisat Advanced Synthetic Aperture Radar (ASAR) performs this function in wave mode.

4.4 **LAND-OBSERVATION MISSIONS**

All imagery missions of the operational meteorological satellites provide information on several geophysical variables characterizing land surface. Specifically:

(a)   VIS/IR imaging instruments: land surface temperature, soil moisture indexes, several vegetation indexes, several fire parameters, radiative parameters, ice and snow cover;

(b)   MW imaging instruments: all-weather land surface temperature, surface-soil moisture, several ice and snow parameters;

(c)   Radar scatterometers: surface-soil moisture, total biomass, snow water equivalent.

However, the design of the instruments flown on operational meteorological satellites is driven by the main objective of describing the surface–atmosphere interface processes, as necessary (and sufficient) for weather analysis and prediction and by the need for the observed spatial-temporal scales to be consistent with climate monitoring requirements. This section focuses on satellite programmes addressing land applications as primary objectives, for geophysical variables such as land cover and use, fraction of vegetated land, vegetation type, lake and glacier cover, topography, small-scale soil moisture and snow parameters for hydrology.

These applications require spatial resolutions at the scale of metres or a few tens of metres, which imply using optical bands (especially VIS) or imaging radar (SAR). Another application of very high-resolution optical imagery or SAR is security, including disaster monitoring, control of compliance with internationally agreed protocols for environmental protection, etc.

4.4.1 **Main operational or near-operational missions**

Land observation has been the second space application, after meteorology, to give rise to operational programmes. The first land-observation satellite, initially named the Earth Resources Technology Satellite (ERTS), thereafter re-named Landsat-1, was launched by the National Aeronautics and Space Administration (NASA) in July 1972. Since then, other space agencies have undertaken land-observation programmes, often in a fairly operational way. Table 4.5 lists the programmes that have a demonstrated heritage of continuity or are designed for long-term continuity.

4.4.2 **The Disaster Monitoring Constellation**

The Disaster Monitoring Constellation (DMC) initiative was originally promoted by the British National Space Centre (BNSC). The principle of the DMC (see Figure 4.5) was to have about five satellites in the same orbit, separated by about 20 min, in such a way that the (narrow) swath of the instruments of one satellite (~600 km) was contiguous with the next, thus ensuring daily

Table 4.5. Land-observation satellite programmes designed for long-term continuity

Acronym	Full name	Responsible	Programme objective/nature
Amazônia	Amazônia	INPE	Vegetation monitoring
ASNARO	Advanced Satellite with New System Architecture for Observation	NEC, USEF	Commercially-oriented programme
CartoSat	Satellite for Cartography	ISRO	Cartography update
CBERS	China-Brazil Earth Resources Satellite	CAST, INPE	Earth resources search and management
GeoEye	GeoEye	GeoEye	Commercial programme
KANOPUS-V	KANOPUS Vulkan	Roscosmos	Vegetation monitoring
Landsat and LDCM	Landsat and Landsat Data Continuity Mission	USGS, NASA	Earth resources search and management
Resurs DK and P	Resurs-DK and Resurs-P	Roscosmos	LEO, high-inclination
Pléiades	Pléiades	CNES	Land-use and hazard management
ResourceSat	Satellite for Earth Resources	ISRO	Earth resources search and management
Sentinel-2	Sentinel-2	ESA, EC	Vegetation monitoring
SPOT 4, 5	Satellite Pour l'Observation de la Terre	CNES	Earth resources search and management
SPOT 6, 7	Satellite Pour l'Observation de la Terre	SpotImage	Commercially-oriented programme
WorldView	World View	DigitalGlobe	Commercial programme

Note:
INPE = National Institute for Space Research (Brazil)
NEC = Nippon Electric Company
USEF = Institute for Unmanned Space Experiment Free Flyer (Japan)
USGS = US Geological Survey

global coverage. The first DMC satellite was AlSat-1, launched in November 2002. A cluster of three satellites, UK-DMC-1, NigeriaSat-1 and Bilten Satellite (BILSat), was placed in orbit by a single launch in September 2003. Over time, more partners joined the constellation, and the instrumentation became more elaborate. Table 4.6 depicts the current situation, which includes satellites not strictly part of the DMC, but close in objective, structure and instrumentation.

4.4.3 All-weather high-resolution monitoring (by synthetic aperture radar)

All missions listed for land observation have a common limitation: observations are not available in the presence of clouds. In most cases, night-time is also a limitation since most instruments use only the VIS spectral range. In an emergency, when high resolution is needed, it is very important to have an all-weather sensing capability, which can be provided only by synthetic aperture radar (SAR). Several SAR missions are available, many of them being managed with a perspective for long-term operational continuity.

The number of SARs in orbit is important, since SAR instruments have a narrow swath, whereas their application to disaster monitoring requires frequent revisit times. In addition, the SAR principle is applicable with a single frequency, whereas various features to be observed have "signatures" at different frequencies. The SIR-C/X-SAR mission (Shuttle Imaging Radar with Payload C/X-SAR), flown twice on the US Space Shuttle in April and September 1994,

Table 4.6. Satellite programmes of the Disaster Monitoring Constellation and similar

Acronym	Full name	Agency/Country	Instrument capability
AlSat	Algeria Satellite	CNTS, Algeria	Multi-spectral and panchromatic
BJ	Beijing	NRSCC, China	Multi-spectral and panchromatic
Deimos	Deimos	CDTI, Spain	Multi-spectral
DubaiSat	Dubai Satellite	EIAST, United Arab Emirates	Multi-spectral and panchromatic
EnMAP	Environmental Mapping and Analysis Programme	DLR, Germany	Hyperspectral
FORMOSAT-2	Formosa Satellite – 2	NSPO, Taiwan Province of China	Multi-spectral and panchromatic
HJ A, B	Huan Jing A and B	CAST, China	Hyperspectral and multispectral
Ingenio (SEOSat)	Ingenio (Spanish Earth Observation Satellite)	CDTI, Spain	Multi-spectral and panchromatic
KOMPSAT	Korea Multi-purpose Satellite	KARI, Republic of Korea	Multi-spectral and panchromatic
NigeriaSat	Nigeria Satellite	NASRDA, Nigeria	Multi-spectral and panchromatic
PRISMA	Precursore Iperspettrale della Missione Applicativa	ASI, Italy	Hyperspectral and panchromatic
RapidEye (5 sats)	RapidEye (5 satellites)	DLR, Germany	Multi-spectral
Rasat	Earth observation satellite	Tübitak-Uzay, Turkey	Multi-spectral and panchromatic
SSOT	Sistema satelital para observación de la tierra	ACE, Chile	Multi-spectral and panchromatic
SumbandilaSat	Sumbandila Satellite	SANSA, South Africa	Multi-spectral
THEOS	Thailand Earth Observation System	GISTDA, Thailand	Multi-spectral and panchromatic
TopSat	TopSat	BNSC, UK	Multi-spectral and panchromatic
UK-DMC	UK Disaster Monitoring Constellation	BNSC, UK	Multi-spectral
X-Sat	X Satellite	NTU, Singapore	Multi-spectral

Note:
CNTS = National Centre of Space Technology
NRSCC = National Remote-sensing Centre of China
CDTI = Centre for the Development of Industrial Technology
EIAST = Emirates Institution for Advanced Science and Technology
NSPO = National Space Organization
KARI = Korea Aerospace Research Institute
NASRDA = National Space Research and Development Agency
ACE = Chilean Space Agency
SANSA = South African National Space Agency
GISTDA = Geo-informatics and Space Technology Development Agency
NTU = Nanyang Technological University

demonstrated the benefit of having simultaneous SAR imagery in the L, C and X bands (L and C provided by NASA, X by the German Aerospace Centre (DLR) and the Italian Space Agency (ASI)).

Table 4.7 lists all current and planned missions equipped with a SAR, grouped by frequency band and responsible agency.

4.5   **MISSIONS ON SOLID EARTH**

Since the early days of space missions, satellites have been used to reconstruct the shape of the geoid by means of various orbits of different heights, inclinations and eccentricity. The main purpose was internal: to support mission analysis for orbiting satellites. As time passed and technology has improved, the purpose has evolved towards the study of the Earth itself.

The satellite objectives for solid Earth are (see Figure 4.6 for definitions):

(a)   To provide a very accurate determination of the geoid, which is the basis for several associated applications, particularly conversion of altimeter measurements into sea level and ocean topography. The most common technique uses radar altimetry from orbits of relatively high altitude and high stability;

(b)   To infer crustal dynamics by monitoring local site positions from satellites in well-known and stable orbits; common techniques are laser ranging and ground-based GPS receivers;

(c)   To infer the dynamics of the outermost layers of the Earth (lithosphere, mantle, upper part of the mesosphere); common techniques use measurements of the gravity field and its anomalies by very low-orbiting satellites, and satellite-to-satellite tracking;

(d)   To collect information on the inner parts of the globe (lower mesosphere, liquid core, solid core) inferred through observation of the magnetosphere in satellite measurements of the magnetic and electric fields.
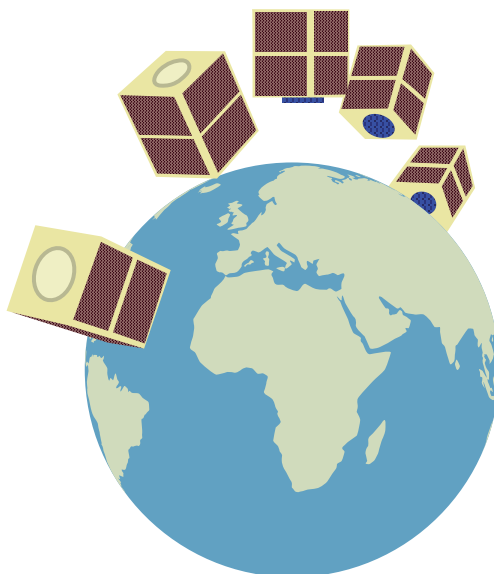
Figure 4.5. Concept of the DMC, based on five satellites dephased by about 20 min

Table 4.7. Current and planned SAR programmes

Acronym	Full name	Agency/Country	Frequency band
ALOS	Advanced Land Observing Satellite	JAXA, Japan	L band
SAOCOM-1	Satélite argentino de observación con microondas – series 1	CONAE, Argentina	L band
SAOCOM-2	Satélite argentino de observación con microondas – series 2	CONAE, Argentina	L band
HJ-1C	Huan Jing 1C	CAST, China	S band
Envisat	Environmental Satellite	ESA	C band
RadarSat	RadarSat	CSA, Canada	C band
RCM	RadarSat Constellation Mission	CSA, Canada	C band
RISAT-1	Radar Imaging Satellite – 1	ISRO, India	C band
Sentinel-1	Sentinel-1	ESA	C band
CSG	Constellation of Small Satellites for Mediterranean Basin Observation (COSMO) SkyMed Second Generation	ASI, Italy	X band
CSK	COSMO-SkyMed	ASI, Italy	X band
KOMPSAT-5	Korea Multi-purpose Satellite – 5	KARI, Republic of Korea	X band
Meteor M and MP	Meteor-M and Meteor-MP	RosHydroMet	X band
Paz (SEOSAR)	Paz (Spanish Earth Observation SAR)	CDTI, Spain	X band
RISAT-2	Radar Imaging Satellite – 2	ISRO, India	X band
TerraSAR-X	TerraSAR-X	DLR, Germany	X band
TanDEM-X	TanDEM-X	DLR, Germany	X band
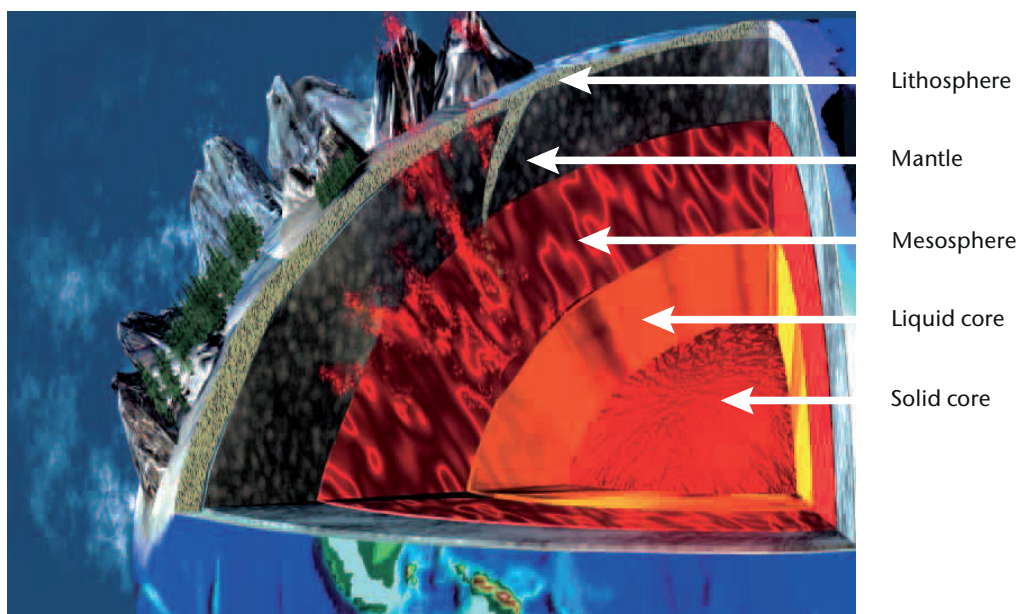
Figure 4.6. Stratification of the solid Earth

Table 4.8. Missions specific to solid Earth

Acronym	Full name	Responsible	Sensing systems
STARLETTE and Stella	Satellite de taille adaptée avec réflecteurs laser pour les études de la terre, and Stella	CNES	Laser ranging
LAGEOS 1 and 2	Laser Geodynamics Satellite, 1 and 2	ASI, NASA	Laser ranging
LARES	Laser Relativity Satellite	ASI	Laser ranging
GOCE	Gravity Field and Steady-state Ocean Circulation Explorer	ESA	Gradiometer, laser ranging
GRACE (2 sats)	Gravity Recovery and Climate Experiment	NASA, DLR, CNES	Accelerometer, laser ranging, satellite-to-satellite ranging
CHAMP	Challenging Mini-satellite Payload	DLR	Accelerometer, laser ranging, magnetometer
Ørsted	Ørsted	DNSC, CNES, NASA	Magnetometers
SAC-C	Satélite de aplicaciones científicas – C	CONAE	Magnetometer
SWARM (3 sats)	The Earth's Magnetic Field and Environment Explorers	ESA, CNES, CSA	Accelerometer, electric field sensor, magnetometers

Note:
DNSC = Danish National Space Center

This section considers two families of missions:

(a) Those referring to the geoid and crustal positioning and movements (space geodesy);

(b) Those referring to the lithosphere and inner layers (Earth interior).

Table 4.8 lists missions specific to solid Earth, for either geodesy or the interior.

4.5.1 Space geodesy

The primary technique for reconstructing the geoid (the equipotential surface which would coincide exactly with the mean ocean equilibrium surface, if the oceans were at rest and extended through the continents) is radar altimetry. Other information on the geoid stems from the precise positioning systems on any satellite. Several of them are worthy of mention:

(a) Laser retro-reflectors, to accurately measure the distance and rate of change for the satellite from the laser source on the ground;

(b) On-board transponder of signals from ground transmitting-receiving stations;

(c) Two-way and dual-frequency microwave tracking system for ground receiving stations;

(d) Global navigation satellite systems (GNSS);

(e) Star trackers, utilized for satellite attitude control but also contributing to precise orbitography.

The primary purpose of these systems is to support precise orbit determination as necessary for certain instruments performing the satellite mission, the most sensitive of which are altimeters and limb sounders. The benefit for the geodetic mission stems from the statistical analysis of the

Earth's gravity field anomalies (milligals)

−50 −40 −30 −20 −10 0 10 20 30 40 50
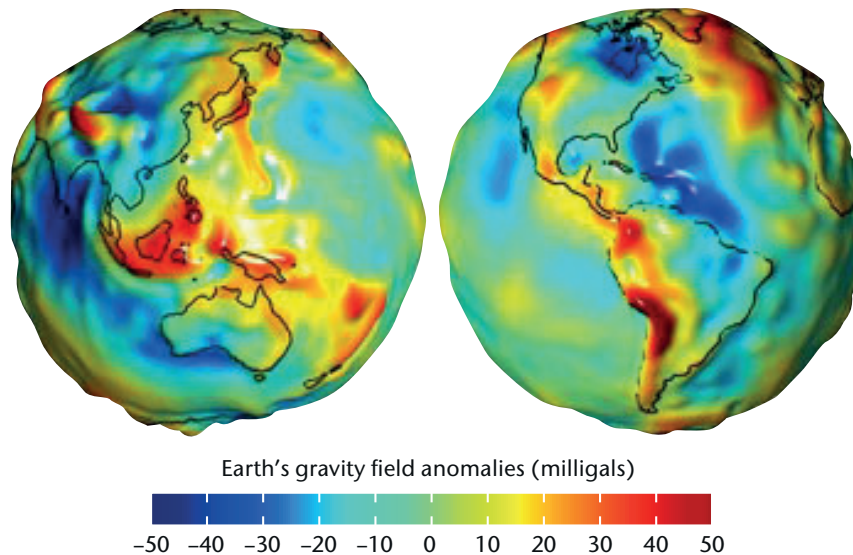
Figure 4.7. Three-dimensional visualization of geoid undulations.
(1 Gal = 0.01 m/s² and 1 mGal ≈ 10^{-6} g_0)

data. In this section the focus is on the application with the opposite objective: to establish the position of a ground station assuming that the orbit is well known. To this effect, an International Terrestrial Reference System for space geodesy has been established to collect and analyse data in a number of coordinated centres. The system includes a few satellites having space geodesy as a unique objective. These are listed in Table 4.8.

4.5.2   **Earth's interior**

The representation of the geoid is now fairly precise, despite its complexity. With the help of mathematical models using spherical harmonics, the achieved accuracy is now in the range of 1 cm or less. Figure 4.7 shows a current view of the geoid. It may be observed that, in this representation, the Earth's surface is not at all a regular ellipsoid, although the vertical range of the geoid height is contained within 200 m. The regularity of the geoid is affected by undulations of different wavelengths ranging from many thousands of kilometres to a few hundred. One objective is to associate these anomalies with the Earth's interior, first of all to the lithosphere because of its relevance to volcanism and earthquakes.

Specific missions for studying the Earth's interior exploit gravity and gravity-gradient observations, representative of the external layers (lithosphere, mantle and upper mesosphere); and magnetic and electric fields, significant for the internal layers (lower mesosphere, liquid core and solid core) (see Figure 4.6). Table 4.8 lists missions on the Earth's interior.

4.6   **MISSIONS ON SPACE WEATHER**

Although the term "space weather" is relatively recent, the relevant activities started with the advent of the space era, if not before, because space weather has a strong impact on the safety of satellites in orbit and of man in space. Awareness and prediction of the space environment has now become a prerequisite for the long-term sustainability of space activities. In addition, there is increasing awareness of the impact of space weather on facilities on the Earth.

Space weather is characterized by electromagnetic bursts from the X to the radio bands, solar energetic particle events, and perturbations in the solar wind density and speed, such as interplanetary coronal mass ejections propagating plasma blobs. In particular, the solar wind modulations compress and shape the magnetosphere, and this effect propagates lower down

to the thermosphere and ionosphere. Telecommunications and even power grids, pipelines and other conducting networks on the Earth's surface are affected (by geomagnetically induced currents, for example). Rapid magnetic changes on the ground, that occur during geomagnetic storms and are associated with space weather, can also be important for activities such as geophysical mapping and hydrocarbon production. Correlations have been discovered between travelling ionospheric disturbances and atmospheric gravity waves in the thermosphere.

Monitoring space weather implies two main aspects: monitoring the electromagnetic and particle solar emission as well as the solar wind to characterize the modulation source (solar activity), and monitoring the effects of this activity within the magnetosphere and down to the Earth's surface.

4.6.1   Solar activity monitoring

There have been space missions to understand solar physics since the early days of the space era, either from deep space orbits or from Earth orbits.

Two "sentinels" of solar wind, the joint NASA/ESA SOHO mission and the NASA Advanced Composition Explorer (ACE) mission, were launched in 1995 and 1998, respectively. SOHO and ACE have been placed at the L1 Lagrangian point (at 1% of the Earth–Sun distance upstream of the Earth). From that vantage point the two satellites measure solar wind and the associated magnetic field approximately one hour before they reach the Earth. In 2006, in collaboration with several European scientific institutes, NASA launched the Solar–Terrestrial Relations Observatory (STEREO), two satellites moving in the Earth's orbit around the Sun, viewing the Sun from changing positions to obtain a stereoscopic view of the dynamics of coronal mass ejection and, at the same time, to measure the local features, at the satellite position, of the solar wind.

Several missions in Earth orbit are also carrying instruments dedicated to continuous monitoring of solar activity. Table 4.9 lists the satellites monitoring solar activity from positions in deep space or in Earth orbit. In addition, some geostationary meteorological satellites (GOES or FY-4 series) contribute or will contribute to solar monitoring.

4.6.2   Magnetosphere and ionosphere monitoring

Closer to the Earth (see Figure 4.8(a) and (b)), the thermosphere and ionosphere are the layers where space weather is more turbulent. The main driver of the ionization state of the ionosphere is solar electromagnetic radiation (extreme ultraviolet and ultraviolet) which, in turn, is modulated by solar activity. The ionosphere is affected by waves, storms and travelling disturbances. Through interaction with magnetic storms, energetic particles and electrical currents can occur, which affect radio propagation. Mapping electron density in the ionospheric "E-region" enables ionospheric conductivity and currents to be inferred. When associated with magnetic field data, this information enables the internal component of the magnetic field (due to the solid Earth) to be discriminated from external components. Small-scale irregularities and eddies of the ionosphere can cause scattering of radio waves (scintillation), which affects the reliability of radio links crossing the ionosphere.

4.6.2.1   *Observation of the magnetosphere*

Missions dedicated to the magnetosphere have a long-standing heritage. Two significant current examples are the Time History of Events and Macroscale Interactions during Substorms (THEMIS) and MMS.

THEMIS is a NASA mission launched in 2007. It consists of a constellation of five small satellites in highly eccentric orbits, crossing the magnetosphere at several altitudes (see Figure 4.9), with periods ranging from 0.8 to 4 days.

Table 4.9. Missions specific to solar activity monitoring

Acronym	Full name	Responsible	Orbit
ACE	Advanced Composition Explorer	NASA	L1 Lagrange point
Aditya-1	Aditya-1	ISRO	LEO, Sun-synchronous
DSCOVR	Deep Space Climate Observatory	NOAA, NASA	L1 Lagrange point
Hinode	Hinode (former name: SOLAR-B)	JAXA	LEO, Sun-synchronous
IRIS	Interface Region Imaging Spectrograph	NASA	LEO, Sun-synchronous
Picard	Picard	CNES	LEO, Sun-synchronous
PROBA 1 and 2	Project for On-board Autonomy 1 and 2	ESA	LEO, Sun-synchronous
RHESSI	Reuven Ramaty High Energy Solar Spectroscopic Imager	NASA	LEO, low-inclination
SDO	Solar Dynamics Observatory	NASA	Geosynchronous, low inclination
SOHO	Solar and Heliospheric Observatory	ESA, NASA	L1 Lagrange point
Solar Orbiter	Solar Orbiter	ESA, NASA	Solar orbit
Solar Probe Plus	Solar Probe Plus	NASA	Solar orbit
STEREO (2 sats)	Solar–Terrestrial Relations Observatory	NASA	Ecliptic plane
TIMED	Thermosphere, Ionosphere, Mesosphere Energetics and Dynamics mission	NASA	LEO, high-inclination
WIND	Comprehensive Solar Wind Laboratory for Long-term Solar Wind Measurements	NASA	L1 Lagrange point
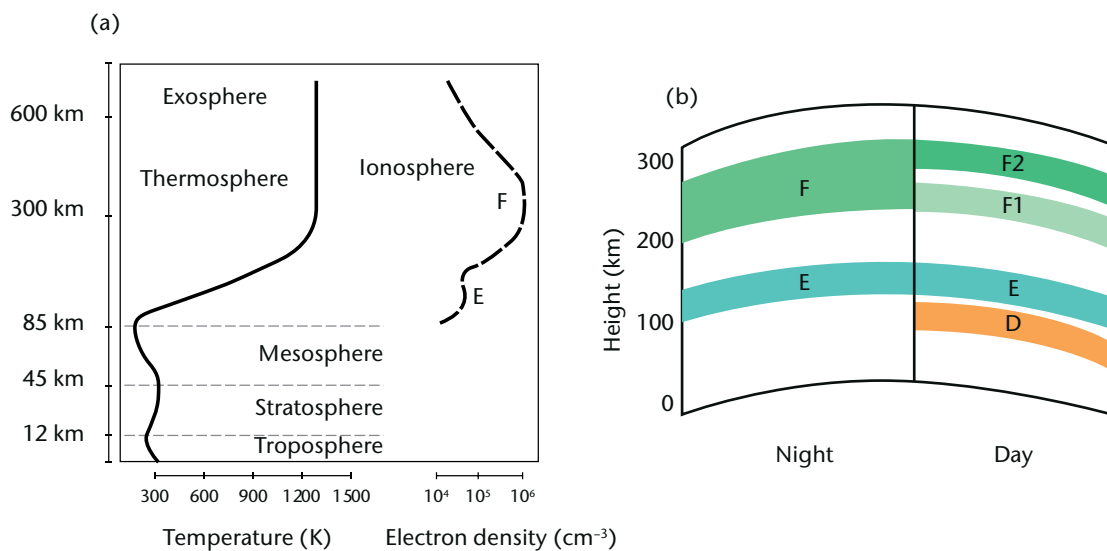
Figure 4.8. (a) Atmospheric stratification below and above the mesopause; (b) Layers of denser electronic content. The densest layer is F2, present day and night.
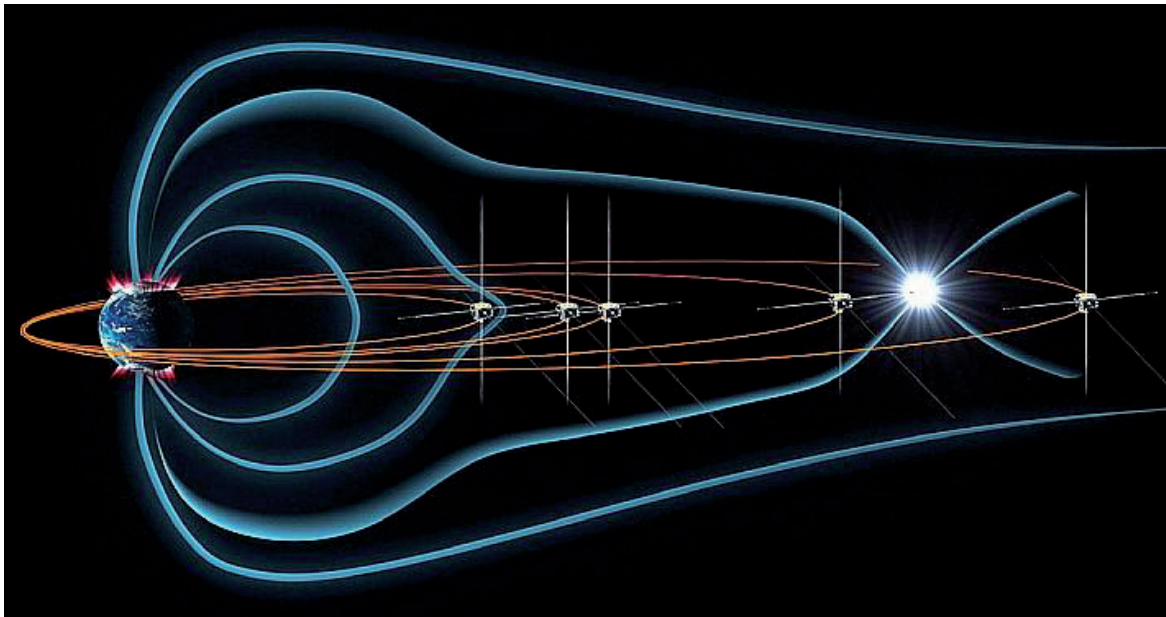
Figure 4.9. The orbits of the five THEMIS satellites in the magnetosphere. The white flash represents the energy released by a magnetospheric substorm.

THEMIS measures the magnetic field, electric fields and charged particles in order to address the physical processes in near-Earth space that initiate the violent eruptions of the aurora occurring during substorms in the Earth's magnetosphere. The system also includes a number of ground stations, to detect auroras and measure the surface magnetic field.

The MMS mission developed by NASA is based on a constellation of four satellites with highly eccentric orbits spread across the magnetosphere, similarly to THEMIS (see Figure 4.10). Plasma analysers, energetic particle detectors, magnetometers, and electric field instruments are used to study the microphysics of magnetic reconnection, the ultimate driver of space weather. Table 4.10 lists a number of missions specifically addressing the magnetosphere.
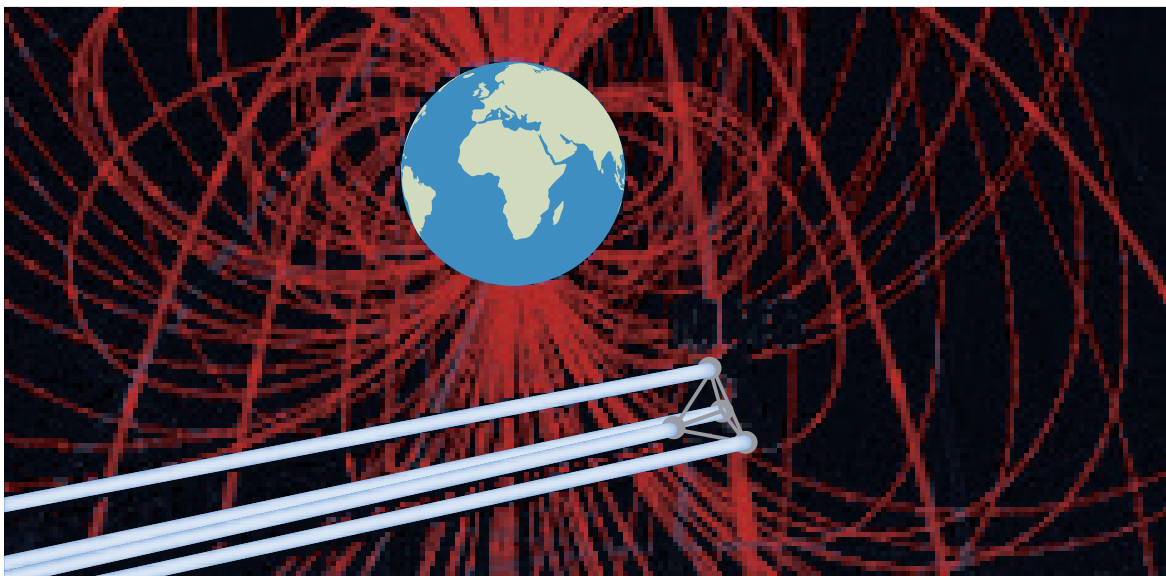
Figure 4.10. The four MMS satellites flying in formation. Tetrahedral pattern is used to capture the 3D structure of the encountered reconnection sites.

Table 4.10. Non-exhaustive list of missions orbiting inside the magnetosphere

Acronym	Full name	Responsible	Orbit
Arctica-M	Arctica-M	RosHydroMet	Molniya orbit
ARTEMIS	Acceleration, Reconnection, Turbulence, and Electrodynamics of the Moon's Interaction with the Sun	NASA	Lunar orbit
C/NOFS	Communication/Navigation Outage Forecasting System	DoD, NASA	LEO, low inclination
CASSIOPE	Cascade SmallSat and Ionospheric Polar Explorer	CSA	Highly elliptic, high inclination, relatively low altitude
Cluster (4 sats)	Cluster	ESA, NASA	Highly elliptic, polar inclination, tetrahedral formation flight
Geotail	Geotail	JAXA, NASA	Extremely elliptic, low inclination, crossing the moon orbit
IBEX	Interstellar Boundary Explorer	NASA	Highly elliptic, low inclination
IMAGE (or Explorer 78)	Imager for Magnetopause-to-Aurora Global Exploration	NASA	High-eccentricity polar orbit
Ionozond (5 sats)	Ionozond	Roscosmos	Four sats in Sun-synchronous orbit, one in drifting orbit
MMS (4 sats)	Magnetospheric Multiscale mission	NASA	Highly elliptic, low inclination, tetrahedral formation flight
SAMPEX (or Explorer 68)	Solar Anomalous and Magnetospheric Particle Explorer	NASA	Polar orbit
THEMIS (5 sats)	Time History of Events and Macroscale Interactions during Substorms	NASA	Highly elliptic, low inclination, apogees at five different altitudes
TWINS (2 sats)	Two Wide-angle Imaging Neutral-atom Spectrometers	NASA, United States Air Force	Molniya orbit
VAP (2 sats)	Van Allen Probe (formerly RBSP, Radiation Belt Storm Probes mission)	NASA	Highly elliptic, low inclination, crossing the radiation belts

Section 4.5 describes a number of missions in lower orbit that also carry instruments relevant to the magnetosphere:

(a) Ørsted: Fluxgate Vector Magnetometer (FVM) and scalar Overhauser Magnetometer (OVM);

(b) SAC-C: Magnetic Mapping Payload/Ørsted-2 (MMC/Ørsted-2);

(c) CHAMP: Magnetometer Instrument Assembly System (MIAS);

(d) SWARM: Absolute Scalar Magnetometer (ASM), Vector Field Magnetometer (VFM) and Electric Field Instrument (EFI).

4.6.2.2 *Observation of the ionosphere*

With the advent of radio occultation sounding, the profile of the electron density across the ionosphere has become the best measurable geophysical variable associated with space weather.

The signal from navigation satellites (GPS, GLONASS, Compass, Galileo) is affected by the rotation of the electric field and the delay induced by the ionosphere. In order to correct for this effect, at least two frequencies are used (now shifting to three): ~1 180 GHz, ~1 580 GHz and, possibly, ~1 250 GHz. Differentiating the two (or three) signals yields information on:

(a)   The total electron content (TEC);

(b)   The electron density profile.

The TEC, although integrated along-view, is measured for changing tangent heights; it is therefore possible to reconstruct the vertical profile by tomography. Several radio occultation payloads are being flown, on both multi-purpose satellites and dedicated facilities (such as the COSMIC constellation).

Radar altimeters also provide TEC observations by exploiting two frequencies, generally ~13.5 GHz and ~5.3 GHz. The coverage is only at nadir and tomography is not possible; however, since altimetry missions are often orbited at high altitude (1 336 km for JASON, for example), the measurement includes the lower part of the plasmasphere (the layer above the thermosphere, from ~1 000 to ~40 000 km altitude).

TEC can also be measured directly by phase-delay analysis of the two or three frequencies transmitted by a GNSS satellite and received by a LEO satellite. In this case TEC is observed along the path from the GNSS satellite (orbit altitude ~20 000 km) to the LEO satellite (orbit altitude ~800 km), thus in the medium plasmasphere. The number of available GNSS satellites is rather large: ~24 each for GPS and GLONASS systems, ~30 for Galileo, ~35 for Compass, with a total close to 110 and a fair global distribution.

4.6.2.3   *Space environment observation from operational meteorological satellites*

The constellations of operational meteorological satellites substantially contribute to space weather monitoring. In many cases the focus is on the in situ detection of energetic particle events, which are a threat to the on-board electronics and other subsystems sensitive to corpuscular radiation. Magnetic and electric fields are also measured in many cases, as well as solar activity. The orbits of meteorological satellites, however, do not meet all the needs of space environment monitoring: for instance the 90 to 300 km height range cannot be covered and Sun-synchronous orbits cannot capture the diurnal cycle, thus introducing a sampling bias. Nonetheless, the long-term, continuous availability of a high number of meteorological satellites constitutes a valuable contribution to space weather monitoring.

Table 4.11 presents the information available from operational meteorological satellite series related to space weather. Radio occultation payloads (see section 4.2.2) are omitted.

**Table 4.11. Operational meteorological missions carrying
instruments relevant to space weather**

Satellite series	Payload for in situ space environment monitoring
GOES 11 to 15	Space Environment Monitor (SEM): suite of instruments for charged particles, solar X-ray and magnetic field Solar X-ray Imager (SXI)
GOES R, S, T, U	Space Environment In Situ Suite (SEISS) for charged particles in solar wind and cosmic rays Extreme Ultraviolet Sensor/X-Ray Sensor Irradiance Sensors (EXIS) Solar Ultraviolet Imager (SUVI) Magnetometer (MAG)
Electro-L Electro-M	GGAK-E: Heliogeophysical Instrument Complex for charged particles of solar wind and cosmic rays
FY-2	SEM for charged particles of solar wind

Satellite series	Payload for in situ space environment monitoring
FY-4	SEM for charged particles of solar wind Solar X-EUV (SXEUV): imaging telescope for incoming X-rays and extreme UV from the Sun
NOAA 15 to 19 Metop A, B	SEM/2 for medium-energy and total-energy proton detection
JPSS	SEM for National Polar-orbiting Operational Environmental Satellite System (SEM-N): including a spectrometer for precipitating electrons and ions, a spectrometer for medium-energy particles, and omni-directional detectors for high-energy particles
DMSP F16 to S20	Special Sensor Ion and Electron Scintillation Monitor (SSIES) Special Sensor Precipitating Electron and Ion Spectrometer (SSJ5) Special Sensor Magnetometer (SSM) Special Sensor Ultraviolet Limb Imager (SSULI) Special Sensor Ultraviolet Spectrographic Imager (SSUSI)
Meteor-M	Geophysical Monitoring System Complex (GGAK-M), including: Spectrometer for Geoactive Measurements (MSGI-MKA) Radiation Monitoring System (KGI-4C)
Meteor-MP	Geophysical Monitoring System Complex, improved after GGAK-M (GGAK-MP)
FY-3 A, B	SEM for charged particles of the solar wind
FY-3 C to G	Space Environment Suite (SES), including: SEM, same as on FY-3A and FY-3B Wide-Field Auroral Imager (WAI) Ionospheric Photometer (IPM)

CHAPTER CONTENTS

CHAPTER 5. SPACE-BASED OBSERVATION OF GEOPHYSICAL VARIABLES

5.1 INTRODUCTION

This chapter offers an overview of the geophysical variables that can be observed from space and of the performance that can be expected for their derivation. The performance is estimated by taking into account the physical principle involved in each measurement technique and the state-of-the-art instrument technology at the time of writing this document and in the foreseeable future. Assumptions are made to provide the most representative estimation in each case. The figures do not necessarily represent the actual performance of a particular instrument, but are intended to illustrate the relative performances of the various remote-sensing techniques.

5.1.1 Processing levels

For the purpose of this Guide, the discussion is limited to geophysical variables that can be retrieved by processing the output from a single instrument or a set of closely associated instruments. Product derivation may involve complex algorithms, physical or statistical models, and supporting information from external sources, either ancillary (necessary for processing) or auxiliary (to help processing). The present chapter focuses on products that can be derived with a limited amount of external information, where this external information only plays a minor role compared with that of the satellite instrument output, and no significant bias can be introduced by a model. For instance, modelling of the physical phenomenon controlling the variable, radiative transfer models, and inversion retrieval models, are within the scope of this chapter. Beyond the scope of this chapter, for example, are assimilations that merge several measurements and background fields, that combine the physics of the phenomenon and the dynamics of the model to the point where the satellite contribution to the output product is barely recognizable, and that can be biased to the model being used.

This chapter will focus on Level 2 products, and some Level 3 and Level 4 products for which there is a well-established and recognized methodology (see the processing levels defined in Part III, Chapter 2, 2.3.2.6, Table 2.11).

5.1.2 Product quality

For satellite imagery used directly for human interpretation, several quality criteria can be considered; these include spatial resolution, geo-location accuracy, calibration stability across consecutive images, and colour constancy in representing a given property within the observed scene in the case of RGB composite imagery. These components of the image product quality are not discussed further here.

In this chapter, the aim is to address the quality of quantitative products with numbers that can be used in automatic procedures and numerical models. This evaluation can then be compared with the requirements for the same products.

Product quality is specified here by:

(a)   Atmospheric volume (for vertical profiles)

(b)   Horizontal resolution (Δx)

(c)   Vertical resolution (Δz) (for vertical profiles)

(d)   Observing cycle (Δt)

(e)   Accuracy (RMS)

(f)   Timeliness (δ)

5.1.2.1   *Atmospheric volumes (relevant to 3D observations)*

User requirements may differ according to the layer of the atmosphere being considered. The figure in this section shows the definitions of the atmospheric volumes used in the WMO observation requirements database.

While users' requirements may change in a stepwise mode when moving along the vertical, the quality of satellite-derived products changes with height in a smooth way, depending mainly on the vertical gradient of the quantity, with better performance being achieved at steeper gradients. A step change occurs when the required vertical resolution cannot be achieved by cross-nadir scanning instruments and limb scanning becomes necessary. For the sake of simplicity, different product performances are taken into account for the troposphere, the stratosphere, and the total atmospheric column (where applicable). It is understood that quality will softly degrade with increasing altitude in the troposphere, and the same in the stratosphere. Product quality is only quoted above the height of 1 km; below 1 km the accuracy is too irregular and difficult to estimate.

5.1.2.2   *Horizontal resolution*

The horizontal resolution (Δx) is the convolution of several features (sampling distance, degree of independence of the information relative to nearby samples, the point spread function, etc.). For simplicity, it is generally agreed to refer to the sampling distance between two successive product values carrying independent information.
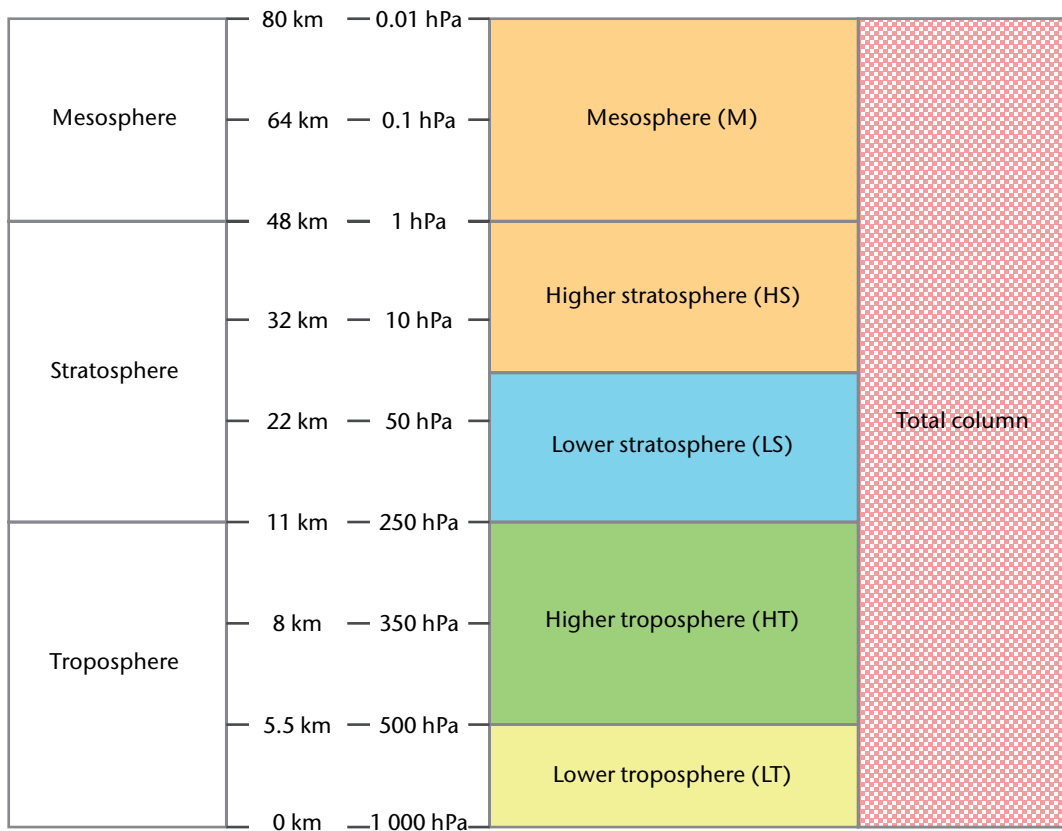
Atmospheric volumes defined by users. The higher stratosphere and mesosphere go together (HS&M). The heights and pressures are qualitative, and refer to mid-latitudes/yearly average. The planetary boundary layer is part of the lower troposphere.

The horizontal resolution of the geophysical variable being measured is controlled by instrument features (primarily the instantaneous field of view (IFOV), the sampling distance, or pixel, and the modulation transfer function) and by the processing scheme that may be designed to take account of interfering effects (such as clouds in the IFOV). For example, if clouds prevent the measurement being useful, it may be convenient to process pixel arrays searching or extrapolating for the less contaminated measurement in the cell of size Δx. The number of pixels to be co-processed depends on the spectral range used to perform the measurement (down to one for all-weather microwaves, for example) and on the available spectral information (when more spectral channels are available, a smaller cluster of pixels is needed). The extreme case is when a large pixel array (32 x 32, for instance) is needed to characterize the geophysical variable (an example is the inference of atmospheric motion vectors from the displacement of highly correlated cloudy pixel arrays within two images at different times).

For parameters such as cloud cover or snow cover, a sufficient number of samples (pixels) in the $\Delta x \cdot \Delta x$ cell is necessary to achieve the required accuracy. For cloud-disturbed surface measurements of slowly-changing variables (such as snow) it may be necessary to apply a multi-temporal analysis that waits for the clouds to move away (this would be a Level 3 product). It is generally possible, within limits, to trade off horizontal resolution against accuracy during product generation. Often, the product horizontal resolution is larger than a single pixel in order to enhance the signal-to-noise ratio (SNR) to meet the product accuracy requirements.

For cross-nadir scanning instruments, the instrument IFOV or pixel size gets larger from the sub-satellite point towards the swath edge; the product horizontal resolution performance must therefore be averaged across the instrument swath.

For conical scanners, the along-scan resolution is constant, but the cross-scan resolution is degraded by the cosine of the azimuth angle (the IFOV is nearly elliptical). The quadratic average in the along- and across-scan directions must be considered, and account has to be taken of the IFOV elongation in the along-scan direction due to the line-of-scan motion during the measurement integration time. If a single antenna is used for several frequencies, the resolution will change with frequency due to diffraction.

For limb sounding, the horizontal resolution is determined by the viewing geometry. The atmospheric path may physically extend for a few thousand kilometres, but the effective path (which accounts for higher atmospheric density around the tangent height) is around 300 km along-view. Across the viewing direction, although the transversal IFOV may be much narrower (tens of kilometres), the product resolution is determined by the number of azimuth views (in most cases only one, fore or aft). For the sake of simplicity, the typical horizontal resolution of limb measurements is taken as 300 km.

5.1.2.3   *Vertical resolution*

The vertical resolution (Δz) is also defined by referring to the vertical sampling distance between two successive product values, carrying independent information.

The vertical resolution of the product depends on the sensing principle, the instrument spectral range and the number of channels or spectral resolution. The weighting function may be more or less broadened in the vertical depending on the spectral resolution and range (worse in microwave (MW), better in the optical ranges). Moreover, the spectral channels may be narrow enough to observe single lines of the absorbing/emitting gas, or a few lines or line bands. If several lines are included in the channel, the weighting function will be broadened since it will average surface emission between the lines (peaking in the lower atmosphere) and atmospheric emission in the lines (peaking at higher altitudes). In general, resolving power $\lambda/\Delta\lambda \approx 100$ enables broad-resolution retrieval of temperature vertical profiles with roughly 2 km vertical resolution; $\lambda/\Delta\lambda \approx 1\,000$ enables higher vertical resolution retrieval of temperature at about 1 km along with total-column retrieval of trace gases; $\lambda/\Delta\lambda \approx 10\,000$ is needed for trace-gas profiles. The gas density has a bearing on the achievable vertical resolution, so that with increasing altitude the vertical measurement resolution degrades, becoming unacceptable in the medium and high stratosphere.

It should be noted that the weighting function shifts to higher altitudes as the instrument viewing angle shifts from nadir to swath edge. This is due to the longer path length through the atmosphere with increasing view angle. The transmittance is an exponential function of the number of absorbing molecules in the path of the escaping radiation; a more oblique angle entails a greater likelihood of encountering more molecules in the upper atmosphere and hence the weighting function moves up in altitude.

The vertical resolution depends on the sensitivity of the wavelength to temperature. Infrared (IR) sensitivity to temperature is higher in the medium-wave infrared (MWIR) range (about 3–6 μm), thus the weighting functions are narrower in the lower troposphere and very broad in the higher troposphere and stratosphere. Short waves are less sensitive to temperature, so the vertical resolution is relatively homogeneous with altitude. MW is relatively more sensitive to cold temperature and the vertical resolution is relatively good in the stratosphere.

In the stratosphere and above, the vertical resolution achievable by cross-nadir scanning is poor. Limb scanning offers better vertical resolution; it is performed by mechanical scanning along the vertical (angular IFOV combined with the scan rate) and is in the range of 1 to 3 km (which is not possible with cross-nadir scanning). The vertical resolution achieved by limb sounding degrades with altitude, as the SNR degrades with decreasing gas concentration. Occultation instruments (including radio occultation) have a vertical resolution that is determined by the sampling rate during the occultation phase. During ground processing, an algorithm performs some vertical integration as a trade-off against product accuracy.

5.1.2.4   *Observing cycle*

The observing cycle (Δt) is defined as the time required to achieve global coverage (for low Earth orbit, LEO) or full disk coverage (for geostationary Earth orbit, GEO). It is closely linked to the scanning capability of the instrument and to the orbital features. The relationship between observing cycle and scanning mechanism has been extensively discussed in Part III, Chapter 3, 3.1.1. However, the instrument observing cycle may not coincide with the product observing cycle since not all observations taken during an instrument observing cycle may be useful for a given product. For example, a clear-sky mapped product may exhibit too many gaps due to cloud-affected observations. Thus the effective product observing cycle is a compromise between the minimum theoretical observing cycle that will have many gaps, and multi-temporal analysis degrading the product observing cycle but producing a more regular product field (generated by a Level 3 process). The compromise takes into account the sensitivity of the spectral band to the disturbing factor and the intrinsic time-variability of the desired geophysical parameter (which might not tolerate delays entailed by multi-temporal analysis). In another example, multi-temporal analysis might be necessary to collect enough signal when the required product accuracy cannot readily be achieved.

For most meteorological variables the required observing cycle prevents multi-temporal analysis. The solution is at system level, by establishing the number of satellites available to measure the geophysical variable. A global observing cycle shorter than 12 h (for measurements in IR and MW) or 24 h (for measurements involving short wave (SW)) requires more satellites in regularly spaced orbits. For a 3 h cycle, four satellites are needed, provided the instrument swath is as large as the decalage (visible/infrared (VIS/IR) imagers, for example). For limited-swath instruments (such as MW radiometers of the Global Precipitation Measurement mission) the 3 h cycle requires eight satellites.

The observing cycle may be shortened at the expense of global coverage by using low-inclination orbits. The extreme limit is Δt < one orbital period for a quasi-equatorial orbit run from E to W. Latitudes beyond the reach of the instrument swath will not be covered.

For satellites in GEO orbits, the observing cycle depends on the instrument refresh cycle. It may be minutes if the observation is unaffected by clouds; otherwise multi-temporal analysis may be needed. A constellation of six regularly-spaced GEO satellites provides coverage of all latitudes below 55°, rising to 70° and above for longitudes close to that of the six GEO locations.

Instruments with only nadir-viewing (non-scanning) provide infrequent global coverage. Limb-scanning instruments, including radio occultation, have a similar drawback (see Part III, Chapter 3, 3.1.1). For these instruments, the observing cycle is difficult to define.

5.1.2.5 *Accuracy (RMS)*

Accuracy is defined as the "closeness of the agreement between a measured quantity value and a true quantity value of the measurand" (from the *International Vocabulary of Metrology – Basic and General Concepts and Associated Terms (VIM)*, JCGM 200: 2012). The quantitative expression corresponding to the accuracy is the uncertainty (see Part I, Chapter 1, 1.6.2). It is the combined result of several instrument features: random error, bias, sensitivity, precision, etc. In this Part (on space-based observations), the uncertainty is generally characterized by the root-mean-square (RMS) error range, namely the RMS difference (observed – true values) of the measurement. The uncertainty of a satellite-derived observation of a geophysical variable is driven by the physical principle linking the satellite measurement to the observed variable, and in particular by the sensitivity of the measurement to variations of this variable.

The radiometric resolution is thus a driving factor of the product uncertainty. It can be characterized by the noise equivalent differential temperature, or the signal-to-noise ratio, or the noise equivalent spectral radiance, as defined in Part III, Chapter 3, 3.1.4. However, the product uncertainty is also strongly affected by the retrieval algorithm and by the trade-off with the other quality features (Δx, Δz and Δt). Furthermore, the nature of the target (intensity of the emitted or scattered signal), the sensitivity of the sensing technique to the geophysical variable, and the efficiency in filtering out disturbing factors (such as clouds) have a pronounced impact on the final product uncertainty.

For a new instrument, evaluating the uncertainty requires sensitivity studies based on complicated simulations.

In this Part, product uncertainty is estimated from the heritage of past and current instruments, and simulation of planned instruments. Some validation of satellite-derived product accuracy (discussed in Part III, Chapter 6) enters into estimates for past and current instruments; for future instruments a theoretical calculation is performed.

5.1.2.6 *Timeliness*

Timeliness (δ) is defined as the time elapsed between the moment the observation is taken and the availability of the product assuming routine operations. Timeliness depends on the satellite transmission facilities, the availability of acquisition stations, the processing time required to generate the product, and the overall data management.

In this Guide, the timeliness δ of the various products has not been evaluated because it is a system feature that is not determined solely by the instrument.

5.1.3 **Evaluation of satellite product quality**

This chapter provides an overview of the satellite products that can potentially be retrieved from current or planned instruments, for geophysical variables of the following eight themes:

(a)   Basic atmospheric (3D and 2D) variables

(b)   Cloud and precipitation variables

(c)   Aerosols and radiation

(d)   Ocean and sea ice

(e)   Land surface (including snow)

(f)   Solid Earth

(g)   Atmospheric chemistry

(h)   Space weather

This list of observation products is limited to "elementary" geophysical variables; it does not include products that can be derived from other products.

For each satellite product, the applicable remote sensing principles are indicated, together with any observing conditions or limitations. The annex to this chapter contains an evaluation of the achievable quality in terms of RMS error,[1] Δx, Δz and Δt, based on the characteristics of state-of-the art instruments that are being developed at the time of writing this Guide, and expected to be operational by 2020.

5.2   BASIC ATMOSPHERIC 3D AND 2D VARIABLES

Table 5.1 lists basic variables for weather prediction, including numerical weather prediction (NWP), that are observable from space.

Table 5.1. Geophysical variables considered under the theme "Basic atmospheric (3D and 2D) variables"

Atmospheric temperature	Wind (horizontal)	Height of the top of the planetary boundary layer	Height of the tropopause
Specific humidity	Wind vector over the surface (horizontal)	Temperature of the tropopause	

Other basic variables such as atmospheric pressure, temperature and humidity at surface; and wind vertical component are not included because they cannot be reliably measured from space with current technology.

5.2.1   Atmospheric temperature

Definition: 3D field of the atmospheric temperature – Required from surface to top of atmosphere (TOA) (layers: LT, HT, LS, HS&M) – Physical unit: [K] – Uncertainty unit: [K].

Method 1: IR spectroscopy – Principle: IR emission from different atmospheric layers, selected by using spectral intervals of different absorption strength in bands of CO_2 (~4.3 and 15 μm). Applicable in both LEO and GEO.

Method 2: MW/sub-mm radiometry – Principle: MW and sub-millimetre wave emission from different atmospheric layers, selected by using spectral intervals of different absorption strength in bands of O_2 (~54, 118 and potentially 425 GHz). Applicable in both LEO and potentially GEO.

Method 3: Global navigation satellite system (GNSS, consisting of the Global Positioning System (GPS) and the Russian satellite navigation system, GLONASS) radio-occultation – Principle: Atmospheric refraction of L-band signals from the global navigation satellite system received by a LEO satellite during the occultation phase. Applicable only in LEO.

---

[1]   Note that RMS error used in this Part corresponds approximately to an expanded uncertainty with a coverage factor of $k = 1$, while in the rest of this Guide a coverage factor of $k = 2$ is generally used (see Part I, Chapter 1, 1.6.4.3 and the *Evaluation of Measurement Data – Guide to the Expression of Uncertainty in Measurement* (JCGM 100:2008)).

Method 4: Limb sounding – Principle: Emission by lines (in IR or MW) or line broadening (in SW) as observed by high-resolution spectrometers intended for atmospheric chemistry operating in the Earth's limb. Applicable only in LEO.

5.2.2   **Specific humidity**

Definition: 3D field of the specific humidity in the atmosphere – Required from surface to TOA (layers: LT, HT, LS, HS&M) + total column – Physical units: [g/kg] for layers, [kg/m²] for total column – Uncertainty unit: [%] for layers, [kg/m²] for total column.

Method 1: IR spectroscopy – Principle: IR emission from different atmospheric layers, selected by using spectral intervals of different absorption strength in bands of H_2O (~6 and potentially ~18 μm) with support of CO_2 (~4.3 and 15 μm). Applicable in both LEO and GEO.

Method 2: MW/sub-mm radiometry – Principle: MW and sub-mm wave emission from different atmospheric layers, selected by using spectral intervals of different absorption strength in bands of H_2O (183 and potentially 324, 380 GHz and others at higher frequencies) with necessary support of O_2 (~54, 118 and potentially 425 GHz). Applicable in LEO and potentially in GEO.

Method 3: GNSS radio-occultation – Principle: Atmospheric refraction of L-band signals from the GNSS received by a LEO satellite during the occultation phase. Applicable only in LEO.

Method 4: Differential absorption lidar (DIAL) – Principle: Backscattered radiation in a near infrared (NIR) water-vapour absorption band (~935 nm for example) and a side window by DIAL. Applicable only in LEO.

Method 5: Limb sounding – Principle: Emission (in IR or MW/sub-mm), absorption (in Sun or star occultation of SW) or scattering (in SW) by lines as observed by high-resolution spectrometers intended for atmospheric chemistry operating in the Earth's limb. Applicable only in LEO.

Method 6: IR split window – Principle: By-product of the retrieval of surface temperatures from IR images (split-windows such as 11 and 12 μm). Suitable only for total column. Applicable in both LEO and GEO.

Method 7: MW imaging (23 GHz) – Principle: MW emission in a weak H_2O band (~23 GHz), associated with a nearby window (19 or 37 GHz). Suitable only for total column over the sea. Applicable in LEO and potentially in GEO.

Method 8: NIR imaging (935 nm) – Principle: Differential reflectance between an NIR water-vapour absorption band (~935 nm for example) and a side window by narrow-bandwidth radiometers. Suitable only for total column. Applicable in both LEO and GEO.

5.2.3   **Wind (horizontal)**

Definition: 3D field of the horizontal vector component (2D) of the 3D wind vector – Required from surface to TOA (layers: LT, HT, LS, HS&M) – Physical unit: [m/s] – Uncertainty unit: [m/s] intended as vector error, in other words the module of the vector difference between the observed vector and the true vector.

Method 1: Doppler lidar – Principle: Motion of atmospheric eddies "signed" by aerosol or molecular scattering, tracked by means of Doppler lidar. Applicable only in LEO.

Method 2: VIS/IR image sequences – Principle: Motion of atmospheric cells of determined size "signed" by clouds and water-vapour patches (and possibly ozone patches) recognized and tracked in VIS/IR image sequences. Applicable in both LEO and GEO.

Method 3: IR imager-sounder – Principle: Motion of water-vapour patches tracked in frequent sounding by IR imaging spectrometers operating in absorption bands of H_2O (~6 μm) with support of CO_2 (~4.3 and 15 μm). Applicable in both LEO and GEO.

Method 4: Limb sounding – Principle: Doppler shift and broadening of spectral lines of O_2, O_3, OH^- observed by high-resolution VIS spectrometers operating in the Earth's limb. Applicable only in LEO.

5.2.4   Wind vector over the surface (horizontal)

Definition: Horizontal vector component (2D) of the 3D wind vector, conventionally measured at 10 m height – Required over sea and land surface (all methods below apply over sea). Physical unit: [m/s] – Uncertainty unit: [m/s] intended as vector error, namely the module of the vector difference between the observed vector and the true vector.

Method 1: Radar scatterometry – Principle: Backscattered radiation from capillary waves by medium-frequency radar (about 5 or 11 GHz). More viewing angles are used to determine direction. Applicable only over the sea. Applicable only in LEO.

Method 2: Polarimetric MW radiometry – Principle: Emitted and scattered MW radiation in atmospheric windows at several frequencies (10, 19, 37 GHz for example). Three Stokes parameters to be measured (at least four polarizations, for example), preferably four (requiring six polarizations). Applicable only over the sea. Applicable only in LEO.

Method 3: MW imagery – Principle: Emitted and scattered MW radiation in atmospheric windows at several frequencies (such as 10, 19, 37 GHz). At least two polarizations needed. Applicable only over the sea. Only speed measured. Applicable only in LEO.

Method 4: Radar altimetry – Principle: Backscattered radiation from sea surface by medium-frequency radar (~13 GHz). Wind speed associated with echoes scattered from capillary waves. Applicable only over the sea. Only speed measured. Only nadir. Applicable only in LEO.

5.2.5   Height of the top of the planetary boundary layer

Definition: Height of the surface separating the planetary boundary layer from the free atmosphere – Physical unit: [km] – Uncertainty unit: [km].

Method 1: Backscatter lidar – Principle: Backscattered radiation in ultraviolet (UV), VIS or NIR by lidar. Applicable only in LEO.

Method 2: From IR sounding – Principle: Derived from IR sounding of temperature and humidity. Applicable in both LEO and GEO.

Method 3: From GNSS sounding – Principle: Derived from GNSS radio-occultation sounding of temperature and humidity. Applicable only in LEO.

5.2.6   Height of the tropopause

Definition: Height of the surface separating the troposphere from the stratosphere – Physical unit: [km] – Uncertainty unit: [km].

Method 1: Backscatter lidar – Principle: Backscattered radiation in UV, VIS or NIR by lidar. Two wavelengths preferred. Applicable only in LEO.

Method 2: From IR sounding – Principle: Derived from IR sounding of temperature. Applicable in both LEO and GEO.

Method 3: From GNSS sounding – Principle: Derived from GNSS radio-occultation sounding of temperature. Applicable only in LEO.

5.2.7   Temperature of the tropopause

Definition: Atmospheric temperature at the height of the surface separating the troposphere from the stratosphere – Physical unit: [K] – Uncertainty unit: [K].

Method 1: From IR sounding – Principle: Derived from IR sounding of temperature. Applicable in both LEO and GEO.

Method 2: From GNSS sounding – Principle: Derived from GNSS radio-occultation sounding of temperature. Applicable only in LEO.

Method 3: From limb sounding – Principle: Derived from limb sounding of temperature. Applicable only in LEO.

5.3   CLOUD AND PRECIPITATION VARIABLES

This theme includes the basic variables observable from space for actual weather analysis, and for short-term prediction and nowcasting, as well as for hydrology. Table 5.2 lists these variables.

**Table 5.2. Geophysical variables considered under the theme
"Cloud and precipitation variables"**

Cloud-top temperature	Cloud-base height	Cloud ice	Precipitation (liquid or solid)
Cloud-top height	Cloud optical depth	Cloud-ice effective radius	Precipitation intensity at surface (liquid or solid)
Cloud type	Cloud liquid water	Freezing-level height in clouds	Accumulated precipitation (over 24 h)
Cloud cover	Cloud-droplet effective radius	Melting-layer depth in clouds	Lightning detection

5.3.1   Cloud-top temperature

Definition: Temperature of upper surface of cloud – Physical unit: [K] – Uncertainty unit: [K].

Method 1: IR radiometry – Principle: Derived from IR imagery in a number of channels including "windows" and others (in water-vapour absorption bands) as necessary to evaluate cloud emissivity. Applicable in both LEO and GEO.

Method 2: From IR sounding – Principle: Derived as a by-product of temperature/humidity sounding retrieval from IR spectroscopy. The different brightness temperature at different wavelengths sensitive to CO_2 enables retrieval of cloud-top temperature within the sounded IFOV. Applicable in both LEO and GEO.

5.3.2   Cloud-top height

Definition: Height of the upper surface of the cloud – Physical unit: [km] – Uncertainty unit: [km].

Method 1: IR radiometry – Principle: Derived from cloud-top pressure converted to height and temperature using a forecast temperature profile after viewing the cloud through an 11 and 13.4 μm channel pair (comparison with "window", measures the columnar defect of CO_2 above cloud top). Applicable in both LEO and GEO.

Method 2: From IR sounding – Principle: Derived as a by-product of temperature/humidity sounding retrieval from IR spectroscopy. The different radiative transfer at different wavelengths enables retrieval of cloud-top height within the sounded IFOV. Applicable in both LEO and GEO.

Method 3: Backscatter lidar – Principle: Backscattered radiation in UV, VIS or NIR by lidar. Two wavelengths preferred. Applicable only in LEO.

Method 4: Cloud radar – Principle: Backscattered radiation in MW (~94 GHz) by radar. Applicable only in LEO.

Method 5: A-band spectroscopy – Principle: Observed defect of columnar O_2 above the cloud top by spectroscopy of the 760 nm A-band and nearby "window". Applicable in both LEO and GEO.

5.3.3   **Cloud type**

Definition: Comprehensive properties of the observed cloud. The list of types of interest is predetermined – Uncertainty expressed as number of discriminated types [classes].

Method 1: VIS/IR radiometry – Principle: Multi-spectral analysis of cloud reflectance, top-surface temperature, optical depth, emissivity, phase, drop size, over different backgrounds, observed in a few discrete channels of relatively large bandwidths (5–10 cm^{-1}). Applicable in both LEO and GEO.

5.3.4   **Cloud cover**

Definition: 3D field of fraction of sky where clouds are detected. Required as a 3D field in the troposphere (assumed height: 12 km) and also as a single layer (total column) to provide the total cloud cover – Physical unit: [%] – Uncertainty unit: [%].

Method 1: VIS/IR radiometry – Principle: Derived from cloud imagery in a few discrete channels selected so as to detect all cloud types. The fractional cover refers to the number of cloudy pixels in a given pixel array. Applicable in both LEO and GEO.

Method 2: From IR sounding – Principle: Derived as a by-product of temperature/humidity sounding retrieval from IR spectroscopy. The different radiative transfer at different wavelengths enables retrieval of cloud fraction times cloud emissivity within the sounded IFOV. Applicable in both LEO and GEO.

Method 3: Cloud radar – Principle: Backscattered radiation from cloud droplets observed by high-frequency radar (~94 GHz). Applicable only in LEO.

5.3.5   **Cloud-base height**

Definition: Height of the bottom surface of the cloud – Physical unit: [km] – Uncertainty unit: [km].

Method 1: Cloud radar – Principle: Derived as lower level of the backscattered radiation from cloud droplets observed by high-frequency radar (~94 GHz). Applicable only in LEO.

5.3.6   **Cloud optical depth**

Definition: Effective depth of the cloud from the viewpoint of radiation propagation. The definition is $OD = e^{-K \Delta z}$. K is the extinction coefficient [km^{-1}], Δz the optical path [km] between the base and the top of the cloud. It depends on the wavelength but is usually referred to visible radiation. Physical unit: [dimensionless] – Uncertainty unit: [dimensionless].

Method 1: Backscatter lidar – Principle: Backscattered radiation in UV, VIS or NIR by lidar. Two wavelengths preferred. Applicable only in LEO.

Method 2: SW polarimetry – Principle: Scattered solar radiation in several narrowband channels of UV, VIS, NIR and short-wave infrared (SWIR), some with polarimetric measurements to determine three Stokes parameters. Applicable only in LEO.

Method 3: Short-wave/thermal infrared (SW/TIR) radiometry – Principle: Scattered solar radiation in several narrowband channels of VIS, NIR and SWIR, and emitted radiation in several window channels of TIR. Applicable in both LEO and GEO.

5.3.7   **Cloud liquid water**

Definition: 3D field of atmospheric water in the liquid phase (precipitating or not). Required in the troposphere (assumed height: 12 km) and for total column – Physical unit: [g/kg] for layers, [g/m^2] for total column – Uncertainty unit: [%] for layers, [g/m^2] for total column.

Method 1: Cloud radar – Principle: Backscattered radiation from cloud droplets observed by high-frequency radar (~94 GHz). Applicable only in LEO.

Method 2: Precipitation radar – Principle: Backscattered radiation from cloud droplets observed by medium-frequency radar (dual-frequency preferred, 14 and 35 GHz). Applicable only in LEO.

Method 3: MW/sub-mm sounding – Principle: MW/sub-mm radiation in window channels (typically, ~10, 19, 37, 90, 150 GHz) with dual polarization, and absorption bands (typically, ~54, 118, 183 GHz). Applicable in LEO and potentially in GEO.

5.3.8   **Cloud-droplet effective radius**

Definition: 3D field of the size distribution of liquid water droplets, assimilated to spheres of the same volume. Required in the troposphere (assumed height: 12 km), and at the cloud-top surface – Physical unit: [μm] – Uncertainty unit: [μm].

Method 1: Cloud radar – Principle: Backscattered radiation from cloud droplets by high-frequency radar (~94 GHz). Applicable only in LEO.

Method 2: Precipitation radar – Principle: Backscattered radiation from cloud droplets by medium-frequency radar (dual-frequency preferred, 14 and 35 GHz). Applicable only in LEO.

Method 3: MW/sub-mm sounding – Principle: MW/sub-mm radiation in window channels (typically, ~10, 19, 37, 90, 150 GHz) with dual polarization, and absorption bands (typically, ~54, 118, 183 GHz). Actually, the cloud-droplet effective radius profile is retrieved with the help of an associated NWP model, possibly cloud-resolving. Applicable in LEO and potentially in GEO.

Method 4: Backscatter lidar – Principle: Backscattered radiation in UV, VIS or NIR by lidar. Essentially limited to cloud top. Applicable only in LEO.

Method 5: SW polarimetry – Principle: Scattered solar radiation in several narrowband channels of UV, VIS, NIR and SWIR, some with polarimetric measurements to determine three Stokes parameters. Essentially limited to cloud top. Applicable only in LEO.

Method 6: VIS/IR radiometry – Principle: Scattered solar radiation in several narrowband channels of VIS, NIR, SWIR and MWIR. Also, differential emission in several channels of thermal infrared (TIR, for cirrus clouds). Essentially limited to cloud top. Applicable in both LEO and GEO.

5.3.9   **Cloud ice**

Definition: 3D field of atmospheric water in the solid phase (precipitating or not). Required in the troposphere (assumed height: 12 km) and for total column – Physical unit: [g/kg] for layers, [g/m^2] for total column – Uncertainty unit: layers [%], [g/m^2] for total column.

Method 1: Cloud radar – Principle: Backscattered radiation from ice particles observed by high-frequency radar (~94 GHz). Applicable only in LEO.

Method 2: Precipitation radar – Principle: Backscattered radiation from ice particles by medium-frequency radar (dual-frequency preferred, 14 and 35 GHz). Applicable only in LEO.

Method 3: MW/sub-mm sounding – Principle: MW/sub-mm radiation in window channels (typically, ~37, 90, 150 GHz) with dual polarization, and absorption bands (typically, ~54, 118, 183, and potentially 380, 425 GHz). Actually, the cloud-ice profile is retrieved with the help of an associated NWP model, possibly cloud-resolving. Applicable in LEO and potentially in GEO.

Method 4: Sub-mm imagery – Principle: Emitted and scattered radiation in MW atmospheric windows (243, 664, 874 GHz) in dual polarization supported by channels in H$_2$O absorption bands (183, 325, 448 GHz). Suitable only for total column. Applicable only in LEO.

Method 5: Far IR (FIR) imagery – Principle: Emitted and scattered radiation in several atmospheric windows of FIR (18.2, 24.4, 52, 87 μm) as compared to TIR (8.7, 11, 12 μm). Suitable only for total column. Applicable only in LEO.

5.3.10   **Cloud-ice effective radius**

Definition: 3D field of the size distribution of ice particles, assimilated to spheres of the same volume. Required in the troposphere (assumed height: 12 km), and at the cloud-top surface – Physical unit: [μm] – Uncertainty unit: [μm].

Method 1: Cloud radar – Principle: Backscattered radiation from ice particles by high-frequency radar (~94 GHz). Applicable only in LEO.

Method 2: Precipitation radar – Principle: Backscattered radiation from ice particles by medium-frequency radar (dual-frequency preferred, 14 and 35 GHz). Applicable only in LEO.

Method 3: MW/sub-mm sounding – Principle: MW/sub-mm radiation in window channels (typically, ~10, 19, 37, 90, 150 GHz) with dual polarization, and absorption bands (typically, ~54, 118, 183 GHz). Actually, the cloud-ice effective radius profile is retrieved with the help of an associated NWP model, possibly cloud-resolving. Applicable in LEO and potentially in GEO.

Method 4: Backscatter lidar – Principle: Backscattered radiation in UV, VIS or NIR by lidar. Essentially limited to cloud top. Applicable only in LEO.

Method 5: SW polarimetry – Principle: Scattered solar radiation in several narrowband channels of UV, VIS, NIR and SWIR, some with polarimetric measurements to determine three Stokes parameters. Essentially limited to cloud top. Applicable only in LEO.

Method 6: VIS/IR radiometry – Principle: Scattered solar radiation in several narrowband channels of VIS, NIR, SWIR and MWIR. Also, differential emission in several channels of TIR (for cirrus clouds). Essentially limited to cloud top. Applicable in both LEO and GEO.

5.3.11 Freezing-level height in clouds

Definition: Height of the atmospheric layer in cloud where liquid-solid states transform into each other – Physical unit: [km] – Uncertainty unit: [km].

Method 1: Precipitation radar – Principle: Backscattered radiation from cloud drops by medium-frequency radar (dual-frequency preferred, 14 and 35 GHz). Applicable only in LEO.

Method 2: From MW/sub-mm sounding – Principle: Derived from MW and sub-mm wave sounding of temperature. Applicable in LEO and potentially in GEO.

5.3.12 Melting-layer depth in clouds

Definition: Depth of the atmospheric layer in cloud where liquid-solid states transform into each other – Physical unit: [km] – Uncertainty unit: [km].

Method 1: Precipitation radar – Principle: Backscattered radiation from cloud drops by medium-frequency radar (dual-frequency preferred, 14 and 35 GHz). Applicable only in LEO.

Method 2: From MW/sub-mm sounding – Principle: Derived from MW and sub-mm wave sounding of temperature. Applicable in LEO and potentially in GEO.

5.3.13 Precipitation (liquid or solid)

Definition: 3D field of the vertical flux of precipitating water mass. Required in the troposphere (assumed height: 12 km) – Physical unit: [g · s^{-1} · m^{-2}] (vertical flux of precipitating water mass) – Uncertainty unit: [%].

Method 1: Precipitation radar – Principle: Backscattered radiation from cloud drops by medium-frequency radar (dual-frequency preferred, 14 and 35 GHz). Doppler capability also useful. Applicable only in LEO.

Method 2: MW/sub-mm sounding – Principle: MW/sub-mm radiation in window channels (typically, ~10, 19, 37, 90, 150 GHz) with dual polarization, and absorption bands (typically, ~54, 118, 183, 380, 425 GHz). Actually, the precipitation profile is retrieved with the help of an associated NWP model, possibly cloud-resolving. Applicable in LEO and potentially in GEO

5.3.14 Precipitation intensity at surface (liquid or solid)

Definition: Intensity of precipitation reaching the ground – Physical unit: [mm/h] (if solid, mm/h of liquid water after melting) – Uncertainty unit: [mm/h]. Since uncertainty changes with intensity, it is necessary to specify a reference intensity. Assumed intensity: 5 mm/h.

Method 1: Precipitation radar – Principle: Backscattered radiation from cloud drops by medium-frequency radar (dual-frequency preferred, 14 and 35 GHz). Doppler capability also useful. Applicable only in LEO.

Method 2: MW/sub-mm sounding – Principle: MW/sub-mm radiation in window channels (typically, ~10, 19, 37, 90, 150 GHz) with dual polarization, and absorption bands (typically, ~54, 118, 183, 380, 425 GHz). Actually, the precipitation rate at surface is retrieved from the profile reconstructed with the help of an associated NWP model, possibly cloud-resolving. Applicable in LEO and potentially in GEO.

Method 3: VIS/IR radiometry – Principle: Inferred from cloud imagery in a few discrete channels selected so as to detect all cloud types, assisted by conceptual models, generally more responsive to convective rain. Applicable in GEO.

Method 4: Fusion between MW from LEO and IR from GEO – Principle: Combined product of LEO/MW-derived accurate/infrequent measurements with GEO/IR frequent images used either to be "calibrated" by MW measurements or to enable dynamical interpolation between MW-derived precipitation data. Requiring both LEO and GEO.

5.3.15   **Accumulated precipitation (over 24 hours)**

Definition: Integration of precipitation intensity reaching the ground in given time intervals. The reference requirement refers to integration over 24 h – Physical unit: [mm] – Uncertainty unit: [mm].

Method 1: From fusion between MW from LEO and IR from GEO – Principle: Derived by time integration of frequent precipitation rate measured by merging MW precipitation rate data from LEO with IR imagery from GEO. Requiring both LEO and GEO.

Method 2: From MW/sub-mm sounding – Principle: Derived by time integration of frequent precipitation rate measured by MW/sub-mm sounders in GEO. Applicable in GEO (potentially).

5.3.16   **Lightning detection**

Definition: Mapping of lightning events as number of flashes in a given time interval over a given area – Physical unit: [counts] – Uncertainty expressed as hit rate (HR) and false-alarm rate (FAR).

Method 1: Lightning mapping – Principle: Detection of flashes by a charge-coupled device camera in a very narrow channel in a NIR oxygen absorption band (generally at 777.4 nm) for operability also in daylight. The number of flashes in a given time over a given area, and their intensity, are related to the maturity of the convective process in cloud. Applicable in both LEO and GEO.

5.4   **AEROSOL AND RADIATION**

This theme comprises variables that affect the Earth radiation budget versus space, cloud–radiation interaction, cloud formation, air quality and several characterizing factors of climate and climate change. The variables observable from space are listed in Table 5.3.

Table 5.3. Geophysical variables considered under the theme "Aerosol and radiation"

Aerosol optical depth	Upward spectral radiance at TOA	Earth's surface albedo
Aerosol concentration	Upward LW irradiance at TOA	Earth's surface SW bi-directional reflectance
Aerosol effective radius	Upward SW irradiance at TOA	Upward LW irradiance at Earth's surface
Aerosol type	Short-wave cloud reflectance	Long-wave Earth-surface emissivity
Volcanic ash	Downward LW irradiance at Earth's surface	Photosynthetically active radiation
Downward solar irradiance at TOA	Downward SW irradiance at Earth's surface	Fraction of absorbed photosynthetically active radiation

Further variables such as aerosol absorption optical depth, aerosol extinction coefficient, aerosol single scattering albedo and aerosol phase function have not been considered since they are closely linked to the selected ones (optical thickness, concentration, effective radius, and type), which are more understandable to the general user.

5.4.1 Aerosol optical depth

Definition: Effective depth of the aerosol column from the viewpoint of radiation propagation. The definition is $OD = \exp(-K \Delta z)$. K is the extinction coefficient [km^{-1}], Δz the optical path [km] between the Earth's surface and TOA. It depends on the wavelength – Physical unit: [dimensionless] – Uncertainty unit: [dimensionless].

Method 1: Backscatter lidar – Principle: Backscattered radiation in UV, VIS or NIR by lidar. Applicable only in LEO.

Method 2: SW polarimetry – Principle: Scattered solar radiation in several narrowband channels of UV, VIS, NIR and SWIR, some with polarimetric measurements to determine three Stokes parameters. Also, multi-viewing at different incident angles. Applicable only in LEO.

Method 3: SW spectroscopy (cross-nadir) – Principle: Scattered radiation in UV, VIS, NIR and SWIR observed cross-nadir with high spectral resolution. Applicable in both LEO and GEO.

Method 4: VIS/IR radiometry – Principle: Scattered solar radiation in several channels of VIS, NIR and SWIR. Some information, relevant to absorbing aerosol, also available in thermal IR windows. Applicable in both LEO and GEO.

5.4.2 Aerosol concentration

Definition: 3D field of the mass mixing ratio of condensed particles in the atmosphere (other than water) – Required from surface to TOA (layers: LT, HT, LS, HS&M) + total column – Physical units: [g/kg] for layers, [g/m^2] for total column – Uncertainty unit: [%] for layers, [g/m^2] for total column.

Method 1: Backscatter lidar – Principle: Backscattered radiation in UV, VIS or NIR by lidar. Applicable only in LEO.

Method 2: SW polarimetry – Principle: Scattered solar radiation in several narrowband channels of UV, VIS, NIR and SWIR, some with polarimetric measurements to determine three Stokes parameters. Also, multi-viewing at different incident angles. Applicable only in LEO.

Method 3: SW spectroscopy (cross-nadir) – Principle: Scattered radiation in UV, VIS, NIR and SWIR observed cross-nadir with high spectral resolution. Applicable in both LEO and GEO.

Method 4: SW spectroscopy (limb) – Principle: Scattered radiation in UV, VIS, NIR and SWIR observed in limb mode with high spectral resolution. Also, absorbed radiation from Sun or stars during occultation. Applicable only in LEO.

Method 5: VIS/IR radiometry – Principle: Scattered solar radiation in several channels of VIS, NIR and SWIR. Some information, relevant to absorbing aerosol, also available in thermal IR windows. Suitable only for total column. Applicable in both LEO and GEO.

5.4.3 Aerosol effective radius

Definition: 3D field of the mean size of the aerosol particles, assimilated to spheres of the same volume. Required in the troposphere (assumed height: 12 km) and as columnar average – Physical unit: [μm] – Uncertainty unit: [μm].

Method 1: Backscatter lidar – Principle: Backscattered radiation in UV, VIS or NIR by lidar. Applicable only in LEO.

Method 2: SW polarimetry – Principle: Scattered solar radiation in several narrowband channels of UV, VIS, NIR and SWIR, some with polarimetric measurements to determine three Stokes parameters. Also, multi-viewing at different incident angles. A priori information and intensive modelling necessary. Applicable only in LEO.

Method 3: SW spectroscopy (cross-nadir) – Principle: Scattered radiation in UV, VIS, NIR and SWIR observed cross-nadir with high spectral resolution. A priori information and intensive modelling necessary. Applicable in both LEO and GEO.

5.4.4   Aerosol type

Definition: 3D field. Comprehensive properties of the aerosol being observed. The list of types of interest is predetermined – Required in the troposphere (assumed height: 12 km) and as columnar average – Uncertainty expressed as number of types that can actually be resolved [classes].

Method 1: Backscatter lidar – Principle: Backscattered radiation in UV, VIS or NIR by lidar. Applicable only in LEO.

Method 2: SW polarimetry – Principle: Scattered solar radiation in several narrowband channels of UV, VIS, NIR and SWIR, some with polarimetric measurements to determine three Stokes parameters. Also, multi-viewing at different incident angles. A priori information and intensive aerosol modelling absolutely necessary. Applicable only in LEO.

Method 3: SW spectroscopy (cross-nadir) – Principle: Scattered radiation in UV, VIS, NIR and SWIR observed cross-nadir with high spectral resolution. A priori information and intensive aerosol modelling absolutely necessary. Applicable in both LEO and GEO.

Method 4: VIS/IR radiometry – Principle: Scattered solar radiation in several channels of VIS, NIR and SWIR. Some information also available in thermal IR windows. A priori information and intensive aerosol modelling necessary. Suitable only for total column. Applicable in both LEO and GEO.

5.4.5   Volcanic ash

Definition: 3D field of concentration of volcanic ash – Required from surface to TOA (layers: LT, HT, LS, HS&M) + total column – Physical units: [g/kg] for layers, [g/m^2] for total column – Uncertainty unit: [%] for layers, [g/m^2] for total column.

Method 1: Backscatter lidar – Principle: Backscattered radiation in UV, VIS or NIR by lidar. Applicable only in LEO.

Method 2: SW polarimetry – Principle: Scattered solar radiation in several narrowband channels of UV, VIS, NIR and SWIR, some with polarimetric measurements to determine three Stokes parameters. Also, multi-viewing at different incident angles. Applicable only in LEO.

Method 3: SW spectroscopy (cross-nadir) – Principle: Scattered radiation in UV, VIS, NIR and SWIR observed cross-nadir with high spectral resolution. Applicable in both LEO and GEO.

Method 4: SW spectroscopy (limb) – Principle: Scattered radiation in UV, VIS, NIR and SWIR observed in limb mode with high spectral resolution. Also, absorbed radiation from Sun or stars during occultation. Applicable only in LEO.

Method 5: VIS/IR radiometry – Principle: Scattered solar radiation in several channels of VIS, NIR and SWIR. Some information also available in thermal IR windows. Suitable only for total column. Applicable in both LEO and GEO.

5.4.6 Downward solar irradiance at top of atmosphere

Definition: Flux density of the solar radiation at the top of the atmosphere – Physical unit: [W/m^2] – Uncertainty unit: [W/m^2].

Method 1: Cavity radiometer – Principle: Trapping of total downward solar radiation at satellite altitude into devices such as active cavities. Absolute measurement. Applicable in LEO, GEO, or outer-space orbits, at the L1 Lagrange libration point, for instance.

5.4.7 Upward spectral radiance at top of atmosphere

Definition: Level 1 product. Spectral range 0.2–200 μm. Resolving power $\lambda/\Delta\lambda = 1\,000$. Uncertainty quoted as signal-to-noise ratio.

Method 1: Wide-range spectroscopy – Principle: Measurement of the radiation in the interval 0.2–200 μm emitted by the Earth–atmosphere system towards space. Several spectrometers are needed to cover short wave and long wave. The objective is to monitor climate change by using the spectrum as an absolute "signature". Applicable only in LEO.

5.4.8 Upward long-wave irradiance at top of atmosphere

Definition: Flux density of terrestrial radiation emitted to space by the Earth's surface, atmosphere and clouds at the top of the atmosphere – Physical unit: [W/m^2] – Uncertainty unit: [W/m^2].

Method 1: Broadband radiometry – Principle: Measurement of the radiation in the interval 4–200 μm emitted by the Earth–atmosphere system towards space by means of detectors with as flat a response in the interval as possible. Applicable in both LEO and GEO.

5.4.9 Upward short-wave irradiance at top of atmosphere

Definition: Flux density of terrestrial radiation reflected to space by the Earth's surface, atmosphere and clouds at the top of the atmosphere – Physical unit: [W/m^2] – Uncertainty unit: [W/m^2].

Method 1: Broadband radiometry – Principle: Measurement of the radiation in the interval 0.2–4.0 μm reflected by the Earth–atmosphere system towards space by means of detectors with as flat response in the interval as possible. Information on bi-directional reflectance and modelling are required in order to convert radiance into irradiance. Applicable in both LEO and GEO.

5.4.10 Short-wave cloud reflectance

Definition: Reflectance of the solar radiation from clouds – Physical unit: [%] – Uncertainty unit: [%].

Method 1: SW radiometry – Principle: Scattered solar radiation in several channels of VIS, NIR and SWIR. Multi-viewing geometry useful. Applicable in both LEO and GEO.

5.4.11 Downward long-wave irradiance at Earth's surface

Definition: Flux density of long-wave (LW) radiation from Sun, atmosphere and clouds to the Earth's surface – Physical unit: [W/m^2] – Uncertainty unit: [W/m^2].

Method 1: From IR/MW sounding – Principle: High-level product derived mostly from atmospheric temperature and water-vapour profiles. Contributions also from cloud cover profile, specifically cloud-base height. Atmospheric modelling necessary. Applicable in both LEO and GEO.

5.4.12   Downward short-wave irradiance at Earth's surface

Definition: Flux density of short-wave radiation from Sun, atmosphere and clouds to the Earth's surface – Physical unit: [W/m²] – Uncertainty unit: [W/m²].

Method 1: SW radiometry – Principle: High-level product derived from observation of scattered solar radiation in several narrowband channels of VIS, NIR and SWIR to estimate attenuation from clouds and aerosol. Multiple viewing and multi-polarization help. Applicable in both LEO and GEO.

5.4.13   Earth's surface albedo

Definition: Hemispherically integrated reflectance of the Earth's surface in the range 0.4–0.7 μm (or other specific short-wave ranges) – Physical unit: [%] – Uncertainty unit: [%].

Method 1: Multi-view SW radiometry – Principle: High-level product after measuring scattered solar radiation in several channels of VIS under several viewing angles and solar angles to estimate anisotropy effects and improve radiative flux computations. Channels for atmospheric corrections also included. Applicable only in LEO

Method 2: VIS radiometry – Principle: Measurement of scattered solar radiation in several channels of VIS, including those for atmospheric corrections. Anisotropy effects for hemispheric integration computed by modelling. Applicable in both LEO and GEO.

5.4.14   Earth's surface short-wave bi-directional reflectance

Definition: Reflectance of the Earth's surface as a function of the viewing angle and the illumination conditions in the range 0.4–0.7 μm (or other specific short-wave ranges) – Physical unit: [%] – Uncertainty unit: [%].

Method 1: SW radiometry – Principle: Scattered solar radiation in several channels of VIS, NIR and SWIR observed under several viewing angles and solar angles to estimate anisotropy effects and improve radiative flux computations. Channels for atmospheric corrections also included. Applicable only in LEO.

5.4.15   Upward long-wave irradiance at Earth's surface

Definition: Flux density of long-wave radiation emerging from the Earth's surface – Physical unit: [W/m²] – Uncertainty unit: [W/m²].

Method 1: Broadband radiometry – Principle: Measurement of the radiation in the interval 4–200 μm emitted by the Earth's surface towards the atmosphere and ultimately to space. Detectors are needed, with as flat response in the interval as possible. Atmospheric corrections, mostly for water vapour and clouds, are necessary. Applicable in both LEO and GEO.

5.4.16   Long-wave Earth-surface emissivity

Definition: Emissivity of the Earth's surface in the thermal IR, function of the wavelength – Physical unit: [%] – Uncertainty unit: [%].

Method 1: IR radiometry – Principle: Emitted radiation in several relatively narrowband IR window channels, to determine equivalent black-body temperatures at several wavelengths. Applicable in both LEO and GEO.

Method 2: IR spectroscopy – Principle: Multiple determination of equivalent black-body temperatures in highest number of narrow windows through the IR spectrum. Applicable in both LEO and GEO.

5.4.17   Photosynthetically active radiation

Definition: Flux density of downward photons of wavelength 0.4–0.7 μm at surface – Physical unit: [μ einstein $\cdot$ m^{-2} s^{-1}] (1 einstein = 6 $\cdot$ 10^{23} photons); most frequently used: [W/m^2] – Uncertainty unit: [W/m^2].

Method 1: VIS radiometry – Principle: High-level product similar to "downwelling short-wave irradiance at Earth surface" except that it refers to the interval 0.4–0.7 μm used by vegetation for photosynthesis. Applicable in both LEO and GEO.

5.4.18   Fraction of absorbed photosynthetically active radiation

Definition: Fraction of absorbed photosynthetically active radiation that is absorbed by vegetation (land or marine) for photosynthesis processes (generally around the "red") – Physical unit: [%] – Uncertainty unit: [%].

Method 1: VIS radiometry – Principle: Computed from the observed photosynthetically active radiation and one measure in the "red" region (~670 nm). Applicable in both LEO and GEO.

5.5   OCEAN AND SEA ICE

This theme comprises variables that characterize the ocean surface, including waves and sea ice. The variables observable from space are listed in Table 5.4.

Table 5.4. Geophysical variables considered under the theme "Ocean and sea ice"

Ocean chlorophyll concentration	Oil-spill cover	Coastal sea level (tide)	Wave directional-energy frequency spectrum
Colour dissolved organic matter	Sea-surface temperature	Significant wave height	Sea-ice cover
Ocean suspended sediments concentration	Sea-surface salinity	Dominant wave direction	Sea-ice thickness
Ocean diffuse attenuation coefficient	Ocean dynamic topography	Dominant wave period	Sea-ice type

Many variables have not been considered: underwater profiles of temperature and salinity (impossible to measure from space), currents (derivable from ocean topography as for the geostrophic component, otherwise impossible or too inaccurate), iceberg extension or height (special case of ice cover and thickness), and ice drift (product of multi-temporal analysis).

5.5.1   Ocean chlorophyll concentration

Definition: Indicator of living phytoplankton biomass, extracted from ocean-colour observation. Required in both open ocean and coastal zone – Physical unit: [mg/m^3] – Uncertainty unit: [mg/m^3] at a specific concentration (1 mg/m^3, for example).

Method 1: VIS radiometry – Principle: Measurement of reflected solar radiation in several channels (most significant: 442.5 nm, 490 nm, 560 nm, 665 nm, 681.25 nm). Spectral resolution of the order of 2%. Applicable in both LEO and GEO.

5.5.2 Colour dissolved organic matter

Definition: Former name: "Yellow substance absorbance". Variable extracted from ocean-colour observation. Indicative of biomass undergoing decomposition processes. Required in both open ocean and coastal zone – Physical unit: $[m^{-1}]$ – Uncertainty unit: $[m^{-1}]$ at a specific concentration (such as $1\ m^{-1}$).

Method 1: VIS radiometry – Principle: Measurement of reflected solar radiation in several channels (most significant: 412.5 nm). Spectral resolution of the order of 2%. Applicable in both LEO and GEO.

5.5.3 Ocean suspended sediments concentration

Definition: Variable extracted from ocean-colour observation. Indicative of river outflow, re-suspension or pollution of other-than-biological origin. Required in both open ocean and coastal zone – Physical unit: $[g/m^3]$ – Uncertainty unit: $[g/m^3]$ at a specific concentration (such as $2\ g/m^3$).

Method 1: VIS radiometry – Principle: Measurement of reflected solar radiation in several channels (most significant: 510 nm, 560 nm, 620 nm). Spectral resolution of the order of 2%. Applicable in both LEO and GEO.

5.5.4 Ocean diffuse attenuation coefficient

Definition: Former name: "Water clarity". Indicator of water turbidity and vertical processes in the ocean, extracted from ocean-colour observation. Required in both open ocean and coastal zone – Physical unit: $[m^{-1}]$ – Uncertainty unit: $[m^{-1}]$.

Method 1: VIS radiometry – Principle: Measurement of reflected solar radiation in several channels of the range 400–700 nm. Spectral resolution of the order of 2%. Applicable in both LEO and GEO.

5.5.5 Oil-spill cover

Definition: The fraction of an ocean area polluted by hydrocarbons released from ships, accidentally or deliberately. Oil spills are impacting on ocean-atmosphere exchanges. Required in both open ocean and coastal zone – Physical unit: [%] – Uncertainty unit: [%].

Method 1: VIS/NIR radiometry – Principle: Measurement of reflected solar radiation in several channels of the range 400–1 000 nm. Spectral resolution of the order of 2%. Applicable in both LEO and GEO.

Method 2: SW polarimetry – Principle: Scattered solar radiation in several narrowband channels of VIS, NIR and SWIR, some with dual polarization. Applicable only in LEO.

Method 3: High-resolution optical imagery – Principle: Reflected solar radiation in VIS/NIR/SWIR observed in several discrete channels of relatively narrow bandwidths (1%–5%). Applicable only in LEO.

Method 4: SAR imagery – Principle: Backscattered MW radiation at frequencies of 1.3, 5 or 11 GHz collected by synthetic aperture radar (SAR). Polarimetric capability is useful. Applicable only in LEO.

5.5.6   Sea-surface temperature

Definition: Temperature of the sea water at surface. The "bulk" temperature refers to the depth of typically 2 m, the "skin" temperature refers to values within the upper 1 mm. – Physical unit: [K] – Uncertainty unit: [K].

Method 1: IR radiometry – Principle: Derived from IR imagery in multiple channels including "windows" and others (in water-vapour absorption bands) as necessary to evaluate atmospheric attenuation. Dual-view reduces the uncertainty of atmospheric correction. Applicable in both LEO and GEO.

Method 2: IR spectroscopy – Principle: Derived from a high number of very narrow channels through the IR spectrum, associated with other channels providing all the information needed for atmospheric corrections. Applicable in both LEO and GEO.

Method 3: MW radiometry – Principle: Emitted and scattered MW radiation in atmospheric windows at low to medium frequencies (5, 10 GHz, for example). More polarizations are needed, to correct for roughness effects. Applicable only in LEO.

5.5.7   Sea-surface salinity

Definition: Salinity of sea water in the surface layer, which is the layer affected by turbulence associated with wind stress, waves and diurnal solar heating cycle. (The layer is a few metres deep but a microwave observation would be representative of the upper ~1 m). In the open ocean the correct term should be "halinity" in order to make reference to the most common anion, chlorine – Physical unit: practical salinity unit [PSU], close to 1‰, or 1 g of salt per 1 litre of solution – Uncertainty unit: [PSU].

Method 1: MW radiometry – Principle: Emitted and scattered MW radiation at low frequencies (such as 1.4 GHz). More polarizations are needed, to correct for roughness effects. More channels are desirable, to correct for temperature. Applicable only in LEO.

5.5.8   Ocean dynamic topography

Definition: Deviation of sea level from the geoid caused by ocean currents (after corrections for tides and atmospheric pressure effects) – Physical unit: [cm] – Uncertainty unit: [cm].

Method 1: Radar altimetry – Principle: Backscattered radiation from sea surface by medium-frequency radar (dual-frequency preferred, 13 and 3 or 5 GHz). Associated with two or three channels of passive MW radiometry (23 and 37 and/or 19 GHz) needed for tropospheric path correction from water vapour and ionosphere-induced rotation. Ocean topography is extracted by filtering the fluctuation of wave heights out of the satellite-to-surface measured range. Applicable only in LEO.

5.5.9   Coastal sea level (tide)

Definition: Deviation of sea level from local references in coastal zones, caused by local currents and tides (astronomical and wind-induced) – Physical unit: [cm] – Uncertainty unit: [cm].

Method 1: Radar altimetry – Principle: Backscattered radiation from sea surface by medium-frequency radar (dual-frequency preferred, 13 and 3 or 5 GHz). Associated with two or three channels of passive MW radiometry (23 and 37 and/or 19 GHz) needed for tropospheric path correction from water vapour and ionosphere-induced rotation. Sea level is extracted by filtering the fluctuation of wave heights out of the satellite-to-surface measured range. Applicable only in LEO.

5.5.10 Significant wave height

Definition: Average amplitude of the highest 30 of 100 waves – Physical unit: [m] – Uncertainty unit: [m].

Method 1: Radar altimetry – Principle: Backscattered radiation from sea surface by medium-frequency radar (dual-frequency preferred, 13 and 3 or 5 GHz). Wave height is linked to the statistical dispersion of the radar-measured ranges. Applicable only in LEO.

Method 2: From SAR spectra – Principle: From spectral analysis of SAR images at frequencies of 1.3 or 5 GHz by processing spectrum power, wavelength and direction with the help of boundary conditions. Applicable only in LEO.

5.5.11 Dominant wave direction

Definition: One feature of the ocean wave spectrum. It is the direction of the most energetic wave in the spectrum – Physical unit: [degrees] – Uncertainty unit: [degrees].

Method 1: From SAR spectra – Principle: From spectral analysis of SAR images at frequencies of 1.3, 5 or 11 GHz. Applicable only in LEO.

5.5.12 Dominant wave period

Definition: One feature of the ocean wave spectrum. It is the period of the most energetic wave in the spectrum – Physical unit: [s] – Uncertainty unit: [s].

Method 1: From SAR spectra – Principle: From spectral analysis of SAR images at frequencies of 1.3, 5 or 11 GHz. Applicable only in LEO.

5.5.13 Wave directional-energy frequency spectrum

Definition: 2D variable colloquially referred to as "wave spectrum". Describes the wave energy travelling in each direction and frequency band (such as 24 distinct azimuth sectors each 15° wide, and 25 frequency bands) – Physical unit: $[m^2 \cdot Hz^{-1} \cdot rad^{-1}]$ – Uncertainty unit: $[m^2 \cdot Hz^{-1} \cdot rad^{-1}]$.

Method 1: From SAR spectra – Principle: From spectral analysis of SAR images at frequencies of 1.3, 5 or 11 GHz. Applicable only in LEO.

5.5.14 Sea-ice cover

Definition: The fraction of an ocean area where ice is detected – Physical unit: [%] – Uncertainty unit: [%].

Method 1: VIS/IR radiometry – Principle: Reflected solar radiation in VIS/NIR/SWIR or emitted radiation in MWIR/IR observed in a few discrete channels of relatively large bandwidths (5%–10%). The fractional cover refers to the number of pixels classified as ice in a given pixel array. Applicable in both LEO and GEO.

Method 2: MW radiometry – Principle: Emitted and scattered MW radiation in atmospheric windows at medium-high frequencies (such as 37, 90 GHz). More polarizations are needed (signal from sea is strongly polarized). The fractional cover refers to the number of pixels classified as ice in a given pixel array. Applicable only in LEO.

Method 3: High-resolution optical imagery – Principle: Reflected solar radiation in VIS/NIR/SWIR observed in several discrete channels. High-resolution is prioritized at the expense of the observing cycle. Applicable only in LEO.

Method 4: SAR imagery – Principle: Backscattered MW radiation at frequencies of 1.3, 5 or 11 GHz collected by synthetic aperture radar. The fractional cover refers to the number of pixels classified as ice in a given array. Applicable only in LEO.

5.5.15 Sea-ice thickness

Definition: Thickness of the ice sheet. It is related to sea-ice elevation and ice density – Physical unit: [cm] – Uncertainty unit: [cm].

Method 1: Radar altimetry – Principle: Backscattered radiation from sea surface by medium-frequency radar (dual-frequency preferred, 13 and 3 or 5 GHz). Associated with two-channel passive MW radiometry (23 and 37 GHz) needed for tropospheric path correction from water vapour. Applicable only in LEO.

Method 2: Lidar altimetry – Principle: Backscattered VIS/NIR radiation by lidar. Two wavelengths preferred, such as 532 and 1 064 nm. Applicable only in LEO.

Method 3: SAR interferometry – Principle: Backscattered MW radiation at frequencies of 1.3, 5 or 11 GHz collected by synthetic aperture radar. Height of observed surface determined by interferometry between images from more passes. Applicable only in LEO.

5.5.16 Sea-ice type

Definition: Comprehensive properties (age, roughness, density, etc.) of the observed sea ice. The list of types of interest is predetermined – Uncertainty expressed as number of discriminated types [classes].

Method 1: Radar scatterometry – Principle: Backscattered radiation by medium-frequency radar scatterometry (around 5 or 11 GHz). Calibrated radar reflectivity depends on roughness and surface conductivity (linked to age). Applicable only in LEO.

Method 2: MW radiometry – Principle: Emitted and scattered MW radiation in atmospheric windows at medium frequencies (such as 19, 37 GHz). Three Stokes parameters (in other words at least four polarizations) desirable. Applicable only in LEO.

Method 3: SAR imagery – Principle: Backscattered MW radiation at frequencies of 1.3, 5 or 11 GHz collected by synthetic aperture radar. Applicable only in LEO.

5.6 LAND SURFACE (INCLUDING SNOW)

This theme comprises variables that characterize the land surface, including vegetation, fire, glaciers and snow. The variables observable from space are listed in Table 5.5.

A few variables have not been considered, such as groundwater (considered covered by soil moisture, snow, glaciers; and land cover); river discharge (products are of too high a level); subsoil temperature profile (impossible from space); snow and lake surface temperature; permafrost (specific cases of surface temperature observation); coastlines (too obvious); biomass (too generic).

**Table 5.5. Geophysical variables considered under the theme
"Land surface (including snow)"**

Land surface temperature	Leaf area index	Snow status (wet/dry)	Land surface topography
Soil moisture at surface	Normalized difference vegetation index	Snow cover	Glacier cover
Soil moisture (in the roots region)	Fire fractional cover	Snow water equivalent	Glacier topography
Fraction of vegetated land	Fire temperature	Soil type	
Vegetation type	Fire radiative power	Land cover	

5.6.1   Land surface temperature

Definition: Temperature of the apparent surface of land (bare soil or vegetation) – Physical unit: [K] – Uncertainty unit: [K].

Method 1: IR radiometry – Principle: Derived from IR imagery in multiple channels including "windows" and others as needed to evaluate emissivity and atmospheric attenuation (from water vapour). Dual-view reduces the uncertainty of atmospheric correction. Applicable in both LEO and GEO.

Method 2: IR spectroscopy – Principle: Derived from a high number of very narrow window channels through the IR spectrum, associated with other channels providing all the information needed for atmospheric corrections. This enables emissivity to be estimated. Applicable in both LEO and GEO.

Method 3: MW radiometry – Principle: Emitted and scattered MW radiation in atmospheric windows at low to medium frequencies (such as 5, 10 GHz). More polarizations are needed to correct for wetness effects. Applicable only in LEO.

5.6.2   Soil moisture at surface

Definition: Fractional content of water in a volume of wet soil. Surface layer (upper few centimetres) – Physical unit: $[m^3/m^3]$ – Uncertainty unit: $[m^3/m^3]$.

Method 1: MW radiometry – Principle: Emitted MW radiation at low frequencies (1.4 and 2.7 GHz, for example). Multiple polarizations needed, to correct for roughness effects. Multiple channels desirable, to correct for temperature. Higher frequencies (5, 10 GHz) also useful, particularly for bare soil. Applicable only in LEO.

Method 2: Radar scatterometry – Principle: Backscattered MW radiation at relatively low frequencies (such as 5 GHz). The multiple viewing angle capability is exploited to correct for roughness. Applicable only in LEO.

Method 3: SAR imagery – Principle: Backscattered MW radiation at frequencies of 1.3, 5 or 11 GHz collected by synthetic aperture radar. Applicable only in LEO.

Method 4: VIS/IR radiometry – Principle: Several proxies are possible. Examples: damping of reflectivity from VIS/NIR to SWIR; from apparent thermal inertia derived by measuring the delay in land temperature rising in response to incoming solar radiation (valid for bare soil). Applicable in both LEO and GEO.

5.6.3 Soil moisture (in the roots region)

Definition: Subsoil 3D field of the fractional content of water in a volume of wet soil. Required from surface down to ~3 m – Physical unit: $[m^3/m^3]$ – Uncertainty unit: $[m^3/m^3]$.

Method 1: L-band MW radiometry – Principle: Emitted MW radiation at low frequencies (such as 1.4 GHz). More polarizations are needed, to correct for roughness effects. Applicable only in LEO.

Method 2: L-band SAR imagery – Principle: Backscattered MW radiation at low frequency (typically 1.3 GHz) collected by SAR. P band (~400 MHz) and S band (~2.7 GHz) are also possible. Applicable only in LEO.

5.6.4 Fraction of vegetated land

Definition: The fraction of a land area where vegetation is present – Physical unit: [%] – Uncertainty unit: [%].

Method 1: High-resolution optical imagery – Principle: Reflected solar radiation in VIS/NIR/SWIR observed in several discrete channels of relatively narrow bandwidths (1%–5%). Hyperspectral (several hundred channels) possible. Applicable in LEO and potentially in GEO.

Method 2: SAR imagery – Principle: Backscattered MW radiation at frequencies of 1.3, 5 or 11 GHz collected by synthetic aperture radar. Applicable only in LEO.

5.6.5 Vegetation type

Definition: Observed vegetal species or families. The list of types of interest is predetermined – Uncertainty is expressed as number of identified types [classes].

Method 1: High-resolution optical imagery – Principle: Reflected solar radiation in VIS/NIR/SWIR observed in several discrete channels of relatively narrow bandwidths (1%–5%). Hyperspectral (several hundred channels) possible. Applicable in LEO and potentially in GEO.

Method 2: SAR imagery – Principle: Backscattered MW radiation at frequencies of 1.3, 5 or 11 GHz collected by synthetic aperture radar. Applicable only in LEO.

5.6.6 Leaf area index

Definition: One half of the total projected green leaf fractional area in the plant canopy within a given area. Representative of total biomass and health of vegetation – Physical unit: [%] – Uncertainty unit: [%].

Method 1: SW radiometry – Principle: Scattered solar radiation through VIS/NIR and deeply into SWIR (up to 2.4 μm, for example). Several channels needed, relatively narrow (2%–3%). Applicable in both LEO and GEO.

Method 2: Radar scatterometry – Principle: Backscattered radiation by medium-frequency radar scatterometry (about 5 or 11 GHz). Calibrated radar reflectivity depends on surface conductivity (linked to biomass). Applicable only in LEO.

Method 3: High-resolution optical imagery – Principle: Reflected solar radiation in VIS/NIR/SWIR observed in several discrete channels of relatively narrow bandwidths (1%–5%). Hyperspectral (several hundred channels) possible. Applicable in LEO and potentially in GEO.

5.6.7   Normalized difference vegetation index

Definition: Difference between maximum (in NIR) and minimum (around the "red") vegetation reflectance, normalized to the summation. Representative of total biomass, supportive for computing leaf area index if not directly measured – Physical unit: [%] – Uncertainty unit: [%].

Method 1: VIS/NIR radiometry – Principle: Scattered solar radiation in VIS ("red", minimum reflectance from vegetation) and NIR (typically, 865 nm, high reflectance). Applicable in both LEO and GEO.

Method 2: High-resolution optical imagery – Principle: Scattered solar radiation in VIS ("red", minimum reflectance from vegetation) and NIR (typically, 865 nm, high reflectance). Applicable in LEO and potentially in GEO.

5.6.8   Fire fractional cover

Definition: The fraction of a land area where fire is present – Physical unit: [%] – Uncertainty unit: [%].

Method 1: VIS/NIR radiometry – Principle: Reflected solar radiation in VIS/NIR/SWIR or emitted radiation in MWIR/IR observed in a few discrete channels of relatively large bandwidths (5%–10%). The fractional cover refers to the number of pixels classified as fire in a given pixel array. Applicable in both LEO and GEO.

Method 2: High-resolution optical imagery – Principle: Reflected solar radiation in VIS/NIR/SWIR observed in several discrete channels. Useful post factum for damage inventory. High resolution is prioritized at the expense of the observing cycle. Applicable only in LEO.

Method 3: SAR imagery – Principle: Backscattered MW radiation at frequencies of 1.3, 5 or 11 GHz collected by SAR. The fractional cover refers to the number of pixels classified as fire in a given array. Useful post factum for damage inventory. Applicable only in LEO.

5.6.9   Fire temperature

Definition: Temperature of the fire occurring within an area – Physical unit: [K] – Uncertainty unit: [K].

Method 1: IR radiometry – Principle: Derived from IR imagery in a number of window channels. MWIR (3.7 μm) most sensitive. Applicable in both LEO and GEO.

5.6.10   Fire radiative power

Definition: Power radiated by the fire occurring within an area – Physical unit: [kW · m^{-2}] – Uncertainty unit: [kW · m^{-2}].

Method 1: IR radiometry – Principle: Derived from IR imagery in a number of window channels. MWIR (3.7 μm) most sensitive. Applicable in both LEO and GEO.

5.6.11   Snow status (wet/dry)

Definition: Binary product (dry or melting/thawing) expressing the presence of liquid water in a snow layer – Uncertainty expressed as hit rate [HR] and false-alarm Rate [FAR] when classifying the status as either wet or dry.

Method 1: MW radiometry – Principle: Emitted and scattered MW radiation in atmospheric windows at medium-high frequencies (such as 37, 90 GHz). More polarizations are needed. Since wet snow can be confused with underlying soil, preventive snow detection (mask) is necessary. Applicable only in LEO.

Method 2: SAR imagery – Principle: Backscattered MW radiation collected by synthetic aperture radar at relatively high frequencies, such as ~10 GHz (X band), possibly ~19 GHz (K band), since dry snow tends to be transparent to SAR. More useful for change detection during thawing and freezing cycles. Applicable only in LEO.

5.6.12 Snow cover

Definition: The fraction of a given area which is covered by snow – Physical unit: [%] – Uncertainty unit: [%].

Method 1: VIS/IR radiometry – Principle: Reflected solar radiation in VIS/NIR/SWIR or emitted radiation in MWIR/IR observed in a few discrete channels of relatively large bandwidths (5%–10%). The fractional cover refers to the number of pixels classified as snow in a given pixel array. Alternatively, retrieval can be carried out at pixel level by exploiting the "defect" of brightness due to mixed snow/no-snow in the pixel ("effective snow cover"). Applicable in both LEO and GEO.

Method 2: MW radiometry – Principle: Emitted and scattered MW radiation in atmospheric windows at medium-high frequencies (such as 37, 90 GHz). More polarizations are needed. The fractional cover refers to the number of pixels classified as snow in a given pixel array. Snow surface status (dry or wet) is also determined. Applicable only in LEO.

Method 3: High-resolution optical imagery – Principle: Reflected solar radiation in VIS/NIR/ SWIR observed in several discrete channels. High-resolution is prioritized at the expense of the observing cycle. Applicable in LEO and potentially in GEO.

5.6.13 Snow water equivalent

Definition: Vertical depth of the water that would be obtained by melting a snow layer. The snow depth may be inferred by exploiting auxiliary information on the density of the snow layer – Physical unit: [mm] – Uncertainty unit: [mm].

Method 1: MW radiometry – Principle: Emitted and scattered MW radiation in atmospheric windows at medium-high frequencies (such as 37, 90 GHz), preferred because at low frequency dry snow is transparent. More polarizations are needed. Applicable only in LEO.

Method 2: Radar scatterometry – Principle: Backscattered MW radiation at low-medium frequencies (5, 13 GHz). Higher frequency preferred over dry snow. The multiple viewing angle capability is exploited to correct for roughness. Applicable only in LEO.

Method 3: SAR imagery – Principle: Backscattered MW radiation collected by SAR at relatively high frequencies (dry snow is transparent to SAR). An optimal frequency would be ~19 GHz (K_u band). Lower frequencies can be used for monitoring changes by interferometry. Applicable only in LEO.

5.6.14 Soil type

Definition: Observed soil composition or structure (acid, alkaline, rough, etc.). The list of types of interest is predetermined – Uncertainty is expressed as number of discriminated types [classes].

Method 1: High-resolution optical imagery – Principle: Reflected solar radiation in VIS/NIR/SWIR observed in several discrete channels of relatively narrow bandwidths (1%–5%). Hyperspectral (several hundred channels) possible. Applicable in LEO and potentially in GEO.

Method 2: SAR imagery – Principle: Backscattered MW radiation at frequencies of 1.3, 5 or 11 GHz collected by synthetic aperture radar. Applicable only in LEO.

5.6.15 Land cover

Definition: Observed land utilization (urban, cultivated, desertic, etc.). The list of types of interest is predetermined – Uncertainty expressed as the number of identified types [classes].

Method 1: High-resolution optical imagery – Principle: Reflected solar radiation in VIS/NIR/SWIR observed in several discrete channels of relatively narrow bandwidths (1%–5%). Hyperspectral (several hundred channels) possible. Applicable in LEO and potentially in GEO.

Method 2: SAR imagery – Principle: Backscattered MW radiation at frequencies of 1.3, 5 or 11 GHz collected by synthetic aperture radar. Applicable only in LEO.

5.6.16 Land surface topography

Definition: Map of land surface heights – Physical unit: [m] – Uncertainty unit: [m].

Method 1: High-resolution VIS stereoscopy – Principle: Reflected solar radiation in VIS observed in one or more channels of relatively narrow bandwidths (1%–5%) from at least two viewing directions, generally from successive orbits, so as to implement stereoscopy. Applicable only in LEO.

Method 2: SAR interferometry – Principle: Backscattered MW radiation at frequencies of 1.3, 5 or 11 GHz collected by synthetic aperture radar. Interferometry from successive orbital passes. Applicable only in LEO.

Method 3: Radar altimetry – Principle: Backscattered radiation from land surface by medium-frequency radar (dual-frequency preferred, 13 and 3 or 5 GHz). Associated with two or three channels of passive MW radiometry (23 and 37 and/or 19 GHz) needed for tropospheric path correction from water vapour and ionosphere-induced rotation. Along-track SAR processing is needed for acceptable resolution. Only nadir view. Applicable only in LEO.

Method 4: Lidar altimetry – Principle: Backscattered VIS/NIR radiation by lidar. Two wavelengths preferred, such as 532 and 1 064 nm. Only nadir view. Applicable only in LEO.

5.6.17 Glacier cover

Definition: The fraction of a land area covered by permanent ice – Physical unit: [%] – Uncertainty unit: [%].

Method 1: High-resolution VIS stereoscopy – Principle: Reflected solar radiation in VIS/NIR/SWIR observed in several discrete channels of relatively narrow bandwidths (1%–5%). Applicable in LEO and potentially in GEO.

Method 2: SAR imagery – Principle: Backscattered MW radiation at frequencies of 1.3, 5 or 11 GHz collected by synthetic aperture radar. Interferometry used to detect changes. Applicable only in LEO.

5.6.18 **Glacier topography**

Definition: Map of the height of the glacier surface – Physical unit: [cm] – Uncertainty unit: [cm].

Method 1: SAR interferometry – Principle: Backscattered MW radiation at frequencies of 1.3, 5 or 11 GHz collected by synthetic aperture radar. Interferometry from successive orbital passes. Applicable only in LEO.

5.7 **SOLID EARTH**

This theme comprises variables that characterize the solid Earth (space geodesy and Earth interior). The variables observable from space are listed in Table 5.6.

Table 5.6. Geophysical variables considered under the theme "Solid Earth"

Geoid	Crustal plates positioning	Crustal motion (horizontal and vertical)	Gravity field	Gravity gradients

5.7.1 **Geoid**

Definition: Equipotential surface which would coincide exactly with the mean ocean surface of the Earth, if the oceans were in equilibrium, at rest, and extended through the continents (such as with very narrow channels) – Physical unit: [cm] – Uncertainty unit: [cm].

Method 1: Radar altimetry – Principle: Backscattered radiation from sea surface by medium-frequency radar (dual-frequency preferred, 13 and 3 or 5 GHz). Associated with two or three channels of passive MW radiometry (23 and 37 and/or 19 GHz) needed for tropospheric path correction from water vapour and ionosphere-induced rotation. Highly stable orbits needed (relatively high altitude, 50°–70° inclination and accurate repeat cycle). Multi-orbital analysis enables transient perturbations to be filtered out of waves, ocean currents and tides. Applicable only in LEO.

Method 2: Gravity-field observation – Principle: Observation of the gravity field at satellite altitude by accelerometers, gradiometers, satellite–satellite tracking (coupled satellites or with GPS satellites). Low orbits are used, changing during mission time. Applicable only in LEO.

5.7.2 **Crustal plates positioning**

Definition: Basis for monitoring the evolution of the lithosphere dynamics – Physical unit: [cm] – Uncertainty unit: [cm].

Method 1: Laser ranging – Principle: Accurate measurement of the satellite–ground distance by pointing the satellite using a surface-based laser that collects the light reflected by cube-corner mirrors covering the surface of the satellite. A worldwide network can provide both precision orbitography and the position of the crustal plates supporting the laser ranging stations. Applicable only in LEO.

Method 2: GPS receiver – Principle: Statistical analysis of the position of a surface-based GPS receiver localized by the constellations of navigation satellites (GPS, GLONASS, Compass, Galileo). Applicable only in LEO.

5.7.3   Crustal motion (horizontal and vertical)

Definition: Changes over time of the position and height of the Earth's plates. Indicative of the lithosphere dynamics, thus useful for earthquake prediction – Physical unit: [mm/y] – Uncertainty unit: [mm/y].

Method 1: Laser ranging – Principle: Analysis of changes in crustal plate positioning, accurately measured by satellite-ground distance through a surface-based laser that collects the light reflected by cube-corner mirrors covering the surface of the satellite. A worldwide network of laser-ranging stations enables this analysis to be performed. Applicable only in LEO.

Method 2: GPS receiver – Principle: Analysis of changes in crustal plate positioning, accurately measured by surface-based GPS receivers localized by the constellations of navigation satellites (GPS, GLONASS, Compass, Galileo). Applicable only in LEO.

5.7.4   Gravity field

Definition: 3D field, actually measured in situ at orbital height. Indicative of the statics and dynamics of the lithosphere and the mantle – Physical unit: [mGal] (1 Gal = 0.01 m/s^2, so 1 mGal ≈ 10^{-6} g$_0$. "Gal" stands for Galileo) – Uncertainty unit: [mGal].

Method 1: Gradiometry – Principle: Appropriate network of accelerometers sensitive to anomalies in the gravity field crossed by the satellite during its motion in orbit. Applicable only in LEO.

Method 2: Satellite-to-satellite tracking – Principle: Continuous monitoring of the distance between satellites in coordinated orbits, for example by means of K-band radar or lidar. Applicable only in LEO.

5.7.5   Gravity gradients

Definition: 3D field, actually measured in situ at orbital height. Indicative of fine details of the statics and dynamics of the lithosphere and the mantle – Physical unit: [E], Eötvös (1 E = 1 mGal/10 km) – Uncertainty unit: [E].

Method 1: Gradiometry – Principle: Appropriate network of accelerometers sensitive to anomalies of the gravity field crossed by the satellite during its motion in orbit. Applicable only in LEO.

Method 2: Satellite-to-satellite tracking – Principle: Continuous monitoring of the distance between satellites in coordinated orbits by means of K-band radar or lidar, for example. Applicable only in LEO.

5.8   ATMOSPHERIC CHEMISTRY

This theme deals with species that impact the ozone cycle, and/or provoke the greenhouse effect and/or affect air quality. The species observable from space and which are so far the subject of explicit requirements are listed in Table 5.7.

Table 5.7. Geophysical variables considered under the theme "Atmospheric chemistry"

O_3	C_2H_2	CFC–11	CH_2O	ClO		CO	COS	HCl	HNO_3	N_2O_5	NO_2	Peroxyacetyl nitrate	SF_6
BrO	C_2H_6	CFC–12	CH_4		$ClONO_2$	CO_2	H_2O	HDO	N_2O	NO	OH	Polar stratospheric cloud occurrence	SO_2

5.8.1 Ozone (O₃)

Definition: 3D field of dry-air mole fraction of O_3. Required from surface to TOA (layers: LT, HT, LS, HS&M) + total column – Physical unit: [nmol/mol] for layers, Dobson unit [DU] for total column (1 DU = 2.69 · 10^{20} molecules/m²) – Uncertainty unit: [nmol/mol] for layers, [DU] for total column.

Method 1: SW spectroscopy (cross-nadir) – Principle: Scattered radiation in UV and VIS observed with high spectral resolution in several bands by cross-nadir spectrometers. Applicable in both LEO and GEO.

Method 2: IR spectroscopy (cross-nadir) – Principle: Emitted radiation in TIR (~9.7 μm) observed with medium-high spectral resolution by cross-nadir spectrometers. Applicable in both LEO and GEO.

Method 3: SW spectroscopy (limb) – Principle: Scattered radiation in UV and VIS observed in limb mode with high spectral resolution. Also, missing lines from the spectrum of the Sun, moon or stars during occultation. Applicable only in LEO.

Method 4: IR spectroscopy (limb) – Principle: Emitted radiation in TIR (~9.7 μm) observed with high spectral resolution by limb-sounding spectrometers. Applicable only in LEO.

Method 5: MW/sub-mm spectroscopy (limb) – Principle: Emitted radiation in MW/sub-mm (such as ~240, 300 and 500 GHz) observed with high spectral resolution by limb-sounding spectrometers. Applicable only in LEO.

Method 6: DIAL – Principle: Backscattered radiation in a UV, VIS or TIR ozone-absorption band and a side window by differential absorption lidar. Applicable only in LEO.

5.8.2 Bromine monoxide (BrO)

Definition: 3D field of dry-air mole fraction of BrO. Required from surface to TOA (layers: LT, HT, LS, HS&M) – Physical unit: [nmol/mol] – Uncertainty unit: [nmol/mol].

Method 1: UV spectroscopy (cross-nadir) – Principle: Scattered radiation in UV observed with high spectral resolution in the 300 nm region by cross-nadir spectrometers. Applicable in both LEO and GEO.

Method 2: UV spectroscopy (limb) – Principle: Scattered radiation in UV (300 nm region) observed in limb mode with high spectral resolution. Also, missing lines from the spectrum of the Sun, moon or stars during occultation. Applicable only in LEO.

Method 3: MW/sub-mm spectroscopy (limb) – Principle: Emitted radiation in MW/sub-mm (such as ~640 GHz) observed with high spectral resolution by limb-sounding spectrometers. Applicable only in LEO.

5.8.3 Acetylene (C₂H₂)

Definition: 3D field of dry-air mole fraction of C_2H_2. Required in the troposphere (layers: LT, HT) – Physical unit: [nmol/mol] – Uncertainty unit: [nmol/mol].

Method 1: TIR spectroscopy (cross-nadir) – Principle: Emitted radiation in TIR (~7.5 and 13.7 μm) observed with high spectral resolution by cross-nadir spectrometers. Applicable in both LEO and GEO.

5.8.4   Ethane (C$_2$H$_6$)

Definition: 3D field of dry-air mole fraction of C$_2$H$_6$. Required in the troposphere (layers: LT, HT) – Physical unit: [nmol/mol] – Uncertainty unit: [nmol/mol].

Method 1: TIR spectroscopy (cross-nadir) – Principle: Emitted radiation in TIR (~3.3 and 12 μm) observed with high spectral resolution by cross-nadir spectrometers. Applicable in both LEO and GEO.

5.8.5   Trichlorofluoromethane (CFC–11 = Freon–11)

Definition: 3D field of dry-air mole fraction of CFC–11. Required from surface to TOA (layers: LT, HT, LS, HS&M) – Physical unit: [nmol/mol] – Uncertainty unit: [nmol/mol].

Method 1: TIR spectroscopy (cross-nadir) – Principle: Emitted radiation in TIR (~9.2 and 11.7 μm) observed with medium-high spectral resolution by cross-nadir spectrometers. Applicable in both LEO and GEO.

Method 2: TIR spectroscopy (limb) – Principle: Emitted radiation in TIR (~9.2 and 11.7 μm) observed with medium-high spectral resolution by limb-sounding spectrometers. Applicable only in LEO.

5.8.6   Dichlorodifluoromethane (CFC–12 = Freon–12)

Definition: 3D field of dry-air mole fraction of CFC–12. Required from surface to TOA (layers: LT, HT, LS, HS&M) – Physical unit: [nmol/mol] – Uncertainty unit: [nmol/mol].

Method 1: TIR spectroscopy (cross-nadir) – Principle: Emitted radiation in TIR (~8.8 and 10.8 μm) observed with medium-high spectral resolution by cross-nadir spectrometers. Applicable in both LEO and GEO.

Method 2: TIR spectroscopy (limb) – Principle: Emitted radiation in TIR (~8.8 and 10.8 μm) observed with medium-high spectral resolution by limb-sounding spectrometers. Applicable only in LEO.

5.8.7   Formaldehyde (CH$_2$O = HCHO)

Definition: 3D field of dry-air mole fraction of CH$_2$O. Required in the troposphere (layers: LT, HT) + total column – Physical unit: [nmol/mol] for layers, units of [$1.3 \cdot 10^{15}$ molecules/cm^2] for total column – Uncertainty unit: [nmol/mol] for layers, [$1.3 \cdot 10^{15}$ cm^{-2}] for total column.

Method 1: UV spectroscopy (cross-nadir) – Principle: Scattered radiation in UV (~350 nm) observed with high spectral resolution by cross-nadir spectrometers. Applicable in both LEO and GEO.

5.8.8   Methane (CH$_4$)

Definition: 3D field of dry-air mole fraction of CH$_4$. Required from surface to TOA (layers: LT, HT, LS, HS&M) + total column – Physical unit: [nmol/mol] for layers, units of [$1.3 \cdot 10^{15}$ molecules/cm^2] for total column – Uncertainty unit: [nmol/mol] for layers, [$1.3 \cdot 10^{15}$ molecules/cm^2] for total column.

Method 1: SWIR spectroscopy (cross-nadir) – Principle: Scattered radiation in SWIR (~2.3 μm) observed with high spectral resolution by cross-nadir spectrometers. Applicable in both LEO and GEO.

Method 2: TIR spectroscopy (cross-nadir) – Principle: Emitted radiation in TIR (~3.4, 4.3 and 7.7 μm) observed with medium-high spectral resolution by cross-nadir spectrometers. Applicable in both LEO and GEO.

Method 3: SWIR spectroscopy (limb) – Principle: Scattered radiation in SWIR (~2.3 μm) observed in limb mode with high spectral resolution. Also, missing lines from the spectrum of the Sun, moon or stars during occultation. Applicable only in LEO.

Method 4: TIR spectroscopy (limb) – Principle: Emitted radiation in TIR (~3.4, 4.3 and 7.7 μm) observed with high spectral resolution by limb-sounding spectrometers. Applicable only in LEO.

5.8.9 Chlorine monoxide (ClO = hypochlorite)

Definition: 3D field of dry-air mole fraction of ClO. Required from surface to TOA (layers: LT, HT, LS, HS&M) – Physical unit: [nmol/mo] – Uncertainty unit: [nmol/mol].

Method 1: UV spectroscopy (cross-nadir) – Principle: Scattered radiation in UV observed with high spectral resolution in the 300 nm region by cross-nadir spectrometers. Applicable in both LEO and GEO.

Method 2: UV spectroscopy (limb) – Principle: Scattered radiation in UV (300 nm region) observed in limb mode with high spectral resolution. Also, missing lines from the spectrum of the Sun, moon or stars during occultation. Applicable only in LEO.

Method 3: MW/sub-mm spectroscopy (limb) – Principle: Emitted radiation in MW/sub-mm (such as ~640 GHz) observed with high spectral resolution by limb-sounding spectrometers. Applicable only in LEO.

5.8.10 Chlorine nitrate (ClONO$_2$)

Definition: 3D field of dry-air mole fraction of ClONO$_2$. Required from mid-troposphere to TOA (layers: HT, LS, HS&M) – Physical unit: [nmol/mol] – Uncertainty unit: [nmol/mol].

Method 1: TIR spectroscopy (cross-nadir) – Principle: Emitted radiation in TIR (~5.7, 7.7 and 12.5 μm) observed with high spectral resolution by cross-nadir spectrometers. Applicable in both LEO and GEO.

Method 2: TIR spectroscopy (limb) – Principle: Emitted radiation in TIR (~5.7, 7.7 and 12.5 μm) observed with high spectral resolution by limb-sounding spectrometers. Applicable only in LEO.

5.8.11 Carbon monoxide (CO)

Definition: 3D field of dry-air mole fraction of CO. Required from surface to low stratosphere (layers: LT, HT, LS) + total column – Physical unit: [nmol/mol] for layers, units of [1.3 · 10^{15} molecules/cm^2] for total column – Uncertainty unit: [nmol/mol] for layers, [1.3 · 10^{15} molecules/cm^2] for total column.

Method 1: SWIR spectroscopy (cross-nadir) – Principle: Scattered radiation in SWIR (~2.3 μm) observed with high spectral resolution by cross-nadir spectrometers. Applicable in both LEO and GEO.

Method 2: TIR spectroscopy (cross-nadir) – Principle: Emitted radiation in TIR (~4.6 μm) observed with medium-high spectral resolution by cross-nadir spectrometers. Applicable in both LEO and GEO.

Method 3: SWIR spectroscopy (limb) – Principle: Scattered radiation in SWIR (~2.3 μm) observed in limb mode with high spectral resolution. Also, missing lines from the spectrum of the Sun, moon or stars during occultation. Applicable only in LEO.

Method 4: TIR spectroscopy (limb) – Principle: Emitted radiation in TIR (~4.6 μm) observed with high spectral resolution by limb-sounding spectrometers. Applicable only in LEO.

5.8.12   Carbon dioxide (CO$_2$)

Definition: 3D field of dry-air mole fraction of CO$_2$. Required from surface to TOA (layers: LT, HT, LS, HS&M) + total column – Physical unit: [nmol/mol] for layers, units of [1.3 · 10^{15} molecules/cm^2] for total column – Uncertainty unit: [nmol/mol] for layers, [1.3 · 10^{15} molecules/cm^2] for total column.

Method 1: SWIR spectroscopy (cross-nadir) – Principle: Scattered radiation in SWIR (~1.6 and 2.1 μm) observed with high spectral resolution by cross-nadir spectrometers. Applicable in both LEO and GEO.

Method 2: TIR spectroscopy (cross-nadir) – Principle: Emitted radiation in TIR (~4.3 and 15 μm) observed with medium-high spectral resolution by cross-nadir spectrometers. Applicable in both LEO and GEO.

Method 3: SWIR spectroscopy (limb) – Principle: Scattered radiation in SWIR (~1.6 and 2.1 μm) observed in limb mode with high spectral resolution. Also, missing lines from the spectrum of the Sun, moon or stars during occultation. Applicable only in LEO.

Method 4: TIR spectroscopy (limb) – Principle: Emitted radiation in TIR (~4.3 and 15 μm) observed with high spectral resolution by limb-sounding spectrometers. Applicable only in LEO.

Method 5: DIAL – Principle: Backscattered radiation in a CO$_2$ absorption band and a side window by differential absorption lidar. Several bands are available, around 1.6 and 2.0 μm, for example. Only total column feasible. Integration over large area and long time necessary to achieve the required uncertainty (~0.3%). Applicable only in LEO.

5.8.13   Carbonyl sulphide (COS)

Definition: 3D field of dry-air mole fraction of COS. Required from surface to low stratosphere (layers: LT, HT, LS) – Physical unit: [nmol/mol] – Uncertainty unit: [nmol/mol].

Method 1: TIR spectroscopy (cross-nadir) – Principle: Emitted radiation in TIR (~4.8 and 11.6 μm) observed with high spectral resolution by cross-nadir spectrometers. Applicable in both LEO and GEO.

Method 2: TIR spectroscopy (limb) – Principle: Emitted radiation in TIR (~4.8 and 11.6 μm) observed with high spectral resolution by limb-sounding spectrometers. Applicable only in LEO.

5.8.14   Water vapour (H$_2$O)

Definition: 3D field of dry-air mole fraction of H$_2$O (intended as a chemical species relevant for atmospheric chemistry). Required from surface to TOA (layers: LT, HT, LS, HS&M) – Physical unit: [nmol/mol] – Uncertainty unit: [nmol/mol].

Method 1: SW spectroscopy (cross-nadir) – Principle: Scattered radiation in VIS, NIR and SWIR observed with high spectral resolution in several bands by cross-nadir spectrometers. Applicable in both LEO and GEO.

Method 2: IR spectroscopy (cross-nadir) – Principle: Emitted radiation in TIR (~6.3 μm) observed with medium-high spectral resolution by cross-nadir spectrometers. Applicable in both LEO and GEO.

Method 3: Far IR spectroscopy (cross-nadir) – Principle: Emitted radiation in FIR (~18 μm) observed with medium-high spectral resolution by cross-nadir spectrometers. Applicable in both LEO and GEO.

Method 4: GNSS radio-occultation – Principle: Atmospheric refraction of L-band signals from the GNSS received by a LEO satellite during the occultation phase. Applicable only in LEO.

Method 5: SW spectroscopy (limb) – Principle: Scattered radiation in VIS, NIR and SWIR observed in limb mode with high spectral resolution. Also, missing lines from the spectrum of the Sun, moon or stars during occultation. Applicable only in LEO.

Method 6: IR spectroscopy (limb) – Principle: Emitted radiation in TIR (~6.3 μm) observed with high spectral resolution by limb-sounding spectrometers. Applicable only in LEO.

Method 7: MW/sub-mm spectroscopy (limb) – Principle: Emitted radiation in several bands of the MW/sub-mm range observed with high spectral resolution by limb-sounding spectrometers. Applicable only in LEO.

Method 8: DIAL – Principle: Backscattered radiation in a UV, VIS or TIR absorption band and a side window by differential absorption lidar. Applicable only in LEO.

5.8.15   Hydrogen chloride (HCl)

Definition: 3D field of dry-air mole fraction of HCl. Required from mid-troposphere to TOA (layers: HT, LS, HS&M) – Physical unit: [nmol/mol] – Uncertainty unit: [nmol/mol].

Method 1: MW/sub-mm spectroscopy (limb) – Principle: Emitted radiation in MW/sub-mm (such as ~625 GHz) observed with high spectral resolution by limb-sounding spectrometers. Applicable only in LEO.

5.8.16   HDO

Definition: 3D field of dry-air mole fraction of HDO = water vapour (with one hydrogen nucleus replaced by its deuterium isotope). Required from low stratosphere to TOA (layers: LS and HS&M) – Physical unit: [nmol/mol] – Uncertainty unit: [nmol/mol].

Method 1: MW/sub-mm spectroscopy (limb) – Principle: Emitted radiation in MW/sub-mm (such as ~1 000 GHz) observed with high spectral resolution by limb-sounding spectrometers. Applicable only in LEO.

5.8.17   Nitric acid (HNO$_3$)

Definition: 3D field of dry-air mole fraction of HNO$_3$. Required from surface to TOA (layers: LT, HT, LS, HS&M) + total column – Physical unit: [nmol/mol] for layers, units of [1.3 · 10^{15} molecules/cm^2] for total column – Uncertainty unit: [nmol/mol] for layers, [1.3 · 10^{15} molecules/cm^2] for total column.

Method 1: IR spectroscopy (cross-nadir) – Principle: Emitted radiation in TIR (~5.9, 7.6 and 11.3 μm) observed with high spectral resolution by cross-nadir spectrometers. Applicable in both LEO and GEO.

Method 2: IR spectroscopy (limb) – Principle: Emitted radiation in TIR (~5.9, 7.6 and 11.3 μm) observed with high spectral resolution by limb-sounding spectrometers. Applicable only in LEO.

Method 3: MW/sub-mm spectroscopy (limb) – Principle: Emitted radiation in MW/sub-mm (such as ~345 GHz) observed with high spectral resolution by limb-sounding spectrometers. Applicable only in LEO.

5.8.18 Nitrous oxide (N_2O)

Definition: 3D field of dry-air mole fraction of N_2O. Required from surface to TOA (layers: LT, HT, LS, HS&M) – Physical unit: [nmol/mol] – Uncertainty unit: [nmol/mol].

Method 1: SWIR spectroscopy (cross-nadir) – Principle: Scattered radiation in SWIR (~2.3 μm) observed with high spectral resolution by cross-nadir spectrometers. Applicable in both LEO and GEO.

Method 2: TIR spectroscopy (cross-nadir) – Principle: Emitted radiation in TIR (~4.5 and 7.7 μm) observed with medium-high spectral resolution by cross-nadir spectrometers. Applicable in both LEO and GEO.

Method 3: SWIR spectroscopy (limb) – Principle: Scattered radiation in SWIR (~2.3 μm) observed in limb mode with high spectral resolution. Also, missing lines from the spectrum of the Sun, moon or stars during occultation. Applicable only in LEO.

Method 4: TIR spectroscopy (limb) – Principle: Emitted radiation in TIR (~4.5 and 7.7 μm) observed with high spectral resolution by limb-sounding spectrometers. Applicable only in LEO.

Method 5: MW/sub-mm spectroscopy (limb) – Principle: Emitted radiation in MW/sub-mm (such as ~300 and 500 GHz) observed with high spectral resolution by limb-sounding spectrometers. Applicable only in LEO.

5.8.19 Nitrogen pentoxide (N_2O_5)

Definition: 3D field of dry-air mole fraction of N_2O_5. Required in the troposphere (layers: LT, HT) – Physical unit: [nmol/mol] – Uncertainty unit: [nmol/mol].

Method 1: TIR spectroscopy (cross-nadir) – Principle: Emitted radiation in TIR (~5.8 and 8.0 μm) observed with high spectral resolution by cross-nadir spectrometers. Applicable in both LEO and GEO.

5.8.20 Nitric oxide (NO)

Definition: 3D field of dry-air mole fraction of NO. Required from surface to TOA (layers: LT, HT, LS, HS&M) – Physical unit: [nmol/mol] – Uncertainty unit: [nmol/mol].

Method 1: SW spectroscopy (cross-nadir) – Principle: Scattered radiation in UV (~250 nm) observed with high spectral resolution by cross-nadir spectrometers. Applicable in both LEO and GEO.

Method 2: IR spectroscopy (cross-nadir) – Principle: Emitted radiation in TIR (~5.3 μm) observed with high spectral resolution by cross-nadir spectrometers. Applicable in both LEO and GEO.

Method 3: SW spectroscopy (limb) – Principle: Scattered radiation in UV (~250 nm) observed in limb mode with high spectral resolution. Also, missing lines from the spectrum of the Sun, moon or stars during occultation. Applicable only in LEO.

Method 4: IR spectroscopy (limb) – Principle: Emitted radiation in TIR (~5.3 μm) observed with high spectral resolution by limb-sounding spectrometers. Applicable only in LEO.

5.8.21   Nitrogen peroxide (NO$_2$)

Definition: 3D field of dry-air mole fraction of NO$_2$. Required from surface to TOA (layers: LT, HT, LS, HS&M) + total column – Physical unit: [nmol/mol] for layers, units of [$1.3 \cdot 10^{15}$ molecules/cm^2] for total column – Uncertainty unit: [nmol/mol] for layers, [$1.3 \cdot 10^{15}$ cm^{-2}] for total column.

Method 1: SW spectroscopy (cross-nadir) – Principle: Scattered radiation in UV and VIS observed with high spectral resolution in several bands by cross-nadir spectrometers. Applicable in both LEO and GEO.

Method 2: IR spectroscopy (cross-nadir) – Principle: Emitted radiation in TIR (~6.1 μm) observed with high spectral resolution by cross-nadir spectrometers. Applicable in both LEO and GEO.

Method 3: SW spectroscopy (limb) – Principle: Scattered radiation in UV and VIS observed in limb mode with high spectral resolution. Also, missing lines from the spectrum of the Sun, moon or stars during occultation. Applicable only in LEO.

Method 4: IR spectroscopy (limb) – Principle: Emitted radiation in TIR (~6.1 μm) observed with high spectral resolution by limb-sounding spectrometers. Applicable only in LEO.

5.8.22   Hydroxyl radical (OH)

Definition: 3D field of dry-air mole fraction of OH. Required from surface to TOA (layers: LT, HT, LS, HS&M) – Physical unit: [nmol/mol] – Uncertainty unit: [nmol/mol].

Method 1: Sub-mm spectroscopy (limb) – Principle: Emitted radiation in sub-mm (~2 500 GHz) observed with high spectral resolution by limb-sounding spectrometers. Applicable only in LEO.

Method 2: FIR spectroscopy (limb) – Principle: Emitted radiation in the Far IR (several lines in the range 28–182 μm, best at ~84 μm) observed with high spectral resolution by limb-sounding spectrometers. Applicable only in LEO.

5.8.23   Peroxyacetyl nitrate

Definition: 3D field of dry-air mole fraction of peroxyacetyl nitrate. Required in the troposphere (layers: LT, HT) – Physical unit: [nmol/mol] – Uncertainty unit: [nmol/mol].

Method 1: TIR spectroscopy (cross-nadir) – Principle: Emitted radiation in TIR (~5.7, 8.6 and 12.5 μm) observed with high spectral resolution by cross-nadir spectrometers. Applicable only in LEO.

5.8.24   Polar stratospheric cloud occurrence

Definition: 3D field of polar stratospheric cloud occurrence. Required in the lower stratosphere (layer: LS) – Uncertainty expressed as hit rate [HR] and false-alarm rate [FAR].

Method 1: SW spectroscopy (cross-nadir) – Principle: Scattered radiation in UV and VIS observed with moderate spectral resolution by cross-nadir spectrometers. Applicable in both LEO and GEO.

Method 2: SW spectroscopy (limb) – Principle: Scattered radiation in UV and VIS observed in limb mode with moderate spectral resolution. Applicable only in LEO.

Method 3: IR spectroscopy (limb) – Principle: Emitted radiation in TIR observed with moderate spectral resolution by limb-sounding spectrometers. Applicable only in LEO.

Method 4: Backscatter lidar – Principle: Backscattered radiation in UV, VIS or NIR by lidar. Applicable only in LEO.

5.8.25 Sulphur hexafluoride (SF$_6$)

Definition: 3D field of dry-air mole fraction of SF$_6$. Required from low stratosphere to TOA (layers: LS and HS&M) – Physical unit: [nmol/mol] – Uncertainty unit: [nmol/mol].

Method 1: TIR spectroscopy (cross-nadir) – Principle: Emitted radiation in TIR (~10.5 μm) observed with high spectral resolution by cross-nadir spectrometers. Applicable in both LEO and GEO.

Method 2: TIR spectroscopy (limb) – Principle: Emitted radiation in TIR (~10.5 μm) observed with high spectral resolution by limb-sounding spectrometers. Applicable only in LEO.

5.8.26 Sulphur dioxide (SO$_2$)

Definition: 3D field of dry-air mole fraction of SO$_2$. Required from surface to lower stratosphere (layers: LT, HT, LS) + total column – Physical unit: [nmol/mol] for layers, units of [$1.3 \cdot 10^{15}$ molecules/cm^2] for total column – Uncertainty unit: [nmol/mol] for layers, [$1.3 \cdot 10^{15}$ cm^{-2}] for total column.

Method 1: UV spectroscopy (cross-nadir) – Principle: Scattered radiation in UV (~350 nm) observed with high spectral resolution by cross-nadir spectrometers. Applicable in both LEO and GEO.

Method 2: TIR spectroscopy (cross-nadir) – Principle: Emitted radiation in TIR (~7.3 and 8.6 μm) observed with medium-high spectral resolution by cross-nadir spectrometers. Applicable in both LEO and GEO.

5.9 SPACE WEATHER

This theme comprises variables that characterize space weather. The variables relevant to this theme are classified below according to three categories:

(a)   Solar processes monitoring (Table 5.8);

(b)   Sun–Earth interplanetary space, dominated by the solar wind (Table 5.9);

(c)   Earth proximity: the magnetosphere and ionosphere (Table 5.10).

Table 5.8. Satellite observations relevant to solar processes monitoring

Variable	Details	Physical unit
Solar gamma rays, X-rays, EUV, UV, VIS	Integrated flux density Flux spectrum Flux image	W $\cdot$ m^{-2} W $\cdot$ m^{-2} $\cdot$ nm^{-1} W $\cdot$ m^{-2} $\cdot$ arcsec^{-2}
Solar Ca II-K image	K-line of Ca-II (393.4 nm)	W $\cdot$ m^{-2} $\cdot$ arcsec^{-2}
Solar H-alpha image	Hydrogen-alpha transition (656.3 nm)	W $\cdot$ m^{-2} $\cdot$ arcsec^{-2}
Solar Lyman-alpha image	Hydrogen Lyman-alpha transition (121.6 nm)	W $\cdot$ m^{-2} $\cdot$ arcsec^{-2}
Solar Lyman-alpha flux	Hydrogen Lyman-alpha transition (121.6 nm)	W $\cdot$ m^{-2} $\cdot$ nm^{-1}
Solar magnetic field	Magnetic field at the solar surface (photosphere)	nT

Variable	Details	Physical unit
Solar radio flux spectrum	Radio flux integrated over the solar disk	$W \cdot m^{-2} \cdot Hz^{-1}$
Solar radio flux image	Radio flux received from the solar disk	$W \cdot m^{-2} \cdot Hz^{-1} \cdot arcsec^{-2}$
Solar velocity fields	3D map of plasma velocity in the photosphere	$m \cdot s^{-1} \cdot arcsec^{-2}$
Solar electric field	Map of the electric field in the photosphere	$mV \cdot m^{-1} \cdot arcsec^{-2}$
Solar corona image	Image of the corona surrounding the Sun	$W \cdot m^{-2} \cdot arcsec^{-2}$

**Table 5.9. Satellite observations relevant
to Sun–Earth interplanetary space and solar wind**

Variable	Details	Physical unit
Electrons, protons, neutrons, alpha-particles	Integrated flux density Differential directional flux Integral directional flux	$particles \cdot m^{-2} \cdot s^{-1}$ $particles \cdot m^{-2} \cdot s^{-1} \cdot sr^{-1} \cdot eV^{-1}$ $particles \cdot m^{-2} \cdot s^{-1} \cdot sr^{-1}$
Heavy ions [2(He) < Z ≤ 26(Fe)]	Angular flux energy and mass spectrum Integral directional flux	$particles \cdot m^{-2} \cdot s^{-1} \cdot sr^{-1}$ $(MeV/nucleon)^{-1}$ $particles \cdot m^{-2} \cdot s^{-1} \cdot sr^{-1}$
Cosmic rays	Neutron flux	$neutron \cdot m^{-2} \cdot s^{-1}$
Gamma rays, X-rays, EUV, UV, VIS, NIR, SWIR	Flux Flux spectrum Sky image	$W \cdot m^{-2}$ $W \cdot m^{-2} \cdot nm^{-1}$ $W \cdot m^{-2} \cdot arcsec^{-2}$
Radio waves	Integrated flux density	$W \cdot m^{-2} \cdot Hz^{-1}$
Heliospheric image	Image of the solar wind environment	$W \cdot m^{-2} \cdot arcsec^{-2}$
Interplanetary magnetic field	Magnetic field in the solar wind	nT
Solar wind density	Density of the solar wind plasma	$particles \cdot cm^{-3}$
Solar wind temperature	Temperature of solar wind plasma	K
Solar wind velocity	Velocity of the solar wind plasma	$km \cdot s^{-1}$

Table 5.10. Satellite observations specific to the magnetosphere and ionosphere

Variable	Details	Physical unit
Ionospheric plasma velocity	Velocity of bulk plasma or electrons, a function of altitude	$km \cdot s^{-1}$
Ionospheric scintillation	Random fluctuations of radio waves and refractive index	dimensionless
Ionospheric total electron content	Number of electrons between two points	TECU
Electron density	3D distribution of the electron density in the ionosphere	$electrons \cdot m^{-3}$
Magnetic field	Magnetic field in the Earth environment (magnetosphere)	nT
Electric field	Magnitude and direction of the Earth's electric field	$mV \cdot m$
Electrostatic charge	Accumulated electric charge on a satellite platform	$pA \cdot cm^{-2}$
Radiation dose rate	3D field of the dose rate of energetic particles	$mSv \cdot h^{-1}$

In the following sections, some details are given for a few variables that are relevant to the ionosphere and magnetosphere.

5.9.1   Ionospheric total electron content

Definition: Number of electrons along a path between two points. Observed under different viewing angles so as to generate vertical profiles by tomography. Required in the ionosphere and plasmasphere – Physical unit: [electrons/m^2]; practical unit: TECU = 10^{16} electrons/m^2 – Uncertainty unit: [%].

Method 1: GNSS radio-occultation – Principle: Differential refraction between two frequencies (~1.2 and 1.6 GHz) transmitted by a navigation satellite and received by a LEO satellite during the occultation phase. Path-integrated content observed at changing tangent heights so as to provide vertical profile. Applicable only in LEO.

Method 2: Radar altimetry – Principle: Differential phase delay between signals from dual-frequency radar altimeter (~13 GHz and ~3 or 5 GHz). Phase rotation measurement, primarily needed to correct the altimeter ranging measurement, is also used to infer the column-integrated total electron content. Applicable only in LEO.

Method 3: GPS–LEO signal phase delay – Principle: Differential phase delay between signals from two-frequency GPS transmitters (~1.2 and 1.6 GHz) and a receiver in LEO using GPS for navigation. In principle, any satellite equipped with a GPS navigation system is suitable. The information refers to the topside ionosphere and plasmasphere, namely the layer between the satellite altitude and the GPS altitude (~20 000 km). Applicable only in LEO.

5.9.2   Electron density

Definition: 3D distribution of the electron density. Required in the ionosphere and plasmasphere – Physical unit: [electrons/m^3] – Uncertainty unit: [%].

Method 1: GNSS radio-occultation – Principle: Differential refraction between two frequencies (~1.2 and 1.6 GHz) transmitted by a navigation satellite and received by a LEO satellite during the occultation phase. Derived by tomography of the total electron content. Applicable only in LEO.

5.9.3   Magnetic field

Definition: Magnitude and direction of the Earth's magnetic field. Indicative of the degree of geomagnetic disturbance within the magnetosphere, and also in the Earth's interior. Required in the magnetosphere – Physical unit: [nT] (1 tesla = 10^4 gauss) – Uncertainty: [nT].

Method 1: Magnetometry – Principle: more magnetometers for in situ measurement along the orbit as the satellite moves. Applicable in LEO, in GEO and in highly elliptical orbits.

5.9.4   Electric field

Definition: Magnitude and direction of the Earth's electric field. Required in the ionosphere – Physical unit: [mV · m^{-1}] – Uncertainty: [mV · m^{-1}].

Method 1: Ion drift – Principle: Measurement of magnitude and direction of the incoming ion flux. The electric field is derived from the relationship between electric field, measured ion drift velocity and measured magnetic field strength. In situ measurement along the orbit as the satellite moves. Applicable in LEO and in highly elliptical orbits.

———————

ANNEX. ACHIEVABLE QUALITY OF SATELLITE PRODUCTS

This annex indicates the achievable quality in terms of RMS error,[1] horizontal resolution (Δx), vertical resolution (Δz) and observing cycle (Δt), with assumptions made on the number of satellites needed for the quoted observing cycle Δt, and the main possible observing conditions or limitations. These quality estimates are based on the characteristics of state-of-the art instruments that are being developed at the time of writing this Guide, and expected to be operational by 2020.

This estimate is made for each applicable remote-sensing principle for geophysical variables of the eight following themes:

(a)   Basic atmospheric 3D and 2D variables

(b)   Cloud and precipitation variables

(c)   Aerosols and radiation

(d)   Ocean and sea ice

(e)   Land surface (including snow)

(f)   Solid Earth

(g)   Atmospheric chemistry

(h)   Space weather

1. BASIC ATMOSPHERIC 3D AND 2D VARIABLES

**Table 5.A.1. Geophysical variables considered under the theme
"Basic atmospheric 3D and 2D variables"**

Atmospheric temperature	Wind (horizontal)	Height of the top of the planetary boundary layer	Height of the tropopause
Specific humidity	Wind vector over the surface (horizontal)	Temperature of the tropopause	

---

[1]   Note that RMS error used in this Part corresponds approximately to an expanded uncertainty with a coverage factor of $k = 1$, while in the rest of this Guide a coverage factor of $k = 2$ is generally used (see Part 1, Chapter 1, 1.6.4.3 and the *Evaluation of Measurement Data – Guide to the Expression of Uncertainty in Measurement* (JCGM 100:2008).

Table 5.A.1.1. Estimated potential quality of product "Atmospheric temperature" (by 2020)

Layer	Orbit	Technique	Uncertainty (RMS)	Δx (km)	Δz (km)	Δt (h)	Number of sats	Conditions
Troposphere (at ~500 hPa)	LEO	IR spectroscopy	1 K	20	1	4	3	Clear-air
	GEO	IR spectroscopy	1 K	20	1	0.5	6	Clear-air
	LEO	MW/sub-mm radiometry	1.5 K	30	1.5	4	3	Nearly all weather
	GEO	MW/sub-mm radiometry	1.5 K	30	1.7	0.5	6	Nearly all weather
	LEO	GNSS radio-occultation	1 K	300	0.5	12	12	All weather
Stratosphere (at ~30 hPa)	LEO	IR spectroscopy	3 K	20	3	4	3	–
	GEO	IR spectroscopy	4 K	20	4	0.5	6	–
	LEO	MW/sub-mm radiometry	4 K	30	4	4	3	–
	GEO	MW/sub-mm radiometry	4 K	30	4	0.5	6	–
	LEO	GNSS radio-occultation	2 K	300	1	12	12	–
	LEO	Limb sounding	2 K	300	2	72	1	–

Table 5.A.1.2. Estimated potential quality of product "Specific humidity" (by 2020)

Layer	Orbit	Technique	Uncertainty (RMS)	Δx (km)	Δz (km)	Δt (h)	Number of sats	Conditions
Troposphere (at ~500 hPa)	LEO	IR spectroscopy	10%	20	1.5	4	3	Clear-air
	GEO	IR spectroscopy	10%	20	2	0.5	6	Clear-air
	LEO	MW/sub-mm radiometry	15%	30	2.5	4	3	Nearly all weather
	GEO	MW/sub-mm radiometry	15%	30	2.5	0.5	6	Nearly all weather
	LEO	GNSS radio-occultation	10%	300	0.5	12	12	All weather
	LEO	DIAL (non-scanning)	2%	50	0.3	360	1	Clear-air
Stratosphere (at ~30 hPa)	LEO	IR spectroscopy	15%	20	4	4	3	–
	GEO	IR spectroscopy	20%	20	5	0.5	6	–
	LEO	MW/sub-mm radiometry	30%	30	5	4	3	–
	GEO	MW/sub-mm radiometry	30%	30	5	0.5	6	–
	LEO	GNSS radio-occultation	20%	300	5	12	12	–
	LEO	DIAL (non-scanning)	10%	50	2	360	1	–
	LEO	Limb sounding	20%	300	2	72	1	–

Layer	Orbit	Technique	Uncertainty (RMS)	Δx (km)	Δz (km)	Δt (h)	Number of sats	Conditions
Total column	LEO	From IR sounding	2 kg · m⁻²	20	–	4	3	Clear-air
	GEO	From IR sounding	2 kg · m⁻²	20	–	0.5	6	Clear-air
	LEO	From MW sounding	3 kg · m⁻²	30	–	4	3	All weather
	GEO	From MW sounding	3 kg · m⁻²	30	–	0.5	6	All weather
	LEO	From DIAL (non-scanning)	1 kg · m⁻²	50	–	360	1	Clear-air
	LEO	IR split-window	4 kg · m⁻²	1	–	4	3	Clear-air
	GEO	IR split-window	4 kg · m⁻²	4	–	0.1	6	Clear-air
	LEO	MW imaging (23 GHz)	2 kg · m⁻²	20	–	3	8 (GPM)[a]	All weather, sea
	LEO	NIR imaging (935 nm)	3 kg · m⁻²	8	–	8	3	Clear-air, daylight
	GEO	NIR imaging (935 nm)	3 kg · m⁻²	16	–	0.25	6	Clear-air, daylight

Note:

a   Contributing to the Global Precipitation Measurement (GPM) mission.

Table 5.A.1.3. Estimated potential quality of product "Wind (horizontal)" (by 2020)

Layer	Orbit	Technique	Uncertainty (RMS)	Δx (km)	Δz (km)	Δt (h)	Number of sats	Conditions
Troposphere (at ~500 hPa)	LEO	Doppler lidar (non-scanning)	1 m · s⁻¹	50	0.5	180	1	Clear-air
	LEO	VIS/IR image sequences	6 m · s⁻¹	15	6	4	3	Need for tracers, polar regions
	GEO	VIS/IR image sequences	5 m · s⁻¹	50	6	1	6	Need for tracers
	LEO	IR imager-sounder	5 m · s⁻¹	160	2	4	3	Clear-air, polar regions
	GEO	IR imager-sounder	4 m · s⁻¹	160	2	1	6	Clear-air
Stratosphere (at ~30 hPa)	LEO	Doppler lidar (non-scanning)	4 m · s⁻¹	50	2	180	1	Non-scanning
	LEO	Doppler shift (limb mode)	5 m · s⁻¹	300	2	72	1	Daylight

**Table 5.A.1.4. Estimated potential quality of product
"Wind vector over the surface (horizontal)" (by 2020)**

Layer	Orbit	Technique	Uncertainty (RMS)	Δx (km)	Δz (km)	Δt (h)	Number of sats	Conditions
Surface	LEO	Radar scatterometer	2 m · s⁻¹	20	–	12	3	Over sea, all weather
	LEO	Polarimetric MW radiometry	3 m · s⁻¹	10	–	8	3	Over sea, all weather
	LEO	MW imagery	3 m · s⁻¹	10	–	8	3	Over sea, all weather, speed only
	LEO	Radar altimetry (non-scanning)	3 m · s⁻¹	100	–	120	2	Over sea, all weather, speed only

**Table 5.A.1.5. Estimated potential quality of product
"Height of the top of the planetary boundary layer" (by 2020)**

Layer	Orbit	Technique	Uncertainty (RMS)	Δx (km)	Δz (km)	Δt (h)	Number of sats	Conditions
N/A	LEO	Backscatter lidar (non-scanning)	0.1 km	50	–	360	1	Clear-air
	LEO	From IR sounding	0.5 km	20	–	4	3	Clear-air
	GEO	From IR sounding	0.5 km	20	–	0.5	6	Clear-air
	LEO	From GNSS sounding	0.3 km	300	–	12	12	All weather

**Table 5.A.1.6. Estimated potential quality of product
"Height of the tropopause" (by 2020)**

Layer	Orbit	Technique	Uncertainty (RMS)	Δx (km)	Δz (km)	Δt (h)	Number of sats	Conditions
N/A	LEO	Backscatter lidar (non-scanning)	0.1 km	50	–	360	1	Clear-air
	LEO	From IR sounding	2 km	20	–	4	3	Clear-air
	GEO	From IR sounding	2 km	20	–	0.5	6	Clear-air
	LEO	From GNSS sounding	0.5 km	300	–	12	12	All weather

**Table 5.A.1.7. Estimated potential quality of product
"Temperature of the tropopause" (by 2020)**

Layer	Orbit	Technique	Uncertainty (RMS)	Δx (km)	Δz (km)	Δt (h)	Number of sats	Conditions
N/A	LEO	From IR sounding	2 K	20	–	4	3	Clear-air
	GEO	From IR sounding	2.5 K	20	–	0.5	6	Clear-air
	LEO	From GNSS sounding	1 K	300	–	12	12	All weather
	LEO	From limb sounding	1.5 K	300	–	72	1	Clear-air

2. CLOUD AND PRECIPITATION VARIABLES

Table 5.A.2. Geophysical variables considered under the theme "Cloud and precipitation variables"

Cloud-top temperature	Cloud-base height	Cloud ice	Precipitation (liquid or solid)
Cloud-top height	Cloud optical depth	Cloud-ice effective radius	Precipitation intensity at surface (liquid or solid)
Cloud type	Cloud liquid water	Freezing-level height in clouds	Accumulated precipitation (over 24 h)
Cloud cover	Cloud-droplet effective radius	Melting-layer depth in clouds	Lightning detection

Table 5.A.2.1. Estimated potential quality of product "Cloud-top temperature" (by 2020)

Layer	Orbit	Technique	Uncertainty (RMS)	Δx (km)	Δz (km)	Δt (h)	Number of sats	Conditions
N/A	LEO	IR radiometry	2 K	1	–	4	3	–
	GEO	IR radiometry	2 K	4	–	0.1	6	–
	LEO	From IR sounding	0.5 K	20	–	4	3	Within sounded IFOV
	GEO	From IR sounding	1 K	20	–	0.5	6	Within sounded IFOV

Table 5.A.2.2. Estimated potential quality of product "Cloud-top height" (by 2020)

Layer	Orbit	Technique	Uncertainty (RMS)	Δx (km)	Δz (km)	Δt (h)	Number of sats	Conditions
N/A	LEO	IR radiometry	0.5 km	1	–	4	3	–
	GEO	IR radiometry	0.5 km	4	–	0.1	6	–
	LEO	From IR sounding	0.3 km	20	–	4	3	Within sounded IFOV
	GEO	From IR sounding	0.3 km	20	–	0.5	6	Within sounded IFOV
	LEO	Backscatter lidar (non-scanning)	0.1 km	50	–	360	1	Multi-orbit
	LEO	Cloud radar (non-scanning)	0.3 km	50	–	360	1	Multi-orbit
	LEO	A-band spectroscopy	0.3 km	4	–	8	3	Daylight
	GEO	A-band spectroscopy	0.3 km	8	–	0.25	6	Daylight

Table 5.A.2.3. Estimated potential quality of product "Cloud type" (by 2020)

Layer	Orbit	Technique	Uncertainty (RMS)	Δx (km)	Δz (km)	Δt (h)	Number of sats	Conditions
N/A	LEO	VIS/IR radiometry	10 classes	4	–	4	3	Degraded at night (no VIS)
	GEO	VIS/IR radiometry	8 classes	12	–	0.1	1	Degraded at night (no VIS)

Table 5.A.2.4. Estimated potential quality of product "Cloud cover" (by 2020)

Layer	Orbit	Technique	Uncertainty (RMS)	Δx (km)	Δz (km)	Δt (h)	Number of sats	Conditions
Troposphere	LEO	From IR sounding	10%	10	6	4	3	Within sounded IFOV
	GEO	From IR sounding	10%	10	6	0.1	6	Within sounded IFOV
	LEO	Cloud radar (non-scanning)	10%	250	1	720	1	Multi-orbit
Total column	LEO	VIS/IR radiometry	3%	5	–	4	3	Degraded at night (no VIS)
	GEO	VIS/IR radiometry	3%	30	–	0.1	6	Degraded at night (no VIS)
	LEO	From IR sounding	10%	10	–	4	3	Within sounded IFOV
	GEO	From IR sounding	10%	10	–	0.1	6	Within sounded IFOV

Table 5.A.2.5. Estimated potential quality of product "Cloud-base height" (by 2020)

Layer	Orbit	Technique	Uncertainty (RMS)	Δx (km)	Δz (km)	Δt (h)	Number of sats	Conditions
N/A	LEO	Cloud radar (non-scanning)	0.3 km	50	–	360	1	Multi-orbit

Table 5.A.2.6. Estimated potential quality of product "Cloud optical depth" (by 2020)

Layer	Orbit	Technique	Uncertainty (RMS)	Δx (km)	Δz (km)	Δt (h)	Number of sats	Conditions
	LEO	Backscatter lidar (non-scanning)	0.1	50	–	360	1	Multi-orbit
Total column	LEO	SW polarimetry	0.5	20	–	48	1	Daylight
	LEO	SW/TIR radiometry	2	4	–	8	3	–
	GEO	SW/TIR radiometry	2	12	–	0.1	6	–

Table 5.A.2.7. Estimated potential quality of product "Cloud liquid water" (by 2020)

Layer	Orbit	Technique	Uncertainty (RMS)	Δx (km)	Δz (km)	Δt (h)	Number of sats	Conditions
Troposphere	LEO	Cloud radar (non-scanning)	10%	50	0.3	360	1	Multi-orbit
	LEO	Precipitation radar	20%	5	0.5	120	1	Precipitating clouds
	LEO	MW/sub-mm sounding	40%	20	3	3	8 (GPM)	–
	GEO	MW/sub-mm sounding	60%	30	4	0.5	6	–

Layer	Orbit	Technique	Uncertainty (RMS)	Δx (km)	Δz (km)	Δt (h)	Number of sats	Conditions
Total column	LEO	Cloud radar (non-scanning)	100 g · m^{-2}	50	–	360	1	Multi-orbit
	LEO	Precipitation radar	200 g · m^{-2}	5	–	120	1	Precipitating clouds
	LEO	MW/sub-mm sounding	200 g · m^{-2}	20	–	3	8 (GPM)	–
	GEO	MW/sub-mm sounding	300 g · m^{-2}	30	–	0.5	6	–

**Table 5.A.2.8. Estimated potential quality of product
"Cloud-droplet effective radius" (by 2020)**

Layer	Orbit	Technique	Uncertainty (RMS)	Δx (km)	Δz (km)	Δt (h)	Number of sats	Conditions
Troposphere	LEO	Cloud radar (non-scanning)	3 μm	50	0.3	360	1	Non-precipitating clouds
	LEO	Precipitation radar	10 μm	5	0.3	120	1	Precipitating clouds
	LEO	MW/sub-mm sounding	30 μm	20	3	3	8 (GPM)	Heavily model-aided
	GEO	MW/sub-mm sounding	30 μm	30	3	0.5	6	Heavily model-aided
Cloud top	LEO	Cloud radar (non-scanning)	3 μm	50	–	360	1	Multi-orbit
	LEO	MW/sub-mm sounding	10 μm	20	–	3	8 (GPM)	–
	GEO	MW/sub-mm sounding	10 μm	30	–	0.5	6	–
	LEO	Backscatter lidar (non-scanning)	0.2 μm	50	–	360	1	Multi-orbit
	LEO	SW polarimetry	1 μm	10	–	48	1	Daylight
	LEO	VIS/IR radiometry	2 μm	1	–	4	3	Degraded at night (no VIS)
	GEO	VIS/IR radiometry	2 μm	4	–	0.1	6	Degraded at night (no VIS)

Table 5.A.2.9. Estimated potential quality of product "Cloud ice" (by 2020)

Layer	Orbit	Technique	Uncertainty (RMS)	Δx (km)	Δz (km)	Δt (h)	Number of sats	Conditions
Troposphere	LEO	Cloud radar (non-scanning)	10%	50	0.3	360	1	Non-precipitating clouds
	LEO	Precipitation radar	20%	5	0.3	120	1	Precipitating clouds
	LEO	MW/sub-mm sounding	50%	20	3	3	8 (GPM)	Heavily model-aided
	GEO	MW/sub-mm sounding	50%	30	3	0.5	6	Heavily model-aided

Layer	Orbit	Technique	Uncertainty (RMS)	Δx (km)	Δz (km)	Δt (h)	Number of sats	Conditions
Total column	LEO	Cloud radar (non-scanning)	20 g · m⁻²	50	–	360	1	Non-precipitating clouds
	LEO	Precipitation radar	20 g · m⁻²	5	–	120	1	Precipitating clouds
	LEO	MW/sub-mm sounding	40 g · m⁻²	20	–	3	8 (GPM)	Model-aided
	GEO	MW/sub-mm sounding	40 g · m⁻²	30	–	0.5	6	Model-aided
	LEO	Sub-mm imagery	20 g · m⁻²	10	–	24	1	–
	LEO	FIR imagery	20 g · m⁻²	10	–	24	1	–

**Table 5.A.2.10. Estimated potential quality of product
"Cloud-ice effective radius" (by 2020)**

Layer	Orbit	Technique	Uncertainty (RMS)	Δx (km)	Δz (km)	Δt (h)	Number of sats	Conditions
Troposphere	LEO	Cloud radar (non-scanning)	3 µm	50	0.3	360	1	Non-precipitating clouds
	LEO	Precipitation radar	10 µm	5	0.3	120	1	Precipitating clouds
	LEO	MW/sub-mm sounding	30 µm	20	3	3	8 (GPM)	Heavily model-aided
	GEO	MW/sub-mm sounding	30 µm	30	3	0.5	6	Heavily model-aided
Cloud top	LEO	Cloud radar (non-scanning)	3 µm	50	–	360	1	Multi-orbit
	LEO	MW/sub-mm sounding	10 µm	20	–	3	8 (GPM)	–
	GEO	MW/sub-mm sounding	10 µm	30	–	0.5	6	–
	LEO	Backscatter lidar (non-scanning)	0.2 µm	50	–	360	1	Multi-orbit
	LEO	SW polarimetry	1 µm	10	–	48	1	Daylight
	LEO	VIS/IR radiometry	4 µm	1	–	4	3	Degraded at night (no VIS)
	GEO	VIS/IR radiometry	4 µm	4	–	0.1	6	Degraded at night (no VIS)

**Table 5.A.2.11. Estimated potential quality of product
"Freezing-level height in clouds" (by 2020)**

Layer	Orbit	Technique	Uncertainty (RMS)	Δx (km)	Δz (km)	Δt (h)	Number of sats	Conditions
	LEO	Precipitation radar	0.3 km	5	–	120	1	–
N/A	LEO	MW/sub-mm sounding	1.5 km	30	–	4	3	–
	GEO	MW/sub-mm sounding	1.5 km	30	–	0.5	6	–

**Table 5.A.2.12. Estimated potential quality of product
"Melting-layer depth in clouds" (by 2020)**

Layer	Orbit	Technique	Uncertainty (RMS)	Δx (km)	Δz (km)	Δt (h)	Number of sats	Conditions
	LEO	Precipitation radar	0.3 km	5	–	120	1	–
N/A	LEO	MW/sub-mm sounding	1.5 km	30	–	4	3	–
	GEO	MW/sub-mm sounding	1.5 km	30	–	0.5	6	–

**Table 5.A.2.13. Estimated potential quality of product
"Precipitation (liquid or solid)" (by 2020)**

Layer	Orbit	Technique	Uncertainty (RMS)	Δx (km)	Δz (km)	Δt (h)	Number of sats	Conditions
	LEO	Precipitation radar	10%	5	0.3	120	1	–
Troposphere	LEO	MW/sub-mm sounding	30%	20	3	3	8 (GPM)	Heavily model-aided
	GEO	MW/sub-mm sounding	30%	30	3	0.5	6	Heavily model-aided

**Table 5.A.2.14. Estimated potential quality of product
"Precipitation intensity at surface (liquid or solid)" (by 2020)**

Layer	Orbit	Technique	Uncertainty (RMS)	Δx (km)	Δz (km)	Δt (h)	Number of sats	Conditions
	LEO	Precipitation radar	0.5 mm h^{-1}	5	–	120	1	–
	LEO	MW/sub-mm sounding	1 mm h^{-1}	10	–	3	8 (GPM)	Heavily model-aided
Surface	GEO	MW/sub-mm sounding	1.5 mm h^{-1}	10	–	0.5	6	Heavily model-aided
	GEO	VIS/IR radiometry	5 mm h^{-1}	10	–	0.1	6	Convection only
	GEO	LEO/MW + GEO/IR fusion	2.5 mm h^{-1}	10	–	0.1	6	Product from data-fusion

**Table 5.A.2.15. Estimated potential quality of product
"Accumulated precipitation (over 24 hours)" (by 2020)**

Layer	Orbit	Technique	Uncertainty (RMS)	Δx (km)	Δz (km)	Δt (h)	Number of sats	Conditions
	GEO	LEO/MW + GEO/IR fusion	5 mm	10	–	3	3 (LEO) + 6 (GEO)	Product from data-fusion
Surface	GEO	MW/sub-mm sounding	2 mm	10	–	3	6	Heavily model-aided

Table 5.A.2.16. Estimated potential quality of product "Lightning detection" (by 2020)

Layer	Orbit	Technique	Uncertainty (RMS)	Δx (km)	Δz (km)	Δt (h)	Number of sats	Conditions
N/A	LEO	Lightning mapping	0.10/0.95 FAR/HR	5	–	12	3	–
	GEO	Lightning mapping	0.15/0.90 FAR/HR	10	–	0.01	6	–

3. AEROSOL AND RADIATION

Table 5.A.3. Geophysical variables considered under the theme "Aerosol and radiation"

Aerosol optical depth	Upward spectral radiance at TOA	Earth's surface albedo
Aerosol concentration	Upward LW irradiance at TOA	Earth's-surface SW bi-directional reflectance
Aerosol effective radius	Upward SW irradiance at TOA	Upward LW irradiance at Earth's surface
Aerosol type	Short-wave cloud reflectance	Long-wave Earth-surface emissivity
Volcanic ash	Downward LW irradiance at Earth's surface	Photosynthetically active radiation
Downward solar irradiance at TOA	Downward SW irradiance at Earth's surface	Fraction of absorbed photosynthetically active radiation

Table 5.A.3.1. Estimated potential quality of product "Aerosol optical depth" (by 2020)

Layer	Orbit	Technique	Uncertainty (RMS)	Δx (km)	Δz (km)	Δt (h)	Number of sats	Conditions
Total column	LEO	Backscatter lidar (non-scanning)	0.01	50	–	360	1	Clear-air
	LEO	SW polarimetry	0.03	20	–	48	1	Clear-air, daylight
	LEO	SW spectroscopy	0.04	20	–	8	3	Clear-air, daylight
	GEO	SW spectroscopy	0.04	20	–	1	6	Clear-air, daylight
	LEO	VIS/IR radiometry	0.05	5	–	8	3	Clear-air, daylight
	GEO	VIS/IR radiometry	0.05	2	–	0.1	6	Clear-air, daylight

Table 5.A.3.2. Estimated potential quality of product "Aerosol concentration" (by 2020)

Layer	Orbit	Technique	Uncertainty (RMS)	Δx (km)	Δz (km)	Δt (h)	Number of sats	Conditions
Troposphere (at ~500 hPa)	LEO	Backscatter lidar (non-scanning)	1%	50	0.1	360	1	Clear-air
	LEO	SW polarimetry	5%	20	3	48	1	Clear-air, daylight
	LEO	SW spectroscopy (cross-nadir)	5%	20	3	8	3	Clear-air, daylight
	GEO	SW spectroscopy (cross-nadir)	10%	20	3	1	6	Clear-air, daylight

Layer	Orbit	Technique	Uncertainty (RMS)	Δx (km)	Δz (km)	Δt (h)	Number of sats	Conditions
Stratosphere (at ~30 hPa)	LEO	Backscatter lidar (non-scanning)	2%	50	0.5	360	1	–
	LEO	SW polarimetry	20%	20	7	48	1	Daylight
	LEO	SW spectroscopy (cross-nadir)	20%	20	8	8	3	Daylight
	GEO	SW spectroscopy (cross-nadir)	20%	20	10	1	6	Daylight
	LEO	SW spectroscopy (limb)	10%	300	2	144	1	Daylight
Total column	LEO	Backscatter lidar (non-scanning)	$0.1\ g \cdot m^{-2}$	50	–	360	1	Clear-air
	LEO	SW polarimetry	$0.4\ g \cdot m^{-2}$	20	–	48	1	Clear-air, daylight
	LEO	SW spectroscopy	$1\ g \cdot m^{-2}$	20	–	8	3	Clear-air, daylight
	GEO	SW spectroscopy	$1\ g \cdot m^{-2}$	20	–	1	6	Clear-air, daylight
	LEO	VIS/IR radiometry	$4\ g \cdot m^{-2}$	4	–	8	3	Clear-air, daylight
	GEO	VIS/IR radiometry	$4\ g \cdot m^{-2}$	8	–	0.1	6	Clear-air, daylight

Table 5.A.3.3. Estimated potential quality of product "Aerosol effective radius" (by 2020)

Layer	Orbit	Technique	Uncertainty (RMS)	Δx (km)	Δz (km)	Δt (h)	Number of sats	Conditions
Troposphere	LEO	Backscatter lidar (non-scanning)	$0.2\ \mu m$	50	0.3	360	1	Clear-air
	LEO	SW polarimetry	$0.5\ \mu m$	20	3	48	1	Clear-air, daylight, model-aided
	LEO	SW spectroscopy	$1\ \mu m$	20	3	8	3	Clear-air, daylight, model-aided
	GEO	SW spectroscopy	$1\ \mu m$	20	3	1	6	Clear-air, daylight, model-aided
Total column	LEO	Backscatter lidar (non-scanning)	$0.1\ \mu m$	50	–	360	1	Clear-air
	LEO	SW polarimetry	$0.3\ \mu m$	20	–	48	1	Clear-air, daylight, model-aided
	LEO	SW spectroscopy	$0.5\ \mu m$	20	–	8	3	Clear-air, daylight, model-aided
	GEO	SW spectroscopy	$0.5\ \mu m$	20	–	1	6	Clear-air, daylight, model-aided

Table 5.A.3.4. Estimated potential quality of product "Aerosol type" (by 2020)

Layer	Orbit	Technique	Uncertainty (RMS)	Δx (km)	Δz (km)	Δt (h)	Number of sats	Conditions
Troposphere	LEO	Backscatter lidar (non-scanning)	6 classes	50	0.3	360	1	Clear-air
	LEO	SW polarimetry	4 classes	20	3	48	1	Clear-air, daylight, model-aided
	LEO	SW spectroscopy	4 classes	20	3	8	3	Clear-air, daylight, model-aided
	GEO	SW spectroscopy	4 classes	20	3	1	6	Clear-air, daylight, model-aided
Total column	LEO	Backscatter lidar (non-scanning)	6 classes	50	–	360	1	Clear-air
	LEO	SW polarimetry	4 classes	20	–	48	1	Clear-air, daylight, model-aided
	LEO	SW spectroscopy	4 classes	20	–	8	3	Clear-air, daylight, model-aided
	GEO	SW spectroscopy	4 classes	20	–	1	6	Clear-air, daylight, model-aided
	LEO	VIS/IR radiometry	2 classes	4	–	8	3	Clear-air, daylight, model-aided
	GEO	VIS/IR radiometry	2 classes	8	–	0.1	6	Clear-air, daylight, model-aided

Table 5.A.3.5. Estimated potential quality of product "Volcanic ash" (by 2020)

Layer	Orbit	Technique	Uncertainty (RMS)	Δx (km)	Δz (km)	Δt (h)	Number of sats	Conditions
Troposphere	LEO	Backscatter lidar (non-scanning)	1%	50	0.1	360	1	Clear-air
	LEO	SW polarimetry	5%	20	3	48	1	Clear-air, daylight
	LEO	SW spectroscopy (cross-nadir)	5%	20	3	8	3	Clear-air, daylight
	GEO	SW spectroscopy (cross-nadir)	10%	20	3	1	6	Clear-air, daylight
Stratosphere	LEO	Backscatter lidar (non-scanning)	2%	50	0.5	360	1	Clear-air
	LEO	SW polarimetry	20%	20	7	48	1	Clear-air, daylight
	LEO	SW spectroscopy (cross-nadir)	20%	20	8	8	3	Clear-air, daylight
	GEO	SW spectroscopy (cross-nadir)	20%	20	10	1	6	Clear-air, daylight
	LEO	SW spectroscopy (limb)	10%	300	2	144	1	–

Layer	Orbit	Technique	Uncertainty (RMS)	Δx (km)	Δz (km)	Δt (h)	Number of sats	Conditions
Total column	LEO	Backscatter lidar (non-scanning)	$0.5\ g \cdot m^{-2}$	50	–	360	1	Clear-air
	LEO	SW polarimetry	$2\ g \cdot m^{-2}$	20	–	48	1	Clear-air, daylight
	LEO	SW spectroscopy	$4\ g \cdot m^{-2}$	20	–	8	3	Clear-air, daylight
	GEO	SW spectroscopy	$4\ g \cdot m^{-2}$	20	–	1	6	Clear-air, daylight
	LEO	VIS/IR radiometry	$10\ g \cdot m^{-2}$	4	–	8	3	Clear-air, over sea
	GEO	VIS/IR radiometry	$10\ g \cdot m^{-2}$	8	–	0.1	6	Clear-air, over sea

Table 5.A.3.6. Estimated potential quality of product "Downward solar irradiance at TOA" (by 2020)

Layer	Orbit	Technique	Uncertainty (RMS)	Δx (km)	Δz (km)	Δt (h)	Number of sats	Conditions
TOA	LEO	Cavity radiometer	$0.2\ W \cdot m^{-2}$	N/A	–	24	1	Multi-orbit integration
TOA	GEO	Cavity radiometer	$0.15\ W \cdot m^{-2}$	N/A	–	24	6	Daily integration

Table 5.A.3.7. Estimated potential quality of product "Upward spectral radiance at TOA" (by 2020)

Layer	Orbit	Technique	Uncertainty (unit)	Δx (km)	Δz (km)	Δt (h)	Number of sats	Conditions
TOA	LEO	SW+LW spectroscopy	100 SNR	50	–	720	1	Non-scanning
				10	–	168	1	Limited swath

Table 5.A.3.8. Estimated potential quality of product "Upward long-wave irradiance at TOA" (by 2020)

Layer	Orbit	Technique	Uncertainty (RMS)	Δx (km)	Δz (km)	Δt (h)	Number of sats	Conditions
TOA	LEO	Broadband radiometry	$4\ W \cdot m^{-2}$	20	–	4	3	–
	GEO	Broadband radiometry	$4\ W \cdot m^{-2}$	30	–	0.25	6	–

Table 5.A.3.9. Estimated potential quality of product "Upward short-wave irradiance at TOA" (by 2020)

Layer	Orbit	Technique	Uncertainty (RMS)	Δx (km)	Δz (km)	Δt (h)	Number of sats	Conditions
TOA	LEO	Broadband radiometry	$10\ W \cdot m^{-2}$	20	–	4	3	Model-aided
	GEO	Broadband radiometry	$15\ W \cdot m^{-2}$	30	–	0.25	6	Model-aided

**Table 5.A.3.10. Estimated potential quality of product
"Short-wave cloud reflectance" (by 2020)**

Layer	Orbit	Technique	Uncertainty (RMS)	Δx (km)	Δz (km)	Δt (h)	Number of sats	Conditions
TOA	LEO	SW radiometry	5%	4	–	4	3	–
	GEO	SW radiometry	7%	8	–	0.1	6	–

**Table 5.A.3.11. Estimated potential quality of product
"Downward LW irradiance at Earth's surface" (by 2020)**

Layer	Orbit	Technique	Uncertainty (RMS)	Δx (km)	Δz (km)	Δt (h)	Number of sats	Conditions
Surface	LEO	From IR/MW sounding	10 W · m^{-2}	20	–	4	3	Model-aided
	GEO	From IR/MW sounding	10 W · m^{-2}	20	–	0.5	6	Model-aided

**Table 5.A.3.12. Estimated potential quality of product
"Downward SW irradiance at Earth's surface" (by 2020)**

Layer	Orbit	Technique	Uncertainty (RMS)	Δx (km)	Δz (km)	Δt (h)	Number of sats	Conditions
Surface	LEO	SW radiometry	20 W · m^{-2}	4	–	4	3	Clear-air, model-aided
	GEO	SW radiometry	30 W · m^{-2}	8	–	0.1	6	Clear-air, model-aided

Table 5.A.3.13. Estimated potential quality of product "Earth's surface albedo" (by 2020)

Layer	Orbit	Technique	Uncertainty (RMS)	Δx (km)	Δz (km)	Δt (h)	Number of sats	Conditions
Surface	LEO	Multi-view SW radiometry	1%	10	–	168	1	Clear-air, model-aided
	LEO	VIS radiometry	3%	4	–	168	3	Clear-air, heavily model-aided
	GEO	VIS radiometry	5%	8	–	72	6	Clear-air, heavily model-aided

**Table 5.A.3.14. Estimated potential quality of product
"Earth's-surface SW bi-directional reflectance" (by 2020)**

Layer	Orbit	Technique	Uncertainty (RMS)	Δx (km)	Δz (km)	Δt (h)	Number of sats	Conditions
Surface	LEO	Multi-view SW radiometry	3%	8	–	168	1	Clear-air

**Table 5.A.3.15. Estimated potential quality of product
"Upward long-wave irradiance at Earth's surface" (by 2020)**

Layer	Orbit	Technique	Uncertainty (RMS)	Δx (km)	Δz (km)	Δt (h)	Number of sats	Conditions
Surface	LEO	Broadband radiometry	15 W · m^{-2}	20	–	4	3	Clear-air, model-aided
	GEO	Broadband radiometry	15 W · m^{-2}	30	–	0.25	6	Clear-air, model-aided

**Table 5.A.3.16. Estimated potential quality of product
"Long-wave Earth-surface emissivity" (by 2020)**

Layer	Orbit	Technique	Uncertainty (RMS)	Δx (km)	Δz (km)	Δt (h)	Number of sats	Conditions
Surface	LEO	IR radiometry	3%	4	–	168	3	Clear-air
	GEO	IR radiometry	6%	12	–	72	6	Clear-air
	LEO	IR spectroscopy	1%	10	–	168	3	Clear-air
	GEO	IR spectroscopy	1%	10	–	72	6	Clear-air

**Table 5.A.3.17. Estimated potential quality of product
"Photosynthetically active radiation" (by 2020)**

Layer	Orbit	Technique	Uncertainty (RMS)	Δx (km)	Δz (km)	Δt (h)	Number of sats	Conditions
Surface	LEO	VIS radiometry	10 W · m^{-2}	4	–	4	3	Clear-air, model-aided
	GEO	VIS radiometry	10 W · m^{-2}	8	–	0.1	6	Clear-air, model-aided

**Table 5.A.3.18. Estimated potential quality of product "Fraction of absorbed
photosynthetically active radiation" (by 2020)**

Layer	Orbit	Technique	Uncertainty (RMS)	Δx (km)	Δz (km)	Δt (h)	Number of sats	Conditions
Surface	LEO	VIS radiometry	10%	4	–	4	3	Clear-air, model-aided
	GEO	VIS radiometry	10%	8	–	0.1	6	Clear-air, model-aided

4. OCEAN AND SEA ICE

Table 5.A.4. Geophysical variables considered under the theme "Ocean and sea ice"

Ocean chlorophyll concentration	Oil-spill cover	Coastal sea level (tide)	Wave directional-energy frequency spectrum
Colour dissolved organic matter	Sea-surface temperature	Significant wave height	Sea-ice cover
Ocean suspended sediments concentration	Sea-surface salinity	Dominant wave direction	Sea-ice thickness
Ocean diffuse attenuation coefficient	Ocean dynamic topography	Dominant wave period	Sea-ice type

Table 5.A.4.1. Estimated potential quality of product "Ocean chlorophyll concentration" (by 2020)

Layer	Orbit	Technique	Uncertainty (RMS)	Δx (km)	Δz (km)	Δt (h)	Number of sats	Conditions
Surface	LEO	VIS radiometry	0.1 mg · m^{-3}	4	–	8	3	Clear-air, daylight, model-aided
	GEO	VIS radiometry	0.2 mg · m^{-3}	8	–	0.25	6	Clear-air, daylight, model-aided

Table 5.A.4.2. Estimated potential quality of product "Colour dissolved organic matter" (by 2020)

Layer	Orbit	Technique	Uncertainty (RMS)	Δx (km)	Δz (km)	Δt (h)	Number of sats	Conditions
Surface	LEO	VIS radiometry	0.01 m^{-1}	4	–	8	3	Clear-air, daylight, model-aided
	GEO	VIS radiometry	0.02 m^{-1}	8	–	0.25	6	Clear-air, daylight, model-aided

Table 5.A.4.3. Estimated potential quality of product "Ocean suspended sediments concentration" (by 2020)

Layer	Orbit	Technique	Uncertainty (RMS)	Δx (km)	Δz (km)	Δt (h)	Number of sats	Conditions
Surface	LEO	VIS radiometry	0.05 g · m^{-3}	4	–	8	3	Clear-air, daylight, model-aided
	GEO	VIS radiometry	0.1 g · m^{-3}	8	–	0.25	6	Clear-air, daylight, model-aided

Table 5.A.4.4. Estimated potential quality of product "Ocean diffuse attenuation coefficient" (by 2020)

Layer	Orbit	Technique	Uncertainty (RMS)	Δx (km)	Δz (km)	Δt (h)	Number of sats	Conditions
Surface	LEO	VIS radiometry	0.5 m^{-1}	4	–	8	3	Clear-air, daylight, model-aided
	GEO	VIS radiometry	1 m^{-1}	8	–	0.25	6	Clear-air, daylight, model-aided

Table 5.A.4.5. Estimated potential quality of product "Oil-spill cover" (by 2020)

Layer	Orbit	Technique	Uncertainty (RMS)	Δx (km)	Δz (km)	Δt (h)	Number of sats	Conditions
Surface	LEO	VIS/NIR radiometry	15%	4	–	8	3	Clear-air, daylight
	GEO	VIS/NIR radiometry	15%	8	–	0.25	6	Clear-air, daylight
	LEO	SW polarimetry	10%	20	–	48	1	Clear-air, daylight
	LEO	High-resolution optical imagery	20%	0.3	–	168	4	Clear-air, daylight
	LEO	SAR imagery	5%	1	–	360	2	All weather

Table 5.A.4.6. Estimated potential quality of product "Sea-surface temperature" (by 2020)

Layer	Orbit	Technique	Uncertainty (RMS)	Δx (km)	Δz (km)	Δt (h)	Number of sats	Conditions
Surface	LEO	IR radiometry	0.4 K	8	–	4	3	Clear-air
	GEO	IR radiometry	0.8 K	24	–	0.1	6	Clear-air
	LEO	IR spectroscopy	0.3 K	20	–	4	3	Clear-air
	GEO	IR spectroscopy	0.5 K	20	–	0.25	6	Clear-air
	LEO	MW radiometry	1 K	50	–	8	3	All weather

Table 5.A.4.7. Estimated potential quality of product "Sea-surface salinity" (by 2020)

Layer	Orbit	Technique	Uncertainty (RMS)	Δx (km)	Δz (km)	Δt (h)	Number of sats	Conditions
Surface	LEO	L-band MW radiometry	0.3 PSU	200	–	240	1	All weather, space-time integrated

Table 5.A.4.8. Estimated potential quality of product "Ocean dynamic topography" (by 2020)

Layer	Orbit	Technique	Uncertainty (RMS)	Δx (km)	Δz (km)	Δt (h)	Number of sats	Conditions
Surface	LEO	Radar altimetry (non-scanning)	3 cm	50	–	240	2	All weather

Table 5.A.4.9. Estimated potential quality of product "Coastal sea level (tide)" (by 2020)

Layer	Orbit	Technique	Uncertainty (RMS)	Δx (km)	Δz (km)	Δt (h)	Number of sats	Conditions
Surface	LEO	Radar altimetry (non-scanning)	3 cm	50	–	240	2	All weather

Table 5.A.4.10. Estimated potential quality of product "Significant wave height" (by 2020)

Layer	Orbit	Technique	Uncertainty (RMS)	Δx (km)	Δz (km)	Δt (h)	Number of sats	Conditions
Surface	LEO	Radar altimetry (non-scanning)	0.1 m	50	–	240	2	All weather
	LEO	From SAR spectra	0.5 m	50	–	240	2	All weather

**Table 5.A.4.11. Estimated potential quality of product
"Dominant wave direction" (by 2020)**

Layer	Orbit	Technique	Uncertainty (RMS)	Δx (km)	Δz (km)	Δt (h)	Number of sats	Conditions
Surface	LEO	From SAR spectra	10 degrees	50	–	240	2	All weather

**Table 5.A.4.12. Estimated potential quality of product
"Dominant wave period" (by 2020)**

Layer	Orbit	Technique	Uncertainty (RMS)	Δx (km)	Δz (km)	Δt (h)	Number of sats	Conditions
Surface	LEO	From SAR spectra	10 s	50	–	240	2	All weather

**Table 5.A.4.13. Estimated potential quality of product
"Wave directional-energy frequency spectrum" (by 2020)**

Layer	Orbit	Technique	Uncertainty (RMS)	Δx (km)	Δz (km)	Δt (h)	Number of sats	Conditions
Surface	LEO	From SAR spectra	$0.1 \ m^2 \cdot Hz^{-1} \cdot rad^{-1}$	50	–	240	2	All weather

Table 5.A.4.14. Estimated potential quality of product "Sea-ice cover" (by 2020)

Layer	Orbit	Technique	Uncertainty (RMS)	Δx (km)	Δz (km)	Δt (h)	Number of sats	Conditions
	LEO	VIS/IR radiometry	10%	5	–	48	3	Clear-air
	GEO	VIS/IR radiometry	20%	15	–	6	6	Clear-air
Surface	LEO	MW radiometry	20%	20	–	3	8 (GPM)	All weather
	LEO	High-resolution optical imagery	5%	1	–	168	4	Clear-air, daylight
	LEO	SAR imagery	3%	3	–	360	2	All weather

Table 5.A.4.15. Estimated potential quality of product "Sea-ice thickness" (by 2020)

Layer	Orbit	Technique	Uncertainty (RMS)	Δx (km)	Δz (km)	Δt (h)	Number of sats	Conditions
	LEO	Radar altimetry (non-scanning)	25 cm	30	–	720	1	All weather
Surface	LEO	Lidar altimetry (non-scanning)	10 cm	30	–	720	1	Clear-air
	LEO	SAR interferometry	100 cm	1	–	360	2	All weather

Table 5.A.4.16. Estimated potential quality of product "Sea-ice type" (by 2020)

Layer	Orbit	Technique	Uncertainty (RMS)	Δx (km)	Δz (km)	Δt (h)	Number of sats	Conditions
	LEO	Radar scatterometry	5 classes	20	–	12	3	All weather
Surface	LEO	MW radiometry	3 classes	10	–	3	8 (GPM)	All weather
	LEO	SAR imagery	4 classes	1	–	360	2	All weather

5. LAND SURFACE (INCLUDING SNOW)

Table 5.A.5. Geophysical variables considered under the theme "Land surface (including snow)"

Land surface temperature	Leaf area index	Snow status (wet/dry)	Land surface topography
Soil moisture at surface	Normalized difference vegetation index	Snow cover	Glacier cover
Soil moisture (in the roots region)	Fire fractional cover	Snow water equivalent	Glacier topography
Fraction of vegetated land	Fire temperature	Soil type	
Vegetation type	Fire radiative power	Land cover	

Table 5.A.5.1. Estimated potential quality of product "Land surface temperature" (by 2020)

Layer	Orbit	Technique	Uncertainty (RMS)	Δx (km)	Δz (km)	Δt (km)	Number of sats	Conditions
	LEO	IR radiometry	2 K	8	–	4	3	Clear-air
	GEO	IR radiometry	4 K	24	–	0.1	6	Clear-air
Surface	LEO	IR spectroscopy	1 K	20	–	4	3	Clear-air
	GEO	IR spectroscopy	1 K	20	–	0.25	6	Clear-air
	LEO	MW radiometry	1 K	50	–	8	3	All weather

Table 5.A.5.2. Estimated potential quality of product "Soil moisture at surface" (by 2020)

Layer	Orbit	Technique	Uncertainty (RMS)	Δx (km)	Δz (km)	Δt (h)	Number of sats	Conditions
	LEO	MW radiometry	0.05 m^3 · m^{-3}	30	–	8	3	All weather, vegetation-sensitive
	LEO	Radar scatterometry	0.05 m^3 · m^{-3}	20	–	36	1	All weather, vegetation-sensitive
Surface	LEO	SAR imagery	0.1 m^3 · m^{-3}	0.1	–	360	2	All weather, vegetation-sensitive
	LEO	VIS/IR radiometry	0.5 m^3 · m^{-3}	4	–	4	3	Clear-air, vegetation-sensitive
	GEO	VIS/IR radiometry	0.5 m^3 · m^{-3}	12	–	0.1	6	Clear-air, vegetation-sensitive

Table 5.A.5.3. Estimated potential quality of product "Soil moisture (in the roots region)" (by 2020)

Layer	Orbit	Technique	Uncertainty (RMS)	Δx (km)	Δz (km)	Δt (h)	Number of sats	Conditions
	LEO	L-band MW radiometry	0.05 m^3 · m^{-3}	50	0.0001	72	1	All weather, model-aided
Surface	LEO	L-band SAR imagery	0.1 m^3 · m^{-3}	0.1	0.0001	1 440	1	All weather, model-aided

**Table 5.A.5.4. Estimated potential quality of product
"Fraction of vegetated land" (by 2020)**

Layer	Orbit	Technique	Uncertainty (RMS)	Δx (km)	Δz (km)	Δt (h)	Number of sats	Conditions
Surface	LEO	High-resolution optical imagery	10%	1	–	168	4	Clear-air, daylight
	LEO	SAR imagery	20%	5	–	360	2	All weather

Table 5.A.5.5. Estimated potential quality of product "Vegetated type" (by 2020)

Layer	Orbit	Technique	Uncertainty (RMS)	Δx (km)	Δz (km)	Δt (h)	Number of sats	Conditions
Surface	LEO	High-resolution optical imagery	20 classes	0.1	–	2 160	4	Clear-air, daylight
	LEO	SAR imagery	10 classes	0.2	–	2 160	2	All weather

Table 5.A.5.6. Estimated potential quality of product "Leaf area index" (by 2020)

Layer	Orbit	Technique	Uncertainty (RMS)	Δx (km)	Δz (km)	Δt (h)	Number of sats	Conditions
Surface	LEO	SW radiometry	10%	2	–	168	3	Clear-air, daylight
	GEO	SW radiometry	10%	4	–	72	6	Clear-air, daylight
	LEO	Radar scatterometry	30%	20	–	12	3	All weather
	LEO	High-resolution optical imagery	10%	0.1	–	168	4	Clear-air, daylight

**Table 5.A.5.7. Estimated potential quality of product
"Normalized difference vegetation index" (by 2020)**

Layer	Orbit	Technique	Uncertainty (RMS)	Δx (km)	Δz (km)	Δt (h)	Number of sats	Conditions
Surface	LEO	VIS/NIR radiometry	5%	2	–	168	3	Clear-air, daylight
	GEO	VIS/NIR radiometry	5%	4	–	72	6	Clear-air, daylight
	LEO	High-resolution optical imagery	5%	0.1	–	168	4	Clear-air, daylight

Table 5.A.5.8. Estimated potential quality of product "Fire fractional cover" (by 2020)

Layer	Orbit	Technique	Uncertainty (RMS)	Δx (km)	Δz (km)	Δt (h)	Number of sats	Conditions
Surface	LEO	VIS/IR radiometry	12%	4	–	4	3	Degraded at night (no VIS)
	GEO	VIS/IR radiometry	25%	12	–	0.1	6	Degraded at night (no VIS)
	LEO	High-resolution optical imagery	10%	0.1	–	168	4	Clear-air, daylight
	LEO	SAR imagery	10%	0.1	–	360	2	All weather

Table 5.A.5.9. Estimated potential quality of product "Fire temperature" (by 2020)

Layer	Orbit	Technique	Uncertainty (RMS)	Δx (km)	Δz (km)	Δt (h)	Number of sats	Conditions
Surface	LEO	IR radiometry	10 K	2	–	4	3	Clear-air
	GEO	IR radiometry	20 K	6	–	0.1	6	Clear-air

Table 5.A.5.10. Estimated potential quality of product "Fire radiative power" (by 2020)

Layer	Orbit	Technique	Uncertainty (RMS)	Δx (km)	Δz (km)	Δt (h)	Number of sats	Conditions
Surface	LEO	IR radiometry	$10\ \mathrm{kW \cdot m^{-2}}$	2	–	4	3	Clear-air
	GEO	IR radiometry	$20\ \mathrm{kW \cdot m^{-2}}$	6	–	0.1	6	Clear-air

Table 5.A.5.11. Estimated potential quality of product "Snow status (wet/dry)" (by 2020)

Layer	Orbit	Technique	Uncertainty (RMS)	Δx (km)	Δz (km)	Δt (h)	Number of sats	Conditions
Surface	LEO	MW radiometry	0.15/0.90 FAR/HR	10	–	3	8 (GPM)	All weather
	LEO	SAR imagery	0.25/0.80 FAR/HR	1	–	360	2	All weather

Table 5.A.5.12. Estimated potential quality of product "Snow cover" (by 2020)

Layer	Orbit	Technique	Uncertainty (RMS)	Δx (km)	Δz (km)	Δt (h)	Number of sats	Conditions
Surface	LEO	VIS/IR radiometry	10%	5	–	48	3	Clear-air
	GEO	VIS/IR radiometry	10%	10	–	6	6	Clear-air
	LEO	MW radiometry	20%	20	–	3	8 (GPM)	All weather
	LEO	High-resolution optical imagery	1%	1	–	168	4	Clear-air, daylight

Table 5.A.5.13. Estimated potential quality of product "Snow water equivalent" (by 2020)

Layer	Orbit	Technique	Uncertainty (RMS)	Δx (km)	Δz (km)	Δt (h)	Number of sats	Conditions
Surface	LEO	MW radiometry	20 mm	10	–	8	3	All weather
	LEO	Radar scatterometry	20 mm	20	–	12	3	All weather
	LEO	SAR imagery	30 mm	0.1	–	360	2	All weather

Table 5.A.5.14. Estimated potential quality of product "Soil type" (by 2020)

Layer	Orbit	Technique	Uncertainty (RMS)	Δx (km)	Δz (km)	Δt (h)	Number of sats	Conditions
Surface	LEO	High-resolution optical imagery	20 classes	0.01	–	8 760	4	Clear-air, daylight
	LEO	SAR imagery	20 classes	0.01	–	8 760	2	All weather

Table 5.A.5.15. Estimated potential quality of product "Land cover" (by 2020)

Layer	Orbit	Technique	Uncertainty (RMS)	Δx (km)	Δz (km)	Δt (h)	Number of sats	Conditions
Surface	LEO	High-resolution optical imagery	20 classes	0.01	–	8 760	4	Clear-air, daylight
	LEO	SAR imagery	10 classes	0.01	–	8 760	2	All weather

Table 5.A.5.16. Estimated potential quality of product "Land surface topography" (by 2020)

Layer	Orbit	Technique	Uncertainty (RMS)	Δx (km)	Δz (km)	Δt (h)	Number of sats	Conditions
Surface	LEO	High-resolution VIS stereoscopy	2 m	0.01	–	8 760	4	Clear-air, daylight
	LEO	SAR interferometry	1 m	0.01	–	8 760	2	All weather
	LEO	Radar altimetry (non-scanning)	0.2 m	0.2	–	43 800	1	All weather
	LEO	Lidar altimetry (non-scanning)	0.1 m	0.1	–	43 800	1	Clear-air

Table 5.A.5.17. Estimated potential quality of product "Glacier cover" (by 2020)

Layer	Orbit	Technique	Uncertainty (RMS)	Δx (km)	Δz (km)	Δt (h)	Number of sats	Conditions
Surface	LEO	High-resolution optical imagery	10%	0.01	–	8 760	4	Clear-air, daylight
	LEO	SAR imagery	10%	0.01	–	8 760	2	All weather

Table 5.A.5.18. Estimated potential quality of product "Glacier topography" (by 2020)

Layer	Orbit	Technique	Uncertainty (RMS)	Δx (km)	Δz (km)	Δt (h)	Number of sats	Conditions
Surface	LEO	SAR interferometry	100 cm	0.01	–	8 760	2	All weather

6. SOLID EARTH

Table 5.A.6. Geophysical variables considered under the theme "Solid Earth"

Geoid	Crustal plates positioning	Crustal motion (horizontal and vertical)	Gravity field	Gravity gradients

Table 5.A.6.1. Estimated potential quality of product "Geoid" (by 2020)

Layer	Orbit	Technique	Uncertainty (RMS)	Δx (km)	Δz (km)	Δt (h)	Number of sats	Conditions
Surface	LEO	Radar altimetry (non-scanning)	10 cm	500	–	8 760	2	All weather, model-aided
	LEO	Gravity field	1 cm	100	–	17 520	1	All weather, heavily model-aided

Table 5.A.6.2. Estimated potential quality of product "Crustal plates positioning" (by 2020)

Layer	Orbit	Technique	Uncertainty (RMS)	Δx (km)	Δz (km)	Δt (h)	Number of sats	Conditions
Surface	LEO	Laser ranging	2 cm	500	–	8 760	5	Night time, clear-air
	LEO	GPS receiver	2 cm	100	–	8 760	24	All weather

Table 5.A.6.3. Estimated potential quality of product "Crustal motion (horizontal and vertical)" (by 2020)

Layer	Orbit	Technique	Uncertainty (RMS)	Δx (km)	Δz (km)	Δt (h)	Number of sats	Conditions
Surface	LEO	Laser ranging	$2\ mm \cdot y^{-1}$	500	–	8 760	5	Night time, clear-air
	LEO	GPS receiver	$2\ mm \cdot y^{-1}$	100	–	8 760	24	All weather

Table 5.A.6.4. Estimated potential quality of product "Gravity field" (by 2020)

Layer	Orbit	Technique	Uncertainty (RMS)	Δx (km)	Δz (km)	Δt (h)	Number of sats	Conditions
Orbit height	LEO	Gradiometry	2 mGal	300	–	8 760	1	Orbit to change during mission
	LEO	Sat–sat ranging	2 mGal	300	–	8 760	2	Orbit to change during mission

Table 5.A.6.5. Estimated potential quality of product "Gravity gradients" (by 2020)

Layer	Orbit	Technique	Uncertainty (RMS)	Δx (km)	Δz (km)	Δt (h)	Number of sats	Conditions
Orbit height	LEO	Gradiometry	0.1 E	300	–	8 760	1	Orbit to change during mission
	LEO	Sat–sat ranging	0.1 E	300	–	8 760	2	Orbit to change during mission

7. ATMOSPHERIC CHEMISTRY

Table 5.A.7. Geophysical variables considered under the theme "Atmospheric chemistry"

O_3	C_2H_2	CFC–11	CH_2O	ClO	CO	COS	HCl	HNO_3	N_2O_5	NO_2	Peroxyacetyl nitrate	SF_6
BrO	C_2H_6	CFC–12	CH_4	$ClONO_2$	CO_2	H_2O	HDO	N_2O	NO	OH	Polar stratospheric cloud occurrence	SO_2

Table 5.A.7.1. Estimated potential quality of product "O$_3$" (by 2020)

Layer	Orbit	Technique	Uncertainty (RMS)	Δx (km)	Δz (km)	Δt (h)	Number of sats	Conditions
Troposphere (at ~500 hPa)	LEO	SW spectroscopy (cross-nadir)	10 nmol mol^{-1}	20	3	8	3	Clear-air, daylight
	GEO	SW spectroscopy (cross-nadir)	15 nmol mol^{-1}	20	4	1	6	Clear-air, daylight
	LEO	IR spectroscopy (cross-nadir)	10 nmol mol^{-1}	20	3	4	3	Clear-air
	GEO	IR spectroscopy (cross-nadir)	15 nmol mol^{-1}	20	4	0.5	6	Clear-air
	LEO	DIAL (non-scanning)	3 nmol mol^{-1}	50	0.5	360	1	Clear-air
Stratosphere (at ~30 hPa)	LEO	SW spectroscopy (cross-nadir)	20 nmol mol^{-1}	20	5	8	3	Daylight
	GEO	SW spectroscopy (cross-nadir)	30 nmol mol^{-1}	20	6	1	6	Daylight
	LEO	IR spectroscopy (cross-nadir)	20 nmol mol^{-1}	20	6	4	3	–
	GEO	IR spectroscopy (cross-nadir)	30 nmol mol^{-1}	20	8	0.5	6	–
	LEO	SW spectroscopy (limb)	10 nmol mol^{-1}	300	2	144	1	Daylight
	LEO	IR spectroscopy (limb)	10 nmol mol^{-1}	300	2	72	1	–
	LEO	Sub-mm spectroscopy (limb)	10 nmol mol^{-1}	300	2	72	1	–
	LEO	DIAL (non-scanning)	5 nmol mol^{-1}	50	1	360	1	–
Total column	LEO	SW spectroscopy	6 DU	20	–	8	3	Clear-air, daylight
	GEO	SW spectroscopy	9 DU	20	–	1	6	Clear-air, daylight
	LEO	IR spectroscopy	12 DU	20	–	4	3	Clear-air
	GEO	IR spectroscopy	15 DU	20	–	0.5	6	Clear-air

Table 5.A.7.2. Estimated potential quality of product "BrO" (by 2020)

Layer	Orbit	Technique	Uncertainty (RMS)	Δx (km)	Δz (km)	Δt (h)	Number of sats	Conditions
Troposphere (at ~500 hPa)	LEO	UV spectroscopy (cross-nadir)	40 nmol · mol^{-1}	50	5	8	3	Clear-air, daylight
	GEO	UV spectroscopy (cross-nadir)	40 nmol · mol^{-1}	50	6	1	6	Clear-air, daylight

Layer	Orbit	Technique	Uncertainty (RMS)	Δx (km)	Δz (km)	Δt (h)	Number of sats	Conditions
Stratosphere (at ~30 hPa)	LEO	UV spectroscopy (cross-nadir)	50 nmol · mol^{-1}	50	8	8	3	Daylight
	GEO	UV spectroscopy (cross-nadir)	50 nmol · mol^{-1}	50	10	1	6	Daylight
	LEO	UV spectroscopy (limb)	30 nmol · mol^{-1}	300	2	144	1	Daylight
	LEO	Sub-mm spectroscopy (limb)	20 nmol · mol^{-1}	300	2	72	1	–

Table 5.A.7.3. Estimated potential quality of product "C$_2$H$_2$" (by 2020)

Layer	Orbit	Technique	Uncertainty (RMS)	Δx (km)	Δz (km)	Δt (h)	Number of sats	Conditions
Troposphere (at ~500 hPa)	LEO	TIR spectroscopy (cross-nadir)	30 nmol · mol^{-1}	50	3	4	3	Clear-air
	GEO	TIR spectroscopy (cross-nadir)	50 nmol · mol^{-1}	50	4	0.5	6	Clear-air

Table 5.A.7.4. Estimated potential quality of product "C$_2$H$_6$" (by 2020)

Layer	Orbit	Technique	Uncertainty (RMS)	Δx (km)	Δz (km)	Δt (h)	Number of sats	Conditions
Troposphere (at ~500 hPa)	LEO	TIR spectroscopy (cross-nadir)	30 nmol · mol^{-1}	50	4	4	3	Clear-air
	GEO	TIR spectroscopy (cross-nadir)	50 nmol · mol^{-1}	50	5	0.5	6	Clear-air

Table 5.A.7.5. Estimated potential quality of product "CFC–11" (by 2020)

Layer	Orbit	Technique	Uncertainty (RMS)	Δx (km)	Δz (km)	Δt (h)	Number of sats	Conditions
Troposphere (at ~500 hPa)	LEO	IR spectroscopy (cross-nadir)	10 nmol · mol^{-1}	50	4	4	3	Clear-air
	GEO	IR spectroscopy (cross-nadir)	15 nmol · mol^{-1}	50	5	0.5	6	Clear-air
Stratosphere (at ~30 hPa)	LEO	IR spectroscopy (cross-nadir)	15 nmol · mol^{-1}	50	6	4	3	–
	GEO	IR spectroscopy (cross-nadir)	20 nmol · mol^{-1}	50	8	0.5	6	–
	LEO	IR spectroscopy (limb)	10 nmol · mol^{-1}	300	2	72	1	–

Table 5.A.7.6. Estimated potential quality of product "CFC–12" (by 2020)

Layer	Orbit	Technique	Uncertainty (RMS)	Δx (km)	Δz (km)	Δt (h)	Number of sats	Conditions
Troposphere (at ~500 hPa)	LEO	IR spectroscopy (cross-nadir)	10 nmol · mol^{-1}	50	4	4	3	Clear-air
	GEO	IR spectroscopy (cross-nadir)	15 nmol · mol^{-1}	50	5	0.5	6	Clear-air
Stratosphere (at ~30 hPa)	LEO	IR spectroscopy (cross-nadir)	15 nmol · mol^{-1}	50	6	4	3	–
	GEO	IR spectroscopy (cross-nadir)	20 nmol · mol^{-1}	50	8	0.5	6	–
	LEO	IR spectroscopy (limb)	10 nmol · mol^{-1}	300	2	72	1	–

Table 5.A.7.7. Estimated potential quality of product "CH$_2$O" (by 2020)

Layer	Orbit	Technique	Uncertainty (RMS)	Δx (km)	Δz (km)	Δt (h)	Number of sats	Conditions
Troposphere (at ~500 hPa)	LEO	UV spectroscopy (cross-nadir)	25 nmol · mol^{-1}	50	3	8	3	Clear-air, daylight
	GEO	UV spectroscopy (cross-nadir)	30 nmol · mol^{-1}	50	4	1	6	Clear-air, daylight
Total column	LEO	UV spectroscopy	1.5 · 1.3 · 10^{15} cm^{-2}	20	–	8	3	Clear-air, daylight
	GEO	UV spectroscopy	2 · 1.3 · 10^{15} cm^{-2}	20	–	1	1	Clear-air, daylight

Table 5.A.7.8. Estimated potential quality of product "CH$_4$" (by 2020)

Layer	Orbit	Technique	Uncertainty (RMS)	Δx (km)	Δz (km)	Δt (h)	Number of sats	Conditions
Troposphere (at ~500 hPa)	LEO	SWIR spectroscopy (cross-nadir)	10 nmol · mol^{-1}	50	4	8	3	Clear-air, daylight
	GEO	SWIR spectroscopy (cross-nadir)	15 nmol · mol^{-1}	50	5	0.5	6	Clear-air, daylight
	LEO	TIR spectroscopy (cross-nadir)	15 nmol · mol^{-1}	50	3	4	3	Clear-air
	GEO	TIR spectroscopy (cross-nadir)	20 nmol · mol^{-1}	50	4	0.25	6	Clear-air

Layer	Orbit	Technique	Uncertainty (RMS)	Δx (km)	Δz (km)	Δt (h)	Number of sats	Conditions
Stratosphere (at ~30 hPa)	LEO	SWIR spectroscopy (cross-nadir)	30 nmol · mol^{-1}	50	6	8	3	Daylight
	GEO	SWIR spectroscopy (cross-nadir)	40 nmol · mol^{-1}	50	7	0.5	6	Daylight
	LEO	TIR spectroscopy (cross-nadir)	30 nmol · mol^{-1}	50	6	4	3	–
	GEO	TIR spectroscopy (cross-nadir)	40 nmol · mol^{-1}	50	10	0.25	6	–
	LEO	SWIR spectroscopy (limb)	10 nmol · mol^{-1}	300	2	144	1	Daylight
	LEO	TIR spectroscopy (limb)	10 nmol · mol^{-1}	300	2	72	1	–
Total column	LEO	SWIR spectroscopy	$2 \cdot 1.3 \cdot 10^{15}$ cm^{-2}	20	–	8	3	Clear-air, daylight
	GEO	SWIR spectroscopy	$3 \cdot 1.3 \cdot 10^{15}$ cm^{-2}	20	–	1	6	Clear-air, daylight
	LEO	TIR spectroscopy	$4 \cdot 1.3 \cdot 10^{15}$ cm^{-2}	20	–	4	3	Clear-air
	GEO	TIR spectroscopy	$5 \cdot 1.3 \cdot 10^{15}$ cm^{-2}	20	–	0.5	6	Clear-air

Table 5.A.7.9. Estimated potential quality of product "ClO" (by 2020)

Layer	Orbit	Technique	Uncertainty (RMS)	Δx (km)	Δz (km)	Δt (h)	Number of sats	Conditions
Troposphere (at ~500 hPa)	LEO	UV spectroscopy (cross-nadir)	40 nmol · mol^{-1}	50	5	8	3	Clear-air, daylight
	GEO	UV spectroscopy (cross-nadir)	40 nmol · mol^{-1}	50	6	1	6	Clear-air, daylight
Stratosphere (at ~30 hPa)	LEO	UV spectroscopy (cross-nadir)	50 nmol · mol^{-1}	50	5	8	3	Daylight
	GEO	UV spectroscopy (cross-nadir)	50 nmol · mol^{-1}	50	6	1	6	Daylight
	LEO	UV spectroscopy (limb)	30 nmol · mol^{-1}	300	2	144	1	Daylight
	LEO	Sub-mm spectroscopy (limb)	30 nmol · mol^{-1}	300	2	72	1	–

Table 5.A.7.10. Estimated potential quality of product "ClONO$_2$" (by 2020)

Layer	Orbit	Technique	Uncertainty (RMS)	Δx (km)	Δz (km)	Δt (h)	Number of sats	Conditions
Troposphere (at ~500 hPa)	LEO	IR spectroscopy (cross-nadir)	10 nmol · mol^{-1}	50	4	4	3	Clear-air
	GEO	IR spectroscopy (cross-nadir)	15 nmol · mol^{-1}	50	5	0.5	6	Clear-air

Layer	Orbit	Technique	Uncertainty (RMS)	Δx (km)	Δz (km)	Δt (h)	Number of sats	Conditions
Stratosphere (at ~30 hPa)	LEO	IR spectroscopy (cross-nadir)	15 nmol · mol^{-1}	50	6	4	3	–
	GEO	IR spectroscopy (cross-nadir)	20 nmol · mol^{-1}	50	8	0.5	1	–
	LEO	IR spectroscopy (limb)	10 nmol · mol^{-1}	300	2	72	1	–

Table 5.A.7.11. Estimated potential quality of product "CO" (by 2020)

Layer	Orbit	Technique	Uncertainty (RMS)	Δx (km)	Δz (km)	Δt (h)	Number of sats	Conditions
Troposphere (at ~500 hPa)	LEO	SWIR spectroscopy (cross-nadir)	20 nmol · mol^{-1}	50	3	8	3	Clear-air, daylight
	GEO	SWIR spectroscopy (cross-nadir)	25 nmol · mol^{-1}	50	4	0.5	6	Clear-air, daylight
	LEO	TIR spectroscopy (cross-nadir)	10 nmol · mol^{-1}	50	3	4	3	Clear-air
	GEO	TIR spectroscopy (cross-nadir)	30 nmol · mol^{-1}	50	4	0.25	6	Clear-air
Stratosphere (at ~30 hPa)	LEO	SWIR spectroscopy (cross-nadir)	30 nmol · mol^{-1}	50	5	8	3	Daylight
	GEO	SWIR spectroscopy (cross-nadir)	40 nmol · mol^{-1}	50	6	0.5	6	Daylight
	LEO	TIR spectroscopy (cross-nadir)	30 nmol · mol^{-1}	50	5	4	3	–
	GEO	TIR spectroscopy (cross-nadir)	50 nmol · mol^{-1}	50	6	0.25	6	–
	LEO	SWIR spectroscopy (limb)	10 nmol · mol^{-1}	300	2	144	1	Daylight
	LEO	TIR spectroscopy (limb)	10 nmol · mol^{-1}	300	2	72	1	–
Total column	LEO	SWIR spectroscopy	4 · 1.3 · 10^{15} cm^{-2}	20	–	8	3	Clear-air, daylight
	GEO	SWIR spectroscopy	5 · 1.3 · 10^{15} cm^{-2}	20	–	1	1	Clear-air, daylight
	LEO	TIR spectroscopy	5 · 1.3 · 10^{15} cm^{-2}	20	–	4	3	Clear-air
	GEO	TIR spectroscopy	6 · 1.3 · 10^{15} cm^{-2}	20	–	0.5	1	Clear-air

Table 5.A.7.12. Estimated potential quality of product "CO$_2$" (by 2020)

Layer	Orbit	Technique	Uncertainty (RMS)	Δx (km)	Δz (km)	Δt (h)	Number of sats	Conditions
Troposphere (at ~500 hPa)	LEO	SWIR spectroscopy (cross-nadir)	10 nmol · mol^{-1}	100	3	8	3	Clear-air, daylight
	GEO	SWIR spectroscopy (cross-nadir)	15 nmol · mol^{-1}	100	4	0.5	6	Clear-air, daylight
	LEO	TIR spectroscopy (cross-nadir)	10 nmol · mol^{-1}	100	3	4	3	Clear-air
	GEO	TIR spectroscopy (cross-nadir)	15 nmol · mol^{-1}	100	4	0.25	6	Clear-air
Stratosphere (at ~30 hPa)	LEO	SWIR spectroscopy (cross-nadir)	20 nmol · mol^{-1}	100	3	8	3	Clear-air, daylight
	GEO	SWIR spectroscopy (cross-nadir)	30 nmol · mol^{-1}	100	4	0.5	6	Clear-air, daylight
	LEO	TIR spectroscopy (cross-nadir)	20 nmol · mol^{-1}	100	3	4	3	Clear-air
	GEO	TIR spectroscopy (cross-nadir)	30 nmol · mol^{-1}	100	4	0.25	6	Clear-air
	LEO	SWIR spectroscopy (limb)	10 nmol · mol^{-1}	300	2	144	1	Daylight
	LEO	TIR spectroscopy (limb)	10 nmol · mol^{-1}	300	2	72	1	–
Total column	LEO	SWIR spectroscopy	1 · 1.3 · 10^{15} cm^{-2}	50	–	8	3	Clear-air, daylight
	GEO	SWIR spectroscopy	1.5 · 1.3 · 10^{15} cm^{-2}	50	–	1	6	Clear-air, daylight
	LEO	TIR spectroscopy	2 · 1.3 · 10^{15} cm^{-2}	50	–	4	3	Clear-air
	GEO	TIR spectroscopy	2.5 · 1.3 · 10^{15} cm^{-2}	50	–	0.5	6	Clear-air
	LEO	DIAL (non-scanning)	0.3 · 1.3 · 10^{15} cm^{-2}	500	–	8 760	1	Clear-air

Table 5.A.7.13. Estimated potential quality of product "COS" (by 2020)

Layer	Orbit	Technique	Uncertainty (RMS)	Δx (km)	Δz (km)	Δt (h)	Number of sats	Conditions
Troposphere (at ~500 hPa)	LEO	TIR spectroscopy (cross-nadir)	10 nmol · mol^{-1}	50	3	4	3	Clear-air
	GEO	TIR spectroscopy (cross-nadir)	30 nmol · mol^{-1}	50	4	0.25	6	Clear-air
Stratosphere (at ~30 hPa)	LEO	TIR spectroscopy (cross-nadir)	30 nmol · mol^{-1}	50	5	4	3	–
	GEO	TIR spectroscopy (cross-nadir)	50 nmol · mol^{-1}	50	6	0.25	6	–
	LEO	TIR spectroscopy (limb)	10 nmol · mol^{-1}	300	2	72	1	–

Table 5.A.7.14. Estimated potential quality of product "H₂O" (by 2020)

Layer	Orbit	Technique	Uncertainty (RMS)	Δx (km)	Δz (km)	Δt (h)	Number of sats	Conditions
Troposphere (at ~500 hPa)	LEO	SW spectroscopy (cross-nadir)	5 nmol · mol^{-1}	10	3	8	3	Clear-air, daylight
	GEO	SW spectroscopy (cross-nadir)	6 nmol · mol^{-1}	10	4	0.5	6	Clear-air, daylight
	LEO	TIR spectroscopy (cross-nadir)	7 nmol · mol^{-1}	10	1.5	4	3	Clear-air
	GEO	TIR spectroscopy (cross-nadir)	8 nmol · mol^{-1}	10	2	0.25	6	Clear-air
	LEO	FIR spectroscopy	5 nmol · mol^{-1}	10	2	168	1	Clear-air
	LEO	GNSS radio-occultation	10 nmol · mol^{-1}	300	0.5	12	12	All weather
	LEO	DIAL (non-scanning)	2 nmol · mol^{-1}	50	0.5	360	1	Clear-air
Stratosphere (at ~30 hPa)	LEO	SW spectroscopy (cross-nadir)	15 nmol · mol^{-1}	10	5	8	3	Daylight
	GEO	SW spectroscopy (cross-nadir)	20 nmol · mol^{-1}	10	6	0.5	6	Daylight
	LEO	TIR spectroscopy (cross-nadir)	20 nmol · mol^{-1}	10	5	4	3	–
	GEO	TIR spectroscopy (cross-nadir)	30 nmol · mol^{-1}	10	6	0.25	6	–
	LEO	FIR spectroscopy	10 nmol · mol^{-1}	10	4	168	1	–
	LEO	GNSS radio-occultation	20 nmol · mol^{-1}	300	1	12	12	–
	LEO	SW spectroscopy (limb)	10 nmol · mol^{-1}	300	2	144	1	Daylight
	LEO	TIR spectroscopy (limb)	10 nmol · mol^{-1}	300	2	72	1	–
	LEO	Sub-mm spectroscopy (limb)	10 nmol · mol^{-1}	300	2	72	1	–
	LEO	DIAL (non-scanning)	7 nmol · mol^{-1}	50	1	360	1	–

Table 5.A.7.15. Estimated potential quality of product "HCl" (by 2020)

Layer	Orbit	Technique	Uncertainty (RMS)	Δx (km)	Δz (km)	Δt (h)	Number of sats	Conditions
Stratosphere (at ~30 hPa)	LEO	Sub-mm spectroscopy (limb)	30 nmol · mol^{-1}	300	2	72	1	–

Table 5.A.7.16. Estimated potential quality of product "HDO" (by 2020)

Layer	Orbit	Technique	Uncertainty (RMS)	Δx (km)	Δz (km)	Δt (h)	Number of sats	Conditions
Stratosphere (at ~30 hPa)	LEO	Sub-mm spectroscopy (limb)	15 nmol · mol^{-1}	300	2	72	1	–

Table 5.A.7.17. Estimated potential quality of product "HNO$_3$" (by 2020)

Layer	Orbit	Technique	Uncertainty (RMS)	Δx (km)	Δz (km)	Δt (h)	Number of sats	Conditions
Troposphere (at ~500 hPa)	LEO	IR spectroscopy (cross-nadir)	30 nmol · mol^{-1}	50	3	4	3	Clear-air
	GEO	IR spectroscopy (cross-nadir)	40 nmol · mol^{-1}	50	4	0.5	6	Clear-air
Stratosphere (at ~30 hPa)	LEO	IR spectroscopy (cross-nadir)	50 nmol · mol^{-1}	50	6	4	3	–
	GEO	IR spectroscopy (cross-nadir)	60 nmol · mol^{-1}	50	8	0.5	6	–
	LEO	IR spectroscopy (limb)	30 nmol · mol^{-1}	300	2	72	1	–
	LEO	Sub-mm spectroscopy (limb)	30 nmol · mol^{-1}	300	2	72	1	–
Total column	LEO	IR spectroscopy	3 · 1.3 · 10^{15} cm^{-2}	20	–	4	3	Clear-air
	GEO	IR spectroscopy	5 · 1.3 · 10^{15} cm^{-2}	20	–	0.5	6	Clear-air

Table 5.A.7.18. Estimated potential quality of product "N$_2$O" (by 2020)

Layer	Orbit	Technique	Uncertainty (RMS)	Δx (km)	Δz (km)	Δt (h)	Number of sats	Conditions
Troposphere (at ~500 hPa)	LEO	SWIR spectroscopy (cross-nadir)	10 nmol · mol^{-1}	50	3	8	3	Clear-air, daylight
	GEO	SWIR spectroscopy (cross-nadir)	15 nmol · mol^{-1}	50	4	0.5	6	Clear-air, daylight
	LEO	TIR spectroscopy (cross-nadir)	10 nmol · mol^{-1}	50	3	4	3	Clear-air
	GEO	TIR spectroscopy (cross-nadir)	15 nmol · mol^{-1}	50	4	0.25	6	Clear-air
Stratosphere (at ~30 hPa)	LEO	SWIR spectroscopy (cross-nadir)	20 nmol · mol^{-1}	50	6	8	3	Daylight
	GEO	SWIR spectroscopy (cross-nadir)	30 nmol · mol^{-1}	50	8	0.5	6	Daylight
	LEO	TIR spectroscopy (cross-nadir)	30 nmol · mol^{-1}	50	6	4	3	–
	GEO	TIR spectroscopy (cross-nadir)	40 nmol · mol^{-1}	50	8	0.25	6	–
	LEO	SWIR spectroscopy (limb)	15 nmol · mol^{-1}	300	2	144	1	Daylight
	LEO	TIR spectroscopy (limb)	15 nmol · mol^{-1}	300	2	72	1	–
	LEO	Sub-mm spectroscopy (limb)	10 nmol · mol^{-1}	300	2	72	1	–

Table 5.A.7.19. Estimated potential quality of product "N$_2$O$_5$" (by 2020)

Layer	Orbit	Technique	Uncertainty (RMS)	Δx (km)	Δz (km)	Δt (h)	Number of sats	Conditions
Troposphere (at ~500 hPa)	LEO	TIR spectroscopy (cross-nadir)	30 nmol · mol^{-1}	50	3	4	3	Clear-air
	GEO	TIR spectroscopy (cross-nadir)	50 nmol · mol^{-1}	50	4	0.5	1	Clear-air

Table 5.A.7.20. Estimated potential quality of product "NO" (by 2020)

Layer	Orbit	Technique	Uncertainty (RMS)	Δx (km)	Δz (km)	Δt (h)	Number of sats	Conditions
Troposphere (at ~500 hPa)	LEO	SW spectroscopy (cross-nadir)	20 nmol · mol^{-1}	50	3	8	3	Clear-air, daylight
	GEO	SW spectroscopy (cross-nadir)	30 nmol · mol^{-1}	50	4	1	6	Clear-air, daylight
	LEO	IR spectroscopy (cross-nadir)	20 nmol · mol^{-1}	50	3	4	3	Clear-air
	GEO	IR spectroscopy (cross-nadir)	30 nmol · mol^{-1}	50	4	0.5	6	Clear-air
Stratosphere (at ~30 hPa)	LEO	SW spectroscopy (cross-nadir)	50 nmol · mol^{-1}	50	6	8	3	Daylight
	GEO	SW spectroscopy (cross-nadir)	60 nmol · mol^{-1}	50	8	1	6	Daylight
	LEO	IR spectroscopy (cross-nadir)	50 nmol · mol^{-1}	50	6	4	3	–
	GEO	IR spectroscopy (cross-nadir)	60 nmol · mol^{-1}	50	8	0.5	6	–
	LEO	SW spectroscopy (limb)	20 nmol · mol^{-1}	300	2	144	1	Daylight
	LEO	IR spectroscopy (limb)	20 nmol · mol^{-1}	300	2	72	1	–

Table 5.A.7.21. Estimated potential quality of product "NO$_2$" (by 2020)

Layer	Orbit	Technique	Uncertainty (RMS)	Δx (km)	Δz (km)	Δt (h)	Number of sats	Conditions
Troposphere (at ~500 hPa)	LEO	SW spectroscopy (cross-nadir)	20 nmol · mol^{-1}	50	3	8	3	Clear-air, daylight
	GEO	SW spectroscopy (cross-nadir)	30 nmol · mol^{-1}	50	4	1	6	Clear-air, daylight
	LEO	IR spectroscopy (cross-nadir)	20 nmol · mol^{-1}	50	3	4	3	Clear-air
	GEO	IR spectroscopy (cross-nadir)	30 nmol · mol^{-1}	50	4	0.5	6	Clear-air

Layer	Orbit	Technique	Uncertainty (RMS)	Δx (km)	Δz (km)	Δt (h)	Number of sats	Conditions
Stratosphere (at ~30 hPa)	LEO	SW spectroscopy (cross-nadir)	50 nmol · mol^{-1}	50	6	8	3	Daylight
	GEO	SW spectroscopy (cross-nadir)	60 nmol · mol^{-1}	50	8	1	6	Daylight
	LEO	IR spectroscopy (cross-nadir)	50 nmol · mol^{-1}	50	6	4	3	–
	GEO	IR spectroscopy (cross-nadir)	60 nmol · mol^{-1}	50	8	0.5	6	–
	LEO	SW spectroscopy (limb)	20 nmol · mol^{-1}	300	2	144	1	Daylight
	LEO	IR spectroscopy (limb)	20 nmol · mol^{-1}	300	2	72	1	–
Total column	LEO	SW spectroscopy	$2 \cdot 1.3 \cdot 10^{15}$ cm^{-2}	20	–	8	3	Clear-air, daylight
	GEO	SW spectroscopy	$2 \cdot 1.3 \cdot 10^{15}$ cm^{-2}	20	–	1	6	Clear-air, daylight
	LEO	IR spectroscopy	$3 \cdot 1.3 \cdot 10^{15}$ cm^{-2}	20	–	4	3	Clear-air
	GEO	IR spectroscopy	$3 \cdot 1.3 \cdot 10^{15}$ cm^{-2}	20	–	0.5	6	Clear-air

Table 5.A.7.22. Estimated potential quality of product "OH" (by 2020)

Layer	Orbit	Technique	Uncertainty (RMS)	Δx (km)	Δz (km)	Δt (h)	Number of sats	Conditions
Stratosphere (at ~30 hPa)	LEO	Sub-mm spectroscopy (limb)	30 nmol · mol^{-1}	300	2	72	1	–
	LEO	FIR spectroscopy (limb)	20 nmol · mol^{-1}	300	2	72	1	–

Table 5.A.7.23. Estimated potential quality of product "Peroxyacetyl nitrate" (by 2020)

Layer	Orbit	Technique	Uncertainty (RMS)	Δx (km)	Δz (km)	Δt (h)	Number of sats	Conditions
Troposphere (at ~500 hPa)	LEO	TIR spectroscopy (cross-nadir)	30 nmol · mol^{-1}	50	3	4	3	Clear-air
	GEO	TIR spectroscopy (cross-nadir)	40 nmol · mol^{-1}	50	4	0.5	6	Clear-air

**Table 5.A.7.24. Estimated potential quality of product
"Polar stratospheric cloud occurrence" (by 2020)**

Layer	Orbit	Technique	Uncertainty (RMS)	Δx (km)	Δz (km)	Δt (h)	Number of sats	Conditions
Stratosphere (at ~30 hPa)	LEO	SW spectroscopy (cross-nadir)	0.30/0.80 FAR/HR	50	4	8	3	Daylight
	GEO	SW spectroscopy (cross-nadir)	0.40/0.70 FAR/HR	50	4	8	6	Daylight
	LEO	SW spectroscopy (limb)	0.20/0.85 FAR/HR	300	2	144	1	Daylight
	LEO	IR spectroscopy (limb)	0.25/0.80 FAR/HR	300	2	72	1	–
	LEO	Backscatter lidar (nadir-viewing)	0.10/0.95 FAR/HR	50	0.1	360	1	–

Table 5.A.7.25. Estimated potential quality of product "SF_6" (by 2020)

Layer	Orbit	Technique	Uncertainty (RMS)	Δx (km)	Δz (km)	Δt (h)	Number of sats	Conditions
Stratosphere (at ~30 hPa)	LEO	TIR spectroscopy (cross-nadir)	25 nmol · mol^{-1}	50	6	4	3	–
	GEO	TIR spectroscopy (cross-nadir)	30 nmol · mol^{-1}	50	8	0.25	6	–
	LEO	TIR spectroscopy (limb)	15 nmol · mol^{-1}	300	2	72	1	–

Table 5.A.7.26. Estimated potential quality of product "SO_2" (by 2020)

Layer	Orbit	Technique	Uncertainty (RMS)	Δx (km)	Δz (km)	Δt (h)	Number of sats	Conditions
Troposphere (at ~500 hPa)	LEO	UV spectroscopy (cross-nadir)	20 nmol · mol^{-1}	50	3	8	3	Clear-air, daylight
	GEO	UV spectroscopy (cross-nadir)	25 nmol · mol^{-1}	50	4	1	1	Clear-air, daylight
	LEO	IR spectroscopy (cross-nadir)	30 nmol · mol^{-1}	50	3	4	3	Clear-air
	GEO	IR spectroscopy (cross-nadir)	35 nmol · mol^{-1}	50	4	0.5	1	Clear-air
Stratosphere (at ~30 hPa)	LEO	UV spectroscopy (cross-nadir)	30 nmol · mol^{-1}	50	6	8	3	Daylight
	GEO	UV spectroscopy (cross-nadir)	35 nmol · mol^{-1}	50	8	1	1	Daylight
	LEO	IR spectroscopy (cross-nadir)	40 nmol · mol^{-1}	50	6	4	3	–
	GEO	IR spectroscopy (cross-nadir)	50 nmol · mol^{-1}	50	8	0.5	1	–

Layer	Orbit	Technique	Uncertainty (RMS)	Δx (km)	Δz (km)	Δt (h)	Number of sats	Conditions
Total column	LEO	UV spectroscopy	$1.5 \cdot 1.3 \cdot 10^{15}$ cm^{-2}	20	–	8	3	Clear-air, daylight
	GEO	UV spectroscopy	$2 \cdot 1.3 \cdot 10^{15}$ cm^{-2}	20	–	1	1	Clear-air, daylight
	LEO	TIR spectroscopy	$2.5 \cdot 1.3 \cdot 10^{15}$ cm^{-2}	20	–	4	3	Clear-air
	GEO	TIR spectroscopy	$3 \cdot 1.3 \cdot 10^{15}$ cm^{-2}	20	–	0.5	1	Clear-air

8. SPACE WEATHER

Table 5.A.8. Selected variables from the theme "Space weather" addressing the magnetosphere and ionosphere

Ionospheric total electron content	Electron density	Magnetic field	Electric field

Table 5.A.8.1. Estimated potential quality of product "Ionospheric total electron content" (by 2020)

Layer	Orbit	Technique	Uncertainty (RMS)	Δx (km)	Δz (km)	Δt (h)	Number of sats	Conditions
	LEO	GNSS radio-occultation	5%	300	3	12	12	90–800 km altitude
Ionosphere	LEO	Radar altimetry (non-scanning)	10%	100	200	120	2	90–1 300 km altitude
	LEO	GPS–LEO signal phase delay	20%	300	4 000	12	12	1 000–20 000 km altitude

Table 5.A.8.2. Estimated potential quality of product "Electron density" (by 2020)

Layer	Orbit	Technique	Uncertainty (RMS)	Δx (km)	Δz (km)	Δt (h)	Number of sats	Conditions
Ionosphere	LEO	GNSS radio-occultation	10%	300	10	12	12	90–800 km altitude

Table 5.A.8.3. Estimated potential quality of product "Magnetic field" (by 2020)

Layer	Orbit	Technique	Uncertainty (RMS)	Δx (km)	Δz (km)	Δt (h)	Number of sats	Conditions
Magnetosphere	LEO	Magnetometry	0.3 nT	100	–	240	1	Limited to satellite orbit
	GEO	Magnetometry	1 nT	100	–	0.25	6	Limited to satellite orbit

Table 5.A.8.4. Estimated potential quality of product "Electric field" (by 2020)

Layer	Orbit	Technique	Uncertainty (RMS)	Δx (km)	Δz (km)	Δt (h)	Number of sats	Conditions
Magnetosphere	LEO	Ion drift	10 mV·m^{-1}	100	–	240	1	Limited to satellite orbit
	GEO	Ion drift	10 mV·m^{-1}	100	–	0.25	6	Limited to satellite orbit

————————

CHAPTER CONTENTS

CHAPTER 6. CALIBRATION AND VALIDATION

6.1 INSTRUMENT CALIBRATION

6.1.1 Introduction

Calibration is the process of quantitatively defining the satellite instrument response to known, controlled signal inputs.[1] The calibration information is contained in a calibration formula or in calibration coefficients that are then used to convert the instrument output (measured in "counts", or, previously, "analogue signals") into physical units (for example, radiance values). Instrument calibration is critical for any higher-level data processing, especially for deriving quantitative products or when data from different instruments need to be merged (such as for composite imagery). For climate applications, the requirement for accurate calibration is particularly stringent[2] since detection of small trends over long periods requires the ability to compare different instruments flown on different satellites at different times. Building homogeneous climate data records is contingent on very stable calibration and error characterization.

The following considerations apply to passive and active instruments alike.

Five calibration domains should be generally considered: radiometric, spectral, spatial, temporal, and polarization. A complete calibration record should include estimates of uncertainties in calibration parameters. Satellite instrument calibration should take into account all phases of an instrument's lifetime: from design and pre-launch phases to post-launch and on-orbit operations.

The intercalibration of instruments against a common reference instrument allows for consistency among satellite measurements at a given point in time. By comparing model-simulated and observed satellite radiances in data assimilation schemes, major numerical weather prediction (NWP) centres can also help determine relative biases between instruments. Calibration to absolute standards is, nevertheless, necessary to allow traceability of errors and to detect any long-term drift over time unambiguously.

Calibration using well-characterized, stable Earth targets (called vicarious calibration) is a fallback when a satellite instrument cannot be directly traceable to an agreed reference standard,[3] for example due to the absence of a reliable on-board calibration device. Data records from past instruments can be "recalibrated" retrospectively, if additional information on the state of these instruments becomes available, for example through comparison with reprocessed, well-known historical time series.

6.1.2 Factors affecting calibration

The response of an instrument to signal input, i.e. the relationship between the irradiance the instrument is exposed to and the numerical value assigned to the measurement (in physical units, for example, W m^{-2}) depends on several elements, such as:

(a) The viewing geometry, shielding effects, stray light, and antenna pattern;

(b) Detector sensitivity and ageing;

(c) Filter optics, as well as the possible contamination and stability of the filter;

---

[1] From the Committee on Earth Observation Satellites (CEOS) Working Group on Calibration and Validation. (The terms defined in this Part differ in some instances from those defined in JCGM, 2012).
[2] See, for example, Ohring (2007).
[3] For guidance on reference standards, see, for example, Fox (2010).

(d)   The temperature of all parts of the instrument, including the front-end optics, detector and back-end electronics (focal plane electronics, preamplifier, etc.);

(e)   The signal-processing system (gain, analogue-to-digital converter, etc.).

All of these elements help to determine the spectral response function and the point spread function that characterize the instrument from a radiometric and geometric viewpoint, respectively. They must be modelled before launch and monitored in flight by a set of on-board internal measurements (the housekeeping system). The instrument model and the housekeeping system are useful for understanding the status of the instrument and its trend as well as for predicting and correcting biases. However, it is generally not possible to analytically describe the exact variation of the instrument response resulting from these factors. Reference measurements are mandatory to characterize the actual calibration.

6.1.3   **Pre-launch calibration**

The pre-launch calibration of an instrument is performed in the laboratory, by using accurately known radiation sources under controlled conditions. Simulating all possible instrument states and stress factors before launch is very important because it is the only way to accurately characterize and model the instrument before it is exposed to the harsh orbital environment. Housekeeping systems and instruments need to be robust enough to withstand physical stress incurred during the launch, commissioning and exploitation phases. Housekeeping data, in combination with post-launch calibration information, will then allow operators to infer the calibration status of the instrument in orbit and to resolve on-orbit anomalies.

6.1.4   **On-board calibration**

On-board calibration involves monitoring the instrument performance (and stability) while in orbit. It is performed using reference targets (such as black bodies in the infrared, solar diffusers, and lamp line sources in short wave) for passive instruments, or by internal calibration systems (such as gain monitors) for active instruments. Some heritage instruments have been in operation without adequate means of on-board calibration, such as the Advanced Very High Resolution Radiometer (AVHRR), which provides long-term observations in the visible and near-infrared regions. Other means of calibration (e.g. vicarious, intercalibration) need to be used for characterizing such instruments. The accuracy of in-flight instrument calibration is a function of the stability of the on-board calibration systems throughout the instrument's lifetime. Therefore, the calibration itself must be regularly checked by intercalibration against highly accurate references.

In the case of infrared instruments, if the radiometer detectors are assumed to have linear response, the output voltage is given as:

$$V = \alpha R + V_0$$

where R is the input radiance, α is the radiometer responsivity and V_0 is the system offset. Calibration consists of determining α and V_0, which is accomplished by exposing the radiometer to at least two reference targets with significantly different brightness temperatures.

For infrared and microwave instruments, one reference target is deep space, at a temperature of 2.725 K. Direct viewing of deep space is not always possible for instruments on a satellite platform. For instance, pushbroom instruments constantly pointing to the Earth's surface need to be equipped with a sub-reflector to supply the deep space view at intervals. A second target is usually a well-characterized source with temperature in the medium to upper dynamic range, often a black body, which is ideally traceable to the International System of Units (SI), i.e. to a radiance scale provided by a national metrology institute.

If the instrument response is not linear across the dynamic range, this needs to be accounted for in the pre-launch instrument characterization, for example by using a quadratic function, or through linearization in different parts of the dynamic range and the possible addition of a second black body kept at a different temperature.

For ultraviolet, visible and near-infrared instruments, on-board calibration is more challenging since it is affected by many factors. At the low-signal extreme, deep space is a useful reference, provided that disrupting effects (for example, reflections from other parts of the satellite) are avoided. At the high-signal end, an absolute source is generally replaced by solar diffusers that provide a relatively stable reference. The moon also may be used as a reference target, with the advantage that it can be viewed without an attenuator; however, it must be used in conjunction with an accurate model of the moon's brightness. Neither the solar diffuser nor the moon provides an absolute calibration. Another system often used is a bench of lamp line sources of well-controlled intensity. Spectrally-dependent polarization effects induced by the reflecting surfaces of the instrument optics also need to be taken into account.

Another problem with on-board calibration is that often the instrument structure does not allow illumination of the full primary optics with reference sources. For example, a spin-stabilized radiometer in geostationary Earth orbit uses an internal black body requiring a model of the contributions of the telescope and foreoptics to the background radiation. Often, the reference source only illuminates a fraction of the total instrument optics and, therefore, is more used for stability monitoring than for absolute calibration.

6.1.5   Vicarious calibration

On-board calibration can be complemented by stable ground targets used as references in a process termed vicarious calibration. The target needs to be well characterized in order to infer the emitted or reflected radiance towards space. The combined effects of the viewing geometry and, in short wave, the bidirectional reflectance distribution function of the surface and atmosphere must be taken into account. The radiative transfer through the atmosphere between the satellite and the ground reference source must be accurately known at the time of the satellite overpass. In a cloud-free case, the short-wave spectrum is particularly affected by aerosols, whereas the long-wave spectrum is particularly influenced by the presence of water vapour.

Vicarious calibration can involve different kinds of targets: polar ice fields as a black body for microwave radiometers; snow fields, sunglint, homogeneous desert areas, and deep convective cloud tops for the upper end of the visible dynamic range; cloud-free ocean surface for dark targets in the visible spectrum; cube-corner reflectors for synthetic aperture radars; the rainforest as a black body for radar scatterometers; etc. Calibration field sites equipped with in situ observations are used for the calibration of high spatial resolution space-based instruments. During initial payload commissioning or at regular intervals, aircraft overflights of a target area synchronous with the satellite overpass offer additional vicarious calibration data.

6.1.6   Intercalibration by simultaneous observations

The intercalibration of satellite instruments involves relating the measurements of one instrument to those of another. This is done for the dual purposes of:

(a)   Providing vicarious calibration to instruments that have no or a defective internal calibration device (intercalibration being performed against a high-quality, well-calibrated instrument serving as a reference);

(b)   Merging the data from several instruments to generate consistent time-series.

The intercalibration of instruments operated during the same period requires careful collocation wherein instrument outputs are compared when the instruments are viewing the same Earth scenes, at the same times and from the same viewing angles. As part of the International Satellite Cloud Climatology Project of the World Climate Research Programme, simultaneous

observations from collocations between geostationary Earth orbit (GEO) imagers and a low Earth orbit reference imager have been performed on a monthly basis for almost 30 years as a means to normalize GEO satellite imagery. More recently, the Global Space-based Inter-calibration System (GSICS) has developed an operational methodology for such intercalibrations, specifically for simultaneous collocated observations. The methodology considers the trade-off between accurate spatial–temporal co-registration of the instruments and the frequency of such events, and takes into account the corrections to be applied for:

(a)   Different viewing geometries (with regard to both the instrument scan angle and the solar position);

(b)   Different atmospheric states in the line of sight, including aerosols and clouds;

(c)   Different spectral response functions.

It should be noted that simultaneous observations between two Sun-synchronous satellites can only occur at the intersections of their orbital planes, which are always located at a given local solar time and at a given, generally high north or south, latitude.[4]

6.1.7   Bias adjustment of long-term data records

An alternative approach for instrument intercalibration, which is less demanding in computation and applicable a posteriori to long data series, is to simply compare the statistical distribution of overlapping time-series of two satellite instrument data records without imposing individual matches of individual scenes. Using this approach, it is possible to identify the relative bias between the two data records. The observed bias is analysed so that the different conditions of observation (for example, different local solar times) are accounted for, leaving the remaining bias as the part that is actually due to the difference in instrument calibration. One successful example of this approach is the intercalibration of the nine microwave sounding units on board the early National Oceanic and Atmospheric Administration satellites, representing a 26-year record of global tropospheric temperatures.

6.1.8   Using calibration information

The type of calibration information available depends on the processing level and on the instrument considered. Each instrument has its own operating mode and calibration cycle, which includes regular measurements of calibration targets each time a certain number of observations are performed. For instance, the table in this section indicates the calibration cycles of the Advanced Microwave Sounding Unit – A (AMSU-A), the Microwave Humidity Sounder (MHS) and the High-resolution Infrared Sounder 4 (HIRS/4).

Examples of observation/calibration cycles

	AMSU-A	MHS	HIRS/4
Number of Earth views	1 line of 30 pixels	1 line of 90 pixels	38 lines of 56 pixels
Number of warm target views	2 (~300 K)	4 (~273 K)	48 (~290 K)
Number of cold target views	2 (deep space ~2.73 K)	4 (deep space ~2.73 K)	56 (deep space ~2.73 K)
Overall duration of the cycle	8 s	8/3 s	256 s

---

4   For a 98° inclination, the crossing latitude is above 70° when the equatorial crossing times (ECT) of the two orbits differ by less than 8 h, and only drops significantly when the ECT difference increases towards 12 h.

An important step in the pre-processing from Level 0 to Level 1b data (see Part III, Chapter 2, 2.3.2.6) is to extract the calibration information in the form of warm/cold view counts and then to compute the resulting calibration coefficients in accordance with the calibration model (such as a linear or quadratic calibration function, or a lookup table) defined by the satellite operator for that particular instrument. This provides the operational calibration for that instrument.

For applications requiring high accuracy and consistency among different instrument data records, a correction can be applied on top of the operational calibration to take into account the latest results of the intercalibration activities. Such corrections are provided by GSICS. The corrected calibration coefficients may be included in the Level 1.b/Level 1.5 data formats as additional calibration information.

6.1.9　　Traceability of space-based measurements

While intercalibration can ensure consistency between satellite instruments, it does not necessarily provide traceability to SI unless a reference instrument in orbit is SI-traceable. There are major challenges to achieving SI traceability in orbit as most sensors degrade physically during and after launch. Achieving SI traceability poses instrument design challenges and remains a research topic for all but a few measurement types.

The Climate Absolute Radiance and Refractivity Observatory (CLARREO) mission proposed by the United States National Research Council consists of a highly accurate infrared interferometer with a high-emissivity reference black body using multiple phase-change cells for SI-traceable thermometer calibration, an ultraviolet, visible and near-infrared spectrometer calibrated by Sun and moon views, a cryogenically cooled active cavity radiometer, and radio occultation measurements. This suite of instruments is intended to provide fully traceable measurements of the entire Earth-emitted and -reflected solar spectrum. Implementing and maintaining such a mission would provide an anchor point in support of the calibration and traceability of the whole fleet of operational radiometers.

For measurement traceability, one should take advantage of instruments that do not depend on radiometric calibration, such as radio occultation and Sun or star occultation sensors (see Part III, Chapter 2, 2.2.4.3 and 2.2.5.1).

6.2　　PRODUCT VALIDATION

6.2.1　　Factors to be accounted for in validation

Validation is the process of assessing, by independent means, the quality of the data products derived from satellite instrument measurements.[5] Product validation should be performed by product developers, downstream of instrument calibration, and should be documented in instrument-specific product validation plans. Guidelines for documenting product quality are provided in the Quality Assurance Framework for Earth Observation (QA4EO).

Geophysical products are generated from satellite data (often radiance measurements) by applying an algorithm that is either physically or empirically based. Comparing the retrieved products and their trends with in situ observations or model outputs is an important part of the process to assess and document the reliability of given retrieval algorithms and define their domain of applicability.

If a particular trend is detected, it may relate to the instrument's performance; a careful analysis of the satellite instrument's calibration and environmental data must be performed before any empirical correction can be applied.

---

[5]　From the CEOS Working Group on Calibration and Validation.

For many products, validation is a complex problem since the comparison between products derived from satellite measurements and independent reference products often from in situ measurements is subject to several errors: (i) an inherent satellite-derived product error, (ii) the error in the reference data, and (iii) the error introduced by the comparison methodology, often due to non-collocation in time and space. In general, different measurement techniques measure different things: a satellite observation usually refers to a relatively large area (the instantaneous field of view) and nearly-instantaneous measurements (within milliseconds); ground (in situ) measurements are generally very local and integrated over a relatively long time. Surface-based remote-sensing usually provides information representative of the atmospheric column. Comparison of the different types of measurements requires downscaling or upscaling methods that can introduce spatially or temporally dependent errors.

A validation assessment model can be used to improve comparisons by understanding and accounting for these differences and to better appreciate the advantages and disadvantages of different validation approaches. Validation campaigns run by satellite operators are usually accompanied by such an assessment model.

It should be noted that for certain satellite products, independent validation measurements may not exist, and validation can only be performed by evaluating the impact of the product when used in an application (for example, when assimilated in an NWP model).

6.2.2   Validation strategies

The validation of satellite-derived products should follow defined best-practice and variable-dependent protocols, such as those developed by the CEOS Working Group on Calibration and Validation. The validation of satellite-derived parameters and products can be carried out using the following sources:

(a)   Surface-based in situ measurements;

(b)   Surface-based remote-sensing measurements;

(c)   Model comparison and assimilation;

(d)   Other satellite-derived or blended products of a similar type.

To use such validation sources, it is essential that:

(a)   Measurement errors be well known;

(b)   Temporal and spatial sampling follow best-practice protocols;

(c)   Sampling be representative of the typical application-dependent environment (e.g. climatic zones, marine regimes, atmospheric regions, land-cover types).

For example, to support validated generation of combined sea-surface temperature satellite products, the Group for High Resolution Sea Surface Temperature has developed a comprehensive validation strategy,[6] which includes detailed descriptions of protocols, strategies to harmonize validation concepts for different satellite sensors contributing to sea-surface temperature measurements, needs for in situ (buoy) measurements as in situ data sources, and metrics to monitor product quality.

---

[6]   https://www.ghrsst.org/products-and-services/product-validation/

6.2.3   **Impact studies**

Experience shows that the results of direct validation are less significant for some satellite-derived products than for others. Since validation tests combine the effects of different error sources (satellite product, ground measurement, comparison method), the error due to the satellite product itself may be difficult to single out. For certain geophysical variables, ground measurements may be rather inaccurate. For others, the comparison method may depend too much on the observation environment.

One option for evaluating a product for a particular application is thus to assess its impact on the application skill. In this case, the evaluation reflects the quality of the product combined with the ability of the application to use it. For example, NWP models showed marginal impact for a couple of decades from atmospheric temperature–humidity soundings; this changed to a significant positive impact only when direct radiance assimilation was introduced. An opposite example is the assimilation of cloud-motion winds, which exhibited a strong positive impact at first, although the initial validation exercises were disappointing.

In summary, validation requires rigorous analysis of all error sources and of all steps in the comparison method. If the analysis shows that the error of the satellite product cannot be singled out, performing an impact study is a remaining validation mechanism.

———————————

REFERENCES AND FURTHER READING

Fox, N., 2010: *QA4EO – A Quality Assurance Framework for Earth Observation: A guide to "reference standards" in support of Quality Assurance requirements of GEO* (M.C. Greening, ed.). QA4EO-QAEO-GEN-DQK-003, Group on Earth Observations (available from http://www.qa4eo.org/docs/QA4EO-QAEO-GEN-DQK-003_v4.0.pdf).

Joint Committee for Guides in Metrology, 2012: *International Vocabulary of Metrology – Basic and General Concepts and Associated Terms (VIM)*. JCGM 200:2012.

Ohring, G. (ed.), 2007: *Achieving Satellite Instrument Calibration for Climate Change (ASIC³)*. Report of a workshop organized by the National Oceanic and Atmospheric Administration, National Institute of Standards and Technology, National Aeronautics and Space Administration, National Polar-orbiting Operational Environmental Satellite System-integrated Program Office, and Space Dynamics Laboratory of Utah State University, 16–18 May 2006. Landsdowne, VA.

CHAPTER CONTENTS

CHAPTER 7. CROSS-CUTTING ISSUES

7.1 FREQUENCY PROTECTION ISSUES

7.1.1 Overall frequency management

A critical issue for sustaining space-based Earth observations is whether the radio-frequency spectrum in the microwave range (1 to 300 GHz and above) remains available. This is important for:

(a) Passive observations of the Earth surface (in atmospheric windows) and atmospheric gases in absorption bands;

(b) Active observations with radar (altimeters, scatterometers, synthetic aperture radars);

(c) Communications necessary for data downloading and satellite control.

The use of the radio-frequency spectrum is coordinated at the global level by the International Telecommunication Union (ITU). Radio Regulations are adopted by ITU Members at the World Radiocommunication Conferences (WRC) every four years. The ITU regulates the allocation of radio-frequency bands to the different applications known as services, such as fixed and mobile telecommunications, broadband mobile applications, radio navigation, ground-based radars, short-range devices and electronic news gathering. Earth observation applications are identified by ITU as two particular services: the Earth exploration-satellite service (EESS) and Meteorological satellite (Metsat) service. While some bands are allocated to a service on an exclusive basis, most bands are allocated to several services with certain conditions (such as the limitation of the number, the emitting power and the geographical distribution of sources) that aim at avoiding harmful interference.

With the rapid expansion of the telecommunication sector and its increasing spectrum needs, the protection of frequencies required for EESS and Metsat has become very critical. Concerns include:

(a) Interference from uncontrolled emissions within exclusive EESS or Metsat bands, or to out-of-band emissions from nearby frequency bands;

(b) Sharing bands under conditions that are not stringent enough to guarantee reliable protection;

(c) The desire of other services to expand to bands formerly allocated to EESS or Metsat;

(d) The need of EESS or Metsat to use new bands arising due to the evolving remote-sensing technology (for example, microwave above 300 GHz), growing data rates or expanding telecommunication bandwidths.

In addressing these issues, it should be noted that frequencies used for passive measurements cannot be selected in any part of the spectrum: they are determined by the physics and must correspond to either absorption peaks of atmospheric components or window channels. Natural emissions are extremely weak compared to most artificial sources, and hence are easily corrupted. Therefore, passive radiometric bands must be considered as a natural heritage to be preserved.

7.1.2 Passive microwave radiometry

The spectral microwave range used for Earth observation stretches from ~1.4 GHz (e.g. for ocean salinity) to ~2 500 GHz and beyond. The most critical issues are for frequencies below 300 GHz. The use of frequencies above ~300 GHz is still emerging; moreover, since the water vapour continuum prevents viewing the lower troposphere, most of the instruments operating at those frequencies are designed for atmospheric chemistry and exploit limb viewing, which makes them less prone to interferences from ground sources. The ITU has identified a limited number of bands allocated to EESS, of which active uses are either prohibited or limited. As the radio-frequency spectrum becomes more crowded and users have a need for higher data rates, there is increasing pressure on higher frequencies, leading the ITU to share EESS bands with active services. Only a few narrowbands are assigned to EESS on an exclusive basis ensuring reliable legal protection. This has the following effects:

(a) The position of the allocated microwave channels often does not coincide with the sensitivity peak for the needed geophysical variable or with a spectral area free of contamination from other effects;

(b) The protected bandwidth may be so narrow that the signal-to-noise ratio is poor; this may force consideration of an unprotected band where a wider bandwidth is available, accepting the risk of interference.

Unfortunately, the pressure from other users of the spectrum, including commercial and mobile services, is continuously increasing; specialized groups from WMO, the Coordination Group for Meteorological Satellites, and space agencies must continuously monitor the situation at each update of the ITU Regulations.

7.1.3 Active microwave sensing

The problem of frequency protection also holds for active sensing (altimeters, scatterometers or synthetic aperture radars). For some applications of radar backscattering, like precipitation measurement, the sensing frequency has to be chosen in relation with the target properties. In other cases, like altimetry or synthetic aperture radar imagery, it is not very selective and there is some flexibility to find a frequency allocation in any of the L, S, C, X, K_u, K, K_a, V or W bands (see Part III, Chapter 2, Table 2.8 for definitions).

7.1.4 Satellite operation and communication frequencies

Frequency allocation for satellite–ground communications is another critical issue. As this involves active usage, the ITU Regulations are very restrictive in terms of allowed frequency, bandwidth and emitted power. The consequences are:

(a) Higher cost for a ground receiving station that works with low signals;

(b) Higher cost because the insufficient bandwidth available in one band for the data rate to be handled forces relocation to higher-frequency bands that require more challenging technology and antenna pointing;

(c) Ultimately, more difficulty to secure a frequency, particularly for real-time transmission; fewer frequencies are available, and sometimes this provokes interferences between satellites of the same family that are in orbit simultaneously.

In any event, frequency protection is difficult to guarantee, and users are experiencing problems, especially in industrialized areas. The table in this section provides the frequency bands allocated to data transmission to and from meteorological satellites (from WMO/ITU, 2008). It also takes into account the band 7 850–7 900 MHz, which was added at WRC-12.

Frequency bands for use by meteorological satellites for data transmission

Frequency band (MHz)	Metsat allocations
137–138	Primary for space-to-Earth direction
400.15–401	Primary for space-to-Earth direction
401–403	Primary for Earth-to-space direction
460–470	Secondary for space-to-Earth direction
1 670–1 710	Primary for space-to-Earth direction
7 450–7 550	Primary for space-to-Earth direction, geostationary satellites only
7 750–7 900	Primary for space-to-Earth direction, non-geostationary satellites only
8 025–8 400	Primary for space-to-Earth direction for Earth exploration-satellites[a]
8 175–8 215	Primary for Earth-to-space direction
18 000–18 300	Primary for space-to-Earth direction in Region 2,[b] geostationary satellites only
18 100–18 400	Primary for space-to-Earth direction in Regions 1 and 3,[b] geostationary satellites only
25 500–27 000	Primary for space-to-Earth direction for Earth exploration-satellites[a]

Notes:
a Since Metsat is a sub-class of the Earth exploration-satellite service, Earth exploration-satellite service allocations (as an example: 25 500–27 000 MHz) can also be used for the operation of Metsat applications.
b Regions 1, 2 and 3 refer to the ITU radiocommunication Regions.

7.2 INTERNATIONAL COORDINATION

7.2.1 The Coordination Group for Meteorological Satellites

Focusing on long-term sustained missions, the Coordination Group for Meteorological Satellites (CGMS), in accordance with an agreed baseline, coordinates satellite constellations in geostationary and low Earth orbit in support of WMO and co-sponsored programmes. Established in 1972 with a focus on weather monitoring by geostationary satellites for weather forecasting, CGMS initially defined common standards for low-resolution image dissemination in weather facsimile (WEFAX) format and for the International Data Collection System to support mobile stations viewed by the different satellites. The scope of CGMS was extended in 1992 to polar-orbiting meteorological satellites, and CGMS is now increasingly addressing key climate observations. The agreed baseline describes the missions to be maintained on a long-term basis; it serves as a reference for the intended contributions of the participating members to the Global Observing System (GOS) in response to the WMO Vision for the GOS in 2025. CGMS defines technical standards or best practices to ensure interoperability across the global system. It has developed contingency plans which provide a framework for action in case of satellite outage or other unexpected difficulties in fully implementing the agreed baseline.

The Coordination Group for Meteorological Satellites operates through working groups dedicated to: (i) satellite systems and telecommunications, (ii) satellite products, (iii) continuity and contingency planning, and (iv) global data dissemination. Together with WMO, CGMS launched major collaboration initiatives including the Global Space-based Inter-calibration System (GSICS), the Sustained and Coordinated Processing of Environmental Satellite Data for Climate Monitoring project (SCOPE-CM), and the Virtual Laboratory for Education and Training in Satellite Meteorology. CGMS works in partnership with several international science groups, is active on a continuous basis, and helps to organize working group meetings at two-year intervals, including for:

(a) The International TIROS Operational Vertical Sounder (TOVS) Working Group;

(b) The International Winds Working Group;

(c)   The International Precipitation Working Group;

(d)   The International Radio Occultation Working Group.

7.2.2   The Committee on Earth Observation Satellites

The Committee on Earth Observation Satellites (CEOS) was established in 1984 by the Group of Seven (most industrialized countries of the world). Unlike CGMS, CEOS first focused on land observation satellites (initially Landsat, then also the Satellite pour l'Observation de la Terre (SPOT) and the Indian Remote-sensing Satellite (IRS)), and specifically on new technologies such as synthetic aperture radars. Later, the scope of CEOS was extended to all Earth observation programmes but with less emphasis on meteorology until a new interest arose for climate issues. An important activity since its establishment has been calibration and validation through the Working Group on Calibration and Validation. Other CEOS working groups are the Working Group on Information Systems and Services, the Working Group on Capacity Building and Data Democracy, and the new CEOS/CGMS Working Group on Climate.

The coordination activity of CEOS is now articulated around the concept of constellations, to share experience in the development of algorithms, standardize data products and formats, exchange information regarding the calibration and validation of measurements, facilitate the timely exchange of and access to data products from existing and planned missions, and facilitate the planning of new missions. There are currently seven virtual constellations:

(a)   Atmospheric composition;

(b)   Land surface imaging;

(c)   Ocean surface topography;

(d)   Precipitation;

(e)   Ocean colour radiometry;

(f)   Ocean surface vector wind;

(g)   Sea-surface temperature.

7.3   SATELLITE MISSION PLANNING

7.3.1   Satellite programme life cycle

In the early days of satellite meteorology, the life cycle of a satellite mission was only a few years. Mission definition, satellite design, system development and science demonstration happened in one or two years each; the exploitation period was short and the ground segment often under-dimensioned.

Nowadays, an operational programme (e.g. for meteorological purposes) generally proceeds with the following phases:

Phase 0: Definition of user requirements, involving the user community, and of mission requirements, i.e. identification of the possible techniques to fulfil the user requirements. This lasts about three to four years;

Phase A: Feasibility assessment at system level (including a preliminary definition of the ground segment) and of critical instruments (possibly including instrument simulations), and rough order-of-magnitude cost estimation. The duration is about two years;

Phase B: Preliminary design, preparatory activities (including airborne campaigns) and detailed cost estimation. This takes about another two years;

Phase C: Detailed design and development and testing of all systems (including the ground segment) and subsystems. This phase is the longest, requiring about five years;

Phase D: Integration of all subsystems, testing of the whole satellite and launch campaign. This is often accomplished in one year.

Adding some time for the decision-making and approval processes, and for in-orbit commissioning, the duration of the development phase is of the order of 15 years.

Phase E: The exploitation phase is generally aimed at 15 years for an operational programme including a series of three or four satellites, with some overlap for contingency purposes (the typical lifetime of a low Earth orbit satellite is five years, and seven years for a geostationary Earth orbit (GEO) satellite). The duration of a satellite generation is a trade-off between the need for a long series to offset the development cost and the user learning curve, and the need to develop a new generation of satellite instruments to benefit from state-of-the-art technology.

The organization of a space programme involves many participants: the applications community, scientific institutes, space agencies focused on research and development, industry, and governments with their industrial policy and budget constraints. In the case of Earth observation programmes with worldwide scope, there must be as much coordination as possible with international partners, which may further complicate the decision-making process.

7.3.2 Continuity and contingency planning

The continuity of space-based observations has been a critical requirement for the meteorological satellite constellation in geostationary orbit ever since nowcasting and severe weather forecasting, including tropical cyclone warning, began relying on satellite monitoring. The operational continuity of GEO imagery entails round-the-clock operation, high availability, near-real-time data dissemination, and long-term continuity guaranteed by a robust programme that includes provisions for in-orbit backup. When the polar-orbiting constellation was established, and numerical weather prediction models were increasingly relying on satellite sounding (infrared, microwave and radio-occultation) and other key satellite observations such as ocean surface winds, a similar requirement for operational continuity was applied to the morning and afternoon satellites that became the core meteorological constellation in polar orbit. A baseline configuration of the operational space-based observing system was defined and undertaken by the satellite operators contributing to WMO programmes.

While satellite operators committed to give their best efforts to maintain the geostationary and polar Sun-synchronous constellations, CGMS developed a Global Contingency Plan (see section 7.2.1 and box below) providing a technical and legal framework for contingency measures to be taken on a "help your neighbour" basis in case of deficiency of one of the elements of the operational configuration.

For geostationary satellites, contingency support can be provided if the number of satellites is sufficiently high and their nominal positions are appropriately spaced along the Equator (see, for instance, Part III, Chapter 4, Figure 4.1). Moving a satellite from one longitude to another requires little fuel if implemented at a slow pace. As per the contingency plan, several satellites are maintained in backup positions and it is possible to relocate a satellite to fill a gap through a manoeuvre lasting a few days or weeks depending on the urgency and the fuel available on board. Several examples have taken place: a spare Meteosat satellite was moved to cover the West Atlantic Ocean when the Geostationary Operational Environmental Satellite (GOES) system suffered a launch delay in the early 1990s; a spare GOES satellite filled the gap in the Western Pacific Ocean during the transition from the Geostationary Meteorological Satellite (GMS) to the Multifunctional Transport Satellite (MTSAT) in the early 2000s; and in the last two decades the Indian Ocean position has been covered on occasions by GOES and Meteosat satellites.

For Sun-synchronous satellites, contingency is more complicated. Changing the orbital plane of a satellite requires a very large amount of fuel and is not envisaged apart from the natural drift of the orbital plane due to precession or orbit-keeping manoeuvres to correct this drift. The contingency plan therefore focuses on the availability of backup satellites in each orbital plane along with regular spacing of the equatorial crossing times of these planes.

When WMO adopted its Vision for the GOS in 2025, the scope of the operational space-based observing system was extended to climate monitoring, reflecting both the requirement to monitor the climate on a continuing basis and the maturity of space-based systems evolving from research and development to an operational status. In response, a new baseline was subsequently defined and adopted by CGMS that incorporates a number of climate-oriented missions. Continuity is as crucial for climate monitoring as for operational weather forecasting; however, the requirements are different because climate monitoring involves different timescales. First, near-real-time availability and short-term gaps in a daily cycle are not driving requirements. Second, major importance is attached to long-term continuity and stability of measurements throughout decades. The Global Climate Observing System (GCOS) Climate Monitoring Principles require systematic overlap between all consecutive satellites to allow for intercalibration and traceability. Stability and traceability could also be achieved by maintaining one highly secured reference mission, with in-orbit backup, that serves as a calibration reference standard for all the others (as discussed in Part III, Chapter 6, 6.1.9). Such a provision should be a major element in the definition of the Architecture for Climate Monitoring from Space.

CGMS continuity and contingency planning

The CGMS baseline defines (i) a geostationary constellation comprising six satellites nominally located at fixed longitudes (135°W, 75°W, 0°, 76°E, 105°E, 140°E) and performing a set of agreed missions, (ii) a core meteorological constellation in polar Sun-synchronous orbit performing imagery and sounding, and (iii) different constellations dedicated to additional missions in either Sun-synchronous or inclined low Earth orbits. The CGMS Working Group on Operational Continuity and Contingency Planning keeps under review the implementation of the baseline, the availability of in-orbit backups and the risks of interruption of key missions.

The Coordination Group for Meteorological Satellites has adopted a Global Contingency Plan which includes guidelines to ensure continuity, for example, in terms of in-orbit backup and re-launch policy, sets criteria for entering into contingency mode and identifies actions to be taken in such contingency situations. In particular, the Global Contingency Plan defines a generic procedure for relocating a spare geostationary satellite to take over from a failing satellite, which is referred to as the "help your neighbour" strategy. This global plan is supplemented by bilateral contingency agreements between geostationary satellite operators. On several occasions, over the past three decades, such contingency relocations have been essential to preserve the continuity of vital operational missions.

7.3.3   Long-term evolution

The evolving user requirements for satellite data and the dramatic progress of space and remote-sensing technology call for continuous improvements to satellite systems and instrumentation.

At the same time, the strong pressure on resources stresses the need to seek an optimization of the global effort to assure the availability of a comprehensive observing system and avoid unnecessary redundancy beyond the required margins for robustness. Optimization is also needed in the development, validation and sustained processing of derived products, and requires data sharing, interoperability and quality assurance. Global coordination under the auspices of WMO aims at ensuring such optimization under the overall context of the WMO Integrated Global Observing System, building on the Rolling Review of Requirements, the high-level guidance provided by the Vision for the GOS, the Statement of Guidance in each application area, and the Implementation Plan for the Evolution of Global Observing Systems which consolidates the recommendations addressed to agents implementing observing systems.

A notable initiative is also the Architecture for Climate Monitoring from Space, promoted by WMO, CEOS and CGMS, which aims to provide an end-to-end response from the space-based observing system to the climate monitoring requirements.

REFERENCES AND FURTHER READING

Bizzarri, B., 1982: Satellite data for numerical weather prediction. *Rivista di Meteorologia Aeronautica*, 42(4):369–382.

———, 1986: Basic principles of remote sensing. *Proceedings of the Course on Satellite Meteorology and its Extension to Agriculture* (Erice, ed.). EUMETSAT, EUM P03, pp. 1–10.

Bizzarri, B. and C. Tomassini, 1976: Retrieval of information from high-resolution images. *Proceedings of the Symposium on Meteorological Observations from Space*, Committee on Space Research, Philadelphia, pp. 140–144.

Chander, G., T.J. Hewison, N. Fox, X. Wu, X. Xiong and W.J. Blackwell, 2013: Overview of intercalibration of satellite instruments. *IEEE Transactions on Geoscience and Remote Sensing*, 51(3):1056–1080.

Committee on Earth Observation Satellites: Mission, Instruments and Measurements database online (available from http://database.eohandbook.com, updated yearly).

Datla, R.V., J.P. Rice, K.R. Lykke, C. Johnson, J.J. Butler and X. Xiong, 2009: *Best Practice Guidelines for Pre-launch Characterization and Calibration of Instruments for Passive Optical Remote Sensing.* NIST IR 7637, National Institute of Standards and Technology.

European Space Agency: Sharing Earth Observation Resources (available from https://directory.eoportal.org/web/eoportal/satellite-missions, updated at intervals).

Fox, N., 2010: *QA4EO – A Quality Assurance Framework for Earth Observation: A guide to "reference standards" in support of Quality Assurance requirements of GEO* (M.C. Greening, ed.). QA4EO-QAEO-GEN-DQK-003, Group on Earth Observations (available from http://www.qa4eo.org/docs/QA4EO-QAEO-GEN-DQK-003_v4.0.pdf).

Joint Committee for Guides in Metrology, 2012: *International vocabulary of metrology – Basic and general concepts and associated terms (VIM).* JCGM 200:2012.

Klein, M. and A.J. Gasiewski, 2000: The sensitivity of millimeter and sub-millimeter frequencies to atmospheric temperature and water vapor variations. *Journal of Geophysical Research: Atmospheres*, 13:17481–17511.

Kramer, H.J., 2002: *Observation of the Earth and its Environment – Survey of Missions and Sensors*, Springer (CD-ROM inclusive of survey on airborne sensors and campaigns).

Ohring, G. (ed.), 2007: *Achieving Satellite Instrument Calibration for Climate Change (ASIC^3).* Report of a workshop organized by the National Oceanic and Atmospheric Administration, National Institute of Standards and Technology, National Aeronautics and Space Administration, National Polar-orbiting Operational Environmental Satellite System-integrated Program Office, and Space Dynamics Laboratory of Utah State University, 16–18 May 2006. Landsdowne, VA.

Parkinson, C.L., A. Ward and M.D. King (eds.), 2006: *Earth Science Reference Handbook*. NASA Goddard Space Flight Center.

Tobin, D.C., H.E. Revercomb, R.O. Knuteson, F.A. Best, W.L. Smith, N.N. Ciganovich, R.G. Dedecker, S. Dutcher, S.D. Ellington, R.K. Garcia, H.B. Howell, D.D. LaPorte, S.A. Mango, T.S. Pagano, J.K. Taylor, P. van Delst, K.H. Vinson and M.W. Werner, 2006*a*: Radiometric and spectral validation of Atmospheric Infrared Sounder observations with the aircraft-based Scanning High-Resolution Interferometer Sounder. *Journal of Geophysical Research: Atmospheres*, 111(D09S02).

Tobin, D.C., H.E. Revercomb, C.C. Moeller and T.S. Pagano, 2006*b*: Use of Atmospheric Infrared Sounder high-spectral resolution spectra to assess the calibration of Moderate Resolution Imaging Spectroradiometer on EOS Aqua. *Journal of Geophysical Research: Atmospheres*, 111(D09S05).

World Meteorological Organization, 2001: *Applications with Meteorological Satellites* (W.P. Menzel). SAT-28 (WMO/TD-No. 1078). Geneva.

———, 2014: Observing Systems Capability Analysis and Review (OSCAR) database and tool (available from http://www.wmo-sat.info/oscar/, regularly updated).

World Meteorological Organization/International Telecommunication Union, 2008: *Handbook on Use of Radio Spectrum for Meteorology: Weather, Water and Climate Monitoring and Prediction*. Geneva.

———————

PART IV. QUALITY ASSURANCE AND MANAGEMENT OF OBSERVING SYSTEMS

PART CONTENTS

CHAPTER CONTENTS

CHAPTER 1. QUALITY MANAGEMENT

1.1   GENERAL

This chapter is general and covers operational meteorological observing systems of any size or nature. Although the guidance it gives on quality management is expressed in terms that apply to large networks of observing stations, it should be read to apply even to a single station.

Quality management

Quality management provides the principles and the methodological frame for operations, and coordinates activities to manage and control an organization with regard to quality. Quality assurance and quality control are the parts of any successful quality management system. Quality assurance focuses on providing confidence that quality requirements will be fulfilled and includes all the planned and systematic activities implemented in a quality management system so that quality requirements for a product or service will be fulfilled. Quality control is associated with those components used to ensure that the quality requirements are fulfilled and includes all the operational techniques and activities used to fulfil quality requirements. This chapter concerns quality management associated with quality control and quality assurance and the formal accreditation of the laboratory activities, especially from the point of view of meteorological observations of weather and atmospheric variables.

The ISO 9000 family of standards is discussed to assist understanding in the course of action during the introduction of a quality management system in a National Meteorological and Hydrological Service (NMHS); this set of standards contains the minimum processes that must be introduced in a quality management system for fulfilling the requirements of the ISO 9001 standard. The total quality management concept according to the ISO 9004 guidelines is then discussed, highlighting the views of users and interested parties. The ISO/IEC 17025 standard is introduced. The benefits to NMHSs and the Regional Instrument Centres (RICs) from accreditation through ISO/IEC 17025 are outlined along with a requirement for an accreditation process.

The ISO/IEC 20000 standard for information technology (IT) service management is introduced into the discussion, given that every observing system incorporates IT components.

Quality assurance and quality control

Data are of good quality when they satisfy stated and implied needs. Elsewhere in this Guide explicit or implied statements are given of required accuracy, uncertainty, resolution and representativeness, mainly for the synoptic applications of meteorological data, but similar requirements can be stated for other applications. It must be supposed that minimum total cost is also an implied or explicit requirement for any application. The purpose of quality management is to ensure that data meet requirements (for uncertainty, resolution, continuity, homogeneity, representativeness, timeliness, format, and so on) for the intended application, at a minimum practicable cost. All measured data are imperfect, but, if their quality is known and demonstrable, they can be used appropriately.

The provision of good quality meteorological data is not a simple matter and is impossible without a quality management system. The best quality management systems operate continuously at all points in the whole observing system, from network planning and training, through installation and station operations to data transmission and archiving, and they include feedback and follow-up provisions on timescales from near-real-time to annual reviews and end-to-end process. The amount of resources required for an effective quality management system is a proportion of the cost of operating an observing system or network and is typically a few per cent of the overall cost. Without this expenditure, the data must be regarded as being of unknown quality, and their usefulness is diminished.

An effective quality management system is one that manages the linkages between preparation for data collection, data collection, data assurance and distribution to users to ensure that the user receives the required quantity. For many meteorological quantities, there are a number of these preparation-collection-assurance cycles between the field and the ultimate distribution to the user. It is essential that all these cycles are identified and the potential for divergence from the required quantity minimized. Many of these cycles will be so closely linked that they may be perceived as one cycle. Most problems occur when there are a number of cycles and they are treated as independent of one another.

Once a datum from a measurement process is obtained, it remains the datum of the measurement process. Other subsequent processes may verify its worth as the quantity required, use the datum in an adjustment process to create the quality required, or reject the datum. However, none of these subsequent processes changes the datum from the measurement process. Quality control is the process by which an effort is made to ensure that the processes leading up to the datum being distributed are correct, and to minimize the potential for rejection or adjustment of the resultant datum.

Quality assurance includes explicit control of the factors that directly affect the data collected and processed before distribution to users. For observations or measurements, this includes equipment, exposure, measurement procedures, maintenance, inspection, calibration, algorithm development, redundancy of measurements, applied research and training. In a data transmission sense, quality control is the process established to ensure that for data that is subsequently transmitted or forwarded to a user database, protocols are set up to ensure that only acceptable data are collected by the user.

Quality control is the best-known component of quality management systems, and it is the irreducible minimum of any system. It consists of all the processes that are put in place to generate confidence and ensure that the data produced will have the required quality and also include the examination of data at stations and at data centres to verify that the data are consistent with the quality management system goals, and to detect errors so that the data may be either flagged as unreliable, corrected or, in the case of gross errors, deleted. A quality management system should include procedures for feeding back into the measurement and quality control process to prevent the errors from recurring. Quality assurance can be applied in real-time post measurement, and can feed into the quality control process for the next process of a quality system, but in general it tends to operate in non-real time.

Real-time quality control is usually performed at the station and at meteorological analysis centres. Delayed quality assurance may be performed at analysis centres for the compilation of a refined database, and at climate centres or databanks for archiving. In all cases, the results should be returned to the observation managers for follow-up.

A common component of quality control is quality monitoring or performance monitoring, a non-real-time activity in which the performance of the network or observing system is examined for trends and systematic deficiencies. It is typically performed by the office that manages and takes responsibility for the network or system, and which can prescribe changes to equipment or procedures. These are usually the responsibility of the network manager, in collaboration with other specialists, where appropriate.

Modern approaches to data quality emphasize the advantages of a comprehensive system for quality assurance, in which procedures are laid down for continuous interaction between all parties involved in the observing system, including top management and others such as designers and trainers who may otherwise have been regarded as peripheral to operational quality concerns after data collection. The formal procedures prescribed by the International Organization for Standardization (ISO) for quality management and quality assurance, and other detailed procedures used in manufacturing and commerce, are also appropriate for meteorological data.

1.2   THE ISO 9000 FAMILY, ISO/IEC 17025, ISO/IEC 20000 AND THE WMO QUALITY MANAGEMENT FRAMEWORK

The chapter gives an explanation of the related ISO standards and how they interconnect.

Proficiency in ISO quality systems is available through certification or accreditation, and usually requires external auditing of the implemented quality management system. Certification implies that the framework and procedures used in the organization are in place and used as stated. Accreditation implies that the framework and procedures used in the organization are in place, used as stated and technically able to achieve the required result. The assessment of technical competence is a mandatory requirement of accreditation, but not of certification. The ISO 9001 is a standard by which certification can be achieved by an organization, while accreditation against the ISO/IEC 17025 is commonly required for laboratories and routine observations.

The ISO 9000 standard has been developed to assist organizations of all types and sizes to implement and operate quality management systems. The ISO 9000 standard describes the fundamentals of quality management systems and gives definitions of the related terms (for example, requirement, customer satisfaction). The main concept is illustrated in Figure 1.1. The ISO 9001 standard specifies the requirements for a quality management system that can be certified in accordance with this standard. The ISO 9004 standard gives guidelines for continual improvement of the quality management system to achieve a total quality management system. The ISO 19011 standard provides the guidance on auditing the quality management system. All these standards are described in more detail in the related documents of the WMO Quality Management Framework.

1.2.1   ISO 9000: Quality management systems – Fundamentals and vocabulary

The following eight quality management principles are the implicit basis for the successful leadership of NMHSs of all sizes and for continual performance improvement:

(a)   Customer focus;
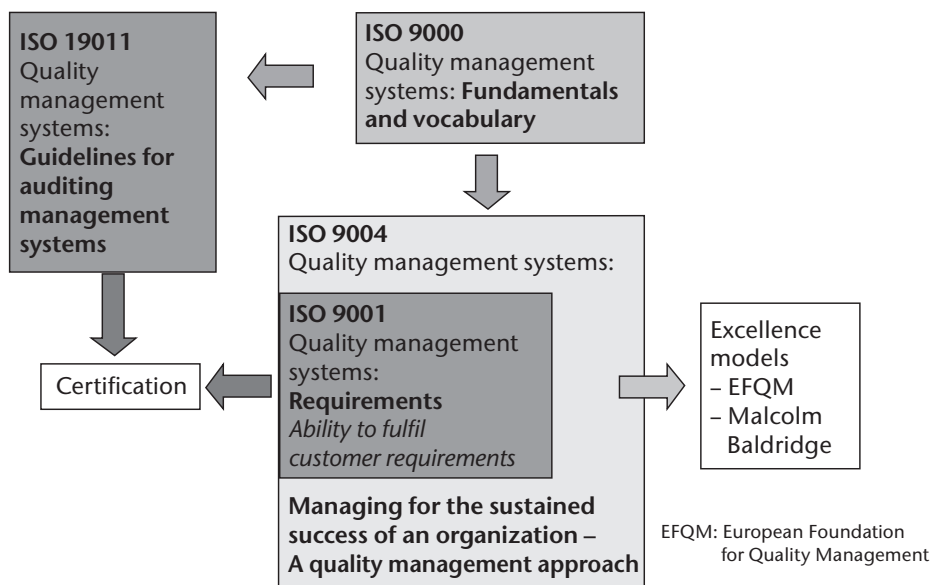
(b)   Leadership;

(c)   Involvement of people;

Figure 1.1. The main concept of the ISO 9000 standards and the dependencies

(d)   Process approach;

(e)   System approach to management;

(f)   Continual improvement;

(g)   Factual approach to decision-making;

(h)   Mutually beneficial supplier relationships.

All these principles must be documented and put to practice to meet the requirements of the ISO 9000 and 9001 standards to achieve certification. The main topic of these standards is the process approach, which can simply be described as activities that use resources to transform inputs into outputs.

The process-based quality management system is simply modelled in Figure 1.2. The basic idea is that of the mechanism likely to obtain continual improvement of the system and customer satisfaction through measuring the process indices (for example, computing time of a GME model, customer satisfaction, reaction time, and so forth), assessing the results, making management decisions for better resource management and obtaining inevitably better products.

1.2.2   ISO 9001: Quality management systems – Requirements

The basic requirements for a quality management system are given by this standard, including processes for improvement and complaint management and carrying out management reviews. These processes are normally incorporated in the quality manual. The ISO 9001 standard focuses on management responsibility rather than technical activities.

To achieve certification in ISO 9001, six processes must be defined and documented by the organization (NMHS), as follows:

(a)   Control of documents;

(b)   Control of records;

(c)   Control of non-conforming products;

(d)   Corrective action;
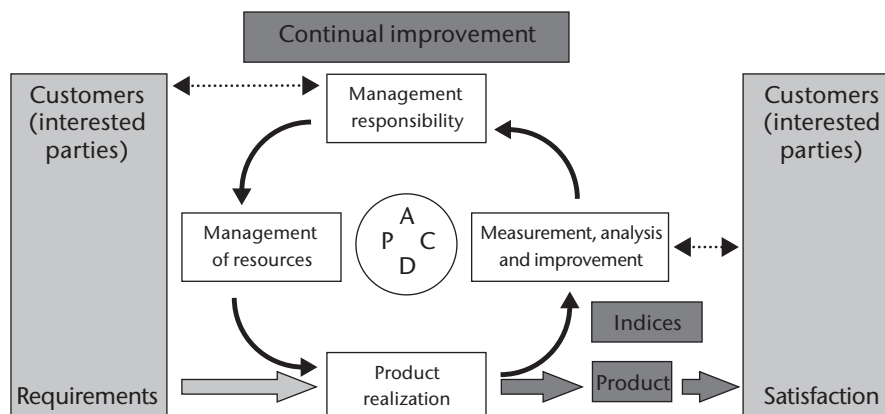
P = Plan, D = Do, C = Check, A = Act

Figure 1.2. The PDCA control circuit (also named the Deming-circuit)

(e)   Preventive action;

(f)   Internal audit.

Furthermore, there must be a quality manual which states the policy (for example, the goal is to achieve regional leadership in weather forecasting) and the objectives of the organization (for example, improved weather forecasting: reduce false warning probability) and describes the process frameworks and their interaction. There must be statements for the following:

(a)   Management;

(b)   Internal communication;

(c)   Continual improvement;

(d)   System control (for example, through management reviews).

Exclusions can be made, for example, for development (if there are no development activities in the organization).

The documentation pyramid of the quality management system is shown in Figure 1.3. The process descriptions indicate the real activities in the organization, such as the data-acquisition process in the weather and climate observational networks. They provide information on the different process steps and the organizational units carrying out the steps, for cooperation and information sharing purposes. The documentation must differentiate between periodic and non-periodic processes. Examples of periodic processes are data acquisition or forecast dissemination. Examples of non-periodic processes include the installation of measurement equipment which starts with a user or component requirement (for example, the order to install a measurement network).

Lastly, the instructions in ISO 9001 give detailed information on the process steps to be referenced in the process description (for example, starting instruction of an AWS). Forms and checklists are helpful tools to reduce the possibility that required tasks will be forgotten.

1.2.3   **ISO 9004: Managing for the sustained success of an organization –
A quality management approach**

The guidelines for developing the introduced quality management system to achieve business excellence are formulated in ISO 9004. The main aspect is the change from the customer position to the position of interested parties. Different excellence models can be developed by the
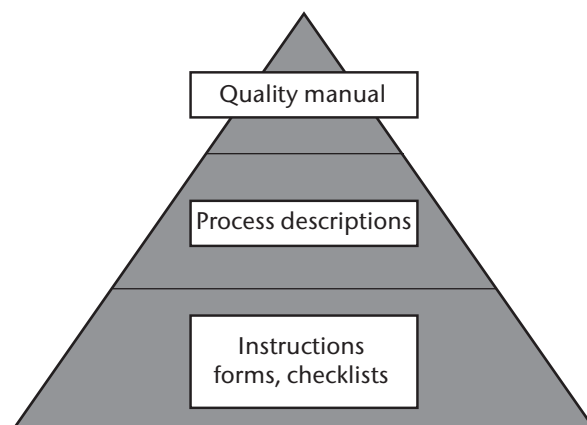

Figure 1.3. The documentation pyramid of a quality management system

ISO 9004 guidelines, for example, the Excellence Model of the European Foundation for Quality Management (EFQM)[1] or the Malcolm Baldrige National Quality Award.[2] Both excellence models are appropriately established and well respected in all countries of the world.

The EFQM Excellence Model contains the following nine criteria which are assessed by an expert team of assessors:

(a) Leadership;

(b) People;

(c) Policy and strategy;

(d) Partnerships and resources;

(e) Processes;

(f) People results;

(g) Customer results;

(h) Society results;

(i) Key performance results.

The Malcolm Baldrige model contains seven criteria similar to the EFQM Excellence Model, as follows:

(a) Leadership;

(b) Strategic planning;

(c) Customer and market focus;

(d) Measurement, analysis, and knowledge management;

(e) Human resources focus;

(f) Process management;

(g) Results.

There is no certification process for this standard, but external assessment provides the opportunity to draw comparisons with other organizations according to the excellence model (see also Figure 1.1).

1.2.4   ISO 19011: Guidelines for auditing management systems

This standard is a guide for auditing management systems and does not have any regulatory character. The following detailed activities are described for auditing the organization:

(a) Principles of auditing (ethical conduct, fair presentation, due professional care, independence, evidence-based approach);

(b) Audit planning (establishing and implementing the audit programme);

---

[1]   See EFQM website at http://www.efqm.org.
[2]   See the NIST website at http://www.nist.gov/baldrige/.

(c)   Audit activities (initiating the audit, preparing and conducting on-site audit activities, preparing the audit report);

(d)   Training and education of the auditors (competence, knowledge, soft skills).

The manner in which audits are conducted depends on the objectives and scope of the audit which are set by the management or the audit client. The primary task of the first audit is to check the conformity of the quality management system with the ISO 9001 requirements. Further audits give priority to the interaction and interfaces of the processes.

The audit criteria are the documentation of the quality management system, the process descriptions, the quality manual and the unique individual regulations.

The audit planning published by the organization should specify the relevant departments of the organization, the audit criteria and the audit objectives, place, date and time to ensure a clear assignment of the audits.

1.2.5   ISO/IEC 17025: General requirements for the competence of testing and calibration laboratories

This set of requirements is applicable to facilities, including laboratories and testing sites, that wish to have external accreditation of their competence in terms of their measurement and testing processes.

The ISO/IEC 17025 standard aligns its management requirements with those of ISO 9001. This standard is divided into two main parts: management requirements and technical requirements. Hence, the quality management system must follow the requirements of the ISO 9001 standard, which include described processes, a management handbook that provides a connection between processes and goals and policy statements, and that these aspects be audited regularly. All laboratory processes must be approved, verified and validated in a suitable manner to meet the requirements. Furthermore, the roles of the quality management representative (quality manager) and the head of the laboratory must be determined.

An essential component of the technical requirements is the development of uncertainty analyses for each of the measurement processes, including documented and verified traceability to international metrology standards.

1.2.6   ISO/IEC 20000: Information technology – Service management

NMHSs make use of IT equipment to obtain data from the measuring networks to use in GME/LM models and to provide forecasters with the outputs of models. The recommendations of this standard are helpful for the implementation of reliable IT services. The new ISO/IEC 20000 standard summarizes the old British standard BS-15000 and the IT Infrastructure Library (ITIL) recommendations. The division of requirements follows the ITIL structure.

The ITIL elements are divided into service delivery and service support with the following processes:

Service delivery:

(a)   Service-level management;

(b)   Financial management;

(c)   IT service continuity management;

(d)   Availability management;

(e)   Capacity management.

Service support:

(a)   Change management;

(b)   Incident management;

(c)   Problem management;

(d)   Release management;

(e)   Configuration management.

Security management is common to both areas.

All these require that:

(a)   The processes be adapted to the NMHS's organization;

(b)   Particular attention be paid to user support.

Special attention has been placed on the change-management process, which can contain release and configuration management. Incident and problem management is normally covered by the implementation of a user help desk.

1.2.7   **WMO Quality Management Framework**

The WMO Quality Management Framework gives the basic recommendations that were based on the experiences of NMHSs. The necessary conditions for successful certification against ISO 9001 are explained in WMO (2005*a*, 2005*b*).

The Quality Management Framework is the guide for NMHSs, especially for NMHSs with little experience in a formal quality management system. The introduction of a quality management system is described only briefly in the following section, noting that WMO cannot carry out any certification against ISO 9001.

1.3   **INTRODUCTION OF QUALITY MANAGEMENT**

The introduction of successful quality management depends heavily on the cooperation of senior management. The senior management of the NMHS must be committed to the quality management system and support the project team. The necessary conditions for successful certification are summarized and the terms of ISO 9001 standards are explained in ISO 20000.

Senior-level management defines a quality policy and the quality objectives (including a quality management commitment), and staff have to be trained in sufficient quality management topics to understand the basis for the quality management process (see section 1.2.2). Most importantly, a project team should be established to manage the transition to a formal quality management system including definition and analysis of the processes used by the organization.

To assist the project team, brief instructions can be given to the staff involved in the process definition, and these would normally include the following:

(a)   To document (write down) what each group does;

(b)   To indicate the existing documentation;

(c)   To indicate the proof or indicators of what is done;

(d)   To identify what can be done to continually improve the processes.

Given that the documentation specifies what the organization does, it is essential that the main processes reflect the functions of the organization of the NMHS. These can be a part of the named processes (see Figure 1.4), for example:

(a)   Weather forecasting (including hydrometeorological, agrometeorological, human biometeorological aspects) and weather warnings;

(b)   Consulting services (including climate and environment);

(c)   Data generation (from measurement and observational networks);

(d)   International affairs;

(e)   Research and development (global modelling, limited area models, instrumentation);

(f)   Technical infrastructure (computing and communications, engineering support, data management and IT support);

(g)   Administration processes (purchasing, financial and personnel management, organization, administration offices and immovables, knowledge management, central planning and control and legal affairs).

Even though these processes will meet the individual needs of NMHSs and provide them with subprocesses, normally there should be regulations for remedying incidents (for example, system failures, staff accidents).

The processes must be introduced into the organization with clear quality objectives, and all staff must be trained in understanding the processes, including the use of procedures and checklists and the measurement of process indicators.
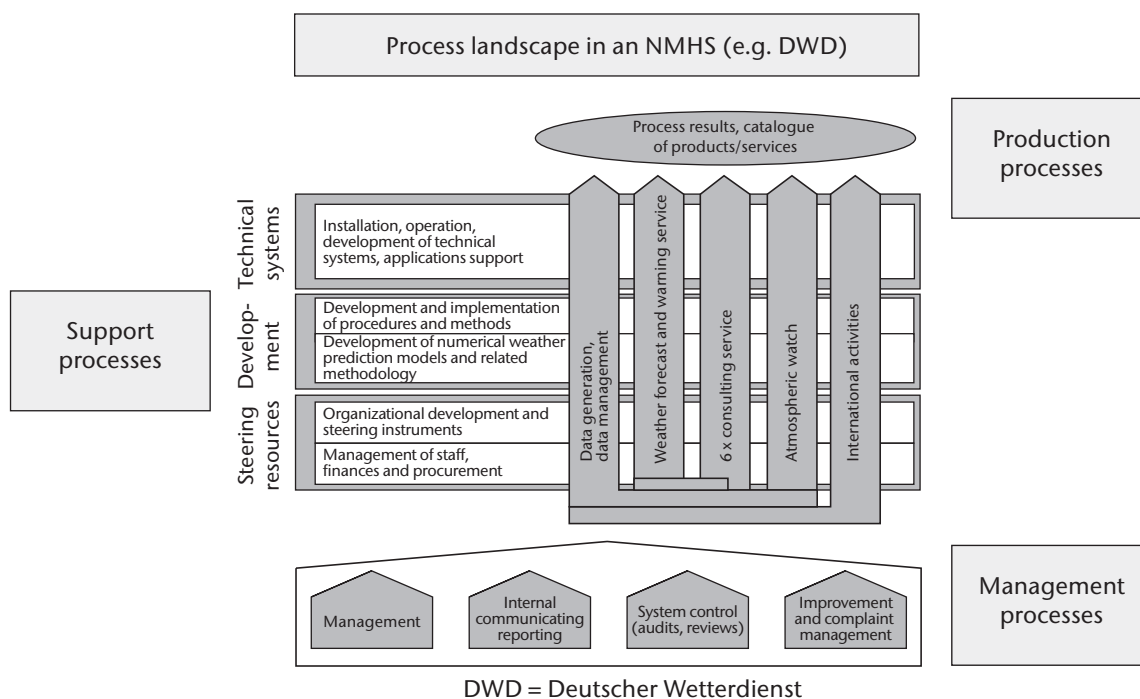

Figure 1.4. Process landscape of an NMHS (example: DWD, WMO 2005*a*)

Before applying for certification, the quality management system must be reviewed by carrying out internal audits in the departments and divisions of the organization, to check conformity of the quality management system as stated and as enacted. These documented reviews can be performed on products by specialized and trained auditors. The requirements and recommendations for these reviews are given in ISO 19011 (see section 1.2.4).

The management review of the quality management system will include the following:

(a)   Audit results;

(b)   Customer feedback;

(c)   Process performance based on performance indicators;

(d)   Status of preventive and corrective actions;

(e)   Follow-up actions from previous management reviews;

(f)   Changes in the quality management system (policy of the organization);

(g)   Recommendations for improvement.

1.4   **ACCREDITATION OF LABORATORIES**

Accreditation requires additional processes and documentation and, most importantly, evidence that laboratory staff have been trained and have mastered the processes and methods to be accredited.

The documentation must contain the following aspects:

(a)   A management manual for the laboratory;

(b)   The process descriptions mentioned in section 1.2;

(c)   The documentation of all processes and methods;

(d)   Work instructions for all partial steps in the processes and methods;

(e)   Equipment manuals (manual including calibrating certificates);

(f)   Maintenance manuals.

Since procedures and methods are likely to change more frequently than the management aspects of the accreditation, the methods are usually not included in the management manual. However, there is specific reference to the procedures and methods used in the management manual.

As it is unlikely that all aspects of the accreditation will be covered once the quality management system is introduced, it is recommended that a pre-audit be conducted and coordinated with the certifying agency. In these pre-audits it would be normal for the certifying agency:

(a)   To assess staff and spatial prerequisites;

(b)   To assess the suitability of the management system;

(c)   To check the documentation;

(d)   To validate the scope of the accreditation.

The accreditation procedure consists of assessments by an expert panel (external to the organization), which includes a representative from the certifying agency. The assessment panel will focus on two main areas as follows:

(a)   Documentation;

(b)   An examination of the facilities included in the scope of the accreditation (for example, laboratories, special field sites).

The assessment of documentation covers verification of the following documents:

(a)   A management manual (or laboratory guide);

(b)   Procedure instructions;

(c)   Work instructions;

(d)   Test instructions;

(e)   Equipment manuals;

(f)   Maintenance manuals;

(g)   Uncertainty analyses of specific quantities, test results and calibrations;

(h)   Proof documents (for example, that staff training has occurred and that quantities are traceable);

(i)   Records (for example, correspondence with the customer, generated calibration certificates).

The external expert team could request additional documents, as all aspects of the ISO/IEC 17025 standard are checked and in more detail than a certification under ISO 9001.

Besides the inspection of the measurement methods and associated equipment, the assessment of the facilities in the scope of the accreditation will include the following:

(a)   Assessment of the staff (including training and responsibility levels);

(b)   Assessment of the infrastructure that supports the methods (for example, buildings, access).

The following are also checked during the assessment to ensure that they meet the objectives required by management for accreditation:

(a)   Organizational structure;

(b)   Staff qualifications;

(c)   Adequacy of the technological facilities;

(d)   Customer focus.

In addition, the assessment should verify that the laboratory has established proof of the following:

(a)   Technical competence (choice and use of the measuring system);

(b)   Calibration of measurement equipment;

(c)   Maintenance of measurement equipment;

(d)   Verification and validation of methods.

Benefits and disadvantages of accreditation

Through initial accreditation by an independent certifying agency NMHSs prove their competence in the area of meteorological measuring and testing methods according to a recognized standard. Once accreditation is established, there is an ongoing periodic external audit, which provides additional proof that standards have been maintained, but more importantly it helps the organization to ensure that its own internal quality requirements are met.

An accreditation with suitable scope also provides commercial opportunities for the calibration, verification and assessment of measurement devices.

For organizations that do not have a quality management system in place, the benefits of accreditation are significant. First, it documents the organization's system, and, through that, a process of analysis can be used to make the organization more efficient and effective. For example, one component of accreditation under ISO/IEC 17025 requires uncertainty analyses for every calibration and verification test; such quantitative analyses provide information on where the most benefit can be achieved for the least resources.

Accreditation or certification under any recognized quality framework requires registration and periodic audits by external experts and the certifying agency. These represent additional costs for the organization and are dependent on the scope of the accreditation and certification.

Seeking accreditation before an effective quality management system is in place will lead to an increased use of resources and result in existing resources being diverted to establish a quality management system; there will also be additional periodic audit costs.

1.5   **QUALITY MANAGEMENT TOOLS**

Several well-known tools exist to assist in the processes of a quality management system and its continuous improvement. Three examples of these tools are described below as an introduction: the Balanced Score card, Failure Mode and Effects Analysis, and Six Sigma.

The Balanced Scorecard (Kaplan and Norton, 1996) has at a minimum four points of focus: finances, the customer, processes and employees. Often the general public is added given that public interests must always be taken into account.

Each organization and organization element provides key performance indicators for each of the focus areas, which in turn link to the organization's mission (or purpose, vision or goals) and the strategy (or working mission and vision).

Failure Mode and Effects Analysis is a method for the examination of possible missing causes and faults and the probability of their appearance. The method can be used for analysing production processes and product specification. The aim of the optimization process is to reduce the risk priority number.

The Six Sigma method was developed in the communications industry and uses statistical process controls to improve production. The objective of this method is to reduce process failure below a specific value.

1.6   **FACTORS AFFECTING DATA QUALITY**

The life history of instruments in field service involves different phases, such as planning according to user requirements, selection and installation of equipment, operation, calibration, maintenance and training activities. To obtain data of adequate or prescribed quality, appropriate actions must be taken at each of these phases. Factors affecting data quality are summarized in this section, and reference is made to more comprehensive information available in other chapters of this Guide and in other WMO Manuals and Guides.

User requirements: The quality of a measuring system can be assessed by comparing user requirements with the ability of the systems to fulfil them. The compatibility of user data-quality requirements with instrumental performance must be considered not only at the design and planning phase of a project, but also continually during operation, and implementation must be planned to optimize cost/benefit and cost/performance ratios. This involves a shared responsibility between users, instrument experts and logistic experts to match technical and financial factors. In particular, instrument experts must study the data quality requirements of the users to be able to propose specifications within the technical state of the art. This important phase of design is called value analysis. If it is neglected, as is often the case, it is likely that the cost or quality requirements, or both, will not be satisfied, possibly to such an extent that the project will fail and efforts will have been wasted.

Functional and technical specifications: The translation of expressed requirements into functional specifications and then into technical specifications is a very important and complex task, which requires a sound knowledge of user requirements, meteorological measuring technology, methods of observation, WMO regulations, and relevant operational conditions and technical/administrative infrastructures. Because the specifications will determine the general functioning of a planned measuring system, their impact on data quality is considerable.

Selection of instruments: Instruments should be carefully selected considering the required uncertainty, range and resolution (for definitions see Part I, Chapter 1), the climatological and environmental conditions implied by the users' applications, the working conditions, and the available technical infrastructure for training, installation and maintenance. An inappropriate selection of instruments may yield poor quality data that may not be anticipated, causing many difficulties when they are subsequently discovered. An example of this is an underspecification resulting in excessive wear or drift. In general, only high quality instruments should be employed for meteorological purposes. Reference should be made to the relevant information given in the various chapters in this Guide. Further information on the performance of several instruments can be found in the reports of WMO international instrument intercomparisons and in the proceedings of WMO/CIMO and other international conferences on instruments and methods of observation.

Acceptance tests: Before installation and acceptance, it is necessary to ensure that the instruments fulfil the original specifications. The performance of instruments, and their sensitivity to influence factors, should be published by manufacturers and are sometimes certified by calibration authorities. However, WMO instrument intercomparisons show that instruments may still be degraded by factors affecting their quality which may appear during the production and transportation phases. Calibration errors are difficult or impossible to detect when adequate standards and appropriate test and calibration facilities are not readily available. It is an essential component of good management to carry out appropriate tests under operational conditions before instruments are used for operational purposes. These tests can be applied both to determine the characteristics of a given model and to control the effective quality of each instrument.

When purchasing equipment, consideration should be given to requiring the supplier to set up certified quality assurance procedures within its organization according to the requirements of the NMHS, thus reducing the need for acceptance testing by the recipient. The extra cost when purchasing equipment may be justified by consequent lower costs for internal testing or operational maintenance, or by the assured quality of subsequent field operations.

Compatibility: Data compatibility problems can arise when instruments with different technical characteristics are used for taking the same types of measurements. This can happen, for example, when changing from manual to automated measurements, when adding new instruments of different time-constants, when using different sensor shielding, when applying different data reduction algorithms, and so on. The effects on data compatibility and homogeneity should be carefully investigated by long-term intercomparisons. Reference should be made to the various WMO reports on international instrument intercomparisons.

Siting and exposure: The density of meteorological stations depends on the timescale and space scale of the meteorological phenomena to be observed and is generally specified by the users, or set by WMO regulations. Experimental evidence exists showing that improper local siting and exposure can cause a serious deterioration in the accuracy and representativeness of measurements. General siting and exposure criteria are given in Part I, Chapter 1, and detailed information appropriate to specific instruments is given in the various chapters of Part I. Further reference should be made to the regulations in WMO (2010*c*). Attention should also be paid to external factors that can introduce errors, such as dust, pollution, frost, salt, large ambient temperature extremes or vandalism.

Instrumental errors: A proper selection of instruments is a necessary, but not sufficient, condition for obtaining good-quality data. No measuring technique is perfect, and all instruments produce various systematic and random errors. Their impact on data quality should be reduced to an acceptable level by appropriate preventive and corrective actions. These errors depend on the type of observation; they are discussed in the relevant chapters of this Guide (see Part I).

Data acquisition: Data quality is not only a function of the quality of the instruments and their correct siting and exposure, but also depends on the techniques and methods used to obtain data and to convert them into representative data. A distinction should be made between automated measurements and human observations. Depending on the technical characteristics of a sensor, in particular its time constant, proper sampling and averaging procedures must be applied. Unwanted sources of external electrical interference and noise can degrade the quality of the sensor output and should be eliminated by proper sensor-signal conditioning before entering the data-acquisition system. Reference should be made to sampling and filtering in Part II, Chapter 1 and in Part II, Chapter 2. In the case of manual instrument readings, errors may arise from the design, settings or resolution of the instrument, or from the inadequate training of the observer. For visual or subjective observations, errors can occur through an inexperienced observer misinterpreting the meteorological phenomena.

Data processing: Errors may also be introduced by the conversion techniques or computational procedures applied to convert the sensor data into Level II or Level III data. Examples of this are the calculation of humidity values from measured relative humidity or dewpoint and the reduction of pressure to mean sea level. Errors also occur during the coding or transcription of meteorological messages, in particular if performed by an observer.

Real-time quality control: Data quality depends on the real-time quality-control procedures applied during data acquisition and processing and during the preparation of messages, in order to eliminate the main sources of errors. These procedures are specific to each type of measurement but generally include gross checks for plausible values, rates of change and comparisons with other measurements (for example, dewpoint cannot exceed temperature). Special checks concern manually entered observations and meteorological messages. In AWSs, special built-in test equipment and software can detect specific hardware errors. The application of these procedures is most important since some errors introduced during the measuring process cannot be eliminated later. For an overview of manual and automatic methods in use, refer to other paragraphs of this chapter as well as to Part II, Chapter 1 and WMO (1993*a*, 2010*a*, 2010*b*, 2010*c*).

Performance monitoring: As real-time quality-control procedures have their limitations and some errors can remain undetected, such as long-term drifts in sensors and errors in data transmission, performance monitoring at the network level is required at meteorological analysis centres and by network managers. This monitoring is described in section 1.8 of this chapter. Information

can also be found in Part II, Chapter 1 and in WMO (2010*a*). It is important to establish effective liaison procedures between those responsible for monitoring and for maintenance and calibration, to facilitate rapid response to fault or failure reports from the monitoring system.

Testing and calibration: During their operation, the performance and instrumental characteristics of meteorological instruments change for reasons such as the ageing of hardware components, degraded maintenance, exposure, and so forth. These may cause long-term drifts or sudden changes in calibration. Consequently, instruments need regular inspection and calibration to provide reliable data. This requires the availability of standards and of appropriate calibration and test facilities. It also requires an efficient calibration plan and calibration housekeeping. See Part IV, Chapter 4 for general information about test and calibration aspects and to the relevant chapters of Part I for individual instruments.

Maintenance: Maintenance can be corrective (when parts fail), preventive (such as cleaning or lubrication) or adaptive (in response to changed requirements or obsolescence). The quality of the data provided by an instrument is considerably affected by the quality of its maintenance, which in turn depends mainly on the ability of maintenance personnel and the maintenance concept. The capabilities, personnel and equipment of the organization or unit responsible for maintenance must be adequate for the instruments and networks. Several factors have to be considered, such as a maintenance plan, which includes corrective, preventive and adaptive maintenance, logistic management, and the repair, test and support facilities. It must be noted that the maintenance costs of equipment can greatly exceed its purchase costs (see Part II, Chapter 1).

Training and education: Data quality also depends on the skills of the technical staff in charge of testing, calibration and maintenance activities, and of the observers making the observations. Training and education programmes should be organized according to a rational plan geared towards meeting the needs of users, and especially the maintenance and calibration requirements outlined above, and should be adapted to the system; this is particularly important for AWSs. As part of the system procurement, the manufacturer should be obliged to provide very comprehensive operational and technical documentation and to organize operational and technical training courses (see Part IV, Chapter 5) in the NMHS.

Metadata: A sound quality assurance entails the availability of detailed information on the observing system itself and in particular on all changes that occur during the time of its operation. Such information on data, known as metadata, enables the operator of an observing system to take the most appropriate preventive, corrective and adaptive actions to maintain or enhance data quality. Metadata requirements are further considered in section 1.9. For further information on metadata, see Part I, Chapter 1 (and Annex 1.C).

1.7   QUALITY ASSURANCE (QUALITY CONTROL)

WMO (2010*c*) prescribes that certain quality-control procedures must be applied to all meteorological data to be exchanged internationally. Level I and Level II data, and the conversion from one to the other, must be subjected to quality control. WMO (2010*b*) prescribes that quality-control procedures must be applied by meteorological data processing centres to most kinds of weather reports exchanged internationally, to check for coding errors, internal consistency, time and space consistency, and physical and climatological limits, and it specifies the minimum frequency and times for quality control.

WMO (2010*a*) gives general guidance on procedures. It emphasizes the importance of quality control at the station, because some errors occurring there cannot be subsequently corrected, and also points out the great advantages of automation. WMO (1993*a*) gives rather detailed descriptions of the procedures that may be used by numerical analysis centres, with advice on climatological limits, types of internal consistency checks, comparisons with neighbouring stations and with analyses and prognoses, and provides brief comments on the probabilities of rejecting good data and accepting false data with known statistical distributions of errors.
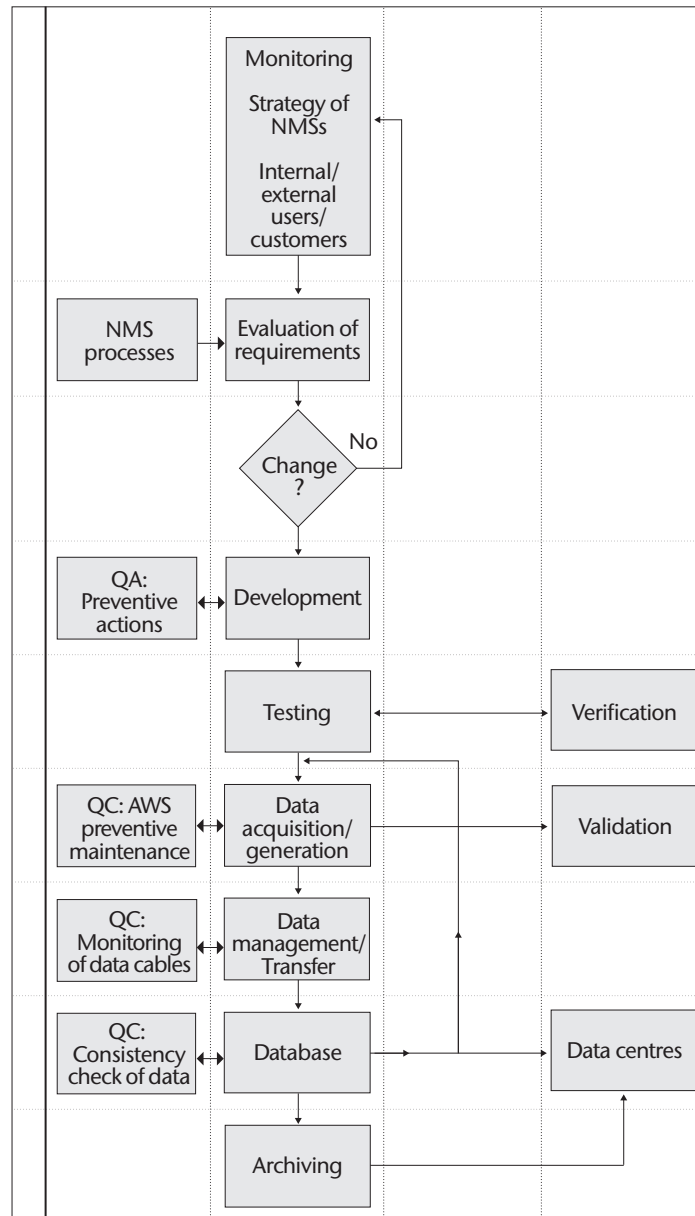
NMS: National Meteorological or Hydrological Service
QA: Quality assurance
QC: Quality control

Figure 1.5. Process for observation generation

Quality control, as specifically defined in section 1.1, is implemented in real time or near real time to data acquisition and processing. In practice, responsibility for quality control is assigned to various points along the data chain. These may be at the station, if there is direct manual involvement in data acquisition, or at the various centres where the data are processed.

Quality assurance procedures must be introduced and reassessed during the development phases of new sensors or observing systems (see Figure 1.5).

1.7.1   Surface data

1.7.1.1   *Manual observations and staffed stations*

The observer or the officer in charge at a station is expected to ensure that the data leaving the station have been quality controlled, and should be provided with established procedures for attending to this responsibility. This is a specific function, in addition to other maintenance and record-keeping functions, and includes the following:

(a)   Internal consistency checks of a complete synoptic or other compound observation: In practice, they are performed as a matter of course by an experienced observer, but they should nevertheless be an explicit requirement. Examples of this are the relations between the temperature, the dewpoint and the daily extremes, and between rain, cloud and weather;

(b)   Climatological checks: These for consistency: The observer knows, or is provided with charts or tables of, the normal seasonal ranges of variables at the station, and should not allow unusual values to go unchecked;

(c)   Temporal checks: These should be made to ensure that changes since the last observation are realistic, especially when the observations have been made by different observers;

(d)   Checks of all arithmetical and table look-up operations;

(e)   Checks of all messages and other records against the original data.

1.7.1.2   *Automatic weather stations*

At AWSs, some of the above checks should be performed by the software, as well as engineering checks on the performance of the system. These are discussed in Part II, Chapter 1.

1.7.2   Upper-air data

The procedures for controlling the quality of upper-air data are essentially the same as those for surface data. Checks should be made for internal consistency (such as lapse rates and shears), for climatological and temporal consistency, and for consistency with normal surface observations. For radiosonde operations, it is of the utmost importance that the baseline initial calibration be explicitly and deliberately checked. The message must also be checked against the observed data.

The automation of on-station quality control is particularly useful for upper-air data.

1.7.3   Data centres

Data should be checked in real time or as close to real time as possible, at the first and subsequent points where they are received or used. It is highly advisable to apply the same urgent checks to all data, even to those that are not used in real time, because later quality control tends to be less effective. If available, automation should of course be used, but certain quality-control procedures are possible without computers, or with only partial assistance by computing facilities. The principle is that every message should be checked, preferably at each stage of the complete data chain.

The checks that have already been performed at stations are usually repeated at data centres, perhaps in more elaborate form by making use of automation. Data centres, however, usually have access to other network data, thus making a spatial check possible against observations from surrounding stations or against analysed or predicted fields. This is a very powerful method and is the distinctive contribution of a data centre.

If errors are found, the data should be either rejected or corrected by reference back to the source, or should be corrected at the data centre by inference. The last of these alternatives may evidently introduce further errors, but it is nevertheless valid in many circumstances; data so corrected should be flagged in the database and should be used only carefully.

The quality-control process produces data of established quality, which may then be used for real-time operations and for a databank. However, a by-product of this process should be the compilation of information about the errors that were found. It is good practice to establish at the first or subsequent data-processing point a system for immediate feedback to the origin of the data if errors are found, and to compile a record for use by the network manager in performance monitoring, as discussed below. This function is best performed at the regional level, where there is ready access to the field stations.

The detailed procedures described in WMO (1993*a*) are a guide to controlling the quality control of data for international exchange, under the recommendations of WMO (2010*b*).

1.7.4 Interaction with field stations

If quality is to be maintained, it is absolutely essential that errors be tracked back to their source, with some kind of corrective action. For data from staffed stations this is very effectively done in near real time, not only because the data may be corrected, but also to identify the reason for the error and prevent it from recurring.

It is good practice to assign a person at a data centre or other operational centre with the responsibility for maintaining near-real-time communication and effective working relations with the field stations, to be used whenever errors in the data are identified.

1.8 PERFORMANCE MONITORING

The management of a network, or of a station, is greatly strengthened by keeping continuous records of performance, typically on a daily and monthly schedule. The objective of performance monitoring is to review continually the quality of field stations and of each observing system, such as for pressure measurement, or the radiosonde network.

There are several aspects to performance monitoring, as follows:

(a)   Advice from data centres should be used to record the numbers and types of errors detected by quality-control procedures;

(b)   Data from each station should be compiled into synoptic and time-section sets. Such sets should be used to identify systematic differences from neighbouring stations, both in spatial fields and in comparative time series. It is useful to derive statistics of the mean and the scatter of the differences. Graphical methods are effective for these purposes;

(c)   Reports should be obtained from field stations about equipment faults, or other aspects of performance.

These types of records are very effective in identifying systematic faults in performance and in indicating corrective action. They are powerful indicators of many factors that affect the data, such as exposure or calibration changes, deteriorating equipment, changes in the quality of consumables or the need for retraining. They are particularly important for maintaining confidence in automatic equipment.

The results of performance monitoring should be used for feedback to the field stations, which is important to maintain motivation. The results also indicate when action is necessary to repair or upgrade the field equipment.

Performance monitoring is a time-consuming task, to which the network manager must allocate adequate resources. WMO (1988) describes a system to monitor data from an AWS network, using a small, dedicated office with staff monitoring real-time output and advising the network managers and data users. Miller and Morone (1993) describe a system with similar functions, in near real time, making use of a mesoscale numerical model for the spatial and temporal tests on the data.

1.9 DATA HOMOGENEITY AND METADATA

In the past, observational networks were primarily built to support weather forecasting activities. Operational quality control was focused mainly on identifying outliers, but rarely incorporated checks for data homogeneity and continuity of time series. The surge of interest in climate change, primarily as a result of concerns over increases in greenhouse gases, changed this situation. Data homogeneity tests have revealed that many of the apparent climate changes can be attributed to inhomogeneities in time series caused only by operational changes in observing systems. This section attempts to summarize these causes and presents some guidelines concerning the necessary information on data, namely, metadata, which should be made available to support data homogeneity and climate change investigations.

1.9.1 Causes of data inhomogeneities

Inhomogeneities caused by changes in the observing system appear as abrupt discontinuities, gradual changes, or changes in variability. Abrupt discontinuities mostly occur due to changes in instrumentation, siting and exposure changes, station relocation, changes in the calculation of averages, data reduction procedures and the application of new calibration corrections. Inhomogeneities that occur as a gradually increasing effect may arise from a change in the surroundings of the station, urbanization and gradual changes in instrumental characteristics. Changes in variability are caused by instrument malfunctions. Inhomogeneities are further due to changes in the time of observations, insufficient routine inspection, maintenance and calibration, and unsatisfactory observing procedures. On a network level, inhomogeneities can be caused by data incompatibilities. It is obvious that all factors affecting data quality also cause data inhomogeneities.

The historical survey of changes in radiosondes (WMO, 1993b) illustrates the seriousness of the problem and is a good example of the careful work that is necessary to eliminate it.

Changes in the surface-temperature record when manual stations are replaced by AWSs, and changes in the upper-air records when radiosondes are changed, are particularly significant cases of data inhomogeneities. These two cases are now well recognized and can, in principle, be anticipated and corrected, but performance monitoring can be used to confirm the effectiveness of corrections, or even to derive them.

1.9.2 Metadata

Data inhomogeneities should, as far as possible, be prevented by appropriate quality-assurance procedures with respect to quality control. However, this cannot always be accomplished as some causes of inhomogeneities, such as the replacement of a sensor, can represent real improvements in measuring techniques. It is important to have information on the occurrence, type and, especially, the time of all inhomogeneities that occur. After obtaining such information, climatologists can run appropriate statistical programs to link the previous data with the new data in homogeneous databases with a high degree of confidence. Information of this kind is commonly available in what is known as metadata — information on data — also called station histories. Without such information, many of the above-mentioned inhomogeneities may not be identified or corrected. Metadata can be considered as an extended version of the station administrative record, containing all possible information on the initial set-up, and type and times of changes that occurred during the life history of an observing system. As computer

data management systems are an important aspect of quality data delivery, it is desirable that metadata should be available as a computer database enabling computerized composition, updating and use.

1.9.3 Elements of a metadata database

A metadata database contains initial set-up information together with updates whenever changes occur. Major elements include the following:

(a) Network information:

   (i) The operating authority, and the type and purpose of the network;

(b) Station information:

   (i) Administrative information;

   (ii) Location: geographical coordinates, elevation(s);[3]

   (iii) Descriptions of remote and immediate surroundings and obstacles;[3]

   (iv) Instrument layout;[3]

   (v) Facilities: data transmission, power supply, cabling;

   (vi) Climatological description;

(c) Individual instrument information:

   (i) Type: manufacturer, model, serial number, operating principles;

   (ii) Performance characteristics;

   (iii) Calibration data and time;

   (iv) Siting and exposure: location, shielding, height above ground;[3]

   (v) Measuring or observing programme;

   (vi) Times of observations;

   (vii) Observer;

   (viii) Data acquisition: sampling, averaging;

   (ix) Data-processing methods and algorithms;

   (x) Preventive and corrective maintenance;

   (xi) Data quality (in the form of a flag or uncertainty).

1.9.4 Recommendations for a metadata system

The development of a metadata system requires considerable interdisciplinary organization, and its operation, particularly the scrupulous and accurately dated record of changes in the metadata base, requires constant attention.

---

[3] It is necessary to include maps and plans on appropriate scales.

A useful survey of requirements is given in WMO (1994), with examples of the effects of changes in observing operations and an explanation of the advantages of good metadata for obtaining a reliable climate record from discontinuous data. The basic functional elements of a system for maintaining a metadata database may be summarized as follows:

(a) Standard procedures must be established for collecting overlapping measurements for all significant changes made in instrumentation, observing practices and sensor siting;

(b) Routine assessments must be made of ongoing calibration, maintenance, and homogeneity problems for the purpose of taking corrective action, when necessary;

(c) There must be open communication between the data collector and the researcher to provide feedback mechanisms for recognizing data problems, the correction or at least the potential for problems, and the improvement of, or addition to, documentation to meet initially unforeseen user requirements (for example, work groups);

(d) There must be detailed and readily available documentation on the procedures, rationale, testing, assumptions and known problems involved in the construction of the dataset from the measurements.

These four recommendations would have the effect of providing a data user with enough metadata to enable manipulation, amalgamation and summarization of the data with minimal assumptions regarding data quality and homogeneity.

1.10 NETWORK MANAGEMENT

All the factors affecting data quality described in section 1.6 are the subject of network management. In particular, network management must include corrective action in response to the network performance revealed by quality-control procedures and performance monitoring.

Networks are defined in WMO (2010c), and guidance on network management in general terms is given in WMO (2010a), including the structure and functions of a network management unit. Network management practices vary widely according to locally established administrative arrangements.

It is highly desirable to identify a particular person or office as the network manager to whom operational responsibility is assigned for the impact of the various factors on data quality. Other specialists who may be responsible for the management and implementation of some of these factors must collaborate with the network manager and accept responsibility for their effect on data quality.

The manager should keep under review the procedures and outcomes associated with all of the factors affecting quality, as discussed in section 1.6, including the following considerations:

(a) The quality-control systems described in section 1.1 are operationally essential in any meteorological network and should receive priority attention by the data users and by the network management;

(b) Performance monitoring is commonly accepted as a network management function. It may be expected to indicate the need for action on the effects of exposure, calibration and maintenance. It also provides information on the effects of some of the other factors;

(c) Field station inspection described below, is a network management function;

(d) Equipment maintenance may be a direct function of the network management unit. If not, there should be particularly effective collaboration between the network manager and the office responsible for the equipment;

(e)   The administrative arrangements should enable the network manager to take, or arrange for, corrective action arising from quality-control procedures, performance monitoring, the inspection programme, or any other factor affecting quality. One of the most important other factors is observer training, as described in Part IV, Chapter 5, and the network manager should be able to influence the content and conduct of courses and how they are conducted or the prescribed training requirements.

1.10.1 Inspections

Field stations should be inspected regularly, preferably by specially appointed, experienced inspectors. The objectives are to examine and maintain the work of the observers, the equipment and instrument exposure, and also to enhance the value of the data by recording the station history. At the same time, various administrative functions, which are particularly important for staffed stations, can be performed. The same principles apply to staffed stations, stations operated by part-time, voluntary or contract observers and, to a certain degree, to AWSs. Requirements for inspections are laid down in WMO (2010c), and advice is given in WMO (2010a).

Inspections reports are part of the performance monitoring record.

It is highly advisable to have a systematic and exhaustive procedure fully documented in the form of inspections and maintenance handbooks, to be used by the visiting inspectors. Procedures should include the details of subsequent reporting and follow-up.

The inspector should attend, in particular, to the following aspects of station operations:

(a)   *Instrument performance*: Instruments requiring calibration must be checked against a suitable standard. Atmospheric pressure is the prime case, as all field barometers can drift to some degree. Mechanical and electrical recording systems must be checked according to established procedures. More complex equipment such as AWSs and radars need various physical and electrical checks. Anemometers and thermometer shelters are particularly prone to deterioration of various kinds, which may vitiate the data. The physical condition of all equipment should be examined for dirt, corrosion and so on;

(b)   *Observing methods*: Bad practice can easily occur in observing procedures, and the work of all observers should be continually reviewed. Uniformity in methods recording and coding is essential for synoptic and climatological use of the data;

(c)   *Exposure*: Any changes in the surroundings of the station must be documented and corrected in due course, if practicable. Relocation may be necessary.

Inspections of manual stations also serve the purpose of maintaining the interest and enthusiasm of the observers. The inspector must be tactful, informative, enthusiastic and able to obtain willing cooperation.

A prepared form for recording the inspection should be completed for every inspection. It should include a checklist on the condition and installation of the equipment and on the ability and competence of the observers. The inspection form may also be used for other administrative purposes, such as an inventory.

It is most important that all changes identified during the inspection should be permanently recorded and dated so that a station history can be compiled for subsequent use for climate studies and other purposes.

An optimum frequency of inspection visits cannot be generally specified, even for one particular type of station. It depends on the quality of the observers and equipment, the rate at which the equipment and exposure deteriorates, and changes in the station staff and facilities.

An inspection interval of two years may be acceptable for a well-established station, and six months may be appropriate for automatic stations. Some kinds of stations will have special inspection requirements.

Some equipment maintenance may be performed by the inspector or by the inspection team, depending on the skills available. In general, there should be an equipment maintenance programme, as is the case for inspections. This is not discussed here because the requirements and possible organizations are very diverse.

———————————

REFERENCES AND FURTHER READING

Deming, W.E., 1986: *Out of the Crisis: Quality, Productivity and Competitive Position*. University of Cambridge Press, Cambridge.

International Organization for Standardization, 2005: *Quality Management Systems – Fundamentals and Vocabulary*, ISO 9000:2005. Geneva.

———, 2008: *Quality Management Systems – Requirements*, ISO 9001:2008. Geneva.

———, 2009: *Managing for the Sustained Success of an Organization – A Quality Management Approach*, ISO 9004:2009. Geneva.

———, 2011: *Guidelines for Auditing Management Systems*, ISO 19011:2011. Geneva.

International Organization for Standardization/International Electrotechnical Commission, 2005: *General Requirements for the Competence of Testing and Calibration Laboratories*, ISO/IEC 17025:2005. Geneva.

———, 2011: *Information Technology – Service Management – Part 1: Service Management System Requirements*, ISO/IEC 20000-1:2011. Geneva.

———, 2012: *Information Technology – Service Management – Part 2: Guidance on the Application of Service Management Systems*, ISO/IEC 20000-2:2012. Geneva.

Kaplan, R.S. and D.P. Norton, 1996: *The Balanced Scorecard: Translating Strategy into Action*. Harvard Business School Press, Boston.

Miller, P.A. and L.L. Morone, 1993: Real time quality control of hourly reports from the automated surface observing system. *Preprints of the Eighth Symposium on Meteorological Observations and Instrumentation*. American Meteorological Society, Boston, pp. 373-378.

World Meteorological Organization, 1988: Practical experience of the operation of quality evaluation programmes for automated surface observations both on land and over the sea (M. Field and J. Nash). *Papers Presented at the WMO Technical Conference on Instruments and Methods of Observation (TECO-1988)*. Instruments and Observing Methods Report No. 33 (WMO/TD-No. 222). Geneva.

———, 1993*a*: *Guide on the Global Data-Processing System* (WMO-No. 305). Geneva.

———, 1993*b*: *Historical Changes in Radiosonde Instruments and Practices* (D.J. Gaffen). Instruments and Observing Methods Report No. 50 (WMO/TD-No. 541). Geneva.

———, 1994: Homogeneity of data and the climate record (K.D. Hadeen and N.B. Guttman). *Papers Presented at the WMO Technical Conference on Instruments and Methods of Observation (TECO-94)*. Instruments and Observing Methods Report No. 57 (WMO/TD-No. 588). Geneva.

———, 2005*a*: *WMO Quality Management Framework (QMF)*. First WMO Technical Report (revised edition), (WMO/TD-No. 1268). Geneva.

———, 2005*b*: *Guidelines on Quality Management Procedures and Practices for Public Weather Services*. PWS-11 (WMO/TD-No. 1256). Geneva.

———, 2010*a*: *Guide to the Global Observing System* (WMO-No. 488). Geneva.

———, 2010*b*: *Manual on the Global Data-processing and Forecasting System* (WMO-No. 485), Volume I. Geneva.

———, 2010*c*: *Manual on the Global Observing System* (WMO-No. 544), Volume I. Geneva.

———————

CHAPTER CONTENTS

CHAPTER 2. SAMPLING METEOROLOGICAL VARIABLES

2.1   GENERAL

The purpose of this chapter is to give an introduction to this complex subject, for non-experts who need enough knowledge to develop a general understanding of the issues and to acquire a perspective of the importance of the techniques.

Atmospheric variables such as wind speed, temperature, pressure and humidity are functions of four dimensions – two horizontal, one vertical, and one temporal. They vary irregularly in all four, and the purpose of the study of sampling is to define practical measurement procedures to obtain representative observations with acceptable uncertainties in the estimations of mean and variability.

Discussion of sampling in the horizontal dimensions includes the topic of areal representativeness, which is discussed in Part I, Chapter 1, in other chapters on measurements of particular quantities, and briefly below. It also includes the topics of network design, which is a special study related to numerical analysis, and of measurements of area-integrated quantities using radar and satellites; neither of these is discussed here. Sampling in the vertical is briefly discussed in Part I, Chapters 12 and 13 and Part II, Chapter 5. This chapter is therefore concerned only with sampling in time, except for some general comments about representativeness.

The topic can be addressed at two levels as follows:

(a)   At an elementary level, the basic meteorological problem of obtaining a mean value of a fluctuating quantity representative of a stated sampling interval at a given time, using instrument systems with long response times compared with the fluctuations, can be discussed. At the simplest level, this involves consideration of the statistics of a set of measurements, and of the response time of instruments and electronic circuits;

(b)   The problem can be considered more precisely by making use of the theory of time-series analysis, the concept of the spectrum of fluctuations, and the behaviour of filters. These topics are necessary for the more complex problem of using relatively fast-response instruments to obtain satisfactory measurements of the mean or the spectrum of a rapidly varying quantity, wind being the prime example.

It is therefore convenient to begin with a discussion of time series, spectra and filters in sections 2.2 and 2.3. Section 2.4 gives practical advice on sampling. The discussion here, for the most part, assumes digital techniques and automatic processing.

It is important to recognize that an atmospheric variable is actually never sampled. It is only possible to come as close as possible to sampling the output of a sensor of that variable. The distinction is important because sensors do not create an exact analogue of the sensed variable. In general, sensors respond more slowly than the atmosphere changes, and they add noise. Sensors also do other, usually undesirable, things such as drift in calibration, respond non-linearly, interfere with the quantity that they are measuring, fail more often than intended, and so on, but this discussion will only be concerned with response and the addition of noise.

There are many textbooks available to give the necessary background for the design of sampling systems or the study of sampled data. See, for example, Bendat and Piersol (1986) or Otnes and Enochson (1978). Other useful texts include Pasquill and Smith (1983), Stearns and Hush (1990), Kulhánek (1976), and Jenkins and Watts (1968).

2.1.1   Definitions

For the purposes of this chapter the following definitions are used:

Sampling is the process of obtaining a discrete sequence of measurements of a quantity.

A *sample* is a single measurement, typically one of a series of spot readings of a sensor system. Note that this differs from the usual meaning in statistics of a set of numbers or measurements which is part of a population.

An *observation* is the result of the sampling process, being the quantity reported or recorded (often also called a measurement). In the context of time-series analysis, an observation is derived from a number of samples.

The ISO definition of a *measurement* is a "set of operations having the object of determining the value of a quantity". In common usage, the term may be used to mean the value of either a sample or an observation.

The *sampling time* or *observation period* is the length of the time over which one observation is made, during which a number of individual samples are taken.

The *sampling interval* is the time between successive observations.

The *sampling function* or *weighting function* is, in its simplest definition, an algorithm for averaging or filtering the individual samples.

The *sampling frequency* is the frequency at which samples are taken. The *sample spacing* is the time between samples.

Smoothing is the process of attenuating the high frequency components of the spectrum without significantly affecting the lower frequencies. This is usually done to remove noise (random errors and fluctuations not relevant for the application).

A *filter* is a device for attenuating or selecting any chosen frequencies. Smoothing is performed by a *low-pass* filter, and the terms *smoothing* and *filtering* are often used interchangeably in this sense. However, there are also *high-pass* and *band-pass* filters. Filtering may be a property of the instrument, such as inertia, or it may be performed electronically or numerically.

2.1.2   Representativeness in time and space

Sampled observations are made at a limited rate and for a limited time interval over a limited area. In practice, observations should be designed to be sufficiently frequent to be representative of the unsampled parts of the (continuous) variable, and are often taken as being representative of a longer time interval and larger area.

The user of an observation expects it to be representative, or typical, of an area and time, and of an interval of time. This area, for example, may be "the airport" or that area within a radius of several kilometres and within easy view of a human observer. The time is the time at which the report was made or the message transmitted, and the interval is an agreed quantity, often 1, 2 or 10 min.

To make observations representative, sensors are exposed at standard heights and at unobstructed locations and samples are processed to obtain mean values. In a few cases, sensors, for example transmissometers, inherently average spatially, and this contributes to the representativeness of the observation. The human observation of visibility is another example of this. However, the remaining discussion in this chapter will ignore spatial sampling and concentrate upon time sampling of measurements taken at a point.

A typical example of sampling and time averaging is the measurement of temperature each minute (the samples), the computation of a 10 min average (the sampling interval and the sampling function), and the transmission of this average (the observation) in a synoptic report every 3 h. When these observations are collected over a period from the same site, they themselves become samples in a new time sequence with a 3 h spacing. When collected from a large number of sites, these observations also become samples in a spatial sequence. In this sense, representative observations are also representative samples. In this chapter we discuss the initial observation.

2.1.3   **The spectra of atmospheric quantities**

By applying the mathematical operation known as the Fourier transform, an irregular function of time (or distance) can be reduced to its spectrum, which is the sum of a large number of sinusoids, each with its own amplitude, wavelength (or period or frequency) and phase. In broad contexts, these wavelengths (or frequencies) define "scales" or "scales of motion" of the atmosphere.

The range of these scales is limited in the atmosphere. At one end of the spectrum, horizontal scales cannot exceed the circumference of the Earth or about 40 000 km. For meteorological purposes, vertical scales do not exceed a few tens of kilometres. In the time dimension, however, the longest scales are climatological and, in principle, unbounded, but in practice the longest period does not exceed the length of records. At the short end, the viscous dissipation of turbulent energy into heat sets a lower bound. Close to the surface of the Earth, this bound is at a wavelength of a few centimetres and increases with height to a few metres in the stratosphere. In the time dimension, these wavelengths correspond to frequencies of tens of hertz. It is correct to say that atmospheric variables are bandwidth limited.

Figure 2.1 is a schematic representation of a spectrum of a meteorological quantity such as wind, notionally measured at a particular station and time. The ordinate, commonly called energy or spectral density, is related to the variance of the fluctuations of wind at each frequency n. The spectrum in Figure 2.1 has a minimum of energy at the mesoscale around one cycle per hour, between peaks in the synoptic scale around one cycle per four days, and in the microscale around one cycle per minute. The smallest wavelengths are a few centimetres and the largest frequencies are tens of hertz.
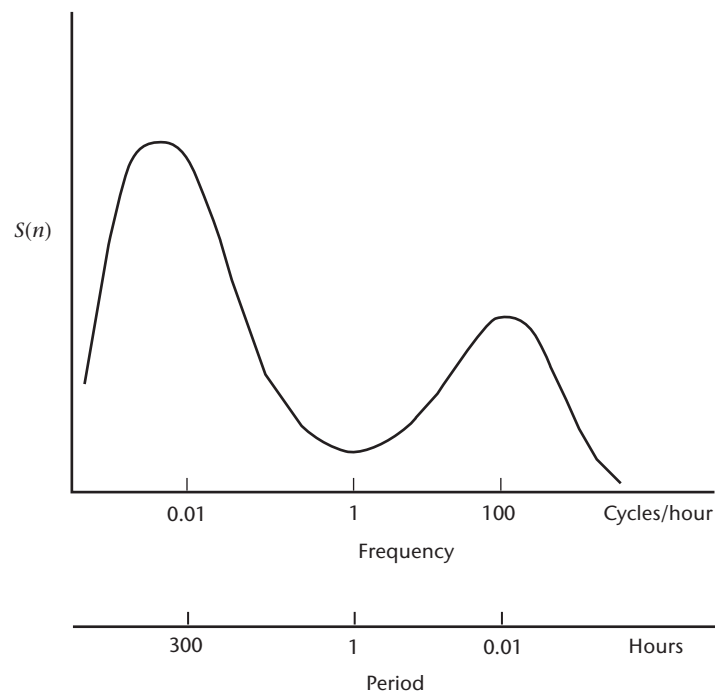

Figure 2.1. A typical spectrum of a meteorological quantity

2.2 TIME SERIES, POWER SPECTRA AND FILTERS

This section is a layperson's introduction to the concepts of time-series analysis which are the basis for good practice in sampling. In the context of this Guide, they are particularly important for the measurement of wind, but the same problems arise for temperature, pressure and other quantities. They became important for routine meteorological measurements when automatic measurements were introduced, because frequent fast sampling then became possible. Serious errors can occur in the estimates of the mean, the extremes and the spectrum if systems are not designed correctly.

Although measurements of spectra are non-routine, they have many applications. The spectrum of wind is important in engineering, atmospheric dispersion, diffusion and dynamics. The concepts discussed here are also used for quantitative analysis of satellite data (in the horizontal space dimension) and in climatology and micro-meteorology.

In summary, the argument is as follows:

(a)   An optimum sampling rate can be assessed from consideration of the variability of the quantity being measured. Estimates of the mean and other statistics of the observations will have smaller uncertainties with higher sampling frequencies, namely, larger samples;

(b)   The Nyquist theorem states that a continuous fluctuating quantity can be precisely determined by a series of equispaced samples if they are sufficiently close together;

(c)   If the sampling frequency is too low, fluctuations at the higher unsampled frequencies (above the Nyquist frequency, defined in section 2.2.1) will affect the estimate of the mean value. They will also affect the computation of the lower frequencies, and the measured spectrum will be incorrect. This is known as aliasing. It can cause serious errors if it is not understood and allowed for in the system design;

(d)   Aliasing may be avoided by using a high sampling frequency or by filtering so that a lower, more convenient sampling frequency can be used;

(e)   Filters may be digital or analogue. A sensor with a suitably long response time acts as a filter.

A full understanding of sampling involves knowledge of power spectra, the Nyquist theorem, filtering and instrument response. This is a highly specialized subject, requiring understanding of the characteristics of the sensors used, the way the output of the sensors is conditioned, processed and logged, the physical properties of the elements being measured, and the purpose to which the analysed data are to be put. This, in turn, may require expertise in the physics of the instruments, the theory of electronic or other systems used in conditioning and logging processes, mathematics, statistics and the meteorology of the phenomena, all of which are well beyond the scope of this chapter.

However, it is possible for a non-expert to understand the principles of good practice in measuring means and extremes, and to appreciate the problems associated with measurements of spectra.

2.2.1   Time-series analysis

It is necessary to consider signals as being either in the time or the frequency domain. The fundamental idea behind spectral analysis is the concept of Fourier transforms. A function, $f(t)$, defined between $t = 0$ and $t = \tau$ can be transformed into the sum of a set of sinusoidal functions:

$$f(t) = \sum_{j=0}^{\infty} \left[A_j \sin(j\omega t) + B_j \cos(j\omega t) \right] \tag{2.1}$$

where $\omega = 2\pi/\tau$. The right-hand side of the equation is a Fourier series. A_j and B_j are the amplitudes of the contributions of the components at frequencies $n_j = j\omega$. This is the basic

transformation between the time and frequency domains. The Fourier coefficients A_j and B_j relate directly to the frequency $j\omega$ and can be associated with the spectral contributions to $f(t)$ at these frequencies. If the frequency response of an instrument is known – that is, the way in which it amplifies or attenuates certain frequencies – and if it is also known how these frequencies contribute to the original signal, the effect of the frequency response on the output signal can be calculated. The contribution of each frequency is characterized by two parameters. These can be most conveniently taken as the amplitude and phase of the frequency component. Thus, if equation 2.1 is expressed in its alternative form:

$$f\left(t\right) = \sum_{j=0}^{\infty} \alpha_j \sin\left(j\omega t + \phi_j\right) \tag{2.2}$$

the amplitude and phase associated with each spectral contribution are α_j and ϕ_j. Both can be affected in sampling and processing.

So far, it has been assumed that the function $f(t)$ is known continuously throughout its range $t = 0$ to $t = \tau$. In fact, in most examples this is not the case; the meteorological variable is measured at discrete points in a time series, which is a series of N samples equally spaced Δt apart during a specified period $\tau = (N–1)\Delta t$. The samples are assumed to be taken instantaneously, an assumption which is strictly not true, as all measuring devices require some time to determine the value they are measuring. In most cases, this is short compared with the sample spacing Δt. Even if it is not, the response time of the measuring system can be accommodated in the analysis, although that will not be addressed here.

When considering the data that would be obtained by sampling a sinusoidal function at times Δt apart, it can be seen that the highest frequency that can be detected is $1/(2\Delta t)$, and that in fact any higher frequency sinusoid that may be present in the time series is represented in the data as having a lower frequency. The frequency $1/(2\Delta t)$ is called the Nyquist frequency, designated here as n_y. The Nyquist frequency is sometimes called the folding frequency. This terminology comes from consideration of aliasing of the data. The concept is shown schematically in Figure 2.2. When a spectral analysis of a time series is made, because of the discrete nature of the data, the contribution to the estimate at frequency n also contains contributions from higher frequencies, namely from $2jn_y \pm n$ ($j = 1$ to ∞). One way of visualizing this is to consider the frequency domain as if it were folded, in a concertina-like way, at $n = 0$ and $n = n_y$ and so on in steps of n_y. The spectral estimate at each frequency in the range is the sum of all the contributions of those higher frequencies that overlie it.

The practical effects of aliasing are discussed in section 2.4.2. It is potentially a serious problem and should be considered when designing instrument systems. It can be avoided by minimizing, or reducing to zero, the strength of the signal at frequencies above n_y. There are a couple of ways of achieving this. First, the system can contain a low-pass filter that attenuates contributions at frequencies higher than n_y before the signal is digitized. The only disadvantage of this approach is that the timing and magnitude of rapid changes will not be recorded well, or even at all. The second approach is to have Δt small enough so that the contributions above the Nyquist frequency are insignificant. This is possible because the spectra of most meteorological variables fall off very rapidly at very high frequencies. This second approach will, however, not always be practicable, as in the example of three-hourly temperature measurements, where if Δt is of the order of hours, small scale fluctuations, of the order of minutes or seconds, may have relatively large spectral ordinates and alias strongly. In this case, the first method may be appropriate.

2.2.2   **Measurement of spectra**

The spectral density, at least as it is estimated from a time series, is defined as:

$$S\left(n_j\right) = \left(A_j^2 + B_j^2\right)\Big/n_y = \alpha_j^2\Big/n_y \tag{2.3}$$

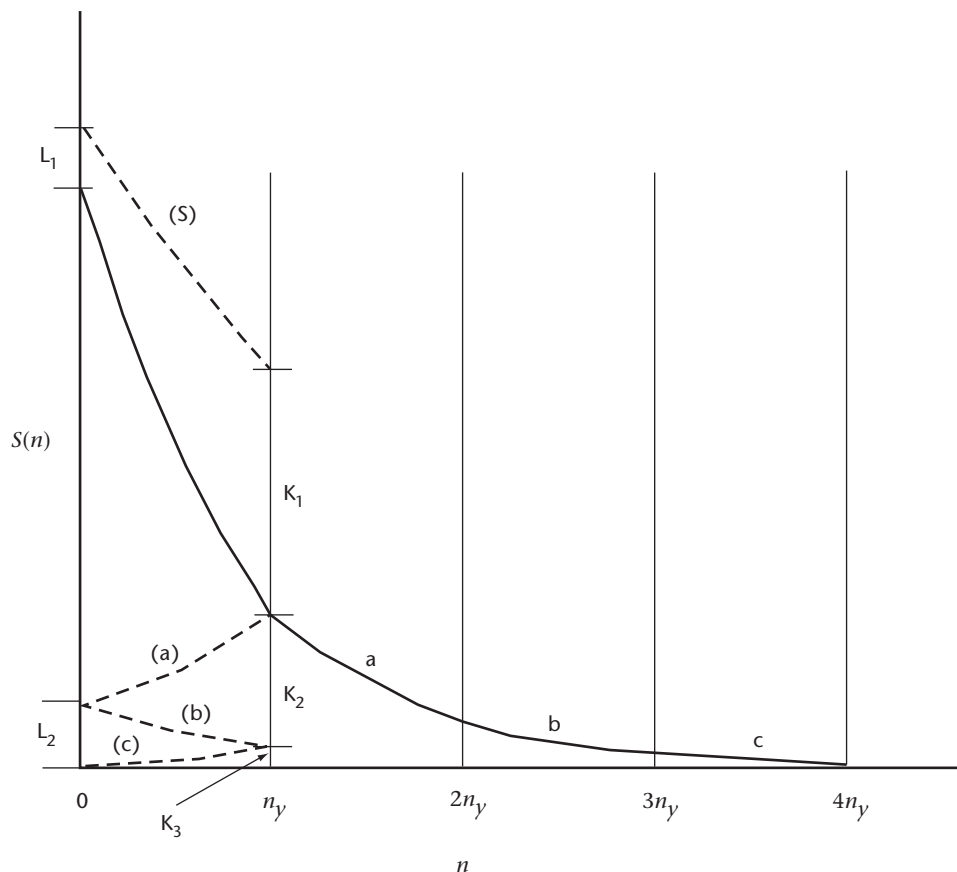It will be noted that phase is not relevant in this case.

Figure 2.2. A schematic illustration of aliasing a spectrum computed from a stationary time-series. The spectrum can be calculated only over the frequency range zero to the Nyquist frequency n_y. The true values of the energies at higher frequencies are shown by the sectors marked a, b and c. These are "folded" back to the $n = 0$ to n_y sector as shown by the broken lines (a), (b), (c). The computed spectrum, shown by the bold broken line (S), includes the sum of these.

The spectrum of a fluctuating quantity can be measured in a number of ways. In electrical engineering it was often determined in the past by passing the signal through band-pass filters and by measuring the power output. This was then related to the power of the central frequency of the filter.

There are a number of ways of approaching the numerical spectral analysis of a time series. The most obvious is a direct Fourier transform of the time series. In this case, as the series is only of finite length, there will be only a finite number of frequency components in the transformation. If there are N terms in the time series, there will be $N/2$ frequencies resulting from this analysis. A direct calculation is very laborious, and other methods have been developed. The first development was by Blackman and Tukey (1958), who related the auto-correlation function to estimates of various spectral functions. (The auto-correlation function $r(t)$ is the correlation coefficient calculated between terms in the time series separated by a time interval t). This was appropriate for the low-powered computing facilities of the 1950s and 1960s, but it has now been generally superseded by the so-called fast Fourier transform (FFT), which takes advantage of the general properties of a digital computer to greatly accelerate the calculations. The main limitation of the method is that the time series must contain 2^k terms, where k is an integer. In general, this is not a serious problem, as in most instances there are sufficient data to conveniently organize the series to such a length. Alternatively, some FFT computer programs can use an arbitrary number of terms and add synthetic data to make them up to 2^k.

As the time series is of finite duration (N terms), it represents only a sample of the signal of interest. Thus, the Fourier coefficients are only an estimate of the true, or population, value.

To improve reliability, it is common practice to average a number of terms each side of a particular frequency and to assign this average to the value of that frequency. The confidence interval of the estimate is thereby shrunk. As a rule of thumb, 30 degrees of freedom is suggested as a satisfactory number for practical purposes. Therefore, as each estimate made during the Fourier transform has 2 degrees of freedom (associated with the coefficients of the sine and cosine terms), about 15 terms are usually averaged. Note that 16 is a better number if an FFT approach is used as this is 2^4 and there are then exactly $2^k/2^4$ ($= 2^{k-4}$) spectral estimates; for example, if there are 1 024 terms in the time series(so $k = 10$), there will be 512 estimates of the As and Bs, and 64 ($= 2^{10-4}$) smoothed estimates.

Increasingly, the use of the above analyses is an integral part of meteorological systems and relevant not only to the analysis of data. The exact form of spectra encountered in meteorology can show a wide range of shapes. As can be imagined, the contributions can be from the lowest frequencies associated with climate change through annual and seasonal contributions through synoptic events with periods of days, to diurnal and semi-diurnal contributions and local mesoscale events down to turbulence and molecular variations. For most meteorological applications, including synoptic analysis, the interest is in the range minutes to seconds. The spectrum at these frequencies will typically decrease very rapidly with frequency. For periods of less than 1 min, the spectrum often takes values proportional to $n^{-5/3}$. Thus, there is often relatively little contribution from frequencies greater than 1 Hz.

One of the important properties of the spectrum is that:

$$\sum_{j=0}^{\infty} S\left(n_j\right) = \sigma^2 \tag{2.4}$$

where σ^2 is the variance of the quantity being measured. It is often convenient, for analysis, to express the spectrum in continuous form, so that equation 2.4 becomes:

$$\int_0^{\infty} S\left(n\right) dn = \sigma^2 \tag{2.5}$$

It can be seen from equations 2.4 and 2.5 that changes caused to the spectrum, say by the instrument system, will alter the value of σ^2 and hence the statistical properties of the output relative to the input. This can be an important consideration in instrument design and data analysis.

Note also that the left-hand side of equation 2.5 is the area under the curve in Figure 2.2. That area, and therefore the variance, is not changed by aliasing if the time series is stationary, that is if its spectrum does not change from time to time.

2.2.3   **Instrument system response**

Sensors, and the electronic circuits that may be used with them comprising an instrument system, have response times and filtering characteristics that affect the observations.

No meteorological instrument system, or any instrumental system for that matter, precisely follows the quantity it is measuring. There is, in general, no simple way of describing the response of a system, although there are some reasonable approximations to them. The simplest can be classified as first and second order responses. This refers to the order of the differential equation that is used to approximate the way the system responds. For a detailed examination of the concepts that follow, there are many references in physics textbooks and the literature (see MacCready and Jex, 1964).

In the first order system, such as a simple sensor or the simplest low-pass filter circuit, the rate of change of the value recorded by the instrument is directly proportional to the difference between the value registered by the instrument and the true value of the variable. Thus, if the true value at time t is $s(t)$ and the value measured by the sensor is $s_0(t)$, the system is described by the first order differential equation:

$$\frac{ds_0(t)}{dt} = \frac{s(t) - s_0(t)}{T_I} \tag{2.6}$$

where T_I is a constant with the dimension of time, characteristic of the system. A first order system's response to a step function is proportional to $\exp(-t/T_I)$, and T_I is observable as the time taken, after a step change, for the system to reach 63% of the final steady reading. Equation 2.6 is valid for many sensors, such as thermometers.

A cup anemometer is a first order instrument, with the special property that T_I is not constant. It varies with wind speed. In fact, the parameter $s_0 T_I$ is called the distance constant, because it is nearly constant. As can be seen in this case, equation 2.6 is no longer a simple first order equation as it is now non-linear and consequently presents considerable problems in its solution. A further problem is that T_I also depends on whether the cups are speeding up or slowing down; that is, whether the right-hand side is positive or negative. This arises because the drag coefficient of a cup is lower if the airflow is towards the front rather than towards the back.

The wind vane approximates a second order system because the acceleration of the vane towards the true wind direction is proportional to the displacement of the vane from the true direction. This is, of course, the classical description of an oscillator (for example, a pendulum). Vanes, both naturally and by design, are damped. This occurs because of a resistive force proportional to, and opposed to, its rate of change. Thus, the differential equation describing the vane's action is:

$$\frac{d^2\phi_0(t)}{dt^2} = k_1\left[\phi_0(t) - \phi(t)\right] - k_2 \frac{d\phi_0(t)}{dt} \tag{2.7}$$

where ϕ is the true wind direction; ϕ_0 is the direction of the wind vane; and k_1 and k_2 are constants. The solution to this is a damped oscillation at the natural frequency of the vane (determined by the constant k_1). The damping of course is very important; it is controlled by the constant k_2. If it is too small, the vane will simply oscillate at the natural frequency; if too great, the vane will not respond to changes in wind direction.

It is instructive to consider how these two systems respond to a step change in their input, as this is an example of the way in which the instruments respond in the real world. Equations 2.6 and 2.7 can be solved analytically for this input. The responses are shown in Figures 2.3 and 2.4. Note how in neither case is the real value of the element measured by the system. Also, the choice of the values of the constants k_1 and k_2 can have great effect on the outputs.
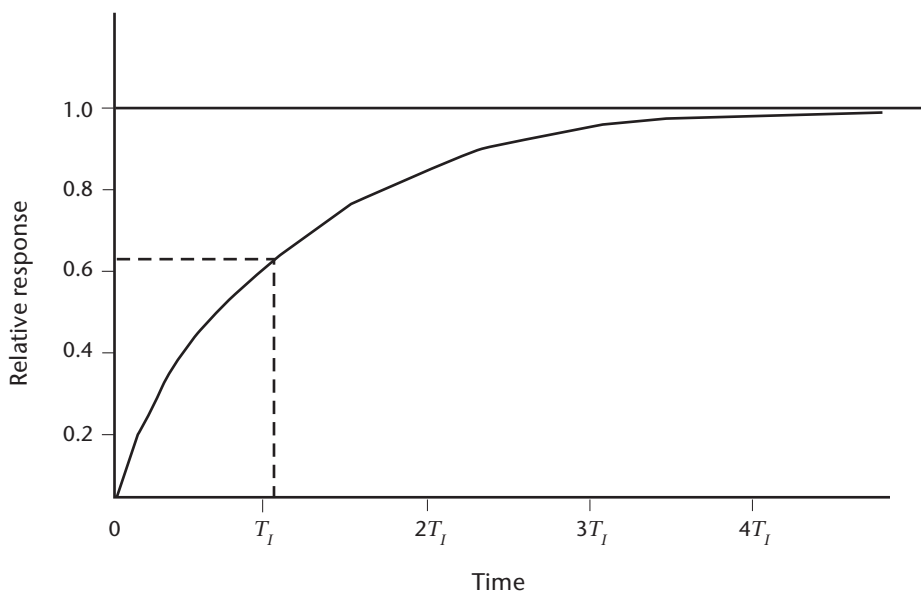

Figure 2.3. The response of a first order system to a step function. At time T_I the system has reached 63% of its final value.
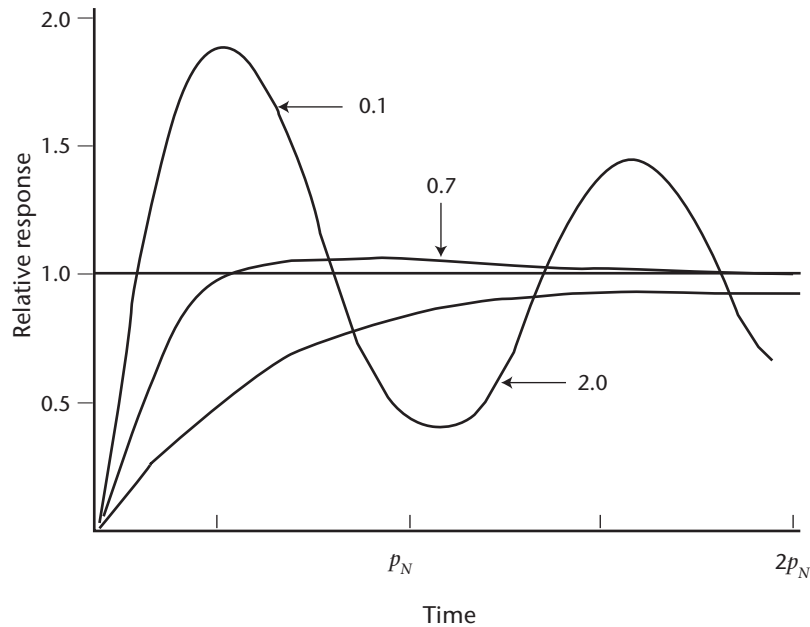
Figure 2.4. The response of a second order system to a step function. p_N is the natural period, related to k_1 in equation 2.7, which, for a wind vane, depends on wind speed. The curves shown are for damping factors with values 0.1 (very lightly damped), 0.7 (critically damped, optimum for most purposes) and 2.0 (heavily damped). The damping factor is related to k_2 in equation 2.7.

An important property of an instrument system is its frequency response function or transfer function $H(n)$. This function gives the amount of the spectrum that is transmitted by the system. It can be defined as:

$$S(n)_{\text{out}} = H(n)S(n)_{\text{in}} \tag{2.8}$$

where the subscripts refer to the input and output spectra. Note that, by virtue of the relationship in equation 2.5, the variance of the output depends on $H(n)$. $H(n)$ defines the effect of the sensor as a filter, as discussed in the next section. The ways in which it can be calculated or measured are discussed in section 2.3.

2.2.4   **Filters**

This section discusses the properties of filters, with examples of the ways in which they can affect the data.

Filtering is the processing of a time series (either continuous or discrete, namely, sampled) in such a way that the value assigned at a given time is weighted by the values that occurred at other times. In most cases, these times will be adjacent to the given time. For example, in a discrete time-series of N samples numbered 0 to N, with value y_i, the value of the filtered observation $\bar{y}_i$ might be defined as:

$$\bar{y}_i = \sum_{j=-m}^{m} w_j\, y_{i+j} \tag{2.9}$$

Here there are $2m + 1$ terms in the filter, numbered by the dummy variable j from $-m$ to $+m$, and $\bar{y}_i$ is centred at $j = 0$. Some data are rejected at the beginning and end of the sampling time. w_j is commonly referred to as a weighting function and typically:

$$\sum_{j=-m}^{m} w_j = 1 \tag{2.10}$$

so that at least the average value of the filtered series will have the same value as the original one.

The above example uses digital filtering. Similar effects can be obtained using electronics (for example, through a resistor and capacitor circuit) or through the characteristics of the sensor (for example, as in the case of the anemometer, discussed earlier). Whether digital or analogue, a filter is characterized by $H(n)$. If digital, $H(n)$ can be calculated; if analogue, it can be obtained by the methods described in section 2.3.

For example, compare a first order system with a response time of T_1, and a "box car" filter of length T_s on a discrete time-series taken from a sensor with much faster response. The forms of these two filters are shown in Figure 2.5. In the first, it is as though the instrument has a memory which is strongest at the present instant, but falls off exponentially the further in the past the data goes. The box car filter has all weights of equal magnitude for the period T_s, and zero beyond that. The frequency response functions, $H(n)$, for these two are shown in Figure 2.6.

In the figure, the frequencies have been scaled to show the similarity of the two response functions. It shows that an instrument with a response time of, say, 1 s has approximately the same effect on an input as a box car filter applied over 4 s. However, it should be noted that a box car filter, which is computed numerically, does not behave simply. It does not remove all the higher frequencies beyond the Nyquist frequency, and can only be used validly if the spectrum falls off rapidly above n_y. Note that the box car filter shown in Figure 2.6 is an analytical solution for w as a continuous function; if the number of samples in the filter is small, the cut-off is less sharp and the unwanted higher frequency peaks are larger.

See Acheson (1968) for practical advice on box car and exponential filtering, and a comparison of their effects.

A response function of a second order system is given in Figure 2.7, for a wind vane in this case, showing how damping acts as a band-pass filter.

It can be seen that the processing of signals by systems can have profound effects on the data output and must be expertly done.
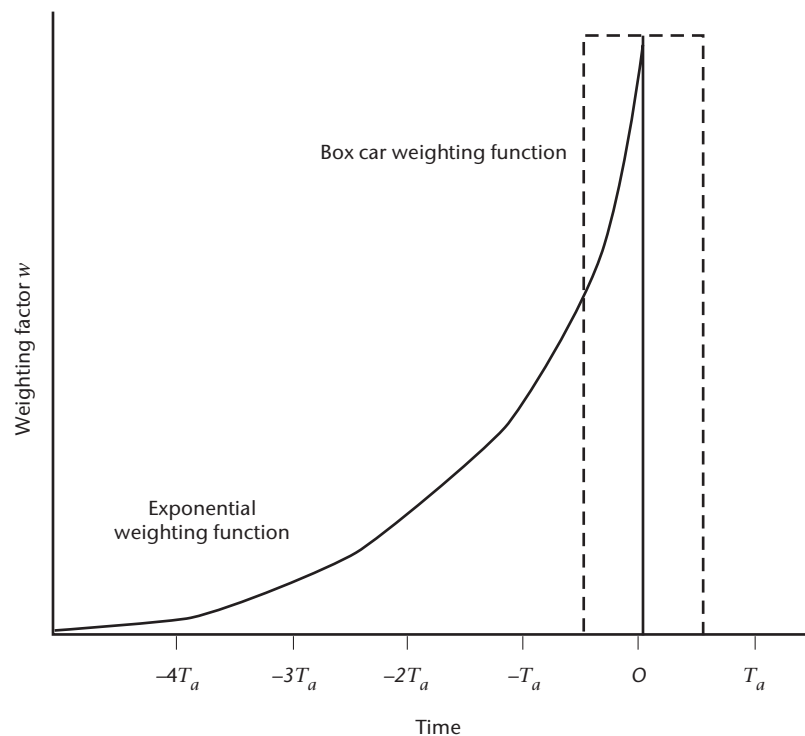

Figure 2.5. The weighting factors for a first order (exponential) weighting function and a box car weighting function. For the box car T_a is T_s, the sampling time, and $w = 1/N$. For the first order function T_a is T_1, the time constant of the filter, and $w(t) = (1/T_1) \exp(-t/T_1)$.
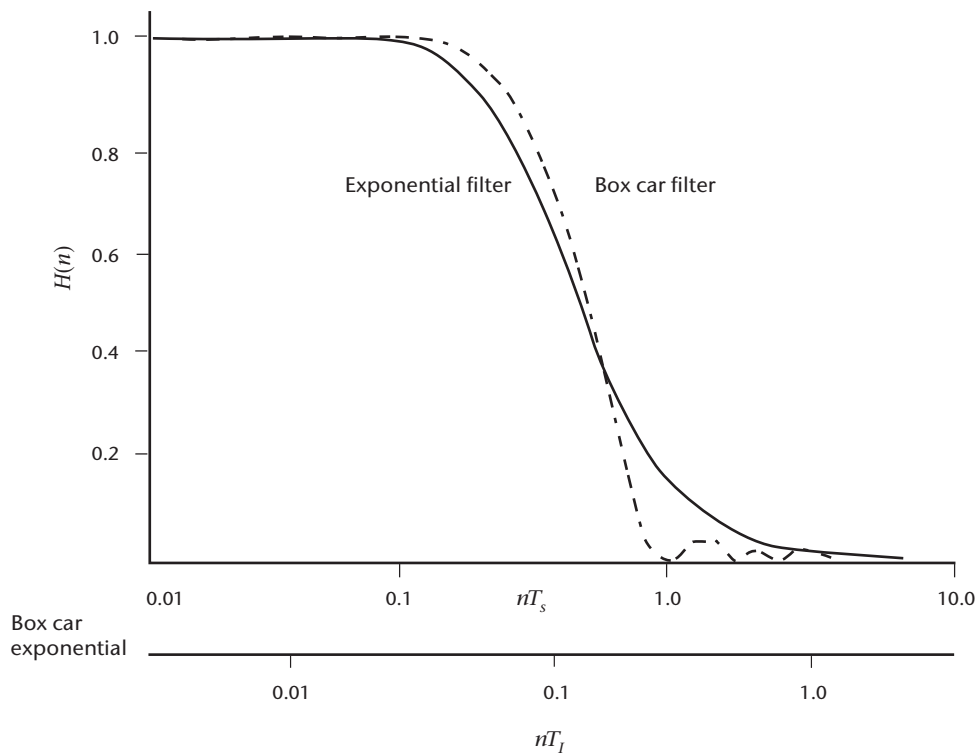
Figure 2.6. Frequency response functions for a first order (exponential) weighting function and a box car weighting function. The frequency is normalized for the first order filter by T_I, the time constant, and for the box car filter by T_s, the sampling time.

Among the effects of filters is the way in which they can change the statistical information of the data. One of these was touched on earlier and illustrated in equations 2.5 and 2.8. Equation 2.5 shows how the integral of the spectrum over all frequencies gives the variance of the time series, while equation 2.8 shows how filtering, by virtue of the effect of the transfer function, will change the measured spectrum. Note that the variance is not always decreased by filtering. For example, in certain cases, for a second order system the transfer function will amplify parts of the spectrum and possibly increase the variance, as shown in Figure 2.7.

To give a further example, if the distribution is Gaussian, the variance is a useful parameter. If it were decreased by filtering, a user of the data would underestimate the departure from the mean of events occurring with given probabilities or return periods.

Also, the design of the digital filter can have unwanted or unexpected effects. If Figure 2.6 is examined it can be seen that the response function for the box car filter has a series of maxima at frequencies above where it first becomes zero. This will give the filtered data a small periodicity at these frequencies. In this case, the effect will be minimal as the maxima are small. However, for some filter designs quite significant maxima can be introduced. As a rule of thumb, the smaller the number of weights, the greater the problem. In some instances, periodicities have been claimed in data that only existed because the data had been filtered.

An issue related to the concept of filters is the length of the sample. This can be illustrated by noting that, if the length of record is of duration T, contributions to the variability of the data at frequencies below $1/T$ will not be possible. It can be shown that a finite record length has the effect of a high-pass filter. As for the low-pass filters discussed above, a high-pass filter will also have an impact on the statistics of the output data.
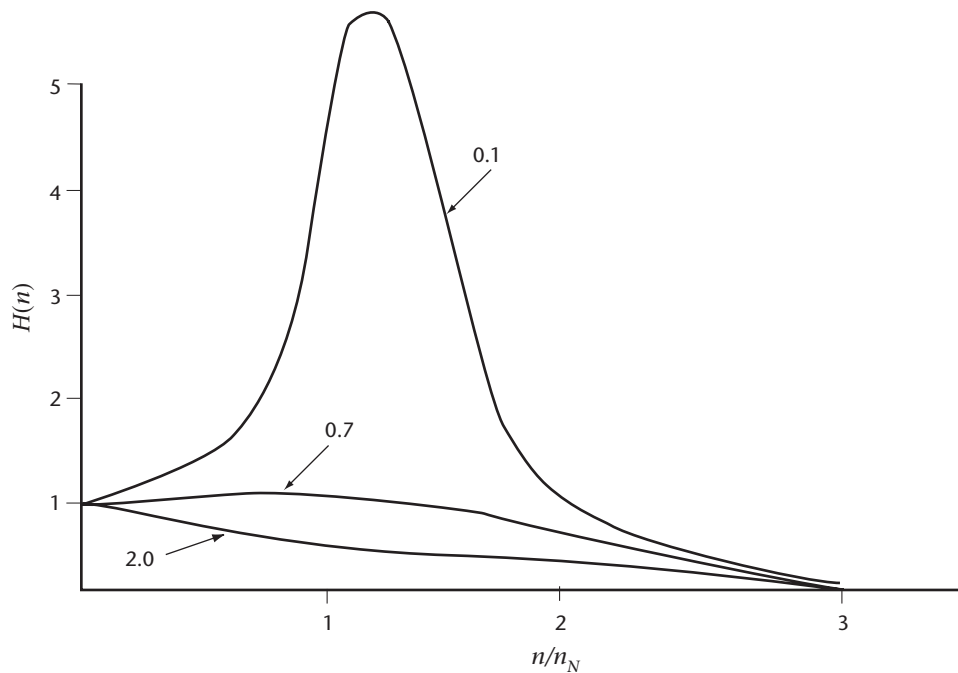
Figure 2.7. Frequency response functions for a second order system, such as a wind vane. The frequency is normalized by n_N, the natural frequency, which depends on wind speed. The curves shown are for damping factors with values 0.1 (very lightly damped), 0.7 (critically damped, optimum for most purposes) and 2.0 (heavily damped).

2.3   DETERMINATION OF SYSTEM CHARACTERISTICS

The filtering characteristics of a sensor or an electronic circuit, or the system that they comprise, must be known to determine the appropriate sampling frequency for the time series that the system produces. The procedure is to measure the transfer or response function $H(n)$ in equation 2.8.

The transfer function can be obtained in at least three ways – by direct measurement, calculation and estimation.

2.3.1   Direct measurement of response

Response can be directly measured using at least two methods. In the first method a known change, such as a step function, is applied to the sensor or filter and its response time measured; $H(n)$ can then be calculated. In the second method, the output of the sensor is compared to another, much faster sensor. The first method is more commonly used than the second.

A simple example of how to determine the response of a sensor to a known input is to measure the distance constant of a rotating-cup or propeller anemometer. In this example, the known input is a step function. The anemometer is placed in a constant velocity air-stream, prevented from rotating, then released, and its output recorded. The time taken by the output to increase from zero to 63% of its final or equilibrium speed in the air-stream is the time "constant" (see section 2.2.3).

If another sensor, which responds much more rapidly than the one whose response is to be determined, is available, then good approximations of both the input and output can be measured and compared. The easiest device to use to perform the comparison is probably a modern, two-channel digital spectrum analyser. The output of the fast-response sensor is input to one channel, the output of the sensor being tested to the other channel, and the transfer function automatically displayed. The transfer function is a direct description of the sensor as a filter. If the device whose response is to be determined is an electronic circuit, generating

a known or even truly random input is much easier than finding a much faster sensor. Again, a modern, two-channel digital spectrum analyser is probably most convenient, but other electronic test instruments can be used.

2.3.2 Calculation of response

This is the approach described in section 2.2.3. If enough is known about the physics of a sensor/filter, the response to a large variety of inputs may be determined by either analytic or numerical solution. Both the response to specific inputs, such as a step function, and the transfer function can be calculated. If the sensor or circuit is linear (described by a linear differential equation), the transfer function is a complete description, in that it describes the amplitude and phase responses as a function of frequency, in other words, as a filter. Considering response as a function of frequency is not always convenient, but the transfer function has a Fourier transform counterpart, the impulse response function, which makes interpretation of response as a function of time much easier. This is illustrated in Figures 2.3 and 2.4 which represent response as a function of time.

If obtainable, analytic solutions are preferable because they clearly show the dependence upon the various parameters.

2.3.3 Estimation of response

If the transfer functions of a transducer and each following circuit are known, their product is the transfer function of the entire system. If, as is usually the case, the transfer functions are low-pass filters, the aggregate transfer function is a low-pass filter whose cut-off frequency is less than that of any of the individual filters.

If one of the individual cut-off frequencies is much less than any of the others, then the cut-off frequency of the aggregate is only slightly smaller.

Since the cut-off frequency of a low-pass filter is approximately the inverse of its time constant, it follows that, if one of the individual time constants is much larger than any of the others, the time constant of the aggregate is only slightly larger.

2.4 SAMPLING

2.4.1 Sampling techniques

Figure 2.8 schematically illustrates a typical sensor and sampling circuit. When exposed to the atmosphere, some property of the transducer changes with an atmospheric variable such as temperature, pressure, wind speed or direction, or humidity and converts that variable into a useful signal, usually electrical. Signal conditioning circuits commonly perform functions such as converting transducer output to a voltage, amplifying, linearizing, offsetting and smoothing. The low-pass filter finalizes the sensor output for the sample-and-hold input. The sample-and-hold and the analogue-to-digital converter produce the samples from which the observation is computed in the processor.

It should be noted that the smoothing performed at the signal conditioning stage for engineering reasons, to remove spikes and to stabilize the electronics, is performed by a low-pass filter; it reduces the response time of the sensor and removes high frequencies which may be of interest. Its effect should be explicitly understood by the designer and user, and its cut-off frequency should be as high as practicable.

So-called "smart sensors", those with microprocessors, may incorporate all the functions shown. The signal conditioning circuitry may not be found in all sensors, or may be combined with other circuitry. In other cases, such as with a rotating-cup or propeller anemometer, it may be easy

to speak only of a sensor because it is awkward to distinguish a transducer. In the few cases for which a transducer or sensor output is a signal whose frequency varies with the atmospheric variable being measured, the sample-and-hold and the analogue-to-digital converter may be replaced by a counter. But these are not important details. The important element in the design is to ensure that the sequence of samples adequately represents the significant changes in the atmospheric variable being measured.

The first condition imposed upon the devices shown in Figure 2.8 is that the sensor must respond quickly enough to follow the atmospheric fluctuations which are to be described in the observation. If the observation is to be a 1, 2 or 10 min average, this is not a very demanding requirement. On the other hand, if the observation is to be that of a feature of turbulence, such as peak wind gust, care must be taken when selecting a sensor.

The second condition imposed upon the devices shown in Figure 2.8 is that the sample-and-hold and the analogue-to-digital converter must provide enough samples to make a good observation. The accuracy demanded of meteorological observations usually challenges the sensor, not the electronic sampling technology. However, the sensor and the sampling must be matched to avoid aliasing. If the sampling rate is limited for technical reasons, the sensor/filter system must be designed to remove the frequencies that cannot be represented.

If the sensor has a suitable response function, the low-pass filter may be omitted, included only as insurance, or may be included because it improves the quality of the signal input to the sample-and-hold. As examples, such a filter may be included to eliminate noise pick-up at the end of a long cable or to further smooth the sensor output. Clearly, this circuit must also respond quickly enough to follow the atmospheric fluctuations of interest.
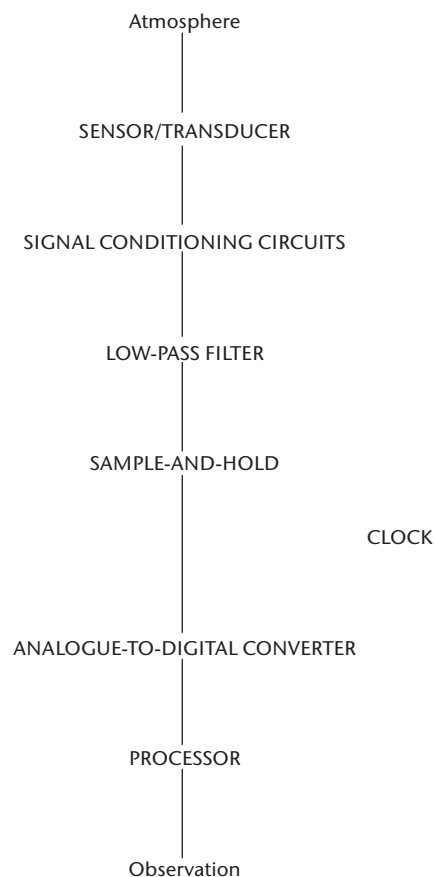
Atmosphere

SENSOR/TRANSDUCER

SIGNAL CONDITIONING CIRCUITS

LOW-PASS FILTER

SAMPLE-AND-HOLD

CLOCK

ANALOGUE-TO-DIGITAL CONVERTER

PROCESSOR

Observation

Figure 2.8. An instrument system

2.4.2 Sampling rates

For most meteorological and climatological applications, observations are required at intervals of 30 min to 24 hours, and each observation is made with a sampling time of the order of 1 to 10 min. Part I, Chapter 1, Annex 1.E gives a recent statement of requirements for these purposes.

A common practice for routine observations is to take one spot reading of the sensor (such as a thermometer) and rely on its time constant to provide an approximately correct sampling time. This amounts to using an exponential filter (Figure 2.6). Automatic weather stations commonly use faster sensors, and several spot readings must be taken and processed to obtain an average (box car filter) or other appropriately weighted mean.

A practical recommended scheme for sampling rates is as follows:[1]

(a) Samples taken to compute averages should be obtained at equispaced time intervals which:

   (i) Do not exceed the time constant of the sensor; or

   (ii) Do not exceed the time constant of an analogue low-pass filter following the linearized output of a fast-response sensor; or

   (iii) Are sufficient in number to ensure that the uncertainty of the average of the samples is reduced to an acceptable level, for example, smaller than the required accuracy of the average;

(b) Samples to be used in estimating extremes of fluctuations, such as wind gusts, should be taken at rates at least four times as often as specified in (i) or (ii) above.

For obtaining averages, somewhat faster sampling rates than (i) and (ii), such as twice per time constant, are often advocated and practised.

Criteria (i) and (ii) derive from consideration of the Nyquist frequency. If the sample spacing $\Delta t \leq T_I$, the sampling frequency $n \geq 1/T_I$ and $nT_I \geq 1$. It can be seen from the exponential curve in Figure 2.6 that this removes the higher frequencies and prevents aliasing. If $\Delta t = T_I$, $n_y = 1/2T_I$ and the data will be aliased only by the spectral energy at frequencies at $nT_I = 2$ and beyond, that is where the fluctuations have periods of less than $0.5T_I$.

Criteria (i) and (ii) are used for automatic sampling. The statistical criterion in (iii) is more applicable to the much lower sampling rates in manual observations. The uncertainty of the mean is inversely proportional to the square root of the number of observations, and its value can be determined from the statistics of the quantity.

Criterion (b) emphasizes the need for high sampling frequencies, or more precisely, small time-constants, to measure gusts. Recorded gusts are smoothed by the instrument response, and the recorded maximum will be averaged over several times the time constant.

The effect of aliasing on estimates of the mean can be seen very simply by considering what happens when the frequency of the wave being measured is the same as the sampling frequency, or a multiple thereof. The derived mean will depend on the timing of the sampling. A sample obtained once per day at a fixed time will not provide a good estimate of mean monthly temperature.

For a slightly more complex illustration of aliasing, consider a time series of three-hourly observations of temperature using an ordinary thermometer. If temperature changes smoothly with time, as it usually does, the daily average computed from eight samples is acceptably stable. However, if a mesoscale event (a thunderstorm) has occurred which reduced the temperature by many degrees for 30 min, the computed average is wrong. The reliability of daily averages

---

[1] As adopted by the Commission for Instruments and Methods of Observation at its tenth session (1989) through Recommendation 3 (CIMO-X).

depends on the usual weakness of the spectrum in the mesoscale and higher frequencies. However, the occurrence of a higher-frequency event (the thunderstorm) aliases the data, affecting the computation of the mean, the standard deviation and other measures of dispersion, and the spectrum.

The matter of sampling rate may be discussed also in terms of Figure 2.8. The argument in section 2.2.1 was that, for the measurement of spectra, the sampling rate, which determines the Nyquist frequency, should be chosen so that the spectrum of fluctuations above the Nyquist frequency is too weak to affect the computed spectrum. This is achieved if the sampling rate set by the clock in Figure 2.8 is at least twice the highest frequency of significant amplitude in the input signal to the sample-and-hold.

The wording "highest frequency of significant amplitude" used above is vague. It is difficult to find a rigorous definition because signals are never truly bandwidth limited. However, it is not difficult to ensure that the amplitude of signal fluctuations decreases rapidly with increasing frequency, and that the root-mean-square amplitude of fluctuations above a given frequency is either small in comparison with the quantization noise of the analogue-to-digital converter, small in comparison with an acceptable error or noise level in the samples, or contributes negligibly to total error or noise in the observation.

Section 2.3 discussed the characteristics of sensors and circuits which can be chosen or adjusted to ensure that the amplitude of signal fluctuations decreases rapidly with increasing frequency. Most transducers, by virtue of their inability to respond to rapid (high-frequency) atmospheric fluctuations and their ability to replicate faithfully slow (low-frequency) changes, are also low-pass filters. By definition, low-pass filters limit the bandwidth and, by Nyquist's theorem, also limit the sampling rate that is necessary to reproduce the filter output accurately. For example, if there are real variations in the atmosphere with periods down to 100 ms, the Nyquist sampling frequency would be 1 per 50 ms, which is technically demanding. However, if they are seen through a sensor and filter which respond much more slowly, for example with a 10 s time constant, the Nyquist sampling rate would be 1 sample per 5 s, which is much easier and cheaper, and preferable if measurements of the high frequencies are not required.

2.4.3   **Sampling rate and quality control**

Many data quality control techniques of use in automatic weather stations depend upon the temporal consistency, or persistence, of the data for their effectiveness. As a very simple example, two hypothetical quality-control algorithms for pressure measurements at automatic weather stations should be considered. Samples are taken every 10 s, and 1 min averages computed each minute. It is assumed that atmospheric pressure only rarely, if ever, changes at a rate exceeding 1 hPa per minute.

The first algorithm rejects the average if it differs from the previous one by more than 1 hPa. This would not make good use of the available data. It allows a single sample with as much as a 6 hPa error to pass undetected and to introduce a 1 hPa error in an observation.

The second algorithm rejects a sample if it differs from the previous one by more than 1 hPa. In this case, an average contains no error larger than about 0.16 (1/6) hPa. In fact, if the assumption is correct that atmospheric pressure only rarely changes at a rate exceeding 1 hPa per minute, the accept/reject criteria on adjacent samples could be tightened to 0.16 hPa and error in the average could be reduced even more.

The point of the example is that data quality control procedures that depend upon temporal consistency (correlation) for their effectiveness are best applied to data of high temporal resolution (sampling rate). At the high frequency end of the spectrum in the sensor/filter output, correlation between adjacent samples increases with increasing sampling rate until the Nyquist frequency is reached, after which no further increase in correlation occurs.

Up to this point in the discussion, nothing has been said which would discourage using a sensor/ filter with a time constant as long as the averaging period required for the observation is taken as

a single sample to use as the observation. Although this would be minimal in its demands upon the digital subsystem, there is another consideration needed for effective data quality control. Observations can be grouped into three categories as follows:

(a) Accurate (observations with errors less than or equal to a specified value);

(b) Inaccurate (observations with errors exceeding a specified value);

(c) Missing.

There are two reasons for data quality control, namely, to minimize the number of inaccurate observations and to minimize the number of missing observations. Both purposes are served by ensuring that each observation is computed from a reasonably large number of data quality-controlled samples. In this way, samples with large spurious errors can be isolated and excluded, and the computation can still proceed, uncontaminated by that sample.

––––––––––––––

REFERENCES AND FURTHER READING

Acheson, D.T., 1968: An approximation to arithmetic averaging for meteorological variables. *Journal of Applied Meteorology*, 7:548–553.

Bendat, J.S. and A.G. Piersol, 1986: *Random Data: Analysis and Measurement Procedures*. Second edition, John Wiley and Sons, New York.

Blackman, R.B. and J.W. Tukey, 1958: *The Measurement of Power Spectra*. Dover Publications, New York.

Jenkins, G.M. and D.G. Watts, 1968: *Spectral Analysis and its Applications*. Holden-Day, San Francisco.

Kulhánek, O., 1976: *Introduction to Digital Filtering in Geophysics*. Elsevier, Amsterdam.

MacCready, P.B. and H.R. Jex, 1964: Response characteristics and meteorological utilization of propeller and vane wind sensors. *Journal of Applied Meteorology*, 3(2):182–193.

Otnes, R.K. and L. Enochson, 1978: *Applied Time Series Analysis. Volume 1: Basic techniques*. John Wiley and Sons, New York.

Pasquill, F. and F.B. Smith, 1983: *Atmospheric Diffusion*. Ellis Horwood, Chichester.

Stearns, S.D. and D.R. Hush, 1990: *Digital Signal Analysis*. Prentice Hall, New Jersey.

———————

CHAPTER CONTENTS

CHAPTER 3. DATA REDUCTION

3.1 GENERAL

This chapter discusses in general terms the procedures for processing and/or converting data obtained directly from instruments into data suitable for meteorological users, in particular for exchange between countries. Formal regulations for the reduction of data to be exchanged internationally have been prescribed by WMO, and are laid down in WMO (2010*c*). Part I, Chapter 1, contains some relevant advice and definitions.

3.1.1 Definitions

In the discussion of the instrumentation associated with the measurement of atmospheric variables, it has become useful to classify the observational data according to data levels. This scheme was introduced in connection with the data-processing system for the Global Atmospheric Research Programme, and is defined in WMO (2010*b*, 2010*c*).

Level I data, in general, are instrument readings expressed in appropriate physical units, and referred to with geographical coordinates. They require conversion to the normal meteorological variables (identified in Part I, Chapter 1). Level I data themselves are in many cases obtained from the processing of electrical signals such as voltages, referred to as raw data. Examples of these data are satellite radiances and water-vapour pressure.

The data recognized as meteorological variables are Level II data. They may be obtained directly from instruments (as is the case for many kinds of simple instruments) or derived from Level I data. For example, a sensor cannot measure visibility, which is a Level II quantity; instead, sensors measure the extinction coefficient, which is a Level I quantity.

Level III data are those contained in internally consistent datasets, generally in grid-point form. They are not within the scope of this Guide.

Data exchanged internationally are Level II or Level III data.

3.1.2 Meteorological requirements

Observing stations throughout the world routinely produce frequent observations in standard formats for exchanging high-quality information obtained by uniform observing techniques, despite the different types of sensors in use throughout the world, or even within nations. To accomplish this, very considerable resources have been devoted over very many years to standardize content, quality and format. As automated observation of the atmosphere becomes more prevalent, it becomes even more important to preserve this standardization and develop additional standards for the conversion of raw data into Level I data, and raw and Level I data into Level II data.

3.1.3 The data reduction process

The role of a transducer is to sense an atmospheric variable and convert it quantitatively into a useful signal. However, transducers may have secondary responses to the environment, such as temperature-dependent calibrations, and their outputs are subject to a variety of errors, such as drift and noise. After proper sampling by a data-acquisition system, the output signal must be scaled and linearized according to the total system calibration and then filtered or averaged. At this stage, or earlier, it becomes raw data. The data must then be converted to measurements of the physical quantities to which the sensor responds, which are Level I data or may be Level II

data if no further conversion is necessary. For some applications, additional variables must be derived. At various stages in the process the data may be corrected for extraneous effects, such as exposure, and may be subjected to quality control.

Data from conventional and automatic weather stations (AWSs) must, therefore, be subjected to many operations before they can be used. The whole process is known as data reduction and consists of the execution of a number of functions, comprising some or all of the following:

(a) Transduction of atmospheric variables;

(b) Conditioning of transducer outputs;

(c) Data acquisition and sampling;

(d) Application of calibration information;

(e) Linearization of transducer outputs;

(f) Extraction of statistics, such as the average;

(g) Derivation of related variables;

(h) Application of corrections;

(i) Data quality control;

(j) Data recording and storage;

(k) Compilation of metadata;

(l) Formatting of messages;

(m) Checking message contents;

(n) Transmission of messages.

The order in which these functions are executed is only approximately sequential. Of course, the first and the last function listed above should always be performed first and last. Linearization may immediately follow or be inherent in the transducer, but it must precede the extraction of an average. Specific quality control and the application of corrections could take place at different levels of the data-reduction process. Depending on the application, stations can operate in a diminished capacity without incorporating all of these functions.

In the context of this Guide, the important functions in the data-reduction process are the selection of appropriate sampling procedures, the application of calibration information, linearization when required, filtering and/or averaging, the derivation of related variables, the application of corrections, quality control, and the compilation of metadata. These are the topics addressed in this chapter. More explicit information on quality management is given in Part IV, Chapter 1, and on sampling, filtering and averaging in Part IV, Chapter 2.

Once reduced, the data must be made available through coding, transmission and receipt, display, and archiving, which are the topics of other WMO Manuals and Guides. An observing system is not complete unless it is connected to other systems that deliver the data to the users. The quality of the data is determined by the weakest link. At every stage, quality control must be applied.

Much of the existing technology and standardized manual techniques for data reduction can also be used by AWSs, which, however, make particular demands. AWSs include various sensors, standard computations for deriving elements of messages, and the message format itself. Not all sensors interface easily with automated equipment. Analytic expressions for

computations embodied in tables must be recovered or discovered. The rules for encoding messages must be expressed in computer languages with degrees of precision, completeness and unambiguousness not demanded by natural language instructions prepared for human observers. Furthermore, some human functions, such as the identification of cloud types, cannot be automated using either current or foreseeable technologies.

Data acquisition and data-processing software for AWSs are discussed at some length in Part II, Chapter 1, to an extent which is sufficiently general for any application of electrical transducers in meteorology. Some general considerations and specific examples of the design of algorithms for synoptic AWSs are given in WMO (1987).

In processing meteorological data there is usually one correct procedure, algorithm or approach, and there may be many approximations ranging in validity from good to useless. Experience strongly suggests that the correct approach is usually the most efficient in the long term. It is direct, requires a minimum of qualifications, and, once implemented, needs no further attention. Accordingly, the subsequent paragraphs are largely limited to the single correct approach, as far as exact solutions exist, to the problem under consideration.

3.2   SAMPLING

See Part IV, Chapter 2 for a full discussion of sampling. The following is a summary of the main outcomes.

It should be recognized that atmospheric variables fluctuate rapidly and randomly because of ever-present turbulence, and that transducer outputs are not faithful reproductions of atmospheric variables because of their imperfect dynamic characteristics, such as limited ability to respond to rapid changes. Transducers generally need equipment to amplify or protect their outputs and/or to convert one form of output to another, such as resistance to voltage. The circuitry used to accomplish this may also smooth or low-pass filter the signal. There is a cut-off frequency above which no significant fluctuations occur because none exist in the atmosphere and/or the transducer or signal conditioning circuitry has removed them.

An important design consideration is how often the transducer output should be sampled. The definitive answer is: at an equispaced rate at least twice the cut-off frequency of the transducer output signal. However, a simpler and equivalent rule usually suffices: the sampling interval should not exceed the largest of the time constants of all the devices and circuitry preceding the acquisition system. If the sampling rate is less than twice the cut-off frequency, unnecessary errors occur in the variance of the data and in all derived quantities and statistics. While these increases may be acceptable in particular cases, in others they are not. Proper sampling always ensures minimum variance.

Good design may call for incorporating a low-pass filter, with a time constant about equal the sampling interval of the data-acquisition system. It is also a precautionary measure to minimize the effects of noise, especially 50 or 60 Hz pick-up from power mains by cables connecting sensors to processors and leakage through power supplies.

3.3   APPLICATION OF CALIBRATION FUNCTIONS

The WMO regulations (WMO, 2010c) prescribe that stations be equipped with properly calibrated instruments and that adequate observational and measuring techniques are followed to ensure that the measurements are accurate enough to meet the needs of the relevant meteorological disciplines. The conversion of raw data from instruments into the corresponding meteorological variables is achieved by means of calibration functions. The proper application of calibration functions and any other systematic corrections are most critical for obtaining data that meet expressed accuracy requirements.

The determination of calibration functions should be based on calibrations of all components of the measurement chain. In principle at least, and in practice for some meteorological quantities such as pressure, the calibration of field instruments should be traceable to an international standard instrument, through an unbroken chain of comparisons between the field instrument and some or all of a series of standard instruments, such as a travelling standard, a working standard, a reference standard and a national standard (see Part I, Chapter 1 for definitions).

A description of the calibration procedures and systematic corrections associated with each of the basic meteorological variables is contained in each of the respective chapters in Part I.

Field instruments must be calibrated regularly by an expert, with corresponding revisions to the calibration functions. It is not sufficient to rely on calibration data that is supplied along with the calibration equipment. The supplier's calibration equipment often bears an unknown relationship to the national standard, and, in any case, it must be expected that calibration will change during transport, storage and use. Calibration changes must be recorded in the station's metadata files.

3.4   LINEARIZATION

If the transducer output is not exactly proportional to the quantity being measured, the signal must be linearized, making use of the instrument's calibration. This must be carried out before the signal is filtered or averaged. The sequence of operations "average then linearize" produces different results from the sequence "linearize then average" when the signal is not constant throughout the averaging period.

Non-linearity may arise in the following three ways (WMO, 1987):

(a)   Many transducers are inherently nonlinear, namely, their output is not proportional to the measured atmospheric variable. A thermistor is a simple example;

(b)   Although a sensor may incorporate linear transducers, the variables measured may not be linearly related to the atmospheric variable of interest. For example, the photodetector and shaft-angle transducer of a rotating beam ceilometer are linear devices, but the ceilometer output signal (backscattered light intensity as a function of angle) is non-linear in cloud height;

(c)   The conversion from Level I to Level II may not be linear. For example, extinction coefficient, not visibility or transmittance, is the proper variable to average in order to produce estimates of average visibility.

In the first of these cases, a polynomial calibration function is often used. If so, it is highly desirable to have standardized sensors with uniform calibration coefficients to avoid the problems that arise when interchanging sensors in the field. In the other two cases, an analytic function which describes the behaviour of the transducer is usually appropriate.

3.5   AVERAGING

The natural small-scale variability of the atmosphere makes smoothing or averaging necessary for obtaining representative observations and compatibility of data from different instruments. For international exchange and for many operational applications, the reported measurement must be representative of the previous 2 or 10 min for wind, and, by convention, of 1 to 10 min for other quantities. The 1 min practice arises in part from the fact that some conventional meteorological sensors have a response of the order of 1 min and a single reading is notionally a 1 min average or smoothed value. If the response time of the instrument is much faster, it is

necessary to take samples and filter or average them. This is the topic of Part IV, Chapter 2. See Part I, Chapter 1, (Annex 1.E), for the requirements of the averaging times typical of operational meteorological instrument systems.

Two types of averaging or smoothing are commonly used, namely, arithmetic and exponential. The arithmetic average conforms with the normal meaning of average and is readily implemented digitally; this is the box car filter described in Part IV, Chapter 2. An exponential average is the output of the simplest low-pass filter representing the simplest response of a sensor to atmospheric fluctuations, and it is more convenient to implement in analogue circuitry than the arithmetic average. When the time constant of a simple filter is approximately half the sampling time over which an average is being calculated, the arithmetic and exponential smoothed values are practically indistinguishable (see Part IV, Chapter 2, and also Acheson, 1968).

The outputs of fast-response sensors vary rapidly thus necessitating high sampling rates for optimal (minimum uncertainty) averaging. To reduce the required sampling rate and still provide the optimal digital average, it could be possible to linearize the transducer output (where that is necessary), exponentially smooth it using analogue circuitry with time constant t_c, and then sample digitally at intervals t_c.

Many other types of elaborate filters, computed digitally, have been used for special applications.

Because averaging non-linear variables creates difficulties when the variables change during the averaging period, it is important to choose the appropriate linear variable to compute the average. The table in section 3.6 lists some specific examples of elements of a synoptic observation which are reported as averages, with the corresponding linear variable that should be used.

3.6   RELATED VARIABLES AND STATISTICS

Besides averaged data, extremes and other variables that are representative for specific periods must be determined, depending on the purpose of the observation. An example of this is wind gust measurements, for which higher sampling rates are necessary.

Also, other quantities have to be derived from the averaged data, such as mean sea-level pressure, visibility and dewpoint. At conventional manual stations, conversion tables are used. It is common practice to incorporate the tables into an AWS and to provide interpolation routines, or to incorporate the basic formulae or approximations of them. See the various chapters of Part I for the data conversion practices, and Part II, Chapter 1 for AWS practice.

Quantities for which data conversion is necessary when averages are being computed

Quantity to be reported	Quantity to be averaged
Wind speed and direction	Cartesian components
Dewpoint	Absolute humidity
Visibility	Extinction coefficient

3.7   CORRECTIONS

The measurements of many meteorological quantities have corrections applied to them either as raw data or at the Level I or Level II stage to correct for various effects. These corrections are described in the chapters on the various meteorological variables in Part I. Corrections to raw data, for zero or index error, or for temperature, gravity and the like are derived from the calibration and characterization of the instrument. Other types of corrections or adjustments

to the raw or higher level data include smoothing, such as that applied to cloud height measurements and upper-air profiles, and corrections for exposure such as those sometimes applied to temperature, wind and precipitation observations. The algorithms for these types of corrections may, in some cases, be based on studies that are not entirely definitive; therefore, while they no doubt improve the accuracy of the data, the possibility remains that different algorithms may be derived in the future. In such a case, it may become necessary to recover the original uncorrected data. It is, therefore, advisable for the algorithms to be well documented.

3.8 QUALITY MANAGEMENT

Quality management is discussed in Part IV, Chapter 1. Formal requirements are specified by WMO (2010c) and general procedures are discussed in WMO (2010a).

Quality-control procedures should be performed at each stage of the conversion of raw sensor output into meteorological variables. This includes the processes involved in obtaining the data, as well as reducing them to Level II data.

During the process of obtaining data, the quality control should seek to eliminate both systematic and random measurement errors, errors due to departure from technical standards, errors due to unsatisfactory exposure of instruments, and subjective errors on the part of the observer.

Quality control during the reduction and conversion of data should seek to eliminate errors resulting from the conversion techniques used or the computational procedures involved. In order to improve the quality of data obtained at high sampling rates, which may generate increased noise, filtering and smoothing techniques are employed. These are described earlier in this chapter, as well as in Part IV, Chapter 2.

3.9 COMPILING METADATA

Metadata are discussed in Part I, Chapter 1, in Part IV, Chapter 1, and in other chapters concerning the various meteorological quantities. Metadata must be kept so that:

(a) Original data can be recovered to be re-worked, if necessary (with different filtering or corrections, for instance);

(b) The user can readily discover the quality of the data and the circumstances under which it was obtained (such as exposure);

(c) Potential users can discover the existence of the data.

The procedures used in all the data-reduction functions described above must therefore be recorded, generically for each type of data, and individually for each station and observation type.

_____

REFERENCES AND FURTHER READING

Acheson, D.T., 1968: An approximation to arithmetic averaging for meteorological variables. *Journal of Applied Meteorology*, 7(4):548–553.

World Meteorological Organization, 1987: *Some General Considerations and Specific Examples in the Design of Algorithms for Synoptic Automatic Weather Stations* (D.T. Acheson). Instruments and Observing Methods Report No. 19 (WMO/TD-No. 230). Geneva.

———, 2010*a*: *Guide to the Global Observing System* (WMO-No. 488). Geneva.

———, 2010*b*: *Manual on the Global Data-Processing and Forecasting System* (WMO-No. 485), Volume I. Geneva.

———, 2010*c*: *Manual on the Global Observing System* (WMO-No. 544), Volume I. Geneva.

CHAPTER CONTENTS

CHAPTER 4. TESTING, CALIBRATION AND INTERCOMPARISON

4.1   **GENERAL**

One of the purposes of WMO, set forth in Article 2 (c) of the WMO Convention, is "to promote standardization of meteorological and related observations and to ensure the uniform publication of observations and statistics". For this purpose, sets of standard procedures and recommended practices have been developed, and their essence is contained in this Guide.

Valid observational data can be obtained only when a comprehensive quality assurance programme is applied to the instruments and the network. Calibration and testing are inherent elements of a quality assurance programme. Other elements include clear definition of requirements, instrument selection deliberately based on the requirements, siting criteria, maintenance and logistics. These other elements must be considered when developing calibration and test plans. On an international scale, the extension of quality assurance programmes to include intercomparisons is important for the establishment of compatible datasets.

Because of the importance of standardization across national boundaries, several WMO regional associations have set up Regional Instrument Centres (RICs)[1] to organize and assist with standardization and calibration activities. Their terms of reference and locations are given in Part I, Chapter 1, Annex 1.A. Similarly, on the recommendation of JCOMM,[2] a network of Regional Marine Instrument Centres has been set up to provide for similar functions regarding marine meteorology and related oceanographic measurements. Their terms of reference and locations are given in Part II, Chapter 4, Annex 4.A, respectively.

National and international standards and guidelines exist for many aspects of testing and evaluation, and should be used where appropriate. Some of them are referred to in this chapter.

4.1.1   Definitions

Definitions of terms in metrology are given in the *International Vocabulary of Metrology – Basic and General Concepts and Associated Terms (VIM)* by the Joint Committee for Guides in Metrology (JCGM, 2012). Many of them are reproduced in Part I, Chapter 1, and some are repeated here for convenience. They are not universally used and differ in some respects from terminology commonly used in meteorological practice. However, the JCGM definitions are recommended for use in meteorology. The JCGM document is a joint production with the International Bureau of Weights and Measures (BIPM), the International Electrotechnical Commission (IEC), the International Federation of Clinical Chemistry and Laboratory Medicine (IFCC), the International Laboratory Accreditation Cooperation (ILAC), the International Organization for Standardization (ISO), the International Union of Pure and Applied Chemistry (IUPAC), the International Union of Pure and Applied Physics (IUPAP) and the International Organization of Legal Metrology (OIML).

The VIM terminology differs from common usage in the following respects in particular:

Accuracy (of a measurement): A qualitative term referring to the closeness of agreement between a measured quantity value and a true quantity value of a measurand. The accuracy of a measurement is sometimes understood as the closeness of agreement between measured quantity values that are being attributed to the measurand. It is possible to refer to an instrument or a measurement as having a high accuracy, but the quantitative measure of the accuracy is expressed in terms of uncertainty.

---

[1]   Recommended by the Commission for Instruments and Methods of Observation at its ninth session (1985) through Recommendation 19 (CIMO-IX).

[2]   Recommended by the Joint WMO/IOC Technical Commission for Oceanography and Marine Meteorology at its third session (2009) through Recommendation 1 (JCOMM-III).

Uncertainty: A non-negative parameter characterizing the dispersion of the quantity values being attributed to a measurand, based on the information used.

The error of a measurement: The measured quantity value minus a reference quantity value (the deviation has the other sign). It is composed of the random and systematic errors (the term bias is commonly used for systematic error).

Repeatability: The closeness of agreement between indications or measured quantity values obtained on the same or similar objects under a set of conditions that includes the same measurement procedure, same operators, same measuring system, same operating conditions and same location, and replicate measurements over a short period of time.

Reproducibility: The closeness of agreement between indications or measured quantity values obtained on the same or similar objects under a set of conditions that includes different locations, operators and measuring systems, and replicate measurements.

4.1.2 Testing and calibration programmes

Before using atmospheric measurements taken with a particular sensor for meteorological purposes, the answers to a number of questions are needed as follows:

(a)   What is the sensor or system accuracy?

(b)   What is the variability of measurements in a network containing such systems or sensors?

(c)   What change, or bias, will there be in the data provided by the sensor or system if its siting location is changed?

(d)   What change or bias will there be in the data if it replaces a different sensor or system measuring the same weather element(s)?

To answer these questions and to assure the validity and relevance of the measurements produced by a meteorological sensor or system, some combination of calibration, laboratory testing and functional testing is needed.

Calibration and test programmes should be developed and standardized, based on the expected climatic variability, environmental and electromagnetic interference under which systems and sensors are expected to operate. For example, considered factors might include the expected range of temperature, humidity and wind speed; whether or not a sensor or system must operate in a marine environment, or in areas with blowing dust or sand; the expected variation in electrical voltage and phase, and signal and power line electrical transients; and the expected average and maximum electromagnetic interference. Meteorological Services may purchase calibration and test services from private laboratories and companies, or set up test organizations to provide those services.

It is most important that at least two like sensors or systems be subjected to each test in any test programme. This allows for the determination of the expected variability in the sensor or system, and also facilitates detecting problems.

4.2 TESTING

4.2.1 The purpose of testing

Sensors and systems are tested to develop information on their performance under specified conditions of use. Manufacturers typically test their sensors and systems and in some cases

publish operational specifications based on their test results. However, it is extremely important for the user Meteorological Service to develop and carry out its own test programme or to have access to an independent testing authority.

Testing can be broken down into environmental testing, electrical/electromagnetic interference testing and functional testing. A test programme may consist of one or more of these elements.

In general, a test programme is designed to ensure that a sensor or system will meet its specified performance, maintenance and mean-time-between-failure requirements under all expected operating, storage and transportation conditions. Test programmes are also designed to develop information on the variability that can be expected in a network of like sensors, in functional reproducibility, and in the comparability of measurements between different sensors or systems.

Knowledge of both functional reproducibility and comparability is very important to climatology, where a single long-term database typically contains information from sensors and systems that through time use different sensors and technologies to measure the same meteorological variable. In fact, for practical applications, good operational comparability between instruments is a more valuable attribute than precise absolute calibration. This information is developed in functional testing.

Even when a sensor or system is delivered with a calibration report, environmental testing and possibly additional calibration should be performed. An example of this is a modern temperature measurement system, where at present the probe is likely to be a resistance temperature device. Typically, several resistance temperature devices are calibrated in a temperature bath by the manufacturer and a performance specification is provided based on the results of the calibration. However, the temperature system which produces the temperature value also includes of power supplies and electronics, which can also be affected by temperature. Therefore, it is important to operate the electronics and probe as a system through the temperature range during the calibration. It is good practice also to replace the probe with a resistor with a known temperature coefficient, which will produce a known temperature output and operate the electronics through the entire temperature range of interest to ensure proper temperature compensation of the system electronics.

Users should also have a programme for testing randomly selected production sensors and systems, even if pre-production units have been tested, because even seemingly minor changes in material, configurations or manufacturing processes may affect the operating characteristics of sensors and systems.

The International Organization for Standardization has standards (ISO, 1999, 2013) which specify sampling plans and procedures for the inspection of lots of items.

4.2.2   **Environmental testing**

4.2.2.1   *Definitions*

The following definitions serve to introduce the qualities of an instrument system that should be the subject of operational testing:

Operational conditions: Those conditions or a set of conditions encountered or expected to be encountered during the time an item is performing its normal operational function in full compliance with its performance specification.

Withstanding conditions: Those conditions or a set of conditions outside the operational conditions which the instrument is expected to withstand. They may have only a small probability of occurrence during an item's lifetime. The item is not expected to perform its operational function when these withstanding conditions exist. The item is, however, expected to be able to survive these conditions and return to normal performance when the operational conditions return.

Outdoor environment: Those conditions or a set of conditions encountered or expected to be encountered during the time that an item is performing its normal operational function in an unsheltered, uncontrolled natural environment.

Indoor environment: Those conditions or a set of conditions encountered or expected to be encountered during the time that an item is energized and performing its normal operational function within an enclosed operational structure. Consideration is given to both the uncontrolled indoor environment and the artificially controlled indoor environment.

Transportation environment: Those conditions or a set of conditions encountered or expected to be encountered during the transportation portion of an item's life. Consideration is given to the major transportation modes – road, rail, ship and air transportation, and also to the complete range of environments encountered – before and during transportation, and during the unloading phase. The item is normally housed in its packaging/shipping container during exposure to the transportation environment.

Storage environment: Those conditions or a set of conditions encountered or expected to be encountered during the time an item is in its non-operational storage mode. Consideration is given to all types of storage, from the open storage situation, in which an item is stored unprotected and outdoors, to the protected indoor storage situation. The item is normally housed in its packaging/shipping container during exposure to the storage environment.

The International Electrotechnical Commission also has standards (IEC, 2002) to classify environmental conditions which are more elaborate than the above. They define ranges of meteorological, physical and biological environments that may be encountered by products being transported, stored, installed and used, which are useful for equipment specification and for planning tests.

4.2.2.2 *Environmental test programme*

Environmental tests in the laboratory enable rapid testing over a wide range of conditions, and can accelerate certain effects such as those of a marine environment with high atmospheric salt loading. The advantage of environmental tests over field tests is that many tests can be accelerated in a well-equipped laboratory, and equipment may be tested over a wide range of climatic variability. Environmental testing is important; it can give insight into potential problems and generate confidence to go ahead with field tests, but it cannot replace field testing.

An environmental test programme is usually designed around a subset of the following conditions: high temperature, low temperature, temperature shock, temperature cycling, humidity, wind, rain, freezing rain, dust, sunshine (insolation), low pressure, transportation vibration and transportation shock. The ranges, or test limits, of each test are determined by the expected environments (operational, withstanding, outdoor, indoor, transportation, storage) that are expected to be encountered.

The purpose of an environmental test programme document is to establish standard environmental test criteria and corresponding test procedures for the specification, procurement, design and testing of equipment. This document should be based on the expected environmental operating conditions and extremes.

For example, the United States prepared its National Weather Service standard environmental criteria and test procedures (NWS, 1984), based on a study which surveyed and reported the expected operational and extreme ranges of the various weather elements in the United States operational area, and presented proposed test criteria (NWS, 1980). These criteria and procedures consist of three parts:

(a) Environmental test criteria and test limits for outdoor, indoor, and transportation/storage environments;

(b) Test procedures for evaluating equipment against the environmental test criteria;

(c)   Rationale providing background information on the various environmental conditions to which equipment may be exposed, their potential effect(s) on the equipment, and the corresponding rationale for the recommended test criteria.

4.2.3   Electrical and electromagnetic interference testing

The prevalence of sensors and automated data collection and processing systems that contain electronic components necessitates in many cases the inclusion in an overall test programme for testing performance in operational electrical environments and under electromagnetic interference.

An electrical/electromagnetic interference test programme document should be prepared. The purpose of the document is to establish standard electrical/electromagnetic interference test criteria and corresponding test procedures and to serve as a uniform guide in the specification of electrical/electromagnetic interference susceptibility requirements for the procurement and design of equipment.

The document should be based on a study that quantifies the expected power line and signal line transient levels and rise times caused by natural phenomena, such as thunderstorms. It should also include testing for expected power variations, both voltage and phase. If the equipment is expected to operate in an airport environment, or other environment with possible electromagnetic radiation interference, this should also be quantified and included in the standard. A purpose of the programme may also be to ensure that the equipment is not an electromagnetic radiation generator. Particular attention should be paid to equipment containing a microprocessor and, therefore, a crystal clock, which is critical for timing functions.

4.2.4   Functional testing

Calibration and environmental testing provide a necessary but not sufficient basis for defining the operational characteristics of a sensor or system, because calibration and laboratory testing cannot completely define how the sensor or system will operate in the field. It is impossible to simulate the synergistic effects of all the changing weather elements on an instrument in all of its required operating environments.

Functional testing is simply testing in the outdoor and natural environment where instruments are expected to operate over a wide variety of meteorological conditions and climatic regimes, and, in the case of surface instruments, over ground surfaces of widely varying albedo. Functional testing is required to determine the adequacy of a sensor or system while it is exposed to wide variations in wind, precipitation, temperature, humidity, and direct, diffuse and reflected solar radiation. Functional testing becomes more important as newer technology sensors, such as those using electro-optic, piezoelectric and capacitive elements, are placed into operational use. The readings from these sensors may be affected by adventitious conditions such as insects, spiders and their webs, and the size distribution of particles in the atmosphere, all of which must be determined by functional tests.

For many applications, comparability must be tested in the field. This is done with side-by-side testing of like and different sensors or systems against a field reference standard. These concepts are presented in Hoehne (1971, 1972, 1977).

Functional testing may be planned and carried out by private laboratories or by the test department of the Meteorological Service or other user organization. For both the procurement and operation of equipment, the educational and skill level of the observers and technicians who will use the system must be considered. Use of the equipment by these staff members should be part of the test programme. The personnel who will install, use, maintain and repair the equipment should evaluate those portions of the sensor or system, including the adequacy of the instructions and manuals that they will use in their job. Their skill level should also be considered when preparing procurement specifications.

4.3   **CALIBRATION**

4.3.1   **The purpose of calibration**

Sensor or system calibration is the first step in defining data validity. In general, it involves comparison against a known standard to determine how closely instrument output matches the standard over the expected range of operation. Performing laboratory calibration carries the implicit assumption that the instrument's characteristics are stable enough to retain the calibration in the field. A calibration history over successive calibrations should provide confidence in the instrument's stability.

Specifically, calibration is the operation that, under specified conditions, in a first step, establishes a relation between the quantity values with measurement uncertainties provided by measurement standards and corresponding indications with associated measurement uncertainties, and, in a second step, uses this information to establish a relation for obtaining a measurement result from an indication (JCGM, 2012). It should define a sensor/system's bias or average deviation from the standard against which it is calibrated, its random errors, the range over which the calibration is valid, and the existence of any thresholds or non-linear response regions. It should also define resolution and hysteresis. Hysteresis should be identified by cycling the sensor over its operating range during calibration. The result of a calibration is often expressed as a calibration factor or as a series of calibration factors in the form of a calibration table or calibration curve. The results of a calibration must be recorded in a document called a calibration certificate or a calibration report.

The calibration certificate or report should define any bias that can then be removed through mechanical, electrical or software adjustment. The remaining random error is not repeatable and cannot be removed, but can be statistically defined through a sufficient number of measurement repetitions during calibration.

4.3.2   **Standards**

The calibration of instruments or measurement systems is customarily carried out by comparing them against one or more measurement standards. These standards are classified according to their metrological quality. Their definitions (see also JCGM, 2012) are given in Part I, Chapter 1 and may be summarized as follows:

Primary standard: A measurement standard established using a primary reference measurement procedure, or created as an artefact, chosen by convention.

Note: When these standards are relevant to NMHS' calibration laboratories or RICs they should also be traceable to the International System of Units (SI).

Secondary standard: A measurement standard established through calibration with respect to a primary measurement standard for a quantity of the same kind.

International standard: A measurement standard recognized by signatories to an international agreement and intended to serve worldwide.

National standard: A measurement standard recognized by national authorities to serve in a State or economy as the basis for assigning quantity values to other measurement standards for the kind of quantity concerned.

Reference standard: A measurement standard designated for the calibration of other measurement standards for quantities of a given kind in a given organization or at a given location.

Working standard: A measurement standard that is used routinely to calibrate or verify measuring instruments or measuring systems.

Transfer device: A device used as an intermediary to compare measurement standards.

Travelling standard: A measurement standard, sometimes of special construction, intended for transport between different locations.

Primary standards reside within major international or national metrological institutions. In pressure measurements (see Part I, Chapter 3), this term is used for instruments based on physical principles, such as mercury barometers or dead weight sensors, although these standards should be called secondary standards according to the calibration and measurement capabilities (CMCs). Secondary standards often reside in major calibration laboratories and are usually not suitable for field use. These standards are generally called reference measurement standards, according to ISO/IEC 17025 (ISO/IEC, 2005). Working standards are usually laboratory instruments that have been calibrated against a secondary standard. Working standards that may be used in the field are known as travelling standards. Travelling standard instruments may also be used to compare instruments in a laboratory or in the field. All of these standards used for a meteorological purpose and relevant to NMHS' calibration laboratories or RICs should be traceable to SI.

4.3.3　　**Traceability**

Traceability is defined by JCGM (2012) as a: "property of a measurement result whereby the result can be related to a reference through a documented unbroken chain of calibrations, each contributing to the measurement uncertainty".

In meteorology, it is common practice for pressure measurements to be traceable through travelling standards, working standards and secondary standards to national standards, and the accumulated uncertainties therefore are known (except for those that arise in the field, which have to be determined by field testing). Temperature measurements lend themselves to the same practice.

The same principle must be applied to the measurement of any quantity for which measurements of known uncertainty are required.

4.3.4　　**Calibration practices**

The calibration of meteorological instruments is normally carried out in a laboratory where appropriate measurement standards and calibration devices are located. They may be Regional Instrument Centres, national laboratories, private laboratories, or laboratories established within the Meteorological Service or other user organization. A calibration laboratory is responsible for maintaining the necessary qualities of its measurement standards and for keeping records of their traceability. Such laboratories can also issue calibration certificates that should also contain an estimate of the uncertainty of calibration. In order to guarantee traceability, the calibration laboratory should be recognized and authorized by the appropriate national authorities.

Manufacturers of meteorological instruments should deliver their quality products, for example, standard barometers or thermometers, with calibration certificates or calibration reports. These documents may or may not be included in the basic price of the instrument, but may be available as options. Calibration certificates given by authorized calibration laboratories may be more expensive than factory certificates. As discussed in the previous section, environmental and functional testing, and possibly additional calibration, should be performed.

Users may also purchase calibration devices or measurement standards for their own laboratories. A good calibration device should always be combined with a proper measurement standard, for example, a liquid bath temperature calibrator with certified resistance thermometers and/or a set of certified liquid-in-glass thermometers. For the example above, further considerations, such as the use of non-conductive silicone fluid, should be applied. Thus, if a temperature-measurement device is mounted on an electronic circuit board, the entire board may be immersed in the bath so that the device can be tested in its operating configuration.

Not only must the calibration equipment and standards be of high quality, but the engineers and technicians of a calibration laboratory must be well trained in basic metrology and in the use of available calibration devices and measurement standards.

Once instruments have passed initial calibration and testing and are accepted by the user, a programme of regular calibration checks and calibrations should be instituted. Instruments, such as mercury barometers, are easily subject to breakage when transported to field sites. At distant stations, these instruments should be kept stationary as far as possible, and should be calibrated against more robust travelling standards that can be moved from one station to another by inspectors. Travelling standards must be compared frequently against a working standard or reference standard in the calibration laboratory, and before and after each inspection tour.

Details of laboratory calibration procedures of, for example, barometers, thermometers, hygrometers, anemometers and radiation instruments are given in the relevant chapters of this Guide or in specialized handbooks. These publications also contain information concerning recognized international standard instruments and calibration devices. Calibration procedures for automatic weather stations require particular attention, as discussed in Part II, Chapter 1.

Field inspection practices

Field inspection offers the user the ability to check the instrument on site. Leaving the instrument installed at a meteorological station eliminates any downtime that would occur while removing and reinstalling the instrument in the field. Inspection is usually done at one point against the working standard by placing the working standard as close to the instrument under inspection (IUI) as possible. Stabilization time must be allowed to reach temperature equilibrium between the working standard and the IUI. Attention must be paid to the proximity of the working standard to the IUI, the temperature gradients, the airflow, the pressure differences and any other factors that could influence the inspection results. This field inspection is an effective way to verify the instrument quality. The most important disadvantage is that the inspection is usually limited to one point. The second disadvantage is that if an error is reported, the IUI should be removed and replaced by a new calibrated sensor. Then the IUI has to be calibrated and adjusted if possible in a laboratory. It should also be noted that the field inspection provides additional valuable information as it involves testing the whole instrumental set-up in the field, including cabling, etc. When performing field inspections, it is important that the metadata of the conditions at the time of the inspection be recorded, including all details on the changes made to the instrumental set-up (see additional details provided in Part II, Chapter 1, 1.7).

Inter-laboratory comparisons

An inter-laboratory comparison (ILC) is defined as the organization, performance and evaluation of calibration results for the same instrument by two or more laboratories in accordance with predetermined conditions. A laboratory's participation in an ILC enables the laboratory to assess and demonstrate the reliability of the resultant measurement data by comparison with results from other participating laboratories. Each accredited laboratory will be expected to participate in a minimum of one proficiency test/inter-laboratory comparison at least every five years for each major sub-discipline of the main disciplines of the laboratory's scope of accreditation. Participation in at least one proficiency test/inter-laboratory comparison is required prior to the granting of accreditation. As mentioned in the RICs' terms of reference (Part I, Chapter 1), a RIC must participate in or organize inter-laboratory comparisons of standard calibration instruments and methods.

4.4 INTERCOMPARISONS OF INSTRUMENTS

Intercomparisons of instruments and observing systems, together with agreed quality-control procedures, are essential for the establishment of compatible datasets. All intercomparisons should be planned and carried out carefully in order to maintain an adequate and uniform

quality level of measurements of each meteorological variable. Many meteorological quantities cannot be directly compared with metrological standards and hence to absolute references — for example, visibility, cloud-base height and precipitation. For such quantities, intercomparisons are of primary value.

Comparisons or evaluations of instruments and observing systems may be organized and carried out at the following levels:

(a)　International comparisons, in which participants from all interested countries may attend in response to a general invitation;

(b)　Regional intercomparisons, in which participants from countries of a certain region (for example, WMO Regions) may attend in response to a general invitation;

(c)　Multilateral and bilateral intercomparisons, in which participants from two or more countries may agree to attend without a general invitation;

(d)　National intercomparisons, within a country.

Because of the importance of international comparability of measurements, WMO, through one of its constituent bodies, from time to time arranges for international and regional comparisons of instruments. Such intercomparisons or evaluations of instruments and observing systems may be very lengthy and expensive. Rules have therefore been established so that coordination will be effective and assured. These rules are reproduced in Annexes 4.A and 4.B.[3] They contain general guidelines and should, when necessary, be supplemented by specific working rules for each intercomparison (see the relevant chapters of this Guide).

Reports of particular WMO international comparisons are referenced in other chapters in this Guide (see, for instance, Part I, Chapters 3, 4, 9, 12, 14 and 15). Annex 4.C provides a list of the international comparisons which have been supported by the Commission for Instruments and Methods of Observation and which have been published in the WMO technical document series.

Reports of comparisons at any level should be made known and available to the meteorological community at large.

––––––––––––

[3]　Recommendations adopted by the Commission for Instruments and Methods of Observation at its eleventh session (1994), through the annex to Recommendation 14 (CIMO-XI) and Annex IX.

ANNEX 4.A. PROCEDURES OF WMO GLOBAL AND REGIONAL INTERCOMPARISONS OF INSTRUMENTS

1.   A WMO intercomparison of instruments and methods of observation shall be agreed upon by the WMO constituent body concerned so that it is recognized as a WMO intercomparison.

2.   The Executive Council will consider the approval of the intercomparison and its inclusion in the programme and budget of WMO.

3.   When there is an urgent need to carry out a specific intercomparison that was not considered at the session of a constituent body, the president of the relevant body may submit a corresponding proposal to the President of WMO for approval.

4.   In good time before each intercomparison, the Secretary-General, in cooperation with the president of CIMO and possibly with presidents of other technical commissions or regional associations, or heads of programmes concerned, should make inquiries as to the willingness of one or more Members to act as a host country and as to the interest of Members in participating in the intercomparison.

5.   When at least one Member has agreed to act as host country and a reasonable number of Members have expressed their interest in participating, an international organizing committee should be established by the president of CIMO in consultation with the heads of the constituent bodies concerned, if appropriate.

6.   Before the intercomparison begins, the organizing committee should agree on its organization, for example, at least on the main objectives, place, date and duration of the intercomparison, conditions for participation, data acquisition, processing and analysis methodology, plans for the publication of results, intercomparison rules, and the responsibilities of the host(s) and the participants.

7.   The host should nominate a project leader who will be responsible for the proper conduct of the intercomparison, the data analysis, and the preparation of a final report of the intercomparison as agreed upon by the organizing committee. The project leader will be a member ex officio of the organizing committee.

8.   When the organizing committee has decided to carry out the intercomparison at sites in different host countries, each of these countries should designate a site manager. The responsibilities of the site managers and the overall project management will be specified by the organizing committee.

9.   The Secretary-General is invited to announce the planned intercomparison to Members as soon as possible after the establishment of the organizing committee. The invitation should include information on the organization and rules of the intercomparison as agreed upon by the organizing committee. Participating Members should observe these rules.

10.   All further communication between the host(s) and the participants concerning organizational matters will be handled by the project leader and possibly by the site managers unless other arrangements are specified by the organizing committee.

11.   Meetings of the organizing committee during the period of the intercomparison could be arranged, if necessary.

12.   After completion of the intercomparison, the organizing committee shall discuss and approve the main results of the data analysis of the intercomparison and shall make proposals for the utilization of the results within the meteorological community.

13.   The final report of the intercomparison, prepared by the project leader and approved by the organizing committee, should be published in the WMO Instruments and Observing Methods Report series.

_____

ANNEX 4.B. GUIDELINES FOR ORGANIZING WMO INTERCOMPARISONS OF INSTRUMENTS

## 1.	INTRODUCTION

1.1	These guidelines are complementary to the procedures of WMO global and regional intercomparisons of meteorological instruments. They assume that an international organizing committee has been set up for the intercomparison and provide guidance to the organizing committee for its conduct. In particular, see Part I, Chapter 12, Annex 12.C.

1.2	However, since all intercomparisons differ to some extent from each other, these guidelines should be considered as a generalized checklist of tasks. They should be modified as situations so warrant, keeping in mind the fact that fairness and scientific validity should be the criteria that govern the conduct of WMO intercomparisons and evaluations.

1.3	Final reports of other WMO intercomparisons and the reports of meetings of organizing committees may serve as examples of the conduct of intercomparisons. These are available from the World Weather Watch Department of the WMO Secretariat.

## 2.	OBJECTIVES OF THE INTERCOMPARISON

The organizing committee should examine the achievements to be expected from the intercomparison and identify the particular problems that may be expected. It should prepare a clear and detailed statement of the main objectives of the intercomparison and agree on any criteria to be used in the evaluation of results. The organizing committee should also investigate how best to guarantee the success of the intercomparison, making use of the accumulated experience of former intercomparisons, as appropriate.

## 3.	PLACE, DATE AND DURATION

3.1	The host country should be requested by the Secretariat to provide the organizing committee with a description of the proposed intercomparison site and facilities (location(s), environmental and climatological conditions, major topographic features, and so forth). It should also nominate a project leader.[1]

3.2	The organizing committee should examine the suitability of the proposed site and facilities, propose any necessary changes, and agree on the site and facilities to be used. A full site and environmental description should then be prepared by the project leader. The organizing committee, in consultation with the project leader, should decide on the date for the start and the duration of the intercomparison.

3.3	The project leader should propose a date by which the site and its facilities will be available for the installation of equipment and its connection to the data-acquisition system. The schedule should include a period of time to check and test equipment and to familiarize operators with operational and routine procedures.

---

[1]	When more than one site is involved, site managers shall be appointed, as required. Some tasks of the project leader, as outlined in this annex, shall be delegated to the site managers.

4.   PARTICIPATION IN THE INTERCOMPARISON

4.1   The organizing committee should consider technical and operational aspects, desirable features and preferences, restrictions, priorities, and descriptions of different instrument types for the intercomparison.

4.2   Normally, only instruments in operational use or instruments that are considered for operational use in the near future by Members should be admitted. It is the responsibility of the participating Members to calibrate their instruments against recognized standards before shipment and to provide appropriate calibration certificates. Participants may be requested to provide two identical instruments of each type in order to achieve more confidence in the data. However, this should not be a condition for participation.

4.3   The organizing committee should draft a detailed questionnaire in order to obtain the required information on each instrument proposed for the intercomparison. The project leader shall provide further details and complete this questionnaire as soon as possible. Participants will be requested to specify very clearly the hardware connections and software characteristics in their reply and to supply adequate documentation (a questionnaire checklist is available from the WMO Secretariat).

4.4   The chairperson of the organizing committee should then request:

(a)   The Secretary-General to invite officially Members (who have expressed an interest) to participate in the intercomparison. The invitation shall include all necessary information on the rules of the intercomparison as prepared by the organizing committee and the project leader;

(b)   The project leader to handle all further contact with participants.

5.   DATA ACQUISITION

5.1   Equipment set-up

5.1.1   The organizing committee should evaluate a proposed layout of the instrument installation prepared by the project leader and agree on a layout of instruments for the intercomparison. Special attention should be paid to fair and proper siting and exposure of instruments, taking into account criteria and standards of WMO and other international organizations. The adopted siting and exposure criteria shall be documented.

5.1.2   Specific requests made by participants for equipment installation should be considered and approved, if acceptable, by the project leader on behalf of the organizing committee.

5.2   Standards and references

The host country should make every effort to include at least one reference instrument in the intercomparison. The calibration of this instrument should be traceable to national or international standards. A description and specification of the standard should be provided to the organizing committee. If no recognized standard or reference exists for the variable(s) to be measured, the organizing committee should agree on a method to determine a reference for the intercomparison.

5.3 Related observations and measurements

The organizing committee should agree on a list of meteorological and environmental variables that should be measured or observed at the intercomparison site during the whole intercomparison period. It should prepare a measuring programme for these and request the host country to execute this programme. The results of this programme should be recorded in a format suitable for the intercomparison analysis.

5.4 Data-acquisition system

5.4.1 Normally the host country should provide the necessary data-acquisition system capable of recording the required analogue, pulse and digital (serial and parallel) signals from all participating instruments. A description and a block diagram of the full measuring chain should be provided by the host country to the organizing committee. The organizing committee, in consultation with the project leader, should decide whether analogue chart records and visual readings from displays will be accepted in the intercomparison for analysis purposes or only for checking the operation.

5.4.2 The data-acquisition system hardware and software should be well tested before the comparison is started and measures should be taken to prevent gaps in the data record during the intercomparison period.

5.5 Data-acquisition methodology

The organizing committee should agree on appropriate data-acquisition procedures, such as frequency of measurement, data sampling, averaging, data reduction, data formats, real-time quality control, and so on. When data reports have to be made by participants during the time of the intercomparison or when data are available as chart records or visual observations, the organizing committee should agree on the responsibility for checking these data, on the period within which the data should be submitted to the project leader, and on the formats and media that would allow storage of these data in the database of the host. When possible, direct comparisons should be made against the reference instrument.

5.6 Schedule of the intercomparison

The organizing committee should agree on an outline of a time schedule for the intercomparison, including normal and specific tasks, and prepare a time chart. Details should be further worked out by the project leader and the project staff.

6. DATA PROCESSING AND ANALYSIS

6.1 Database and data availability

6.1.1 All essential data of the intercomparison, including related meteorological and environmental data, should be stored in a database for further analysis under the supervision of the project leader. The organizing committee, in collaboration with the project leader, should propose a common format for all data, including those reported by participants during the intercomparison. The organizing committee should agree on near-real-time monitoring and quality-control checks to ensure a valid database.

6.1.2 After completion of the intercomparison, the host country should, on request, provide each participating Member with a dataset from its submitted instrument(s). This set should also contain related meteorological, environmental and reference data.

6.2 Data analysis

6.2.1 The organizing committee should propose a framework for data analysis and processing and for the presentation of results. It should agree on data conversion, calibration and correction algorithms, and prepare a list of terms, definitions, abbreviations and relationships (where these differ from commonly accepted and documented practice). It should elaborate and prepare a comprehensive description of statistical methods to be used that correspond to the intercomparison objectives.

6.2.2 Whenever a direct, time-synchronized, one-on-one comparison would be inappropriate (for example, in the case of spatial separation of the instruments under test), methods of analysis based on statistical distributions should be considered. Where no reference instrument exists (as for cloud base, meteorological optical range, and so on), instruments should be compared against a relative reference selected from the instruments under test, based on median or modal values, with care being taken to exclude unrepresentative values from the selected subset of data.

6.2.3 Whenever a second intercomparison is established some time after the first, or in a subsequent phase of an ongoing intercomparison, the methods of analysis and the presentation should include those used in the original study. This should not preclude the addition of new methods.

6.2.4 Normally the project leader should be responsible for the data-processing and analysis. The project leader should, as early as possible, verify the appropriateness of the selected analysis procedures and, as necessary, prepare interim reports for comment by the members of the organizing committee. Changes should be considered, as necessary, on the basis of these reviews.

6.2.5 After completion of the intercomparison, the organizing committee should review the results and analysis prepared by the project leader. It should pay special attention to recommendations for the utilization of the intercomparison results and to the content of the final report.

7. FINAL REPORT OF THE INTERCOMPARISON

7.1 The organizing committee should draft an outline of the final report and request the project leader to prepare a provisional report based on it.

7.2 The final report of the intercomparison should contain, for each instrument, a summary of key performance characteristics and operational factors. Statistical analysis results should be presented in tables and graphs, as appropriate. Time-series plots should be considered for selected periods containing events of particular significance. The host country should be invited to prepare a chapter describing the database and facilities used for data-processing, analysis and storage.

7.3 The organizing committee should agree on the procedures to be followed for approval of the final report, such as:

(a) The draft final report will be prepared by the project leader and submitted to all organizing committee members and, if appropriate, also to participating Members;

(b) Comments and amendments should be sent back to the project leader within a specified time limit, with a copy to the chairperson of the organizing committee;

(c) When there are only minor amendments proposed, the report can be completed by the project leader and sent to the WMO Secretariat for publication;

(d)   In the case of major amendments or if serious problems arise that cannot be resolved by correspondence, an additional meeting of the organizing committee should be considered (the president of CIMO should be informed of this situation immediately).

7.4   The organizing committee may agree that intermediate and final results may be presented only by the project leader and the project staff at technical conferences.

8.   RESPONSIBILITIES

8.1   Responsibilities of participants

8.1.1   Participants shall be fully responsible for the transportation of all submitted equipment, all import and export arrangements, and any costs arising from these. Correct import/export procedures shall be followed to ensure that no delays are attributable to this process.

8.1.2   Participants shall generally install and remove any equipment under the supervision of the project leader, unless the host country has agreed to do this.

8.1.3   Each participant shall provide all necessary accessories, mounting hardware, signal and power cables and connectors (compatible with the standards of the host country), spare parts and consumables for its equipment. Participants requiring a special or non-standard power supply shall provide their own converter or adapter. Participants shall provide all detailed instructions and manuals needed for installation, operation, calibration and routine maintenance.

8.2   Host country support

8.2.1   The host country should provide, if asked, the necessary information to participating Members on temporary and permanent (in the case of consumables) import and export procedures. It should assist with the unpacking and installation of the participants' equipment and provide rooms or cabinets to house equipment that requires protection from the weather and for the storage of spare parts, manuals, consumables, and so forth.

8.2.2   A reasonable amount of auxiliary equipment or structures, such as towers, shelters, bases or foundations, should be provided by the host country.

8.2.3   The necessary electrical power for all instruments shall be provided. Participants should be informed of the network voltage and frequency and their stability. The connection of instruments to the data-acquisition system and the power supply will be carried out in collaboration with the participants. The project leader should agree with each participant on the provision, by the participant or the host country, of power and signal cables of adequate length (and with appropriate connectors).

8.2.4   The host country should be responsible for obtaining legal authorization related to measurements in the atmosphere, such as the use of frequencies, the transmission of laser radiation, compliance with civil and aeronautical laws, and so forth. Each participant shall submit the necessary documents at the request of the project leader.

8.2.5   The host country may provide information on accommodation, travel, local transport, daily logistic support, and so forth.

8.3 **Host country servicing**

8.3.1 Routine operator servicing by the host country will be performed only for long-term intercomparisons for which absence of participants or their representatives can be justified.

8.3.2 When responsible for operator servicing, the host country should:

(a) Provide normal operator servicing for each instrument, such as cleaning, chart changing, and routine adjustments as specified in the participant's operating instructions;

(b) Check each instrument every day of the intercomparison and inform the nominated contact person representing the participant immediately of any fault that cannot be corrected by routine maintenance;

(c) Do its utmost to carry out routine calibration checks according to the participant's specific instructions.

8.3.3 The project leader should maintain in a log regular records of the performance of all equipment participating in the intercomparison. This log should contain notes on everything at the site that may have an effect on the intercomparison, all events concerning participating equipment, and all events concerning equipment and facilities provided by the host country.

9. **RULES DURING THE INTERCOMPARISON**

9.1 The project leader shall exercise general control of the intercomparison on behalf of the organizing committee.

9.2 No changes to the equipment hardware or software shall be permitted without the concurrence of the project leader.

9.3 Minor repairs, such as the replacement of fuses, will be allowed with the concurrence of the project leader.

9.4 Calibration checks and equipment servicing by participants, which requires specialist knowledge or specific equipment, will be permitted according to predefined procedures.

9.5 Any problems that arise concerning the participants' equipment shall be addressed to the project leader.

9.6 The project leader may select a period during the intercomparison in which equipment will be operated with extended intervals between normal routine maintenance in order to assess its susceptibility to environmental conditions. The same extended intervals will be applied to all equipment.

_____

ANNEX 4.C. REPORTS OF INTERNATIONAL COMPARISONS CONDUCTED UNDER THE AUSPICES OF THE COMMISSION FOR INSTRUMENTS AND METHODS OF OBSERVATION[1,2]

Topic	Instruments and Observing Report No.	Title of report
Sunshine duration	16	*Radiation and Sunshine Duration Measurements: Comparison of Pyranometers and Electronic Sunshine Duration Recorders of RA VI* (Budapest, Hungary, July–December 1984), G. Major, WMO/TD-No. 146 (1986).
Radiation	16	*Radiation and Sunshine Duration Measurements: Comparison of Pyranometers and Electronic Sunshine Duration Recorders of RA VI* (Budapest, Hungary, July–December 1984), G. Major, WMO/TD-No. 146 (1986).
Precipitation	17	*International Comparison of National Precipitation Gauges with a Reference Pit Gauge* (1984), B. Sevruk and W.R. Hamon, WMO/TD-No. 38 (1984).
Radiosondes	28	*WMO International Radiosonde Comparison, Phase I* (Beaufort Park, United Kingdom, 1984), A.H. Hooper, WMO/TD-No. 174 (1986).
Radiosondes	29	*WMO International Radiosonde Intercomparison, Phase II* (Wallops Island, United States, 4 February–15 March 1985), F.J. Schmidlin, WMO/TD-No. 312 (1988).
Radiosondes	30	*WMO International Radiosonde Comparison* (United Kingdom, 1984/United States, 1985), J. Nash and F.J. Schmidlin, WMO/TD-No. 195 (1987).
Cloud-base height	32	*WMO International Ceilometer Intercomparison* (United Kingdom, 1986), D.W. Jones, M. Ouldridge and D.J. Painting, WMO/TD-No. 217 (1988).
Humidity	34	*WMO Assmann Aspiration Psychrometer Intercomparison* (Potsdam, German Democratic Republic, 1987), D. Sonntag, WMO/TD-No. 289 (1989).
Humidity	38	*WMO International Hygrometer Intercomparison* (Oslo, Norway, 1989), J. Skaar, K. Hegg, T. Moe and K. Smedstud, WMO/TD-No. 316 (1989).
Radiosondes	40	*WMO International Radiosonde Comparison, Phase III* (Dzhambul, USSR, 1989), A. Ivanov, A. Kats, S. Kurnosenko, J. Nash and N. Zaitseva, WMO/TD-No. 451 (1991).
Visibility	41	*The First WMO Intercomparison of Visibility Measurements* (United Kingdom, 1988/1989), D.J. Griggs, D.W. Jones, M. Ouldridge and W.R. Sparks, WMO/TD-No. 401 (1990).
Radiation	43	*First WMO Regional Pyrheliometer Comparison of RA II and RA V* (Tokyo, Japan, 23 January–4 February 1989), Y. Sano, WMO/TD-No. 308 (1989).

---

[1]   For the most recent reports see: http://www.wmo.int/pages/prog/www/IMOP/publications-IOM-series.html.

[2]   The reports of the WMO International Pyrheliometer Intercomparisons, conducted by the World Radiation Centre at Davos (Switzerland) and carried out at five-yearly intervals, are also distributed by WMO.

Topic	Instruments and Observing Report No.	Title of report
Radiation	44	*First WMO Regional Pyrheliometer Comparison of RA IV* (Ensenada, Mexico, 20–27 April 1989), I. Galindo, WMO/TD-No. 345 (1989).
Pressure	46	*The WMO Automatic Digital Barometer Intercomparison* (de Bilt, Netherlands, 1989–1991), J.P. van der Meulen, WMO/TD-No. 474 (1992).
Radiation	53	*Segunda Comparación de la OMM de Pirheliómetros Patrones Nacionales AR III* (Buenos Aires, Argentina, 25 November–13 December 1991), M. Ginzburg, WMO/TD-No. 572 (1992).
Radiosondes	59	*WMO International Radiosonde Comparison, Phase IV* (Tsukuba, Japan, 15 February–12 March 1993), S. Yagi, A. Mita and N. Inoue, WMO/TD-No. 742 (1996).
Wind	62	*WMO Wind Instrument Intercomparison* (Mont Aigoual, France, 1992–1993), P. Gregoire and G. Oualid, WMO/TD-No. 859 (1997).
Radiation	64	*Tercera Comparación Regional de la OMM de Pirheliómetros Patrones Nacionales AR III – Informe Final* (Santiago, Chile, 24 February–7 March 1997), M.V. Muñoz, WMO/TD-No. 861 (1997).
Precipitation	67	*WMO Solid Precipitation Measurement Intercomparison – Final Report*, B.E. Goodison, P.Y.T. Louie and D. Yang, WMO/TD-No. 872 (1998).
Present weather	73	*WMO Intercomparison of Present Weather Sensors/Systems – Final Report* (Canada and France, 1993–1995), M. Leroy, C. Bellevaux, J.P. Jacob, WMO/TD-No. 887 (1998)
Radiosondes	76	*Executive Summary of the WMO Intercomparison of GPS Radiosondes* (Alcantâra, Maranhão, Brazil, 20 May–10 June 2001), R.B. da Silveira, G. Fisch, L.A.T. Machado, A.M. Dall'Antonia Jr., L.F. Sapucci, D. Fernandes and J. Nash, WMO/TD-No. 1153 (2003).
Radiosondes	83	*WMO Intercomparison of Radiosonde Systems*, Vacoas, Mauritius, 2–25 February 2005, J. Nash, R. Smout, T. Oakley, B. Pathack and S. Kurnosenko, WMO/TD-No. 1303 (2006).
Rainfall intensity	84	*WMO Laboratory Intercomparison of Rainfall Intensity Gauges* – Final Report, France, The Netherlands, Italy, September 2004–September 2005, L. Lanza, L. Stagi, M. Leroy, C. Alexandropoulos, W. Wauben, WMO/TD-No. 1304 (2006)
Humidity	85	*WMO Radiosonde Humidity Sensor Intercomparison* – Final Report of Phase I and Phase II, Phase I: Russian Federation, 1995–1997, Phase II: USA, 8–26 September 1995, Phase I: A. Balagurov, A. Kats, N. Krestyannikova, Phase II: F. Schmidlin, WMO/TD-No. 1305 (2006)
Radiosondes	90	*WMO Intercomparison of GPS Radiosondes* – Final Report, Alcantâra, Brazil, 20 May to 10 June 2001, R. da Silveira, G. F. Fisc, L.A. Machado, A.M. Dall'Antonia Jr., L.F. Sapucci, D. Fernandes, R. Marques, J. Nash, WMO/TD-No. 1314 (2006)
Pyrheliometers	91	*International Pyrheliometer Comparison* – Final Report, Davos, Switzerland, 26 September–14 October 2005, W. Finsterle, WMO/TD-No. 1320 (2006)
Pyrheliometers	97	*Second WMO Regional Pyrheliometer Comparison of RA II* (Tokyo, 22 January–2 February 2007), H. Sasaki, WMO/TD-No. 1494 (2009)

Topic	Instruments and Observing Report No.	Title of report
Pyranometers	98	*Sub-Regional Pyranometer Intercomparison of the RA VI members from South-Eastern Europe* (Split, Croatia, 22 July–6 August 2007), K. Premec, WMO/TD-No. 1501 (2009)
Rainfall intensity	99	*WMO Field Intercomparison of Rainfall Intensity Gauges* (Vigna di Valle, Italy, October 2007–April 2009), E. Vuerich, C. Monesi, L. Lanza, L. Stagi, E. Lanzinger, WMO/TD-No. 1504 (2009)
Thermometer screens and humidity	106	*WMO Field Intercomparison of Thermometer Screens/Shields and Humidity Measuring Instruments*, Ghardaïa, Algeria, November 2008–October 2009 Final Report, M. Lacombe, D. Bousri, M. Leroy, M. Mezred, WMO/TD-No. 1579 (2011)
Radiosondes	107	*WMO Intercomparison of High Quality Radiosonde Systems*, Yangjiang, China, 12 July–3 August 2010, J. Nash, T. Oakley, H. Vömel, LI Wei, WMO/TD-No. 1580 (2011)
Pyrheliometers	108	*WMO International Pyrheliometer Comparison – Final Report*, Davos, Switzerland, 27 September to 15 October 2010, W. Finsterle (2011), http://www.wmo.int/pages/prog/www/IMOP/publications/IOM-108_IPC-XI_Davos.pdf
Pyrheliometers	112	*Baltic Region Pyrheliometer Comparison 2012*, 21 May–1 June 2012, Norrköping, Sweden, T. Carlund (2013)
Pyrheliometers	113	*Third WMO Regional Pyrheliometer Comparison of RA II*, Tokyo, 23 January to 3 February 2012, N. Ohkawara, H. Tatsumi, O. Ljima, H. Koide, S. Yamada (2013), http://www.wmo.int/pages/prog/www/IMOP/publications/IOM-113_RA-II-RPC-2012.pdf

REFERENCES AND FURTHER READING

Hoehne, W.E., 1971: *Standardizing Functional Tests*. NOAA Technical Memorandum, NWS T&EL-12, United States Department of Commerce, Sterling, Virginia.

———, 1972: Standardizing functional tests. *Preprints of the Second Symposium on Meteorological Observations and Instrumentation*, American Meteorological Society, pp. 161–165.

———, 1977: *Progress and Results of Functional Testing*. NOAA Technical Memorandum, NWS T&EL-15, United States Department of Commerce, Sterling, Virginia.

International Electrotechnical Commission, 2002: *Classification of Environmental Conditions – Part 1: Environmental Parameters and their Severities*. IEC 60721-1. Geneva.

International Organization for Standardization, 1999: *Sampling Procedures for Inspection by Attributes – Part 1: Sampling Schemes Indexed by Acceptance Quality Limit (AQL) for Lot-by-Lot Inspection*. ISO 2859-1:1999. Geneva.

———, 2013: *Sampling Procedures for Inspection by Variables – Part 1: Specification for Single Sampling Plans Indexed by Acceptance Quality Limit (AQL) for Lot-by-Lot Inspection for a Single Quality Characteristic and a Single AQL*. ISO 3951-1:2013. Geneva.

International Organization for Standardization/ International Electrotechnical Commission, 2005: *General Requirements for the Competence of Testing and Calibration Laboratories*. ISO/IEC 17025:2005/ Cor 1:2006. Geneva.

Joint Committee for Guides in Metrology, 2012: *International Vocabulary of Metrology – Basic and General Concepts and Associated Terms (VIM)*. JCGM 200:2012.

National Weather Service, 1980: *Natural Environmental Testing Criteria and Recommended Test Methodologies for a Proposed Standard for National Weather Service Equipment*. United States Department of Commerce, Sterling, Virginia.

———, 1984: *NWS Standard Environmental Criteria and Test Procedures*. United States Department of Commerce, Sterling, Virginia.

World Meteorological Organization, 1989: *Analysis of Instrument Calibration Methods Used by Members* (H. Doering). Instruments and Observing Methods Report No. 45 (WMO/TD-No. 310). Geneva.

World Meteorological Organization/International Council of Scientific Unions, 1986: *Revised Instruction Manual on Radiation Instruments and Measurements* (C. Fröhlich and J. London, eds.). World Climate Research Programme Publications Series No. 7 (WMO/TD-No. 149). Geneva.

––––––––––––––

CHAPTER CONTENTS

CHAPTER 5. TRAINING OF INSTRUMENT SPECIALISTS

5.1 INTRODUCTION

5.1.1 General

Given that the science and application of meteorology are based on continuous series of measurements using instruments and systems of increasing sophistication, this chapter is concerned with the training of those specialists who deal with the planning, specification, design, installation, calibration, maintenance and application of meteorological measuring instruments and remote-sensing systems. This chapter is aimed at technical managers and trainers and not least at the instrument specialists themselves who want to advance in their profession.

Training skilled personnel is critical to the availability of necessary and appropriate technologies in all countries so that the WMO Global Observing System can produce cost-effective data of uniform good quality and timeliness. However, more than just technical ability with instruments is required. Modern meteorology requires technologists who are also capable as planners and project managers, knowledgeable about telecommunications and data processing, good advocates for effective technical solutions, and skilled in the areas of financial budgets and people management. Thus, for the most able instrument specialists or meteorological instrument systems engineers, training programmes should be broad-based and include personal development and management skills as well as expertise in modern technology.

Regional Training Centres (RTCs) have been established in many countries under the auspices of WMO, and many of them offer training in various aspects of the operation and management of instruments and instrument systems. Regional Training Centres are listed in the annex. Similarly, Regional Instrument Centres (RICs) and Regional Marine Instrument Centres (RMICs) have been set up in many places, and some of them can provide training. Their locations and functions are listed in Part I, Chapter 1, Annex 1.A, and Part II, Chapter 4, Annex 4.A and are discussed briefly in sections 5.5.1.2, and 5.5.1.3, respectively.

5.1.2 Technology transfer

Training is a vital part of the process of technology transfer, which is the developmental process of introducing new technical resources into service to improve quality and reduce operating costs. New resources demand new skills for the introductory process and for ongoing operation and maintenance. This human dimension is more important in capacity building than the technical material.

As meteorology is a global discipline, the technology gap between developed and developing nations is a particular issue for technology transfer. Providing for effective training strategies, programmes and resources which foster self-sustaining technical infrastructures and build human capacity in developing countries is a goal that must be kept constantly in view.

5.1.3 Application to all users of meteorological instruments

This chapter deals with training mainly as an issue for National Hydrometeorological Services. However, the same principles apply to any organizations that take meteorological measurements, whether they train their own staff or expect to recruit suitably qualified personnel. In common with all the observational sciences, the benefits of training to ensure standardized measurement procedures and the most effective use and care of equipment, are self-evident.

5.2 APPROPRIATE TRAINING FOR OPERATIONAL REQUIREMENTS

5.2.1 Theory and practice

Taking measurements using instrument systems depends on physical principles (for example, the thermal expansion of mercury) to sense the atmospheric variables and transduce them into a standardized form that is convenient for the user, for example, a recorded trace on a chart or an electrical signal to input into an automatic weather station. The theoretical basis for understanding the measurement process must also take into account the coupling of the instrument to the quantity being measured (the representation or "exposure") as well as the instrumental and observational errors with which every measurement is fraught. The basic measurement data is then often further processed and coded in more or less complex ways, thus requiring further theoretical understanding, for example, the reduction of atmospheric pressure to mean sea level and upper-air messages derived from a radiosonde flight.

Taking the measurement also depends on practical knowledge and skill in terms of how to install and set up the instrument to take a standardized measurement, how to operate it safely and accurately, and how to carry out any subsequent calculations or coding processes with minimal error.

Thus, theoretical and practical matters are closely related in achieving measurement data of known quality, and the personnel concerned in the operation and management of the instrument systems need theoretical understanding and practical skills which are appropriate to the complexity and significance of their work. The engineers who design or maintain complex instrumentation systems require a particularly high order of theoretical and practical training.

5.2.2 Matching skills to the tasks

Organizations need to ensure that the qualifications, skills and numbers of their personnel or other contractors (and thus training) are well matched to the range of tasks to be performed. For example, the training needed to read air temperature in a Stevenson screen is at the lower end of the range of necessary skills, while theoretical and practical training at a much higher level is plainly necessary in order to specify, install, operate and maintain automatic weather stations, meteorological satellite receivers and radars.

Therefore, it is useful to apply a classification scheme for the levels of qualification for operational requirements, employment, and training purposes. The national grades of qualification in technical education applicable in a particular country will be important benchmarks. To help the international community achieve uniform quality in their meteorological data acquisition and processing, WMO recommends the use of its own classification of personnel with the accompanying duties that they should be expected to carry out competently.

5.2.3 WMO classification of personnel

The WMO classification scheme[1] identifies two broad categories of personnel: graduate professionals and technicians (WMO, 2001). For meteorological and hydrological personnel, these categories are designated as follows: meteorologist and meteorological technician, and hydrologist and hydrological technician, respectively. The recommended syllabus for each class includes a substantial component on instruments and methods of observation related to the education, training and duties expected at that level. The WMO classification of personnel also sets guidelines for the work content, qualifications and skill levels required for instrument specialists. Section 7.3 of WMO (2001) includes an example of competency requirements, while WMO (2002) offers detailed syllabus examples for the initial training and specialization

---

[1] Classification scheme approved by the WMO Executive Council at its fiftieth session (1998), and endorsed by the World Meteorological Congress at its thirteenth session (1999).

of meteorological personnel. These guidelines enable syllabi and training courses to be properly designed and interpreted; they also assist in the definition of skill deficits and aid the development of balanced national technical skill resources.

5.3 SOME GENERAL PRINCIPLES FOR TRAINING

5.3.1 Management policy issues

5.3.1.1 *A personnel plan*

It is important that National Meteorological Services have a personnel plan that includes instrument specialists, recognizing their value in the planning, development and maintenance of adequate and cost-effective weather observing programmes. The plan would show all specialist instrument personnel at graded levels (WMO, 2001) of qualification. Skill deficits should be identified and provision made for recruitment and training.

5.3.1.2 *Staff retention*

Every effort should be made to retain scarce instrumentation technical skills by providing a work environment that is technically challenging, has opportunities for career advancement, and has salaries comparable with those of other technical skills, both within and outside the Meteorological Service.

5.3.1.3 *Personnel development*

Training should be an integral part of the personnel plan. The introduction of new technology and re-equipment imply new skill requirements. New recruits will need training appropriate to their previous experience, and skill deficits can also be made up by enhancing the skills of other staff. This training also provides the path for career progression. It is helpful if each staff member has a career profile showing training, qualifications and career progression, maintained by the training department, in order to plan personnel development in an orderly manner.

5.3.1.4 *Balanced training*

National training programmes should aim at a balance of skills over all specialist classes giving due attention to the training, supplementation and refresher phases of training, and which result in a self-sustaining technical infrastructure.

5.3.2 Aims and objectives for training programmes

In order to achieve maximum benefits from training it is essential to have clear aims and specific objectives on which to base training plans, syllabi and expenditure. The following strategic aims and objectives for the training of instrument specialists may be considered.

5.3.2.1 *For managers*

Management aims in training instrument specialists should be, among others:

(a) To improve and maintain the quality of information in all meteorological observing programmes;

(b) To enable National Meteorological and Hydrological Services (NMHSs) to become self-reliant in the knowledge and skills required for the effective planning, implementation

and operation of meteorological data-acquisition programmes, and to enable them to develop maintenance services ensuring maximum reliability, accuracy and economy from instrumentation systems;

(c)   To realize fully the value of capital invested in instrumentation systems over their optimum economic life.

5.3.2.2   *For trainers*

The design of training courses should aim:

(a)   To provide balanced programmes of training which meet the defined needs of the countries within each region for skills at graded levels;

(b)   To provide effective knowledge transfer and skill enhancement in National Meteorological Services by using appropriately qualified tutors, good training aids and facilities, and effective learning methods;

(c)   To provide for monitoring the effectiveness of training by appropriate assessment and reporting procedures;

(d)   To provide training at a minimum necessary cost.

5.3.2.3   *For trainers and instrument specialists*

The general objective of training is to equip instrument specialists and engineers (at graded levels of training and experience):

(a)   To appreciate the use, value and desirable accuracy of all instrumental measurements;

(b)   To understand and apply the principles of siting instrument enclosures and instruments so that representative, homogeneous and compatible datasets are produced;

(c)   To acquire the knowledge and skill to carry out installations, adjustments and repairs and to provide a maintenance service ensuring maximum reliability, accuracy and economy from meteorological instruments and systems;

(d)   To be able to diagnose faults logically and quickly from observed symptoms and trace and rectify systematically their causes;

(e)   To understand the sources of error in measurements and be competent in the handling of instrument standards and calibration procedures in order to minimize systematic errors;

(f)   To keep abreast of new technologies and their appropriate application and acquire new knowledge and skills by means of special and refresher courses;

(g)   To plan and design data-acquisition networks, and manage budgets and technical staff;

(h)   To manage projects involving significant financial, equipment and staff resources and technical complexity;

(i)   To modify, improve, design and make instruments for specific purposes;

(j)   To design and apply computer and telecommunications systems and software, control measurements and process raw instrumental data into derived forms and transmit coded messages.

5.3.3   **Training for quality**

Meteorological data acquisition is a complex and costly activity involving human and material resources, communication and computation. It is necessary to maximize the benefit of the information derived while minimizing the financial and human resources required in this endeavour.

The aim of quality data acquisition is to maintain the flow of representative, accurate and timely instrumental data into the national meteorological processing centres at the least cost. Through every stage of technical training, a broad appreciation of how all staff can affect the quality of the end product should be encouraged. The discipline of total quality management (Walton, 1986, and Imai, 1986) considers the whole measurement environment (applications, procedures, instruments and personnel) in so far as each of its elements may affect quality. In total quality management, the data-acquisition activity is studied as a system or series of processes. Critical elements of each process, for example, time delay, are measured and the variation in the process is defined statistically. Problem-solving tools are used by a small team of people who understand the process, to reduce process variation and thereby improve quality. Processes are continuously refined by incremental improvement.

WMO (1990) provides a checklist of factors under the following headings:

(a)   Personnel recruitment and training;

(b)   Specification, design and development;

(c)   Instrument installation;

(d)   Equipment maintenance;

(e)   Instrument calibration.

All of the above influence data quality from the instrument expert's point of view. The checklist can be used by managers to examine areas over which they have control to identify points of weakness, by training staff within courses on total quality management concepts, and by individuals to help them be aware of areas where their knowledge and skill should make a valuable contribution to overall data quality.

The International Organization for Standardization provides for formal quality systems, defined by the ISO 9000 group of specifications (ISO, 2005, 2008, 2009, 2011), under which organizations may be certified by external auditors for the quality of their production processes and services to clients. These quality systems depend heavily on training in quality management techniques.

5.3.4   **How people learn**

5.3.4.1   *The learning environment*

Learning is a process that is very personal to the individual, depending on a person's needs and interests. People are motivated to learn when there is the prospect of some reward, for example, a salary increase. Nonetheless, job satisfaction, involvement, personal fulfilment, having some sense of power or influence, and the affirmation of peers and superiors are also strong motivators. These rewards come through enhanced work performance and relationships with others on the job.

Learning is an active process in which the student reacts to the training environment and activity. A change of behaviour occurs as the student is involved mentally, physically and emotionally. Too much mental or emotional stress during learning time will be counterproductive.

Trainers and managers should attempt to stimulate and encourage learning by creating a conducive physical and psychological climate and by providing appropriate experiences and methods that promote learning. Students should feel at ease and be comfortable in the learning environment, which should not provide distractions. The "psychological climate" can be affected by the student's motivation, the manner and vocabulary of the tutor, the affirmation of previously-acquired knowledge, avoiding embarrassment and ridicule, establishing an atmosphere of trust, and the selection of teaching methods.

5.3.4.2   *Important principles*

Important principles for training include the following:

(a)   *Readiness*: Learning will take place more quickly if the student is ready, interested and wants to learn;

(b)   *Objectives*: The objectives of the training (including performance standards) should be clear to those responsible and those involved;

(c)   *Involvement*: Learning is more effective if students actively work out solutions and do things for themselves, rather than being passively supplied with answers or merely shown a skill;

(d)   *Association*: Learning should be related to past experiences, noting similarities and differences;

(e)   *Learning rate*: The rate of training should equal the rate at which an individual can learn (confirmed by testing), with learning distributed over several short sessions rather than one long session being more likely to be retained;

(f)   *Reinforcement*: Useful exercises and repetition will help instil new learning;

(g)   *Intensity*: Intense, vivid or dramatic experiences capture the imagination and make more impact;

(h)   *Effectiveness*: Experiences which are satisfying are better for learning than those which are embarrassing or annoying. Approval encourages learning;

(i)   *Support*: The trainee's supervisor must be fully supportive of the training and must be able to maintain and reinforce it;

(j)   *Planning and evaluation*: Training should be planned, carried out and evaluated systematically, in the context of organizational needs.

5.3.4.3   *Varying the methods*

People in a group will learn at different speeds. Some training methods (see section 5.4) will suit some individuals better than others and will be more effective under different circumstances. Using a variety of training methods and resources will help the group learn more rapidly.

Research (Moss, 1987) shows that, through the senses, our retention of learning occurs from the following:

(a)   Sight (83%);

(b)   Hearing (11%);

(c)   Other senses (6%).

However, we learn best by actually performing the task. Methods or training media in general order of decreasing effectiveness are:

(a)   Real experience;

(b)   Simulated practical experience;

(c)   Demonstrations and discussions;

(d)   Physical models and text;

(e)   Film, video and computer animation;

(f)   Graphs, diagrams and photographs;

(g)   Written text;

(h)   Lectures.

These methods may, of course, be used in combination. A good lecture may include some of the other methods.

Traditional educational methods rely heavily on the spoken and written word, whereas evidence shows that visual and hands-on experience are far more powerful.

Training for instrument specialists can take advantage of the widest range of methods and media. The theoretical aspects of measurement and instrument design are taught by lectures based on text and formulae and supported by graphs and diagrams. A working knowledge of the instrument system for operation, maintenance and calibration can be gained by the use of photographs with text, films or videos showing manual adjustments, models which may be disassembled, demonstrations, and ultimately practical experience in operating systems. Unsafe practices or modes of use may be simulated.

5.3.5   **Personal skills development**

A meteorological instrument systems engineering group needs people who are not only technically capable, but who are broadly educated and are able to speak and write well. Good personal communication skills are necessary to support and justify technical programmes and particularly in management positions. Skilled technologists should receive training so that they can play a wider role in the decisions that affect the development of their Meteorological Service.

There is a tendency for staff who are numerate and have practical, manual ability to be less able with verbal and written linguistic skills. In the annual personal performance review of their staff, managers should identify any opportunities for staff to enhance their personal skills by taking special courses, for example, in public speaking, negotiation, letter and report writing or assertiveness training. Some staff may need assistance in learning a second language in order to further their training.

5.3.6   **Management training**

Good management skills are an important component of engineering activity. These skills involve time management; staff motivation, supervision and performance assessment (including a training dimension); project management (estimation of resources, budgets, time, staff and materials, and scheduling); problem solving; quality management; and good verbal and written communication skills. Instrument specialists with leadership aptitude should be identified for management training at an appropriate time in their careers.

Today's manager may have access to a personal computer and be adept in the use of office and engineering software packages to be used, for example, for word processing, spreadsheets, databases, statistical analysis with graphics, engineering drawing, flow charting, and project management. Training in the use of these tools can add greatly to personal productivity.

5.3.7   A lifelong occupation

5.3.7.1   *Three training phases*

Throughout their working lives, instrument specialists should expect to be engaged in repeated cycles of personal training, both through structured study and informal on-the-job training or self-study. Three phases of training can be recognized as follows:

(a)   A developmental, training phase when the trainee acquires general theory and practice at graded levels;

(b)   A supplementation phase where the training is enhanced by learning about specific techniques and equipment;

(c)   A refresher phase where some years after formal training the specialist needs refresher training and updates on current techniques and equipment.

5.3.7.2   *Training*

For instrument specialists, the training phase of technical education and training usually occurs partly in an external technical institute and partly in the training establishment of the NMHS where a basic course in meteorological instruments is taken. Note that technical or engineering education may extend over both WMO class levels.

5.3.7.3   *Specialist training*

The supplementation phase will occur over a few years as the specialist takes courses on special systems, for example, automatic weather stations, or radar, or on disciplines like computer software or management skills. Increasing use will be made of external training resources, including WMO-sponsored training opportunities.

5.3.7.4   *Refresher training*

As the instrument specialist's career progresses there will be a need for periodic refresher courses to cover advances in instrumentation and technology, as well as other supplementary courses.

There is an implied progression in these phases. Each training course will assume that students have some prerequisite training on which to build.

5.4   THE TRAINING PROCESS

5.4.1   The role of the trainer

Most instrument specialists find themselves in the important and satisfying role of trainer from time to time and for some it will become their full-time work, with its own field of expertise. All trainers need an appreciation of the attributes of a good trainer.

A good trainer is concerned with quality results, is highly knowledgeable in specified fields, and has good communication skills. He or she will have empathy with students, and will be patient and tolerant, ready to give encouragement and praise, flexible and imaginative, and practised in a variety of training techniques.

Good trainers will set clear objectives and plan and prepare training sessions well. They will maintain good records of training prescriptions, syllabi, course notes, courses held and the results, and of budgets and expenditures. They will seek honest feedback on their performance and be ready to modify their approach. They will also expect to be always learning.

5.4.2 Task analysis

The instrument specialist must be trained to carry out many repetitive or complex tasks for the installation, maintenance and calibration of instruments, and sometimes for their manufacture. A task analysis form may be used to define the way in which the job is to be done, and could be used by the tutor in training and then as a checklist by the trainee. First, the objective of the job and the required standard of performance is written down. The job is broken down into logical steps or stages of a convenient size. The form might consist of a table whose columns are headed, for example with: steps, methods, measures, and reasons:

(a) Steps (what must be done): These are numbered and consist of a brief description of each step of the task, beginning with an active verb;

(b) Methods (how it is to be done): An indication of the method and equipment to be used or the skill required;

(c) Measures (the standard required): Includes a qualitative statement, reference to a specification clause, test, or actual measure;

(d) Reasons (why it must be done): A brief explanation of the purpose of each step.

A flow chart would be a good visual means of relating the steps to the whole task, particularly when the order of the steps is important or if there are branches in the procedure.

5.4.3 Planning the training session

The training process consists of four stages, as shown in the figure:

(a) Planning:

　(i) Review the training objectives, established by the employing organization or standards-setting body (for example, WMO);

　(ii) Analyse the features of the body of knowledge, task or skill that is the subject of the session;

　(iii) Review the characteristics of the students: qualifications, work experience, language ability, specific problems;

　(iv) Assess the required level of training (Which students may need special attention?);

　(v) Determine the objectives for the session (What results are required? How can they be measured?);

(b) Preparation:

　(i) Select course content: Assemble information, organize it in a logical sequence;
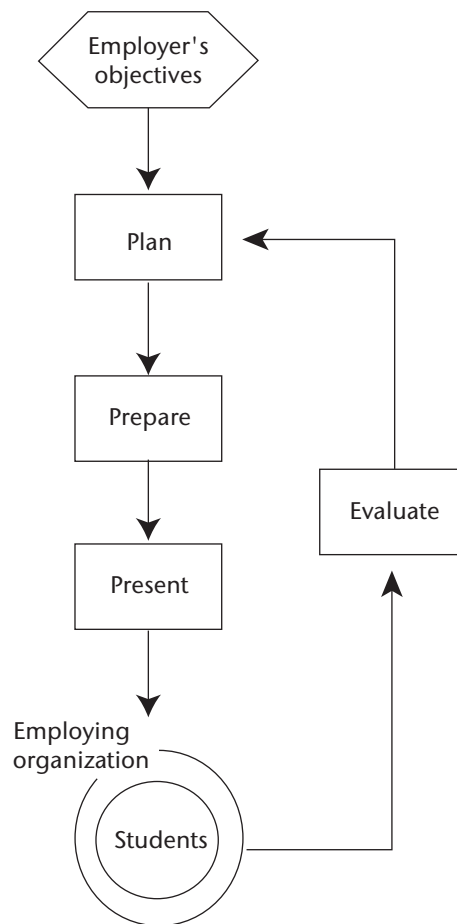
Stages in the training process

    (ii)   Determine training methods and media: appropriate to the topic, so as to create and maintain interest (see section 5.4.5);

    (iii)   Prepare a session plan: Set out the detailed plan with the time of each activity;

    (iv)   Plan evaluation: What information is required and how is it to be collected? Select a method and prepare the questions or assignment;

(c)   Presentation:

    (i)   Carry out training, using the session plan;

    (ii)   Encourage active learning and participation;

    (iii)   Use a variety of methods;

    (iv)   Use demonstrations and visual aids;

(d)   Evaluation:

    (i)   Carry out the planned evaluation with respect to the objectives;

    (ii)   Summarize results;

    (iii)   Review the training session for effectiveness in light of the evaluation;

    (iv)   Consider improvements in content and presentation;

(v)   Write conclusions;

(vi)   Apply feedback to the next planning session.

All training will be more effective if these stages are worked through carefully and systematically.

5.4.4   Effectiveness of training

5.4.4.1   *Targeted training*

With the limited resources available for training, real effort should be devoted to maximizing the effectiveness of training. Training courses and resources should be dedicated to optimizing the benefits of training the right personnel at the most useful time. For example, too little training may be a waste of resources, sending management staff to a course for maintenance technicians would be inappropriate, and it is pointless to train people 12 months before they have access to new technology.

Training opportunities and methods should be selected to best suit knowledge and skills requirements and trainees, bearing in mind their educational and national backgrounds. To ensure maximum effectiveness, training should be evaluated.

5.4.4.2   *Evaluating the training*

Evaluation is a process of obtaining certain information and providing it to those who can influence future training performance. Several approaches to evaluating training may be applied, depending on who needs the information among the following:

(a)   WMO, which is concerned with improving the quality of data collected in the Global Observing System. It generates training programmes, establishes funds and uses the services of experts primarily to improve the skill base in developing countries;

(b)   The National Meteorological Service, which needs quality weather data and is concerned with the overall capability of the division that performs data acquisition and particular instrumentation tasks within certain staff number constraints. It is interested in the budget and cost-benefit of training programmes;

(c)   The training department or Regional Training Centre, which is concerned with establishing training programmes to meet specified objectives within an agreed budget. Its trainers need to know how effective their methods are in meeting these objectives and how they can be improved;

(d)   Engineering managers, who are concerned with having the work skills to accomplish their area of responsibility to the required standard and without wasting time or materials;

(e)   Trainees, who are concerned with the rewards and job satisfaction that come with increased competence. They will want a training course to meet their needs and expectations.

Thus, the effectiveness of training should be evaluated at several levels. National and Regional Training Centres might evaluate their programmes annually and triennially, comparing the number of trainees in different courses and pass levels against budgets and the objectives which have been set at the start of each period. Trainers will need to evaluate the relevance and effectiveness of the content and presentation of their courses.

5.4.4.3   *Types of evaluation*

Types of evaluation include the following:

(a)   A training report, which does not attempt to measure effectiveness. Instead, it is a factual statement of, for example, the type and the number of courses offered, dates and durations, the number of trainees trained and qualifying, and the total cost of training. In some situations, a report is required on the assessed capability of the student;

(b)   Reaction evaluation, which measures the reaction of the trainees to the training programme. It may take the form of a written questionnaire through which trainees score, at the end of the course, their opinions about relevance, content, methods, training aids, presentation and administration. As such, this method cannot improve the training that they receive. Therefore, every training course should have regular opportunities for review and student feedback through group discussion. This enables the trainer to detect any problems with the training or any individual's needs and to take appropriate action;

(c)   Learning evaluation, which measures the trainee's new knowledge and skills, which are best compared against a pre-training test. Various forms of written test (essay, short answer questions, true or false questions, multiple-choice questions, drawing a diagram or flow chart) can be devised to test a trainee's knowledge. Trainees may usefully test and score their own knowledge. Skills are best tested by a set practical assignment or by observation during on-the-job training (WMO, 1990). A checklist of required actions and skills (an observation form) for the task may be used by the assessor;

(d)   Performance evaluation, which measures how the trainee's performance on the job has changed after some time, in response to training, which is best compared with a pre-training test. This evaluation may be carried out by the employer at least six weeks after training, using an observation form, for example. The training institution may also make an assessment by sending questionnaires to both the employer and the trainee;

(e)   Impact evaluation, which measures the effectiveness of training by determining the change in an organization or work group. This evaluation may require planning and the collection of baseline data before and after the specific training. Some measures might be: bad data and the number of data elements missing in meteorological reports, the time taken to perform installations, and the cost of installations.

5.4.4.4   *Training for trainers*

Trainers also require training to keep abreast of technological advances, to learn about new teaching techniques and media, and to catch a fresh vision of their work. There should be provision in their NMHS's annual budget to allow the NMHS's training staff to take training opportunities, probably in rotation.

Some options are: personal study; short courses (including teaching skills) run by technical institutes; time out for study for higher qualifications; visits to the factories of meteorological equipment manufacturers; visits and secondments to other NMHS and RICs; and attendance at WMO and other training and technical conferences.

5.4.5   **Training methods and media**

The following list, arranged in alphabetical order, contains only brief notes to serve as a reminder or to suggest possibilities for training methods (more details may be found in many other sources, such as Moss (1987) and Craig (1987)):

(a)   Case study:

    (i)   A particular real-life problem or development project is set up for study by individuals, or often a team;

    (ii)   The presentation of the results could involve formal documentation as would be expected in a real situation;

(b)   Classroom lecture:

   (i)   This is most suitable for developing an understanding of information which is best mediated in spoken and written form: basic knowledge, theoretical ideas, calculations, procedures;

   (ii)   Visual media and selected printed handout material are very useful additions;

   (iii) There should be adequate time for questions and discussion;

   (iv)   Lectures tend to be excessively passive;

(c)   Computer-assisted instruction:

   (i)   This uses the capability of the personal computer to store large amounts of text and images, organized by the computer program into learning sequences, often with some element of interactive choice by the student through menu lists and screen selection buttons;

   (ii)   The logical conditions and branching and looping structures of the program simulate the learning processes of selecting a topic for study based on the student's needs, presenting information, testing for understanding with optional answers and then directing revision until the correct answer is obtained;

   (iii) Some computer languages, for example, ToolBook for the IBM personal computer and HyperCard for the Macintosh, are designed specifically for authoring and presenting interactive training courses in what are known as "hypermedia";

   (iv)   Modern systems use colour graphic screens and may include diagrams, still pictures and short moving sequences, while a graphical user interface is used to improve the interactive communication between the student and the program;

   (v)   Entire meteorological instrument systems, for example, for upper-air sounding, may be simulated on the computer;

   (vi)   Elaborate systems may include a laser video disc or DVD player or CD-ROM cartridge on which large amounts of text and moving image sequences are permanently stored;

   (vii) The software development and capital cost of computer-assisted instruction systems range from modest to very great; they are beginning to replace multimedia and video tape training aids;

(d)   Correspondence courses:

   (i)   The conventional course consists of lessons with exercises or assignments which are mailed to the student at intervals;

   (ii)   The tutor marks the assignments and returns them to the student with the next lesson;

   (iii) Sometimes it is possible for students to discuss difficulties with their tutor by telephone;

   (iv)   Some courses may include audio or video tapes, or computer disks, provided that the student has access to the necessary equipment;

   (v)   At the end of the course an examination may be held at the training centre;

(e)   Demonstrations:

   (i)   The tutor demonstrates techniques in a laboratory or working situation;

    (ii)   This is necessary for the initial teaching of manual maintenance and calibration procedures;

    (iii)   Students must have an opportunity to try the procedures themselves and ask questions;

(f)   Distance learning:

    (i)   Students follow a training course, which is usually part-time, in their own locality and at times that suit their work commitments, remote from the training centre and their tutor;

    (ii)   Study may be on an individual or group basis;

    (iii)   Some institutions specialize in distance-learning capability;

    (iv)   Distance learning is represented in this section by correspondence courses, television lectures and distance learning with telecommunications;

(g)   Distance learning with telecommunications:

    (i)   A class of students is linked by special telephone equipment to a remote tutor. They study from a printed text. Students each have a microphone which enables them to enter into discussions and engage in question and answer dialogue. Any reliable communications medium could be used, including satellite, but obviously communications costs will be an issue;

    (ii)   In more elaborate and costly systems, all students have computers that are linked to each other and to the remote tutor's computer via a network; or the tutor teaches from a special kind of television studio and appears on a television monitor in the remote classroom, which also has a camera and microphones so that the tutor can see and hear the students;

(h)   Exercises and assignments:

    (i)   These often follow a lecture or demonstration;

    (ii)   They are necessary so that students actively assimilate and use their new knowledge;

    (iii)   An assignment may involve research or be a practical task;

(i)   Exhibits:

    (i)   These are prepared display material and models which students can examine;

    (ii)   They provide a useful overview when the real situation is complex or remote;

(j)   Field studies and visits:

    (i)   Trainees carry out observing practices and study instrument systems in the field environment, most usefully during installation, maintenance or calibration;

    (ii)   Visits to meteorological equipment manufacturers and other Meteorological Services will expand the technical awareness of specialists;

(k)   Group discussion/problem solving:

    (i)   The class is divided into small groups of four to six persons;

    (ii)   The group leader should ensure that all students are encouraged to contribute;

(iii) A scribe or recorder notes ideas on a board in full view of the group;

(iv) In a brainstorming session, all ideas are accepted in the first round without criticism, then the group explores each idea in detail and ranks its usefulness;

(l) Job rotation/secondment:

(i) According to a timetable, the student is assigned to a variety of tasks with different responsibilities often under different supervisors or trainers in order to develop comprehensive work experience;

(ii) Students may be seconded for a fixed term to another department, manufacturing company or another Meteorological Service in order to gain work experience that cannot be obtained in their own department or Service;

(iii) Students seconded internationally should be very capable and are usually supported by bilateral agreements or scholarships;

(m) Multimedia programmes:

(i) These include projection transparencies, video tapes and computer DVDs and CD-ROMs;

(ii) They require access to costly equipment which must be compatible with the media;

(iii) They may be used for class or individual study;

(iv) The programmes should include exercises, questions and discussion topics;

(v) Limited material is available for meteorological instrumentation;

(n) One-to-one coaching:

(i) The tutor works alongside one student who needs training in a specific skill;

(ii) This method may be useful for both remedial and advanced training;

(o) On-the-job training:

(i) This is an essential component of the training process and is when the trainee learns to apply the formally acquired skills in the wide variety of tasks and problems which confront the specialist. All skills are learnt best by exercising them;

(ii) Certain training activities may be best conducted in the on-the-job mode, following necessary explanations and cautions. These include all skills requiring a high level of manipulative ability and for which it is difficult or costly to reproduce the equipment or conditions in the laboratory or workshop. Examples of this are the installation of equipment, certain maintenance operations and complex calibrations;

(iii) This type of training uses available personnel and equipment resources and does not require travel, special training staff or accommodation, and is specific to local needs. It is particularly relevant where practical training far outweighs theoretical study, such as for training technicians;

(iv) The dangers are that on-the-job training may be used by default as the "natural" training method in cases where more structured training with a sound theoretical component is required to produce fully rounded specialists; that supervisors with indifferent abilities may be used; that training may be too narrow in scope and have significant gaps in skills or knowledge; and that the effectiveness of training may not be objectively measured;

(v) The elements necessary for successful on-the-job training are as follows:

a. A training plan that defines the skills to be acquired;

b. Work content covering the required field;

c. A work supervisor who is a good trainer skilled in the topic, has a good teaching style and is patient and encouraging;

d. Adequate theoretical understanding to support the practical training;

e. A work diary for the trainee to record the knowledge acquired and skills mastered;

f. Progress reviews conducted at intervals by the training supervisor;

g. An objective measure of successfully acquired skills (by observation or tests);

(p) Participative training:

(i) This gives students active ownership of the learning process and enables knowledge and experience to be shared;

(ii) Students are grouped in teams or syndicates and elect their own leaders;

(iii) This is used for generating ideas, solving problems, making plans, developing projects, and providing leadership training;

(q) Peer-assisted learning:

(i) This depends on prior common study and preparation;

(ii) In small groups, students take it in turns to be the teacher, while the other students learn and ask questions;

(r) Programmed learning:

(i) This is useful for students who are not close to tutors or training institutions;

(ii) Students work individually at their own pace using structured prepared text, multimedia or computer-based courses;

(iii) Each stage of the course provides self-testing and revision before moving on to the next topic;

(iv) Training materials are expensive to produce and course options may be limited.

Good teaching is of greater value than expensive training aids.

5.4.6 Television lectures

Some teaching institutions which provide predominantly extramural courses broadcast lectures to their correspondence students over a special television channel or at certain times on a commercial channel.

5.4.7 Video programmes

Video programmes offer a good training tool because of the following:

(a)   They provide a good medium for recording and repeatedly demonstrating procedures when access to the instrument system and a skilled tutor is limited;

(b)   The programme may include pauses for questions to be discussed;

(c)   A video programme can be optimized by combining it with supplementary written texts and group discussions;

(d)   Although professionally made videos are expensive and there is limited material available on meteorological instruments, amateurs can make useful technical videos for local use with modest equipment costs, particularly with careful planning and if a sound track is added subsequently.

5.5   RESOURCES FOR TRAINING

Other than the media resources suggested in the previous section, trainers and managers should be aware of the sources of information and guidance available to them; the external training opportunities which are available; the training institutions which can complement their own work; and, not least, the financial resources which support all training activities.

5.5.1   Training institutions

5.5.1.1   *National education and training institutions*

In general, NMHSs will be unable to provide the full range of technical education and training required by their instrument specialists, and so will have varying degrees of dependence on external educational institutions for training, supplementary and refresher training in advanced technology. Meteorological engineering managers will need to be conversant with the curricula offered by their national institutions so that they can advise their staff on suitable education and training courses. WMO (2001, 2002) give guidance on the syllabi necessary for the different classes of instrument specialists.

When instrument specialists are recruited from outside the NMHS to take advantage of well-developed engineering skills, it is desirable that they have qualifications from a recognized national institution. They will then require further training in meteorology and its specific measurement techniques and instrumentation.

5.5.1.2   *The role of WMO Regional Instrument Centres in training*

On the recommendation of CIMO,[2] several WMO regional associations set up RICs to maintain standards and provide advice. Their terms of reference and locations are given in Part I, Chapter 1, Annex 1.A.

RICs are intended to be centres of expertise on instrument types, characteristics, performance, application and calibration. They will have a technical library on instrument science and practice; laboratory space and demonstration equipment; and will maintain a set of standard instruments with calibrations traceable to international standards. They should be able to offer information, advice and assistance to Members in their Region.

Where possible, these centres will combine with a Regional Radiation Centre and should be located within or near an RTC in order to share expertise and resources.

---

[2]   Recommended by the Commission for Instruments and Methods of Observation at its ninth session (1985) through Recommendation 19 (CIMO-IX).

A particular role of RICs is to assist in organizing regional training seminars or workshops on the maintenance, comparison and calibration of meteorological instruments and to provide facilities and expert advisors.

RICs should aim to sponsor the best teaching methods and provide access to training resources and media which may be beyond the resources of NMHSs. The centres will need to provide refresher training for their own experts in the latest technology available and training methods in order to maintain their capability.

Manufacturers of meteorological instrumentation systems could be encouraged to sponsor training sessions held at RICs.

5.5.1.3   *The role of WMO-IOC Regional Marine Instrument Centres in training*

On the recommendation of the Joint WMO/IOC Technical Commission for Oceanography and Marine Meteorology,[3] a network of RMICs has been set up to maintain standards and provide advice regarding marine meteorology and other related oceanographic measurements. Their terms of reference and locations are given in Part II, Chapter 4, Annex 4.A, respectively.

RMICs are intended to be centres of expertise on instrument types, characteristics, performance, application and calibration. They will have a technical library on instrument science and practice, laboratory space and demonstration equipment, and will maintain a set of standard instruments with calibrations traceable to international standards. They should be able to offer information, advice and assistance to Members in their Region.

RMICs will assist in organizing regional training seminars or workshops on the maintenance, comparison and calibration of marine meteorological and oceanographic instruments and will provide facilities and expert advisors.

RMICs should aim to sponsor the best teaching methods and provide access to training resources and media. In order to maintain their capability the centres will arrange refresher training for their own experts in training methods and the latest technology available.

Manufacturers of marine meteorological and oceanographic instrumentation systems could be encouraged to sponsor training sessions held at RMICs.

5.5.2   **WMO training resources**

5.5.2.1   *WMO education and training syllabi*

WMO (2001, 2002) include syllabi for specialization in meteorological instruments and in meteorological telecommunications. The education and training syllabi are guidelines that need to be interpreted in the light of national needs and technical education standards.

5.5.2.2   *WMO survey of training needs*

WMO conducts a periodic survey of training needs by Regions, classes and meteorological specialization. This guides the distribution and kind of training events sponsored by WMO over a four-year period. It is important that Member countries include a comprehensive assessment of their need for instrument specialists in order that WMO training can reflect true needs.

---

[3]   Recommended by the Joint WMO/IOC Technical Commission for Oceanography and Marine Meteorology at its third session (2009) through Recommendation 1 (JCOMM-III).

5.5.2.3 *WMO education and training publications*

These publications include useful information for instrument specialists and their managers. WMO (1986*b*) is a compendium in two volumes of lecture notes on training in meteorological instruments at technician level which may be used in the classroom or for individual study.

5.5.2.4 *WMO training library*

The library produces a catalogue (WMO, 1986*a*) of training publications, audiovisual aids and computer diskettes, some of which may be borrowed, or otherwise purchased, through WMO.

5.5.2.5 *WMO instruments and observing methods publications*

These publications, including reports of CIMO working groups and rapporteurs and instrument intercomparisons, and so forth, provide instrument specialists with a valuable technical resource for training and reference.

5.5.2.6 *Special WMO-sponsored training opportunities*

The Managers of engineering groups should ensure that they are aware of technical training opportunities announced by WMO by maintaining contact with their training department and with the person in their organization who receives correspondence concerning the following:

(a)   Travelling experts/roving seminars/workshops: From time to time, CIMO arranges for an expert to conduct a specified training course, seminar or workshop in several Member countries, usually in the same Region. Alternatively, the expert may conduct the training event at a RIC or RTC and students in the region travel to the centre. The objective is to make the best expertise available at the lowest overall cost, bearing in mind the local situation;

(b)   Fellowships: WMO provides training fellowships under its Technical Cooperation Programme. Funding comes from several sources, including the United Nations Development Programme, the Voluntary Cooperation Programme, WMO trust funds, the regular budget of WMO and other bilateral assistance programmes. Short-term (less than 12 months) or long-term (several years) fellowships are for studies or training at universities, training institutes, or especially at WMO RTCs, and can come under the categories of university degree courses, postgraduate studies, non-degree tertiary studies, specialized training courses, on-the-job training, and technical training for the operation and maintenance of equipment. Applications cannot be accepted directly from individuals. Instead, they must be endorsed by the Permanent Representative with WMO of the candidate's country. A clear definition must be given of the training required and priorities. Given that it takes an average of eight months to organize a candidate's training programme because of the complex consultations between the Secretariat and the donor and recipient countries, applications are required well in advance of the proposed training period. This is only a summary of the conditions. Full information and nomination forms are available from the WMO Secretariat. Conditions are stringent and complete documentation of applications is required.

5.5.3 Other training opportunities

5.5.3.1 *Technical training in other countries*

Other than WMO fellowships, agencies in some countries offer excellent training programmes which may be tailored to the needs of the candidate. Instrument specialists should enquire about these opportunities with the country or agency representative in their own country.

5.5.3.2   *Training by equipment manufacturers*

This type of training includes the following:

(a)   New data-acquisition system purchase: All contracts for the supply of major data-acquisition systems (including donor-funded programmes) should include an adequate allowance for the training of local personnel in system operation and maintenance. The recipient Meteorological Service representatives should have a good understanding of the training offered and should be able to negotiate in view of their requirements. While training for a new system is usually given at the commissioning stage, it is useful to allow for a further session after six months of operational experience or when a significant maintenance problem emerges.

(b)   Factory acceptance/installation/commissioning: Work concerned with the introduction of a major data-acquisition facility, for example, a satellite receiver or radar, provides unique opportunities for trainees to provide assistance and learn the stringent technical requirements.

Acceptance testing is the process of putting the system through agreed tests to ensure that the specifications are met before the system is accepted by the customer and despatched from the factory.

During installation, the supplier's engineers and the customer's engineers often work together. Other components, such as a building, the power supply, telecommunications and data processing, may need to be integrated with the system installation.

Commissioning is the process of carrying out agreed tests on the completed installation to ensure that it meets all the specified operational requirements.

A bilateral training opportunity arises when a country installs and commissions a major instrumentation system and trainees can be invited from another country to observe and assist in the installation.

5.5.3.3   *International scientific programmes*

When international programmes, such as the World Climate Programme, the Atmospheric Research and Environment Programme, the Tropical Cyclone Programme or the Tropical Ocean and Global Atmosphere Programme, conduct large-scale experiments, there may be opportunities for local instrument specialists to be associated with senior colleagues in the measurement programme and to thereby gain valuable experience.

5.5.3.4   *International instrument intercomparisons sponsored by the Commission for Instruments and Methods of Observation*

From time to time, CIMO nominates particular meteorological measurements for investigation as a means of advancing the state of knowledge. Instruments of diverse manufacture and supplied by Members are compared under standard conditions using the facilities of the host country. An organizing committee plans the intercomparison and, in its report, describes the characteristics and performance of the instruments.

If they can be associated with these exercises, instrument specialists would benefit from involvement in some of the following activities: experimental design, instrument exposure, operational techniques, data sampling, data acquisition, data processing, analysis and interpretation of results. If such intercomparisons can be conducted at RICs, the possibility of running a parallel special training course might be explored.

5.5.4 Budgeting for training costs

The meteorological engineering or instrumentation department of every NMHS should provide an adequate and clearly identified amount for staff training in its annual budget, related to the Service's personnel plan. A lack of training also has a cost: mistakes, accidents, wastage of time and material, staff frustration, and a high staff turnover resulting in poor quality data and meteorological products.

5.5.4.1 *Cost-effectiveness*

Substantial costs are involved in training activities, and resources are always likely to be limited. Therefore, it is necessary that the costs of various training options should be identified and compared, and that the cost-effectiveness of all training activities should be monitored, and appropriate decisions taken. Overall, the investment in training by the NMHS must be seen to be of value to the organization.

5.5.4.2 *Direct and indirect costs*

Costs may be divided into the direct costs of operating certain training courses and the indirect or overhead costs of providing the training facility. Each training activity could be assigned some proportion of the overhead costs as well as the direct operating costs. If the facilities are used by many activities throughout the year, the indirect cost apportioned to any one activity will be low and the facility is being used efficiently.

Direct operating costs may include trainee and tutor travel, accommodation, meals and daily expenses, course and tutor fees, WMO staff costs, student notes and specific course consumables, and trainee time away from work.

Indirect or overhead costs could include those relating to training centre buildings (classrooms, workshops and laboratories), equipment and running costs, teaching and administration staff salaries, WMO administration overheads, the cost of producing course materials (new course design, background notes, audiovisual materials), and general consumables used in training.

In general, overall costs for the various modes of training may be roughly ranked from the lowest to the highest as follows (depending on the efficiency of resource use):

(a)   On-the-job training;

(b)   Correspondence courses;

(c)   Audiovisual courses;

(d)   Travelling expert/roving seminar, in situ course;

(e)   National course with participants travelling to a centre;

(f)   Computer-aided instruction (high initial production cost);

(g)   Regional course with participants from other countries;

(h)   Long-term fellowships;

(i)   Regional course at a specially equipped training centre.

ANNEX. REGIONAL TRAINING CENTRES

Country	Name of centre	WMO Region
Algeria	Hydrometeorological Institute for Training and Research (IHFR), Oran	I
Angola	Instituto Nacional de Meteorologia e Geofísica, Luanda	I
Egypt	Egyptian Meteorological Authority, Cairo	I
Kenya	Institute for Meteorological Training and Research, Nairobi; and Department of Meteorology, University of Nairobi, Nairobi	I
Madagascar	École supérieure polytechnique d'Antananarivo, University of Antananarivo; and École nationale d'enseignement de l'aéronautique et de la météorologie, Antananarivo	I
Niger	African School of Meteorology and Civil Aviation (EAMAC), Niamey; and Regional Training Centre for Agrometeorology and Operational Hydrology and their Applications (AGRHYMET), Niamey	I
Nigeria	Meteorological Research and Training Institute, Lagos; and Department of Meteorology, Federal University of Technology, Akure	I
South Africa	South Africa Weather Service, Pretoria	I
China	Nanjing University of Information, Science and Technology, Nanjing; and China Meteorological Administration Training Centre, Beijing	II
India	Central Training Institute and National Water Academy, Pune; India Meteorological Department Training Centre, New Delhi; and Indian Institute of Technology Roorkee, Roorkee	II
Iran (Islamic Republic of)	Islamic Republic of Iran Meteorological Organization, Tehran	II
Iraq	Iraqi Meteorological Organization, Baghdad	II
Qatar	Qatar Aeronautical College, Doha	II
Republic of Korea	Korea Meteorological Administration, Seoul	II
Uzbekistan	Tashkent Hydrometeorological Professional College, Tashkent	II
Argentina	Department of Atmospheric and Ocean Sciences, University of Buenos Aires, Buenos Aires; and Department of Education and Training of the National Meteorological Service, Buenos Aires	III
Brazil	Department of Meteorology, Federal University of Pará, Belém	III
Peru	Universidad Nacional Agraria La Molina, Lima	III
Venezuela (Bolivarian Republic of)	Department of Meteorology and Hydrology, Central University of Venezuela, Caracas	III
Barbados	Caribbean Institute for Meteorology and Hydrology, affiliated with the University of the West Indies, Bridgetown	IV
Costa Rica	Section of Atmospheric Physics, School of Physics, University of Costa Rica, San José	IV
Indonesia	Meteorology, Climatology and Geophysics Agency, Tangerang; and Research Centre for Water Resources, Bandung	V
Philippines	Department of Meteorology and Oceanography, University of the Philippines; and Training Centre of the Philippine Atmospheric, Geophysical and Astronomical Services Administration (PAGASA), Quezon City	V

Country	Name of centre	WMO Region
Israel	Postgraduate Training Centre for Applied Meteorology, Bet Dagan	VI
Italy	National Research Council Institute of Biometeorology, Florence	VI
Russian Federation	Roshydromet Advanced Training Institute, Moscow; Moscow Hydrometeorological College, Moscow; and Russian State Hydrometeorological University, St Petersburg	VI
Turkey	Turkish State Meteorological Service, Ankara	VI

Note: For the most recent information on RTCs and their components, please visit: https://www.wmo.int/pages/prog/dra/etrp/rtcs.php.

REFERENCES AND FURTHER READING

Craig, R.L. (ed.), 1987: *Training and Development Handbook: A Guide to Human Resource Development*. McGraw-Hill, New York.

Imai, M., 1986: *Kaizen: The Key to Japan's Competitive Success*. Random House, New York.

International Organization for Standardization, 2005: *Quality Management Systems – Fundamentals and Vocabulary*. ISO 9000:2005, Geneva.

———, 2008: *Quality Management Systems – Requirements*. ISO 9001:2008, Geneva.

———, 2009: *Managing for the Sustained Success of an Organization – A Quality Management Approach*. ISO 9004:2009, Geneva.

———, 2011: *Guidelines for Auditing Management Systems*. ISO 19011:2011, Geneva.

Moss, G., 1987: *The Trainer's Handbook*. Ministry of Agriculture and Fisheries, New Zealand.

Walton, M., 1986: *The Deming Management Method*. Putnam Publishing, New York.

World Meteorological Organization, 1986*a*: *Catalogue of Meteorological Training Publications and Audiovisual Aids*. Fourth edition, Education and Training Programme Report No. 4 (WMO/TD-No. 124). Geneva.

———, 1986*b*: *Compendium of Lecture Notes on Meteorological Instruments for Training Class III and Class IV Meteorological Personnel* (D.A. Simidchiev). (WMO-No. 622). Geneva.

———, 1990: *Guidance for the Education and Training of Instrument Specialists* (R.A. Pannett). Education and Training Programme Report No. 8 (WMO/TD-No. 413). Geneva.

———, 2001: *Guidelines for the Education and Training of Personnel in Meteorology and Operational Hydrology* (WMO-No. 258), Volume I: Meteorology. Geneva.

———, 2002: *Initial Formation and Specialisation of Meteorological Personnel: Detailed Syllabus Examples* (WMO/TD-No. 1101). Geneva.

———, 2010: *Guide to the Global Observing System* (WMO-No. 488). Geneva.

———————

JN 142286